



# 9<sup>th</sup> IUPAC International Conference on Green Chemistry

5-9 September 2022, Athens, Greece

Venue: **Zappeion Megaron** | [www.greeniupac2022.org](http://www.greeniupac2022.org)

Physical and Virtual

## CONFERENCE PROCEEDINGS



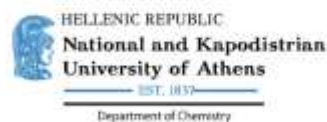
Organized by:

Association of Greek Chemists

In collaboration with:

IUPAC Interdivisional Committee on Green Chemistry for Sustainable Development

Endorsed by :



CONTACT INFORMATION  
GreenIUPAC 2022 Secretariat

- [www.greeniupac2022.org](http://www.greeniupac2022.org)
- [info@greeniupac2022.org](mailto:info@greeniupac2022.org)
- +30 2310 528978
- Enotikon 10 Thessaloniki, Greece, GR - 54627

## Gold Sponsor



**ALFA ANALYTICAL INSTRUMENTS**

## Silver Sponsors



**ACS**  
Chemistry for Life®



## Bronze Sponsors



## Sponsors



**WILEY**

**Global Challenges**



## Supported by



Dear Colleagues,

On behalf of the Association of Greek Chemists (AGC) and the IUPAC Interdivisional Committee on Green Chemistry for Sustainable Development (ICGCSD), we would like to welcome you to the **9th IUPAC International Conference on Green Chemistry (9th ICGC)**, which is taking place on 5-9 September 2022, in Athens, Greece, at Zappeion Megaron, offering the choice of virtual participation. The 9<sup>th</sup> ICGC is endorsed by IUPAC, EuChemS, ACS, the Hellenic Green Chemistry Network, the Green Sciences for Sustainable Development Foundation, and the Departments of Chemistry of Aristotle University of Thessaloniki and of National and Kapodistrian University of Athens. The 9<sup>th</sup> ICGC is the ninth of a series of ICGCSD/IUPAC successful conferences on Green and Sustainable Chemistry that started 16 years ago in Germany (2006), followed by the conferences in Russia (2008), Canada (2010), Brazil (2012), South Africa (2014), Italy (2016), Russia (2017) and Thailand (2018).

The IUPAC ICGC conferences offer the opportunity to discuss the latest developments in green & sustainable chemistry, to expand existing and establish new relations among academia and industry, and to disseminate the philosophy and principles of sustainable development and circular (bio)economy. The topics of the 9<sup>th</sup> ICGC cover the broader field of green chemistry and technology with more emphasis on green solvents, sustainable catalytic and synthetic processes, biomass conversion to fuels, chemicals and polymers, CO<sub>2</sub> utilization, alternative fuels and green energy, benign low-energy chemical processes, nanomaterials for energy and the environment, pollution prevention and remediation, computational chemistry, green chemistry metrics and environmental assessment, sustainable industrial processes, waste recycle and valorization, and circular (bio)economy.

The conference program consists of 9 Plenary and 17 Keynote Lectures, ~200 Oral and ~300 Poster presentations. Five Special Issues will be dedicated to the 9<sup>th</sup> ICGC, in the journals *Pure and Applied Chemistry* (De Gruyter), *ACS Sustainable Chemistry & Engineering* (ACS), *Green Chemistry* (RSC), *Sustainable Chemistry and Pharmacy* (Elsevier), and *Catalysis Today* (Elsevier), featuring selected high-quality papers presented at the conference.

We would like to thank the Plenary and Keynote speakers for accepting our invitation to deliver a lecture, all the authors who have dedicated important time in preparing their abstracts and presentations, as well as all session chairs for ensuring a smooth flow of the programme. We would also like to thank all the organizations and companies that supported the 9<sup>th</sup> ICGC financially and offered the means for organizing a high-quality conference.

We look forward to welcoming you at the 9th ICGC in Athens or on-line and have a fruitful and enjoyable conference!

On behalf of the Organizing Committee,

Konstantinos Triantafyllidis

Chair of the 9th ICGC

# Committees

## ICGCSD/IUPAC Members

<b>Buxing Han, Chinese Academy of Sciences, China – Committee Chair</b>	
<b>Pietro Tundo, Ca' Foscari University of Venice, Italy – Committee Secretary</b>	<b>Michelle Rogers, Cargill, Inc., USA</b>
<b>Jonathan Forman, Pacific Northwest National Laboratory, USA</b>	<b>Tim Wallington, Ford Motor Company, USA</b>
<b>Klaus Kümmerer, Leuphana University Lüneburg, Germany</b>	<b>Quirinus B. Broxterman, InnoSyn B.V., The Netherlands</b>
<b>Natalia P. Tarasova, D. Mendeleev University of Chemical Technology, Russia</b>	<b>Srivari Chandrasekhar, CSIR-Indian Institute of Chemical Technology, India</b>
<b>Florent Allais, URD ABI – AgroParisTech, France</b>	<b>Sylvia Draper, The University of Dublin, Ireland</b>
<b>Aurelia Sorina Visa, Institute of Chemistry Timisoara of the Romanian Academy, Romania</b>	<b>Elisaveta H. Ivanova, Bulgarian Academy of Sciences, Bulgaria</b>
<b>Jane Wissinger, University of Minnesota, USA</b>	<b>Jian Pei, Peking University, China</b>
<b>Ana Aguiar-Ricardo, Universidade NOVA de Lisboa, Portugal (President of the EuChemS – Division of Green and Sustainable Chemistry)</b>	<b>Elena Poverenov, Agricultural Research Organization, Israel</b>
<b>Nadia Kandile, Ain Shams University, Egypt</b>	<b>Adriana Tafrova-Grigorova, University of Sofia, Bulgaria</b>
<b>Liliana Mammìno, University of Venda, South Africa</b>	<b>Supawan Tantayanon, Chulalongkorn University, Thailand</b>

## International Scientific Committee

<b>Pietro Tundo, Ca' Foscari University of Venice, Italy – Chair</b>	
<b>Donato A. G. Aranda, Universidade Federal do Rio de Janeiro, Brazil</b>	<b>Santiago V. Luis, University Jaume I, Spain</b>
<b>Katalin Barta, University of Groningen, The Netherlands</b>	<b>Jeremy Luterbacher, Ecole Polytechnique Fédérale de Lausanne, Switzerland</b>
<b>Hassan S. Bazzi, Texas A&amp;M University at Qatar, Qatar</b>	<b>Michael North, The University of York, UK</b>
<b>Pieter Bruijninx, Utrecht University, The Netherlands</b>	<b>Vasile Parvulescu, University of Bucharest, Romania</b>
<b>Emilio E. Bunel, Pontificia Universidad Católica de Chile, Chile</b>	<b>Elsje Alessandra Quadrelli, Université de Lyon/CNRS, France</b>
<b>Juan Carlos Colmenares, Polish Academy of Sciences, Poland</b>	<b>Daniel Garcia Rivers, University of Havana, Cuba</b>
<b>Fernando Colmenares, Universidad Cooperativa de Colombia, Colombia</b>	<b>Thomas Schaub, Catalysis Research Laboratory, BASF SE, Germany</b>
<b>Claudia Crestini, Ca' Foscari University of Venice, Italy</b>	<b>James Sullivan, University College Dublin, Ireland</b>
<b>Nicholas Gathergood, University of Lincoln, UK</b>	<b>Andreia F. Sousa, University of Aveiro, Portugal</b>
<b>Richard Gosselink, Wageningen University and Research, The Netherlands</b>	<b>Charlotta Turner, Lund University, Sweden</b>
<b>Roger Gläser, University of Leipzig, Germany</b>	<b>Luigi Vaccaro, University of Perugia, Italy</b>
<b>Oliver Kappe, University of Graz, Austria</b>	<b>Dionisios Vlachos, University of Delaware, USA</b>
<b>Arjan Kleij, Institute of Chemical Research of Catalonia, Spain</b>	<b>Dirk De Vos, KU Leuven, Belgium</b>
<b>David Kubicka, University of Chemistry and Technology Prague, Czech Republic</b>	<b>Feng Wang, Dalian Institute of Chemical Physics, Chinese Academy of Sciences, China</b>
<b>Carol S.K. Lin, City University of Hong Kong, Hong Kong</b>	<b>Vadim Yakovlev, Boreskov Institute of Catalysis SB RAS, Russia</b>
<b>Ekaterina S. Lokteva, Lomonosov Moscow State University, Russia</b>	<b>Ning Yan, National University of Singapore, Singapore</b>
<b>Julie Zimmerman, Yale University, USA</b>	

### Local Organizing Committee

<b>Konstantinos Triantafyllidis, Aristotle University of Thessaloniki – Chair</b>	
<b>Panayotis Siskos, National and Kapodistrian University of Athens– Vice Chair</b>	<b>Ioannis Katsoyiannis, Aristotle University of Thessaloniki, President of Association of Greek Chemists (AGC)</b>
<b>Konstantinos Poulos, University of Patras, Coordinator of Hellenic Green Chemistry Network</b>	<b>Athanasios Papadopoulos, International Hellenic University and AGC</b>
<b>Panagiotis Spathis, Chair of Dept. of Chemistry, Aristotle University of Thessaloniki</b>	<b>Christiana Mitsopoulou, Chair of Dept. of Chemistry, National and Kapodistrian University of Athens</b>
<b>Victoria Samanidou, Aristotle University of Thessaloniki and AGC</b>	<b>Eleni Deliyanni, Aristotle University of Thessaloniki and AGC</b>
<b>Adamantini Paraskevopoulou, Aristotle University of Thessaloniki and AGC</b>	<b>Vasileios Koulos, Association of Greek Chemists (AGC)</b>
<b>Yannis Vafeiadis, Association of Greek Chemists (AGC)</b>	<b>Ioannis Sitaras, Association of Greek Chemists (AGC)</b>
<b>Emmanouil Daftsis, Association of Greek Chemists (AGC)</b>	<b>Georgios Iakovou, Aristotle University of Thessaloniki</b>
<b>Dimitrios Giannakoudakis, Aristotle University of Thessaloniki and AGC</b>	<b>Kyriazis Rekos, Aristotle University of Thessaloniki and AGC</b>
<b>Konstantinos Moustakas, National Technical University of Athens</b>	<b>Antigoni Margellou, Aristotle University of Thessaloniki</b>
<b>Christina Pappa, Aristotle University of Thessaloniki</b>	<b>Dimitrios Giliopoulos, Aristotle University of Thessaloniki</b>
<b>Soultana Ioannidou, Aristotle University of Thessaloniki</b>	<b>Eleni Psochia, Aristotle University of Thessaloniki</b>
<b>Eleni Salonikidou, Aristotle University of Thessaloniki</b>	<b>Stylianos Torofias, Aristotle University of Thessaloniki</b>

### Local Scientific Committee

<b>Anastasios Zouboulis, Aristotle University of Thessaloniki (AUTH)</b>	<b>Ioannis Lykakis, Aristotle University of Thessaloniki</b>
<b>Christiana Mitsopoulou, National and Kapodistrian University of Athens</b>	<b>Christoforos Kokotos, National and Kapodistrian University of Athens</b>
<b>Angeliki Lemonidou, Aristotle University of Thessaloniki</b>	<b>Michael Terzidis, International Hellenic University and AGC</b>
<b>George Kyzas, International Hellenic University</b>	<b>Dimitrios Bikiaris, Aristotle University of Thessaloniki</b>
<b>Stella Bezergianni, Centre for Research and Technology-Hellas</b>	<b>Angelos Lappas, Centre for Research and Technology-Hellas (CERTH)</b>
<b>Eleni Iliopoulou, Centre for Research and Technology-Hellas</b>	<b>Eleni Heracleous, International Hellenic University and CERTH</b>
<b>Panagiotis Kougiyas, Hellenic Agricultural Organisation DEMETER</b>	<b>Andreana Assimopoulou, Aristotle University of Thessaloniki</b>

## TABLE OF CONTENTS

### Plenary Lectures..... 28

Circular Chemistry: Catalyzing the Green Economy.....	29
Reaction Mechanisms and Energy Profiles: How Green Chemistry Complies with them. The Case of Dimethyl Carbonate .....	30
Green Chemistry, “...to solve most of the world’s problems.” .....	31
Emerging technologies for a sustainable conversion of lignocellulosic biomass into biobased products .....	32
Conversion of CO <sub>2</sub> and Biomass into Chemicals and Fuels.....	33
EU perspective for biofuels and bioenergy under the European Green Deal and REPowerEU.....	34
How CO <sub>2</sub> -Switchable Materials can Help in Biomass Conversion and Greener Coatings .....	35
Green Synthesis of Metal Nanoparticle Embedded Soft Hybrid Gel from Plant-based materials....	36
Enhancing the Circular Economy in the Water Sector by Addressing the Chemical Contaminants of Concern Present in Wastewater .....	37

### Keynote Lectures..... 38

Sustainable Cross-Couplings: Demetallation of Organometallic Reactions.....	39
Biowaste valorisation: the waste-to-wealth concept .....	40
DES, ES AND ILS: Tailoring Solvents for Sustainable Applications.....	41
Unlocking the potential of crustacean waste: solvent-free pathways to added-value materials ....	42
Teaching global perspectives: Connecting Green Chemistry, the UN SDGs, and Sustainable Polymers.....	43
On the Efficient Transformation of Co <sub>2</sub> to Chemicals and Fuels.....	44
Chemicals from lignin: feasible, safe and sustainable.....	45
European Sustainable Biobased Nanomaterials Community (BIOMAC). From biomass pretreatment for monomers and additives extraction to the synthesis of biobased composites .....	46
Towards Scalable Synthesis of Furanics: Products Purification and Comparative Environmental Assessment.....	48
Design of Biomass Waste-Derived Biochar Catalyst for Glucose Oxidation .....	49
Alternative technologies for the selective conversion of bio-based feedstocks to specialty chemicals.....	50
Solar Fuels: from Mechanistic Understanding to Device Engineering.....	51
The quest to a circular approach to (furanic) polymers.....	52
Biocatalytic solutions for industrial waste glycerol valorization.....	54
Green Analytical Chemistry and Circularity: towards more sustainable processes, materials and outcomes.....	55
Green chemistry and computational chemistry: a wealth of promising synergies .....	56

**Oral presentations.....57****Alternative & benign chemical processes.....58**

Organic Synthetic Photochemistry: Embracing the Needs of Green and Sustainable Chemistry ....	59
Photocatalytic cleavage of lignin C–C bonds by Z-scheme nanocomposite .....	60
Reduction of alkenes to alkanes by ammonia under high frequency ultrasound .....	62
A new concept for the sustainable coupling of catalysis processes: {2-phases 2-reactions 1-catalyst} <sup>†</sup> .....	64
Merging photoflow and Pd-catalysis to synthesized new aminocyclopentenes .....	66
Chiral metal organic frameworks for electrocatalytic water splitting .....	67
A roadmap towards the development of a scalable continuous flow process for the synthesis of a Raf kinase inhibitor, BAY 43-9006 .....	69

**Alternative fuels & biofuels – Green energy .....71**

Light-induced production of biobased fuels and lubricant oils from conjugated dienes .....	72
Bio-crude oil production via hydrothermal liquefaction of agricultural biomass.....	73
Continuous hydroprocessing of nitrogen-rich biocrudes from municipal solid wastes in a graded catalyst bed: Synergetic effect of oxygenates and nitrogenates .....	75
Catalytic hydrodeoxygenation of lignin pyrolysis bio-oil towards transportation fuels .....	76
Biomass to hydrogen: Understanding the factors affecting hydrogen production rate via reforming of bio-oil. ....	78
A flexible and integrated process for treating multiple waste biomass to produce high-value bioproducts and advanced transportation fuel .....	80
Transformation of natural triglycerides into green diesel over Ni-Mo catalysts supported on titania .....	81
Fluidized bed gasification of solid digestate from anaerobic digestion plants – The THERMODIGESTATE project.....	84
Design approaches and mechanistic insights of molecular metal chalcogenides as H <sub>2</sub> evolution catalysts.....	86
Flame Spray Pyrolysis as a Synthesis Platform to Assess Metal Promotion in In <sub>2</sub> O <sub>3</sub> -Catalyzed CO <sub>2</sub> Hydrogenation.....	88
Combustion induced multicomponent Cu based catalysts for CO/CO <sub>2</sub> hydrogenation to methanol in three-phase system: Experimental and Theoretical Insights .....	90
Plasma assisted conversion of CO <sub>2</sub> and CH <sub>4</sub> over promoted catalysts: Comprehension of surface effects.....	92
Tuning the structural and catalytic active sites of TiO <sub>2</sub> /CeO <sub>2</sub> for CO <sub>2</sub> conversion to synthesize a green fuel additive .....	94
Single step synthesis of bio-inspired NiO/C as Pd support catalyst for direct ethanol fuel cell application.....	95
Methane oxidation using earth abundant metals anchored on nodes of a metal-organic framework .....	96

Heterotrophic production of biofuels in marine diatoms.....	98
<b>Biobased monomers, polymers &amp; composites .....</b>	<b>99</b>
Innovative Structural Modification Process of Kraft Lignin Using Flow System Approach.....	100
UV degradation of poly(lactic acid) materials through copolymerisation with a sugar-derived cyclic xanthate .....	102
Itaconic acid as renewable building block for UV-curing polymer resins .....	104
Recyclable, degradable, and high Tg bio-based Polybenzoxazine vitrimers.....	105
Lignin as a renewable resource – a deep dive into structure-property relationship.....	106
Epoxy - Organosolv lignin composites with enhanced properties .....	107
Preparation of lignin-based vinylogous urethane vitrimer materials and their potential use for removable adhesives.....	108
Lipase-catalyzed selective (meth)acrylation of lignin-derived monomers for the protection-group free synthesis of polymers with strong antioxidant properties.....	109
Synthesis of biobased polymers based on isohexide building blocks .....	110
Fully lignocellulose-based PET analogues for the circular economy.....	111
Greener Enzymatic Synthesis of Levoglucosenone-based Polymers .....	112
Degradable Cross-linked Polyesters: Resins to be Cheerful.....	114
D-xylose for a versatile class of bioplastics with tunable properties .....	115
Synthesis, aging and antibacterial tests of di(meth)acrylate composites.....	117
Biobased monomers and polymers from lignin and cellulose .....	119
Synthesis of renewable diblock copolymers by aqueous RAFT polymerisation induced self-assembly of lactic acid-based monomers .....	120
Biobased Boronic Ester Vitrimer Resin from Epoxidized Linseed Oil for Recyclable Carbon Fiber Composites.....	121
<b>Bio-catalysis &amp; bio-processes .....</b>	<b>122</b>
Silymarin derivatization using biocatalytic system based on cold-active lipase biocatalyst.....	123
Enzymatic Preparation of Lipophilic Derivatives of Hydroxytyrosol with Enhanced Oxidative Stability.....	124
Synthesis of novel rearranged stemodane diterpenoids and their biotransformation by <i>Exophiala lecanii-corni</i> .....	126
DES-based biocatalysis for menthol derivatization.....	127
Reactive natural deep eutectic solvents as essential reaction media for lipase catalyzed carbohydrate esterification.....	128
<b>Biomass and renewables valorization .....</b>	<b>130</b>
The Use of Cellulose Nanocrystals as Scaffolds for Nanodevices, Photoreversible and Antimicrobial Self Assemblies; Supramolecular Chemistry Using Nature’s Most Abundant Template .....	131



Crosslinking of Sugar-Derived Polyethers and Boronic Acids: Synthesis of Functional Films and Organogels .....	133
Green dual crosslinking treatments to produce chitosan microspheres based on tripolyphosphate and vanillin: a comparative study of two strategies .....	135
FucoPol-based cosmetic creams: Formulation design, stability evaluation, rheological and texture assessment .....	137
One-Pot and Biomass-Agnostic Syntheses of Biodegradable and Non-Ecotoxic Surfactants from Algal Polysaccharides and Pectins .....	138
Pretreatment of brewers' spent grains via non-thermal plasma for poly(3-hydroxybutyrate) production .....	139
Antibacterial activity of porous hydrogel films from renewable raw materials and their carrier ability for controlled release of flavoring compounds .....	141
Strategies for the production of biorefinery enzymes by the valorisation of lignocellulosic waste	142
Lactic and succinic acid production from lignocellulosic biomass .....	144
Indigenous plants as a source for discovery and synthesis of pharmaceutical products and industrial materials.....	146
. BlueBio mass valorization through analytical techniques for the quest of biostimulants in plant growth .....	147
Solid dispersions as food colorant solutions: a systematic study addressing different natural polymers.....	149
Electrochemical C-H Functionalization of Quinolizidine Alkaloids.....	151
Biobased vitrimers - novel dynamic materials from vegetable oils and their applications .....	152
<b><u>Biomass to chemicals .....</u></b>	<b>153</b>
Metal free heterogeneous catalyst for one pot conversion of fructose/carbohydrate feedstocks into 2,5-diformylfuran.....	154
Predictive model of the biocatalytic synthesis of butyl levulinate from levulinic acid in a continuous flow microreactor .....	155
Butyl-5-(Dibutoxymethyl)-2-Furoate (BDMF): a New Bio-sourced Furanic Platform Molecule for the Green Production of Biodegradable Surfactants and Industrial Chemicals.....	157
Selective condensation of small sugars by reconstructed Hydrotalcite towards the synthesis of polyol-based flame retardants .....	158
Efficient conversion of sucrose to methyl lactate with Sn-USY: the role of water .....	159
Catalytic dehydrative decarbonylation of tall oil-derived fatty acids to linear alpha-olefins.....	161
<b><u>Bio-Waste Valorization &amp; Circular economy .....</u></b>	<b>162</b>
Influence of supercritical CO <sub>2</sub> pretreatment of spent coffee grounds on the yield and composition of polar molecules extracted by subcritical H <sub>2</sub> O extraction under microwave irradiation .....	163
Biphasic green solvents system for a fast "one-pot" simultaneous extraction at room temperature of valuable compounds from tomato pomace waste .....	164

Re-circulation of spent coffee grounds for ‘awaking’ epoxy resins cross-linking and stimulating properties .....	166
Biovalorization of by-products from olive leaf and olive pomace obtained through green extraction methodology .....	167
High-performance or Functional Plant oil-based UV-curable Materials: Green Synthesis, properties, and applications .....	170
The effects of hydrogen peroxide and bleach on cellulose in oxidised sugar beet pulp .....	171
<b>Bio-waste valorization .....</b>	<b>173</b>
How the physio-chemical properties of char from the pyrolysis of Automotive Shredder Residue (ASR) influences its future uses .....	174
Nitrogen-rich waste step gasification: evolution of fuel-nitrogen during the different stages .....	176
Simultaneous nutrient ions recovery from anaerobic digestates of different origin by using Selective Electrodialysis .....	177
Hydrolysis of poly(ethylene terephthalate) using a wide range of Low-Cost Ionic Liquids for chemical plastic recycling .....	179
Optimization of ultrasound-assisted extraction of natural antioxidants from rapeseed cake using deep eutectic solvents.....	180
Extraction of bioactive compounds from fisheries waste streams using natural deep eutectic solvent systems for their therapeutic application .....	182
Adsorption from the liquid and gas phase on biocarbons obtained from residue after supercritical extraction of raw plants .....	184
Biochar and Activated Carbon Derived from Oil Palm Kernel Shell as a Framework for the Preparation of Sustainable Controlled Release Urea Fertilizer .....	186
<b>Catalysis for biomass &amp; sustainable synthesis .....</b>	<b>189</b>
Selective photo-catalytic oxidation of 5-hydroxymethylfurfural (HMF) to 2,5-Diformylfuran (DFF) over reduced graphite oxide-titanate nanotubes composites.....	190
Sustainable one-pot syntheses of functional dyes based on 5-(hydroxymethyl)furfural .....	192
Catalytic conversion of biomass-derived compounds to high added value products using an acid treated natural mordenite .....	194
A green chemistry approach to catalytic synthesis of ethyl levulinate.....	196
Application of copper-containing minerals in preparative organic chemical reactions as catalysts. ....	197
A Comparison of In-situ Reduction of Copper and Nickel-rich Mixed Oxides for Effective Organosolv Lignin Fractionation.....	198
Development of Cr-free hydrogenolysis catalysts .....	199
Mesoporous metal phosphates and zeolites as solid acid catalysts: Stability and catalytic performance in oleic acid esterification.....	201
<b>Catalysis for biomass.....</b>	<b>204</b>

Recovery of monoaromatic compounds from Kraft lignin toward the production of a potential green bisphenol A replacer .....	205
From biomass-derived furans to aromatic compounds catalyzed by WNb-O mixed oxides with controlled acid properties .....	206
Heterogeneous catalytic conversion of 5-Hydroxymethyl furfural to Methoxymethylfurfural .....	208
Catalytic conversion of tetroses to methionine hydroxy analogues.....	210
Synthesis of semi-aromatic polyamides based on renewable 2,5-furandicarboxylic acid (FDCA) .	212
Conversion of biomass derived levulinic acid into $\gamma$ -valerolactone using methanesulfonic acid: An optimization study using response surface methodology .....	214
Promotion of hydroxy bond hydrogenolysis versus aromatic ring hydrogenation by selective poisoning with chlorine of heterogeneous Cu-Co catalysts.....	215
<b>CO<sub>2</sub> utilization.....</b>	<b>217</b>
Effect of Ni Particle Size in the Low-Temperature CO <sub>2</sub> Hydrogenation Over Highly Active Ni/CeO <sub>2</sub> -Nanorods .....	218
Low temperature CO <sub>2</sub> -assisted ethane dehydrogenation for ethylene production:.....	221
chemical looping vs cofeeding .....	221
Reducing Energy Demand by Capturing Carbon in Green Solvents.....	224
Multi-enzyme co-immobilization on Hierarchical Porous Carbon Nanoparticles (HPCs) for the bioconversion of CO <sub>2</sub> to Formic Acid.....	226
Solid Oxide Electrolysis for the production of green-energy carriers.....	229
Electrochemical reduction of uncaptured flue gas in a membrane electrode assembly electrolyzer .....	231
Capture and reuse of CO <sub>2</sub> : from ionic liquids to structured 3DP printed devices.....	233
POSS-porphyrin-imidazolium crosslinked network as catalytic bifunctional platform for the conversion of CO <sub>2</sub> with epoxides. ....	235
<b>Computational chemistry.....</b>	<b>237</b>
A Computational and Testing Toolbox Towards Safe and Sustainable by Design Chemicals .....	238
Experiment-based parameter estimation of an amine solvent for CO <sub>2</sub> hydrogenation using hybrid Gaussian Process Bayesian Optimization.....	240
Machine Learning Assisted Modeling of Interfacial Tension in the System N <sub>2</sub> /Brine.....	242
Computational eco-design and screening of biodegradable renewable polyesters.....	244
Developing Machine Learning Coupled with Group Contribution Models for the Prediction of Densities of Deep Eutectic Solvents .....	245
<b>Education, Society, UN Sustainable Development Goals.....</b>	<b>246</b>
Sustainability in undergraduate practical classes: From green chemistry metrics to environmentally friendly process design.....	247
A rational dimension of Green chemistry and bethical education towards Sustainability .....	248

Pedagogic applications of systems-oriented concept map extension (SOCME) in the education of community college students for a green environment.....	250
Green Chemistry in Secondary Education: Views of Greek Chemistry Teachers.....	251
Green Chemistry Education and Promotion in Taiwan.....	254
<b>Environmental catalysis .....</b>	<b>255</b>
Efficient visible light driven photocatalytic degradation of perfluorooctanoic acid by Bi <sub>7</sub> O <sub>9</sub> I <sub>3</sub> catalyst .....	256
Photocatalytic degradation of Ciprofloxacin antibiotic by doped LaFeO <sub>3</sub> nanopowders .....	258
Catalysis on demand for greening up the battle against agrochemicals: fast, sustainable and versatile .....	260
A Critical Revisit of Zeolites for CO <sub>2</sub> Desorption in Primary Amine Solution Argues its Genuine Catalytic Function.....	262
Rational Design of Manganese Dioxide Catalyst for the Preferential Oxidation of CO in Hydrogen Stream: from Theory to Practice .....	263
Nickel catalysts modified with TiC derived from organic precursor for resource recovery via dry reforming of waste plastics .....	266
Carbonized Bone Waste For Photothermal Desalination .....	268
Studies of different ionic liquids as electrolytes for electrochemical reduction of CO <sub>2</sub> .....	270
<b>Green Analytical Chemistry-(Eco)Toxicology.....</b>	<b>271</b>
Green extraction and quantification of zeaxanthin and lutein in corn grains and their associated by-products .....	272
A green analytical method to characterize unsaturated hydrocarbons in waste polyolefin pyrolysis oil using FTIR.....	274
Insights into ecotoxicity of flavonoids and their mixtures .....	276
bio-Profiles of Chemical Reactions.....	278
Transformation Products of Sulfonamides in aquatic Systems: What can we learn from available environmental Fate and Behaviour data?.....	279
Determination of olive oil aroma profile using Hisorb-TD-GC/MS .....	281
Mapping VOCs from different soils of Cyprus vineyards using HS-SPME-GC/MS analysis .....	282
Evaluation of efficacy of ZnO nanoparticles as nanofertilizers: An alternative agriculture approach .....	283
<b>Green catalysis &amp; synthesis .....</b>	<b>284</b>
Connecting sonication with photocatalysis to intensify a continuous flow photocatalytic processes: A disruptive alternative for lignin valorization.....	285
Key role of ultrasound on the synthesis of TiO <sub>2</sub> nanomaterials and catalytic performance.....	288
Metal Nanoparticles and Metal-based Polymeric Materials as vehicles for Green Organic Synthetic Methodologies .....	290

Tailor-made POLITAG-Pd <sup>0</sup> catalyst for the low-loading Heck cross-coupling in $\gamma$ -valerolactone as safe reaction medium .....	291
The road to intrinsically dynamic materials: disulfide chemistry as a solution .....	293
Chiral iron(II)-catalysts within valinol-grafted metal-organic frameworks for enantioselective reduction of ketones .....	294
Copper oxide supported on red-mud as catalyst for organic conversion reactions: model reactions employing H <sub>2</sub> O <sub>2</sub> as an oxidizing agent in liquid phase oxidation: Selectivity and structure-activity relationship.....	296

## Green Chemistry and Sustainable industrial processes, Metrics, LCA

..... 297

Green assessment of polymer microparticles production processes. Use of bio-based resists derived from renewable monomers for sustainable 3D fabrication of automotive components through two photon polymerization.....	298
Use of bio-based resists derived from renewable monomers for sustainable 3D fabrication of automotive components through two photon polymerization .....	300
Are Lignin-Derived Monomers and Polymers truly sustainable? An In-Depth Green Metrics Calculations Approach.....	302
Life cycle costing for the production of lignin-based adhesives from softwood kraft lignin via base-catalysed depolymerization .....	303
Fruit waste to wealth: Life cycle and Techno economic analysis to develop a sustainable pectin production process.....	305

## Green solvents & sustainable synthesis ..... 307

A new synthetic approach to dialkyl carbonates and their use as green solvents for the preparation of PVDF membranes.....	308
Waste minimized Copper Catalyzed Alkyne-Azide Cycloaddition with heterogeneous metallic Copper(0) and azeotrope CH <sub>3</sub> CN:H <sub>2</sub> O under batch and continuous flow condition .....	309
Enabling nucleophilic fluorination in water .....	311
Preparation of amins (and thioamins) in aqueous media and their remarkable applications..	313
Synthesis and characterization of new BPA-free polycarbonates based on dimethyl carbonate and diphenylmethane derivatives.....	314
Amino Acid-Functionalized Metal-Organic Frameworks for Sustainable Asymmetric Catalysis ....	316
Green Synthesis Promoted by Ionic Liquids.....	318
Natural Deep Eutectic Solvents as Versatile Tools for the Development of Green Processes .....	319
A New Example of Natural Deep Eutectic Solvents as A Green Approach to the Solubilization and Stabilization of Biomolecules .....	320
Affordable Ionic Liquids: A Thermal Investigation .....	321
Bio-derived ionic liquids: synthesis and biological activity .....	323
Optimization of a green extraction method for the recovery of bioactives from cornelian cherry ( <i>Cornus mas</i> L.) fruits using $\beta$ -cyclodextrin as an extraction enhancer .....	324

Sorption of CO <sub>2</sub> in Composite Cellulose Acetate – Ionic Liquid Membranes .....	326
Organonitriles as complexing agents for the double metal cyanide-catalyzed synthesis of polyether, polyester, and polycarbonate polyols .....	328
<b><u>Nanomaterials &amp; Ionic liquids for advanced applications.....</u></b>	<b>329</b>
Electroless plating on 3D printed photocurable resin artifacts without the use of chromium and palladium solutions .....	330
Robust flow synthesis of defect-incorporated ZnO quantum dots and investigation of their structure-property interlink .....	332
Development and Application of Chromogenic Ionic Liquid Crystals .....	334
Ionic Liquids-modified Metal Organic Frameworks: Preparation and Application in Adsorption ..	335
Bioinspired Dendritic Polymer Composites Combining Adsorption and Catalysis for Water Purification .....	336
Tuning the surface chemistry of nanoporous activated carbons towards diesel fuel desulfurization .....	338
Plant based fabrication of CuO/NiO Nanocomposite: A Green Approach for Low-Level Quantification of Vanillin in Food Samples .....	339
<b><u>Nanomaterials for energy &amp; environment .....</u></b>	<b>340</b>
Perovskite BaTaO <sub>2</sub> N: A Promising Candidate for Solar Water Splitting .....	341
Natural mineral lintsite as the base for the new range of functional materials .....	342
Green synthesis of nanosized energy storage electrode materials for lithium-ion batteries .....	344
Galvanic-Replacement Enabled Synthesis of In(OH) <sub>3</sub> /Au/C Nanocomposite and Its Photocatalytic Degradation of Methylene Blue .....	345
Au-Cu <sub>2-x</sub> Te disk-on-dot Hetero-nanostructure Photoelectrocatalysts .....	346
<b><u>Plastic waste recycle and valorization .....</u></b>	<b>347</b>
Chemical recycling of plastic waste towards waxes and lubricants.....	348
Valorization of Polyhydroxyalkanoates as Circular Carbon Feedstock Beyond Bioplastics .....	350
Delamination of polyamide/polyolefin multilayer films by selective glycolysis of polyurethane adhesive .....	352
Back-to-monomer recycling of polycondensation polymers: opportunities for chemicals and enzymes.....	354
Debromination by soxhlet extraction and chemical recycling (pyrolysis) of various plastics collected from waste electric and electronic equipment.....	355
Pre-treatment to remove additives from plastic waste based on the use of biosolvents.....	357
Reductive Depolymerization of Polyesters and Polycarbonates with Hydroboranes by Using a Lanthanum(III) Tris(amide) Catalyst .....	358
Poly(ethyleneterphthalate) and polyethylene targeted solubilization and recovery with green solvents .....	360
<b><u>Pollution prevention &amp; remediation .....</u></b>	<b>361</b>

Sustainable Water Purification Processes using Ionic and Porous Materials .....	362
Bisphenol A adsorption on Hydrophobic Activated Carbon .....	363
The Influence of the Support and the Synthesis Method on the Activity of Pt-Catalysts for the Hydrogenation of Cl-Pollutants in Water .....	364
Nitrogen doped graphene efficiently promotes the reduction of vinyl chloride by nano zero-valent iron .....	366
Photocatalytic removal of methylene blue and thiabendazole by reduced ZnO: influence of oxygen vacancies on adsorption and photocatalytic degradation .....	368
Landfill leachate treatment by using fixed bed columns packed with WWTP sludge porous carbons .....	370
Asymmetric poly(ionic liquid)-ionic liquid membranes for gas separation.....	372
Fast peroxydisulfate oxidation of the antibiotic Norfloxacin catalyzed by cyanobacterial biochar	373
New biodegradable metal complex for photo-Fenton like processes at neutral pH.....	375
Reduce Greenhouse Gas Emissions by optimizing Wastewater Treatment Plants .....	376
Designing of thiourea-functionalized chitosan aerogels for deep cleaning of wastewaters containing heavy metal ions.....	378
A potential biotechnological approach to recover technology-critical elements from complex aqueous mixtures .....	379
Continuous Adsorption Process for Cr(VI) on Hydrothermally Treated Chitosan/Polyvinyl Alcohol Beads .....	382
Effect of blending Methanol with Gasoline on the Exhaust Emissions.....	383
One-pot solvent-free synthesis of renewable plasticizer alcohols/bio-oil from wastewater grown microalgal biomass via. in-situ crystallization of hydroxyapatite .....	385
Effect of water to biomass ratio of hydrothermal carbonization on the adsorption properties of hydrochar from waste seaweed.....	387
Biochemical and antioxidant response modulation by plant growth promoting <i>Bacillus</i> spp strains to improve drought tolerance in maize .....	390
<b><u>Poster presentations .....</u></b>	<b><u>391</u></b>
<b><u>Alternative and benign chemical processes (microwaves, ultrasounds, photochemistry, electrochemistry, flow chemistry, etc.).....</u></b>	<b><u>392</u></b>
Electrochemical synthesis as alternative synthetic strategies for the Manganese phthalocyanine and its graphene quantum dot conjugate.....	393
Microwave- and ultrasound-promoted greener synthesis of tolperisone derivatives and their biological evaluation .....	395
Pre-treatment of beech wood using choline chloride-based deep eutectic solvents .....	396
Cocrystallization through green mechanochemical synthesis: An approach to improve solubility of drugs.....	398
Steroidal fused pyrroles: an environmentally friendly alternative to the synthesis of plant growth promoters.....	400

The radiation chemistry as a green alternative for the synthesis of graphene-supported gold nanoparticles.....	402
Electrochemical Synthesis of Aryl Alcohols in Continuous-Flow.....	403
Direct electrochemical oxidation of abietanes .....	404
Continuous Formation of Bioderived Cyclic Carbonates using Supported Ionic Liquid Based Catalysts and Supercritical Carbon Dioxide (scCO <sub>2</sub> ) as Solvent and Reagent .....	405
Microwave assisted one-pot synthesis of bridgehead bicyclo[4.4.0]boron heterocycles as DNA visible light photo-interacting molecules with possible theranostic applications .....	407
Advancing flow chemistry through continuous API manufacturing: A Process route towards Celecoxib .....	409
Chalcones as alkyne surrogates for the synthesis of pyrazoles through sequential mechanochemical (3+2)-cycloaddition with nitrile imines and deacylative oxidation.....	410
A multistep microflow process towards Selective Serotonin Reuptake Inhibitor (SSRI), Fluoxetine. ....	411
Microreactor based on TiO <sub>2</sub> nanotubes for photocatalytic degradation of organic compounds in water .....	413
<b><u>Alternative fossil fuels and biofuels, green bio-energy .....</u></b>	<b>415</b>
A Comparison Study of Trace Metal Profiles of Biodiesel and Bioglycerol Produced From Heated and Unheated Canola Oil Using High Performance ICP-MS.....	416
Pretreatment of nitrogen-rich hydrothermal liquefaction biocrudes by demetallization: Recalcitrant effect of basic nitrogenates and metalloporphyrins.....	418
Hydrodeoxygenation of oleic acid over Ni catalysts supported on Beta zeolite.....	419
Bio-based production of hydrogen and CO <sub>2</sub> utilization.....	421
Spent coffee grounds conversion to bio-crude oil via hydrothermal liquefaction .....	422
The effect of kaolin and hectorite clay on the Fischer-Tropsch synthesis condensed hydrocarbon products .....	424
Photochemical dimerization of volatile conjugated dienes produced photobiologically.....	426
<b><u>Biomass derived platform &amp; fine chemicals, pharmaceuticals, monomers, polymers, materials .....</u></b>	<b>427</b>
Lignin model compounds hydrogenolysis over base metal catalysts .....	428
Lignin-based benzoxazines: a tunable key-precursor for various applications.....	431
Comparative analysis of the biological activity of proanthocyanidins from fruit and non-fruit trees and shrubs of Northern Europe .....	432
Physicochemical changes of alginate/polyacrylic acid mixture induced by host-guest interactions of the appended units .....	434
Development of olive oil and $\alpha$ -tocopherol containing emulsions stabilized by FucoPol: Rheological and textural analyses.....	435
Cellulose Nanocrystal Modification with Subberin Fatty Acids and Application in Additive Manufacturing Resins Reinforcement.....	436



Bioproduction of 2-Phenylethanol by <i>Acinetobacter soli</i> .....	437
Study of the modification of chitosan structure with 2-methoxy-4-vinylphenol for enhanced antioxidant activity.....	440
Degradation and environmental impact of biodegradable plastics.....	441
How to Design Single Atom Alloy Catalysts towards High-efficient Biomass Conversion .....	442
Development of Sugar-Derived Bioconjugates: A More Sustainable Alternative to PEGylation ....	443
Durability in Sea Water of 3D Printed Materials based on Polyhydroxyalkanoate / Polybutylene Succinate Blends.....	445
Lignocellulose Sustainable Material Preparation Strategy from Biomass Waste .....	446
Biochars and activated carbons obtained from herbs as low-cost and regenerable adsorbents of polymers.....	447
Enzymatic modification of biopolymers with phenolic antioxidants .....	449
Taking advantage of side reactions: the example of furfuryl alcohol polymerization.....	451
Exploration of sulphur incorporation within sugar-derived cyclic monomers to predict reactivity and polymer properties.....	452
Green synthesis and characterization of novel furan-based oligoesters for organogel applications .....	454
Xylose and hemicellulose sugar steams dehydration to furfural in aqueous and biphasic media .	455
Production of value-added furanic compounds via photocatalytic selective oxidation of 5-hydroxymethylfurfural .....	456
Use of V <sub>2</sub> O <sub>5</sub> Sheets as an Efficient Catalyst for the Hydroxyalkylation Alkylation Reaction for the Production of Biofuel Precursors .....	458
Metabolic engineering of <i>Methylovimicrobium alcaliphilum</i> 20Z for production of ectoine from methane and lignocellulosic sugars .....	460
Laccase immobilization onto polymeric supports for synthetic dyes degradation .....	461
Tailored pretreatment/fractionation of forest and agricultural biomass towards selective isolation of lignin, hemicellulose and cellulose.....	463
Solid-catalyst assisted OxiOrganosolv pre-treatment of wheat straw for enzymatic and microbial conversion to bioactive food additives .....	464
Production of bio-based gluconic acid from agro-industrial residues: Experimental analysis, process design and technoeconomic evaluation .....	466
Depolymerisation of lignin in sugarcane bagasse by hydrothermal liquefaction to optimize catechol formation.....	468
Synthesis and color reduction of Lignin nanoparticles encapsulating CeO <sub>2</sub> for safe, anti-oxidant and high SPF sunscreen.....	469
Hydrothermal upgradation and mineralization strategies for synthesis of platform chemicals, pharmaceuticals and biomaterials-The ultimate wastewater grown algal biorefinery approach..	470
Hybridization of chemically modified cellulose and hydroxyapatite applicable to tough biomass materials.....	471
Synthesis and Characterization of Unsaturated Polyester Resins Based on Adipic Acid .....	474

Exploring the potential of itaconic acid based unsaturated polyester resins as high performance green materials for UV 3D printing applications.....	475
Bio-based P-F resins for wood-based panels by substituting phenol and formaldehyde with biomass-derived phenolics and furfural.....	476
Development of an engineered methanotroph-based platform for methane-to-indole 3-acetic acid bioconversion for sustainable agriculture.....	477
The effect of organic acids on the degradation of PLA/PBAT blends .....	480
Cellulose micro/nanoparticles as green polymer reinforcing agents .....	481
Glucose hydrogenation/hydrogenolysis towards sugar alcohols over Pt/Ru catalysts supported on micro/mesoporous activated carbon.....	482
Synthesis and closed-loop recycling of plant oil-based polyamides .....	483
Use of tosylated glycerol carbonate for the preparation of new functionalized pyrazole compounds .....	484
Enzyme-induced crosslinking to tailor chitosan/gelatin-based encapsulation carriers.....	485
Degradation Studies of PLA/PBAT Blends in Simulated Marine Environments .....	487
Flow chemistry synthesis of a potential new class of biorenewable monomers, fuel oxygenates and bio-based lubricants.....	489
A biorefinery approach for integrated recovery of anthocyanins and pectin from blueberry pomace .....	490
Enzymatic modification of a polysaccharides-rich extract from green marine macroalgae <i>Ulva</i> sp. for the enrichment of its biological activity .....	492
Synthesis of profluorescent nitroxide-alginate bioconjugate for biocompatible scavenging and detection of ROS in bone tissue culture.....	494
European Sustainable BIO-based nanoMATERIALS Community (BIOMAC).....	496
The study of a natural antioxidant interaction with a biomaterial substrate.....	498
Towards sustainability: Exploring the properties of novel vanillic acid-based polyesters.....	499
FDCA-based copolyesters modulate the properties of PLA-based blends.....	500
Synthesis and properties of poly(glycerol pimelate), a hyperbranched polyester for ocular drug delivery .....	501
Synthesis and analysis of bio-based epoxy resin from native lignin derived oligomers.....	502
<b><u>Catalytic processes (homogeneous, heterogeneous and bio-catalysis)</u></b>	<b>504</b>
Design of noble-metal-free molecular catalysts and photosensitizers for photocatalytic hydrogen production.....	505
Aluminum metal-organic framework-supported single-site nickel-catalyst for heterogeneous chemoselective hydrogenation of nitro and nitrile compounds.....	506
Feruloyl esterase-catalyzed synthesis of a bioactive sugar ester based on phenolic compounds derived from the halophyte <i>Salicornia</i> spp. ....	508
Utilization of industrial residues as co-capturing agents for enzyme-accelerated CO <sub>2</sub> capture.....	510

Mono-Phosphine Metal-Organic Framework- Supported Cobalt Catalyst for Efficient Borylation Reactions .....	512
Use of Magnetic Cross-Linked Tyrosinase Aggregates for Biocatalytic Processes in Deep Eutectic Solvents .....	514
Suitability of volcanic materials as green catalysts for environmental purposes .....	516
Green Chemicals From Dehydration and Partial Dehydrogenation of Sugar Cane Fusel Oil.....	518
Optimization of furan-based oligoester enzymatic synthesis by design of experiments .....	520
Catalytic dehydration of 1,3-Butanediol into 1,3-Butadiene .....	521
Boosting Bicyclic-Aziridines Potential Through Enzymatic Kinetic Resolution in Flow .....	522
Effect of Aqueous Choline Chloride-Based DES Solutions on the Biocatalytic Performance of Immobilized Hydrolases .....	523
Dry Reforming of Methane over Fe-Co Based Alumina Supported Catalysts .....	525
Catalytic properties of Ni-Cu mixed oxides deposited on stainless steel meshes by plasma jet sputtering .....	526
Bioconversion of daidzin and genistin in seed and roots extracts of Korean wild soybean into daidzein and genistein by $\beta$ -galactosidase from <i>Thermoproteus uzoniensis</i> .....	529
Cobalt-copper oxide catalysts and their performance in total oxidation of ethanol.....	530
Photocatalytic Degradation of Ceftazidime in Wastewaters and Landfill Leachate using Manganese Oxides Supported on TiO <sub>2</sub> -Graphene Nanocomposite Catalysts .....	532
Alternative and greener microwave assisted alkyl levulinate production.....	533
Towards an artificial metalloprotein-controlled enantioselective allylic substitution reaction .....	534
Turning Green Ideas into Industrial Success .....	535
Manganese-Catalyzed Hydrogenation of Sclareolide to Ambradiol .....	536
Hydrogenative Depolymerization of Polyurethanes Catalyzed by a Manganese Pincer Complex .	537
Diffusion and Adsorption Effects in TS-1/SAC Composites Catalysts for the Green Epoxidation of Methyl Oleate with H <sub>2</sub> O <sub>2</sub> .....	538
Photocatalytic degradation of RB5 with modified graphitic carbon nitride (g-C <sub>3</sub> N <sub>4</sub> ) as catalyst....	540
A comparative study of the CO <sub>2</sub> methanation efficiency of dispersed Rh, Ru and Ir nanoparticles: Effect of metal nature and supporting material .....	541
Fabrication of Au nanoparticles supported on one-dimensional (1D) La <sub>2</sub> O <sub>3</sub> nanorods for selective Esterification of Methacrolein to Methyl Methacrylate with Molecular Oxygen.....	542
TiO <sub>2</sub> -ZrO <sub>2</sub> as supports of metal particles for the oxidation or reduction of pollutants in the Water .....	543
Sustainable N-doped basic carbon catalysts for the synthesis of nitrogen heterocycles .....	544
New Strategies for the Conversion of Biobased Furanics into High-value Added Synthons .....	546
Development of Transition-Metal-Free Lewis Acid-Initiated Double Arylation of Aldehyde: A Sustainable Approach Towards the Total Synthesis of Anti-breast Cancer Agent.....	548
Catalytic Activity of Cobalt Schiff-Base Complexes in Hydrosilylation of Alkynes .....	550

A study on the multicycle redox characteristic of La-Fe-oxide for chemical looping CO <sub>2</sub> conversion to CO.....	551
Co-Ce supported SiO <sub>2</sub> for preferential CO oxidation in hydrogen rich gases -influence of the preparation method.....	552
Polyethylene Biodegradation by <i>Bacillus</i> Species from a Landfill Site.....	554
Biodegradation of polystyrene by bacteria from the soil in common environments.....	555
Catalytic oxidation of propane and <i>n</i> -hexane over cobalt loaded hierarchical ZSM-5 zeolite.....	556
Catalytic hydrodeoxygenation (HDO) of lignin-derived phenolic compounds over zeolite-supported nickel catalysts.....	559
<b>CO<sub>2</sub> utilization.....</b>	<b>560</b>
The effect of reaction conditions on CO <sub>2</sub> Hydrogenation with Cu/ZnO/SBA-15 catalyst.....	561
Cu  Ag tandem-operation for highly efficient CO <sub>2</sub> conversion toward C <sub>2</sub> -3 products.....	563
Electrochemical <i>In-situ</i> Analysis of CO <sub>2</sub> Reduction Reaction on Gold Grain Boundary.....	564
Nanosheets of lithium silicate with excellent CO <sub>2</sub> capture kinetics and extraordinary stability at high temperatures.....	565
CO <sub>2</sub> valorization by sorption-enhanced reverse water-gas shift reaction for low-temperature CO synthesis: a kinetic study of the reaction and water adsorption.....	566
Nickel-NHC-complexes for CO <sub>2</sub> Photoreduction using the Cooperative Effect of Ionic Liquids.....	568
New photocatalytic materials for carbon dioxide valorization in carbonylation chemistry using the cooperative effect of ionic liquids.....	569
Syngas Production by Carbon Dioxide Conversion of Methane over Co-based Catalyst with High Stable Activity.....	570
Upgrading biogas, produced from the anaerobic digestion of municipal wastewater treatment sludge, to biomethane by applying membrane gas separation.....	572
Dynamic simulation of biogenic CO <sub>2</sub> methanation in fixed and structured catalytic reactors for decentralized Power-to-Gas applications.....	574
Coupling Reaction of CO <sub>2</sub> with Epoxides by Highly Nucleophile 4-Aminopyridines.....	576
Development of Cu <sub>2</sub> O/BiVO <sub>4</sub> heterojunction photocatalysts for sustainable artificial photosynthesis.....	577
Effect of Interaction between Ru and N dopant in N-doped Titanium Oxide supported Heterogeneous catalyst over CO <sub>2</sub> Hydrogenation to Formate.....	579
Design and application of catalytically active hollow-fiber membrane reactors.....	580
Conversion of glycidol to glycerol carbonate using Halogen-free bio-based organic salts.....	582
Preparation of CO <sub>2</sub> sorption pellets from polyaniline using microwave heating.....	584
Utilization of CO/CO <sub>2</sub> -containing industrial process gas into valuable polyurethane building blocks.....	586
Carbon Nanostructures Obtained through CO <sub>2</sub> Utilization.....	588
Hybrid energy storage based on CO <sub>2</sub> capture and renewable energy sources (RES); Construction and operation of a novel flue gas storage and supply system.....	589

## Computational Chemistry towards greener chemical processes..... 590

Betanidin zwitterionic and nonionic dimer conformers towards DSSCs application: A DFT investigation to optoelectronic and charge transfer properties.....	591
Development of bioplastic disposable food packaging from starch and cellulose .....	592
Physiological Regulation of Antifungal Properties of Agaricomycetes Mushroom <i>Schizophyllum commune</i> .....	593
New bismuth titanates based photocatalysts: a comprehensive DFT and experimental insight ...	594
Pd-catalyzed allylic substitution between C-based nucleophiles and Bicyclic Aziridines .....	596
Characterization of Giant Reed as a Potential Feedstock for Fast Catalytic Pyrolysis .....	597
Synthesis of new class dual functionalized ionic liquids and their performance for effective CO <sub>2</sub> capture: Properties and interaction mechanism analysis.....	599

## Education and societal awareness – UN Sustainable Developments

### Goals ..... 600

Green Chemistry for high school: methoxylation of alpha-pinene over ionic resins.....	601
How green chemistry education can empower chemistry students to be promoters of sustainable substances-handling practices in their communities.....	603

### Green analytical chemistry ..... 605

Determination of air pollutants in confined crowded places .....	606
Impact of UV-B Exposure on Physicochemical Properties of Poly(ethylene terephthalate): On the way to microplastics formation.....	607
A novel device for on-line determination of ammonia/ammonium in ambient air .....	608
Application of green solvents and procedures for analysis of pharmaceuticals in environmental samples.....	610
Green Analytical method for the assay of some selected drugs.....	611
Activity-Guided Isolation and Identification of Metabolites from Endophytic Fungus using HPLC-DAD, Mass Spectrometry and Multidimensional NMR Spectroscopy .....	612
Biochar as a green modifier for the development of electrochemical biosensors .....	614
A protein-based free-standing transparent elastomer and its potential applications .....	616
Beeswax-based waterproof paper as a sustainable substrate for electrochemical sensing platforms .....	617
Application of the SPA analytical method for the determination of tar in pyrolytic gases in the tyres pyrolysis process .....	619
A new environmentally friendly method for the determination of mercury .....	621

### Green Chemistry & UN Sustainable Developments Goals ..... 622

Chemistry in the question of human survival .....	623
---	-----

## Green Chemistry and entrepreneurship – Sustainable industrial processes ..... 624

Effect of NaCl concentration on protein production by submerged cultivation of <i>Pleurotus ostreatus</i> .....	625
A novel device for the carbonate determination, as carbon dioxide, during petroleum and natural gas exploration.....	628
Renewable Reagents for Nucleophilic Fluorination.....	629
Curcumin solid dispersion particles as novel Pickering stabilizers.....	630

## Green solvents – Safe reagents and chemicals – Sustainable organic synthesis ..... 632

Development of a biographene-poly(lactic acid) hybrid material as support for enzyme immobilization.....	633
Dimethyl isosorbide <i>via</i> dimethyl carbonate chemistry: scaling-up, purification and concurrent reaction pathways.....	635
Acidic deep eutectic solvents-based efficient oxidative extractive desulfurization of fuel oil.....	636
An Eco-Friendly Preparations of Pyridoxal Oxime Quaternary Salts in Deep Eutectic Solvents.....	637
Green Synthetic Transformation of Benzimidoyl-cyanides to the Valuable Intermediates Alkyl-N-pyridin-2-yl-benzimidates.....	638
Multi gram scale synthesis of HMF and comparative environmental evaluation.....	639
Nanoarchitectonics of phosphorylated graphitic carbon nitride for sustainable, selective and metal-free synthesis of primary amides.....	640
A greener approach towards coumarin analogues via Natural Deep Eutectic Solvent-mediated Suzuki-Miyaura coupling.....	642
Development of bioactive chitosan-based hydrogels using Natural Deep Eutectic Solvents (NADES) as dissolution and gelling agents.....	643
Natural Deep Eutectic Solvents (NADES) as green alternative solvents for the extraction of bioactive compounds from Greek wild rose ( <i>Rosa canina</i> L.) rosehip shells (hypanthia).....	644
Bioactive chemical space exploration via greener multicomponent reactions.....	646
Synthesis of new succinimide derivatives with potential anticonvulsant activity.....	648
DMAP-catalyzed synthesis of quinazolinone and derivatives <i>via alpha</i> chloroaldehyde <i>O</i> -methanesulfonates and 2-(benzylamino)benzoic acids.....	649
Novel phosphate-containing imidazoles as potential green biologically active substrates.....	650
Solubility of <i>Moringa oleifera</i> L. seed in SFE-CO <sub>2</sub> : a response surface methodology analysis.....	651
Aerobic and Catalyst-free Oxidation of Aldehydes to Acids Promoted by Sunlight or UVA-light...	654
Natural product derivatives through organic synthesis as enhanced antioxidant agents.....	656
A Comprehensive Screening Investigation on using Group Contribution Models for Estimation of the Critical Properties of Deep Eutectic Solvents.....	658

<i>In situ</i> generated chloride, bromide and iodide as catalysts for the oxidation of benzyl halides to benzoic acids in alkaline water using TBHP as oxidant .....	659
Nickel Phosphide Supported on Graphitic Carbon Nitride as Non-Noble Metal Catalyst for Reductive Amination of Carbonyl Compounds by Transfer Hydrogenation.....	661
CO <sub>2</sub> /CH <sub>4</sub> selective hollow fiber and flat sheet membranes based on green solvent.....	663
Aerobic waste-minimized Pd-catalysed C–H alkenylation in GVL using a tube-in-tube heterogeneous flow reactor.....	665
Waste Minimized β-Azidation reaction of α,β-unsaturated carbonyl compounds catalyzed by POLITAG-M-F in azeotrope CH <sub>3</sub> CN:H <sub>2</sub> O under batch and continuous flow condition. ....	666
Density and Refractive Index of Binary Ionic Liquid Mixtures with Common Cations/Anions: Measurement and Modelling.....	668
Total synthesis of (-)-agelastatin A via photochemical transformation of pyridinium salt and early-stage enzymatic resolution .....	669
‘On-Water’ directing groups assisted C–H bond functionalization of ferrocene derivatives .....	670
A novel approach towards expanding the utility of Deep eutectic solvents as a biocompatible co-solvent for α-chymotrypsin. ....	672
<b><u>Nano-materials for energy and environmental applications.....</u></b>	<b>674</b>
Ecological Treatment Processes for Leathers Intended for Medical Applications.....	675
Mixed metal oxide nanoparticles for organic solar cell applications.....	678
Green synthesis of tin sulfide films and effect of annealing .....	679
Surface functionality role in the conductivity of microwave synthesized CQDs thin films.....	681
Effect of Surface Functionalization and Doping of Graphitic Carbon Nitrides on Carbon Dioxide Fixation to Cyclic Carbonates at Atmospheric pressure under Solvent-Free Conditions .....	683
Portable paper sensing platform using novel histidine-stabilized gold nanoclusters for fast naked-eye detection of Fe ions from water .....	685
Nature-inspired nanocomposites with exceptional isotropic mechanical and magneto-responsive properties.....	687
Metabolic response of Murine Fibroblast cells exposed to Green synthesis mediated Silver Nanoparticles .....	689
Biomass derived nanoporous carbons for diesel deep desulfurization .....	691
Synthesis and Applications of Cu <sub>2</sub> O Nanoparticle Functionalized TiO <sub>2</sub> for Photocatalyzed Glaser Coupling.....	692
Synthesis and effect of calcination temperature on the physicochemical properties of porous clay heterostructures (PCH) material .....	694
The Role of Morphology on the Controlled Crazing of Biopolymer Systems.....	696
Bimetallic sulfides derived from bi-metal–organic frameworks as sodium anode material with long-term cycling stability .....	698
Iron-based catalytic materials as energy carriers for carbon dioxide valorization .....	700
Lignocellulose-based membranes for lithium-ion battery separators.....	702

Synthesis, Characterization and UVC-activated Photocatalytic Activity of Superparamagnetic Iron Oxide Decorated Indium Hydroxide Nanocomposite .....	704
Phosphonated Polyetheramine-Coated Magnetic Nanoparticles: A Sustainable Approach for Oilfield scale Management.....	705
Recyclable Magnetic Nanoparticles Coated-Poly(4-styrenesulfonic acid-co-maleic acid) for Oilfield Scale Control.....	707
Synthesis and characterization of Metal-organic framework of Zn (II) modified by magnetic nanoparticles and multi-walls carbon nanotubes for dispersive solid phase extraction of some benzophenones in water samples.....	709
An Electrochemical Oxidation of Wastewaters through Graphene Oxide Coated Electrode.....	711
Green Nanopesticides: An approach for the control of Tea pest, <i>Oligonychus coffeae</i> .....	713
Environmentally friendly, electrically conductive, and versatile emulsion-based ink of carbon nanotubes and silver flakes for distributed tactile sensing.....	714
Investigating the growth profile of different microalgae strains in nanoemulsion based growth media.....	715
A novel Green-Chemistry-inspired approach for lignin-based model compounds valorization by exploiting photocatalytic-microflow reactor .....	716
Surface chemistry of new CQDs produced using a microwave-assisted approach as an effective organic pollution removal agent in water medium .....	718
Synthesis of zinc oxide nanoparticles using Japanese knotweed extract .....	720
Synthesis of Ag/Ag <sub>2</sub> O nanoparticles on cellulose paper and cotton fabric using <i>Eucalyptus globulus</i> leaf extracts: toward the clarification of formation mechanism .....	721
Investigation of photocatalytic properties of titanium dioxide nanoparticles onto ceramic roof tiles .....	724
Harvesting of hot holes and hot electrons generated on plasmonic nanostructures for amine photooxidation reaction.....	726
Versatile synthesis of graphene materials for the removal of copper ions from aqueous solutions .....	727
Synthesis and characterization of modified TiO <sub>2</sub> nanoparticles with enhanced visible-light photocatalytic properties .....	731
Engineering of Au/p-C <sub>3</sub> N <sub>4</sub> nanosheets with Enhanced Charge Separation for Photocatalytic Hydrogen Evolution.....	732
Synthesis of film Cu,F-TiO <sub>2</sub> NTs photocatalysts with a highly ordered structure for wastewater treatment .....	734
Size and shape-controlled synthesis of well-defined iron oxide nanocrystals by investigation of the reaction path mechanism.....	737
Investigating the structural and mechanical properties of innovative polypropylene/nanoadditive composites for heating/cooling pipe systems .....	739
Catalyst nanoparticles stabilization and/or redispersion: A new anti-sintering strategy based on the effect of the O <sup>δ-</sup> electric double layer account of metal-support interactions. ....	740
Cobalt-manganese catalysts supported on ion exchanged clinoptilolite for n-hexane oxidation..	742



Photocatalytic removal of persistent organic pollutants using immobilized titanium dioxide ..... 744

## Pollution prevention and remediation ..... 745

Fatty acids-based Eutectic Solvents Liquid Membranes for Removal of Sodium Diclofenac from Water..... 746

Energy Balance of a Thermophilic Biological Fluidized Bed Reactor During Exothermic Reactions of Sludge Minimization..... 747

Removal of pharmaceuticals on functionalized activated carbons ..... 749

Effect of competing anions on chromate and arsenate adsorption by polyethylenimine functionalized silica-based material..... 750

Oxidation and removal of As(III) and organic contaminants from wastewaters and groundwaters using nano-modified biochar ..... 752

Pilot scale continuous photocatalytic reactor for removal of emerging contaminants from leachates ..... 753

Novel diketopyrrolopyrrole-rhodamine conjugates with sensing ability ..... 754

Visible light-driven degradation Trichloroethylene in aqueous phase with Vanadium-doped TiO<sub>2</sub> photocatalysts..... 755

Absorption of Pollutants by CsPbBr<sub>3</sub> Perovskite ..... 757

Investigation of the degradation of trace substances by combined oxidative-enzymatic wastewater treatment ..... 760

Poly(ionic liquid)s as efficient adsorbents for dyes removal from water streams..... 762

Removing Sulfur Dioxide (SO<sub>2</sub>) by Nanoparticle Piperine Extracted From Piper Nigrum L..... 763

Methane combustion over Pd-MeOx/Al<sub>2</sub>O<sub>3</sub> (Me= Co, Ni or Ce) catalysts ..... 765

Commercial photocatalytic paints for environmental remediation ..... 767

## Toxicology and Ecotoxicology of Chemicals and Products..... 768

Inventory of pesticides used by farmers on paddy fields in peatland area: A case study in Indonesia ..... 769

## Valorization of renewable and natural resources ..... 770

Synthesis and characterization of polysaccharide- and protein-based edible films and modification with zein bilayer coatings..... 771

Photocatalytic transformations of quinic acid derivatives..... 774

Phenol-formaldehyde resins based on lignin functionalized with succinic anhydride ..... 775

Polyolefin-lignin blends: Assessing lignin properties on post-consumer recycled polypropylene . 778

Valorization of limonene in the presence of heterogenous catalysts ..... 781

Valorization of ruminant animal dung fiber: A sustainable natural resource of non-wood material for various applications. .... 783

Reinforcement and protection of marbles with composite epoxy-based adhesives using cellulose micro/nano-particles..... 785

Structural and morphological characterization of xerogels based on agar and gelatin. .... 786

Lignin-containing polymer coatings – synthesis and characterization .....	787
Glycerol-based UV-curable resins for synthesis of vitrimers .....	788
From ferulic acid and lignin to vanillin and other platform chemicals by hydrogen peroxide .....	789
Augmenting the performance of eco-friendly greases using synergistic natural resources .....	790
pH indicator films based on renewable biodegradable polymers for food packaging applications	791
Thermally insulating air- and ice-templated plant-based foams .....	792
Synthesis and characterization of poly(lactic acid)/poly(ethylene adipate) copolymers for paclitaxel controlled delivery .....	793

## Waste recycle and valorization – Circular economy (food waste, hazardous waste, municipal waste, plastic waste) .....

Effect of a compatibilizer on the structural and mechanical properties of recycled HDPE/hemp composite materials.....	795
Laccases catalyzed dephenolization of raw wine lees and wine lees extract .....	796
Laccase production using wine lees by submerged cultivation of <i>Pleurotus ostreatus</i> .....	798
Lab-scale production of grid-grade biomethane via supercritical water gasification of biowastes and sequential gas phase conversion according to a catalytic tandem approach.....	799
Modified cross-linked pectin hydro-films for biomedical applications.....	802
Optimization of enzymatic hydrolysis for utilization of food waste .....	804
Investigation and optimization of heat and enzymatic pretreatments of OFMSW and its combination with beechwood pulp .....	806
Supercritical fluid extraction as a tool to isolate phytochemicals from rice.....	808
( <i>Oryza sativa</i> L.) by-products.....	808
Towards a kiwi waste valorization: optimization of extraction of phenolic compounds assisted by green chemistry tools.....	810
New Compatibilizers from PET Residues.....	811
Techno-economic evaluation and life cycle assessment for sustainable production of bio-based polyurethanes from the organic fraction of municipal solid waste .....	813
Tertiary treatment of municipal wastewater by microalgae technology for utilization in cooling towers of thermal power plants.....	814
Harnessing the potential of seaweed <i>Sargassum</i> spp. by treatment in acidic medium and anaerobic digestion .....	815
A new HPLC method for the detection and quantification of chemically recycled PET monomers in protic ionic liquids .....	817
Circular Economy Electrochemistry: Utilizing recycled materials for the development of 3D-printed electrochemical devices .....	819
Catalytic upgrading of end-of-life tyre pyrolysis vapours for the production of highly aromatic pyrolysis oils .....	821
Synthesis, ageing tests and flammability characterization of composites based on epoxy resin with different curing agents and flame retardant compounds.....	824

From water for the water: food-waste based hydrogels for adsorption and photo-degradation of pollutants. ....	826
Assessment of the H <sub>2</sub> S adsorption capacity of carbonaceous solids produced by pyrolysis of the major organic components of manure digestate.....	828
Determining antibacterial effect of liquid soaps from recycled cooking oil and distinct essential oils .....	830
Sustainable resource recovery from waste printed circuit boards using green solvents .....	832
Transforming CO <sub>2</sub> and Sea Water to Green HYDROGEN & Green CEMENT Using Magnesium Waste Scrap .....	834
Regulation of lignin-modifying enzymes production in lignocellulose fermentation by new white-rot basidiomycete <i>Trametes lactinea</i> .....	836
Bio-based thermoset derived from epoxidized soybean oil and agri-waste .....	838
Bio-based PLA/PHB plasticized blend films with eugenol for active food packaging applications. ....	839
Optimization of production, antioxidant activity and stability of plant-based emulsions.....	842

# Plenary Lectures

# Circular Chemistry: Catalyzing the Green Economy

Javier García-Martínez

Department of Inorganic Chemistry. University of Alicante, 03690, Alicante, Spain. e-mail: [j.garcia@ua.es](mailto:j.garcia@ua.es)

Circular Chemistry is a new concept based on the design of molecules and processes from the very beginning so products can be recovered, recycled, and reused in an economical and efficient way. [1] During my presentation, I will describe some examples of how this not only possible but also urgently needed and, in many cases, profitable. During the last months, our group has published a series of papers [2-4] on the design and fabrication of nanostructured catalysts with controlled porosity using interzeolite transformation, surfactant-templating and control growth that yield outstanding conversion and selectivity towards highly desirable chemicals, biofuels, and pharmaceuticals. More specifically, catalysts prepared by partial zeolite show a 6-fold increase in TOF in the Friedel–Crafts alkylation of indole using a bulky alcohol as alkylating agent over the conventional zeolite. Similar results were obtained in the Claisen–Schmidt condensation. In this case, the best performing hierarchical catalysts displayed a 3-fold enhancement in TOF.

An important advantage of this strategy is that the physicochemical properties and, therefore the performance, of the hierarchical catalysts can be finely tuned by simply stopping the interzeolite transformation at different times. [2] In another example, the evaluation of our self-pillared pentasil zeolites in the Friedel–Crafts alkylation reaction of methylene with benzyl alcohol results in higher conversion and an approximate twofold increase in the selectivity to the desirable product. Similarly, we observed in the MTH reaction that SPPs extend catalyst lifetime and markedly enhance turnovers, as much as fourfold relative to conventional ZSM-5. [4]

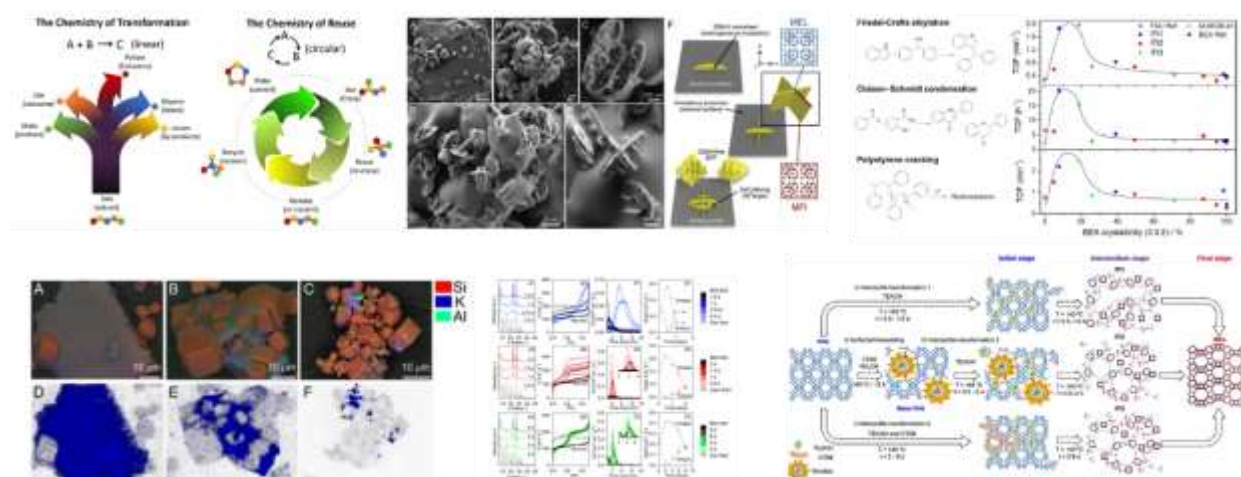


Figure 1. Scheme of linear (transformation) and circular (reuse) chemistry and some examples of the conversion of waste into raw materials using novel catalysts prepared by interzeolite transformation, surfactant-templating and control growth.

Finally, I will briefly mention some of the initiatives we are doing at the International Union of Pure and Applied Chemistry (IUPAC) to teach, promote, and support Green Chemistry, especially in the context of the International Year of Basic Sciences for Sustainable Development. [5] The IUPAC Interdivisional Committee on Green Chemistry for Sustainable Development (ICGCSD) plays a critical role in our efforts to integrate Green Chemistry into all our activities and is leading some important projects that I will briefly present.

## Acknowledgements

J.G.M thanks the European Commission for funding, H2020-MSCARISE-2019 program (Ref. ZEOBIOCHEM – 872102) and the Spanish MINECO and AEI/FEDER, UE for the project ref. RTI2018-099504-B-C21.

## References

1. J. García-Martínez, *Angewandte Chemie* **133**(10), 5008 (2021)
2. M. Mendoza-Castro, E. Jardin, N. Ramírez, C.A. Trujillo, N. Linares, J. García-Martínez\*, *J. Am. Chem. Soc.*, **144**(11), 5163 (2022)
3. H. Dai, J. Claret, E. L. Kunkes, V. Vattipalli, N. Linares, J. García-Martínez, Ahmad Moini, and Jeffrey D. Rimer, *Angewandte Chemie*, **61**(16), e202117742 (2022)
4. R. Jain, A. Chawla, N. Linares, J. García Martínez, Jeffrey D. Rimer, *Adv. Mater.* **33**, 2100897 (2021)
5. F. Gomollón, J. García-Martínez, *Nature Chemistry*, **14**, 113 (2022)

## Reaction Mechanisms and Energy Profiles: How Green Chemistry Complies with them. The Case of Dimethyl Carbonate

Pietro R. Tundo

Research Associate, Institute of Chemistry of Organometallic Compounds - ICCOM  
National Research Council – CNR and President of Green Sciences for Sustainable Development Foundation, Venice –  
[tundop@unive.it](mailto:tundop@unive.it)

An important task for organic chemists toward a sustainable development is to discover and develop new reaction pathways in syntheses; they, coupled with metrics measurement, are the fundamental bases of green and sustainable chemistry.

Due to its benign nature, interest on Dimethyl Carbonate (DMC) has been enormously increasing in the last few decades: it is currently used in many chemical reactions as DMC can substitute chlorine-based chemistry. Green preparations of anti-inflammatory drugs, polymers, fragrances and solvents are widely reported. DMC peculiar reaction outcomes are based on its anisotropic electrophilic nature and because it follows exemplarily the Pearson's HSAB theory; in doing that, DMC and Dialkyl Carbonates (DACs) give unprecedented selectivity.

Comparison among Esters and Carbonates reaction pathways is dramatic in nucleophilic attack as it proceeds very differently: in methyl acetate the reactions take place almost exclusively at the carbonyl  $sp^2$  because  $S_N2$  substitutions on the methyl  $sp^3$  have a higher activation energy; in the dimethyl carbonate, instead, the nucleophilic attack to the  $sp^2$  carbon is more difficult, while the attack to the alkyl carbon is easier; the activation energy of the  $S_N2$  reaction pathway is further decreased by entropic factors if formation of cycles is involved (Figure).

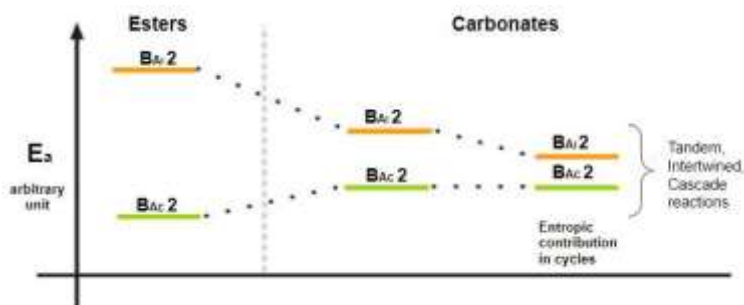


Figure. Activation energies in Esters and Carbonates; only  $B_{Ac}2$  and  $B_{Al}2$  reaction mechanisms are shown.

Ingold's terminology is adopted for esters and carbonates.

So, while in esters only  $sp^2$  carbon is susceptible of a nucleophilic attack, in DACs  $E_a$  of  $B_{Ac}2$  and  $B_{Al}2$  are almost comparable; moreover, because the reagent is modified during the reaction, different reactions can take place in sequence in the same pot. Thus, tandem reaction, cascade, and intertwined reactions are possible in carbonates. This cannot occur in esters and wasn't ever reported.

$S_N2$  Nucleophilic substitution reactions at saturated and acyclic carbons will be discussed; they take place either in basic and acidic-catalyzed conditions and allowed to get > 99% in *mono*-methylation reactions at the methylene carbon. Heterocycles of 5 and 6 atoms were obtained in quantitative yields, thus opening the way to novel compounds through a green chemistry pathway.

Limitations and new results will be presented: when the formation of cycles occurs, and when it doesn't. Moreover, also unimolecular substitutions take place.

Energy constraints and the dual electrophilic character of DACs originate unexpected reactivity and give results which are impossible for Esters.

### References

- [1] P. Tundo and M. Selva, *Acc. Chem. Res.*, 2002, 35, 706.
- [2] P. Tundo, F. Arico and M. Musolino, *Green Chem.*, 2018, 20, 28-85.
- [3] Tundo P. and Arico F. PCT/IB2018/054621 - 22 June 2018. EP Application 18746996.0 - 21 January 2020

## Green Chemistry, “...to solve most of the world’s problems.”

Paul T. Anastas

Center for Green Chemistry and Green Engineering, Yale University, New Haven, CT, USA 06511

\*Paul.anastas@yale.edu

Over thirty years, green chemistry has revolutionized how we design, develop, implement, teach and commercialize the chemistry that we do [1]. As we look forward to the future of chemistry, it is important to expand our understanding that green chemistry is not simply about how we design things to avoid problems, but instead to create new molecules, synthetic/manufacturing methods, new materials, new commercial products, new conceptual frameworks that allow us to achieve the broader goals of our society and civilization.[2] This presentation looks at what is possible (but not practiced) today, and the power and potential of green chemistry in designing a sustainable future for the coming generations.[3]

### References

1. Erythropel, H., et. Al., *Green Chemistry*, 20 (9), 1929-1961 (2018).
2. Anastas, P.T., Zimmerman, J.B., *Green Chemistry*, 21 6545 – 6566, (2019).
3. Zimmerman, J.B., et. al, *Science*, 367, 6476, 397-400. (2021)

## Emerging technologies for a sustainable conversion of lignocellulosic biomass into biobased products

Solange I. Mussatto

*Department of Biotechnology and Biomedicine, Technical University of Denmark, Kongens Lyngby, Denmark*

*\*e-mail: smussatto@dtu.dk*

Innovation and technology are key points in the transition to a greener and more sustainable economy. In this sense, the development of new processes able to result in reduced emissions and levels of CO<sub>2</sub> in the atmosphere are essential to support this transition and, at the same time, promote economic growth. Lignocellulosic biomass has a huge potential to be used as feedstock for a sustainable production of fuels and chemicals by fermentation. However, the recalcitrance of these materials is one of the major hurdles in their efficient utilization. In addition, due to the complexity of the media generated from lignocellulosic biomass, achieving a successful fermentation performance from such complex substrates is a challenge. Process intensification is a promising strategy to improve the techno-economic potential of biobased production. Within this area, different emerging technologies have been proposed, among of which, the use of greener pretreatment methods, the application of high solid loading for biomass saccharification, as well as the development of robust microbial strains and/or application of microbial co-cultures for fermentation are seen today as promising approaches able to accelerate the development of innovative and sustainable biobased processes [1].

### Acknowledgements

Novo Nordisk Foundation, Denmark (BiobaseDK project, grant number NNF20SA0066233).

### References

1. S.I. Mussatto, C.K. Yamakawa, L. van der Maas, G. Dragone, *Renew. Sustain. Energy Rev.*, **152** 111620 (2021).



## Conversion of CO<sub>2</sub> and Biomass into Chemicals and Fuels

Buxing Han<sup>1,2</sup>

1. Institute of Chemistry, Chinese Academy of Sciences, 100190, Beijing, China

2. Shanghai Key Laboratory of Green Chemistry and Chemical Processes, School of Chemistry and Molecular Engineering, East China Normal University, Shanghai 200062, China

\*Email: hanbx@iccas.ac.cn

Carbon dioxide (CO<sub>2</sub>) is the main greenhouse gas, and it is also a renewable, abundant, and cheap C1 feedstock. Biomass is abundant renewable carbon resource. Use of CO<sub>2</sub> and biomass as carbon source to produce fuels and value-added chemicals is of great importance for the sustainable development of our society and achieving the goal carbon neutrality. In recent years, we are very interested in catalytic conversion CO<sub>2</sub> and biomass. In this presentation, I would like to discuss some of the recent results in our group on design of green solvents, green catalysts and their application in conversion of CO<sub>2</sub> and biomass into valuable chemicals and fuels [1-18].

### Acknowledgements

The speaker thanks the National Key Research and Development Program of China (2017YFA0403103), National Natural Science Foundation of China (21733011, 21890761, 22121002), the Chinese Academy of Sciences (QYZDY-SSW-SLH013) for financial support.

### References

- M. Y. He, Y. H. Sun, B. X. Han, *Angew. Chem. Int. Ed.*, DOI: 10.1002/anie.202112835(2022).
- P. S. Li, J. H. Bi, J. Y. Liu, Q. G. Zhu, C. J. Chen, X. F. Sun, J. L. Zhang, B. X. Han, *Nat. Commun.*, 13, 1965(2022).
- C. J. Chen, X. P. Yan, Y. H. Wu, S. J. Liu, X. D. Zhang, X. F. Sun, Q. G. Zhu, H. H. Wu, B. X. Han, *Angew. Chem. Int. Ed.*, DOI:10.1002/anie.202202607(2022).
- Y. F. Sha, J. L. Zhang, X. Y. Chen, M. Z. Xu, Z. Z. Su, Y. Y. Wang, J. Y. Hu, B. X. Han, L. R. Zheng, *Angew. Chem. Int. Ed.*, DOI: 10.1002/anie.202200039(2022).
- R. Z. Wu, Q. L. Meng, J. Yan, H. Z. Liu, Q. G. Zhu, L. R. Zheng, J. Zhang, B. X. Han, *J. Am. Chem. Soc.*, 144, 1556-1571(2022).
- S. L. Liu, M. H. Dong, Y. X. Wu, S. Lan, Y. Xin, J. Du, S. P. Li, H. Z. Liu, B. X. Han, *Nat. Commun.*, 13, 2320(2022).
- W. W. Guo, X. X. Tan, J. H. Bi, L. Xu, D. X. Yang, C. J. Chen, Q. G. Zhu, J. Ma, A. Tayal, J. Y. Ma, Y. Y. Huang, S. F. Sun, S. J. Liu, B. X. Han, *J. Am. Chem. Soc.*, 143, 6877-6885(2021).
- Q. L. Meng, J. Yan, R. Z. Wu, H. Z. Liu, Y. Sun, N. N. Wu, J. F. Xiang, L. R. Zheng, J. Zhang, B. X. Han, *Nat. Commun.*, 12, 4534(2021).
- M. L. Hua, J. L. Song, X. Huang, H. Z. Liu, H. L. Fan, W. T. Wang, Z. H. He, Z. T. Liu, B. X. Han, *Angew. Chem. Int. Ed.*, 60, 21479-21485(2021).
- W. W. Guo, S. J. Liu, X. X. Tan, R. Z. Wu, X. P. Yan, C. J. Chen, Q. G. Zhu, L. R. Zheng, J. Y. Ma, X. F. Sun, B. X. Han, *Angew. Chem. Int. Ed.*, 60, 21979-21987(2021).
- Y. H. Wu, C. J. Chen, X. P. Yan, X. F. Sun, Q. G. Zhu, P. S. Li, Y. M. Li, S. J. Liu, J. Y. Ma, Y. Y. Huang, B. X. Han, *Angew. Chem. Int. Ed.*, 60, 20803-20810(2021).
- B. F. Chen, Z. B. Xie, F. F. Peng, S. P. Li, J. J. Yang, T. B. Wu, H. L. Fan, Z. F. Zhang, M. Q. Hou, S. M. Li, H. Z. Liu, B. X. Han, *Angew. Chem. Int. Ed.*, 60, 14405-14409(2021).
- S. Q. Jia, Q. G. Zhu, M. E. Chu, S. T. Han, R. T. Feng, J. X. Zhai, W. Xia, M. Y. H, He, H. H. Wu, B. X. Han, *Angew. Chem. Int. Ed.*, 60, 10977-10982(2021).
- S. P. Li, M. H. Dong, J. J. Yang, X. M. Cheng, X. J. Shen, S. L. Liu, Z. Q. Wang, X. Q. Gong, H. Z. Liu, B. X. Han, *Nat. Commun.*, 12, 584(2021).
- C. X. Xie, L. F. Lin, L. Huang, Z. X. Wang, Z. W. Jiang, Z. H. Zhang, B. X. Han, *Nat. Commun.* 12, 4823(2021).
- M. Cui, Q. L. Qian, J. J. Zhang, Y. Wang, B. B. A. Bediako, H. Z. Liu, B. X. Han, *Chem*, 7, 726-737(2021).
- H. L. Fan, J. X. Wang, P. P. Wu, L. Zheng, J. F. Xiang, H. L. Liu, B. X. Han, L. Jiang, *Chem*, 7, 1852-1869(2021).
- B. B. A. Bediako, Q. L. Qian, B. X. Han, *Acc. Chem. Res.* 54, 2467-2476(2021).

## **EU perspective for biofuels and bioenergy under the European Green Deal and REPowerEU**

Maria Georgiadou

<sup>1</sup>European Commission, Directorate General Research and Innovation, 21 Rue du Champ de Mars, 1049 Brussels, Belgium,  
\*[maria.georgiadou@ec.europa.eu](mailto:maria.georgiadou@ec.europa.eu)

EU perspective for the role of advanced biofuels and bioenergy under the European Green Deal supporting green and digital development as well as the REPowerEU promoting EU energy security and reducing dependence of fossil fuel imports. The EU policies, the R&I strategy and financing support through the EU programmes will be presented. International cooperation opportunities will be addressed.

### **References**

1. Fit for 55': delivering the EU's 2030 Climate Target on the way to climate neutrality COM(2021) 550 final
2. REPowerEU: Joint European action for more affordable, secure and sustainable energy COM(2022) 108 final

## How CO<sub>2</sub>-Switchable Materials can Help in Biomass Conversion and Greener Coatings

Philip G. Jessop<sup>1\*</sup> and Michael F. Cunningham<sup>1</sup>

<sup>1</sup>Queen's University, Departments of Chemistry and Chemical Engineering, 90 Bader Lane, Kingston, Ontario, Canada  
\*jessop@queensu.ca

Waste CO<sub>2</sub> can be harnessed to lower the environmental and economic cost of important products and processes without the CO<sub>2</sub> being converted into any product. The examples to be presented include A) biomass conversion and B) protective coatings utilize, and utilize CO<sub>2</sub> as a trigger for CO<sub>2</sub>-switchable materials (1).

### How Can CO<sub>2</sub>-Switchable Materials Help Biomass Conversion?

Why does biomass have trouble beating fossil fuels as a feedstock for more products? In many cases, biomass conversion to organic products is more expensive AND more environmentally harmful than fossil fuel conversion to the same products. Why? The energetically-costly removal of water! Biomass contains water, is often grown in water, is often converted in water, and emits water during dehydration reactions to lower the O/C ratio. Thus water removal can be necessary during feedstock preparation, feedstock conversion, and post-reaction separation steps. Life cycle assessments have shown repeated examples where water removal is so environmentally and economically costly that biomass-derived products cannot compete economically OR environmentally against petrochemicals. This situation must change if we are to attain a sustainable society in the future.

I will describe several new processes by which CO<sub>2</sub>-switchable materials can help separate organics from water, including high pressure switchable water (2) and solvent-assisted switchable water (SASW). Examples will include the separation of water from 1,3-propanediol obtained from biomass through biocatalysts, and the separation of water from ethanol and acetone.

### How Can CO<sub>2</sub>-Switchable Materials Help Make Greener Protective Coatings?

Water-based latex coatings are much less harmful than oil-based coatings, because during application of the coating, the 100% of the solvent is released into the environment. Obviously releasing water is environmentally preferable to releasing organic solvents. However, water-based latex coatings suffer from significant drawbacks that limit their use in industry and society. First, surfactants are necessary in latex coatings during the emulsion polymerization step and during storage, but become a liability once the coating is applied to a surface. For example, if the coating is applied to a metal in order to protect the metal from oxidation, then the surfactants will typically concentrate at the coating/metal interface. Their presence there helps water to seep in between the coating and the metal and thereby cause the coating to lift off and allowing the metal to rust. Using CO<sub>2</sub>-switchable surfactants makes it possible to make latex formulations that have active surfactants during emulsion polymerization and formulation storage and yet have the surfactant “turn off” when the formulation is applied to a metal surface.

As another example, the use of CO<sub>2</sub>-switchable solvents will be described for the preparation of latex coatings from biopolymers rather than fossil-fuel derived polymers.

### Acknowledgements

All of the students and postdoctoral fellows involved in the projects are gratefully acknowledged, as is funding from the Natural Sciences and Engineering Research Council of Canada.

### References

1. P. G. Jessop and M. F. Cunningham, *CO<sub>2</sub>-Switchable Materials*, Royal Society of Chemistry, Cambridge, 2020.
2. I. T. Cunha, H. Yang, P. G. Jessop, *Green Chem.* **21** 3996 (2021).

## Green Synthesis of Metal Nanoparticle Embedded Soft Hybrid Gel from Plant-based materials.

Supawan Tantayanon

<sup>1</sup>Department of Chemistry, Faculty of Science, Chulalongkorn University, Bangkok 10330, Thailand

\*supawan.t@chula.ac.th

The unique optical and electronic properties of metal nanoparticles and tunable properties of the organic templates encourage the scientific community to generate metal nanoparticle embedded soft hybrid materials for various novel utilities. The generation of hybrid materials from renewable resources and their utilization in basic and applied areas has been at the forefront of research in recent years for sustainable development. Here, we discuss the in-situ synthesis of metal nanoparticle embedded soft hybrid materials via eco-benign approach which exclude the use of toxic reducing/capping agents or toxic reaction media. In this protocol, the gel matrix composed of benign organic templates act as reducing as well as stabilizing agent for the in-situ generation and stabilization of metal nanoparticles. As the incorporation of metal salts (as nanoparticle precursor) in the gel medium is required in this process, in most of the cases aqueous media were used for the generation of metal nanoparticle embedded soft hybrid materials. This discussion includes interesting findings from our laboratory where hybrid gel matrix composed of renewable chemicals was utilized for the in-situ synthesis of palladium nanoparticle embedded soft trihybrid material. The hybrid gel matrix rich in polyphenols/flavonoids was exploited to generate palladium nanoparticle embedded trihybrid gel through in-situ reduction of doped Pd (II) salts to stable PdNPs. The xerogel of this trihybrid material was utilized as recyclable heterogeneous catalyst for C-C coupling reaction in air under phosphene free condition and reduction reaction. [1,2].



Figure 1. Green synthesis of metal nanoparticle embedded soft hybrid which is used as recyclable heterogeneous catalyst.

### References

1. R. Majumdar, S. Tantayanon, B. G. Bag, *Chemistry-An Asian Journal*, **11**, 2406 (2016).
2. R. Majumdar, S. Tantayanon, *Pure and Applied Chemistry* (2022), <https://doi.org/10.1515/pac-2021-0801>.

## Enhancing the Circular Economy in the Water Sector by Addressing the Chemical Contaminants of Concern Present in Wastewater

Despo Fatta-Kassinou

Department of Civil and Environmental Engineering and Nireas- International Water Research Center, University of Cyprus,  
P.O.Box 20517, 1678, Nicosia, Cyprus  
[dfatta@ucy.ac.cy](mailto:dfatta@ucy.ac.cy)

Even though wastewater reuse is a strategy that is rapidly expanding, there are still several issues to be addressed with respect to the presence of contaminants of emerging concern (CEC) in treated wastewater. The need to look beyond the conventional contaminants when assessing the potential risks of wastewater reuse with respect to ecosystems and human health is recognized as a priority issue in all policy areas at the EU level and beyond. CEC include pharmaceuticals and personal care products' compounds, disinfection by-products (DBPs), etc., as well as their transformation products (TPs) originating during treatment through biotic/abiotic processes [1].

Conventional activated sludge (CAS) currently applied in urban wastewater treatment plants (UWTPs) is inefficient in eliminating CEC, with their removal being highly variable. Membrane bioreactors have been shown to be more effective than CAS in removing only CEC susceptible to biodegradation. In recent years, considerable efforts have been made regarding the application of advanced treatment technologies, such as membrane filtration, adsorption on activated carbon and advanced chemical oxidation processes (AOPs), capable of improving the effluent quality with respect to the presence of CEC. Concerning filtration and separation processes, while the pores in micro- and ultra-filtration are too large to reject CEC, the lower pore sizes used in nanofiltration and reverse osmosis, have been shown to effectively reject significant amounts of CEC. However, the membrane technologies generate a residual stream, thereby creating a need for further proper management. Adsorption using activated carbon has been effectively used for the removal of various CEC, which after reaching its maximum adsorption capacity, should be regenerated, and further reused. AOPs (e.g., UV-C/H<sub>2</sub>O<sub>2</sub>, solar photo-Fenton, ozonation) have gained popularity over the past few decades in pilot-scale applications for their high efficiency in removing CEC, while also providing disinfection of the wastewater. Noteworthy is that several TPs may be formed during the application of AOPs, which may exhibit their own biological effects. Soluble microbial products in wastewater constitute the main precursors to the formation of DBPs which often are biologically potent [2,3].

Recent scientific evidence revealed that the extent of crops' uptake of CEC is mainly influenced by the physicochemical properties of the compounds, the physiological properties of the crop and the soil properties. To date, it is difficult to draw concrete conclusions on the effects of soil and wastewater properties on the uptake of CEC, since data in the literature are available for different plant-growth methods and for different plants and CEC in each study. Moreover, there is lack of data on the health risks associated with the consumption of wastewater-irrigated crops, while predictive models to accurately estimate the concentration of CEC in crops grown in different environmental/agronomic practices would be useful for risk assessment [4].

Summarizing, there are several knowledge gaps and open questions related to the potential effects that the wastewater discharges and reuse practice might induce regarding the CEC. It has become clear that new strategies consistent with the precautionary principle and the "One Health" approach are needed to assess the overall quality of wastewater intended for reuse. Knowledge regarding risks that relate to low-dose exposure of CEC to non-target organisms, the additive/synergistic behavior of various CEC in mixtures, crops' uptake, and antibiotic resistance is only now starting to shape. This talk aims at addressing these important issues.

### References

1. L. Rizzo, S. Malato, D. Antakyali, V. G. Beretsou, M. B. Đolić, W. Gernjak, E. Heath, I. Ivancev-Tumbas, P. Karaolia, A. R. Lado Ribeiro, G. Mascolo, C. S. McArdell, H. Schaar, A. M. Silva, D. Fatta-Kassinou, *Science of the Total Environment*, **655** 986 (2019).
2. S.G. Michael, B. Drigo, I. Michael-Kordatou, C. Michael, T. Jäger, S.C. Aleer, T. Schwartz, E. Donner, D. Fatta-Kassinou, *Journal of Hazardous Materials*, <https://doi.org/10.1016/j.jhazmat.2022.128943> (2022).
3. L. Rizzo, W. Gernjak, P. Krzeminski, S. Malato, C. S. McArdell, J. A. Sanchez Perez, H. Schaar, D. Fatta-Kassinou, *Science of the Total Environment*, **710** 136312 (2020).
4. A. Christou, G. Papadavid, P. Dalias, V. Fotopoulos, C. Michael, J. M. Bayona, B. Piña, D. Fatta-Kassinou, *Environmental Research*, **17** 422 (2019).

# Keynote Lectures

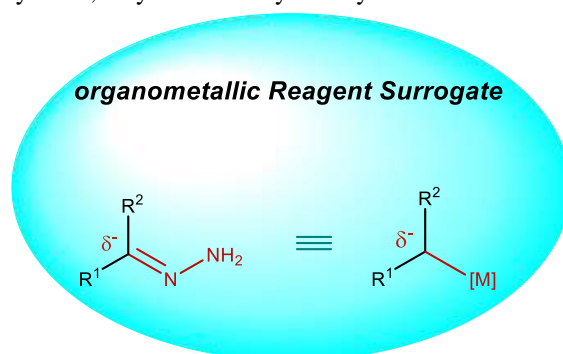
## Sustainable Cross-Couplings: Demetallation of Organometallic Reactions

Chao-Jun Li

<sup>1</sup>Department of Chemistry, and FQRNT Centre for Green Chemistry and Catalysis, McGill University, 801 Sherbrooke Street West, Montreal, Quebec H3A0B8, Canada

\*cj.li@mcgill.ca

The construction of new carbon-carbon bonds is the cornerstone of organic chemistry. Organometallic reagents are amongst the most robust and versatile nucleophiles for this purpose. Polarization of the metal-carbon bonds in these reagents facilitates their reactions with a vast array of electrophiles to achieve chemical diversification. The dependence on stoichiometric quantities of metals and often organic halides as feedstock precursors, which in turn produces copious amounts of metal halide waste, are the key limitations of the classical organometallic reactions. Inspired by the classical Wolff-Kishner reduction converting carbonyl groups in aldehydes or ketones into methylene derivatives, our group has recently developed strategies to couple various alcohols, aldehydes, and ketones with a broad range of both hard and soft carbon electrophiles in the presence of catalytic amounts of transition metals, via the hydrazone derivatives: i.e., as **Organometallic Reagent Surrogates**. This talk will discuss this concept in our research group, leading to a novel carbon-carbon bond-forming strategy. The strategy has been demonstrated by the employment of carbonyl-derived alkyl carbanions in various transition-metal catalyzed chemical transformations, including 1,2-carbonyl/imine addition, conjugate addition, carboxylation, olefination, cross-coupling, allylation, alkylation and hydroalkylation.<sup>1</sup>



### Acknowledgements

I would like to thank NSERC, Canada Research Chair program, CFI, FQRNT, Killam Research Fund of the Canadian Council of Arts and McGill University for support of our research.

### References

- Dai, X.-J.; Li, C.-C.; Li, C.-J. *Chem. Soc. Rev.* **2021**, *50*, 10733-10742; Wang, H.; Dai, X.-J.; Li, C.-J. *Nature Chemistry*, **2017**, *9*, 374-378; Dai, X.-J.; Wang, H.; Li, C.-J. *Angew. Chem. Int. Ed.*, **2017**, *56*, 6302-6306; Chen, N.; Dai, X.-J.; Wang, H.; Li, C.-J. *Angew. Chem. Int. Ed.*, **2017**, *56*, 6260-6263; Cao, D.; Zeng, H.; Peng, Y.; Li, C.-J. *Nat. Commun.*, **2021**, *12*, 3729; Luo, S.; Peng, M.; Querard, P.; Li, C.-C.; Li, C.-J. *J. Org. Chem.*, **2021**, *86*, 13111-13117; Kang, H.; Li, C.-J. *Chem. Sci. Chem. Sci.* **2022**, *13*, 118-122; Lv, L.; Li, C.-J. *Angew. Chem. Int. Ed.*, **2021**, *60*, 13098-13104; Wang, Y.-Z.; Liu, Q.; Cheng, L.; Yu, S.-C.; Liu, L.; Li, C.-J. *Tetrahedron*, **2021**, *80*, No. 131889; Lv, L.; Li, C.-J. *Chem. Sci.*, **2021**, *12*, 2870-2875; Li, C.-C.; Wang, H.; Sim, M. M.; Qiu, Z.; Chen, Z.-P.; Khaliullin, R. Z.; Li, C. J. *Nature. Commun.*, **2020**, *11*, No. 6022; Yao, J.; Chen, Z.; Yu, L.; Lv, L.; Cao, D.; Li, C.-J. *Chem. Sci.* **2020**, *11*, 10759-10763; Yu, L.; Lv, L.; Qiu, Z.; Chen, Z.; Tan, Z.; Liang, Y.-F.; Li, C.-J. *Angew. Chem. Engl. Ed.* **2020**, *59*, 14009-14013; Lv, L.; Yu, L.; Qiu, Z.; Li, C.-J., *Angew. Chem. Engl. Ed.* **2020**, *59*, 6466-6472; Li, C.-C.; Kan, J.; Qiu, Z.; Li, J.; Lv, L.; Li, C.-J. *Angew. Chem. Engl. Ed.* **2020**, *59*, 4544-4549; Lv, L.; Zhu, D.; Qiu, Z.; Li, J.; Li, C.-J., *ACS Catal.* **2019**, *9*, 9199-9205; Zeng, H.; Luo, Z.; Han, X.; Li, C.-J., *Org. Lett.* **2019**, *21*, 5948-5951; Cao, D.; Pan, P.; Zeng, H.; Li, C.-J. *Chem. Commun.* **2019**, *55*, 9323-9326; Li, C.-J.; Huang, J.; Dai, X.; Wang, H.; Chen, N.; Wei, W.; Zeng, H.; Tang, J.; Li, C.; Zhu, D.; Lv, L. *Synlett*, **2019**, *30*, 1508-1524; Zhu, D.; Lv, L.; Qiu, Z.; Li, C.-J., *J. Org. Chem.* **2019**, *84*, 6312-6322; Lv, L.; Zhu, D.; Li, C.-J. *Nat. Commun.* **2019**, *10*, 715; Zhu, D.; Li, C.-C.; Lv, L.; Ung, S.; Gao, J.; Li, C.-J. *Angew. Chem. Int. Ed.*, **2018**, *57*, 16520-16524; Lv, L.; Qiu, Z.; Li, J.; Liu, M.; Li, C.-J. *Nat. Commun.* **2018**, *9*, 4739. Li, C.-C.; Dai, X.-J.; Wang, H.; Zhu, D.; Gao, J.; Li, C.-J. *Org. Lett.* **2018**, *20*, 3801-3805; Yan, S.-S.; Zhu, L.; Ye, J.-H.; Zhang, Z.; Huang, H.; Zeng, H.; Li, C.-J.; Lan, Y.; Yu, D.-G., *Chem. Sci.*, **2018**, *9*, 4873-4878; Lv, L.; Zhu, D.; Tang, J.; Qiu, Z.; Li, C.-C.; Gao, J.; Li, C.-J. *ACS Catal.* **2018**, *8*, 4622-4627; Tang, J.; Lv, L.; Dai, X.-J.; Li, C.-C.; Li, L.; Li, C.-J. *Chem. Commun.* **2018**, *54*, 1750-1753; Kan, J.; Chen, Z.; Qiu, Z.; Lv, L.; Li, C.; Li, C.-J. *Sci. Adv.*, **2022**, *8*, eabm6840.

## **Biowaste valorisation: the waste-to-wealth concept**

Rafael Luque

*Departamento de Química Orgánica, Universidad de Córdoba, Campus de Rabanales, Edificio Marie Curie (C-3), Ctra Nnal IV, Km 396, E14071, Córdoba, Spain  
e-mail: rafael.luque@uco.es*

Society urgently needs to cope with increasing energy demands, extensive pollution concerns and most importantly resource scarcity (water, food) already predicted for the years to come. In order to become a more sustainable society, scientists have to embrace such urgent challenges in the 21st Century, coming up with suitable alternatives for the betterment of humankind. Waste valorisation, going well beyond traditional waste management practises, has the potential to become an alternative for the harvesting of valuable compounds (chemicals, materials, fuels, energy carriers), generating wealth from biowaste, circumventing at the same time environmental hazards and concerns such waste feedstocks have inherently associated.

This contribution is aimed to frame the waste-to-wealth concept as illustrated in a number of biowaste valorisation examples from sewage sludge to coffee waste grounds, slaughterhouse and construction waste as effective sources of valuable chemicals, biomaterials and biofuels.



## DES, ES AND ILS: Tailoring Solvents for Sustainable Applications

João Afonso, Bruna F. Soares, Gabriela Caetano, Isabel M. Marrucho

*Centro de Química Estrutural and Institute of Molecular Sciences and Departamento de Engenharia Química, Instituto Superior Técnico, Universidade de Lisboa, Lisboa, Portugal  
isabel.marrucho@tecnico.ulisboa.pt*

The need to develop new solvents and materials with tailored properties to afford more sustainable and circular processes as prompt a large number of research in recent years. In particular, the establishment of Deep Eutectic Solvents (DES) as a new class of solvents was essentially grounded on naïve comparisons with Ionic Liquids (ILs), since the first DES were composed of solid at room temperature ionic liquids, such as choline chloride. The easiness of DESs preparation afforded the quick preparation and utilization of a massive number of solvents and their use in wide variety of applications with a minimal fundamental knowledge of their thermophysical properties and phase equilibria studies. As time went by, the understanding of DES nature lead to the thermodynamic definition of DES and consequently to its differentiation from other classes of solvents.

This talk aims at dispelling some myths about DES and establish fair comparisons with other classes of solvents, such as ILs, eutectic solvents and volatile organic compounds (VOCs), so that clear and sound conclusions can be withdrawn. Several important parameters typically used to characterize solvents and that have been much used to justify DESs wide range of applications, such as vapor pressure, thermal stability, polarity, toxicity and water miscibility, were accessed for these different solvents and comparisons were established.

Several examples will be used to illustrate the application of each one of these classes of solvents and to demonstrate that the specific properties of each solvent determine their role in advancing the sustainability of chemical processes.

### Acknowledgements

This work was funded by national funds through FCT - Fundação para a Ciência e a Tecnologia - under the projects CQE (UIDB/00100/2020 and UIDP/00100/2020) and PTDC/EAM-AMB/2023/2021.

## Unlocking the potential of crustacean waste: solvent-free pathways to added-value materials

Tony Jin,<sup>1</sup> Juliana L. Vidal,<sup>1</sup> Faezeh Hajiali,<sup>1</sup> Tracy Liu,<sup>1</sup> Edmond Lam,<sup>2</sup> Audrey Moores<sup>1,3</sup>

<sup>1</sup>Centre in Green Chemistry and Catalysis, Dept. of Chemistry, McGill University, 801 Sherbrooke St. West, Montréal, H3A 0B8, Canada

<sup>2</sup>Aquatic and Crop Resource Development Research Centre, National Research Council of Canada, 6100 Royalmount Avenue, Montreal, Quebec, H4P 2R2 Canada

<sup>3</sup>Department of Materials Engineering, McGill University, 3610 University Street, Montreal, Quebec H3A 0C5, Canada  
\*audrey.moores@mcgill.ca

Chitin, the second most abundant biopolymer after cellulose, is present in the shell of crustaceans, in the cuticle of insect and even in some fungi.<sup>1</sup> It can be converted into chitosan, a highly praised material with application as a fertilizer, water treatment flocculant, biomedical fibers and food additive. Yet today's technologies for chitin extraction and chitosan production rely on the use of corrosive treatments, high energy input and large quantities of by product effluents. Herein we are presenting our group's effort to tackle this question, through the use of solvent-free methods, and the road map we have established to access several exciting added-value polymers and nanomaterials. Mechanochemistry is becoming an established method for the sustainable, solid-phase synthesis of scores of nanomaterials and molecules, ranging from active pharmaceutical ingredients to materials for cleantech.<sup>2</sup> Beyond its ability to trigger reactivity through energy delivery to chemical systems, mechanochemistry is also a way to activate precursors and mix reagents that may react further in a subsequent aging phase.<sup>3</sup> We showed that mechanochemistry and aging could be used effectively for the deacetylation of chitin using solid NaOH as reagent.<sup>4</sup> This process yielded high molecular weight chitosan with minimal use of energy and solvent. Moving upstream, we have explored the extraction of chitin from crustacean shells, and demonstrated effective extraction of high quality chitin using milling with various solid acids.<sup>5</sup> Chitin, like cellulose, is a crystalline material, granting access to nanocrystals via acid or oxidative partial hydrolysis.<sup>1</sup> Classic methods being water and chemical intensive, we have developed a mechanochemical version, in which aging done under high humidity in a shaker was needed to afford high yields of excellent quality chitin nanocrystals.<sup>6</sup> This method can be extended to cellulose nanocrystals synthesis. Finally, we have also extended the use of mechanochemistry to the fabrication of chitosan nanocrystals from chitin nanocrystals.<sup>7</sup> We developed hydrogels from chitosan and chitin nanocrystals, with exceptional gelling properties and demonstrated their applicability for slow drug release.

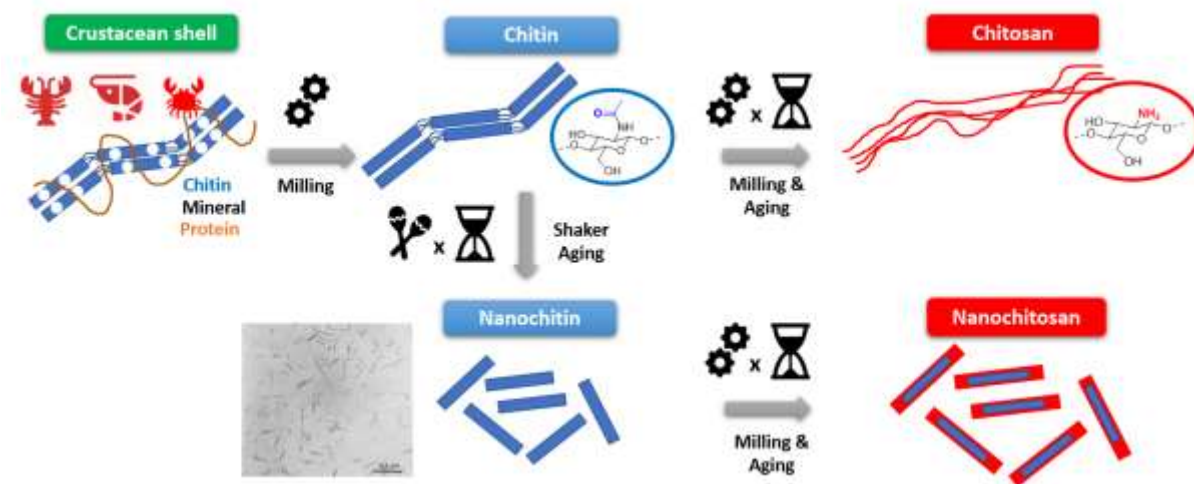


Figure 1. Overall synthetic scheme for access to chitin and chitosan derivatives from crustacean shells by mechanochemistry, as developed in the group.<sup>4, 5, 6, 7</sup>

### References

1. T. Jin, T. Liu, E. Lam, A. Moores, *Nanoscale Horiz.* **2021**, *6*, 505-542
2. J.-L. Do, T. Friščić, *ACS Cent. Sci.* **2017**, *3*, 1, 13–19
3. M. J. Cliffe, C. Mottillo, R.S. Stein, D.-K. Bučar, T. Friščić, *Chem. Sci.*, **2012**, *3*, 2495-2500
4. T. Di Nardo, C. Hadad, A. Nguyen Van Nhien, A. Moores, *Green Chem.* **2019**, *21*, 3276-3285
5. F. Hajiali, J. L. Vidal, T. Jin, L. de la Garza, M. Santos, G. Yang, A. Moores, *submitted*.
6. T. Jin, T. Liu, F. Hajiali, M. Santos, Y. Liu, D. Kurdyla, S. Regnier, S. Hrapovich, E. Lam, A. Moores, *submitted*
7. T. Jin, T. Liu, S. Jiang, V. Michaelis, D. Kurdyla, B.A. Klein, E. Lam, J. Li, A. Moores, *Green Chem.* **2021**, *23*, 6527-6537

## Teaching global perspectives: Connecting Green Chemistry, the UN SDGs, and Sustainable Polymers

Jane E. Wissinger<sup>1</sup>

<sup>1</sup>University of Minnesota, 207 Pleasant St. SE Minneapolis, MN 55455, United States

\*jwiss@umn.edu

### Abstract text:

This presentation will share how the UN Sustainable Development Goals (UN SDGs) and systems thinking were incorporated into an upper division green chemistry course and sustainable polymer laboratory experiments in order to build awareness and provide an appreciation for the vast opportunities a chemistry degree offers to contribute to a sustainable future. Early introduction of these topics provided a platform to use for discussion throughout the course curriculum. The lecture course begins with the U.S. environmental movement through the birth of green chemistry and sets the stage for how green chemistry and sustainable chemistry will be essential for attaining the UN Sustainable Development Goals. These concepts are then reinforced as a breadth of units are taught including green metrics, alternative reaction mechanisms, chemical toxicology, design for hazard reduction, and use of renewable feedstocks and green energy. The theme then transitions to more specific consumer products such as pharmaceuticals, sustainable polymers, nanomaterials, and dyes where life cycle thinking and systems thinking apply. Special emphasis is placed on the dire need to develop more environmentally friendly polymeric materials and recent advances made by the University of Minnesota NSF Center for Sustainable Polymers. A portfolio of experiments engaging students in modern advances in green polymers is shared. Guest lecturers from academia, government agencies, and industry provide real world context for students as they look ahead to the potential impact of their future careers for a sustainable future.

## On the Efficient Transformation of CO<sub>2</sub> to Chemicals and Fuels

Jorge Gascon

<sup>1</sup>King Abdullah University of Science and Technology, KAUST Catalysis Center (KCC), Advanced Catalytic Materials,  
Thuwal 23955, Saudi Arabia  
\*jorge.gascon@kaust.edu.sa

The increasing global CO<sub>2</sub> levels has led to a massive thrust in research on both Carbon Capture and Storage (CCS) and Carbon Capture and Utilization (CCU). It has been posited that, in terms of volume, the contribution of CCU will be significantly less as compared to CCS for avoiding CO<sub>2</sub> emissions and achieving the “2 degree scenario” (2DS) goals. However, what cannot be denied is that the immediate economic potential of CCU far outweighs that of CCS especially considering the fact that large scale capital investment is required in case of the latter.

While it is clear that CCS does need to be implemented in order to realistically achieve the 2DS goals, what is not commonly considered is that instead of approaching CCS and CCU as two separate methods of carbon mitigation, we should think of how CCU can, in fact, help address the problems faced for the implementation of CCS. With research intensifying on CCU, it is not impractical to think of an economic cycle where the profits gained from CCU can help to offset the costs of CCS if an integrated system of CCSU (Carbon Capture Storage and Utilization) is implemented. The reuse of stored CO<sub>2</sub> can become beneficial if consumption of fossil fuels is greatly reduced over the next century and the stored CO<sub>2</sub> becomes the chief feedstock for carbon-based chemicals.

In this presentation, we will present several routes based on careful choice of catalytic components and reactor configuration to increase selectivity and productivity in the direct hydrogenation of CO<sub>2</sub> to methanol, light olefins, aromatics and liquid fuels.

## Chemicals from lignin: feasible, safe and sustainable

Bert F. Sels

<sup>1</sup>CSCE/KULeuven, Chem&Tech Celestijnenlaan 200F 3001 Leuven, Belgium

\*bert.sels@kuleuven.be

Biomass offers a sustainable source of carbon for synthesizing chemicals. In this context, a lot of progress at the level of the biorefinery to disentangle complex lignocellulosic biomass into various fractions has been made recently. Given the high mass content of carbohydrates in the biomass composition, focus of most traditional biorefineries is on isolating those and do useful (material) chemistry with it. However lately, use of lignin, instead of burning it, becomes a massive focus point in recent biomass research as a means to valorize as much as possible of the green carbon [1].

New methods are becoming available and developed giving access to lignin fractions of various sorts. Chemical, structural and physical properties may be different, determining their usages in chemical application later on. A most progressed methodology relies on the lignin-first principle, in which fractionation of lignocellulose in the biorefinery relies on a specific lignin stabilization strategy, either as the polymer itself, or as stable lignin fragments if lignin depolymerization in the refinery conditions is allowed [2, 3]. These lignin-first fractionation strategies allow for selective fractionation and depolymerization of lignin into monomeric phenolics and oligomers [4, 5]. A very successful approach in this aspect is the reductive catalytic fractionation, also called RCF. This lecture will show that the RCF lignin-derived chemicals can potentially be viewed as a new chemicals' platform, originating from a green carbon source, to produce both drop in chemicals, e.g. by applying a chemical funneling concept [6, 7], or to novel chemicals. Especially for the latter, safety of the phenolic chemicals will be highlighted, showing that phenolic alternatives derived from lignin are not only functional, for instance as structural core for additives (plasticizers, flame retardants) and polymers (epoxyresins, polycarbonates, PUR) and sustainable with respect to its green carbon content, but importantly they also are significantly less harmful as a chemical [8 - 11]. This safety aspect is currently underused and underexplored as a motivator in the carbon feedstock transition, despite its importance for the society and the environment.

### Acknowledgements

Financial support from C2 KULeuven, FWO EoS (Biofact), iBOF program (Next Bioref) and SBO Catalyستي (Paddle) are greatly acknowledged.

### References

1. W. Schutyser, T. Renders, S. Van den Bosch, S.F. Koelewijn, G.T. Beckham, B.F. Sels, *Chemical Society Reviews*, **47** (3), 852 (2018).
2. M.M. Abu-Omar, K. Barta, G.T. Beckham, J.S. Luterbacher, J. Ralph., R. Rinaldi, Y. Román-Leshkov, J.S.M. Samec, B.F. Sels, F. Wang, *Energy & Environmental Science* **14** (1), 262 (2021).
3. S. Van den Bosch, S.-F. Koelewijn, T. Renders, G. Van den Bossche, T. Vangeel, W. Schutyser, B.F. Sels, Ed. R. Luque and B.F. Sels, *Lignin Chemistry*, Springer, 129 (2020).
4. T. Renders, E. Cooreman, S. Van den Bosch, W. Schutyser, S.-F. Koelewijn, T. Vangeel, A. Deneyer, G. Van den Bossche, C.M. Courtin, B.F. Sels, *Green Chemistry* **20** (20), 4607 (2018).
5. P. Sudarsanam, D. Ruijten, Y. Liao, T. Renders, S.F. Koelewijn, B.F. Sels, *Trends in Chemistry* **2** (10), 898 (2020).
6. Y. Liao, S.-F. Koelewijn, G. Van den Bossche, J. Van Aelst, S. Van den Bosch, T. Renders, K. Navare, T. Nicolaï, K. Van Aelst, M. Maesen, H. Matsushima, J.M. Thevelein, K. Van Acker, B. Lagrain, D. Verboekend, B.F. Sels, *Science* **367** (6484), 1385 (2020).
7. X. Wu, Y. Liao, J. Bomon, G. Tian, S.-T. Bai, K. Van Aelst, Q. Zhang, W. Vermandel, B. Wambacq, B.U.W. Maes, J. Yu, B. F. Sels, *ChemSusChem*, (accepted 2022).
8. K. Van Aelst, E. Van Sinay, T. Vangeel, E. Cooreman, G. Van den Bossche, T. Renders, J. Van Aelst, S. Van den Bosch, B.F. Sels, *Chemical Science* **11** (42), 11498 (2020).
9. Korneel Van Aelst, Elien Van Sinay, Thijs Vangeel, Yingtuan Zhang, Tom Renders, Sander Van den Bosch, Joost Van Aelst, Bert F Sels, *Chemical Communications* **57** (46), 5642 (2021).
10. S-F Koelewijn, C Cooreman, T Renders, C Andecochea Saiz, S Van den Bosch, W Schutyser, W De Leger, M Smet, P Van Puyvelde, H Witters, B Van der Bruggen, BF Sels, *Green Chemistry* **20** (5), 1050 (2018).
11. L. Trullemans, S.-F. Koelewijn, I. Scodeller, T. Hendrickx, P. Van Puyvelde, B.F. Sels, *Polymer Chemistry* **12** (41), 5870 (2021).

## European Sustainable Biobased Nanomaterials Community (BIOMAC). From biomass pretreatment for monomers and additives extraction to the synthesis of biobased composites

Dimitrios N. Bikiaris<sup>1\*</sup>, Katerina Papadopoulou<sup>1</sup>, Panagiotis A. Klonos<sup>1</sup>, Eleftheria Xanthopoulou<sup>1</sup>, Zoi Terzopoulou<sup>1</sup>, Alexandra Zamboulis<sup>1</sup>, Ondřej Mašek<sup>2</sup>, Anjali Jayakumar<sup>2</sup>, Christian Wurzer<sup>2</sup>, Sofia Makri<sup>3</sup>, Ioanna Deligkiozi<sup>3</sup>, Alexandros Zoikis Karathanasis<sup>3</sup>, Christina Pappa<sup>4</sup>, Antigoni Margellou<sup>4</sup>, Stylianos Torofias<sup>4</sup>, Konstantinos Triantafyllidis<sup>4</sup>

<sup>1</sup>Laboratory of Polymer Chemistry and Technology, Department of Chemistry, Aristotle University of Thessaloniki, GR-54124 Thessaloniki, Greece,

<sup>2</sup>UK Biochar Research Centre, School of GeoSciences, University of Edinburgh, Edinburgh, EH9 3FF, UK

<sup>3</sup>Creative Nano PC, 4 Leventi Street, Peristeri, 12132 Athens, Greece

<sup>4</sup>Laboratory of Chemical and Environmental Technology, Department of Chemistry, Aristotle, University of Thessaloniki, GR-54124 Thessaloniki, Greece

\*[dbic@chem.auth.gr](mailto:dbic@chem.auth.gr)

In recent years, the synthesis of biobased polymers and additives from biomass has received great attention. This is because biomass is produced in abundance from plants every year through photosynthesis, using only CO<sub>2</sub> and water. However, the chemical energy that is stored in biomass in the form of glucose or sugars, is lost during the annual cycle of seasons. Different pretreatments can be applied to convert glucose or other biomass ingredients to building blocks for polymer production or to extract additives for nanocomposite production. Aliphatic monomers, like lactic and succinic acid or diols like ethylene, propylene and butylene glycol are such high added value monomers that can be produced during solvolysis or hydrothermal pretreatment of biomass. They can be used for the synthesis of poly(lactic acid) (PLA), poly(butylene succinate) (PBSu) and other polymer and copolymers.

PLA is a very promising biobased polymer, both because of its biodegradation and its physical characteristics that resemble those of synthetic plastics [1]. PBSu is also an important biobased polyester since it is produced from biobased succinic acid and butanediol by two stage melt polycondensation [2]. Both polyesters are thermoplastic materials, commercially available with completely different physical properties, since PLA can be taken completely amorphous while PBSu is a semicrystalline polyester due to its fast crystallisation rate. They are biodegradable polyesters under specific environmental conditions, fully recyclable and can be used in food packaging applications, single used items, agriculture, automotive, etc., replacing traditional non degradable polymers in many applications.

To improve their properties, two different types of biobased additives i.e., lignin, in its neat, extracted form from biomass and in the form of nanolignin, and biochar were used as reinforcing agents. Two series of polymer-based composites were prepared by melt mixing, using lignin or nanolignin in contents 0.5, 1, 2.5% and 5 wt% in the PLA matrix. Additionally, PBSu nanocomposites with 1, 2.5% and 5 wt% of Miscanthus biochar (MSP 700) [3] were prepared by in situ polymerisation. All composites were characterised by FTIR and NMR spectroscopies, DSC and TGA thermal methods, XRD, mechanical properties and SEM.

From the SEM micrographs it was found that in both polymers a fine dispersion of the additives was achieved, which affects the physical properties of the used polymers. In all cases, a reinforcing effect of additives was observed since tensile strength (Figure 1) and Young's modulus increased by increasing additive content.

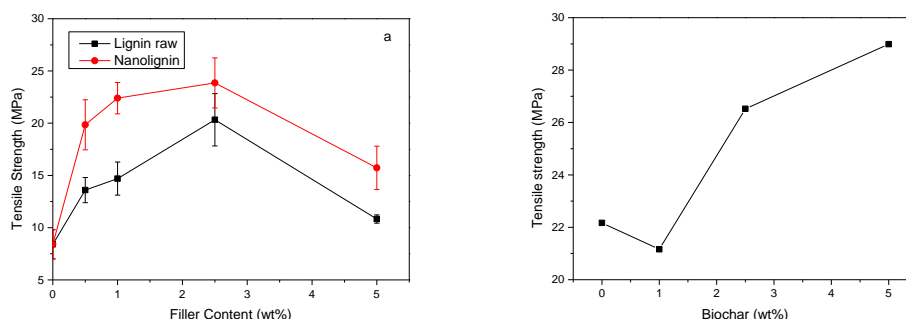


**Figure 1.** Tensile strength of PLA/lignin-nanolignin composites and b) PBSu/Biochar composites at different additive content.

### Acknowledgements

This project has received funding from the European Union's Horizon 2020 Research and Innovation Programme under Grant Agreement No. 952941



## References

1. E. Balla, V. et al. *Polymers* **13**, 1822 (2021). <https://doi.org/10.3390/polym13111822>.
2. G.Z. Papageorgiou, D.N. Bikiaris. *Polymer* **46**, 12081 (2005).
3. O. Mašek et al. *Journal of Analytical and Applied Pyrolysis* **132**, 200 (2018).

## Towards Scalable Synthesis of Furanics: Products Purification and Comparative Environmental Assessment

Fabio Aricò

<sup>1</sup>Ca' Foscari University of Venice, Department of Environmental Sciences, Informatics and Statistics, Via Torino 155, 30172 Venezia (Italy)

\*Fabio.arico@unive.it

5-Hydroxymethylfurfural (HMF) is an archetype of bio-based platform chemicals, molecules derived by biomass that are the focus of Biorefinery research field.[1] HMF can be easily prepared from D-fructose via acid-catalyzed triple dehydration. This synthesis was carried out in the presence of numerous catalysts such as mineral and Lewis acids, metal chlorides, metal oxides, heteropolyacids and ion-exchange resins to mention just a few. [2] Although all these catalysts lead to an efficient conversion of D-fructose into HMF, typical reaction drawbacks include harsh reaction conditions and difficult isolation of the target molecule from the reaction media. Furthermore, despite the large number of publications reported in the literature, only limited attention has been focused on the separation

of HMF from the reaction mixture. As a result, most of syntheses leading to HMF and furanics are based on small scale reactions where separation and isolation strategies are rarely addressed.

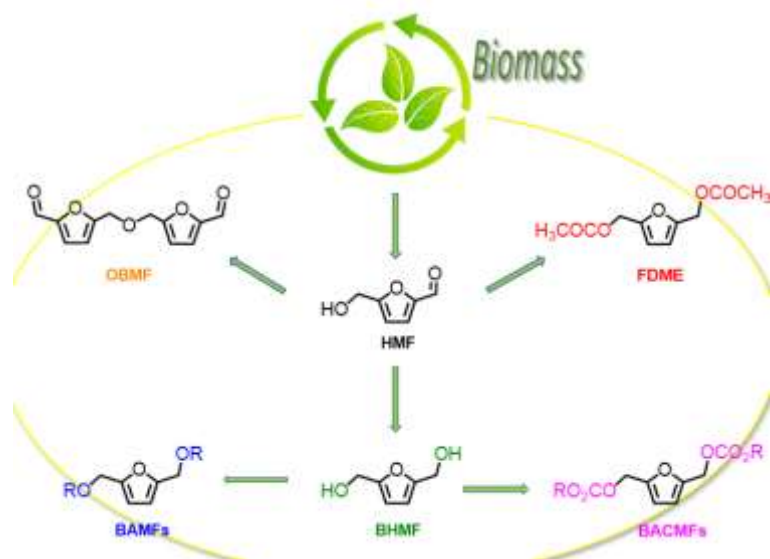


**Figure 1.** Furanics from biomass

Our interest into furanics is related to their upgrading into a variety of value-added derivatives, such as chemicals, materials, bio-based polymers and fuels. In this prospect it is pivotal to develop simple synthetic approaches addressing both isolation and purification of these compounds. In

recent years we have investigated gram to multi-grams scale syntheses of HMF,[3] 5-bis(hydroxymethyl)furan (BHMf), 2,5-bis[(alkoxycarbonyl)oxymethyl]furan (BAMF),[4] 2,5-Bis[(alkoxycarbonyl)oxymethyl] furan (BACMF)[5], 2,5-furandicarboxylic acid dimethyl ester (FDME)[6] and more recently 5,5 '(oxy-bis(methylene)bis-2-furfural (OBMF) and its derivatives. Most of the abovementioned compounds have been achieved employing commercially available catalysts, green solvents, mild reaction conditions and the products were isolated as pure via simple purification procedures. Furthermore, for specific examples green metrics and materials efficiency performance of the reported procedures have also been investigated taking into account E-factor and PMI green metrics.

### Acknowledgements

We want to acknowledge the Organization for the Prohibition of Chemical Weapons (OPCW); Project Number L/ICA/ICB/218789/19 for funding part of this research. The presented work is also within the framework of COST Action FUR4Sustain (CA18220-European network of FURan based chemicals and materials FOR a Sustainable development), supported by COST.

### References

1. A.A. Turkin, E.V. Makshina, B.F. Sels, *ChemSusChem*, e202200412 (2022).
2. H. Xia, S. Xu, H. Hu, J. An, C. Li, *RSC Adv.*, **8**, 30875 (2018).
3. M. Musolino, J. Andraos, F. Aricò, *ChemistrySelect*, **3**, 2359 (2018).
4. M. Musolino, M. J. Ginés-Molina, R. Moreno-Tost, F. Aricò, *ACS Sustainable Chem. Eng.* **7**, 10221 (2019).
5. A. G. Sathicq, M. Annatelli, I. Abdullah, G. Romanelli, *Sustainable Chemistry and Pharmacy*, **19**, 100352 (2021).
6. G. Trapasso, M. Annatelli, D. Dalla Torre, *Green Chem.*, **24**, 2766 (2022).



## Design of Biomass Waste-Derived Biochar Catalyst for Glucose Oxidation

Qiaozhi Zhang<sup>1</sup>, Yang Cao<sup>1</sup>, Daniel C.W. Tsang<sup>1,2,\*</sup>

<sup>1</sup>Department of Civil and Environmental Engineering, The Hong Kong Polytechnic University, Hung Hom, Kowloon, Hong Kong, China.

<sup>2</sup>Research Institute for Future Food, The Hong Kong Polytechnic University, Hung Hom, Kowloon, Hong Kong, China.

\* [dan.tsang@polyu.edu.hk](mailto:dan.tsang@polyu.edu.hk)

As a major renewable and carbon-neutral resource, biomass attracts increasing attention due to fossil resource depletion and carbon emission concerns. Pyrolyzing biomass waste to produce biochar would reduce the environmental pollution and greenhouse gas emission compared to conventional combustion. By varying pyrolysis conditions and introducing active sites, the characteristics of biochar can be manipulated. Furthermore, biochar is a carbon-negative material compared to activated carbon [1], indicating its great potential as support of catalyst. Biomass valorization to chemicals is an important utilization of this renewable resource. This study reports the production of two value-added organic acids, *i.e.*, gluconic acid (GOA) and glucuronic acid (GUA), from biomass waste-derived glucose via microwave-assisted catalytic oxidation. They are versatile in multiple fields, such as food and pharmaceuticals, biodegradable polymers, and construction materials [2]. Noble metal-based catalysts have been extensively investigated for glucose oxidation, where an unfavourable base addition is generally required to achieve ideal performance in a green chemistry sense. Herein, a series of novel wood waste-derived biochar-supported Cu-based catalysts were prepared by varying synthesis conditions (*i.e.*, pyrolysis temperature of 600/800°C and purging with N<sub>2</sub>/CO<sub>2</sub>) for tuning CuO<sub>x</sub> species and functionality of biochar support. The catalytic performances and mechanisms were studied with a view to facilitate glucose conversion and improve product selectivity. The yield of GUA and GOA could reach up to 39.0% and 30.7% within 20 min at 160°C over the CuBC600N catalysts (shown as r1 in **Figure 1b**). By analyzing the microwave-catalyst interactions, the enhanced catalytic performance and reduced energy consumption (**Figure 1a**) are mainly attributed to a high percentage of active Cu<sub>2</sub>O species and abundant O-containing functional groups as well as the less  $\pi$ - $\pi$  conjugated area of the biochar support. The synergistic effects of Cu/Cu<sub>2</sub>O sites (*i.e.*, adsorption and catalysis) and the reaction pathways towards GUA were elucidated by density functional theory (DFT) calculation. In addition, it was found that the catalytic performance was still 70% higher than bare biochar catalysts in the third run of the reaction (**Figure 1b**), demonstrating the importance of the CuO<sub>x</sub> species stabilized on the biochar support for catalytic activity improvement. This study can provide valuable information for the rational design of carbon-negative and microwave-sensitive biochar catalysts for high-efficiency glucose oxidation.

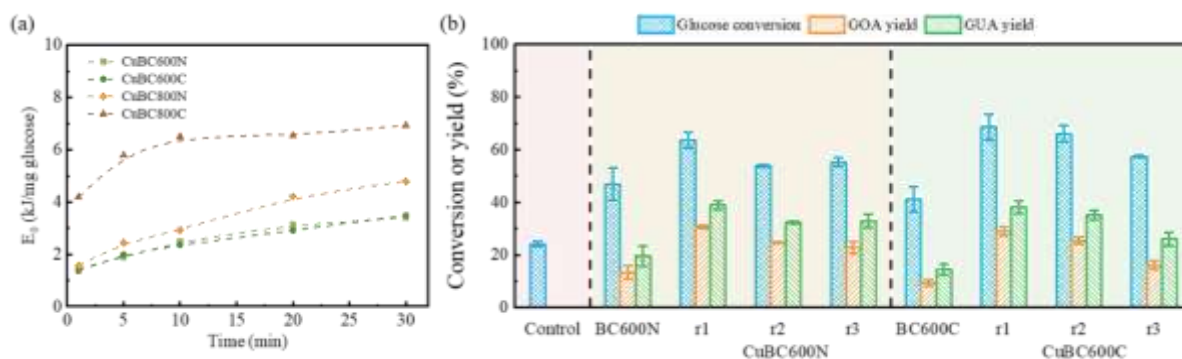


Figure 1. (a) Energy consumption of Cu biochar catalytic systems during glucose oxidation reaction, and (b) Recyclability and stability of CuBC600N and CuBC600C: glucose conversion and GOA and GUA yield in 3 runs (control: reaction without catalyst; reaction conditions: 200 mg glucose, 50 mg biochar, and 1 equiv. H<sub>2</sub>O<sub>2</sub> in 10 mL DI water; 160 °C, 20 min).

### Acknowledgements

This study was financially supported by the Hong Kong Research Grants Council [PolyU 15222020] and Hong Kong International Airport Environmental Fund [Phase 2].

### References

1. H. A. Alhashimi and C. B. Aktas, *Resources, Conservation and Recycling*, **118** 13 (2017).
2. Q. Zhang, Z. Wan, I. K. M. Yu and D. C. W. Tsang, *Journal of Cleaner Production*, **312** 127745 (2021).

## Alternative technologies for the selective conversion of bio-based feedstocks to specialty chemicals

François Jérôme,<sup>1\*</sup> Karine De Oliveira Vigier,<sup>1</sup> Prince N. Amaniampong<sup>1</sup>

<sup>1</sup>University of Poitiers, CNRS, Institut de Chimie des Milieux et Matériaux de Poitiers, 1 rue Marcel Doré, 86073 Poitiers, FRANCE

\*e-mail francois.jerome@univ-poitiers.fr

With the growing concerns of our society about climate change, a strong political impulsion has been given to the defossilization of our industry. In this context, the production of chemicals from biomass waste has become of particular interest. A very important part of the academic and industrial work, during the last 25 years, has focused on the transformation of biobased building blocks (monosaccharides, fatty acids, glycerol ...) to existing bulk chemicals. This approach has the advantage of not disrupting the downstream processes, but it is in conflict with the low cost of fossil-based processes, which often makes these biobased products economically uncompetitive for the end users. A more recent and original approach consists in taking advantage of the chemical functionality and diversity present in biomass to access biobased chemicals with new properties and thus improved performances as compared to existing fossil-based chemicals. Despite of interest, this promising approach requires chemists to revisit catalytic reactions.

Biomass waste is mainly composed of sugars. In the context of chemicals manufacturing, the activation and conversion of sugars at low temperatures is mandatory. Indeed, at temperatures higher than 100°C, sugars are readily degraded in an uncontrolled way, thus lowering the selectivity and reactor productivity but also rapidly deactivating catalysts. Being able to convert (selectively) concentrated feed of biomass to a targeted chemical is a challenging and difficult scientific task that will be partly addressed in this lecture.

First, we will focus on the synthesis of relevant renewable aromatics from bio-based furfural derivatives and cheap alkenes, through a Diels-Alder/aromatization sequence.<sup>1</sup> The prediction and the control of the ortho : meta selectivity in the Diels-Alder step was achieved through a combined experimental-theoretical approach. In particular, we will show that the ortho : meta selectivity at the reaction equilibrium stems from a subtle interplay between charge interactions, favoring the ortho products, and steric interactions, favoring the meta isomers.

In a second part, we will show that the massive electrification of our society now opens new rooms for the development of alternatives technologies, in particular to access biobased chemicals that are hardly obtainable with traditional routes. We will illustrate it through the synthesis of biosurfactants directly from recalcitrant cellulosic biomass.<sup>2</sup> The proposed process, named mechanocatalysis and firstly introduced by Blair and Rinaldi, is based on a synergistic effect between an acid catalyst and mechanical forces. The impact of water and minerals present in biomass on the mechanocatalytic process efficiency will be discussed as well as a life cycle assessment to shed light on the contribution of this technology as compared to the current industrial process. Turning now to reactions in water, an essential solvent for biomass, we will highlight the contribution of ultrasound for the catalyst free biomass processing. We will show that high frequency ultrasound is capable of generating •OH radicals (homolytic dissociation of water inside cavitation bubbles), and thus to initiate chemical reactions at a nearly room temperature with sugars. Transposition of this technology for the activation and conversion of NH<sub>3</sub> (future H<sub>2</sub> carrier) will be also discussed, particularly for the metal free hydrogenation of biobased alkenes in water.<sup>3</sup>

### Acknowledgements

Frederic Guegan, Rapahel Wischert, Ivan Scodeller, Anaëlle Humblot, Ayman Karam, SOLVAY, ARD, the CNRS, the University of Poitiers and the region Nouvelle-Aquitaine are strongly acknowledged for their financial supports and, more importantly, for very fruitful scientific discussions.

### References

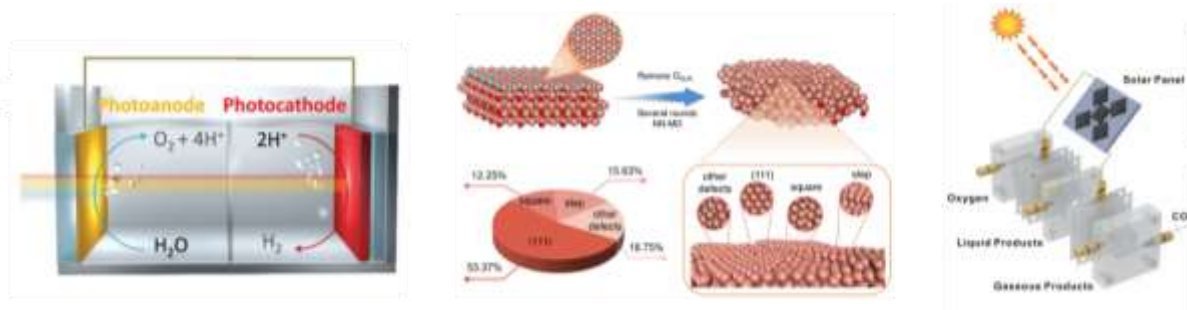
1. a) I. Scodeller, S. Mansouri, D. Morvan, E. Muller, K. de Oliveira Vigier, R. Wischert, F. Jérôme, *Angew. Chem. Int. Ed.*, **57** (33), 10510-10514 (2018) ; b) I. Scodeller, K. De Oliveira Vigier, E. Muller, C. Ma, F. Guégan, R. Wischert, F. Jérôme, *ChemSusChem*, **14** (1), 313-323 (2021).
2. A. Karam, K. De Oliveira Vigier, S. Marinkovic, B. Estrine, C. Oldani, F. Jérôme, *ChemSusChem*, **10** (18), 3604–3610 (2017).
3. A. Humblot, L. Grimaud, A. Allavena, P. N. Amaniampong, K. De Oliveira Vigier, T. Chave, S. Streiff, F. Jérôme, *Angew. Chem. Int. Ed.*, **60** (48), 25230-25234 (2021).

## Solar Fuels: from Mechanistic Understanding to Device Engineering

Jinlong Gong

School of Chemical Engineering and Technology, Tianjin University, Tianjin 300072, China  
Key Laboratory for Green Chemical Technology of Ministry of Education, Tianjin University, Tianjin 300072, China.  
Collaborative Innovation Center of Chemical Science and Engineering (Tianjin), Tianjin 300072, China.  
E-mail: jlgong@tju.edu.cn

Utilizing solar energy and achieving artificial photosynthesis are vital process to building a sustainable society and an effective way to achieve the goal of carbon neutrality. This report presents our research progress in the construction of bias-free water splitting systems and the optimization of CO<sub>2</sub> reduction systems. We have proposed a strategy to spatially decouple the light absorption site from the surface reaction site and developed a method to regulate the bending degree of the energy band, thus constructing an efficient charier transport channel to achieve efficient conversion of solar energy to hydrogen energy. In addition, we have combined theoretical calculations and in-situ spectroscopic techniques to clarify the relationship between active site structures and CO<sub>2</sub> conversion pathways, leading to the development of a series of site-controlled construction methods. By introducing the basic roles of hydrodynamics into the design of reaction systems, we have elucidated the matching principle between solar energy and electrolyzer power. Through modulating the temperature, velocity and concentration fields in the CO<sub>2</sub> reduction system, we have initially achieved the stable production of multi-carbon products under scaling-up conditions.



### References:

- [1] Phil De Luna, Christopher Hahn, Edward H. Sargent et al., *Science*, 2019, 364, eaav3506
- [2] Jin Hyun Kim, Dharmesh Hansora, Pankaj Sharma et al., *Chem. Soc. Rev.* 2019, 48, 1908
- [3] B Liu, S.-J Wang, S.-J Feng, et al. *Adv. Funct. Mater.*, 2020, 2007222
- [4] S.-J Feng, T Wang, B Liu, et al. *Angew. Chem. Int. Ed.* 2020, 59, 2044
- [5] X.-X Chang, T Wang, Z.-J Zhao, et al., *Angew. Chem. Int. Ed.* 2018, 57, 15415
- [6] Z. Q. Chen, T Wang, B Liu, et al., *J. Am. Chem. Soc.* 2020, 142, 6878
- [7] D. F. Cheng, Z. J. Zhao, J. L. Gong, et al., *Nature Commun.* 2021,12,395
- [8] D. Z. Zhong, Z. J. Zhao, J. L. Gong, et al., *Angew. Chem. Int. Ed.*, 2021,60,4879

## The quest to a circular approach to (furanic) polymers

Andreia F. Sousa<sup>1,2\*</sup>

<sup>1</sup>CICECO – Aveiro Institute of Materials University of Aveiro, 3810-193 Aveiro, Portugal

<sup>2</sup>Centre for Mechanical Engineering, Materials and Processes, Department of Chemical Engineering, University of Coimbra  
Rua Silvio Lima – Polo II, 3030-790 Coimbra, Portugal

\*e-mail: [andreiafs@ua.pt](mailto:andreiafs@ua.pt)

Polymeric materials, commonly known as plastics, are ubiquitous in our daily lives. They can be used in making simple household objects as food packages and on more sophisticated materials among biomedicine or electronics. Despite their exceptional properties (e.g., lightweight, durability, and versatility), they are predominantly synthesised from fossil resources, they are overused, and, moreover, they commonly have a non-circular fate after use, hence, raising severe pollution and climate changes issues [1]. In this context, Sousa team started a burgeoning surge for more sustainable approaches to polymers, both in terms of their origin [2–5] and fate via chemical recycling [6].

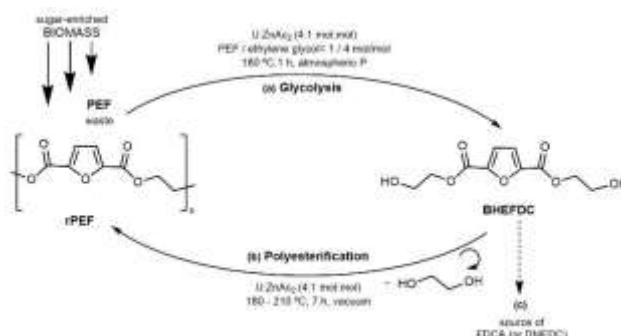


Figure 1. PEF continuous circular recycling method by using a small amount of U : ZnAc<sub>2</sub>, as DES, and mild conditions to catalyse glycolysis (a) and polyesterification (b) reactions [6], reproduced by permission of The Royal Society of Chemistry.

Noteworthy, the basilar work on poly(ethylene 2,5-furandicarboxylate) (PEF) by Sousa [7] relies primarily in the renewable origin of PEF monomers, 2,5-furandicarboxylic acid (typically obtained from C5 or C6 sugars) and ethyleneglycol. To the best of our knowledge, Sousa team, disclosed for the first time the potential of urea : zinc acetate deep eutectic solvent (DES) to assist the continuous, eco-friendly and closed-loop approach for recycling PEF directly into its starting repolymerized polymer (rPEF), without the need of intermediate steps of isolation and purification of monomers and using mild conditions (Fig. 1). Further studies with (furanic) polyesters evidenced even more the suitability, greenness and straightforward of this continuous recycling approach. The whole-value chain of furans has attracted EU funding through the COST Action FUR4Sustain (CA18220).

### Acknowledgements

This work was developed within the scope of CICECO-Aveiro Institute of Materials (UIDB/50011/2020 & UIDP/50011/2020) & LA/P/0006/2020, financed by national funds through the FCT– Fundação para a Ciência e a Tecnologia/MEC (PIDDAC). This research is also sponsored by FEDER funds through the program COMPETE—Programa Operacional Factores de Competitividade—and by national funds through FCT under the project UID/EMS/00285/2020. FCT is also acknowledged for the research contract under Scientific Employment Stimulus to AFS (CEECIND/02322/2020). This work is also supported by COST Action FUR4Sustain- European network of FURan based chemicals and materials FOR a Sustainable development, CA18220, supported by COST (European Cooperation in Science and Technology).

### References

1. C.N. Hamelinck, A.P.C. Faaij, H. Den Uil, H. Boerrigter, *Energy*, **29** 1743 (2004).
2. R. Ash, R. M. Barrer, C.G. Pope, *Proc. R. Soc. London, Ser. A*, **271** 19 (1963).
- [1] A.F. Sousa, A.J.D. Silvestre, *Plastics from renewable sources as green and sustainable alternatives*, *Curr Opin Green Sustain Chem.* **33** (2022) 100557. doi:10.1016/j.cogsc.2021.100557.
- [2] S. Zaidi, M.J. Soares, A. Bougarech, S. Thiagarajan, N. Guigo, S. Abid, M. Abid, A.J.D. Silvestre, A. F. Sousa, *Unravelling the para- and ortho-benzene substituent effect on the glass transition of renewable wholly (hetero-)aromatic polyesters bearing 2,5-furandicarboxylic moieties*, *Eur Polym J.* **150** (2021) 110413. doi:10.1016/j.eurpolymj.2021.110413.
- [3] M. Matos, A.F. Sousa, P.V. Mendonça, A.J.D. Silvestre, *Co-polymers based on Poly(1,4-butylene 2,5-furandicarboxylate) and Poly(propylene oxide) with tuneable thermal properties: Synthesis and*

- characterization, *Materials*. 12 (2019). doi:10.3390/ma12020328.
- [4] M. Matos, A.F. Sousa, A.C. Fonseca, C.S.R. Freire, J.F.J. Coelho, A.J.D. Silvestre, A new generation of furanic copolyesters with enhanced degradability: Poly(ethylene 2,5-furandicarboxylate)-co-poly(lactic acid) copolyesters, *Macromol Chem Phys*. 215 (2014) 2175–2184. doi:10.1002/macp.201400175.
- [5] A.F. Sousa, N. Guigo, M. Pozycka, M. Delgado, J. Soares, P. V. Mendonça, J.F.J. Coelho, N. Sbirrazzuoli, A.J.D. Silvestre, Tailored design of renewable copolymers based on poly(1,4-butylene 2,5-furandicarboxylate) and poly(ethylene glycol) with refined thermal properties, *Polym Chem*. 9 (2018) 722–731. doi:10.1039/c7py01627a.
- [6] B. Agostinho, A. Silvestre, A.F. Sousa, From PEF to rPEF: Disclosing the potential of deep eutectic solvents in biobased polyesters continuous de-/re-polymerization recycling, *Green Chem.* (2022) in press. doi:10.1039/D2GC00074A.
- [7] A. Gandini, A.J.D. Silvestre, C.P. Neto, A.F. Sousa, M. Gomes, The furan counterpart of poly(ethylene terephthalate): An alternative material based on renewable resources, *J Polym Sci Pol Chem*. 47 (2009) 295–298. doi:10.1002/pola.23130.

## **Biocatalytic solutions for industrial waste glycerol valorization**

Magdalena Ripoll<sup>1,2</sup> and Lorena Betancor<sup>1\*</sup>

<sup>1</sup>*Department of Biotechnology, Universidad ORT Uruguay, Mercedes 1237, 11100 Montevideo, Uruguay*

<sup>2</sup>*Graduate Program in Chemistry, Facultad de Química, Universidad de la República, Av. Gral. Flores 2124, 11800 Montevideo, Uruguay*

*\*betancor@ort.edu.uy*

Arguably, the last 10 years have represented the era in which biocatalysis has been best regarded as a tool to serve the needs of green processes. Endorsed by an ever-increasing number of biocatalytic processes applied in the industry, and the surge of innovative technologies for new or improved biocatalysts, there is an intense focus in the field to address less green or impractical processes. Although advancements in line with more sustainable biocatalytic processes have been significant in the last years, many challenges remain in the design and engineering of biotransformations for effective translational biotechnology sustainable solutions. Innovative tools and strategies to overcome biocatalysts limitations are key to enabling intensified processes with substantial improvements in terms of cost, environmental footprint, processing volume and overall safety of the process, compared to purely chemical alternatives.

Crude glycerol is the main by-product of the biodiesel industry, generated in a 10:1 ratio. It is heavily contaminated, reaching maximum purity levels of 60-80%. Due to its large supply and low demand, crude glycerol has an inferior market value. In turn, obtaining pure glycerol from this residue for use in the chemical or food industries (> 99%) is very expensive. Moreover, due to market fluctuations, glycerol prices frequently drop dramatically, forcing companies to take extreme actions such as disposal via incineration generating contamination issues. This presentation will summarize efforts made by our group to intensify the crude glycerol microbial biotransformation into dihydroxyacetone, glyceric acid and serinol, all valuable compounds obtained from this feedstock. Attention to many aspects of process improvement to increase productivity and stability of the biocatalysts has been addressed, including tools and strategies such as biocatalysts immobilization, media simplification, volume reduction and coupling of other biocatalysts for the implementation of biosynthetic cascades.

### **Acknowledgements**

This work was funded by Agencia Nacional de Investigación e Innovación (ANII), Uruguay (POS\_NAC\_2019\_1\_158182, FMV\_1\_2021\_1\_167184), Programa de Desarrollo de Ciencia Básicas (PEDECIBA) and Universidad ORT Uruguay.

## Green Analytical Chemistry and Circularity: towards more sustainable processes, materials and outcomes

Vânia G. Zuin Zeidler<sup>1-3</sup> (Prof. Dr. Dr.)

<sup>1</sup> Institute of Sustainable Chemistry, Leuphana University Lüneburg, Universitätsallee 1, 21335, Lüneburg, Germany.

<sup>2</sup> Green Chemistry Centre of Excellence, University of York, Heslington, York, YO10 5DD, UK.

<sup>3</sup> Department of Chemistry, Federal University of São Carlos, Rod. Washington Luís (SP-310), Km 235, 13565-905, São Carlos, SP, Brazil.

\*vania.zuin@leuphana.de

Green analytical chemistry can be understood as the design and use of analytical methods that provide qualitative and quantitative chemical information in a safe socio-environmental manner, with adequate accuracy and precision to prevent, identify and solve problems in complex contexts or systems (for instance, of environmental, medical, pharmaceutical or agro-industrial origin) [1]. Sample preparation has been identified as one of the main steps negatively impacting both the analytical performance and greenness of the methods, which usually entails using renewable resources, eliminating or reducing chemicals, minimising energy consumption, as well as analytical waste. Currently, the generation of more sustainable processes and materials – including analytical information – requires that green analytical chemistry should be adapted to the circular economy. Thus, aiming at discussing what can and should be circulated and what can and should not be from a chemical point of view [2,3], some selected cases based on greener and more sustainable methods to obtain bioactive organic compounds from agro-industrial waste will be presented, emphasising the fundamental role of sustainable separation.

### Acknowledgements

The author is grateful to the São Paulo Research Foundation (Fapesp-Brazil, 2017/05712-0) and to the organisers of the 9<sup>th</sup> ICGC for their support.

### References

1. V.G Zuin *et al.*, *Pure and Applied Chemistry* **93**, 13 (2021).
2. K. Kümmerer, J.H. Clark, V.G. Zuin, *Science* **367** 369 (2020).
3. V.G. Zuin, L.Z. Ramin, *Topics in Current Chemistry* **376** 3 (2018).

## Green chemistry and computational chemistry: a wealth of promising synergies

Liliana Mammino\*

\*University of Venda, University Road, Thohoyandou 0950, South Africa

\*sasdestria@yahoo.com

The green chemistry principles [1] envisage the design of substances and production processes that are benign for human health and the environment, where ‘benign’ refers to the entire life of a substance, from production through usage and to final disposal. The design of new substances entails the design of new molecules, and the design of more benign processes may entail the design of other substances (besides reactants and products) facilitating the process’ ‘greenness’, from catalysts to green solvents. Computational chemistry is the area of chemistry that has made molecular design rational by being able to predict the properties of not-yet-synthesized molecules, what enables the selection of the promising ones for synthesis and experimental testing, with enormous cost-savings. Synergies between the two areas would appear a natural outcome. On the other hand, their extent remains below their actual potentialities. The presentation proposes to underline the variety of possible synergies and the benefits of each of them, within a perspective considering that ‘knowing about each other’ is the main key to make new interchanges possible. It is also considered that it is important to pursue the ‘knowing about each other’ objective both at the educational level, in the preparation of chemistry experts, and at the professional level, to facilitate the recognition of the synergies that can be useful for specific purposes.

The presentation integrates information from extensive literature review, interactions with specialists in both areas, and the presenter’s direct experience with computational chemistry, green chemistry education, and attempts to explore synergies’ themes and routes [2]. It highlights the importance of fostering cross-disciplinary attitudes at education level and facilitating them within chemistry practices. Already-tested and new potential educational approaches are outlined. The consideration of research-and-practice concrete cases includes examples of themes that are currently focuses of great attention in each of the two areas (e.g., the interest in the action of catalysts) and outlines the advantages that can derive from interchanges of information about needs, approaches and results. The possible roles of typical computational chemistry focuses (such as the study of interactions between molecules, and several others) within green chemistry research are also explored.

Overall, the presentation aims at furthering cross-area interchanges by enlarging the scope for knowing what to “talk to each other” about. This objective is pursued through the selection of expectedly-interesting information and through the ways in which it is presented (which, among other features, do not assume any prior computational chemistry knowledge). The content considers the molecular design requirements directly associated with each of the green chemistry principles, as well as those associated with their implications, both for the production stage and for predictions of significant aspects concerning the useful life of produced substances and their ultimate fate.

The expected take-home messages comprise: increased awareness of the importance and benefits of synergies between the two areas; increased acquaintance with approaches to foster students’ familiarization with the possible synergies (including the confidence inherently deriving from the consideration of concrete illustrative examples); and sufficient information to serve as background reference in the identification of the cross-area themes that could be more constructive for each individual ongoing or planned research.

### References

1. P.T. Anastas, J.C. Warner, *Green Chemistry: Theory and Practice*. New York: Oxford University Press, (1998).
2. L. Mammino, *Green Chemistry and Computational Chemistry: Shared Lessons in Sustainability*. Amsterdam: Elsevier (2021).



# Oral presentations

## Alternative & benign chemical processes

# Organic Synthetic Photochemistry: Embracing the Needs of Green and Sustainable Chemistry

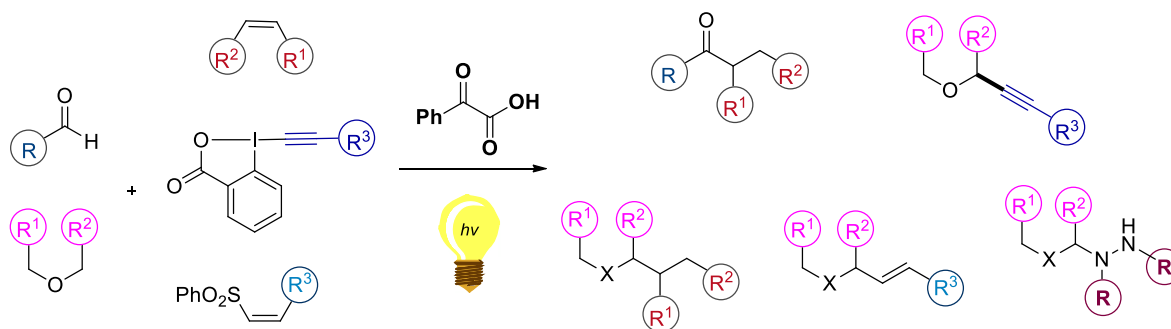
Christoforos G. Kokotos<sup>1\*</sup>

<sup>1</sup>Laboratory of Organic Chemistry, Department of Chemistry, National and Kapodistrian University of Athens, Panepistimiopolis 15771, Athens, Greece  
ckokotos@chem.uoa.gr

The introduction of novel reactivities and new platforms of activation is the ultimate goal in Organic Synthesis. During the last years, Chemistry is continuously seeking new ways to embrace the principles of Green and Sustainable Chemistry. Photochemistry, the use of light to promote organic transformations, is a concept that provides access to alternative activation modes, compared to polar chemistry, and is fully in line with Green Chemistry. In recent years, photoredox catalysis has become a powerful strategy for the activation of small molecules. Photoorganocatalysis, the use of small organic molecules as photocatalysts, is a low-cost and environmentally friendly alternative, which further increases the sustainability options of photochemistry.

Very recently, our group introduced in literature a photochemical protocol that is easy to operate employing cheap household lamps as the source of irradiation and phenylglyoxylic acid as the photoinitiator. Along these lines, very recently, we introduced a sustainable and photochemical protocol for the hydroacylation reaction of unactivated olefins,[1] the C-H functionalization of heterocycles [2-4] and the synthesis of disulfides from sulfides.[5]

## PhCOCOOH: A powerful Photoinitiator



■ Mild, Metal-Free and Photochemical reaction conditions ■ Cheap, easy to execute, simple ■ Environmentally friendly

## Acknowledgements

The author gratefully acknowledges the School of Sciences and the Special Account for Research Grants of the National and Kapodistrian University of Athens for financial support for the participation in this conference.

## References

1. E. Voutyritsa, C. G. Kokotos, *Angew. Chem. Int. Ed.* **59**, 1735, (2020).
2. E. Voutyritsa, M. Garreau, M. G. Kokotou, I. Triandafillidi, J. Waser, C. G. Kokotos, *Chem. Eur. J.* **26**, 14453, (2020).
3. G. N. Papadopoulos, M. G. Kokotou, N. Spiliopoulou, N. F. Nikitas, E. Voutyritsa, D. I. Tzaras, N. Kaplaneris, C. G. Kokotos, *ChemSusChem* **13**, 5934, (2020).
4. N. Spiliopoulou, P. L. Gkizis, I. Triandafillidi, N. F. Nikitas, C. S. Batsika, A. Bisticha, C. G. Kokotos, *Chem. Eur. J.* **28**, e202200023, (2022).
5. N. Spiliopoulou, C. G. Kokotos, *Green Chem.* **23**, 546, (2021).

# Photocatalytic cleavage of lignin C–C bonds by Z-scheme nanocomposite

Xuejiao Wu,<sup>1</sup> Shunji Xie,<sup>2</sup> Ye Wang<sup>2</sup> and Bert F. Sels<sup>1\*</sup>

<sup>1</sup>Center for Sustainable Catalysis and Engineering, Faculty of Bioscience Engineering, KU Leuven, Heverlee 3001, Belgium.

<sup>2</sup>State Key Laboratory of Physical Chemistry of Solid Surfaces, Collaborative Innovation Center of Chemistry for Energy Materials, National Engineering Laboratory for Green Chemical Productions of Alcohols, Ethers and Esters, College of Chemistry and Chemical Engineering, Xiamen University, Xiamen 361005, China.

\*bert.sels@kuleuven.be

*Selective cleavage of recalcitrant C–C linkages in lignin, the largest aromatic feedstock in nature, represents a highly attractive but challenging approach to providing added-value aromatics. Photocatalysis can generate reactive intermediates under mild conditions, and thus is a potential tool for lignin C–C bond cleavage. Here, we demonstrate an effective photocatalytic system based on Z-scheme nanocomposite that can break C–C bonds in lignin model compounds at room temperature under simulated solar light irradiation. Our mechanistic study has shown that the primary pathway for C–C bond cleavage involves an electron-hole coupled photoredox process. The construction of the Z-scheme heterojunction structure endows the catalyst with strong reduction and oxidation capability, which is key for the electron-hole coupled C–C bond cleavage.*

## 1. Introduction

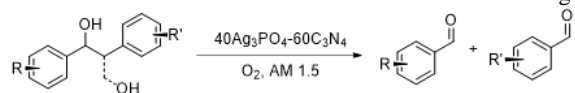
Lignin is a major component of lignocellulosic biomass and a natural aromatic biopolymer, and thus, it is the most abundant source of renewable aromatics.<sup>1</sup> Through selective breakage of lignin C–O, C–C bonds, added-value aromatic compounds can be obtained.<sup>1,2</sup> Great efforts have been devoted to the study of lignin C–O bond cleavage in past decades and considerable success has been achieved.<sup>1-3</sup> In contrast, only a few research progress has been made in the selective cleavage of lignin C–C bonds. The cleavage of recalcitrant C–C bonds remains one of the key challenges for the valorization of lignin. Current studies on lignin C–C bond cleavage are mainly focused on thermocatalysis under relatively severe reaction conditions.<sup>4</sup> The conventional methods not only limit the activity but also lead to low product selectivity. Moreover, additional additives such as expensive oxidants or bases are needed in most cases.<sup>4</sup> Photocatalysis, which utilizes solar energy to drive chemical reactions as nature does for photosynthesis, is a promising method to challenge highly difficult reactions by conventional thermocatalytic approaches.<sup>5,6</sup> However, as a newly emerging and challenging topic, only a few reports have succeeded in breaking lignin C–C bonds by photocatalysis. Moreover, the current understanding of the reaction mechanisms and the knowledge about the photocatalyst structure-performance relation are very limited. It would be highly desirable to develop efficient photocatalytic systems and systematically investigate the key to effective catalysts for the cleavage of lignin C–C bonds.

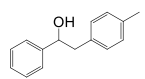
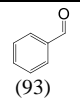
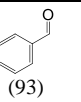
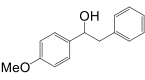
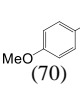
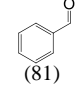
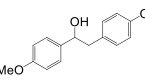
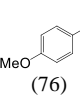
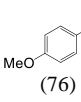
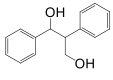
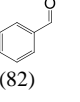
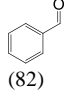
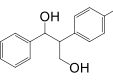
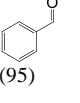
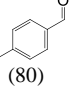
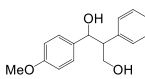
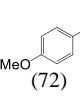
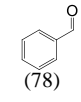
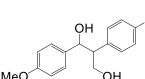
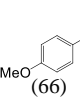
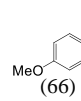
## 2. Results and discussion

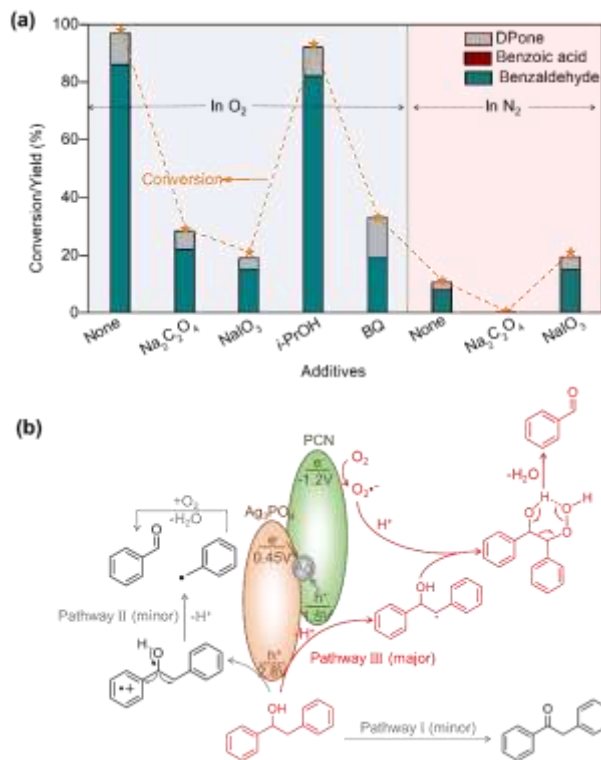
We examined photocatalytic performances of some typical semiconductors including BiVO<sub>4</sub>, Cu<sub>2</sub>O, CeO<sub>2</sub>, BiOCl, BiOI, CdS, and PCN for the conversion of 1,2-diphenylethanol (DPol), a lignin β-1 model compound, at room temperature. Limited activities with conversion lower than 5% were observed for most catalysts. Interestingly, PCN is very unique in catalyzing the cleavage of the C<sub>α</sub>–C<sub>β</sub> bond in DPol, benzaldehyde is the major product with a high selectivity of 68% and yield of 15% after 6 hours under simulated solar light irradiation. To increase the photocatalytic performance of PCN, we have synthesized a series of Ag<sub>3</sub>PO<sub>4</sub>–PCN heterojunction nanocomposites. Among these nanocomposites, 40Ag<sub>3</sub>PO<sub>4</sub>–60PCN (40wt% Ag<sub>3</sub>PO<sub>4</sub>–60wt% PCN) showed the highest benzaldehyde yield, reaching 86%, which was about 5.7 times higher than that of PCN. 40Ag<sub>3</sub>PO<sub>4</sub>–60PCN nanocomposites were powerful catalysts for photocatalytic cleavage of lignin C<sub>α</sub>–C<sub>β</sub> bonds. Aromatic aldehydes

with high yield of 66%–95% were obtained from the conversion of various β-1 lignin model compounds (Table 1).

Characterizations of the catalysts led to structural details of the Z-scheme within Ag<sub>3</sub>PO<sub>4</sub>–PCN composites. Control experiments with different atmospheres, *i.e.*, O<sub>2</sub> and N<sub>2</sub>, and additives, *i.e.*, Na<sub>2</sub>C<sub>2</sub>O<sub>4</sub> as a hole scavenger, NaIO<sub>3</sub> as an electron scavenger, *i*-PrOH as a hydroxyl radical scavenger, and BQ (p-benzoquinone) as a superoxide radical scavenger, were performed (Figure 2a). These control experiments have revealed three reaction pathways for the conversion of DPol (Figure 2b). The relation between the energy band structure and the reaction mechanisms was studied and clarified. The primary pathway involves an electron-hole coupled photoredox process (Figure 2b, pathway III), which requires both holes and electrons with strong oxidation and reduction ability, respectively. The Z-scheme structure allows the Ag<sub>3</sub>PO<sub>4</sub>–PCN catalyst to have strong redox capacity and this is essential to the electron-hole coupled C–C bond cleavage.

**Table 1.** Products from photocatalytic conversions of  $\beta$ -1 lignin models.


Substrate	t (h)	Conv.	Yield (%)	
	6	99	 (93)	 (93)
	6	99	 (70)	 (81)
	6	99	 (76)	 (76)
	6	99	 (82)	 (82)
	10	97	 (95)	 (80)
	10	99	 (72)	 (78)
	12	98	 (66)	 (66)

**Figure 1.** Mechanistic study. (a) Control experiments. (b) Proposed reaction pathways.

## Acknowledgments

This work was supported by the postdoctoral mandate from KU Leuven (PDM/20/117) and Research Foundation-Flanders (FWO post-doctoral fellowship: 12S1822N).

## References

1. W. Schutyser, T. Renders, S. Van den Bosch, S. F. Koelewijn, G. T. Beckham, B. F. Sels, *Chem. Soc. Rev.*, **47** 852 (2018).
2. M. M. Abu-Omar, K. Barta, G. T. Beckham, J. Luterbacher, J. Ralph, R. Rinaldi, Y. Roman-Leshkov, J. Samec, B. F. Sels, F. Wang, *Energy Environ. Sci.*, **14** 262 (2021).
3. X. Wu, X. Fan, S. Xie, J. Lin, J. Cheng, Q. Zhang, L. Chen, Y. Wang, *Nat. Catal.*, **1** 772 (2018).
4. C. Li, X. Zhao, A. Wang, G. W. Huber, T. Zhang, *Chem. Rev.*, **115** 11559 (2015).
5. X. Wu, N. Luo, S. Xie, H. Zhang, Q. Zhang, F. Wang, Y. Wang, *Chem. Soc. Rev.*, **49** 6198 (2020).
6. X. Wu, S. Xie, H. Zhang, Q. Zhang, B. F. Sels, Y. Wang, *Adv. Mater.*, **33** 2007129 (2021).

## Reduction of alkenes to alkanes by ammonia under high frequency ultrasound

Anaëlle Humblot\*<sup>1</sup> and François Jérôme<sup>1</sup>

<sup>1</sup>Institut de Chimie des Milieux et Matériaux de Poitiers, University of Poitiers-CNRS, 1 rue Marcel Doré, TSA 41105, 86073 Poitiers, France.

\*anaelle.humblot@univ-poitiers.fr

When a liquid is subjected to an ultrasonic irradiation at a high frequency, cavitation bubbles are formed. Inside the cavitation bubbles, extreme conditions of temperature and pressure are reached. As a result, gaseous molecules diffusing inside cavitation bubbles are instantaneously pyrolysed, leading to the formation of radicals. At the bubble collapse time, these radicals are propelled into the solution where they can be recombined or react with other compounds in the solution to initiate chemical reactions.

In a previous work, we demonstrated the possibility to use high frequency ultrasound for the activation of ammonia and its subsequent conversion to hydrazine.<sup>[1]</sup> Here, we extended this concept for the reduction of alkenes, which is usually performed by hydrogenation with gaseous hydrogen in the presence of a catalytic amount of transition metal catalyst. We demonstrated that under high frequency ultrasound, it is possible to use ammonia as a source of hydrogen for the reduction of olefins in water, through the formation of diimide  $N_2H_2$ .

A typical experiment was performed using a 5 wt% aqueous solution of ammonia containing a non-activated alkene (1-octene for model reactions) supported on activated charcoal. The solution was subjected to an ultrasonic irradiation at 525 kHz in a high frequency ultrasound reactor. The solution was maintained at 30 °C. The reduction of 1-octene to n-octane was monitored by GC-FID. Under these conditions, the hydrogenation reaction occurred, and n-octane was formed in 52% yield after 6 hours of sonication. The n-octane yield was increased up to 87% after 28 hours of reaction. (Figure 1) In the same system but with gaseous  $H_2$  bubbled in water instead of an ammonia solution, less than 5% of 1-octene was reduced. This is partly due to the low solubility of hydrogen in water, which makes it less available for the hydrogenation reaction. This demonstrates that ammonia can be used as a hydrogen source for an efficient hydrogenation of alkenes in these conditions.

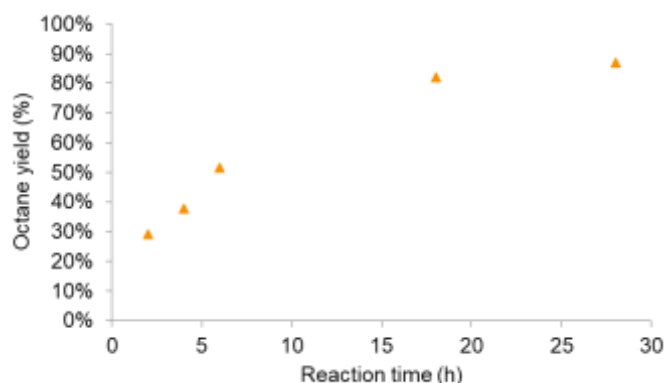


Figure 1. Kinetics of 1-octene reduction with ammonia

To maximize the yield of the hydrogenation reaction in this system, the influence of different parameters was studied: the amount of ammonia, the charge of the alkene on the activated charcoal and the amount of activated charcoal.

Then, the mechanism of the reaction was investigated. Two pathways are possible for the reduction of alkenes from ammonia under high frequency ultrasound:

1) according to our previous work, hydrazine  $N_2H_4$  is formed when aqueous ammonia is submitted to high frequency ultrasound, then hydrazine can be oxidized to diimide  $N_2H_2$  with molecular oxygen from air, and the formed diimide reduces the double bond and releases nitrogen;

2) the pyrolysis of ammonia inside the cavitation bubbles generates the formation of NH radicals, whose presence was confirmed by sonoluminescence analysis<sup>[2]</sup>. Then, NH radicals recombine directly to diimide which reduces the alkene. The second pathway was determined as the main mechanism. Indeed, when the reaction is performed under argon atmosphere, the hydrogenation of 1-octene occurs at the same rate, which indicates that no oxygen is needed to perform the reaction, and the oxidation of hydrazine to diimide is less likely to occur.

In this system, in the presence of activated charcoal as a support for olefins, the phenomenon of heterogeneous cavitation takes place: the cavitation bubbles produced under high frequency ultrasound are formed at the surface of the charcoal particles, grow and implode on the particles, propelling the radicals on the surface. NH radicals formed from the pyrolysis of ammonia in the cavitation bubbles recombine to form diimide  $N_2H_2$  which reduces the alkene on the surface of the activated charcoal particles. (Figure 2)

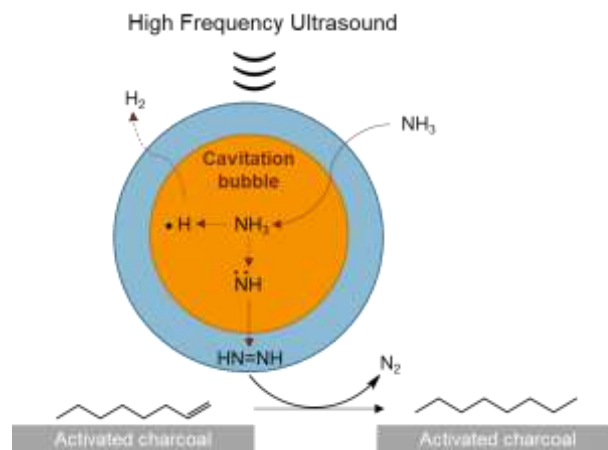


Figure 2. Proposed mechanism for 1-octene reduction with ammonia under high frequency ultrasound

This reduction of olefin using ammonia under high frequency ultrasound was extended to other unsaturated compounds to study the scope of the reaction. Interestingly, other primary or secondary alkenes and alkyne were also successfully reduced in this system.

The technology of high frequency ultrasound is of great interest for the reduction of olefins in water using ammonia, which is more difficult with molecular hydrogen due to its low solubility in aqueous solutions. It is possible thanks to the phenomenon of acoustic cavitation which enables the formation of a diimide that enables the hydrogenation of double or triple C-C bonds with nitrogen as only coproduct.

### Acknowledgements

Authors acknowledge the CNRS, the University of Poitiers and SOLVAY for their financial support.

### References

1. A. Humblot, L. Grimaud, A. Allavena, P. N. Amaniampong, K. De Oliveira Vigier, T. Chave, S. Streiff, F. Jérôme, *Angew. Chem. Int. Ed.*, **60** 25230 (2021).
2. R. Pflieger, T. Ouerhani, T. Belmonte, S. I. Nikitenko, *Phys. Chem. Chem. Phys.*, **19** 26272 (2017).

## A new concept for the sustainable coupling of catalysis processes: {2-phases 2-reactions 1-catalyst}<sup>†</sup>

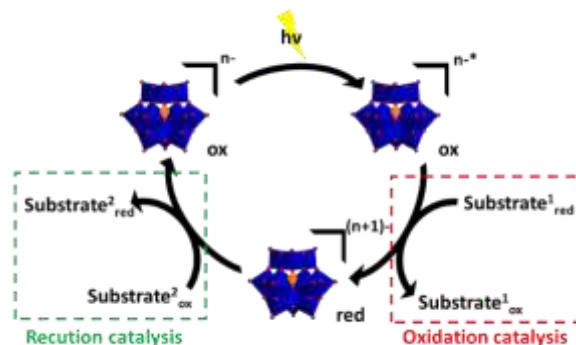
Philipp Schmid<sup>1\*</sup>, Olivier Diat<sup>2</sup>, Arno Pfitzner<sup>1</sup> and Pierre Bauduin<sup>2\*</sup>

<sup>1</sup>Institute of Inorganic Chemistry, University of Regensburg, Universitätsstraße 31, 93053 Regensburg, Germany

<sup>2</sup>ICSM, CEA, CNRS, ENSCM, Univ Montpellier, 34199 Marcoule, France

\*pierre.bauduin@cea.fr

Polyoxometalates (POMs) are anionic metal-oxo clusters of nanometric size, consist of condensed polyhedral transition metal-oxo (mainly V, Mo and W) units and often contain a heteroatom-oxo (*e.g.* B, Si, P, *etc.*) unit.<sup>[1]</sup> POMs are well-known catalysts in diverse processes, such as acid-catalysis and multifunctional catalysis up to photocatalysis, *cf.* scheme 1.<sup>[2,3]</sup> Due to its low energy cost and simplicity, especially photocatalysis has gained high attention recently.<sup>[4]</sup>



**Scheme 1.** Photocatalytic cycle of an  $\alpha$ -Keggin POM. By irradiating, the oxidized POM species is excited. This excited species catalyses an oxidation reaction, while being reduced. The reduced species catalyses a reduction consecutively, while the POM itself is re-oxidized, which closes the catalytic cycle.

Excitation of oxidized POMs is achieved with light between 200-500 nm, producing POMs in an excited state.<sup>[5]</sup> The excited POM can initiate the oxidation of a substrate (Substrate1<sub>red</sub> to Substrate1<sub>ox</sub>), by being reduced. This reduced species may catalyze a reduction reaction (Substrate2<sub>ox</sub> to Substrate2<sub>red</sub>), while the POM is re-oxidized closing the catalytic cycle.<sup>[6]</sup> A major drawback of such catalytic cycles is usually, that (re-)generation of the desired active catalyst species is achieved by a sacrificial reaction, *e.g.* generation of reduced POM species by oxidation of 2-propanol or reoxidation of the POM with O<sub>2</sub>/H<sub>2</sub>O<sub>2</sub>. This sacrificial procedure leads to complex mixtures in solution, *i.e.* catalyst, starting material, product, 2-propanol/acetone, H<sub>2</sub>O<sub>2</sub> and produces a large quantity of side-products.

Another remarkable property of low charge-density POMs, such as the  $\alpha$ -PW12O40<sup>3-</sup> (PW), is their strong association with (hydrated) polymers,<sup>[7]</sup> macrocyclic guest-molecules<sup>[8]</sup> and non-ionic surfactants<sup>[9,10]</sup> in aqueous solution. This binding phenomenon - called the (super-)chaotropic effect - was explained to arise from the partial dehydration of both, the POM and the interacting molecule.<sup>[11,12]</sup> Interestingly, PW turned out to be on the border between superchaotropic and hydrophobic anions.<sup>[13]</sup> Indeed, it was proposed that PW mainly distributes in the hydrophobic pseudo-phase of bicontinuous microemulsions.<sup>[14]</sup> This latter hydrophobic character of PW manifests in its self-assembling property in pure water, analogously to surfactants.<sup>[15,16]</sup>

We exploit here the photocatalytic property of PW to change its total charge, consequently its charge density and therefore its distribution in a biphasic water-hydrophobic alcohol (liquid-liquid) system. For this purpose, we monitored the distribution of POM with inductively coupled plasma-optical emission spectroscopy (ICP-OES) and followed the oxidation state of PW oxidation by 31P-nuclear magnetic resonance (31P-NMR). Reactions were followed by common analytical methods, such as ultraviolet-visible (UV-VIS) spectroscopy and 1H-NMR.

Figure 1a shows the distribution coefficient,  $\log(K_D)$  of POMs,  $\log(K_D^{POM}) = \log\left(\frac{c(POM)_{org.}}{c(POM)_{aq.}}\right)$ , as a function of the initial PW/SiW (in their acidic forms (H3PW12O40, HPW and H4SiW12O40, HSiW)) concentration,  $c_0$ , in the aqueous phase. The  $\log(K_D^{POM})$  is presented in a logarithmic scale, and therefore a negative  $\log(K_D^{POM})$  indicates the preferred distribution in the aqueous phase (below dark dashed line), while a positive  $\log(K_D^{POM})$  refers to the preferred distribution in the organic phase, here 1-Octanol (above dark dashed line). For  $c_0(HPW) \geq 5$  mmol L<sup>-1</sup>, HPW (threefold negatively charged POM) distributes mostly to the organic 1-Octanol phase, whereas HSiW (fourfold negatively charged POM) remains in the aqueous phase regardless of its concentration. The effect of UV-illumination (365 nm) on the distribution coefficient of HPW is shown in Fig. 1b for  $c_0(HPW) = 10$  mmol L<sup>-1</sup> with 1-Octanol as organic phase. Here, PW is reduced from PW12O40<sup>3-</sup> to PW12O40<sup>4-</sup>, while 1-Octanol is



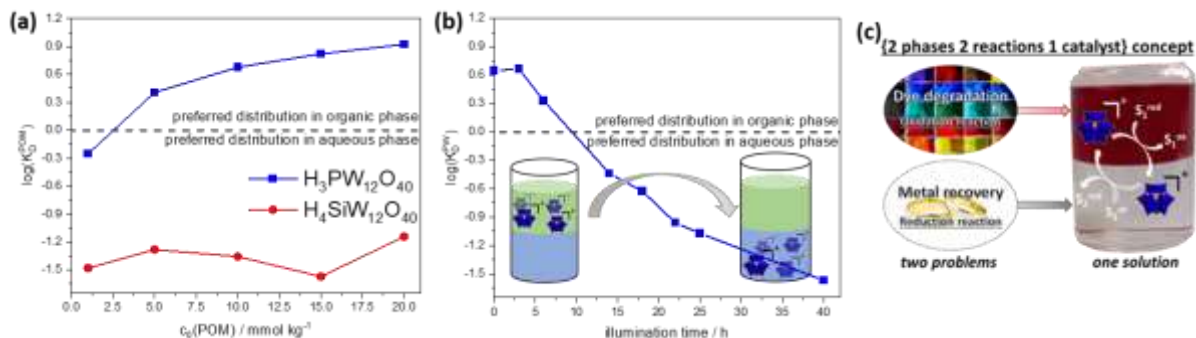


**Figure 2.** (a) Distribution of  $\text{H}_3\text{PW}_{12}\text{O}_{40}$  (HPW) and  $\text{H}_4\text{SiW}_{12}\text{O}_{40}$  (HSiW) between water and an 1-Octanol as an organic phase. (b) shows the evolution of  $10 \text{ mmol L}^{-1}$  HPW distribution in water/1-OctOH as a function of UV illumination ( $\lambda = 365 \text{ nm}$ ). Reoxidation of the reduced POM species is prohibited by excluding oxygen from the system. (c) Schematic representation of the {2-phases 2-reactions 1-catalyst} concept. Two different reactions, i.e. oxidation (dye degradation) and reduction (metal recovery), can be separated in two different phases. Both reactions are catalysed only by one catalyst which cycles between the two phases depending on its oxidation state. The concept can be applied to a vast number of reactions and catalysts.

oxidized as a counter reaction. In the starting system ( $t = 0 \text{ h}$ ) PW distributes mostly in the 1-OctOH phase ( $\log(K_D^{PW}) = 0.67$ , see Fig. 1a). After a period of 4 h, showing a constant  $\log(K_D^{PW})$ ,  $\log(K_D^{PW})$  decreases almost linearly down to -1.6 within 40 h. Therefore, PW is nearly fully transferred to the aqueous phase upon UV-illumination, driven by its transition from  $\text{PW}_{12}\text{O}_{40}^{3-}$  to  $\text{PW}_{12}\text{O}_{40}^{4-}$ , as confirmed by  $^{31}\text{P}$ -NMR. Now, we have a system that enables to separate oxidizing ( $\text{PW}_{12}\text{O}_{40}^{3-}$  in the organic phase) and reducing ( $\text{PW}_{12}\text{O}_{40}^{4-}$  in the aqueous phase) environments with only one catalyst. We can use this system to exemplify our {2-phases 2-reactions 1-catalyst} concept with different standard chemical reactions, such as the coupled oxidative degradation of dyes (organic phase) and reductive metal recovery (aqueous phase), which is schematically presented in Fig. 1c. Further useful coupled reactions are investigated within this study, such as classical oxidation of organic compounds (e.g. alcohol to aldehyde) and UV-light controlled metal-organic complexation reactions.

The {2-phases 2-reactions 1-catalyst} concept can be extended to diverse catalysts, while its challenge lies in the rational choice of a pair of solvents, which are immiscible and allow to separate to active forms of a catalyst. The main advantages of the concept are the (i) self-regeneration of the catalyst, (ii) economy of one reactor and (iii) economy of the non-sustainable production of large amounts of side-products.

## References

- [1] J. J. Borrás-Almenar, E. Coronado, A. Müller, M. Pope, *Polyoxometalate Molecular Science*, Springer, Netherlands, Dordrecht, The Netherlands, **2003**.
- [2] C. L. Hill, *Comprehensive Coordination Chemistry II: From Biology to Nanotechnology*, Elsevier, Oxford, **2004**.
- [3] C. Streb, *Dalt. Trans.* **2012**, *41*, 1651–1659.
- [4] L. Marzo, S. K. Pagire, O. Reiser, B. König, *Angew. Chemie - Int. Ed.* **2018**, *57*, 10034–10072.
- [5] E. Papaconstantinou, *Chem. Soc. Rev.* **1989**, *18*, 1–31.
- [6] C. Streb, K. Kastner, J. Tucher, *Phys. Sci. Rev. Rev.* **2019**, *4*, 1–10.
- [7] T. Buchecker, P. Schmid, I. Grillo, S. Prévost, M. Drechsler, O. Diat, A. Pfitzner, P. Bauduin, *J. Am. Chem. Soc.* **2019**, *141*, 6890–6899.
- [8] Y. Wu, R. Shi, Y. Wu, J. M. Holcroft, Z. Liu, M. Frascioni, M. R. Wasielewski, H. Li, J. F. Stoddart, *J. Am. Chem. Soc.* **2015**, *137*, 4111–4118.
- [9] T. Buchecker, P. Schmid, S. Renaudineau, O. Diat, A. Proust, A. Pfitzner, P. Bauduin, *Chem. Commun.* **2018**, *54*, 1833–1836.
- [10] M. Hohenschutz, I. Grillo, O. Diat, P. Bauduin, *Angew. Chemie - Int. Ed.* **2020**, *59*, 8084–8088.
- [11] B. Naskar, O. Diat, V. Nardello-Rataj, P. Bauduin, *J. Phys. Chem. C* **2015**, *119*, 20985–20992.
- [12] K. I. Assaf, M. S. Ural, F. Pan, T. Georgiev, S. Simova, K. Rissanen, D. Gabel, W. M. Nau, *Angew. Chemie - Int. Ed.* **2015**, *54*, 6852–6856.
- [13] K. I. Assaf, W. M. Nau, *Angew. Chemie - Int. Ed.* **2018**, *57*, 13968–13981.
- [14] P. Schmid, T. Buchecker, A. Khoshshima, D. Touraud, O. Diat, W. Kunz, A. Pfitzner, P. Bauduin, *J. Colloid Interface Sci.* **2021**, *587*, 347–357.
- [15] A. Chaumont, G. Wipff, *Phys. Chem. Chem. Phys.* **2008**, *10*, 6940–6953.
- [16] M. K. Bera, B. Qiao, S. Seifert, B. P. Burton-Pye, M. Olvera De La Cruz, M. R. Antonio, *J. Phys. Chem. C* **2016**, *120*, 1317–1327.

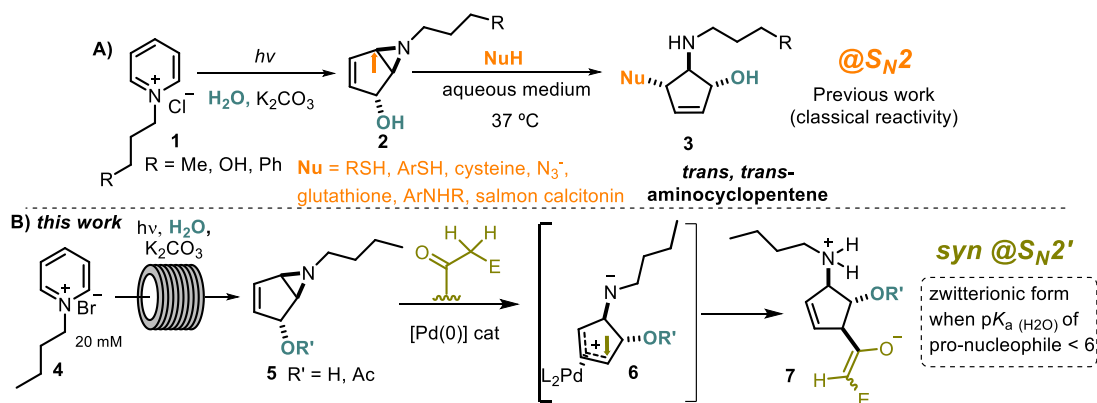
## Merging photoflow and Pd-catalysis to synthesized new aminocyclopentenes

João A. C. Oliveira,<sup>1,2</sup> Milene A. G. Fortunato,<sup>2</sup> Gredy Kiala,<sup>1,2</sup> Julie Oble,<sup>1</sup>  
Giovanni Poli,<sup>1</sup> Filipa Siopa,<sup>1,2\*</sup> and Carlos A. M. Afonso<sup>2</sup>

<sup>1</sup>Sorbonne Université, Faculté des Sciences et Ingénierie, CNRS, Institut Parisien de Chimie Moléculaire, IPCM, 4 place Jussieu, 75005 Paris, France; <sup>2</sup>Research Institute for Medicines (iMed.U LISBOA), Faculty of Pharmacy, Universidade de Lisboa, Av. Prof. Gama Pinto, 1649-003 Lisboa, Portugal

\*[filipasiopa@ff.ulisboa.pt](mailto:filipasiopa@ff.ulisboa.pt)

In 1972 Kaplan et al, reported a pioneer study in photochemical transformation of N-methylpyridinium chlorides to 6-methylazabicyclo[3.1.0]hex-3-en-2-ols (bicyclic aziridine).[1] In 2016, we described the photoreaction of several pyridinium salts **1** into the corresponding bicyclic aziridines **2** under batch conditions with low productivity. S<sub>N</sub>2 ring opening reaction of **2** in water with heteroatom-based nucleophiles allowed the synthesis of new *trans, trans*-aminocyclopentenes (**Scheme 1-A**).[2] This powerful photocyclization, stereo and regioselective S<sub>N</sub>2 aziridine ring opening sequence, was applied to the total synthesis of several natural and non-natural products, like (+)-mannostatin A and (+)-castanospermine.[3] Here will be presented the application of flow on photoreaction of *N*-butyl pyridinium salt **4** (**Scheme 1-B**) allowing to solve the scalability problem of this rearrangement and consequently producing bicyclic aziridine **5** on a gram scale.[4] Furthermore, palladium-catalyzed ring opening of bicyclic aziridine **5** with active methylenes (**Scheme 1-B**) presented a new selectivity due to η<sup>3</sup>-allylpalladium complex formation and nucleophile addition anti to the allylic oxy group **6**, resulting in a new aminocyclopentenes **7**.[5]



Scheme 1: A) Photoreaction of pyridinium salt followed by classical S<sub>N</sub>2 aziridine ring opening reaction. B) Photoflow of pyridinium salts and palladium catalyzed aziridine ring opening reaction.

### Acknowledgements

We thank the Fundação para a Ciência e Tecnologia for financial support (PhD grant 2020.04589.BD) and project (PTDC/QUI-QOR/32008/2017, UIDB/04138/2020, UIDP/04138/2020 and PESSOA 2018/2019 (Proc. 441.00 França and PHC PESSOA 2018 No 40875QJ)). The project leading to this application has received funding from the European Union's Horizon 2020 research and innovation programme under grant agreement No 951996.

### References

1. L. Kaplan, J.W. Pavlik, K.E. Wilzbach, *J. Am. Chem. Soc.*, **94** 3283 (1972).
2. J.R. Vale, F. Siopa, P.S. Branco, C.A.M. Afonso, *Eur. J. Org. Chem.*, 2048 (2016).
3. T. Damiano, D. Morton, A. Nelson, *Org. Biomol. Chem.*, **5** 2735 (2007). J. Zou, P.S. Mariano, *Photochem. Photobiol. Sci.*, **7** 393 (2008).
4. F. Siopa, J.P.M. Antonio, C.A.M. Afonso, *Org. Process Res. Dev.*, **22** 551 (2018). M.A.G. Fortunato, C.-P. Ly, F. Siopa, C.A.M. Afonso, *Methods Protoc.*, **2** 67 (2019).
5. J. Oliveira, K. Gredy, F. Siopa, A. Bernard, G. Gontard, J. Oble, C. A. M. Afonso, G. Poli, *Tetrahedron*, **51** 121182 (2020).

## Chiral metal organic frameworks for electrocatalytic water splitting

Rufaro Kawondera<sup>1</sup>, Wilbert Mtangi<sup>1\*</sup>, Stephen Nyoni<sup>2</sup>, Gift Mehlana<sup>3</sup>

<sup>1</sup>Institute of Materials Science, Processing and Engineering Technology, Chinhoyi University of Technology

<sup>2</sup>Department of Chemistry, School of Natural Sciences and Mathematics, Chinhoyi University of Technology

<sup>3</sup>Department of Chemical Technology, Midlands State University

Corresponding Author email: [wmtangi@cut.ac.zw](mailto:wmtangi@cut.ac.zw)

### Introduction

Although researchers have studied photocatalytic water-splitting extensively, the present methods are not efficient due to slow kinetics, high overpotential and poor stability of the photoelectrodes<sup>[1]</sup>, they are also expensive as they use noble metals<sup>[2]</sup> which are rare and expensive and in some instances the yield is not sustainable. This study seeks to develop an efficient photoelectrode that incorporates chiral metal organic frameworks (MOF) as electrocatalysts for improved hydrogen production from water splitting. Chirality was induced in the Metal organic framework, MIL-53(Fe) using (R-) Camphor Sulphonic Acid and (S+)Camphor Sulphonic Acid. Electrocatalytic water splitting using Linear Sweep Voltammetry yielded a reduction in the onset potential for hydrogen evolution from 1.9 V for bare titanium dioxide to 1.35 V and 1.43V for the MIL-53(Fe) functionalized with R(-) Camphor Sulphonic acid and S (+) Camphor Sulphonic acid, respectively.

### Experimental

Metal organic frameworks were synthesized according to the method reported by Liu<sup>[3]</sup> with terephthalic acid as a linker and Fe as the metal coordinating centre. Chirality was introduced during synthesis by substituting a portion of the terephthalic acid with the chiral linker during one pot synthesis of the chiral MOFs. The functional groups present in the MIL-53 were confirmed using FTIR analysis. The FTIR characterizations were carried out using a Thermo Scientific Nicolet 6700 FTIR machine. The analysis was done from 4000 cm<sup>-1</sup> to 400 cm<sup>-1</sup> on samples prepared by the KBr method. The phase analysis was carried out using a Bruker D2 phaser XRD machine, which uses a copper tube with 1.5418 Angstroms as the X-ray source. The scan mode was continuous PSD fast with scan type two theta/theta with detector Lynxeye XET. The scan step was 0.5 second with 3948 steps and the total time was 2180 seconds. Powdered samples were placed on a zero background sample holder and scanned from 4 to 60, 2 theta positions.

The electrochemical measurements were performed using a CH Instruments, electrochemical analyser Model 608E. Water splitting was performed using TiO<sub>2</sub> nano particulate films deposited on fluorine-doped tin oxide, FTO coated glass, using the electrophoretic deposition (EPD) technique. Chiral electrodes were fabricated by functionalizing 0.1mM slurry solutions on TiO<sub>2</sub> coated FTO substrates. Linear Sweep voltammetry was conducted from 0 to 2.5V using a scan rate of 0.01Vs<sup>-1</sup> in 0.1M Sodium Sulphate. All PEC measurements were carried out in a 3 electrode system using the Ag/AgCl reference electrode and a platinum counter electrode.

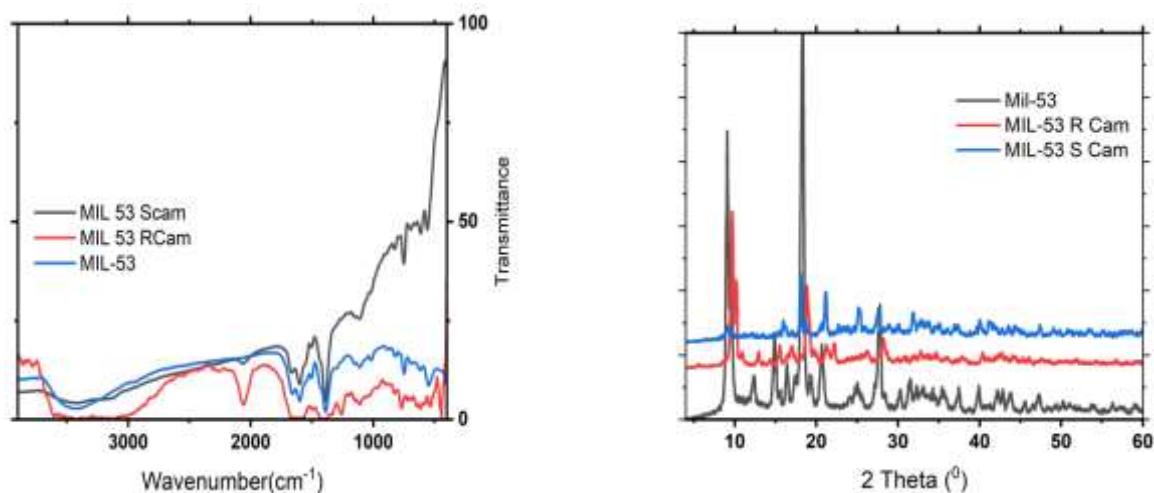


Figure 1. (a) FTIR Spectra of MIL53, MIL- 53-R(-) Camphor sulphonic Acid, MIL-53- S(+)- Camphor Sulphonic Acid

(b) XRD Spectra of MIL53, MIL- 53R(-) Camphor sulphonic Acid, MIL-53-S(+)- Camphor Sulphonic Acid

In the FTIR spectra, bands were noted at 549cm<sup>-1</sup> which can be attributed to the successful formation of the Fe-O bond. The band at 749cm<sup>-1</sup> can be attributed to the aromatic ring stretching, an indication that the terephthalic acid and ferric chloride had successfully reacted to give MIL-53(Fe). The bands at 1515 cm<sup>-1</sup> and at 1659 cm<sup>-1</sup> are due to the asymmetric stretching of the COO bond, while the band around 3200 cm<sup>-1</sup> is due to the OH molecules adsorbed on the MIL-53(Fe) surface.

In the XRD pattern of the synthesized MIL-53(Fe) (Fig. 1b), the diffraction lines appeared at  $2\theta$  of 10, 12.7, 16, 17.5, 25.5, were identical to those reported for standard MIL-53(Fe) [4], indicating that the MIL-53 (Fe) was successfully synthesized.

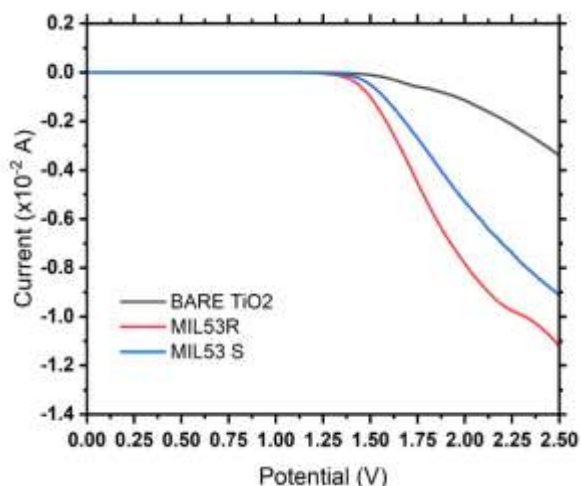


Figure 2. Linear Sweep Voltammogram showing the onset of Hydrogen production

From Linear Sweep Voltammetry, the voltage for the onset potential for hydrogen production was observed to be 1.9 V for bare  $\text{TiO}_2$ , 1.35 V and 1.43 V for the MIL-53(Fe) functionalized with R(-) Camphor Sulphonic acid and S (+) Camphor Sulphonic acid, respectively. The marked reduction in the voltage at which there was an onset of hydrogen production, can be attributed to the presence of the chiral molecules which controlled the spin of the transmitted electrons, thereby minimising the formation of by-products such as hydrogen peroxide.

We have successfully synthesized chiral MOFs and demonstrated that their use in water splitting greatly reduces the over-potential required for the onset of hydrogen.

#### Acknowledgements

Wilbert Mtangi would like to thank the PhosAgro/UNESCO/IUPAC for Green Chemistry for the financial support under grant number 4500415755. Rufaro Kawondera would like to acknowledge financial support from Chinhoyi University of Technology's Vice Chancellor Scholarship.

#### References

- [1] S. Ghosh, B.P. Bloom, Y. Lu, D. Lamont, D. H. Waldeck, *J. Phys Chem C*, **124**,22610-22618 (2020).
- [2] E. Torun, C. Fang, G.A. De Wijs, R.A. De Groot, *J. Phys. Chem. C*, **117**, 6353–6357(2013).
- [3] N. Liu, C. Jing, Z. Li, W. Huang, B. Gao, F. You, X. Zhang, *Matter. Lett.*, **237**,92-95, (2019).
- [4] S. Naeimi, H. Faghihian, *Environ. Toxicol. Pharmacol.*, **53**, 121-132(2017).

# A roadmap towards the development of a scalable continuous flow process for the synthesis of a Raf kinase inhibitor, BAY 43-9006

Faith M Akwi<sup>1\*</sup> and Paul Watts<sup>1</sup>

<sup>1</sup> Department of Chemistry, Nelson Mandela University, University way, Port Elizabeth, 6031, South Africa.

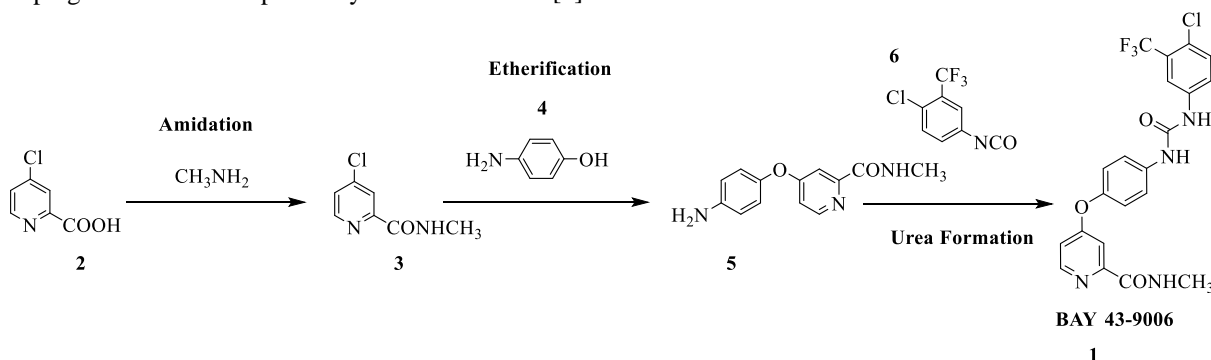
\* s211206296@mandela.ac.za

## Introduction

Over the past 30 years, the batch-based synthesis of chemical compounds has been intensively pursued with many synthetic methodologies and routes being developed, however the synthetic technologies with the capability of scale-up for industrial application in the preparation of important chemical compounds are often not well established. Aspects such as industrial application feasibility, their cost and/or environmental impact are often neglected although they are key issues for industrial scale-up. Continuous flow processing is one kind of synthesis technique that has been reported to enable direct scale-up of reaction processes from lab to plant scale with multi-kilogram quantities of products generated in high throughput [1]. As such, this study is aimed at developing a scalable continuous flow lab-process for the synthesis of BAY 43-9006, a Raf kinase inhibitor used in the treatment of renal cell carcinoma, hepatocellular carcinoma and thyroid cancer [2-4]. Herein, we detail our strategy towards achieving the aforementioned.

## Experimental

Unless otherwise mentioned, all reagents and solvents were obtained commercially and used without further purification. To attain compound **2** (Scheme 1), 2-picolinic acid was subjected to acylation and ring chlorination conditions following a protocol reported by Bankston *et al.* [5] The formed acid chloride was subsequently hydrolyzed, purified and thereafter characterized using <sup>1</sup>H NMR. KF-Alumina was prepared by a simple impregnation method reported by Yamawaki *et al.* [6]



Scheme 1. Synthetic route towards BAY 43-9006

All reaction steps shown in Scheme 1 above were performed in batch mode prior to being translated into continuous flow systems, which included PTFE tubular reactors, a packed bed reactor and Chemtrix® glass chip reactors for the amidation, etherification and urea formation reactions respectively. Synthetic standards obtained from the batch syntheses were characterized by NMR and FTIR. Additionally, relevant reaction parameters such as temperature, residence time and mole equivalents of reacting species were screened and optimized in continuous flow systems and *offline* HPLC was used for reaction monitoring. The amidation of carboxylic acid **2** with methylamine was achieved *via* carbodiimide coupling in the presence of HOBt as an additive in tubular flow reactors (Total volume: 0.44 mL). Etherification of amide **3** with phenol **4** was extensively investigated under microwave conditions using the Monowave® bench-top microwave, after which the synthesis was translated to column flow reactor system. The last step comprising the synthesis of urea **1** was investigated using Chemtrix® glass chip reactors (Total volume: 20 μL). In all the three flow systems used in this study, Chemyx Fusion 2000 syringe pumps were used to deliver reagents that were preloaded into luer lock glass syringes.

## Results and Discussion

A carbodiimide amidation of carboxylic acid **2** was successfully carried out in PTFE tubular flow reactor system without any occurrence of blockages. An investigation of reaction parameters showed 60 °C as the optimum reaction temperature for the synthesis of amide **3** from which 96% yield of **3** was achieved. Ether **5** was thereafter generated from amide **3** and phenol **4** in the presence of a solid supported base (KF-Alumina) and a phase transfer catalyst. The reaction was investigated in batch mode under conventional and microwave heating to ascertain its feasibility. An excellent yield of 98% was attained from the batch microwave synthesis of ether **5** in 40 minutes using tetrabutylphosphonium bromide as a PTC catalyst. Despite the fact that microwave heating is superior to conventional heating, it was not a scalable approach for this reaction step. We thus attempted to translate these optimum conditions to a flow system comprising of a column packed bed flow reactor where on only 70% yield

was attained in 30 minutes. We noted there was a problem of mass transfer and the KF support instead acted like a chromatography purification column because the product was retained on the Alumina. As such, we are currently looking into different supports that can enable the efficient flow synthesis of ether **5**. Finally, Raf kinase inhibitor BAY 43-9006 **1** was synthesized from ether derivative **5** and isocyanate **6**. At 40 °C, 80% yield of urea **1** was attained in 6.34 minutes. The developed modular flow syntheses thus far have the capability of generating urea **1** in a total synthesis time of less than an hour and with good atom economy.

Table 1. A summary of the batch and flow conditions in the synthesis of BAY 43-9006

Reaction Step	Batch Conditions	Flow conditions
Amidation	<b>Conventional round bottomed flask</b> 1 eq DIC, 1 eq amine, 1 eq carboxylic acid and 1.2 eq HOBt Reaction temperature: Room temperature Reaction time: 80 minutes, solvent: THF:DMF Yield: 69%	<b>Home-made PTFE tubular reactors</b> 1 eq EDC, 1 eq amine, 1 eq carboxylic acid and 0.7 eq HOBt Reaction temperature: 60 °C Residence time: 4 minutes, solvent: MeCN:DMF Yield: 96%
	<b>Etherification</b>	<b>Column packed bed flow reactor</b>
	0.44 g of 40% KF-Alumina, 1.5 eq phenol, 0.5 eq PTC and 1 eq amide Reaction temperature: 120 °C Reaction time: 24 hours, Solvent: MeCN Yield: >90%	0.22 g of 40% KF-Alumina, 1.5 eq phenol, 1 eq PTC and 1 eq amide Reaction temperature: 150 °C Reaction time: 30 minutes, solvent: Acetonitrile Yield: 70%
	<b>Microwave heating (Monowave®)</b> 0.22 g of 40% KF-Alumina, 1.5 eq Phenol, 1 eq PTC and 1 eq amide Reaction temperature: 150 °C Reaction time: 40 minutes, solvent: MeCN Stirring rate: 1200 rpm Yield: 98%	
	0.33 g of 30% KF-Alumina, 1.2 eq Phenol, 0.1 eq PTC and 1 eq amide Reaction temperature: 190 °C Reaction time: 40 minutes, solvent: MeCN Stirring rate: 1200 rpm Yield: 98%	
Urea Formation	<b>Conventional round bottomed flask</b> 1.1 eq isocyanate and 1 eq ether Reaction temperature: Room temperature Reaction time: 16 hours, Solvent: Dichloromethane Yield: 80%	<b>Chemtrix glass chip reactors</b> 1.1 eq isocyanate and 1 eq ether Reaction temperature: 40 °C Reaction time: 6.34 minutes, Solvent: MeCN Yield: 80%

## Acknowledgements

We thank the National Research Foundation South Africa for financial support.

## References

1. M. Berton, J.M. de Souza, I. Abdiaj, D.T. Mcquade, D.R. Snead, *J Flow Chem*, **73**(2020).
2. D. Bankston, J. Dumas, R. Natero, B. Riedl, M. Monahan, R. Sibley, *Org Process Res Dev*, **777**(2002).
3. J. Yamawaki, T. Kawate, T. Ando, T. Hanafusa, *Bull Chem Soc Jpn*. **1885**(1983).
4. G. M. Keating, A. Santoro, Sorafenib, *Drugs*, **223**(2009).
5. D. Strumberg, *Expert Opin Pharmacother*, **407**(2012).
6. S.M. Ferrari, U. Politti, R. Spini, G. Materazzi, E. Baldini, S. Ulisse, P. Miccoli, A. Antonelli, P. Fallahi, *Expert Rev Anticancer Ther*, **863**(2015).

# Alternative fuels & biofuels – Green energy

# Light-induced production of biobased fuels and lubricant oils from conjugated dienes

Leandro Cid Gomes,<sup>1</sup> Anup Rana,<sup>1</sup> Per Wiklund<sup>2</sup> and Henrik Ottosson<sup>1\*</sup>

<sup>1</sup>Department of Chemistry—Ångström Laboratory, Box 523, 751 20 Uppsala, Sweden.

<sup>2</sup>Biobase Sweden AB, Götlundagatan 3, 124 71 Bandhagen, Stockholm, Sweden.

\*henrik.ottosson@kemi.uu.se

## Abstract:

Today, the production of high energy density fuels and lubricant oils are heavily dependent on hydrocarbons from fossil sources, yet their replacement for cleaner alternatives are challenging and hydrocarbons are the ideal compounds to be used in such applications.[1] Terpenes are good candidates as feedstock because of their high abundance in nature and due to their possible syntheses by metabolically engineered microorganisms.[2] We addressed the need of more sustainable routes to fuels and lubricant oils by developing light induced routes, using hydrocarbons obtained from renewable sources and converting them into drop-in oil surrogates through photosensitized dimerization reactions (Figure 1).

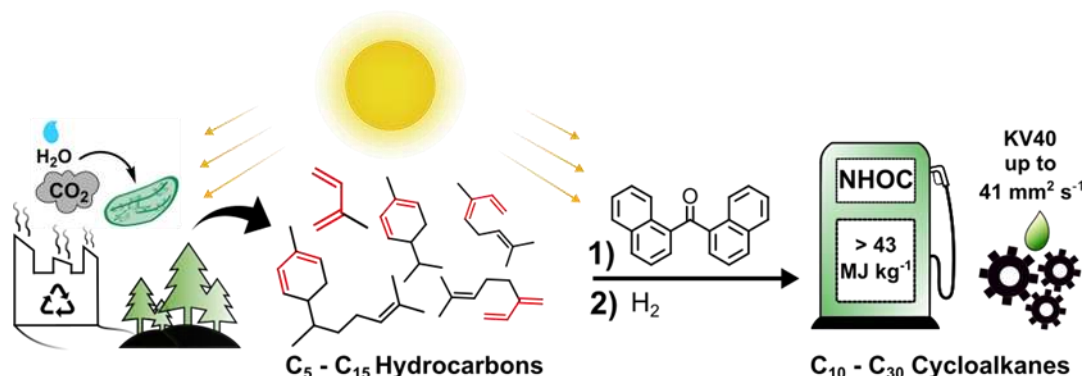


Figure 1. Light-induced production of fuels and lubricant oils from conjugated dienes obtained from renewable sources (e.g., cyanobacteria, industrial waste and rapid-growth forests). NHOC: net heat of combustion (important property of fuels).

KV40: kinematic viscosity at 40 °C (important property of lubricant oils).

The early work on the dimerization of conjugated dienes by Hammond *et al.* [3] has inspired our group to develop a route to jet fuel *via* the photosensitized dimerization of isoprene produced by photosynthetic microorganisms [4]. Herein, we expand the solvent free route to triplet photosensitized dimerization of monoterpenes and sesquiterpenes. Under irradiation at 365 nm, higher conversions in shorter times than previously reported were found (e.g. 96.1 wt.%, 12 h, for  $\alpha$ -phellandrene dimerization). Remarkable results were obtained using simulated and natural sunlight (90.8 wt.% and 46.6 wt.%, respectively). Reasons for the lower reactivities of some monoterpenes were addressed and followed by a cross-dimerization strategy carried out to enhance their conversion and to explore routes from terpenes to C<sub>15</sub> and C<sub>30</sub> hydrocarbons. Selected dimers of monoterpenes and sesquiterpenes were hydrogenated and the cycloalkanes obtained showed physical properties compatible to those of diesel-like fuels and lubricant oils. Therefore, we propose a sustainable route to diesel-like fuels and lubricant oils by using sunlight to dimerize terpenes with a reusable photosensitizer.

## Acknowledgements

Financial support from the Formas agency (grant 2017-00862) and the Swedish Energy Agency (grants 44728-1 and 52576-1) are greatly acknowledged.

## References

1. J. A. Muldoon, B. G. Harvey, *ChemSusChem*, **13**, 5777–5807 (2020).
2. B. Pattanaik and P. Lindberg, *Life*, **5**, 269–293 (2015).
3. G. S. Hammond, N. J. Turro and R. S. H. Liu, *J. Org. Chem.*, **28**, 3297–3303 (1963).
4. A. Rana *et al.*, DOI: 10.26434/chemrxiv.14054564.v1



## Bio-crude oil production via hydrothermal liquefaction of agricultural biomass

D. Liakos<sup>1,2</sup>, K. Triantafyllidis<sup>2</sup>, N. Tourlakidis<sup>1</sup>, V.M. Vasdekis<sup>1</sup>, T. Kokkalis<sup>3</sup>, L. Ntoufas<sup>3</sup>, S. Bezergianni<sup>1\*</sup>

<sup>1</sup>Centre for Research & Technology Hellas (CERTH), Chemical Process & Energy Resources Institute (CPERI), Thessaloniki, 6km Charilaou-Thermi, 57001, Greece

<sup>2</sup>Aristotle University of Thessaloniki (AUTH), Department of Chemistry, University Campus, 54124 Thessaloniki, Greece

<sup>3</sup>Green Innovative Company (GRINCO), 17<sup>th</sup> km Larissa-Thessaloniki Rd, Industrial Area, 41004, Greece

\*sbezerg@certh.gr

Second generation biofuels are considered the future in energy and transportation fuels coverage due to the increased demand and the new government regulations[1]. For residual biomass conversion into liquid biofuel intermediates, there are two main thermo-chemical processes that can be applied, which are pyrolysis and hydrothermal liquefaction (HTL)[1]. HTL prevails over pyrolysis in many aspects, such as the absence of the costly drying step of the feedstock (necessary in pyrolysis), the optional use of catalysts, and the increased oil yield and properties. Also, HTL can convert various feedstocks, including municipal wastes, algae, forest, and agricultural residues which are largely available[1]. Thus, HTL appears as a very promising technology in the biofuel production chain.

In the present study, olive tree branches and wheat straw (agricultural residual biomass) were studied as potential feedstocks for bio-crude oil production via HTL. These types of biomasses are lignocellulosic, meaning that their structure mainly consisted of cellulose, hemicellulose, and lignin. Also, glycerol and crude glycerol, which is a by-product from the transesterification reaction of lipids in the 1<sup>st</sup> generation biodiesel industry, were tested as co-feed. The aim of the study was to find the optimal conditions of the process under which maximum oil yield was produced. The solvent used in the process was deionized water and the experiments were conducted without catalyst addition. The conditions investigated were temperature (280° - 350°C), residence time (10 – 60 min) and the biomass-to-glycerol ratio (from 1/0 to 1/1). The initial pressure of the reactor was 30 bar and the solid-to-liquid ratio was 1/10 in all sets of conditions. Each experiment was conducted twice for better accuracy of the results. The agricultural biomass was collected from Thessaly's plain in Greece and was subjected to milling and sieving prior use to render small particles sized between 185 and 1000 µm. In order to perform a stoichiometric analysis per dry basis, the biomass was dried at 105°C to remove moisture. The results, which include elemental, proximate (moisture and ash) and structural analysis are presented in Table 2. Olive tree branches have higher concentration of cellulose and less lignin compared to wheat straw. Also, carbon content in olive tree branches is slightly higher than wheat straw, although in both types of biomasses it is lower in comparison with liquid fuels.

Table 2: Results of biomass (olive tree branches and wheat straw) analysis

**	Olive Tree	Wheat Straw		Olive Tree	Wheat Straw
<b>Moisture</b>	9.2	8.6	<b>Acetyl Units</b>	4.87	3.03
<b>Ash</b>	3.01	3.04	<b>Carbon</b>	48.75	44.78
<b>Cellulose</b>	48.45	33.08	<b>Hydrogen</b>	5.9	5.54
<b>Hemicellulose</b>	14.9	25.73	<b>Nitrogen</b>	1.35	0.88
<b>Lignin</b>	31.45	35.22	<b>Oxygen*</b>	44	48.8

\*Calculated by difference \*\*All units are measured in wt. %

All the experiments were conducted in a bench top, high-pressure stirred batch reactor with internal vessel volume of 250 mL (Parr 4576A). The reactor is coupled with a J-type thermowell for heating and a U-type cooling coil for rapid temperature dropping. In a typical run, the reactor was loaded with 10g of raw biomass or mix with glycerol and 100 mL of deionized water (for solid to liquid ratio of 1/10). Then, the reactor was sealed and purged 3 times with nitrogen to remove air. Finally, the reactor inlets were compressed to 30 bar with nitrogen (to keep the water in liquid state), then it was heated and kept to the desired temperature, according to the set of conditions before finally cooling to room temperature.

HTL of biomass yields solid, liquid and gas products. Upon decompression of the reactor, a gas sample was collected in a sample bag and analyzed via GC-FID. The collection of the products after the reactor cooldown includes vacuum filtration of the mix in a Buchner funnel with filter paper and the collected liquid is the aqueous phase product containing the solvent with some liquified organics. Then, the filter paper cake was washed with 250 – 300 mL acetone to separate bio-crude oil from solids (hydro-char) and collected in the flask. The solids were dried and weighted, while the acetone was removed in a rotary evaporator at 40°C under reduced pressure to collect the final bio-crude oil product.

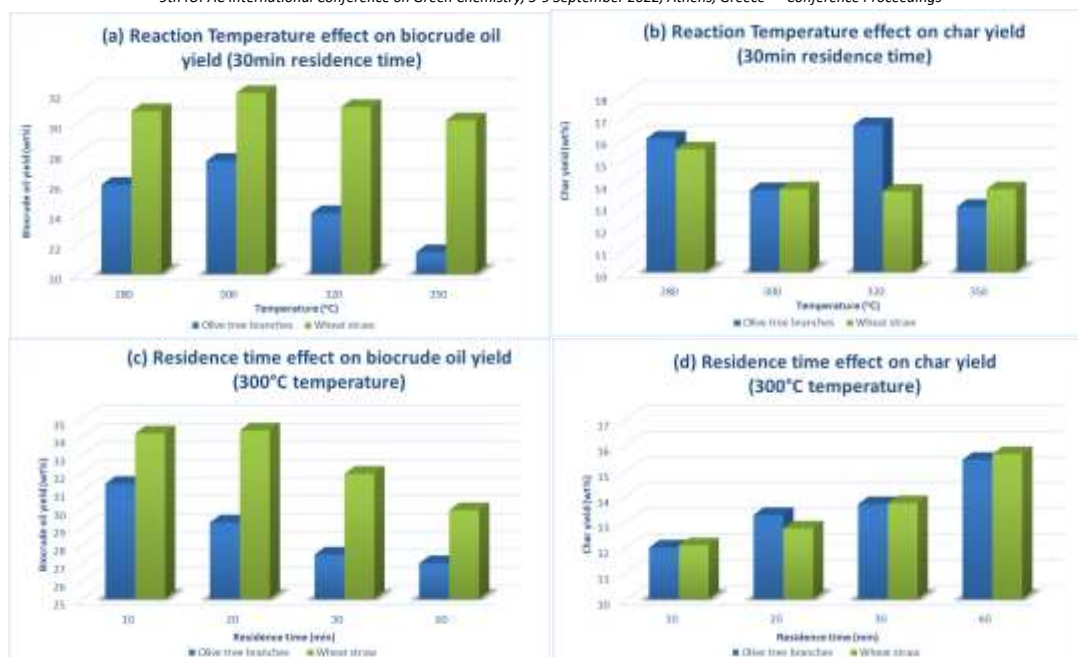


Figure 2: Effect of temperature and residence time on biocrude oil yield((a), (c)) and hydro-char yield ((b), (d))

The effect of each examined parameter is displayed in **Error! Reference source not found.**. The reaction temperature strongly affects the oil yield as lignin starts to liquefy from 280°C, while cellulose and hemicellulose start decomposing in lower temperatures[2]. Also, as the temperature rises, there is competition between depolymerization reactions, repolymerization (leading to solid products) and cracking or decarbonylation reactions, which lead to gaseous products[2]. Wheat straw generates higher oil yield due to its higher lignin content in comparison to olive branches. Also, judging by the oil and solid yield charts, the optimal temperature for oil production is 300°C for liquefaction of these types of biomass (27.46wt% and 31.95wt%). At 280°C the lignin is not fully liquified, while at temperatures above 300°C the conditions favor char formation and mainly gas CO<sub>2</sub> production leading to loss of organic products.

Feedstock residence/reaction time also affects the yield of the products. Wheat straw optimal time is 20 min but the optimal time for olive tree branches is 10min possibly due to the lower lignin content. At longer residence times, depolymerization reactions cease and repolymerization occurs leading to significantly higher solid yield (up to 15.65wt% at 300°C, 60min for wheat straw). So, the maximum yield for HTL of olive tree branches was 31.39wt% and 34.35wt% for wheat straw.

Glycerol addition was also tested as co-feed at 20wt% and 50wt% at optimal conditions. The results showed higher oil yield especially at 1/1 ratio (35.13wt% for olive and 36.65wt% for straw) and significantly lower solid yield (4.16wt% for wheat straw), which is in accordance with literature and leads to the conclusion that lignin is highly soluble in glycerol[3].

Concluding, HTL of biomass leads to high biocrude-oil yield with favorable properties. Wheat straw HTL resulted in higher oil yield and the addition of crude glycerol in the process creates a synergistic effect in reactions, demonstrating further enhancement of oil yield. Finally, the future step for this study is to investigate the potential use of a catalyst to enhance oil yield and properties even more.

## Acknowledgements

This research has been co-financed by the European Union and Greek national funds through the Operational Program Competitiveness, Entrepreneurship, and Innovation, under the call RESEARCH – CREATE – INNOVATE (project code: “AgroFUCHer”).

## References

- [1] A. Dimitriadis, S. Bezergianni, Hydrothermal liquefaction of various biomass and waste feedstocks for biocrude production: A state of the art review, *Renewable and Sustainable Energy Reviews*. 68 (2017) 113–125. <https://doi.org/10.1016/j.rser.2016.09.120>.
- [2] T.H. Seehar, S.S. Toor, A.A. Shah, T.H. Pedersen, L.A. Rosendahl, Biocrude production from wheat straw at sub and supercritical hydrothermal liquefaction, *Energies (Basel)*. 13 (2020). <https://doi.org/10.3390/en13123114>.
- [3] T.H. Pedersen, L. Jasiunas, L. Casamassima, S. Singh, T. Jensen, L.A. Rosendahl, Synergetic hydrothermal co-liquefaction of crude glycerol and aspen wood, *Energy Conversion and Management*. 106 (2015) 886–891. <https://doi.org/10.1016/j.enconman.2015.10.017>.

## Continuous hydroprocessing of nitrogen-rich biocrudes from municipal solid wastes in a graded catalyst bed: Synergetic effect of oxygenates and nitrogenates

Muhammad Salman Haider<sup>1\*</sup>, Daniele Castello<sup>1</sup>, and Lasse Rosendahl<sup>1</sup>

<sup>1</sup> Department of AAU Energy, Aalborg University, Aalborg, Denmark

\*mush@energy.aau.dk

Raising concerns regarding climate change produces an urge to decarbonize the long-haul transportation sector. In this regard, biomass could be a potential renewable source to produce sustainable, carbon-neutral liquid fuels. Hydrothermal liquefaction (HTL) followed by catalytic hydroprocessing is one of the most promising pathways to convert varying feedstocks (organic urban residues, forestry residues, algae etc.) into high quality renewable drop-in fuels. The energetically dense black viscous product from HTL ("biocrude"), contains a diverse organic pool with considerable amount of oxygen (~5-20%), nitrogen (~0-8%) and inorganic content (~0.1-0.6%). The presence of these organic contaminants poses new and exciting scientific challenges (e.g., thermal instability at high temperatures, coke precursors, extensive coking, nitrogen removal, exothermicity, pressure drops), which are indispensable to understand, during hydroprocessing. Therefore, special attention is needed not only to realize this complex biocrude mixture but also to optimally select proper hydrotreating temperatures in graded-catalyst reactor bed (three different types hydrotreating catalysts based on their porosity and nickel loading on  $\gamma$ -Al<sub>2</sub>O<sub>3</sub> support) which can suppress coke formation and reactor plugging. In this work, we comprehensively discuss the missing scientific links which are essential in selecting proper hydrotreating temperatures in graded-catalyst reactor bed and thereby, ensures smooth hydroprocessing with no coking for hundreds of hours (up to 600 hours).

A bench scale continuous hydrotreater (30-80 mL/h) with two reactors in a series was utilized. Based on the biocrude thermal stability, each reactor works at different temperatures and is packed with three different NiMo/Al<sub>2</sub>O<sub>3</sub> commercial catalysts from Haldor Topsøe, to control exothermicity and pressure drop. TGA-DSC was used to determine the thermal stability of HTL biocrudes. Fourier-transform ion cyclotron resonance mass spectrometry (FT ICR MS), GCXGC-MS, GC-MS, inductively coupled plasma optical emission spectroscopy (ICP-OES), elemental analyzer (CHN/O) and higher heating value (HHV) were used for chemical characterization. Furthermore, the drop-in fuel products after true boiling point fraction distillation (ASTM D2892) underwent detailed characterization in accordance with ASTM D1655 (the global standard for aviation fuel) and EN 590 (European standard for diesel).

In brief, some of the main results that were obtained are:

- 1. Oxygenates:** Oxygen functionalities are mostly related to thermal instability of biocrudes and extensive coking at higher hydrotreating temperatures. Both analytical (TGA-DSC) and experimental (extensive polymerization of sludge HTL biocrude at 180°C in pipes during continuous hydroprocessing) work evidently suggest that HTL biocrudes are thermally instable.
- 2. Nitrogenates:** Over longer hydroprocessing times nitrogen functionalities (mostly basic nitrogenates) decrease the catalytic activity to a large extent at mild hydrotreating temperatures. Moreover, HTL biocrudes also have highly reactive organic species e.g., metalloporphyrins (analyzed via FT-ICR MS etc.), which extensively produce coking even at low hydrotreating temperatures.
- 3. Selection of proper hydrotreating temperatures:** The vital key is to identify the coke precursors and have a comprehensive knowledge regarding thermal instability of given HTL biocrude.
- 4. Overcoming the coking propensity:** Stabilization of highly reactive organic species under optimal hydrotreating conditions with carefully selected catalysts in a graded reactor bed.
- 5. Complete nitrogen removal:** 100% nitrogen removal has been achieved for the first time during continuous hydrotreating (e.g., sludge biocrude). This milestone evidently paves the pathway and prospects of future aviation fuel approval from regulatory authorities.
- 6. Compliance with ASTM D1655 and EN 590:** Chemical composition of produced fuels were analyzed by GCXGC-MS. The produced drop-in fuels after the fractional distillation of hydrotreated HTL biocrudes fulfill all specification of Jet-A1 and the stringent sulfur requirements in case of diesel (less than 10 ppm). The results of present work not only represent a great scientific advancement towards better understanding of HTL biocrudes and subsequent hydroprocessing step, but also paves the way toward green, sustainable and energy secure future where we can virtually utilize any kind of biomass source for drop-in fuels.

### Acknowledgements

This work has received funding from European Union's Horizon 2020 research and innovation program under grant no. 818413 (NextGenRoadFuel) and Lowcarbfuels.dk a Danish funded project.

## Catalytic hydrodeoxygenation of lignin pyrolysis bio-oil towards transportation fuels

Antigoni Margellou<sup>1,\*</sup>, Foteini Zormpa<sup>1</sup>, Stylianos Torofias<sup>1</sup>, Evangelia Delli<sup>1,2</sup>, Ana Correa de Araujo<sup>3</sup>, Axel Funke<sup>3</sup>, Leonidas Matsakas<sup>4</sup>, Ulrika Rova<sup>4</sup>, Paul Christakopoulos<sup>4</sup>, Konstantinos Triantafyllidis<sup>1,\*</sup>

<sup>1</sup>Department of Chemistry, Aristotle University of Thessaloniki, Thessaloniki, Greece

<sup>2</sup>Department of Physics, Aristotle University of Thessaloniki, Thessaloniki, Greece

<sup>3</sup>Karlsruhe Institute of Technology, Institute of Catalysis Research & Technology, Eggenstein - Leopoldshafen, Germany

<sup>4</sup>Department of Civil, Environmental and Natural Resources Engineering, Luleå University of Technology, Luleå, Sweden

\*[amargel@chem.auth.gr](mailto:amargel@chem.auth.gr); [ktrianta@chem.auth.gr](mailto:ktrianta@chem.auth.gr)

Lignin is one of the three main structural components of the lignocellulosic biomass. Lignin is widely available in the form of kraft lignin and lignosulphonates, which are derived as by-products of the pulp and paper industry. During the last years and within biorefining approaches, processes aiming to the direct lignin isolation have been developed, e.g. organosolv process. Due to the high aromatic/phenolic nature, lignin can be converted to a wide variety of value-added chemicals towards fuel and polymers. The most widely applied processes of lignin conversion are the fast pyrolysis and the hydrogenolysis process. Fast pyrolysis is performed at relatively high/moderate temperatures (400-600 °C) under inert atmosphere resulting in bio-oils enriched in alkoxy/alkyl-phenol compounds with composition depending mainly on the lignin origin, i.e. hardwood or softwood biomass [1-3]. The obtained bio-oils can be directly utilized in phenol-formaldehyde resins replacing petroleum derived phenol as well as in the production of epoxy resins and polycarbonates replacing conventional bisphenol A derivatives. Alternatively, the thermal pyrolysis bio-oils can be in-situ upgraded to BTX aromatics using acidic, mainly zeolitic, catalysts during the pyrolysis process. Furthermore, the bio-oils can be upgraded to (alkyl)cyclohexanes via downstream hydrodeoxygenation and utilized as drop-in transportation bio-fuels. In this work, lignin streams isolated via the organosolv fractionation process from different forestry/agricultural wastes was initially converted to bio-oils enriched in alkoxy/alkyl-phenols. In a second step, the pyrolysis bio-oils was converted to (alkyl)cyclohexanes via hydrodeoxygenation process. Hydrodeoxygenation of model phenolic compounds was also studied to elucidate the reaction mechanisms involved in the HDO process.

Lignin fractions were isolated from different forestry and agricultural lignocellulosic biomass feedstocks (beechwood, birch, spruce and wheat straw) via organosolv process, in ethanol-water solvent mixtures, with dilute H<sub>2</sub>SO<sub>4</sub> as catalyst, at 180-200 °C. The pretreatment conditions were carefully selected according to the nature of biomass feedstock. Lignins were characterized to obtain their thermal and structural properties. Hardwood (beech, birch) and wheat straw derived lignins consist of both guaiacyl and syringyl units, substituted with one and two methoxy groups, while spruce lignin exhibit only guaiacyl units with one methoxy group. The composition of the parent lignin is usually “transferred” to the bio-oil composition in terms of S/G content and can influence their downstream valorization routes. A fingerprint of pyrolysis bio-oil composition was determined in a Micro-pyrolyzer with on-line GC-MS (Py/GC-MS). All bio-oils are enriched in alkoxy (35-63%) and alkylated phenols (6-20%). Other compounds such as aldehydes and acids are also identified but in lower concentrations. Hardwood derived bio-oils exhibit both guaiacyl and syringyl derived alkoxy phenols while softwood derived bio-oils only guaiacyl compounds. Lignin bio-oils were produced in two lab-scale set-ups, i.e. in a fixed-bed reactor and in a fluidized bed reactor pyrolysis unit, at 500-600°C, with the pyrolysis vapors being condensed at 60 °C or -15°C. The main products of lignin fast pyrolysis are the bio-oil, non-condensable gases and char. The organosolv lignins resulted in 40-47 wt.% bio-oil, 32-49 wt.% solids and 6-14 wt.% gases. Considering the bio-oil composition, alkoxy-phenols are mainly detected (40-71%) as well as alkylated phenols (5-10%). Indicatively, the composition of birch lignin derived bio-oil is shown in Figure 1.

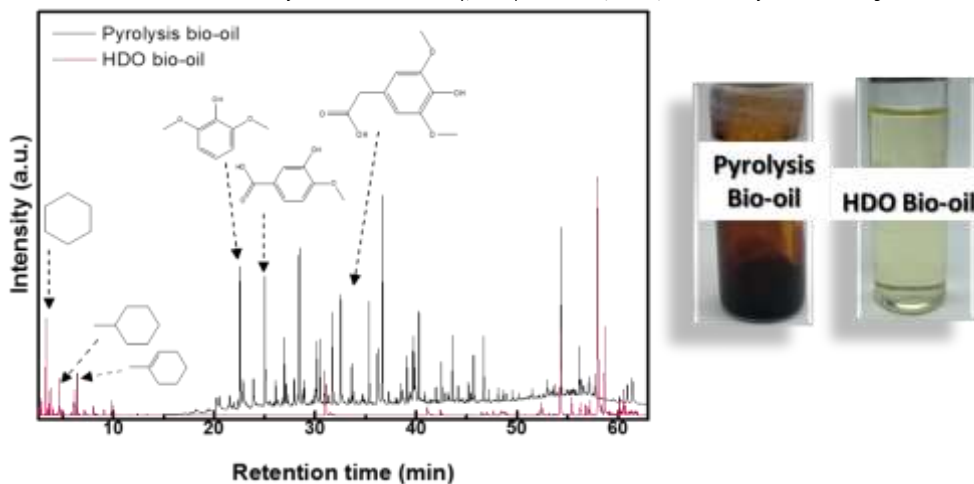


Figure 1. GC-MS of pyrolysis oil and the bio-oil after HDO (10%Ni/Beta catalyst, 220°C, 50 bar H<sub>2</sub>, 1 hr). Regarding the downstream hydrodeoxygenation of thermal pyrolysis bio-oils, the experiments were carried out in a batch autoclave reactor, under the optimized conditions determined for the model phenolic compounds. Optimization of reaction temperature, time, H<sub>2</sub> pressure, catalyst to feed ratio was studied using bifunctional catalysts based on Ni supported on micro/mesoporous aluminosilicate, mainly zeolitic, catalysts with acidic properties. Both the porous properties and the acidity proved to influence the conversion, the products distribution and yield. The most abundant compounds identified in the HDO products were cyclohexane, methyl/ethyl cyclohexane, methyl cyclopentane (via isomerization) and 1,1- bicyclohexyl (via alkylation). Under the optimized reactions, lignin derived bio-oils were hydrodeoxygenated using a bifunctional zeolite catalyst, i.e. 10% Ni/BETA (Si/Al=12.5). As can be observed in Figure 1, the Ni/zeolite catalyst induced deep hydrodeoxygenation of the alkoxy and alkylated phenols towards (alkyl)cyclohexanes. The produced alkylated cyclohexanes exhibit carbon number distribution in the range of C<sub>6</sub>-C<sub>9</sub> and can be utilized as drop-in transportation biofuels.

## Acknowledgements

This project has received funding from the European Union's Horizon 2020 research and innovation programme under Grant Agreement No. 101007130.

## References

- [1] A.G. Margellou, P. Lazaridis, I. Charisteidis, C. Nitsos, C. Pappa, A. Fotopoulos, S. Van den Bosch, B. Sels, K. Triantafyllidis, *Applied Catalysis A: Gen.*, **623** 118298 (2021).
- [2] I. Charisteidis, P. Lazaridis, A. Fotopoulos, E. Pachatouridou, L. Matsakas, U. Rova, P. Christakopoulos, K. Triantafyllidis, *Catalysts*, **9** 935 (2019).
- [3] P. Lazaridis, A. Fotopoulos, S. Karakoulia, K. Triantafyllidis, *Front Chem*, **6** 295 (2018).

## Biomass to hydrogen: Understanding the factors affecting hydrogen production rate via reforming of bio-oil.

Vasileia-Loukia Yfanti<sup>1\*</sup>, Areti Moutsiou<sup>1</sup> and Angeliki A. Lemonidou<sup>1,2</sup>

<sup>1</sup>Department of Chemical Engineering, Aristotle University of Thessaloniki, University campus, Thessaloniki, 54124, Greece

<sup>2</sup>Chemical Process & Energy Resources Institute (CERTH/CPERI), Thessaloniki, 57001, Greece

\*[vasileia@auth.gr](mailto:vasileia@auth.gr)

Every year almost 90Mtn of hydrogen are consumed by the chemical (production of ammonia, methanol) and petrochemical industry (hydrotreating, hydrodesulfurization, hydrocracking). In addition to the above uses, hydrogen is considered as the future energy carrier, due to its high energy content and clean combustion without CO<sub>2</sub> emissions. Currently, hydrogen is produced via endothermic steam reforming of methane, a process with low energy efficiency, high operating cost and high green-house gases emissions [1]. A sustainable alternative for hydrogen production is the utilization and upgrading of biomass derived oxygenates as well as the waste streams of their processes. The Aqueous Phase Reforming (APR) of bio-oil is a promising process for hydrogen production as it is associated by low energy requirements, takes place in a single chemical reactor and generates low levels of carbon monoxide in the effluent gases [2-3]. The present work studies the formation of hydrogen via aqueous phase reforming of miscanthus pyrolysis derived bio-oil. Ethylene glycol, hydroxyacetone and acetic acid were used as model compounds in order to examine the main factors that affect catalyst stability and hydrogen production rate.

The experiments were performed in a batch reactor, using an aqueous mixture of the main bio-oil compounds (13 wt% ethylene glycol + 2.2 wt% hydroxyacetone + 2 wt% acetic acid + 82.8 wt% water) as well as the real aqueous phase of bio-oil as feed. Supported and non-supported Pt, Rh and Ni catalysts (1wt% Pt/C, 1wt% Pt/ZSM-5-23, 2wt% Rh/C, 2wt% Rh/CeO<sub>2</sub>-Al<sub>2</sub>O<sub>3</sub>, 12wt% Ni/ZrO<sub>2</sub>-CeO<sub>2</sub>-La<sub>2</sub>O<sub>3</sub> and NiFeCo with mass ratio of 16.7:53.1:2.8wt% Ni:Fe:Co) were synthesized using wet impregnation and sol-gel preparation methods and evaluated on APR of ethylene glycol (280 – 300 °C, 3 h, 20 bar initial N<sub>2</sub> pressure). The APR of the model compounds mixture and the real bio-oil was tested in a high-pressure batch reactor under the same reaction conditions and over the more promising catalyst, in terms of selectivity to hydrogen. The stability of the catalyst was tested for 3 consecutive runs. The results obtained from the tests using aqueous solution of individual compounds or mixture of them, combined with temperature programming methods (TGA, TPD-He), provided information about the reaction pathways as well as the adsorbed species. In addition, the effect of MgO addition in APR as a means for activity enhancement was also explored.

The results of catalysts screening in APR of ethylene glycol expressed as ethylene glycol consumption rate and hydrogen formation rate are presented in Figure 1. The 1wt% Pt/C catalyst proved as the more selective catalyst towards H<sub>2</sub> as it is active on C-C bond scission, promotes the water gas shift (WGS) reaction and limits the formation of alkanes, resulting in 96.3% hydrogen selectivity in gaseous phase and 87.4% ethylene glycol conversion, at 300 °C. Nickel catalysts are active yet not selective, as they catalyze methanation and promote condensation reactions. Similarly, the Pt/ZSM-5-23 favors the formation of CH<sub>4</sub> and C<sub>2</sub>H<sub>6</sub>.

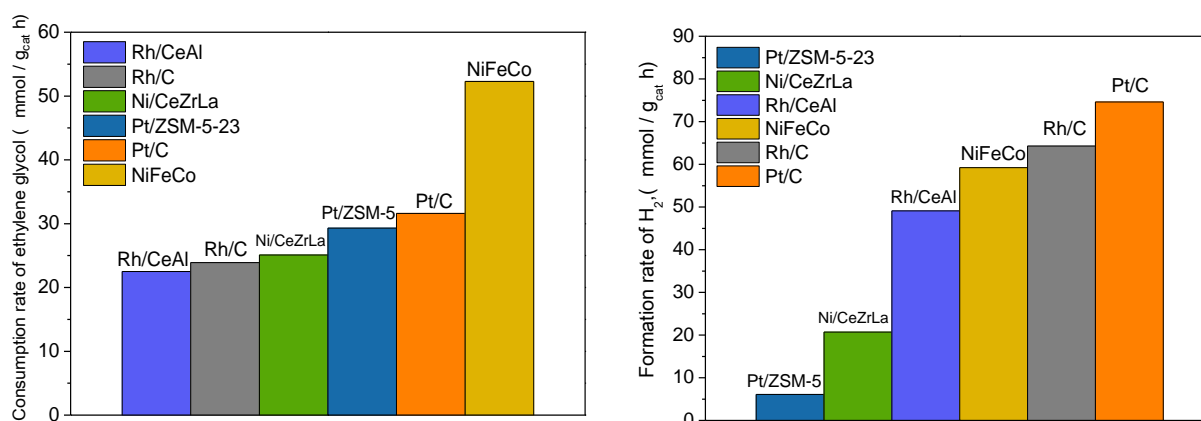


Figure 1: Conversion rate of ethylene glycol (a) and hydrogen formation rate (b), over the tested catalysts

The APR of the surrogate bio-oil mixture was tested over the Pt/C catalyst, at 300 °C, showing 35.5 % hydrogen yield. Besides H<sub>2</sub> and CO<sub>2</sub>, the gas phase is consisted by CH<sub>4</sub>, C<sub>2</sub>H<sub>6</sub> and CO at low concentrations. The main

products in liquid phase are methanol and ethanol, followed by 1-propanol, diethyl ether and acetic acid which is formed as product. The key factor that enhances hydrogen production is the increase of reaction temperature, as not only boosts ethylene glycol conversion and reformation but enhances H<sub>2</sub> formation as well, through the conversion of intermediates bio-products such as ethanol.

Compared with the results of preliminary tests using aqueous solution of individual reactants as feed, in the presence of all three reactants in the feed, the conversion of ethylene glycol and acetic acid is reduced by 35% and 65% respectively, while that of hydroxyacetone remains stable and almost complete. Hydrogen is formed via APR of ethylene glycol and hydroxyacetone, while the contribution of acetic acid to hydrogen formation is negligible. In contrast to the other two reactants, acetic acid shows low reactivity and low reforming rates as the reaction conditions promote its decarboxylation.

The reduced conversion of ethylene glycol is mainly attributed to the presence of acetic acid in the feed. The TGA and TPD-He techniques of the used catalysts proved that under APR of surrogate bio-oil mixture, a strongly adsorbed compound (which is not detected in the absence of acetic acid in the feed) is formed. This compound is considered one of the main causes leading to the reduced catalytic activity. Most likely, its formation is due to the reaction between acetic acid and ethylene glycol or hydroxyacetone derived adsorbed species. Moreover, the above techniques showed that acetic acid is adsorbed on catalyst surface forming strongly adsorbed species, probably derived via ketene, a precursor of carbonaceous deposits. Upon reuse, the catalyst loses 50% of its activity after the first use, while a stabilization is observed afterwards. Besides, of adsorbed species, Pt sintering is considered as another cause for catalyst deactivation.

The addition of MgO in the feed led to doubling of hydrogen yield at almost complete ethylene glycol conversion. The positive role of MgO is associated primarily with the neutralization of acetic acid and secondarily with the adsorption of the produced CO<sub>2</sub>. The positive effect of MgO is also confirmed during the reforming of the real aqueous fraction of bio-oil, as the production of hydrogen was possible only in the presence of MgO. Otherwise, a direct catalyst deactivation was observed due to the complexity of the feedstock.

Summarizing, the formation of a hydrogen rich gas stream with low CO content is realized, via the low energy cost reforming of the aqueous phase of bio-oil. The supported Pt/C catalyst proved to be an active and selective material for APR conditions. However, it suffers from deactivation mainly due to the strong adsorbed compounds that poison its surface. These compounds mainly originate from acetic acid in the feed. Promising results regarding ethylene glycol conversion and hydrogen productivity are achieved working at higher temperature 300 °C and in the presence of MgO as sorbent and acid neutralizing agent. A more in depth mechanistic and deactivation study is in progress. The above results provide valuable basic information for further reforming studies of various types of bio-oils as well as of heavier non-volatile oxygenated bio-molecules.

## References

1. P. Nikolaidis, A. Poullikkas, *Renew. Sust. Energ. Rev.*, 67 597 (2017).
2. T. P. Vispute, G. W. Huber, *Green Chem.*, 11 1433 (2009).
3. A. Arandía, I. Coronado, A. Remiro, A.G. Gayubo, M. Reinikainen, *Int. J. Hydrog.* 44 (26) 13157 (2019).

## **A flexible and integrated process for treating multiple waste biomass to produce high-value bioproducts and advanced transportation fuel**

**Tanmay Chaturvedi<sup>1\*</sup> and Mette H. Thomsen<sup>2</sup>**

<sup>1</sup>AAU Energy, Aalborg University, Niels Bohrs Vej 8 6700 Esbjerg, Denmark

\*tac@energy.aau.dk

Abstract text:

The H2020 Project: FLEXI-GREEN FUELS investigates the production of next generation liquid biofuels for shipping and aviation from sustainable resources by developing and improving integrated technologies for a complete conversion of second generation (2G) types of feedstocks: (1) Lignocellulosic residue biomass focusing on wood waste from forest industries and sawmill wastes and agricultural residues and (2) the organic fraction of municipal waste (OFMSW). FLEXI-GREEN FUELS integrated a flexible yet integrated process to produce high-value bioproducts such as chitin and squalene along-side with advanced transportation biofuels for the shipping and aviation sector. Semi-continuous organosolv pretreatment process using a mixture of ethanol and water as solvent, is used for the separation of the cellulose and hemicellulose fractions from lignin. As lipids are far superior bio-crudes towards hydrocarbon fuels, the intermediate conversion of sugars (being abundant in lignocellulosic biomass and OFMSW) to lipids plays a key role in the proposed integrated technology. Three efficient processes to convert sugars to lipids, namely fungal fermentation, algae dark fermentation, and lipid rich larva production are investigated. Lipids from all these three methods will be further converted via advanced hydrotreatment (HDO/isomerization) processes to diesel range (C16-C18) alkanes, which in turn are optimized for blending with aviation or shipping fuels. The remainder of hydrolysate that is not utilized for lipid production is used as a substrate in a Microbial Electrolysis Cell (MEC) for green hydrogen production. The potential difference needed for the upstart of the MEC is in principle presumed to be provided by the excess energy from wind turbines.

### **Acknowledgements**

This project has received funding from the European Union's Horizon 2020 research and innovation programme under grant agreement No. 101007130



## Transformation of natural triglycerides into green diesel over Ni-Mo catalysts supported on titania

George Petropoulos<sup>1</sup>, John Zafeiropoulos<sup>1</sup>, Eleana Kordouli<sup>1,2</sup>, Christos Kordulis<sup>1,2</sup>, Alexis Lycourghiotis<sup>2</sup> and Kyriakos Bourikas<sup>1\*</sup>

<sup>1</sup>Hellenic Open University, Parodos Aristotelous 18, GR26335, Greece

<sup>2</sup>Department of Chemistry, University of Patras, GR26500, Greece

\*bourikas@eap.gr

### Introduction

Biomass is an excellent source of renewable energy. Plant oils, animal fats, waste cooking oils and microalgal oils constitute a very useful kind of biomass as they comprised from natural triglycerides, which contain smaller amounts of oxygens compared to other kinds of biomass. This kind of biomass is already used for the production of biodiesel. Problems in the production, storage, use of biodiesel and accumulation of large amounts of low quality glycerol have promoted research for alternative upgrading processes of the natural triglycerides, for obtaining hydrocarbons, instead of fatty acid methyl esters. The selective deoxygenation (SDO) is the most important upgrading alternative [1,2]. This is realized by hydrotreatment through decarboxylation (deCO<sub>2</sub>), decarbonylation (deCO) and hydrodeoxygenation (HDO). In the frame of the so called “stand –alone” approach [3] natural triglycerides are hydrotreated separately from the petroleum fractions. In this context, two types of catalysts are proved to be very effective: supported noble metals and conventional sulphided NiMo, CoMo and NiW supported catalysts. However, both kinds of catalysts present several weaknesses. The noble metals have high cost and limited availability. On the other hand, the conventional sulphided NiMo, CoMo and NiW catalysts need to be maintained in the sulphided form by introducing sulphur compound in the feed which presumably results to S-contaminated end products. The aforementioned weakness motivated, in the last years, intensive research on the less expensive transition metal catalysts in their metallic, phosphide, and carbide forms [3]. Studies concerning metallic Ni catalysts have shown that we need supported catalysts with high nickel content and high specific surface area in order to obtain high values of nickel active surface [3]. This is necessary in order to achieve high yields of hydrocarbons in the diesel range. On the other hand, the promotion action of Mo in the nickel catalysts for this process has been well established in the recent literature [4].

In this direction, in the present work we developed Ni catalysts supported on titania with various Ni/(Ni+Mo) ratios in order to find the optimum one. The selection was based on the effectiveness of the catalysts on the transformation of sunflower oil into green diesel. In the next step, we evaluated the most promising catalyst also in other three vegetable oils, namely rapeseed oil, soya oil and *Cynara cardunculus* oil.

### Experimental

From a previous study we had found that the optimum loading for the monometallic Ni/TiO<sub>2</sub> catalyst was the 50 wt. % Ni and the most appropriate synthesis technique was the Deposition – precipitation (D.I.) at high temperature (110°C) using [Ni(H<sub>2</sub>O)<sub>6</sub>]<sup>2+</sup> as the precursor Ni ion and urea as the precipitating agent [5]. Thus, we kept the total loading of the active phases equal to 50 wt. % and we synthesized with this technique various NiMo/TiO<sub>2</sub> catalysts with Ni/(Ni+Mo) ratio equal to 0.91, 0.95, 0.98, 0.99 and 0.994. Moreover, for reasons of comparison we synthesized a Mo/TiO<sub>2</sub> catalyst with 50 wt. % Mo, using the wet impregnation technique. In all cases the deposition of the active phase(s) was followed by drying at 120°C for 2 h, calcination at 400°C for 2 h and reduction at 400°C for 2.5 h. The physicochemical characteristics of the catalysts were studied using various techniques, such as N<sub>2</sub> adsorption-desorption, XRD, TPR, NH<sub>3</sub>-TPD and TGA. The evaluation of the catalysts was performed in a semi-batch reactor at the following conditions: ratio of oil to catalyst mass 100 ml / 1 g, pressure 40 bar, H<sub>2</sub> flow rate 100 ml/min, speed of stirring 2000 rpm, temperature 310°C. A liquid sample was withdrawn from the reactor every hour and analyzed on a GC-MS system. The reaction was monitored for a period of 9h.

## Results and Discussion

In Table 1 we list the values of various textural characteristics of the catalysts prepared with the various Ni/(Ni+Mo) ratios.

Table 1. Values of various textural characteristics of the catalysts prepared with the various Ni/(Ni+Mo) ratios.

Catalyst	Composition (wt. %)	SSA (m <sup>2</sup> /g)	Specific Pore volume (cm <sup>3</sup> /g)	Mean Pore Diameter (nm)	Mean crystallite size of Ni <sup>0</sup> (nm)
0MoTi	50% Mo	94	0.23	8.51	-
0.91NiMoTi	43% Ni, 7% Mo	158	0.33	7.05	14.5
0.95NiMoTi	46% Ni, 4% Mo	158	0.39	8.19	15.5
0.98NiMoTi	48% Ni, 2% Mo	157	0.37	7.66	20.5
0.99NiMoTi	49% Ni, 1% Mo	163	0.38	7.62	14.2
0.994NiMoTi	49.5% Ni, 0.5% Mo	175	0.51	9.14	13.5
1NiTi	50% Ni	156	0.63	13.06	11.5

Concerning the 0MoTi catalyst, a single-peak pore distribution with a center at about 11 nm appears, i.e. with an extension of 2 nm to the right, relative to the center of the peak appeared by the carrier (not shown here). This is expected, because due to the large percentage of Mo loading, the smaller pores become clogged, resulting in this movement of the peak to larger sizes. In this catalyst there is also a significant reduction of its total porosity in relation to the carrier, which justifies the low value of specific surface area (Table 1) and is an indication of the not so good dispersion of Mo. We note that this catalyst has been synthesized by the wet impregnation technique. As for the NiMoTi catalysts, the picture is different. The catalysts exhibit an almost uniform peak pore distribution, with a center of approximately 7 nm (not shown here). This, compared to the center of the single-peak distribution of the Ni catalyst which is around 10 nm, shows that in these catalysts the active phase of Ni is deposited in such a way that fewer small pores are blocked. On the other hand, these catalysts lack the intermediate nickel porosity that had been formed using this technique and which we saw in a previous study giving a significant additional specific surface area to the catalysts [5]. Thus, these catalysts exhibit a similar specific surface area to that of the 1NiTi catalyst (Table 1). The XRD patterns of the catalysts revealed that the predominant phase is Ni<sup>0</sup> with a small contribution from nickel oxide. The addition of Mo does not seem to have a beneficial effect on the dispersion of Ni, on the contrary, the dispersion decreases as the average size of Ni<sup>0</sup> crystallites is increased in NiMoTi catalysts compared to the 1NiTi catalyst (Table 1). Regarding the 0MoTi catalyst, in addition to the main peaks of the anatase, peaks of molybdenum oxide (MoO<sub>2</sub>) are appeared. It seems that under the reduction conditions of the catalysts a reduction of Mo<sup>6+</sup> to Mo<sup>4+</sup> has taken place. No molybdenum oxide (MoO<sub>2</sub>) peaks are observed in NiMoTi catalysts and this can be attributed either to the fact that they have a small percentage of Mo or to the fact that the molybdenum is well dispersed. The TPR study showed that as the percentage of Mo in the catalysts increases, it appears that Mo interacts strongly with nickel, reducing the dispersion of NiO and thus facilitating its reduction to Ni<sup>0</sup>.

All catalysts proved to be very effective, as they show a complete conversion of sunflower oil from just the 2nd hour of the reaction. The most selective for the production of hydrocarbons is the catalyst with ratio Ni/(Ni+Mo) = 0.99 (synergistic ratio), which showed a yield of 72% (Figure 1). Moreover, the four oils of the energy crops (*Cynara cardunculus* oil, rapeseed oil, sunflower oil and soybean oil) appear almost equally suitable for their conversion into green diesel. In the presence of the above optimum catalyst, all four oils were completely converted and led to the production of hydrocarbons in the diesel region (C<sub>15</sub>-C<sub>18</sub>) with a yield of about 70%.

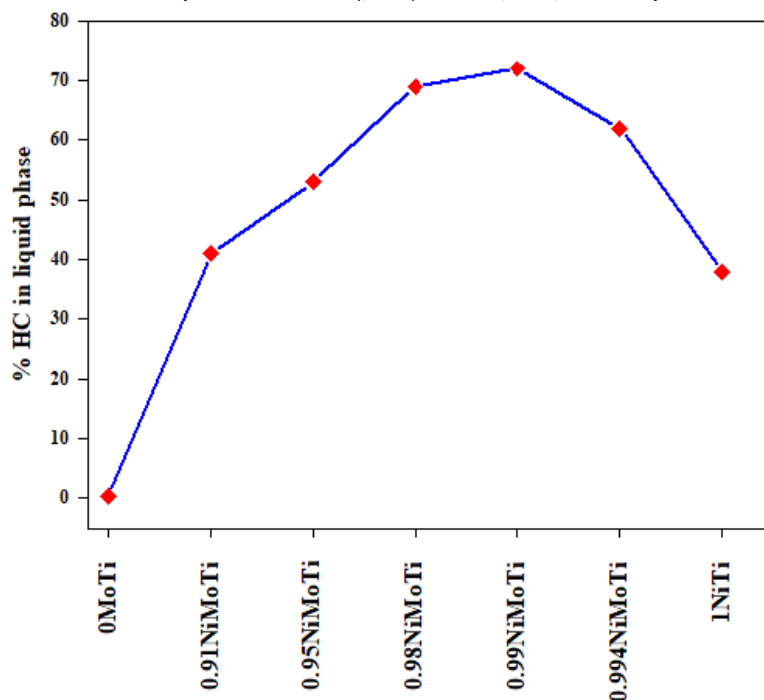


Figure 1. % Hydrocarbons in the liquid phase of the reaction over the various catalysts.

In conclusion, the NiMo/TiO<sub>2</sub> catalysts, evaluated under free solvent conditions and very high ratio of reactant volume to catalyst mass (100 mL /1 g), were proved very active and selective in the transformation of various oils of energy crops into green diesel.

#### References

1. S. Zhao, T. Brück, J.A. Lercher, *Green Chem.* **15**, 1720 (2013).
2. I. Kubickova, D. Kubicka, *Waste Biomass Valor.* **1**, 293 (2010).
3. Ch. Kordulis, K. Bourikas, M. Gousi, E. Kordouli, A. Lycourghiotis, *Appl. Catal. B* **181**, 156 (2016).
4. E. Kordouli, B. Pawelec, K. Bourikas, Ch. Kordulis, J.L.G. Fierro, A. Lycourghiotis, *Appl. Catal. B* **229**, 139 (2018).
5. G. Petropoulos, J. Zafeiropoulos, Ch. Kordulis, A. Lycourghiotis, K. Bourikas, *Int. J. Mechanical Production Eng.* **7**, 123, (2019).

## Fluidized bed gasification of solid digestate from anaerobic digestion plants – The THERMODIGESTATE project

Markos Charsoulas<sup>1</sup>, Dimitrios Mertzis<sup>1\*</sup>, Stefanos Tsiakmakis<sup>1</sup>, Zissis Samaras<sup>2</sup>

<sup>1</sup>Bio-based Energy Technologies PC, Ant. Tritsi 21, 55535 Thessaloniki Greece

<sup>2</sup>Lab of Applied Thermodynamics, Faculty of Engineering, Mech. Eng. Dpt., Aristotle University Thessaloniki, Greece  
jimmer@auth.gr

In anaerobic digestion (AD) biogas plants an average of 60% of the fed dry biomass exits the plant as digestate, which either has to be disposed as waste or is distributed, usually over long distances, as fertiliser. Both solutions involve high logistic costs and greenhouse gas emissions. To counter those difficulties, an innovative system for carbon-neutral energy production from solid digestate is proposed. The solid digestate fraction is characterized by high ash and moisture contents which makes it unsuitable for existing commercial utilization technologies such as downdraft fixed bed gasification systems due to the low ash melting point. In the THERMODIGESTATE project a small scale fluidized bed gasifier is used to convert the solid fraction of digestate from biogas plants into syngas for energy production. Through the adoption of the fluidized bed gasifier, fuels with high moisture and low ash melting points can be utilized as feedstocks. Process temperature in the fluidized bed reactor is kept below 850°C due to intense mixing between the biomass particles and the hot floating sand bed. The proposed system consists of a compact fluidized bed gasifier, a compact hot gas filtration unit and a, simple to maintain and operate, gas cooling system. The produced gas, free from particles and tars is suitable for use in the existing biogas plant gas engines to increase the plant efficiency. The ability to produce energy from biomass through gasification was validated and demonstrated during the Smart-CHP project [1]. The development of the current gasification system was carried out by “Bio-Based Technologies P.C.” (BIO2CHP), an Aristotle University of Thessaloniki (AUTH) spin-off company and was based on 10 years of research conducted at the Laboratory of Applied Thermodynamics of AUTH.

The proposed technology has already operated successfully utilizing olive kernels and grape pomace. The main difference with the solid digestate fraction is the low bulk density and significantly higher ash content of the fuel leading to higher fuel consumption for the same output. Preliminary tests were performed in an existing BIO2CHP pilot unit using densified solid digestate in the form of pellets. In those tests, mixtures of digestate pellets and olive kernels with varying composition were used. Olive kernels have extensively been used as a fuel before, thus limiting the risks of testing a whole new fuel. The results indicate that gasification with digestate is not very different from that with olive kernels, as presented in Figure 3. The main difference is that due to the lower heating value of the first, the heating value of syngas produced is also lower.

Table 3 Properties of olive kernels and digestate pellets used in the experiments

Parameter	Units	Olive kernels	Digestate pellets
Moisture	% wt (ar)	12.8	18.51
ash	% wt (db)	6.74	11.48
HHV	MJ/kg (db)	21.23	13.62
Carbon	% wt (db)	50.62	35.24
Hydrogen	% wt (db)	5.97	4.48
Oxygen	% wt (db)	33.41	40.6
Nitrogen	% wt (db)	2.31	1.18
Apparent density	g/cm <sup>3</sup>	0.65	1.12

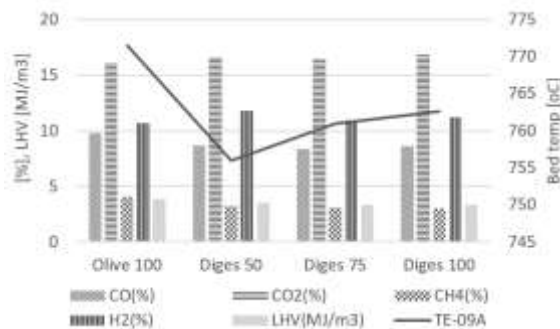


Figure 3 Syngas composition and heating value for different mixtures of olive kernels and digestate pellets

The THERMODIGESTATE project was primarily focused on designing, manufacturing and pilot testing of a modified gasification system suitable for the use of untreated solid digestate. The pilot operation took place at the biogas plant “BIOGAS LAGKADA S.A.”, which is a partner in the project and a technology end user. During the pilot operation, useful operation data were recorded in order to evaluate the efficiency of the system. The working conditions of the equipment (pressure, temperature, mass flows) were continuously monitored and chemical analysis for the feedstock, produced syngas and by-products (ash, condensates) were periodically performed. Finally, based on those data, efficiency metrics such as the potential of energy production from digestate, the expected annual working time of the system and its operational costs were defined.

### Acknowledgements

This research has been co-financed by the European Union and Greek national funds through the Operational Program Competitiveness, Entrepreneurship and Innovation, under the call RESEARCH – CREATE – INNOVATE (project code: T2EDK-05187)

### References

1. D. P. Mertzis, “Mobile biomass gasification unit coupled to an internal combustion engine - Design, realization and investigation:” 2013. doi: 10.26262/heal.auth.ir.133634

## Design approaches and mechanistic insights of molecular metal chalcogenides as H<sub>2</sub> evolution catalysts

Alexander Elliott<sup>1</sup>, James McAllister<sup>1</sup>, Alexey Ganin<sup>1</sup>, Nuno A. G. Bandeira,<sup>3</sup> Carles Bo<sup>2</sup>, and Haralampos N. Miras<sup>1\*</sup>

<sup>1</sup> WestCHEM, School of Chemistry, The University of Glasgow, Glasgow G12 8QQ (UK). <sup>2</sup> Institute of Chemical Research of Catalonia (ICIQ), The Barcelona Institute of Science and Technology, Avda. Països Catalans 16, 43007 Tarragona, Spain.

<sup>3</sup> BioISI – BioSystems and Integrative Sciences Institute, Faculdade de Ciências da Universidade de Lisboa, Campo Grande, 1749-016 Lisboa, Portugal.

\*Charalampos.miras@glasgow.ac.uk

With increased public awareness of the global challenge in relation to alternative clean energy sources, the requirement for novel materials with excellent electrochemical and/or photochemical performance to meet these needs has never been so crucial. Demand for energy is predicted to double by 2050, and although this soar in demand may still be met by fossil fuels, the associated increase in CO<sub>2</sub> emissions could have calamitous effects on the environment.[1] Utilization of hydrogen as energy source is a viable alternative to fossil fuels and is considered as one of the ideal energy carriers of the future. However, the sustainable electrochemical production of hydrogen presents a great challenge.

Metal chalcogenides have attracted tremendous research interest as they play a fundamental role in a wide range of important energy generation and storage applications including catalysis, photovoltaics, batteries and artificial photosynthesis systems.[2] 2D transition metal chalcogenides (TMCs) as well as molecular metal(oxy)chalcogenides present exciting opportunities in green, sustainable energy applications as they contain earth-abundant elements (typically 3d and 4d transition metals).[3] The main driving force behind this work is that many research efforts are focused on the discovery of new catalytic systems aiming to tackle challenging problems, yet little thought is given to the actual strategy and development of new modular systems and most importantly to the deeper understanding of the underlying system-specific processes. Exploring the potential of molecular materials and how can we take advantage of fine tuning of their behaviour is not common. This is due to practical issues related to their stability and/or scalability. In this regard chalcogenides are inorganic molecular units formed by metal centres which linked by chalcogen atoms. The question we try to address here: can we use a robust molecular species and dope it with other elements from the group of chalcogens? Will this improve the properties of the catalyst? Does the doping influence the stability of intermediate catalytic species or alter the mechanistic pathways and the interaction between the active sites and the substrate?

Here, we present an approach showing high efficiency and stability of molecular catalysts and our effort to tune these molecular species for the hydrogen evolution reaction.

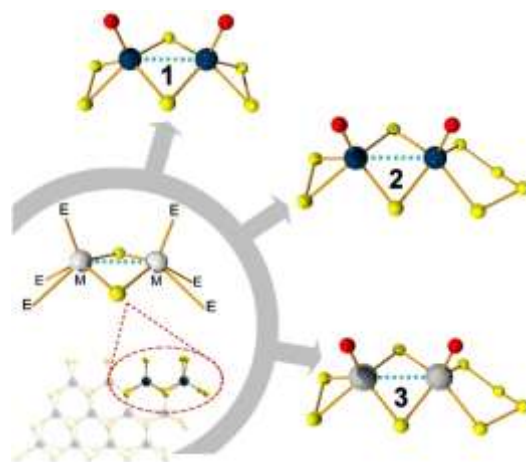


Figure 1. Ball-and-stick representation of representative molecular chalcogenide catalysts discussed here: (A)  $[\text{Mo}_2\text{O}_2(\mu\text{-S})_2(\text{S}_2)_2]^{2-}$  (1), (B)  $[\text{Mo}_2\text{O}_2(\mu\text{-S})_2(\text{S}_2)(\text{S}_4)]^{2-}$  (2) and (C)  $[\text{W}_2\text{O}_2(\mu\text{-S})_2(\text{S}_2)(\text{S}_4)]^{2-}$  (3). Where M: Mo or W and E: chalcogen atom. Colour code: Blue, Mo; Grey, W; yellow, S; red, O; green, N; black, carbon.

More specifically, we explore the fine tuning of molecular catalysts by controlling the stoichiometry and type of earth abundant elements, such as the chalcogen or metal and explore critical aspects of the hydrogen evolution reaction. Electrochemical and other analytical methods show that the employed stoichiometric and structural control leads to energetically efficient evolution of hydrogen, while the molecules responsible for this process remain intact during the course of the investigation. Linear sweep voltammetry (LSV) shows that stoichiometric and structural control lead to the evolution of hydrogen at low onset potential of just  $-114 \pm 3$  mV (at  $j = 10$  mA  $\text{cm}^{-2}$ ) with no catalyst degradation over 1000 cycles (Figure 2).

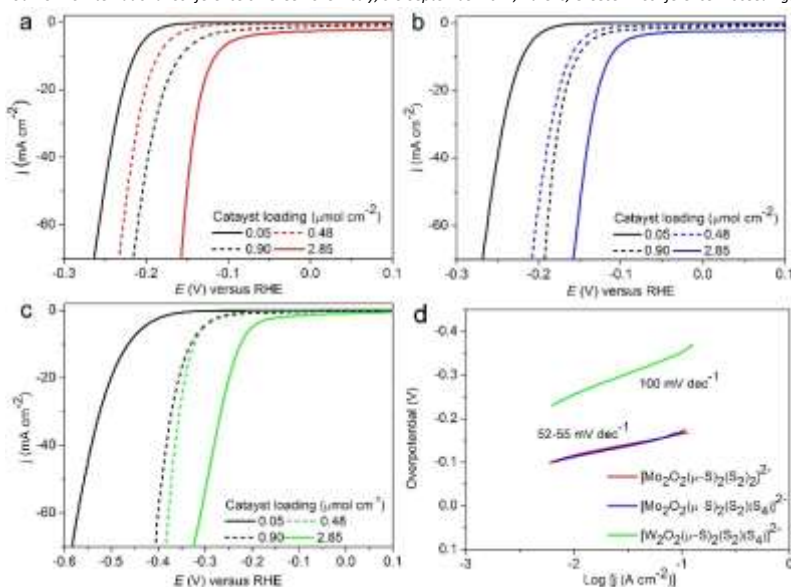


Figure 2. Electrochemical measurements of catalysts **1**, **2** and **3** for HER electrocatalysis in 1 M H<sub>2</sub>SO<sub>4</sub>. Observed polarisation curves as a function of the concentration of the catalyst: **a**. [Mo<sub>2</sub>O<sub>2</sub>(μ-S)<sub>2</sub>(S<sub>2</sub>)<sub>2</sub>]<sup>2-</sup>; **b**. [Mo<sub>2</sub>O<sub>2</sub>(μ-S)<sub>2</sub>(S<sub>2</sub>)(S<sub>4</sub>)]<sup>2-</sup>; **c**. [W<sub>2</sub>O<sub>2</sub>(μ-S)<sub>2</sub>(S<sub>2</sub>)(S<sub>4</sub>)]<sup>2-</sup>; **d**. corresponding Tafel plots.

Density functional calculations[4],[5] reveal the effect of the electronic and structural features and confer plausibility to the existence of a unimolecular mechanism in the HER process based on the tested hypotheses. Crucially, theoretical calculations reveal the effect of the electronic and structural features and provide vital information of the mechanism that potentially takes place in this case. The calculated HER protonation equilibria suggest a reversible cleavage and reformation of S-S or Se-Se bonds assisted by metal induced polarisation. Most importantly, the incorporation of the terminal oxo group seems to mitigate the negative charge density developed on the terminal sulfur or selenium centres due to its electronegativity and ability to form  $\pi$ -bonds. The molecular catalysts can be synthesized at gram scale and show great promise as earth-abundant alternatives for electrocatalytic hydrogen production. The results indicate that the tuning of efficient catalyst-substrate interaction is more important than the presence of a large number of catalytic sites. Our work is part of a worldwide effort towards a hydrogen-based economy. With a surfeit of oxo-chalcogenide clusters available, this work will help us understand further mechanistic aspects of molecular analogues' functionality and pave the way for the design of next-generation noble metal free HER catalysts. We anticipate these findings to be a starting point for further exploration of molecular catalytic systems and inspire others in an effort to tackle challenging scientific issues.

## Acknowledgements

The authors would like to thank EPSRC, the Carnegie Trust, the Spanish Ministerio de Economía y Competitividad, the Portuguese Foundation for Science and Technology and the University of Glasgow for supporting this work.

## References

1. N. S. Lewis, D. G. Nocera. *Proc. Natl. Acad. Sci. USA*, **103**, 15729 (2006).
2. M.-R. Gao, Y.-F. Xu, J. Jiang, S.-H. Yu, *Chem. Soc. Rev.* **42**, 2986 (2013).
3. J. McAllister, N. A. G. Bandeira, J. McGlynn, A. Ganin, Y.-F. Song, C. Bo, H. N. Miras *Nature Commun.* **10**, 370, (2019).
4. M. Álvarez-Moreno, C. de Graaf, N. López, F. Maseras, J. M. Poblet, C. Bo, *J. Chem. Inf. Model.* **55**, 95–103 (2015).
5. A data set collection of computational results is available in the ioChem- BD repository and can be accessed via <http://dx.doi.org/10.19061/iochem-bd-1-99>.

## Flame Spray Pyrolysis as a Synthesis Platform to Assess Metal Promotion in $\text{In}_2\text{O}_3$ -Catalyzed $\text{CO}_2$ Hydrogenation

Thaylan Pinheiro Araújo<sup>1</sup>, Jordi Morales-Vidal<sup>2</sup>, Tangsheng Zou<sup>1</sup>, Rodrigo García-Muelas<sup>2</sup>, Patrik O. Willi<sup>1</sup>, Konstantin M. Engel<sup>1</sup>, Olga V. Safonova<sup>3</sup>, Dario Faust Akl<sup>1</sup>, Frank Krumeich<sup>1</sup>, Robert N. Grass<sup>1</sup>, Cecilia Mondelli<sup>1</sup>, Núria López<sup>2\*</sup>, Javier Pérez-Ramírez<sup>1\*</sup>

<sup>1</sup>Institute of Chemical and Bioengineering, Department of Chemistry and Applied Biosciences, ETH Zurich, Vladimir-Prelog-Weg 1, 8093 Zurich, Switzerland

<sup>2</sup>Institute of Chemical Research of Catalonia (ICIQ), The Barcelona Institute of Science and Technology, Av. Països Catalans 16, 43007 Tarragona, Spain

<sup>3</sup>Paul Scherrer Institute, Forschungsstrasse 111, 5232 Villigen, Switzerland

\*nlopez@iciq.es, jpr@chem.ethz.ch

Back in 2016, indium oxide ( $\text{In}_2\text{O}_3$ ) was uncovered as a highly selective catalyst for the hydrogenation of carbon dioxide to green methanol, a key energy carrier and commodity supporting current worldwide efforts in its sustainable production *via* catalytic routes [1]. Since the ability of  $\text{In}_2\text{O}_3$  to activate  $\text{H}_2$  is limited, a plethora of metal promoters in various forms (nanoparticles of different sizes and down to single atoms) have been investigated to boost its activity, with variable outcomes [2-12]. However, metal promoters have been introduced on differently prepared  $\text{In}_2\text{O}_3$  using distinct synthetic methods and contents, and the resulting catalysts were tested under diverse conditions. This lack of systematic catalyst preparation and evaluation precludes a direct comparison of speciation and promotional effects among metal-promoted  $\text{In}_2\text{O}_3$  catalysts, which is key for the design of an optimal system. In this study, we employ flame spray pyrolysis (FSP) as a standardized synthesis method to introduce nine metal promoters ( $M = 0.5$  wt.%) to  $\text{In}_2\text{O}_3$  [13]. Methanol productivity generally increased on  $M$ - $\text{In}_2\text{O}_3$  with selectivity following  $\text{Pd} \sim \text{Pt} > \text{Rh} \sim \text{Ru} \sim \text{Ir} > \text{Ni} \sim \text{Co} > \text{Ag} \sim \text{In}_2\text{O}_3 > \text{Au}$  (Figure 1). In-depth characterization, kinetic analyses, and theoretical calculations reveal a range of metal-dependent speciation which dictate catalyst architecture and degree of promotion (Figure 2). The first encompasses systems containing atomically-dispersed and well-stabilized, mostly through  $M$ -In bonds, Pd, Pt, Rh, Ru, and Ir species on the  $\text{In}_2\text{O}_3$  surface, which reached a methanol selectivity of up to 95%. The second covers Co- and Ni- $\text{In}_2\text{O}_3$ , with a less boosted methanol selectivity (*ca.* 75%) owing to promoters forming large oxidic and indium alloy-containing clusters, respectively, and in the case of Co, to its partial incorporation into the bulk of  $\text{In}_2\text{O}_3$ . The third family includes Au and Ag, which sinter into nanoparticles, resulting in inferior or similar methanol selectivity (56 and 67%) to undoped  $\text{In}_2\text{O}_3$ , respectively. DFT simulations further elucidated that methanol formation is greatly enhanced over systems containing a high concentration of isolated promoter atoms, particularly Pd and Pt, owing to the creation of  $\text{In}_3M$  and  $\text{In}_2M_2$  ensembles, which strongly facilitate homolytic  $\text{H}_2$  splitting and increase the availability of hydrides, which in turn participate in C-H hydrogenations. As expected, the surface population of the active sites diminishes upon clustering or bulk incorporation of metal promoters such as Ni, Ag, and Co, thereby translating into inferior methanol productivity. Specifically, large Au nanoparticles block the active ensembles for  $\text{CO}_2$  hydrogenation and explains the low activity of Au- $\text{In}_2\text{O}_3$ .

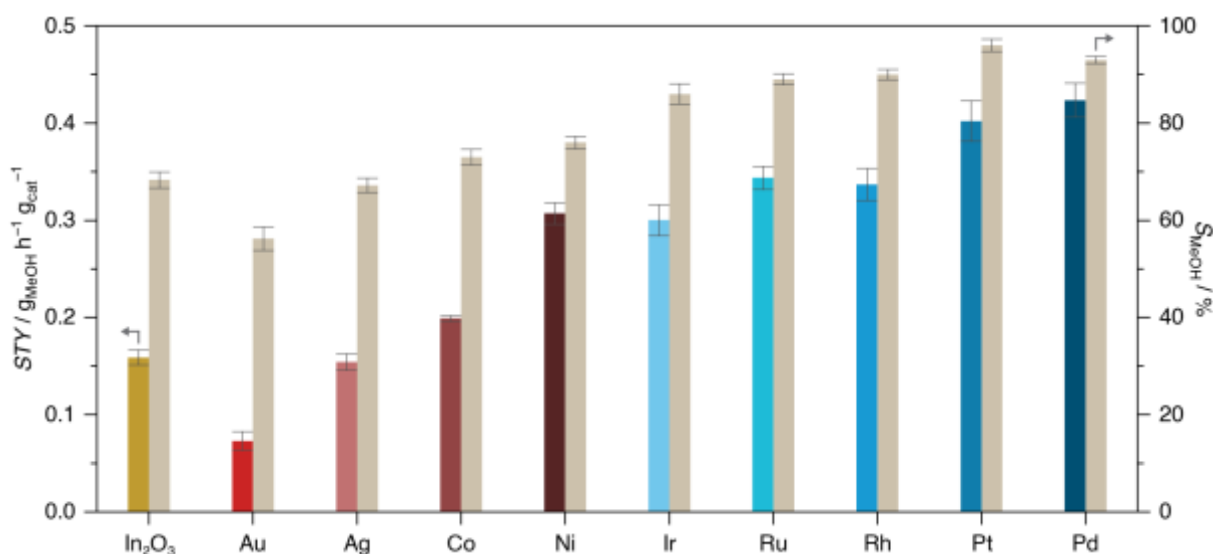


Figure 1. Methanol space-time yield (STY, colored bars) and selectivity ( $S_{\text{MeOH}}$ , beige bars) during  $\text{CO}_2$  hydrogenation over undoped  $\text{In}_2\text{O}_3$  and  $M$ - $\text{In}_2\text{O}_3$  catalysts (0.5 wt.% of metal) prepared by FSP. The methanol STY was assessed at  $GHSV = 24,000 \text{ cm}^3 \text{ h}^{-1} \text{ g}_{\text{cat}}^{-1}$ , while  $S_{\text{MeOH}}$  at constant  $\text{CO}_2$  conversion (*ca.* 3%) and variable  $GHSV$ . Averaged values measured over 24 h on stream are presented with their corresponding error bars. Reaction conditions:  $T = 553 \text{ K}$ ,  $P = 5 \text{ MPa}$ , and  $\text{H}_2/\text{CO}_2 = 4$ .















promoter	speciation	impact on performance	structural and mechanistic insights	
		$\Delta STY$  50–63%	$S_{MeOH}$  86–96%	<ul style="list-style-type: none"> <li>Atomically-dispersed promoter species</li> <li>High density of <math>In_3M</math> or <math>In_2M_2</math> ensembles</li> <li>Higher availability of MH</li> <li>MeOH formation favored</li> </ul>
		 20–48%	 73–76%	<ul style="list-style-type: none"> <li>Clustering and bulk incorporation of promoters</li> <li>Low density of <math>In_3M</math> or <math>In_2M_2</math> ensembles</li> <li>Lower availability of MH</li> <li>MeOH selectivity less boosted</li> </ul>
		 3–54%	 67–56%	<ul style="list-style-type: none"> <li>Sintering into nanoparticles</li> <li>Homolytic <math>H_2</math> splitting hindered</li> <li><math>Au_n</math> ensembles inhibit methanol formation</li> <li>CO formation favored</li> </ul>

Figure 2. Summary of promoter speciation and their associated structural-mechanistic features dictating performance of  $M$ - $In_2O_3$  catalysts.

Overall, this study marks a new step toward the atomic-level understanding of  $In_2O_3$  promotion by relevant metal promoters, revealing that the degree of promotion is metal speciation-dependent and likely dictated by the density and stability of space resolved  $In_3M$  and  $In_2M_2$  ensembles. This offers key guidelines for the design of an optimal system to propel green methanol production. Going beyond  $CO_2$  hydrogenation, our strategy to engineer promotion using a universal and scalable preparation method such as FSP holds great potential for tailoring new or existing catalytic systems applicable in diverse energy conversions

### Acknowledgements

This study was created as part of NCCR Catalysis, a National Centre of Competence in Research funded by the Swiss National Science Foundation. The Scientific Center for Optical and Electron Microscopy (ScopeM) at the ETH Zurich and the SuperXAS beamline at PSI, are thanked for access to their facilities. We are grateful to Prof. Christophe Copéret, Dr. Gina Noh, and Mr. Jan Alfke for assistance with sample preparation for XAS measurements. T.Z. thanks the Agency for Science, Technology and Research (A\*STAR) Singapore for support through a graduate fellowship. The Spanish Ministry of Science and Innovation is acknowledged for financial support (RTI2018-101394-B-I00 and Severo Ochoa Grant CEX2019-000925-S) and the Barcelona Supercomputing Center-MareNostrum (BSC-RES) for providing generous computer resources.

### References

- O. Martín, A. J. Martín, C. Mondelli, S. Mitchell, T. F. Segawa, R. Hauert, C. Drouilly, D. Curulla Ferré, J. Pérez-Ramírez, *Angew. Chem. Int. Ed.* **55** 6261 (2016).
- M. S. Frei, M. Capdevila-Cortada, R. García-Muelas, C. Mondelli, N. López, J. A. Stewart, D. Curulla Ferré, J. Pérez-Ramírez, *J. Catal.* **361** 313 (2018).
- N. Rui, Z. Wang, K. Sun, J. Ye, Q. Ge, C. J. Liu, *Appl. Catal. B* **218** 488 (2017).
- M. S. Frei, C. Mondelli, R. García-Muelas, K. S. Kley, B. Puértolas, N. López, O. V. Safonova, J. A. Stewart, D. Curulla Ferré, J. Pérez-Ramírez, *Nat. Commun.* **10** 3377 (2019).
- Z. Han, C. Tang, J. Wang, L. Li, C. Li, *J. Catal.* **394** 236 (2021).
- K. Sun, N. Rui, Z. Zhang, Z. Sun, Q. Ge, C. J. Liu, *Green Chem.* **22** 5059 (2020).
- J. Wang, K. Sun, X. Jia, C. J. Liu, *Catal. Today*, **365** 341(2021).
- Q. Wu, C. Shen, N. Rui, K. Sun, C. J. Liu, *J. CO<sub>2</sub> Util.* **53** 101720 (2021).
- C. Shen, K. Sun, Z. Zhang, N. Rui, X. Jia, D. Mei, C. J. Liu, *ACS Catal.* **11** 4036 (2021).
- N. Rui, F. Zhang, K. Sun, Z. Liu, W. Xu, E. Stavitski, S. D. Senanayake, J. A. Rodriguez, C. J. Liu, *ACS Catal.* **10** 11307 (2020).
- N. H. M. Dostagir, C. Thompson, H. Kobayashi, A. M. Karim, A. Fukuoka, A. Shrotri, *Catal. Sci. Technol.* **10** 8196 (2020).
- A. Bavykina, I. Yarulina, A. J. Al Abdulghani, L. Gevers, M. N. Hedhili, X. Miao, A. R. Galilea, A. Pustovarenko, A. Dikhtiarenko, A. Cadiau, A. Aguilar-Tapia, J.-L. Hazemann, S. M. Kozlov, S. Oud-Chikh, L. Cavallo, J. Gascon, *ACS Catal.* **9** 6910 (2019).
- T. Pinheiro Araújo, J. Morales-Vidal, T. Zou, R. García-Muelas, P.O. Willi, K.M. Engel, O. V. Safonova, D. Faust Akl, F. Krumeich, R.N. Grass, C. Mondelli, N. López, J. Pérez-Ramírez, *Adv. Energy Mater.* **12** 2103707 (2022).

## Combustion induced multicomponent Cu based catalysts for CO/CO<sub>2</sub> hydrogenation to methanol in three-phase system: Experimental and Theoretical Insights

Vaibhav Pandey<sup>1</sup>, K.K. Pant<sup>2\*</sup>, Sreedevi Upadhyayula

Department of Chemical Engineering, Indian Institute of Technology Delhi, 110016, India

\*Corresponding Author: kkpant@chemical.iitd.ac.in

### Abstract:

Greenhouse gases (GHG) have resulted in adverse climatic conditions impacting humankind and an abundant challenge to reduce the emission. Effective utilization of GHG and finding an alternative cleaner source of energy is a need of an hour. CO and CO<sub>2</sub> hydrogenation to methanol is a one-step-two-target approach to solve climate change and energy deficient challenges of the world. Methanol, an alternative source of hydrogen as well as basic raw material for petrochemical industries, also serves as a fuel, solvent, and energy storage medium and has a great scope in the future. The synergistic interaction between small copper particles and ZnO/MgO supported catalysts synthesized by solvent combustion method, shows a high methanol production rate in the liquid-phase low-temperature methanol synthesis from coal-derived syngas. The possibility of an autocatalytic reaction pathway in slurry reactors was investigated. The space-time yield of methanol (STY) showed a linear relationship with Cu<sup>0</sup> surface area Cu particle size. The effect of various parameters and solvents' effect on CO adsorption in the methanol synthesis reaction was also investigated. Catalytic activity was correlated by the various characterization of catalytic systems like X-Ray Diffraction, Scanning Electron Microscope-Energy Dispersive Spectroscopy, High Resolution- Transmission Electron Microscopy, Temperature-Programmed Reduction, N<sub>2</sub> physisorption, and N<sub>2</sub>O chemisorption techniques. 6CuZnOMgO catalyst shows maximum conversion (45%), selectivity (>99%) at 50 bar pressure, and 240 °C temperature due to larger Cu<sup>0</sup> surface area and greater specific surface area. In addition, Density Functional Theory (DFT) studies of CO adsorption on the tetrahedral Cu<sub>4</sub> cluster on two different supports' (MgO and ZnO) interface were investigated for a better understanding of the promoting effect of MgO on CO activation.

### Experimental:

#### • Catalyst synthesis:

Catalysts are synthesized by the solvent combustion method using organic fuel adopted from [1]. Typically, Cu-ZnO, Cu-MgO, Cu-ZnO-MgO catalysts were prepared from Copper nitrate trihydrate, zinc nitrate hexahydrate, magnesium nitrate. The initial mixture was stirred to form a homogeneous aqueous solution and heated for 2 hours at 50 °C to obtain a slurry. After being heated overnight at 110 °C, the paste was combusted in a muffle furnace at 350 °C for 4 h to produce combusted carbon-free powder.

#### • Activity test:

CO hydrogenation reaction was carried out in a stainless-steel stirred tank slurry reactor with 300 ml volume in continuous mode with a typical 5 weight % slurry concentration in diglyme solvent. Prior to the reaction catalyst was reduced in hydrogen environment at 15 bar and 250 °C for 6 hours at 400 rpm stirring speed. The reactor was cooled to ambient temperature and purged with syngas (CO/H<sub>2</sub>= 0.5) and pressurized up to 50 bar pressures at a gas flow rate of 100 sccm (GHSV = 2564 ml g<sub>cat</sub><sup>-1</sup> h<sup>-1</sup>). The reactor was heated to 220 °C while maintaining the pressure at 50 bar using back pressure regulator. The effluent gaseous products were analyzed using Gas Chromatograph (Agilent technologies 8860 GC) with flame ionization (FID) and thermal conductivity detectors (TCD) and liquid products were analyzed by ALS equipped Gas Chromatograph (Agilent technologies 7820A GC) with flame ionization detector (FID). The syngas conversion and product selectivity were calculated from the following relationships:

$$\% \text{ CO conversion } (X_{\text{CO}}) = \frac{\text{CO}_{\text{in}} - \text{CO}_{\text{out}}}{\text{CO}_{\text{in}}} * 100$$

$$\% \text{ Selectivity}_P = \frac{\text{Total moles of P formed}}{\text{Total moles of CO reacted}}$$

### Results and Discussion:

**XRD:** Powder X-ray Diffraction was used to identify the crystallinity of the calcined catalysts, where all the catalysts showed higher crystallinity. The 6CuZn and 6CuMg showed the characteristic peaks of ZnO, MgO, and also several facets of CuO (JCPDS Card no. 89-5896). The 2θ peaks at 31.8, 35.5, 38.7, 48.8, 58.3 shows the peaks of CuO. the calcined catalysts shows the CuO, ZnO and MgO peaks, indicating that dried precursors were decomposed to CuO, ZnO and MgO. 6CuZnMg shows broader peaks which corresponds to smaller crystallite size than other catalysts. Moreover, the CuO peaks are shifted toward lower angle, corresponds to Cu<sup>+</sup> ions are replaced by Zn<sup>+</sup> ions. However, CuO peaks are shifted towards higher angle in the case of MgO. This is the indication of Mg<sup>+</sup> ions replaced the Zn<sup>+</sup> ions.

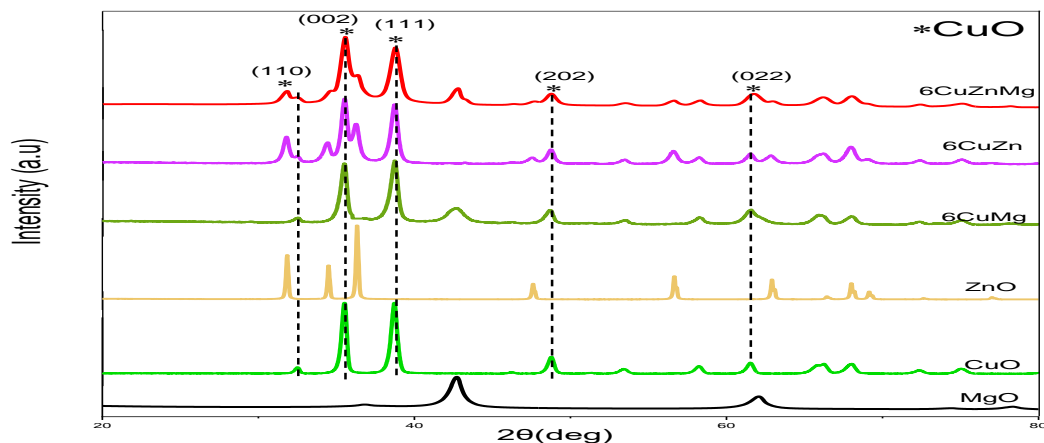
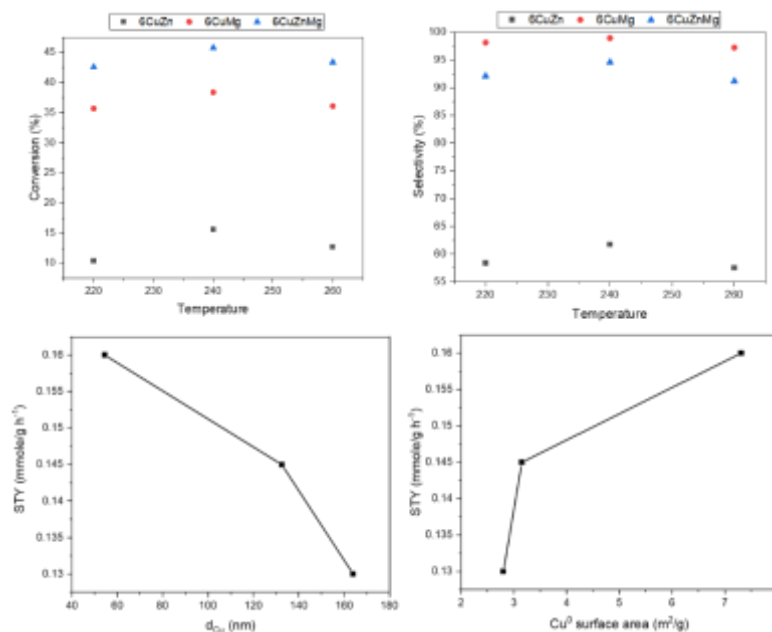


Figure1: XRD of the calcined catalysts

**Activity Test:** The activity of the CuZnOMgO catalyst was measured at different reaction temperatures. The effect of temperature on syngas conversion, and methanol selectivity, was tested in the range of 220-260 °C, and it was found that CuZnOMgO catalyst showed an increase of syngas conversion and methanol selectivity up to 240 °C then decrease for 260 °C. results, it is evident that the presence of both MgO and ZnO played a significant role in CO activation and higher methanol selectivity. Metallic Cu surface area and particle size affects the activity. Higher dispersion, lower particle size and higher CuO surface area of CuZnOMgO results in higher productivity of methanol. Along with these properties, slurry weight % also enhances the productivity of the methanol. As the concentration of the slurry wt% increases, the STY of the methanol increases. Higher Cu content and dispersion can be one of the reasons for better productivity of the methanol.

Figure2: Activity test of the catalysts at 220-260 °C, 50 bar, 1000 rpm, and GHSV = 2564 ml  $g_{cat}^{-1}h^{-1}$ .

## Acknowledgements

Authors thankfully acknowledge the Department of Science and Technology, Government of India under Technology (Sanction no. (RP03506G) TMD/CERI/MDME/2017/001 and (RP03817G) TM/EWO/MI/CCUS/19C), Science and Engineering Research Board, Thermax Ltd, and Federation of Indian Chambers of Commerce & Industry for providing financial support.

## References

- [1] Benzen Yao, Tiancun Xia, Ofentse A. Makgae, Xiangyu Jie, Sergio Gonzalez-Cortes, Shaoliang Guan, Angus I. Kirkland, Jonathan R. Dilworth, Hamid A. Al-Megren, Saeed M. Alshihri, Peter J. Dobson, Gari P. Owen, John M. Thomas & Peter P. Edwards, Nature Communication, **11**, 6395 (2020)

## Plasma assisted conversion of CO<sub>2</sub> and CH<sub>4</sub> over promoted catalysts: Comprehension of surface effects

Shengfei Wang<sup>1</sup>, Vandad Rohani<sup>1\*</sup>, Tongqi Ye<sup>2</sup>, Paul Dupont<sup>1</sup>, Sylvain Pagnon<sup>1</sup>, Laurent Fulcheri<sup>1</sup>

<sup>1</sup>MINES ParisTech, PSL University, Centre Procédés Energies Renouvelables et Systèmes Energétiques (PERSEE), 06904 Sophia Antipolis, France

<sup>2</sup>Anhui Province Key Laboratory of Advanced Catalytic Materials and Reaction Engineering, School of Chemistry and Chemical Engineering, Hefei University of Technology, Hefei, Anhui, 230009 P.R. China

\* e-mail address of corresponding author (Vandad Rohani): vandad-julien.rohani@mines-paristech.fr

### Abstract text:

The large amount of anthropic greenhouse gases (GHG) emission is becoming a serious issue. Dry reforming of methane draws attention since it could not only eliminate two major GHG but also produce valuable chemicals at the same time from them. However, these molecules are thermodynamically stable and require hard conditions to be activated. Non-thermal plasmas (NTP), which are generated under strong electric fields, provide an interesting manner to convert these molecules at ambient conditions by a direct electrical way. NTP are able to electrically produce many reactive species (ions, excited states, radicals). Among them, vibrationally and electronically excited species play an important role because they lower the activation barrier and lead to more efficient global reactions. Most of the works reported in literature on GHG conversion by plasma focus on syngas production but traces of coproducts such as hydrocarbons, alcohols, and organic acids are generally also produced [1,2]. However, the main gaseous organic hydrocarbons obtained until now are ethane and propane which are far less important than unsaturated hydrocarbons in chemical industry. Try to produce molecules other than saturated hydrocarbons is thus a real challenge. Anyway, increase the share of coproducts in the final composition to move toward new processes able to directly convert CO<sub>2</sub>/CH<sub>4</sub> into higher added-value molecules (synthetic fuels or chemicals) has a great interest. In that case, a heavy two-steps process chain consisting in production of syngas then production of synfuels/chemicals could be replaced by a simpler one-step one consisting in direct production of synfuels/chemicals under conditions close to ambient ones. Whereas there are few works focusing on the direct synthesis of high added-value hydrocarbons (e.g., ethene) in plasma surroundings, we developed a new hybrid NTP-catalytic process for the production of value-added unsaturated hydrocarbons and oxygenates.

We prepared the potassium (K) modified Fe-based catalysts according to the reported MOF mediated synthesis approach [3]. Then the catalysts were tested by our home-made plasma fixed bed reactor [1]. The selectivity of products, especially hydrocarbons, were analyzed to show the role of catalysts and promoters. Temperature-programmed desorption (TPD) tests were carried out and illustrated the modification of surface properties after introducing the potassium.

The catalysts exhibit synergistic effects during plasma catalytic process and considerably tune the selectivity of H<sub>2</sub>, CO and liquid oxygenates while decrease the conversion rate slightly. The molar ratio of unsaturated hydrocarbons to saturated hydrocarbons (U/S ratio) and molar ratio of H<sub>2</sub> to CO (H/C ratio) are shown in Figure 1. The unsaturated hydrocarbons products are negligible in the plasma-only process while the K promoted catalysts further improve the unsaturated hydrocarbons production. For Fe-SiO<sub>2</sub> and Fe/C-SiO<sub>2</sub> catalysts, the U/S ratio (represent the molar ratio of ethylene and acetylene to ethane) is 0.19 and 0.07 respectively, nevertheless the U/S ratios rise to 0.35 and 0.90 using K-Fe-SiO<sub>2</sub> and K-Fe/C-SiO<sub>2</sub> catalysts. The H/C ratio increases to around 2.0 which is the most desirable gas composition in F-T synthesis while packing K-Fe/C-SiO<sub>2</sub> catalyst.

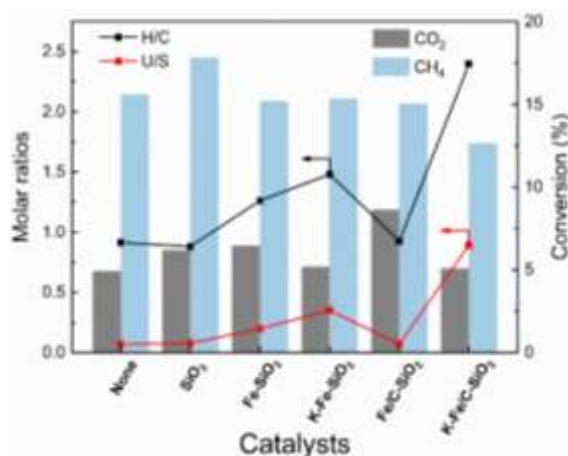


Figure 1. H<sub>2</sub>-TPD profiles of the (a) Fe-SiO<sub>2</sub> and K-Fe-SiO<sub>2</sub>, (b) Fe/C-SiO<sub>2</sub> and K-Fe/C-SiO<sub>2</sub> catalysts.

The CO<sub>2</sub>-TPD results elaborate the influence of K on the CO<sub>2</sub> adsorption properties. As shown in Figure 2, the selected iron-based catalysts exhibit 2 peaks in the temperature range of 100–200 °C and 500–600 °C, which are

ascribed to the desorption of CO<sub>2</sub> on weak and strong basic sites respectively. After the introduction of K promoters, we observed that the desorption peak of CO<sub>2</sub> is much lower since K promoters covered the surface basicity of catalysts. The decreased surface basicity of Fe/C catalysts could correspond to the slight decrease of conversion.

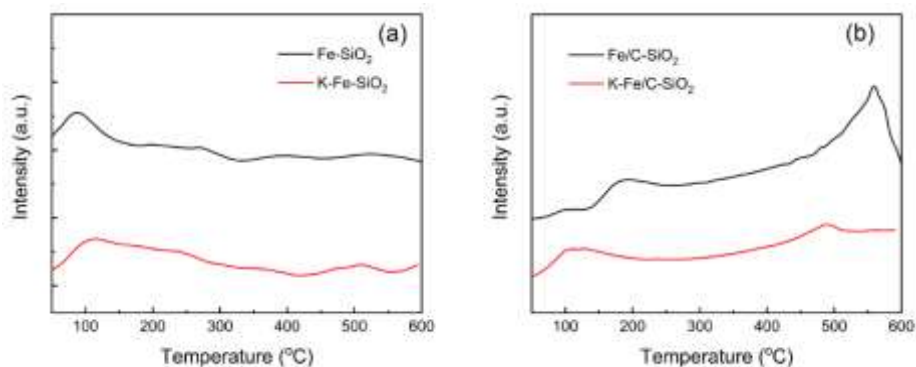


Figure 2. CO<sub>2</sub>-TPD profiles of the (a) Fe-SiO<sub>2</sub> and K-Fe-SiO<sub>2</sub>, (b) Fe/C-SiO<sub>2</sub> and K-Fe/C-SiO<sub>2</sub> catalysts.

The addition of promoters also could suppress the adsorption strength and amount of H<sub>2</sub>. Figure 3 indicates that H<sub>2</sub> adsorption capacity decreased markedly after the modification of K which is in line with the previous literatures. The desorption peak shift to a lower temperature on the K modified surface. According to the reported H<sub>2</sub> chemisorption analysis [3,4], the amount of H<sub>2</sub> adsorption decreased sharply after K promotion while the chemisorption of CO is improved. Owing to less surface H adsorbed on the catalysts, the value-added unsaturated hydrocarbons, formed in the plasma surrounding, would be less converted into the saturated hydrocarbons via the hydrogenation [5].

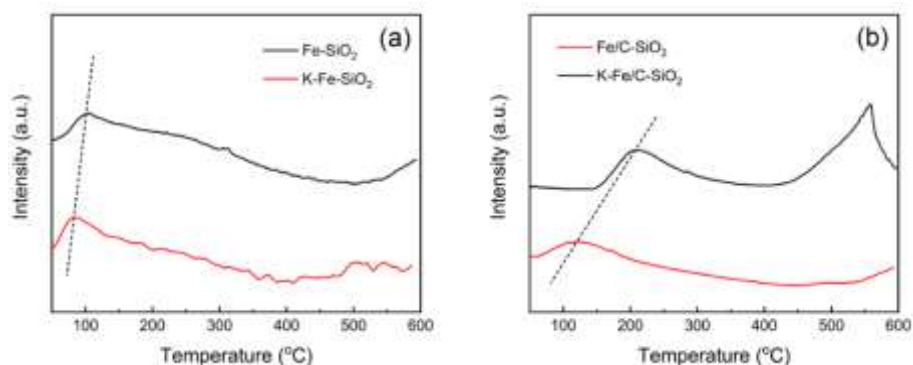


Figure 3. H<sub>2</sub>-TPD profiles of the (a) Fe-SiO<sub>2</sub> and K-Fe-SiO<sub>2</sub>, (b) Fe/C-SiO<sub>2</sub> and K-Fe/C-SiO<sub>2</sub> catalysts.

The plasma-catalytic process considerably tunes the selectivity of H<sub>2</sub>, CO and liquid oxygenates. The highest U/S ratio is 0.90 using K-Fe/C-SiO<sub>2</sub> catalysts while the H/C ratio increases to around 2.0 which is the most desirable. The modification of K promoters adjusted the surface adsorption and basic properties which is attributed to the improvement of certain products selectivities.

## Acknowledgements

This work was supported by MINES ParisTech, Université PSL and Institut Mines-Télécom. Shengfei Wang thanks them for their contribution and support to his PhD scholarship.

## References

1. D. Li, V. Rohani, F. Fabry, A. P. Ramaswamy, M. Sennour, L. Fulcheri, Direct conversion of CO<sub>2</sub> and CH<sub>4</sub> into liquid chemicals by plasma-catalysis, *Appl. Catal. B: Environ.* **261** (2020).
2. R. Snoeckx, A. Bogaerts, Plasma technology - a novel solution for CO<sub>2</sub> conversion? *Chem. Soc. Rev.* **46** (2017).
3. A. Ramirez, L. Gevers, A. Bavykina, S. Ould-Chikh, J. Gascon, Metal Organic Framework-Derived Iron Catalysts for the Direct Hydrogenation of CO<sub>2</sub> to Short Chain Olefins *ACS Catal.* **8** (2018).
4. Y. Han, C. Fang, C. Fang, X. Ji, J. Wei, Q. Ge, J. Sun, Interfacing with Carbonaceous Potassium Promoters Boosts Catalytic CO<sub>2</sub> Hydrogenation of Iron, *ACS Catal.* **10** (2020)
5. W. Wang, X. Jiang, X. Wang, C. Song, Fe-Cu Bimetallic catalysts for selective CO<sub>2</sub> hydrogenation to olefin-rich C<sub>2</sub>+ hydrocarbons, *Ind. Eng. Chem. Res.* **57** (2018).

## Tuning the structural and catalytic active sites of TiO<sub>2</sub>/CeO<sub>2</sub> for CO<sub>2</sub> conversion to synthesize a green fuel additive

Praveen Kumar<sup>1,\*</sup>, Urška Lavrenčič Štangar

<sup>1</sup>Faculty of Chemistry and Chemical Technology, University of Ljubljana, 1000 Ljubljana, Slovenia

\*e-mail: Praveen.Kumar@fkt.uni-lj.si; praveen@engineering.ucsb.edu

Carbon dioxide (CO<sub>2</sub>) is mainly discussed negatively as a greenhouse gas and the main cause of anthropogenic climate change. Recently, CO<sub>2</sub> has received increased attention as an abundant carbon resource and readily available raw material, rather than being treated as an environmentally harmful greenhouse gas. In recent decades, the utilization of CO<sub>2</sub> has attracted the attention of scientific groups, especially those studying industrial and environmental processes. In this direction, CO<sub>2</sub> has been a renewable C1 feedstock for high-value chemicals in recent times. Among various strategies, the carbonylation of alcohols with CO<sub>2</sub> is attractive for the synthesis of alkyl carbonates [1,2].

Our main focus has been on the synthesis of TiO<sub>2</sub>/CeO<sub>2</sub>-based catalysts using a combined exo- and endo-template approach, which are more industrially applicable due to higher activities and lower costs. In this work, the effects of the Ti/Ce molar ratio on the surface properties and structure of the TiO<sub>2</sub>/CeO<sub>2</sub> catalyst, the reaction conditions, and the reusability study of the catalyst for direct conversion of CO<sub>2</sub> were investigated. The catalytic activity of the synthesized TiO<sub>2</sub>/CeO<sub>2</sub> catalysts was closely related to the basic and acidic sites. The basic sites are responsible for CO<sub>2</sub> activation and methoxy group formation, while the acidic sites are responsible for methanol activation in the reaction. Moreover, the reaction mechanism was proposed for dimethyl carbonate synthesis in the conversion of CO<sub>2</sub> with methanol. Optimization of reaction conditions was studied batch-wise reactor at different reaction parameters such as reaction temperature, catalyst dose, and reaction time. The reusability of TiO<sub>2</sub>/CeO<sub>2</sub> catalysts was also investigated. In addition, the heat of reaction and Gibbs free energy were carried out using chemical equilibrium modeling. The relationships between the structure of TiO<sub>2</sub>/CeO<sub>2</sub> and their catalytic activity have created a need for new preparation routes for improved surface properties.

To investigate the Dimethyl carbonate synthesis in presence of synthesized TiO<sub>2</sub>/CeO<sub>2</sub>-based catalysts are shown in Fig. 1.

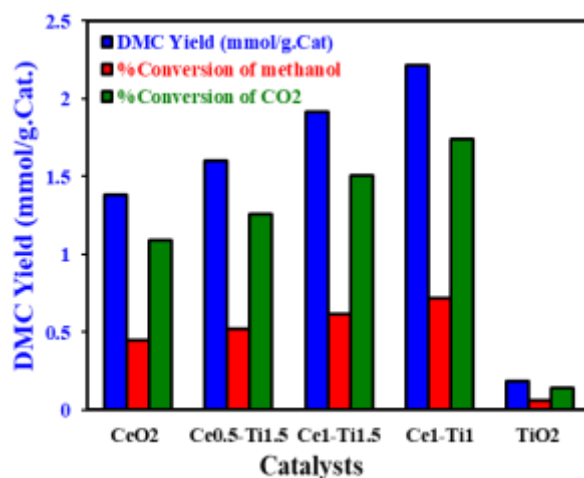


Fig. 1. DMC synthesis from direct conversion of CO<sub>2</sub> and methanol in presence of TiO<sub>2</sub>/CeO<sub>2</sub>-based catalysts

### Acknowledgments

This work was supported by the Ministry of Education, Science and Sports, Slovenia (EU Grant C3330-19-952015), Slovenian Research Agency "Chemistry for Sustainable Development (P1-0134)" and Bilateral Research Project N2-0188.

### References

1. P. Kumar, V.C. Srivastava, U.L. Štangar, B. Mušič, I.M. Mishra, Y. Meng, *Catalysis Reviews*, **63** 363-421 (2021).
2. J.D. Medrano-Garcia, J. Javaloyes-Anton, D. Vazquez, R. Ruiz-Femenia, J.A. Caballero, *Journal of CO<sub>2</sub> Utilization* **45** 101436 (2021).

## Single step synthesis of bio-inspired NiO/C as Pd support catalyst for direct ethanol fuel cell application

Xolile Fuku<sup>\*a</sup>, Mmalewane Modibedi<sup>b</sup>, Nolubabalo Matinise<sup>c</sup>,  
Mkhulu Mathe<sup>a</sup>

<sup>a</sup>*Institute of Nanotechnology and Water Sustainability, College of Science,  
Engineering and Technology, University of South Africa, Florida Science Campus,  
1710, South Africa*

<sup>b</sup>*CSIR Energy Materials, PO Box 395, Pretoria 0001, South Africa*

<sup>c</sup>*Nanosciences African Network (NANOAFNET), Materials Research Department, iThemba LABS-National Research  
Foundation of South Africa, Old Faure Road,  
corresponding Author: Dr Xolile Fuku, \*email: [fukuxg@gmail.com](mailto:fukuxg@gmail.com)*

There is a tremendous interest on ethanol beneficiation as it is largely produced from crops, and it is regarded as a potential candidate for low temperature fuel cell applications. Although ethanol possesses good advantages, its resistant to oxidation poses a threat [1]. The main objective of the study is to synthesis bio-inspired metal oxide–support catalyst which will help enhance the activity, and efficiency of Pd catalyst in Fuel cell performance as well as ethanol oxidation. Here, Pd nanoparticles were supported on NiO/C through a green facile one-step process using pomegranate peel extracts as reducing agent. A series of characterizations were carried out to provide proof for and to quantify the presence of Pd, Ni, O and C in the prepared sample. Microscopic methods confirmed the successful preparation of pure NiO/C and (%5 Pd) Pd-NiO/C, evident by the key elemental components, mixed nanostructures and co-existence of Pd and NiO/C. The resultant Pd-NiO/C nanocatalyst revealed higher activity towards the oxidation of ethanol and that the nanocatalyst is more tolerant to poisoning by intermediate oxidation species. Enhanced cell performance with current and power densities of 66 mA cm<sup>-2</sup> and 26mWcm<sup>-2</sup> relative to the commercial Pd/C were obtained under passive conditions at 1 M ethanol in 1MKOH. While the cell output was 117 mW.

**Keywords:** Green synthesis, Electrocatalyst, Metal oxides, Ethanol electro-oxidation, Alkaline anion exchange membrane fuel cells

### Acknowledgements

The authors are thankful to the CSIR and NRF for funding. We acknowledge the support extended by iThemba Labs, the Department of Materials Division (MRD) and CSIR-Energy material's unit for providing us with state-of-the-art facilities and instrumentation.

### References

[1] R. Modibedi, T. Mehlo, K. Ozoemena, M. Mathe, Synthesis, characterization and application of Pd-based nanoelectrocatalyst in the Alkaline Direct Ethanol Fuel Cell (ADEFC), *Int. J. Hydrogen Energy* 40 (2015) 15605–15612.

## Methane oxidation using earth abundant metals anchored on nodes of a metal-organic framework

Manav Chauhan<sup>1</sup> and Kuntal Manna<sup>1\*</sup>

<sup>1</sup>Department of Chemistry, Indian Institute of Technology, New Delhi, India

\*[kmanna@chemistry.iitd.ac.in](mailto:kmanna@chemistry.iitd.ac.in)

Natural gas is primarily used for domestic cooking/heating, conversion to syn-gas via reforming, and transportation fuels in the form of compressed natural gas (CNG). Methane is the major component of natural gas, and the transportation of natural gas over long distances is economically challenging. Methane leaks from petrochemical industry and coal reserves have risen about 2.5 folds since the pre-industrial times. The industries rather flare this methane into carbon dioxide so that it has less harmful impact on the environment. A total of 143 billion m<sup>3</sup> of methane was flared back in 2012 which would have a market value of 14,000 crores.<sup>1</sup> A solution to this problem is the oxidation of methane into its oxygenates like ethanol, acetic acid and primarily methanol. The use of methanol as a fuel or a fuel additive has increased a lot in the past. A number of alternate technologies and routes are being developed in addition to the traditional two-step syngas route for the synthesis of methanol from methane via steam-reforming process which itself is a temperature and pressure extensive process.<sup>2</sup> We have synthesized a highly active single-site earth abundant metal catalyst supported on a zirconium based metal-organic framework (MOFs) for oxidation of methane to methanol with a very high selectivity. MOFs have recently emerged as an interesting class of porous and tunable molecular material for developing robust and chemoselective single-site base-metal catalysts. MOFs are built from metal-oxo clusters based secondary building units (SBUs) and organic linkers that hold the properties of tunability and reticular synthesis.<sup>3-5</sup> Moreover, MOF-supported catalysts combine both the advantages of homogeneous catalysts such as homogeneity of the active sites, reproducibility and selectivity, and heterogeneous counterparts such as high stability, facile catalyst separation and recovery. This direct approach to methanol production could be adopted not just at mining or refinery sites but also at remote agricultural farmlands which account for about 32% of the total man-made methane emissions.

UiO-66 MOF having the formula of  $Zr_6(\mu_3-OH)_4(\mu_3-O)_4(C_8O_4H_4)_6$  is constructed from zirconium oxide as SBUs and benzene dicarboxylic acid (bdc) as organic linkers via a solvothermal reaction of  $ZrCl_4$  with benzene dicarboxylic acid in DMF at 100 °C for 15 minutes. Deprotonation of  $\mu_3-OH$  with *n*-BuLi was followed by post-synthetic metalation of lithiated UiO-66 with different earth abundant metals. They were tested for methane oxidation, out of which UiO-66-Co turned out to be highly selective and productive. The catalyst was highly effective for the oxidation of methane into C-1 and C-2 oxygenates. Selectivity of over 98% was observed for alcohol formation. 514 m<sup>2</sup>/g of BET surface area was observed for UiO-66-Co in comparison to 808 m<sup>2</sup>/g of UiO-66. BET pore size was 0.57 nm. The cobalt active center was tetra-coordinated with one Cl, two carboxylate O and one  $\mu_4-O$  at 1.94, 1.84, 2.10 and 2.04 respectively as determined by EXAFS and DFT simultaneously. Other characterizations including PXRD, XANES, and TEM were also performed. The uniform distribution of Zr and Co particles throughout the MOF was confirmed by scanning electron microscopy (SEM)-energy-dispersive X-ray (EDX) mapping. The  $Co^{+2}$  edge energy was about 5 eV higher than  $CoCl_2$  indicating higher than +2 oxidation state. All the reactions were performed using 50 mL Parr pressure vessels (4793 (VGR)-T-SS-3000-DVD). The liquid products were analyzed using HPLC equipped with a refractive index detector using a Hi-Plex-H column. The gaseous products were analyzed using gas chromatography (GC) equipped with a mass detector (Agilent 5977B GC/MSD) and a TCD detector.

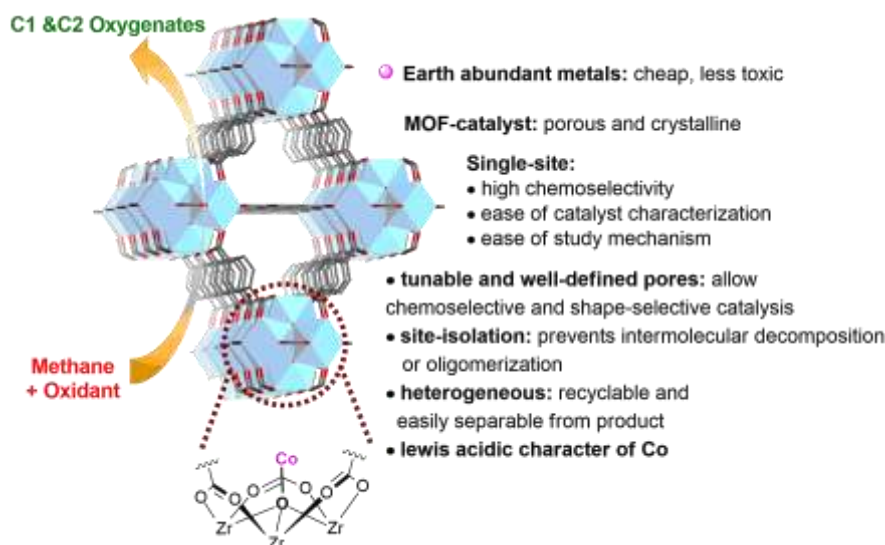


Figure 1. Earth abundant metals anchored onto the SBUs of UiO-66 MOF



We have synthesized a UiO-66 MOF supported cobalt catalyst with the highest ever reported methanol yield, to the best of our knowledge using a non-noble metal, along with more than 90% selectivity and a decent conversion in water along with an oxidant. Mercury test further ruled out the possibility of any activity of leached metal nanoparticles. MOF also showed recyclability and stability with a slight decrease in methanol yield in each run with minimal leaching of post synthetically attached metal or zirconium.

### Acknowledgements

This research is supported by the Science and Engineering Research Board (SERB), India (project ECR/2017/001931). Authors acknowledge the Central Research Facility, IIT Delhi, for instrument facilities.

### References

1. M. Ravi, M. Ranocchiari, J.A. van Bokhoven, *Angew. Chem.*, **56** 16464 (2017).
2. R. Sharma, H. Poelman, G.B. Marin, V.V. Galvita, *Catalysts*, **10** 194 (2020).
3. A. J. Howarth, Y. Liu, P. Li, Z. Li, T.C. Wang, J.T. Hupp, O.K. Farha, *Nat. Rev. Mater.*, **1** 15018 (2016).
4. T. Zhang, K. Manna, W. Lin, *Jacs.*, **138** 3241 (2016).
5. K. Manna, P. Ji, Z. Lin, F.X. Greene, A. Urban, N.C. Thacker, W. Lin, *Nat Commun.*, **7** 12610 (2016).

## Heterotrophic production of biofuels in marine diatoms

Giuliana d'Ippolito<sup>1,\*</sup>, Adelaide Cupo<sup>1</sup>, Salvatore Morra<sup>1</sup>, Simone Landi<sup>2</sup>, Genoveffa Nuzzo<sup>1</sup>, Carmela Gallo<sup>1</sup>, Emiliano Manzo<sup>1</sup> and Angelo Fontana<sup>1,2</sup>

<sup>1</sup>Institute of Biomolecular Chemistry CNR, Via Campi Flegrei 34, 80078, Pozzuoli, Napoli, Italy.

<sup>2</sup>Department of Biology, University of Naples "Federico II", Via Cinthia, I-80126 Napoli, Italy.

\*e-mail address \*gdippolito@icb.cnr.it

### Abstract

The current prices of microalgae oils are much higher than vegetable oils mainly due to the high cost of photoautotrophic cultivation of microalgae. Heterotrophic growth represents a sustainable alternative to overcome light and climatic/geographic dependency, and to reduce cultivation costs [1,2]. Among microalgae, diatoms are excellent lipid accumulators and have characteristics, both conceptual and proven, which make them amenable to large-scale biofuel production [3]. In this context, a repeated-batch process for heterotrophic cultivation of marine diatom *Cyclotella cryptica* for biodiesel production is described. The diatom is cultured under optimized heterotrophic conditions in 6 bioreactors of 10 L each, using glucose as carbon source, harvesting every 7 days 9/10 of the culture, and using 1/10 as seed culture for the next cycle. The whole repeated batch process lasted 42 days for a total of 6 cycles, without using antibiotics along the cultivation. Biomass production ranged from 1.7 g L<sup>-1</sup> to 1.4 g L<sup>-1</sup> with a median value of 1.5 ± 0.1 g L<sup>-1</sup>. Total lipid productivity ranged from 37.87 to 48.57 mg L<sup>-1</sup> day<sup>-1</sup>, with a median value of 39.74 mg L<sup>-1</sup> day<sup>-1</sup>. Triglycerides were the most abundant lipidic pool, representing 54-65 % of total glycerolipids, and negligible level of free fatty acids were detected in the harvested biomass [4]. Main fatty acids in biooil were C16:0 (25%), C16:1 ω-7 (55%) and C20:5 ω-3 (14%), distributed in specific modality as acyl chains in glycerolipids [5]. On these bases, biodiesel properties were estimated in terms of main parameters (iodine value, cetane number, saponification value, etc...) to define the potentiality of diatom oil as biofuel in comparison to vegetable oils. The current technologies for biofuel production from microalgae will be discussed to assess the feasibility of different approaches in the prospective to substitute vegetable oils with microalgal oils.

### References

1. P. Botte, G. d'Ippolito Giuliana\*, C. Gallo, A. Sardo, A. Fontana, *Journal Applied Phycology*, **30**, 1, (2018)
2. F. M Vella. A. Sardo, C. Gallo, S. Landi, A. Fontana and G. d'Ippolito, *Algal Research* **42**, 101553 (2019)
3. G. d'Ippolito, A. Sardo, D. Paris, M. Vella, M.G. Adelfi, P. Botte, C. Gallo, *Biotechnology for Biofuels*, **8**, 28 (2015)
4. S. Morra, A. Cupo, L. Caso, M. Lanzilli, S. Landi, C. Gallo, G. Nuzzo, Emiliano Manzo, A. Fontana and G. d'Ippolito, *Bioresource Technology*, under submission
5. A. Cupo, S. Landi, S. Morra, G. Nuzzo, C. Gallo, E. Manzo, A. Fontana, G. d'Ippolito, *Marine Drugs* **19**, 7, Article Number 355 (2021)

# Biobased monomers, polymers & composites

## Innovative Structural Modification Process of Kraft Lignin Using Flow System Approach

Sílvio Vaz Jr.\*, Carlos Eduardo Salvador

Brazilian Agricultural Research Corporation (Embrapa), Parque Estação Biológica, s/n, Av. W3 Norte, Asa Norte, 70770-901, Brasília, DF, Brazil

\*Corresponding author: [silvio.vaz@embrapa.br](mailto:silvio.vaz@embrapa.br); (+55) 61 3448-2315

### Abstract

An innovative process of structural modification of kraft lignin (KL) followed by the incorporation of the herbicide picloram ( $C_6H_3Cl_3N_2O_2$ ; CAS 1918-02-1) was developed by means the methoxylation reaction in a continuous flow regime. The modified KL-picloram nanoformulation obtained will be used in the study and validation of formulations of controlled release of the herbicide picloram in the subsequent stages in order to prove the environmental gain of this type of formulation against a convention formulation. It is expected that the structural modification will promote an improving of properties as surface area, adsorption and availability of chemical groups for interaction. The modification process, followed by the incorporation of the agrochemical molecule, in addition to being innovative, as it uses flow synthesis, meets the United Nations Sustainable Development Goals.

### Methodology

KL was solubilized in a sodium hydroxide solution followed by formaldehyde (for methylation) and herbicide picloram (for incorporation) additions (Fig. 1). Reactions of KL modification were conduct in a flow system device (Asia, Syrris) with a later herbicide incorporation in a vessel. KL modification and picloram incorporation were confirmed by means FTIR (IRAffinity-1, Shimadzu) and TEM (EM902, Carl Zeiss).

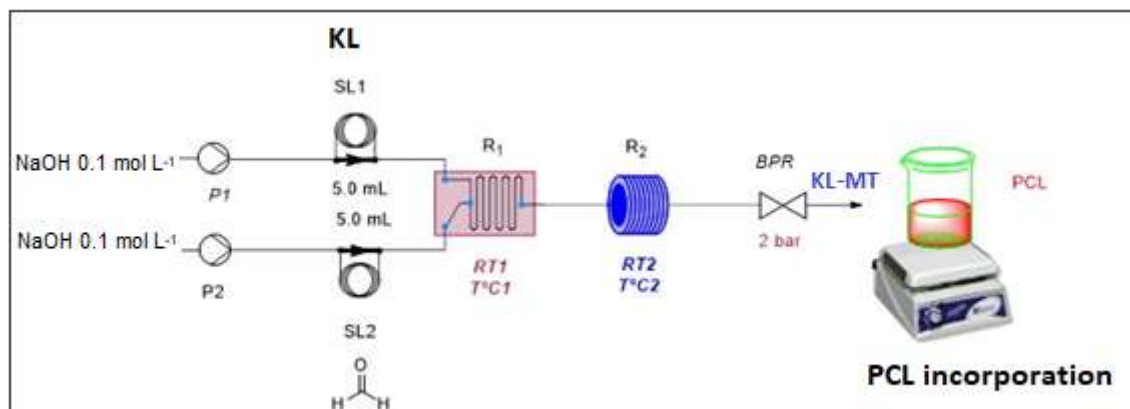


**Fig. 1** Process developed for the structural modification of KL with subsequent incorporation of the herbicide picloram. KL = kraft lignin; Pn = system injection pump pressure in flow; SLn = solvent (formaldehyde) + kraft lignin solubilized in tubular reservoir; Rn = flow system reactors; RTn = reactor temperature; BPR = pressure regulator; KL-MT = methoxylated kraft lignin; PCL = picloram.

### Results and discussions

Fig. 2 shows the confirmation of the modification of KL. Fig. 3 shows the confirmation of the incorporation of picloram to modified KL. The maximum size particle determined for the system modified KL-picloram was 97 nm.

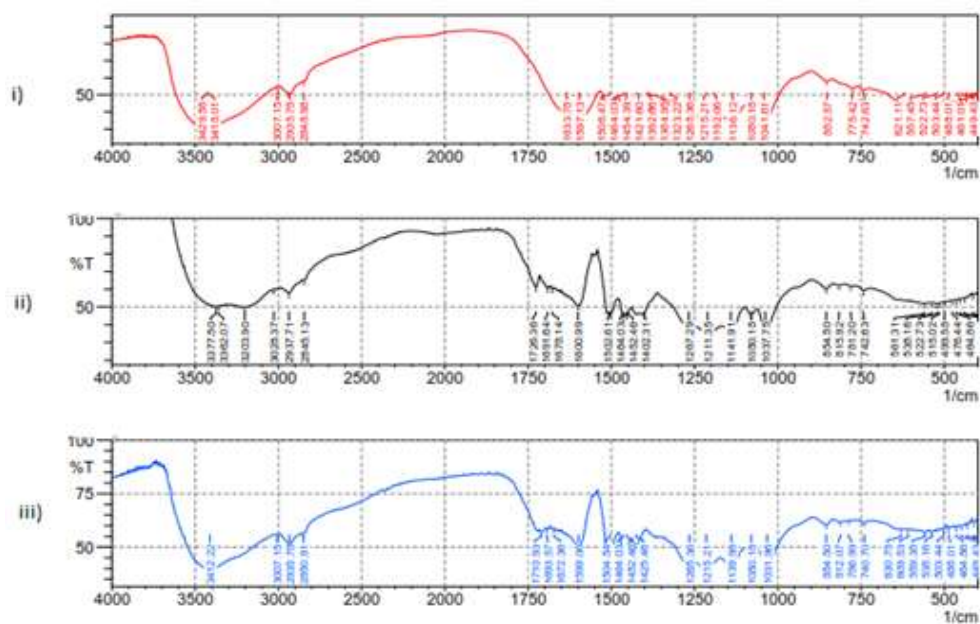


**Fig. 2** FTIR spectrum of unmodified kraft lignin (i, red), batch modified (ii, black) and continuous flow modified (iii, blue). The region between 1750 and 1500  $\text{cm}^{-1}$  stands out, where the alteration in the absorption bands can be observed produced by means the picloram incorporation.

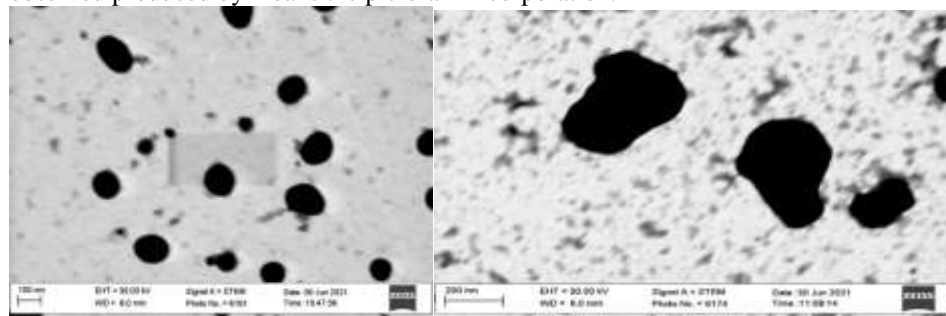


**Fig. 3** Transmission electron microscopy of modified lignin (left) and picloram incorporated into modified kraft lignin (right). The picloram incorporation promoted the swelling of the kraft lignin particle.

It is expected that the structural modification will promote an improving of properties as surface area, adsorption and availability of chemical groups for interaction. Furthermore, the developed process is closely related to the United Nations Sustainable Development Goal 12 for responsible consumption and production.

### Conclusions

It was concluded that the developed process using a methoxylation route in a continuous flow regime produced a modified KL-picloram nanoformulation with satisfactory physicochemical properties (particle size and encapsulation power) for its use in the further validation studies of the controlled release formulation in order to prove environmental gain against conventional formulation.

### Acknowledgments

Authors thank to Brazilian National Council for Scientific and Technological Development (CNPq) for the financial support (The Greenmol Project; grant number 400120/2019-4), and to EMBRAPA-CNPq Scholarship Program for CES's scholarship.

## UV degradation of poly(lactic acid) materials through copolymerisation with a sugar-derived cyclic xanthate

Craig Hardy<sup>1</sup> and Antoine Buchard<sup>1\*</sup>

<sup>1</sup>Centre for Sustainable and Circular Technologies, Department of Chemistry, University of Bath, Bath, BA2 7AY, UK.

\*a.buchard@bath.ac.uk

The production of degradable polymers from sustainable resources has now become essential in order to relieve our dependence on petroleum-based plastics, and subsequently alleviate the increasing damage upon the planet's eco-system.[1][2] Starting from tri-O-acetyl-D-glucal (commercial or easily prepared from the natural product D-glucose) and carbon disulfide (CS<sub>2</sub>), we have successfully developed new synthetic methodologies towards two novel bicyclic xanthate monomers: one retaining the original glucal unsaturation and its hydrogenated, saturated analogue, and begun the exploration of the structure-property relationship on the resulting polymers.[3] Manufactured by reaction of charcoal or natural gas with sulfur, an abundant by-product of the oil and chemical industry, incorporating CS<sub>2</sub> into polymers also has proven benefits in terms of waste valorisation.[4][5]

Under optimised conditions, organocatalytic ring-opening polymerisation (ROP) of the unsaturated monomer proceeds quickly in solution, at room temperature, resulting in monomer conversions up to 90 % and polymers with number-average molar masses in excess of 10,000 g mol<sup>-1</sup>. First order kinetics with respect to monomer concentration was demonstrated, and the thermodynamic parameters of the polymerisation ( $\Delta H_p = -25.6$  kJ mol<sup>-1</sup>;  $\Delta S_p = -80$  J mol<sup>-1</sup> K<sup>-1</sup>) were determined from the equilibrium monomer conversions across a range of temperatures. Due to the ROP equilibrium limitations, the polythiocarbonate polymers exhibit full chemical recyclability back to the monomer, by dilution (0.1 mol L<sup>-1</sup>) at room temperature. The resulting polythiocarbonates possess a regio-regular structure with alternating C(S)S<sub>2</sub> and C(S)O<sub>2</sub> linkages, as well as a reactive alkene function present in the polymer backbone. The unsaturated and saturated polymers are amorphous in nature, with glass transition temperatures ( $T_g$ ) around 65 and 92 °C, and each have an onset of thermal degradation ( $T_{d5\%}$ ) of around 188 and 191 °C. Demonstrating the intrinsic effect, which the addition of unsaturation to the pyranoside ring of the sugar-based cyclic xanthate monomer has upon the thermal properties of the resultant polymers.

In addition, the sulfur-containing linkages, within the polymer backbone, also allow the rapid degradation of polymers under UV radiation ( $\lambda = 365$  nm). This feature was exploited in the copolymerisation of L-Lactide with the cyclic xanthate monomer, used to incorporate thionocarbonate and thioester linkages into a polyester backbone, resulting in UV-degradable PLA materials. Indeed, the poly(lactide-co-xanthate) copolymers show enhanced UV-degradability compared to PLA, with 40% mass loss within 6 hours of UV exposure for as little as 3% xanthate incorporation.

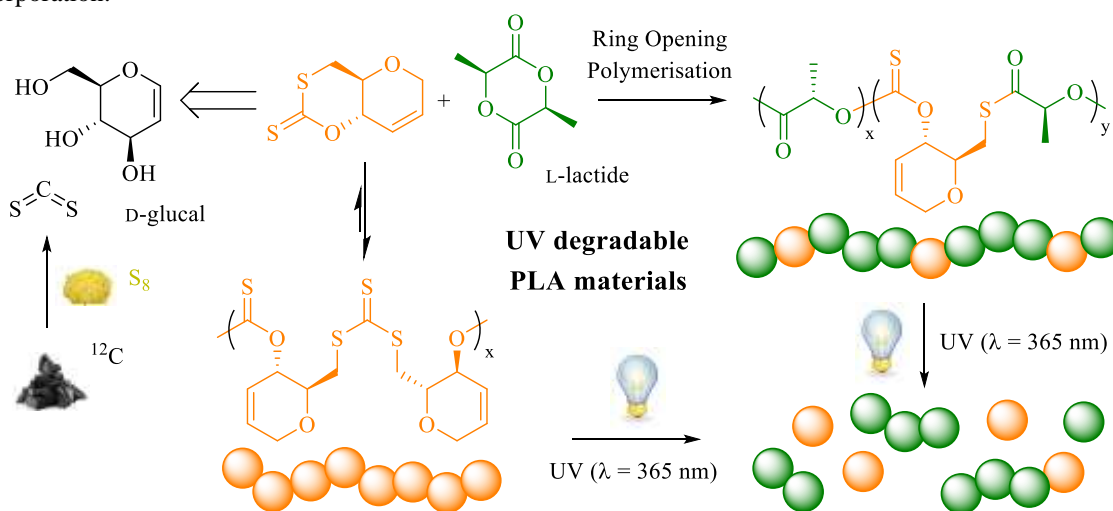


Figure 4. Synthesis and ring-opening polymerisation of a D-glucal-derived bicyclic xanthate to produce chemically recyclable and UV-degradable sugar-based unsaturated polythiocarbonates, in addition to the production of UV degradable PLA materials through the copolymerisation with L-lactide.

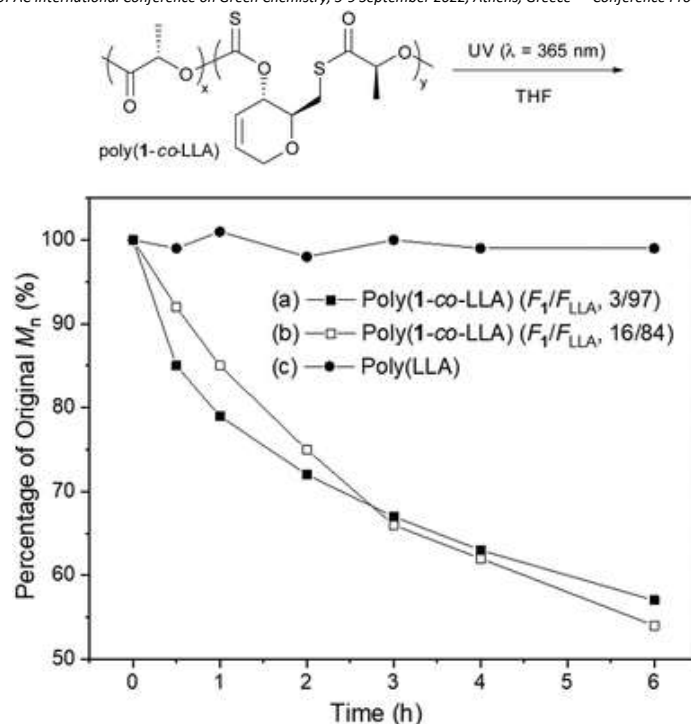


Figure 5. Percentage of original  $M_n$  vs. time, following the exposition of poly(1-co-LLA) copolymers to UV irradiation ( $\lambda = 365$  nm). The reactions were performed at room temperature with  $[\text{poly}(\mathbf{1-co-LLA})]_0 = 0.040 \text{ mol L}^{-1}$ . (a) Poly(1-co-LLA) ( $F_1/F_{LLA}$ , 3/93) ( $M_{n,SEC} = 13,200 \text{ g mol}^{-1}$ ,  $D_M = 1.66$ ), (b) poly(1-co-LLA) ( $F_1/F_{LLA}$ , 16/84) ( $M_{n,SEC} = 15,800 \text{ g mol}^{-1}$ ,  $D_M = 1.80$ ) and (c) poly(LLA) ( $M_{n,SEC} = 12,800 \text{ g mol}^{-1}$ ,  $D_M = 1.12$ ).

### Acknowledgements

We thank the Royal Society (UF\160021, fellowship to AB; RGF\EA\201023; RGF\EA\180028, studentship to CH) for research funding.

### References

1. G. L. Gregory, E. M. López-Vidal and A. Buchard, *Chem. Comm.*, 2017, **53**, 2198–2217.
2. A. T. Lonnecker, Y. H. Lim, and K. L. Wooley, *ACS Macro Lett.*, 2017, **6**, 748–753.
3. C. Hardy, G. Kociok-Köhn and A. Buchard, *Chem. Comm.*, 2022, Advance Article.
4. M. J. H. Worthington, R. L. Kucera and J. M. Chalker, *Green Chem.*, 2017, **19**, 2748–2761.
5. T. M. McGuire and A. Buchard, *Polym. Chem.*, 2021, **12**, 4253–4261.

## Itaconic acid as renewable building block for UV-curing polymer resins

Tobias Robert<sup>1</sup>, Sacha Pérocheau Arnaud<sup>1</sup>, Natalia Malitowski<sup>1</sup>, Marcel Kluge<sup>1</sup>,  
Rim Ouhichi<sup>2</sup>, Lazaros Papadopoulos<sup>3</sup>

<sup>1</sup>Fraunhofer Institute for Wood Research, Bienroder Weg 54E, 38108 Braunschweig, Germany

<sup>2</sup>Laboratoire de Chimie Appliquée H.C.G.P., Faculté des Sciences de Sfax, Université de Sfax, Bp 1171, 3000 Sfax, Tunisia

<sup>3</sup>Department of Chemistry, Laboratory of Polymer Chemistry and Technology, Aristotle University of Thessaloniki, GR-541 24, Thessaloniki, Greece

\*tobias.robert@wki.fraunhofer.de

### Abstract text:

Over the last years itaconic acid has drawn considerable attention as novel and renewable building block for bio-based polymers. It has been used as (co-)monomer in radical polymerization reactions to obtain polyitaconates with different fields of application.[1] However, itaconic acid can also be used as monomer for unsaturated polyesters.[2] Due to the higher reactivity compared to polyesters derived from maleic acid, these materials can also be used in UV-curing applications and have the potential to be a renewable alternative to polyester acrylates. In addition, by using other bio-based building blocks it is possible to obtain polymers of this type that are completely derived from renewable resources.

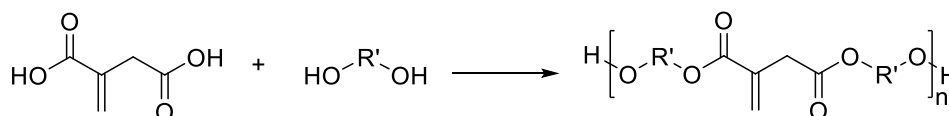


Figure 1. Synthesis of bio-based polyester itaconates.

Herein, the synthesis and properties of novel polyesters and poly(ester amide)s derived from itaconic acid will be reported. Furthermore, the application of these polymer resins as binders for different UV-curing applications, such as printing inks,[3] wood coatings, and materials for additive manufacturing will be presented. In addition, novel small molecules derived from itaconic acid that might have potential to be used as reactive diluents will be discussed. The results suggest that these bio-based resins and monomers can be an alternative to conventional materials derived from acrylic acid. These findings are very intriguing, as itaconic acid usually suffers from lower reactivity towards UV-induced crosslinking in comparison to acrylic acid. In addition, characterization of the properties of the UV-cured materials derived from itaconic acid show that they can compete or even surpass the properties of commercial materials.

### Acknowledgements

All the authors acknowledge financial support from the German Ministry of Education and Research.

### References

1. I. Delidovich, P. J. C. Hausoul, L. Deng, R. Pfützenreuter, M. Rose, R. Palkovits, *Chem. Rev.* 2016, 116, 1540.
2. a) T. Robert, F. Friebe, *Green Chem.* 2016, 18, 2922.; b) S. Brännström, E. Malmström, M. Johansson, *J. Coat. Tech. Res.* 2017, 14, 851; c) T. Farmer, R. Castle, J. Clark, D. Macquarrie, *Int. J. Mol. Sci.* 2015, 78, 49; d) J. Dai, S. Ma, Y. Wu, L. Han, L. Zhang, J. Zhu, X. Liu, *Green Chem.* 2015, 17, 2383.
3. T. Robert, S. Eschig, T. Biemans, F. Scheifler, *J. Coat. Technol. Res.* 2019, 16, 689.



## Recyclable, degradable, and high T<sub>g</sub> bio-based Polybenzoxazine vitrimers

A. Adjaoud<sup>1,2</sup>, L. Puchot<sup>1</sup>, P. Verge<sup>1\*</sup>

<sup>1</sup> Luxembourg Institute of Science and Technology, Esch-sur-Alzette, Luxembourg

<sup>2</sup> University of Luxembourg, Esch-sur-Alzette, Luxembourg

Over the past few decades, the apogee of industrialization has led to a compelling increase in the consumption of thermosets worldwide, resulting in an abundant source of wastes which cannot be recycled or repaired. To address this issue, reversible dissociative or associative bonds have been inserted within the chemical structure of thermosets to create covalent adaptable networks (CANs), enabling self-healability or recyclability. In 2011, Leibler and co-workers successfully introduced dynamic covalent bonds in thermoset polymer networks and developed the first “vitriimer”, combining the antithetical properties of a thermoplastic and a thermoset [1]. At service temperatures, vitrimers behave like a traditional thermoset with high mechanical properties, chemical resistance, and insolubility. At higher temperatures, they display the fluidity and the reprocessing ability of a thermoplastic. Among the different strategies and methodologies used to conceive vitrimers, the dynamic transesterification reaction (TER) occurring between ester bonds and aliphatic OH is the most representative chemistry for vitrimers. Catalysts are required to trigger the dynamic exchanges. They can be either external (the most common is zinc acetate) or internal. The latter is generally achieved by introducing tertiary amines in the chemical structure of the vitrimers. [2][3]

Among the different chemical structures suitable to combine the specifications of traditional thermosets to recyclability, healability and degradability, polybenzoxazines (PBZ) have recently shown their significance. PBZ are monocomponent thermosets constituted by an abundant number of tertiary amines, suitable to design vitrimers relying on TER. They are also a promising alternative to phenolic and epoxy resins due to their unique mechanical and thermal properties, such as a high glass transition temperature, near-zero shrinkage upon polymerization, and high char yield polymers. [4]

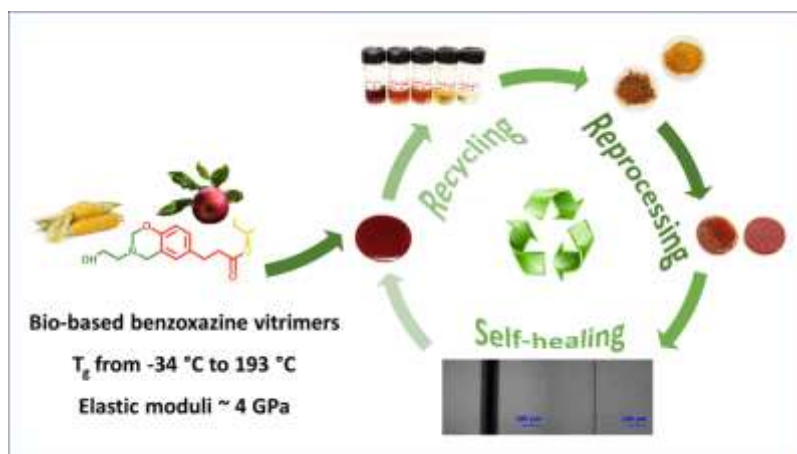


Figure 1. Schematic representation illustrating Polybenzoxazines and their properties

This presentation will illustrate the strategies to conceive degradable, self-healable and recyclable polybenzoxazine vitrimers from bio-based materials such as polyethylene glycol, isosorbide, lignin-like materials, with high thermal and mechanical properties (figure 1). [5][6]

**Keywords:** Vitrimers, Polybenzoxazines, degradable, recyclable, biobased

### References

- [1] D. Montarnal, M. Capelot, F. Tournilhac and L. Leibler, *Science*, **2011**, 334, 965–968.
- [2] J. Han, T. Liu, C. Hao, S. Zhang, B. Guo and J. Zhang, *Macromolecules*, **2018**, 51, 6789–6799.
- [3] C. Hao, T. Liu, S. Zhang, W. Liu, Y. Shan and J. Zhang, *Macromolecules*, **2020**, 53, 3110–3118.
- [4] H. Ishida, in *Handbook of Benzoxazine Resins*, ed. H. Ishida and T. Agag, Elsevier, Amsterdam, **2011**, pp. 3–81.
- [5] A. Adjaoud, A. Trejo-Machin, L. Puchot; P. Verge, et al *Polymer Chemistry* **2021**, 12, 3276 - 3289.pdf
- [6] A. Adjaoud, L. Puchot, P. Verge et al *ACS Sus Chem Eng* **2021**.

## Lignin as a renewable resource – a deep dive into structure-property relationship.

Ola Aleksandra Wróblewska<sup>\*1</sup>, Panagiotis Falireas<sup>1</sup>, Viviana Polizzi<sup>1</sup>, Karolien Vanbroekhoven<sup>1</sup>, Jaime Gracia Vitoria<sup>1</sup>, Elias Feghali<sup>1,2</sup>, Walter Eevers<sup>1,3</sup> and Richard Vendamme<sup>1\*</sup>

<sup>1</sup>VITO, Boeretang 200, 2400 Mol, Belgium

<sup>2</sup>Chemical Engineering Program, Notre Dame University-Louaize, PO Box: 72, Zouk Mosbeh, Lebanon,

<sup>3</sup>Department of Chemistry, University of Antwerp, Groenenborgerlaan 171, 2020 Antwerp, Belgium

[\\*ola.wroblewska@vito.be](mailto:ola.wroblewska@vito.be), [Richard.vendamme@vito.be](mailto:Richard.vendamme@vito.be)

Abstract text:

**Lignin**, a by-product of the pulp and paper industry, that is traditionally extracted from wood in order to produce cellulose, is the most abundant natural source of aromatics on Earth. As such, it shows potential in polymer design, in which currently, the majority of the used resources are still fossil-based. Not only can lignin replace existing harmful and fossil-based monomers, such as bisphenol A (BPA), but because of its unique structure it can improve the material properties for certain applications. The major issue that the field is currently struggling to resolve is lignin implementation because of the challenging structural characteristics that are often displayed; specifically referred to as incompatibility, insolubility and poor esthetics. At the Flemish Institute for Technological Research (VITO), instead of viewing these characteristics as obstacles, we are aiming to exploit them to our advantage; to show that lignin can produce high quality materials. If handled properly, it can lead to high-gloss materials with greatly improved toughness in comparison with fossil-based counterparts or one-to-one sustainable alternatives. Furthermore, utilizing the lignin depolymerization process, that we apply in our pilot plant, and careful characterization of the produced depolymerized lignin oil, we gain new insight into *structure-property relationships*. This highlights the importance of functionality and molecular composition when designing materials specific to application. The focus of this talk will be on the preparation of lignin and depolymerized lignin-based polyurethanes<sup>1</sup> and epoxy resins<sup>2</sup>.



Figure 1. A variety of materials that contain lignin – from natural to man-made.

### Acknowledgements

This project has received funding from the Bio-Based Industries Joint Undertaking under the European Union's Horizon 2020 research and innovation programme under the grant agreement number 101023342.

### References:

<sup>1</sup>M. Rubens, M. Van Wesemael, E. Feghali, L.L. Lufungula, F. Blockhuys, K. Vanbroekhoven, W. Eevers, R.Vendamme, *Ind. Crops Prod.*, 2022, 180, 114703

<sup>2</sup>P. Ortiz, R.Vendamme, W. Eevers, *Molecules* 2020, 25(5), 1158;

## Epoxy - Organosolv lignin composites with enhanced properties

Christina P. Pappa<sup>1,2</sup>, Stylianos A. Torofias<sup>1,2</sup>, Konstantinos S. Triantafyllidis<sup>1,2,\*</sup>

<sup>1</sup>Department of Chemistry, Aristotle University of Thessaloniki (AUTH), 54124 Thessaloniki, Greece

<sup>2</sup>Center for Interdisciplinary Research and Innovation (CIRI-AUTH), Balkan Center, 10th km Thessaloniki-Thermi Rd, P.O. Box 8318, 57001 Thessaloniki, Greece

\*e-mail address of corresponding author: ktrianta@chem.auth.gr

In recent years, lignin has attracted an immense amount of attention due to its potential as a renewable source that can be utilized in the production of fuels, bio-based polymers and chemicals, aromatics etc [1]. Lignin is one of the three main components found in lignocellulosic biomass and is considered as the most abundant natural source of phenolics and aromatics. Nowadays, it is underutilized in biorefineries as it is traditionally used for the in-house production of heat and energy [2]. Its structure renders lignin an excellent potential resource for plenty of currently petroleum-derived materials, like polymers, due to the aromatic structure and the presence of various functional groups like phenolic and aliphatic hydroxyls, carboxyls, aldehydes etc. Organosolv lignin is a technical lignin, isolated from all kinds of lignocellulosic biomass within the biorefinery schemes (Organosolv process). This type of process is very promising since it can selectively isolate organosolv lignins that have desirable properties, such as decreased molecular weights (MW), low polydispersity (PDI), appreciable amounts of  $\beta$ -O-4 interunit bonds and also increased functionality (especially phenolic OHs groups) [2].

Lignins have previously being studied as potential materials for additives in plenty of thermoset and thermoplastic polymers like phenol-formaldehyde resins, PLA and PUs [1] with success. In the past years lignin has also been used in epoxy resins, which are considered as one of the most commonly used thermosetting polymers, due to their superior mechanical and adhesive properties, and chemical resistance [3, 4].

In this work, organosolv lignin was utilized either as a crosslinker or as a reactive additive in epoxy resin towards the production of bio-based epoxy composites. In detail, beechwood biomass (Lignocel) organosolv lignin (OBs) was isolated via hydrothermal treatment in a mixture of EtOH/water and H<sub>2</sub>SO<sub>4</sub> as an acid catalyst. The isolation process was optimized and the obtained OBs lignin had a particle size within the submicron scale. OBs was further characterized using 2D-HSQC and <sup>31</sup>P- NMR, GPC, TGA/DSC analysis. The OBs lignin was then blended with a commercial epoxy resin (Diglycidyl Ether of Bisphenol A, EPON 828) and a glassy curing agent (Jeffamine D-230) replacing either part of the curing agent or substituting part of the resin/curing agent mixture, followed by curing under appropriate conditions. The lignin content in the cured composites was in the range of 3-9 wt.%. All the epoxy-organosolv lignin composites were transparent and exhibited superior mechanical, thermal and antioxidant properties compared to the pristine polymers, proving the high potential of lignin in replacing petroleum derived monomers in relevant polymeric materials.

### Acknowledgements



The research work was supported by the Hellenic Foundation for Research and Innovation (HFRI) under the HFRI PhD Fellowship grant (Fellowship Number: 967)

### References

1. C. Cui, H. Sadeghifar, S. Sen, D. Argyropoulos, *Bioresources* **8** 864-886 (2013).
2. S. Constant, H.L.J. Wienk, A.E. Frissen, P.de Peinder, R. Boelens, D.S. van Es, R.J.H. Grisel, B.M. Weckhuysen, W.J.J. Huijgen, R.J.A. Gosselink, P.C.A. Bruijninx, *Green Chemistry*, **18** 2651-2665 (2016).
3. S. Nikafshar, J. Wang, K. Dunne, P. Sangthongantoi, M. Nejad, *ChemSusChem* **14** 1184 (2021).
4. X. Zhen, H. Li, Z. Xu, Q. Wang, S. Zhu, Z. Wang, Z. Yuan, *Int. J. Biol. Macromol.* **182** 276–285 (2021).

## Preparation of lignin-based vinylogous urethane vitrimer materials and their potential use for removable adhesives

Jian Liu, Andrij Pich, Katrien V. Bernaerts\*

*Maastricht University, Faculty of Science and Engineering, Brightlands Chemelot Campus, Aachen-Maastricht Institute for Biobased Materials (AMIBM), Urmonderbaan 22, 6167 RD Geleen, The Netherlands*

*\*E-mail: katrien.bernaerts@maastrichtuniversity.nl*

### Abstract

Conventional thermosets rely on petrochemical products, and cannot be reprocessed, recycled or reshaped under mild conditions owing to their permanent, highly crosslinked structure. Although some of these materials are down-cycled into lower value products, most thermosets are incinerated, landfilled, or otherwise unaccounted for (i.e. leakage), which intensifies the problem of resource shortage and environmental pollution. In this work, wheat straw lignin (Protobind 1000) was used as a raw material to prepare modified lignin by a non-catalytic reaction with t-butyl acetoacetate. The modified lignin was cross-linked with fatty acid diamine (Priamine 1075), and a fully bio-based vitrimer material was successfully prepared. The vitrimers have high lignin content (40-50 wt%). The mechanical properties of these vitrimers could be adjusted by changing the density of the cross-linked network inside the material, which is determined by the ratio of modified lignin and diamine. In the case of elevated temperature (>100 °C), the dynamic chemical bonds (vinylogous urethane amine exchange) inside the material are activated, which allows the material to be recycled and reused. Rheology was used to study time and temperature dependent stress relaxation dynamics. Experimental results show that the relaxation time of the Vitrimer-1 ranges from 104s at 150 °C to 9s at 180 °C, exhibiting a rapid relaxation throughout the process without the addition of any catalyst. A potential application for this work is removable adhesives. The dry shear stress of the adhesive is 12.7 Mpa, and the wet shear strength is similar under different conditions, with a minimum strength of 3.5MPa. Combining the special solvent swelling behavior of the vitrimer material itself and the rapid exchange of dynamic chemical bonds of the material at high temperatures, we propose to use both solvent removal and heat removal methods to remove the adhesive, and the removed adhesive can be recycled. This work provides a case for bio-based vitrimer to promote the development and utilization of advanced bio-based thermoset materials.

## Lipase-catalyzed selective (meth)acrylation of lignin-derived monomers for the protection-group free synthesis of polymers with strong antioxidant properties

M. Rubens<sup>1,\*</sup>, W. Van Hecke<sup>1</sup>, R. Vendamme<sup>1</sup> and K. Vanbroekhoven<sup>1</sup>

<sup>1</sup>Flemish Institute for Technological Research (Vito N.V.), Boeretang 200, Mol 2400, Belgium

\*maarten.rubens@vito.be

Lubricants, fuels, plastics, and by extension all organic matter is prone to oxidation.<sup>1</sup> Antioxidants, as the name indicates, are compounds that delay or inhibit this destructive oxidative process. Although many known natural antioxidants exist, the most used antioxidants are synthetic petrol-derived hindered phenols. Despite their strengths and widespread use, these synthetic molecules are known to leach from their polymer matrix into the packaged product and surroundings.

Native lignin, made of a complex polyphenolic structure that consists of hindered phenols, is an ideal candidate for serving as a renewable antioxidant. Until now, the use of lignin as an antioxidant has been limited by its heterogeneous nature and its inadequate compatibility with common plastics. Novel depolymerization techniques allow for the deconstruction of lignin into a bio-oil rich in monomers. One of such monomers is dihydroconiferyl alcohol (DCA), which contains both an aromatic and aliphatic hydroxyl group.<sup>2</sup>

In this work, a lipase-catalyzed (meth)acrylation was developed to selectively acrylate the aliphatic hydroxyl group of DCA while keeping its hindered phenol intact. Typically, a protection-deprotection strategy on the phenol is used for the radical polymerization of these monomers.<sup>3</sup> However, we show that under select conditions, the radical polymerization proceeds without the protection of the phenol. An extensive kinetic study using RAFT polymerization, the determination of copolymerization ratios, and block copolymer synthesis were performed to prove this effect. Finally, the antioxidant properties of the developed acrylic polymers were studied, showing a similar antioxidative strength compared to commercial antioxidant additives.

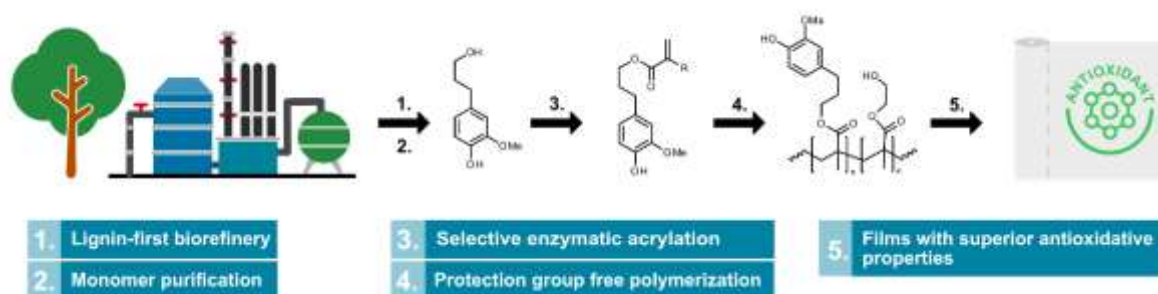


Figure 1. Biobased monomers from lignin bio-oils for the production of acrylic films with antioxidative properties

### References

1. A. M. Pisoschi and G. P. Negulescu, *Biochem & Anal Biochem*, 2012, 1, 1.
2. J.E. Quinsaat, E. Feghali, D.J. van de Pas, R. Vendamme, K.M. Torr, *ACS Applied Polymer Materials*, 2021 3.11, 5845-5856.
3. S.Wang, L. Shuai, B.
4. Saha, D. G. Vlachos and T. H. Epps, *ACS Cent. Sci.*, 2018, 4, 701–708.

## Synthesis of biobased polymers based on isohexide building blocks

Antonios Vasileiadis Vasileiou<sup>1</sup>, Valerio Zullo<sup>2</sup>, Christopher – Peter Kelevendjiev<sup>1</sup>, Mitchell Glas<sup>1,3,4</sup>, Katja Loos<sup>1</sup>

<sup>1</sup> Department of Macromolecular Chemistry and New Polymeric Materials, Zernike Institute of Advanced Materials, University of Groningen, Nijenborgh 4, 9747 AG Groningen, The Netherlands

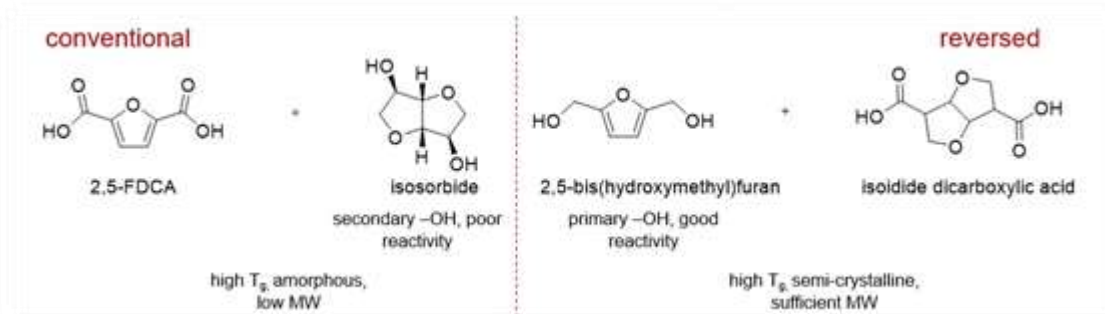
<sup>2</sup> University of Pisa – Department of Chemistry and Industrial Chemistry, Via Moruzzi 13, 56124 Pisa, Italy

<sup>3</sup> Van Hall Larenstein University of Applied Sciences, Agora 1, 8934 CJ Leeuwarden, The Netherlands

<sup>4</sup> NHL Stenden University of Applied Sciences, Rengerslaan 8, 8917 DD Leeuwarden, The Netherlands

Biobased building blocks and biobased polymers have increased their visibility in recent years. However, the most abundant type of biobased building blocks - carbohydrates - is still often unsuitable for high-end industrial chemical processes. Isohexides have a great potential as monomers for polymer preparation since they can provide the polymer structure with rigidity and as a result enhance the glass transition temperature of the material as well as their hydroxyl groups offer functionalization sites. Interestingly in the preparation of polymers, isohexides can be utilized as monomers, in different forms. The most obvious is the use of isohexides as a difunctional diol monomer whereas the less common one is the conversion of the isohexide into the corresponding carboxylic acid and the corresponding diamine.

We report the development of biobased polyesters derived from 2,5-bis(hydroxymethyl furan) (BHMF) and the isohexide derived isoidide dicarboxylic acid (IDA). The polymers derived from this combination of BHMF and IDA have a reversed combination of diol and diacid structures as compared to conventional polycondensates. This reversed combination results in polyesters with a fast crystallization rate (from the high rotational mobility of furan) and a high  $T_g$  and  $T_m$  (from the bulkiness of the IDA). In addition, the structure does not allow the formation of vinyl esters during thermal degradation, and therefore discoloration is minimized. Moreover, we report the synthesis of biobased diamines derived from 2,5-dimethyl furan dicarboxylate and the isohexide based isoidide diamine (IDM).



**Scheme 1:** Proposed synthetic pathway for the synthesis of conventional and reversed polyesters based on isohexide moieties

- (1) Wu, J.; Eduard, P.; Jasinska-Walc, L.; Rozanski, A.; Noordover, B. A. J. J.; Van Es, D. S.; Koning, C. E. Fully Isohexide-Based Polyesters: Synthesis, Characterization, and Structure-Properties Relations. *Macromolecules* **2013**, *46* (2), 384–394. <https://doi.org/10.1021/ma302209f>.
- (2) Wu, J.; Eduard, P.; Thiyagarajan, S.; Van Haveren, J.; Van Es, D. S.; Koning, C. E.; Lutz, M.; Fonseca Guerra, C. Isohexide Derivatives from Renewable Resources as Chiral Building Blocks. *ChemSusChem* **2011**, *4* (5), 599–603. <https://doi.org/10.1002/cssc.201100076>.
- (3) Stubbs, C. J.; Worch, J. C.; Prydderch, H.; Wang, Z.; Mathers, R. T.; Dobrynin, A. V.; Becker, M. L.; Dove, A. P. Sugar-Based Polymers with Stereochemistry-Dependent Degradability and Mechanical Properties. *J. Am. Chem. Soc.* **2022**, *144* (3), 1243–1250. <https://doi.org/10.1021/jacs.1c10278>.
- (4) Wu, J.; Eduard, P.; Thiyagarajan, S.; Noordover, B. A. J.; Van Es, D. S.; Koning, C. E. Semi-Aromatic Polyesters Based on a Carbohydrate-Derived Rigid Diol for Engineering Plastics. *ChemSusChem* **2015**, *8* (1), 67–72. <https://doi.org/10.1002/cssc.201402935>.
- (5) Marubayashi, H.; Ushio, T.; Nojima, S. Crystallization of Polyesters Composed of Isohexides and Aliphatic Dicarboxylic Acids: Effects of Isohexide Stereoisomerism and Dicarboxylic Acid Chain Length. *Polym. Degrad. Stab.* **2017**, *146* (October), 174–183. <https://doi.org/10.1016/j.polymdegradstab.2017.10.005>.
- (6) Zullo, V.; Petri, A.; Iuliano, A. An Efficient and Practical Chemoenzymatic Route to (3R,3aR,6R,6aR)-Hexahydrofuro[3,2-b]Furan-6-Amino-3-ol (6-Aminoisomannide) from Renewable Sources. *SynOpen* **2021**, *5* (3), 161–166. <https://doi.org/10.1055/a-1532-5825>.

## Fully lignocellulose-based PET analogues for the circular economy

Xianyuan Wu<sup>1</sup> and Katalin Barta\*

<sup>1</sup>Stratingh Institute for Chemistry, University of Groningen, Groningen, The Netherlands

\*e-mail address of corresponding author ([katalin.barta@uni-graz.at](mailto:katalin.barta@uni-graz.at))

With an annual production of 70 million tons globally, polyethylene terephthalate (PET) is one of the most widely used polymers worldwide, indispensable for the manufacturing of packaging material, clothing, fibers and single-use beverage bottles. However, its accumulation in landfills and oceans has been estimated to reach up to 530 million tons to date, which accounts for near-catastrophic environmental pollution. Moreover, most of the PET is still, typically, produced from fossil resources by copolymerization of ethylene glycol (EG) and terephthalic acid (TPA).

Thus, there is tremendous incentive to obtain readily recyclable or upcyclable, fully bio-based PET alternatives in order to implement circular economy approaches. This will require the development of new, robust catalytic methods and comprehensive biorefinery strategies:

Here we present a comprehensive biorefinery strategy for constructing PET analogues, as well as gasoline range and jet-range fuels, based entirely on woody biomass (Fig. 1)<sup>1</sup>. In our unique approach, lignin gives the aliphatic diol building block, while cellulose may provide the necessary aromatic diacid components (FDCA or TPA) in the developed polyesters. Central to the method is the catalytic funneling<sup>2</sup> of native lignin by a non-noble metal two step catalytic sequence, which results in 4-(3-hydroxypropyl) cyclohexan-1-ol (PC), obtained as single compound in the excellent isolated yield of 11.7 wt % (on lignin basis), and other product streams are convertible to gasoline range cyclohexane derivatives and high energy density fuel range bicyclic alkane, achieving the total carbon yield of 29.5 %. Notably, this funneling strategy allows overcoming tedious and expensive product isolation and purification protocols, providing a single polymer building block PC from complex biomass feed as well as other usable product streams. This leads to overall excellent lignocellulose utilization and the synthesis of fully wood-based polyesters. The new polyesters poly (PC/TPA) and poly (PC/FDCA) display excellent thermal properties ( $T_g$  = between 75-90 °C) that compare favorably to commercially available PET and are readily recyclable in methanol. Preliminary techno-economic analysis shows feasibility of the developed process, thus overall these fully bio-based polyesters are promising candidates for the circular economy.

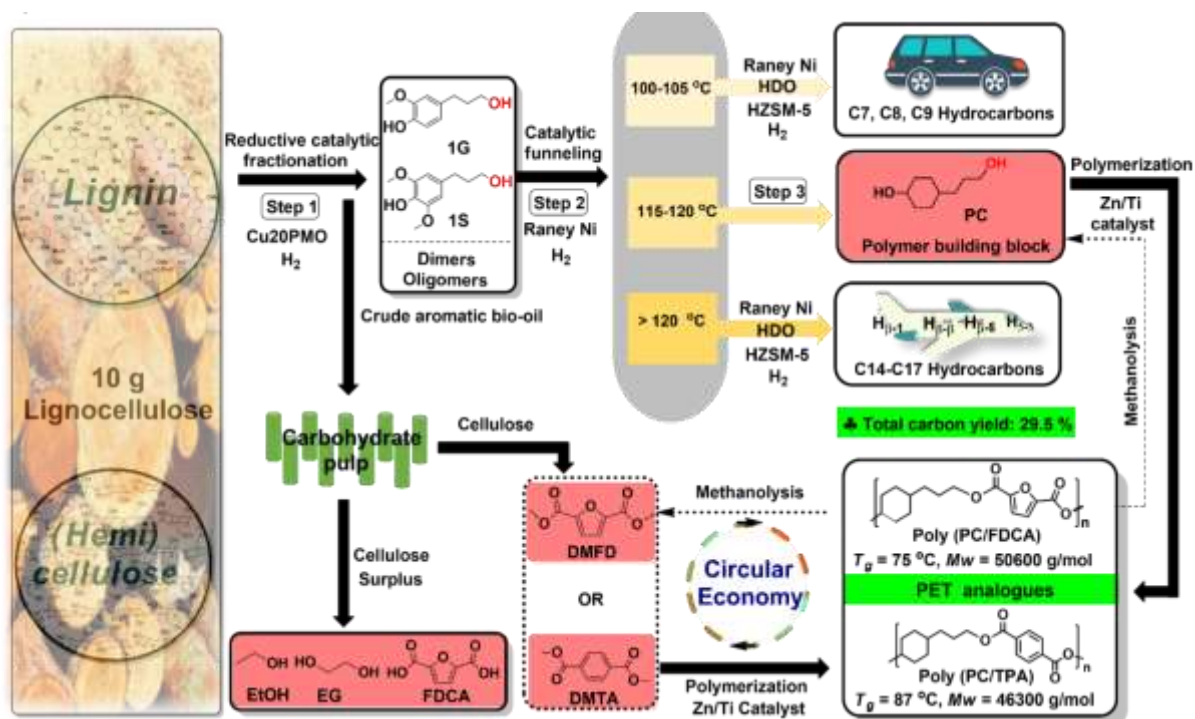


**Fig. 1** A) Our comprehensive biorefinery strategy to produce fully lignocellulose-based, recyclable PET analogues and other valuable products.

### References

1. X.Y. Wu, M.V. Galkina Z. H., Sun, K. Barta, *Nat. Commun.* **13**, 3376 (2022).
2. X.Y. Wu, M.V. Galkina Z. H., Sun, K. Barta, *Chem Catal.*, **1**, 1 (2021).

## Greener Enzymatic Synthesis of Levoglucosenone-based Polymers

Cicely M. Warne<sup>1\*</sup>, Sami Fadlallah<sup>2</sup>, Florent Allais<sup>2</sup>, Georg M. Guebitz<sup>1,3</sup>, Alessandro Pellis<sup>3,4</sup>

<sup>1</sup>Austrian Centre of Industrial Biotechnology (ACIB), Konrad-Lorenz-Strasse 20, 3430 Tulln an der Donau, Austria.

<sup>2</sup>URD Agro-Biotechnologies Industrielles (ABI), CEBB, AgroParisTech, Pomacle 51110 France

<sup>3</sup>Institute of Environmental Biotechnology, University of Natural Resources and Life Sciences Vienna, Konrad-Lorenz-Strasse 20, 3430 Tulln an der Donau, Austria.

<sup>4</sup>Università di Genova, Dipartimento di Chimica e Chimica Industriale, via Dodecaneso 31, 16146, Genova (GE), Italy  
\*cicely.warne@boku.ac.at

Abstract text:

With fossil fuels depleting fast, society needs to find alternatives to the current oil-based plastics. The obvious solution is to utilize biomass as a source of carbon, as much of it is currently discarded as waste. Many bio-derived platform molecules are being used to synthesize polymers, one of which is levoglucosenone (LGO). Derived from cellulose feedstock such as wood pulp<sup>1</sup>, it is a very versatile organic molecule with functionalized chiral structure (Figure 1). This makes it a useful molecule in many reactions, such as in the synthesis of the solvent Cyrene<sup>1</sup>. There have been several previous works that focus on LGO-based polymers<sup>2-4</sup>, however, these methods used traditional metal catalysts or non-green reagents. Enzymes are a more sustainable alternative; they are inherently bio-based and often require mild reaction conditions. Here, the polymerization of several LGO-derived monomers was attempted with the biocatalyst *Candida antarctica* lipase B (CaLB) in the green solvents Cyrene and dioxolane Cygnet.

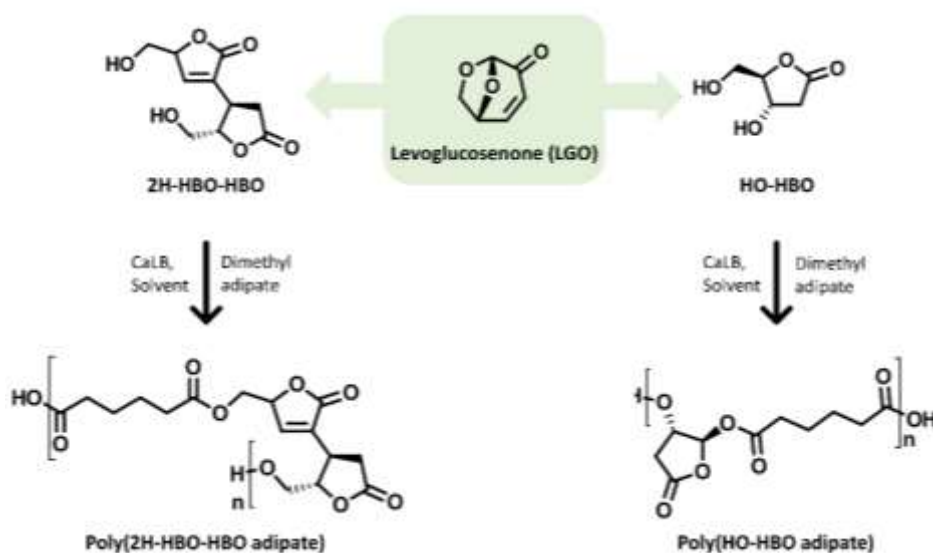


Figure 1. Two monomers derived from LGO were used in this study, as described in previous works<sup>2,3</sup>, and the polyesters were produced from their polycondensation reaction with dimethyl adipate.

Diol monomers were synthesized according to previously published works<sup>2,3</sup>. Several conditions were tested and polymers were successfully synthesized in almost all conditions. 2H-HBO-HBO did not polymerize in the presence of Cyrene as a side reaction resulted in the formation of a brown solid. This monomer has been known to undergo Michael's addition and self-polymerization<sup>4</sup>, and use of the Cyrene derivative Cygnet 0.0 as the reaction solvent eliminated this side reaction.

The yields for Poly(2H-HBO-HBO adipate) were initially very low. Using a less polar anti-solvent such as 2,2,5,5-tetramethyloxolane (TMO) instead of water resulted in a much better yield, up to 81%. TMO is considered a green solvent, and the yield is much improved compared to the previous work of 38%<sup>3</sup>. We have also managed to produce poly(HO-HBO adipate) at a good yield using an enzymatic polycondensation reaction. Although this is at a slightly lower yield (88%) compared to previously published results, where a 90% yield was achieved<sup>2</sup>, this method is greener, as it substitutes diacyl chlorides with diesters.

### Acknowledgements

This work is supported by European Union's Horizon 2020 research and innovation program under grant agreement No 953073, project UPLIFT (sUustainable PLAstIcs for the Food and drink packaging indusTry).

### References

1 J. E. Camp, *ChemSusChem*, 2018, **11**, 3048–3055.



- 2 F. Diot-Néant, L. M. M. Mouterde, J. Couvreur, F. Brunois, S. A. Miller and F. Allais, *European Polymer Journal*, 2021, **159**, 110745.
- 3 F. Diot-Néant, L. Mouterde, S. Fadlallah, S. A. Miller and F. Allais, *ChemSusChem*, 2020, **13**, 2613–2620.
- 4 S. Fadlallah, A. L. Flourat, L. M. M. Mouterde, M. Annatelli, A. A. M. Peru, A. Gallos, F. Aricò and F. Allais, *Macromolecular Rapid Communications*, 2021, **42**, 2100284.

## Degradable Cross-linked Polyesters: Resins to be Cheerful

Theona Şucu<sup>1,2</sup> and Michael P. Shaver<sup>1,2\*</sup>

<sup>1</sup> Department of Materials, School of Natural Sciences, University of Manchester, Manchester, M1 3BB, United Kingdom;

<sup>2</sup> Henry Royce Institute, University of Manchester, Sustainable Materials Innovation Hub, Manchester, M13 9BL, United Kingdom.

\*michael.shaver@manchester.ac.uk

Polyesters such as poly(lactic acid) form the cornerstone of biodegradable thermoplastics due to their excellent mechanical and thermal properties, but their poor solvent resistance, low thermal stability and significant stress softening limit their widespread application. Cross-linking these degradable systems could impart additional dimensional stability, enhancing their tensile and impact strength hence producing materials with improved elasticity and shape retention, while also reducing creep. Traditional thermoplastics can be mechanically and chemically recycled, but these pathways are often not possible for thermoset resins due to their cross-linked structure. The renewed demand for sustainable polymers from public, industry and government stakeholders has increased research into (bio)degradable thermoplastics, but thermosets have often been overlooked.

To address this need for more sustainable thermosets, we have developed novel, bio-based cross-linkers that can be readily copolymerized with commercially available cyclic esters. We use bio-derived feedstocks to synthesize two bifunctional molecules based on the 1,3-dioxolan-4-one moiety, varying the length of the spacer between the two reactive groups. Using a range of cyclic esters ( $\alpha$ -lactide,  $\epsilon$ -caprolactone,  $\delta$ -valerolactone), a family of polyester resins incorporating these novel monomers were then prepared. The structure–property relationships from the two novel cross-linkers were elucidated, and the properties of the resins could be tuned from tough solids to elastomers. Importantly, we demonstrate that these materials are competitive with commercially available thermosets employed for physically demanding applications. Unlike commercial thermosets, however, the triggered degradation of polyester resins can be leveraged to enable more sustainable end-of-life fates such as biodegradation, chemical recycling *via* depolymerization or even reprocessing.

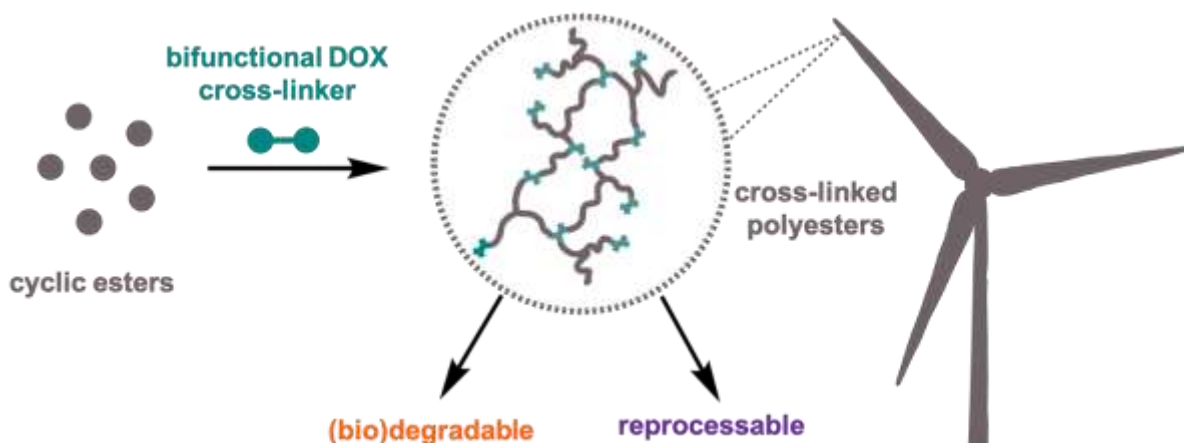


Figure 1. Project scope.

### Acknowledgements

Our current research efforts are supported by the European Regional Development Fund, project reference 15R19P03387. We are also grateful for funding from the EPSRC through the UKRI Plastics and Research Innovation Fund (NE/V01045X/1).

### References

- Şucu, T.; Shaver, M. P. Inherently Degradable Cross-Linked Polyesters and Polycarbonates: Resins to Be Cheerful. *Polym. Chem.* **2020**, *11* (40), 6397–6412.

## D-xylose for a versatile class of bioplastics with tunable properties

Marco Piccini\* and Antoine Buchard

Centre for Sustainable and Circular Technologies, Dept. of Chemistry, University of Bath, Bath BA2 7AY, United Kingdom  
\*m.piccini@bath.ac.uk

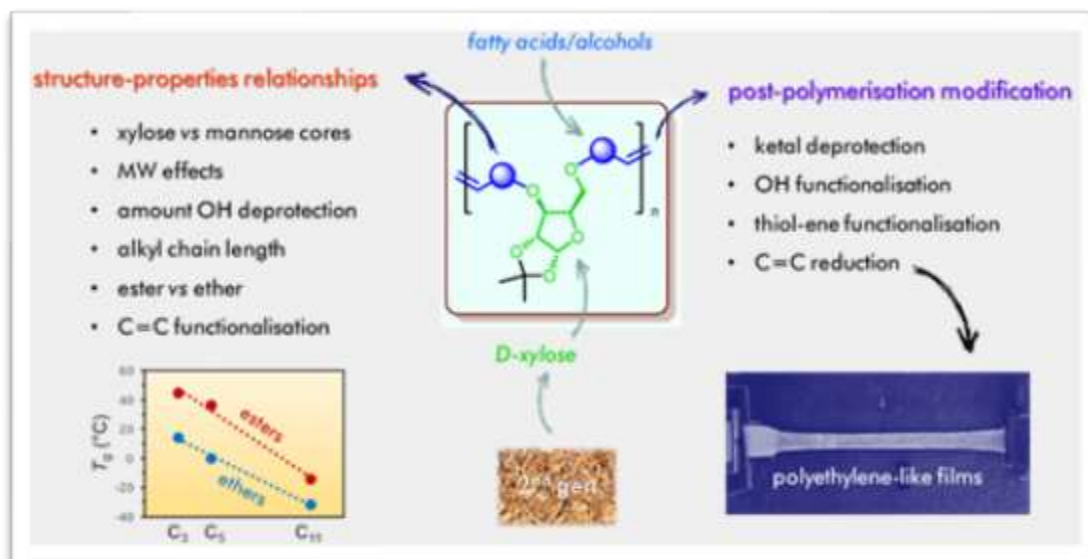


Figure 1. Graphical abstract

In this work we investigate sugars as building blocks for the synthesis of renewable polymers in which monosaccharides, used without structural modification, are incorporated into the main polymer backbone [1]. D-xylose was chosen being one of the most abundant sugars in nature, derived from easy depolymerisation of hemicellulose, including from second generation feedstocks such as agricultural, forestry and paper-making waste streams. The synthetic approach hereby used exploits olefin metathesis chemistry for the polymerisation of alkene-containing monomers. In particular, rigid isopropylidene-functionalised xylofuranose core was combined with biobased flexible 10-undecenoic acid (from castor oil), obtaining renewable  $\alpha,\omega$ -unsaturated glycolipid **1a**. This monomer was polymerised via acyclic diene metathesis (ADMET) with Grubbs second generation catalyst. Using low catalyst loadings (0.1 mol%) and no solvents (with associated sustainability and cost benefits), high molecular weight ( $M_n$  up to 71,000 g mol<sup>-1</sup>) amorphous polyesters were obtained, with high thermal (up to 365 °C) and hydrolytic (pH 7, 0, 14) stability, and relatively low glass transition temperatures (−28 to −8 °C), imparted by the flexible fatty acid chain. Post-polymerisation modification via ketal deprotection revealed hydroxyl groups inducing semicrystallinity, allowing the production of transparent polymer films. Further hydroxyl functionalisation (including with phosphine groups) was demonstrated, opening new possibilities for functional renewable polymers.

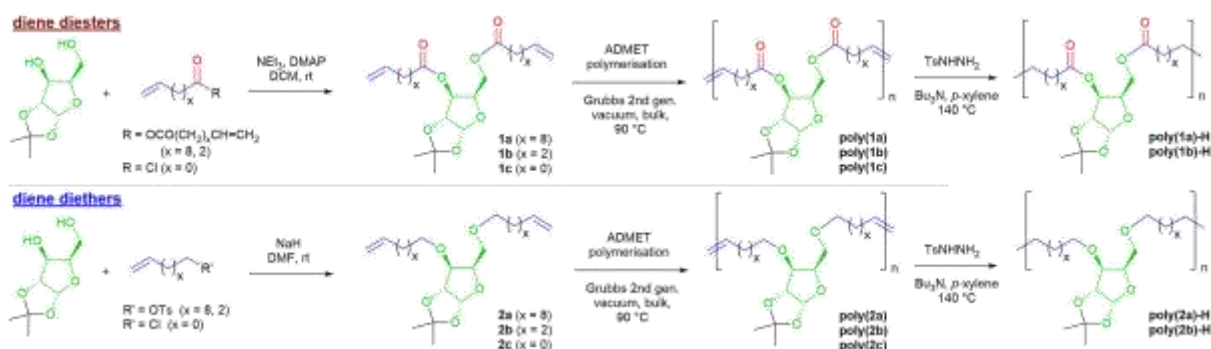


Figure 2. Synthesis of ADMET monomers and polymers from D-xylose and post-polymerisation C=C reduction

Given the promising properties, the study was widened to structural analogues in order to investigate structure-properties relationships [2].  $\alpha,\omega$ -unsaturated diesters and diethers were synthesised from  $\omega$ -unsaturated acids and alcohols ( $C_{11}$ ,  $C_5$  and  $C_3$ ), most of which obtainable from renewable sources. ADMET polymerisation afforded polyesters and polyethers with molecular weights increasing with increasing chain length ( $63,000 - 2,000 \text{ g mol}^{-1}$ ). These were found to be amorphous materials; remarkably,  $T_g$  decreased linearly with increasing chain length for both polyesters ( $-14$  to  $45 \text{ }^\circ\text{C}$ ) and polyethers ( $-32$  to  $14 \text{ }^\circ\text{C}$ ). The newly formed internal olefin bonds were subsequently modified post-polymerisation via C=C hydrogenation and thiol-ene “click” reaction. Hydrogenation turned amorphous  $C_{20}$  polymers into semicrystalline solids ( $T_m$   $44 - 50 \text{ }^\circ\text{C}$ ) and allowed production of transparent flexible films with exceptional polyethylene-like mechanical and gas barrier properties. Thiol-ene modification also proved an effective functionalisation strategy.

In summary, we have developed a versatile class of biobased polymers from D-xylose, whose properties (thermal, mechanical) can be tuned by modulating their structure (chain length, functionality, alternative sugar cores) and via a variety of post-polymerisation modification techniques (OH deprotection and functionalisation, C=C reduction and thiol-ene modification), opening several routes for a range of applications.

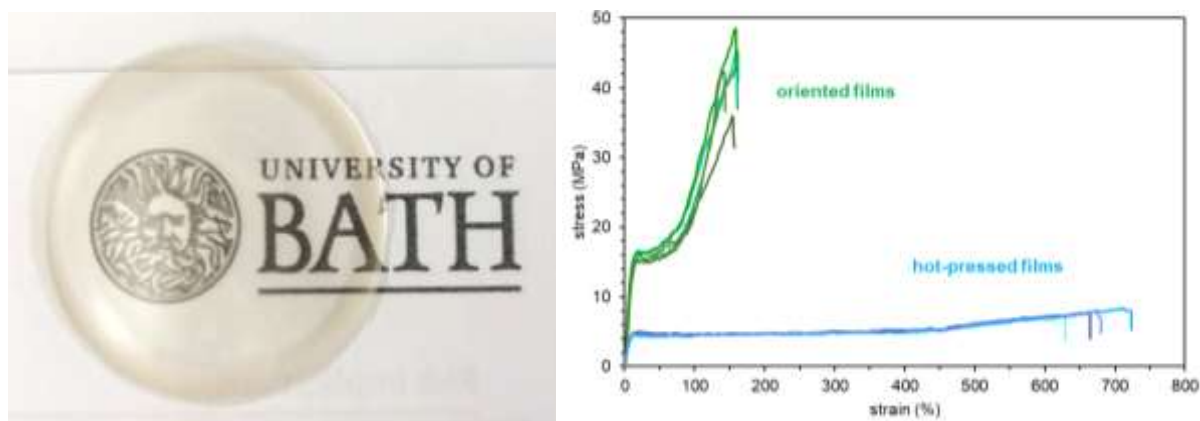


Figure 3. (left) Film from hot-pressed **poly(2a)-H**; (right) Tensile testing (stress vs. strain curves) for the same film (after hot-pressing and after uniaxial stretching)

### Acknowledgements

Analytical facilities were provided through the Material and Chemical Characterisation Facility (MC<sup>2</sup>) and at the University of Bath. This work was supported by the Engineering and Physical Sciences Research Council EP/L016354/1 (Studentship to MP, CDT in Sustainable Chemical Technologies). AB acknowledges Roger and Sue Whorrod (Whorrod Research Fellowship) and the Royal Society (UF/160021 fellowship) for research funding.

### References

1. M. Piccini, A. Buchard et al., *Polymer Chemistry* **2020**, *11*, 2681
2. M. Piccini A. Buchard et al., *ACS Applied Polymer Materials* **2021**, *3*, 5870

## Synthesis, aging and antibacterial tests of di(meth)acrylate composites

Karolina Młynarczyk<sup>1\*</sup>, Beata Podkościelna<sup>1</sup> and Magdalena Jaszek<sup>2</sup>

<sup>1</sup> Department of Polymer Chemistry, Maria Curie-Skłodowska University in Lublin, Gliniana 33, PL-20614 Lublin, Poland

<sup>2</sup> Department of Biochemistry and Biotechnology, Maria Curie-Skłodowska University in Lublin, Akademicka 19, PL-20033 Lublin, Poland

\*e-mail address of corresponding author: karolina.mlynarczyk@mail.umcs.pl

The fact that antibiotics are increasingly widely used has caused many strains of bacteria to become resistant to their effects. Increasingly, scientists are looking for compounds that exhibit antimicrobial activity. Examples include zinc oxide and benzethonium chloride, which is a quaternary ammonium salt that is synthetically derived. Synthesis of composites with potential antimicrobial properties may be the answer to the problem of bacterial resistance to antibiotics [1, 2].

Zinc oxide has antibacterial and antifungal properties. Due to the physicochemical properties of ZnO, it is widely used in many scientific and industrial fields. It is used as an ingredient in salves and ointments (pharmaceutical industry), as well as in toothpaste. In combination with eugenol, it is used as a filling for dental cavities. Zinc white is a white pigment used in the paint industry. It can also be used as a catalyst for organic synthesis, for the production of semiconductors, sensors, or in optoelectronics. ZnO exhibits strong antibacterial activity for a wide range of bacterial types. The mechanism of its action is not fully understood. It is assumed that it may be photocatalytic generation of reactive oxygen species. The inhibition of bacterial growth may be due to the penetration and disorganization of the cell membrane by the interaction of ZnO nanoparticles [3-5].

Benzethonium chloride is otherwise known as hyamine. It has surfactant, antiseptic, and anti-infective properties. It is used as an antibacterial agent in disinfectant fluids. It is found in the composition of cosmetic and toilet products (soap, mouthwash, disinfectant wipes). Its properties allow to use it as food preservative and disinfectant of hard surfaces [6].

Activities aimed at more frequent use of compounds with antimicrobial properties are very important in relation to the SARS-CoV-2 virus pandemic. It is very important to systematically disinfect surfaces - tables, doorknobs, handrails, or containers for disinfectant liquids that are made of plastic. An interesting idea is the synthesis of composites, which in their structure contain a protective agent against microorganisms.

Composites containing bisphenol A diacrylate (BPA.DA) as the main monomer were synthesized. As an active solvents 2-ethylhexyl acrylate (AEH), butyl acrylate (BA) and methyl methacrylate (MMA) were used. Benzethonium chloride (BEN) and zinc oxide (ZnO) were used as fillers having antimicrobial properties. The monomer ratio was 70:30. 2,2-Dimethoxy-2-phenylacetophenone (IQ) was applied as photoinitiator. Composites containing 1, 2, 5% by weight of antimicrobial filler were prepared. Appropriate amounts of substrates were mixed in a glass beaker, then the mixture was transferred into 10 x 12 x 0.2 cm glass molds with a teflon spacer. The mixtures were placed in a UV lamp for 30 minutes.

Aging studies of the materials were performed. For this purpose, the obtained composites were cut into 10 x 10 x 2 mm squares and placed in different organic and inorganic solvents. The aging test lasted for 16 weeks. During this time, systematically (one time by week) the samples were weighed after removal from the solvent, dried for two hours and weighed again. The swelling factor was also calculated from the formula:

Biological testing of the samples was also carried out. For this purpose, the samples were prepared in an appropriate manner and sterilized. Then the antimicrobial properties were determined with respect to selected Gram-positive and Gram-negative bacteria. Additionally, the effect of the obtained composites on the adhesion, i.e. biofilm formation of the tested bacterial strains was examined using the method with TTC. In the last stage of the study, the fungicidal and fungistatic properties were determined using the liquid (broth) culture. The following test organisms were used: and *Escherichia coli*, *Staphylococcus aureus*, *Candida albicans* and *Aspergillus niger*.

In order to confirm the structure of the composites, ATR-FT/IR spectra were performed before and after the aging process, which also allowed us to observe the changes resulting from the degradation of the composites. The hardness of the materials before and after the aging process was also measured. Additionally, differential scanning calorimetry (DSC) analysis was performed.

### References

1. D. R. Monteiro, L. F. Gorup, A. S. Takamiya, A. C. Ruvollo-Fihlo, E. Rodrigues de Camargo i D. B. Barbosa, *Int. J. Antimicrob. Agents*, **2**, 103-110, (2009).
2. S. Imazato, *Dent Mater.*, **19**(6), 449-457, (2003).

3. S. Anandan, A. Vinu, N. Venkatachalam, B. Arabindoo, V. Murugesan, *J. Mol. Catal. A Chem.*, **256**, 312-320, (2006).
4. X. L. Guo, H. Tabata, T. Kawai, *J. Cryst. Growth*, **237**, 554-547, (2002).
5. Y. Liu, J. Zhou, A. Larbot, M. Persin, *J. Mater. Process. Technol.*, **189**, 379-383, (2007).
6. K. Gałuszek, *Stud. Med.*, **19**, 13-23, (2010).

**Biobased monomers and polymers from lignin and cellulose**

Kei. Saito\*

Graduate School of Advanced Integrated Studies in Human Survivability

Kyoto University

Higashi-Ichijo-Kan, Yoshida-nakaadachicho 1, Sakyo-ku, Kyoto, 606-8306, Japan

saito.kei.1y@kyoto-u.ac.jp

Lignin is the second most abundant biopolymer just after cellulose. Its structure is a complex 3D network of phenol compounds linked by C-C (carbon-carbon) or C-O-C (carbon-oxygen-carbon) bonds, thus representing a promising source of aromatic compounds. The first part of this study focused on the depolymerisation of lignin using the redistribution mechanism with phenols under oxidative conditions in water in the presence of Cu catalyst. We have previously demonstrated that poly(2,6-dimethyl-1,4-phenylene oxide) (PPO) can be successfully depolymerised both in water and in ionic liquid involving the redistribution mechanism under mild condition (at 50-80°C, atmospheric pressure). The redistribution mechanism is one of the pathways in PPO preparation from the oxidative polymerisation of phenols, in which the carbon-oxygen bond (aryl ether bond) formed between phenols can dissociate under oxidative conditions to build the polymer chains and most importantly, this reaction is known to be an equilibration reaction. Considering the equilibrium involved in the redistribution mechanism in the polymerisation, we have found that depolymerisation is likely to occur simultaneously by adding phenol compounds to PPO under oxidative conditions. As lignin has a similar aryl ether structure to PPO in its network, our hypothesis is that this selective depolymerisation mechanism can be used to depolymerise lignin by breaking aryl ether bonds in its structure under mild condition.

We also have developed the novel oxidative degradation of lignin using MnO<sub>2</sub> with blue-light with a formate ionic liquid to produce ethyl acetate and also water soluble depolymerised lignin products.<sup>1</sup> The β-O-4 bonds in lignin were oxidised, which were then depolymerised by a green and recyclable ionic liquid, 2-hydroxy ethylammonium formate, under mild conditions. At last, we have developed the photo-responsive materials from lignin degraded products.<sup>2</sup>

The second part of this study focused on using Cyrene<sup>TM</sup>, a bio-based green solvent. Cyrene<sup>TM</sup> has been transformed into its methacrylic derivative (m-Cyrene) for the first time and its polymerisation was studied using different polymerisation techniques such as bulk, solution and emulsion polymerisation.<sup>3</sup> The new m-Cyrene monomer was found to undergo rapid polymerisation compared to isobornyl methacrylate (IBMA), another bio-derived monomer with a close structural similarity, and the highest polymerisation rate was obtained in Cyrene<sup>TM</sup> as the polymerisation solvent media. Cytotoxicity test confirmed the non-toxic nature of the bio-derived monomer, making it a green bio-derived methacrylic monomer for synthesising polymers where high thermal stability and mechanical properties are required.

**References**

<sup>1</sup> J. Dai, G. N. Styles, A. F. Patti,\* K. Saito, *Green Chem.*, **2019**, *21*, 2005-2014

<sup>2</sup> P. S. Roy, M. M. Mention, M. AP. Turner, F. Brunissen, V. G. Stavros, G. Garnier, F. Allais, K. Saito, *Green Chem.* **2021**, *23*, 10050-10061.

<sup>3</sup> P. Ray, C. Smith, K. Saito, G. P. Simon, *Polym. Chem.*, **2019**, *10*, 3334-3341.

## Synthesis of renewable diblock copolymers by aqueous RAFT polymerisation induced self-assembly of lactic acid-based monomers

Sarah E. Woods<sup>1</sup>, James D. Tinkler<sup>1</sup>, Nabil Bensabeh<sup>2</sup>, Marc Palà<sup>2</sup>, Simon. J. Martin<sup>1</sup>, Gerard Lligadas<sup>2\*</sup> and Fiona L. Hatton<sup>1\*</sup>

<sup>1</sup>Department of MATERIALS, Loughborough University, Epinal Way, Loughborough, Leicestershire, UK, LE11 3TU  
\*f.hatton@lboro.ac.uk

<sup>2</sup>Laboratory of Sustainable Polymers, Department of Analytical Chemistry and Organic Chemistry, University Rovira i Virgili, C/ Marcel·lí Domingo 1, 43007 Tarragona, Spain  
\*gerard.lligadas@urv.cat

In 2016, 90% of all plastics were made from fossil fuels and it's estimated that at the current rate of consumption crude oil and natural gas will have run out by 2070.<sup>[1,2]</sup> With 350 million tonnes of plastic produced worldwide in 2017 alone, it is clear that the sustainability of this area requires attention.<sup>[3]</sup> Renewable feedstocks, or biomass, are generally plant or biologically-based materials that replenish as they are used.<sup>[4]</sup> The monomers *N,N*-dimethyl lactamide acrylate (DMLA) and ethyl lactate acrylate (ELA) are sourced from lactic acid, which is made through the fermentation of carbohydrates.

The aim of this project was to conduct reversible addition-fragmentation chain-transfer (RAFT) polymerisation to make the hydrophilic poly(DMLA). This was then used as a macroRAFT agent in a RAFT-mediated polymerisation induced self-assembly (PISA) reaction in water to chain extend the hydrophobic poly(ELA) forming the diblock copolymer PDMLA-*b*-PELA. PISA allows for simultaneous synthesis and self-assembly as the PELA grows, reducing the number of steps required and potentially improving the reactions 'green' credentials.<sup>[4]</sup> PDMLA<sub>x</sub> was synthesised at numerous degrees of polymerisation (DP<sub>x</sub> = 25 to 400), all with narrow molecular dispersity's (M<sub>w</sub>/M<sub>n</sub> = 1.14 to 1.28) and glass transition temperatures (T<sub>g</sub>) between 73 and 78 °C. PDMLA-*b*-PELA<sub>x</sub> (DP<sub>x</sub> = 10 to 400), also achieved narrow molecular dispersity's (M<sub>w</sub>/M<sub>n</sub> = 1.18 to 1.54). Data collected so far show two T<sub>g</sub>'s present, at 10 and 60°C, representative of PELA and PDMLA, respectively.<sup>[5]</sup> Dynamic light scattering (DLS) analysis shows particle Z-average diameters between 14 and 74 nm (Đ = 0.0362 to 0.197). All reactions reached high monomer conversions with short reaction times (<6 hours). These polymers have also shown evidence of a temperature response. Through a visual examination, PDMLA<sub>x</sub> (DP<sub>x</sub> ≥ 100) show a transition from clear to cloudy above 90 °C, with this temperature increasing with DP. The same behaviour was observed in PDMLA-*b*-PELA, with DLS data collected so far showing an increase in particle size once a critical temperature has been reached.

### Acknowledgements

Financial support from Loughborough University and the Engineering and Physical Sciences Research (EPSRC) (EP/R513088/1) is gratefully acknowledged. We thank the Loughborough University department of MATERIALS department and the Laboratory of Sustainable Polymers, Department of Analytical Chemistry and Organic Chemistry, University Rovira i Virgili. We also thank the Loughborough University department of CHEMISTRY and the University of Nottingham school of CHEMISTRY for use of their <sup>1</sup>H NMR. The authors are grateful for the Strategic Equipment Grant (EP/T006412/1) provided by the EPSRC, which funded the atomic force microscopy (AFM) use for this project.

### References

1. World economic forum, *The New Plastics Economy Rethinking the future of plastics*, World economic forum technical report, 2016.
2. BP, *BP Statistical Review of World Energy June 2016*, BP technical report, 2016.
3. PlasticsEurope, *Plastics – the Facts 2018, Plasticseurope technical report*, 2018.
4. K. Yao and C. Tang, *Macromolecules*, 2013, **46**, 1689–1712.
5. N.Bensabeh et al. *ACS Sustainable chemistry & engineering*, 2020, **8**, 1276-1284.



## Biobased Boronic Ester Vitrimer Resin from Epoxidized Linseed Oil for Recyclable Carbon Fiber Composites

Davide Sangaletti<sup>a</sup>, Arkadiusz Zych<sup>a</sup>, Luca Ceseracciu<sup>a,b</sup>, Lara Marini<sup>a</sup>, Athanassia Athanassiou<sup>a</sup>

<sup>a</sup> Smart Materials, Istituto Italiano di Tecnologia (IIT), via Morego 30, 16163 Genoa, Italy

<sup>b</sup> Materials Characterization Facility, Istituto Italiano di Tecnologia (IIT), via Morego 30, 16163 Genoa, Italy

In the last decades, fibers reinforced polymer composites (FRPC) have experienced a continuously rising demand, since they are widely employed in various applications. Most commonly used matrices are the epoxy thermosets, since they have excellent thermomechanical properties and they are lightweight.<sup>1</sup> However, those materials cannot be reprocessed or recycled at the end of their lifetime, which causes a rapid consumption of fossil-based feedstocks and environmental concerns. Moreover, the permanent cross-linking of the matrix makes very difficult the recovery of the valuable reinforcements inside the composite.<sup>2-3</sup>

To overcome these drawbacks, we propose a new bio-based, vitrimer resin for carbon fiber reinforced composites that can be thermally reprocessed multiple times, keeping unaltered its physicochemical properties thanks to the dynamic boronic ester exchange. The new composite materials can also be easily recycled by vitrimer hydrolysis under mild conditions, making possible the full recovery of the carbon fibers contributing to “circular economy”. The developed material is synthesized by the reaction between the epoxidized linseed oil and a diboronic ester dithiol dynamic cross-linker, through a thiol-epoxy “click” reaction.<sup>4-6</sup> Both the syntheses of the cross-linker and the vitrimer have been developed following green chemistry principles. In particular, the synthesis of the new vitrimer takes advantages of a catalyst and is a solvent free process.

1. <https://www.grandviewresearch.com/press-release/global-fiber-reinforced-polymer-frp-composites-market>
2. Hongwei S., Lin Z., Yeping W., Lixian S., Ming K., Xiuli Z., Mao C., Rapidly reprocessable, degradable epoxy vitrimer and recyclable carbon fiber reinforced thermoset composites relied on high contents of exchangeable aromatic disulfide crosslinks, *Comp. Part B* 199 (2020) 108278
3. Yu-Yao L., Jia H., Yi-D. L., Xiao-Li Z., Jian-Bing Z., Biobased epoxy vitrimer from epoxidized soybean oil for reprocessable and recyclable carbon fiber reinforced composite, *Comp. Comm.* 22 (2020) 100445
4. <https://www.vitrimat.eu/>
5. Zych A, Tellers J, Bertolacci L, Ceseracciu L, Marini L, Mancini G, Athanassiou A. Biobased, Biodegradable, Self-Healing Boronic Ester Vitrimers from Epoxidized Soybean Oil Acrylate, *ACS Appl. Polym. Mater.* 2021, 3, 1135–1144. <https://dx.doi.org/10.1021/acsapm.0c01335>
6. Chen, Y.; Tang, Z.; Zhang, X.; Liu, Y.; Wu, S.; Guo, B. Covalently Cross-Linked Elastomers with Self-Healing and Malleable Abilities Enabled by Boronic Ester Bonds. *ACS Appl. Mater. Interfaces* 2018, 10, 24224–24231.

# Bio-catalysis & bio-processes

## Silymarin derivatization using biocatalytica system based on cold-active lipase biocatalyst

Gheorghita G.R.<sup>1</sup>, Ion S.<sup>1</sup>, Ftodiev A.<sup>1</sup>, Paun I.<sup>2</sup>, Purcarea C.<sup>2</sup>, Tudorache M.<sup>1\*</sup>

<sup>a</sup> Department of Organic Chemistry, Biochemistry and Catalysis, Faculty of Chemistry, University of Bucharest, Romania

<sup>b</sup> Institute of Biology Bucharest of the Romanian Academy, Bucharest, Romania

\*e-mail: madalina.sandulescu@g.unibuc.ro

Silymarin is a natural mixture of flavonolignans extracted from *Silybum marianum* L. Gaertn (milk thistle) seeds, a species originated from Europe and Asia and extensively cultivated worldwide. *In vivo*, Silymarin is synthesized by radical coupling between flavonoids and coniferyl alcohol [1], determining from a compositional point of view a great diversity of related compounds such as silybin or silybinin (33.4%), silychristin (12.9%), silydianin (3.5%) and isosilybin (8.35%) [2]. These flavonoid-like compounds are responsible for the therapeutic activity of the plant extract [3].

Silybin, as one of the most biologically active compounds within the silymarin mixture [4]. Silybin has low liposolubility, thus consisting its drawback on cellular adsorption in the context of bioavailability strategy. So that, silybin fatty acid esters could be a valuable alternative.

We propose a biocatalytic cold-active lipase-mediated system for the acylation of silybin A/B with proper fatty acids or esters [5]. The biocatalyst consists of the protein material extracellularly produced by a novel *Psychrobacter sp.* extracted from perennial ice deposits of Scarisoara Ice Cave (Romania). The lipolytic effect of the protein material is considered for the catalysed reaction, as many extracellular putative lipases are attributed to species draft genome.

The relative enzyme activity was evaluated for both free and immobilized biocatalyst specimens and the optimization of the biocatalytic system has been achieved. The developed immobilized biocatalysts exhibited between 80 and 128% recovery of the catalytic activity for protein loading in the range 90–99% and this led to an immobilization yield up to 89%. A comparison of the FTIR spectra confirmed the enzyme attachment to the support surface. Additionally, the protein content on the functionalized particle layer was highlighted by SEM analysis.

Kinetics measurements were performed for the immobilized lipase fraction and compared to a free lipase biocatalyst. The kinetic constants  $K_m$  and  $V_{max}$ , and particularly  $k_{cat}$ , were calculated for 25 and 37 °C to confirm the cold-active behavior of the lipase. Lipolytic activity of free and immobilized enzymes was detected for both tested temperatures (25 and 37 °C). According to the  $K_m$  values at 25 °C, lipase biocatalysts exhibited cold-active behavior, without substantial changes to the substrate's apparent affinity for a higher temperature (37 °C). In the case of the catalytic constant ( $k_{cat}$ ), similar values were recorded for both temperatures. For catalytic efficiency ( $k_{cat}/K_m$ ), the close values for both temperatures support the structural and functional stability of the proteinaceous material.

The developed biocatalytic process based on cold-active lipase activity involved the acylation of silybin as the main component of silymarin with methyl fatty acid esters (e.g., methyl decanoate, methyl laurate, methyl myristate, and methyl palmitate) for both free and immobilized biocatalysts. A maximum of 67% silybin conversion was reached for the immobilized biocatalyst and methyl decanoate as the acylating agent.

A valuable biocatalytic process based on the enzyme activity of a cold-active lipase fraction was successfully elaborated for silymarin. This biocatalytic system could offer several advantages for silymarin valorization such as (i) energy saving by the cold-active behavior of the biocatalyst, (ii) derivatization of the silybin structure with fatty acid residue leading to a more hydrophobic product, (iii) curative features of silybin esters when omega acid residues are used as the acylation agent, and (iv) improving the efficiency of the cold-pressed milk thistle oil technology by considering the corresponding residues as a silybin and fatty acid source.

### Acknowledgements

This work was financially supported by PNCDI III PED project (contract no. 356PED/2020) from UEFISCDI, Romania.

### References

1. Kropacova K, Misurova E, Hakova H (1998) Radiats. Biol. Radioecol. 38, 411-415.
2. Lu C, Lu Y, Chen J, Zhang W, Wu W (2007) Eur. J. Pharm. Biopharm. 66, 210-219.
3. Lee DY-W, Liu Y (2003) J. Nat. Prod. 66, 1171-1174.
4. Liang Q, Wang C, Li BB, Zhang AH (2015) Pharmacog. Mag. 43, 586-593.
5. Singh RP, Agarwal R (2006) Mol. Carcinogen 45, 436-442.
6. Gheorghita GR, Paun VI, Neagu SE, Maria G, Enache M, Purcarea C, Parvulescu VI, Tudorache, M (2021) Catalysts 11(11), 1390.

## Enzymatic Preparation of Lipophilic Derivatives of Hydroxytyrosol with Enhanced Oxidative Stability

Renia Fotiadou, Dimitrios C. Lefas, Myrto G. Bellou, Angeliki C. Polydera, Haralambos Stamatis\*.  
Laboratory of Biotechnology, Department of Biological Applications and Technologies, University of Ioannina, 45110  
Ioannina, Greece

\*Corresponding author: [hstamati@uoi.gr](mailto:hstamati@uoi.gr)

### Abstract

Natural compounds such as vanillyl alcohol (VA) and hydroxytyrosol (Htyr) exhibit strong antioxidant and other biological activities capturing much scientific and industrial attention. However, their widespread use is limited due to insufficient solubility in lipophilic media<sup>1</sup>. Meanwhile, common edible oils consist of mono- and polyunsaturated fatty acids that are susceptible to precocious auto-oxidation. Hence, transesterification of oils with natural antioxidant compounds is a promising approach that strengthens the potential to fully exploit the advantageous activities of natural phenols in lipophilic solutions. These functional oils could be used for different applications from cosmetics to food sector, as they would combine the beneficial properties of both components<sup>1,2</sup>. In this regard, a nanobiocatalytic system (NBS, immobilized enzyme on nanosized material) was developed for the targeted modification of pomace olive oil (POO) with two natural phenolic compounds. More specifically, lipase from *Thermomyces lanuginosus* was immobilized on the functionalized surface of green hybrid magnetic nanoparticles derived from an aqueous olive leaf extract (Zinc oxide-Iron oxide Nanoparticles, ZnOFe). The aim of this work was to investigate the ability of the nanobiocatalytic system, ZnOFe-TLL, to modify POO with antioxidants in solvent free conditions and assess its reusability. Reaction variables such as time, temperature, substrate concentration and enzyme quantity were evaluated. For an in-depth study, specific oxidative markers were investigated after accelerated oxidation of POO and modified POO for 14 days at 90 °C.

The results of this study reinforce the possibility of using immobilized biocatalysts for the preparation of "functionalized" oils with sufficient activity and recyclability. Moreover, "functionalized" oils were exhibited higher antioxidant activity (mg Trolox mg<sup>-1</sup> oil) than the control oil. The oxidative properties indicated that the control oil was more prone to auto-oxidation than the two modified according to conjugated dienes (CD) and TBARS values. Furthermore, POO modified with hydroxytyrosol was incredibly stable in contrast to control oil and POO modified with vanillyl alcohol. The observed differences were significantly ( $p < 0.05$ ). From the results of this study, it can be concluded that natural antioxidants can substitute synthetic antioxidants, as they reinforce shelf life of oils, have beneficial health effects, and promote sustainability. Moreover, a fully green nanobiocatalytic system was developed and applied to solvent-free biocatalytic reactions of interest conforming to the principles of green chemistry.

### Methods

Lipase from *Thermomyces lanuginosus* was kindly provided from Novozymes. Pomace olive oil was purchased from the local market. Hydroxytyrosol (CarboSynth), vanillyl alcohol (CarboSynth), 2-thiobarbituric acid (TBA, Sigma-Aldrich), malondialdehyde tetra-butylammonium salt (MDA, Sigma), 2,2-diphenyl-1-picrylhydrazyl (DPPH, Sigma), isooctane (LAB-SCAN), acetic acid (Sigma) were of analytical grade. Methanol, hexane, heptane, water were for liquid or gas chromatography and purchased from Fisher.

The fatty acid profile of pomace olive oil was estimated by gas chromatography-mass spectroscopy. Fatty acid methyl esters (FAMES) were prepared according to AOCS Official method Ce 2-66 and analyzed using a GCMS-QP2010 SE (Shimadzu). The modification of the fatty acids of POO with antioxidants was monitored and quantified by high performance liquid chromatography (HPLC) as previously described<sup>3</sup>. Fluorescence spectra of all samples were acquired in a quartz cuvette on a luminescence spectrofluorometer Jasco-8300 (Tokyo, Japan) at  $\lambda_{ex} = 400$  nm, as an excitation wavelength, with a scan speed of 100 nm min<sup>-1</sup> at room temperature. The samples were diluted in isooctane. Emission fluorescence of all samples was recorded at 600-750 nm in duplicate.

Antioxidant activity, conjugated dienes and thiobarbituric reactive substances were measured according to known methodologies. Immobilization of TLL on the surface of ZnOFe nanoparticles and transesterification reactions were conducted as previously described with minor modifications<sup>3</sup>.

### Results

Specific key results of this work are presented in Figures 1, 2 and Table 1. Green synthesized magnetic nanoparticles were used as carrier for the immobilization of TLL. The novel nanobiocatalytic system, ZnOFe-TLL, was applied to the targeted transesterification of pomace olive oil with two natural antioxidants. Because of the complex fatty acid composition of POO, four main products were produced and identified in any case. Conversion yields up to 90% were achieved with 20 mM of antioxidant and 10 mg mL<sup>-1</sup> nanobiocatalyst, as shown in Figure 1. Moreover, reactions were time dependent with similar rates.

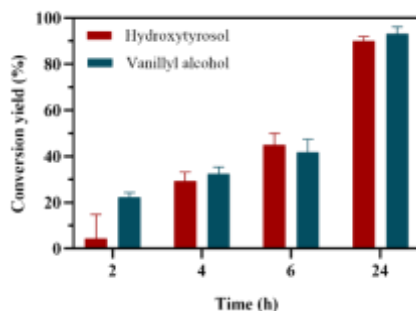


**Figure 6.** Time course of hydroxytyrosol (Htyr) and vanillyl alcohol (VA) esterification/transesterification with pomace olive oil. The reactions were conducted by ZnOFe-TLL ( $10\text{mg mL}^{-1}$ ) at  $50\text{ }^{\circ}\text{C}$  in solvent free conditions.

Thiobarbituric acid reactive substances (TBARS) assay and fluorescence spectroscopy were used as markers for lipid peroxidation of control and modified oils. TBARS assay assess the concentration of the secondary oxidation products that are formed during oxidation, while fluorescence spectroscopy gives a thorough insight about the adulteration of oils at  $\lambda_{\text{em}}=670\text{ nm}$  (decrease of chlorophyll peaks). As shown in Table 1, the oxidation of control oil proceeds rapidly in contrast to the modified oils ( $p<0.05$ ). Antioxidants were able to maintain POO stability under accelerated oxidation. More specifically, according to TBARS assay control oil fully oxidized after 14 days at  $90\text{ }^{\circ}\text{C}$ , whereas modified oils had much lower TBARS values. Moreover, fluorescence spectroscopy revealed a more rapidly deterioration of control oil pigments (Figure 2a) in contrast to Htyr modified oil (Figure 2b).

**Table 4.** Thiobarbituric acid reactive substances (TBARS) in control and modified oils with natural antioxidants. The values with the symbol (\*) differ significantly from those of the control oil.

Days	TBARS ( $\mu\text{M g}^{-1}\text{ oil}$ )		
	POO	POO modified with VA	POO modified with Htyr
1	$13.44 \pm 2.92$	$15.9 \pm 2.92$	$14.26 \pm 1.72$
4	$80.66 \pm 0.56$	$73.28 \pm 5.24$	$19.39 \pm 2.34^*$
7	$357.7 \pm 28.38$	$124.1 \pm 5.24^*$	$74.92 \pm 16.78^*$
10	$410.57 \pm 9.83$	$126.97 \pm 7.51^*$	$89.26 \pm 2.87^*$
14	$438.03 \pm 19.68$	$124.92 \pm 4.66^*$	$97.05 \pm 3.5^*$

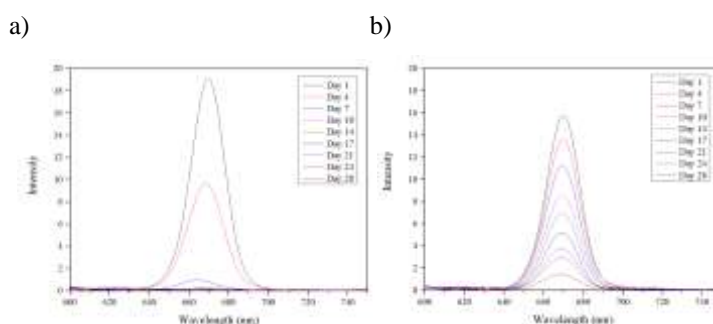


**Figure 7.** Fluorescence spectra of control oil (a) and Htyr modified oil (b) after accelerated oxidation at  $90\text{ }^{\circ}\text{C}$  for 28 days.

To sum up, ZnOFe-TLL, a fully green NBS can be effectively utilized for the targeted modification of antioxidant compounds in order to acquire lipophilic derivatives with enhanced oxidative stability.

## Acknowledgements

This research has been co-financed by the European Regional Development Fund of the European Union and Greek national funds through the Operational Program Competitiveness, Entrepreneurship, and Innovation, under the call RESEARCH-CREATE-INNOVATE (project code: T2EDK-03599).

## References

1. H. Zhang, M. Zheng, J. Shi, H. Tang, Q. Deng, F. Huang, D. Luo., *Food Chem.*, **248**, 272 (2018).
2. M. Ćorović, A. Milivojevic, M. Simovic, K. Banjanac, P. Pjanovic, D. Bezbradica., *Sustain Chem Pharm.*, **15**, 100231 (2020).
3. R. Fotiadou, A. V. Chatzikonstantinou, M. A. Hammami, N. Chalmpes, D. Moschovas, K. Spyrou, A. C. Polydera, A. Avgeropoulos, D. Gournis, H. Stamatis., *Nanomaterials*, **11**, 458 (2021).

## Synthesis of novel rearranged stemodane diterpenoids and their biotransformation by *Exophiala lecanii-corni*

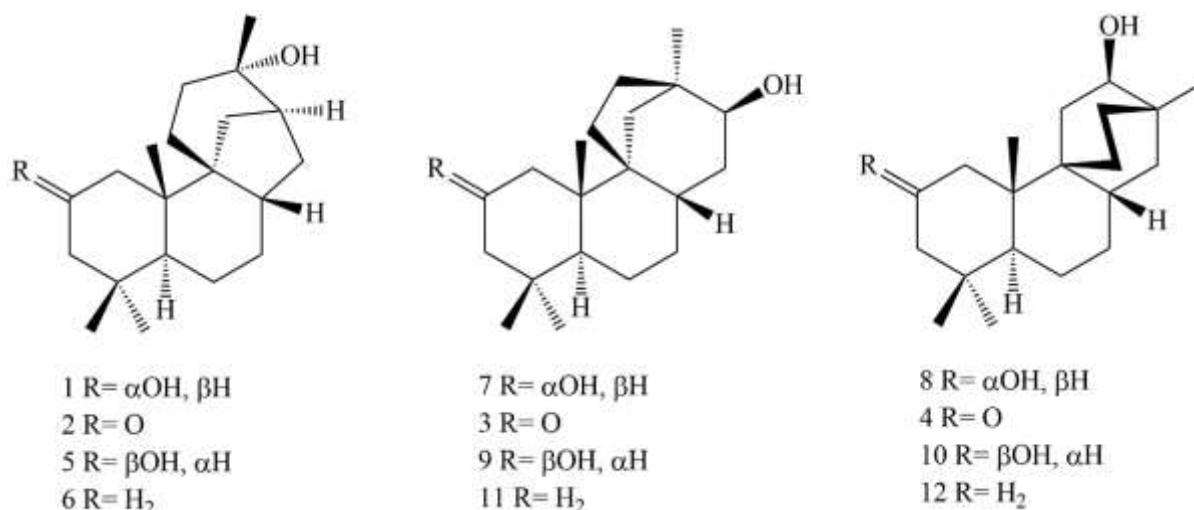
Ricaldo K. Pryce<sup>1</sup> and Paul B. Reese<sup>2\*</sup>

Department of Chemistry, The University of the West Indies, Mona, Kingston 7, Jamaica.  
ricaldopryce@gmail.com

Stemodin (**1**) is a biologically active natural product from *Stemodia maritima*. The compound possesses cytotoxic and antiviral properties and can be obtained in relatively large quantities from the plant.<sup>1</sup> Stemodinone (**2**), also isolated from *S. maritima* (albeit in lower quantities), can be generated by simple oxidation of **1**. In the presence of aqueous acid, **2** undergoes solvolytic rearrangement to form 15(13→12)*abeo*-13 $\beta$ -hydroxystemaran-2-one (**3**) and 15(8→9)*abeo*-8 $\beta$ (H)-12 $\beta$ -hydroxystemaran-2-one (**4**).<sup>2</sup> The skeleton of **3** is similar to that of the scopadulanes, which inhibit the porcine H<sup>+</sup>, K<sup>+</sup>-ATPase enzyme, and possess antitumour and antiviral activities against the *Herpes simplex* virus type 1. These natural products also interfere with the nutrient transport of the malarial parasite *Plasmodium falciparum*.<sup>3</sup> The biological activity of compounds bearing the skeleton of **4** have not been explored.

Diterpene **2** is readily chemically converted to analogues **5** and **6**. The solvolyses of **1**, **5** and **6** were carried out in order to generate similar products of rearrangement. The biological properties of these novel analogues were assessed and found to possess antioxidant and antianalgesic properties while their efficacies against various cancer cell lines are being assessed. The analogues also served as substrates for transformation by the fungus *Exophiala lecanii-corni*. The aim is the production of a series of novel compounds for bioassay. *E. lecanii-corni* has previously been exploited as a catalyst for steroid biotransformation. However, its potential for microbial functionalization of terpenes is yet to be investigated.

Figure 1: Rearranged stemodane analogues



### Acknowledgements

I would like to thank Professor Muraleedharan Nair from Michigan State University for the COX-1 and COX-2 inhibitory bioassays as well as the antioxidant studies. I would also like to thank the Office of Graduate Studies and Research at UWI for the research grant which was used to fund the purchase of reagents and glassware for the research.

### References

1. F. Russell, V. Mulabagal, D. Thompson, M. Singh-Wilmot, W. Reynolds, M. Nair, V. Langer and P. Reese, *Phytochemistry*, 2011, **72**, 2361-2368.
2. G. Martin, W. Reynolds and P. Reese, *Phytochemistry*, 2005, **66**, 901-909.
3. M. Riel, D. Kyle and W. Milhous, *J. Nat. Prod.*, 2002, **65**, 614-615.

## DES-based biocatalysis for menthol derivatization

Ciorici A.M., Sabina I., Parvulescu V.I., Tudorache M.\*

Department of Organic Chemistry, Biochemistry and Catalysis, Faculty of Chemistry, University of Bucharest, Sos. Panduri, No. 90-92, sector 5, Bucharest, Romania

\*email: madalina.sandulescu@g.unibuc.ro

Terpenes derivatization based on the biocatalytic (enzymatic) process is a widely used method due to the good efficiency, high enantio-specificity and also cost-effectiveness, especially for the use of immobilized enzyme. However, the polarity of the aqueous phase requested by the enzyme activity is in contrast with the low water solubility of the reagents (e.g. menthol). This is an important limitation aspect especially for the industrial esterification/ transesterification process. Enzymatic processes are not only restricted by low solubilities of the interested substrates and solvent-based inhibition of the enzyme activity, but also by a lack of enzyme stability in the chosen solvent.

To overcome these drawbacks, enzymatic reactions have been performed in non-conventional reaction media (e.g. ionic liquids, supercritical fluids, deep eutectic solvents - DES). DESs are eutectic mixtures of at least two components coupled by hydrogen bond interactions. The resulted mixture is liquid at room temperature, comfortable used as solvent and with lower freezing point compared to the initial constituents. DES involvement in enzymatic biocatalysis has been first described by Abbott and co-workers in 2003 and gained attention as alternative reaction media for biocatalytic process.

We developed a DES-based biocatalytic method for (-)-menthol acylation with methyl fatty acids (FAME) using immobilized lipase enzyme as biocatalyst. The mixture of menthol and FAME in a certain molar ratio was the DES solvent phase of the proposed biocatalytic process. Chemical interaction between DES components started by adding a lipase in DES phase. Optimization and validation of the developed method has been performed. The experimental data and their scientific message will be detailed in a poster presentation.

### Acknowledgements

This work was financially supported by PNCDI III PED project (contract no. 376PED/2020) from UEFISCDI, Romania.

### References

- A.P. Abbott, G. Capper, D.L. Davies, R.K. Rasheed, V. Tambyrajah, *Chem. Comm.* **2003**, 70.
- J.T. Gorke, F. Srienc, R.J. Kazlauskas, *Chem. Comm.* **2008** 10.
- P. Patzold, A. Weimer, A. Liese, D. Holtmann, *Biotechnol Reports* **2019**, 22, e00333.
- M. Hummer, S. Kara, A. Liese, I. Huth, J. Schader, D. Holtmann, *Molec. Catal.* **2018**, 458, 67.

## Reactive natural deep eutectic solvents as essential reaction media for lipase catalyzed carbohydrate esterification

Carmen Gabriela Boeriu<sup>1,2\*</sup>, Alina Ramona Buzatu<sup>1,3</sup>, Ioan Bîtcă<sup>1</sup>, Diana Maria Dreavă<sup>1</sup>, Anamaria Todea<sup>1</sup>, Francisc Peter<sup>1</sup>

<sup>1</sup> Faculty of Industrial Chemistry and Environmental Engineering, Polytechnic University Timisoara, Romania;

<sup>2</sup> Wageningen Food & Biobased Research, Wageningen, The Netherlands; <sup>3</sup> Department of Biochemistry and Pharmacology, "Victor Babes" University of Medicine and Pharmacy, Timisoara, Romania;

\*carmengabriela.boeriu@upt.ro, carmen.boeriu@wur.nl

Biocatalytic routes for carbohydrate esterification show the important advantage of carrying out the reactions in a single step, without protection/deprotection of the hydroxyl groups, but also face some challenges, one of the most important being the selection of the appropriate solvent, as the solubilization of sugars, the stability and regioselectivity of lipases in the reaction medium as well as the environmental issues must be solved [1, 2]. Natural deep eutectic solvents (NADES) emerged as a novel class of green solvents and a possible solution for most of the problems related to the reaction media in biocatalytic transformations, being nontoxic, biodegradable and biocompatible [3, 4]. In this study, a new concept for the enzymatic synthesis of fatty acid esters of carbohydrates and carbohydrate polyols has been explored, using a reactive NADES as reaction medium, where the deep eutectic solvent has a double role, as a solvent and as a reagent pool. The research focused on three main directions: (i) preparation and characterization of a broad range of NADES, (ii) evaluation of the effects of NADES composition and properties on the esterification activity and operational stability of free and immobilized enzymes and (iii) estimation of the synthetic capacity of selected enzymes for the synthesis of fatty acid esters of carbohydrates and carbohydrate polyols in reactive NADES.

Binary and ternary hydrophilic NADES based on choline chloride (ChCl) as hydrogen bond acceptors (HBA) and different hydrogen bond donors (HBD) such as urea (U), monomethyl urea (MU), sugar alcohols (sorbitol, xylitol, arabitol), monosaccharides (glucose), and disaccharides (sucrose, maltose), were prepared and characterized by DSC, TGA and dynamic rheology to determine the freezing temperature ( $T_f$ ), the thermal stability and the viscosity-temperature profile. NADES based on urea/glucose 2:1, MU/glucose 2:1, ChCl/urea/glucose 1:1:1 and ChCl/urea/glucose 1:2:1 were liquid at room temperature (RT), with low viscosity in a broad temperature range. All other NADES of ChCl with sugars and polyols were gels at RT and viscous fluids above 60 °C.

Thirteen native lipases from different microbial sources and the commercial immobilized *Candida antarctica* B lipase (N435) were efficient in the synthesis of propyl laurate in both the generally used tert-butanol/DMSO solvent mixture and in the ChCl:glucose (2:1) NADES. However, only few could convert sugars into lauryl esters. The most active enzymes, e.g. the lipases from *Candida antarctica* B (CalB), *Candida antarctica* A (CalA), *Pseudomonas stutzeri* (*Ps. stutzeri*), and *Aspergillus oryzae* and N435, showed significant esterification activity in all 18 different binary and ternary ChCl-based NADES prepared. Moreover, the selected enzymes showed relatively high thermal stability in NADES at 70°C (Figure 1A). The highest stability was observed in the first 24 hours for native *A. oryzae* and *C. antarctica* A lipases. The immobilized CalB (N435) showed not only high activity in the selected NADES, but also exceptionally high thermal stability, maintaining 92% of activity upon incubation at 70°C for 72 h (Figure 1A).

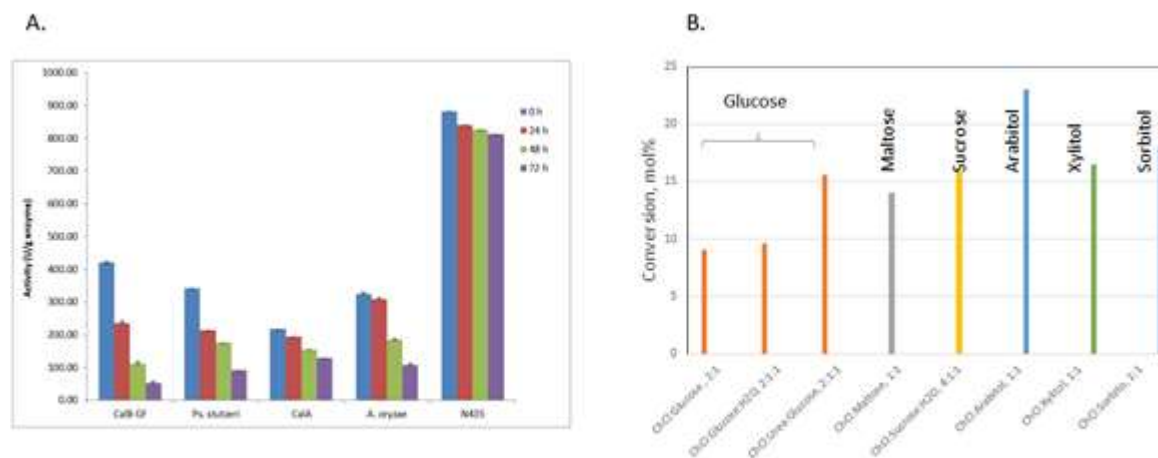


Figure 1. A) Esterification activity of selected native lipases in ChCl/glucose 2:1 NADES, upon incubation at 70°C, in time.

B) Substrate conversion during esterification of carbohydrates and carbohydrate polyols with immobilized CalB lipase (N435), in reactive NADES, at 70 °C.



Synthesis of mono-lauryl and di-lauryl esters of carbohydrates (e.g. glucose, sucrose, maltose) and polyols (e.g. arabitol, xylitol, sorbitol) catalyzed by immobilized *C. antarctica* lipase B (N435) in the corresponding ChCl/sugar or ChCl/polyol reactive NADES was demonstrated by HPLC, MALDI-TOF-MS and 1D and 2D NMR. Highest conversion (23 mol%) was obtained for the arabitol lauryl esters (Figure 1B). The type and properties of the NADES has a high influence on the progress of reaction, as shown for glucose esterification, when the highest conversion (16%) was obtained for the low viscosity ChCl/urea/glucose 2:1:1 NADES (Figure 1B).

In conclusion, in this study a large spectrum of choline chloride based reactive NADES with physical and fluid properties suited for biocatalysis were successfully obtained and evaluated as reaction media for the synthesis of lauric esters of monosaccharides, disaccharides and carbohydrate polyols. Several enzymes showed significant activity and high thermal stability in NADES, and were able to efficiently convert carbohydrates and polyols into their lauryl esters. The results are very promising and open the way to further explore the potential of NADES as reaction medium for the enzymatic synthesis of long alkyl chain esters of oligosaccharides.

### Acknowledgements

This work was supported by a grant of the Romanian Ministry of Education and Research, CCCDI-UEFISCDI, project number PN-III-P4-ID-PCE-2020-2177, within PNCDI III, contract number PCE 157/2021.

### References

1. Van Kempen S.E.H.J., Boeriu C.G., Schols H.A., de Waard P., van der Linden E., Sagis L.M.C., *Food Chemistry*, **138** 1884 (2013)
2. Ter Haar R., Schols H.A., van den Broek L.A.M., Sağlam D., Frissen A.E., **Boeriu C.G.**, Gruppen H. *J. Mol. Cat. B. Enzymatic*. **62** 183 (2010)
3. Pätzold M., Siebenhaller S., Kara S., Liese A., Syldatk C., Holtmann D. *Trends Biotechnol.* **37** 943, (2019)
4. Tan J.-N., Dou Y., *Appl. Microbiol. Biotechnol.* **104**, 1481 (2020).

# Biomass and renewables valorization

# The Use of Cellulose Nanocrystals as Scaffolds for Nanodevices, Photoreversible and Antimicrobial Self Assemblies; Supramolecular Chemistry Using Nature's Most Abundant Template

Dimitris S. Argyropoulos; Reza Ghiladi, Frank Scholle, I. Fillponnen, H. Sadeghifar,

*Departments of Chemistry & Forest Biomaterials*

*North Carolina State University*

*Raleigh, NC, 27695-8005*

*USA*

*E mail: dsargyro@ncsu.edu*

*http://www4.ncsu.edu/~dsargyro/*

## Abstract

Over a number of years work in our laboratory has been exploring the use of cellulose nanocrystals (CNC) as scaffolds for the creation of novel nanomaterials with unique and stimuli responsive characteristics. The forces responsible for the spatial organization within cellulose, coupled with traditional chemistry are aimed at creating structures via molecular self assembly; These concepts have been the inspiration for our supramolecular research. In this lecture we will report on our systematic efforts aimed at functionalizing CNCs by using both grafting from and grafting onto approaches. The selective creation and activation of a nano-pattern on CNC will be described and the chemical methods used to create the foundation for novel CNC based materials (including self-assembled Cellulose NanoPlatelet Gels), photo reversible light induced and novel antimicrobial assemblies will be described.

## Introduction

The modification of polysaccharides plays a central role in the field of sustainable chemistry. By the virtue of their large abundancy and the structural and superstructural diversity polysaccharides are ideal starting materials for defined modifications and specific applications. The chemical modification of polysaccharides provides a versatile route for the structure and property design of such materials. Due to the chemical functionality of polysaccharides (bearing hydroxyl and/or carboxylic acid groups) the esterification and etherification are the most common approaches for the modification reactions of polysaccharides. Moreover, the oxidation and homogenous nucleophilic substitution reactions are applied but to a lesser extent. Cellulose and dextran are the most commonly used starting materials for the creation of highly engineered nanoparticles.

In general, 1,3-dipolar cycloaddition reactions have long been popular in the generation of carbohydrate mimetics in homogeneous reaction environment. More precisely, the thermally induced cycloaddition (Huisgen reaction) occurs between an azide and a triple bond and is nowadays often referred as a member of the click-reaction family because of its robustness. The reaction has gained increasing attention after discovering that the 1,3-dipolar cycloaddition between azides and terminal alkynes can be catalysed by Cu(I) salts. In fact, the Huisgen reaction has become the most popular click reaction to date by the virtue of its high yields, rapidity, high regio- and stereoselectivity, mild reaction conditions and experimental simplicity. Several authors have described the use of this novel click-chemistry concept for the generation of carbohydrate mimetics and derivatives

## Results and Discussion

In this paper we describe the formation of nano-platelet gel-like nanomaterials formed using cellulose nanocrystals (CNC) as the starting material. Initially, the primary hydroxyl groups on the surfaces of the CNCs were selectively activated to carboxylic acids by using TEMPO-mediated hypohalite oxidation. In the next step, compounds carrying terminal amine functionality were grafted on to the surface activated oxidized CNC's via the carbodiimide-mediation, creating an amide linkage between the amine and the carboxylic groups on the CNC's surfaces. The grafted amine compounds contained terminal alkyne or azide functionalities and as such two sets of precursors were prepared. The alkyne and azide, surface functionalized CNC precursors, were then brought together via the "Click"-chemistry creating, for the first time, unique nano-platelet gels as evidenced by detailed transmission electron microscopic investigations (TEM).

These approaches were followed and evaluated for the creation for novel CNC based materials (including self-assembled Cellulose NanoPlatelet Gels), photo reversible light induced and novel antimicrobial assemblies.

"Click"-chemistry has been shown effective for the preparation of new gel-like cellulose nanomaterials. The primary hydroxyl groups in cellulose nanocrystals were first selectively activated by their conversion to carboxylic acids. These regularly spaced surface functionalities were further used as reactive sites for amidation reactions, providing the essential precursors to "Click"-chemistry. TEM images of the produced materials showed evidence of the crystals being packed in an organized manner.

Furthermore, our work has shown and will report the synthesis of fluorescent cellulose nanocrystals (CNCs) by covalently linking of fluorescence chromophores to the cellulose surface. First, the primary hydroxyl groups on

the surface of the CNCs were converted to carboxylic acids by using TEMPO-mediated hypohalite oxidation. In the next step, a compound (propargylamine) carrying a terminal amine functionality was grafted on to the oxidized CNCs via carbodiimide-mediated formation of an amide linkage between an amine and the carboxylic groups on the CNC's surface. The grafted amine also contained an alkyne functionality which was then used as the reaction site for further modification. These modified CNCs were finally subjected to Click chemistry reaction conditions i.e. Copper(I)-catalyzed Azide-Alkyne Cycloaddition (CuAAC) with an azide-bearing fluorescent coumarin and anthracene chromophores resulting in highly fluorescent nano cellulosic materials. Finally, the produced materials were subjected to photochemical irradiation inducing [2+2] and [4+4] cycloaddition reactions respectively between the installed coumarin and anthracene side chains, causing the photo-induced formation of cellulosic based crystalline nano-arrays. Current efforts to reverse these reactions at lower wavelengths will pave the way toward the creation of photo induced tunable cellulosic based nanomaterials.

Finally, we will demonstrate our efforts toward the development of textile materials through the covalent attachment of commercially available phenothiazine and porphyrin-based photosensitizers (PS) to nanofibrillated cellulose (NFC) and paper (Pap), imparting antimicrobial activity on them via a photodynamic mode of action. The facile covalent attachment of the free-base 5-aminophenyl-10,15,20-tris-(4-methylpyridin-4-ium-1-yl)porphyrin (A3B) and metallated 5-aminophenyl-10,15,20-tris-(4-methylpyridin-4-ium-1-yl)porphyrin zinc(II) (A3B-Zn) was accomplished by cyanuric chloride coupling. Materials characterization and the degree of photosensitizer loading were determined by FTIR, elemental & TGA Analyses, SEM, and UV-Visible Diffuse Reflectance Spectroscopy (UV-Vis DRS). The antimicrobial potency of the PS-NFC and PS-Pap materials was determined under controlled, illumination conditions against four strains of bacteria recognized by the World Health Organization (WHO) as either critical or high priority pathogens: Gram-positive strains methicillin-resistant *S. aureus* (MRSA; ATCC-44) and vancomycin-resistant *E. faecium* (VRE; ATCC-2320), and Gram-negative strains multidrug-resistant *A. baumannii* (MDRAB; ATCC-1605) and *K. pneumoniae* (KP; ATCC-2146). Our results demonstrated broad photodynamic inactivation of all strains studied upon illumination (30 min; 65±5 mW/cm<sup>2</sup>; 400-700 nm) by a minimum of 99.9999%, although it was noted that the Gram-negative strains required greater PS concentrations or longer incubation times to achieve this level of inactivation. Antiviral studies employing the nanofibrillated cellulose conjugates against two enveloped viruses, Dengue-1 (DENV) and Vesicular Stomatitis Virus (VSV), revealed complete inactivation by both materials. Differences between the photobiocidal efficacies of the PS employed in this study will also be discussed.

## Conclusions

Cellulose nanocrystals offer tremendous possibilities for the creation of novel materials and assemblies with designed characteristics. The chemistry and the potential of these most abundant natural templates will be explored and various novel applications will be demonstrated

## Crosslinking of Sugar-Derived Polyethers and Boronic Acids: Synthesis of Functional Films and Organogels

*Emma L. Daniels*<sup>1</sup>, Dr. Antoine P. Buchard<sup>\*1,3</sup>, Dr Hannah S. Leese<sup>\*2,3</sup>, and Prof Steve Parker<sup>1,3</sup>

<sup>1</sup> Department of Chemistry, University of Bath, Claverton Down, Bath, BA2 7AY, UK

<sup>2</sup> Department of Chemical Engineering, University of Bath, Claverton Down, Bath, BA2 7AY, UK

<sup>3</sup> Centre for Sustainable and Circular Technology, CSCT, University of Bath, Claverton Down, Bath, BA2 7AY, UK

\**apb46@bath.ac.uk, hsl25@bath.ac.uk*

Polymers are vital materials in today's society and are used in a wide range of advanced applications. However, many commodity polymers such as polypropylene and polyesters are derived from fossil fuels, accounting for 7% of global oil and gas usage, and contribute significantly to plastic pollution [1, 2]. Replacing such functional polymers with renewable, potentially biodegradable polymers is therefore crucial. Several renewably-sourced polymers have been developed, including those derived from sugars such as D-Mannose and D-xylose [2-5]. In this work, we will discuss the synthesis of sugar-derived polyesters and their development into functional materials. Namely, the development of conductive films and crosslinked hydro/organogels.

Polyethers can be derived from xylose sugars (**Figure 1**). After polymerization, removal of acetal protecting groups can be achieved through treatment with aqueous acid. The degree of deprotection is controllable [5] and reveals hydroxyl groups along the polymer backbone. 1,2-diols such as these are known to react with boronic acids to form cyclic boronate esters [6 - 8]. In this work, this chemistry has been exploited to achieve polymer crosslinking with difunctional boronic acids (**Figure 1**).

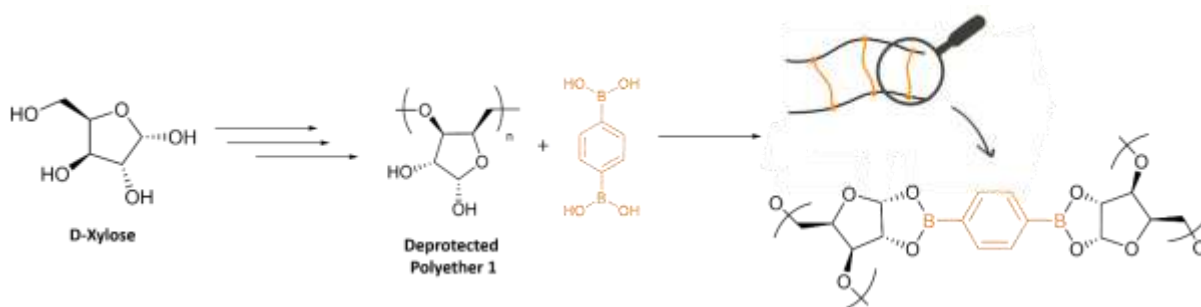


**Figure 1** Polymer crosslinking; reaction of a deprotected sugar-derived polymer with 1,4-diboric acid as a difunctional

Crosslinking of deprotected polyethers with 1,4-benzene diboric acid (DBA) in dimethyl sulphoxide (DMSO) results in the formation of crosslinked organogel networks. These gels show viscoelastic properties that can be tuned by altering the degree of crosslinking (**Figure 2a**). Similar boronic acid-based gels have applications within healthcare technologies as glucose sensors, drug release materials, and cell culture media [5]. Furthermore, crosslinking in the presence of lithium counter cations enables hydrogel derivatives to be produced, and introduces conductivity. The utility of crosslinked gels as gel polymer electrolytes has been explored: initial electrochemical impedance spectroscopy (EIS) measurements show typical Nyquist behaviour, indicating conductivity [9].

Various crosslinked films have been synthesised: deprotected polyethers are reacted with borax, lithiated DBA, or lithiated boric acid in aqueous conditions. After purification by dialysis, films are obtained by solvent casting (**Figure 2b**). Initial EIS measurements show these materials to be promising candidates for solid polymer electrolytes (SPEs). By performing crosslinking in the presence of a small molecule template, the utilization of these gels and/or films as platforms for boronic-acid based molecular imprinting technologies will also be discussed [7].

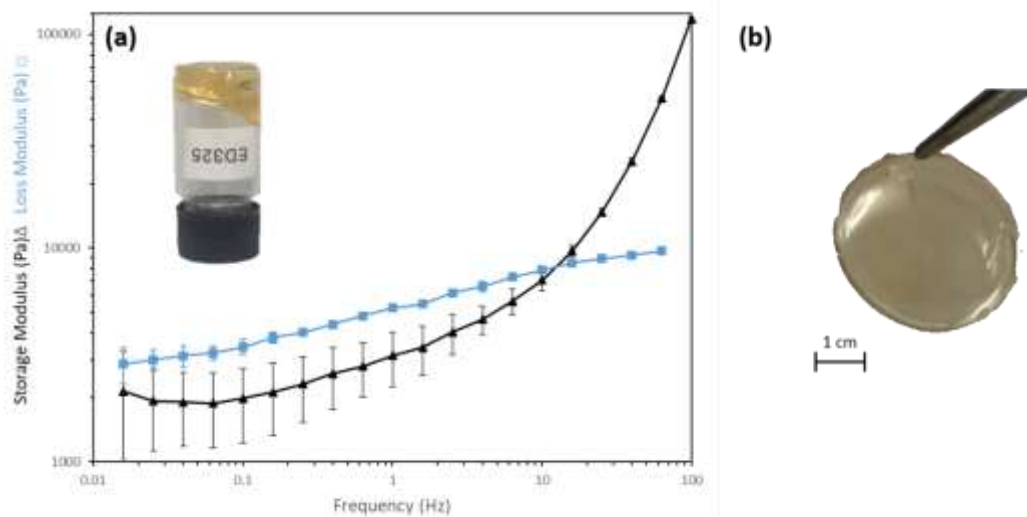


**Figure 2** Crosslinked (a) organogels showing viscoelastic behaviour and (b) solvent cast films, suitable for EIS analysis.

## Acknowledgements

This work was supported by the Engineering and Physical Sciences Research Council grant, EP/L016354/1. The authors gratefully acknowledge the Material and Chemical Characterisation Facility (MC<sup>2</sup>) at University of Bath.

## References

1. Y. Zhu, C. Romain, and C. K. Williams, *Nature Review*, 2016, **540** (10), 354-362
2. J-G. Rosenboom, R. Langer, and G. Traverso, *Nature Reviews Materials*, 2022, **7**, 117-137
3. G. L. Gregory, L. M. Jenisch, B. Charles, G. Kociok-Köhn, A. Buchard, *Macromolecules*, 2016, **49**, 7165-7169
4. T. M. McGuire, C. Pérale, R. Castaing, G. I. Kociok-Köhn, A. Buchard, *Journal of the American Chemical Society*, 2019, **141**, 13301-13305
5. T. M. McGuire, J. Bowels, E. Deane, E. Farrar, M. N. Grayson, A. Buchard, *Angew. Chem. Int. Ed.*, 2021, **60**, 4524-4528
6. Y. Guan and Y. Zhang, *Chem. Soc. Rev.*, 2013, **42** (20), 8160-8121
7. W. L. A. Brooks, and B. S. Sumerlin, *Chemical Reviews*, 2016, **116** (3), 1375-1397
8. A. Pettignano, S. Grijalvo, M. Haring, R. Eritja, N. Tanchoux, F. Quignard, D. D. Diaz, *Chem. Comm.*, 2017, **53** (23), 3350-3353
9. K. Dai, Y. Zheng, W. Wei, *Adv. Funct. Mater.*, 2021, **31**, 2008632

## Green dual crosslinking treatments to produce chitosan microspheres based on tripolyphosphate and vanillin: a comparative study of two strategies

Rodolpho F. Correa<sup>1,2</sup>, Giovana Colucci<sup>1</sup>, Nouredine Halla<sup>3</sup>, João A. Pinto<sup>1</sup>, Arantzazu Santamaria-Echart<sup>1,\*</sup>, Silvia P. Blanco<sup>2</sup>, Isabel P. Fernandes<sup>1</sup>, Maria-Filomena Barreiro<sup>1,\*</sup>

<sup>1</sup>*Centro de Investigação de Montanha (CIMO), Campus de Santa Apolónia, Instituto Politécnico de Bragança, 5300-253 Bragança, Portugal*

<sup>2</sup>*Universidade Tecnológica Federal do Paraná, Av. Dos Pioneiros, 3131-Jardim Morumbi, Londrina 86036-370, Brazil*

<sup>3</sup>*Laboratory of Biototoxicology, Pharmacognosy and Biological Recovery of Plants, Department of Biology, Faculty of Sciences, University of Saida, Saida 20000, Algeria*

\*asantamaria@ipb.pt (A.S-E.); barreiro@ipb.pt (M-F.B.)

Microencapsulation procedures have recently focused attention on designing novel sustainable microspheres to be used in several application fields, including food, pharmaceuticals, and cosmetics [1,2]. The broad range of possibilities to design microspheres, together with the recent focus on green strategies, has evolved to solutions involving biopolymers [2,3] and avoiding toxic chemicals [4,5]. Among biopolymers, chitosan (CS) is presented as an attractive candidate considering its renewable character along with its antibacterial, antifungal, antioxidant, and anticancer properties, biodegradability, and non-toxicity [6]. Nevertheless, CS solubility in acidic medium ( $\text{pH} < 6.3$ ), implying instability in aqueous and physiological environments [7], can limit CS application in specific scenarios. Therefore, crosslinking through physical, chemical, or combined strategies has gained attention to overcome this challenge [8]. Particularly, those based on green routes and highlighting the combination of physical and chemical crosslinking routes to modulate the structure, of the CS microspheres.

In this context, this work aims to address the dual crosslinking strategy of CS (brand 90/200/A1; deacetylation degree of 91.9%) based on the potential of sodium tripolyphosphate (TPP) [9], Generally Recognized as a Safe Substance (GRAS), and vanillin (VA) natural compound [10]. In the first ionically crosslinking step, the CS microspheres were prepared by spray-coagulation, atomizing an acidic CS solution in a TPP coagulation bath (3, 5 and 10 TPP (w/v) concentrations were used) at pH 6 allowing to be consolidated for 3.5 h. The base CS microspheres were coded as CS3, CS5, and CS10, corresponding to 3, 5, and 10% TPP (w/v), respectively. In the second step, a chemical crosslinking was conducted using a 1% (w/v) VA solution following through two alternative strategies: in-situ and post-treatment methods. In the in-situ crosslinking, the VA solution was added directly to the coagulation bath and the coagulation bath was heated to 50 °C for 2 h. In the post-treatment, the ionically crosslinked microspheres were recovered by vacuum filtration, and washed with distilled H<sub>2</sub>O. Then, the microspheres were transferred to a VA solution (neutral pH) and the crosslinking reaction occurred at 50 °C for 2 h. By both strategies, the produced microspheres were recovered by vacuum filtration, washed with distilled H<sub>2</sub>O, and lyophilized. The dual crosslinked CS microspheres were coded according to the first step codification followed by “VA<sub>in-situ</sub>” or “VA<sub>post</sub>”, according to the corresponding covalent crosslinking strategy.

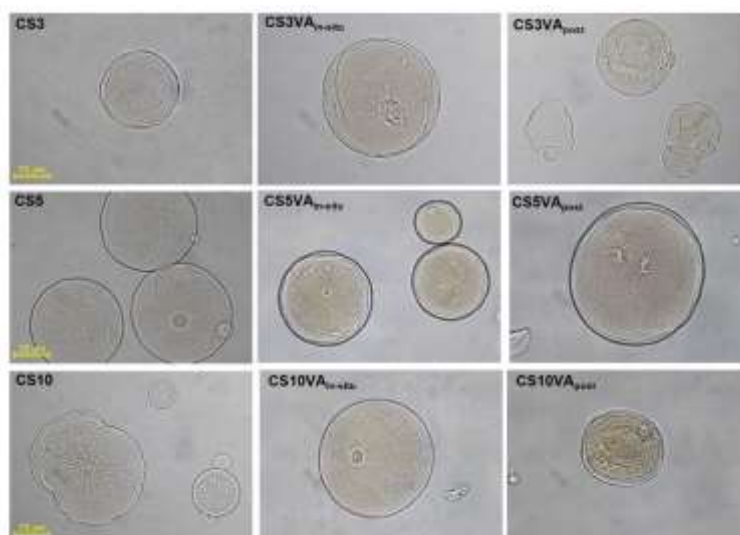


Figure 1. OM images of the produced microspheres at 400x magnifications (scale bar 25  $\mu\text{m}$ ).

Figure 1 shows the morphology of the obtained microspheres, including the physically crosslinked and the covalently crosslinked systems by both strategies. When 3% of TPP was employed (CS3), the microspheres exhibited a more fragile and unregular shape, showing the lowest values of particle size, evidencing that this TPP concentration was not enough to provide an effective crosslinking [11]. As the TPP concentration increased, microspheres become more spherical and better consolidated, which was accompanied by an increase in the

particle size for the particles produced with 5% TPP. Nevertheless, at high TPP concentration (10%), the higher crosslinking level induced the formation of denser microspheres whose hydrodynamic volume was reduced [12].

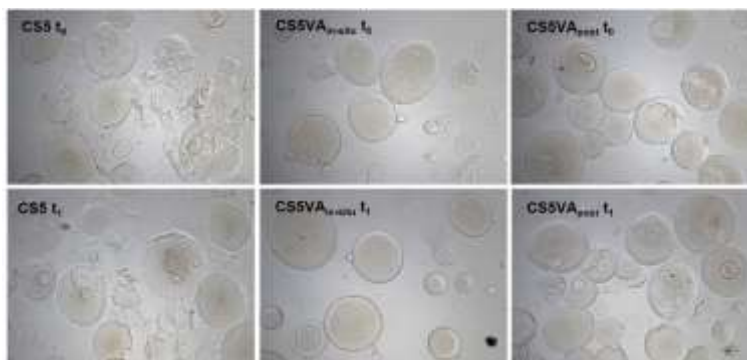


Figure 2. OM images of 5% w/v TPP microspheres swelling tests after 1 h (t0) and 1 day (t1) at 100× magnification.

The microspheres were subjected to swelling in acidic medium (pH 3.2) and analyzed after 1 h (t0) and 1 day (t1). Figure 2 shows the behavior of the systems based on 5 % w/v of TPP. It was generally observed that microspheres subjected to the ionic crosslinking with TPP were not stable in acidic medium, resulting in their disruption. The covalent crosslinking with VA decreased the disaggregation of the microspheres. Both formulations (CS5VA<sub>in-situ</sub> and CS5VA<sub>post</sub>) maintained their shape and appearance in comparison to the physically crosslinked counterpart (CS5). Particularly CS5VA<sub>in-situ</sub> due to the more effective crosslinking through this strategy, where the reaction of the remaining free amine groups after the ionic crosslinking is favored when VA is directly added to the TPP coagulation bath.

### Acknowledgements

Financial support by national funds FCT/MCTES to CIMO (UIDB/00690/2020). National funding by the FCT-Foundation for Science and Technology, through the institutional scientific employment program-contract with I.P.F and A.S.E. Further support was obtained through the Valor Natural project (Mobilized Project Norte-01-0247-FEDER-024479) and the GreenHealth project (Norte- 01-0145-FEDER-000042).

### References

1. S.K. Ghosh, Wiley: Weinheim, Germany, ISBN 352731296X (2006)
2. I.M. Martins, M.F. Barreiro, M. Coelho, A.E. Rodrigues, *Chem. Eng. J.* **245**, 191 (2014)
3. J. Kozłowska, W. Prus, N. Stachowiak, *Int. J. Biol. Macromol.* **129** 952 (2019)
4. B.N. Estevinho, F. Rocha, Elsevier Inc. Amsterdam, The Netherlands, ISBN 9780128114490 (2018)
5. F. Nazzaro, P. Orlando, F. Fratianni, R. Coppola, *Curr. Opin. Biotechnol.* **23** 182 (2012)
6. I. Aranaz, M. Mengibar, R. Harris, I. Panos, B. Miralles, N. Acosta, G. Galed, A. Heras, *Curr. Chem. Biol.* **3** 203 (2012)
7. A. Aljawish, I. Chevalot, J. Jasniewski, J. Scher, L. Muniglia, *J. Mol. Catal. B Enzym.* **112** 25 (2015)
8. H. Mittal, S.S. Ray, B.S. Kaith, J.K. Bhatia, Sukriti, J. Sharma, *Eur. Polym. J.* **109** 402 (2018)
9. T. Józwiak, U. Filipkowska, P. Szymczyk, J. Rodziewicz, A. Mielcarek, *Funct. Polym.* **114**, 58 (2017)
10. E.A. Borges da Silva, M. Zabkova, J.D. Araújo, C.A. Cateto, M.F. Barreiro, M.N. Belgacem, A.E. Rodrigues, *Chem. Eng. Res. Des.* **87** 1276 (2009)
11. S. Hassani, A. Laouini, H. Fessi, C. Charcosset, *Colloids Surfaces A Physicochem. Eng. Asp.* **482** 34 (2015).
12. J. Li, Q. Huang, *Carbohydr. Polym.* **87** 1670 (2012)



## FucoPol-based cosmetic creams: Formulation design, stability evaluation, rheological and texture assessment

Sílvia Baptista<sup>1,2,3</sup>, Filomena Freitas<sup>1,2\*</sup>, Maria A.M. Reis<sup>1,2</sup>

<sup>1</sup> Associate Laboratory i4HB - Institute for Health and Bioeconomy, School of Science and Technology, NOVA University Lisbon, Caparica, Portugal

<sup>2</sup> UCIBIO – Applied Molecular Biosciences Unit, Department of Chemistry, School of Science and Technology, NOVA University Lisbon, 2819-516 Caparica, Portugal

<sup>3</sup> 73100, Lda. Edifício Arcis, Rua Ivone Silva, 6, 4º piso, 1050-124 Lisboa, Portugal

\* a4406@fct.unl.pt; Tel.: +351 212948357

**Abstract:** Production of topical formulations based on sustainable ingredients is receiving widespread attention from researchers and industry – driven by the costumers' growing awareness for environmental issues. Although numerous sustainable ingredients (natural, organic, or green chemistry-derived) have been investigated, there is a lack of comparative studies between conventional ingredients and sustainable alternatives. In this study, olive oil (30 wt.%) and  $\alpha$ -tocopherol (2.5 wt.%) containing oil-in-water (O/W) emulsions stabilized with the bacterial fucose-rich polysaccharide FucoPol were formulated envisaging their validation as cosmetic creams. Formula composition was designed using Response Surface Methodology (RSM) to determine the contents of FucoPol (1.5 wt.%), cetyl alcohol (1.5 wt.%) and glycerin (3.0 wt.%) that resulted in high emulsification index after 24 hours ( $E_{24} \geq 97.56\%$ ), concomitant with an apparent viscosity of 8.72 Pa.s. The optimized FucoPol emulsion was formulated with 1.5 wt.% FucoPol, 1.5 wt.% cetyl alcohol, and 3.0 wt.% glycerine, with 8.72 Pa.s of viscosity (at a shear rate  $2.3 \text{ s}^{-1}$ ), droplet size and zeta potential of 6.12  $\mu\text{m}$  and 97.9 mV, respectively. After comparison with several available commercial products, the optimized formulation showed the desired criteria of the thin emulsion system and the physicochemical properties and stability indicate its suitability for cosmeceutical applications.

**Keywords:** polysaccharide; FucoPol; natural emulsifier; oil-in-water emulsion; experimental design; cosmetics; rheology; texture

## One-Pot and Biomass-Agnostic Syntheses of Biodegradable and Non-Ecotoxic Surfactants from Algal Polysaccharides and Pectins

Durand L.<sup>1</sup>, Wong T.<sup>1</sup>, Perocheau Arnaud S.<sup>1</sup>, **Noirbent G.<sup>1</sup>**, Renault L.<sup>1</sup>, Wang Y.<sup>1</sup>, Benvegnu T.<sup>1</sup>, Pessel F.<sup>2</sup>, Boyere C.<sup>2</sup>

<sup>1</sup>Ecole Nationale Supérieure de Chimie de Rennes, 11 allée de Beaulieu, 35708 Rennes

<sup>2</sup>SurfactGreen, 11 allée de Beaulieu, 35708 Rennes

\*Corresponding author: Thierry BENVENU / thierry.benvegnu@ensc-rennes.fr

Abstract text:

During past decades, thanks to the use of renewable resources in chemical production, the focus has shifted towards the development of fully bio-based surfactants. These surfactants have been widely studied due to their good biodegradability and low toxicity and ecotoxicity. The most common ones are the alkyl polyglucosides (APG) which are non-ionic compounds with a production about 85000 t/a.<sup>1</sup> However, the examples of anionic surfactants derived from renewable resources are scarce and the use of novel building blocks derived from sustainable resources to obtain the targeted properties is a major challenge for the surfactant industry. Therefore, the ENSCR has led researches on the development of novel surfactants and green/blue chemical processes, using biomass from terrestrial or marine origin. These researches allowed the development of one-pot and Biomass-Agnostic syntheses of anionic or non-ionic surfactants derived from algal polysaccharides (ulvans, alginates, agarose) and pectins.<sup>1-5</sup> Physicochemical studies of these original sugar-based molecules have been achieved and clearly highlight the potential of these original materials as surface-active agents and emulsifying products. In addition, the readily biodegradability and the absence of aquatic ecotoxicity make these surfactants very promising for cosmetic or personal care applications.

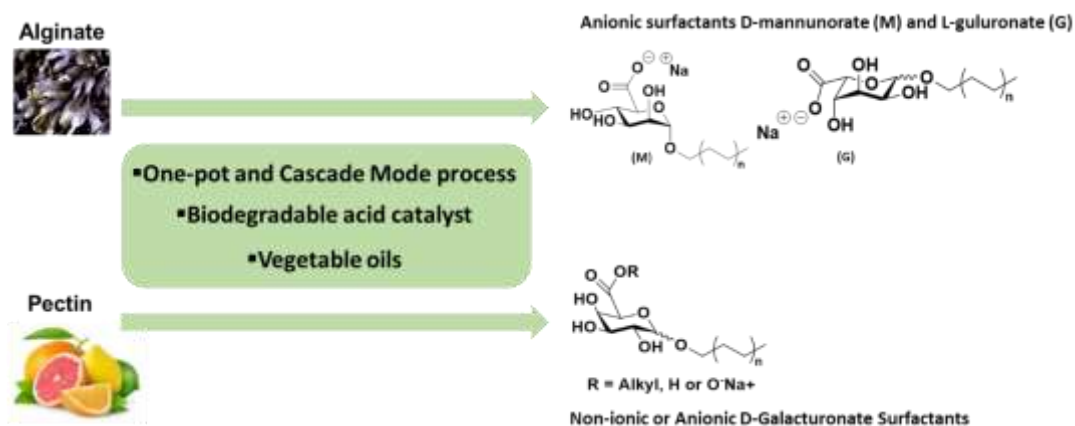


Figure 8 : Biobased Surfactants from alginates and pectins

### Acknowledgments

- CD35, Région Bretagne, BpiFrance, ADEME

### References

- Milliasseau, D., Jeftić, J., Pessel, F., Plusquellec, D. & Benvegnu, T. Transformation of Pectins into Non-Ionic or Anionic Surfactants Using a One-Pot and Cascade Mode Process. *Molecules* **26**, 1956 (2021).
- Sari-Chmayssem, N. *et al.* Direct and one-pot conversion of polyguluronates and alginates into alkyl-l-guluronamide-based surfactant compositions. *Green Chem.* **18**, 6573–6585 (2016).
- Benvegnu, T., Sari-Chmayssem, N., Taha, S. & Mawlawi, H. Procédé de préparation de compositions tensioactives comprenant des L-Iduronamides, D-Glucuronamides et L-Rhamnosides d'alkyle a partir d'ulvanes. FR3060005-A1 (2016).
- Wang, Y., Renault, L., Guégan, J. P. & Benvegnu, T. Direct Conversion of Agarose into Alkyl Mono- and Disaccharide Surfactants Based on 3,6-Anhydro L- and D-Galactose Units. *ChemistrySelect* **6**, 389–395 (2021).
- Boyere Cédric, Galle Francis, Pessel Freddy, R. X. Procédé d'obtention de compositions tensioactives à partir de matières végétales brutes. WO2022/013500A1 (2022).

## Pretreatment of brewers' spent grains via non-thermal plasma for poly(3-hydroxybutyrate) production

Chrysanthi Argeiti<sup>1\*</sup>, Eleni Stylianou<sup>1</sup>, Dimitrios Ladakis<sup>1</sup>, Apostolis Koutinas<sup>1</sup>

<sup>1</sup> Agricultural University of Athens, Department of Food Science and Human Nutrition, Iera Odos 75, Athens, Greece.

\*[chrysa.argeiti@gmail.com](mailto:chrysa.argeiti@gmail.com)

Brewers' spent grains (BSG) account for ca. 85% of the total byproducts produced by breweries. BSG is a lignocellulosic material containing high quantities of oligosaccharides and polysaccharides, which could be used as carbon source for microbial fermentations. Biopolymers are among the most important products that can be obtained from renewable resources, such as lignocellulosic biomass [1]. Poly(3-hydroxybutyrate) (PHB) is a polyester produced from renewable resources via bacterial fermentation as a secondary intracellular product. Novel technologies for efficient pretreatment of lignocellulosic biomass should be developed in order to improve the sustainable production of PHB. Dielectric barrier discharge (DBD) air plasma pretreatment of lignocellulosic biomass has emerged as a novel technology that could become a viable alternative to conventional pretreatment technologies using high pressure and temperatures and acids or alkalis. Depending on the gas used, plasma treatment leads to partial ionization of the gas causing the production of various reactive species that stimulate both chemical and physical changes in the lignocellulose structure. The main advantages of plasma treatment are the fact that the process is carried out at ambient pressure and temperature, while no chemicals are used [2].

BSG pretreatment with non-thermal plasma at different operating conditions was evaluated, followed by enzymatic hydrolysis of the lignocellulosic biomass. The BSG used in this study contained 20% protein, 27% cellulose, 33% hemicellulose and 17% lignin. BSG was suspended in deionised water in a Duran bottle with 1 L working volume at a concentration of 50 g/L. Air was supplied at a flow rate of 1 L/min. All experimental runs were carried out at ambient temperature and 60 Hz frequency under continuous stirring (300 rpm) using a magnetic stirrer. The first set of experiments was carried out at three different voltage values (100, 150, 200 V) and four different pretreatment durations (10, 30, 60, 120 min) at 500 Hz discharge frequency and 5% duty cycle (50 usec). The highest glucan hydrolysis yield (96%) was achieved when DBD plasma was performed for 120 min (Figure 1B). The second set of experiments was performed at 200 V and 30 min pre-treatment duration, 1000 Hz discharge frequency and three different duty cycles (5%, 10% or 116 usec and 15% or 183 usec). Figure 1 shows that the glucan hydrolysis yield was increased with increasing pretreatment duration. The highest xylan hydrolysis yield was obtained when the lowest pre-treatment duration (10 min) was applied at all voltage values (Figure 1).

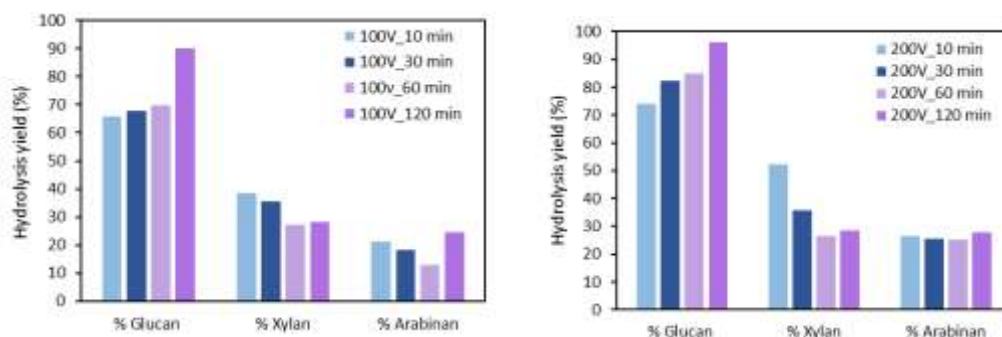


Figure 1. Hydrolysis yield after non-thermal DBD plasma pretreatment of BSG at 100 V and 200 V using different pretreatment durations (10, 30, 60 and 120 min)

After DBD plasma pretreatment, the remaining BSG solids were subjected to enzymatic hydrolysis using a commercial enzymatic cocktail. Bacterial fermentations for PHB production were conducted with the bacterial strain *Paraburkholderia sacchari* DMSZ 17165. Bacterial stock cultures were maintained at 4°C in petri dishes. Inoculum preparation was carried out in Erlenmeyer flasks containing, 20 g/L glucose, (NH<sub>4</sub>)<sub>2</sub>SO<sub>4</sub> 1 g/L, Na<sub>2</sub>HPO<sub>4</sub> 4.5 g/L, KH<sub>2</sub>PO<sub>4</sub> 1.5 g/L, MgSO<sub>4</sub> 0.2 g/L, yeast extract 1 g/L and trace elements 1 mL. The inoculum was incubated in a rotary shaker incubator at 250 rpm agitation at 30°C for 24 h. The fed-batch fermentation was carried out in a 2 L stirred-tank bioreactor (Eppendorf, Bioflo 120) with 1.2 L working volume. Fermentation pH was controlled at 6.8 with 2 M HCl and NH<sub>3</sub>. Inoculum size was 10% (v/v). The temperature was maintained at 30°C and agitation was set at cascade mode (400-1200 rpm) depending on the dissolved oxygen concentration (20% of saturation). Continuous supply of air at a flow rate of 2.5 vvm was applied.

Plasma pre-treated BSG hydrolysate was used as fermentation medium. Figure 2A shows that the plasma pre-treated BSG hydrolysate contained a high free amino nitrogen (FAN) concentration (854 mg/L) at the beginning of fermentation. The FAN was consumed after 20 h, while inorganic nitrogen (IN) was still present until the end of fermentation. The inorganic phosphorus (IP) was consumed at around 15 h. The use of plasma pre-treated BSG

hydrolysate led to 95.6 g/L PHB concentration and 163 g/L DCW that corresponds to 58.5% intracellular PHB content. The yield and productivity were 0.27 g<sub>PHB</sub>/g<sub>consumed sugars</sub> and 2.77 g/(L·h), respectively.

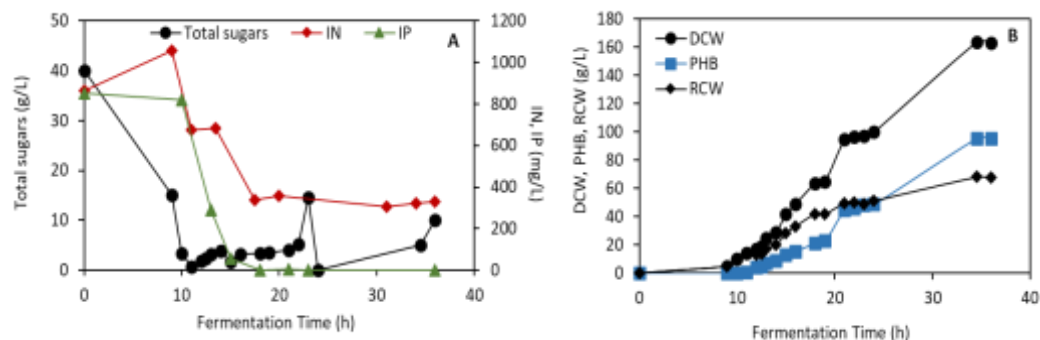


Figure 2. PHB production in *P. sacchari* fed-batch bioreactor culture carried out using BSG hydrolysate produced after non-thermal plasma pretreatment

Table 1. PHB production efficiency in *P. sacchari* fed-batch fermentation carried out using BSG hydrolysate produced after non-thermal plasma pretreatment

Time (h)	DCW (g/L)	PHB (%)	PHB (g/L)	Yield (g <sub>PHB</sub> /g <sub>consumed sugars</sub> )	Productivity (g/L/h)
34	163	58.5	95.6	0.27	2.77

## Acknowledgements

This work is part of the European project BIOSUPPACK - ‘Demonstrative process for the production and enzymatic recycling of environmentally safe, superior and versatile PHA-based rigid packaging solutions by plasma integration in the value chain. This project has received funding from the Bio Based Industries Joint Undertaking under the European Union’s Horizon 2020 research and innovation program.

## References

- Dávila, J. A., Rosenberg, M., & Cardona, C. A. (2016). A biorefinery approach for the production of xylitol, ethanol and polyhydroxybutyrate from brewer’s spent grain. *AIMS Agriculture and Food*, 1(1), 52-66.
- Vanneste, J., Ennaert, T., Vanhulsel, A., & Sels, B. (2017). Unconventional pretreatment of lignocellulose with low-temperature plasma. *ChemSusChem*, 10(1), 14-31.

## Antibacterial activity of porous hydrogel films from renewable raw materials and their carrier ability for controlled release of flavoring compounds

Irina E. Raschip\* and Maria V. Dinu

“Petru Poni” Institute of Macromolecular Chemistry, Grigore Ghica Voda Alley 41A, Iasi 700487, Romania

\*e-mail address of corresponding author: [iecoj@icmpp.ro](mailto:iecoj@icmpp.ro)

The development of new advanced bioactive packaging materials, especially based on polymeric compounds, is a priority direction of modern chemistry aimed to improve the existing food technologies. In particular, the use of antimicrobial-loaded edible films was proved to be an effective tool for foodstuff protection against bacterial spoilage organisms [1]. The biocompatible and biodegradable character of polysaccharides, associated with the presence of specific interaction sites in their structure, make them very attractive as carriers of various additives, such as antioxidant, antimicrobial, or flavoring agents [1,2].

Nowadays, one of the major problems is that some food products are found to be contaminated by pathogenic bacteria such as *Escherichia coli* and *Staphylococcus aureus* reducing so, their shelf life. Our research aims to demonstrate the antibacterial activity of some biodegradable formulation xanthan gum (XG)-lignin hydrogel films (Figure 1a, 1b) and their potential application as carriers for controlled release of flavoring compounds [3].

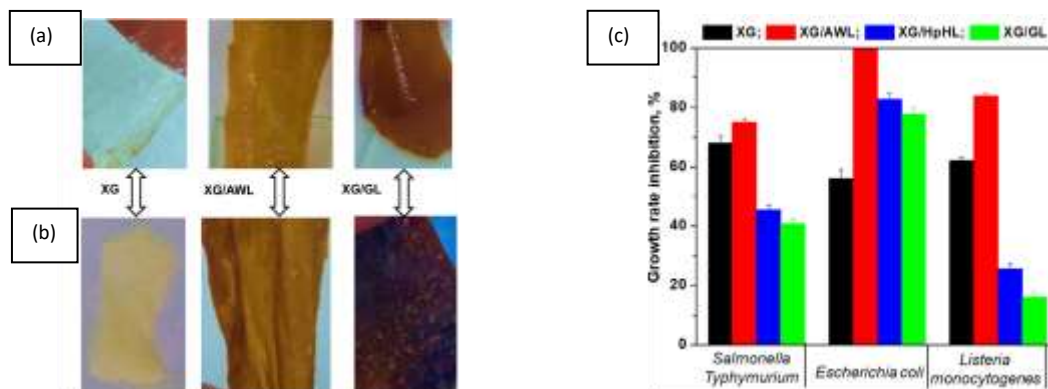


Figure 1. Optical images of the XG-based hydrogel films after synthesis (a) and lyophilization (b) growth rate inhibition of bacteria by XG, XG/AWL, XG/HpHL, and XG/GL hydrogels after 48 h (c).

The XG-lignin films containing an aspen wood lignin type showed a high antibacterial activity against *Salmonella Typhymurium*, *Escherichia coli* and *Listeria monocytogenes* bacteria (Figure 1c) compared with those containing softwood lignin, or lignin from annual plants [3]. Additionally, near infrared chemical imaging technique was used as nondestructive method to observe the spatial distribution of the polymeric components and vanillin into the hydrogel films as well as its release profile. The vanillin release rate dependence on the lignin type was also evidenced, a retarded release of vanillin being observed. These results give an important insight into the use of XG, lignin, and vanillin for the development of new edible films for active packaging materials. In this context, we develop new green hydrogels from XG and various types of waste lignin as starting materials with improved properties.

**Keywords:** green hydrogels, antibacterial activity, vanillin release

### Acknowledgements

The PN-III-P1-1.1-TE2021-1683 project is gratefully acknowledged.

### References

1. P. Cazon, G. Velazquez, J.A. Ramirez, M. Vázquez, *Food Hydrocolloids*, **68**, 136 (2017).
2. I.E. Raschip, N. Fifere, M.V. Dinu, Polysaccharide-based materials as promising alternatives to synthetic-based plastics for food packaging applications; *Bioplastics for Sustainable Development*; (Eds.) M. Kuddus, Roohi; Springer Nature Publisher, 19, 515-554 (2021).
3. I.E. Raschip, O.M. Paduraru-Mocanu, L.E. Nita, M.V. Dinu, *Journal of Applied Polymer Science*, **137**, e49111 (2020).

## Strategies for the production of biorefinery enzymes by the valorisation of lignocellulosic waste

Vladimir Elisashvili\*, Mikheil D. Asatiani, and Eva Kachlishvili

Institute of Microbial Biotechnology, Agricultural University of Georgia, 240 Aghmashenebeli alley, Tbilisi, Georgia

\*v.elisashvili@agrni.edu.ge

Lignocellulosic biomass is the cheapest and inexhaustible renewable resource for the production of organic chemicals and biofuels through microbial and enzymatic conversion. Among microorganisms, wood-rotting and litter-decomposing fungi belonging to the division of *Basidiomycota* are one of the best decomposers of lignocellulosic materials. In order to use the remnants of lignocellulose as a substrate for growth, and as sources of energy and nutrients, these fungi secrete a large amount of hydrolytic and oxidative enzymes for depolymerization of cellulose, hemicelluloses and lignin. Their major hydrolytic enzymes are exo-1,4- $\beta$ -D-glucanase, endo-1,4- $\beta$ -D-glucanase, and xylanase and these fungi secrete one or more extracellular lignin-modifying enzymes (LME): lignin peroxidase, manganese-dependent peroxidase, and laccase. These lignocellulose-degrading enzymes (LCDE) are fundamental for efficient bioconversion of plant residues and the supply of nutrients to fungi. Besides, they are necessary for a variety of industrial and biotechnological applications including pulp and paper, food, textile and dye industries, cosmetics, agriculture, bioremediation, and analytical biochemistry. Therefore, the search for fungi with outstanding enzyme activity and properties, as well as elucidation of the growth conditions that regulate LCDE production, is of fundamental importance to hundreds of laboratories and companies.

The saprotrophic white-rot basidiomycetes (WRB) are the major agents of wood bio-deterioration in natural ecosystems, producing hydrolytic and lignin-modifying enzymes to completely mineralize native lignocellulosic biomass without association with other microbes. Moreover, some of them have shown exceptional potential for the production of individual groups of hydrolytic and oxidative enzymes under appropriate cultivation conditions. However, an analysis of literature data clearly shows a wide intra- and interspecies diversity in the ability of WRB to produce LCDE [1, 2]. Thus, in the submerged fermentation of mandarin pomace, we showed the laccase activity of *Ganoderma* spp. varied from 2.0 U/mL to 75.4 U/mL while the MnP activity of *Trametes* spp. strains ranged from 0 to 0.9 U/mL. Endoglucanase activity in the Avicel-containing medium varied from 0.2 U/mL in *Ganoderma appplanatum* 258 to 61.5 U/mL in *Pycnoporus coccineus* 310 cultures. Moreover, the WRB manifested different responses to the used carbon sources. Among them, *Cerrena* spp., *Corioloropsis gallica*, *Pseudotrametes gibbosa*, and *T. versicolor* produced significant laccase activity in synthetic medium, whereas the presence of lignocellulosic material was a prerequisite for the enzyme production by *Ganoderma* spp., *Phlebia radiata*, *Pycnoporus coccineus*, and *Trametes ochracea*.

To increase enzyme yields, various approaches and strategies, such as exploitation of cheap plant raw materials as growth substrates, the addition of specific inducers of enzyme synthesis, optimization of fermentation media and cultivation conditions, and development of better bioprocess technologies have been widely exploited. The lignocellulosic growth substrate has the greatest effect on LCDE secretion, so the choice of a suitable substrate with an adequate content of carbon, nitrogen, and a potential inducer is an important criterion for enhanced cellulase production. In particular, wheat straw followed by wheat bran supported an efficient secretion of endoglucanase by *Irpex lacteus*, whereas mandarin pomace provided maximum secretion of this enzyme by *Schizophyllum commune*. Likewise, the submerged fermentation of kiwi residue stimulated MnP secretion by *Phellinus robustus* while walnut pericarp 12-fold augmented activity of this enzyme in *Cerrena unicolor*. These data indicate that for each enzyme producer, fungus-specific lignocellulosic substrate ensuring the highest enzyme activity must be established.

Co-cultivation of different WRB species has also been explored since it ensures better utilization of substrate, enhanced enzyme yield and provides a complete set of target enzymes required for specific applications. However, compatibility between microorganisms is the main issue in mixed cultures. For example, co-cultivation of *Irpex lacteus* and *S. commune* resulted in increased cellulase production as compared to the corresponding monocultures, while co-cultivation of *Pycnoporus coccineus* or *Trametes hirsuta* with *S. commune* had negative effects on cellulase production. Likewise, co-cultivation of *C. unicolor* with *Trametes versicolor*, *Lenzites betulina*, and *Panus lecomtei* led to up-regulation of laccase activity. Moreover, the interspecific interaction of *C. unicolor* and *T. versicolor* induced the production of two new laccase isoenzymes. By contrast, interactions of *C. unicolor* with *Trametes coccineus* and *T. hirsuta* resulted in a multiple decreased ability of *C. unicolor* to produce laccase.

Regulatory mechanisms controlling LCDE synthesis have been studied in some model fungi. It is worth noting that for cellulase and xylanase production, the growth medium usually includes cellulosic substrates as these enzymes' synthesis is activated only when inducers are present. When readily metabolizable carbon sources are available in the medium, the synthesis of these enzymes undergoes catabolite repression. Several examples of the regulation of cellulase and xylanase synthesis will be presented in the report. As for the regulation of the synthesis of lignin-modifying enzymes, the regulating effect of aromatic compounds and metal ions on the enzyme activity

and gene expression in WRB is well established. In the submerged fermentation of mandarin squeeze by *T. multicolor* 511, veratryl alcohol and guaiacol two-fold increased the specific laccase activity compared with the control medium, guaiacol 4-fold increased the fungus MnP activity, while veratryl alcohol favoured LiP secretion. Copper is the most important and commonly used metal ion for laccase production. However, the effect of these compounds in enzyme activity expression depends on their concentrations and fungal strain peculiarities. In our study, in the submerged fermentation of mandarin pomace, an augmentation in copper concentration from 0 to 0.5 mM increased 18-fold the activity of *T. multicolor* laccase but did not significantly affect the activity of manganese peroxidase (MnP) and lignin peroxidase (LiP), which indicated that the inductive effect of copper was specific for laccase. It is interesting that iron ions at the concentration of 0.1 mM almost 8-fold increased both volumetric and specific activity of laccase compared with the control medium. In the same culture, an increase in the concentration of manganese from 0 to 0.5 mM only slightly increased the activity of *T. multicolor* laccase and decreased the activity of LiP, but this metal 13-14 times specifically increased the volumetric and specific activity of MnP when it was added to the control medium at a concentration of 0.5 mM.

Overall, extensive work has been done to enhance the synthesis and yields of lignocellulolytic enzymes. However, elucidation of the factors hindering the production of these enzymes is also one of the most challenging tasks.

### Acknowledgements

This work was supported by the Estonian Environmental Investment Center (Project number Kliima.3.01.20-0082).

### References

1. V. Elisashvili, M.D. Asatiani, E. Kachlishvili, *Microbial Enzymes and Biotechniques*, (P. Shukla, ed). Springer, Singapore, 107-130 (2020).
2. J.A. Bentil, A. Thygesen, M. Mensah, L. Lange, A.S. Meyer, *Appl. Microbiol. Biotechnol.*, **102** 5827-5839 (2021).

## Lactic and succinic acid production from lignocellulosic biomass

Agata Olszewska-Widdrat<sup>1\*</sup>, Roland Schneider<sup>1</sup> and Joachim Venus<sup>1</sup>

<sup>1</sup>Leibniz Institute for Agricultural Engineering and Bioeconomy (ATB), Max-Eyth-Allee 100 14469 Potsdam, Germany

\*aolszewska-widdrat@atb-potsdam.de

### Abstract

The production of biobased chemicals plays a crucial role in the formation of circular bioeconomy. Platform chemicals, such as succinic (SA) and lactic acid (LA) are one of the main key-factors in the transition from fossil-based plastic industry into biobased and green production. Additionally, the biomass valorization is of high importance concerning platform chemicals [1]. Market projections showed an estimation that the value of LA will rise from \$2.64 billion in 2018 to over \$9 billion by 2025 [2]. According to market needs and sustainable development, we propose a biotechnological way of LA and SA production from lignocellulosic biomass. The enzymatic hydrolysis, followed by the microbial conversion of sugars into organic acids and their purification to monomers show a huge potential in the development of new, environmentally friendly process with a capability of converting biomass into added-value goods. *Bacillus coagulans* and *Actinobacillus succinogenes*, used in this study, produce lactic and succinic acid respectively. Both strains showed a very promising performance. Their productivities are listed in Table 1. Additionally, the optical purity of L-LA was detected reaching 99,5 %. Several *Bacillus coagulans* strains, belonging to the strain library of ATB were evaluated firstly in  $\mu$ -scale using a Bioscreen method and then two best candidates were used for small-scale fermentation experiments (Table 1). All microbial strains used in this study were homofermentative and thermophilic L-LA producers. In the case of succinic acid production, two strains were evaluated and *Actinobacillus succinogenes* was chosen for small scale fermentations due to its better performance. Sugar content and acid production were measured via High-performance liquid chromatography (HPLC). Sawdust hydrolysis was carried out at the different dosages of the enzyme and compared with the mathematical model.

Table 1. Strains used in the small-scale fermentations

Strain	Temp (°C)	Species	Productivity (g/l*h)
A541	52	n.d.	2.03
A211	52	<i>B. coagulans</i>	0.95
B1	37	<i>Actinobacillus succinogenes</i>	1.22

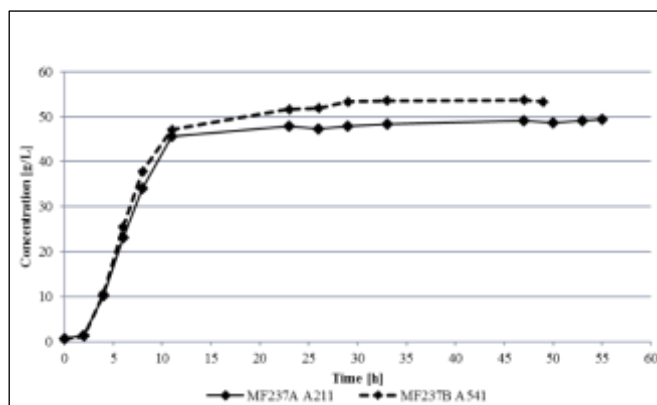


Figure 1. Lactic acid production from birch sawdust hydrolysate



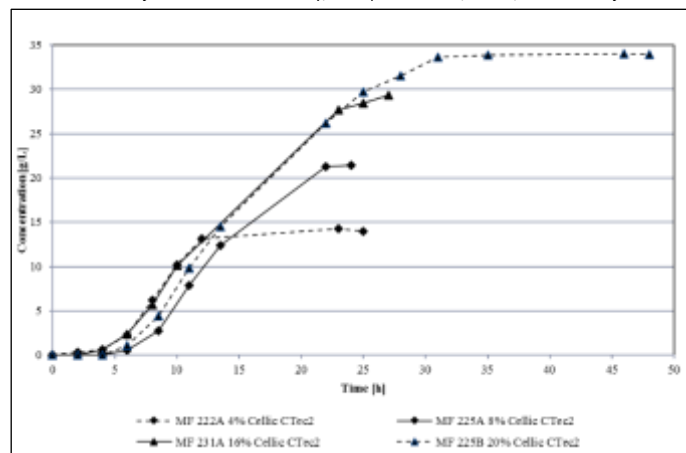


Figure 2 Succinic acid production from birch sawdust hydrolysate at different enzyme dosage

It was demonstrated that lignocellulosic biomass can be successfully used for the production of two main platform chemicals, such as, lactic and succinic acid. Both processes enable the utilization of C5 and C6 sugars, leading to the homofermentative production of pure monomers. The fermentation broth can be purified ending up with the optically pure lactic and succinic acid that will be further used for bioplastic production.

### Acknowledgements

I would like to thank Giovanna Rehde for her contribution in the HPLC analysis of samples.

### References

1. M. Alexandri, R. Schneider, H. Papapostolou, D. Ladakis, A. Koutinas, J. Venus, *ACS Sustainable Chem. Eng.*, 7, 7, 6569–6579 (2019).
2. 271 19 (1963). Grand view research, Lactic Acid Market Size, Share & Trends Analysis Report By Raw Material, By Application, And Segment Forecast, 2018 – 2025, San Francisco, 2019. <https://www.grandviewresearch.com/industry-analysis/lactic-acid-and-poly-lactic-acid-market>.

## Indigenous plants as a source for discovery and synthesis of pharmaceutical products and industrial materials

Upenyu Guyo\*, Pimpernel Garanganga, Evelyn Mariwowo, Blessing Nyamukuta, Fidelis Chigondo

*Department of Chemical Sciences, Midlands State University, P. Bag 9055, Gweru, Zimbabwe South Africa.  
guyou@staff.msu.ac.zw*

Plants are rich and sustainable sources of natural compounds in the form of terpenoids, alkaloids, tannins, flavonoids, and other classes of phytochemicals. Unlike animals, plants do not have an adaptive immunity but rely on chemical molecules for their survival, propagation, and reproduction. Plants tend to evolve producing new chemical structures and enhancing abundances of phytochemicals hence availing an opportunity to obtain new compounds with novel applications in improving the quality of life and health. Zimbabwe has a vast repository of diverse indigenous fruit and herbal plants with more than 5000 plant species consumed as food, medicine, or used otherwise. These indigenous species have been utilised for nutritional, palatability, therapeutic, and materials applications in Zimbabwean ethnobotany. Ten percent of these species have been documented to have medicinal properties and used as traditional medicines leaving about ninety percent of the indigenous species available for other applications. This research provides an ethnobotanical survey of indigenous plants in Zimbabwe which will inform the discovery and synthesis of active compounds to complement the conventional synthetic methods based on catalysis and various chemical reactions. Target-oriented discovery of new compounds from indigenous plants is being done coupled with the development of new strategies to isolate and synthesise the compounds. Structure-based in silico identification of novel natural compounds for the treatment of malaria bedevilling local people in Zimbabwe communities is being conducted. Molecules from indigenous plants have been isolated and used in the formulation of health creams. To fully realise the impact of indigenous plants on the sustainable development of the nation, novel materials are being fabricated for various applications such as water treatment.

### References

- 1.Sharma V, Janmeda P. Arab J Chem 2017;10:509–14
- 2.Asha Devi NK, Rajendran R, Karthik Sundaram S Indian J Nat Prod Resour 2011;2:59–64.
- 3·Altemimi A, Lakhssassi N, Baharlouei A, Watson DG, Lightfoot DA. Plants 2017;6.
- 4.Dawurung CJ, Nguyen MTH, Pengon J, Dokladda K, Bunyong R, Rattanajak R, et al. BMC Complement Med Ther 2021;21:1–12.
- 5.Raks V, Al-Suod H, Buszewski B. Chromatographia 2018;81:189–202.
- 6.Akther N. Biomed J Sci Tech Res 2018;10.
- 7.Nharingo T, Zivurawa MT, Guyo U. Int J Environ Sci Technol 2015;12:3791–802.
- 8.Moyo M, Guyo U, Mawenyiyo G, Zinyama NP, Nyamunda BC J Ind Eng Chem 2015;27:126–32.

## . BlueBio mass valorization through analytical techniques for the quest of biostimulants in plant growth

Matsia, S.<sup>1\*</sup> Maroulis, M.<sup>1,2</sup> Perikli, M.<sup>1,2</sup> Parvulescu, O.C.<sup>3</sup> Ion, V.A.<sup>4</sup> Løes, A.-K.<sup>5</sup> Cabell, J.<sup>5</sup>  
Salifoglou, A.<sup>1</sup>

<sup>1</sup> *Laboratory of Inorganic Chemistry and Advanced Materials, School of Chemical Engineering, Aristotle University of Thessaloniki, Thessaloniki 54124, Greece*

<sup>2</sup> *Modern Analytics Testing Laboratories, Themi 57500, Thessaloniki, Greece*

<sup>3</sup> *Chemical and Biochemical Engineering Department, University Politehnica of Bucharest, 1-3 Gheorghe Polizu, Bucharest, Romania*

<sup>4</sup> *Research Center for Studies of Food Quality and Agricultural Products, USAMV, 59, Marasti Blvd., Bucharest 011464, Romania*

<sup>5</sup> *Norwegian Centre for Organic Agriculture (NORSØK), Gunnars veg 6, Tingvoll N-6630, Norway*

\*E-mail: srmatsia@cheng.auth.gr

### Abstract

Significant research and innovation activities, all over the world, have been and are currently being carried out to develop high-value products for pharmaceutical or nutritional purposes. This universal drive has led to the establishment of a new industry, however, there are still appreciably valuable residual materials, which are underused, emerging especially from the capture of wild fish, raising fish in aquaculture, and the seaweed and shellfish industries [1].

The importance of BlueBio materials in agricultural activities, targeting new fertilizers and biostimulants of plant growth, attract keen interest from the scientific community. There are different types, defined as biostimulants, including humic acid (HA) and fulvic acid (FA), protein hydrolysates (PHs), seaweed extracts, chitosan, inorganic compounds, beneficial fungi, and bacteria. The primary sources of biostimulants also reflect origin and physiological characteristics, much the same way as the ones extracted from macro- and micro-algae [2,3,4].

Bearing in mind the ambitious goals of the European Union about the organically-driven management of agricultural land, to be reached by 2030, and the economic significance of such products to the entire continent, this project aspires to study available residual materials from fish capture, the brown algae industry, the mussel industry, and organic aquaculture. Relevant materials were provided by five Scandinavian industry partners (**Figure 1**). The materials are chemically characterized and compounds with potential biostimulant effects on crop plants are to be investigated, while concurrently checking for possible biotoxicity.

The goal, therefore, is the development of expert analytical tools in the characterization of Low and High Nitrogen Algal Cake and possibly other marine-derived residual products. Parameters include cellulose content, for which a classical Weende-based approach have been implemented. The Macro and Micro Nutrients, including K, Ca, Mg, P, Fe, Mn, etc., as well as potential toxic elements (PTEs) As, Cd, Cr, Hg, Pb have been perused through Inductively Coupled Plasma (ICP) methodologies. Key to such an endeavor is sample preparation, involving dry ashing as well as microwave assisted digestion. PTEs are also determined via ICP-MS approaches, thus seeking to achieve lower levels of detection. Moreover, screening for organic compounds emerges prominently in the study and is pursued through GC-MS methods on extracts of varying polarity solvents. Using those extracts, the lipid content in the title materials is explored through GC-FID. Collectively, promising materials (assessed through chemical characterization) will be tested under real growing conditions in greenhouses and fields. The logistics and related costs required for establishing a relevant value chain for producing fertilizers and/or biostimulants will be assessed by interviewing collaborating industry partners and surveying potential customers.

### Materials and Methods

Methods used for extractions of raw materials include the following: Accelerated solvent extraction (ASE) and GREEN solvent (e.g. ethanol, ethylacetate, hydrotrope mixtures, ionic liquids), ultrasonic assisted extraction and microwave assisted extraction. Extracts obtained through the above processes have been analyzed for their elemental composition and organic compounds composition [GC-MS, LC-ESI-MS, (<sup>1</sup>H, <sup>13</sup>C)-NMR, FT-IR]. The desired compounds expected to appear include antioxidants, organic acids, proteins, amino acids, PUFAs, etc., depending on the nature of the raw materials used.



**Figure 1:** Raw materials from BlueBio resources

## Results

Our efforts to identify the various components of raw materials, including low nitrogen seaweeds (LNSW), high nitrogen seaweeds (HNSW) and grinding fish residues (GFB), started by determining total C, N concentration of the samples, and protein-fat content, with the results shown in **Table 1**.

**Table 1:** Total carbon, hydrogen and nitrogen

Analysis	LNSW	HNSW	GFB
Total C %	12.1	12.1	7.85
Total N %	0.16	0.42	2.05
Protein %	1.0	2.6	12.8
Fat %	2.3	1.5	0.2

The collective results formulate a well-defined profile for both Low and High Nitrogen Algal Cake materials, thus signifying the importance of a) screening for key ingredients in raw materials, and b) identification of both organic and inorganic components in algal materials, which could be used in agricultural practices for crop plant growth enhancement. It is worth emphasizing the fact that past studies have shown a positive effect of high N algal cake on ryegrass growth [5]. What boosted production of dry matter with algal cake, across five harvests, higher than non-fertilized soil control, was a long-term effect, with yields maintaining a quite stable level even in the final harvest and control yields leveling off. In the final harvest, the yield with algal fiber was higher than that with the same amount of N applied in mineral N fertilizer (Calcinit). The algal cake has a rather slow, yet long-term growth effect.

Poised to pursue the physicochemically and biologically supported effort for the search on crop plant biostimulants, the presently ongoing research attests to the importance of raw materials of marine industries in their added value as BlueBio products in contemporary agricultural activities and beyond.

## Acknowledgements

This work is part of the project MARIGREEN, which has received funding from the European Union's Horizon 2020 research and innovation program under agreement 817992 and GSRI (T12EPA5-00071).

## References

- [1] L. Xu, D. Geelen, *Frontiers in Plant Science*, 9 1567 (2018).
- [2] O.I. Yakhin, A.A. Lubyaynov, I.A. Yakhin, P.H. Brown, *Front. Plant Sci.*, 7 2049 (2016).
- [3] P. du Jardin, *Sci. Hortic.*, 196 3–14 (2015).
- [4] D.J. McHugh, *A Guide to the Seaweed Industry*. Rome: Food and Agriculture Organization of the United Nations (2013).
- [5] I. Ahuja, A.-K. Løes, Effect of fish bones and algae fibre as fertilisers for ryegrass. Norwegian Centre for Organic Agriculture (NORSØK) Report Vol. 4 No. 7 2019, 64 p. Tingvoll, Norway.

## Solid dispersions as food colorant solutions: a systematic study addressing different natural polymers

Stephany C. de Rezende<sup>1,2,3</sup>, Arantzazu Santamaria-Echart<sup>1</sup>, Olga Ferreira<sup>1</sup>, Madalena M. Dias<sup>2,3</sup> and Maria Filomena Barreiro<sup>1\*</sup>

<sup>1</sup>Centro de Investigação de Montanha (CIMO), Instituto Politécnico de Bragança, Campus de Santa Apolónia, 5300-253 Bragança, Portugal

<sup>2</sup>LSRE-LCM - Laboratory of Separation and Reaction Engineering - Laboratory of Catalysis and Materials Faculdade de Engenharia, Universidade do Porto, Rua Dr. Roberto Frias, 4200-465 Porto, Portugal

<sup>3</sup>ALiCE - Associate Laboratory in Chemical Engineering Faculdade de Engenharia, Universidade do Porto, Rua Dr. Roberto Frias, 4200-465 Porto, Portugal  
\*barreiro@ipb.pt

Considering new consumer's trends and restrictions placed on the use of synthetic colorants, the food industry has a strong demand for natural analogs, particularly carotenoids, which are responsible for the colors red and yellow, representing around 90% of the total amount of colorants added to foods [1,2]. Nonetheless, their low water solubility and stability make their use limited. In this context, solid dispersion (SD) technique, which comprises a system containing at least two components, commonly a hydrophobic active material and a hydrophilic carrier, usually a polymer, is a promising strategy to overcome this constraint. In SD the active material is molecularly dispersed into the polymer, promoting hydrogen bonding between the components and resulting in particles formation. The process uses high-energy mixing devices to induce molecular interactions, then the solvent is evaporated, being the spray-drying and freeze-drying considered efficient methodologies [3]. The main objective of this method is to allow the change in the crystallin profile of the active material. The transformation of the crystalline substance into amorphous improves the water solubility/dissolution rates, enhancing also the stability.

This work aims to develop food colorant formulations based on curcumin (65% purity) by testing five natural polymers, including K-carrageenan (KC), maltodextrin (MD, dextrose equivalent of 18), Arabic gum (AG), potato starch (PS) and pectin (PC), in comparison with the synthetic polyvinylpyrrolidone (PVP), in the preparation of particles using the SD technique [4]. For that, an aqueous solution (100 mL of citric acid/sodium citrate aqueous buffer solution (pH 6)) containing the polymer (0.4 g) and Tween 80 (15% w/w, polymer-basis) was poured into ethanol (50 mL) comprising curcumin (15% w/w, polymer-basis). The mixture was sonicated at 70% potency for 10 min (30 s on and 10 s off) and after, submitted to solvent evaporation to remove the ethanol using a vacuum rotary evaporator at 40 °C and 175 mbar. The samples were frozen at -20 °C and dried using a freeze-dryer at -106 °C. The corresponding physical mixtures (PMs) were prepared by mimicking the proportions used in the SDs. In order to evaluate the effect of the pH control on the formulations' crystallinity and water solubility, reference formulations were produced without the buffer, following the same SDs production process. The samples were coded as CX-Y, where "X" corresponds to the polymer abbreviation and "Y" refers to pH controlled (pH) or uncontrolled (Ref).

The SDs samples were analyzed by Differential scanning calorimetry (DSC) and X-ray powder diffraction analysis, according to Figure 1.

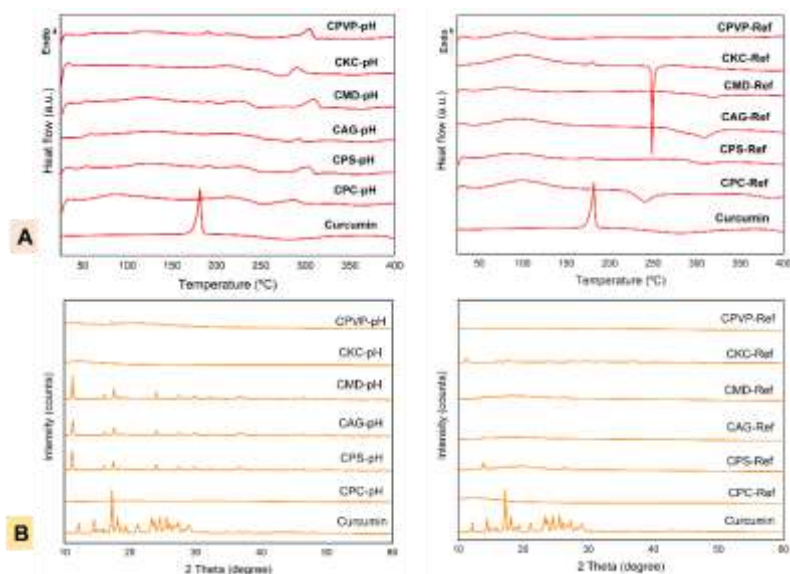


Figure 1. DSC thermograms (A) and X-ray analysis (B) of curcumin and SDs under pH controlled and uncontrolled conditions.

Concerning thermal analysis by DSC, it is perceived that the curcumin presented an endothermic peak at 181.8 °C, corresponding to the most stable crystalline polymorphism of commercial curcumin, cited in the literature as Form 1 [5]. In general, all the SDs with pH control indicated a shift in the melting peak related to curcumin to higher temperatures. For the reference formulations, lower or even the disappearance of the melting peak of the curcumin was observed, this behavior can be associated with the transformation of the crystalline form of the curcumin into more amorphous systems or less stable forms, namely Forms 2 and 3 [6]. Regarding the X-ray analysis, the curcumin presented the typical crystalline pattern of curcumin in Form 1. For the SDs, while specific polymers facilitated the modification of curcumin's crystalline structure under pH controlled environment, others enhanced the conversion under pH-uncontrolled. It is worth highlighting that the results obtained with both characterizations corroborate that most systems obtained without pH control are characterized by lower ordered structures.

Furthermore, a water solubility study was carried out [7,8] for all the samples. The SDs provide higher increase (25 to 37 µg/mL) in the curcumin water solubility, when compared with PMs (7 to 8 µg/mL). Depending on the used polymer, there were some relevant differences between the SDs with and without pH control. The systems produced with k-carrageenan and pectin presented better solubility when prepared under controlled pH, differently from the other polymers, where higher solubility values were found in the preparations without pH control. For the Arabic gum, the solubility was similar for both conditions, independent of the used pH. The relationship between the solubility and the molecular level curcumin-polymer interactions is inherent, supporting the DSC and X-ray analysis results.

### Acknowledgements

The authors are grateful to the Foundation for Science and Technology (FCT, Portugal) and FEDER under Programme PT2020 for financial support to CIMO (UIDB/00690/2020), LSRE-LCM (UIDB/50020/2020) and ALiCE (LA/P/0045/2020). FCT for the Research grant SFRH/BD/147326/2019 of Stephany C. de Rezende and national funding by FCT, PI, through the institutional scientific employment program-contract for Arantzazu Santamaria-Echart. In addition, to the technical support provided by I3Bs- Research Institute on Biomaterials, Biodegradables and Biomimetics of University of Minho is also acknowledged.

### References

1. J.A. Fernández-López, V. Fernández-Lledó, J.M., Angosto. New insights into red plant pigments: more than just natural colorants. *RSC Advances*, **10** 24669-24682 (2020)
2. B. Gordillo, G.T. Sigurdson, F. Lao, M.L. González-Miret, F.J. Heredia, M.M. Giusti. Assessment of the color modulation and stability of naturally copigmented anthocyanin-grape colorants with different levels of purification. *Food Research International*, **106** 791-799 (2018)
3. Y. Umemoto, S. Uchida, T. Yoshida, K. Shimada, H. Kojima, A. Takagi, S. Tanaka, Y. Kashiwagura, N. Namiki. An effective polyvinyl alcohol for the solubilization of poorly water-soluble drugs in solid dispersion formulations. *Journal of Drug Delivery Science and Technology*. **55** 101401 (2020)
4. F.V. Leimann, O.H. Gonçalves, G.D. Sorita, S. Rezende, E. Bona, I.P.M. Fernandes, I.C.F.R. Ferreira, M.F. Barreiro. Heat and pH stable curcumin-based hydrophilic colorants obtained by the solid dispersion technology assisted by spray-drying. *Chemical Engineering Science*. **205** 248-258 (2019)
5. P. Sanphui, N.R. Goud, U.B.R. Khandavilli, S. Bhanoth, A. Nangia. New polymorphs of curcumin. *Chemical Communications*. **47** 5013-5015 (2011)
6. K.U. Pandey, S.V. Dalvi. Understanding stability relationships among three curcumin polymorphs. *Advanced Powder Technology*. **30** 266-276 (2019)
7. N.N.S. Mai, R. Nakai, Y. Kawano, T. Hanawa. Enhancing the Solubility of Curcumin Using a Solid Dispersion System with Hydroxypropyl- $\beta$ -Cyclodextrin Prepared by Grinding, Freeze-Drying, and Common Solvent Evaporation Methods. *Pharmacy*. **8** 1-14 (2020)
8. S. Nogami, K. Minoura, N. Kiminami, y. Kitaura, H. Uchiyama, K. Kadota, Y. Tozuka. Stabilizing effect of the cyclodextrins additive to spray-dried particles of curcumin/polyvinylpyrrolidone on the supersaturated state of curcumin. *Advanced Powder Technology*. **32** 1750-1756 (2021).

## Electrochemical C-H Functionalization of Quinolizidine Alkaloids

Raquel M. Durão<sup>a,\*</sup>, Jaime A. S. Coelho<sup>b</sup>, Svilen. P. Simeonov<sup>a</sup>, Carlos A. M. Afonso<sup>a</sup>

<sup>a</sup>Instituto de Investigação do Medicamento (iMed.Ulisboa), Faculty of Pharmacy, University of Lisbon, Av. Prof. Gama Pinto, 1649-003 Lisboa, Portugal. <sup>b</sup>Centro de Química Estrutural, Institute of Molecular Sciences, Faculty of Sciences, University of Lisbon, Campo Grande, 1749-016 Lisboa, Portugal

\*raquel-durao@campus.ul.pt

Quinolizidine alkaloids (QA) are largely abundant in the *Leguminosae* family, especially in the genera *Lupinus* [1]. Maulide and Afonso's groups developed a process for the extraction of lupanine from *Lupinus albus* seeds wastewater and the preparation of sparteine [2]. These natural products are known for their pharmacological activities, which includes antimicrobial, antihypertensive, antimuscarinic and antidiabetic, as hyperglycemia agents, effects on the central nervous system and uses in asymmetric organic synthesis [3]. Motivated by the potential added value of novel QA derivatives, we explored the selective C-H functionalization of QA using electrochemistry. Herein we present a new methodology for the cyanation of lupanine (Figure 1), which offers an efficient and greener alternative to conventional methods.

The electrochemistry equipment used in this work were an ElectraSyn 2.0 system by IKA.

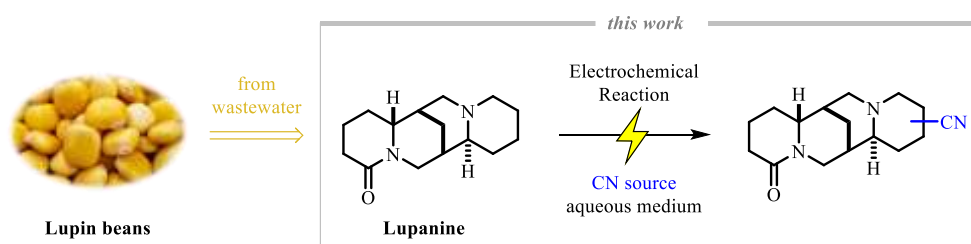


Figure 1: Electrochemical cyanation methodology.

### Acknowledgements

We thank the Fundação para a Ciência e a Tecnologia (FCT) for financial support (Ref. 2020/06352/BD, UIDB/04138/2020 and UIDP/04138/2020), COMPETE Programme (SAICTPAC/0019/2015) and PTDC/QUI-QOR/1786/2021. The project leading to this application has received funding from the European Union's Horizon 2020 research and innovation programme under grant agreement No 951996. J.A.S.C. thanks FCT for Scientific Employment Stimulus 2020/02383/CEECIND.

### References

1. S. Bunsupa, M. Yamazaki, and K. Saito, "Quinolizidine alkaloid biosynthesis: Recent advances and future prospects," *Front. Plant Sci.*, vol. 3, no. OCT, pp. 1–7, 2012.
2. R. F. M. F. N. Maulide, B. Peng, C. A. M. Afonso, "Process for converting lupanine into sparteine, EP2808326A1; WO2014191261A1; 3-12-2013."
3. (a) J. Pothier, S. L. Cheav, N. Galand, C. Dormeau, and C. Viel, "A comparative study of the effects of sparteine, lupanine and lupin extract on the central nervous system of the mouse," *J. Pharm. Pharmacol.*, vol. 50, no. 8, pp. 949–954, 1998. (b) F. V. Romeo, S. Fabroni, G. Ballistreri, S. Muccilli, A. Spina, and P. Rapisarda, "Characterization and antimicrobial activity of alkaloid extracts from seeds of different genotypes of *Lupinus* spp," *Sustain.*, vol. 10, no. 3, pp. 6–10, 2018. (c) M. Wiedemann, C. M. Gurrola-Díaz, B. Vargas-Guerrero, M. Wink, P. M. García-López, and M. Düfer, "Lupanine improves glucose homeostasis by influencing KATP channels and insulin gene expression," *Molecules*, vol. 20, no. 10, pp. 19085–19100, 2015. (d) S. Carmalia, V. D. Alves, I. M. Coelho, L. M. Ferreira, and A. M. Lourenço, "Recovery of lupanine from *Lupinus albus* L. leaching waters," *Sep. Purif. Technol.*, vol. 74, no. 1, pp. 38–43, 2010.

**Biobased vitrimers - novel dynamic materials from vegetable oils and their applications**

A. Zych<sup>1\*</sup>, D. Sangaletti<sup>1,2</sup>, G. Spallanzani<sup>1,3</sup>, J. Tellers<sup>4</sup>, L. Bertolacci<sup>1</sup>, L. Ceseracciu<sup>5</sup>, A. Athanassiou<sup>1</sup>

<sup>1</sup> Smart Materials, Istituto Italiano di Tecnologia, Via Morego 30, Genova 16163, Italy

<sup>2</sup> DIBRIS, University of Genoa, via Opera Pia 13, Genoa, Italy

<sup>3</sup> Dipartimento di fisica, Politecnico di Milano, Piazza Leonardo da Vinci 32, 20133, Milano, Italy

<sup>4</sup> Institut de Chimie de Nice, Université Côte d'Azur CNRS, UMR 7272, Nice 06108, France

<sup>5</sup> Materials Characterization Facility, Istituto Italiano di Tecnologia, Via Morego 30, Genova 16163, Italy

\*E-mail: arkadiusz.zych@iit.it

**Abstract**

The global production of thermosets has been increasing in recent years, causing rapid consumption of fossil-based feedstocks and contributing to the plastic waste accumulation in the environment, especially because they cannot be easily reprocessed or recycled at the end of their lifetime. To overcome those issues, dynamic crosslinks capable of exchange reactions can be introduced, enabling network rearrangements, malleability, and reprocessability [1]. Those dynamic thermosets form a new class of materials, called vitrimers, since they flow like a vitreous silica (quartz glass) following the Arrhenius law [2]. At service temperatures they behave like permanently crosslinked polymers but at elevated temperatures the exchange reactions speed up making flow possible while maintaining constant number of chemical bonds and crosslinks. Thanks to that, vitrimers can be repaired, reshaped and reprocessed decreasing significantly the cost and environmental impact. Facile way to produce biobased vitrimers from vegetable oils and a diboronic ester dithiol vitrimer crosslinker will be presented [3]. The synthesis of the cross-linker and the production process of the vitrimers has been done following green chemistry principles. The developed vitrimer materials can be reprocessed multiple times like a thermoplastic, without compromising its mechanical properties. Moreover they can be conveniently recycled by reversible hydrolysis in 90% ethanol and subsequent solvent evaporation, regenerating the original vitrimer. In case of an accidental release into the environment, the materials are able to biodegrade, solving the problem of waste accumulation. Properties of the final materials can be tuned from soft and flexible to rigid and hard by varying the vegetable oil type and crosslink density. The use of those materials in self-healing coatings, strain sensors and carbon fiber composites will be demonstrated.

**Keywords:** Biobased vitrimers; dynamic thermosets; boronic esters; vegetable oils; carbon fibre composites.

**References** (Not more than 5, please follow the below reference style if any).

1. D. Montarnal, M. Capelot, F. Tournilhac, L. Leibler, *Science*, **2011**, 334 (6058), 965.
2. W. Denissen, J. M. Winne, F. E. Du Prez, *Chemical Science*, **2016**, 7 (1), 30-38.
3. A. Zych, J. Tellers, L. Bertolacci, L. Ceseracciu, L. Marini, G. Mancini, A. Athanassiou, *ACS Applied Polymer Materials*, **2021**, 3 (2), 1135–1144.



# Biomass to chemicals

## Metal free heterogeneous catalyst for one pot conversion of fructose/carbohydrate feedstocks into 2,5-diformylfuran

Arvind Singh Chauhan<sup>1,2</sup> and Pralay Das<sup>1,2,\*</sup>

<sup>1</sup>Chemical Technology Division, CSIR-Institute of Himalayan Bioresource Technology, Palampur-176061, H.P., India.  
Fax: +91-1894-230433. \*E-mail: pdas@ihbt.res.in, pralaydas1976@gmail.

<sup>2</sup>Academy of scientific and innovative research (AcSIR), Ghaziabad- 201002, India.

The sustainable valorization of naturally abundant renewable biomass into valuable fine chemicals has gained global attention. 2,5-diformylfuran (DFF) is a valuable furan-based entity derived from biomass carbohydrates that has numerous applications in pharmaceuticals, polymeric materials, fungicides, organic conductors.<sup>1</sup> Traditionally, DFF has been synthesized primarily from 5-HMF using a variety of metal-based catalysts and stoichiometric oxidants.<sup>2</sup> However, the high price and low stability of 5-HMF limits bulk DFF production to this day. As a result, development of a one-step approach for DFF synthesis directly from fructose/carbohydrate feedstocks has become a challenging task for both academic and industrial researchers.

From last few years, our research group has been dedicatedly working on the conversion of lignocellulosic biomass into high value chemicals.<sup>3</sup> In this context, we have developed a metal catalyst free solid acid catalysed and highly chemoselective one pot approach for the synthesis of DFF directly from low cost fructose/carbohydrate feedstocks. The user-friendly solid acid catalyst was explored for the transformation of fructose to DFF to achieve highest yield. The crucial role of developed catalytic and reagent systems was investigated thoroughly with detailed mechanistic studies supported by identification of intermediate and control experiments. The developed process is scalable, easily to operate, highly chemo-selective and does not require any tedious purification techniques to achieve high purity. The ability to produce DFF in acceptable quantities from low-cost feed-stocks including sugar, sugarcane molasses, and jaggery, highlighted the developed process simplicity and efficiency.

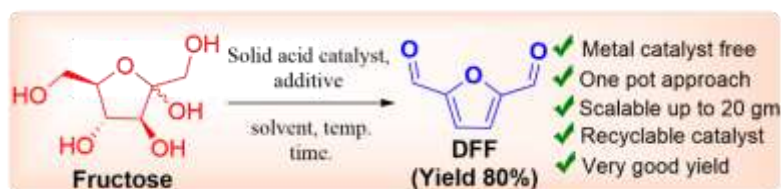


Figure 1. One pot synthesis of DFF from fructose.

### Highlights:

- A user friendly, commercially available solid acid catalyst was used for the synthesis of DFF.
- Metal catalyst free oxidation approach and less hazard produce.
- Highly chemo-selective, scalable approach and recyclable catalyst up to seven cycles.
- The process is also applied successfully on various low-cost carbohydrate feedstocks including sugar, sugarcane molasses and jaggery.

### Acknowledgements

We are grateful to the Director, CSIR IHBT for providing necessary facilities during the work. A. S. Chauhan thank DST INSPIRE, New Delhi for awarding fellowships and financial support as part of the project number MLP0203.

### References

1. a) Z. Chen, S. Liao, L. Ge, P. N. Amaniampong, Y. Min, C. Wang, K. Li, J.-M. Lee, *Chem. Eng. J.*, **379** 122284-122294 (2020). 379, 122284–122292; b) P. Pal, S. Saravanamurugan, *ChemSusChem*, **12** 145-163 (2019).
2. a) I. Sadaba, Y. Y. Gorbanev, S. Kegnaes, S. S. R. Putluru, R. W. Berg, A. Riisager, *ChemCatChem*, **5** 284-293 (2013); b) R. Fang, R. Luque, Y. Li, *Green Chem.*, **18** 3152-3157 (2016) 18, 3152–3157.
3. a) A. Kumar, A. S. Chauhan, Shaifali, P. Das, *Cellulose*, **28** 3967-3980 (2021); b) A. S. Chauhan, A. Kumar, P. Das, *Org. Process Res. Dev.*, **25** 892–899 (2021); c) A. S. Chauhan, A. Kumar, A. K. Sharma, P. Das, *Chem.Eur. J.*, **27** 12971– 12975 (2021); d) A. Kumar, A. S. Chauhan, R. Bains, P. Das, *J. Ind. Eng. Chem.*, **101** 214-226 (2021).

## Predictive model of the biocatalytic synthesis of butyl levulinate from levulinic acid in a continuous flow microreactor

Cordier A.<sup>1,2</sup> Legros J.<sup>1</sup>, Held C.<sup>3</sup>, Leveueur S.<sup>2\*</sup>,

<sup>1</sup>Lab COBRA, CNRS, University of Rouen, 76000 Rouen, France

<sup>2</sup> Normandie Univ, INSA Rouen, UNIROUEN, LSPC, EA4704, 76000 Rouen, France

\* [sebastien.leveueur@insa-rouen.fr](mailto:sebastien.leveueur@insa-rouen.fr)

<sup>3</sup> TU Dortmund University, EMIL-FIGGE-STR. 70, Dortmund, Deutschland

Abstract text:

Due to the coming soon peak and scarcity of petroleum resources, the straightforward production of biobased functionalized organic compounds is required [1]. Thanks to its ketone and carboxylic acid group, levulinic acid is a good candidate for the synthesis of non-petroleum product particularly into biodiesel through levulinate esters [2] and gamma-valerolactone [3]. For an efficient and greener synthesis, we aim to develop intensified miniaturized flow reactor [4], with recyclable supported catalyst. Flow systems allow a better temperature control, to limit the concentration gradient [5], and consequently a better selectivity and productivity [6]. As catalyst, we chose Novozym 435, the well-know supported Cal-B used for the synthesis or hydrolysis of amide and ester [7]. In this context, our work is about developing predictive model for the synthesis of levulinate esters by Novozymes 435 with a microreactor under continuous flow.

The kinetic study of levulinate ester synthesis were performed with a mixture of levulinic acid, 1-butanol and Novozym 435 used as biocatalyst and placed in an Omnifit column which allow to carry out the reaction under continuous flow with a PTFE tubing and a syringe pump (Figure 1).

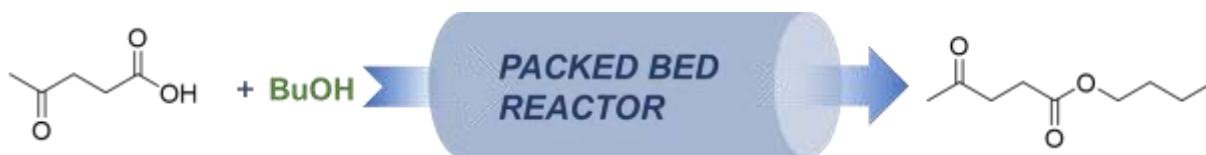


Figure 1. Biocatalytic butyl levulinate synthesis into a microfluidic system

Sample were analyzed by GC-FID and Athena Visual Studio® software, using a Bayesian framework [6], is used for the modelling.

Based on experimental data, internal and external mass transfer can be neglected as well as immobilized Cal-B deactivation which is negligible for 10 hours. The comparison between different kinetic model show that a Ping-Pong Bi-Bi mechanism [8] with alcohol inhibition is the most adequate. Figures 2 and 3 show, respectively, the fit of the model with one equivalent of BuOH at 50°C and the parity plot which compare the experimental data with the predicted data.

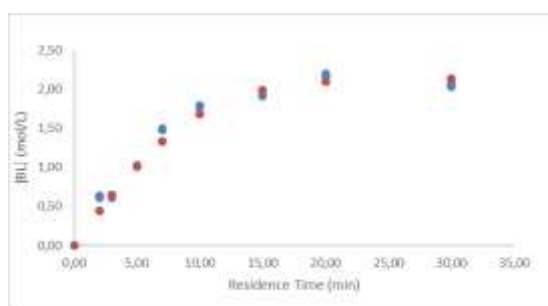


Figure 2. Fit of model to the experimental concentration of BL at 50°C and [LA]<sub>inlet</sub>=5.16 mol/L (red dot: simulated; blue dot: experimental)

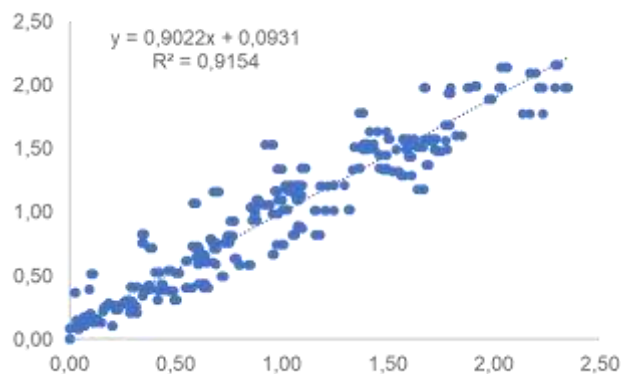


Figure 3. Parity plot for the model

Thanks to this applied and fundamental study we have been able to describe a biocatalytic mechanism and a predictive model by developing an original method, assessed by Bayesian inference, for the synthesis of a biobased product with a continuous flow microreactor.

### Acknowledgements

This research was funded, in whole or in part, by the ANR (French National Research Agency) and the DFG (German Research Foundation) through the project MUST (Microfluidics for Structure-reactivity relationships aided by Thermodynamics & kinetics) [ANR-20-CE92- 0002-01 - Project number 446436621].

### References

1. T. Bennich; S. Belyazid, *Sustainability*, **9** 887 (2017).
2. F. D. Pileidis; M.M. Titirici, *ChemSusChem*, **9** 562 (2016).
3. J. Delgado; S.N. Vasquez Salcedo; G. Bronzetti; C. Moreno; M. Mignot; J. Legros; C. Held; H. Grénman; S. Leveueur, *Chemical Engineering Journal*, **3** 430 (2022)
4. J. A. Bennett; Z. S. Campbell; M. Abolhasani, *Current Opinion in Chemical Engineering*, **26** 9 (2019).
5. S. Mansour; A. Delaune; M. Manneveau; B. Picard; A. Claudel; C. Vallières; L. Sigot; P.-Y. Renard; J. Legros, *Green Chem*, **23** 7522 (2021).
6. B.M. Plutschack; B. Pieber; K. Gilmore; P.H. Seeberger, *Chemical Reviews* **117** 11796 (2017).
7. W. E. Stewart; M. Caracotsios, "Athena Visual Studio," (2010).
8. M. N. Varma; G. Madras, *Journal of Chemical Technology an Biotechnology*, **83** 1135 (2008).
9. A. Cordier; manuscript in progress

# Butyl-5-(Dibutoxymethyl)-2-Furoate (BDMF): a New Bio-sourced Furanic Platform Molecule for the Green Production of Biodegradable Surfactants and Industrial Chemicals

Pérocheau Arnaud S.<sup>1</sup>, Wong T.<sup>1</sup>, Noirbent G.<sup>1</sup>, Durand L.<sup>1</sup>, Renault L.<sup>1</sup>, Roussel X.<sup>2</sup>, Benvegnu T.<sup>1,\*</sup>.

<sup>1</sup> Ecole Nationale Supérieure de Chimie de Rennes, 11 Allée de Beaulieu, 35708 Rennes, France.

<sup>2</sup> SurfactGreen, 11 Allée de Beaulieu, 35708 Rennes, France.

\* E-mail: thierry.benvegnu@ensc-rennes.fr



Figure 1: Graphical abstract: BDMF as bio-based platform molecule.

With increasing awareness of environmental issues brought by the use of petroleum-based compounds, a recent growing interest in sustainable chemistry for the development of novel molecules derived from renewable resources has been witnessed. This translates into the need for the development of platform molecules obtained from biomass feedstocks through environmentally friendly synthesis in accordance with green chemistry principles.

To this end, platform molecules such as 5-(hydroxymethyl)-furfural (HMF) [1] and 5-(chloromethyl)-furfural (CMF) [2] have been the focus of numerous studies as they can be transformed into different building blocks for various applications. While the former exhibits a problematic instability and high water miscibility, preventing an efficient extraction, the latter requires the use of chlorinated chemicals.

We herein report the robust conversion of homo- and hetero- uronate polysaccharides through a one-pot process into a novel more stable bio-based furanic derivate with lower water miscibility, the butyl 5-(dibutoxymethyl)-2-furoate (BDMF) [3]. This derivate exhibits two different and already protected functional groups allowing to access a furanic ester or carboxylic acid without the oxidation of HMF. BDMF can in turn be converted to higher value chemicals in one or two easy steps to reach the targeted functional groups such as aldehyde, acid, oxime, amine or nitrile. These simple transformations allow their use for various applications as monomers, coating additives, polymers, pharmaceutical compounds, agrochemistry and surfactants. Fully bio-based, biodegradable and non-ecotoxic anionic surfactants were obtained using an eco-friendly synthesis and their characterisation showed that these surfactants are promising anionic moieties with efficient surface tension reduction and high foaming power.

**Keywords:** butyl 5-(dibutoxymethyl)-2-furoate, 5-(hydroxymethyl)-furfural, biomass, sustainable chemistry, platform molecule, surfactant.

## Acknowledgements

The Région Bretagne and SurfactGreen company are acknowledged for supporting and funding this work.

## References

- [1] J. J. Bozell and G. R. Petersen, "Technology development for the production of biobased products from biorefinery carbohydrates-the US Department of Energy's "Top 10" revisited," *Green Chem.*, vol. 12, pp. 539-554, 2010.
- [2] M. Maskal, "5-(Chloromethyl)furfural (CMF): A Platform for Transforming Cellulose into Commercial Products," *ACS Sustainable Chemistry & Engineering*, vol. 7, pp. 5588-5601, 2019.
- [3] L. Renault, R. Marchal, B. Le Guennic, X. Roussel, P.-Y. Divet and T. Benvegnu, "Direct Conversion of Alginate Oligo- and Polysaccharides into Biodegradable Non-Ecotoxic Anionic Furanic Surfactants - An Experimental and Mechanical Study," *Advanced Sustainable Systems*, vol. 5, no. 7, p. 2100108, 2021.

## Selective condensation of small sugars by reconstructed Hydrotalcite towards the synthesis of polyol-based flame retardants

Fatima Rammal<sup>1</sup>, Ibrahim Khalil<sup>1</sup>, Ward Lorenz<sup>1</sup>, Beau Van Vaerenbergh<sup>2</sup>, Bert De Schrijver<sup>2</sup>, Ekaterina Makshina<sup>1</sup>, Bert Sels<sup>1\*</sup>

<sup>1</sup> CSCE, Katholieke Universiteit Leuven, Celestijnenlaan 200F, Leuven 3001, Belgium

<sup>2</sup> Oleon NV, Assenedestraat 2, Evergem 9940, Belgium

\*Bert.Sels@kuleuven.be

Aside from their use as precursors in a variety of chemical materials ranging from surfactants and plasticizers to polymer crosslinkers, branched polyols have gained additional interest due to their ability to be converted by esterification into lubricants and moisturizers or, more importantly, into green flame retardants by phosphorylation reaction as a direct replacement for bromine and chlorine-containing alternatives [1].

Therefore, the development of an efficient and sustainable approach for the synthesis of branched polyols is of great interest. Thus, the objective of this work is to realize the condensation of dihydroxyacetone into branched sugars (dendroketoose) by means of a stable and robust heterogeneous catalysis in order to obtain the corresponding branched polyols via hydrogenation. In terms of heterogeneous basic catalysts, hydrotalcite is one of the most important candidates to realize the base-catalyzed condensation of dihydroxyacetone. This is due to their interesting structural properties, their ease of synthesis, and the various active sites that lead to a selective aldolization [2].

Our approach consists in studying the activity and selectivity of hydrotalcite in condensation chemistry as a function of its composition, layered structure, and porous characteristics. These different parameters define the strength, nature, and accessibility of the different active basic sites which have been investigated by means of FT-IR spectroscopy, CO<sub>2</sub> temperature-programmed desorption, nitrogen physisorption, and XRD measurements. Interestingly, additional optimization studies were conducted in order to improve the stability of the catalyst and subsequently promote a successful hydrogenation process.

Thus, the gain in mechanistic insights allowed the selection of an adapted pretreatment process that improves the properties and stability of hydrotalcites as heterogeneous catalysts, which was successfully applied for the formation of branched sugars under mild conditions and suitable for late-stage functionalization. The catalyst characterization, as well as mechanistic studies, will be discussed in this presentation.

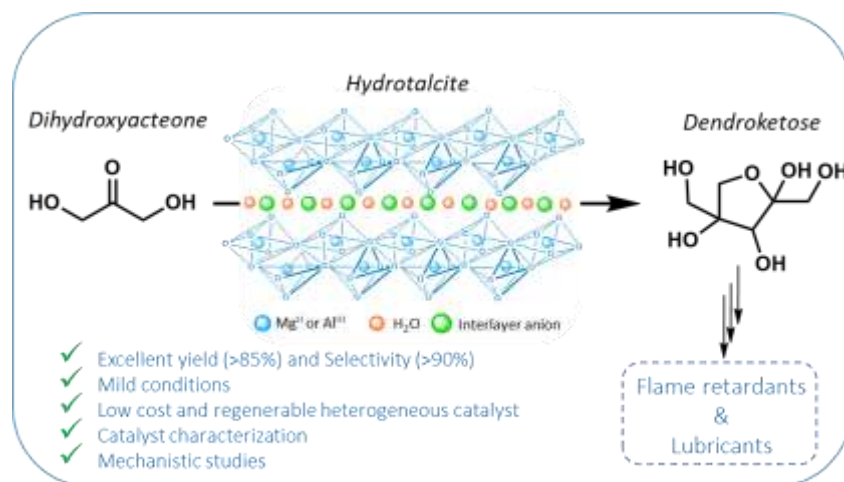


Figure 1. DHA as precursor for flame retardants and lubricants

### References

1. A. Deneyer, S. Tlatli, M. Dusselier, Bert F. S. *ACS Sustainable Chem. Eng.* **6** 7940 (2018).
2. B. M. Choudary, M. Lakshmi Kantam, Ch. Venkat Reddy, K. Koteswara Rao, F. Figueras, *Green Chem.*, **1** 187 (1999).

## Efficient conversion of sucrose to methyl lactate with Sn-USY: the role of water

Jose M. Jimenez-Martin, Maia Montaña, María Linares, Alicia García, Jose Iglesias\*

Chemical & Environmental Engineering Group. Universidad Rey Juan Carlos, C/ Tulipan s/n, 28933, Madrid, Spain

\*jose.iglesias@urjc.es

The development of tin functionalized zeolites has been a major breakthrough in catalysis science related to Lewis acid heterogeneous catalysts, because of the extraordinary versatility and selectivity these materials show in a wide variety of transformations, including Baeyer-Villiger oxidations, Meerwein-Ponndorf-Verley hydrogen transfer reductions or retroaldolic condensation of sugar monosaccharides. This last transformation is especially relevant because it has revealed to be an excellent alternative to anaerobic fermentations for the production of lactic acid and related derivatives [1]. Lactic acid is a highly interesting bioproduct because it is the starting point in the synthesis of a wide variety of important chemicals, both commodities and drop-ins, such as acrylic acid (monomer), alkyl lactates (green solvents), poly-lactic acid or PLA (biopolymer). Current industrial process used for the production of lactic acid is based on a fermentation process associated to a high waste generation -1 kg of  $\text{CaSO}_4$  is produced per kg of lactic acid- [2]. Chemo-catalytic routes for the production of lactic acid based on the use of highly active and selective Sn-zeolites, are known to proceed through efficient pathways (Figure 1) and require of a reduced number of steps as compared to fermentation routes [3]. However, this synthetic pathway still require of highly active, selective and robust catalysts and their validation in the conversion of complex carbohydrate feedstock, showing a high concentration of sugars, whose conversion would eventually require of small-sized chemical reactors. Sn- $\beta$  and Sn-USY zeolites have demonstrated to be highly active catalysts and, under certain conditions, stable enough to conduct the direct transformation of carbohydrates to alkyl lactates in a single step under continuous flow conditions. Nevertheless, the afore mention questions on their capability to process complex mixtures of carbohydrates at high concentration values still need to be addressed. This work presents the most relevant results achieved in the evaluation of a Sn-USY-based catalytic system in the conversion of highly concentrated sucrose methanolic solutions into methyl lactate [4-5]. The work also provides the results on the effect of water in the overall catalytic performance of the Sn-USY zeolite, whose intrinsic catalytic activity and reusability is enhanced in the presence of small quantities of water.

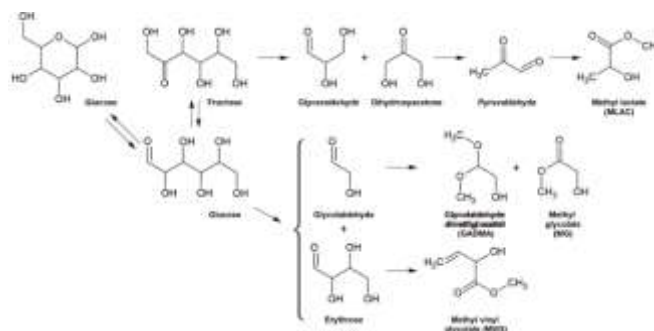


Figure 1. Reaction Scheme on the conversion of glucose into methyl lactate in the presence of Sn-USY catalysts

The synthesis of the Sn-USY zeolite starts from a commercial USY zeolite (CBV 712), which is subjected to a two-step dealumination using aqueous  $\text{HNO}_3$  solution ( $10 \text{ mol}\cdot\text{L}^{-1}$ ;  $20 \text{ mL}\cdot\text{g}^{-1}_{\text{zeo}}$ ; 1h). Tin was incorporated by grafting  $\text{SnCl}_4$  onto the hydroxyl nests created at the aluminum vacancies. The material was calcinated at  $550^\circ\text{C}$  and ion exchanged with  $\text{KCl}$  aqueous solutions ( $0.5 \text{ M}$ ,  $100 \text{ mL}\cdot\text{g}^{-1}_{\text{zeo}}$ ,  $50^\circ\text{C}$ ) to neutralize Brønsted acid sites. The prepared material was thoroughly characterized by different techniques, including  $\text{N}_2$  adsorption isotherms, XRD, TEM,  $\text{NH}_3$ -TPD, DRIFT with  $\text{ACN-D}_3$  and pyridine as molecular probes, among others. Catalytic tests were conducted in a batch reactor loaded with  $75 \text{ mL}$  of methanolic solutions of carbohydrates (glucose, sucrose,  $0.14$ - $0.28 \text{ mol}\cdot\text{L}^{-1}$ ) together with  $0.75 \text{ g}$  of catalyst, and the mixture was heated up to  $150^\circ\text{C}$  (time zero) for 6 h under continuous stirring. The presence of water in the reaction media was varied by substituting of methanol with water (1-8 wt%). The reaction media was analyzed with a gas chromatograph fitted with a CP-WAX 52CB column and a liquid chromatograph equipped with a Shodex  $\text{NH}_2\text{P-50 4E}$  column.

The catalytic activity of the Sn-USY catalyst was initially evaluated in the transformation of glucose and sucrose methanolic solutions at different concentration levels. Reaction results from the transformation of both carbohydrates in methanol, in the presence of Sn-USY, reflected scarce differences in the performance of the catalysts when operating at the lower value of the sugar concentration range. Results indicated a 70% yield towards methyl lactate can equally be achieved either from glucose or from sucrose. The rest of the identified products were ascribed to retro-aldol transformation pathways involving glucose, leading to the formation of GADMA and MVG as main side reactions (Figure 1). Identified reaction products totalized >95% of the starting feedstock. Catalytic tests performed at a higher substrate concentration level ( $0.28 \text{ mol/L}$ ) were conducted solely with sucrose (Figure 2). As expected, a large drop in the yields calculated for all the detected products, was observed. Obviously, processing concentrated sucrose methanolic solutions seems to require of longer operation times. Under these

conditions, a yield of 34% towards methyl lactate was obtained after reacting for 6 h. This result was accompanied with a great production of methyl glycosides, especially during the early beginning of the catalytic tests, which are later converted, but a slow reaction rate. These results demonstrate the fast rate of glycosidation, but they also reveal the difficulties found in the transformation of glycosides towards retroaldol-derived products.

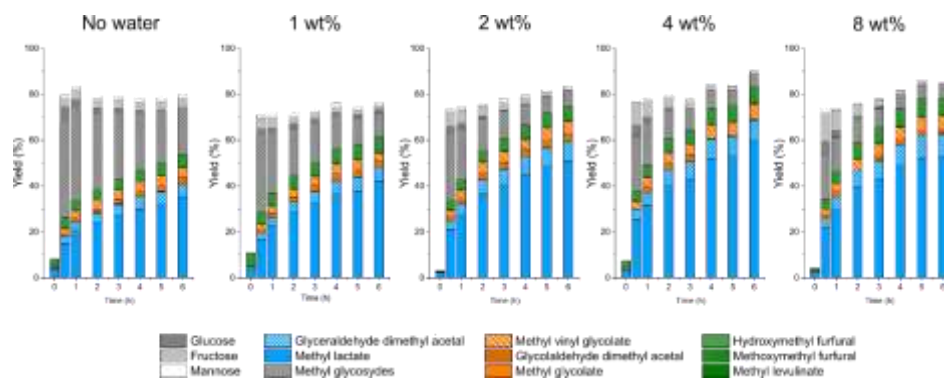


Figure 2. Product distribution obtained with different water concentration in the reaction media 7.2 g sucrose, 0.75 g catalyst, 75 mL methanol, 150°C)

In order to limit the formation of glycosides, favoring the presence of sucrose or its constituents glucose and fructose, small quantities of water were added to the reaction media (Figure 2). The presence of water reduces the concentration of methyl glycosides, leading to higher concentrations of fructose and glucose at the beginning of the transformation, presumably due to higher rate of sucrose hydrolysis as compared to methanolysis. [6]. This effect has strong consequences on the retro-aldol condensation of the sugar monosaccharides, since the formation of methyl lactate is promoted, rising to 42% when 1 wt% water is added to the reaction media, to nearly 55% at 8 wt% water concentration. The higher availability of free monosaccharides, instead of alkyl glycosides, seems to be one of the reasons for the higher methyl lactate yield achieved in the presence of small quantities of water. However, alkyl glycosides are also much faster converted, a result which seems to be related to a higher intrinsic catalytic activity of the Sn-USY zeolite. This is in accordance with previous results, which suggest that the addition of water to the reaction media prevents the deactivation of the catalytic sites through different pathways [7].

In order to evaluate if catalyst deactivation takes place, and if it is playing a role in the studied transformation, catalyst reutilization tests were conducted. Results evidence the catalyst tested in pure methanol solvent almost lost all of the starting catalytic activity, providing very low yields towards retroaldol condensation products (<5%). On the contrary, catalysts tested in the presence of increasing water contents, reflected a much better reusability in a second catalytic run. In this way, the presence of water not only modifies the composition of the reaction media in terms of monosaccharides speciation (free sugars vs glycosides), but it also seems to exert an important role in the preservation of the catalytic activity of Sn-USY zeolites. Further insights on the performance the addition of water as a solution to catalyst deactivation are being conducted through catalyst recycling tests.

The presence of water in the reaction media when converting highly concentrated methanolic solutions of sucrose in the presence of tin containing zeolites improves methyl lactate production, reducing side products such as methyl glycosides and preserving the catalytic activity during the reaction, achieving a total yield of 55%, a result scarcely reported for the considered substrate concentration.

## Acknowledgements

This project has received funding from the Bio Based Industries Joint Undertaking (JU) under the European Union's Horizon 2020 research and innovation program under grant agreement No 101023202.

This research was funded by the Spanish Ministry of Science, Innovation and Universities (projects RTI2018-094918-B-C41 & RTI2018-094918-B-C42)

## References

1. M.S. Holm, S. Saravanamurugan, E. Taarning, *Science*, 2010, 328, 602-605
2. P.V. Wouwe, M. Dusselier, E. Vanleeuw, B. Sels, *ChemSusChem*, 2016, 9, 907-921
3. M.S. Holm, Y.J.Pagan-Torres, S. Saravanamurugan, A. Riisager, J.A. Dumesic, E. Taarning, *Green Chem.*, 2012, 14, 702-706
4. J. Iglesias, J. Moreno, G. Morales, J.A. Melero, P. Juarez, M. Lopez-Granados, R. Mariscal, I. Martinez-Salazar, *Green Chem.*, 2019, 21, 5876
5. J.M. Jimenez-Martin, A. Orozco-Saumel, H. Hernando, M. Linares, R. Mariscal, M. Lopez-Granados, A. Garcia, J. Iglesias, *Sus. Chem. Eng.*, -submitted-
6. I. Tosi, A. Riisager, E. Taarning, P. R. Jensen, S. Meier, *Catal. Sci. Technol.*, 2018, 8, 2137-2145
7. D. Padovan, S. Tolborg, L. Botti, E. Taarning, I. Sádaba, C. Hammond, *React. Chem. Eng.*, 2018, 3, 155-163

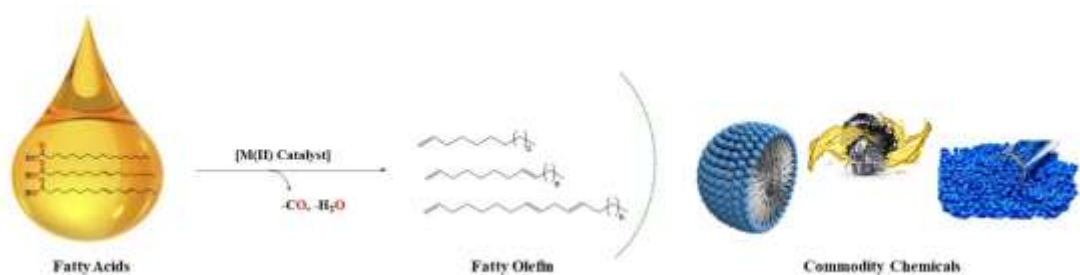


## Catalytic dehydrative decarbonylation of tall oil-derived fatty acids to linear $\alpha$ -olefins

Sibongile Pikoli<sup>1</sup> and Banothile C. E. Makhubela<sup>2\*</sup>

Chemistry Department, University of Johannesburg, Auckland Park Kingsway Campus, Auckland Park 2006, South Africa  
\*bmakhubela@uj.ac.za

Long-chain (C9 to C18) linear  $\alpha$ -olefins - used in producing chemical products like surfactants<sup>1,2</sup>, lubricants<sup>3</sup> and polymers<sup>1,4</sup> - have traditionally been synthesized from petroleum-based feedstocks. A more sustainable way to access linear  $\alpha$ -olefins of the chain length required for surfactant and lubricant applications is by using triglyceride-derived fatty acid feedstocks. Fatty acids provide a suitable hydrocarbon chain length and carboxylic acid handle that can be converted to a terminal olefin using catalytic decarbonylation in the presence of acetic anhydrides.<sup>5,6</sup> The most effective catalysts for decarbonylation include expensive rhodium and palladium metals. Non-noble metal catalysts like nickel and iron are also used, however, these operate at extremely high temperatures (200 - 300 °C) and require stoichiometric amounts of additives such as potassium iodide.<sup>4,7</sup> Metal catalysts like those incorporating inexpensive nickel and cobalt would be of interest if they catalyze decarbonylation reactions efficiently, especially if they give high linear  $\alpha$ -olefin yields without the need for additives.



Scheme 1: Metal catalysed conversion of fatty acids to form fatty olefins

Herein, we present the synthesis of new nickel(II) and cobalt(II) complexes bearing aminophosphine ligands and their use as precatalysts for the dehydrative decarbonylation of fatty acids at lower temperatures without the need for additives.

### References:

- 1 Z. Zhou, H. Liu, Z. Chen, W. Zhu and Z. Liu, *ACS Catal.*, 2021, **11**, 4077–4083.
  - 2 S. H. Hopen Eliasson, A. Chatterjee, G. Occhipinti and V. R. Jensen, *ACS Sustain. Chem. Eng.*, 2019, **7**, 4903–4911.
  - 3 A. Chatterjee and V. R. Jensen, *ACS Catal.*, 2017, **7**, 2543–2547.
  - 4 X. Zhang, F. Jordan and M. Szostak, *Org. Chem. Front.*, 2018, **5**, 2515–2521.
  - 5 M. A. Ortuño, B. Dereli and C. J. Cramer, *Inorg. Chem.*, 2016, **55**, 4124–4131.
  - 6 S. H. Hopen Eliasson and V. R. Jensen, *Faraday Discuss.*, 2019, **220**, 231–248.
  - 7 F. Cataldo, *Eur. Chem. Bull.*, 2019, **8**, 88–95.
  - 8 (accessed 31-03-2022)
- [https://www.kindpng.com/imgv/hRRimbR\\_clip-art-oil-drop-png-drop-oil-png/](https://www.kindpng.com/imgv/hRRimbR_clip-art-oil-drop-png-drop-oil-png/)  
[https://favpng.com/png\\_view/soap-micelle-surfactant-soap-molecule-chemistry-png/KNBiXCnc](https://favpng.com/png_view/soap-micelle-surfactant-soap-molecule-chemistry-png/KNBiXCnc)  
<https://www.volkswagen.com.my/volkswagen-service/parts-and-accessories/engine-oil-and-fluids/engine-oil>  
<https://www.kaysun.com/blog/material-selection-tips-resin-trends-part-1>

# Bio-Waste Valorization & Circular economy

# Influence of supercritical CO<sub>2</sub> pretreatment of spent coffee grounds on the yield and composition of polar molecules extracted by subcritical H<sub>2</sub>O extraction under microwave irradiation

Alexandre VANDEPONSEELE, Manon MAILLET, Philippe FANGET, Micheline DRAYE,  
Christine PIOT and Gregory CHATEL\*

Univ. Savoie Mont Blanc, CNRS, EDYTEM, F-73000 Chambéry, France

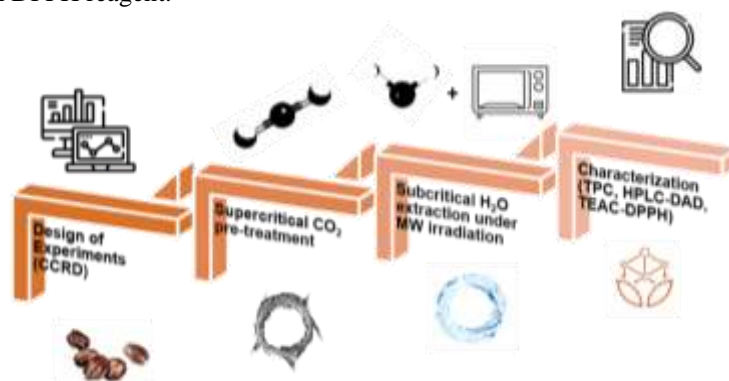
\* gregory.chatel@univ-smb.fr

Spent coffee grounds (SCG) is the most significant coffee by-product with approximately 6 Mt of SCG generated each year worldwide due to coffee brewing stage. The SCG is a bioresource of great interest to produce bioactive ingredients thanks to its composition in high value lipids, caffeine and polyphenols. Then, the valorization of SCG has been intensively investigated these last years with disruptive technologies such as ultrasound, microwave, subcritical H<sub>2</sub>O or supercritical CO<sub>2</sub> [1].

The supercritical CO<sub>2</sub> (SC-CO<sub>2</sub>) and subcritical H<sub>2</sub>O (SCW) are both green solvents under high pressure to give new properties to H<sub>2</sub>O and CO<sub>2</sub>. Above the critical point of CO<sub>2</sub> at 31°C and 74 bars, SC-CO<sub>2</sub> gets hybrid properties between a gas viscosity and a liquid's solvation capacity. Therefore, SC-CO<sub>2</sub> is particularly suitable for lipids extraction from dry SCG without extracting caffeine and polyphenols. Previous work shows that supercritical CO<sub>2</sub> from wet SCG allow the selective extraction of caffeine [2]. Thereby, the solid residue of SCG can be defatted and decaffeinated before further extraction to produce decaffeinated polar molecules extracts, which can be used as bioactive ingredients in nutraceutical, with high antioxidants properties and without the drawbacks about health issues related to caffeine,

Subcritical H<sub>2</sub>O (SCW) corresponds to liquid water under pressure and at high temperature between 100-374 °, which possesses unique properties in those conditions. SCW benefits from an increase of the diffusion coefficient of water, increase of the solubility of solutes, increase of the diffusion of solutes, reduction of dielectric constant of water to become closer to that of ethanol and acidification of water. SCW can be used to replace hydroalcoholic solvents for the production polar bioactive ingredients from SCG

Therefore, the aim of this work is i) to investigate the role and influence of supercritical CO<sub>2</sub> pretreatment on dry or wet SCG at 300 bars, 40 °C on the yield, composition and properties of polar molecules extracted by subcritical H<sub>2</sub>O and ii) to optimize the full process including supercritical CO<sub>2</sub> pretreatment and subcritical H<sub>2</sub>O extraction by modifying conditions as cycles of decaffeination, temperature, solid/liquid ratio, time of extraction and microwave irradiation thanks to a Design of Experiments (DoE) with a Central Composite Rotatable Design (CCRD). To do this, polar molecules extracts were characterized by their mass yield after lyophilization, by their chemical composition thanks to Total Polyphenols Content (TPC) and HPLC-DAD analyses to define the caffeine and hydroxycinnamic acids content and by their antioxidant properties with Trolox Equivalent Antioxidant Capacity (TEAC) with DPPH reagent.



## Acknowledgements

The authors gratefully acknowledge the Auvergne Rhône Alpes French Region for the awarding of the PhD scholarship to Alexandre Vandeponseele and for equipment funding through the Pack Ambition Recherche program (VALORWaste project). They also acknowledge the TRIALP company and the Université Savoie Mont Blanc Foundation for their financial supports through soMAR project.

## References

1. A. Vandeponseele et al., 2020, Green Chemistry, 22, 8544–8571.
2. A. Vandeponseele et al., J. Supercrit. Fluids, In preparation (unpublished results)

## Biphasic green solvents system for a fast “one-pot” simultaneous extraction at room temperature of valuable compounds from tomato pomace waste

F.Contillo<sup>1</sup>, M. Marone<sup>1</sup>, P. Marasco<sup>1</sup>, D. Racca<sup>1</sup>, M. Monteleone<sup>1</sup>, M Caroprese<sup>2</sup>, M. Francavilla<sup>1\*</sup>

<sup>1</sup>STAR\*Research Group, Department of Agriculture, Food, Natural Resources and Engineering (DAFNE), University of Foggia, Via Napoli 25, 71122 Foggia, Italy;

<sup>2</sup>Department of Agriculture, Food, Natural Resources and Engineering (DAFNE), University of Foggia, Via Napoli 25, 71122 Foggia, Italy;

\*matteo.francavilla@unifg.it

Climate change and growing populations are a threat to sustainable development around the world. Strategies to improve global sustainability, including the biorefinery process in the agro-food sector designed to minimise waste and transform every fraction of raw biomass into valuable compounds and materials, need to be adopted [1].

Tomato [*Lycopersicon esculentum* (L.)] is one of the most cultivated horticultural species in the World. Italy is the leading country in the production of canned and processed tomatoes, producing 13% of the entire world's production. At the same time, Italy is the main producer at the European level with over 6 million tons, followed by Spain with 4.14 million tons, Turkey with 2.10 million tons and Portugal with 1.56 million tons [2]. The tomato industry generates a huge amount of by-products (Tomato Pomace, TP), corresponding approximately to 2-5% of the total biomass entering the industrial process. According to the Circular Economy approach, the TP, composed of skin and seeds, represents an intriguing substrate for further valorisation process. It is rich in structural polysaccharides, such as hemicellulose and cellulose, non-structural polysaccharides (pectin) and biomolecules with antioxidant, antimicrobial, antitumor, anti-fungal, anti-neurodegenerative, etc., widely used in the food and pharmaceutical industries [3]. Several studies on TP valorisation have been previously reported, focusing on the extraction of a single class of compounds at a time, such as pigments (lycopene and  $\beta$ -carotene) [4], polysaccharides (pectin), fatty acids or proteins [5]. In the light of our knowledge, only a few studies investigated biorefinery models consisting of cascading extraction processes for the production of multiple compounds. Between them, Kehili et al. [6], proposed the integration of supercritical CO<sub>2</sub> extraction of pigments from TP with the subsequent separation of proteins from the residue or anaerobic digestion of residue for bioenergy production [7, 8]. Azobou et al. [9] suggested a sequential extraction of polyphenols and lycopene from tomato skins, the extraction of edible oil from tomato seeds, and the valorisation of the solid residue by producing a low-cost bio-sorbent for dye removal. Moreover, Nagarajn et al. [10] investigated the extraction of a hydrocolloid complex composed of lipids and pectin from TP.

With the aim to set up a new sequential (scalable) process inspired by the Green Chemistry principles and using eco-friendly solvents and techniques, we investigated in this study the use of a biphasic green solvents system for a fast “one-pot” simultaneous extraction of valuable compounds from tomato pomace at room temperature. The investigated biorefinery model consisted of simultaneous extraction of lycopene oleoresin, polyphenols and pectin from TP, by means of a biphasic system (BPS) composed of two immiscible green and safe solvents (ethyl acetate and water), followed by microwave assisted extraction (MAE) of cutin (poly-hydroxy fatty acids) from the resulting solid residue (SR) (Figure 1).

The *one-pot* extraction with BPS was tested at different temperatures (25, 40 and 60 °C) and homogenising times (1, 5 and 10 minutes). At the best experimental conditions (time = 1 min; temperature = 25 °C), it generated a three phases system (Figure 1): the Red Phase (RP, ethyl acetate), the White Phase (WP) and the Solid Residue (SR), with a yield of 7.5% dw, 17.8% dw and 74% dw of tomato pomace respectively, and an extraction efficiency higher than 99%.

The RP was composed of lipids that contained a high amount of unsaturated fatty acid (82% wt), valuable pigments such as *all-trans* lycopene (1.24 mg g<sup>-1</sup> dw of tomato pomace) and  $\beta$ -carotene (0.18 mg g<sup>-1</sup> dw of TP), and polyphenols (0.25 mg GAE g<sup>-1</sup> dw of TP). Lycopene was easily purified from fatty acids and polyphenols by crystallisation (purity > 99%, recovery of 90%).

The WP was composed mainly of high-quality pectin (70% dw) that formed a polymeric gelatinous structure at the interface between water and ethyl acetate, making it easy to be separated by filtration. A certain amount of proteins (25% dw) was also found in the polymer.

The microwave-assisted extraction (MAE) of cutin from the solid residue SR was optimised by varying extraction temperature (from 100 °C to 160 °C) and time (from 10 to 30 minutes). The highest cutin yield (~20% dw of TP) was found operating MAE with an alkaline solution (0.5M NaOH) at 120 °C for 30 minutes. Interestingly, the yield of compounds extracted with our *one-pot* simultaneous biphasic extraction process at room temperature and MAE was higher than the yield achieved by conventional methods.

In conclusion, the preliminary results of the proposed cascading process seem to demonstrate the effectiveness of green sequential extractions of high-value compounds from tomato pomace, converting a by-product/waste into a multi-products source. Further investigations will aim at the production of functionalised biopolymers and platform compounds.

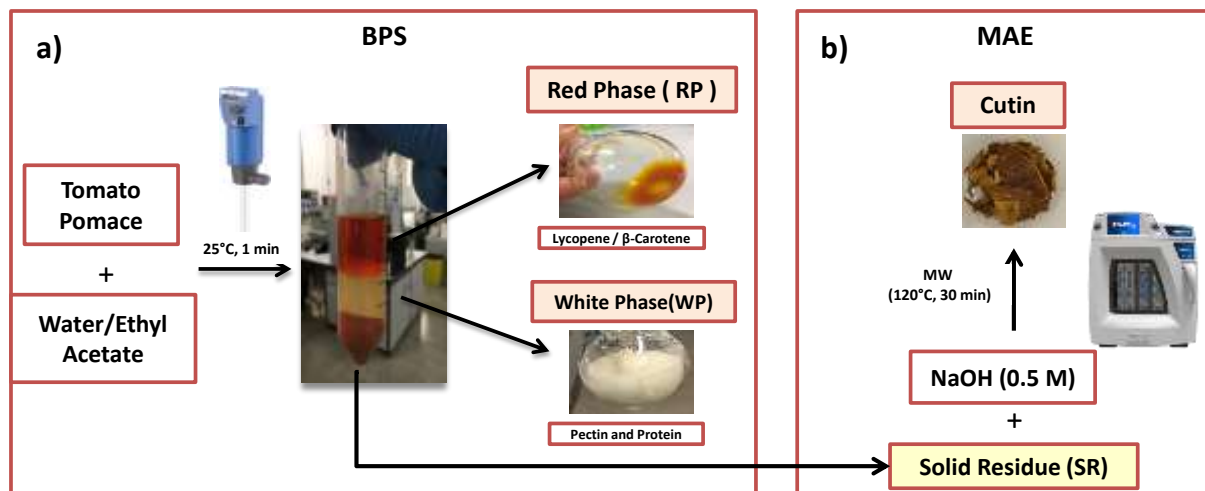


Figure 1. The integrated bio-refinery process designed for valorization of tomato pomace: **a)** “One-pot” simultaneous extraction of lipids, pigments (lycopene and  $\beta$ -carotene), phenols and pectin with a biphasic solvent system BPS (ethyl acetate and water); **b)** Microwave assisted extraction (MAE) of cutin from solid residue.

### Acknowledgements

This research was funded by PRINCES Industrie Alimentar., Mitsubishi Corporation. (PhD project: *Bio-refinery processes for the valorization of industrial waste from Tomato processing*)

### References

1. C.A. Cardona-Alzate, J.C. Solarte-Toro, Á. Peña, *Catal. Today* **302** 61 (2018).
2. FAOSTAT. *Food and agriculture Organization of the united Nations*. Available at <https://www.fao.org/faostat/en/#data>. (2020).
3. F. Boccia, P. Di Donato, C. Covino, A. Poli, *Journal of Cleaner Production* **227** 424 (2019).
4. Y. Deng, S. Zhao, X. Yang, F. Hou, L. Fan, W. Wang, E. Xu, H. Cheng, M. Guo, D. Liu, *Trends in Food Science and Technology* **115** (2021).
5. A.N. Grassino, M. Brnčić, D. Vikić-Topić, S. Roca, M. Dent, S.R. Brnčić, *Food Chemistry* **198** 93 (2015).
6. M. Kehili, L.M. Schmidt, W. Reynolds, A. Zammel, C. Zetzl, I. Smirnova, N. Allouche, S. Sayadi, *Biotechnol Biofuels* **9** 261 (2016).
7. B. Scaglia, P. D’Incecco, P. Squillace, M. Dell’Orto, P. De Nisi, L. Pellegrino, A. Botto, C. Cavicchi, F. Adani, *Journal of Cleaner Production* **243** (2020).
8. B.J. Allison, C.W. Simmons, *Biomass and Bioenergy* **105** 331 (2017).
9. S. Azabou, I. Louati, F.B. Taheur, M. Nasri, T. Mechichi, *Environmental Science and Pollution Research*. **24** 1 (2020).
10. J. Nagarajan, H. PuiKay, N.P. Krishnamurthy, N.R. Ramakrishnan, T.M.S. Aldawoud, C.M. Galanakis, O.C. Wei, *Biomolecules* **10** 1019 (2020).

## Re-circulation of spent coffee grounds for ‘awaking’ epoxy resins cross-linking and stimulating properties

Jonathan Tellers<sup>1</sup>, Mona Jamali<sup>1</sup>, Philippe Willems<sup>2</sup>, Bôke Tjeerdsma<sup>2</sup>, Nicolas Sbirrazzuoli<sup>1</sup>, and Nathanael Guigo<sup>1\*</sup>

<sup>1</sup>Institut de Chimie de Nice, Université Côte d'Azur, CNRS, UMR 7272, 06108 Nice, France.

<sup>2</sup>ORINEO – original renewables, Acaciastraat 14, B-3071 Erps-Kwerps, Belgium.

\*Nathanael.Guigo@univ-cotedazur.fr

### Abstract text:

Spent Coffee Grounds (SCGs) are part of coffee wastes obtained during the brewing process of coffee (i.e. after the consumption of coffee) and these SCGs are usually discarded as waste material. Therefore, there are great opportunities for re-circulating SCGs due to their low cost and large availabilities. In this communication, we will showcase how SCGs were incorporated in a biobased epoxy resins and what was the impact of such incorporation on the curing behavior and on cross-linked material properties.

First, the communication will focus on the fully biobased and non-toxic epoxy/hardener system that we have used. The epoxy resin was Epoxidized Linseed Oil (ELO) and the cross-linking system was composed of a so-called eutectic hardener.[1] This innovative technology consists of preparing an eutectic mixture between e.g. citric acid and a liquefier, e.g. ethyl lactate. The advantage is that the citric acid in combination with the liquefier is liquid at room temperature thus facilitating its incorporation and cross-linking capability compared to a solid citric acid that would face some dispersion issues. The resulting cross-linked matrix between ELO and the eutectic hardeners presents interesting properties and most importantly can be cured at room temperature. [1, 2]

In a second part, the communication will highlight the influence of SCGs' incorporation in the ELO/eutectic hardener system. Different SCG content e.g. 25 to 35 wt% and various curing time and temperature were employed. [3] SCGs and hexane extracted SCGs (25 wt%) have a slight catalytic effect particularly in the initial stages of the polymerization reaction conducted at room temperature (i.e. 24 °C). The effect can be correlated with the presence of remaining caffeine in SCGs that can somehow slightly accelerate the curing. Such acceleration is interesting as room temperature curing requires several days. On top of that, addition of e.g. 35 wt% SCGs lead to an increased hardness compared to raw resin. SCGs are found to heavily increase stiffness of the final material, especially when oils present in SCGs are previously extracted, raising the rubber plateau modulus from around 5 MPa to 14 MPa. This investigation paves the way for sustainable re-circulation of SCGs in biobased epoxy system with positive impact on the value chain of coffee and its waste management.



Figure 1. Overview of raw materials and obtained flexible thermosets. [adapted from ref. 3].

### Acknowledgements

This work benefited from financial support from the French government, managed by the National Research Agency (ANR) under the UCAJEDI Future Investments project with reference number ANR-15-IDEX-01 " and financial support of "La Maison de la Chimie".

### References

1. J. Tellers, P. Willems, B. Tjeerdsma, N. Guigo, N. Sbirrazzuoli, *Green Chem.*, **22**, 3104 (2020).
2. J. Tellers, M. Jamali, P. Willems, B. Tjeerdsma, N. Sbirrazzuoli, N. Guigo, *Green Chem.*, **23**, 536 (2021).
3. J. Tellers, P. Willems, B. Tjeerdsma, N. Sbirrazzuoli, N. Guigo, *Macromol. Mater. Eng.*, **306**, 2100323 (2021).

## Biovalorization of by-products from olive leaf and olive pomace obtained through green extraction methodology.

Isabel M. Martins<sup>1,2\*</sup>, Yaidelin A. Manrique<sup>1,2</sup>, Rharyne França<sup>1,2</sup>, Ricardo C. Calhela<sup>3</sup>, Lillian Barros<sup>3</sup> and Madalena M. Dias<sup>1,2</sup>

<sup>1</sup>LSRE-LCM - Laboratory of Separation and Reaction Engineering – Laboratory of Catalysis and Materials, Faculty of Engineering, University of Porto, Rua Dr. Roberto Frias, 4200-465 Porto, Portugal

<sup>2</sup>ALiCE - Associate Laboratory in Chemical Engineering, Faculty of Engineering, University of Porto, Rua Dr. Roberto Frias, 4200-465 Porto, Portugal

<sup>3</sup>Centro de Investigação da Montanha (CIMO), Instituto Politécnico de Bragança, Campus de Santa Apolónia, 5300-253 Bragança, Portugal

\*isa@fe.up.pt

The population of the Mediterranean region have been cultivating olive trees and extracting their oil for thousands of years [1]. The consumption of olive oil is associated with several health benefits, especially the reduction of degenerative and cardiovascular diseases and cancer [2]. Being a popular food in several countries, its production has grown increasingly with the corresponding increase in residues, such as the olive leaf and olive pomace [3]. The large-scale production of these residues, without appropriate treatment, increasingly represents a high polluting potential [4].

The olive leaf and olive pomace are residues rich in phenolic compounds, with recognized bioactive activity, mainly through the presence of three bioactive compounds: oleuropein, hydroxytyrosol and tyrosol [1, 5]. These phenolic compounds have bioactivity towards cancer cells, tumors, and lowering blood sugar, among others. Thus, their recovery represents a way to valorize the by-products of olive oil production since they present themselves as compounds with high added value [5].

To increase the selectivity and preserve the substances of interest, a suitable and greener technology has been recently introduced, namely supercritical fluid extraction using carbon dioxide as solvent (SFE-CO<sub>2</sub>) [6, 7]. Thus, the evaluation of extracts obtained using this methodology, as well as research around the parameters that provide better yields for extraction, are of interest in the nutraceutical and food industries [8, 9].

The present work aims to evaluate the bioactivity of olive leaf and olive pomace extracts, rich in bioactive compounds with functional properties and optimize the extraction conditions using supercritical fluid extraction. In the future, it is expected to incorporate these bio-compounds into fruit and vegetable preparations, jams, and sweets.

The extracts obtained from SFE-CO<sub>2</sub> were evaluated by high-performance liquid chromatography (HPLC) for their phenolic composition to assess the presence of three bioactive compounds: oleuropein, hydroxytyrosol and tyrosol. Their fatty acid composition was also evaluated by gas chromatography-mass spectrometry (GC-MS). The bioactive capacity of the extracts was evaluated concerning their cytotoxic and anti-inflammatory activity.

Extractions were carried out using a 200 mL extractor, with pressure of 200 bar, temperature of 40 °C and 2.5 h of extraction time, in a dynamic process (continuous circulation of CO<sub>2</sub>). Extraction yields of circa 2.5 % for olive leaf and 1.5 % for olive pomace were obtained.

The chemical composition of the obtained extracts was evaluated by liquid chromatography (HPLC) and gas chromatography-mass spectrometry (GC-MS), and their toxicity was evaluated through a non-tumor cell line.

The phenolic composition of the olive pomace extract was performed by HPLC and allowed to identify the hydroxytyrosol and tyrosol (data not shown). On the other hand, olive leaf extract revealed the presence of residual amount of oleuropein. Olive leaf extract was also analyzed by GC-MS and Figure 1 presents the chromatographic profile of the extract. Concerning the chemical composition (Table 1), GC-MS analysis revealed the presence of D-limonene, palmitic acid, linoleic acid, oleic acid, stearic acid, erucic acid amide, cis-9-hexadecenal, oleamide, tetracosane and vitamin E.

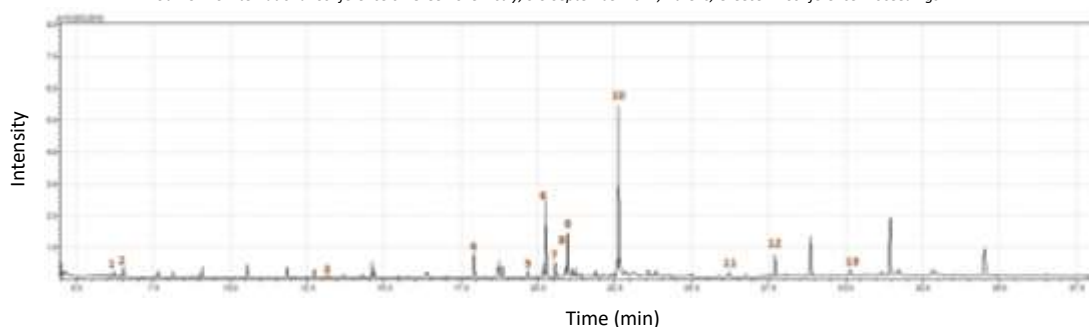


Figure 1. Chromatographic profile of the olive leaf extract analysed in GC-MS.

Table 5. List of the main compound identified in the olive leaf extract analysed in GC-MS.

n°	Compounds	Relative concentration (%)
1	Carene	0.49
2	D-Limonene	1.04
3	<i>p</i> -Cresol	0.05
4	Palmitic acid	3.81
5	Linoleic acid	1.82
6	Oleic acid	11.36
7	Stearic acid	1.72
8	Erucic acid amide	1.46
9	cis-9-Hexadecenal	5.42
10	Oleamide	21.32
11	Tetracosane	9.24
12	Squalene	4.76
13	Vitamin E	0.84

The cytotoxicity analysis was performed in the olive pomace and olive leaf extracts (Table 2) and the results were expressed in GI<sub>50</sub> values (concentration that inhibited 50 % of the cell proliferation). The non-tumour cell line PLP2 (primary pig liver culture) was used, and the olive leaf extracts did not reveal cytotoxicity up to 400 µg/mL.

Table 2. Cytotoxic activities of olive pomace and leaf extracts and respective positive controls (mean ± SD).

	Olive Pomace Extract – SFE-CO <sub>2</sub>	Olive Leaf Extract – SFE-CO <sub>2</sub>	Positive Control
GI <sub>50</sub> (µg·mL <sup>-1</sup> )	197 ± 11	>400	1.4 ± 0.1

## Acknowledgements

The authors are thankful for the samples provided by Acushla (www.acushla.pt). This work was funded by the European Regional Development Fund (ERDF) through the Regional Operational Program North 2020, within the scope of Project Mobilizador POCI-01-0247-FEDER-046112: BIOma - BIOeconomy integrated solutions for Mobilization of the Agrofood chain. This work was financially supported by LA/P/0045/2020 (ALiCE), UIDB/50020/2020 and UIDP/50020/2020 (LSRE-LCM), funded by national funds through FCT/MCTES (PIDDAC).

## References

1. S. Dermechea, M. Nadoura, C. Larroche, F. Moulti-Mati, P. Michaud, Olive mill wastes: Biochemical characterizations and valorization strategies, *Process Biochemistry*, **48**(10) 1532 (2013).
2. J. J.Gaforio, F. Visioli, C. Alarcón-de-la-Lastra, O. Castañer, M. Delgado-Rodríguez, M. Fitó, et al., Virgin Olive Oil and Health: Summary of the III International Conference on Virgin Olive Oil and Health Consensus Report, JAEN (Spain) 2018, *Nutrients*, **11**(9) 2039 (2019).
3. M. Barbanera, E. Lascaro, V. Stanzione, A. Esposito, R. Altieri, M. Bufacchi, Characterization of pellets from mixing olive pomace and olive tree pruning, *Renewable Energy*, **88** 185 (2016).
4. J. M .Romero-García, L. Niño, C. Martínez-Patiño, C. Álvarez, E. Castro, M. J. Negro, Biorefinery based on olive biomass. State of the art and future trends, *Bioresource Technology*, **159** 421 (2014).
5. B. Gullón, P. Gullón, G. Eibes, C. Cara, A. Torres, J. C. López-Linares, E. Ruiz, E. Castro, Valorisation of olive agro-industrial by-products as a source of bioactive compounds. *Science of The Total Environment*, **645** 533 (2018).
6. J. C. Kessler, V. Vieira, I. M. Martins, Y. A. Manrique, et al, Chemical and organoleptic properties of bread enriched with *Rosmarinus officinalis* L.: The potential of natural extracts obtained through green extraction methodologies as food ingredients. *Food Chemistry*, **384** 132514 (2022).



7. J. C. Kessler, V. Vieira, I. M. Martins, Y. A. Manrique, et al, Obtaining Aromatic Extracts from Portuguese *Thymus mastichina* L. by Hydrodistillation and Supercritical Fluid Extraction with CO<sub>2</sub> as Potential Flavouring Additives for Food Applications, *Molecules*, **27**(3) 694 (2022).
8. J. Azmir, I. S. M. Zaidul, M. M. Rahman, K. M. Sharif, A. Mohamed, et al., Techniques for extraction of bioactive compounds from plant materials: A review. *Journal of Food Engineering*, **117**(4) 426 (2013).
9. T. Arumugham, R. K. S. W. Hasan, P. L. Show, et al., Supercritical carbon dioxide extraction of plant phytochemicals for biological and environmental applications – A review. *Chemosphere*, **271**: 129525 (2021).

## High-performance or Functional Plant oil-based UV-curable Materials: Green Synthesis, properties, and applications

Chengguo Liu\*, Qianqian Shang, Yun Hu, Yonghong Zhou

Institute of Chemical Industry of Forest Products, Chinese Academy of Forestry, Nanjing 210042, P. R. China

\*liuchengguo@icifp.cn

Ultraviolet (UV)-curing technique are widely utilized in industrial areas such as coatings, adhesives, and 3D-printing materials thanks to their advantages like fast curing speed at ambient temperature, low energy consumption, low volatile organic chemical (VOC) emissions, etc. [1-2]. The value of UV-curable resins and formulated products in the global market was approximate 4.27 Billion USD in 2019 and is expected to amount 8.66 Billion USD by 2027 with an annual compound growth rate of 9.2% during 2020–2027. However, due to the dramatic price fluctuations of fossil resources and stricter environmental regulations, there is a growing interest in developing polymeric materials from renewable resources, such as cellulose, lignin, protein, and carbohydrates. Of all the biobased feedstocks, plant oils are one of the most frequently used bioresources in developing UV-curable materials because of their abundance, low toxicity, triglyceride structures suitable for further modification, and potential biodegradability. In the past decade, several major issues have been revealed in the study of plant oil-based UV-curable materials, such as: conventional properties like stiffness and glass transition temperature ( $T_g$ ) are far inferior to similar petroleum-based products; materials cannot be recycled or simply repaired while damaged or abandoned; the synthesis procedures are usually not ecofriendly and inefficient; etc. Therefore, in our works, by using plant oils and/or other biobased resources as starting materials and employing newly-developed green synthesis strategies or high-efficiency synthesis technologies (e.g. microwave technology), we synthesized a set of biobased monomers or oligomers, and then prepared novel biobased UV-curable materials with high conventional properties or self-healing and recyclable properties. Meanwhile, structure–property relationships, UV-curing kinetics, and self-healing mechanisms were investigated. At last, the obtained UV-curable materials were applied into coatings or 3D printings. In general, our studies can not only provide new ideas and strategies for the design and preparation of biobased UV-curable materials with high-performance or with self-healing and recyclability, but also offer good theoretical foundation for the application of such materials.

### Acknowledgements

The financial support from the Fundamental Research Funds of CAF (CAFYBB2020QA005) and the National Natural Science Foundation of China (31822009 and 31770615) are greatly appreciated.

### References

1. L. Fertier, H. Koleilat, M. Stemmelen, O. Giani, C. Joly-Duhamel, V. Lapinte, J.J. Robin, *Prog. Polym. Sci.*, **38** 932 (2013).
2. M. Layani, X.F. Wang, S. Magdassi, *Advanced Materials*, **30** 1706344 (2018).

## The effects of hydrogen peroxide and bleach on cellulose in oxidised sugar beet pulp

Christian Donohoe<sup>1\*</sup>, Stephen C. Fry<sup>1</sup>, Eric Whale<sup>2</sup>

<sup>1</sup> The Edinburgh Cell Wall Group, Institute of Molecular Plant Sciences, The University of Edinburgh, Daniel Rutherford Building, Edinburgh EH9 3BF, United Kingdom

<sup>2</sup> CelluComp, Unit 3 West Docks KY3 9DW, United Kingdom

\*C.Donohoe@sms.ed.ac.uk

The valorisation of biomass is a key step towards reducing the dependence of chemical production streams on non-renewable sources and for the development of a green economy. Sugar beet pulp (SBP), a secondary biomass product from sugar extraction, can be oxidised with hydrogen peroxide and bleach to produce an industrially valuable, viscous, cellulose-rich material called Curran® which is currently used as a rheology modifier for plastics, paints and cardboard preparative mixtures [1,2]. This study investigates the effects these oxidants have on cellulose within the plant cell wall of SBP.

The physical and chemical properties of Curran® are affected by the oxidation of cellulose in SBP and these changes have been measured according to the degree of oxidation and surface accessibility of the cellulose and the monosaccharide composition and viscosity of the total SBP in comparison with similarly oxidised Whatman paper. This has been achieved using methods such as conductometric titrations [3], novel [<sup>3</sup>H]cellopentaitol adsorption measurements, and successive ammonium oxalate and sodium hydroxide extractions [4,5], alongside dynamic viscometric measurements and quantification of endo β 1-4 glucanase digest products.

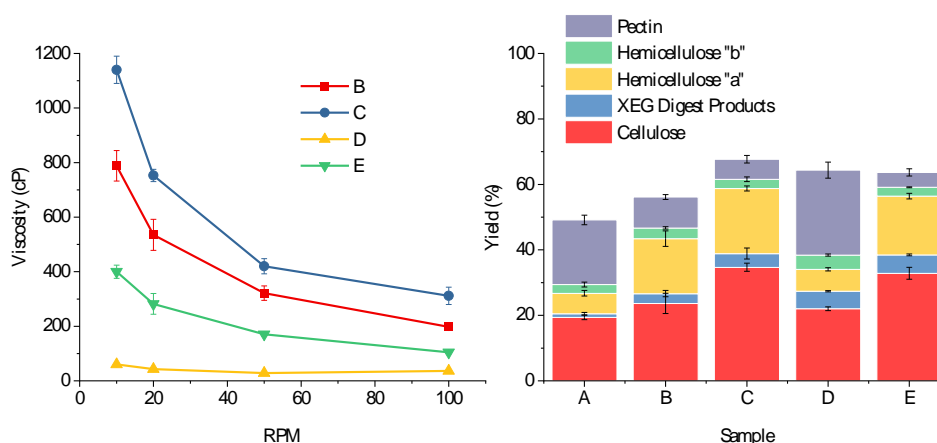


Figure 9: **Left:** Dynamic viscosity of variously treated sugar beet pulp samples (100 ml of 1% wt. suspension in water at 20°C)

**Right:** Yield of plant cell wall components obtained from H<sub>2</sub>O<sub>2</sub>- and bleach-treated SBP

**Key:** A, untreated sample; B, H<sub>2</sub>O<sub>2</sub> treated; C, H<sub>2</sub>O<sub>2</sub> then NaOCl (comparable to commercial Curran®); D, NaOCl; E, NaOCl then H<sub>2</sub>O<sub>2</sub>

Under the two-step oxidations employed, up to 5% of all cellulosic glucose residues in SBP were expected to be oxidised due to measurements taken from similarly oxidised Whatman paper. The oxidised cellulose was found in the (NaOH-soluble) hemicellulose “a” fraction of the material. Both oxidation treatments in either order were required to produce carboxy (RCOOH) groups preferentially over oxo groups (e.g., RCHO); carboxy groups are preferable for further functionalisation. Hydrogen peroxide has been shown in this reaction to solubilise pectin, convert cellulose into hemicellulose-like polysaccharides, and to give Curran® shear-thinning viscometric properties. Bleach further enhanced the viscosity of sugar beet pulp without significantly affecting the overall composition of the material. Surface accessibility of the cellulose in sugar beet pulp to tritiated cellopentaitol improved with any oxidising treatment, but endo-cellulase accessibility only improved in hydrogen peroxide-treated Curran®. This cellulase treatment solubilised both homogalacturonan and rhamnogalacturonan-I in SBP but only RG-I in all hydrogen peroxide treated Curran® samples. The viscosity of these samples during cellulase digestion decreased over time, the rate dependent on the oxidative treatment of the sugar beet pulp.

The sum of these observations suggests that hydrogen peroxide fractures the surface of cellulose during oxidation, solubilising pectin that was non-covalently bound to the cellulose surface. This modification of the surface of the microfibrils by hydrogen peroxide would create acidic cellulosic fragments that are now still water insoluble but NaOH-extractable. Bleach oxidation is important for whiteness and viscosity improvement, but this introduces a chlorine-based oxidant into the production stream and its use should be limited. For viscosity control, the key step of this process is the change in surface of the cellulose during hydrogen peroxide treatment. Similar secondary biomass sources should be explored for potential utilisation using this method.

## Acknowledgements

Special thanks to the EPSRC and Cellucomp for the funding of this research.

## References

- [1] D. Hepworth, E. Whale, Cellulose particulate material, US10246522B2, (2019).
- [2] Curran® | Sustainable Materials & Solutions | CelluComp, <https://www.cellucomp.com/products/curran> .
- [3] E. Lasseguette, *Cellulose*, **15**, 571 (2008).
- [4] C. O'Rourke, T. Gregson, L. Murray, I.H. Sadler, S.C. Fry, *Ann Bot*, **116**, 225 (2015).
- [5] K. Herburger, L. Franková, M. Pičmanová, J.W. Loh, M. Valenzuela-Ortega, F. Meulewaeter, A.D. Hudson, C.E. French, and S.C. Fry, *Molecular Plant*, **13**, 1047 (2020).

# Bio-waste valorization

## How the physio-chemical properties of char from the pyrolysis of Automotive Shredder Residue (ASR) influences its future uses.

Peter Bentley<sup>1</sup>, Karl Williams<sup>1\*</sup> and Ala Khodier<sup>2\*</sup>

<sup>1</sup>University of Central Lancashire, School of Engineering, Preston, Lancashire, PR12HE, UK.

<sup>2</sup>Recycling Lives Ltd, Longridge Road, Preston, Lancashire, PR25BX, UK.

\* [KSWilliams@uclan.ac.uk](mailto:KSWilliams@uclan.ac.uk)

\* [ala.khodier@recyclinglives.com](mailto:ala.khodier@recyclinglives.com)

### Abstract text:

The continuing challenge facing the End-of-life Vehicle (ELV) recycling industry is the treatment of Automotive Shredder Residue (ASR), where landfill is still the preferred option. With the introduction of the ELV Directive, the EU have challenged both the recycling and automotive industry to recycle or recover materials at a minimum value of 95% [1]. The difficulty in meeting these targets is caused by limited markets for certain fractions, such as plastics. Therefore, processing of ASR is key to meeting these targets. This, along with the drive for circularity in the use of resources, has resulted in pursuit of thermal treatment of ASR as a viable commercial solution. Not only does it support the principles of the circular economy, but it also supports the climate emergency by potentially reducing the industrial carbon footprint.

An emerging commercial technology is pyrolysis. This process not only provides energy but also produces a valuable resource in the form of pyrolysis char. This has a number of potential commercial outlets, such as activated carbon, a soil remediation and conditioner, and a filler material. Before it can be used, it is critical to understand the chemical and physical composition and the implications this may have on any future application. However, there is a large knowledge gap which is inhibiting the uptake of this material in commercial applications, where the feedstock and pyrolysis conditions play a major role on the both the chemical and physical characterisation. There is an added complication that the char comprises different fractions with unique characteristics [2]. By detailed analysis of these chars, it would be possible to develop or modify them for specific applications.

This paper will explore how the physical and chemical properties of char from different pyrolysis temperatures and fractions influence their secondary use. ASR was pyrolysed in a pilot scale unit capable of processing 100 kg hr<sup>-1</sup> at 900 °C. This produced 480 kg of char from which samples were taken for analysis. By processing a large amount of ASR, this reduced the sampling error associated with the heterogenous nature of ASR. Three types of pyrolysis char were identified. The following chars were analysed: (i) coarse char (CC) was collected directly from the reaction chamber; (ii) medium char (MC) and (iii) fine char (FC) were collected further down the system.

Testing of the three chars comprised (i) physical (particle size, moisture content, density, porosity) and (ii) chemical (calorific value, organic and inorganic elemental analysis). Initial findings indicated a number of physical and chemical differences. The CC had the highest particle size (800 µm), mean average 353.5 µm and calorific value (14,544 kcal g<sup>-1</sup>), where the relationship was CC > MC > FC. However, the loss on ignition (LOI) was highest in the FC (98%), where FC > MC > CC. For all the chars, the moisture content ranged from 0.6-1.6%. The chemical analysis for 17 key elements by ICP-OES indicated that the concentration of the analyte was higher generally in the CC fraction and reduced through the MC and FC. These results were mirrored in the EDAX analysis, where metal and halogenated elements were determined at higher concentrations in CC. Organic elemental analysis indicated that %C and %H was highest under FC (80.29 and 2.19% respectively) and %S was highest in CC (1.04%). This would be expected for the FC as there are lower concentrations of inorganic products present.

The findings from this experiment provided an initial insight into the differences in properties of fractions of char from ASR pyrolysis. The differences were highlighted in the case of the CC which had larger metal composition and higher S and Cl concentration. This will require further treatment before it can be used as a commercial product. The lower rates of contamination, higher %C and smaller pore structure determined in MC and FC chars indicate that they could be utilised as an activated carbon or filler. Advanced pretreatment of ASR to remove metal fibres may reduce the contamination within chars and improve utilisation.

Table 1. Physical and chemical composition of pyrolytic char from ASR feedstock (CC = Coarse Char; MC = Medium Char; FC = Fine Char)

	CC	MC	FC
moisture content (%)	0.60	1.64	0.95
calorific value (kcal g <sup>-1</sup> )	14544	10489	10012
loss on ignition (%)	21.83	48.89	98.28
%C	31.83	48.36	78.04
%H	0.43	0.71	1.42
%N	0.39	0.46	0.61
%S	1.04	0.87	0.27
%O*	66.30	49.60	19.65

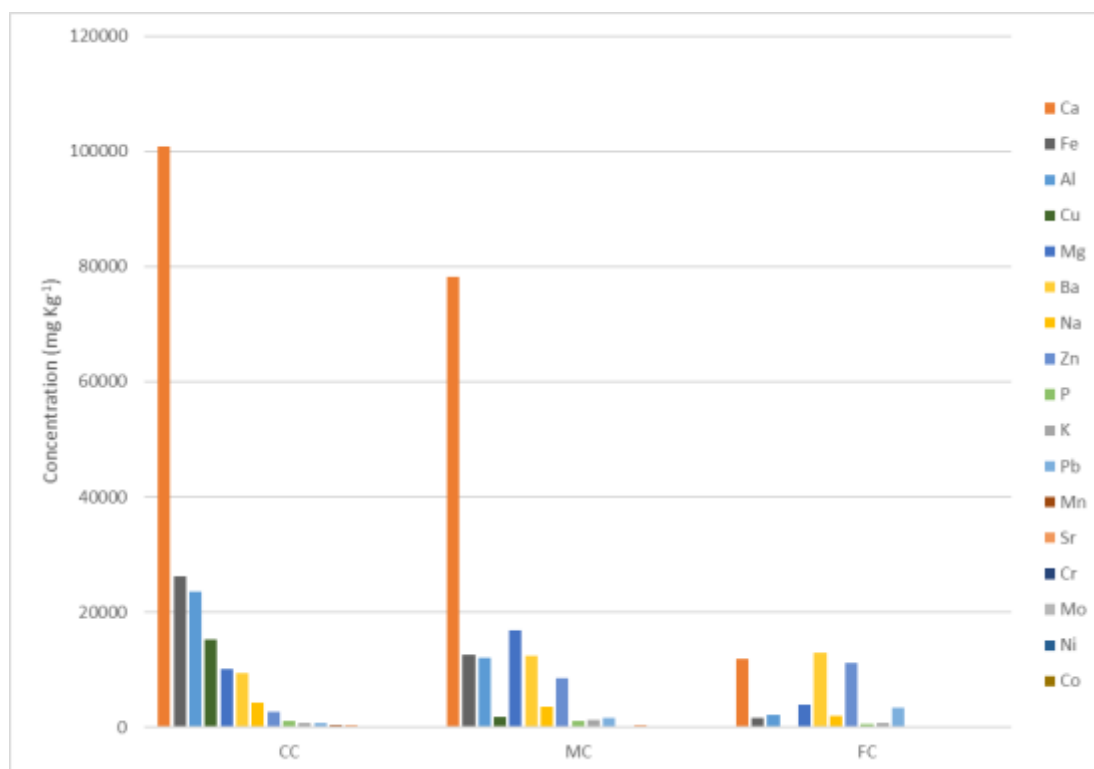


Figure 1. Inorganic elemental concentration of pyrolytic char derived from ASR feedstock. CC = Coarse Char; MC = Medium Char; FC = Fine Char.

## Acknowledgements

The authors gratefully acknowledge Innovate UK via the Knowledge Transfer Partnership (KTP) and Recycling Lives Limited, Preston, UK for the financial support provided.

## References

1. EC, (2000) Directive 2000/53/EC of the European Parliament and the European Council of 18 September 2000 on End-of-Life Vehicles – Commission Statements. *Off. J. Eur. Comm.* **L269**, 0034–0043, Brussels.
2. Williams, K. S., Khodier, A., (2020) Meeting EU ELV targets: Pilot scale pyrolysis automotive shredder residue investigation of PAHs, PCBs, and environmental contaminants in the solid residue products. *Waste Management*, **105**, 233-239.

## Nitrogen-rich waste step gasification: evolution of fuel-nitrogen during the different stages

Fernando Léo<sup>1,2</sup>, Noemí Gil-Lalaguna<sup>1</sup>, Zainab Afailal<sup>1</sup>, Rubenildo Andrade<sup>2</sup>, Electo Lora<sup>2</sup>, Isabel Fonts<sup>1\*</sup>

<sup>1</sup>Thermochemical Processes Group, Aragon Institute for Engineering Research (I3A), Chemical and Environmental Engineering Department, University of Zaragoza, C/ Mariano Esquillor s/n, 50.018 Zaragoza, Spain.

<sup>2</sup>Center for Excellence in Thermal and Distributed Generation (NEST), Institute of Mechanical Engineering, Federal University of Itajubá, Av. BPS, 1303, Block L7, 37500-903 Itajubá, Brazil.

\*isabelfo@unizar.es

### Abstract

Ammonia, one of the most produced chemicals in the world (176 Mt per year [1]), is synthesized industrially by the Haber-Bosch process ( $\text{N}_2(\text{g}) + 3\text{H}_2(\text{g}) \leftrightarrow 2\text{NH}_3(\text{g})$ ), requiring 28 GJ per ton  $\text{NH}_3$  even when using the best available techniques to produce the  $\text{H}_2$  [2]. To obtain  $\text{H}_2$  sustainably, biomass gasification or water electrolysis using renewable energies are studied. In addition, novel methods in which  $\text{NH}_3$  synthesis does not take place by the Haber-Bosch process are on a basic research stage, e.g.  $\text{NH}_3$  production by a catalytic electrochemical process from  $\text{N}_2$  and  $\text{H}_2\text{O}$  [1]. The Haber-Bosch process and these newfangled processes also present drawbacks due to the excessive fixation of stable atmospheric  $\text{N}_2$ , which is one of the anthropogenic causes of the imbalance in the biogeochemical N cycle [3]. Nitrogen-rich biological wastes are a possible source of H and N.

Our research group proposed a strategy in which  $\text{NH}_3$  could be produced by gasification of meat and bone meal (MBM) (9.9 wt.% of N), while the waste was energetically valorized [4]. It was achieved a fuel-N conversion to  $\text{NH}_3$  of 67%, and a potential energy production (gasification gas) up to 102 GJ-per ton  $\text{NH}_3$ . Optimizing the gasification operating conditions to maximize  $\text{NH}_3$  production is complicated due to the large number of reactions involved. The final fuel-N distribution obtained from gasification can be understood as the joint contribution of its stages: pyrolysis, char-N gasification, tar-N cracking and reforming, and gas phase reactions. This work's main objective is to determine experimentally the role of the aforementioned stages on the production of  $\text{NH}_3$  in the gasification of MBM with  $\text{O}_2$ -steam.

The pyrolysis experiments conducted in this work have shown that the yield of  $\text{NH}_3$ -N (calculated over fuel-N) was around 33-35%. It means that around 50% (33/67) of the  $\text{NH}_3$  generated in the whole gasification process is due to the contribution of the pyrolysis and that the stages of char-N gasification and gas phase reactions do not entail a net conversion of  $\text{NH}_3$ , but an additional formation. Moreover, it has been found that the gasification of the pyrolysis char with only  $\text{O}_2$  as gasifying does not incorporate more  $\text{NH}_3$  to the final production, while 3.0% of  $\text{NH}_3$ -N with respect to the original MBM-N is generated under the presence of steam in the gasifying agent. The MBM pyrolysis and char gasification (with  $\text{O}_2$ -steam) stages explain 54.5% of the  $\text{NH}_3$  generated in the overall gasification process.

### Acknowledgements

The authors would like to express their gratitude to the Aragon Government and European Social Fund (Ref. T22-17R) and to Agencia Estatal de Investigación in Spain (Project PID2019-107200RB-I00) for financial support. I. Fonts acknowledges the MINECO, European Social Fund, AEI and Unizar for the post-doctoral contract awarded (RYC2020-030593-I).

### References

1. Ammonia: zero-carbon fertiliser, fuel and energy store, Policy Briefing (2020).
2. I. Rafiqul, C. Weber, B. Lehmann and A. Voss, *Energy*, **30**, 2487 (2005).
3. N. Gil-Lalaguna, Z. Afailal, M. Aznar and I. Fonts, *J. Cleaner Prod.*, **282**, 124417 (2021).
4. D. Jędrejek, J. Levic, J. Wallace and W. Oleszek, *J. of Anim. Feed Sci.*, **25**, 189 (2016).



## Simultaneous nutrient ions recovery from anaerobic digestates of different origin by using Selective Electrodialysis

Vera Proskynitopoulou<sup>1,2</sup>, Souzana Lorentzou<sup>1</sup>, Konstantinos Plakas<sup>1</sup>, Panagiotis Kougiaris<sup>3</sup>, Kyriakos D. Panopoulos<sup>1,\*</sup> and Anastasios Zouboulis<sup>2</sup>

<sup>1</sup> Chemical Process and Energy Resources Institute (CPERI), Centre for Research and Technology Hellas (CERTH), 6th km Charilaou-Thermi Road, Thessaloniki, 57001, Greece

<sup>2</sup> Department of Chemistry, Aristotle University of Thessaloniki, Thessaloniki, 54124, Greece

<sup>3</sup> Hellenic Agricultural Organisation- DEMETER, Soil and Water Resources Institute, Thessaloniki, 57001, Greece

\* Corresponding e-mail panopoulos@certh.gr

### ABSTRACT

Water scarcity and depletion of mineral resources are major global issues, while food demand and consequently need for cultivation is constantly increasing. Recovery of nutrients from waste streams is an alternative, environmental-friendly approach for the replacement of chemical fertilizers, the common production of which is associated with high GHG emissions, and simultaneously leads to appropriate wastewater purification, aiming to surface and groundwater protection [1].

Anaerobic digestion (AD) transforms several organic wastes, such as agricultural waste, animal residues, food waste and municipal sludge, which otherwise would commonly end-up in landfills, into energy (renewable biogas), producing digestate as a by-product. The generated digestate is known to be rich in nutrients (e.g. nitrogen, phosphorus and potassium) and is frequently applied in agricultural soils for enrichment with inorganic and organic components [2].

However, the digestate has variable chemical composition based on the variations of raw materials used as feed in the anaerobic digesters of biogas plants [3, 4]. This creates issues, regarding the utilization of digestate and consequently, a major management issue for storage or disposal of large amounts of materials, which may pose a serious threat to the environment. If this is not managed properly, then the direct disposal in the soil may result in the uncontrolled leaching of nutrients that may cause serious surface and groundwater pollution [5].

Nowadays, water purification and the concept of nutrients extraction and recovery from waste streams has become technically and economically more feasible. Innovations in membrane technologies are attracting considerable attention and are preferential over other alternatively applied methods, due to low chemicals' consumption and cost-effectiveness. Therefore, their role in many industrial sectors, e.g. food production, chemical synthesis and water/wastewater treatment, is vital. Pressure-driven processes such as ultrafiltration, nanofiltration and reverse osmosis have been examined quite widely for the treatment of wastes with nutrient content and the obtained results showed that they can separate and concentrate nitrogen or phosphorus from the feed solution into a solution with higher fertilizer value. Nevertheless, the high concentrations of suspended solids and dissolved organic matter of digestate makes it rather hard and energy consuming to be treated with these technologies, due to common membrane fouling [6].

Electrodialysis (ED) is an electrochemical membrane process that uses the electric field as a driving force to separate selectively and concentrate ions from water sources by using ion-exchange membranes (IEMs). ED is commonly used for seawater desalination, wastewater and brackish water treatment. By reversing the polarity of the system with reverse electrodialysis (EDR) several times during the operation of this process, fouling and scaling can be minimized and thus, the need for lower chemical addition is achieved. The convenient operation, low operating and maintenance costs and high selective separation efficiency are certain specific advantages, which can make ED an attractive treatment method with significant environmental benefits [7].

Previous studies showed that ED can efficiently extract nutrients from wastewater, manure and digestate with fluctuating nutrient content [8]. Moreover, the selective ion separation with the application of anion and cation monovalent membranes for the recovery of several ions has already been investigated successfully in small scale operations and can produce high value fertilizers for land use, which is beneficial to the sustainable agricultural industry [9].

The present study aims to investigate a system of simultaneous selective separation and recovery of nutrient ions ( $\text{PO}_4^{3-}$ ,  $\text{NH}_4^+$ ,  $\text{K}^+$ ,  $\text{Ca}^{2+}$ ,  $\text{Mg}^{2+}$ ) by using selective ED (SED) from the liquid fraction of digestate residue from the biogas plants, using different feedstock materials. Monovalent selective anion exchange membranes and monovalent selective cation exchange membranes are usually integrated into a conventional electrodialysis stack. The current configuration is fractionating  $\text{PO}_4^{3-}$  into the anionic product stream, whereas bivalent cations ( $\text{Ca}^{2+}$  and  $\text{Mg}^{2+}$ ) are extracted in the cationic product stream and the monovalent cations ( $\text{NH}_4^+$  and  $\text{K}^+$ ) are concentrated

in the brine stream. The operational parameters including applied potential, flow rate, products-to-brine volume ratio and electrolyte concentration are investigated both in synthetic and real digestate samples, originating from different sources, e.g. agricultural or animal residues, food and municipal wastes. By mixing the different products of SED in specific proportions, it is also possible to produce high value products without the use of inherent chemicals for precipitation/separation purposes.

## Acknowledgements

This research is conducted within the scope of the Horizon 2020 EU funded project NOMAD (GA 863000).

## References

1. C. Katarzyna, K. Moustakas, A. Witwk-Krowiak. *Bioresour. Technol*, **295** 122223 (2020).
2. R. Nkoa, *Agron Sustain Dev* **34** (2):473–92, (2014).
3. Y. Li, A. Manandhar, G. Li, A. Shah, *Waste Manag.*, **76** 294-305 (2018).
4. T. Rehl, J. Müller, *Resour Conserv Recycl*, **56** 92–104 (2011).
5. J. Huang, X. Chang Chun, R. G. Bradley, W. Xue Chun, R. Pin, *J. Clean. Prod.*, **159** 171–79 (2017).
6. L. Shi, Lin, S. Xie, Z. Hu, G. Wu, L. Morrison, P. Croot, H. Hu, X. Zhan, *J. Membr. Sci.*, **573** 560–69, (2019).
7. L. Gurreri, A. Tamburini, A. Cipollina, G. Micale, *Membranes*, **10**, 146. (2020).
8. Y. Zhang, B. Van Der Bruggen, L. Pinoy, B. Meesschaert, *J. Membr. Sci.*, **332** 104–12 (2009).
9. Z.L. Ye, K. Ghyselbrecht, A. Monballiu, L. Pinoy, B. Meesschaert, *Water Res.*, **60** 424-434 (2019).

## Hydrolysis of poly(ethylene terephthalate) using a wide range of Low-Cost Ionic Liquids for chemical plastic recycling

Maariyah Y Suleman<sup>1</sup>, Panos Bexis<sup>1</sup> and Agnieszka Brandt-Talbot<sup>1\*</sup>

<sup>1</sup>Department of Chemistry, Imperial College London, 80 Wood Lane, W12 0BZ, UK

\*agi@imperial.ac.uk

Modern society heavily utilizes plastic. In 2015, the annual production of plastic reached 381 million tonnes.<sup>1</sup> Common uses are food packaging, construction and single-use disposable equipment. The current waste management of plastic disposal is insufficient, and plastic accumulates in landfill and particularly concerning, it also makes its way into the environment, including the ocean. Hence, plastic pollution has become an alarming global issue that requires various strategies to tackle the fast-growing problem. One strategy is to make recycling and reuse of plastic an attractive alternative to dispersion in the environment. Mechanical recycling techniques are used today however, degradation of material properties, such as mechanical (strength/stiffness) and optical properties (colour, transparency) and contamination are challenges for achieving high quality recycled plastic via mechanical means only. In this research, ionic liquids are employed as more catalytic solvents to depolymerize a common polyester. Depolymerization of the polymer yielding a purifiable monomer would allow recycled plastic raw materials to remain in circulation for longer, encouraging recycling and conserving resources. In our research, we focus on hydrolysis as the chemical recycling pathway using ionic liquids (Fig.1).

Ionic liquids are liquids composed of a cation and anion, with a melting point at or near room temperature and vast opportunity to modulate solvent characteristics to suit a target application.<sup>2</sup> They have been shown to have catalytic properties and seen successful use in various applications, for example the BASIL process. Poly(ethylene terephthalate), (PET), accounts for 13% of global plastic production and is the most recovered and recycled polymer. Despite this, recycled PET is often used in lower-grade applications due to deterioration of low material properties.<sup>3</sup> Depolymerization of PET via hydrolysis produces the monomer terephthalic acid, (TPA), which can be fed into existing polymerization processes.<sup>4</sup>

In this work, a screening protocol was established for determining conversion and yield of PET hydrolysis. A rational selection of low-cost protic ionic liquids, covering a range of anions and three distinct cations, was then employed to evaluate their promise as catalytic solvents for depolymerization of PET. The conversion, crude yield and purity of the product were correlated with the solvent properties. Parameters beyond anion and cation selection investigated are solid loading, PET particle size and effect of acid base ratio of the ionic liquid.

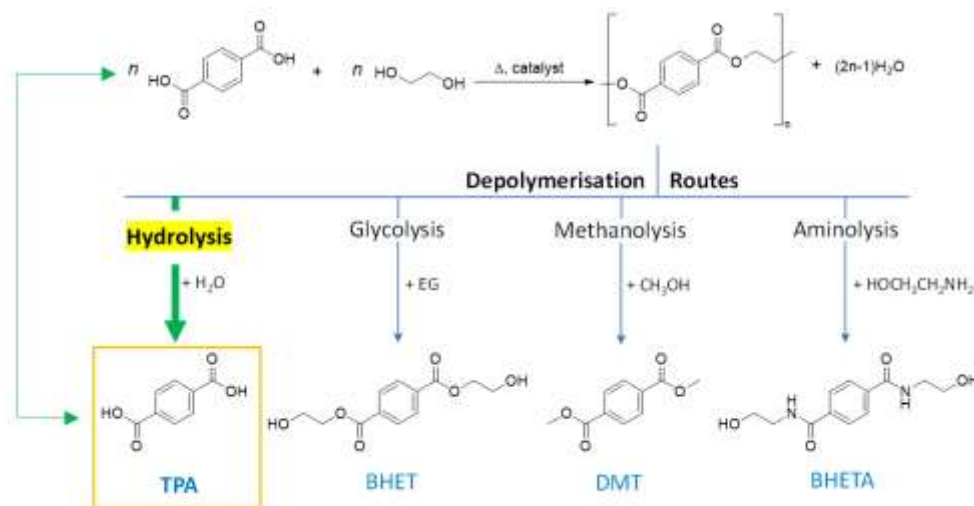


**Figure 1.** Industrial production of PET and various depolymerisation routes producing terephthalic acid (TPA), bis(2-hydroxyethyl) terephthalate (BHET), dimethyl terephthalate (DMT), and bis(2-hydroxyethyl) terephthalamide (BHETA).

### References

1. MacArthur, E. Foundation, The new plastics economy: Rethinking the future of plastics, 2016.
2. Welton, T. Ionic Liquids: A brief history. *Biophys. Rev.* 10, 691-706 (2018).
3. A. C. Castillo, M. Malakkal, P. Bexis and K. Brophy, Enabling a greener plastic future through molecular science, Imperial College London, Institute for Molecular Sciences and Engineering, 2020. <https://spiral.imperial.ac.uk/>
4. A. Aguado, L. Martínez, L. Becerra, M. Arieta-araunabeña, S. Arnaiz, A. Asueta and I. Robertson, *J. Mater. Cycles Waste Manag.*, 2013, 16, 201-210.

## Optimization of ultrasound-assisted extraction of natural antioxidants from rapeseed cake using deep eutectic solvents

Alicja Tymczewska<sup>1\*</sup>, Karolina Gajewska<sup>1</sup> and Aleksandra Szydłowska-Czeraniak<sup>1</sup>

<sup>1</sup>Nicolaus Copernicus University, Faculty of Chemistry, Department of Analytical and Applied Spectroscopy, Gagarina Street 7, Torun, Poland

\*tymczewska@doktorant.umk.pl

Rapeseed is the third most abundant oil plant worldwide and the primary oil seed crop in Poland. During rapeseed processing, several wastes such as rapeseed cake (RK), are generated. Recently, with the increasing interest in circular economy and “zero waste” movements, there is an intense effort to revalorize food by-products. Therefore, the future direction of research could focus on using RK as a source of active (antioxidant and antimicrobial) substances for the development of innovative food packaging materials [1].

On the other hand, most often applied conventional extraction techniques for the isolation of bioactive substances from plant material, require the use of organic solvents. However, traditional organic solvents are toxic, flammable and hazardous to human health and the environment. Therefore, as alternatives to organic solvents, green solvents have received increased attention in the past decade because of their low toxicity [2].

Deep eutectic solvents (DESs) are regarded as a new class of green solvents that became incredibly popular in the past decade. DESs are mixtures of hydrogen bond donors (HBD) and hydrogen bond acceptors (HBA), which are characterized by relatively easy preparation, usually determined by personal preference [3]. Typically, the development of DES is based on heating and stirring the chemical components until formation of a homogenous liquid. It is noteworthy that additional solvent or special conditions are not required. Additionally,

DESs are Generally Recognized as Safe (GRAS) which makes them more suitable to use in the food industry [4]. The most common DESs consist of choline chloride (ChCl) (HBA) and carboxylic acids, polyols or urea and its derivatives (HBD). They occur as clear, homogenous liquids, and their main feature is the possibility of creating a vast number of mixtures with various properties by changing one or both components and their molar ratio. The physical and chemical properties of ChCl-based DESs such as viscosity, polarity or density could be tailored to optimize the extraction process and obtain targeted compounds.

Currently, possible applications of DESs are being explored by researchers. One such possibility of using DES could be an isolation of natural compounds from plant-based products. The number of research papers published in this field is continuously growing (about 10 articles in 2014 and over 160 in 2020), which indicates an urgent desire to find optimal green solvents [4]. Moreover, it was found that DESs could act as eco-friendly plasticizers for biopolymer films [5,6]. Against this background, the application of food waste extracts prepared with DES could act as a multi-functional agent in novel and biodegradable packaging materials.

The main objective of this study was to identify green solvents for the extraction of antioxidants from oil cakes – by-products of fat industries. For this purpose, an ultrasound-assisted extraction (UAE) procedure based on the use of DESs was established. The extraction abilities of four different DESs were evaluated and compared with frequently used, conventional solvents such as methanol. The antioxidant activity (AA) of extracts was evaluated using three different analytical methods: 2,2-diphenyl-1-picrylhydrazyl (DPPH), 2,2'-azino-bis(3-ethylbenzothiazoline-6-sulfonic acid) (ABTS) and cupric ion-reducing antioxidant capacity (CUPRAC). DES 3 based on choline chloride, lactic acid and water in molar ratio 1:1:6 was selected as the most sufficient solvent for UAE in the screening for DESs. To optimize the extraction of antioxidants from RK, a central composite design (CCD) with two factors and three levels was constructed. UAE from RK performed in optimal conditions (time (t) = 7.4 min. and temperature (T) = 80°C) resulted in satisfactory and high AA (AA<sub>DPPH</sub> = 37.70 ± 0.03 mmol TE/100g; AA<sub>ABTS</sub> = 88.28 ± 0.03 mmol TE/100g; AA<sub>CUPRAC</sub> = 16.33 ± 0.04 mmol TE/100g). Moreover, experimental AA values are in good agreement with those drawn from the mathematical models.

Finally, the results demonstrated that the optimized process of UAE using DES could be an eco-friendly and competitive method for the extraction of antioxidants from RK.

Table 1. Compositions and solvent code for the studied DESs.

Solvent code	Constituents	Molar ratio
DES 1	Choline chloride:glycerol:water	1:1:6
DES 2	Choline chloride:glycerol:water	1:2:6
DES 3	Choline chloride:lactic acid:water	1:1:6
DES 4	Choline chloride:lactic acid:water	1:2:6

## Acknowledgments

This research was financially supported by “Grants4NCUStudents” (NCU Excellence Initiative — Research University).

## References

1. A. Szydłowska-Czerniak, S. Poliński, M. Momot, *Appl. Sci.*, **11** 1558 (2021).
2. X.-Q. Chen, et al. *LWT Food Sci. Technol.*, **148** 111708 (2021).
3. S. Cunha, J. O. Fernandes, *TrAC – Trend. Anal. Chem.*, **105** 225-239 (2018).
4. F. Mohd Fuad, M. Mohd Nadzir, A. Harun@Kamaruddin, *J. Mol. Liq.*, **339** 116923 (2021).
5. R. Chandra, et al.. *J. Clean. Prod.*, **284**, 125417 (2021).
6. E. Jakubowska, et al. *Carbohydr. Polym.*, **255**, 117527 (2021)

## Extraction of bioactive compounds from fisheries waste streams using natural deep eutectic solvent systems for their therapeutic application

Maha Abdallah<sup>1,2</sup>, Inês Leonardo<sup>1,2</sup>, Luna Krstić<sup>3</sup>, Frédéric B. Gaspar<sup>1,2</sup>, Amalia Enríquez-de-Salamanca<sup>3,4</sup>, Yolanda Diebold<sup>3,4</sup>, Maria González-García<sup>3,4</sup>, Ana A. Matias<sup>2</sup>, Maria R. Bronze<sup>1,2,5</sup>, Naiara Fernández<sup>2\*</sup>

<sup>1</sup>Instituto de Tecnologia Química e Biológica António Xavier, Universidade Nova de Lisboa, Av. da República, 2780-157 Oeiras, Portugal

<sup>2</sup>iBET, Instituto de Biologia Experimental e Tecnológica, Apartado 12, 2781-901 Oeiras, Portugal

<sup>3</sup>Institute of Applied Ophthalmobiology (IOBA), University of Valladolid, Valladolid, Spain

<sup>4</sup>Biomedical Research Networking Center in Bioengineering, Biomaterials and Nanomedicine (CIBER-BBN), Av. Monforte de Lemos, 3-5, 28029, Madrid, Spain

<sup>5</sup>Faculdade de Farmácia da Universidade de Lisboa, Av. Prof. Gama Pinto, 1649-003 Lisboa, Portugal

\*[naiara.fernandez@ibet.pt](mailto:naiara.fernandez@ibet.pt)

The total mass of marine generated by-products is estimated to be approximately 20 million tons globally<sup>1</sup>. Marine wastes were largely investigated for their valorization and use in industrial applications due to abundance, low-cost and environmental advantages<sup>2</sup>. Therefore, their use as a source for the isolation of bioactive compounds has great advantages as nowadays the integration of natural products in pharmaceutical and cosmetic industries has remarkably increased, as their biological activity and structural properties may differ from the synthetic molecules<sup>3,4</sup>.

Within this project, a green technique was developed to extract bioactives from codfish bones, mussel meat and tuna vitreous humor (Figure 1). Deep eutectic solvents (DES) were prepared using natural compounds, including lactic acid (LA), fructose (F) and urea (U). The extracts obtained using these DES were characterized to define their composition. Proteins and lipids were mainly present in extracts obtained from mussels, while ash content was highest in the extracts obtained from CB.



Figure 1. Bioactive extraction process.

The biocompatibility of the synthesized DES and the soluble fractions (SF) of the raw materials in DES was evaluated and it was possible to conclude that the soluble ingredients obtained from the raw materials improved the biocompatibility of DES.

Extracts obtained from TVH were further evaluated for their potential application as ophthalmological therapeutic active ingredients.<sup>5</sup> In vitro experiments were performed with the DES, the SF and the precipitated extracts (PE) on human corneal epithelial (HCE) cell line. The influence of the samples on the HCE viability, their intracellular reactive oxygen species (ROS) scavenging capacity, and inflammatory response. Moreover, the effect on dry eye-associated microorganisms was studied.

According to the results, all samples displayed an antioxidant effect, which was significantly higher for PE in comparison to SF. Figure 2 shows the percentage of ROS in comparison to the control (represented in the dashed line) for the samples of the extraction process obtained (a) using deep eutectic solvents synthesized using LA:F and LA:U. Their corresponding soluble fractions of TVH in  $DES_{LA:F}$  and  $DES_{LA:U}$  are  $SF_{LA:F}$  and  $SF_{LA:U}$ , respectively. Their corresponding precipitated extracts from  $DES_{LA:F}$  and  $DES_{LA:U}$  are  $PE_{LA:F}$  and  $PE_{LA:U}$ , respectively.

Furthermore, most of the tested samples did not induce an inflammatory response in cells, which suggests the safety in ophthalmic formulations. In addition, the DES and SF proved to be efficient against the studied bacterial strains, while PE did not show an antimicrobial effect. Hence, both DES, SF at defined concentrations could be used as potential compounds in dry eye disease management.

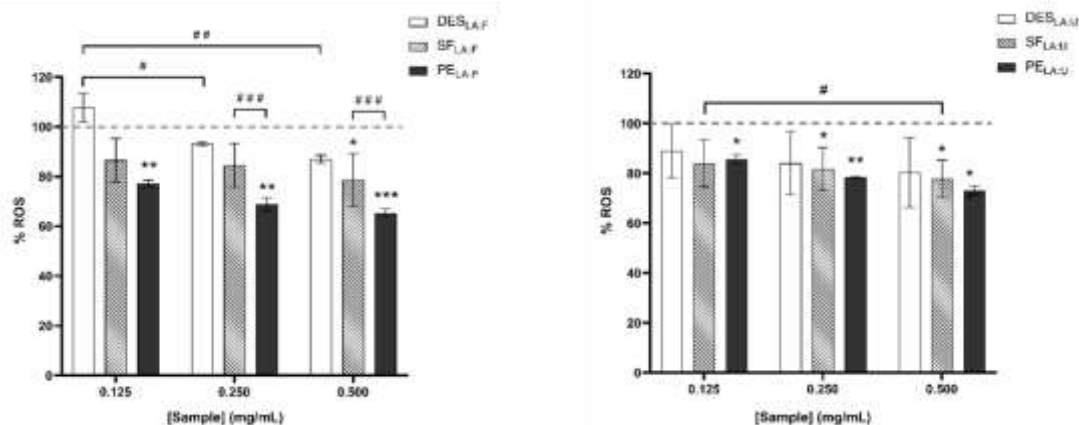


Figure 2. Percentage of ROS in comparison to the control (represented in the dashed line) for the samples of the extraction process obtained. (a) using deep eutectic solvents synthesized using lactic acid (LA) and fructose (F) and (b) LA and urea (U). \*P < 0.05, \*\*P < 0.01, \*\*\*P < 0.001 in comparison to UV-stimulated control cells. # P < 0.05, ## P < 0.01, ### P < 0.001 in comparison between the compounds and different doses.

## Acknowledgements

The authors acknowledge the financial support received from the European Union's H2020-MSCA program, IT-DED3 project grant agreement: 765608. iNOVA4Health – UIDB/04462/2020 and UIDP/04462/2020, a program financially supported by Fundação para a Ciência e Tecnologia/ Ministério da Ciência, Tecnologia e Ensino Superior, through national funds is acknowledged. Funding from INTERFACE Programme, through the Innovation, Technology and Circular Economy Fund (FITEC), is gratefully acknowledged.

## References

1. Food and Agriculture Organization. World fisheries and aquaculture (2018).
2. C. Jiménez, *ACS Med. Chem. Lett.*, **9**, 959 (2018).
3. N. Amberg, C. Fogarassy, *Resources*, **8**, 137 (2019).
4. R. A. Khan, *Saudi Pharm. J.*, **26**, 739 (2018).
5. M.M. Abdallah, I.C. Leonardo, L. Krstić, A. Enríquez-de-Salamanca, Y. Diebold, M.J. González-García, F.B. Gaspar, A.A. Matias, M.R. Bronze, N. Fernández, *Foods*, **11**, 342 (2022).

## Adsorption from the liquid and gas phase on biocarbons obtained from residue after supercritical extraction of raw plants

Aleksandra Bazan-Wozniak\* and Robert Pietrzak

*Adam Mickiewicz University in Poznań, Faculty of Chemistry, Uniwersytetu Poznańskiego 8, 61-614 Poznań, Poland*

*\*aleksandra.bazan@amu.edu.pl*

Undesirable changes in the bacteriological, physical and chemical properties of water are a consequence of introduction of excessive amounts of inorganic and organic materials to it. These pollutants limit or prevent the use of water for drinking, food production and household purposes. The greatest amounts of pollutants enter the water system with sewage [1]. Also the pesticides, surfactants, organic dyes, artificial fertilizers along with municipal and industrial waste can easily enter water system and threaten the organisms living there [2]. Another, equally important problem is the pollution of atmospheric air. Emission of solid liquid or gas pollutants to the atmosphere has been proved to have significant impact on human health, climate and nature [3]. That is why the search for new and more effective technologies for the environment purification is a continuous challenge. Recently, increasingly often carbon materials are used as effective adsorbents of pollutants from liquid and gas phases [4].

Therefore, the primary objective of this study was to obtain a series of low-cost biocarbons by chemical activation of residues after supercritical extraction of raw plants such as: green tea leaves and marigold flowers. The obtained materials were tested as sorbents for the removal of organic pollutant (malachite green) from water and hydrogen sulfide from the air. We also analyzed the effect of precursor on the physicochemical and sorption properties of the biocarbons obtained.

The precursors of the biocarbons were residue after supercritical extraction of green tea leaves (T) and marigold flowers (M) in a form of powder with size range of 0.10 – 0.80 mm and moisture content in air-dry state of 5.2 wt. % (green tea) and 4.9 wt. % (marigold). The precursors were impregnated with 50 % H<sub>3</sub>PO<sub>4</sub> solution (weight ratio 2:1 and 3:1, activator:precursor), dried to constant mass at 110 °C and then subjected to thermal treatment in nitrogen atmosphere with a flow rate of 0.300 L/min. The impregnated samples were heated (5 °C/min) from room temperature to 500 °C and kept at the final activation temperature for 30 min and then cooled down in nitrogen flow (AC). After that, biocarbons were washed distilled water. All biocarbons obtained in microwave muffle furnace (Phoenix, CEM Corporation, Matthews, USA). The obtained biocarbons were designated **TAC2** and **MAC2**, which means biocarbons impregnated with 50 % H<sub>3</sub>PO<sub>4</sub> at weight ratio activator:precursor 2:1 and **TAC3**, **MAC3**, which means biocarbons impregnated with 50 % H<sub>3</sub>PO<sub>4</sub> at weight ratio activator:precursor 3:1.

The porous structures of biocarbons were characterized on the basis of nitrogen adsorption/desorption measured by AutosorbQ analyzer made by Quantachrome. The surface area of samples was found on the basis of the multilayer adsorption BET (Brunauer-Emmett-Teller) theory. The pore size distribution and total pore volume were determined on the basis of the BJH (Barrett-Joyner-Halenda) model. The micropore volume and surface area were found by the t-plot method. The elemental analysis of each biocarbon sample was performed using a Vario EL III elemental analyzer (ElementarAnalysensysteme GmbH, Langenselbold, Germany). The content of surface oxygen functional groups was determined according to the Boehm method (Boehm, 1994).

The evaluation of H<sub>2</sub>S sorption capacity: samples in the form of granules (0.80 - 1.75 mm in diameter) were packed into a glass column (length 300 mm internal diameter, 9 mm bed volume 3cm<sup>3</sup>). The samples were tested in dry and wet conditions. Dry or wet air (70 % humidity) with 0.1 % of H<sub>2</sub>S was passed through the bed of the adsorbent at 0.450 L/ min. The concentration of H<sub>2</sub>S was monitored using Multi-Gas Monitor Q-RAE PLUS PGM-2000/2020 (RAE Systems, Sunnyvale, USA ). The tests were stopped at the breakthrough concentration of 100 ppm (for H<sub>2</sub>S) because of the electrochemical sensor limits. The capacities of each sorbent in terms of milligram of H<sub>2</sub>S per gram of adsorbent were calculated by integration of the area above the breakthrough curves and H<sub>2</sub>S concentration in the inlet gas, flow rate, breakthrough time and mass of the adsorbent [4].

To determine the adsorption capacity of the biocarbons adsorption tests were conducted using model aqueous solutions of malachite green. Stock solutions 1000 mg/L of the adsorbate was prepared and thereafter, working solutions were made to the desired concentrations through serial dilution. The influences of the experimental parameters, such as the initial concentration, pH and adsorption temperature on the sorption capacity of the biocarbons obtained was investigated in details. All experiments were performed at 23 °C.

The biocarbons obtained by chemical activation of residues after supercritical extraction of raw plants with the use of microwave heating can be effective adsorbents of liquid and gas pollutants. The surface area and degree of porous structure development were found to depend on the type of precursor and activator. Chemical activation



leads to prevalent formation of acidic groups on the biocarbons. The effectiveness of malachite green removal from its water solutions depended on type of precursor and activator, initial concentration of the dye, time of contact of the adsorbent and the adsorber, pH and temperature of the reaction. Basic environment is favorable for the dye adsorption. With increasing temperature the activation barrier is overcome and the sorption capacity of the obtained biocarbons increases. Sorption capacities of the samples studied vary in the range from 128 to 330 mg/g adsorbent (Figure 1).

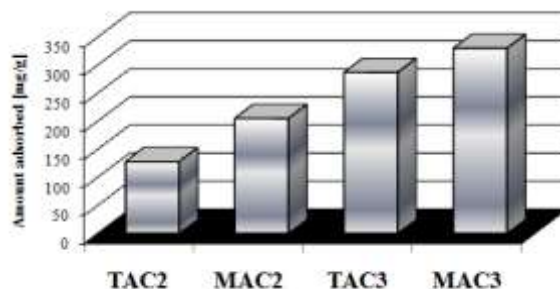


Figure 1. Adsorption of malachite green of the biocarbons obtained.

The sorption capacities of the biocarbons studied towards hydrogen sulfide depend on the conditions of the process and type of precursor. They are greater when adsorption takes place in the presence of steam. The sorption capacity of samples in dry conditions were 33-54 mg, while in wet conditions it was 46-89 mg (Table 1). The efficiency of hydrogen sulfide removal also depended on the surface area and degree of porous structure development of the biocarbons; the larger the surface area and the more developed the porous structure, the greater the sorption capacity toward H<sub>2</sub>S.

Table 1. H<sub>2</sub>S breakthrough capacities of the biocarbons obtained.

Sample	Dry conditions [mg/g]	Wet conditions [mg/g]
TAC2	33	46
MAC2	41	57
TAC3	48	72
MAC3	54	89

## References

1. Z.U. Ahmad, L. Yao, J. Wang, D.D. Gang, F. Islam, Q. Lian, M.E. Zappi, *Chem. Eng. J.* **359** 814 (2019).
2. R.A. Canales-Flores, F. Prieto-García, *Diam. Relat. Mater.* **109** 108027 (2020).
3. A. Bazan-Wozniak, P. Nowicki, R. Pietrzak, *Chem. Eng. Res. Des.* **166** 67 (2021).
4. A. Bazan-Wozniak, R. Pietrzak, *Chem. Eng. J.* **393** 124785 (2020).

## Biochar and Activated Carbon Derived from Oil Palm Kernel Shell as a Framework for the Preparation of Sustainable Controlled Release Urea Fertilizer

Pravin Vejan<sup>\*1</sup>, Rosazlin Abdullah<sup>1,2</sup>, Noraini Ahmad<sup>3</sup> and Tumirah Khadiran<sup>4</sup>

<sup>1</sup> Institute of Biological Sciences, Faculty of Science, University of Malaya, 50603 Kuala Lumpur, Malaysia

<sup>2</sup> Centre for Research in Biotechnology for Agriculture (CEBAR), Institute of Biological Sciences, Faculty of Science, University of Malaya, 50603 Kuala Lumpur, Malaysia

<sup>3</sup> Department of Chemistry, Faculty of Science, University of Malaya, 50603 Kuala Lumpur, Malaysia.

<sup>4</sup> Forest Products Division, Forest Research Institute Malaysia, 52109, Kepong, Selangor, Malaysia.

\*Corresponding author: vcpravin8@gmail.com; s2002032@siswa.um.edu.my

Food security globally in high risk because agricultural food needed to feed the booming human population and in early 2020, the unprecedented nature of COVID-19 prompted whole world to give extra attention on their nation's agricultural food stock up. Moreover, the prolonged and excessive application of conventional fertilizer pave ways to large economic losses due to leaching issues (40–70%) [1]. To solve this ever-increasing issue, there is a need to introduce new fertilizers which provide nutrients to plants slowly thereby reducing nutrient loss and promoting enhanced crop yield [2]. The application of nitrogen fertilizers has increased significantly in the past few decades, from 32 million tons in 1970 to about 111.6 million tons in 2016 [3], with a future projection of 130–150 million tons per year by 2050. The widespread application of nitrogen fertilizers leads to serious environmental pollution, including downstream degradation of water quality, eutrophication of coastal ecosystems, the formation of photochemical smog, and elevated concentration of atmospheric nitrous oxide [4]. Urea is the most widely used fertilizer globally because of its high nitrogen content (46%), low cost, and ease of application [5]. As a solution, controlled release fertilizers (CRFs) are discovered whereby could release nutrients gradually, which try to coincide with the nutrient demand during crop growth. Among CRF's products, biochar and activated carbon is one of the carbon-based frameworks that can be used as a host to encapsulate fertilizer. Biochar and activated carbon can be produced from lignocellulosic biomass such as from different feed stocks like crop residues, grasses, woody biomass, manure, and agriculture waste (oil palm husks, coconut shells, etc.). Among all the agriculture products, biochar is a carbon-rich material obtained from the pyrolysis of biomass in the absence of oxygen. Activated carbon is an adsorbent obtained from carbonaceous materials with a disorganized crystallographic structure, constituted by randomly distributed microcrystals. Consequently, these materials present a high specific surface area (500–1500 m<sup>2</sup>/g), a wide variety of functional groups (carboxylates, carbonyls, hydroxyls, amines) and a pore size distribution (<1–100 nm). All these characteristics give them an extraordinary capacity to adsorb a great diversity of molecules [6]. The characteristics of activated carbon as an adsorbent, both in capacity and in selectivity towards the species to be adsorbed, depend on the degree of disorganization of the microcrystalline structure, which is conditioned by both the nature of the precursor material and the process to which it has been subjected for transformation into activated carbon. The activated carbon from oil palm biomass is found to be sustainable and economically viable. The oil palm biomass was produced by the mill and available in the mill site thus raw material, transportation and operating cost can be minimized [7]. The oil palm kernel shell (OPKS) is a suitable precursor for activated carbon production due to its high density, high carbon content and low ash content [7]. However, very few activated carbon-based CRUFs have been reported, and none in combining OPKS-AC with urea to produce CRUFs. Hence, the feasibility of OPKS-B and OPKS-AC to adsorb urea, the potential of OPKS-AC as the primary sustainable biomaterial used to produce CRUF and the adsorption kinetics and isotherm models of OPKS-B and OPKS-AC towards urea are investigated.

OPKS-B and OPKS-AC were obtained from Malaysian Palm Oil Board (MPOB). The OPKS biochar was produced using a pilot-scale microwave reactor system with temperature reached a maximum set value of 250 °C and residence time of 4 h [7]. Then, the biochar was activated using a double insulated carbonisation-activation system with typical steam temperature in the range of 800-1000 °C to produce OPKS-AC [7]. The surface texture and microstructure of the OPKS-B and OPKS-AC were examined using FESEM (TM3000; Hitachi High-Technologies Co., Tokyo, Japan) at an accelerated voltage of 5 kV. The surface chemistry of OPKS biochar and OPKS activated carbon samples were detected by Fourier Transform Infra-Red spectrometer (FTIR-Spectrum 400 model, Perkin Elmer, USA). The porous structure and surface area of OPKS biochar and OPKS activated carbon were characterized using the nitrogen gas adsorption-desorption method at 77 K using an accelerated surface area and porosimeter, Micromeritics Tristar II plus (Micromeritics, Norcross, GA, USA). The specific surface area and pore size distribution of the samples was calculated using the Brunauer-Emmet-Teller (BET) and BJH (Barrett-Joyner-Halenda) equations, respectively. In the preparation of encapsulated urea/OPKS biochar and urea /OPKS activated carbon, batch absorption experiment utilizing both OPKS-B and OPKS-AC were carried out to investigate and compare the efficacy of OPKS-B and OPKS-AC as an organic framework to encapsulate urea. The entire batch sorption samples were shaken continuously for 24 hours at 150 rpm using digital orbital shaker (SK-O330-Pro, DLAB Scientific) at room temperature. The flasks were then taken off from the shaker and sample was pipetted out to be analysed using a Cary 60 UV-visible spectrophotometer (Agilent Technologies, Santa Clara, CA, USA) at 430 nm [8]. The amount of urea adsorbed per unit mass of adsorbent (OPKS-B and OPKS-AC) at equilibrium,  $Q_e$  (mg g<sup>-1</sup>), were calculated using Eq. (1).

$$Q_e = \frac{(C_0 - C_e)V}{m} \text{ ---- (1)}$$

As for the sorption kinetic study, 0.2 g of each OPKS-B and OPKS-AC was mixed with 150 ml of 1000 mg/L concentration of urea solution in 250 mL conical flasks in the single solute system. Pseudo-first-order and pseudo-second-order kinetic models were introduced to study the adsorption kinetics of urea onto OPKS-B and OPKS-AC, whereas the intra-particle diffusion model was utilized to further analyze the adsorption kinetic results and to validate whether the intra-particle diffusion was the only rate limiting step. For the adsorption isotherm studies, 0.2 g of OPKS-B and OPKS-AC were added to 150 mL of urea solution with varying concentrations, ranging from 200 mg/L to 20 000 mg/L, and were then shaken for 18 hours at 150 rpm to reach equilibrium. The experimental isotherm data were fitted using Freundlich and Langmuir isotherm models to optimize the adsorption process and forecast adsorption.

Table 1. Isotherms parameters for the adsorption of urea onto OPKS-B and OPKS-AC

	Langmuir			Freundlich		
	$q_m$ , ( $\text{mg g}^{-1}$ )	$K_L$ ( $\text{L mg}^{-1}$ )	$R^2$	$K_F$ ( $\text{mg g}^{-1}$ ) ( $\text{L mg}^{-1}$ ) <sup>1/n</sup>	$N$	$R^2$
OPKS-B	-269.02	-0.00032	0.9886	0.0965	0.978	0.9585
OPKS-AC	-239.68	-0.00026	0.9380	0.0212	0.807	0.8784

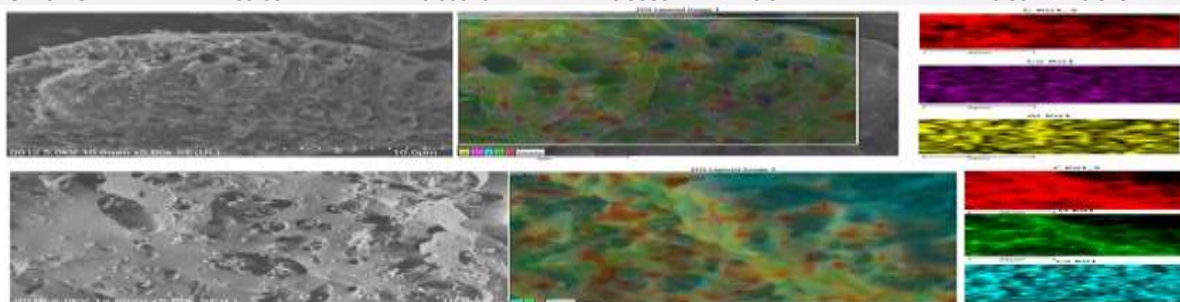


Figure 1. FESEM image and EDX mapping: (a) OPKS-B; (b) OPKS-AC

The present research revealed that the OPKS-B and OPKS-AC both has the potential to be used as a framework to encapsulate urea for preparation of sustained controlled release fertilizer through adsorption method with OPKS-AC has a better advantage comparatively. The high surface area and well-developed porous structure making OPKS-AC a better framework candidate compared than OPKS-B. The pores of various sizes are visible for both carbons OPKS-B and OPKS-AC as shown in Figure 1. Based on the EDX mapping, there are abundance of C, O and Ca detected on the surface of the OPKS biochar. On the other hand, there are presence of C, Ca and Al found on the surface of OPKS-AC based on the EDX mapping performed. For the adsorption process for both OPKS-B and OPKS-AC, the pseudo-second-order kinetic model best fitted the experimental sorption outcome with the high  $R^2$  values of (>65.1%) and (>74.5%), respectively. For urea sorption on OPKS-B and OPKS-AC, the Langmuir isotherm best fitted the experimental isotherm data with higher  $R^2$  values (>0.9886) and (>0.938), respectively, presented in Table 1. The Langmuir model can explain the monolayer absorption of urea on OPKS-B and OPKS-AC well, and no interaction exists between the urea molecules with OPKS-B and OPKS-AC. The validation results analyzed clearly indicated that the utilization of OPKS-AC as the sustainable framework choice of CRUFs production towards a sustainably better agricultural practices and environmentally friendly fertilizer application.

## Acknowledgements

This research was financially supported by the Ministry of Higher Education Malaysia (FRGS-FP074-2019A). The authors would like to thank the University of Malaya and FRIM for the research facilities.

## References

1. Ditta, A. and M. Arshad, *Applications and perspectives of using nanomaterials for sustainable plant nutrition*. Nanotechnology Reviews, 2016. **5**(2): p. 209-229.
2. Liu, R. and R. Lal, *Potentials of engineered nanoparticles as fertilizers for increasing agronomic productions*. Science of the total environment, 2015. **514**: p. 131-139.
3. Association, I.F. *Fertilizer Outlook 2019—2023*. in *Proceedings of the IFA Annual Conference, Montreal, QC, Canada*. 2019.
4. Lyu, Y., et al., *Impact of fertilization schemes with different ratios of urea to controlled release nitrogen fertilizer on environmental sustainability, nitrogen use efficiency and economic benefit of rice production: A study case from Southwest China*. Journal of Cleaner Production, 2021: p. 126198.
5. Gil-Ortiz, R., et al., *Agronomic Assessment of a Controlled-Release Polymer-Coated Urea-Based Fertilizer in Maize*. Plants, 2021. **10**(3): p. 594.
6. Hassan, N.a., et al., *Biochar derived from oil palm trunk as a potential precursor in the production of high-performance activated carbon*. Biomass Conversion and Biorefinery, 2021: p. 1-17.
7. Zainal, N.H., et al., *Microwave-assisted pre-carbonisation of palm kernel shell produced charcoal with high heating value and low gaseous emission*. Journal of cleaner production, 2017. **142**: p. 2945-2949.

8. With, T., T.D. Petersen, and B. Petersen, *A simple spectrophotometric method for the determination of urea in blood and urine*. Journal of clinical pathology, 1961. **14**(2): p. 202.

# Catalysis for biomass & sustainable synthesis

## Selective photo-catalytic oxidation of 5-hydroxymethylfurfural (HMF) to 2,5-Diformylfuran (DFF) over reduced graphite oxide-titanate nanotubes composites

Dimitrios A. Giannakoudakis<sup>1,\*</sup>, Zoi-Lina Koutsogianni<sup>1</sup>, Ioanna Ntekouli<sup>1</sup>, Teresa J. Bandosz<sup>2</sup>, Juan Carlos Colmenares<sup>3</sup>, Konstantinos S. Triantafyllidis<sup>1,4,\*</sup>

<sup>1</sup> Department of Chemistry, Aristotle University of Thessaloniki, Thessaloniki, Greece

<sup>2</sup> Department of Chemistry and Biochemistry, The City College of New York, New York, NY 10031, USA

<sup>3</sup> Institute of Physical Chemistry, Polish Academy of Sciences, Kasprzaka 44/52, Warsaw, Poland

<sup>4</sup> Center for Interdisciplinary Research and Innovation (CIRI-AUTH), Balkan Center, 57001 Thessaloniki, Greece

\*e-mail addresses of corresponding authors: [dagchem@gmail.com](mailto:dagchem@gmail.com), [ktrianta@chem.auth.gr](mailto:ktrianta@chem.auth.gr)

### Abstract:

The continuously amplifying demand in merchandises, fuels and energy necessitates the need to adopt modern and sustainable production approaches. One strategy which concentrates the last decades the research attention is the valorization of abundant and renewable feedstocks, such as biomass, to valuable chemicals [1]. Towards this direction, the design and development of innovative, energy-efficient and environmental-friendly processes, such as the catalytic conversion of biomass to added value chemicals, is of a paramount importance [2]. Solar light assisted photocatalytic methods are considered amongst the most benign alternative technologies, considering the enormous amount of sunlight energy available. In addition to the engineering aspects, the design of novel nanomaterials with enhanced photocatalytic properties plays a key role [3,4].

Various materials based on titanium dioxide have been recognized as efficient photocatalysts for applications in which the unselective oxidative decomposition of organic compounds, like organic pollutants in water, is desired. In the case of synthetic applications, both catalyst properties and reaction parameters need to be tailored towards controlled photocatalytic activity and selective formation of targeted products.

Within the frame of this work, we presented the synthesis and physicochemical characterization of titanium oxide nanotubes (TiO-NTbs) derived from scrolled titanate nanosheets ( $H_2Ti_3O_7$ ) and their nanocomposites with various amounts of (reduced) graphite oxide (rGO), as well as S and N doped counterparts (**Figure 1**) [5,6]. The photoreactivity of the novel nanomaterials was evaluated by monitoring the selective partial and additives-free oxidation of a cellulose/hemicellulose derived compound, 5-hydroxymethylfurfural (5-HMF) to 2,5-diformylfuran (DFF), with the reaction to take place under ambient conditions using low power LED-emitted light (ultraviolet, 365 nm).

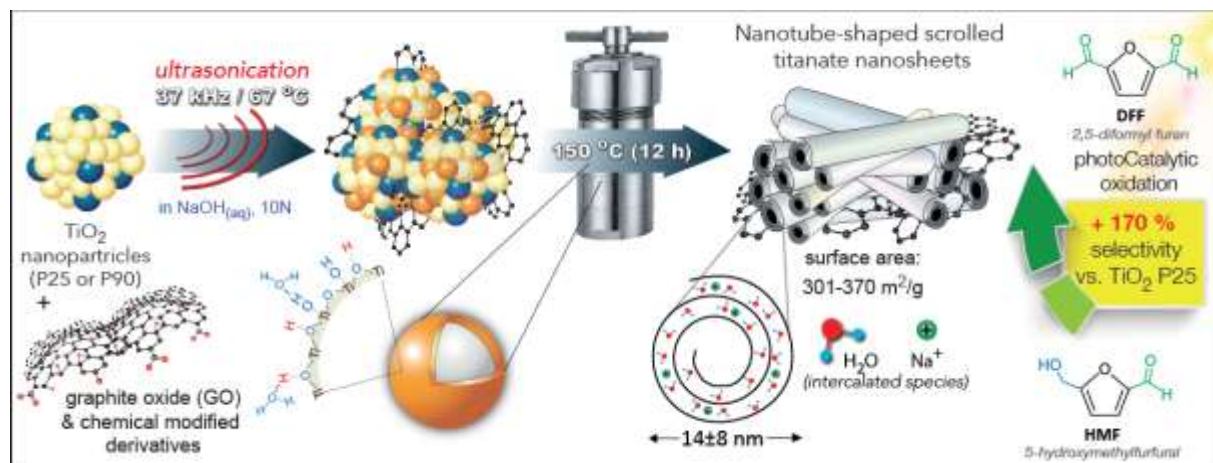


**Figure 1.** The involved steps of the synthesis of the composites consisting of titanate nanotubes and graphite oxide derivatives utilized for the additive-free photocatalytic selective partial oxidation of 5-hydroxymethylfurfural to 2,5-diformylfuran.

TiO-NTbs based materials revealed an elevated photocatalytic HMF partial oxidation activity, with the composite of the optimum amount of rGO (4 wt.%), referred to as TiNTbs@GO10%, presenting higher DFF selectivity by 170% and 72 % compared to the benchmark TiO<sub>2</sub> P25 and pure TiO-NTbs, respectively. The addition of graphitic phase did not affect the dimensions of the formed open-end nanotubes (external diameter  $14 \pm 8$  nm and length  $100 \pm 50$  nm), although it has a positive impact on the textural features, with the specific surface area and total pore volume reaching  $360 \text{ m}^2/\text{g}$  and  $1.05 \text{ cm}^3/\text{g}$ , respectively.

Going a step forward on materials design, the pristine GO was doped with S and N by treatment with sulfanilic acid ( $\text{NH}_2\text{-C}_6\text{H}_4\text{SO}_3\text{H}$ ) prior the synthesis of the composite. This approach led a nanomaterial with similar physicochemical properties with TiNTbs@GO10%. Regarding the HMF-2-DFF photocatalytic efficiency (**Figure**

2), the DFF yield was increased by 3.9 and 2.5 times compared to P25 and TiNTbs, respectively, while by +74% comparing to TiNTbs@GO10%.

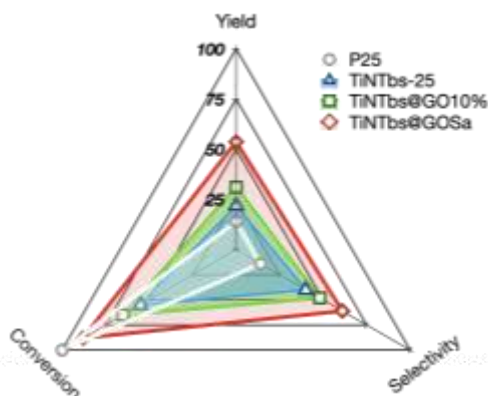


**Figure 2.** The results (CSY triangles) of the photocatalytic HMF to DFF oxidation after 2 h of irradiation with low-power UV light (365 nm) under ambient conditions and without the use of any reagent.

To determine the involved mechanisms, various supplementary experiments were performed by varying each parameter separately. The main conclusion was that different reaction pathways are catalyzed by the commercial TiO<sub>2</sub> P25 nanoparticles and different ones by nanotubes and their composites. The dissolved molecular oxygen plays a key role, as well as does the pre-adsorbed humidity. Another critical conclusion was that the reaction should be also assumed as “self-catalyzed” or “self-promoted” since the photocatalytic formation of DFF promote the HMF conversion. DFT calculations showed that the coupling of HMF with DFF is favourable, with this interaction leading to HOMO-LUMO energy difference decrease and hence promoting the HMF oxidation.

## Conclusions

The main take-home messages are:

1. Titanium oxide nanotubes (TiO-NTbs) present a significant higher selectivity for the photocatalytic partial oxidation of the biomass derived HMF to DFF compared to the benchmark commercial TiO<sub>2</sub> P25 nanoparticles.
2. Designing composite materials of TiO-NTbs with graphite oxide (GO) can have a positive impact on the photocatalytic reactivity.
3. Doping of GO with heteroatoms and especially with S and N can further promote both the HMF conversion as well as the DFF selectivity.
4. The formed DFF has a direct role on the HMF conversion by forming HMF-DFF dimers and lowering the HOMO-LUMO energy difference of HMF as revealed by DFT calculations.

## References

- [1] R. Behling, S. Valange, G. Chatel, Heterogeneous catalytic oxidation for lignin valorization into valuable chemicals: What results? What limitations? What trends?, *Green Chem.* 18 (2016) 1839–1854. doi:10.1039/c5gc03061g.
- [2] D.A. Giannakoudakis, J.C. Colmenares, D. Tsiplakides, K.S. Triantafyllidis, Nanoengineered Electrodes for Biomass-Derived 5-Hydroxymethylfurfural Electrocatalytic Oxidation to 2,5-Furandicarboxylic Acid, *ACS Sustain. Chem. Eng.* 9 (2021) 1970–1993. doi:10.1021/acssuschemeng.0c07480.
- [3] D.A. Giannakoudakis, F.F. Zormpa, A.G. Margellou, A. Qayyum, R.F. Colmenares-Quintero, C. Len, J.C. Colmenares, K.S. Triantafyllidis, Carbon-Based Nanocatalysts (CnCs) for Biomass Valorization and Hazardous Organics Remediation, *Nanomaterials.* 12 (2022) 1679. doi:10.3390/nano12101679.
- [4] D.A. Giannakoudakis, V. Nair, A. Khan, E.A. Deliyanni, J.C. Colmenares, K.S. Triantafyllidis, Additive-free photo-assisted selective partial oxidation at ambient conditions of 5-hydroxymethylfurfural by manganese (IV) oxide nanorods, *Appl. Catal. B Environ.* 256 (2019) 117803. doi:10.1016/j.apcatb.2019.117803.
- [5] D.A. Giannakoudakis, G. Chatel, J.C. Colmenares, Mechanochemical Forces as a Synthetic Tool for Zero- and One-Dimensional Titanium Oxide-Based Nano-photocatalysts, *Top. Curr. Chem.* 378 (2020) 2. doi:10.1007/s41061-019-0262-3.
- [6] D.A. Giannakoudakis, K. Vikrant, A.P. LaGrow, D. Lisovytskiy, K.-H. Kim, T.J. Bandosz, J. Carlos Colmenares, Scrolled titanate nanosheet composites with reduced graphite oxide for photocatalytic and adsorptive removal of toxic vapors, *Chem. Eng. J.* 415 (2021) 128907. doi:10.1016/j.cej.2021.128907.

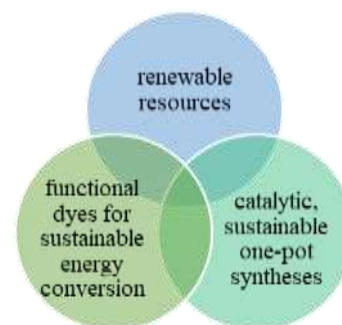
## Sustainable one-pot syntheses of functional dyes based on 5-(hydroxymethyl)furfural

Anita Vißers\* and Thomas J. J. Müller

Heinrich-Heine-Universität, Universitätsstr. 1, 40225 Düsseldorf, Germany

\*anita.vissers@hhu.de

In a material world, chemistry, as the science of transformation and the properties of substances, has a special significance in the pursuit of sustainable goals. The combination of three different factors, which can be summarized as the use of renewable resources, the establishment of sustainable one-pot syntheses and the preparation of functional dyes for sustainable energy conversion, proves to be a goal worth striving for. The polyfunctional, renewable molecule 5-(hydroxymethyl)furfural (HMF) [1] sets the starting point for developing sustainable catalytic one-pot syntheses of functional dyes. Diversity-oriented syntheses of functional dyes as well as systematic structure-property relationships in principle set the stage for the production of these components by sustainable one-pot processes [2]. Dyes are important functional constituents in molecular electronics and photonics, which, in addition to a steady miniaturization, can also avail and realize the efficient conversion of energy [3].



Starting from HMF and unsaturated carbonyl compounds, a substance library of 1,4-diketones was established, which can be used as diverse pivotal building blocks for the synthesis of functional dyes, such as novel pyrroles and pyridazines.

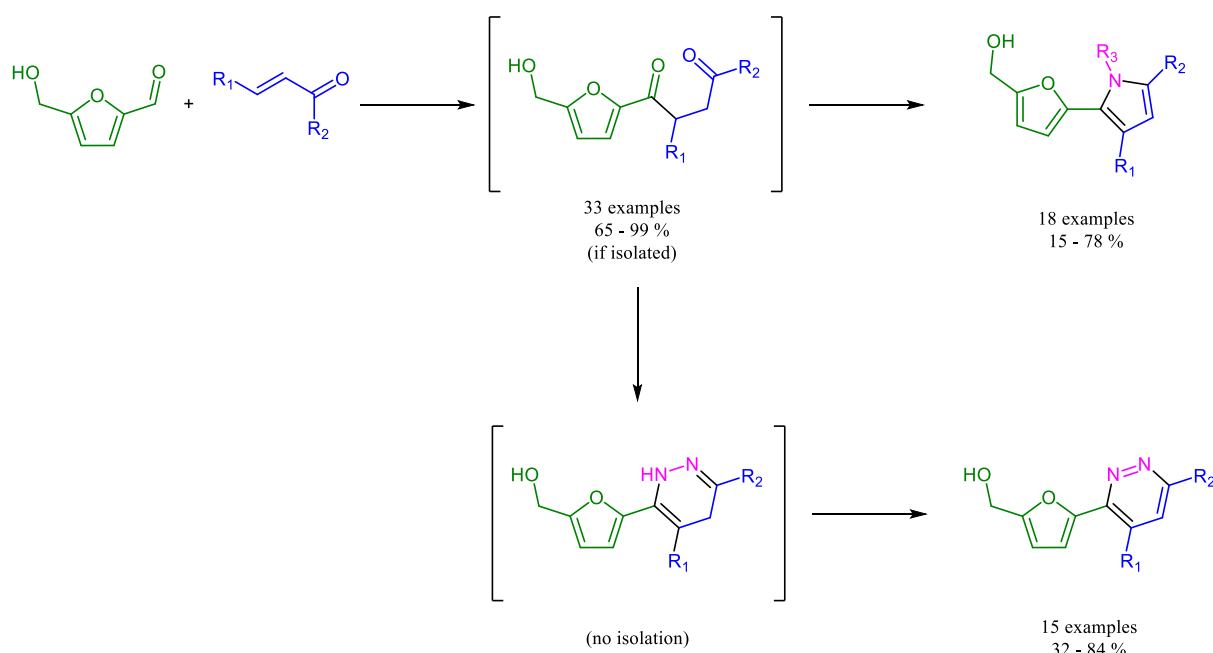


Figure 1: Sustainable one-pot syntheses of substituted pyrroles and pyridazines based on HMF.

For the pyrroles a compound library of 18 examples has been constructed in yields ranging from 15 to 78 % including electronically diverse substituents on the pyrrole core. In addition, a variation of the amine was performed, which led to a divergence of the nitrogen substituent of the pyrrole core from aromatic to aliphatic to unsubstituted. Moreover, beyond the novel green one-pot synthesis, these particular pyrroles are novel in literature.

Photophysical characterization of all pyrrole compounds by absorption and emission spectroscopy indicates a tunable fluorescence from blue to yellowish upon photonic excitation. The fluorescence maxima range from 400 up to 500 nm. Electron withdrawing groups and their positioning moreover exert a strong influence on the emission characteristics.



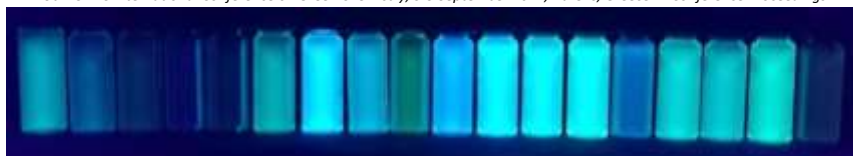


Figure 2: Solution of the 18 pyrroles in  $\text{CH}_2\text{Cl}_2$  under UV-lamp ( $c = 10^{-5}$  mol/L,  $\lambda_{\text{exc}} = 365$  nm).

The resulting Stokes shifts, which were calculated from the longest wavelength absorption maxima and the emission maxima, are in the range of 4600 up to 12100  $\text{cm}^{-1}$ , which serve as an indicator for changes in the electronic structure of the pyrroles during photonic excitation from the ground state to the vibrationally relaxed excited states.

Furthermore, the quantum yield in solution was determined, showing a strong correlation with the substituent and the substitution pattern, which was particularly evident in the case of a discrete cyano-substitution, as a strong acceptor, which dramatically increases the quantum yield up to 95 %.

Extensive solvatochromism studies have been performed on the pyrroles to gain a deeper understanding of the excited state, showing a positive solvatochromism with a bathochromic shift of the emission maximum with increasing solvent polarity and an increasing Stokes shift from 5300 to 8400  $\text{cm}^{-1}$  for the chosen molecule.



Figure 3: Fluorescence of pyrrole in different solvents (from left to right: CH, Toluol, THF, EA,  $\text{CH}_2\text{Cl}_2$ , DMSO, ACN, iPro, EtOH under UV-lamp,  $c = 10^{-5}$  mol/L,  $\lambda_{\text{exc}} = 365$  nm).

Due to the presence of electron-withdrawing groups some of the synthesized pyrroles not only show fluorescence in solution, but they are also emissive in the solid state appearing with emission maxima ranging from 450 to 600 nm. The two singly cyano-substituted pyrroles show the highest quantum yields up to 16 %.

For the pyridazines a compound library of 15 examples has been constructed in yields ranging from 32 to 84 % including electronically diverse substituents on the pyridazine core. The newly established one-pot synthesis includes a final oxidation step, which is carried out under aerobic conditions without further additives and thus particularly represents the principles of sustainability.

## Acknowledgements

We cordially thank the Deutsche Bundesstiftung Umwelt for financial support (scholarship for A.V.).

## References

1. A. A. Rosatella, S. P. Simeonov, R. F. M. Frade, C. A. M. Afonso, *Green Chem.*, **13** 754 (2011).
2. M. Marson, *Chem. Soc. Rev.*, **41** 7712 (2012).
3. X. Huang, T. Li, *J. Mater. Chem.*, **8** 821 (2020).

## Catalytic conversion of biomass-derived compounds to high added value products using an acid treated natural mordenite

Dimitra Makarouni<sup>1,2</sup>, Chara Dimitriadi Evgenidi<sup>2</sup>, Christos Kordulis<sup>1,3,4</sup> and Vassilios Dourtoglou<sup>2\*</sup>

<sup>1</sup> Department of Chemistry, University of Patras, GR-26504, Patras, Greece

<sup>2</sup>VIORYL, Chemical and Agricultural industry, Scientific Research S.A., 28th km. Athens-Lamia national road, GR-19014, Afidnes, Greece

<sup>3</sup>School of Science and Technology, Hellenic Open University, Tsamadou 13-15, GR-26222, Patras, Greece

<sup>4</sup>Foundation of Research and Technology-Institute of Chemical Engineering Science (FORTH/ICE-HT) Stadiou Str. Platani, P.O. Box 1414, GR-26500, Patras, Greece

\*vdourtoglou@vioryl.gr

### Abstract text:

A sustainable chemical industry cannot exist at scale without sustainable and renewable feedstocks. The utilization of minerals as “natural” catalysts for producing useful products through green processes is very important for sustainable development in the frame of cyclic economy. Mordenite is a well-known zeolite material for its shape selectivity, making it a very important catalyst with several applications in the chemical industry. In the present work, a catalyst (named TECHNOSA-H2) based on natural mordenite originated from volcanic soils in Greek islands is utilized for the synthesis of high added value organic products starting from renewable raw materials.

TECHNOSA-H2 was prepared via treatment of natural mordenite with hydrochloric acid [1,2]. In our previous research, we have proved that this catalyst is efficient for the synthesis of several interesting organic molecules such as terpenes and cyclic ethers with great industrial importance [1,3]. In the present study, we want to take this research one-step forward and evaluate the reactivity of the above mordenite-derived catalyst for additional organic synthesis reactions leading to fine chemicals. Focus is given on the utilization of the above mordenite catalyst for the production of valued products like difurfuryl ether (DFE), furfuryl ethyl ether (FEE), d-2-furylmethane (DFM), citral propylene glycol acetal (Citral PGA), citral diethyl acetal (Citral DEA), campholenic aldehyde (CA) and isopulegol (IP) from suitable biomass derivatives (Figure 1).

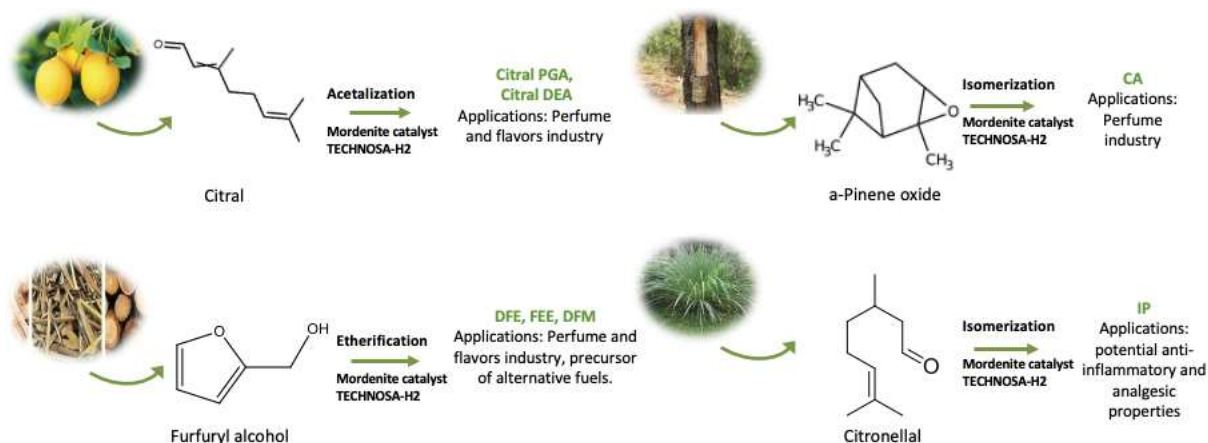


Figure 1. Conversion of biomass-derived compounds to high added value products over the mordenite catalyst TECHNOSA-H2 by the means described in the present research.

Furfuryl alcohol (FA) is industrially obtained in large quantities from the hydrogenation of furfural [4-6], which is produced in bulk in lignocellulosic bio-refineries from crop and wood waste [5]. FA is one of the most important furan derivatives and widely considered as one of the most important biomass-derived platform compounds [7-10]. FA has proved to be a remarkable eco-sustainable bio-derived compound [11]. In addition, the FA derivatives, like DFE, FEE and DFM, have shown great promise as flavoring agents and precursors for alternative fuels and polymers [12-16]. From sustainability standpoint, applying a natural mordenite catalyst for the synthesis of commercially interesting FA ether derivatives can be a promising alternative to the previously recorded methods. Indeed, the findings of the present work showed that both symmetric and non-symmetric ether derivatives of FA can be synthesized using TECHNOSA-H2 catalyst. More specifically, the synthesis of DFE and DFM was achieved in yields 30% and 11%, respectively, by the conversion of FA over TECHNOSA-H2 at 130°C for 3 h. In the presence of the same catalyst, using FA and ethanol as reactants, a yield of furfuryl ethyl ether of 60% at 3h and 150 °C, without high polymer byproducts production can be achieved.

Another important biomass derivative is Citral. Citral is a monoterpene found naturally as a predominant component of the oil in varying citrus plants. Citral propylene glycol acetal (Citral PGA) and Citral diethyl acetal (Citral DEA) have been extensively studied due to their important applications in the food industry [17], [18], however, their synthesis may involve orthoformic triethylester in the presence of perchloric acid, or acid solutions,

such as H<sub>2</sub>SO<sub>4</sub> [19]. In the framework of Green Chemistry, it is important to replace corrosive reagents with natural renewable ones. Hence, the substitution of homogeneous catalysts by the TECHNOSA-H2 catalyst would be a sustainable improvement to previously reported methods. In the present work, we proved that TECHNOSA-H2 can be used for the production of Citral PGA with yields of up to 50% in a reaction time equal to 20 min and a temperature of 60 °C. At the same time and reaction temperature, the production of 50% Citral DEA is achieved by the reaction of the Citral with ethanol in the presence of TECHNOSA-H2.

Other interesting reactions with terpenes are the conversion of  $\alpha$ -pinene to campholenic aldehyde and the cyclization of citronellal to isopulegol. These two reactions draw a lot of attention not only because of the industrial importance of the products formed, but also because they are the two most frequently used catalytic test reactions for differentiating Brønsted and Lewis acidity of solid catalysts [20-22]. In the present work, we investigated the performance of the acid activated mordenite catalyst TECHNOSA-H2 in the reactions of  $\alpha$ -pinene isomerization and citronellal cyclization. Our aim was to examine the potential of TECHNOSA-H2 being an active catalyst for the production of campholenic aldehyde and isopulegol from their biomass derived substrates respectively, and at the same time investigate the nature of the active sites of the catalyst through these two probe reactions. In addition, with regards to the isomeric composition of citral, we also examined the catalytic action of the acid-activated mordenite TECHNOSA-H2 in reactions that reveal shape selectivity properties between stereo-isomers, which include the conversion of the (E)-, (Z)- isomers of Citral. The successful isomerization of  $\alpha$ -pinene oxide over TECHNOSA-H2 for the one-step synthesis of campholenic aldehyde in yields up to 57% at 10min and room temperature was proved, as well as the one-step cyclization of citronellal over TECHNOSA-H2 to isopulegol in yields up to 57% at 140°C and reaction time equal to 10min. Considering the product distribution in the two probe reactions studied and the available literature [20-22], we can conclude that the active sites on TECHNOSA-H2 are a combination of Lewis and Brønsted acid sites. Finally, shape selectivity was tested by the application of TECHNOSA-H2 over the (E)-, (Z)- isomers of citral. It was shown that TECHNOSA-H2 is an effective catalyst for the cyclization of neral i.e. the E-isomer of citral to afford p-cymene, dehydro p-cymene and terpinolene in 60min at 130°C. However, when TECHNOSA-H2 is applied, geranial i.e. the Z-isomer of citral, remains intact. This proves the shape selectivity of the TECHNOSA-H2 catalyst over the E- and Z- isomers of citral.

Based on the findings of the current study, it is proven that TECHNOSA-H2 can be a very promising catalyst for various applications in organic synthesis, while some of these applications include acetalization, isomerization and etherification reactions, as well as reactions where shape selectivity between reactants is desired.

## References

1. Makarouni, D. et al. *Appl. Catal. B: Environ.* **224**, 740–750 (2018).
2. Lycourghiotis, S. et al. *Mol Catal* **450**, 95–103 (2018).
3. Makarouni, D., Kordulis, C., Dourtoglou, V. *Catal. Lett.* **152**, (2022).
4. Fang, R. et al. *Green Chem* **17**, 4183–4188 (2015).
5. Selishcheva, S. et al. *Catal Ind* **11**, 216–223 (2019).
6. O'Driscoll, Á., Leahy, J.J., Curtin, T. *Catal Today* **279**, 194–201 (2017).
7. Sharma, R.V. et al. *Appl. Catal. A: Gen.* **454**, 127–136. (2013).
8. Wang, T. et al. (2019). *Catal Lett* **149**, 1845–1855.
9. Gómez Millán, G. et al. *Fuel Process. Technol.* **182**, 56–67 (2018).
10. Zhao, T. et al. *Fuel Process. Technol.* **180**, 14–22 (2018).
11. Iroegbu, A.O., Hlangothi, S.P., *Chem Africa* **2**, 223–239 (2019).
12. Bressanello, D. et al. *Food Chem* **214**, 218–226 (2017).
13. Yang, N. et al. *Food Chem* **211**, 206–214 (2016).
14. Vanderhaegen, B. et al. *J Agric Food Chem* **52**, 1661–1668 (2004).
15. Vanderhaegen, B., et al. *J Agric Food Chem* **52**, 6755–6764 (2004).
16. Mulik, N.L., Niphadkar, P.S., Bokade, V.V. *Res Chem Intermed* **46**, 2309–2325 (2020).
17. Shahzadi, P. et al. *J Antiviral Antiretroviral* **6**. (2014).
18. Erythropel, H.C. et al. *Nicotine Tob Res* **21**, 1248–1258 (2018).
19. Kroshtal', G.V. et al. *Russ Chem Bull* **35**, 838–840 (1986).
20. Alaerts, L. et al. *Chem. Eur. J.* **12**, 7353–7363 (2006).
21. Vandichel, M. et al. *J. Catal.* **305**, 118–129 (2013).
22. Cirujano, F.G., Llabrés i Xamena, F.X., Corma, A. *Dalton Trans* **41**, 4249–4254 (2012)

## A green chemistry approach to catalytic synthesis of ethyl levulinate

Małgorzata E. Zakrzewska<sup>1\*</sup>, Martina Jakovljević Kovač<sup>2</sup>, Ana R.C. Duarte<sup>1</sup> and Maja Molnar<sup>2</sup>

<sup>1</sup> LAQV, REQUIMTE, Departamento de Química, Faculdade de Ciências e Tecnologia, Universidade Nova de Lisboa, 2829-516 Caparica, Portugal

<sup>2</sup> Faculty of Food Technology Osijek, Josip Juraj Strossmayer University of Osijek, Franje Kuhača 18, 31000 Osijek, Croatia

\* [ma.zakrzewska@campus.fct.unl.pt](mailto:ma.zakrzewska@campus.fct.unl.pt)

Biofuels, understood as derived from biomass, are essential to meet fast-growing demand for transportation and alleviate the negative impact of vehicles emissions. Alkyl levulinates can be produced from levulinic acid, one of the top 12 platform chemicals produced from biomass, and have been proposed as both gasoline and diesel additives capable of enhancing fuel quality, such as reduction in toxicity and sulfur content, improvement in lubricity, stability in flash point and viscosity [1]. Ethyl levulinate is the most widely studied alkyl levulinate that is already being used in flavoring and fragrance industry, plasticizers or as a solvent. Potentially produced from bioethanol constitutes a particularly attractive high value-added chemical from sustainability point of view.

Conventionally, the Fischer esterification is carried out with strong mineral acid leading to corrosion, environmental pollution, and troublesome catalyst recyclability [2]. On the other hand, heterogenous catalyst are associated with lower reaction rates, side products or catalyst deactivation. Ionic liquids, although emerged as a green solution, are often characterized by complex preparation, possible toxicity, low biodegradability and high cost limiting their applications to a large extent.

In this context, deep eutectic systems (DES) offer a pronounced advantage [3,4]. They are recognized by their straightforward and reproducible preparation, 100% atom economy, low-price, and often biodegradability and non-toxicity, especially in case of natural deep eutectic systems (NADES) that are composed of primary metabolites like, i.e., organic acids, sugars, amino acids or choline chloride.

In the undergoing project, we investigated several NADES as catalyst for the esterification of levulinic acid with ethanol. The influence of various parameters, i.e., temperature, time, alcohol to acid ratio, catalyst loading, on the catalytic activity was studied in a batch mode. The green synthetic methods, including mechanochemical, microwave, and ultrasound-assisted organic synthesis were tested in order to optimize the conversion and selectivity towards the desired product. The obtained products were analyzed using HPLC with UV detector, TLC and NMR spectroscopy. The obtained results show that using NADES as catalyst for the synthesis of ethyl levulinate is very promising and can bring numerous advantages to the process.

### Acknowledgements

This project has received funding from the European Union's Horizon 2020 (European Research Council) under grant agreement No ERC-2016-CoG 725034. This work was further supported by the Fundação para a Ciência e Tecnologia FCT/MCTES projects PTDC/EQU-EPQ/1039/2021 and UIDB/50006/2020 of the Associate Laboratory for Green Chemistry – LAQV. The authors also thanks to the Croatian Science Foundation Under the project UIP-2017-05-6593. The NMR spectrometers at FCT NOVA are part of Rede Nacional de RMN (PTNMR), supported by FCT/MCTES through ROTEIRO/0031/2013 - PINFRA/22161/2016 and co-financed by FEDER through COMPETE 2020, POCI, and PORL and FCT through PIDDAC.

### References

1. J.F. Leal Silva, R. Grekin, A. Pinto Mariano, R. Maciel Filho, *Energy Technol.*, **6** 613 (2018).
2. E. Ahmad, Md. Imteyaz Alam, K.K. Pant, M. Ali Haider, *Green Chem.*, **18** 480 (2016).
3. A. Paiva, A.A. Matias, A.R.C. Duarte, *Curr. Opin. Green Sustain. Chem.*, **11** 81 (2018).
4. M. Komar, T.Gazivoda Kraljević, I. jerkovič, M. Molnar, *Molecules*, **27** 558 (2022).

## Application of copper-containing minerals in preparative organic chemical reactions as catalysts.

Gábor Györke, Balázs Volk and Mátyás Milen

Egis Pharmaceuticals PLC, P. O. Box 100, H-1475 Budapest, Hungary,  
gyorke.gabor@egis.hu, volk.balazs@egis.hu, milen.matyas@egis.hu

Our Earth is built up from rocks which consist of minerals with well-defined structure, chemical composition and which are, apart from few exceptions, inorganic compounds. Based on their composition they can be assigned to 10 groups (Strunz system).[1] As of today, more than 5700 minerals are known in the nature, of which at least 770 are copper containing, [2] therefore we can safely say that copper is one of the most abundant metals. Although based on tonnage it is mainly used elsewhere, [3] copper catalysis has great significance in preparative organic chemistry and is widely used to prepare a large variety of biologically active compounds or even marketed medicines. [4] As copper production is a highly polluting process, bypassing it by the usage of minerals can lead to more economical, environmentally friendly methods.

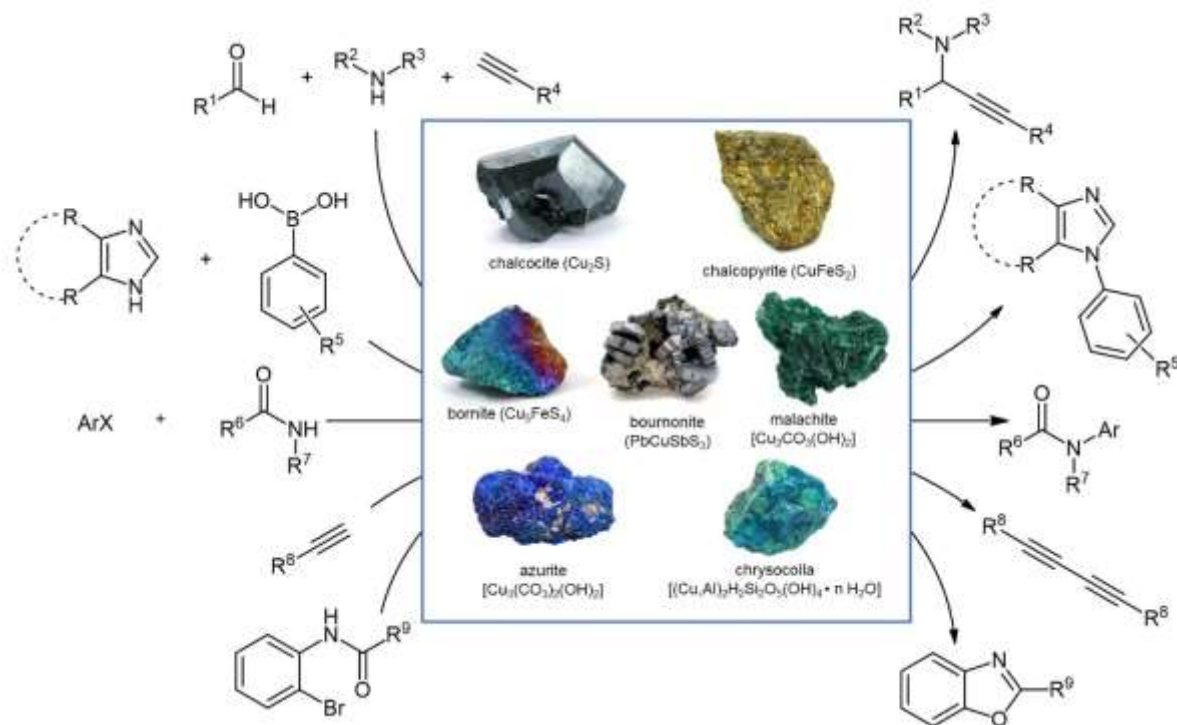


Figure 1. Copper mineral catalyzed organic chemical reactions.

In our present study we wish to showcase five examples for copper mineral catalyzed organic reactions. These highly versatile and thoroughly investigated reactions are preparation of propargylamines via A<sup>3</sup> reaction, [5] Chan–Lam arylation of benzimidazoles, [6] Goldberg arylation of amides, [7] Glaser–Hay coupling of terminal alkynes [8], and the preparation of benzoxazoles and benzothiazoles in an Ullmann type intramolecular coupling reaction. Furthermore, as minerals are formed in the nature, their composition can have some inconsistencies, therefore we compared minerals from multiple origins as well as, when possible, their synthetic variants. ICP, XRF, XRPD, light microscopy, SEM, titration, IR and BET measurements were also carried out to fully characterize the minerals.

### References

1. H. Strunz, *Mineralogische Tabellen*, Akademische Verlagsgesellschaft Becker & Erler Kom.-Ges. (1941).
2. International Mineralogical Association Database of Mineral Properties. <https://rruff.info/ima>
3. J. Emsley, *Nature's building blocks: an A–Z guide to the elements*, Oxford University Press, pp. 121–125 (2003).
4. G. Anilkumar, S. Saranya, *Copper Catalysis in Organic Synthesis*, Wiley-VCH Verlag GmbH & Co. KGaA, (2020).
5. M. Milen, G. Györke, A. Dancsó, B. Volk *Tetrahedron Letters*, **61** 151544 (2020).
6. G. Györke, A. Dancsó, B. Volk, M. Milen *ChemistrySelect*, **6** 802–806 (2021).
7. G. Györke, A. Dancsó, B. Volk, L. Bezúr, D. Hunyadi, I. Szalóki, M. Milen *Catalysis Letters* (2022).
8. G. Györke, A. Dancsó, B. Volk, D. Hunyadi, I. Szalóki, M. Milen *ChemistrySelect* (2022) *in press*.

## A Comparison of In-situ Reduction of Copper and Nickel-rich Mixed Oxides for Effective Organosolv Lignin Fractionation

Iqra Zubair Awan<sup>1,2,3\*</sup>, Olinda Gimello<sup>2</sup>, Thomas Cacciaguerra<sup>2</sup>, Nathalie Tanchoux<sup>2</sup>, Stefania Albonetti<sup>1</sup>, Fabrizio Cavani<sup>1</sup> and Francesco Di Renzo<sup>2</sup>

<sup>1</sup>Department of Industrial Chemistry, Alma Mater Studiorum Università di Bologna, Via Zamboni, 40126 Bologna, Italy

<sup>2</sup>ICGM, University of Montpellier - CNRS - ENSCM, 641 Av. du Doyen Gaston Giraud, 34000 Montpellier, France

<sup>3</sup>Department of Chemistry, Lahore Garrison University, DHA Phase VI, Lahore, Pakistan

\*iqrazubair@gmail.com

Lignin fractionation for the purpose of obtaining functional aromatics is a top trend in Green Chemistry. [1] Out of multiple routes available for the depolymerization of this renewable resource, we studied the catalytic reduction of  $\alpha$ -O-4 lignin model molecule by using methanol/ethanol as a hydrogen donor solvent at temperature less than conventional, in the presence of calcined hydrotalcites of  $A(II)_3B(III)O_x$  with  $A = Cu$  or  $Ni$  and  $B = Al$  or  $Fe$ .

Typically, two reduction pathway schemes; Meerwein–Ponndorf–Verley (MPV) reduction and  $\alpha$ -O-4 hydrogenolysis with subsequent C-C and C-O hydrogenolysis were observed. The function of the catalyst composition and reaction media gave an insight on the competition between solvolysis, hydrogenation from solvent reforming, hydrogen transfer and hydrodeoxygenation reactions. The benchmark single oxide catalysts showed weak conversion with selective MPV hydrogen transfer. The nickel-rich mixed oxides gave 80% of conversion among which complete MPV hydrogenation, very weak  $\alpha$ -O-4 hydrogenolysis, and effective C-O and aliphatic C-C hydrogenation was seen. The copper-rich mixed oxide showed 99% of conversion with nearly total  $\alpha$ -O-4 hydrogenolysis, complete MPV hydrogenation and effective hydrogenation and hydrodeoxygenation. [2] This activity and selectivity data have been related to the in-situ evolution of the heterogeneous catalysts.

The post catalytic characterization of the catalysts indicated that in case of nickel-rich catalysts, the in-situ reduction of CuO to Cu had just begun at 200°C whereas in case of Cu-rich catalysts complete reduction of CuO to Cu and graphite was seen. Moreover, in the  $H_2$ -TPR of NiCuFe and NiCuAl catalysts, CuO was found to be more easily reducible in comparison to NiO in the presence of iron. The reduction of CuO started exactly at 200°C, just at the temperature used for the catalytic reaction.

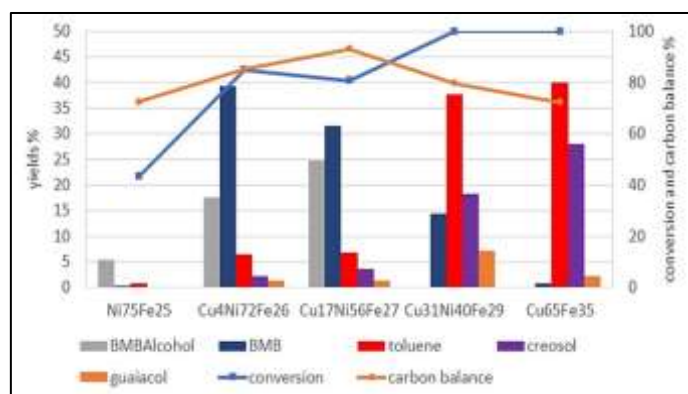


Figure 1. Activity and Selectivity vs. Cu/Ni ratio of calcined oxides

Looking on the overall results, it was concluded that the presence of copper in the catalyst is critical for hydrogenation reactions, leading to yields increased by an order of magnitude. Fe-bearing catalysts got higher activity but introducing consecutive reaction with char formation and worse carbon balance than Al-bearing ones. The hydrogen-donor activity of the solvent is critical, either by direct exchange or by in-situ hydrogen generation, and a strict control of the redox environment of the system is required. The stability of the catalytic materials in different reaction media has proven to be a critical item for the implementation of the processes.

### Acknowledgements

This work was supported by the SINICHEM Joint Doctorate programme selected under the Erasmus Mundus Action 1 Programme (FPA 2013-0037).

### References

1. N. Zhou, W.P.D.W. Thilakarathna, Q.S. He, H.P.V. Rupasinghe, *Front. Energy Res*, **9**, 758744 (2022).
2. I.Z. Awan, G. Beltrami, D. Bonincontro, O. Gimello, T. Cacciaguerra, N. Tanchoux, A. Martucci, S. Albonetti, F. Cavani, F. Di Renzo, *Applied Catalysis A: General*, **609**, 117929 (2021).

## Development of Cr-free hydrogenolysis catalysts

Jaroslav Aubrecht<sup>1\*</sup> and David Kubička<sup>1</sup>

<sup>1</sup>Department of Petroleum Technology and Alternative Fuels, University of Chemistry and Technology Prague, Technická 5, Prague 6, Czech Republic

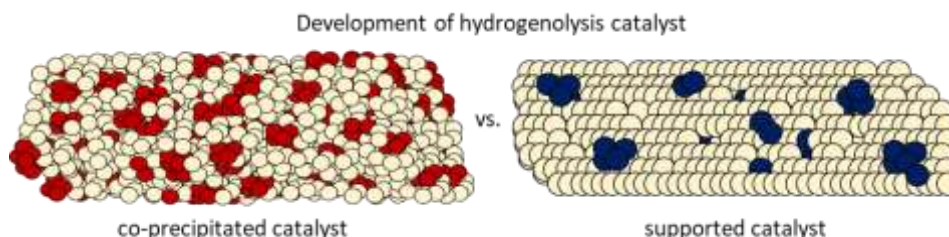
\*aubrechj@vscht.cz

### Introduction

The ester hydrogenolysis is a key process in the production of a wide range of alcohols. There is large applicability of those alcohols in pharmaceutical and cosmetic industries as well as in polyurethane synthesis. The global market of fatty, C<sub>6</sub>-C<sub>22</sub>, alcohols annually raises about 5 % which underlines the importance of the process. Industrially, it is catalysed by Adkins catalysts that are based on copper chromite (CuO.CuCr<sub>2</sub>O<sub>4</sub>) [1]. Although Cr<sub>2</sub>O<sub>3</sub> works as a structural promoter and contributes to i) better CuO dispersion, ii) stabilization of Cu active sites and iii) its higher thermal stability, it is also associated with significant environmental risks. Wastewaters containing Cr salt residues are produced in large volumes when manufacturing Adkins catalysts. These salts need to be later efficiently and costly removed. Also, there is a difficult catalyst reactivation or disposal at the end of its life cycle. Finally, the hydrogenolysis catalysed by Adkins catalyst requires severe reaction conditions such as pressures >200 bar and temperatures >250°C that make the process energy- and cost- demanding. Consequently, the motivation to find new environmentally-friendly alternative for Adkins catalysts is enormous. Our work provides a comprehensive study related to the development of such alternative catalyst for ester hydrogenolysis.

### Methodology:

A large set of Cu-based catalysts was prepared using co-precipitation [2], impregnation [3], deposition-precipitation [4] and chemisorption-hydrolysis [3]. ZnO, ZnO-Al<sub>2</sub>O<sub>3</sub>, MgO and ZnO-MgO were used as promoters in co-precipitated catalysts. Supported catalysts were prepared using Al<sub>2</sub>O<sub>3</sub>, SiO<sub>2</sub>, TiO<sub>2</sub>, ZnO, ZrO<sub>2</sub>, MCM-41, SBA-15 supports. The catalysts were reduced in hydrogen/nitrogen 10 v/v % (99.9%, SIAD Czech, s.r.o., Czech Republic) atmosphere at 220 °C and used in hydrogenolysis of dimethyl adipate (99%, Sigma-Aldrich, United States) at *T* = 160-250°C and *p* = 100 bar.



### Results and discussion:

In this work, a wide range of catalyst promoters and supports, to replace Cr<sub>2</sub>O<sub>3</sub>, were investigated. A large number of co-precipitated (Cu loading of 40-50 wt%) and supported (Cu loading of 8 wt% Cu) catalysts were synthesized. We used rational design to evaluate the structure – synthesis – activity relationship, which in fact will help to design an optimized alternative catalyst.

Catalyst structural and textural properties, in particular CuO/Cu nanoparticle size, catalyst surface area and specific copper surface area, were deeply investigated using XRD, TEM, N<sub>2</sub>-physisorption and N<sub>2</sub>O-chemisorption. Using co-precipitation, small Cu crystallites of 4-6 nm were formed, because of the structural promoters. They also increased the copper surface area compared to the unpromoted CuO catalyst. On the other hand, when depositing Cu on supports, the final Cu crystallite size was strongly dependent on the choice of both synthesis method and support. The smallest crystallites of 2-5 nm were observed when using ZrO<sub>2</sub> or SiO<sub>2</sub> as support. In contrast, TiO<sub>2</sub> or MgO were not suitable supports for the stabilization of Cu nanoparticles. We have identified chemisorption-hydrolysis and deposition-precipitation as the most suitable methods that resulted in catalysts with a high copper surface area.

The catalyst activity (Figure 1) and selectivity were investigated in dimethyl adipate hydrogenolysis to hexane-1,6-diol (HDOL). Besides HDOL, the desired reaction product, a large range of by-products was formed by transesterification. Using pyr-TPD and CO<sub>2</sub>-TPD, we have found a dependence between acid-base sites and the catalyst selectivity to the reaction products. Catalyst activity and selectivity were compared with unpromoted CuO/Cu catalyst at given reaction conditions (*T* = 175°C & *p* = 160 bar for co-precipitated catalysts; *T* = 250°C & *p* = 100 bar for supported catalysts). The addition of ZnO-Al<sub>2</sub>O<sub>3</sub> significantly increased the hydrogenolysis activity among the co-precipitated catalysts, when Cu nanoparticles were due to their interaction with the oxide promoters well dispersed and stabilized. In supported catalysts, the use of ZrO<sub>2</sub> and SiO<sub>2</sub> enhanced the

hydrogenolysis activity of the Cu species. The strong copper – support interaction contributed to the formation of small and stable particles highly active in ester hydrogenolysis.

In conclusion, we have investigated a wide range of promoters and supports. Their characterization and catalytic data will help us to tailor the final catalyst superior to Adkins catalysts both from performance as well as environmental point of view.

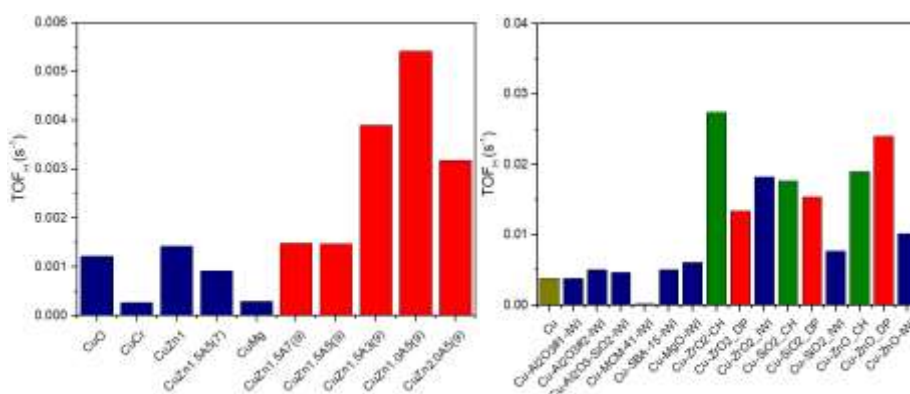


Figure 1. Hydrogenolysis activity of co-precipitated and supported catalysts [5]

## Acknowledgements

Financial support from the Czech Science Foundation (project No. GA20-28093S) is greatly acknowledged. The reactive frontal chromatography results were accomplished by using Large Research Infrastructure ENREGAT supported by the Ministry of Education, Youth and Sports of the Czech Republic under project no. LM2018098.

## References

1. Adkins, H. and K. Folkers, *The catalytic hydrogenation of esters to alcohols*. Journal of the American Chemical Society, 1931. **53**(3): p. 1095-1097.
2. Aubrecht, J., et al., *Do metal-oxide promoters of Cu hydrogenolysis catalysts affect the Cu intrinsic activity?* Applied Catalysis A: General, 2020. **608**: p. 117889.
3. Pospelova, V., et al., *Towards efficient Cu/ZnO catalysts for ester hydrogenolysis: The role of synthesis method*. Applied Catalysis A: General, 2021. **624**: p. 118320.
4. Aubrecht, J., et al., *Critical evaluation of parameters affecting Cu nanoparticles formation and their activity in dimethyl adipate hydrogenolysis*. Catalysis Today, 2022. **387**: p. 61-71.
5. Aubrecht, J., *Dissertation Thesis: Modified Cu-based catalysts: from their preparation to application in dimethyl adipate hydrogenolysis*, in University of Chemistry and Technology Prague. 2022.



## Mesoporous metal phosphates and zeolites as solid acid catalysts: Stability and catalytic performance in oleic acid esterification

S.A. Karakoulia<sup>1\*</sup>, A.A. Marianou<sup>1</sup>, C.M. Michailof<sup>1</sup>, M. Sountourlis<sup>2</sup>, E.F. Iliopoulou<sup>1</sup>, A.A. Lappas<sup>1</sup>

<sup>1</sup>Chemical Process and Energy Resources Institute, Centre for Research and Technology Hellas, Thessaloniki, 6th km. Charilaou – Thermi Road, GR-570 01 Thermi, Greece

<sup>2</sup>Newenergy S.A., Paralimni, GR 62100, Serres, Greece

\*matoula@certh.gr

Biodiesel is an important alternative renewable fuel as it is environmentally friendly, non-toxic and has lower emission gases when used for combustion. Last years a lot of efforts had driven to the improvement of biodiesel production sustainability via the development of a value chain which includes the recycling and valorization of liquid waste from the vegetable oil refining industry (soap stock and fatty acids-FFA) via chemocatalytic processes. Catalytic esterification of fatty acids is a proposed key process for its production [1]. The current work presents the esterification of oleic acid, as a representative fatty acid, with C2 to C4 alcohols, using various types of zeolites and mesoporous metal phosphates as heterogeneous catalysts. In order to enhance the dispersion of active acid sites, hierarchical zeolites of type Y were also synthesized via desilication/dealumination procedures following the top-down method inducing thus additional intra-crystal mesoporosity.

Concerning microporous materials, various zeolites were studied including MFI structures with molar ratios of SiO<sub>2</sub>/Al<sub>2</sub>O<sub>3</sub> (SAR) 23, 50 and 80 (ZSM-5-23, ZSM-5-50, ZSM-5-80), zeolites of type Y with SAR 30 (USY-30) and 60 (USY-60), BEA zeolites with SAR 25 and 75 (Beta-25 and Beta-75) and a Mordenite with SAR 10 (Mordenite-10). Those zeolites, provided from Zeolyst, were initially in NH<sub>4</sub><sup>+</sup> form and converted to their final H<sup>+</sup> form by calcination at 550 °C for 3 hours under air flow. In order to induce mesoporosity, hierarchical zeolites of type Y were also explored. More specifically, desilication step was applied with the presence of C<sub>16</sub>H<sub>33</sub>N(CH<sub>3</sub>)<sub>3</sub>Br (CTAB). Thus, a clear solution of CTAB (0.7g CTAB/g zeolite in 37ml DD H<sub>2</sub>O) was added in an alkaline aqueous solution of 0.2M NaOH (30ml/g zeolite) and stirring was followed for 30 minutes at 65°C. Desilication step was rapidly terminated in an ice bath. The modified solid powder was obtained after filtering and washing with distilled water. Furthermore, dealumination was processed by using 50 ml/g of aqueous 3M HNO<sub>3</sub> under stirring at 65 °C for one hour. After filtering and washing, ion-exchange was followed by stirring the desired quantity of the zeolite with aqueous solution of 2M NH<sub>4</sub>NO<sub>3</sub> at 75-80°C for 2 hours in order to activate the NH<sub>4</sub>-form of the hierarchical zeolite. Calcination at 550°C for 3hours under air was finally executed in order to regenerate H-form of the zeolite. The obtained powder was designated as Z/DS/DA or Z/DS where Z is the initial zeolite used for the modification with (DS-DA) or without (DS) dealumination step.

Metal phosphates have long received significant attention as active catalysts because of their bifunctional signature (solid acidity and redox capability). They have shown promising results on acid catalyzed reactions in liquid media making them ideal candidates for esterification reaction [2]. A series of that type of catalysts, such as Sn/P/O, Zr/P/O and Sn/S/O have been synthesized via soft-templating route with the use of Pluronic 123 (P123) and a parallel hydrothermal treatment [3]. In detail, P123 (2 g) and H<sub>3</sub>PO<sub>4</sub> (2.3 g, 20 mmol) were dissolved in H<sub>2</sub>O (30 g) and stirred for 2 h. Tin chloride pentahydrate (7 g, 20 mmol) dissolved in H<sub>2</sub>O (10 g) was added to the H<sub>3</sub>PO<sub>4</sub> solution. A white colloidal precipitate was slowly formed and then other 20 g of H<sub>2</sub>O were added. The whole mixture was stirred for another 3 hours and kept inside a polypropylene bottle at 100°C for 72 h. The white powder was collected by filtration and washing with distilled water. The mesostructured material was calcined at 500 °C for 5 h under air (SnP-P123). Similar method was followed for zirconium phosphate (ZrP-P123) and tin sulphate (SnS-P123) by using the respective metal sources with molar ratio of 1/1.

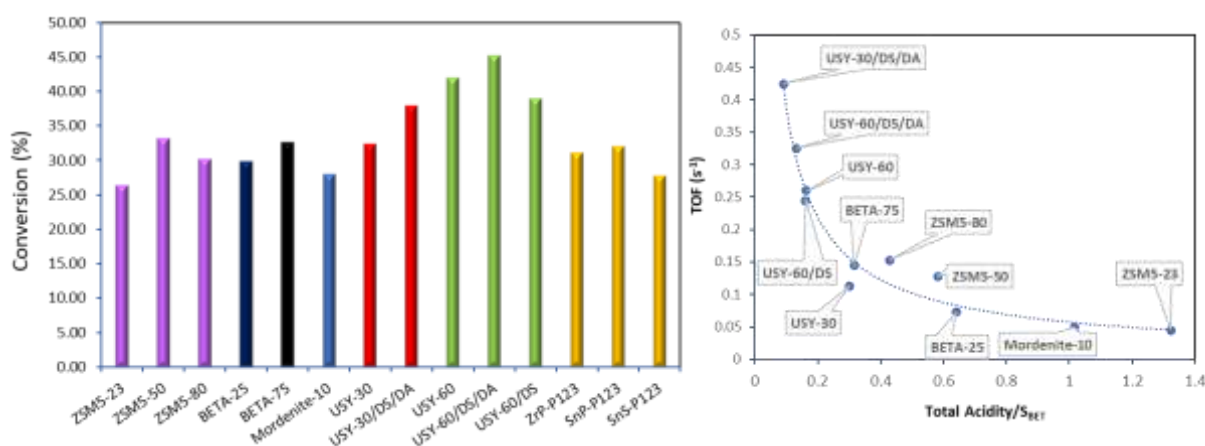
All synthesized materials were fully characterized using ICP-AES, XRD, N<sub>2</sub> porosimetry and in-situ pyridine-FTIR. Screening of the above catalysts was applied for oleic acid esterification with ethanol (EtOH) in an autoclave reactor, at standard reaction conditions (150 °C, 60 min, molar ratio of oleic/EtOH= 1/6, weight ratio of oleic/catalyst=100).

Porosity and acidity characteristics of the catalysts are presented in Table 1. Regarding commercial zeolites, the highest total surface area was noticed for Y type catalysts, while MFI (ZSM-5 zeolites) structure possesses the lowest surface area. In the case of Beta zeolites, besides microporous, an increased mesoporosity is also noticed. As it concerns acidity, it is well known that increase in Al quantity in zeolite structure (SAR decrease) leads to increase in total acidity. For similar SARs, ZSM-5 structure showed the highest number. Hierarchical zeolites were successfully synthesized (USY/DS and USY/DS/DA series) showing induced mesoporosity in any case. As expected, desilication and further dealumination of USY-30 and USY-60 zeolites (USY-30/DS/DA and USY-60/DS/DA) led to decreased number of both Lewis and Brönsted sites due to the partial removal of Al content. Noticeably, lack of dealumination step (USY-60/DS) retained initial total acidity altering however Brönsted/Lewis ratio value (Table 1). Among metal phosphates, SnP-P123 proved to be the catalyst with the highest surface area inducing thus the formation of higher number of acid sites mainly, however, of Lewis type.

Among commercial zeolites, USY-60 showed the best catalytic performance, while metal phosphate catalysts resulted to much lower conversion values (Fig.1). It seems that the presence of much less Bronsted acid sites, noticed in that catalyst category, was not sufficient enough for the desired reaction activation. Moreover, increased surface area, achieved for hierarchical zeolites of Y type with induced mesoporosity, further enhanced catalyst performance. Actually, esterification results, obtained from the studied acid catalysts, revealed a direct correlation of conversion degree with the dispersion of active acid sites. More specifically, the desired catalyst should have high surface area with specific number of acid sites in order to have the potential for optimal dispersion to be utilized to a greater extent upon contact with the reactant molecules. Besides catalyst activity, Turnover Frequency (TOF) proved to be even more beneficial for highly dispersed acid catalysts with low values of Total Acidity/ $S_{\text{BET}}$  ratio (Fig.1b). It must be noted here, that all the above synthesized acid catalysts showed high stability since no metal loss was noticed during the reaction in any case. The optimal catalyst was selected for further study regarding the effect of reaction conditions and catalyst concentration. In addition, the effect of alcohols  $>C_3$  (glycerol, 1-propanol, butanol) was also examined, with the aim of evaluating the influence of the carbon's chain length and the location of OH on esterification performance.

Table 1. Porosity and acidity characteristics of the esterification catalysts

Catalyst	BET				FTIR pyridine		
	S.A.	Total Pore Vol.	Textural Vol.	Meso-pore Vol.	Total	Brønsted Acid Sites	Lewis Acid Sites
	m <sup>2</sup> /g	ml/g			(μmol/g)		
ZSM-5-23	418	0.21	0.02	0.04	553.2	429.8	123.4
ZSM-5-50	427	0.31	0.09	0.13	248.4	196.7	51.7
ZSM-5-80	451	0.27	0.04	0.10	193.2	170.8	22.4
USY-30	885	0.52	0.11	0.16	267.2	184.4	82.8
USY-30/DS/DA	1007	0.90	0.05	0.75	91.1	68.7	22.4
USY-60	918	0.55	0.09	0.23	150.5	118.2	32.2
USY-60/DS/DA	953	0.78	0.20	0.32	127.0	105.5	21.2
USY-60/DS	936	2.63	1.79	0.74	151.0	83.0	68.0
Beta-25/cal	609	1.06	0.11	0.32	389.8	179.6	210.1
Beta-75/cal	679	0.94	0.40	0.37	213.9	132.6	81.4
Mordenite	528	0.28	0.06	0.04	536.3	431.8	104.5
SnP-P123	184	0.34	0.99	0.65	236.2	51.5	184.7
ZrP-P123	107	0.43	0.30	0.13	72.8	11.9	60.9

Figure 1. (a) Oleic acid esterification over acid catalysts and (b) correlation between the ratio of total acidity to  $S_{\text{BET}}$  with TOF

## Acknowledgements

This research has been co-financed by the European Union and Greek national funds through the Operational Program Competitiveness, Entrepreneurship and Innovation, under the call RESEARCH – CREATE – INNOVATE (project code:T1EDK-02864, ProperDiesel).

## References

1. M. Canakci, H. Sanli, *J. Ind. Micr. Biotech.* **35** 431 (2008).
2. A.E.R.S. Khder, S.A. Ahmed, B.M. Altass, *Reac. Kinet. Mech. Cat.* **117** 745 (2016).
3. A. Dutta, D. Gupta, A.K. Patra, B. Saha, A. Bhaumik, *ChemSusChem* **7** 925 (2014).

# Catalysis for biomass

## Recovery of monoaromatic compounds from Kraft lignin toward the production of a potential green bisphenol A replacer

Omar Y. Abdelaziz<sup>1,2\*</sup>, Elson D. Gomes<sup>2</sup>, Smita V. Mankar<sup>3</sup>, Carina A. E. Costa<sup>2</sup>, Baozhong Zhang<sup>3</sup>, Alírio E. Rodrigues<sup>2</sup> and Christian P. Hulteberg<sup>1</sup>

<sup>1</sup>Department of Chemical Engineering, Lund University, P.O. Box 124, SE-221 00 Lund, Sweden

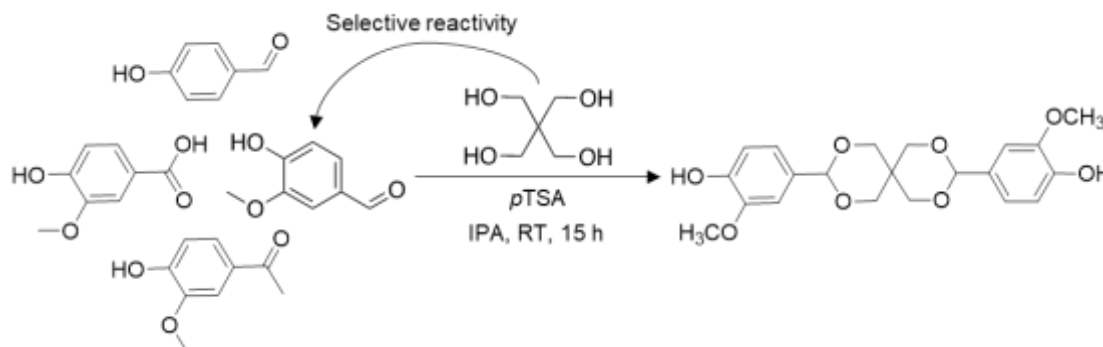
<sup>2</sup>Laboratory of Separation and Reaction Engineering–Laboratory of Catalysis and Materials (LSRE-LCM), Department of Chemical Engineering, Faculty of Engineering, University of Porto, Rua Dr. Roberto Frias, 4200-465 Porto, Portugal

<sup>3</sup>Centre for Analysis and Synthesis, Department of Chemistry, Lund University, P.O. Box 124, SE-221 00 Lund, Sweden

\*omar.abdelaziz@chemeng.lth.se

Biobased molecules with exceptional chemical functionalities can be obtained by the selective transformations of biomass and other non-fossil resources [1]. Such molecules have significant potential as feedstocks for the production of novel polymers to replace those produced from fossil-based counterparts. A biomass component of particular interest is lignin, being the largest renewable source of aromatic building blocks on Earth. The main use of lignin today is limited to combustion for energy production, and its valorization is pivotal in realizing more competitive and sustainable biorefineries. Although different kinds of lignin and lignin model compounds have been explored in the literature, the valorization of technical lignin is prioritized from an industrial standpoint [2].

In the present study, alkaline oxidative depolymerization was applied for the conversion of a technical softwood Kraft lignin stream, LignoBoost lignin (LB), into monoaromatic compounds. The reaction conditions were 50 g/L LB, 2 M NaOH aqueous solution, 150 °C, 5 bar O<sub>2</sub>, 10 min. The concentrations of monoaromatics in the generated product mixture were calculated for vanillin 1.023 (± 0.013) g/L, vanillic acid 0.454 (± 0.007) g/L, acetovanillone 0.156 (± 0.001) g/L, and *p*-hydroxybenzaldehyde 0.019 (± 0.000) g/L. A sequence of membrane filtration and chromatographic separation was then used to recover the monoaromatics produced. About 96% of the major monoaromatic product, i.e. vanillin, was recovered in the water phase resulting from adsorptive separation. It was also possible to recover, in the same phase, approximately 91% of *p*-hydroxybenzaldehyde, 64% of acetovanillone, and 13% of vanillic acid. Moreover, we have demonstrated that a monoaromatic mixture containing the chemical composition of the water phase could react with biobased pentaerythritol, selectively yielding a vanillin-based bisphenol with a spirocyclic acetal structure under green reaction conditions (Scheme 1). This spiro-bisphenol can potentially replace bisphenol A in various applications, e.g., in the production of biobased epoxy resins, thermosets, polyesters, and polycarbonates [3]. The findings of this study present a proof of concept of the use of lignin-derived monoaromatics, for the production of performance-advantaged, biobased polymers.



Scheme 1. Synthesis of spiro-bisphenol from lignin-derived monoaromatics. (*p*TSA, *para*-toluenesulfonic acid; IPA, isopropyl alcohol; RT, room temperature)

### Acknowledgements

This work was supported by the Swedish Foundation for Strategic Environmental Research (2019/1822) within the framework of the research program STEPS – Sustainable Plastics and Transition Pathways at Lund University. The work was based on the Short Term Scientific Mission (STSM) of Dr. Omar Abdelaziz, COST Action LignoCOST (CA17128-46109), supported by COST (European Cooperation in Science and Technology).

### References

1. R. M. Cywar, N. A. Rorrer, C. B. Hoyt, G. T. Beckham, E. Y.-X. Chen, *Nature Reviews Materials*, **7** 83–103 (2022).
2. P. Zhu, O. Y. Abdelaziz, C. P. Hulteberg, A. Riisager, *Current Opinion in Green and Sustainable Chemistry*, **21** 16–21 (2020).
3. S. V. Mankar, M. N. G. Gonzalez, N. Warlin, N. G. Valsange, N. Rehnberg, S. Lundmark, P. Jannasch, B. Zhang, *ACS Sustainable Chemistry & Engineering*, **7** 19090–19103 (2019).

## From biomass-derived furans to aromatic compounds catalyzed by WNb-O mixed oxides with controlled acid properties

Madalina G. Idriceanu<sup>1</sup>, Jaime Mazarío<sup>1</sup>, Daniel Delgado<sup>1</sup>, José M. López Nieto<sup>1</sup> and Marcelo E. Domine<sup>1\*</sup>

<sup>1</sup>Instituto de Tecnología Química (UPV – CSIC). Universitat Politècnica de València. Consejo Superior de Investigaciones Científicas. Avda. Los Naranjos S/N, 46022, Valencia, Spain

\*e-mail: [mdomine@itq.upv.es](mailto:mdomine@itq.upv.es)

### Introduction

The present work is within the framework of the current energy transition, which proposes the progressive substitution of fossil-based raw materials to renewable sources, to produce both chemicals and fuels. In this context of a gradual transition to renewables, and considering the latest forecasts, biomass-derived products will play an essential role during the change. Furanic compounds obtained from biomass primary treatment (i.e. pyrolysis, cellulose hydrolysis and sugars dehydration) become interesting intermediates for high added-value chemicals production, for example aromatic compounds. BTXs (benzene, toluene and xylenes) compounds play an essential and unique role in areas ranging from fine synthetic chemistry to industrial chemical manufacturing. Diels-Alder cyclo-addition of biomass-derived furans with short chain alkenes and subsequent dehydration of the condensed intermediate is a promising route for the sustainable production of some of these aromatic compounds, such as p-xylene (PX). In the case of PX, which presents numerous industrial applications as solvent, component for fuels, synthetic intermediate, etc., could be obtained by reacting a biomass-derived furanic (2,5-dimethylfuran, DMF) and an alkene (ethylene) over solid acid (Brønsted/Lewis) catalyst. Zeolites (H-Y, H-Beta, H-ZSM-5)[1] and M-zeolites (M = Fe, Ga, etc.) with both Brønsted (Br) and Lewis (Le) acidity were active catalysts in the aromatization of furans to PX, although a strong catalytic deactivation by micro-pores blocking mainly due to carbonaceous compounds deposition becomes an important drawback. Other solid acids, such as metallic oxides (i.e. SiO<sub>2</sub>, Al<sub>2</sub>O<sub>3</sub>, TiO<sub>2</sub>, ZrO<sub>2</sub>, Nb<sub>2</sub>O<sub>5</sub>, etc.), also including supported heteropolyacids (HPAs), were used as catalysts for PX production from furans with low conversion and moderate selectivity, leaching of metals being one of the main problems encountered [2-4].

In this work, the aromatization of DMF with ethylene via Diels-Alder route is studied by using hydrothermally prepared WNb-O mixed oxides with pseudo-crystalline Bronze-type structure, enhanced acid properties with adequate Br/Le ratio, and high both thermal and chemical resistance as catalysts [5,6]. The catalytic activity of WNb-O materials with different composition is evaluated under moderated reaction conditions, and compared with H-ZSM-5 commercial zeolite.

### Experimental Procedure

WNb-O mixed oxides were synthesized from their corresponding metals precursors by using the hydrothermal synthesis method [6]. WO<sub>3</sub> and Nb<sub>2</sub>O<sub>5</sub> oxides were also hydrothermally synthesized [6], while commercial zeolites, such as H-ZSM5 (CBV-3024E, Si/Al=13.7), among others, were purchased from Zeolyst Co. and used as reference catalysts. The materials were characterized by different techniques (XRD, ICP, N<sub>2</sub> adsorption, FTIR, NH<sub>3</sub>-TPD...), and activated (calcined in air at 550 °C) prior their use in catalytic tests. The latter were carried out in 12 mL autoclave reactors with carbon reinforced peek interior vessel, and equipped with temperature and pressure controllers, and valves for liquids and gaseous samples extraction/injection. DMF (0.30 g) in 1,4-dioxane (3.00 g) and catalyst (0.15 g) were introduced into reactor, which was hermetically sealed and pressurized with C<sub>2</sub>H<sub>4</sub> at 20 bar, and then heated until 250 °C during 6 h. Gases and liquid products were taken off from the reactor and analyzed by GC-TCD and GC-FID, respectively, while solid fraction (catalyst+residue) was analyzed by TGA.

### Results and Discussion

The aromatization process for obtaining aromatics (i.e. p-xylene, PX) from biomass-derived furans with short-chain alkenes (i.e. ethylene) involves basically a two steps mechanism including: i) a first Diels-Alder cyclo-addition step, where a cyclo-adduct (oxa-norbornene) is formed mainly in the presence of Lewis (Le) acid sites; followed by ii) a second step of selective dehydration of the cyclo-adduct catalyzed by the presence of mainly Brønsted (Br) acid sites. In this complex process other competitive side reactions, such as DMF hydrolysis, olefins and cyclo-adduct polymerization, could also take place, their inhibition or minimization being required to achieve high selectivity to the desired aromatic product (PX).

In a first attempt, catalytic tests were performed with hydrothermally WO<sub>3</sub> and Nb<sub>2</sub>O<sub>5</sub> oxides, and their results in terms of DMF conversion and liquids, gases and PX yields compared to those attained with H-ZSM5 (Si/Al = 13.7) commercial zeolite possessing both Br and Le acidity. As can be seen in Figure 1, H-ZSM-5 reference catalyst gave 70% conversion of DMF with 39% selectivity to PX (yield <20% on liquids basis), these results being slightly higher than those observed with Nb<sub>2</sub>O<sub>5</sub> (DMF conversion = 72%, PX yield ≈10%). On the contrary, although lower conversions of DMF were reached with WO<sub>3</sub> material, PX yield was higher than the values obtained with the zeolite. In addition, WNb-O mixed oxides with different W/Nb compositions were essayed, and the catalytic results are shown in Figures 1 y 2. Results clearly showed that the incorporation of small amounts of Nb species

into the Bronze-type structure of the  $\text{WO}_3$  lead to materials that increased their catalytic activity for aromatization reaction compared to H-ZSM-5 catalyst, thus arriving to an optimal composition for WNb-O materials ( $\text{Nb}_{0.1}\text{W}_{0.9}\text{O}_x$ ) that provide even higher activities and selectivities to PX (with PX yields  $\approx 25\%$ ) than those achieved with  $\text{WO}_3$  sample (see Figure 2).

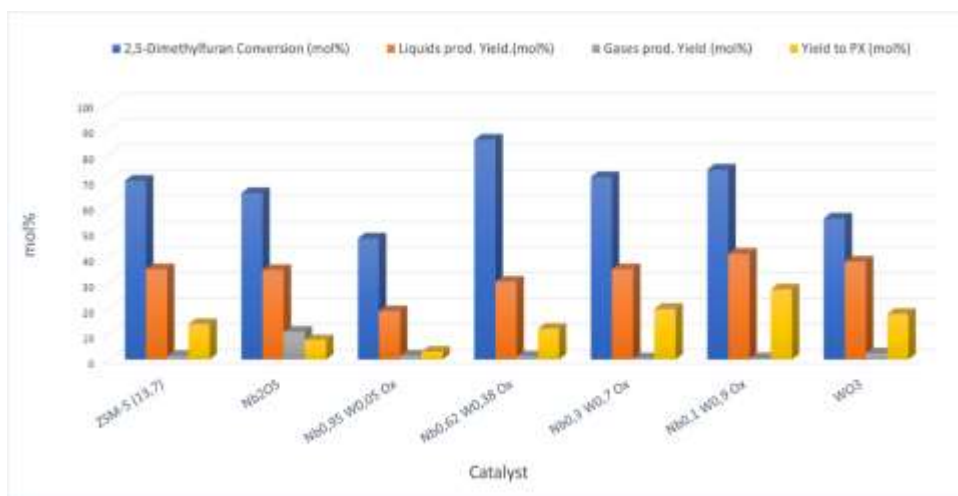


Figure 10. DMF conversion, liquids, gases and PX yields in the catalytic aromatization of DMF with ethylene over WNb-O mixed oxides (H-ZSM-5 as reference catalyst).

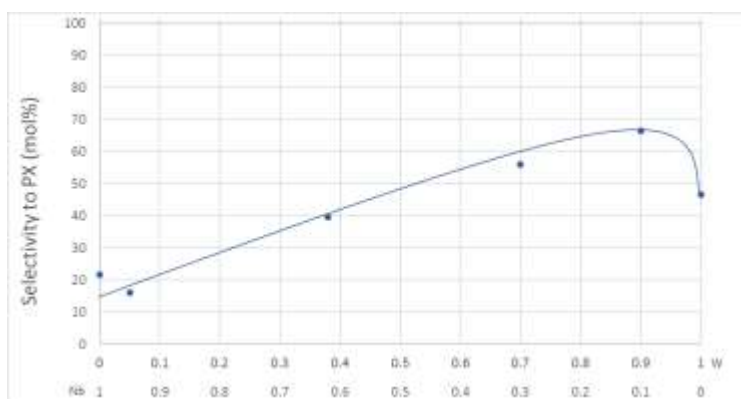


Figure 11. Effect of WNb-O mixed oxide composition on the selectivity to p-xylene (PX) desired product.

The results indicate the necessity of presence of both type of acid sites, Br and Le, to develop efficient catalysts for PX production from biomass-derived furans.  $\text{WO}_3$  based solids modified by incorporation of small amounts of Nb showed an excellent level of PX formation, even higher than that presented by the H-ZSM-5 (reference catalyst). The study of W/Nb composition in the WNb-O mixed oxides allows inferring the degree of dependence between Br/Le ratios and the catalytic performance. Moreover, correlation of the catalytic behavior observed for WNb-O materials with their acid properties evidences that not only the amount and type of acid sites, but also an adequate Br/Le acid sites ratio is needed to reach high selectivity for the desired aromatic product.

Summarizing, this work shows how the study of novel multifunctional solid catalysts with specific and controlled properties, and under adequate reaction conditions, allows developing catalytic processes to transform biomass derivatives into aromatic compounds useful as platforms for the production of numerous high value-added chemicals.

### Acknowledgements

Financial support by CSIC (COOPB 20415) and MICINN of Spanish government (PGC2018-097277-B-100) are gratefully acknowledged.

### References

1. X. Feng, C. Shen, K. Ji, J. Yin T. Tan, *Catal. Sci. Technol.*, **7** 5540 (2017).
2. J. Yin, C. Shen, X. Feng, K. Ji, L. Du; *ACS Sustainable Chem. Eng.*, **6** 1891 (2018).
3. Y.P. Wijaya, H.P. Winoto, Y-K. Park, D.J. Suh, H. Lee, J-M. Ha, J. Jae, *Catal. Today*, **293-294** 167 (2017).
4. A. Settle, L. Bertis, N. Rorrer, Y. Roman-Leshkov, G. Beckham, R. Richards, D. Vardon, *Green Chem.*, **19** 3468 (2017).
5. M.E. Domine, J.M. López Nieto, D. Delgado, A. Fernández-Arroyo, *WO 2017162900 A1* (2017).
6. D. Delgado, A. Fernández-Arroyo, M.E. Domine E. García-González, J.M. López-Nieto, *Catal. Sci. Tech.*, **9** 3126 (2019).

## Heterogeneous catalytic conversion of 5-Hydroxymethyl furfural to Methoxymethylfurfural

P. Diaz-Maizkurrena\*, J. Requies, A. Iriondo, P.L. Arias

Faculty of Engineering of Bilbao (UPV/EHU), Plaza Ingeniero Torres Quevedo, Bilbao (Spain)

\*e-mail address of corresponding author: paula.diaz@ehu.eus

Abstract text:

5-Methoxymethylfurfural (MMF) can be used as fuel or fuel additive due to its appropriate physical and chemical properties [1], in addition to this MMF can be converted into 2,5-furandicarboxylic acid, which can replace terephthalic acid as a monomer to prepare polyethylene terephthalate [2]. The MMF can be obtained by the etherification of HMF (platform molecules) using methanol as reagent, for this reaction HMF as well as methanol, both can be produced from biomass, and in the case of the methanol, is the cheapest aliphatic alcohol, therefore MMF production has significant application prospects. For MMF production acid catalysts are required. The heterogeneous acid catalysts present higher advantages than homogeneous acid catalysts, and one of the main problems associated to the use of platform molecules as raw material is the high number of reactions that can be produced.

Concretely, in this work catalytic conversion of biomass, derived 5-hydroxymethylfurfural to produce MMF have been studied. For this purpose, different zeolites were employed as catalysts: ZSM-5, CBV2314 (SiO<sub>2</sub>/Al<sub>2</sub>O<sub>3</sub> mole ratio = 23), CBV8014 (SiO<sub>2</sub>/Al<sub>2</sub>O<sub>3</sub> mole ratio = 80), CBV5524G (SiO<sub>2</sub>/Al<sub>2</sub>O<sub>3</sub> mole ratio = 50), β zeolite CP814E (SiO<sub>2</sub>/Al<sub>2</sub>O<sub>3</sub> mole ratio = 25), H-Y zeolite, H-β zeolite, MCM-41 (Si/Al=5), and MCM-41 (Si/Al=10). In addition to this, CBV2314 and ZSM-5 were also modified with the addition of 3 % of different metals such as Cu, Co and Mn by wetness impregnation methods.

All experiments were carried out in a 50 mL (±5 mL) batch-type lined with a 30 mL (±5 mL) glass vessel. The production of MMF from HMF was carried out using 15 g solution of HMF/MeOH (1/99 in wt. ratio) and 0.05 g of the selected catalyst. After loading this mixture in the reactor, it was sealed and pressurized by 2 MPa of N<sub>2</sub> and heated to the experiment temperature (from 120 °C to 220 °C). Once the reaction time has been completed, to ensure the end of the reaction, the autoclave was cooled down by placing it in an ice bath, then, the pressure was released.

The catalysts were characterized by N<sub>2</sub> adsorption-desorption isotherms, and by Temperature-programmed desorption of ammonia (TPD-NH<sub>3</sub>). The catalysts with metals, they were also characterized by inductively coupled plasma-optical emission spectroscopy (ICP-OES) to determinate the amount of metal.

All the studied catalysts presented a high surface area and low average pore diameter, (from 2.61 to 5.76). The incorporation of the Co and Cu on CBV2314 decreased a little bit the surface area, which can be attributed to the blocking of the pores by the metallic Cu and Co clusters present on the surface. Regarding the metal loading of the catalysts, the experimental value was found to be similar than the nominal one.

Table 1. BET and acidity results

Sample	S <sub>BET</sub> (m <sup>2</sup> /g)	Pore volume (cm <sup>3</sup> /g)	Average pore diameter (nm)	mmol NH <sub>3</sub> /gcat
H-Y zeolite	328.10	0.0799	3.43	0.24
H-β zeolite	324.50	0.3112	5.18	0.17
MCM – 41 Si/Al:5	n.a.	n.a.	n.a.	0.10
MCM – 41 Si/Al:10	n.a.	n.a.	n.a.	0.13
CBV8014	295.20	0.0889	2.70	0.12
CBV5524G	236.00	0.2489	5.76	0.17
CBV2314	298.90	0.0918	2.96	0.46
CBV2314+3%Co	271.00	0.0721	2.66	0.43
CBV2314+3%Cu	288.00	0.0816	2.61	0.36
CBV2314+3%Mn	n.a.	n.a.	n.a.	0.35



The acidic properties were studied by  $\text{NH}_3$ -TPD. Table 1 shows that the zeolites presented different acidity, the highest value was reached by CBV2314, with a value of 0.46 mmol  $\text{NH}_3/\text{gcat}$ . The acidity decreased when Cu was loaded onto the support. The incorporated Cu particles could be partially covering acid sites on the support, thus decreasing the catalyst's total acidity<sup>3,4</sup>. The behavior of Mn and Co incorporation was similar; therefore, similar effect can be expected.

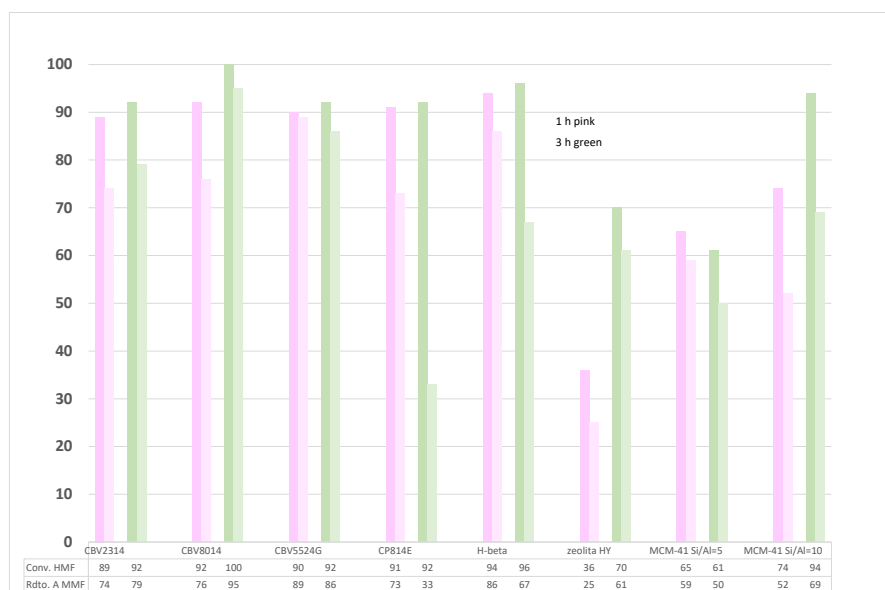


Figure 1. Activity results of the different zeolites

The best HMF conversion and MMF yield were reached for the CBV zeolites. Probably they presented an adequate porosity and acidity for this reaction. The CBV8014 presented the best results, full conversion and a yield of MMF of 95 %. The second one was the CBV5524G, although the yield decrease with the time. The last one was the CBV2314 with a conversion of HMF of 92% and a yield of 79 %. There is a clear relationship between  $\text{SiO}_2/\text{Al}_2\text{O}_3$  mole ratio and the catalyst activity and selectivity. When  $\text{SiO}_2/\text{Al}_2\text{O}_3$  mole ratio higher was increased, the activity and selectivity were also increased. This effect can be also observed in the MCM family. Therefore, it seems that the catalyst with an optimum  $\text{SiO}_2/\text{Al}_2\text{O}_3$  ratio favors the MMF yield.

## Acknowledgements

This work was supported by the University of the BasqueCountry (EHU/UPV), the Spanish Ministry of Economy andInnovation and the European Union though the EuropeanRegional Development Fund (ERDF) (projects: RTI2018-094918-B-C43)

## References

1. Viil, I.; Bredihhin, A.; Mäeorg, U.; Vares, L.RSC Adv.,4, 5689–5693 (2014)
2. Carro, J.; Fernandez-Fueyo, E.; Fernandez-Alonso, C.; Canada,J.; Ullrich, R.; Hofrichter, M.; Alcalde, M.; Ferreira, P.; Martinez, A. T.,11,86–95 (2018).
3. Zang, Z.; Liu, Y.; Liu, D.; Meng, X.; Liu, C. Hydroisomerizationof n -octane over bimetallic Ni-Cu/SAPO-11 catalysts.Appl. Catal., A,543, 274–282 (2017)
4. Fu, Z.; Wang, Z.; Lin, W.; Song, W.; Li, S. High efficientconversion of furfural to 2-methylfuran over Ni-Cu/ $\text{Al}_2\text{O}_3$ catalystwith formic acid as a hydrogen donor.Appl. Catal., A,547, 248–255 (2017)

## Catalytic conversion of tetroses to methionine hydroxy analogues

Sergio Calderon-Ardila<sup>1\*</sup>, Joost Matthijssen<sup>1</sup>, Olivier Péruch<sup>2</sup>, Didier Morvan<sup>2</sup>, Virginie Bellière-Baca<sup>2</sup>, Michiel Dusselier<sup>1\*</sup>, Bert Sels<sup>1\*</sup>

<sup>1</sup> Center for sustainable catalysis and engineering (CSCE), KU Leuven, Celestijnenlaan 200F, 3001 Heverlee, Belgium.

<sup>2</sup> Adisseo France SAS, 10 Place du Général de Gaulle, Antony, France.

\*[sergio.calderon@kuleuven.be](mailto:sergio.calderon@kuleuven.be); \*[michiel.dusselier@kuleuven.be](mailto:michiel.dusselier@kuleuven.be); \*[bert.sels@kuleuven.be](mailto:bert.sels@kuleuven.be)

### Introduction

D- and L-methionine (DL-Met) and 2-hydroxy-4-(methylthio)butyric acid (HMTBA), methionine hydroxy analogue (MHA), are key to achieve a future with zero hunger and with responsible productions of animal protein since these compounds are used to supplement animal feed to achieve optimal development and protein yields in livestock for human consumption<sup>[1]</sup> while minimizing livestock waste<sup>[2,3]</sup>. Currently, the industrial chemical synthesis of these compounds relies on non-renewable feedstock such as propylene or acrolein, making these processes rather unsustainable. The direct conversion of carbohydrates to MHAs could improve the sustainability of the processes but it has been little explored<sup>[4]</sup>. Here we present our findings concerning the conversion of tetroses to MHAs catalyzed by homogeneous and heterogeneous Lewis acid Sn catalysts.

### Experimental

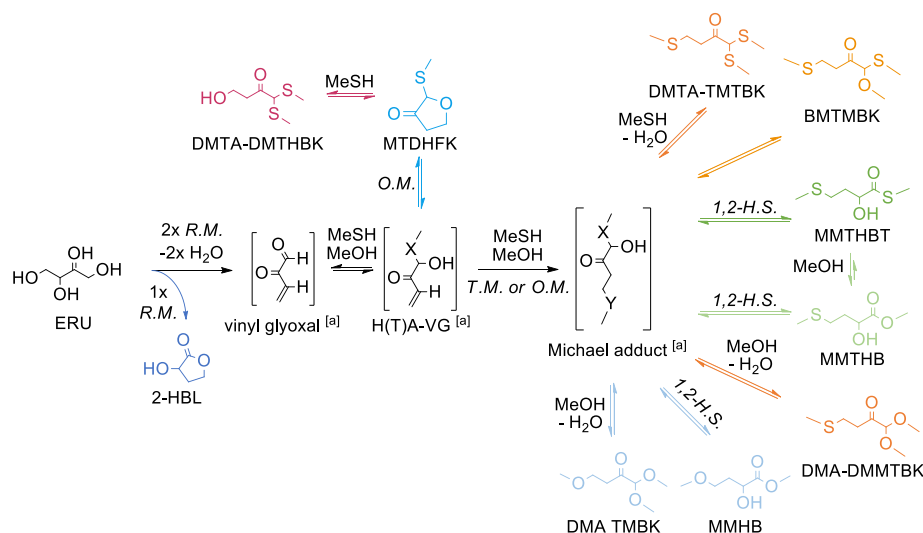
In a typical experiment at 50 mL Parr<sup>®</sup> reactor is loaded with a tetrose (7.5 mmol), Sn-BEA (790 mg equivalent to 0.12 mmol of Sn(IV)), methanol (11.88 g) and naphthalene (120 mg) that is used as internal standard. The reactor is closed, purged three times with nitrogen gas and cooled to 258 K prior to the addition of MeSH (e.g. 368.2 mg) through a mass flow controller. The reactor is pressurized to 40 bar-g with nitrogen and finally it is heated to 373 K and allowed to react for 3 hours with mechanical stirring at 800 rpm. The reaction is quenched by placing the reactor in an ice-water bath for 15 minutes. Afterwards, the reactor is depressurized, flushed three times with nitrogen gas, opened and the reaction mixture is collected for analysis. Reaction products were quantified through GC-FID and HPLC analysis. Compound characterization was performed through GC-MS and NMR spectrometry.

### Results and Discussion

In a first study, we established the main reaction pathways involved in the conversion of erythrose to sulphides of alpha hydroxy thioesters and esters (SAH(T)Es) in the presence of butanethiol and Lewis acid catalysts<sup>[5]</sup>. These SAH(T)Es are MHAs where the terminal sulphide contains a butyl chain instead of a methyl chain. We established that the formation of thioacetals was the main limiting factor for the reaction's selectivity towards SAH(T)Es. The addition of base, water or polar protic solvents to the system increased the selectivity towards SAH(T)Es and decreased the formation of thioacetals. Yield and selectivity of 23% towards SAH(T)Es were obtained in a reaction catalyzed by SnCl<sub>4</sub>·5H<sub>2</sub>O in a butanethiol/methanol mixture at 353K during 6 hours.

We also studied the conversion of tetroses to MHAs in the presence of methanethiol (MeSH), methanol (MeOH) and SnCl<sub>4</sub>·5H<sub>2</sub>O. We could corroborate that the major reaction pathways established in the presence of butanethiol also hold true for the synthesis of MHA in the presence of MeSH (see Scheme 1). These reaction pathways are coherent with the results obtained in parameter variation experiments and offered a roadmap to improve the reaction's selectivity towards MHAs. For instance, the MeSH to MeOH ratio and the water content affect the reaction performance strongly. Especially, the addition of small amounts of water to the solvent mixture increased the yield of MHAs from 24% to 38% by hindering the thioacetalization reactions involved in the formation of by-products.

Finally, we studied the conversion of tetroses to MHAs catalyzed by Sn-deAlBEA zeolites. We found that the balance between Sn Lewis acidity (LA<sub>Sn</sub>) and Al Brønsted acidity (BA<sub>Al</sub>) in the catalyst affects the selectivity towards MHAs. A Sn-deAlBEA with a LA<sub>Sn</sub> / BA<sub>Al</sub> ratio of 4 allowed to obtain the highest yield of MHAs of 39% (selectivity of 42%) at temperatures as low as 373K in reaction times as short as 3 hours (see Fig 1). We believe that this LA<sub>Sn</sub> / BA<sub>Al</sub> ratio allows a fast conversion of the tetrose to vinyl glyoxal through BA catalyzed retro-Michael reactions while LA<sub>Sn</sub> effectively catalyzes the final 1,2-hydride shift reaction needed to form MHAs. We also observed that the addition of water produced a modest increase in yield of MHAs. A kinetic profile, NMR spectroscopy of reaction mixtures and the analysis of used catalysts through pyridine probe FT-IR spectroscopy and elemental analysis by ICP-AES allowed us to establish the effects of our chemistry on the Sn-deAlBEA catalyst. We found a direct relation between thiol content in the reaction and leaching of Sn from the catalyst. We also found that the catalyst suffered a major decrease in BA and a minor decrease in LA during the course of the reaction, affecting its LA<sub>Sn</sub> / BA<sub>Al</sub> ratio and hence its catalytic activity. Catalyst regeneration proved to be effective to recover LA<sub>Sn</sub> but not BA<sub>Al</sub>.

**Scheme 3.** Reaction pathways for the Sn Lewis acid catalyzed conversion of tetroses to methionine hydroxy analogues.

[a] Intermediate not detected. X and Y are independently a sulphur or oxygen atom. R.M. = retro-Michael reaction. T.M. = Thiol-Michael reaction. O.M. = Oxa-Michael reaction. 1,2-H.S. = 1,2-hydride shift.

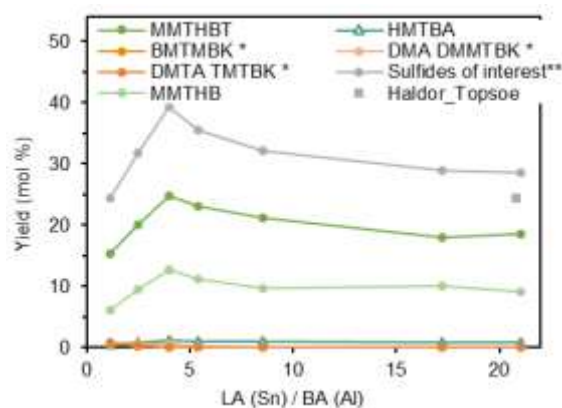


**Figure 12.** Effect of Lewis and Brønsted acidity balance in Sn-deAlBEA zeolites in the conversion of ERU to methionine hydroxy analogues during 3 hours at 373 K (ERU=1g, catalyst =0.890g, molar ratios ERU/Sn=58 and ERU/MeSH=1). Acidity quantified by FT-IR spectroscopy of adsorbed pyridine. The sulfides of interest correspond to the sum of yield of MHAs, namely MMTHB, MMTHBT and HMTBA. The square marker corresponds to the benchmark yield of MHAs obtained by Haldor Topsoe in WO 2016174231 for the conversion of ERU catalyzed by Sn-BEA (1.6 wt% Sn) at 373K during 4 hours (ERU/Sn=65).

## Conclusions

Our studies of the Sn Lewis acid catalyzed conversion of tetroses to methionine hydroxy analogues (MHAs) allowed us to establish the main reaction pathways involved in these transformations. These reaction pathways become a powerful tool to propose improvements to the selectivity of the reaction such as the addition of base or water to the reaction mixture to disfavor the formation of undesired thioacetals. Likewise, we found that an heterogeneous Sn-BEA catalyst with LA<sub>Sn</sub>/BA<sub>Al</sub> ratio of 4 allowed to obtain the highest yield of MHAs of 39% (selectivity of 42%) at temperatures as low as 373K in reaction times as short as 3 hours. This result is in agreement with our reaction pathways that suggest that some BA would favor the transformation of the carbohydrate to a crucial vinyl glyoxal intermediate through BA catalyzed retro-Michael reactions, while LA<sub>Sn</sub> catalyzes a final 1,2-hydride shift required to form MHAs. We could also establish that the presence of MeSH in the reaction mixture causes Sn leaching from the Sn-BEA catalyst. We found that the catalyst suffers a major decrease in BA and a minor decrease in LA during the course of the reaction, affecting its LA<sub>Sn</sub>/BA<sub>Al</sub> ratio and hence its catalytic activity. Catalyst regeneration proved to be effective to recover LA<sub>Sn</sub> but not BA<sub>Al</sub>.

## References

- [1] W. G. Pond, D. B. Church, K. R. Pond, P. A. Schoknecht, *Basic Animal Nutrition and Feeding*, John Wiley & Sons, Hoboken, N.J., **2004**.
- [2] W. K. Kim, C. A. Froelich, P. H. Patterson, S. C. Ricke, *Worlds. Poult. Sci. J.*, **62**, 338 (2006).
- [3] M. Alagawany, M. E. Abd El-Hack, M. Arif, E. A. Ashour, *Environ. Sci. Pollut. Res.*, **23**, 22906 (2016).
- [4] I. Sadaba Zubiri, E. Taarning, D. Tzoulaki, WO2016174231A1 (2016).
- [5] S. Calderon-Ardila, J. Matthijssen, B. Van Huffel, O. Péruch, D. Morvan, V. Bellière-Baca, M. Dusselier, B. F. Sels, *ChemCatChem*, DOI 10.1002/cctc.202101730 (2022).

# Synthesis of semi-aromatic polyamides based on renewable 2,5-furandicarboxylic acid (FDCA)

Muhammad Kamran<sup>1\*</sup>, Matthew G. Davidson<sup>1</sup>, Sicco De Vos<sup>2</sup>

<sup>1</sup> Centre for Sustainable and Circular Technologies, University of Bath, Claverton Down, BA2 7AY, UK.

<sup>2</sup> Corbion Biochem B.V., Gorinchem, The Netherlands.

\*corresponding author: m.kamran@bath.ac.uk

## Introduction

Semi-aromatic polyamides, also termed as polyphthalamides (PPAs), are high performance engineering plastics commonly employed in applications where performance at elevated temperatures is pivotal. Due to their exceptional thermomechanical properties, chemical resistance, low moisture absorption and improved dimensional stability, the use of PPAs in the automotive, electronics and oil and gas sectors is expected to grow significantly.<sup>1,2</sup> At present, most of the commercially available PPA grades are produced using terephthalic acid (TPA) and isophthalic acid (IPA) as the aromatic diacid source. Both of these monomers are derived from unsustainable petroleum resources. 2,5-furandicarboxylic acid (FDCA) which can be obtained from a variety of biobased resources, has a strong potential to be utilized as a renewable replacement to these dicarboxylic acids. However, the current synthetic approaches to produce furan-based polyamides (FPAs) have shown limitations to provide polymers with a reasonably high molecular weight having analogous properties to their petroleum-derived counterparts.<sup>3-5</sup> In this work, we have investigated an environmentally benign approach towards the synthesis of high molecular weight FPAs using a solvent-free melt polymerization technique in the presence of various organometallic catalysts.

## Materials and Methods

In a typical run, equimolar amounts of dimethyl furan-2,5-dicarboxylate (DMFDC) and the respective diamine, e.g., hexamethylenediamine (HMDA) for PA6F; were weighed into a vial with magnetic stirrer. Calculated amount of the catalyst was injected from a stock solution. After transferring all the reactants, vials were sealed and purged with dry argon. Sealed vials were then placed into the reactor heating block. For the oligomerization step, the reaction was performed at a pre-determined temperature and time until the mixture solidified. In the polycondensation step, the vials were placed within the same reactor but fitted with an external argon / vacuum distillation assembly. After sealing the reactor, cycles of vacuum and argon were applied to ensure no oxygen was left in the system. Heating was started initially under argon. The contents were heated to a desired temperature and the pressure was reduced to less than 1 mbar. Reaction was carried out under these conditions for 5 hours. Finally, argon was introduced into the reactor and sample vials were removed for analysis without purification.

## Results and Discussion

Synthesis of poly(hexamethylene furanamide) (PA6F) was carried out as a model biobased semi-aromatic furanic polyamide. A range of environmentally benign, inexpensive and commercially available catalysts were tested following a two-step melt polymerization approach in the absence of any solvent. The initial catalyst screening revealed that incorporation of titanium-based catalysts, such as titanium (IV) isopropoxide (TIPT) and titanium (IV) citrate (TIC) can significantly improve the molecular weight and glass transition temperature of the ensued PA6F polymer when compared with uncatalyzed sample (Figure 1).<sup>6</sup> Following this approach, PA6F polyamide having a  $M_n \sim 15 \text{ kg mol}^{-1}$  and  $M_w \sim 46 \text{ kg mol}^{-1}$  was produced using very low catalyst loadings. To the best of our knowledge, such molecular weights for PA6F synthesised by melt polymerization procedure, have not been reported elsewhere. The PA6F polymer synthesised in this study also showed a significantly high  $T_g$  ( $\sim 130 \text{ }^\circ\text{C}$ ) in comparison to those synthesised using conventional nylon-salt route and other solvent-based methods. The synthesis protocol was subsequently applied to other FPAs utilizing various aliphatic diamines differing in their carbon chain lengths. Consistently, high molecular weight FPAs were obtained. In most cases, these FPAs exhibited promising properties that were comparable to their petroleum derived counterparts (Figure 2).

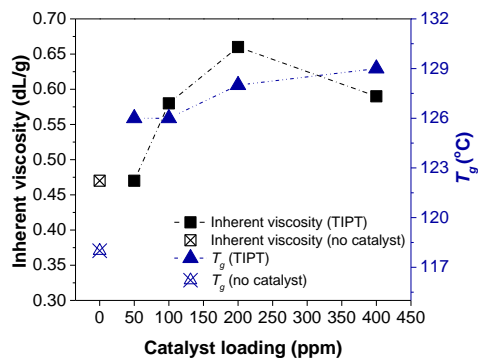


**Figure 1.** Inherent viscosity and glass transition temperatures ( $T_g$ ) for PA6F samples synthesised without any catalyst and titanium isopropoxide.

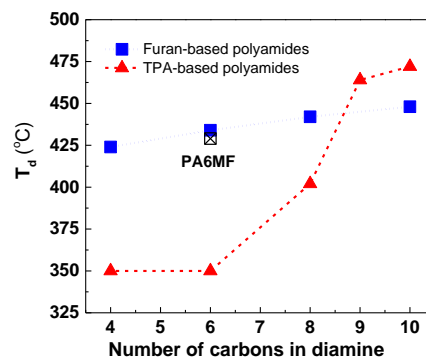


**Figure 2.** Thermal degradation temperature ( $T_d$ ) comparison of furan-based polyamides (FPAs) and TPA based semi-aromatic polyamides possessing different chain length diamines.

## Significance

The incorporation of renewable monomers, such as FDCA, into the polymer backbone is highly desirable in the transition towards more sustainable resources. This study provides insights into an elegant approach to produce furan-based semi-aromatic polyamides with high molecular weight and interesting properties via a catalytic melt polymerization technique. The straightforward and environmentally friendly synthesis approach presents an attractive concept for the industrial-scale manufacturing of FPAs.

## References

1. Zhang, C. *e-Polymers* **2018**, *18*, 373.
2. Kemmish, D. J. In *Practical Guide to High Performance Engineering Plastics*; Smithers Rapra, **2011**; pp 47.
3. Fehrenbacher, U.; Grosshardt, O.; Kowollik, K.; Tübke, B.; Dingenouts, N.; Wilhelm, M. *Chemie Ing. Tech.* **2009**, *81*, 1829.
4. Cousin, T.; Galy, J.; Rousseau, A.; Dupuy, J. *J. Appl. Polym. Sci.* **2018**, *135*, 1.
5. Cao, M.; Zhang, C.; He, B.; Huang, M.; Jiang, S. *Macromol. Res.* **2017**, *25*, 722.
6. Kamran, M. Towards sustainable engineering plastics: Synthesis and characterisation of semi-aromatic polyamides based on renewable 2,5-furandicarboxylic acid (FDCA), PhD thesis, University of Bath, **2021**.

## Conversion of biomass derived levulinic acid into $\gamma$ -valerolactone using methanesulfonic acid: An optimization study using response surface methodology

Lethiwe D. Mthembu<sup>1\*</sup>, David Lokhat,<sup>2</sup>Rishi Gupta,<sup>3</sup> and Nirmala Deenadayalu<sup>1</sup>

<sup>1</sup>Department of Chemistry, Durban University of Technology, Steve Biko Road, Berea, Durban, 4001, South Africa.

<sup>2</sup>Discipline of Chemical Engineering, University of KwaZulu-Natal, Durban 4041, South Africa.

<sup>3</sup>Anton Paar India Pvt Ltd., Udyog Vihar, Gurugram, Haryana, India.

\*lethiwem@dut.ac.za

Biomass derived levulinic acid (LA) can act as a platform chemical for the development of other secondary chemicals such as  $\gamma$ -Valerolactone (GVL), which subsequently can be used for the synthesis of biofuels and biochemicals. To the best of our knowledge, this is the first study to optimize the effect of various process conditions on GVL production from LA using methanesulfonic acid (MsOH). The process parameters comprising temperature (25-200 °C), time (2-10 h), and catalyst loading (0.5-5 g) were investigated for the GVL production from LA. Under optimized conditions, LA derived from depithed sugarcane bagasse (DSB) was able to yield 77.6% GVL. The hydrogen required for the reduction of LA to GVL was formed in-situ by formic acid and triethylamine in the presence of MsOH. Besides, process conditions, different solvents (including water and alcohols) were also tested to determine their effect on GVL yield, and out of which, water yielded the highest GVL conversion of 78.6 %. An attempt was also made to study the impact of different types of catalysts (mineral acids and ionic liquids) on GVL yield, and to develop a benchmark against MsOH. Figure 1 illustrates the reaction steps of GVL production from depithed sugarcane bagasse (DSB), the first reaction includes the production of LA from DSB using 1-ethyl-3-methylimidazolium hydrogen sulfate [EMim][HSO<sub>4</sub>] as a catalyst and the second reaction include the production of GVL from LA using methanesulfonic acid (MsOH) as a catalyst, and formic acid as the hydrogen donor with trimethylamine (Et<sub>3</sub>N) as a stabilizer.<sup>[1,2]</sup>

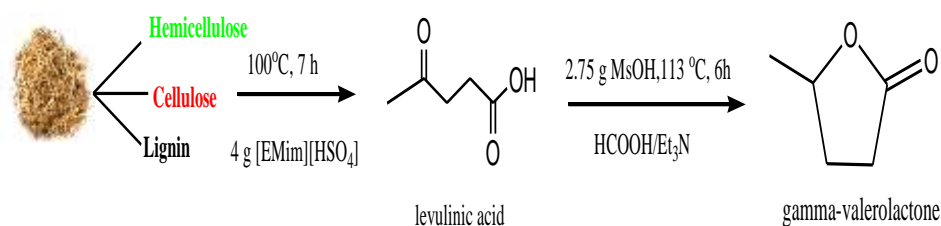


Figure 1. GVL production from LA derived from DSB

### Acknowledgements

The authors are grateful to Council for Scientific and Industrial Research (CSIR) Forestry and Forest Products Research Centre, Durban for the facility to upscale levulinic acid production from depithed sugarcane bagasse. National Research Foundation (NRF), Durban University of Technology, and L'Oréal-UNESCO for Women in Science Sub-Saharan Africa Regional fellowships for financial support.

### References

1. C. Ortiz-Cervantes, J.J. Garcia, *Inorg. Chim. Acta*, **397**, 124-128 (2013).
2. L.D. Mthembu, D. Lokhat, R. Gupta, N. Deenadayalu, *Waste Biomass Valor*, **12**, 199-209 (2021).

## Promotion of hydroxy bond hydrogenolysis versus aromatic ring hydrogenation by selective poisoning with chlorine of heterogeneous Cu-Co catalysts

Alberto Barranca<sup>1</sup>, Iker Agirrezabal-Tellería<sup>1</sup>, Pedro L. Arias<sup>1</sup>, Marcos Rellán-Piñeiro<sup>2</sup>, Manuel A. Ortuño<sup>2</sup>, I. Gandarias<sup>1\*</sup>

<sup>1</sup>Faculty of Engineering Bilbao. University of the Basque Country (UPV/EHU). Plaza Ingeniero Torres Quevedo 1. 48013 Bilbao (Spain). <sup>2</sup>Centro Singular de Investigación en Química Biolóxica e Materiais Moleculares (CIQUS), Universidade de Santiago de Compostela, 15782 Santiago de Compostela, Spain

\*inaki.gandarias@ehu.eus

### Abstract text:

Hydrogenation reactions are common for the valorization of biomass derived platform chemicals, such as furfural (FUR), 5-(hydroxymethyl)furfural (5-HMF) or lignin derived compounds, in order to decrease their O/C ratio [1]. In these upgrading processes, selectivity is very relevant as the C-O bond hydrogenolysis competes with the hydrogenation of aromatic ring. 2-methylfuran (2-MF) is a biomass derived molecule with uses as pesticide, antimalarial drug, and in the cosmetic industry [2]. It is also considered an excellent gasoline bio-additive due to its high octane number (103) and heat capacity [3]. The reaction route (Figure 1) involves the initial furfural hydrogenation into furfuryl alcohol (FAL). Subsequently, hydrogenolysis of the hydroxy group gives rise to 2-MF (route 1). This route competes with the hydrogenation of the furanic ring (route 2), which produces tetrahydrofurfuryl alcohol (THFA), which, in turn, can be transformed into pentanediols (1,5- and 1,2-PDO) through a ring-opening hydrogenolysis of the C-O bond. Ring hydrogenation derived products (RHDP), i.e. THFA and PDOs, are gathered together for a better discussion of the selectivity results.

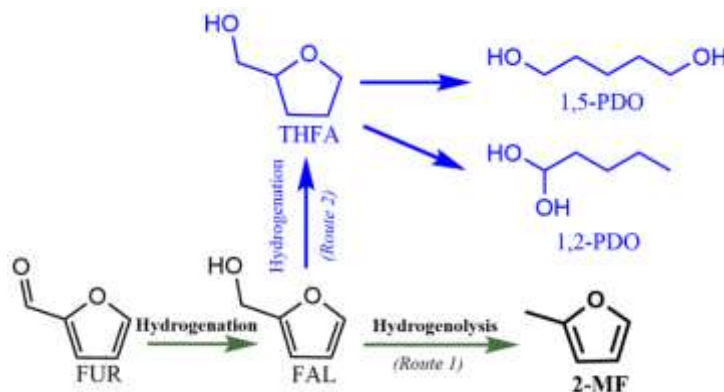


**Figure 1.** Reaction routes for the transformation of furfural into 2-methylfuran and into main byproducts. Compounds in blue (route 2) are gathered under the acronym RHDP (Ring Hydrogenation Derived Products).

Herein, we analyze surface chlorine effect on the activity and selectivity of Cu-Co catalysts supported on  $\gamma$ -Al<sub>2</sub>O<sub>3</sub>. Two different sources of chlorine were studied. First, bimetallic catalysts with a total fixed nominal metal content of 35 wt.% were prepared from different salts, chlorides and/or nitrates by the wetness impregnation technique. These catalysts are named as Cu<sup>(Cl/N)</sup>-Co<sup>(Cl/N)</sup>, "Cl" refers to the chloride precursor and "N" to the nitrate precursor. Next, and in order to tune the surface chlorine content, different concentrations of HCl aqueous solution, i.e. 0.25 M, 0.50 M and 1.00 M, were used during the wet impregnation of the precursors on the support. All the catalysts were treated under the same calcination and pre-reduction conditions. The activity tests were carried out in 50 mL batch reactors at different reaction temperatures and an initial hydrogen pressure of 30 bar. Prepared catalysts were characterized by XRD, XPS, TPR and TPD-NH<sub>3</sub>. Moreover, Periodic Density Functional Theory (DFT) calculations were carried out with the Vienna Ab-Initio Simulation Package (VASP) [4].

Figure 2.A depicts the relationship between the selectivity, or the 2-MF yield, and the surface Cl wt.% (measured by XPS) for all the bimetallic catalysts tested. For the Cu<sup>N</sup>-Co<sup>N</sup> catalyst (0 wt% residual chlorine in the surface), the RHDP/2-MF ratio is higher than one, indicative that the aromatic ring hydrogenation is favored. In contrast, for all the catalysts with surface chlorine, which were prepared using at least one chlorine salt and/or HCl in the impregnating step, this ratio is practically zero. These results indicate that surface chlorine inhibits the ring hydrogenation reactions.

For a better understanding of these activity test results, DFT calculations were performed on ferromagnetic Co(111) and Co(0001) slabs, and examined the adsorption of FUR and FAL under different coverages of Cl. FAL can interact with the catalyst surface via flat (label **a**) or tilted (label **b**) adsorption modes. In the absence of Cl ( $\theta = 0.00$ ), configuration **a** is clearly favored over **b** by 0.84 eV. The same scenario is found when one Cl ( $\theta = 0.06$ ) is included (Figure 2B), obtaining a difference of 0.80 eV. Interestingly, this trend dramatically changes at higher coverages. With four Cl, both configurations are almost isoenergetic, being **a** favored over **b** by only 0.20 eV. With five Cl (Figure 2B), the trend is eventually reversed, and **b** is now preferred over **a** by 0.63 eV. We expect that **a**

would lead to hydrogenation and possibly opening of the aromatic ring, while **b** would result in reactivity focused on the aldehyde (alcohol) group of FUR (FAL).

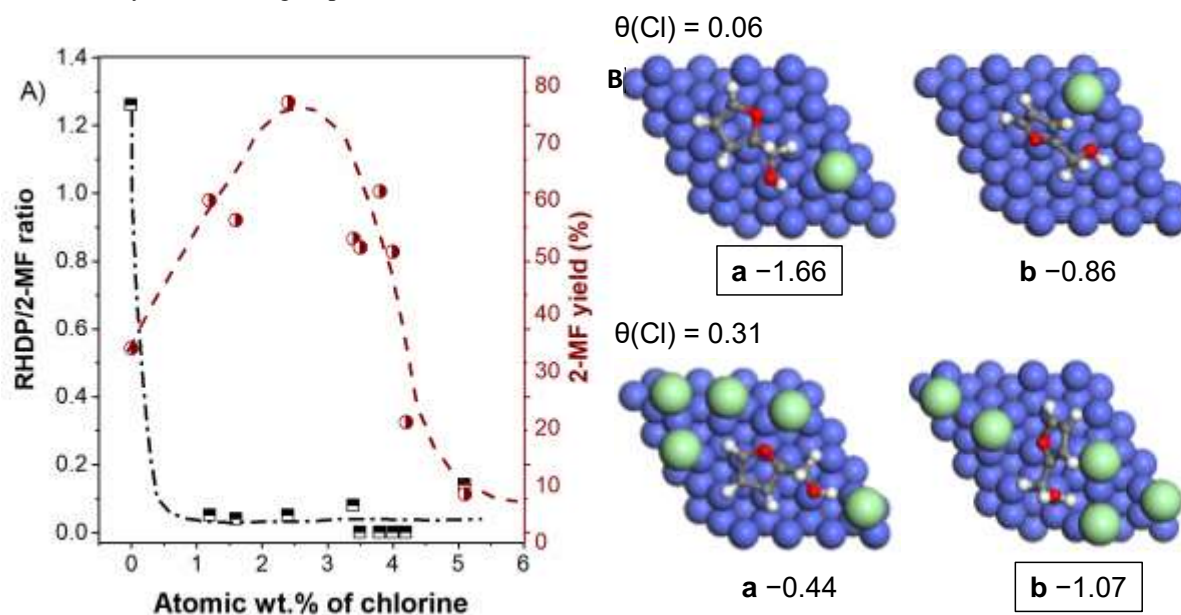


**Figure 2.** A) Effect of surface chlorine (wt%) on RDHP/2-MF ratio and on 2-MF yield for all tested bimetallic catalysts. 453 K, 3 MPa hydrogen,  $0.125 \text{ g}_{\text{cat}} \text{ g}_{\text{FUR}}^{-1}$ , 3.5 h reaction time and 2-MTHF solvent. B) Structures and adsorption energies (in eV) of FAL on Co(111) at different Cl coverages. Atom legend: Co (blue), Cl (green), O (red), C (grey), H (white).

In order to relate activity test results and DFT calculations, it has to be considered that the surface  $\text{Cl}/(\text{Cu}+\text{Co})$  ratio for the nine catalysts presenting chlorine lies between 0.31 to 0.67. Therefore, they all presents  $\theta(\text{Cl})$  coverages for Co near or above 0.31, in which the tilted FAL adsorption mode is favored. In contrast, the  $\text{Cu}^{\text{N}}\text{-Co}^{\text{N}}$  catalyst, with a  $\theta$  coverage value of zero, will favor the flat FAL adsorption and the formation of RHDP.

2-MF yield and the atomic Cl content (wt.%) follows a volcano-shaped data distribution (Figure 2A), with a maximum around 2-3 wt.% of Cl. For surface Cl values above 4 wt.%, the 2-MF yield significantly reduces. Hence, there is an optimum surface chlorine content that maximizes 2-MF yield. The presence of chlorine in the catalyst affects the Cu/Co interactions, as confirmed by XRD. When one or two chloride metal precursors were used in the synthesis of the catalysts, there was a displacement of the diffraction peak identified as Cu/Co phase towards 2-theta positions closer to Co(C), and isolated hexagonal and cubic Co phases were detected. Surface chlorine, coming either from the precursor or from HCl, also affected the TPR profiles of the calcined catalysts, and there was an increment in the reduction temperature of cobalt. The presence of surface chlorine might reduce the hydrogen activation capacity of copper, and/or the spillover of hydrogen atoms from copper to cobalt.

In summary, there is an optimum surface chlorine value in which the adsorption mode of FAL changes from flat to tilted, which favor the transformation of FUR and FAL into 2-MF, but it is not high enough to negatively affect the Cu-Co interactions and the activation of molecular hydrogen. The amount of surface chlorine can be tuned by adjusting the concentration of HCl during the synthesis of the catalyst.

## Acknowledgements

This work was supported by the University of the Basque Country (UPV/EHU), European Union, through the European Regional Development Fund (ERDF) (Spanish MINECOR Project: RTI2018-094918-BC43), and the Basque Government (IT993-16).can be mentioned here.

## References

- 1 Y.S. Yun, C.E. Berdugo-Díaz, D.W. Flaherty, *ACS Catal*, **11** 11193–11232 (2021).
- 2 R. Mariscal, P. Maireles-Torres, M. Ojeda, I. Sádaba, M. López Granados, *Energy Environ. Sci*, **9** 1144–1189 (2016).
- 3 J.P. Lange, E. van der Heide, J. van Buijtenen, R. Price, *ChemSusChem*, **5** 150–166 (2012).
- 4 G. Kresse, J. Furthmüller, *Phys. Rev. B*, **54** 11169–11186 (1996).



## CO<sub>2</sub> utilization

## Effect of Ni Particle Size in the Low-Temperature CO<sub>2</sub> Hydrogenation Over Highly Active Ni/CeO<sub>2</sub>-Nanorods

<sup>1\*</sup> Georgios Varvoutis, <sup>2</sup> Maria Lykaki, <sup>2</sup> Sofia Stefa, <sup>1,3</sup> George E. Marnellos, <sup>2</sup> Michalis Konsolakis

<sup>1</sup> Department of Mechanical Engineering, University of Western Macedonia, Kozani, Greece

<sup>2</sup> School of Production Engineering and Management, Technical University of Crete, Chania, Greece

<sup>3</sup> Chemical Process & Energy Resources Institute, Centre for Research & Technology Hellas, Thessaloniki, Greece

\* gvarvoutis@uowm.gr

### Abstract

The structure sensitivity of CO<sub>2</sub> hydrogenation reaction was explored over nickel particles (10-25 nm) supported on CeO<sub>2</sub> nanorods. An optimum Ni particle size of 20 nm was revealed, with the corresponding sample demonstrating remarkable activity, i.e., 187 μmol CH<sub>4</sub>·g<sup>-1</sup>·s<sup>-1</sup> and 92% CH<sub>4</sub> yield at 275 °C, which is among the highest ever reported. Notably, the intrinsic activity on the basis of the exposed Ni sites or Ni-ceria perimeter is largely independent of the Ni size, showcasing that neither the exposed Ni sites nor the Ni-ceria interface can be employed as activity descriptors. A compromise between the length of the metal-support perimeter and the competitive presence of larger Ni particles is necessary for the optimum activity. On the grounds of a structure-sensitivity analysis, the superior activity of larger Ni particles could be attributed to the presence of under-coordinated step and kink sites, instead of largely inactive terrace sites.

### Introduction

The coupling of a Carbon Capture and Utilization process with a RES-powered water electrolysis unit producing H<sub>2</sub> can potentially provide an integrated scheme that not only prevents large amounts of CO<sub>2</sub> from being released into the atmosphere, but at the same time it exploits the intermittency of renewable energy generation by eventually storing it into chemicals like synthetic natural gas [1]. A multitude of catalysts has been studied for CO<sub>2</sub> methanation, though CeO<sub>2</sub> nanoparticles in particular are widely employed as catalytic support, owing to enhanced characteristics like oxygen storage capacity, oxygen mobility, strong metal-support interactions and interchangeability between Ce<sup>3+</sup> and Ce<sup>4+</sup> [2]. However, there still exists great ambiguity in the literature regarding the effect of Ni particle size, given the contradicting reports of both hindrance [3] and enhancement [4] of the CO<sub>2</sub> methanation activity by an increase in Ni size. In light of the above, in our previous work [5] we demonstrated the superiority of a nickel catalyst supported on CeO<sub>2</sub> nanorods compared to Cu, Co or Fe. Herein, we report on the further fine-tuning and structure-sensitivity of Ni-ceria samples by exploring the effect of Ni particle size and interphase of Ni catalysts supported on ceria nanorods with variable Ni loadings.

### Materials and Methods

Bare ceria nanorods (CeO<sub>2</sub>-NR) were synthesized in our previous work [5]. Subsequently, nickel was added into CeO<sub>2</sub>-NR via the wet impregnation method, by employing various Ni/Ce atomic ratios of  $x = 0.10, 0.25, 0.50, 1.00, 1.50$ , through appropriate amounts of Ni(NO<sub>3</sub>)<sub>2</sub>·6H<sub>2</sub>O. The as-obtained powders were dried at 90 °C overnight, calcined at 500 °C for 2h under static air and were reduced at 400 °C for 1 h under pure H<sub>2</sub> and are designated as NiCe- $x$ . The samples were characterized by N<sub>2</sub> physisorption, ICP-AES, XRD, Raman Spectroscopy and TEM. Catalytic evaluation experiments were conducted at 1 bar and in the temperature range of 200-450 °C in a quartz fixed-bed U-shaped reactor, placed inside a temperature-controlled furnace. The reactant gases were fed at a ratio H<sub>2</sub>:CO<sub>2</sub> = 4 and at WHSV of 30, 60 or 120 L·g<sup>-1</sup>·h<sup>-1</sup>. The analysis of the gases was performed by a gas chromatograph, while a cold trap submerged in a water bath was connected to the reactor effluent for water condensation.

### Results and Discussion

The results of the physicochemical characterization of the as-prepared samples are summarized in Table 1. More specifically, the actual Ni loading was very close to the nominal values, whereas the BET surface area decreased monotonically with increasing Ni loading. Also, the lattice parameter of ceria (calculated from XRD) is lower for all NiCe- $x$  samples. Interestingly, the reduction is drastic in the case of NiCe-0.10, followed by a slight expansion upon further increasing nickel content. Moreover, the oxygen vacancy concentration was calculated by the I<sub>D</sub>/I<sub>F2g</sub> ratio from Raman spectroscopy and it was observed that Ni addition into ceria significantly increases the formation of oxygen vacancies, although the values are more or less constant for  $x \geq 0.25$ . Besides, TEM analysis confirmed the distinct nanorod shape of ceria in all samples, along with a progressive increase in Ni particle size by increasing Ni loading, leading to decreased dispersion values. Also, HR-TEM confirmed the presence of cuboctahedral-like Ni particles submerged into CeO<sub>2</sub> nanorods.

Table 1. Physicochemical characterization results of the as-prepared samples.

Sample	Ni loading (wt. %)	BET surface area (m <sup>2</sup> /g)	Lattice parameter CeO <sub>2</sub> (111) (nm)	I <sub>D</sub> /I <sub>F2g</sub>	Ni particle size (nm)	Ni dispersion (%)
CeO <sub>2</sub> -NR	-	79.2	0.5430	0.08	-	-
NiCe-0.10	3.6	76.9	0.5406	0.22	9.7	10.4
NiCe-0.25	8.0	72.0	0.5408	0.62	10.4	9.7
NiCe-0.50	13.8	65.3	0.5407	0.60	14.4	7.1
NiCe-1.00	23.5	56.5	0.5408	0.66	20.3	5.0
NiCe-1.50	32.5	51.3	0.5410	0.68	24.6	4.1

The results from catalytic experiments are presented in Figure 1a. For the sake of comparison, complementary experiments were conducted over commercial CeO<sub>2</sub> and NiO samples. The beneficial effect of Ni addition onto CeO<sub>2</sub>-NR is evident, since a drastic improvement in the catalytic activity was demonstrated for all NiCe-x samples, even in the case of the catalyst with the lowest nickel loading, namely NiCe-0.10. The observed CH<sub>4</sub> yield trend indicates the existence of an optimum Ni loading equal to 23.5 wt. % (Table 1). Noteworthy, in the case of NiCe-1.00, CH<sub>4</sub> yield reached its maximum value of ca. 92% at 275 °C, which is among the best CO<sub>2</sub> methanation performances in relevant nickel-ceria systems in the literature. Besides CH<sub>4</sub>, CO and light olefins were also detected at minor quantities. Furthermore, the intrinsic characteristics and structure sensitivity of the as-prepared Ni/CeO<sub>2</sub> catalysts was examined. Noteworthy, the site time yield values are almost independent of the Ni loading (Figure 1b), showcasing that the population of the exposed Ni sites alone is not a descriptor for the differences in the catalytic activity. However, the STY values normalized by a single Ni crystallite site (STY<sub>b</sub>) shown in Figure 1c perfectly match the catalytic results, demonstrating the high intrinsic activity of the samples with larger Ni particle size, even when accounting for the differences in the total perimeter between Ni and ceria induced by the variabilities in the content and dispersion of the nickel phase. The latter is better depicted in Figure 1d, where the mass-normalized reaction rates are plotted as a function of the length of the Ni-CeO<sub>2</sub> perimeter.

## Conclusions

The as-synthesized NiCe-1.00 sample, with a Ni particle size of 20 nm, exhibited a remarkable low-temperature catalytic activity, attaining 92% CH<sub>4</sub> yield at 275 °C and a WHSV of 120 L·g<sup>-1</sup>·h<sup>-1</sup>, one of the highest rates ever reported in the literature. Also, structure-sensitivity analysis revealed that neither the exposed Ni surface area nor the total nickel-ceria perimeter can be directly correlated with the catalytic activity. However, although the existence of larger Ni particles inevitably decreased the length of the Ni-CeO<sub>2</sub> periphery, the values for the site time yield expressed in terms of a single Ni crystallite was maximized at ca. 20 nm, in complete agreement with experimental results. Thus, a compromise between the general increase in the metal-support perimeter and the competitive presence of larger Ni particles is necessary for optimum catalytic activity. In any case, the original findings of the present work may be used as a starting point for the fine-tuning of Ni-CeO<sub>2</sub> catalysts with optimum characteristics for the low-temperature CO<sub>2</sub> methanation, via adjusting catalytic features such as the Ni particle size, the length of metal-support interface and the distribution of the more active localized sites upon the catalyst's surface.

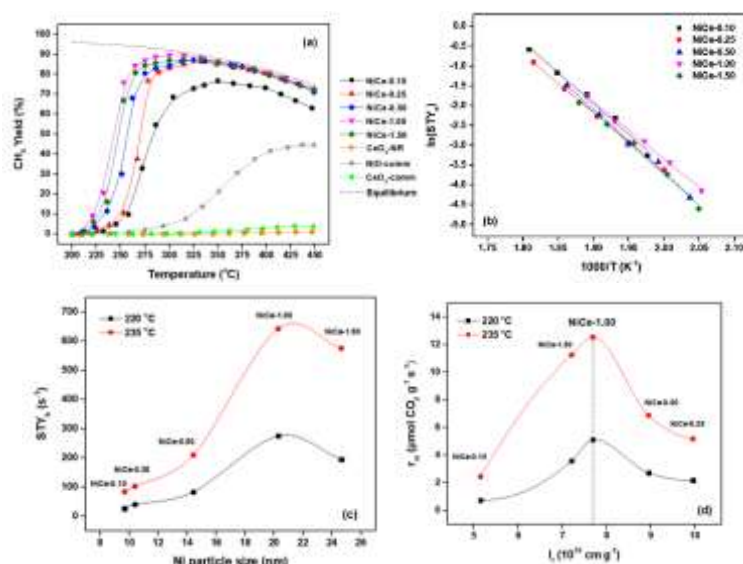


Figure 1. (a) Catalytic evaluation results, (b) Arrhenius plots, (c) Ni crystallite-normalized STY vs. Ni particle size, (d) reaction rates as a function of the nickel-ceria interface perimeter.

## Acknowledgments

This research has been co-financed by the European Union and Greek national funds through the Greece 2.0 National Recovery and Resilience Fund, under the call RESEARCH - CREATE - INNOVATE (project code: T2EDK-01378).

## References

1. D. Hidalgo, J.M. Martin-Marroquin, *Renew. Sustain. Energy Rev.* **132** 110057 (2020).
2. K. Chang, H. Zhang, M.J. Cheng, Q. Lu, *ACS Catal.* **10** 613-631 (2020).
3. Z. Hao, J. Shen, S. Lin, X. Han, X. Chang, J. Liu, M. Li, X. Ma, *Appl. Catal. B, Environ.* **286** 119922 (2021).
4. C. Vogt, E. Groeneveld, G. Kamsma, M. Nachtegaal, L. Lu, C.J. Kiely, P.H. Berben, F. Meirer, B.M. Weckhuysen, *Nat. Catal.* **1** 127-134 (2018).
5. G. Varvoutis, M. Lykaki, S. Stefa, E. Papista, S.A.C. Carabineiro, G.E. Marnellos, M. Konsolakis, S.A.C. Carabineiro, *Catal. Commun.* **142** 106036 (2020).

## Low temperature CO<sub>2</sub>-assisted ethane dehydrogenation for ethylene production: chemical looping vs cofeeding

Stavros A. Theofanidis<sup>1,\*</sup>, Emmanuelle de Clermont Gallerande<sup>2</sup>, Anastasia Christodoulou<sup>1</sup>,  
Alessandro Longo<sup>2,3\*</sup>, Maria Tasioula<sup>1</sup>, Christoph Sahle<sup>2</sup>, Angeliki A. Lemonidou<sup>1</sup>

<sup>1</sup>Department of Chemical Engineering, Aristotle University of Thessaloniki, University Campus, 54124 Thessaloniki, Greece, <sup>2</sup>ID20 beamline, European Synchrotron Radiation Facility, 71, avenue des Martyrs, CS 40220, 38043 Grenoble Cedex 9, France, <sup>3</sup>Istituto per lo Studio dei Materiali Nanostrutturati (ISMN)-CNR, UOS Palermo, Via Ugo La Malfa, 153, 90146 Palermo, Italy.

\*stheofan@cheng.auth.gr; \*alessandro.longo@esrf.fr;

### Introduction

Ethylene is a widely-used petrochemically derived monomer, with an annual estimated production growth of 2.4%, due to the population increase and the rising living standards. It is a valuable building block for many chemicals ranging from solvents to plastics. Nowadays, the non-catalytic steam cracking of naphtha is considered as the dominant process for ethylene production, mainly due to the “economy of scale” [1]. However, the abundance of the stranded gas reserves, combined with the so-called “shale gas revolution”, have revitalized the research interest for the employment of underutilized ethane towards the “*on-purpose*” ethylene production routes. The use of oxygen as an oxidant for the ethane dehydrogenation (EDH) process has been extensively investigated in literature, due to the exothermicity of the reaction [2]. However, the use of oxygen results in low ethylene yields due to the undesired total oxidation reactions towards CO<sub>x</sub>. CO<sub>2</sub> can act as a soft oxidant for EDH, shifting the thermodynamic equilibrium through H<sub>2</sub> consumption via the reverse water gas shift (RWGS) reaction. Utilization of CO<sub>2</sub> from large stationary points is in alignment with EU green deal and can significantly contribute to CO<sub>2</sub> emissions curbing towards 2050. Iron- and/or nickel- oxide based catalysts, supported on different oxides, have been previously investigated for the tandem reactions of EDH and CO<sub>2</sub> reduction elucidating the role of an interface between iron oxide and nickel oxide [3, 4]. The latter interface was found to contribute to the enhanced performance. The goal of this study is to *unravel the role of gaseous feedstock admission mode* over an environmentally-friendly iron-oxide catalyst at 600°C: chemical looping vs cofeeding. In chemical looping, a conventional catalytic reaction is decoupled into sub-reactions with intermediates that react and are regenerated in a cyclic way. The latter reactions make use of a metal oxide (e.g., iron oxide) as oxygen storage material (OSM) (reduced form: M; oxidized form: MO), supplying lattice oxygen to the reductant (e.g., C<sub>2</sub>H<sub>6</sub>). The lattice oxygen is then replenished by the gas phase oxidant (e.g., CO<sub>2</sub>). Since the global reaction is split into two, the reduced and oxidized products can inherently be separated by performing the two reactions at two different points in time or space [5].

### Materials and methods

One pot synthesis protocol: 14wt% Fe<sub>2</sub>O<sub>3</sub>-10wt% NiO-MgO-ZrO<sub>2</sub> catalyst was prepared using a *sol-gel auto-combustion method*. The catalyst was calcined under constant air flow at 800°C for 5h, hereafter named “fresh” FeNiMgZr. Two-steps synthesis protocol: 10wt% NiO-MgO-ZrO<sub>2</sub> support materials were prepared using a *sol-gel auto-combustion method*. The support was calcined under constant air flow at 800°C for 4h. At second step, 14 wt% Fe<sub>2</sub>O<sub>3</sub> was deposited on the abovementioned support by wetness impregnation. The catalyst was calcined under constant air flow at 700°C for 5 h, hereafter named “fresh” Fe/NiMgZr.

### Catalyst characterization: X-ray Raman Spectroscopy (XRS - ID20 ESRF)

All XRS data were gathered at the beamline ID20 of the ESRF (Grenoble, France). The pink beam from four U26 undulators was monochromatized, using a cryogenically cooled Si (111) monochromator and focused to a spot size of approximately 10 μm × 20 μm (V × H) at the sample position using a mirror system in Kirkpatrick-Baez geometry. The large solid angle spectrometer at ID20 was used to collect XRS data with 36 spherically bent Si (660) analyzer crystals. All measurements at O K- and Mg L<sub>2,3</sub>-edges were collected at room temperature.

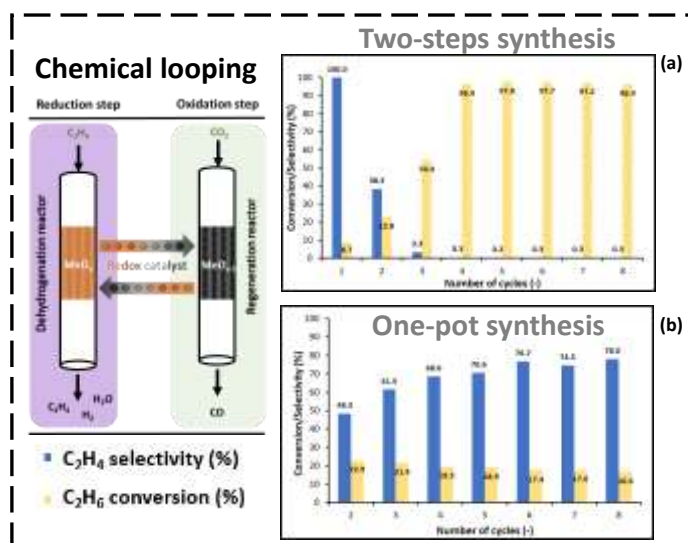
### Catalytic tests

Chemical looping activity measurements were performed at 600°C and atmospheric pressure, in a U-shaped quartz fixed bed reactor, which was housed inside an electric furnace. A sample with particle size fraction 106-180 μm was diluted with inert SiC (~180 μm) for improved heat conductivity. A mixture of 10 vol% C<sub>2</sub>H<sub>6</sub> + Ar and CO<sub>2</sub>+Ar (CO<sub>2</sub>:C<sub>2</sub>H<sub>6</sub> = 1:1, Ar internal standard) were applied during the CO<sub>2</sub>-EDH chemical looping, reaching a W<sub>cat</sub>/F<sub>tot</sub> = 11 kg·s·mol<sup>-1</sup>, while the reactor outlet was analyzed using a calibrated quadrupole OmniStar Pfeiffer mass spectrometer (MS). MS signals were recorded for all major fragments. A correction was applied to remove contributions from unavoidable interference with fragmentation peaks of other gases.

Steady state activity measurements were performed in a quartz fixed bed reactor under the same applied conditions with the chemical looping tests. The reactor outlet leads to an Agilent® 7890A GC system for online analysis, equipped with one TCD and two in-series columns: Porapaq Q and Molecular Sieve 5A. Conversions and selectivities were calculated on a carbon basis. Closure of the carbon mass balance was better than ±2%.

## Results and Discussion

To assess the effect of feed admission mode, i.e., chemical looping vs cofeeding (steady-state experiment), a series of activity tests were performed at 600°C. During the chemical looping CO<sub>2</sub>-EDH process, a series of isothermal redox cycles were applied in a fixed-bed reactor in order to investigate the catalytic performance: diluted C<sub>2</sub>H<sub>6</sub> is fed during the reduction half-cycle, resulting in C<sub>2</sub>H<sub>4</sub>, H<sub>2</sub> and H<sub>2</sub>O production along with a reduced metal-oxide, while the oxidation half-cycle, involved the reaction of CO<sub>2</sub> with the reduced metal oxide generating CO. Between the latter half-cycles the reactor was purged by inert Ar. Figure 1 highlights the effect of catalyst physicochemical properties, originating from the different synthesis method, on catalytic activity (C<sub>2</sub>H<sub>6</sub> conversion) and selectivity towards C<sub>2</sub>H<sub>4</sub>. The Fe/NiMgZr (two-step synthesis protocol) was found to be active and selective for CO<sub>2</sub>-EDH, as it was reported elsewhere [6], under the co-feeding admission mode. DFT calculations elucidated that an interface between iron- and nickel- oxide could be responsible for the enhanced performance, compared to the sample without NiO into the support. However, Figure 1(a) shows a different behavior when the same sample was used during chemical looping: the selectivity towards C<sub>2</sub>H<sub>4</sub> drastically decreases during the first 3 cycles from 100% to 3.3%. The latter demonstrates a change in the active sites, due to deep reduction of iron oxide. Stabilization of iron oxide, in order to avoid its deep reduction under reaction conditions, was achieved by



modifying the protocol and applying the one-pot synthesis. Figure 1 (b) shows the conversion of ethane and the selectivity towards ethylene for FeNiMgZr (prepared by one-pot protocol) during 8 cycles. The catalyst lost 28% of its initial activity during the 8 cycles, reaching a C<sub>2</sub>H<sub>6</sub> conversion of 16.6% and C<sub>2</sub>H<sub>4</sub> selectivity equal to 78%, i.e., 13% C<sub>2</sub>H<sub>4</sub> yield. During the oxidation half cycle, CO<sub>2</sub> conversion was only decreased from 18.1% at the 1<sup>st</sup> cycle to 16.0% at the 8<sup>th</sup>. Accumulation of carbon was examined by means of O<sub>2</sub>-TPO and it was found to be negligible and equal to 0.1 mol<sub>C</sub>/kg<sub>cat</sub>, implying the carbon-resistance of Fe-based catalysts [3]. Steady-state experiments were also conducted for the best candidate, FeNiMgZr (not shown), for comparison purposes, using the same conditions with those applied during the

chemical looping experiments. Significantly lower C<sub>2</sub>H<sub>6</sub> conversion was attained, varying from 5% to 3%, for 40 mins time-on-stream during the co-feeding admission mode. C<sub>2</sub>H<sub>4</sub> productivity was also calculated in order to better compare the catalytic performance between the two different admission modes. An almost two-fold increase of C<sub>2</sub>H<sub>4</sub> productivity was found in case of chemical looping:  $2.8 \cdot 10^{-5} \text{ mol} \cdot \text{s}^{-1} \cdot \text{g}_{\text{cat}}^{-1}$  for cofeeding vs  $4.2 \cdot 10^{-5} \text{ mol} \cdot \text{s}^{-1} \cdot \text{g}_{\text{cat}}^{-1}$  for chemical looping.

To better understand the primary differences between the catalyst structure that can lead to the stabilization of iron and nickel oxides into the lattice and thus result in a stable performance during the CO<sub>2</sub>-EDH chemical looping, systematic XRS measurements were performed at ID20 of ESRF, focusing on the local environment of light elements, i.e., Mg and O. Preliminary results highlighted the difference between

**Figure 13: Activity tests during CO<sub>2</sub>-EDH chemical looping at 600°C. The duration of each cycle was 10 mins (reduction for 5 mins-oxidation for 5 mins). (a) Fe/NiMgZr synthesized by the two-steps protocol, (b) FeNiMgZr synthesized by one-pot.**

10wt% NiO-MgO-ZrO<sub>2</sub> support and the reference cubic MgO: presence of a strong pre-edge, different intensity ratio of the main edge. Modelling of latter support XRS data at Mg L<sub>2,3</sub> and O K edges showed that NiO and MgO form a solid solution, where NiO is homogeneously distributed in the support structure and Mg occupies octahedral sites. The impregnation of Fe results in nano-sized γ-Fe<sub>2</sub>O<sub>3</sub> particles at the fresh state (Fe in octahedral sites), as it was exemplified by EXAFS analysis at Fe K edge, while Mg remains at octahedral sites. However, upon CO<sub>2</sub>-EDH reaction, Mg coordination changes from octahedral-only to mixture of octahedral and tetrahedral. The latter tetrahedral coordination of Mg was found to occur close to the Fe sites, being responsible for the stable catalytic performance.

The present work highlights the effect of feed admission mode on ethylene productivity during the CO<sub>2</sub>-assisted ethane dehydrogenation reaction: chemical looping resulted in a two-fold increase compared to cofeeding. Advanced characterization techniques, focusing on light elements such as Mg, combined with activity tests can elucidate the pivot role of support on drastically enhancing the catalytic performance.

## Acknowledgements

This research was supported by Hellenic Foundation Research & Innovation (II-CUDET, HFRI-FM17-1899).

## References

- [1] I. Amghizar, L.A. Vandewalle, K.M. Van Geem, G.B. Marin, *Eng. J.*, 3 (2017) 171-178.
- [2] E. Heracleous, A.A. Lemonidou, *J. Catal.*, 237 (2006) 162-174.
- [3] S.A. Theofanidis, C. Loizidis, E. Heracleous, A.A. Lemonidou, *J. Catal.*, 388 (2020) 52-65.
- [4] B. Yan, S. Yao, S. Kattel, Q. Wu, Z. Xie, E. Gomez, P. Liu, D. Su, J.G. Chen, *Proc. Natl. Acad. Sci.*, 115 (2018) 8278-8283.
- [5] L. Zeng, Z. Cheng, J.A. Fan, L.-S. Fan, J. Gong, *Nat. Rev. Chem.*, 2 (2018) 349-364.
- [6] S.A. Theofanidis, G.T.K.K. Gunasooriya, I. Itskou, M. Tasioula, A.A. Lemonidou, *ChemCatChem*, (2022).

## Reducing Energy Demand by Capturing Carbon in Green Solvents

Jochem J. B. van Duin<sup>1</sup>, Pieter C. A. Bruijninx<sup>1\*</sup>

<sup>1</sup> Organic Chemistry & Catalysis, Debye Institute for Nanomaterials Science, Utrecht University, Universiteitsweg 99, 3584CG Utrecht, The Netherlands

\*p.c.a.bruijninx@uu.nl

Abstract text:

In 2021 the IPCC released their sixth assessment report, where the need to reduce our greenhouse gas emissions to limit global warming was gravely stressed.[1] To reduce the amount of atmospheric CO<sub>2</sub>, our economy needs to transfer from a linear economy to a circular economy and eventually make use of CO<sub>2</sub> as a carbo-circular chemical building block. However, CO<sub>2</sub> utilization does generally require rather pure streams of CO<sub>2</sub> which are not readily available since the carbon capture and release process is energy intensive. Currently, the industrial capture of (point sourced) CO<sub>2</sub> involves the use aqueous monoethanolamine (MEA). CO<sub>2</sub> desorption then occurs at elevated temperatures, where the high heat capacity of water causes most of the energy penalty.[2] Reducing the energy demand of the desorption step can make the implementation of capture and utilization more attractive.

Here, we compare different green solvents regarding their carbon capture and release capacity, with most of the solvents having half the heat capacity of water. Analysis of the adsorption capacity and adsorption kinetics allowed the identification of multiple green, and in some cases even bio-derived, alternatives to water as a solvent for CO<sub>2</sub> capture with MEA. **Figure 1** depicts the capture capacity of the different solvents in mol CO<sub>2</sub> captured per mol MEA. Among the different possibilities butyl levulinate, a bio-derived, high boiling, solvent synthesized from (hemi)cellulosic feedstock stands out. CO<sub>2</sub> capture in butyl levulinate resulted in 0.53 mols of greenhouse gas captured per mol of scrubber, almost matching the aqueous system with a respective value of 0.60. Most of the herein tested green solvents showed 100% adsorption of CO<sub>2</sub> until minutes before saturation, proving their viability as contenders for the replacement of the aqueous system.

With respect to utilization of CO<sub>2</sub>, the green solvents possess distinct advantages. Beyond the lower heat capacities, the use of green solvents like butyl levulinate, also enable a wider range of substrates and catalysts for utilization, given their different polarities and the absence of water. With high concentrations of CO<sub>2</sub> already dissolved in the system, catalysis could occur at milder pressures and temperatures. Ultimately the goal is to arrive at a system where carbon capture and utilization in green solvents can be combined in one, as shown in **Figure 2**.

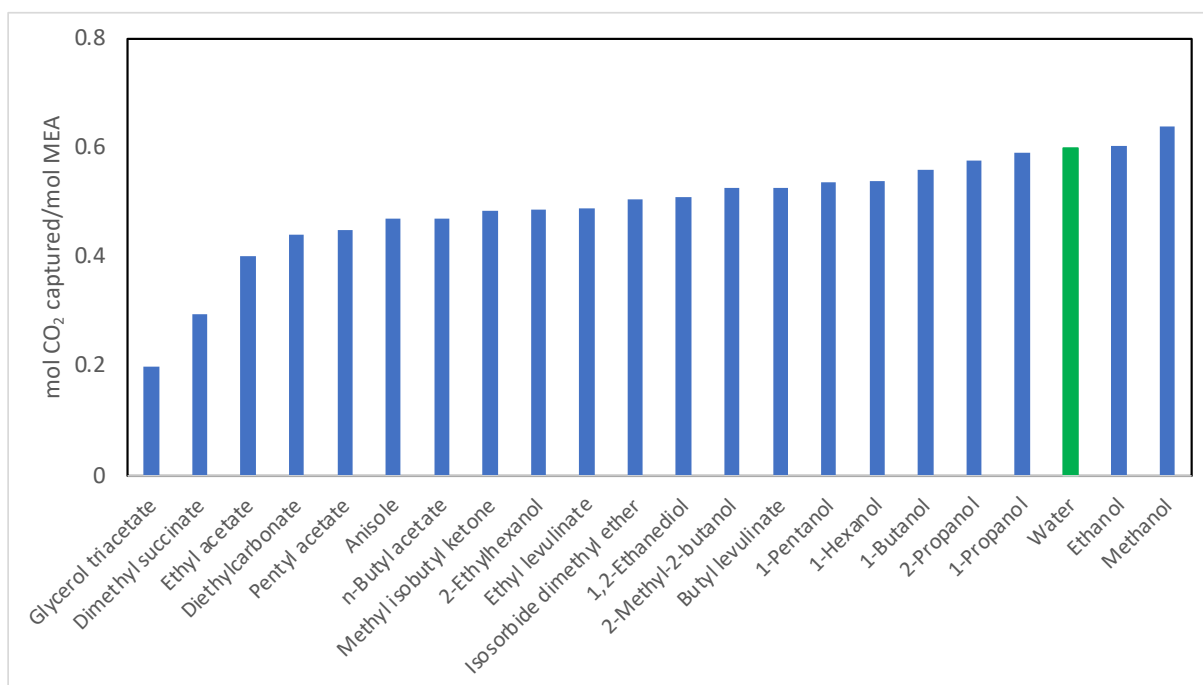


**Figure 1.** CO<sub>2</sub> capture capacities in mol CO<sub>2</sub>/mol MEA for different green solvents. All solvents were measured with a total liquid volume of 10 mL and 30 wt.% MEA, the green bar shows the capture capacity of the industrial standard, aqueous MEA.



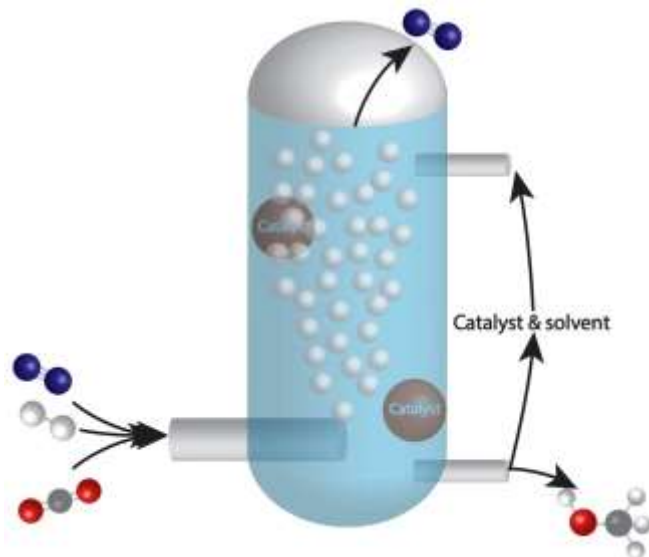


**Figure 2.** Integrated carbon capture and utilization, where CO<sub>2</sub> is first selectively captured from a diluted point source, followed by hydrogenation to, e.g., methanol.

### Acknowledgments

This work was supported by the Netherlands Center for Multiscale Catalytic Energy Conversion, an NWO gravitation programme funded by the Ministry of Education, Culture and Science of the government of the Netherlands.

### References

- [1] IPCC, 2021: Climate Change 2021: The Physical Science Basis. Contribution of Working Group I to the Sixth Assessment Report of the Intergovernmental Panel on Climate Change
- [2] Rochelle, G. T. Amine Scrubbing for CO<sub>2</sub> Capture. *Science* **2009**, 325 (5948), 1652–1654.

## Multi-enzyme co-immobilization on Hierarchical Porous Carbon Nanoparticles (HPCs) for the bioconversion of CO<sub>2</sub> to Formic Acid

Archontoula Giannakopoulou<sup>1</sup>, Christos Gakis<sup>1</sup>, Konstantinos Spyrou<sup>2</sup>, Dimitrios Gournis<sup>2</sup> and Haralambos Stamatis<sup>1\*</sup>

<sup>1</sup>*Biotechnology Laboratory, Department of Biological Applications and Technologies, University of Ioannina, 45110 Ioannina, Greece*

<sup>2</sup>*Department of Materials Science & Engineering, University of Ioannina, 45110 Ioannina, Greece*

\*[hstamati@uoi.gr](mailto:hstamati@uoi.gr)

### Abstract

The ever-growing increase of atmospheric CO<sub>2</sub> concentration along with the continuous demand in fossil fuels requires the development of green and sustainable ways for the conversion of CO<sub>2</sub> into valuable commodities. Furthermore, CO<sub>2</sub> emissions are the main culprit for the deterioration of the greenhouse effect and subsequently the climate change. For these reasons, scientific research focuses on the development of innovative methodologies aimed at reducing the concentration of this pollutant in the atmosphere. The enzymatic reduction of CO<sub>2</sub> is of significant importance and could be achieved through efficient multienzymatic cascade reactions [1]. The application of such systems offers significant advantages, such as the rapid and high-efficiency production of products, the reduction of operating costs and the reduced energy requirements. In the present work, we report the simultaneous co-immobilization of carbonic anhydrase (CA), formate dehydrogenase (FDH) and glutamate dehydrogenase (GDH) onto hierarchical porous carbon (HPC) nanoparticles for the development of a nanobiocatalytic system able to produce formic acid from CO<sub>2</sub>. HPC nanoparticles are characterized by large surface area and porosity that facilitate the immobilization of multiple enzymes, thus enhancing the mass transfer effects of the substrates [2]. The prepared nanobiocatalyst was characterized by various spectroscopic techniques and was evaluated in terms of its activity and operational stability. Compared with the free enzymes, the immobilized enzymes using bubbled CO<sub>2</sub> as substrate exhibited almost 12 times higher formate production, suggesting its possible future exploitation in industrial applications concerning the CO<sub>2</sub> utilization. Also, the incorporation of GDH into the system facilitated the co-factor regeneration, a main challenge in multi-step cascade reactions and yielded higher amounts of formic acid compared with the amount produced when applying only FDH and CA.

### Materials

Carbonic Anhydrase from bovine erythrocytes (> 2,000 U/mg protein, lyophilized) and Glutamate Dehydrogenase from beef liver (15.5 U/mg, lyophilized) were purchased from Sigma-Aldrich (St. Louis, MO, USA). Formate dehydrogenase from *Candida boidinii* (75 U/mL, liquid) was purchased from Megazyme (Chicago, IL, USA). β-Nicotinamide adenine di-nucleotide, reduced disodium salt (\*H<sub>2</sub>O) (β-NADH) and L-Glutamic acid (>99%) were all purchased from Sigma-Aldrich (St. Louis, MO, USA). The HPCs nanoparticles were synthesized and provided from the Ceramics and Composite Materials Lab (Department of Materials Science & Engineering, University of Ioannina).

### Methods

#### *Non-Covalent Co-Immobilization of CA, FDH and GDH onto HPCs nanoparticles*

In a typical protocol, 2 mg of HPC nanomaterials (Figure 1) were dispersed in sodium phosphate buffer (5 mL, 50 mM, pH 7.0) and the mixture was incubated in an ultrasonic bath for 30 min. After 30 min, an enzyme cocktail (total protein content of 4 mg) containing CA, FDH and GDH (in a typical mass ratio of 2:1:1) was added into the solution. Then, the mixture was incubated for 2 h at 30 °C. After incubation, the immobilization suspension was centrifuged for 10 minutes at 4,000 rpm, the supernatant was discarded, and the co-immobilized enzymes were washed twice with sodium phosphate buffer (50 mM, pH 7.0) to remove any unbound enzymes. Finally, the immobilized suspension was vacuum dried at room temperature, for approximately 2 hours and stored at 4 °C for further use.

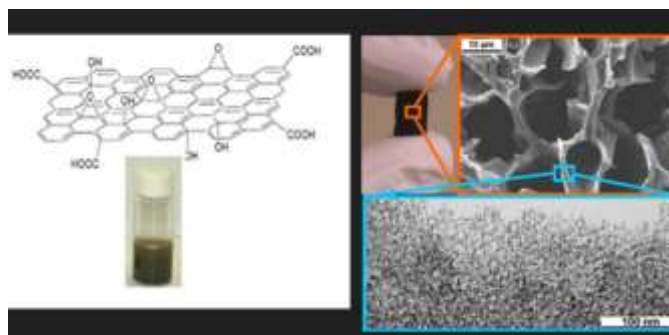


Figure 1. Graphite oxide (GO) (left) and Hierarchical porous carbons (right).

### Conversion of CO<sub>2</sub> to Formic Acid

The biotransformation of CO<sub>2</sub> to formic acid can be described as a two-step cascade reaction involving the synergistic action of several enzymes. For example, formate dehydrogenase (FDH) converts CO<sub>2</sub> to formic acid, while the incorporation of another enzyme, carbonic anhydrase (CA), into the system could accelerate the hydration of CO<sub>2</sub>. In addition, as CO<sub>2</sub> is a thermodynamically stable molecule, its reduction requires energy provided by a cofactor, the adenine nicotinamide dinucleotide (NADH) [3,4]. The development of an integrated system could include the incorporation of another enzyme, glutamate dehydrogenase (GDH) for the successful regeneration of the cofactor for successive reaction cycles. Under these conditions, the biocatalytic in vitro reduction of CO<sub>2</sub> to formic acid consists a "green" process. The prepared nanobiocatalyst consisting of CA, FDH and GDH co-immobilized onto HPCs was applied for the bioconversion of bubbled CO<sub>2</sub> into formic acid (Figure 2). Briefly, 10 mL of phosphate buffer 50 mM, pH 7.0 were bubbled with CO<sub>2</sub> for 1 h. Then, the pH of the CO<sub>2</sub> bubbled buffer was adjusted back to the original solution's pH with the addition of aliquots of 2.0 M NaOH solution. For the enzymatic catalysis of bubbled CO<sub>2</sub>, a mixture solution containing bubbled buffer, 10 mM L-glutamate, 4 mM NADH, and 6 mg of immobilized enzymes in a total reaction volume of 2 mL was incubated at 30 °C, 800 rpm, for 5 hours. Then, the reaction was cooled for 2 minutes, centrifuged at 15,000 rpm, for 4 minutes and the produced formic acid was determined in aliquots of 50 µL of the reaction supernatant according to Lang & Lang protocol [5].

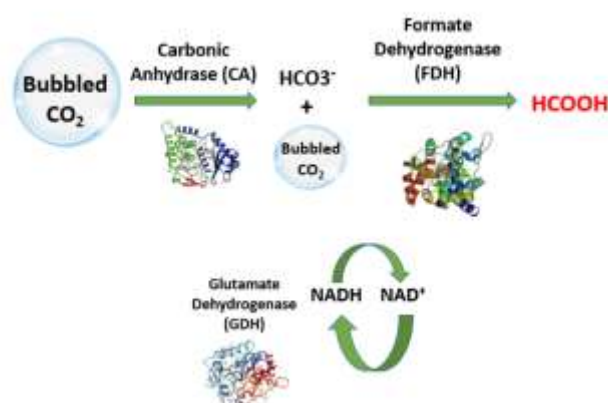


Figure 2. Schematic representation of the enzymatic reduction of CO<sub>2</sub> to formic acid and the co-factor regeneration by GDH.

### Conclusions

In the present study Hierarchical Porous Carbon (HPC) nanoparticles served as an ideal support for the simultaneous co-immobilization of three enzymes, CA, FDH and GDH. The developed nanobiocatalytic system was applied for the sequential reduction of CO<sub>2</sub> to formic acid through a two-step cascade reaction along with the continuous regeneration of the NADH co-factor. The nanobiocatalyst was characterized by various spectroscopic techniques as well as in terms of its operational stability. Finally, the nanobiocatalyst yielded a maximum formic acid production of 1.25 mM, which is almost 12 times higher than the amount produced when a mixture of the free enzymes was used.

### References

1. A. Giannakopoulou, E. Gkantzou, A. Polydera and H. Stamatis, *Trends in Biotechnology*, **38** 202 (2020).
2. L. Estevez, D. Barpaga, J. Zheng, S. Sabale, R. L. Patel, J. G. Zhang, B. P. McGrail and R. K. Motkuri, *Industrial and Engineering Chemistry Research*, **57** 1262 (2018).
3. R. K. Singh, R. Singh, D. Sivakumar, S. Kondaveeti, T. Kim, J. Li, B. H. Sung, B. K. Cho, D. R. Kim, S. C. Kim, V. C. Kalia, Y. H. P. J. Zhang, H. Zhao, Y. C. Kang and J. K. Lee, *ACS Catalysis*, **8** 11085 (2018).
4. C. G. C. Marques Netto, L. H. Andrade and H. E. Toma, *Anais da Academia Brasileira de Ciencias*, **90** 593 (2018).
5. Lang, E. ; Lang, H., *Analytical Chemistry*, **260** 8 (1972).

## Acknowledgements

This research has been co-financed by Greece and the European Union (European Social Fund-ESF) through the Operational Programme «Human Resources Development, Education and Lifelong Learning» in the context of the Act “Enhancing Human Resources Research Potential by undertaking a Doctoral Research” Sub-action 2: IKY Scholarship Programme for PhD candidates in the Greek Universities».



## Solid Oxide Electrolysis for the production of green-energy carriers

N. Bimpiri<sup>1,2\*</sup>, A. Konstantinidou<sup>1,2</sup>, M.E. Farmaki<sup>2</sup>, K.M. Papazisi<sup>2</sup>, S. Balomenou<sup>2</sup>, D. Tsiplakides<sup>1,2</sup>

<sup>1</sup>Department of Chemistry, Aristotle University of Thessaloniki, Thessaloniki 54124, Greece

<sup>2</sup>Centre for Research and Technology Hellas, 6<sup>th</sup> km Charilaou-Thermi road, Thessaloniki 57001, Greece

\*nbimpiri@certh.gr

### Introduction

Global carbon dioxide emissions are increasing over the years, as energy demands increase and fossil fuels remain the main source of energy. The release of the greenhouse gases by consuming fossil fuels will cause the global temperature to exceed the 2°C threshold created by the Intergovernmental Panel on Climate Change (IPCC) by the year of 2050. In the meantime, renewable energy is slowly gaining ground in the energy industry while fossil fuels are running out. For all the reasons, it is of a great importance to speed up the production and therefore the utilization of green energy carriers. Hydrogen can be produced by few easily accessible methods and is one of the most popular green energy carriers due to its clean combustion. However, its storage as a fuel gas has some difficulties. Electrolysis of carbon dioxide and steam (H<sub>2</sub>O-CO<sub>2</sub> co- electrolysis) [1] is a promising method for the production of green-energy carriers: the syngas (CO-H<sub>2</sub> mixture) and a series of carbon-based fuels that can be produced by the Firscher-Tropsch, while making good use of the high levels of carbon dioxide produced by the industrial and energy sectors. Energy can this way be stored in chemical form and then be converted to electrical energy and vice versa, due to the reversible operation in Solid Oxide Fuel Cell/ Solid Oxide Electrolysis Cell systems. In this work, perovskite structure La<sub>0.75</sub>Sr<sub>0.25</sub>Cr<sub>0.9</sub>Fe<sub>0.1</sub>O<sub>3</sub> material was used for the fuel (cathode) electrode of the SOECs, where electrochemical and catalytic reactions take place.

### Experimental

Co-electrolysis was studied with electrolyte-supported button cells, where each layer was deposited by means of screen printing and the active electrode area was 0.785 or 1.766 cm<sup>2</sup>. The electrolyte substrates employed were 8% mol Y<sub>2</sub>O<sub>3</sub> stabilized ZrO<sub>2</sub> (8YSZ) with thicknesses of 1.5±0.5 mm (CoorsTek) and a diameter of 20±0.5 mm, while La<sub>0.75</sub>Sr<sub>0.25</sub>Cr<sub>1-x</sub>Fe<sub>x</sub>O<sub>3-δ</sub> (LaSrCrFe) and 50% wt. (La<sub>0.80</sub>Sr<sub>0.20</sub>)<sub>0.95</sub>MnO<sub>3-x</sub> - 50% wt. (Y<sub>2</sub>O<sub>3</sub>)<sub>0.08</sub>(ZrO<sub>2</sub>)<sub>0.92</sub> (LSM-YSZ, Fuel Cell Materials) were used as fuel and oxygen electrodes, respectively. The perovskite material that was used as fuel electrode was synthesized with the sol-gel method modified with citric acid [2]. A thin gadolinium-doped ceria (GDC10, Cerpotech) interlayer was applied between the LaSrCrFe electrode and the YSZ electrolyte to avoid formation of the non-conducting phase La<sub>2</sub>Zr<sub>2</sub>O<sub>7</sub>, thus ensuring high cell efficiency and prolonged lifetime. A mixture of LaSrCrFe with GDC was also evaluated as fuel electrode. The button cells were mounted in a two chambers test fixture with a standard two electrode setup and platinum meshes/ wires as current leads (ProboStat™ by NorECs). Fuel and oxygen compartments (cathode and anode, respectively) can be fed with various gas mixtures, through mass flowmeters (Bronkhorst), under a controllable (ambient) pressure. Saturated inert or feed gas (passing through a heated humidifier) was used for steam supply to the cathode chamber. A potentiostat/ galvanostat (Autolab PGSTAT302N, Metrohm), integrated with a frequency response analyzer, was used for the electrochemical measurements including recording of the current-potential (i-V) curves and the electrochemical impedance spectroscopy (EIS). The cells that were tested were characterized by terms of electrochemical performance, while the production of syngas was monitored as well by means of a 4-channel non-dispersive infrared analyzer (Fuji), a gas chromatograph (Varian) and a mass spectrometer (Pfeiffer Vacuum).

### Results and Discussion

The cells were operated in co-electrolysis mode with a mixture of CO<sub>2</sub> and steam, in various H<sub>2</sub>O: CO<sub>2</sub> ratios (0.5-2), balanced with He or with H<sub>2</sub>: He of 1:1. The i-V curves recorded under co-electrolysis with H<sub>2</sub> present in the feed stream for two button cells bearing fuel electrodes of LaSrCrFe and mixed LaSrCrFe-GDC, respectively, at 800-900°C are presented in **Figure 1a**. The results show that the mixed 50% LaSrCrFe – 50% GDC electrode has similar performance with the pure LaSrCrFe electrode, indicating that the pure perovskite material has adequate conductivity (ionic and electronic) and electrocatalytic activity, which is not further improved by the addition of the GDC electrolyte material.

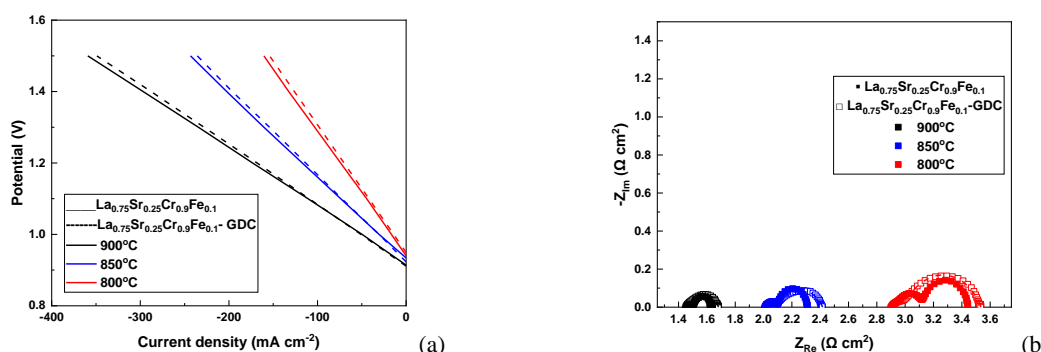


Figure 1. (a) Polarization (i-V) curves and (b) Nyquist plot of impedance spectra measured at -100 mA cm<sup>-2</sup> (100 kHz-10 mHz, 20 mA amplitude) under co-electrolysis conditions in 21% CO<sub>2</sub>, 31% H<sub>2</sub>O in 24% H<sub>2</sub>/ He reactant gas composition.

The polarization resistance ( $R_p$ ) of the cell with the LaSrCrFe electrode ( $0.20 \Omega \text{ cm}^2$ ) is lower than that of the cell with the LaSrCrFe-GDC mixed electrode ( $0.26 \Omega \text{ cm}^2$ ) at  $900^\circ\text{C}$  as shown in the galvanostatic impedance measurements presented in **Figure 1b**. The performance decreases, while the ohmic resistance ( $R_s$ ) increases with the temperature drop, for both cells, as expected.

**Figure 2a** presents the performance of a cell comprising LaSrCrFe cathode under three different  $\text{H}_2\text{O}:\text{CO}_2$  ratios (0.5, 1 and 2) in a balance of  $\text{H}_2/\text{He}$  while **Figure 2b** under mixtures of  $\text{CO}_2\text{-H}_2\text{O}$  in pure He, at  $900^\circ\text{C}$ . The total energy demand ( $\Delta H$ ) of steam electrolysis is lower than that of the other endothermic reduction ( $\text{CO}_2$  electrolysis) and the co-electrolysis has the lowest [3]. The performance of the cell is not affected by the different  $\text{CO}_2\text{-H}_2\text{O}$  ratio, as depicted from the slopes of the  $i\text{-V}$  curve. Based on our previous study on SOECs bearing LaSrCrFe fuel electrodes, these exhibit a similar high performance for both steam and  $\text{CO}_2$  electrolysis processes; however, these are competitive processes and in the case of co-electrolysis, steam electrolysis is dominating, while  $\text{CO}_2$  is converted to CO almost exclusively via the catalytic reverse water gas-shift reaction (RWGS) [4]. This is supported by the cathode outlet gas analysis, where it was observed that the produced  $\text{H}_2:\text{CO}$  ratio increases with increasing temperature, while CO production is favored at higher temperature, when  $\text{H}_2$  is not co-fed to the cathode.

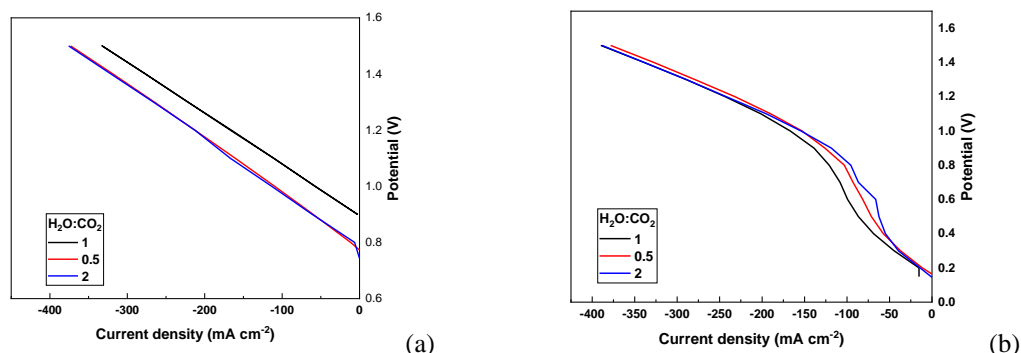


Figure 2. Polarization ( $i\text{-V}$ ) curves for the cell comprising LaSrCrFe cathode at  $900^\circ\text{C}$  under co-electrolysis in three reactant gas compositions: 31%  $\text{H}_2\text{O}/\text{CO}_2$ , 31%  $\text{H}_2\text{O}-62\%\text{CO}_2$  and 62%  $\text{H}_2\text{O}-31\%\text{CO}_2$ : (a) in  $\text{H}_2/\text{He}$  and (b) in He.

Perovskite materials due to their mixed conductivity show high electrocatalytic activity, even when hydrogen is absent from the feed and at the same time they can operate and maintain the activity under both reducing and oxidating conditions (redox stability) [5]. Exsolution, i.e., the phenomenon in which the catalytically active transition metals (in this case Fe), which are incorporated on the B site of the perovskite oxide are segregated from the oxide lattice to the surface under reducing atmosphere, is a key feature and a promising method to design advanced electrocatalysts for SOEC. The exsolved metal nanoparticles are pinned on the surface of the perovskite, and contribute to the electrocatalytic process [6]. Furthermore, it is quite remarkable that SOECs utilizing Ni-metal free electrodes which do not favor carbon deposition can produce green energy carriers, without the need of  $\text{H}_2$  supply and at the same time with the utilization of renewable energy sources with no environmental cost.

## Acknowledgements

The research work was supported by the Hellenic Foundation for Research and Innovation (HFRI) under the HFRI PhD Fellowship grant (Fellowship Number: 1311). The research leading to part of these results has received funding from the Fuel Cells and Hydrogen 2 Joint Undertaking under the project NewSOC (Grant Agreement No: 874577). This Joint Undertaking receives support from the European Union's Horizon 2020 Research and Innovation Programme and Denmark, France, Italy, Spain, Poland, Netherlands, Greece, Finland, Estonia, Germany, United Kingdom, Switzerland.

## References

1. L. Dittrich, M. Nohl, E.E. Jaekel, S. Foit, L.G.J. de Haart and R.-A. Eichel, High-Temperature Co-Electrolysis: A Versatile Method to Sustainably Produce Tailored Syngas Compositions, *J. Electrochem. Soc.* **166** (2019) F971
2. K. M. Papazisi, S. Balomenou, D. Tsiplakides, Synthesis and characterization of  $\text{La}_{0.75}\text{Sr}_{0.25}\text{Cr}_{0.9}\text{M}_{0.1}\text{O}_3$  perovskites as anodes for CO-fuelled solid oxide fuel cells, *J Appl Electrochem* **40** (2010) 1875
3. Y. Zheng, J. Wang, Bo Yu, W. Zhang, J. Chen, J. Qiao, J. Zhang, A review of high temperature co-electrolysis of  $\text{H}_2\text{O}$  and  $\text{CO}_2$  to produce sustainable fuels using solid oxide electrolysis cells (SOECs): advanced materials and technology, *Chemical Society Reviews*, **46** (2017) 1427
4. D.J. Deka, J. Kim, S. Gunduz, M. Ferree, A.C. Co, U.S. Ozkan, Temperature-induced changes in the synthesis gas composition in a high temperature  $\text{H}_2\text{O}$  and  $\text{CO}_2$  co-electrolysis system, *Applied Catalysis A, General* **602** (2020) 117697
5. L. Shu, J. Sunarso, S. S. Hashi, J. Mao, W. Zhou, F. Liang, Advanced perovskite anodes for solid oxide fuel cells: A review, *International Journal of Hydrogen Energy* **44** (2019) 31275
6. Q. A. Islam, S. Paydar, N. Akbar, B. Zhu, Y. Wu, Nanoparticle exsolution oxide and its sustainable electrochemical energy systems, *Journal of Power Sources* **492** (2021) 229626

# Electrochemical reduction of uncaptured flue gas in a membrane electrode assembly electrolyzer

Ung Lee<sup>1\*</sup>, Yun Jeong Hwang<sup>2</sup> and Da Hye Won<sup>1</sup>

<sup>1</sup>Clean Energy Research Center, Korea Institute of Science and Technology, Hwarang Ro 14 Gil 5 Seong Buk Gu Seoul, Republic of Korea

<sup>2</sup>Department of Chemistry, Seoul National University, Seoul 08826, Republic of Korea

\*e-mail ulee@kist.re.kr

Abstract text:

Electrochemical CO<sub>2</sub> reduction (CO<sub>2</sub>R) producing valuable chemicals is a promising technology for mitigating the global climate crisis and developing new processes for chemical production. The recent development of an electrolyzer gave a remarkable advancement of CO<sub>2</sub>R performance in production rate and selectivity. Most research, however, has been conducted using a pure CO<sub>2</sub> stream (>99%) as the feedstock, but flue gases generally contain 5–40% of CO<sub>2</sub>. The direct conversion of flue gas has economic advantages, but technological issues must be overcome, including competitive oxygen reduction reactions, poisoning by toxic impurities, and poor CO<sub>2</sub>R performance limited by low concentrations of the CO<sub>2</sub> feedstock.

Among the CO<sub>2</sub>R products, CO has been considered an attractive product for practical applications because of its wide applicability and high efficiency. As a representative catalyst, Ag is one of the most extensively studied materials, achieving high CO selectivity (>95% CO Faradaic efficiency, FECO) via material engineering. Furthermore, an Ag catalyst on a gas diffusion electrode (GDE) demonstrated high current density and long-term stability, suggesting that a scaled-up system is feasible. However, under low concentration CO<sub>2</sub> conditions, the Ag catalysts displayed a drastically decreased CO<sub>2</sub>R performance. The Kenis group reported that an Ag catalyst in a flow-cell system showed a 45% decrease in the partial current density for CO when the CO<sub>2</sub> concentration was diluted from 100% to 10%. [1]

As an alternative CO production catalyst, a Ni single-atom catalyst (Ni-N/C) has recently attracted attention because of its competitively superior CO selectivity associated with a preferable intermediate interaction for the CO<sub>2</sub>R over the hydrogen evolution reaction (HER) in comparison to other metal-incorporated single-atom catalysts. Ni-N/C demonstrated its outstanding performance, giving an FECO value of ~80% with a current density of -2.9 mA cm<sup>-2</sup> at 15% CO<sub>2</sub> concentration in a H-cell system. [2](34) However, further systematic studies are required to understand the dependence of the behavior on the CO<sub>2</sub> concentration and the controlling fundamentals in the MEA system, the most promising system for practical applications. Herein, we explored the CO<sub>2</sub> reduction with various CO<sub>2</sub> concentrations in a zero-gap MEA electrolyzer and found that suppressing the hydrogen evolution reaction (HER) became more critical at low concentrations of CO<sub>2</sub>. We demonstrate that a Ni single-atom (Ni-N/C) catalyst exhibits a high tolerance toward low CO<sub>2</sub> partial pressure (PCO<sub>2</sub>) because of the intrinsically large activation energy of the HER. Ni-N/C outperformed the CO productivity of Ag nanoparticles, especially at low concentrations of CO<sub>2</sub> in the zero-gap MEA. When the PCO<sub>2</sub> was lowered from 1.0 to 0.1 atm, Ni-N/C maintained >93% of CO Faradaic efficiency (FECO), but Ag nanoparticles showed a decrease in FECO from 94% to 40%. Furthermore, on the basis of a computational fluid dynamics simulation, we developed extrinsic operating conditions controlling the water transfer from the anolyte to the catalyst layer and improved CO selectivity at low CO<sub>2</sub> concentrations in the MEA electrolyzer.

To understand the different performances observed with Ag NPs and Ni-N/C, we investigated the intrinsic properties of each catalyst in the MEA. Activation energy of two reactions (that is, CO<sub>2</sub> to CO and the HER) were measured by temperature-dependent activities from 303 to 343 K. Under all voltage conditions, Ni-N/C showed a lower CO E<sub>act</sub> than Ag NPs, indicating that the intrinsic CO production capability of Ni-N/C was superior to that of the Ag NPs. Meanwhile, Ni-N/C exhibited a notably higher HER activation energy value in comparison to the Ag NPs under all voltage conditions, supporting its particularly sluggish HER. The activation energy gap between CO and the HER further hinted at the reaction selectivity of each active site developed on the Ag NPs and Ni-N/C. Consequently, Ni-N/C intrinsically preferred CO<sub>2</sub> to CO and had an extremely poor HER. These results corresponded well with several previous studies that theoretically suggested the intrinsic catalytic properties of Ni-N/C through density functional theory calculations, [3,4](36,40,47,48) and furthermore it was experimentally demonstrated that the unique intrinsic property of Ni-N/C is still valid in the MEA electrolyzer. Most of the possible Ni-N<sub>x</sub> sites required a higher binding energy for \*H adsorption in comparison the Ag metal surface, implying that it is especially difficult for the HER to occur on Ni-N/C. Therefore, this unique catalytic activity of Ni-N/C could guarantee selective CO production performance, while protons were not attracted to the active surface, even under low-PCO<sub>2</sub> conditions.

To numerically validate this concept, we performed a CFD simulation to estimate the amount of water crossover from the anode to the cathode under typical experimental conditions and its variation with operating conditions.

The CFD simulation predicts a rapid FECO drop when a diluted CO<sub>2</sub> feed is introduced to Ag NPs while Ni-N/C maintains a high FECO regardless of PCO<sub>2</sub>. The consistency of the results of the CFD simulations with experiments demonstrates that not only is the developed model suitable to describe the electrochemical reaction in the zero-gap MEA but also Ni-N/C is far less sensitive to the CO<sub>2</sub> concentration changes. The CFD simulation results indicated that the water crossover can be suppressed at a high CO<sub>2</sub> flow rate and a low aqueous anolyte flow rate, due to a higher interfacial pressure from the cathode to the AEM. In comparison to the typical conditions (i.e., 200 mL min<sup>-1</sup> CO<sub>2</sub> flow rate and 70 mL min<sup>-1</sup> anolyte flow rate), a lower concentration of fluid was visually observed at the cathode/membrane interface under the modified conditions (i.e., 800 mL min<sup>-1</sup> CO<sub>2</sub> flow rate and 7 mL min<sup>-1</sup> anolyte flow rate). This implied the amount of water at the cathode could be controlled by the experimental conditions: that is, the extrinsic environment for the HER could be controlled in the MEA.

Eventually, we performed the CO<sub>2</sub>R on Ag NPs and Ni-N/C with a PCO<sub>2</sub> of 0.1 atm and the specific operating conditions predicted using the CFD simulation to induce different water contents in the cathode part: that is, 0.32, 0.34, and 0.35 mL min<sup>-1</sup>. As the water content at the cathode decreased, the FECO values of the Ag NPs increased from 37% to 69% with an increase in the CO current density value from -56.7 to -118.2 mA cm<sup>-2</sup>. This demonstrated that controlling the the HER can be a rational strategy to achieve high CO selectivity under low-PCO<sub>2</sub> conditions. Interestingly, Ni-N/C showed similar performances for the CO<sub>2</sub>R and HER in terms of FE and partial current density, regardless of water crossover. In other words, the catalytic performance of Ni-N/C was insensitive to water/proton concentration, indicating that the uniqueness of Ni-N/C could be attributed to stable CO<sub>2</sub>R performance under various PCO<sub>2</sub> conditions. Therefore, a poor proton affinity can be a key characteristic for the development of advanced catalysts for the direct intake of low concentrations of CO<sub>2</sub> feed.

## References

1. Kim, B.; Ma, S.; Molly Jhong, H.-R.; Kenis, P. J. A. Influence of dilute feed and pH on electrochemical reduction of CO<sub>2</sub> to CO on Ag in a continuous flow electrolyzer. *Electrochim. Acta* 2015, 166, 271–276
2. Jiao, L.; Yang, W.; Wan, G.; Zhang, R.; Zheng, X.; Zhou, H.; Yu, S.; Jaing, H. Single-Atom Electrocatalysts from Multivariate Metal–Organic Frameworks for Highly Selective Reduction of CO<sub>2</sub> at Low Pressures. *Angew. Chem., Int. Ed.* 2020, 59 (9), 20589–20595.
3. Yan, C.; Li, H.; Ye, Y.; Wu, H.; Cai, F.; Si, R.; Xiao, J.; Miao, S.; Xie, S.; Yang, F.; et al. Coordinatively unsaturated nickel–nitrogen sites towards selective and high-rate CO<sub>2</sub> electroreduction. *Energy Environ. Sci.* 2018, 11 (5), 1204–1210.
4. Möller, T.; Ju, W.; Bagger, A.; Wang, X.; Luo, F.; Ngo Thanh, T.; Varela, A. S.; Rossmeisl, J.; Strasser, P. Efficient CO<sub>2</sub> to CO electrolysis on solid Ni–N–C catalysts at industrial current densities. *Energy Environ. Sci.* 2019, 12 (2), 640–647.



## Capture and reuse of CO<sub>2</sub>: from ionic liquids to structured 3DP printed devices

Marcileia Zanatta<sup>1\*</sup>, Eduardo Garcia-Verdugo,<sup>2</sup> David Valverde,<sup>2</sup> Victor Sans<sup>1</sup>

<sup>1</sup>Institute of Advanced Materials (INAM), Universitat Jaume I, Avda Sos Baynat s/n, 12071, Castellón, Spain

<sup>2</sup>Departamento de Química Inorgánica y Orgánica, Jaume I, E-12071 Castellón, Spain

e-mail: [zanatta@uji.es](mailto:zanatta@uji.es)

Carbon dioxide is the largest contributor to greenhouse gas emission, one of the responsible for the global warming and the climate change. However, the abundance of CO<sub>2</sub> can be also viewed as an opportunity to source the C1 building block of the future for fuels and chemicals. Despite the large number of reports related to strategies for CO<sub>2</sub> capture and activation, a viable solution with potential industrial applicability is lacking due to the harsh conditions, catalyst durability and loses activity at diluted sources of CO<sub>2</sub>. In this context, an ideal material would capture CO<sub>2</sub> at near atmospheric pressure and catalyse the conversion into products of aggregate values, as cyclic carbonate.

Currently, the most common CO<sub>2</sub> industrial capture technology is based on aqueous monoethanolamine (MEA) solutions. However, this process suffers from serious environmental, technological, and safety limitations. Regarding the CO<sub>2</sub> reuse, one of the most studied added-value products is the cyclic carbonate. This because the cycloaddition of CO<sub>2</sub> to epoxide presents an advantage because the CO<sub>2</sub> is directly incorporated to the substrate without necessity of braking bonds of this gas. In addition, cyclic carbonates are widely applied as polar aprotic solvents, organic synthesis intermediates, electrolytes in lithium-ion batteries, cosmetic formulations, and monomers. In this context, the catalysis plays a key role in the development of efficient and sustainable processes to produce the cyclic carbonate. In general, 3 strategies are used: CO<sub>2</sub> activation, epoxide activation or both. Viable solutions combining the activation of both substrates still rare in literature and needs the design of advanced materials with tailored properties.[1]

Ionic liquids (ILs) and their covalently supported (SILs) or polymeric (PILs) analogues are multifunctional materials with the capacity to capture and activate CO<sub>2</sub> at low pressure and temperature. The adsorption in PILs and ILs can occurs via physisorption and/or formation of HCO<sub>3</sub><sup>-</sup>/CO<sub>3</sub><sup>2-</sup>, which can be used as CO<sub>2</sub> local source for further reuse reaction (Figure 1a). [2] With the correct combination of the cation/anion/solvent IL-based materials present buffer-like behavior in solution, acting as very mild bases that shift the thermodynamic equilibrium to the product side, creating an adequate environment to activate the CO<sub>2</sub> and efficiently convert in value products. Additionally, the design of hydrogen bond functionalities allows the efficiently CO<sub>2</sub> cycloaddition to a broad range of epoxides, yielding cyclic carbonates. [3]

Here, multifunctional IL-based materials applied to CO<sub>2</sub> capture and conversion in cyclic carbonate reactions are reported (Figure 1). The balance between the catalyst functionalities is the key to decrease thermodynamic barriers and to selectively convert CO<sub>2</sub> into values products. Currently, we have been working to cross from batch reactions to continuous flow, combing the catalytic ability of ILs and SILs and the structured reactors prepared by additive manufacturing (Figure 1b).[3] The combination of the catalyst structure, buffering environment, hydrogen bond ability and flow chemistry resulted in promising catalytic activity in CO<sub>2</sub> valorisation reaction. [2-3]

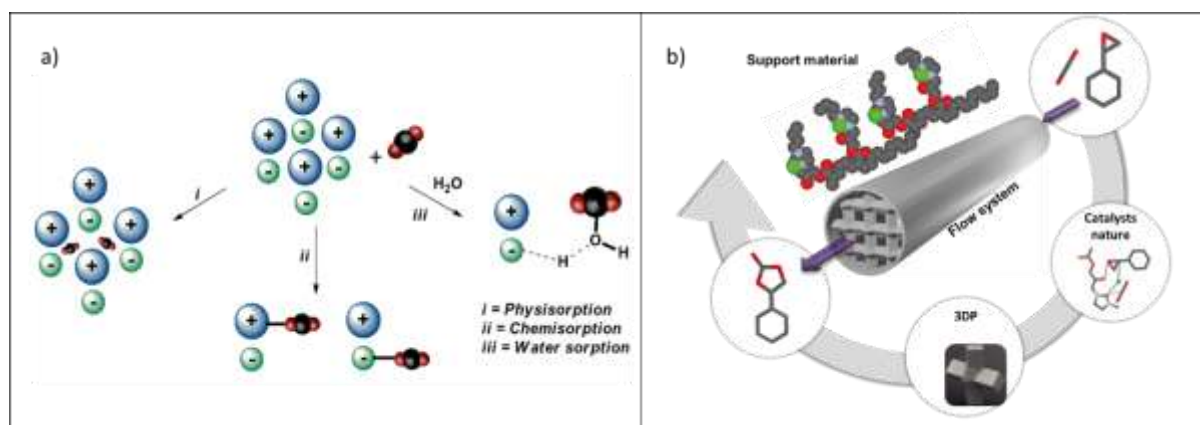


Figure 14. a) Mechanism of CO<sub>2</sub> capture using ILs-based materials. b) Continuous-flow 3D printed SIL-based structured reactors for CO<sub>2</sub> cycloaddition to cyclic carbonates.

### Acknowledgements

This project has received funding from the European Union's Horizon 2020 research and innovation programme under the Marie Skłodowska-Curie grant agreement No 101026335.

## References

1. L. Guo, K. J. Lamb M. North. *Green Chem.*, **2021**, 23, 77–118.
2. a) M. Zanatta, N. M. Simon, J Dupont, *ChemSusChem*, **2020**, 13, 310; b) M. Zanatta, M. Lopes, C. Bernardes, E. Cabrita, M. Corvo, *J. CO2 Util.*, **2020**, 41, 101225. (c) R. V. Barrulas, M. Zanatta, T. Casimiro, M. C. Corvo, *Chem. Eng. J.*, 411, **2021**, 128528.
3. D. Valverde, R. Porcar, M, Zanatta, S, Alcalde, B. Altava, V. Sans, E. García-Verdugo, *Green Chem*, **2022** (doi.org/10.1039/D1GC04593H)

## POSS-porphyrin-imidazolium crosslinked network as catalytic bifunctional platform for the conversion of CO<sub>2</sub> with epoxides.

A. Morena<sup>1,2</sup>, F. Giacalone<sup>2\*</sup>, M. Gruttadauria<sup>2\*</sup>, C. Aprile<sup>1\*</sup>

<sup>1</sup>Unit of Nanomaterials Chemistry, Department of Chemistry, NISM, University of Namur, 61 rue de Bruxelles, 5000 Namur, Belgium

<sup>2</sup>Department of Biological, Chemical and Pharmaceutical Sciences and Technologies, University of Palermo, Viale delle Scienze, Ed. 17, 90128, Palermo, Italy

[anthony.morena@unamur.be](mailto:anthony.morena@unamur.be) or [anthony.morena@unipa.it](mailto:anthony.morena@unipa.it), [francesco.giacalone@unipa.it](mailto:francesco.giacalone@unipa.it)\*; [michelangelo.gruttadauria@unipa.it](mailto:michelangelo.gruttadauria@unipa.it)\*; [carmela.aprile@unamur.be](mailto:carmela.aprile@unamur.be)\*

The high environmental impact of CO<sub>2</sub> today has motivated the scientific community to find effective alternatives to reuse this waste and transform it in s added value chemicals. One of the most relevant pathways is represented by the reaction between CO<sub>2</sub> and epoxides to give the corresponding cyclic carbonates [1]. This is a process that highly satisfies the principles of green chemistry. The reaction displays an atom economy of 100%. Moreover, it can be performed under solvent-free conditions and it can display a potentially low E-factor [1]. The use high energy starting materials, as espoxides, is essential for making the process thermodynamically favourable. In addition, a catalyst with a nucleophilic species, capable of opening the three-membered ring by nucleophilic attack, is required for the process to take place. In further details, the high energy input needed for the carbon dioxide transformation can be further reduced through the use of a co-catalyst that coordinates the epoxide oxygen with a metal centre acting as a Lewis acid or through the formation of hydrogen bonds [3]. In order to improve the performance of this process, several catalytic systems, both homogeneous and heterogeneous, were developed and recently, CO<sub>2</sub> conversion into cyclic carbonates has been successfully obtained combining a Lewis acidic metal and a nucleophile such as a halogen anion in the same bifunctional material [4].

With the intention of following the promising path of heterogeneous two-component materials and exploiting the proximity effect that Polyhedral Oligomeric Silsesquioxanes (POSS) benefit [5-6], two new catalytic materials were synthesized by radical copolymerization of a tetraarylporphyrin aluminum chloride monomer (TSP-AlCl) with a bis-vinylimidazolium salt (bis-imi) carrying bromide anions as counter ion and the Octavynilsilsesquioxane as inorganic core building block.

All the materials prepared have been fully characterized by means of different analytic and spectroscopic techniques, and they have been tested in the synthesis of cyclic carbonates starting from CO<sub>2</sub> and several epoxides. The results obtained show excellent TON values even at temperature ranges below 100 °C, indicating how highly promising this class of materials is.

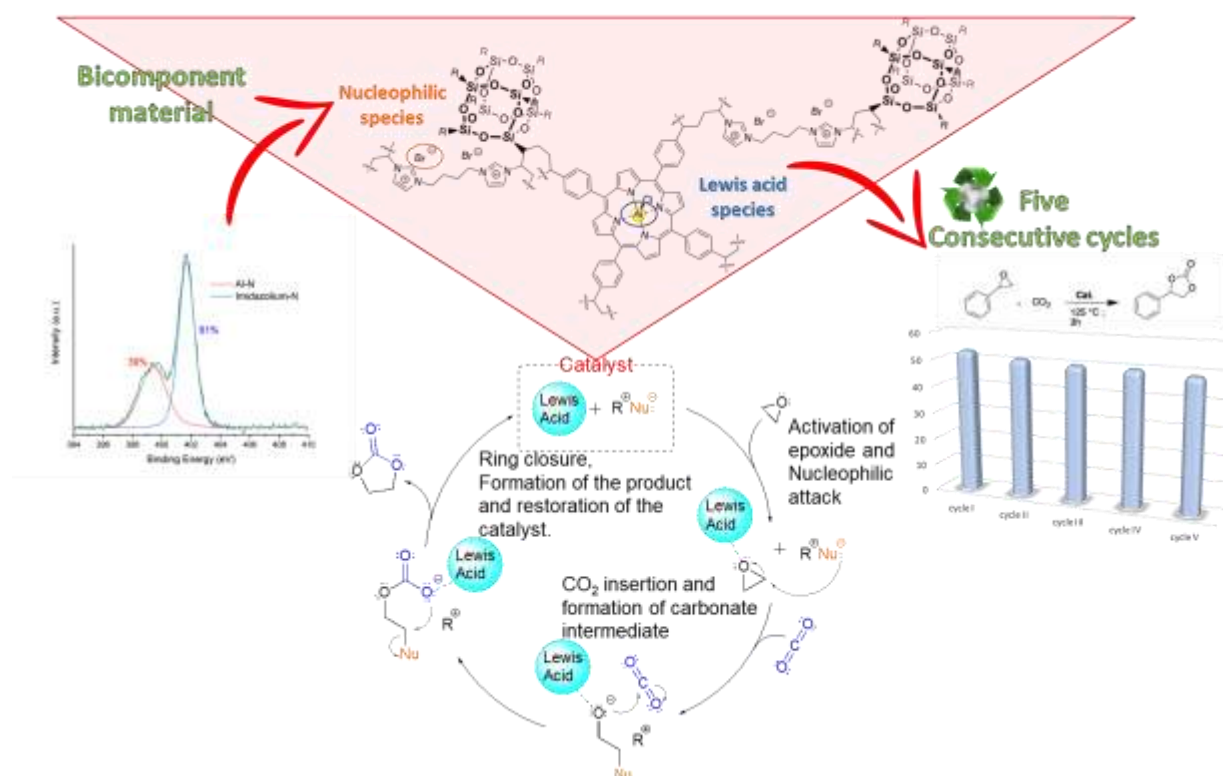


Figure 1. Bicomponent catalytic system for CO<sub>2</sub> conversion (top), Mechanism of catalysed and co-catalysed reaction between CO<sub>2</sub> and epoxides (bottom), N1s high resolution XPS (left), Recycling tests (right).

## Acknowledgements

The authors acknowledge the University of Palermo and the University of Namur. A.M. gratefully acknowledges the University of Palermo and University of Namur for a co-funded PhD fellowship. This research is supported by the F.R.S-FNRS via the funding grants GEQ U.G014.19 and EQP U.N034.17. This research used resources of the PC2 and the MORPH-IM platforms located at the University of Namur.

## References

1. J. Artz, T. E. Müller, K. Thenert, J. Kleinekorte, R. Meys, A. Sternberg, A. Bardow, W. Leitner, *Chem. Rev.*, **118**, 434-504 (2018).
2. V. B. Saptal, B. M. Bhanage, *Curr Opin Green Sustain Chem.*, **3**, 1-10 (2017)
3. P. P. Pescarmona, M. Taherimehr, *Catal. Sci. Technol.*, **2**, 2169-2187 (2012).
4. V. Campisciano, L. Valentino, A. Morena, A. Santiago-Portillo, N. Saladino, M. Gruttadauria, C. Aprile, F. Giacalone, *J. CO2 Util.*, **57**, 101884 (2022).
5. C. Calabrese, C. Aprile, M. Gruttadauria, F. Giacalone, *Catal. Sci. Technol.*, **10**, 7415-7447 (2020).
6. C. Calabrese, L. Fusaro, L. F. Liotta, F. Giacalone, A. Comès, V. Campisciano, C. Aprile, M. Gruttadauria, *ChemPlusChem*, **84**, 1536-1543 (2019).

# Computational chemistry

## A Computational and Testing Toolbox Towards Safe and Sustainable by Design Chemicals

Denis A. Sarigiannis<sup>1,2,3,\*</sup>, Spyros P. Karakitsios<sup>1,2,4</sup> and Antonios Gypakis<sup>5</sup>

<sup>1</sup> HERACLES Research Center on the Exposome and Health, Center for Interdisciplinary Research and Innovation, Aristotle University of Thessaloniki, 10 km Thessaloniki-Thermi Road, Greece

<sup>2</sup> Environmental Engineering Laboratory, Department of Chemical Engineering, Aristotle University of Thessaloniki, University Campus, Thessaloniki, Greece

<sup>3</sup> Environmental Health Engineering Laboratory, Science, Technology and Society Department, Institute for Advanced Study IUSS, Pavia, Italy

<sup>4</sup> ENVE.X P.C., Kalamaria, Greece

<sup>5</sup> Ministry of Development and Investments, General Secretariat for Research and Innovation, Athens, Greece

\*sarigiannis@cheng.auth.gr

### Abstract text:

In December 2020 the European Commission issued its new chemicals strategy for sustainability (CSS) setting out a vision for the EU chemical policy, to strive for a “toxic-free environment” and reduce environmental pollution to zero (the Zero Pollution ambition). The reduction of the net negative impact on ecosystems and people without burden shifting between different sectorial policy objectives, requires a clear departure from current practice. We need to move towards a more holistic approach, enabling the assessment of combined risks (by improving the methods for chemical testing and predictive toxicology) caused by exposures from different sources (by improving exposure assessment) under different regulatory frameworks, following the “one substance one assessment” principle. More interestingly for sustainable chemical innovation, the other key pillar of the CSS is the transition to chemicals that are Safe and Sustainable-by-Design. The SSbD concept is defined as a process to accelerate widespread market uptake of new and alternative chemical products and technologies that deliver greater consumer confidence in their safety, environmental and societal benefits and advance the transition towards a circular economy and climate-neutral society. Currently SSbD is at the core of institutional, process and technological systems innovation in the chemical industry and in chemical engineering in Europe and it has been integrated in the national research and innovation agenda in Greece.

In this context, the most important action of Horizon Europe, the new framework instrument for research and innovation in Europe in vigour for the next seven years, in chemical engineering innovation to date is the creation of the EU-wide partnership on assessment of the risk of chemicals (PARC). PARC is an EU alliance bringing together 200 public institutions aiming to support the implementation of the “Green Deal”, the “Chemicals Strategy for Sustainability Towards a Toxic-Free Environment (CSS)”, including the “Industrial Strategy”, and the “New Circular Economy Action Plan”. Even though the criteria defining specifically the SSbD concept are currently being coined by the European Commission and are expected to be issued in October 2022, the need to move towards the operationalisation of SSbD is a key objective of PARC. Thus, a SSbD toolbox integrating tools for safety and sustainability assessment coming from different policy areas and strategies as well as new tools developed in PARC is being designed to integrate the state of the art in computational tools supporting the SSbD concept implementation.

Examples of the SSbD methodology on major industrial chemicals such as plasticisers (chemicals existing in the market and their alternatives) will be demonstrated, including a broad array of interconnected methodological tools that allow the refinement of the assessment of chemical risks, including their entire life cycle. In this study we also present an innovative tool for integrated health risk assessment of plastic products and of plastic-containing goods during their whole life cycle until their final disposal as waste. The INTEGRA LCA software couples the integrated external and internal exposure assessment capabilities of the INTEGRA computational platform with life cycle impact assessment. The integrated software platform allowed us to perform a first-of-its-kind analysis of adverse health outcomes attributable to chronic exposure to persistent organic pollutants associated with plastic material use and disposal. Our analysis focused on plastic waste generated in the two main metropolitan centers in Greece, Athens and Thessaloniki. A comprehensive review of up-to-date information on plastic products and plasticizers used by the urban population was performed to build up the application-specific release/emissions inventory. This review included both plastic products (e.g. PET bottles, PVC material, polycarbonate products) and plasticizers used in food packaging.

Compounds of interest in this regard include bisphenol A, phthalates such as DEHP and its metabolites, DINCH, di-(2-ethylhexyl)adipate. Integration of all human exposure routes and pathways to the toxic compounds contained in plastic was done at the level of systemic internal dose, that was linked with adverse health outcomes reported in the literature to quantitatively assess the related health risk. Our analysis highlights that landfilling is the worst waste management strategy on a global scale. At the same time, the investigated options for waste treatment coupled with energy and material recovery would result in very important benefits in terms of greenhouse gas

emission reduction. However, not all options are equally benign to the local environment and to the health of the local population, since both the former and the latter are still affected by non-negligible local emissions. Regarding public health impacts, adverse effects on the endocrine system with cascade impacts on human reproduction, metabolic syndrome and, even, neurotoxicity after chronic exposure to the persistent organic chemicals found in plastic products and waste were estimated. The coupled integrated exposure and life cycle assessment methodology developed herein and translated into the INTEGRA LCA platform is a significant step towards the direction of comprehensive, precise and transparent estimation potential health risks associated with use, management and disposal of plastics in urban settings and for the implementation of the SSbD concept in the design, manufacturing and end-of-life management of plastic products or of plastic-containing consumer goods. The incorporation of life cycle analysis produces different conclusions than a simple environmental impact assessment based only on estimated or measured emissions. Taking into account the overall life cycle of both the waste streams and of the technological systems and facilities envisaged under the plausible scenarios analyzed herein, alters the relative attractiveness of the solutions considered and enhances the robustness of the health impact assessment.

INTEGRA LCA is empowered through the use of quantitative structure-activity relationship models for property prediction supported by a machine learning-based search engine that explores the relevant chemical space for alternative molecules that would eventually minimize the environmental and human health hazards associated with their use in consumer products. Thus an integrated framework for selection of chemicals for product redesign has been coined; the computer-aided workflow we present supports the redesigning of these chemicals to achieve the sought out environmental and human health objectives using *in silico* generated structure suggestions. The case study selected in this study allows us to give an overview of the methodological and computational process proposed to identify chemicals suitable for redesign, including the available alternatives and essentiality of the respective properties for sustainable plastic product development. The last step in the methodological procedure laid out in this study is the application of multi-criteria optimisation techniques to (a) define the viability kernel of the proposed solutions in terms of product redesign; and (b) proceed towards the synthesis of complex yet sustainable solutions supporting the multi-criteria analysis process in order to ensure that the finally proposed solution(s) satisfy the multiple criteria put forward by the stakeholders involved in plastic product synthesis, generation and finally disposal (when they become waste) adopting a circular economy paradigm.

### **Acknowledgements**

The support of the European Commission and of the General Secretariat for Research and Innovation of the Hellenic Government through the European Partnership on Assessment of Risk of Chemicals (PARC) is gratefully recognized.

## Experiment-based parameter estimation of an amine solvent for CO<sub>2</sub> hydrogenation using hybrid Gaussian Process Bayesian Optimization

Changsoo Kim<sup>1</sup>, Hee Won Lee<sup>1</sup>, and Ung Lee<sup>1\*</sup>

<sup>1</sup>Korea Institute of Science and Technology, Seoul 02792, Republic of Korea

\*ulee@kist.re.kr

CO<sub>2</sub> mitigation has been receiving a lot of spotlight recently, due to the fact that it is one of the main objectives to effectively delay and overcome the global climate crisis. Carbon capture and utilization (CCU), which is the process of producing useful chemicals from CO<sub>2</sub> captured from absorbents, is deemed as a practical solution of CO<sub>2</sub> mitigation. However, practical application of CCU technologies is hindered by the profitability of the processes, mainly owing to large amounts of energy usage, leading to high utility costs. Other than the utilization section, the largest consumer of energy is the amine regeneration section, and various studies have been conducted to develop amines that show low regeneration energy as well as good capture performance, especially water-lean amines [1]. Consequently, various studies have been conducted to discover new amines that are capable of reducing the regeneration energy, or to develop novel processes that minimize the overall energy usage required for CO<sub>2</sub> utilization.

CO<sub>2</sub> hydrogenation to produce formic acid, has been considered as an economically viable option of CCU, due to the fact that CO<sub>2</sub> is reacted with H<sub>2</sub> directly from its captured state, greatly reducing the energy required by the overall process. While various amines are known to retain high CO<sub>2</sub> capture rates and low regeneration energy, such as monoethanolamine or K<sub>2</sub>Sol [2], they are inappropriate to be used in CO<sub>2</sub> hydrogenation applications since the CO<sub>2</sub> has to be captured in a bicarbonate form for effective hydrogenation to formate. Thus it is important to assess and find new amines appropriate for this purpose, which have high capture rates as well as bicarbonate forming properties. Also, considering the fact that the final goal of CCU is commercialization for large scale CO<sub>2</sub> mitigation, it is essential to learn the thermodynamic and kinetic properties of the CO<sub>2</sub> capture process. However, since new amines lack reaction data on reaction properties, numerous experiments based on varying reaction conditions are required, which is difficult to be performed consistently in a bench-scale process such as the CO<sub>2</sub> capture column. Thus applying machine learning methods to effectively make use of a minimal set of experimental data to estimate the reaction parameters are essential when studying a new amine.

In this study, a new amine candidate for CO<sub>2</sub> hydrogenation, n-methylpyrrolidine (NMPI), is studied for its CO<sub>2</sub> capture capability and CO<sub>2</sub> hydrogenation potential. First, using a capture column 3.6m in height and 3in in diameter, the CO<sub>2</sub> capture rate of 5M NMPI is tested, with respect to a gas mixture with compositions similar to industrial flue gas (15% CO<sub>2</sub>). Multiple sessions of capture experiments are conducted with varying liquid-to-gas (L/G) ratios, to minimize experimental error and to obtain sufficient data for effective parameter estimation. Secondly, thermodynamic and kinetic parameters of NMPI are estimated using the hybrid Gaussian process Bayesian optimization (hGPBO) method, which integrates the Gaussian process Bayesian optimization with a deep learning-based surrogate model to effectively estimate reaction parameters with small number of experiments [3]. A total of nine parameters, including the Gibbs free energy and enthalpy of formation of NMPI, Arrhenius constants and activation energy values for CO<sub>2</sub> capture reaction, and the equilibrium regression parameters for the NMPI hydration reaction, are estimated using the hGPBO in this study. Experimental results of the NMPI show great performance, with over 85% CO<sub>2</sub> absorption when L/G ratios are larger than 1.4. Using the CO<sub>2</sub> absorption rates and column temperature profile data, hGPBO is applied by integrating the process simulator Aspen Plus V11 with Matlab. After developing a surrogate model, hGPBO is applied to estimate the nine parameters, where the results showed good accordance with respect to the experiment results, with the values falling in the 95% confidence interval of the estimated parameters. The results of this study shows that NMPI is indeed a viable amine capable of effectively capturing CO<sub>2</sub> and can be used for CO<sub>2</sub> hydrogenation reactions, and provides estimated parameter values that may be implemented for large scale simulation of related processes which can lead to a commercialized CCU application.



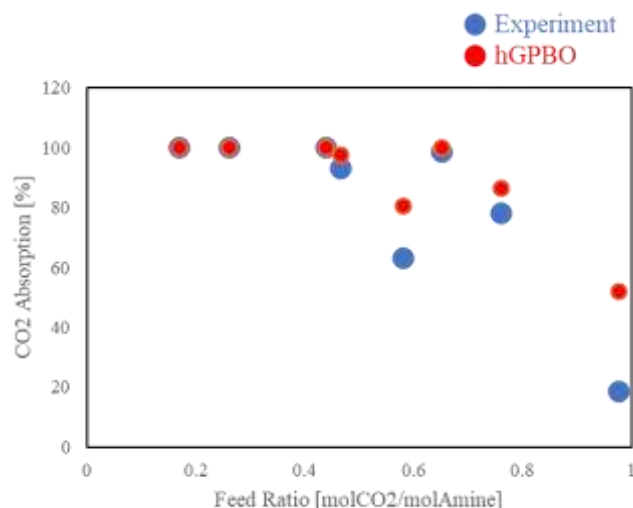


Figure 15. CO<sub>2</sub> absorption rate of the NMPI solvent with respect to varying feed ratio. Red dots show simulation results after hGPBO application

Table 1. CO<sub>2</sub> capture experimental data using NMPI, with respect to various L/G ratios.

Amine [L/hr]	Gas [m <sup>3</sup> /hr]	L/G	CO <sub>2</sub> absorption [%]	CO <sub>2</sub> /Amine [mol/mol]
5	1	5	100	0.149
3	1	3	100	0.248
3	1	3	100	0.248
3	1.5	2	100	0.112
2	1.5	1.3	100	0.167
2	1.5	1.3	18.86	0.977
3	1.5	2	98.8	0.651
3	1.8	1.7	78.24	0.759
3	1.7	1.8	100	0.438
2	1.5	1.3	63.37	0.580
2.5	1.5	1.7	93.27	0.464

## Acknowledgements

This work was supported by the National Research Foundation of Korea (NRF) grant funded by the Korean government (MSIT) (no. NRF-2020M3H7A1098259).

## References

- Heldebrant, D. J., Koech, P. K., Glezakou, V. A., Rousseau, R., Malhotra, D., & Cantu, D. C. (2017). Water-lean solvents for post-combustion CO<sub>2</sub> capture: fundamentals, uncertainties, opportunities, and outlook. *Chemical reviews*, 117(14), 9594-9624.
- Hwang, J., Kim, J., Lee, H. W., Na, J., Ahn, B. S., Lee, S. D., ... & Lee, U. (2019). An experimental based optimization of a novel water lean amine solvent for post combustion CO<sub>2</sub> capture process. *Applied Energy*, 248, 174-184.
- Kim, J., Na, J., Kim, K., Bak, J. H., Lee, H., & Lee, U. (2021). Learning the properties of a water-lean amine solvent from carbon capture pilot experiments. *Applied Energy*, 283, 116213.

## Machine Learning Assisted Modeling of Interfacial Tension in the System N<sub>2</sub>/Brine

G. Reza Vakili-Nezhaad<sup>1\*</sup>, Adel Al Ajmi<sup>1</sup>, Ahmed Al Shaaili<sup>1</sup>, Farzaneh Mohammadi<sup>2</sup>, and Alireza Kazemi<sup>1</sup>

<sup>1</sup>Petroleum & Chemical Engineering Department, College of Engineering, Sultan Qaboos University, Muscat 123, Oman

<sup>2</sup>Department of Environmental Health Engineering, School of Health, Isfahan University of Medical Sciences (MUI), Isfahan, Iran

\*e-mail: Vakili@dqu.edu.om

Flue gases contain large amounts of CO<sub>2</sub> and N<sub>2</sub>. For the purpose of CO<sub>2</sub> sequestration in depleted reservoirs or saline aquifers, a deep understanding about the interaction between these components with brine is vital. Among the most important parameters which should be investigated for such applications is interfacial tension (IFT) in these systems. In the current study we have measured IFT between N<sub>2</sub> and different brines including monovalent and divalent ions at various temperatures and pressures at different salinity ranges. Various brines containing salts such as NaCl, Na<sub>2</sub>SO<sub>4</sub>, KCl, MgCl<sub>2</sub>, and CaCl<sub>2</sub> were synthesized in the range of salinity between 10000 ppm to 50000 ppm. IFT700 (Vinci, France) instrument was used for our experiments. The obtained experimental data were then analyzed using different machine learning algorithms. The prediction of IFT (mN/m) as a response variable with independent variables including temperature (K), pressure (Mpa), and molar concentrations of different anions and cations (M) was carried out using adaptive neuro-fuzzy inference system (ANFIS) and artificial neural network (ANN) with feed-forward architecture models. ANFIS is a powerful approach to modeling the input and output relationship in complex and nonlinear systems. It converges much faster and has the most efficient learning algorithm, compared with other models. On the other hand, the artificial neural network (ANN) is used as one of the most efficient and attractive non-linear multivariate modeling methods for laboratory works. ANN can learn from existing data. One of the benefits of ANN is that the operator does not need to look for a suitable fit function and the ANN can identify and predict any nonlinear correlation [1]. Due to the lack of comparison of the ability of these two powerful models in predicting the IFT in other studies, it was decided to compare the results of IFT modeling with both ANN and ANFIS models. The ANFIS and *mntool* toolboxes were used for model implementation in MATLAB R2017a software.

Based on the present study results, the IFT was predicted accurately by ANFIS and ANN with good performance parameters. The coefficient of determination (R<sup>2</sup>), mean squared error (MSE), mean absolute error (MAE), and average absolute relative deviation (AARD%) were calculated to assess the accuracy of the models. Both models showed very good performance, with R<sup>2</sup> coefficient above 98% for test data. The final regression of test data is illustrated in Figure 1. Therefore, ANFIS and ANN can be used for accurate prediction of IFT in the studied systems [2]. Sensitivity analysis was also performed by Pearson's correlation method to determine the most influential variables on the response parameter, which could be seen in Figure 2 [3]. According to Figure 2, the molar concentrations of different ions including AN1, CA3, CA4 and CA1 were the most influential variables on IFT, respectively.

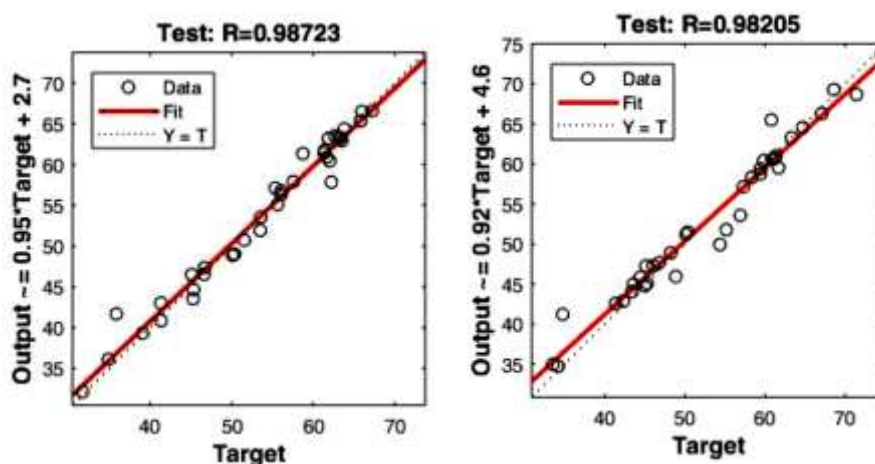
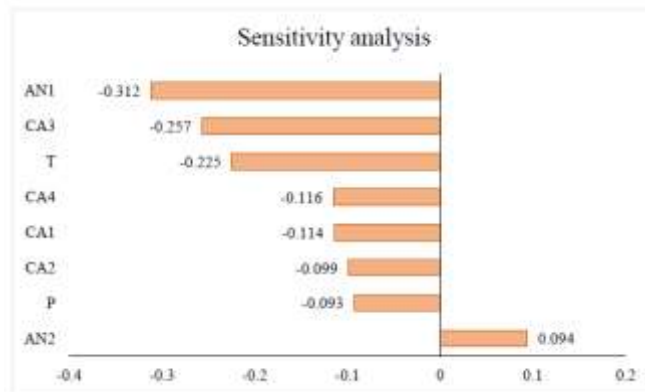


Figure 1. Test data regression output based on ANFIS and ANN models.



**Figure 2.** Sensitivity analysis using Pearson correlation.

As it can be seen from the results, ANFIS and ANN methods were very successful for predicting the behavior of the complex systems studied in this work.

### Acknowledgements

The authors are thankful to Sultan Qaboos University and Isfahan University of Medical Science for supporting this research.

### References

1. K.S.M.H. Ibrahim, Y.F. Huang, A.N. Ahmed et al., *Alexandria Engineering Journal*, **61** 279 (2022).
2. B. Han, X. Bian, *Petroleum*, **4** 43 (2018).
3. C. Germann, G. Marbach, F. Civardi, *Investigative Radiology*, **55** 499 (2020).

## Computational eco-design and screening of biodegradable renewable polyesters

Anamaria Todea<sup>1\*</sup>, Danilo Di Stefano,<sup>2</sup> Sara Fortuna<sup>1</sup>, Fioretta Asaro<sup>1</sup>, Federico Zappaterra<sup>1</sup>, Lucia Gardossi<sup>1</sup>

<sup>1</sup> Dipartimento di Scienze Chimiche e Farmaceutiche, Università degli Studi di Trieste, Piazzale Europa 1, 34127, Trieste, Italy

<sup>2</sup> ESTECO SpA, Trieste, Italy

\* atodea@units.it

Plastic pollution, specifically plastics derived from fossil fuels, is one of the most challenging environmental issues of the past years. The solution offered by bioeconomy is represented by renewable bio-based polymers [1]. Even though several bio-based plastics have been commercialized in the last years, e.g. polylactic acid, polyhydroxy-alkanoates, and more recently polybutylene succinate, the range of monomers derived from renewable resources expands [2]. Biocatalysis can boost such innovation, leveraging on enzymes that overcome the limitations of conventional chemical strategies by catalyzing, under highly selective and mild conditions, the targeted modification, synthesis or degradation of polymers and, most importantly, biobased polymers [3]. Hydrolases, such as lipases and cutinases, were successfully used by several groups for *in vitro* polycondensation of bio-based diacids and polyols, leading to biodegradable polyesters with controlled structures [4].

However, the experimental screening of new enzymes could be very expensive and time-consuming. *In silico* screening, using appropriate bioinformatics tools, can be an effective aid in reducing the number of experiments. From this perspective, *in silico* developing and screening virtual new enzymes can accelerate the optimization process [5]. The possibility to correlate structural features of a polymer and its biodegradability is important in terms of environmental safety and for new tailor-made biodegradable plastics design. Both polymers and enzymes informatics efforts succeed in the recent years by utilization of modern data approaches inspired by artificial intelligence and machine learning methods [6].

The aim of RenEcoPol project is to develop a computational procedure able to analyze and evaluate the ability of different hydrolases to interact and to accept short chain substrates either for synthetic or degradative processes. In this respect specific modelling software's for proteins and protein-ligands interactions such as molecular dynamics and docking were selected and integrated into an automatic workflow. A series of bio-based monomers and enzymes were screened up to now and the computational studies results were correlated with some available experimental data and the results indicate that ability of enzymes to hydrolyze or synthesize polyesters can rationally be selected by integrating different computational tools.

### Acknowledgements



This project has received funding from the European Union's Horizon 2020 research and innovation programme under the Marie Skłodowska-Curie grant agreement No 101029444.

### References

1. A. Pellis, M. Malinconico, A. Guarneri, L. Gardossi, *N Biotechnol*, 60, 146-158 (2021)
2. Todea A, Dreavă DM, Benea IC, Bîcan I, Peter F, Boeriu CG, *Processes*, 9(4), 646, 1-26 (2021).
3. Guarneri A, Cutifani V, Cespugli M, Pellis A, Vassallo R, Asaro F, Ebert C., Gardossi L., *Adv Synth Catal* 361, 2559-73 (2019).
4. Pellis A, Corici L, Sinigoi L., D'Amelio N., Fattor D., Ferrario V., Ebert C., Gardossi L., *Green Chem.*, 17, 1756-1766, (2015).
5. Truppo M.C., *ACS Med Chem Lett.* 11; 8(5): 476–480 (2017.)
6. Chen L., Pilania G., Batra R., Huan T. D., Kim C., Kuenneth C., Ramprasad R., *Mater. Sci. Eng. R Rep.*, 144, 100595, (2021).

## Developing Machine Learning Coupled with Group Contribution Models for the Prediction of Densities of Deep Eutectic Solvents

Reza Haghbakhsh<sup>1,2</sup>, AhmadReza Roosta<sup>3</sup>, Ana Rita C. Duarte<sup>2</sup> and Sona Raeissi<sup>3\*</sup>

<sup>1</sup> Department of Chemical Engineering, Faculty of Engineering, University of Isfahan, 81746-73441, Isfahan, Iran

<sup>2</sup> LAQV, REQUIMTE, Departamento de Química da Faculdade de Ciências e Tecnologia, Universidade Nova de Lisboa, 2829-516 Caparica, Portugal

<sup>3</sup> School of Chemical and Petroleum Engineering, Shiraz University, Shiraz 71345-51154, Iran

\*raeissi@shirazu.ac.ir

Solvents play an important role in the framework of green chemistry. Many organic solvents are hazardous, poisonous, and destructive to the environment. As a result, their usage endangers both human health and the environment. Understanding solvent properties is essential for sustainable development, hence various solvents have been evaluated according to their environmental, safety, and health features. To qualify as a green medium, the solvents must have several criteria, including biodegradability, recyclability, non-toxicity, and low cost. Deep eutectic solvents (DESs), a new category of green solvents, are rapidly becoming popular in the scientific communities. DESs are made up of hydrogen bond acceptors (HBAs), such as halides or ammonium salts and hydrogen bond donors (HBDs), such as carboxylic acids, amides, and alcohols. DESs possess low volatilities and tunable structures, and are found to be cost-effective and easier to synthesize in comparison to the ionic liquids. They have little or insignificant toxicity, and are biodegradable and easily recyclable. These characteristics make DES superior to traditional solvents used in extraction techniques and because of their extraordinary properties, DESs have gained popularity as viable solvents for a variety of industrial applications.

To use a new solvent on any scale, from experimental to large industrial applications, it is necessary to know their fundamental properties, including the thermophysical properties. Density is a most important thermophysical property. It is quite easily measured experimentally. However, in the case of DESs, because of a significantly large number of potential DESs, not only due to the wide range of possible HBAs and HBDs, but also their various molar ratios, measuring the densities of all DESs is impossible. Thus, it is vital to have reliable thermodynamic models to predict the densities of various DESs.

Artificial intelligence (AI) approaches may be viewed as clever instruments for comprehending various phenomenon and answering related inquiries. These strategies attempt to create a machine capable of solving even the most complex issues. The simplicity, flexibility, fast speed, and good learning ability of AI-based techniques are the most promising features [1]. Machine learning (ML) is a subset of artificial intelligence that enables computer systems to recognize patterns, learn from data, and make decisions without explicit instructions. Machine learning has also emerged as a new tool in chemical engineering over the last decade. Indeed, there is a strong and growing interest in machine learning among chemical engineers, owing to its execution speed, flexibility, and user-friendly applications [2]. However, the greatest concern of machine learning models is their correlative nature, which cannot be applied for predictions. To overcome this issue, in this study machine learning and group contribution are merged. The groups of the HBA and HBD compounds are considered as the input parameters of the model. Then training is carried out, so the learned machine can find the relations among the groups and their effects on the final desired DES property of density.

In this study, a large data bank, including 1239 density data points for 149 various DESs, has been developed. The two different machine learning techniques of MLP neural network and LSSVM were applied to develop global density models for DESs. In these models, the groups of the HBA and HBD compounds, their molar ratio, and temperature are considered as the input parameters. The AARD% results below 0.2% for both of the developed models show the reliability and accuracy of the models.

### Acknowledgements

The authors are grateful to Shiraz University, the University of Isfahan, and Universidade Nova de Lisboa for providing facilities. This project has received funding from the European Union's Horizon 2020 - European Research Council (ERC) - under grant agreement No ERC-2016-CoG 725034.

### References

1. B. Daryayehsalameh, M. Nabavi, and B. Vaferi, *Environ. Technol. Innov.*, **22** 101484 (2021).
2. M. R. Dobbelaere, P. P. Plehiers, R. Van De Vijver, C. V. Stevens, and K. M. Van Geem, *Engineering*, **7** 1201–1211 (2021).

# Education, Society, UN Sustainable Development Goals

## Sustainability in undergraduate practical classes: From green chemistry metrics to environmentally friendly process design

Thomas A. Logothetis<sup>1\*</sup>

<sup>1</sup>University of Southampton, Chemistry, Highfield, Southampton, SO17 1BJ, United Kingdom

\*Corresponding author: [thomas.logothetis@soton.ac.uk](mailto:thomas.logothetis@soton.ac.uk)

### Abstract

Scientists from chemistry and chemical engineering and beyond have always sought to improve reactions and processes. This gained impetus when a framework in the form of the twelve principles of green chemistry has been circulated [1], followed by the formulation of the seventeen United Nations Sustainable Development Goals[2]. Chemists have ever since pursued more environmentally friendly pathways and this has translated to Green Chemistry Education, in theory and practice.

The motivation might have been as diverse as a financial stimulus, an indefensible waste problem, an improved awareness of energy consumption, recognition[3] and competition between institutions and, of course, the desire to promote chemistry in a sustainable fashion, fit for future's challenges. This appreciation of a possibility of a better future for all has stimulated a response with a mindfulness for limited resources and driven green topics in research and education.

To advance consciousness about environmental solutions and green chemistry a concerted effort must start at entry level, and it is crucial to address green chemistry as well as sustainable processes, apart from highlighting improved laboratory efficiency. Examples for the latter include water saving laboratory equipment (*i.e.* recirculating or air-cooling condensers[4]) that significantly reduce the carbon-footprint; whereas a project to improve an industrial process can be introduced already in undergraduate laboratory classes in a novel heterogeneous catalyst for nylon production.[5]

This presentation will underscore examples from undergraduate laboratory chemistry education and include established approaches involving green chemistry metrics, *e.g.* E-factor, atom economy, reaction efficiency, selectivity and turn-over. A focus is set, though, at the variation of trajectories to achieve the same target molecule and, moreover, through modifying chemical processes. Students are directed at assessing different engineering aspects, variables in methodology and identify pathways that are scalable, all from a selection of mechanochemical approaches, microwave and flow reactions, sonochemistry versus thermochemistry; and in the process[*sic*] identify sustainable batch and continuous conditions to synthesise a given target.

In summary, the latest ideas how to raise awareness of green chemistry in chemistry education through engaging chemistry laboratory classes will be appraised against the backdrop of current undergraduate provision, while future developments will be shaped via ensuing dialogue

### Acknowledgements

Education in the teaching laboratories at Southampton would not be possible without the generous support provided by academic colleagues, teaching assistants and technicians, all of whom are gratefully acknowledged. Special thank you to all those students, who went beyond their studies and suggested improvements during their lab classes, discussions, and presentation.

### References

1. P. T. Anastas, J. C. Warner, *Green Chemistry: Theory and Practice*, OUP, New York, 1998.
2. UN Sustainable Development Goals – <https://www.un.org/sustainabledevelopment/> [accessed 07/03/2022]
3. The Laboratory Efficiency Assessment Framework – <https://www.ucl.ac.uk/sustainable/staff/leaf> [accessed 07/03/2022]
4. E. W. Baum, J. J. Esteb, A. M. Wilson, *J. Chem. Educ.*, **2014**, *91*, 1087-1088.
5. S. Chapman, J. M. Herniman, G. J. Langley, R. Raja, T. A. Logothetis, *J. Chem. Educ.*, **2019**, *96*, 2937-2946 – *Redox Aluminophosphates: Applying Fundamental Undergraduate Theory To Solve Global Challenges in the Chemical Industry*

## A rational dimension of Green chemistry and bethical education towards Sustainability

Mani Omprakash Srivastava , Chemistry Educator  
Tilak College and DAV Kharghar , Navi Mumbai , India  
\*mane11in@yahoo.com

An amalgamation of GREEN CHEMISTRY and ethical education to prepare leaners and spread the green culture with an army of green tender hearts to conserve Mother Earth and respect Nature's serenity, tranquility and magnificence.

Ethical and green sustainability pledge with joint research projects is to prepare the subsequent generation of learners for persuading and propagating principled and responsible revolutions which will empower learners and will result in no more disastrous constituents in substance of a viable Planet.

A novel approach towards GREEN Chemistry education and Moral Code in Chemistry Education is TO CREATE ETHICAL IDEOLOGY. Shifting the Paradigm by **embracing an interdisciplinary approach of ethical imagination and invention**. Designed and implemented different researches towards a greener prospective program with full involvement of students, teachers and local communities.

It's to Initiate and prepare the subsequent generation of chemists and scientist by empowering them towards a fundamental change in society by bringing a radical revolution in human mind to develop an understanding that Chemistry is to **CREATE NOT DESTROY**.

Developed a zero-tolerance approach towards ignorance and negligence in scientific inventions by highlighting the understanding towards whose responsibility is deadly plastics which has become threatening to all life, CFC generated broad spectrum thinning of ozone layers, heavy metal hazards, oil spill, COVID-19... many like these represents a big concern towards our planet and makes big inventions in vain. Inducing every learner and teachers towards the protection of environment and to protect humanity on Planet earth. The students were instilled with the oft repeated thought that, 'We have not inherited this earth from our fore-fathers; we have borrowed it from our children'.

Bridging the gap between green chemistry and sustainable education through ethical **green expansions** is by connecting the dots across as individuals, society, community, country and world.

Through an approach that provides a framework to integrate sustainability principles and grow their minds to innovate and become curator of our Universe, with their skill to protect our planet's peace, calmness and radiance for future generations. Ethical Imagination and invention transform the way of education is experienced inspiring young people to discover that there is far more within them than they think, to discover their grand passion in life and to explore what it means to live from a strong sense of responsibility.

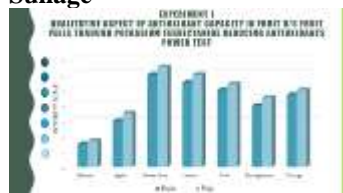
It's an approach to aim and design a "Sustainable World" with Green Curriculum and Green Pledge and to put a stop on the IGNORANCE in scientific INVENTIONS.

### Summary:

**Undertook various projects covering a wide expanse of soil and water, wherein the stress was not on the staple move of removing the irritants but to utilize them in a better manner so as to fulfill our dreams of a Healthy and Green World.**

Working on this line, we tried to use the industrial waste, discarded objects and contaminated water in an exhaustive manner to get rid of their evils and utilize them in a better way for sustainable development. The major Projects are as following:

**Free Radical scavenging activity by investigating Tagetes Erecta a scavenger of Sullage**



**Nutraceutical: Peel of fruits Antioxidants a hero component terminates the free radical chain reactions before the cell components are destroyed! Removal of Heavy Toxic Metal From waste water:**To make potable water (devoid of Toxic Effluents) and make it available for masses.

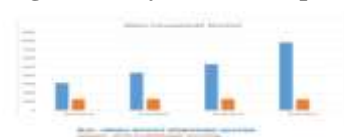
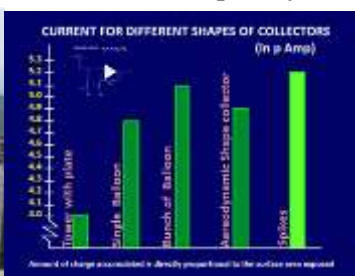






**Designed hydrophobic solution to Solve the Water Crisis:PMMA and SiO<sub>2</sub> coating Used in Urinal to use water in flushing. A Nano solution to a Giga Nano problem which can save gallons of Water.**

**ATMO POWER: Design a sustainable world with consideration to environmental impact by harnessing electricity from atmosphere.**



**Developed Nutrameal A planetary Health diet to Save Earth before its too late and also for lower starta people:**

Nutrimeal from weeds a cost-effective food supplement to combat dietary

deficiencies and malnutrition as it provides balance diet in single food

**Bio Fuel:** To create most valuable form of renewable energy a transportation fuel options to establish safe, clean and sustainable hydrocarbon.

**Offsetting Carbon Emission with Emerging Technologies;** To reduce dependency on hydrocarbon for fueling the transportation and other sector; to provide more economic opportunities for the development of the country' to reduce carbon foot print and save our environment for the future generation.



**In an ideal world,** Education for **GREEN Viable Advancement** should pervade the entire school curriculum, with every subject area, at every year level, dealing with aspects of sustainability in broader way.



**Acknowledgement:**

- Indian Institute of Metrology, Pune, Maharashtra
- Indian Institute of Geomagnetism, Navi Mumbai Maharashtra
- Nehru science Centre, Mumbai, Maharashtra
- Agriculture university: Rauri Krishi Vidya Peeth, Ahmednagar Maharashtra
- Agriculture university Pune, Maharashtra
- Subodh laboratories, Turbhe Maharashtra
- Infinity lab solutions, Nerul, Maharashtra
- Maharashtra pollution control department.
- Bokarpada water purification Centre
- DAV Kharghar

**Reference:**

Green chemistry Education Paul T. Irvin Jay Levy, Kathryn E. Parent American Chemical Society, 2009  
Sustainable Education ,Stephen Sterling  
Scholar.google.com

## Pedagogic applications of systems-oriented concept map extension (SOCME) in the education of community college students for a green environment

Wang-Kin Chiu<sup>1\*</sup>, Ben Y.F. Fong<sup>1</sup> and Wing-Yi Ho<sup>2</sup>

<sup>1</sup>Division of Science, Engineering and Health Studies, College of Professional and Continuing Education, The Hong Kong Polytechnic University, Hong Kong, China

<sup>2</sup>School of Professional Education and Executive Development, The Hong Kong Polytechnic University, Hong Kong, China  
\*oscar.chiu@cpce-polyu.edu.hk

### Abstract text:

Advancement in the scientific development of sustainable chemistry and innovations regarding the principles of green chemistry are important to the world's sustainable development [1, 2]. Chemistry, being a central science, has its vital roles in the collaborative efforts across disciplines for the achievement of Sustainable Development Goals and to address the emerging global challenges including those impacting the environmental sustainability [3]. A green environment, which is of particular significance regarding the worldwide growth of ageing population, is essential to human health and well-being [4]. In recent years, there have been strong advocations calling for reforms in chemical education based on systems thinking and its importance for nurturing the future generations to find the solutions the world needs [5, 6]. Recent reports have also described the efforts in the development of the IUPAC systems thinking framework in chemical education and demonstrated the remarkable application potentials by the use of systems-oriented concept map extension (SOCME) diagrams and integration with the molecular basis of sustainability [7-9].

We now describe the design of SOCME visualizations and incorporation of systems thinking in the teaching and learning of chemistry in a community college in Hong Kong. In this study, three SOCME diagrams have been designed with relevance to the subject content and learning objectives of a general-education (GE) chemistry course at sub-degree level. The SOCME materials focus on polyethylene (PE), polypropylene (PP), and polyethylene terephthalate (PETE), which are common examples of daily-life thermoplastics. Adopting a systems thinking approach, interconnections of the impact of chemicals with the dynamic systems of human and environmental health are identified. Pedagogic design for applying the SOCME visualizations in a technology-enhanced environment of learning chemicals will also be presented.

### Acknowledgements

The work described was partially supported by a research grant from the College of Professional and Continuing Education, an affiliate of The Hong Kong Polytechnic University (project reference no.: SEHS-TF-2021-005(J)).

### References

1. K. Kümmerer, *Angew. Chem. Int. Ed.*, **56** 16420 (2017).
2. J.B. Zimmerman, P.T. Anastas, H.C., Erythropel, W. Leitner, *Science*, **367** 397 (2020).
3. S.A. Matlin, G. Mehta, H. Hopf, A. Krief, *Nat. Chem.*, **7** 941 (2015).
4. B.Y.F. Fong, W.-K. Chiu, W.F.M. Chan, T.Y. Lam, *Int. J. Environ. Res. Public Health*, **18** 8024 (2021).
5. P.G. Mahaffy, A. Krief, H. Hopf, G. Mehta, S.A. Matlin, *Nat. Rev. Chem.*, **2** 1 (2018).
6. E. Dobbelaar, J. Richter, *Pure Appl. Chem.*, **94** 1 (2022).
7. P.G. Mahaffy, S.A. Matlin, J.M. Whalen, T.A. Holme, *J. Chem. Edu.*, **96** 2730 (2019).
8. S.A. Matlin, G. Mehta, H. Hopf, A. Krief, L. Keßler, K. Kümmerer, *Sustain. Chem. Pharm.*, **17**, 100312 (2020).
9. T. Holme, *Sustain. Chem. Pharm.*, **16** 100234 (2020).

## Green Chemistry in Secondary Education: Views of Greek Chemistry Teachers

Katerina Paschalidou<sup>1</sup>, Dionysios Koulougliotis<sup>2</sup>, and Katerina Salta<sup>1\*</sup>

<sup>1</sup>National and Kapodistrian University of Athens, Greece, <sup>2</sup>Ionian University, Greece  
\*ksalta@chem.uoa.gr

### Introduction

The philosophy of Green Chemistry is based on a cohesive set of 12 principles [1] and has served as a foundation for the development and establishment of Education for Sustainable Development (ESD) [2,3]. During the last few years, based on the Green Chemistry philosophy, the principles of Green Chemistry have become an important part of educational practice in secondary education. This fact stimulated the development of a considerable number of curricular materials that aim to develop students' ability for societal decision making by considering all factors driving Green Chemistry and Sustainable Development [4].

Burmeister et al. [2] identified four basic models on how Green Chemistry (GC) can be diffused in Chemistry Education (CE), which refer to: (I) adoption of Green Chemistry principles into school science laboratory, (II) using Green Chemistry issues as content in Chemistry Education, (III) addressing chemistry teaching and learning through Green Chemistry in an socio-scientific issues (SSI)-based context, and (IV) an understanding of Green Chemistry Education, as part of sustainability-driven development of school life. Furthermore, Jegstad and Sinnes [3] have modified Burmeister et al.'s model [2], resulting to a refined one for planning Green and Sustainable Chemistry Education that encompasses five different categories which represent different aspects of a complex whole and partly overlap to achieve a holistic perspective of Green Chemistry Education. The above mentioned four models can be classified as possessing differing degrees (weak to strong) of chemistry *environ-mentalization* which is a term used to describe the extent at which chemistry takes into consideration the interests of society in combination with the corresponding environmental and health threats [5].

There is a lot of research documenting that students' knowledge-building in science classrooms should have some relationship to the way that science knowledge is developed in the scientific community and in fact the 'doing science like a scientist' approach has shifted from a focus on the individual to a focus on social context. Research focusing on learning theories in the last decades has offered a series of student-centered teaching strategies, including argumentation-based, case-based, context-based, problem-based, project-based, SSI-based, inquiry-based, and a hands-on approach to teaching and learning [6].

Regardless of the teaching-learning approach, chemistry teaching and learning goals focus on four domains: (a) the affective domain that incorporates attitudes, motivation, interests, self-efficacy, and values [7]; (b) the cognitive domain which involves the conceptual structures and cognitive processes used when reasoning scientifically; (c) the epistemic domain which includes the frameworks used when developing and evaluating scientific knowledge; and (d) the social domain that relates with processes and contexts that shape how knowledge is communicated, represented, argued, and debated [8].

The integration of the cognitive and affective domain constitutes a cornerstone of Environmental Education fostering awareness at several levels, including: (a) self-awareness, that reflects how one's lifestyle choices impact on the environment; (b) social awareness, that depicts how people interact socially to influence individual choices; (c) environmental awareness that refers to how society impacts on ecosystems through political choices [9].



Figure 1. Factors addressing Green Chemistry in secondary Chemistry Education.

While many chemistry departments have already incorporated the principles of Green Chemistry and the concept of sustainability in their curricula, the integration of Green Chemistry in secondary school curricula seems to be rare. Given its relative novelty to chemistry curricula, we treat Green Chemistry instruction as a school innovation that is being adopted by chemistry teachers. Teachers are ‘agents of change’ of educational reform, and their beliefs must not be ignored. Indeed, their pedagogical beliefs are at the ‘core of educational change’ [10]. Thus, this exploratory research study was designed to address two research questions:

1. To what extent do secondary school chemistry teachers conceptualize what Green Chemistry Education is and how Green Chemistry can be diffused in Chemistry Education?
2. What are secondary school chemistry teachers’ views related to how Green Chemistry can be incorporated in chemistry lessons?

### Method

Because this study aims to describe and theorize chemistry teachers’ concerns about Green Chemistry instruction, we employed a qualitative design that allowed for the emergence of teachers’ ideas. Data analysis employed a grounded theory approach via which patterns emerged from teachers’ own words and were constantly compared with each other to generate larger themes [11].

#### Sample

A total of 10 chemistry teachers participated in the study, accepting an invitation to attend a single interview which was no longer than 90 minutes in length. The participants were selected using an opportunity snowball sampling approach [12]. All research participants taught chemistry at the high school level and held bachelor’s degrees.

#### Data Collection

An authors-designed semi-structured interview protocol was developed. Each interview began with three open-ended, free-response questions, given to the participants ahead of time. These questions gave the participants opportunities to describe their general views regarding the research theme, phrasing responses in whatever way they saw fit. Given that we were seeking to gain views on a complex matter for which ready views might not have been offered in a typical question and answer interview format, in the second part of the interview we used a bank of statements to elicit further participant comments, aiming at participants to organize the expression of their views to decide whether to agree or disagree with each statement presented. The statement card-sorting exercise acted as a component of the analytical tool known as Q methodology [13, 14] to support the process of discourse analysis. A set of 24 statements that represented a range of ways in which Green Chemistry principles are integrated in Chemistry Education have been utilized in literature as it pertains to this study. The full card set was presented to each participant who sorted the statements according to a five-point scale ranging from strongly disagree to strongly agree. Then, participants were asked (a) to report the way in which they had decided to categorize the statements, and (b) to put in order of importance their agreement regarding statements placed under each of the five choices, incorporating a think-aloud process [15].

#### Data Analysis

Data analysis was guided by a grounded theory approach. First, the constant comparative method [11, 16] was employed to code the interview transcripts. After open coding the transcripts, categories including these codes were developed and elaborated with respect to properties and dimensions [11, 16]. The boundaries, properties, and dimensions of these categories were explicitly defined in initial code notes and participant exemplars. The two authors reviewed 25 % of the transcripts using the detailed code notes and participant exemplars to determine the

extent to which analyses inferences were reliable. After a discussion of differences between two coders, a revised taxonomy and the final set of code notes were developed.

### Results, Discussion and Conclusion

Given that data analysis has not been completed, the results, discussion, and conclusions of this study will be presented in the conference

### References

1. P. Anastas and N. Eghbali, *Chem. Soc. Rev.*, **39** 301 (2010).
2. M. Burmeister, F. Rauch, I. Eilks, *Chem. Educ. Res. Pract.*, **13** 59 (2012).
3. K. M. Jegstad, A. T. Sinnes, *Int. J. Sci. Educ.*, **37** 655 (2015).
4. D. Koulougliotis, L. Antonoglou, K. Salta, *Int. J. Sci. Educ.*, **43** 298 (2021).
5. J. Sjöström, I. Eilks, V.G. Zuin, *Sci & Educ*, **25** 321(2016).
6. M. Jurišević, M. Vrtačnik, M. Kwiatkowski, N. Gros, *Chem. Educ. Res. Pract.*, **13** 237 (2012).
7. A. A. Flaherty, *Chem. Educ. Res. Pract.*, **21** 698 (2020).
8. R. A. Duschl, *Rev. Res. Educ.*, **32** 268 (2008).
9. M. Littledyke, *Environ. Educ. Res.*, **14** 1 (2008).
10. N. Mansour, *Res. Sci. Educ.*, **43** 347 (2013).
11. J.M. Corbin, A. Strauss, *Qual. Sociol.*, **13** 3 (1990).
12. L. Cohen, L. Manion, K. Morrison, *Research Methods in Education*, Routledge (2013).
13. S. Ramlo, *J. Mix Methods Res.*, (2022).
14. A. Lundberg, R.R. de Leeuw, R. Aliani, *Educ. Res. Rev.*, **31** 100361 (2020).
15. M. Koro-Ljungberg, E. Douglas, D. Therriault, Z. Malcolm, N. McNeill, *Qual. Res.*, **13** 735 (2013).
16. K. Salta, M. Gekos, I. Petsimeri, D. Koulougliotis, *Chem. Educ. Res. Pract.*, **13** 437 (2012).

## Green Chemistry Education and Promotion in Taiwan

Pao-Kuei Hsiao<sup>1\*</sup>, Yu-Chun Wang<sup>2</sup>, Yu-Kai Lin<sup>3</sup>, Yi-Kuen Liu<sup>1</sup>, Chun-Sheng Wu<sup>1</sup>, Yen-Ju Hsieh<sup>1</sup>

<sup>1</sup> Toxic and Chemical Substances Bureau, No.1, Aly. 35, Ln. 132, Sec. 2, Da'an Rd., Da'an Dist., Taipei City 10667, Taiwan (R.O.C.)

<sup>2</sup> Chung Yuan Christian University, No. 200, Zhongbei Rd., Zhongli Dist., Taoyuan City 320314, Taiwan (R.O.C.)

<sup>3</sup> University of Taipei Tian-Mu Campus, No.101, Sec. 2, Zhongcheng Rd., Shilin Dist., Taipei City 111036, Taiwan (R.O.C.)

\* paokuei.hsiao@epa.gov.tw

### Abstract

To achieve better environmental quality and reduce human health risks, the Toxic and Chemical Substances Bureau (TCSB) under the Taiwan Environmental Protection Administration substantially enhanced the management of chemical substances in Taiwan since its establishment in 2016. TCSB collaborating with the Ministry of Education, promoted green chemistry (GC) education in colleges and primary schools and held the second *Green Chemistry Creativity Competition for Universities*. TCSB also provided a GC research fund for universities and NGOs to apply. In addition, TCSB collaborated with the Ministry of Science and Technology, research institutions, and private sectors to study the policy and techniques for safer alternatives for hazardous chemicals. Furthermore, TCSB launched the *Green Chemistry Application and Innovation Award* to encourage industries to develop green chemistry. Lastly, TCSB conducted education and promotion of GC to the public through community propaganda, media, Internet, publication, etc.

For GC education in the primary schools, TCSB finished more than six sets of environmental education materials and was promoted in 10 primary schools, with participants of more than 300 students and teachers. In addition, by cooperating with NGOs, TCSB held four green chemistry seed training camps for elementary school teachers, with 116 teachers trained.

TCSB completed 16 green-chemistry teaching materials for the general education course for GC education in the universities. After analyzing 237 questionnaires from students who took the course, over 80% of students agreed that they could gain green chemistry knowledge. Furthermore, in holding the *Second Green Chemistry Creativity Competition for Universities*, 46 teams from 27 schools and 40 departments participated in the competition.

TCSB offered a fund for colleges and NGOs to apply scientific green-chemistry studies, such as substituting toxic chemicals. By cooperating with the Ministry of Science and Technology, research institutions, and private sectors, TCSB has been developing a safe alternative screening system for hazardous chemicals since 2020. In addition, some information technologies, such as Python, artificial intelligence, machine learning, and the interconnection of international data banks, were applied to the system.

In all, TCSB strives to manage chemicals well and safeguard human health.

# Environmental catalysis

## Efficient visible light driven photocatalytic degradation of perfluorooctanoic acid by $\text{Bi}_7\text{O}_9\text{I}_3$ catalyst

Jhimli Paul Guin<sup>1,\*</sup>, K. Ravindranathan Thampi<sup>1</sup>, James A. Sullivan<sup>2</sup>

<sup>1</sup>School of Chemical and Bioprocess Engineering, University College Dublin, Belfield, Dublin 4, Ireland

<sup>2</sup>School of Chemistry, University College Dublin, Belfield, Dublin 4, Ireland

\*jhimli.paulguin@ucd.ie; paul.jhimli@gmail.com

Perfluorooctanoic acid (PFOA) is one of the most commonly used perfluoroalkyls in various industries, fire-fighting training sites and household products due to their special oleophobic and hydrophobic properties and their chemical inertness. These are known as persistent organic pollutants as they are resistant to degradation by natural processes. As a result, they are quite often detected in surface and ground waters causing adverse health hazards to living beings [1]. Photocatalysis is an emerging advanced oxidation process where inclusion of sunlight as a renewable source of energy makes their decomposition reaction sustainable [2]. Reactive oxygen species generated from photocatalysis have the potential to degrade PFOA effectively. This study reveals the possibility of using bismuth oxyiodide, composed of earth-abundant Bi (0.00002% by mass in the earth's crust) as a photocatalyst for the degradation of PFOA in water without the addition of any external reagents.

Bismuth nitrate pentahydrate (>98% pure) ( $\text{Bi}(\text{NO}_3)_3 \cdot 5\text{H}_2\text{O}$ ) and perfluorooctanoic acid (PFOA) (>95% pure) were purchased from Sigma Aldrich. Potassium iodide (>97%) was obtained from BDH Ltd., Poole, U.K. Ethylene glycol of analytical grade of purity 99% was used. All the chemicals were used as such without any purification. 2.0 mmol of  $\text{Bi}(\text{NO}_3)_3 \cdot 5\text{H}_2\text{O}$  and 2 mmol of potassium iodide (KI) were dissolved in 20 mL of ethylene glycol separately by ultrasonication to ensure the complete dissolution of the substances. Then, the KI solution was added slowly to the former solution and the resultant yellow-coloured transparent solution was transferred into 50 mL Teflon liners and heated in a muffle furnace at 160 °C for 12 h. The product was washed several times with ethanol and water and dried in air at 80 °C. An aliquot of the product was calcined at 400 °C with a temperature ramp of 10 °C/min for an optimised time of 2 h.

The crystalline structures of the photocatalyst were analyzed by X-ray diffraction (XRD) (Siemens D500 Kristalloflex Diffractometer) with a scanning range between 5 - 80°. The optical properties of the catalysts were measured by UV-Visible diffuse reflectance spectroscopy (UV-Vis DRS) (Jasco V-650 Spectrophotometer) with  $\text{BaSO}_4$  as the reflectance standard and the scanning range was set between 300 - 900 nm. The thermal stability of the catalyst was investigated by a thermogravimetry analyser (TGA Q 500) with a heating range and rate of 30 - 1200 °C and 10 °C/min, respectively. The elemental composition was determined by X - ray photoelectron spectroscopy (Kratos AXIS Ultra DLD monochromatic) with a 150 W Al  $\text{K}\alpha$  x-ray source.

The bismuth oxyiodide catalyst (1 g/L) was dispersed in 10 mL of 1 ppm PFOA solution in 50 mL glass vials. The vials were kept overnight to reach an adsorption-desorption equilibrium and later were placed inside an Atlas Suntest™ CPS+ solar simulator for irradiation, using a 700 W Xe lamp for different time intervals. After irradiation with the simulated solar spectrum (AM1.5), the solutions were centrifuged and the supernatant collected and stored for further studies. The control experiment was conducted without the addition of any catalysts. The photocatalytic degradation of PFOA was determined by negative ion mode electrospray ionization quadrupole time-of-flight mass spectrometry (Agilent 6546 LC/Q-TOF).

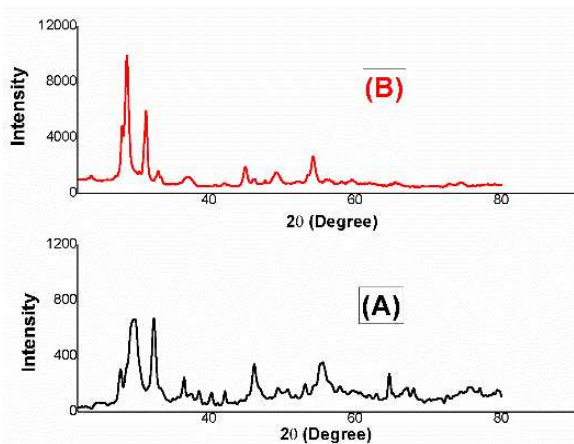


Figure 1. XRD pattern of (A) BiOI and (B)  $\text{Bi}_7\text{O}_9\text{I}_3$ .

Figure 1 shows the XRD pattern of uncalcined (A) and calcined bismuth oxyiodides (B). The three major characteristic diffraction peaks of the uncalcined sample at  $2\theta = 29.8^\circ$ ,  $32.3^\circ$  and  $55.5^\circ$  correspond to (102), (110) and (122) planes of tetragonal BiOI (JCPDS no. 10-0445) [3]. The diffraction peaks of the calcined sample at  $2\theta$



= 28.7°, 31.3°, 37.1°, 44.9°, 49.1° and 54.2° correspond to the (102), (110), (103), (200), (114) and (202) planes of tetragonal phase Bi<sub>7</sub>O<sub>9</sub>I<sub>3</sub> [4]. The slight shift of the diffraction peak of (102) plane of BiOI from 29.8° to a lower angle of 28.7° in Bi<sub>7</sub>O<sub>9</sub>I<sub>3</sub> is attributed to the distortion of the crystal structure. On the other hand, the intense narrow peaks in the Bi<sub>7</sub>O<sub>9</sub>I<sub>3</sub> profile confirm better crystallinity compared to BiOI. The XPS survey spectra of Bi<sub>7</sub>O<sub>9</sub>I<sub>3</sub> confirms the presence of only Bi, O and I, and no other impurities have been observed. The UV-Vis DRS shows that Bi<sub>7</sub>O<sub>9</sub>I<sub>3</sub> has satisfactory visible light absorption with an absorption edge about 532 nm. The material shows a blue-shift compared to the absorption spectra of BiOI (absorption edge at 667 nm) (spectra not shown). The band gap energy of Bi<sub>7</sub>O<sub>9</sub>I<sub>3</sub> was calculated as 2.33 eV from a Tauc plot. Calcination removes defects from the crystal structure of Bi<sub>7</sub>O<sub>9</sub>I<sub>3</sub> resulting in this observed blue-shift. The catalyst shows very high thermal stability with only a mass loss of ~16 % following heating to 1000 °C as confirmed by the TGA analysis.

PFOA showed resistance to degradation under the simulated solar light irradiation in the absence of any catalyst. On the other hand, 80.0% degradation of 1 ppm PFOA in the presence of 1 g/L Bi<sub>7</sub>O<sub>9</sub>I<sub>3</sub> after 4 h of photocatalysis was noted (Figure 2). Analysis of the valence band XPS data confirms that the more negative conduction band potential of Bi<sub>7</sub>O<sub>9</sub>I<sub>3</sub> than E<sup>0</sup> O<sub>2</sub>/O<sub>2</sub><sup>-</sup> (-0.33 V vs NHE) allows the photoexcited electrons to react with oxygen to form superoxide radical anions (O<sub>2</sub><sup>-</sup>) under visible light irradiation. On the other hand, the more negative valence band potential of Bi<sub>7</sub>O<sub>9</sub>I<sub>3</sub> than E<sup>0</sup> ·OH/OH<sup>-</sup> (+1.99 V vs NHE) restricts the oxidation of H<sub>2</sub>O to form hydroxyl radicals (·OH). This study presents the potential for development of sustainable and efficient photocatalysts for removal of PFOA from contaminated water. Some of the challenges and opportunities in such catalytic system developments have been discussed in a recent publication [2].

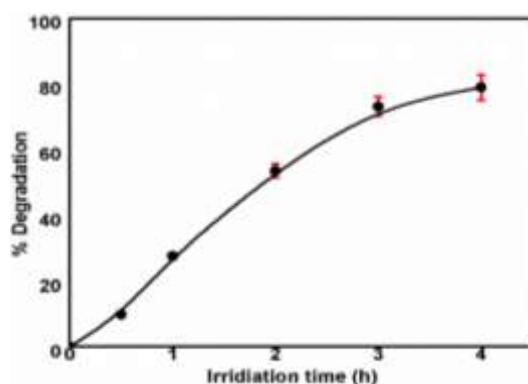


Figure 2. Photocatalytic performance of Bi<sub>7</sub>O<sub>9</sub>I<sub>3</sub> for the degradation of 1 ppm PFOA under 700 W simulated solar light irradiation (catalyst load: 1 g/L).

### Acknowledgements

The study is funded by Irish Research Council Government of Ireland Postdoctoral Fellowship 2020 under the project GOIPD/2020/266.

### References

1. J. L. Domingo, M. Nadal, *Environmental Research*, **177** 108648 (2019).
2. J. Paul Guin, J.A. Sullivan, K.R. Thampi, *ACS Engineering Au* <https://doi.org/10.1021/acsengineeringau.1c00031> (2022).
3. N. Wang, L. Shi, L. Yao, C. Lu, Y. Shi, J. Sun, *RSC Advances*, **8** 537 (2018).
4. J. Yin, D. Gao, X. Zhu, X. Liu, H. Li, *Ceramics International* **47** 19556 (2021).

## Photocatalytic degradation of Ciprofloxacin antibiotic by doped LaFeO<sub>3</sub> nanopowders

Renato Pelosato<sup>1\*</sup>, Isabella Bolognino<sup>1</sup>, G. Marci<sup>2</sup>, Isabella Natali Sora<sup>1</sup>

<sup>1</sup>Department of Engineering and Applied Sciences, University of Bergamo, Viale Marconi 5, 24044 Dalmine (BG), Italy

<sup>2</sup> "Schiavello-Grillone" Photocatalysis Group, Department of Engineering, University of Palermo, Viale delle Scienze, 90128 Palermo, Italy

\*renato.pelosato@unibg.it

Photocatalytic oxidation is considered a promising and green alternative to the conventional methods of organic pollutants degradation in wastewater. Antibiotics are often detected in wastewater media in developed countries, especially molecules as tetracyclines, penicillins, fluoroquinolones and macrolides, together with analgesics [1]. Pure semiconducting oxides photocatalysts are infrequently used. One problem is the rapid recombination of excited electron-hole pairs, which are generated when the semiconductor is irradiated by light with an energy that matches or exceeds the band gap energy of the semiconductor. Metal and/or non-metal doping has shown promising results in diminishing the electron-hole recombination. In this work photocatalytic oxidation of ciprofloxacin (CP) antibiotic using heterogeneous semiconductor oxides such as lanthanum ferrite LaFeO<sub>3</sub> (LF) and 10 different metal-doped LaFeO<sub>3</sub> nanopowders is presented. The bandgap energies of LF and doped-LF are in the range of visible light energies.

In this study ciprofloxacin ( $\geq 98\%$ ) is used as model pollutant. LaFeO<sub>3</sub> (LF), 10 mol% Cu-doped LF (LFC10), 5 mol% Mg-doped LF (LFM05), 10 mol% Mg-doped LF (LFM10), 20 mol% Mg-doped LF (LFM20), 10 mol% Ga-doped LF (LF G10), 3 mol% Pd-doped LF (LFP03), 5 mol% Pd-doped LF (LFP05), 10% mol Y-doped LF (LFY10), 20 mol% Y-doped LF (LFY20) nanopowders are prepared by citrate auto-combustion method [2] and characterized by Powder X-ray diffraction using a Bruker D8-Advance powder diffractometer equipped with a Cu  $\alpha$  source and a Lynxeye XE-T® solid state detector. Crystallite sizes of the powders are calculated using the Williamson-Hall method using SRM676a corundum sample as a reference. The peak broadening of the individual peaks is determined by fitting the peak shape with a Lorentzian profile function by the software EVA DiffracPlus. Brunauer–Emmett–Teller (BET) specific surface area (SSA) of samples is determined using a Micrometric Tristar 3000 automated gas adsorption analyzer. Scanning electron microscopy (SEM) is performed by using a FEI Quanta 200 ESEM microscope, operating at 20 kV on specimens upon which a thin layer of gold had been evaporated.

The photocatalytic degradation reactions are performed using a Ryonet reactor equipped with six lamps (8 W, GE lighting 10055-F8T5/D) emitting in the visible region. The temperature is kept constant at temperature of  $28 \pm 1$  °C through liquid cooling system. Photocatalyst powder (ca. 2.6 mg) and H<sub>2</sub>O<sub>2</sub> (4 drops) are added to 20 mL of a  $5 \times 10^{-6}$  M CP aqueous solution. After stirring for 20 minutes in dark conditions, the six lamps are turned on. All experiments are performed in 4 hours. At different time intervals (t = 0, 30, 60, 120 and 240 minutes) small aliquots of the solution are drawn and centrifugated for 5 minutes at 3500 rpm. The resulting clear solutions are analysed with a UV-Vis spectrophotometer (Jasco V-650). The degradation of CP is calculated by evaluating the absorption peak of CP at 270 nm.

### Results:

All the synthesized samples crystallize in an orthorhombic perovskite crystal structure similar to LF. No traces of side phases are found, except for a tiny trace of PdO in the 5%Pd-doped sample. The recorded XRD patterns are shown in Figure 1A.

Photocatalytic degradation results after 4 h of irradiation under visible light in the presence of H<sub>2</sub>O<sub>2</sub> are summarized in Figure 1B. ('blank' refers to the irradiated CP solution without any addition; 'H<sub>2</sub>O<sub>2</sub>' refers to the irradiated CP solution with H<sub>2</sub>O<sub>2</sub> but without the photocatalyst).

Doped-LF mediated heterogeneous photocatalysis is faster than photolysis (22% degradation, blank sample) and also outperforms the activity of hydrogen peroxide (only the Ga-doped LF has nearly no effect on the degradation rate with respect to H<sub>2</sub>O<sub>2</sub>). 10% Mg-doped LF and 10 and 20% Y-doped LF show the best results with a degradation of 78, 70 and 71% of the initial CP respectively, followed by 3% Pd-doped LF and 5%-Mg-doped with 69 and 67%.

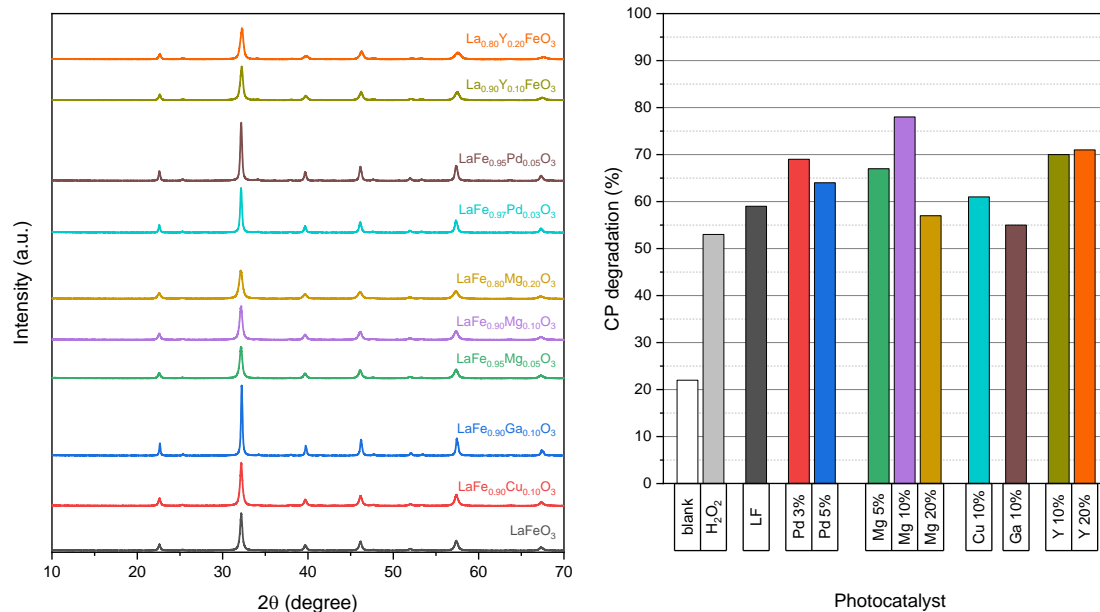


Figure 1. X-Ray Diffraction patterns of the prepared photocatalysts (left) and CP degradation after 4h of visible light illumination (right).

Also, the degradation of CP was analysed against the SSA of the photocatalysts and the calculated crystallite size. The results show that the extent of the degradation is uncorrelated with the microstructural features. In the applied experimental conditions (pH = 6.2) CP is mainly in its zwitterionic form. Complexation with positively charged sorbents can occur with the deprotonated carboxylate and the keto groups [3]. Likely, the degradation mechanism of CP is mediated via surface complexation. Physical mechanisms such as van der Waals forces attraction and hydrogen bonding between CP molecules and OH groups on the surface of the photocatalyst may also contribute in adsorption.

The degradation kinetic parameters with the most performing photocatalyst (10% Mg-doped LF) is shown in Figure 2

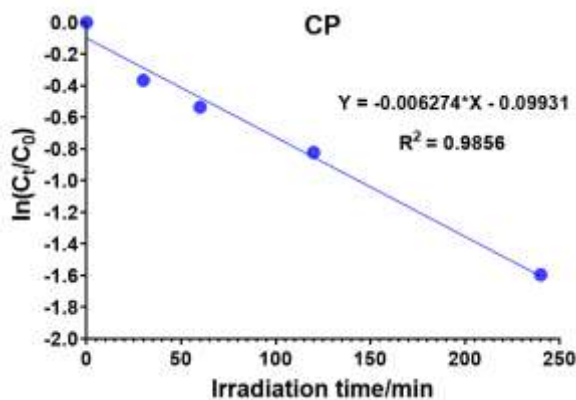


Figure 2. Pseudo-first order kinetics for the photocatalytic degradation of CP ( $5 \times 10^{-6}$  M) in the presence of 10% Mg-doped photocatalyst. Rate constant  $k = 0.0063 \text{ min}^{-1}$  ( $R^2 > 0.98$ ).

## Acknowledgements

One author (I.B.) was supported by University of Bergamo, Project STARS1718AZ1.

## References

1. B. Blair, A. Nikolaus, C. Hedman, R. Klaper, T. Grundl, *Chemosphere* **2015**, *134*, 395–401.
2. T. Caronna, F. Fontana, I.N. Sora, R. Pelosato, *Mater. Chem. Phys.* **2009**, *116*, 645–648.
3. C. Gu, K.G. Karthikeyan, *Environ. Sci. Technol.* **2005**, *39*, 9166–9173, doi:10.1021/es051109f.

## Catalysis on demand for greening up the battle against agrochemicals: fast, sustainable and versatile

Valmir B. Silva, Yane H. Santos, André H. G. Martinez, Renata Hellinger, Alex R. Teixeira, Patrícia Soares, José G. L. Ferreira, Willian Takarada, Mariana H. Nazareno, Aldo J. G. Zarbin and Elisa S. Orth\*

*Departamento de Química, Universidade Federal do Paraná (UFPR), CP 19032, CEP 81531-980, Curitiba, PR, Brasil*  
\*elisaorth@ufpr.br

How safe are we from agrochemicals? They are extensively used worldwide (and necessary for nourishment) but can be highly toxic. Their improper abusive use together with the problematic of threatening stockpiles (unused or prohibited) are of great concern, which require efficient neutralization and monitoring methods. Catalysts-by-design is a promising approach for neutralizing toxic organophosphates (*e.g.* agrochemicals and chemical warfare), since these reactions are extremely slow. Our group has been focused in combating organophosphates, mainly seeking: (i) milder conditions for the neutralization/synthetic processes; (ii) catalysts derived from nanomaterials and sustainable sources (rice husk and shrimp shell); (iii) portable and colorimetric detectors.

The organophosphates and imidazole-derivatives were obtained commercially or synthesized when necessary. [1-2] Chemical functionalization was carried out in order to anchor different functional groups (imidazole, hydroxamate, thiol) on the backbone of various complex materials, such as graphene oxide, carbon nanotubes, gum arabic (commercial and industrial waste) and cellulosic wastes (rice husk and shrimp shell), (Figure 1). All materials were thoroughly characterized by several techniques. The efficiency of the catalysts was evaluated by following the kinetics of the neutralization reactions by UV-Vis spectroscopy. Mechanistic studies were based on magnetic resonance and mass spectroscopy.

Figure 1 summarizes some of the results. The destruction of over 5 pesticides (paraoxon, ethylparathion, methylparathion, diazinon, glyphosate, methylparaoxon, isopropylparathion, acephate) were carried out in the presence of several catalysts. Homogeneous catalysts derived from imidazole (methylated, hydroxylated and carboxylated) showed to be highly versatile in the reaction with an interesting leaving group and thio effect (organophosphates with P=O or P=S), where the mechanism can be modulated and shifted. In general, for P=O, reactions occur exclusively on the phosphorus but for P=S, competitive pathways can occur, which ultimately influences the destruction process (less toxic?).[2] Indeed, these mechanistic studies have shown to be a valuable tool for modulating towards less toxic products. A bilinear variation of the Brønsted equation is proposed, which evaluates concomitantly the effect of the leaving and non-leaving groups. This optimized understanding of the structure-reactivity relationship allows to predict further neutralization processes and is key for chemical security. Moreover, the structure of neutralizing agents derived from imidazoles can be strategically designed for promoting a milder reaction, for example at neutral pH and in aqueous.[3] A myriad of catalysts (> 30 homogeneous and heterogenous) has been developed by the functionalization of various scaffolds under mild conditions (aqueous, neutral pH, ambient condition) anchoring imidazoles, hydroxamates, amidoximes and thiols, giving: (i) nanocatalysts derived from graphene and carbon nanotubes and (ii) sustainable biocatalysts derived from rice husk, gum arabic, shrimp shell and other cellulose-based materials.[4] The catalysts are able to act as neutralizing agents for organophosphates, accelerating the process to less than 1 day, that otherwise could take millions of years. The process guarantees less toxic products and is selective and recyclable. We highlight their easy handling and separation, particularly with thin films (derived from graphene) and magnetic catalysts (derived from carbon nanotubes).[5] Rice husk functionalized with hydroxamate is highly effective, despite its low degree of functionalization and constitutes a sustainable catalyst derived from waste. The bifunctionalized catalysts (with both thiol and imidazole moieties) derived from graphene oxide showed an interesting relationship between coverage degree, group identity and neighboring effects. The materials with the highest degree of functionalization were not the best catalysts. This was attributed to cooperative effects between neighboring groups that promote multiple catalyses (acid, basic and nucleophilic). An elegant bioinspired bifunctional catalysis with both thiol and imidazole is proposed. In addition, a higher coverage by functional groups can disturb or even inhibit possible catalytic mechanisms, either by steric effect or non-ideal positioning of the groups. This finding was extremely important since it shows that the functionalization process pursued should be driven by the application wanted since not always what we expect as a better functionalization methodology will lead to the best response for a specific application. The nanocatalysts also showed a dual function: could be used as sensors (surface enhanced Raman spectroscopy, electrochemical) for detecting these toxic agents. Finally, a portable, simple and compact colorimetric detector has been developed based on a led architecture, ideal for field analysis. The detector benefits from a colorimetric signal triggered from a reaction (neutralization or derivatization), which has been successfully validated for some agrochemicals (Parathion, Paraoxon and Glyphosate) in less than 10 min. This has great potential for food and field analysis.



Figure 1 – Overall summary of the studies carried out herein

Overall, we have shown how greening up the process by promoting faster reactions, under room temperatures, with low amounts of catalysts, using waste materials, carrying out environmentally friendly reactions can effectively tackle the worldwide concern with agrochemicals.[4] The combat against agrochemicals can benefit from peaceful and catalytic strategies- catalysis on demand-which are paramount to guarantee the chemical security of humankind towards such hazardous agents. Albeit versatility is sometimes considered an unwanted promiscuity, we show a variety of catalytic processes that can undergo specific pathways and this can be strategically used to project monitoring and destroying apparatus for various agrochemicals, and can also be extended to chemical weapons. It's important to note that many sensors rely on the same method towards various different pesticides and we show here that this should be specific for each organophosphate.

### Acknowledgements

The authors are grateful to CNPq, CAPES, L'Oréal-UNESCO-ABC, Fundação Araucária, PhosAgro/IUPAC/UNESCO, INCT-Nanocarbon and UFPR for financial support.

### References

1. L. Hostert, R.B. Campos, J.E.S. Fonsaca, V.B. Silva, S.F. Blaskiewicz, J.G.L. Ferreira, W. Takarada, N. Naidek, Y.H. Santos, L.L.Q. Nascimento, A.J.G. Zarbin, E.S. Orth, E. S. *Pure Appl. Chem.* **90**, 1593 (2018)
2. V.B. Silva, L. Nascimento, M. Nunes, R. Campos, A.Oliveira, E.S. Orth, *Chem.: Eur. J.*, **25**, 817 (2019)
3. V. B. Silva, R. B. Campos, P. Pavez, M. Medeiros, E. S. Orth. *Chem. Rec.*, **21**, 2638 (2021).
4. V. B. Silva, Y. H. Santos, R. Hellinger, S. Mansour, A. Delaune, J. Legros, S. Zinoviev, E.S.Nogueira, E. S. Orth. *Green Chem.*, **24**, 585 (2022)
5. S.F.Blaskiewicz, W.G. Endo, A.J.G. Zarbin, E.S. Orth. *Appl. Catal. B*, **264**, 118496 (2020)

# A Critical Revisit of Zeolites for CO<sub>2</sub> Desorption in Primary Amine Solution Argues its Genuine Catalytic Function

Cheng Zhou<sup>1</sup>, Ibrahim Khalil<sup>1</sup>, Ekaterina Makshina<sup>1</sup>, Michiel Dusselier<sup>\*1</sup>, Yuhe Liao<sup>\*2</sup>, Bert F Sels<sup>\*1</sup>

<sup>1</sup>Center for Sustainable Catalysis and Engineering, KU Leuven, Celestijnenlaan 200F, 3001 Heverlee, Belgium. E-mail: bert.sels@kuleuven.be

<sup>2</sup>Guangzhou Institute of Energy Conversion, Chinese Academy of Sciences, 510640 Guangzhou, P. R. China. Email: liaoyh@ms.giec.ac.cn; yuhe.liao20@gmail.com

Abstract text:

Zeolites are the first and most widely reported solid materials that are used in primary amine containing post-combustion CO<sub>2</sub> capture (PCC) processes for quicker solvent regeneration at lower energy consumption. A catalytic solvolysis of the carbamate intermediate, assisted by the Brønsted acid sites (BAS), is commonly accepted as explanation. However, there is little, if any, attention given to the regeneration of BAS in such basic amine-rich solution. Herein, we revisit the role of zeolite for CO<sub>2</sub> desorption in primary amine solution at room to moderately elevated temperature ranges. We noticed indeed an accelerating effect on the CO<sub>2</sub> desorption rate in the presence of BAS. Both their numbers as well as their accessibility for the amine-CO<sub>2</sub> adduct (i.e. carbamate) are important. However, we also noticed, using spectroscopic techniques and by zeolite reuse, a very strong chemical interaction between BAS and the regenerated amine. This suggests that BAS recovery to close the catalytic cycle is difficult and that zeolites can hardly be considered as genuine catalysts, but rather this study concludes a largely stoichiometric effect of the zeolites for the overall desorption process, and this in contrast to reference oxides such as TiO(OH)<sub>2</sub>, as shown in Figure 1.

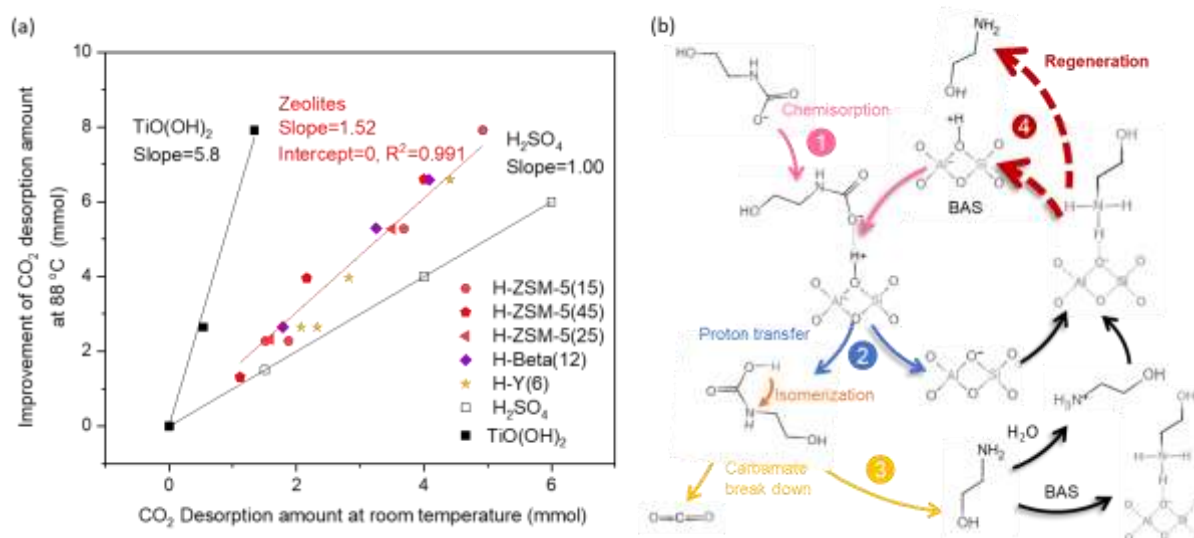


Figure 1. (a) Correlation between CO<sub>2</sub> desorption amount after adding different catalyst with different amount (0 to 16 g) at room temperature and CO<sub>2</sub> desorption amount (blank deducted) for different systems when reaching 88 °C. (b) Proposed mechanism of BAS from zeolite aiding CO<sub>2</sub> desorption in MEA solvent.

This work revisits the role of acid zeolites in the reported ‘fast desorption of CO<sub>2</sub>’ from aqueous primary amine, viz. MEA, solutions. Our kinetic and spectroscopic study confirm that the zeolitic protons can assist, if sufficiently accessible, alike solubilized protons, quick decomposition of the typical carbamate intermediate into CO<sub>2</sub> and amine, and this already at room temperature. However, the proton is rapidly inactivated by the released amine, as demonstrated spectroscopically and by a detailed study of spent acid zeolites, and therefore (almost) no catalytic turn-over is observed in a typical low temperature CO<sub>2</sub> desorption experiment with acid zeolites. Other types of sites, able to assist the decomposition of the carbamate, but more tolerable for the amine, should be investigated in order to realize the efficient and effective (true) catalyzed CO<sub>2</sub> desorption after its capture in aqueous amine solutions.

## Acknowledgements

We thank Walter Vermandel for kindly technical support. Cheng Zhou thanks the Chinese Scholarship Council (NO. 201906310137) for financial support. Ibrahim Khalil thanks the Research Foundation—Flanders (FWO Vlaanderen) for funding (grant 1260321N). Bert F Sels acknowledges KU Leuven for C2 finding and TOTAL for financial support.

# Rational Design of Manganese Dioxide Catalyst for the Preferential Oxidation of CO in Hydrogen Stream: from Theory to Practice

F. Arena<sup>1,\*</sup>, F. Ferrante<sup>2</sup>, L. Gueci<sup>2</sup>, G. Bonura<sup>3</sup>, M. Bertini<sup>2</sup>, S. Todaro<sup>3</sup>, F. Frusteri<sup>3</sup>, C. Nania<sup>2</sup>, D. Duca<sup>2</sup>

<sup>1</sup>Dip.to di Ingegneria, Università di Messina, C.da Di Dio 1, 98765 Messina, Italy

<sup>2</sup>Dip.to di Chimica e Fisica "Emilio Segrè", Università di Palermo, V.le delle Scienze Ed. 17, I-90128 Palermo, Italy

<sup>3</sup>Istituto CNR-ITAE "Nicola Giordano", Salita S. Lucia 39, I-98126 S. Lucia, Messina, Italy Italy

\*Francesco.Arena@unime.it

## Abstract

The CO and H<sub>2</sub> oxidation functionality of the MnO<sub>2</sub> system has been assessed by density functional theory (DFT) analysis of the adsorption and activation energies on a *model* Mn<sub>4</sub>O<sub>8</sub> cluster, in both absence and presence of O<sub>2</sub>. Computational data signal a strong interaction of Mn(IV) centers with CO triggering a stepwise redox cycle involving both catalyst and gas-phase oxygen species, while weak adsorption and high energy barrier hinder the H<sub>2</sub> oxidation functionality. Accordingly a MnO<sub>2</sub>/CeO<sub>x</sub> catalyst with large availability of Mn(IV) sites shows high CO oxidation activity, resulting inactive toward H<sub>2</sub> oxidation below 393K. Empiric kinetics and reducibility data confirm that CO oxidation occurs *via* an easy abstraction of catalyst oxygen (E<sub>app</sub>≈45 kJ/mol), while a high H<sub>2</sub> oxidation energy barrier (E<sub>app</sub>≈70 kJ/mol) shapes the preferential CO oxidation (PROX) pattern of the studied catalyst. Conversion-selectivity of 100%, great stability during 72h of reaction time and moderate inhibiting effects of H<sub>2</sub>O-CO<sub>2</sub> co-feeding document the reliability of MnO<sub>2</sub> materials as efficient, robust and low-cost PROX catalysts.

## Introduction

Proton-exchange membrane fuel cells (PEMFC) are attracting an ever-increasing attention for small-medium scale energy generation purposes, because of high energy-efficiency and zero-pollutant emission. Nevertheless, the production of hydrogen by the steam reforming of hydrocarbons or alcohols in combination with water-gas-shift (WGS) unit(s) implies a residual CO content (0.5–1%), which is detrimental for the Pt-anode because of the poisoning effect at the operative temperature of PEMFC (~353K). Thus, a clean-up system is further required to reduce the CO level to less than 50 ppm [1]. Among the viable options for H<sub>2</sub> purification, the preferential CO oxidation (PROX) appears the most appealing one, mostly for small-scale and mobile power applications [1]. However, none of catalysts currently under scrutiny, included supported noble metals (e.g., Pt, Pd, Ir, Ru, Rh), nano-gold and base metal oxides, meet the necessary requirements for commercial exploitation because of severe drawbacks like high cost, complex synthesis procedures, low selectivity, and poor stability in presence of CO<sub>2</sub> and/or H<sub>2</sub>O [2,3]. Therefore, considering the significant CO oxidation activity of MnO<sub>2</sub> catalysts [4], a comparative DFT analysis of the functionality of Mn(IV) sites toward CO and H<sub>2</sub>, in both absence and presence of O<sub>2</sub>, has been carried out. Since DFT calculations predicting a typical PROX behavior of Mn(IV) centers under any condition, a nanostructured MnO<sub>2</sub>/CeO<sub>x</sub> catalyst with large availability of Mn(IV) sites was synthesized to assess the practical suitability of MnO<sub>2</sub>-based catalysts for the PROX reaction at T≤423K.

## Results and Discussion

**DFT analysis.** Tailored from a pyrolusite lattice, a model Mn<sub>4</sub>O<sub>8</sub> cluster has been selected to assess the oxidative functionality of Mn(IV) sites toward CO and H<sub>2</sub> (Fig. 1, left) [3]. Its geometry was optimized considering all possible spin multiplicity states, with values ranging in-between 1 and 17 (i.e., having S value in the range 0-8). In its most stable configuration, the Mn<sub>4</sub>O<sub>8</sub> cluster has a C<sub>2h</sub> symmetry with two topologically different A and B Mn(IV) sites, three not equivalent O-atoms, and 12 unpaired electrons (Fig. 1, left). Mimicking the structure of defective Mn(IV) sites at the surface of MnO<sub>2</sub> materials, the DFT analysis unveils that CO adsorbs on both A and B atoms of the Mn<sub>4</sub>O<sub>8</sub> cluster. However, the calculated adsorption and activation energy values show that the favored CO oxidation path involves only the Mn(B) site of the cluster (Fig. 1, center). Overcoming an energy barrier of 52.1 kJ mol<sup>-1</sup>, this triggers the formation of the first CO<sub>2</sub> molecule by the shift of the dangling oxygen of the Mn(B) atom to the adsorbed CO.

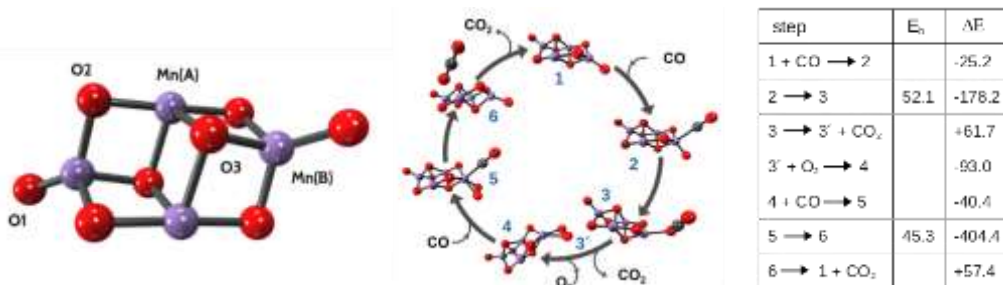


Figure 1. The model  $\text{Mn}_4\text{O}_8$  cluster (left) and DFT-based mechanism energy ( $\text{kJ}\cdot\text{mol}^{-1}$ ) diagrams for the oxidation of CO (center): Mn (purple), O (red), C (grey) atoms involved in the reaction steps are highlighted. Energy barriers ( $E_b$ ) and reaction energies ( $\Delta E$ ) in the Table (right) are in  $\text{kJ}\cdot\text{mol}^{-1}$ .

Then, the remaining O-vacancy prompts the adsorption of  $\text{O}_2$  ( $\Delta E$ ,  $-93.0 \text{ kJ mol}^{-1}$ ) and CO that give rise to a 2<sup>nd</sup>  $\text{CO}_2$  molecule restoring the stoichiometric  $\text{Mn}_4\text{O}_8$  cluster (Fig. 1, center). At variance, DFT calculations indicate that all the reaction paths involving the  $\text{H}_2$  molecules are not competitive with the oxidation of CO owing to much weaker surface interactions and higher (by ca.  $35 \text{ kJ mol}^{-1}$ ) reaction barriers, substantiating a typical preferential CO oxidation behavior of Mn(IV) centers in presence of  $\text{H}_2$  [5].

**From theory to practice.** According to theoretical predictions, a ceria-promoted  $\text{MnO}_2$  catalyst was designed as real counterpart of the model  $\text{Mn}_4\text{O}_8$  cluster. In fact, a low ceria loading ( $\text{Mn}_{\text{at}}/\text{Ce}_{\text{at}}\sim 5$ ) prevents the clustering of the active phase favoring the exposure of Mn(IV) sites [4]. The catalyst was synthesized via the redox-precipitation route and characterized by several techniques indicating the physico-chemical properties summarized in Table 1.

Table 1. Physico-chemical properties of the studied catalyst.

Chemical Composition			Textural Properties			Surface Analysis			
<sup>a</sup> Mn	Ce	K	<sup>a</sup> Mn/Ce	SA	PV	APD	<sup>b</sup> Mn/Ce	<sup>b-c</sup> Mn	<sup>b</sup> Mn(IV) - Mn(III) - Mn(II)
(wt %)			(at/at)	( $\text{m}^2/\text{g}$ )	( $\text{cm}^3/\text{g}$ )	(nm)	(at/at)	AON	(%)
42.8	23.0	3.9	4.73	159	0.55	30	5.12	$3.65\pm 0.02$	77 13 10

a) from XRF analysis; b) from XPS analysis; c) from TPR analyses.

As expected, the  $\text{MnO}_2/\text{CeO}_x$  catalyst features a large surface area and a typical mesoporous texture along with a surface Mn enrichment, mostly in the +4 oxidation state. The surface Mn(IV) sites shape the redox activity of the catalyst, although a crucial influence of the reducing species is evident from the CO-TPR and  $\text{H}_2$ -TPR profiles, shown in Fig. 2A. These display similar features consisting of a main peak partly convoluted with a small component at higher temperature, although a gap of ca. 100K in the onset reduction and 1<sup>st</sup>-maximum indicates a much stronger reducibility of Mn(IV) sites under CO. This substantiates a different reactivity of lattice-oxygen towards CO and  $\text{H}_2$ , which is at the origin of peculiar activity-selectivity pattern of the  $\text{MnO}_2/\text{CeO}_x$  catalyst. Indeed, CO oxidation ( $p_{\text{CO}}/p_{\text{O}_2}$ , 1) tests in  $\text{H}_2$  atmosphere ( $p_{\text{H}_2}/p_{\text{CO}}$ , 10-60) show a remarkable CO oxidation activity probed by conversion values rising steadily to maximum levels of 70-85% in the range of 293-533K, depending on the  $p_{\text{H}_2}/p_{\text{CO}}$  ratio (Fig. 2B).

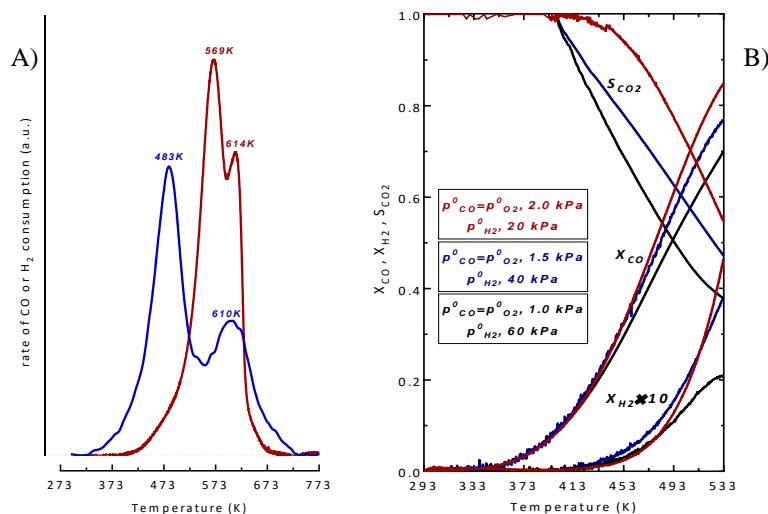


Figure 2. (A) CO-TPR and  $\text{H}_2$ -TPR patterns of the  $\text{MnO}_2/\text{CeO}_x$  catalyst; (B) Activity-selectivity pattern under CO and  $\text{H}_2$  co-feeding conditions (the various colors refer to data at  $p_{\text{H}_2}/p_{\text{CO}}$  ratio; GHSV,  $180,000 \text{ h}^{-1}$ ).

On the other hand, an incipient  $\text{H}_2$  oxidation occurs only at  $T > 393\text{K}$  (Fig. 2B), similarly to that observed in the absence of  $\text{O}_2$  (Fig. 2A). Consequently, the  $\text{MnO}_2/\text{CeO}_x$  catalyst ensures  $\text{O}_2$ -to- $\text{CO}_2$  selectivity levels of 100% in the range of 293-413K, although the maximum CO conversion is only ca. 18% at 413K. Matching previous theoretical findings, this evidence suggests that the oxidation of the two substrates occurs via parallel reaction paths, implying a negligible influence of the contact time on the activity-selectivity pattern of the studied catalyst. In fact, PROX tests under real process conditions ( $\text{GHSV} \leq 3600 \text{ h}^{-1}$ ) show conversion-selectivity levels of 100%, high stability during 72h of reaction time and minor inhibiting effects of  $\text{H}_2\text{O}$  and/or  $\text{CO}_2$  co-feeding in the range of 353-423K, substantiating the suitability of the  $\text{MnO}_2/\text{CeO}_x$  catalyst for practical applications.

## References

1. A.F. Ghenciu, *Current Opinion in Solid State and Materials Science* **6** 389 (2002).
2. K. Liu, A. Wang, T. Zhang, *ACS Catal.*, **2** 1165 (2012).
3. P. Jing, X. Gong, B. Liu, J. Zhang, *Catal. Sci. Tech.* **10** 919 (2020).



4. F. Arena, R. Di Chio, A. Palella, L. Spadaro, L. Frusteri, B. Fazio, S. Morandi, G. Martra, *Appl. Catal. A* **610** 117917 (2021).
5. F. Arena, F. Ferrante, R. Di Chio, G. Bonura, F. Frusteri, L. Frusteri, A. Prestianni, S. Morandi, G. Martra, D. Duca, *Appl. Catal. B* **300** 120715 (2022).

## Nickel catalysts modified with TiC derived from organic precursor for resource recovery via dry reforming of waste plastics

Ewelina Pawelczyk\*, Izabela Wysocka, Jacek Gębicki

<sup>1</sup> Department of Process Engineering and Chemical Technology, Faculty of Chemistry, Gdansk University of Technology, Narutowicza 11/12 St., 80-233 Gdansk, Poland

\*ewelina.pawelczyk@pg.edu.pl

Climate change as well as growing amount of plastic waste are threats of global importance, that require urgent solutions. In 2020, the world plastic production reached 367 Mt [1]. The high global demand for plastic leads to the generation of enormous amount of plastic waste which need proper management. During the last six decades, only 9% of the generated waste plastic has been recycled [2]. Currently implemented waste plastic treatment methods are based on landfilling or incineration, which results in the release of the toxic gases and leaching of harmful substances into soil and groundwater [3,4]. Moreover, these conventional ways of plastic waste treatment do not allow for resource recovery. According to the European Union sustainable development policy, the landfilling and incineration of waste must be progressively reduced and recycling is promoted instead [5]. The European Union target addressed to the circular economy is to achieve the municipal waste recycling of 55% and 65% by 2025 and 2035, respectively. Furthermore, the upper limit of plastic waste storage at landfills cannot exceed 10% by 2035. Therefore, effective methods of waste plastic recycling are highly sought. Another emerging environmental problem is the emission of greenhouse gases, which contributes to climate change [6–8]. Carbon dioxide is one of the main greenhouse gases, hence suitable approach to its management is essential. In this view, carbon capture and utilization technologies are under extensive attention. Development of the pro-environmental technology of plastic waste processing as well as CO<sub>2</sub> utilization is fundamental in terms of sustainable development and circular economy.

Pyrolysis-catalytic-dry reforming (PCDR) process is a promising way of utilization of both carbon dioxide and plastic remains. PCDR allows for resource recovery and valorization of plastic waste - hydrocarbon carrier, that may be suitable raw material for production of valuable products, such as hydrogen and synthesis gas, widely used in the industry [9–11]. However, PCDR technology needs further development and optimization to be successfully implemented in the industrial scale. A key area that must be refined to achieve industrially mature process are catalysts. Currently used catalysts are not effective enough and suffer from deactivation [12,13]. This issue can be potentially overcome by use of metal carbide-based catalyst, due to its reported catalytic activity and stability in dry reforming of not only of methane, but also of other hydrocarbons [14–17]. Accordingly, the combination of a carbide catalyst with the conventional metal oxide-based nickel catalyst can be a solution that allows for an efficient and stable process of high-quality synthesis gas production.

Therefore, nickel catalysts supported on MgAl<sub>2</sub>O<sub>4</sub> were modified with TiC and examined in pyrolysis combined with dry reforming of waste plastic for syngas production. TiC was prepared from various organic precursors to determine the impact of carbon source on catalyst structure, hence its catalytic activity. Commercially available TiC was also used for comparison. The prepared catalysts were characterized with BET surface area, total pore volume and pore size distribution, X-ray diffraction (XRD), scanning electron microscopy (SEM), temperature-programmed reduction (H<sub>2</sub>-TPR) and desorption (CO<sub>2</sub>-TPD) methods. Catalytic activity of investigated catalysts was examined in pyrolysis-catalytic-dry reforming processes of a set of various polymers representing plastic waste in the environment: low-density polyethylene (LDPE), polypropylene (PP), polystyrene (PS), polyethylene terephthalate (PET). PCDR processes were carried out in two-stage reactor system. The experimental system consisted of two separate fixed bed reactors with two separate furnaces. Pyrolysis of plastic sample was performed in the first stage reactor with argon as carrier gas. Pyrolysis gases were passed directly into the dry reforming stage reactor, where catalyst was placed and carbon dioxide stream was fed. The pyrolysis stage reactor was heated with 10°C/min heating rate to temperature of 500°C and the dry reforming reactor was held at a constant temperature of 800°C. Qualitative and quantitative analysis of outlet stream was performed using gas chromatography-mass spectrometry (GC-MS) and gas chromatography with flame-ionization detection (GC-FID). The performance of catalysts was discussed with emphasis on the influence on synthesis gas yield, product distribution, H<sub>2</sub>:CO molar ratio as well as catalyst stability and deactivation. BET and XRD techniques were also performed on used catalysts after the PCDR processes in order to determine changes in their structure and possible deactivation. Additionally, catalytic activity of Ni-TiC/MgAl<sub>2</sub>O<sub>4</sub> were compared to other commonly examined carbide catalysts Ni-Mo<sub>2</sub>C/MgAl<sub>2</sub>O<sub>4</sub> and Ni-WC/MgAl<sub>2</sub>O<sub>4</sub> to compare effect of different transition metal on catalyst performance.

The obtained results indicate that metal carbides have potential as alternative catalysts for syngas production from waste plastics. It was found that carbon source for TiC affects morphological properties of obtained catalyst, including the pore structure, size and shape, hence its catalytic activity as well as stability of obtained catalysts. The investigation has revealed that TiC prepared using organic precursors may be promising alternative to its commercial counterpart, thus can reduce its cost. Depending on the transition metal the catalytic properties differ, due to various changes in the structure of carbides, leading to different syngas yields. It was established that plastic

feedstock type has strong effect on process output including syngas yield and quality. Moreover, PCDR process leads to different distribution and composition of products depending on the type of plastic feedstock.

## Acknowledgements

The financial support for this study from Gdańsk University of Technology by the DEC-23/2020/IDUB/I.3.3 grant under the ARGENTUM—“Excellence Initiative—Research University” program is gratefully acknowledged.

## References

1. Plastics Europe, *Plastics—The Facts 2021*; Plastics Europe: Brussels, Belgium, 2021.
2. R. Geyer, J.R. Jambeck, K.L. Law, *Sci. Adv.*, **3** 19 (2017).
3. S.M. Al-Salem, P. Lettieri, J. Baeyens, *Waste Manag.* **29** 2625 (2009).
4. S.D. Anuar Sharuddin, F. Abnisa, W.M.A. Wan Daud, M.K. Aroua, *Energy Convers. Manag.*, **115** 308 (2016).
5. European Parliament, The Council of the European Union, Official Journal of the European Union L 150: Legislation, *Off. J. Eur. Union.* **2018** 26 (2018).
6. K.O. Yoro, M.O. Daramola, *CO<sub>2</sub> Emission Sources, Greenhouse Gases, and the Global Warming Effect*, Elsevier Inc.: Amsterdam, The Netherlands, 2020; ISBN 9780128196571.
7. W.F. Lamb, T. Wiedmann, J. Pongratz, R. Andrew, M. Crippa, J.G.J. Olivier, D. Wiedenhofer, G. Mattioli, A. Al Khourdajie, J. House, S. Pachauri, M. Figueroa, Y. Saheb, R. Slade, K. Hubacek, L. Sun, S.K. Ribeiro, S. Khennas, S. De La Rue Du Can, L. Chapungu, S.J. Davis, I. Bashmakov, H. Dai, S. Dhakal, X. Tan, Y. Geng, B. Gu, J. Minx, *Environ. Res. Lett.*, **16** 073005 (2021).
8. E. Moe, J.K. S. Røttereng, *Energy Res. Soc. Sci.*, **44** 199 (2018).
9. E. Pawelczyk, I. Wysocka, J. Gębicki, *Catalysts*, **12** 362 (2022).
10. J.M. Saad, P.T. Williams, *Fuel*, **193** 7 (2017).
11. J.M. Saad, P.T. Williams, *Waste Manag.*, **58** 214 (2016).
12. A. Ochoa, J. Bilbao, A.G. Gayubo, P. Castaño, *Renew. Sustain. Energy Rev.*, **119** 109600 (2020).
13. J.M. Saad, M.A. Nahil, C. Wu, P.T. Williams, *Fuel Process. Technol.*, **138** 156 (2015).
14. M.D. Porosoff, M.N.Z. Myint, S. Kattel, Z. Xie, E. Gomez, P. Liu, J.G. Chen, *Angew. Chem. Int. Ed.*, **54** 15501 (2015).
15. F. Solymosi, R. Németh, A. Oszkó, *Stud. Surf. Sci. Catal.*, **136** 339 (2001).
16. M. Ronda-Lloret, V.S. Marakatti, W.G. Sloof, J.J. Delgado, A. Sepúlveda-Escribano, E. V. Ramos-Fernandez, G. Rothenberg, N.R. Shiju, *ChemSusChem*, **13** 6401 (2020).
17. M.M. Sullivan, A. Bhan, *J. Catal.*, **357** 195 (2018).

## Carbonized Bone Waste For Photothermal Desalination

Muhammad Shajih Zafar<sup>1,2</sup>, Athanassia Athanassiou<sup>1</sup>, Despina Fragouli<sup>1</sup>

<sup>1</sup>Smart Materials, Istituto Italiano di Tecnologia, via Morego 30, 16163 Genoa, Italy

<sup>2</sup>Dipartimento di Informatica, Bioingegneria, Robotica e Ingegneria dei Sistemi (DIBRIS), Università degli Studi di Genova, Via Opera Pia 13, 16145 Genoa, Italy

<sup>1,2</sup>[muhammad.zafar@iit.it](mailto:muhammad.zafar@iit.it), <sup>1</sup>[Athanassia.Athanassiou@iit.it](mailto:Athanassia.Athanassiou@iit.it), <sup>1</sup>[Despina.Fragouli@iit.it](mailto:Despina.Fragouli@iit.it)

**Keywords:** biomass, hydroxyapatite, porous device, waste and water management

### Abstract

Solar steam generation is an appealing approach to compete the worldwide freshwater shortage, and for this reason various types of materials have been developed. Herein we present a low-cost attainable alternative to the so far proposed systems, made by cattle bone waste, for steam generation and desalination. This is achieved via thermal treatment, in a controlled environment, of bone samples for their conversion into highly porous photothermal materials. The carbonized bone (CB) is not only composed of intrinsically intertwined meso and microporous channels, for productive water transportation and vapor escape, but exhibits outstanding optical absorption (99%) of the solar irradiation, solar light-to-heat conversion, and low vaporization enthalpy. The CB device demonstrates a solar evaporation rate of  $1.82 \text{ kg m}^{-2} \text{ h}^{-1}$  under 1 sun illumination, and this is attributed not only to its interaction with the sunlight but also to the enhanced evaporation rate in the dark, with the solar-to-vapor conversion efficiency of 80%. Moreover, the desalination efficiency of CB reaches 99.99%. This biowaste-based highly porous photothermal system is a promising material for the efficient collection of freshwater from seawater, because of its outstanding performance coupled with the wide availability of the biosource, the straightforward fabrication approach, and the thermal and chemical stability of the final material. With such valuable alternatives, new paths for managing the continuously rising food waste are opened.

### Materials and Methods

**Materials:** Cattle bone waste was bought from a local market in Genoa, Italy. To develop artificial seawater, synthetic sea-salt (S9883) was purchased from Sigma-Aldrich. Deionized (DI) water was used for whole experiments.

**Materials fabrication:** The bone waste was heated in water for 15 min to eliminate meat remains and other organic scums. Afterward, the boiled bone was kept in a freezer at  $-18 \text{ }^\circ\text{C}$  in an airtight plastic bag until further use. For preparation of the CB, bones were cut transversally into thin slices, vertical to the bone axis by a hacksaw. Sandpaper was used to set the dimensions of the slices such as thickness: 4.0 mm and diameter: 9.5-10.0 mm. These bone pieces were then carbonized in a tube furnace under nitrogen atmosphere (gas flow:  $5 \text{ cm}^3 \text{ min}^{-1}$ ) at temperatures of  $600 \text{ }^\circ\text{C}$  for 1 h, with a heating rate of  $5 \text{ }^\circ\text{C min}^{-1}$ . After carbonization, the CBs were cooled down naturally till the room temperature is reached.

### Results and discussion

For the real assessment of the light-to-heat conversion ability of the CB600, the surface temperature increase was measured under 1 sun illumination using an IR camera. Under disclosure for 18 min, the temperature of the dry sample increases reaching  $35.7 \text{ }^\circ\text{C}$ , showing for that the CB600 relates better with the light transforming it into heat more resourcefully.

One main aspect to evaluate the viability of a material for water harvesting is the solar evaporation rate (SER), which is clearly linked to the amount of purified water collected through the material via steam generation and consequent condensation. The determined evaporation rate after getting the steady-state condition is  $1.81 \text{ kg m}^{-2} \text{ h}^{-1}$ , 6.2 times higher than the rate of the bulk water and 2.7 times higher than the evaporation rate of the CB600 under dark. Based on these points, and after deducting the evaporation rate in dark situations, the SER of the CB600 touches  $1.17 \text{ kg m}^{-2} \text{ h}^{-1}$ , with solar-to-vapor conversion efficiency of 80 % [1,2]. The amount of the water collected from the condensation of the vapors produced via solar evaporation of synthetic seawater with a rate of  $\sim 0.65 \text{ L m}^{-2} \text{ h}^{-1}$ , discloses that the concentration of the five primary ions originally shows in seawater has been pointedly decreased by about three to four orders of magnitude, with ions elimination efficiency higher than 99.99 % as compared to the saline water. Indeed, after the desalination experiment the ions concentration of  $\text{Na}^+$ ,  $\text{Mg}^{2+}$ ,  $\text{K}^+$ ,  $\text{Ca}^{2+}$ , and  $\text{Sr}^+$  in the collected water are 8.6, 0.8, 0.74, 0.44, and  $0 \text{ mgL}^{-1}$ , respectively lower than the values set by WHO (World Health Organization) for the drinking water such as (100, 50, 10, and  $3 \text{ mgL}^{-1}$ ) [3,4].

### Conclusion

The inherent light absorption capability, adequate thermal conductivity and improved surface wettability coupled with the interlinked microchannels and classified porous structure of the CB600 lead to its upgraded light-harvesting and steam-generation capacity. Since the low-cost and higher availability of bone waste, a CB-based solar steam generation and desalination device explicitly intended in order to host and join multiple pieces of the active material can work as a suitable tool to alleviate the water scarcity issue. Effective use of bone waste into a useful photothermal device, handle numerous issues elevated in the United Nation's sustainable development goals. In particular, the current work not only deals with the inhibition of water scarcity problems contributing to

SDG6 but also exhibits an state-of-the-art and ecological way for food waste management participating to the SDG12.

### References

- [1] C. Wang, J. Wang, Z. Li, K. Xu, T. Lei, W. Wang, Superhydrophilic porous carbon foam as a self-desalting monolithic solar steam generation device with high energy efficiency, *J. Mater. Chem. A*. 8 (2020) 9528–9535. <https://doi.org/10.1039/D0TA01439G>.
- [2] Y. Guo, H. Lu, F. Zhao, X. Zhou, W. Shi, G. Yu, Biomass-Derived Hybrid Hydrogel Evaporators for Cost-Effective Solar Water Purification, *Adv. Mater.* 32 (2020) 1907061. <https://doi.org/https://doi.org/10.1002/adma.201907061>.
- [3] L. Yang, G. Chen, N. Zhang, Y. Xu, X. Xu, Sustainable Biochar-Based Solar Absorbers for High-Performance Solar-Driven Steam Generation and Water Purification, *ACS Sustain. Chem. Eng.* 7 (2019) 19311–19320. <https://doi.org/10.1021/acssuschemeng.9b06169>.
- [4] M. Zhu, A. Xia, Q. Feng, X. Wu, C. Zhang, D. Wu, H. Zhu, Biomass Carbon Materials for Efficient Solar Steam Generation Prepared from Carbonized *Enteromorpha Prolifera*, *Energy Technol.* 8 (2020) 1–6. <https://doi.org/10.1002/ente.201901215>.

## Studies of different ionic liquids as electrolytes for electrochemical reduction of CO<sub>2</sub>

S. Messias<sup>1</sup>, C.M. Rangel<sup>2</sup>, V. Paz<sup>1</sup>, L. C. Branco<sup>1</sup>, A. S. Reis Machado\*<sup>1</sup>

<sup>1</sup>LAQV, REQUIMTE, Departamento de Química, Faculdade de Ciências e Tecnologia, Universidade Nova de Lisboa, Caparica, 2829-516, Portugal

<sup>2</sup>Laboratório Nacional de Energia e Geologia, Estrada do Paço do Lumiar, 22 Lisboa, 1649-038, Portugal

\*ams.machado@fct.unl.pt

Ionic liquids have been considered among one of the most promising materials under investigation for integration of CO<sub>2</sub> capture and electrochemical reduction, due to their recognized sustainability and tunable properties, such as non-volatility, high CO<sub>2</sub> solubility, high conductivity, and large electrochemical window. Electrochemical CO<sub>2</sub> reduction is a CCU (Carbon Capture and Utilization) research technology that is being intensively investigated not only for obtaining chemical building blocks and fuels, but as an excellent future option to store energy from renewable sources, such as solar and wind energy, that are seasonal, intermittent and geographical dependent [1,2].

In previous works, the development of a process to produce syngas (CO+H<sub>2</sub>) using electrolytes based on 1-ethyl-3-methyl-imidazolium trifluoromethanesulfonate [EMIM][OTF] was reported [3-4]. In a more recent work, the effect of replacing the 1-ethyl-3-methyl-imidazolium cation [EMIM] by 1-ethyl-3-picolinium [C<sub>2</sub>-3-pic] and 1-ethyl-4-picolinium [C<sub>2</sub>-4-pic] cations as electrolyte for electrochemical reduction of CO<sub>2</sub> at pressures higher than atmospheric was published [5]. The objective of this work is to proceed the study of the influence of ionic liquid-based electrolytes in electrochemical CO<sub>2</sub> reduction. In this context, protic ionic liquids prepared by direct protonation of methylimidazole and picoline scaffolds using suitable organic acids have been investigated.

All electrolytes are characterized by cyclic voltammetry and electrochemical impedance spectroscopy in order to evaluate their electrochemistry behavior for CO<sub>2</sub> electroreduction processes. Productivities of gaseous products resulting from the co-electrolysis of CO<sub>2</sub> and water together with their faradaic efficiencies have been also determined.

### Acknowledgements

This work was supported by the project “CO2RED – Understanding CO<sub>2</sub> Electro-REDuction in Porous Materials” with reference PTDC/EQU-EPQ/2195/2021, funded by FCT – Fundação para a Ciência e Tecnologia. S. Messias is thankful to FCT for the fellowship SFRH/BD/147219/2019.

### References

1. M. Alvarez-Guerra, J. Albo, E. Alvarez-Guerra and A. Irabien, *Energy Environ. Sci.*, **8** 2574 (2015)
2. G. Zhao, T. Jiang, B. Han, Z. Li, J. Zhang, Z. Liu, J. He, W. Wu, *J. of Supercritical Fluids*, **32** 287-291 (2004).
3. T. Pardal, S. Messias, M. Sousa, A.S. Reis Machado, C. M. Rangel, D. Nunes, J.V. Pinto, R. Martins, M. Nunes da Ponte, *J. of CO<sub>2</sub> Utilization*, **18**, 62-72 (2017)
4. S. Messias, M.M. Sousa, M. Nunes da Ponte, C. M. Rangel, T. Pardal, A.S. Reis Machado, *React. Chem. Eng.*, **4**, 1982-1989 (2019)
5. S. Messias, V. Paz, H. Cruz, C. M. Rangel, L. C. Branco, A.S. Reis Machado, *Energy Advances*, in press (2022), DOI:10.1039/D2YA00001F.

# Green Analytical Chemistry- (Eco)Toxicology

## Green extraction and quantification of zeaxanthin and lutein in corn grains and their associated by-products

Ariadne M. Carneiro,<sup>1</sup> Bruna R. Lima,<sup>1</sup> Lucas A. Chibli,<sup>1</sup> Renato L. Carneiro<sup>2</sup> and Cristiano S. Funari<sup>1\*</sup>

<sup>1</sup>Green Biotech Network, São Paulo State University, Av. Universitária, 3780, CEP 18605-525, Botucatu, São Paulo, Brazil

<sup>2</sup>Department of Chemistry, Federal University of São Carlos, Rod. Washington Luiz, s/n, CEP 13565-905, São Carlos, São Paulo, Brazil

\*e-mail: cristiano.funari@unesp.br

Corn (*Zea mays* L.) is the only crop in the world to exceed 1 billion tons of grains per year, since it is cultivated in almost all countries [1]. The corn grain is formed by endosperm, germ, pericarp and tip. The endosperm contains the carotenoids zeaxanthin, lutein, beta-cryptoxanthin, alpha and beta carotenes, among others [2]. Both zeaxanthin and lutein are extremely beneficial to human health as they are compounds that accumulate in the macula, the central part of the retina, helping to maintain eyes' best functions [3]. Choosing appropriate solvents for analytical methods of quantification of carotenoids is an important step and takes into account factors such as solvent polarity, carotenoid chain length, sample matrix and moisture content. The most commonly used solvents are hexane, for less polar carotenoids, and acetone, for more polar ones such as zeaxanthin and lutein [4]. This work aimed to develop a green method for extraction and quantification of these compounds in corn grains and their associated by-products. First, two high-performance liquid chromatography coupled to PDA/UV/Vis methods were selected in the literature and transposed to ultra-high-performance liquid chromatography coupled to PDA/UV/Vis (UHPLC-PAD/UV/Vis) to serve as benchmark methods [5-7]. Then, a new UHPLC-PAD/UV/Vis as well as a new dynamic maceration-based extraction method were developed using Design of Experiments (DoE). The screened organic solvents were those classified as recommended in the CHEM21 solvent selection guide, such as ethanol, acetone, ethyl acetate, anisole, butanol, butyl acetate, dimethyl carbonate, ethyl lactate, heptane, isopropanol and isopropyl acetate [8]. For both the extraction and separation processes, procedures containing only water and ethanol presented the best performances, which were superior than the benchmark methods (Figure 1). The whole new procedure was validated. For instrumental precision, the relative standard deviations (RSDs) observed for retention time and peak area were 0.79 and 1.11% for zeaxanthin, respectively, and 0.77% and 0.67% for lutein. The maximum RSDs in a single day observed for retention time and peak area were 0.09 and 5.88% for zeaxanthin, respectively, and 0.09 and 6.74% for lutein. For inter-day experiments, the RSDs for zeaxanthin were 0.26 and 7.66% for retention time and peak area, respectively. They were 0.25 and 8.36% for lutein. Finally, for intermediate precision, the RSDs for retention time and peak area were 0.13 and 6.65% for zeaxanthin, respectively, and 0.12 and 5.96% for lutein. From the optimized method,  $0.077 \pm 0.005$  and  $0.055 \pm 0.003$  mg/g of zeaxanthin and lutein were found, respectively, in corn grains. The same optimized procedure will be applied to corn by-products in order to know if there is an accumulation of these compounds in such materials.

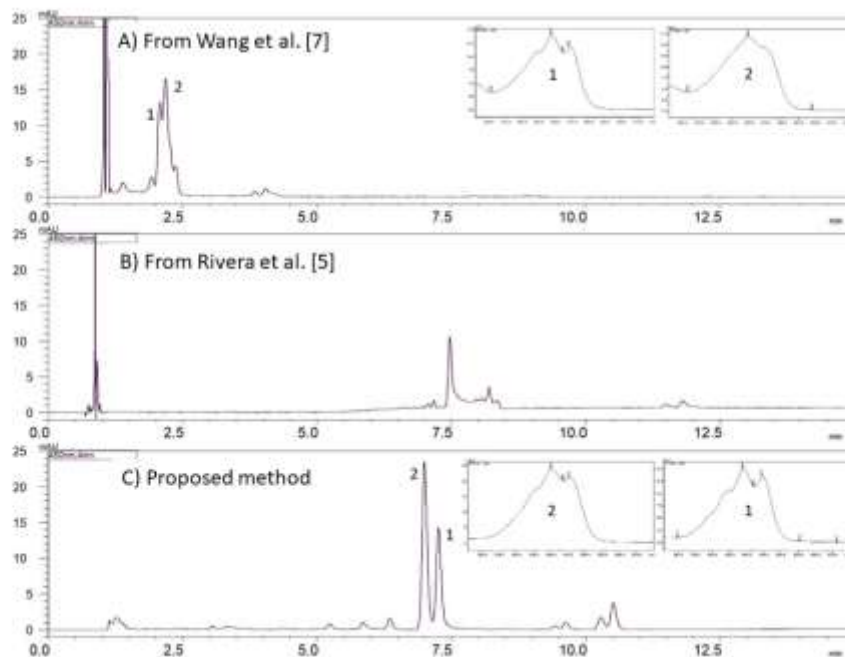


Figure 1: UHPLC-PAD/UV/Vis chromatograms at 450 nm of a representative corn grain extract analyzed under different separation conditions. Columns in A) and B): C18,  $150 \times 2.1$ ,  $1.7 \mu\text{m}$  (Kinetex, Phenomenex), in C) C18  $150 \times 3.0$  mm,  $1.8 \mu\text{m}$  (Zorbax Eclipse XDB-C18, Agilent, USA). Mobile phases: in A) water and ACN:MeOH 7:3 (v/v), in the following gradient: 80-100% ACN:MeOH 7:3 (v/v) (0-12.42 min), 100% ACN:MeOH 7:3 (v/v) (12.42-17.82 min.), in B) ACN:DCM 95:5 (v/v), in C) water and EtOH, in the following gradient: 80-100% EtOH (0-20, 30 min). Flow rates: A) 0.6 ml/min, B) 0.3



ml/min, C) 0.45 ml/min. Injection volumes: 5  $\mu$ L. Analysis temperatures: 35°C. On-line UV spectra of (1) lutein and (2) zeaxanthin are indicated over the chromatograms.

## Acknowledgements

This study was financed by the Coordenação de Aperfeiçoamento de Pessoal de Nível Superior – Brasil (CAPES) and São Paulo Research Foundation / FAPESP (grants 2017/06216-6 and 2018/01786-1).

## References

1. EMBRAPA, A. Aragão, E. Contini, *Embrapa SIRE*, 1 (2007).
2. J. Johnson, T. C. Wallace, *Whole grains and their bioactives: Composition and health*, Wiley (2019)
3. F. Khachik, F. F. De Moura, D. Y. Zhao, C. P. Aebischer, P. S. Bernstein, *Investig. Ophthalmol. Vis. Sci.*, **43**, 3383 (2002).
4. R. K. Saini, Y. S. Keum, *Food Chem.*, **240**, 90 (2018).
5. S. Rivera, R. Canela, *Molecules*, **17**, 11255 (2012).
6. M. M. Maurer, J. R. Mein, S. K. Chaudhuri, H. L. Constant, *Food Chem.*, **165**, 475 (2014).
7. L. Wang, W. Lu, J. Li, J. Hu, R. Ding, Lv, M., Q. Wang, *Molecules*, **24**, 2994 (2019).
8. D. Prat, A. Wells, J. Hayler, H. Sneddon, R. McElroy, S. Abou-Shehada, P. J. Dunn, *Green Chemistry*, **18**, 288 (2016).

## A green analytical method to characterize unsaturated hydrocarbons in waste polyolefin pyrolysis oil using FTIR.

Trang Thi Bui, Sven Janssens, Pieter Billen, Christophe Vande Velde, and Serge M.F. Tavernier\*

*iPRACS group, Faculty of Applied Engineering, University of Antwerp, Antwerp, Belgium*

\* *serge.tavernier@uantwerpen.be*

### Abstract text:

Polyolefin makes up approximately 50% of plastics consumed in Western Europe [1]. Chemical recycling is one of the preferred methods to recycle waste plastics by cracking them into basic chemical substances which can be reused in the petrochemical industry[2]. Characterizing alkenes in waste polyolefin pyrolysis oil is the key to chemical recycling, especially in the pyrolysis processes. In this way, deciding the chemical route and amount of reagents for the next process steps can be estimated correctly and easily. However, characterization is not easy because of the presence of a wide variety of different molecules and functionalities after cracking long chain hydrocarbons during the pyrolysis process of waste plastic, especially in PE (or PP) with no other functional groups, unlike other polymers (PS or PET). Moreover, feedstock for pyrolysis can come from LLDPE, LDPE, HDPE, PP, or even a mixture of them, which can lead to a big challenge to characterize each type of alkene in waste polyolefin pyrolysis oil.

Therefore, in this study, we propose a simple analysis method only using FT-IR to determine the kind and quantity of double bonds in pyrolysis oils. By studying different characteristic absorption peaks in the fingerprint region in the FT-IR spectrum between known and unknown samples, together with the estimated carbon number and molecular weight of those materials through the mass of methylene group (CH<sub>2</sub>), one main equation is proposed (EQ1'). This equation can give directly an amount of alkenes of an unknown sample under the form of "mole of double bonds per gram of sample". In addition, our method can also give a ratio between monosubstituted and 1,1 disubstituted alkenes, which are the two main alkenes in waste PE and PP pyrolysis oil, through the relationship of C-H bending at 910cm<sup>-1</sup> and 885cm<sup>-1</sup> on IR spectrum. To confirm the accuracy of the method proposed in this study, 1H-NMR has been used.

Without sample preparations and solvent consumption, as necessary for titration, GC, or NMR, our research aims for an analytical method following the green chemistry concept. Furthermore, this technique is simple, fast, low cost, and accessible for use in any general lab. We expect this could support the expansion of the application of recycling waste polymer in an industrial context.

### Materials and methods

Waste PE and PP pyrolysis oil from the pyrolysis process of waste plastic from Indaver ( Belgium). Standard alkenes and alkanes (tetradecane, tetradecene, octadecene, decane, decene, 2-methyl-1-undecene...) were obtained from Acros Organics and Sigma Aldrich. All reagents of analytical grade were used directly without further purification.

Fourier transform-infrared (FT-IR and Nuclear magnetic resonance spectroscopy (H-NMR) were recorded on a Bruker FT/IR LUMOS spectrometer with ATR crystal (Bruker, US) and at 400 MHz with a Bruker Advance III HD 400 MHz spectrometer, respectively.

### Key results

From our study, we proposed the main equation (EQ1') for the measurement of double bonds in PE&PP pyrolysis oil:

$$\frac{\text{Mole of double bond}}{\text{Mass of sample}} = \underbrace{\left( \frac{\text{Double bond}}{\text{Carbon}} \right) * \frac{\text{Number of Carbon in sample } (\Sigma Cn)}{\text{Molecular weight of sample}}}_{\text{EQ 1}} = \underbrace{\left( \frac{\text{Double bond}}{\text{Carbon}} \right) * \left( \frac{1}{\text{CH}_2} \right)}_{\text{EQ 1'}}$$

Where the detection of double bonds per carbon (DB/C) has been investigated by FT-IR of standard alkenes.

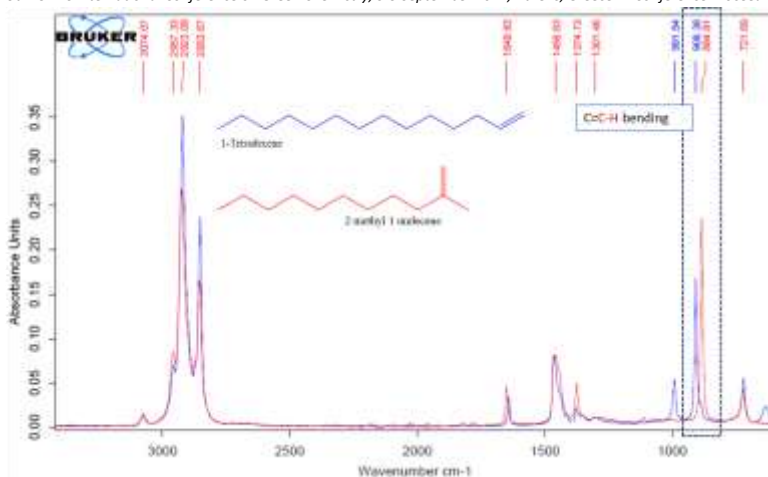


Figure 1. FT-IR spectrums of 1-tetradecene and 2-methyl 1-undecene.

Figure 1 shows the strong peaks of C-H bending vibration at 910 $\text{cm}^{-1}$  for 1-tetradecene and 885 $\text{cm}^{-1}$  for 2-methyl-1-undecene. Therefore, these peaks were selected to go study the relationship of the number of double bonds/carbon (DB/C) with the peak height of monosubstituted and 1,1 disubstituted alkenes. In the next step, different mixtures of the standard alkenes were prepared and analyzed on FT-IR to obtain peak height of the mentioned peaks, following the external standard calibration. Afterward, as shown in Figures 2 A and B, two calibration curves were obtained for the specific type of alkenes which correspond to PE and PP.

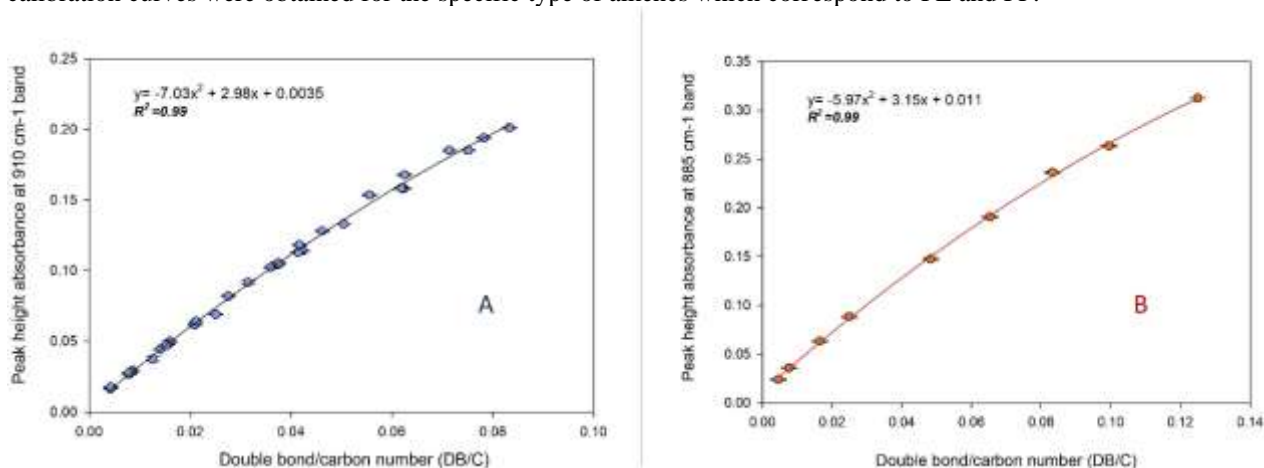


Figure 2. (A) The calibration plot of monosubstituted alkenes analyzed at the 910  $\text{cm}^{-1}$  band and (B) 1,1 disubstituted alkenes analyzed at the 885  $\text{cm}^{-1}$  band, using the Bruker FT/IR LUMOS spectrometer with ATR crystal.

After fitting two equations of DB/C measurement to equation EQ1', three practical methods for the different cases of olefin pyrolysis oil were developed. Afterward, our new method was applied to detect the mole of double bonds per kilogram of the standard mixtures and waste PE&PP pyrolysis oil to check the efficiency of this method. NMR was also used to confirm the accuracy. Overall, obtained results show that our method worked sufficiently well with RSD below 10% in the carbon range from C10 to C20.

In addition, to expand our method, EQ1 is suggested to use for complex mixtures (diene or triene), where gel permeation chromatography (GPC) can be used to quantify #C and MW. Nevertheless, in our study, for most of the oil fractions from waste polyolefin pyrolysis, EQ1' is sufficient to apply.

## Acknowledgements

This work was supported by the VLAIO Catalisti-ICON project P2PC (Plastics To Precious Chemicals; project HBC.2019.0003)

## References

1. Plastics Europe Market Research Group (PEMRG) and Conversio Market & Strategy GmbH 2019
2. Sasse, F. E. (1998). Chemical Recycling of Polymer Materials. *Chemical Engineering & Technology*, 21(10), 777-789

## Insights into ecotoxicity of flavonoids and their mixtures

Lena Schnarr<sup>1\*</sup>, Oliver Olsson<sup>1</sup> and Klaus Kümmerer<sup>1</sup>

<sup>1</sup>Institute of Sustainable Chemistry, Leuphana University Lüneburg, Universitätsallee 1, 21335 Lüneburg, Germany

\*lena.schnarr@leuphana.de

Flavonoids are a class of natural products that are investigated for several applications in pharmacy and agriculture [1,2]. They are present in agricultural and food wastes and thus could be obtained as high value chemicals in a biorefinery process [3]. In addition to their production from renewable resources, natural products are often associated with low ecotoxicity and non-persistence [4,5]. Nonetheless, understanding bioactivities of flavonoids is important in regard of possible applications and ecotoxicity evaluation. Therefore, the objective of this study was to provide ecotoxicity data to enable a better risk assessment. We investigated the algae growth inhibition of flavonoids, mixtures of flavonoids and the stability of test compounds during the test.

Growth inhibition of the green freshwater algae *Raphidocelis subcapitata* was measured according to OECD guideline 201 with a miniaturized test system using 24 well plates. Cell density was measured at 24 hour intervals for a total duration of 72 h via chlorophyll a fluorescence (excitation: 450 nm/ emission 680 nm) using a plate reader (Synergy HT, BioTek Instruments). For the determination of EC<sub>50</sub> values  $\geq 6$  different test substance concentrations were used to obtain dose-response curves which were fitted with a linear regression of selected data points of the slope. Flavonoid concentration (initial concentration 5 mg/L) during the algae growth inhibition test was followed by analysis with HPLC-UV/vis (Shimadzu).

We found that flavonoids have a moderate algae growth inhibition with EC<sub>50</sub> values in the range of 1 to 23 mg/L (table 1). The results of the 1:1-mixtures of flavonoids indicated synergistic effects for 5 out of 10 tested mixtures (table 1). However, the overall growth inhibition effect was not increased since most active mixtures were as active as most active flavonoids. Occurrence of synergistic effects suggests different modes of actions for different flavonoids.

Analysis of concentration of 12 flavonoids during the algae growth inhibition test showed that the majority of flavonoids are instable at the test conditions (table 1). These initial observations suggest that there is no link between stability and activity. Growth inhibition of instable flavonoids raises the question if degradation products contribute to the observed effects.

Table 1. Overview of investigated substances, 1:1-mixtures and their half effect concentrations (EC<sub>50</sub>) presented as average value with standard deviation (n=4). For single substances, stability is evaluated. For mixtures, occurrence of synergistic effects is evaluated.

substances	EC <sub>50</sub> [mg/L]	Stability during algae growth inhibition test (duration 72 h)
Eriodictyol	0.70 ± 0.08	Instable
Luteolin	0.94 ± 0.08	Instable
Gossypetin	1.4 ± 0.2	n.d.
Flavone	1.57 ± 0.02	Stable
3-Hydroxyflavone	1.8 ± 0.3	Instable
3,5-Dihydroxyflavone	2.2 ± 0.8	n.d.
Luteoloside	2.3 ± 0.2	n.d.
Quercetin	2.6 ± 0.3	Instable
7,3',4'-Trihydroxyflavone	2.7 ± 0.4	n.d.
Myricetin	3.7 ± 0.6	Instable
Morin	4.5 ± 0.7	Instable
Diosmetin	5 ± 2	Stable
Fisetin	5.4 ± 0.5	n.d.
Dihydroxymyricetin	5.8 ± 0.4	Instable
Taxifolin	8.1 ± 0.5	Instable
Hyperoside	13 ± 5	n.d.
Hesperetin	22.2 ± 0.6	stable
mixtures	EC <sub>50</sub> [mg/L]	indication for synergy
Luteolin-quercetin	1.1 ± 0.1	No
Luteolin-morin	2.6 ± 0.2	No
Luteolin-taxifolin	0.8 ± 0.2	Yes
Luteolin-hesperetin	1.0 ± 0.2	Yes
Quercetin-morin	3.5 ± 0.5	No
Quercetin-taxifolin	5 ± 1	No
Quercetin-hesperetin	4.0 ± 0.7	Yes

Taxifolin-hesperetin	8.4 ± 0.6	Yes
Luteolin-eriodictyol	0.7 ± 0.1	No
Luteolin-taxifolin-hesperetin	1.1 ± 0.1	Yes

Taken together, the moderate growth inhibition effect and instability of flavonoids indicate low ecotoxicity. However, environmental risks cannot be excluded due to the formation of degradation products.

### Acknowledgements

This research was funded by the EU within the European Regional Development Fund (ERDF), support measure INTERREG V in the Upper Rhine as part of the NAVEBGO project 5.3 (sustainable reduction of biocide inputs to groundwater in the Upper Rhine region; grand agreement number: 66300015).

### References

1. A.N. Panche, A. D. Diwan, S.R. Chandra, *Journal of Nutritional Science*, **5** e47(2016)
2. L. Schnarr, M. L. Segatto, O. Olsson, V. G. Ziun, K. Kümmerer, *Science of the Total Environment*, **824** 153781 (2022).
3. J. Banerjee, R. Singh, R. Vijayaraghavan, D. MacFarlane, A. F. Patti, A. Arora, *Food Chemistry*, **225** 10-22 (2017).
4. R. Manda, V. A. Addanki, S. Srivastava, *Plant Cell Biotechnology and Molecular Biology*, **21** 61-62 (2020).
5. A. Sharma, A. Shukla, K. Attri, M. Kumar, P. Kumar, A. Suttee, G. Singh, R. P. Barnwal, N. Singla, *Ecotoxicology and Environmental Safety*, **201** 110812 (2020).

## bio-Profiles of Chemical Reactions

Ksenia S. Egorova<sup>1\*</sup> and Valentine P. Ananikov<sup>1\*</sup>

<sup>1</sup> N.D. Zelinsky Institute of Organic Chemistry, Russian Academy of Sciences, Leninsky prospect 47, Moscow, Russia 119991

\*egorova-ks@ioc.ac.ru

In recent decades, many metrics have been developed and accepted for evaluation of environmental effects of chemical processes. However, obtaining a reliable overview of possible influence of a given process on various organisms is a very tricky task. In this work, we propose the concept of bio-Profiles of chemical reactions and describe its application for fast preliminary assessment of the impact of these reactions on living organisms by the example of the Suzuki reaction. The concept relies on our recent idea of tox-Profiles built on the basis of median lethal doses of chemical substances in various mammal species [1]. It suggests the usage of bio-Profiles built on the basis of cytotoxicity of all the components participating or forming in a particular chemical process (Figure 1). We also introduce bio-Factors of chemical reactions. bio-Profiles allow visual assessment of the contribution of various compounds to the “overall cytotoxicity” of a given reaction, whereas bio-Factors provide quantitative evaluation of changes in “overall cytotoxicity” during the reaction [2]. These data can be used for subsequent optimization of the chemical process from the viewpoint of toxicity of its participants.

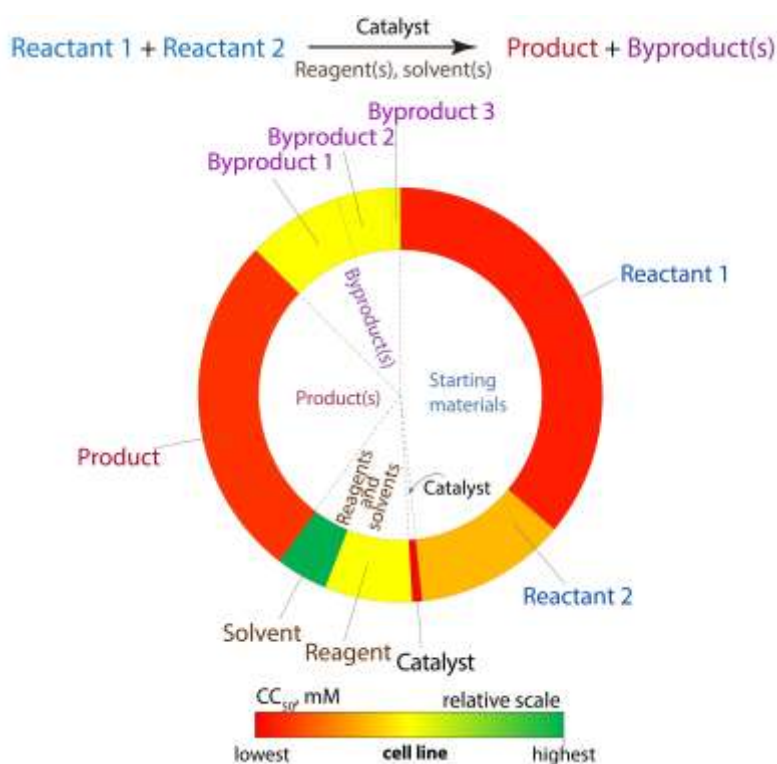


Figure 1. bio-Profile of an exemplary chemical reaction. Adapted and reproduced from [2].

### Acknowledgements

The work was supported by the Russian Science Foundation (RSF Grant 21-13-00049).

### References

1. K.S. Egorova, A.S. Galushko, V.P. Ananikov. *Angew. Chem. Int. Ed.*, **59** 22296 (2020).
2. K.S. Egorova, A.S. Galushko, L.U. Dzhemileva, V.A. D'yakonov, V.P. Ananikov. *Green Chem.*, **23** 6414 (2021).

## Transformation Products of Sulfonamides in aquatic Systems: What can we learn from available environmental Fate and Behaviour data?

Neele Puhlmann<sup>1</sup>, Oliver Olsson<sup>1</sup>, and Klaus Kümmerer<sup>1\*</sup>

<sup>1</sup>Centre/University/Company, Complete address, Country, Times New Roman 9

\*klaus.kuemmerer@leuphana.de

Sulfonamides (SUAs) and their transformation products (TPs) contribute to environmental pollution [1,2,3]. Importance of research on TPs' properties has been emphasised, e.g. allowing a comprehensive environmental risk assessment of their parent compounds. However, TPs' properties have been discussed in reviews on SUAs only marginally, if at all [3-8]. Therefore, we want to discuss the current state of knowledge on SUA-TPs including research gaps, and commonalities of SUA-TPs and TPs in general based on a recent literature review.

Literature on SUA-TPs was consulted systematically to collect data on occurrence, physicochemical properties, degradability, and (eco)toxicity. TPs of 14 SUAs were reviewed, and aspects applicable for TPs in general were identified to guide future handling of TPs as a complex category of compounds. The data of sulfamethoxazole (SMX), the main representative, was analysed in more detail to discuss insights on a chemical level.

Literature search resulted in 607 SUA-TPs reported in 222 publications. Only for 4%, 4%, 31%, and 35% of these TPs, data on occurrence in aquatic systems, on physicochemical properties, degradation, and toxicity, respectively, was found (Figure 16).

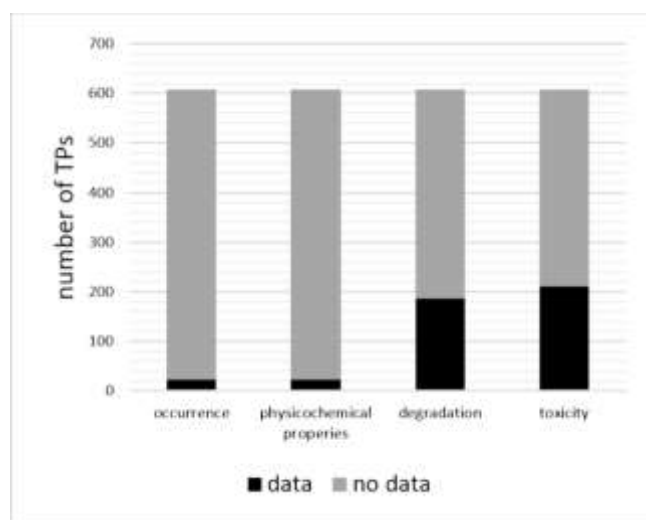


Figure 16: Overview of TPs with data entries regarding occurrence and properties.

Several mixtures of SUA-TPs were more ecotoxic than their parent compounds, e.g. 10 of 15 mixtures of SMX-TPs, consisting of 28 TPs. Only few TPs were tested as a single substance (Figure 17).

Although several TPs could be eliminated experimentally (Figure 18), their mineralisation rate remained often unknown. Thus, further transformation to persistent TPs could not be ruled out. Standardised biodegradability tests of individual TPs would monitor their mineralisation rate, but are almost completely lacking. Reasons are likely poor availability of TPs, but also the focus on abiotic water treatment.

Data assessment demonstrated that data of high significance according to standard methods, e.g. OECD methods for chronic (eco)toxicity and ready biodegradability, is needed to assess environmental risks of prioritised TPs, but also to redesign their parent pharmaceutical for complete environmental mineralisation in a long-term (Benign by Design) [9].

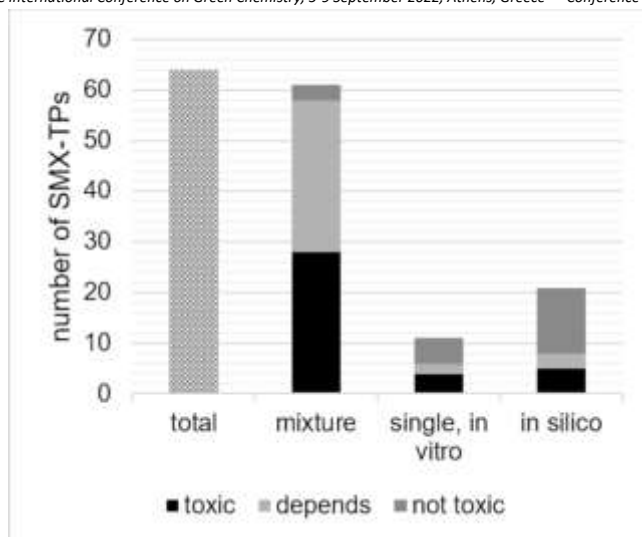


Figure 17: Number of SMX-TPs with data entries on (eco)toxicity, grouped by test approach (test of mixture, of single substances in vitro or in silico) subdivided according to the classification “toxic”, “depends”, and “not toxic”. The result was classified as “depends” in the case of different (eco)toxicities per TP, due to the dependence on different endpoints.

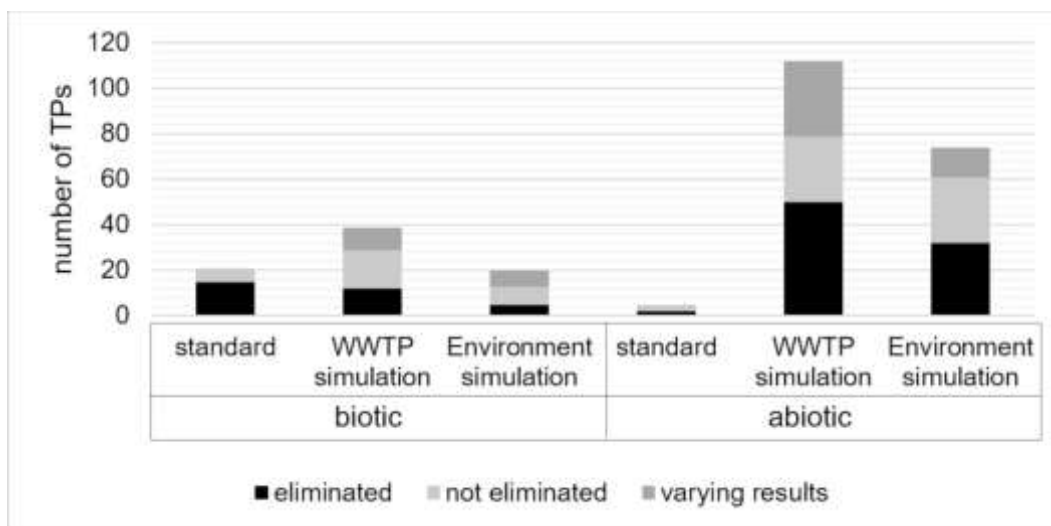


Figure 18: Number of TPs with data on degradation during different degradation tests with further classification, i.e. “not eliminated”, “eliminated” or “varying results” during degradation tests, mostly derived from kinetics. It depends strongly on the test conditions.

#### Highlights:

- 607 transformation products (TPs) of sulfonamides reported in 222 paper
- Data on occurrence, physicochemical properties, degradation, and (eco)toxicity found for 4%, 4%, 31%, and 35% of these TPs, respectively
- TP-mixtures can be more toxic than the single parent compounds
- Lack of data of high informative value by standard methods
- Mineralisation of TPs often unknown due to data gaps, especially for individual TPs

#### References

1. J.L. Wilkinson, A.B.A. Boxall, et al, C. Teta, *Proceedings of the National Academy of Sciences*, **119** 8 (2022).
2. K. Kümmerer, D.D. Dionysiou, O. Olsson, D. Fatta-Kassinos, *Science*, **361** 6399 (2018).
3. S. Tian, C. Zhang, D. Huang, R. Wang, G. Zeng, M. Yan, W. Xiong, C. Zhou, M. Cheng, W. Xue, Y. Yang, W. Wang, *Chemical Engineering Journal*, **389** (2020).
4. L. Charuaud, E. Jarde, A. Jaffrezic, M.-F. Thomas, B. Le Bot, *Journal of Hazardous Materials*, **361**, (2019).
5. A. Ezzariai, M. Hafidi, A. Khadra, Q. Aemig, L. El Fels, M. Barret, G. Merlina, D. Patureau, E. Pinelli, *Journal of Hazardous Materials*, **359** (2018).
6. A. Spielmeier, *Sustainable Chemistry and Pharmacy*, **9** (2018).
7. J. Wang, S. Wang, *Applied Microbiology and Biotechnology*, **102** 8 (2018).
8. Wohde et al., 2016 Wohde, M., Berkner, S., Junker, T., Konradi, S., Schwarz, L., Düring, R.-A., *Environmental sciences Europe*, **28** 1 (2016).
9. K. Kümmerer, *Sustainable Chemistry and Pharmacy*, **12** 100136 (2019).



## Determination of olive oil aroma profile using Hisorb-TD-GC/MS

Panagiota Fella, Marinos Stylianou, Agapios Agapiou\*

*Department of Chemistry, University of Cyprus, P.O.Box 20537, 1678 Nicosia, Cyprus*

*\*E-mail: agapiou.agapios@ucy.ac.cy, Tel.: +357-22-895432, Fax: +357-22-895088*

Solid phase microextraction (SPME) has been successfully applied for over 30 years in a wide variety of food and beverages applications. The limitations of SPME fiber over these years (*e.g.* small surface area, a limited amount of sorptive phase, the fragility of the fiber, *etc.*) are potentially overcome by the Hisorb tool (Markes Int.) that promises higher sensitivity. Therefore, a Hisorb sorptive extraction Thermal Desorption-Gas Chromatography-Mass spectrometry (Hisorb-TD-GC-MS) method was developed for the analysis of volatile organic compounds (VOCs) of olive oil samples derived from four different olive mills in Cyprus last year (blend of different cultivars). Different factors were examined to optimize the Hisorb extraction conditions, such as the sample amount, sample agitation, equilibration time, extraction time, and temperature. In total, more than 80 VOCs were identified and semi-quantified, belonging to several chemical classes, such as hydrocarbons, aldehydes, ketones, alcohols, terpenes, esters, acids, and others. Aldehydes and hydrocarbons were the main chemical classes. Among aldehydes, (E)-2-Hexenal was the prominent compound (ranging from 0.52 to 2.83 mg/kg); it derives from the lipoxygenase pathway and is responsible for the green, fruity, and bitter sensory characteristics. Other important aldehydes are nonanal and hexanal, ranging from 0.41 to 2.83, and from 0.27 to 2.11 mg/kg, respectively. The overall method remains green, and non-invasive, offering the preconcentration ability as SPME, but requires a TD-GC-MS system.

## Mapping VOCs from different soils of Cyprus vineyards using HS-SPME-GC/MS analysis

Kyriaki Kaikiti<sup>1</sup>, Michalis Omirou<sup>2</sup>, Savvas Savvides<sup>2</sup>, Ioannis M. Ioannides<sup>2</sup>, Agapios Agapiou\*<sup>1</sup>

<sup>1</sup>Department of Chemistry, University of Cyprus, P.O.Box 20537, 1678 Nicosia, Cyprus

<sup>2</sup>Department of Agrobiotechnology, Agricultural Research Institute, P.O.Box 22016, Nicosia 1516, Cyprus

\*E-mail: [agapiou.agapios@ucy.ac.cy](mailto:agapiou.agapios@ucy.ac.cy), Tel.: +357-22-895432, Fax: +357-22-895088

Soil volatile organic compounds (VOCs) are one of the main molecules that are affecting soil ecology and function, while several studies suggest that on a regional and global scale, they may affect atmospheric chemistry. Besides, VOCs are key compounds contributing to the communication between plants, insects, animals, soil organisms, subsoil. Cyprus has a long history in wine production and vineyards are a significant component of rural areas and the agricultural ecosystem of the country. In this work, soil samples from 45 different vineyards of Cypriot main wine-making areas were studied for their VOC profile and classified through the headspace solid-phase microextraction gas chromatography/mass spectrometry (HS-SPME-GC/MS) analysis. Multi variety analysis showed significant differences among sites, and the differential abundance of the various VOCs determined was associated with the physicochemical and biological properties of the sampled soils.

**Keywords:** VOCs, soil, Cyprus vineyards, soil nutrients, soil DNA

## Evaluation of efficacy of ZnO nanoparticles as nanofertilizers: An alternative agriculture approach

Arfana Mallah<sup>\*1,2</sup>, Bindia Junejo<sup>3</sup>, Amber R. Solangi<sup>3</sup>, Iqleem H. Taqvi<sup>4</sup>

<sup>1</sup>M.A.Kazi Institute of Chemistry, University of Sindh, 76080 Jamshoro, Pakistan

<sup>2</sup>Department of Chemistry, Norwegian University of Science and Technology, (NTNU) Trondheim, Norway

<sup>3</sup>National Centre of Excellence in Analytical Chemistry, University of Sindh, 76080 Jamshoro, Pakistan

<sup>4</sup>Dept. of Chemistry, Govt. College University Hyderabad, Pakistan

\*Email address of Corresponding Author: arfana30@gmail.com

### Abstract

As with the increasing population, the increase in food resources is a major concern worldwide which requires the use of modern technologies in agriculture. There is a need for a more innovative fertilizer approach that can increase the productivity of food in agricultural systems and be more environmental friendly than synthetic fertilizers. Nanoparticles as nano fertilizers have the potential to promote sustainable agriculture and increase overall crop productivity, mainly by increasing the nutrient use efficiency (NUE) of field and greenhouse crops. These novel materials can release their nutrients at a slow and steady pace, either when applied alone or in combination with synthetic or organic fertilizers. Plant growth significantly depends on Zn nutrition because Zn is a structural component co-factor for various proteins and enzymes. Zinc nanoparticles in the form of ZnO are frequently used in modern agriculture, since they are more efficient and cost-effective than synthetic Zn fertilizers. In this study, zinc oxide nanoparticles were prepared by aqueous chemical growth method. The obtained material was characterized by X-ray diffraction (XRD), Transmission electron microscopy (TEM) and scanning electron microscopy (SEM) and Energy dispersive X-ray spectroscopy (EDX). The average size was found in the range of 10 to 20 nm. The synthesized material was applied in pots and in field in different concentrations for the growth of maize crop. The effects on the growth of maize crop through pot and field experiments were evaluated. The growth parameters such as plant height, root and shoot ratio, dry and fresh weight of the maize plants were studied. The maximum increase in growth and zinc accumulation was observed in the case of ZnO nanoparticles as compared to the ZnSO<sub>4</sub> application. The data containing growth parameters and accumulation of zinc in the maize plants was also compared with that of the control samples (with no zinc application) and those with ZnSO<sub>4</sub> which is a commercial fertilizer used by the farmers.

**Keywords:** Zinc oxide nanoparticles, nano fertilizers, agriculture.

# Green catalysis & synthesis

## Connecting sonication with photocatalysis to intensify a continuous flow photocatalytic processes: A disruptive alternative for lignin valorization

Juan Carlos Colmenares<sup>1\*</sup>, Marta Paszkiewicz-Gawron<sup>1</sup>, Swaraj R. Pradhan<sup>1</sup>, Dariusz Łomot<sup>1</sup>, Abdul Qayyum<sup>1</sup>

<sup>1</sup>Institute of Physical Chemistry, Polish Academy of Sciences, Kasprzaka 44/52 01-224 Warsaw, Poland

\*e-mail address of corresponding author: [jcarloscolmenares@ichf.edu.pl](mailto:jcarloscolmenares@ichf.edu.pl)

The studies for “greener” and economically feasible approaches such as photocatalysis, sonochemistry and flow chemistry for the selective transformation of organic-waste-derived compounds like aromatic alcohols (for instance: coming from underutilized lignin) by avoiding the drastic reaction-conditions/reagents concentrate the focus of attention of the last decade [1-3].

In this work, to get insight into the mechanism of ultrasound-assisted methods, the whole spectrum of materials characterization techniques and basic kinetic studies and photocatalysts’ stability/recycling studies (using the appropriate flow (sono)-(photo)-reactors) have been carried out. The use of ultrasound-based procedures offer a facile, versatile synthetic tool for the preparation of composite nanophotocatalysts, often inaccessible through routine methods. Sonochemistry is the use of ultrasound to facilitate chemical reactions [4]. It has been shown to be effective in enabling various polymer chemistries and forming nanomaterials [5]. In this context, ultrasound is a mechanical wave that locally changes the fluid’s density, which is often measured as pressure perturbations. Designing/fabricating photocatalysts by a sonochemical approach and testing them in an appropriate flow sono-photo-reactors towards sustainable selective transformations of key organic model compounds of lignin, is what we want to achieve.

The design and fabrication of novel photocatalysts are very challenging withing the lignin valorization concept. In this research work, the synthesis of TiO<sub>2</sub> (both as a powder and a layer incorporated in the internal wall of a flow micro-reactor) and metal-free carbon-based photocatalysts were performed by the ultrasound-promoted precipitation, sol-gel-immobilization and hydrosolvothermal methods, respectively. The physicochemical features were determined by a plethora of well-selected technical methods such as N<sub>2</sub> sorption, HR-TEM, HAADF-STEM, EDX, XPS, XRD, EDX, thermal analysis, and diffuse reflectance absorption. The additive-free photoactivity showed that TiO<sub>2</sub> (powder or layer inside the microreactor) and carbophotocatalysts revealed the highest yield of the target product than commercial TiO<sub>2</sub> and g-C<sub>3</sub>N<sub>4</sub>.

More specifically the work will be on:

a. **Design and development of monometal-containing TiO<sub>2</sub> coated microflow reactor for photocatalytic partial oxidation of benzyl alcohol (BnOH) to benzaldehyde (BnAld):** The presented investigation concerns an efficient ultrasound-based monometal (Fe, Cu, Co)-containing TiO<sub>2</sub> deposition on the inner walls of a perfluoroalkoxy alkanes (PFA) microtube under mild conditions. The experiments were carried out using commercial TiO<sub>2</sub> and sol-gel synthesized TiO<sub>2</sub>. The rough surface formed during ultrasonication is the site for the deposition of these nanoparticles in the internal walls of the microtube. The photocatalytic activities of these semiconductor coated fluoropolymer based microreactors were evaluated for the selective oxidation of BnOH to BnAld in liquid flow phase. The analysis of the results showed that various features/parameters are crucial, and by tuning them, it is feasible to improve the conversion of BnOH and BnAld selectivity. Among all the metal-containing TiO<sub>2</sub> samples, the 0.5 at% Fe/TiO<sub>2</sub> (both, iron and titanium, as cheap, safe and abundant metals) photocatalyst exhibited the highest BnOH conversion under visible light (515 nm) in a microflow system. This could be explained by the higher crystallite size, high porosity, and flake-like morphology (Figure 1) [6].

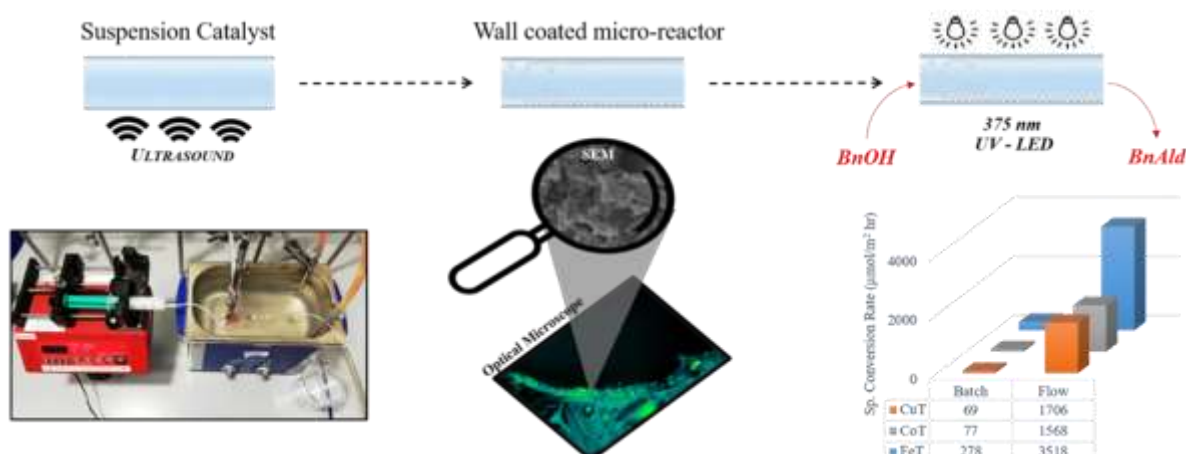


Figure 1. Schematic of the method of monometal-containing TiO<sub>2</sub> internally coated flow microreactor and its photocatalytic activity in benzyl alcohol (BnOH) selective oxidation to benzaldehyde (BnAld).

**b. Designing/fabricating photocatalysts by a sonochemical approach, and testing them in the appropriate flow sonophotoreactor towards sustainable selective oxidation of key organic model compounds of lignin:**

The objective is to prepare metal-free carbon-based and TiO<sub>2</sub>-based photocatalytic materials through the physicochemical effects of low/high-frequency sonication (e.g., effective mass transfer, microstreaming, cross-linked radical polymerization, etc., effects often inaccessible through conventional methods). It will be presented out the study of the physicochemical properties of carbon-based and TiO<sub>2</sub>-based materials (before and after flow (sono)-(photo)-catalytic test reactions), and testing them in the selective sonophotocatalytic oxidation and C-C sonophoto-reductive coupling of bio-oil-inspired model compounds (in flow liquid-phase) as a futuristic approach of bio-oil-based molecules valorization (for instance: 2-phenoxy-1-phenylethanol, 2,6-dimethoxyphenol, benzyl alcohol). Ultrasonication (US)-assisted precipitation (Figure 2b) [7] and US-assisted hydrosolvothermal (Figure 2a) methods were used for the synthesis of metal-oxide-based and metal-free-carbon-based photocatalysts, respectively. Additionally, we report selected experiments of intensification of a flow photocatalytic selective oxidation through the use of ultrasonic waves. The effort of our research is focused on the utilization of flow sonophotocatalysis for the selective transformation of lignin-based model molecules by nanostructured metal oxides (e.g. TiO<sub>2</sub>), and metal-free carbocatalysts. A plethora of parameters that affects the acoustic cavitation phenomena, and as a result the potential of sonication were investigated (e.g. ultrasound frequency and power). Various important photocatalytic parameters such as the wavelength and intensity of the irradiated light, photocatalyst loading, type of solvent, mixture of solvents, and solution pH were also optimized.

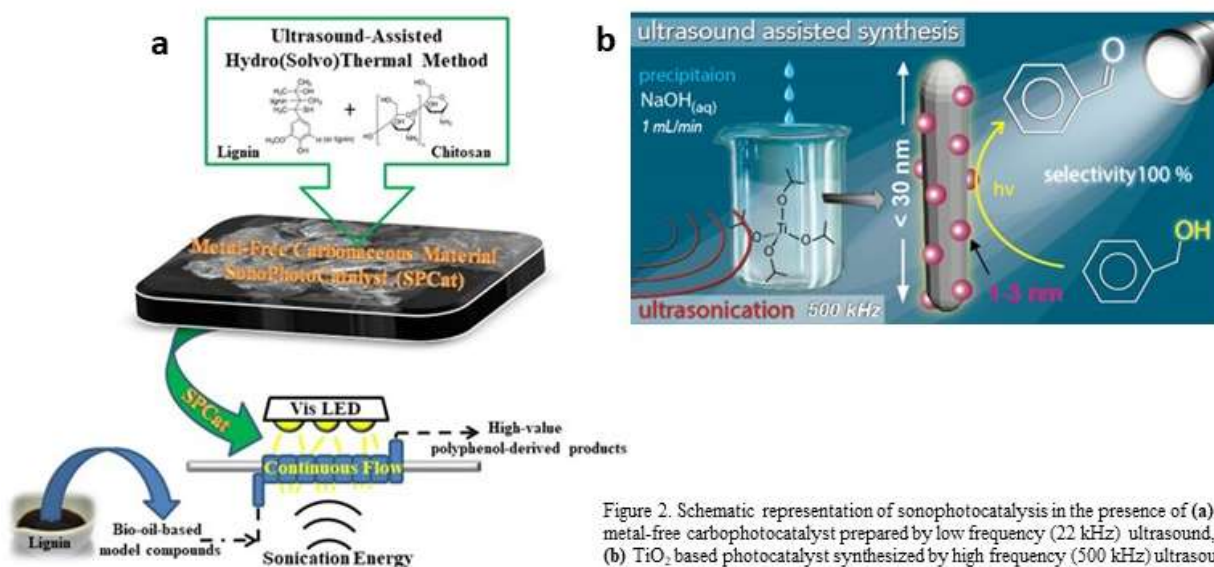


Figure 2. Schematic representation of sonophotocatalysis in the presence of (a) metal-free carbophotocatalyst prepared by low frequency (22 kHz) ultrasound, and (b) TiO<sub>2</sub> based photocatalyst synthesized by high frequency (500 kHz) ultrasound.

## Acknowledgements

This research is supported by the National Science Center (NCN) in Poland within research projects OPUS 20 No. 2020/39/B/ST5/00076, Sonata Bis project nr 2015/18/E/ST5/00306 and OPUS-13 no. 2017/25/B/ST8/01592. (<https://photo-catalysis.org/view.php?id=1282> <https://photo-catalysis.org/view.php?id=917> <https://photo-catalysis.org/view.php?id=1139> ).

## References

1. E. Kuna, R. Behling, S. Valange, G. Chatel, J.C. Colmenares, *Top. Curr. Chem.* 41 (Z) 375 (2017).
2. J.C. Colmenares, R.S. Varma, V. Nair, *Chem. Soc. Rev.*, 46 6675 (2017).
3. X. Liu, X. Duan, W. Wei, S. Wang, B.-J. Ni, *Green Chem.*, 21 4266 (2019).
4. R.J. Wood, J. Lee, M.J. Bussemaker, *Ultrason. Sonochem.*, 38 351 (2017).
5. H. Xu, B.W. Zeiger, K.S. Suslick, *Chem. Soc. Rev.*, 42 2555 (2013).
6. S.R. Pradhan, D. Lisovytskiy, J.C. Colmenares, *Catal. Commun.*, 162 106375 (2022).
7. A. Qayyum, D.A. Giannakoudakis, A.P. LaGrow, O. Bondarchuk, D. Łomot, J.C. Colmenares, *Catal. Commun.*, 163 106406 (2022).

## Key role of ultrasound on the synthesis of TiO<sub>2</sub> nanomaterials and catalytic performance

Abdul Qayyum<sup>1,\*</sup>, Dimitrios A. Giannakoudakis<sup>1</sup>, Darius Lomot<sup>1</sup>, Juan Carlos Colmenares<sup>1,\*</sup>

<sup>1</sup>*Institute of Physical Chemistry, Polish Academy of Sciences, Kasprzaka 44/52, 01-224 Warsaw, Poland.*

*\*[aqayyum@ichf.edu.pl](mailto:aqayyum@ichf.edu.pl), [icarloscolmenares@ichf.edu.pl](mailto:icarloscolmenares@ichf.edu.pl)*

### Abstract

Biomass is assumed as a prosperous renewable feedstock since a plethora of high value platforms and chemicals can be derived by its catalytic transformation [1]. Specifically, lignocellulosic biomass is one of the largest raw source of aromatic chemicals in nature. Lignin is made up of aromatic subunits that are mainly linked to each other through C–O–C or C–C bonds. The selective catalytic conversion of lignin into value-added aromatics is important for providing sustainable development. Efficient and selective conversion of lignin to high-value products is still a challenging field of research because of its inherent heterogeneity and variability [2].

Advanced oxidation processes based on heterogeneous photocatalysis using metal oxide semiconductors gain a continual increment of interest, especially for lignin valorization [3]. Titanium dioxide (TiO<sub>2</sub>) is considered as a promising candidate for heterogeneous catalysis due to its unique physicochemical properties. Different synthesis methods such as hydrothermal, pyrolysis, sol-gel, etc. are being used for the synthesis of TiO<sub>2</sub> [4]. The precipitation-based methods have advantages over the aforementioned methods due to the ability to control various physicochemical features, such as the particle size and size distribution [5]. In addition, the use of ultrasonication as one of the mechano-chemical approaches that has been proven as a promising and versatile tool for the synthesis of novel titanium oxide nanostructures TiO<sub>2</sub> [6]. The key advantage of sonication is the generation and growth of acoustic cavitation, leading to localized hotspots, where the local temperature and pressure can reach up to 5000 K and 500 atm, respectively. Moreover, sonochemistry also has positive effects on other physical or/and chemical phenomena such as better mass transfer phenomenon, de-aggregations, and the formation of free radicals, with all these factors to play a key role in the synthesis of nanomaterials [3]. From the point of view of sustainable catalytic processes, coupling of sonocatalysis with photocatalysis, known as sonophotocatalysis, also presents some advantages over photocatalysis, such as more efficient use of photocatalyst and increased amount of free radical species in aqueous medium and turbulence induced by cavitation phenomenon, which lead to the increase of catalytic activity [7].

Considering all the above-mentioned, TiO<sub>2</sub> catalysts were synthesized following an ultrasound-assisted precipitation method [8]. The ultrasound of 22 kHz frequency varying each time the power, such as 8, 24, 40, 56 and 72 W was used during the synthesis step. A sample of TiO<sub>2</sub> (MagS) was also synthesized by using magnetic stirring instead of ultrasound irradiation in order to study the effect of ultrasonication on the physicochemical properties and photocatalytic performance. A commercial TiO<sub>2</sub> catalyst (P25) was additionally examined for the sake of comparison. These synthesized and commercial TiO<sub>2</sub> catalysts were characterized using various characterization techniques. The photocatalytic performance of all the catalysts was investigated for the partial selective oxidation of a lignin-based model compound i.e. benzyl alcohol (BnOH) to benzyl aldehyde (PhCHO), under low-intensity of UV light irradiation (365 nm, irradiance 100 W/m<sup>2</sup>) and without the use of additives/reagents. The TiO<sub>2</sub> sample synthesized by using 24 W power of ultrasound showed the highest conversion of BnOH and yield of PhCHO as compared to all other synthesized TiO<sub>2</sub> samples. Hence, it was selected among all other ultrasound assisted synthesized TiO<sub>2</sub> samples for studying sonophotocatalytic performance along with MagS and P25 catalysts.



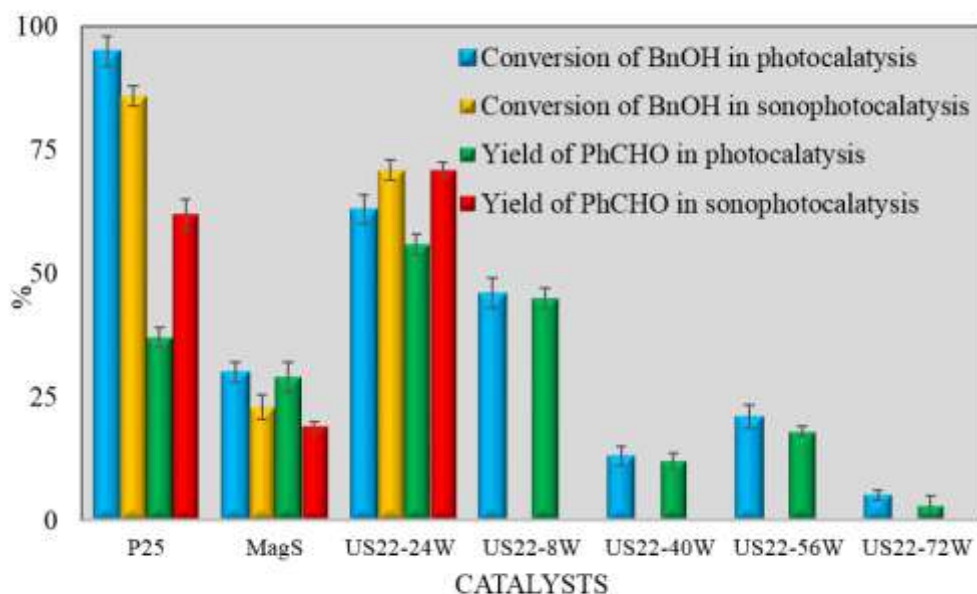


Figure 1. Catalytic performance of synthesized and commercial TiO<sub>2</sub>

Regarding the physicochemical features, US22-24W showed the highest specific surface area (319 m<sup>2</sup>/g) and total pore volume (0.339 cm<sup>3</sup>/g) as compared to MagS and P25. Electron microscopy analysis revealed that the use of ultra-sonication during the synthesis led to the formation of nanorods. XPS analysis showed the presence of some reduced Ti sites on the ultrasound-assisted TiO<sub>2</sub> compared to MagS, while MagS possess a higher amount of sodium than US22-24W.

When low power ultrasound of 22 kHz frequency was coupled to photocatalysis by replacing the magnetic stirring then the increased yield of PhCHO was found as compared to yield obtained in photocatalysis (Figure 1). The increment in the yield led to enhanced the selectivity toward the PhCHO. The research work showed that the physicochemical properties, as well as photo-oxidation performance of synthesized TiO<sub>2</sub>, can be tuned by optimizing the power of ultrasound used during the synthesis step. By coupling ultrasound to photocatalysis, the yield of PhCHO was found higher as a result of the synergistic effect.

### Acknowledgements

This research is funded by the National Science Center (NCN) in Poland within research project OPUS-13 no. 2017/25/B/ST8/01592. More information about the project can be found: <https://photo-catalysis.org/view.php?id=1139>

### References

1. Y. Ma, Z. Du, J. Liu, F. Xia, J. Xu, *Green Chem.*, 17 4968 (2015).
2. Y. Ma, Z. Du, F. Xia, J. Ma, J. Gao, J. Xu, *RSC Adv.*, 6 110229 (2016).
3. G. Chatel, S. Valange, R. Behling, J.C. Colmenares, *ChemCatChem.*, 9(14) 2615-2621 (2017).
4. M. T. Noman, M. A. Ashraf, A. Ali, *Environ. Sci. Pollut. Res.*, 26(4) 3262 (2019).
5. A. Pottier, S. Cassaignon, C. Chanéac, F. Villain, E. Tronc, J. P. Jolivet, *J. Mater. Chem.*, 13(4) 877 (2003).
6. D.A. Giannakoudakis, G. Chatel, J.C. Colmenares, *Top. Curr. Chem.* 378 (2020).
7. D.A. Giannakoudakis, D., Łomot, J.C. Colmenares, *Green Chem.*, 22(15) 4896 (2020).
8. A. Qayyum, D.A. Giannakoudakis, A.P. LaGrow, O. Bondarchuk, D., Łomot, J.C. Colmenares, *Catal. Commun.*, 163 106406 (2022).

# Metal Nanoparticles and Metal-based Polymeric Materials as vehicles for Green Organic Synthetic Methodologies

Ioannis N. Lykakis<sup>1\*</sup> and George E. Kostakis<sup>2</sup>

<sup>1</sup>Department of Chemistry, Aristotle University of Thessaloniki, University Campus, GR-54124 Thessaloniki, Greece

<sup>2</sup>Department of Chemistry, School of Life Sciences, University of Sussex, Brighton BN1 9QJ, U.K  
 lykakis@chem.auth.gr

The use of a recyclable catalyst and environmentally friendly reagents is an elegant route for organic transformations. In general, for catalytic processes, an attractive approach is the use of supported catalysts and/or polymeric materials, which based on their structural/chemical properties offer several advantages on the regio- and chemo-selectivity of the catalytic organic process. Thus, Chemistry Over Materials can play a crucial role Forward the selective Organic Reaction Transformations (COMFORT). Based on this, herein we outline a research study aimed into the photo- and thermal catalytic applications of new AuNPs and AgNPs heterogeneous systems,<sup>1</sup> to afford green catalytic organic redox transformations, towards the synthesis of biological interesting heterocyclic compounds.<sup>2</sup> Alongside, Cu-based 1D coordination polymers<sup>3</sup> have been used successfully for the synthesis of several *N*-heterocyclic cores, using common starting materials and under one-pot process (Figure 1).<sup>3</sup>

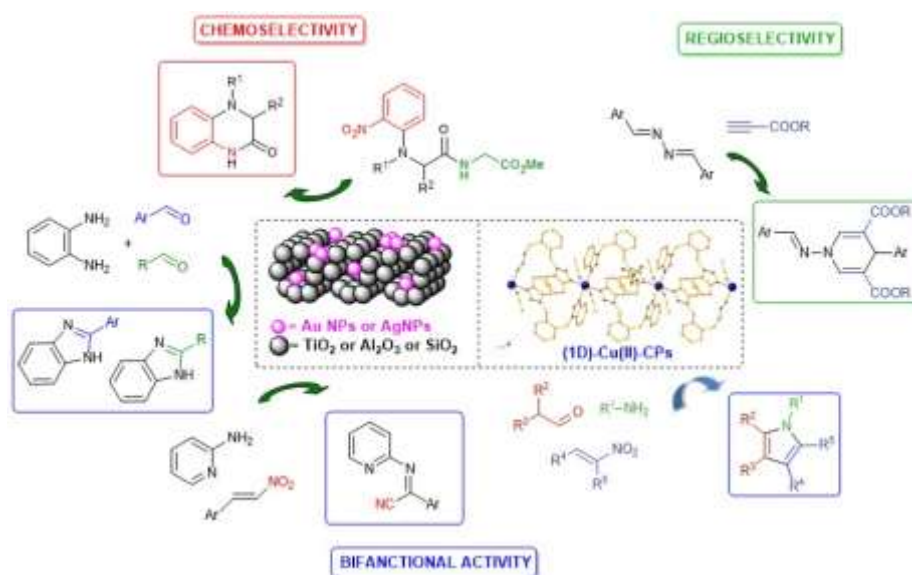


**Figure 1.** New catalytic strategies for the synthesis of *N*-heterocyclics

## Acknowledgements

Financial support of the photo-transformations by the project “PhotoTransform” (MIS: 5047897), NSRF 2014-2020, which is co-financed by the European Social Fund (ESF). Synthetic procedures found support by the project “OPENSREEN-GR” (MIS 5002691) which is implemented under the Action “Reinforcement of the Research and Innovation Infrastructure” (NSRF 2014-2020) and co-financed by Greece and the European Union (KA94150)

## References

- (a) M. Stratakis, I. N. Lykakis, *Synthesis*, 2019. (b) T. Mitsudome, K. Kaneda, *Green Chem.* **15** 2636 (2013). (c) M. Stratakis, H. Garcia, *Chem. Rev.* **112** 4469 (2012). (d) A. Corma, P. Serna, *Science* **313** 332 (2006).
- (a) S. Fountoulaki, V. Daikopoulou, P. L. Gkizis, I. Tamiolakis, G. S. Armatas, I. N. Lykakis, *ACS Catalysis*, **4** 3504 (2014). (b) E. Charistoudi, M. G. Kallitsakis, I. Charisteidis, K. S. Triantafyllidis, I. N. Lykakis, *Adv. Synth. Catal.* **359** 2949 (2017). (c) M. A. Tzani, M. G. Kallitsakis, T. S. Symeonidis, I. N. Lykakis, *ACS Omega* **3** 16005 (2018). (d) M. A. Tzani, C. Gabriel, I. N. Lykakis, *Nanomaterials*, 2045 (2020). (e) M. G. Kallitsakis, D. I. Ioannou, M. A. Terzidis, G. E. Kostakis, I. N. Lykakis, *Org. Lett.*, **22** 4339 (2020).
- (a) M. Kallitsakis, E. Loukopoulos, A. Abdul-Sada, G. J. Tizzard, S. J. Coles, G. E. Kostakis, I. N. Lykakis *Adv. Synth. Catal.* **359** 138 (2017). (b) D. Andreou, M. G. Kallitsakis, E. Loukopoulos, C. Gabriel, G. E. Kostakis, I. N. Lykakis, *J. Org. Chem.* **83** 2104 (2018). (c) M. G. Kallitsakis, D. I. Ioannou, M. A. Terzidis, G. E. Kostakis, I. N. Lykakis, *Org. Lett.*, **22** 4339 (2020).

## Tailor-made POLITAG-Pd<sup>0</sup> catalyst for the low-loading Heck cross-coupling in $\gamma$ -valerolactone as safe reaction medium

Luigi Carpisassi, Federica Valentini, Adrien Comès, Carmela Aprile and Luigi Vaccaro\*

<sup>1</sup> Laboratory of Green Synthetic Organic Chemistry (Green S.O.C.) Department of Chemistry, Biology and Biotechnology Università Degli Studi di Perugia, Via Elce Di Sotto 8 06123-Perugia, Italy

\*luigi.vaccaro@unipg.it

Herein we report a new family of tunable, heterogenous, fully-recoverable catalysts called POLITAG-Pd(0) for the low loading Heck-Mizoroki reaction. This type of catalytic systems are obtained by employing a polystyrene-based gel-type support functionalized with ionic pincer-type ligand for palladium stabilization [1], [2]. By changing the ratio between the supported matrix and the ionic tag moiety 3 different type of supports were obtained (POLITAG-L, M, H). subsequently loaded with different amount of metal in order to obtain 5 different types of catalysts (POLITAG-LL, LM, MM, HM, HH). Furthermore all the systems were fully characterized (EA, XPS, TEM, HR-TEM).

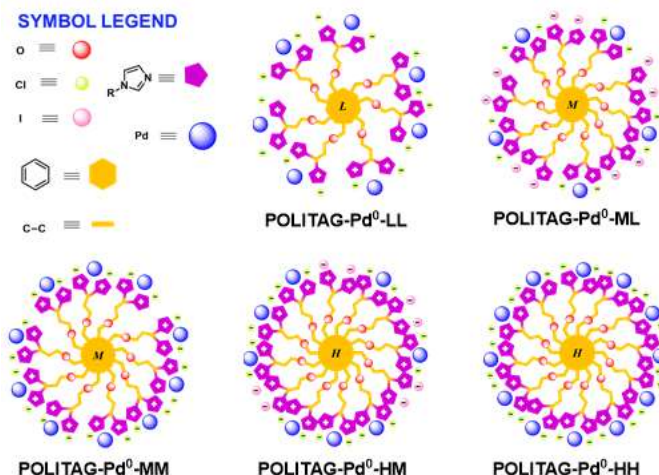
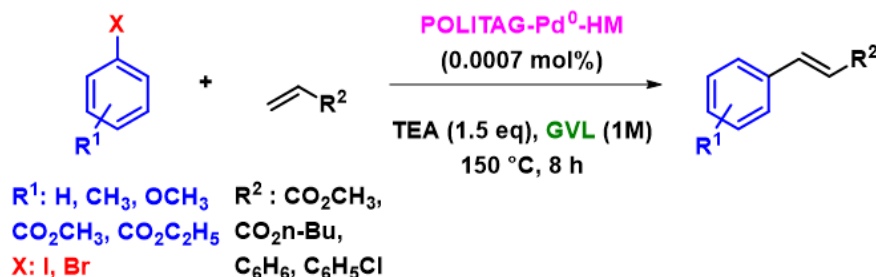


Figure 19. Schematic representation of the five POLITAGs-Pd<sup>0</sup> here synthesized and studied.

In order to test the efficiency of the POLITAGs-Pd<sup>0</sup> synthesized, all the catalytic systems were tested on a Heck-Mizoroki coupling first by using optimized reaction conditions already developed within our research group. In general all the catalytic systems has shown very low metal loss and, between them, the selected POLITAG-Pd<sup>0</sup>-HM is characterized by a high TOF value (26786 h<sup>-1</sup>), affording the desired products in high isolated yields using only 0.0007 mol% of Pd. Moreover, this high catalytic activity coupled with the utilization of  $\gamma$ -valerolactone as green reaction medium led to the definition of a waste-minimized protocol. To fully demonstrate the advantages in customized catalyst-synthesis, Amiloxate, a widely used sunscreen agent, was synthesized with negligible metal contamination and low E-factor.



Scheme 4. Representative Heck reaction with POLITAG-HM as catalyst

### Acknowledgements

The Università degli Studi di Perugia and MUR are acknowledged for financial support for the project AMIS, through the program “Dipartimenti di Eccellenza - 2018-2022”. This research used resources of PC2 (Plateforme Technologique Physico-Chimique Characterization), MORPH-IM (Morphology & Imaging) and SIAM (Synthesis, Irradiation & Analysis of Materials) technology platforms located at the University of Namur.

## References

1. F. Valentini, H. Mahmoudi, L. A. Bivona, O. Piermatti, M. Bagherzadeh, L. Fusaro, C. Aprile, A. Marrocchi, L. Vaccaro. *ACS Sustainable Chem. Eng.*, **7**, 6939-6946 (2019).
2. H. Mahmoudi, F. Valentini, F. Ferlin, L. A. Bivona, I. Anastasiou, L. Fusaro, C. Aprile, A. Marrocchi L. Vaccaro. *Green Chem.*, **21**, 355-360 (2019).

## The road to intrinsically dynamic materials: disulfide chemistry as a solution

Qi Zhang\*

Stratingh Institute for Chemistry, University of Groningen, Nijenborgh 4, 9747 AG Groningen, The Netherlands

\*email: qi.zhang@rug.nl

Understanding dynamic chemistry systems in Nature inspires chemists to design biomimetic synthetic materials. Disulfide bonds, the bonds that tie peptides, feature their dynamic covalent nature, that is reversible covalent bonds. Here we propose that making polymers with disulfide bonds can be a solution towards intrinsically dynamic materials. Unlike traditional plastics and noncovalent (supramolecular) polymers, poly(disulfides) can simultaneously exhibit chemical recycling ability and excellent mechanical performances. We will focus on the poly(disulfides) derived from thioctic acid, a natural small molecule, to show the promising applications of these intrinsically dynamic materials in self-healing elastomers, adhesives, and actuators [1-5]. Then I will move to our recent discovery that hydrogen bonds are essential in the control of disulfide chirality and enable stereodivergent chirality transfer. We find that the formation of S-S---H-N hydrogen bonds in solution can drive conformational adaption to allow intramolecular chirality transfer, while the formation of C=O---H-N hydrogen bonds results in supramolecular chirality transfer to form antiparallel helically self-assembled solid-state architectures [6].

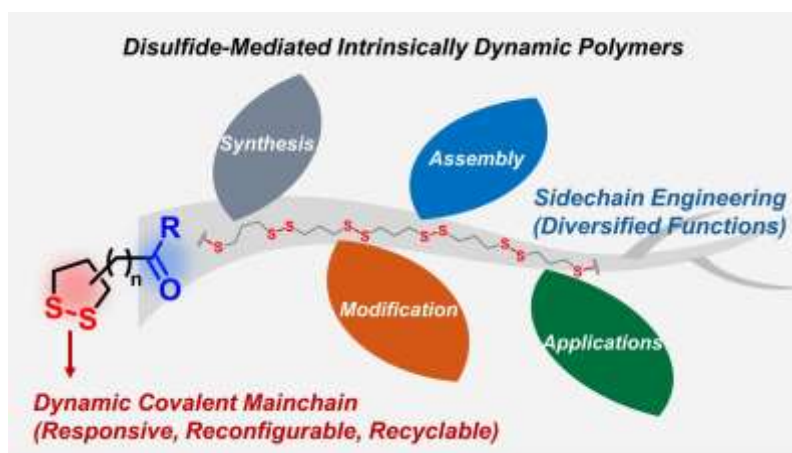


Figure 1. Dynamic disulfide chemistry for sustainable polymers

### Acknowledgements

This project has received funding from the European Union's Horizon 2020 research and innovation programme under the Marie Skłodowska-Curie actions grant agreement grant 101025041.

### References

1. Q. Zhang, C. Shi, D. H. Qu\*, Y. Long, B. L. Feringa\*, H. Tian\*, *Science Advances*, **4**, eaat8192 (2018).
2. Q. Zhang, Y. Deng, H. Luo, C. Shi, G. M. Geise, B. L. Feringa\*, H. Tian, D. H. Qu\*, *J. Am. Chem. Soc.* **141**, 12804-12814 (2019).
3. Q. Zhang, Y. Deng, C. Shi, B. L. Feringa\*, H. Tian, D. H. Qu\*, *Matter*, **4**, 1352-1364 (2021).
4. Y. Deng†, Q. Zhang†, C. Shi, R. Toyoda, D. H. Qu\*, H. Tian, B. L. Feringa\*, *Science Advances*, **8**, abk3286 (2022).
5. Q. Zhang, D. H. Qu\*, B. L. Feringa, H. Tian\*, *J. Am. Chem. Soc.* **144**, 2022–2033 (2022).
6. Q. Zhang, S. Crespi, R. Toyoda, R. Costil, W. R. Browne, D. H. Qu\*, H. Tian, B. L. Feringa\*, *J. Am. Chem. Soc.* **144**, 4376–4382 (2022).

## Chiral iron(II)-catalysts within valinol-grafted metal-organic frameworks for enantioselective reduction of ketones

Naved Akhtar<sup>1</sup> and Kuntal Manna<sup>1\*</sup>

<sup>1</sup>Department of Chemistry, Indian Institute of Technology, New Delhi, India

\*Kuntal.Manna@chemistry.iitd.ac.in

The stereochemistry of an organic compound can have a profound influence on many of its most important properties. For example, the enantiomeric forms of a drug molecule can have completely different biological effects, and polymers that differ only in the stereochemistry of their backbones can have quite dissimilar macroscopic physical characteristics. Control over the stereochemical outcome of organic reactions has thus long been recognized as a central concern across multiple sectors of modern synthetic chemistry. Asymmetric catalysis with single-site solid catalysts continues to attract great interest owing to the importance of heterogeneous catalysis in the production of commodity chemicals, and the lack of similar processes for the synthesis of optically active molecules. Naturally occurring amino acids, protected amino acids or amino alcohols are an important class of chiral ligands in asymmetric metal catalysis as they are cheap, affordable, scalable, and also easily tunable, and air-stable.<sup>1-2</sup> However, the usage of amino acids as chiral ligands to construct robust single-site earth-abundant metal catalysts is very limited due to their lack of steric bulkiness and limited solubility in common organic solvents. Chiral amino alcohols, prepared by reducing chiral amino acids, are an important class of organic compounds containing both an alcohol and an amine functional group. Although optically active amino alcohols are primarily used to synthesize chiral oxazolines,<sup>3-4</sup> their application in asymmetric metal catalysis as chiral ligands is limited due to lack of steric substituents leading to the formation of multinuclear catalytic species.

Hence, we have developed amino alcohol functionalized metal-organic frameworks (MOFs) that are used as solid chiral ligands to prepare robust single-site earth-abundant metal catalysts via site-isolation for asymmetric organic transformations. vol-UiO-68 are constructed from L-valinol functionalized linear dicarboxylate linkers and Zr<sub>6</sub>O<sub>4</sub>(OH)<sub>4</sub> secondary building units (SBUs) to afford UiO-frameworks.<sup>5-6</sup> vol-UiO-68 were synthesized following a similar procedure via synthesizing the aldehyde-functionalized UiO-68-CHO MOFs, respectively, followed by the grafting of L-valinol within these MOFs. The condensation reaction between the aldehyde moiety of MOF and amino group of L-valinol furnished the valinol-grafted chiral vol-UiO MOFs through the formation of imine linkages.<sup>7-8</sup> The deprotonation of hydroxyl group of valinol moiety by LiN[Si(Me)<sub>3</sub>]<sub>2</sub> (LiHMDS) followed by salt metathesis reaction with FeCl<sub>2</sub> in THF afforded iron-metalated L-vol-UiO-FeCl.

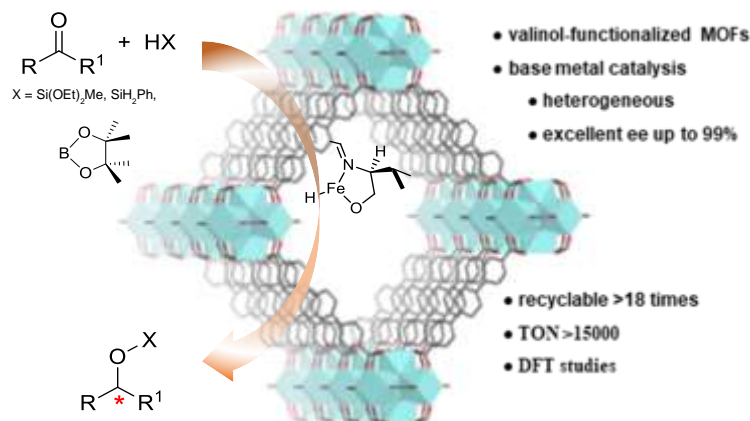


**Figure 1.** Design of amino alcohol-functionalized metal-organic frameworks to develop robust single-site earth-abundant metal catalysts for heterogeneous asymmetric catalysis.<sup>9</sup>

Synthesized MOF catalyst was characterized using PXRD, BET, and TEM. Transmission electron micrograph of vol-UiO-68-FeCl displayed octahedron particles having the average diameter of 1.0  $\mu\text{m}$ . Inductively coupled plasma optical emission spectroscopy (ICP-OES) showed Zr/Fe ratios of 1.66 and 1.44, corresponding to the Fe-loadings of 60% and 71% with respect to the valinol moiety of vol-UiO-68. Metal loading ICP-OES data of Fe-functionalized MOF were obtained with an Agilent 5110 ICP-OES and analyzed using Dichroic Spectral Combiner (DSC). The oxidation state and the coordination environment of the iron-center within L-vol-UiO-Fe were established by XPS, XANES and EXAFS studies. The XANES spectroscopy of vol-UiO-FeCl indicates the Fe<sup>II</sup> oxidation state as its pre-edge position aligned well with that of FeCl<sub>2</sub>. The assignment of +2-oxidation state of iron was further supported by XPS spectroscopy based on Fe<sup>II</sup> 2p<sub>3/2</sub> binding energy of 709.4 eV and 2p<sub>1/2</sub> binding energy of 722.9 eV. XPS was recorded on an X-ray photoelectron spectrometer, PHI 5000 Versa Probe III using Al-K $\alpha$  (h $\nu$ =1486.6eV) X-ray source.

At a 0.5 mol% Fe-loading, L-vol-UiO-Fe was an active heterogeneous catalyst in the hydrosilylation and hydroboration of a range of ketones at room temperature to afford the corresponding chiral alcohols with high yields and excellent enantiomeric excesses up to 99%. The conversions of the reactions and enantiomeric excess of products were determined by gas chromatography (GC) using Agilent 7890B gas chromatograph equipped with a flame ionization detector (FID) and a mass detector (Agilent 5977B GC/MSD) and, high-performance liquid chromatography (HPLC) using Agilent 1260 Infinity II liquid chromatograph equipped with Diode array detector (Agilent 1260 Infinity II). The MOF-catalysts could be recycled and reused multiple times, and the leaching of iron into the supernatant was very low. L-vol-UiO-Fe catalyst have high turnover number of upto 15000 and could be reused at least 10 times without any loss in activity and enantioselectivity. Further, the detailed mechanistic investigation of the catalytic hydrosilylation reactions by kinetic, spectroscopic, and computational studies were also carried out.

### Acknowledgements

This research is funded by the Science and Engineering Research Board (SERB), India (project ECR/2017/001931). Authors acknowledge the Central Research Facility, IIT Delhi, for instrument facilities.

### References:

1. S. Otto, J.B.F.N. Engberts, *J. Am. Chem. Soc.*, **121** (29), 6798-6806 (1999).
2. Q. Shao, K. Wu, Z. Zhuang, S. Qian, J.-Q. Yu, *Acc. Chem. Res.*, **53** (4), 833-851 (2020).
3. S.-G. Kim, H. Seong, J. Kim, K.H. Ahn, *Tetrahedron Lett.*, **45**, 6835-6838 (2004).
4. R. Hassani, Y. Kacem, H. Ben Mansour, H. Ben Ammar, B. Ben Hassine, *Chem. Biol. Interact.*, **217**, 41-48 (2014).
5. Y. Bai, Y. Dou, L.-H. Xie, W. Rutledge, J.-R. Li, H.-C. Zhou, *Chem. Soc. Rev.*, **45** (8), 2327-2367 (2016).
6. S. Yuan, J.-S. Qin, C.T. Lollar, H.-C. Zhou, *ACS Cent. Sci.*, **4** (4), 440-450 (2108).
7. K. Manna, T. Zhang, M. Carboni, C.W. Abney, W. Lin, *J. Am. Chem. Soc.*, **136** (38), 13182-13185 (2014).
8. R. Newar, W. Begum, N. Antil, S. Shukla, A. Kumar, N. Akhtar, Balendra, K. Manna, *Inorg. Chem.*, **59** (15), 10473-10481 (2020).
9. N. Antil, N. Akhtar, R. Newar, W. Begum, A. Kumar, M. Chauhan, K. Manna, *ACS Catal.*, **11** (16), 10450-10459 (2021).

## Copper oxide supported on red-mud as catalyst for organic conversion reactions: model reactions employing H<sub>2</sub>O<sub>2</sub> as an oxidizing agent in liquid phase oxidation: Selectivity and structure-activity relationship

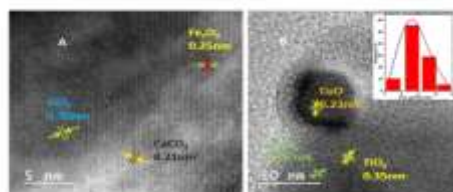
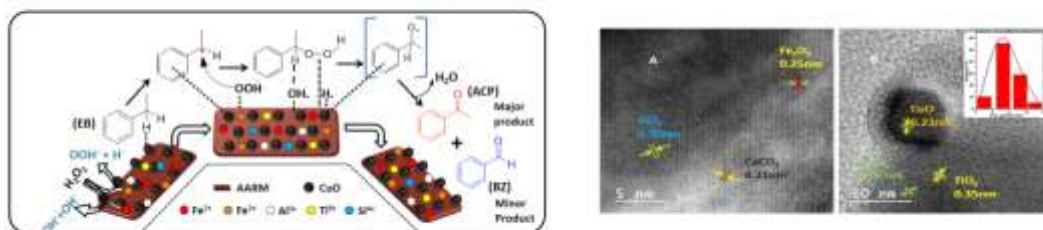
Subhashree Mishra<sup>1</sup>, Rajaram Bal<sup>2</sup>, **Ratan Kumar Dey**<sup>1\*</sup>

<sup>1</sup>.Department of Chemistry, Central University of Jharkhand, Ranchi – 835 205, INDIA

<sup>2</sup>CSIR-Indian Institute of Petroleum, Dehradun – 248 005, INDIA

\*E-mail:ratan.dey@cuja.ac.in, rkdey@rediffmail.com, Contact: +91-8917570944

Acetophenone is important for production of various commodity chemicals/material synthesis like resins, esters, alcohols, aldehydes and a range of fine chemicals.[1] Acetophenone is produced industrially by oxidation of ethyl benzene in presence of molecular oxygen as oxidant and cobalt cycloalkanecarboxylate/cobalt acetate [Co(OAc)<sub>2</sub>·4H<sub>2</sub>O] as catalyst in acetic acid solvent.[2] The process resulted in formation of μ-oxodimers that could deactivate catalyst. Transition metal-based heterogeneous catalysts are recognized as environmentally benign, capable of generating powerful hydroxyl radicals [E°(\*OH/H<sub>2</sub>O) = +2.8 V<sub>NHE</sub>]. The present research work reports facile synthesis of a new heterogeneous catalyst (CuO supported on activated red-mud, CuO\_AARM) for oxidative conversion of ethylbenzene to acetophenone using H<sub>2</sub>O<sub>2</sub> as oxidant. The catalyst promotes benzylic C – H bond oxidation in ethyl benzene to form acetophenone in optimized reaction conditions (Temp.: 75°C; solvent: mixture of H<sub>2</sub>O and acetonitrile (1:1)). Mechanistically, as shown in Scheme-1, the electron deficient metal species could abstract hydrogen from hydroperoxide to produce alkyl peroxide which rapidly decompose to yield acetophenone. DFT study shows that the optimized geometrical structure favor the reaction *via* hydroperoxyl radical formation in an endergonic process. The catalyst shows good kinetic control over the decomposition of H<sub>2</sub>O<sub>2</sub>. The synergy between the atomically dispersed CuO nano-particles and components in red-mud support promotes a facile and robust approach towards development of a recyclable and reusable heterogeneous catalyst with 86.0% conversion efficiency and 74.0% selectivity, thus indicating potential commercial use in a sustainable industrial process.



**Scheme-1:** Mechanism of surface catalyzed oxidation of ethyl benzene to acetophenone using CuO-AARM.

### References:

1. S B. Gutmann, P. Elsner, D. Roberge, C. Oliver Kappe, *ACS Catalysis*, **3** 2669 (2013)
2. C. Parmeggiani, F. Cardona, *Green Chem.*, **14** 547 (2012).



# Green Chemistry and Sustainable industrial processes, Metrics, LCA

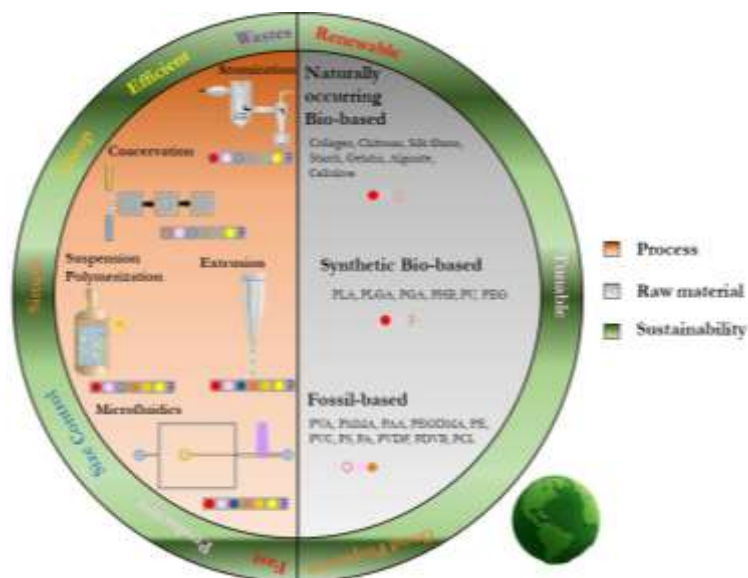
## Green assessment of polymer microparticles production processes. Use of bio-based resists derived from renewable monomers for sustainable 3D fabrication of automotive components through two photon polymerization

Hassan El Itawi,\*<sup>1</sup> Sami Fadlallah,\*<sup>2</sup> Florent Allais<sup>2</sup>, Patrick Perré<sup>1</sup>

<sup>1</sup> Université Paris-Saclay, CentraleSupélec, Laboratoire de Génie des Procédés et Matériaux, SFR Condorcet FR CNRS 3417, Centre Européen de Biotechnologie et de Bioéconomie (CEBB), 3 rue des Rouges Terres, Pomacle 51110, France.

<sup>2</sup> URD Agro-Biotechnologies Industrielles (ABI), CEBB, AgroParisTech, 51100, Pomacle, France  
\*hassan.el-itawi@centralesupelec.fr, sami.fadlallah@agroparistech.fr

Polymer microparticles are polymeric matrices containing an immobilized active compound to control its release for wide range of applications like food industry, cosmetics, and pharmaceuticals. Their production is either by a chemical process like suspension polymerization and coacervation or by a physical process like atomization, extrusion, and microfluidics. The choice of the production process depends on the targeted application, production rate, and microparticles size dispersion. Applications that do not require a narrow size distribution of the microparticles but do require a high production rate, like milk powder, powder juice, or coffee, are often produced by spray-drying atomization due to its 100% yield at an industrial scale. In contrast, the control of size distribution is vital in applications requiring a controlled release like drug delivery flavors and aromas release. Apart from the process, the sustainable production requires the employment of renewable raw materials. In a recent submitted review, we discussed pros, cons, and sustainability challenges of production processes and raw materials. We also introduced the environmental factor (*E factor*) as another crucial parameter for the process choice criteria [1].



We showed that suspension polymerization, an easy to operate process to produce microparticles with wide size distribution at a low cost, requires an excessive use of organic and aqueous solvents. The usage of less solvents showed microparticles with weaker characteristics. The coacervation process produces stable capsules with high encapsulation efficiency but always with a wide size distribution. This process is relatively slow, necessitates a slow and energy-consuming post-processing step like freeze-drying, very sensitive to physical parameters, and employs toxic crosslinkers like glutaraldehyde. The atomization process allows 100% yield large-scale production at an industrial scale. However, the size distribution is wide, the energy consumed is high, and toxic solvents are used. The addition of spinning disk allows the size control but requires a larger reactor surface and will result in satellite droplets that meaning a loss of matter. Microfluidic processes propose a fast, efficient, and less expensive wide range of possibilities to produce microparticles with controlled size and conditions. However, the microparticle size is dependent on the flow rates, which in turn fixes the quantity of solvent wastes generated by the process. This conditions the greenness of the process and makes it sustainable if and only if the continuous phase and solvents are recycled. Concerning the employed raw materials, we showed that fossil-based materials cannot be candidates for sustainable production due to the depletion of their source and their environmental consequences. Naturally occurring and synthetic bio-based materials were shown to be either mechanically or thermally weak or inappropriate for many applications. As a conclusion, we described the importance of discovering bio-based platform molecules that can produce tunable raw material with competitive characteristics while keeping the renewability advantage. The combination of the optimized microfluidic process and bio-based tunable material is a sustainable area of improvement for polymer microparticles production.

## References

[1] Hassan El Itawi and others, 'Green Assessment of Polymer Microparticles Production Processes: A Critical Review', *Green Chem.*, 2022 <<https://doi.org/10.1039/D2GC00578F>>.

## Use of bio-based resists derived from renewable monomers for sustainable 3D fabrication of automotive components through two photon polymerization

F. Gontad<sup>1\*</sup>, M. Rostagno<sup>2</sup> and T. Robert<sup>3</sup>

<sup>1</sup>AIMEN Laser Technology Centre, Polígono Industrial de Cataboi SUR-PPI-2 (Sector) 2, Parcela 3 - O Porriño, Spain

<sup>2</sup>DIAD, Via Nicola Fabrizi 136, Torino 10145, Italy

<sup>3</sup>Fraunhofer WKL, Bienroder Weg 54E, 38108 Braunschweig, Germany

\*Francisco.gontad@aimen.es

### Abstract text:

Polymers have become one of the most researched materials for the structure, performance, and safety of automobiles in recent years, particularly with the development of electric cars with the aim of reducing the total automobile weight and carbon footprint. Bio - plastics represents nowadays less than 1 percent of worldwide plastic production. However, significant growth is expected in future years, following the more and more stringent normative about emissions reduction. It is foreseen that the bioplastic market will grow from 6 billion dollars in 2018 to about 20 billion dollars in 2026 [1]. Besides weight reduction, their high absorption properties also allow the vehicle to meet stricter safety standards with a larger design freedom compared to metals. Anyway, the challenge in their development and production is not over yet, as the conversion to net shape production processes are strongly recommended for well-known environmental issues.

Additionally, the use of these materials can be also applied not only for structural pieces, but also for the fabrication of interior parts with enhanced functional properties such as hydrophobicity, hydrophilicity, optical functionalities for increased driver safety (such as antiglare/antireflective) or even aesthetic applications (like personalised diffractive effects, see Figure 20).



Figure 20 Diffractive logo of AIMEN fabricated on polymeric through Two Photon Polymerization.

Most of the polymers used on the automotive industry are fabricated with conventional replication techniques, which are especially suited for the fabrication of large batches. However, the fabrication of very complex 3D pieces can be very difficult with such techniques, requiring the use of many fabrication and alignment steps for the fabrication of this kind of parts, particularly for those with re-entering features. To this regard, the latest developments of resin-based 3D printers, with higher accuracy and fabrication speeds, represents a valid solution for the fabrication of these complex 3D parts.

There are several alternatives for resin-based 3D printing techniques, such as Stereolithography, Direct Light Printing or Two Photon Polymerization (TPP) with variable resolution and fabrication speeds. Amongst them, TPP is the 3D printing technique that provides a higher resolution, enabling the fabrication of functional micro/nanostructures for different applications [2,3] as has been already demonstrated for demanding applications such as the fabrication of 3D scaffolds for tissue engineering [4] or optical surfaces [5].

Currently, many commercial resists used for TPP have a synthetic origin. Therefore, despite the low waste generated with this technique, developing a biobased, eco-friendly, alternative resists is a strong requirement for the establishment of a sustainable and viable fabrication technique.

In this work, bio-based materials derived from renewable monomers have been synthesized and formulated. These materials were also examined on their ability to be fabricated with a dedicated 3D-TTP printer available at AIMEN (Figure 21), with the aim of producing parts with 3D microstructured surfaces with diffractive colourful effects. The possibility of introducing advanced laser parallelization techniques such as the use of Diffractive Optical Elements or Spatial Light Modulators for an increased technique productivity will be also presented and discussed.



Figure 21 Optical setup for TPP available at AIMEN facilities

## TOPIC: 17. Green Chemistry and entrepreneurship – Sustainable industrial processes

### Acknowledgements

This project has received funding from the European Union's Horizon 2020 Research and Innovation Programme under Grant Agreement No. 952941. BIOMAC is an Innovation Action (IA) started in January 2021 that will run until December 2024. The project EU's contribution is € 14 807 314,50 on a total budget of € 16 596 702,50.



### References

1. [https://www.marketsandmarkets.com/Market-Reports/biodegradable-plastics-93.html?gclid=EAIaIQobChMIr7zU1JbD9wIVNxxkGAB3a9QvUEAAYASAAEgIqMvD\\_BwE](https://www.marketsandmarkets.com/Market-Reports/biodegradable-plastics-93.html?gclid=EAIaIQobChMIr7zU1JbD9wIVNxxkGAB3a9QvUEAAYASAAEgIqMvD_BwE)
2. J. Serbin, A. Egbert, A. Ostendorf, B.N. Chichkov, R. Houbertz, G. Dommann, J. Schulz, C. Cronauer, L. Fröhlich, M. Popall, *Optics Letters*, **28** 301 (2003).
3. S. Waheed, J.M. Cabot, N.P. Macdonald, T. Lewis, R.M. Gijit, B. Paull, M.C. Breadmore, *Lab on a Chip*, **16** 1993 (2016)
4. A. Ovsianikov, A. Deiwick, A. Van Vlierberghe, P. Dubrue, L. Möller, G. Dräger, B. Chichkov, *Biomacromolecules*, **12**.851 (2011).
5. A. She, S. Zhang, S. Shian, D.R. Clarke, F. Capasso, *Optics Express*, **26** 1573 (2018)

## Are Lignin-Derived Monomers and Polymers truly sustainable? An In-Depth Green Metrics Calculations Approach

Sami Fadlallah,\*<sup>1</sup> Pallabi Sinha Roy,<sup>2,3</sup> Gil Garnier,<sup>1,2</sup> Kei Saito,\*<sup>2,3,4</sup> Florent Allais\*<sup>1,2</sup>

<sup>1</sup> URD Agro-Biotechnologies Industrielles (ABI), CEBB, AgroParisTech, 51100, Pomacle, France

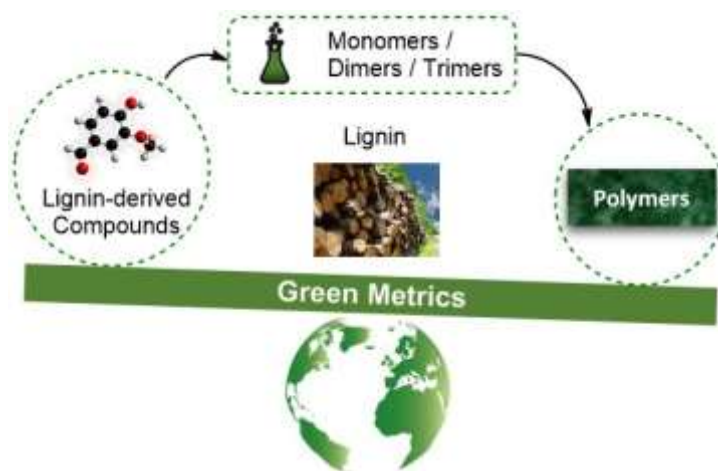
<sup>2</sup> BioPRIA, Department of Chemical Engineering, Monash University, Clayton 3800, VIC, Australia

<sup>3</sup> School of Chemistry, Monash University, Clayton 3800, VIC, Australia

<sup>4</sup> Graduate School of Advanced Integrated Studies in Human Survivability, Kyoto University, Higashi-Ichijo-Kan, Yoshida-nakaadachicho 1, Sakyo-ku, Kyoto, 606-8306, Japan

\*sami.fadlallah@agroparistech.fr, saito.kei.1y@kyoto-u.ac.jp, florent.allais@agroparistech.fr

Lignin is an aromatic biomacromolecule with enormous potential for the synthesis of bio-based materials. The production of monomers and polymers from lignin has been investigated for years and keeps on expanding, as proven by the flourishing literature.<sup>[1]</sup> However, the sustainability of the synthetic procedures has not been systematically analyzed. Green chemistry plays an essential role in this field and provides several tools to design environmentally friendly production methods. In a recent work,<sup>[2]</sup> we have thoroughly investigated the environmental aspects of 175 key monomer synthetic methods and 32 polymerization procedures based on selected criteria, including waste generation, atomic efficiency, energy efficiency, safer solvent use and biocatalytic methodology. Indeed, we strived to achieve three main objectives. First, to measure using green metrics, such as environmental factor (*E* factor) the greenness of plethora of authoritative published monomers and polymers. Second, to highlight from our findings how lignin can be more efficiently transformed through greener processes to provide genuine sustainable polymers. Finally, we wanted to: *i*) convince researchers to consider the green aspects of the synthetic methods, *ii*) redesign the current methods towards more efficient ones, and *iii*) include the sustainability factors along with the renewability in their future investigations.



Our analysis showed that the usage of carbon from renewable resources should not be the only criterion in assessing alternatives to fossil-derived materials. Usage of excess solvents or reagents, multi-step reactions, low atom utilization, high temperature and time-consuming synthetic process have undeniable effects on the sustainability. On the other hand, although many of the existing synthetic methods in the literature show relatively high *E* factor values, the decision for sustainable development cannot be taken merely looking at these numbers. A thoughtful analysis for each factor contributing to the generated waste needs to be considered. Indeed, we have noticed that the reagent quantity and the amount of solvent used were not always optimized at the lab scale and for most of the cases, these are the reasons for higher wastage values. Furthermore, if one process has low wastage, but has high energy consumption, this can also affect the socio-economic development process. Generally, the time and temperature for any process are optimized at the lab scale and high energy, time-consuming or/and costly processes have less opportunity for further improvement in pilot or industrial scale. Due to the increasing awareness of the green synthetic methods, this study could be a major research foundation in the field of biomass-derived monomers and polymers. The calculated green metrics and the sustainable overview provided in this work will conclusively help future researchers to develop and design more sustainable and green synthesis procedures.

### References

1. Brianna M. Upton, Andrea M. Kasko, *Chemical Reviews*, **116**, 2275 (2016).
2. Sami Fadlallah, Pallabi Sinha Roy, Gil Garnier, Kei Saito, Florent Allais, *Green Chemistry*, **23**, 1495 (2021).

## Life cycle costing for the production of lignin-based adhesives from softwood kraft lignin via base-catalysed depolymerization

Dimitrios Ladakis<sup>1\*</sup>, Sofia Maria Ioannidou<sup>1</sup>, Ioannis K. Kookos<sup>2</sup>, Christina P. Pappa<sup>3</sup>, Konstantinos S. Triantafyllidis<sup>3</sup>, Apostolis Koutinas<sup>1</sup>

<sup>1</sup>Department of Food Science and Human Nutrition, Agricultural University of Athens, Iera Odos 75, 11855, Athens, Greece

<sup>2</sup>Department of Chemical Engineering, University of Patras, Rio, Patras, 26504, Greece

<sup>3</sup>Department of Chemistry, Aristotle University of Thessaloniki, 54124 Thessaloniki, Greece

\*e-mail address of the corresponding author: [ladakisdimitris@gmail.com](mailto:ladakisdimitris@gmail.com)

### Abstract:

Lignin is one of the most abundant natural biopolymers on Earth and accounts for approximately 30% of the organic carbon in the biosphere [1]. The alkylphenolic structure of the lignin molecule can be catalytically transferred into low molecular weight compounds such as phenols, alkylphenols, and phenol resins to replace those obtained from fossil resources [2]. Thus, the valorization of lignin is one of the most important challenges for the development of cost-effective biorefinery processes based on lignocellulosic biomass. This study focuses on the evaluation of the techno-economic feasibility and the environmental performance of lignin-based adhesives production from softwood kraft lignin via base-catalyzed depolymerization (BCD).

The design of the lignin-based adhesives production process is a mandatory step for the calculation of the mass and energy balances that will be used in techno-economic assessment and the environmental performance evaluation. The processing steps in this study were designed and simulated employing the UniSim Design software. The high-pressure catalytic reaction efficiency and the yields of the downstream separation and purification process are selected by identifying relevant literature-cited publications [2].

The conducted techno-economic evaluation employed discounted cash flow analysis to compare the profitability and process viability of lignin-based adhesives as compared to appropriate reference products. The methodology for the estimation of fixed capital investment (FCI) and the cost of manufacture (COM) is implemented following well-known procedures and rules of thumb and these metrics are calculated for various plant capacities [3,4]. Based on FCI and COM, a discounted cash flow (DCF) analysis is carried out in order to estimate the minimum selling price (MSP) of the process, by determining the market price of the product where the NPV is zero at the end of the plant lifetime. Moreover, the discounted payback period (DPP) as well as the optimum plant capacity (OPC) for the investment plant are defined. The End-of-Life (EoL) options of PBS will also be evaluated to recycle the material back into secondary value chains. The conversion routes and the EoL option will be environmentally evaluated by the Life Cycle Assessment approach. Key impact categories such as global warming potential and cumulative energy demand will be considered. A holistic evaluation of the sustainability was subsequently carried out that integrates the environmental and techno-economic pillars into a unified life cycle cost by monetizing the environmental externalities [5].

The base-catalysed depolymerization (BCD) process results into two different products from lignin, the BCD-oil (liquid phenolic fraction) and the BCD-oligomers (solid phenolic fraction) which were used for adhesive production. The techno-economic metrics for these products indicate a MSP for the BCD-oligomers at 0.6 \$/kg and for the BCD\_oil of 0.8 \$/kg at the optimum annual plant capacities of 40 kt and 20 kt, respectively. The global warming potential (GWP) was estimated at 2.16 kg CO<sub>2</sub>-eq for the BCD-oligomers and for the BCD\_oil at 2.36 kg CO<sub>2</sub>-eq. The abiotic depletion fossil (AP) at 40.25 and 46.00 MJ for BCD-oligomers and BCD\_oil, respectively. The aforementioned technoeconomic and environmental metrics of the proposed process are lower than the petroleum counterparts (GWP 3.13 kg CO<sub>2</sub>-eq and AP 64 MJ).

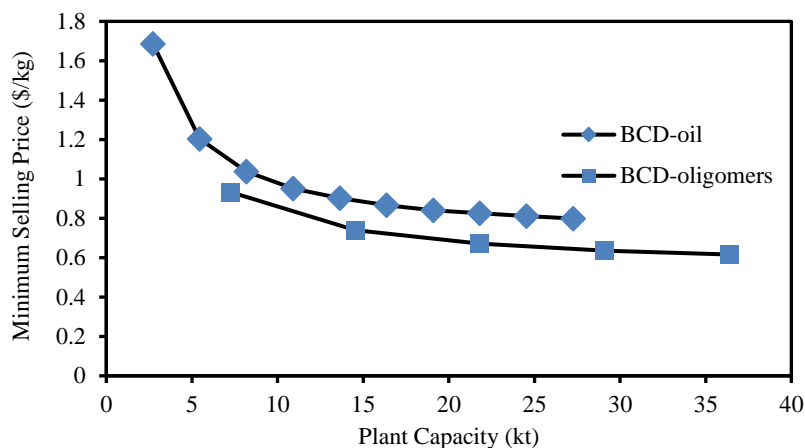


Figure 1. The minimum selling price of the base-catalyzed depolymerization products oil and oligomers.

Keywords: lignin, adhesives, base-catalysed depolymerization, techno-economic, life cycle assessment

### Acknowledgements

CA17128 LignoCOST is a networking Action, supported by COST, to stimulate and financially contribute to the organisation of short term scientific missions between partner institutions, networking events, workshops, and training schools. No support is available to perform research & development activities.

### References

1. Moretti, C., Corona, B., Hoefnagels, R., Vural-Gürsel, I., Gosselink, R., & Junginger, M. (2021). Review of life cycle assessments of lignin and derived products: Lessons learned. *Science of the Total Environment*, 770, 144656.
2. Röbiger, B., Röver, R., Unkelbach, G., & Pufky-Heinrich, D. (2017). Production of bio-phenols for industrial application: Scale-up of the base-catalyzed depolymerization of lignin. *Green and Sustainable Chemistry*, 7(03), 193.
3. M.S. Peters, K.D. Timmerhaus, R.E. West, *McGraw-Hill*, 5th ed. (2003).
4. R. Turton, R.C. Baile, W.B. Whiting, J.A. Shaeiwitz, D. Bhattacharyya, *Prentice Hall*, 5th ed., New Jersey (2018).
5. S. de Bruyn, M. Bijleveld, L. de Graaff, E. Schep, A. Schroten, , R. Vergeer, S. Ahdour, *CE Delft report* (2018).



## Fruit waste to wealth: Life cycle and Techno economic analysis to develop a sustainable pectin production process

Cresha Gracy Nadar<sup>1,2,3\*</sup>, Yogendra Shastri<sup>4</sup>, Amit Arora<sup>2</sup>, Antonio Patti<sup>3</sup>, and Victoria Haritos<sup>5</sup>

<sup>1</sup>IITB-Monash Research Academy, Mumbai, Maharashtra 400076, India

<sup>2</sup>Bioprocessing Laboratory, CTARA, Indian Institute of Technology Bombay, Mumbai, Maharashtra, India

<sup>3</sup>School of Chemistry, Monash University, Wellington Road, Clayton, Victoria, 3800, Australia

<sup>4</sup>Department of Chemical Engineering, Indian Institute of Technology Bombay, Mumbai, Maharashtra, India

<sup>5</sup>Department of Chemical Engineering, Monash University, Wellington Road, Clayton, Victoria, 3800, Australia

\*cresha.nadar@monash.edu

Over the years, the disposal of fruit processing waste (FPW) has posed significant environmental concerns. Owing to their high organic and moisture content, FPW generates substantial amounts of greenhouse gases (GHGs) when disposed of in landfills. This biomass is a rich source of bio-actives that can be extracted using sustainable approaches to develop a green biorefinery. Pectin is a valuable high-demand polysaccharide extracted from fruit peels and widely explored in various sectors due to its unique structural properties. Pectin is majorly used as a gelling, stabilizing, and emulsifying agent by food industries.

The conventional pectin production process is acid-assisted, energy-intensive, and generates acid waste effluents. This existing process was studied using life cycle assessment (LCA) and techno-economic analysis (TEA) methodology considering literature data to understand the challenges and opportunities to make the process sustainable.

Ethanol reduction and elimination of acids were identified to be the major factors to address the sustainability issues. Based on the findings, a sustainable approach was designed to extract pectin from orange peels using an acid-free hydrothermal process. It was observed from the optimization data that the hydrothermal process reduced the extraction time by 75% compared to the conventional process, along with the elimination of acids. Moreover, the use of membrane-assisted purification of pectin solution can reduce the ethanol requirements significantly. Presently, we are performing quality assessment and further characterization of the purified pectin.

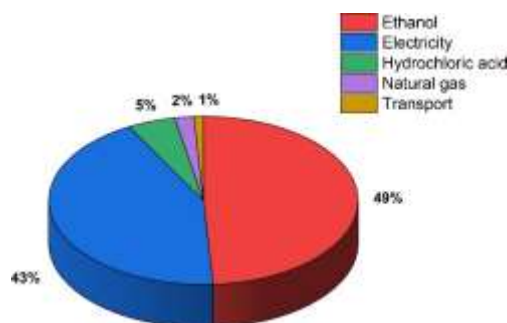


Figure 1. Major contributors to climate change impact categories in the base case.

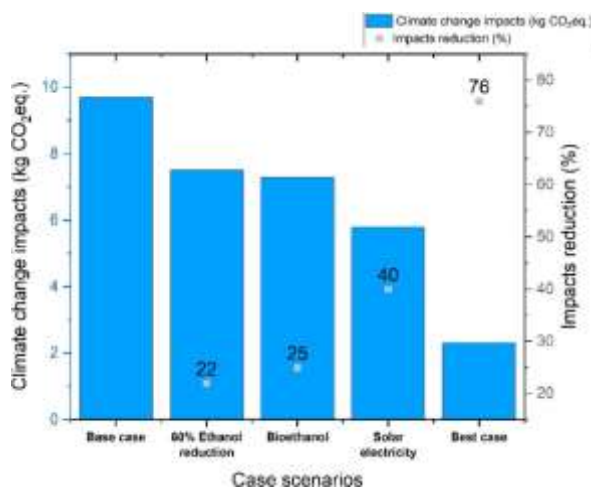


Figure 2. Comparison of climate change impact for different scenarios.

The proposed pectin production process is a green, sustainable, and economical process that successfully addresses the sustainability challenges associated with the conventional process.

## Acknowledgements

All the authors are grateful to IITB-Monash Research Academy and BASF, Navi Mumbai, Maharashtra, India, for providing a fellowship for C.G.N.'s doctoral study.

## References

1. Nadar, C. G., Arora, A., & Shastri, Y. (2022). Sustainability Challenges and Opportunities in Pectin Extraction from Fruit Waste. *ACS Engineering Au*, 2(2), 61-74.
2. Casas-Orozco, D., Villa, A. L., Bustamante, F., & González, L. M. (2015). Process development and simulation of pectin extraction from orange peels. *Food and Bioproducts Processing*, 96, 86-98.

# Green solvents & sustainable synthesis

## A new synthetic approach to dialkyl carbonates and their use as green solvents for the preparation of PVDF membranes

G. Trapasso<sup>1\*</sup>, C. Salaris<sup>2</sup>, M. Reich<sup>3</sup>, E. Logunova<sup>3</sup>, C. Salata<sup>2</sup>, K. Kümmerer<sup>3</sup>, F. Galiano<sup>4</sup>, F. Russo<sup>4</sup>, C. R. McElroy<sup>5</sup>, J. Sherwood<sup>5</sup>, A. Figoli<sup>4</sup>, F. Aricò<sup>1</sup>

<sup>1</sup> Department of Environmental Sciences, Informatics and Statistics, Ca' Foscari University, Scientific Campus Via Torino 155, 30170 Venezia Mestre, Italy.

<sup>2</sup> Department of Molecular Medicine, Padua University, via Gabelli 63, 35121 Padova (IT).

<sup>3</sup> Institute for Sustainable and Environmental Chemistry, Leuphana University Lüneburg, Universitätsallee 1/C13.311b, 21335 Lüneburg, Germany.

<sup>4</sup> Institute on Membrane Technology, ITM-CNR, Via P. Bucci 17c, Rende (CS), 87036, Italy.

<sup>5</sup> Green Chemistry Centre of Excellence, Department of Chemistry, University of York, Heslington, York YO10 5DD, UK.

\* e-mail address of corresponding author: giacomo.trapasso@unive.it

Dialkyl carbonates (DACs) are well-known green solvents and reagents that have been extensively investigated as safe alternatives to chlorine-based compounds. In fact, they can replace alkyl halides and dimethyl sulfate in alkylation and carbonylation reactions as well as phosgene and its derivatives in alkoxy-carbonylation ones [1]. Recently we have developed a high yielding scale-up synthesis of non-commercially available or expensive DACs via transcarybonylation reactions of an alcohol with dimethyl carbonate (DMC) promoted by the nitrogen-based organocatalyst 1,5,7-triazabicyclo[4.4.0]dec-5-ene TBD [2]. Compared to previously published works, [3] the proposed procedure has been customized for DACs large scale production (up to 100 mL of product obtained). Purification of these compounds has been achieved by fractional distillation and the exceeding reagents have been recovered and recycled. Selected DACs for this study include both symmetrical and unsymmetrical compounds, incorporating several alkyl, alkoxyalkyl, alkylamino and alkylthio functional groups. Chemical-physical properties of the new DACs have been also evaluated, as well as their water solubility. Furthermore, biodegradability and cytotoxicity tests have been carried out to investigate the effects of the different substituents on the greenness of these potential solvents and reagents. DACs application as green solvents for membrane preparation was next investigated, using non-solvent induced phase separation (NIPS) and vapor induced phase separation (VIPS) techniques, achieving both porous and plain membranes [4]. Morphology, additives effect, physical-chemical and mechanical proprieties as well as their performances in terms of water permeability and rejection were evaluated and compared to membranes obtained using commercially available cyclic carbonates (namely ethylene carbonate – EC and propylene carbonate – PC).

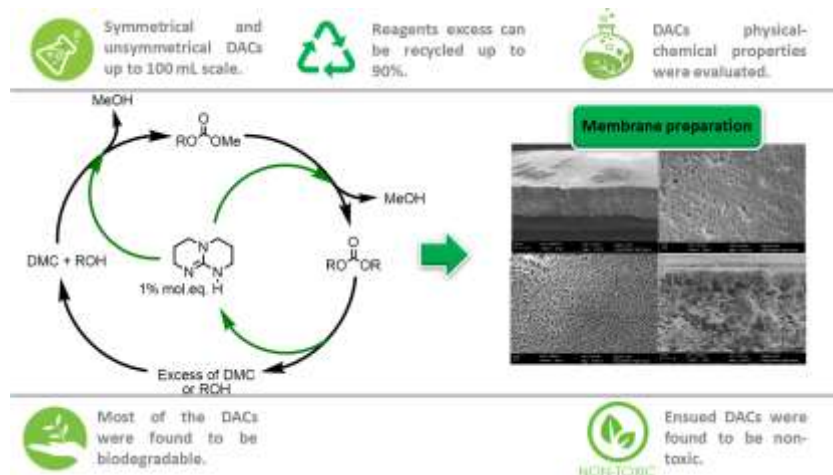


Figure 22 – DACs synthesis and application as green solvents for membrane preparation.

### Acknowledgements

We want to acknowledge Istituto nazionale della previdenza sociale (INPS) for funding the PhD fellowship of Giacomo Trapasso.

### References

- [1] P. Tundo, M. Musolino, F. Aricò, *Green Chem.*, **20** 28-85 (2018).
- [2] G. Trapasso, C. Salaris, M. Reich, E. Logunova, C. Salata, K. Kümmerer, A. Figoli, F. Aricò, *Sustain. Chem. Pharm.*, **26** 100639 (2022).
- [3] a) D. Chevella, A. K. Macharla, R. Banothu, K. S. Gajula, V. Amrutham, M. Boosa, N. Nama, *Green Chem.*, **21** 2938–2945 (2019); b) H. Mutlu, J. Ruiz, S. C. Solleder and M. A. R. Meier, *Green Chem.*, **14** 1728-1735 (2012).
- [4] G. Trapasso, F. Russo, F. Galiano, C. R. McElroy, J. Sherwood, A. Figoli, F. Aricò, *J. Membr. Sci* [Submitted].

# Waste minimized Copper Catalyzed Alkyne-Azide Cycleaddition with heterogeneous metallic Copper(0) and azeotrope CH<sub>3</sub>CN:H<sub>2</sub>O under batch and continuous flow condition

Gabriele Rossini,<sup>1</sup> Giulia Brufani,<sup>1</sup> Federica Valentini,<sup>1</sup> Luigi Vaccaro\*<sup>1</sup>

Università degli Studi di Perugia, Dipartimento di Chimica, Biologia e Biotecnologie, Via Elce di Sotto 8, 06123 Perugia (PG), Italia

\*luigi.vaccaro@unipg.it

Here is reported a waste minimized protocol for Copper Catalyzed Alkyne-Azide Cycleaddition (CuAAC) for the obtainment of a novel class of 1,4-disubstituted  $\beta$ -keto-1,2,3-triazoles using the azeotrope CH<sub>3</sub>CN:H<sub>2</sub>O and heterogeneous metallic copper (0) catalyst, under batch and its application in flow with a Copper Tube Flow Reactor. In the field of heterocycle chemistry, triazoles have emerged as one of the most studied structures, thanks also to the bioavailability and to the biological activity (anti-HIV, antibiotics, antiviral and antibacterial activities). [1, 2] Organic azides represent a versatile synthons to obtain 1,2,3-triazoles via click reactions which is a common strategy in the synthesis of triazoles. [1,2] Many efforts have been done to find new economically and environmentally sustainable processes for the obtainment of this class of compounds. [3] The goal of this project is to optimize the environmental footprint of the Copper Catalyzed Azide-Alkyne Cycleaddition (CuAAC) process. Recently, our research group developed a novel protocol to obtain  $\beta$ -azidocarbonyls from  $\alpha,\beta$ -unsaturated carbonyl compounds via  $\beta$ -azidation reaction, catalyzed by a novel heterogeneous organocatalyst, named POLITAG-F [4] (Polymeric Ionic-Tag with fluoride as counterion), in CH<sub>3</sub>CN:H<sub>2</sub>O azeotrope as recoverable reaction medium. Here is reported an efficient protocol for the synthesis of a novel class of 1,2,3-triazoles-1,4-disubstituted, starting from  $\beta$ -azidocarbonyl compounds previously synthesized with POLITAG-F and various functionalized terminal alkynes using heterogeneous metallic Cu(0) as catalyst in CH<sub>3</sub>CN:H<sub>2</sub>O azeotrope as recoverable reaction medium. The use of azeotropic mixture allows to reduce drastically the E-Factor values for the synthesis of the interested triazoles. The application in flow using a reactor completely made of copper allows to increase the efficiency of the protocols obtaining the interested triazoles with good yields and a reduced environmental footprint. Furthermore, the application in flow allows to reduce drastically the copper content on the final product. Finally, the study has been completed with a comprehensive evaluation of the environmental performance of the developed protocols by considering the principal mass green metrics: E-factor, process mass intensity (PMI), atom economy (AE), reaction mass efficiency (RME).

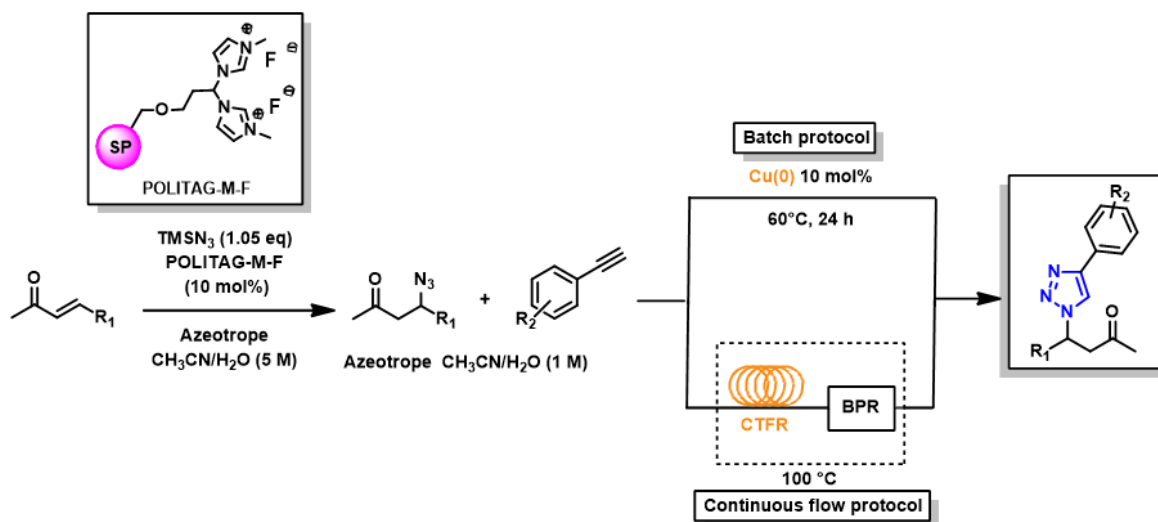


Figure 1. Copper Catalyzed Alkyne-Azide Cycleaddition with heterogeneous metallic Copper(0) and azeotrope CH<sub>3</sub>CN:H<sub>2</sub>O of previously synthesized  $\beta$ -azido carbonyls using POLITAG-M-F under batch and continuous flow condition

## Acknowledgements

The Università degli Studi di Perugia and MIUR are acknowledged for financial support for the project AMIS through the program “Dipartimenti di Eccellenza 2018-2022.”

## References

1. (a) Rani, A., Singh, G., Singh, A., Maqbool, U., Kaur, G., & Singh, J. (2020). CuAAC-enssembled 1,2,3-triazole-linked isosteres as pharmacophores in drug discovery: Review. In *RSC Advances* (Vol. 10, Issue 10, pp. 5610–5635). Royal Society of Chemistry. <https://doi.org/10.1039/c9ra09510a>
2. (a) Malah, T. el, Nour, H. F., Satti, A. A. E., Hemdan, B. A., & El-Sayed, W. A. (2020). Design, synthesis, and antimicrobial activities of 1,2,3-triazole glycoside clickamers. *Molecules*, 25(4). <https://doi.org/10.3390/molecules25040790> (b) Gao, F., Ye, L., Kong, F., Huang, G., & Xiao, J. (2019). Design, synthesis and antibacterial activity evaluation of moxifloxacin-amide-1,2,3-triazole-isatin hybrids. *Bioorganic Chemistry*, 91. <https://doi.org/10.1016/j.bioorg.2019.103162> (c) B. Li China, CN109503694 A 2019-03-22; (d) Tian, Y., Liu, Z., Liu, J., Huang, B., Kang, D., Zhang, H., de Clercq, E., Daelemans, D., Pannecouque, C., Lee, K. H., Chen, C. H., Zhan, P., & Liu, X. (2018). Targeting the entrance channel of NNIBP: Discovery of diarylnicotinamide 1,4-disubstituted 1,2,3-triazoles as novel HIV-1 NNRTIs with high potency against wild-type and E138K mutant virus. *European Journal of Medicinal Chemistry*, 151, 339–350. <https://doi.org/10.1016/j.ejmech.2018.03.059> (e) Fu, N., Wang, S., Zhang, Y., Zhang, C., Yang, D., Weng, L., Zhao, B., & Wang, L. (2017). Efficient click chemistry towards fatty acids containing 1,2,3-triazole: Design and synthesis as potential antifungal drugs for *Candida albicans*. *European Journal of Medicinal Chemistry*, 136, 596–602. <https://doi.org/10.1016/j.ejmech.2017.05.001>
3. (a) Rasina, D., Lombi, A., Santoro, S., Ferlin, F., & Vaccaro, L. (2016). Searching for novel reusable biomass-derived solvents: Furfuryl alcohol/water azeotrope as a medium for waste-minimised copper-catalysed azide-alkyne cycloaddition. *Green Chemistry*, 18(23), 6380–6386. <https://doi.org/10.1039/c6gc01941b> (b) Luciani, L., Goff, E., Lanari, D., Santoro, S., & Vaccaro, L. (2018). Waste-minimised copper-catalysed azide-alkyne cycloaddition in Polarclean as a reusable and safe reaction medium. *Green Chemistry*, 20(1), 183–187. <https://doi.org/10.1039/c7gc03022c>
4. Ferlin, F., Valentini, F., Brufani, G., Lanari, D., Vaccaro, L. (2021) *ACS Sustainable Chem. Eng.*, 9, 16, 5740–5749

## Enabling nucleophilic fluorination in water

K. Sharma<sup>1\*</sup>, B. N. Nguyen<sup>2</sup>, J. Blacker<sup>3</sup> and N. Kapur<sup>4</sup>

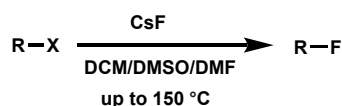
*School of Chemistry, University of Leeds, Leeds LS2 9JT, U.K.*

\*K.Sharma1@leeds.ac.uk

Currently, 25% of the marketed drugs and 30% of agrochemicals contain at least one fluorine atom, highlighting the importance of organofluorine molecules.<sup>1</sup> However, the existing protocols for the preparation of these fluorine-containing molecules rely heavily on the use of toxic organic solvents and reagents (Figure 1a).<sup>2</sup> Hence, the development of effective sustainable protocols for incorporating fluorine atoms in organic molecules is of utmost importance to pharmaceutical industries.

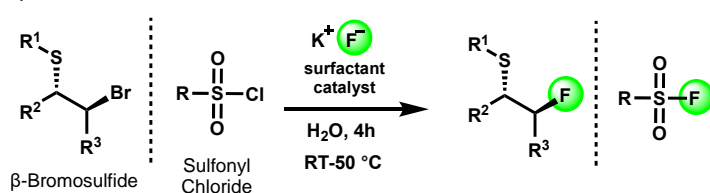
Water is widely considered to be an environmentally benign reaction media which can enable sustainable and economical routes to access pharmaceutically relevant drug molecules.<sup>3</sup> However, its application to nucleophilic fluorination reactions has been prevented mainly due to the inactivation of fluoride as a nucleophile in water. By employing a surfactant-based catalytic system we have enabled nucleophilic fluorination in water (Figure 1b). We have successfully demonstrated its application to fluorinate  $\beta$ -bromosulfide and sulfonyl chloride substrates giving good conversions to the desired fluorinated products (up to 90%). This was achieved through an extensive optimisation of reaction parameters such as surfactant, temperature, fluoride source, and substrate concentration (Figure 1c). Further work is currently underway to extend its application to other substrates of pharmaceutical importance.

### a) Traditional approaches to nucleophilic fluorination



- Hazardous reaction conditions
- High costs
- Requirement for drying of reagents/solvents

### b) This work



- 'Green Fluorination'
- Environmentally-benign reaction conditions
- Economical
- No requirement for drying of reagents/solvents

### c) Optimization of reaction parameters

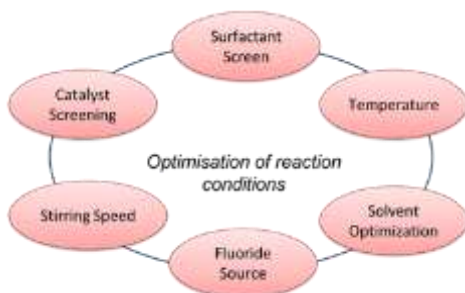


Figure 1. a) Traditional approaches to nucleophilic fluorination. b) This work: the development of an efficient sustainable nucleophilic fluorination reaction of  $\beta$ -bromosulfide and sulfonyl chlorides in water. c) Optimization of various reaction parameters to obtain an efficient sustainable nucleophilic fluorination protocol.

We have developed an effective sustainable protocol for nucleophilic fluorination of  $\beta$ -bromosulfide and sulfonyl chloride substrates using water as the reaction media. This protocol occurs under environmentally-benign reaction conditions, utilizes a sustainable fluoride source, is economical, and does not require any drying of the reagents or solvents.

## Acknowledgements

We gratefully acknowledge EPSRC Research Grant EP/S013768/1.

## References

1. *J. Fluorine Chem.*, **239** 109639 (2020).
2. *Green Chem.*, **19** 3951 (2017).
3. *Chemical Reviews*, **109** 725 (2009).



## Preparation of aminsals (and thioaminsals) in aqueous media and their remarkable applications

Juliana G. Pereira<sup>1)</sup>, Lúcia A. S. Cavaca<sup>1)</sup>, João P. M. António<sup>1)</sup>, Rafael F. A. Gomes<sup>1)\*</sup>, Carlos A. M. Afonso<sup>1)\*\*</sup>

1) Research Institute for Medicines (iMed.Ulisboa), Faculty of Pharmacy, Universidade de Lisboa, Av. Prof. Gama Pinto, 1649-003, Lisboa, Portugal

\*rafael.gomes@campus.ul.pt; \*\*carlosafonso@ff.ulisboa.pt

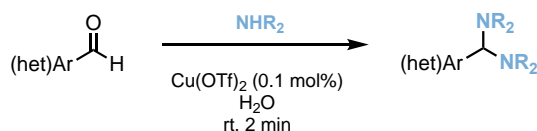
Aminsals are the condensation product of aldehydes and secondary amines. Structurally similar to acetals, these compounds have been used as intermediates, chiral auxiliaries and protection groups in reactions and in the biology field.<sup>1</sup>

The most common methodology for the formation of aminsals involves the condensation of aldehydes with amines in ethanol or toluene under high temperatures using dehydrating agents to remove the water in the reaction, shifting the equilibrium to the product.<sup>2</sup> However, performing the reaction in aqueous media instead of organic solvents is an environmentally competitive process for the preparation of aminsals.

This work reports on the formation of aminsals, from aromatic aldehydes and furfural derivatives with different secondary amines in water under mild conditions (**Figure 1a**) as well as the formation of several thioaminsals with yields up to 97% (**Figure 1b**).<sup>3</sup> This is followed by the stability studies of different aminsals and their use as protection group for aldehydes. Applying this approach together with the advantages of a continuous flow system allowed us to develop a new, simple and rapid methodology for selective removal of genotoxic aldehydes from APIs (Active Pharmaceutical Ingredient). Our method uses the diamine scavenging resin in a continuous flow system, generating the aminsal within the microreactor efficiently (**Figure 2**).<sup>4</sup>

The described aminsal compounds were prepared with a more sustainable methodology allowing the use of these interesting molecules as protection group and presenting a noteworthy role on the removal of genotoxic impurities of the APIs.

(a)



(b)

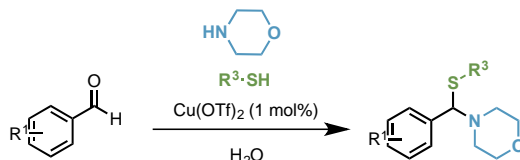


**Figure 1.** (a) Preparation of aminsals from aromatic aldehydes and furfural derivatives with different secondary amines and (b) preparation of thioaminsals from aromatic aldehydes with alkyl and aryl thiols, and morpholine in water under mild conditions.

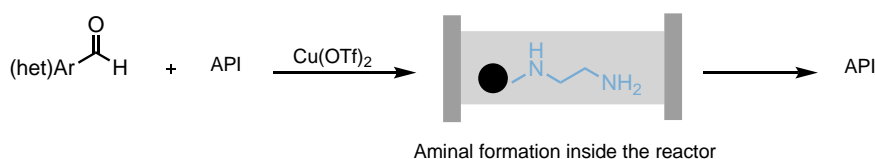


**Figure 2.** A new strategy for selective removal of genotoxic aldehydes from APIs.

### Acknowledgements

We thank the Fundação para a Ciência e Tecnologia (PD/BD/128316/2019, UIDB/04138/2020 and UIDP/04138/2020), COMPETE Programme (SAICTPAC/0019/2015) for financial support. The project leading to this application has received funding from the European Union's Horizon 2020 research and innovation programme under grant agreement No 951996.

### References

1. A. Alexakis, N. Lensen, P. Mangeney, *Tetrahedron Letters*, **32** 1171 (1991).
2. M. A. Ramirez, G. Ortiz, G. Levin, McCormack, W. M. M. Blanco, I. A. Perillo, A. Salerno, *Tetrahedron Letters*, **55** 4774 (2014).
3. L. A. Cavaca, R. F. A. Gomes, C. A. M. Afonso, *Molecules*, **27** 1673 (2022).
4. J. G. Pereira, J. P. M. António, R. Mendonça, R. F. A. Gomes, C. A. M. Afonso, *Green Chemistry*, **22**, 7484 (2020)

## Synthesis and characterization of new BPA-free polycarbonates based on dimethyl carbonate and diphenylmethane derivatives

Krystyna Wnuczek<sup>1\*</sup> and Beata Podkościelna<sup>1</sup>, Andrzej Puszka<sup>1</sup>

<sup>1</sup>Maria Curie-Skłodowska University, Institute of Chemical Sciences, Faculty of Chemistry, Department of Polymer Chemistry, Gliniana 33, 20-614, Lublin, Poland

\*krystyna.wnuczek@poczta.umcs.lublin.pl

Polycarbonates (PC) are widely used as engineering plastics due to their amalgamation of properties like clarity, toughness, low moisture absorption, good thermal stability and high mechanical durability. From a chemical point of view, PC are polyesters of carbonic acid [1–3]. Bisphenol A polycarbonates (BPA-PC) derived from petroleum is one of the most important and widely commercialized polycarbonates. However, bisphenol A is a toxic compound that can induce chronic toxicity and environmental problems [4]. The use of bisphenol A as a diol for the synthesis of polycarbonates is controversial. The detection of bisphenol A in the environment and food products has been the subject of much recent research. Some studies prove that thermal treatment of any product containing can bisphenol A makes it be released into food [5]. New methods of obtaining polycarbonates without the use of BPA are being sought. The best strategy for large-scale preparation of aliphatic polycarbonates is the two-step condensation polymerization of dimethyl carbonate (DMC) and aliphatic diols with more than three carbon atoms. Oligomers are obtained in the first, initial condensation step, due to the low equilibrium constant. In the second step, polymer chains propagated by transesterification, while high temperature and high vacuum are required to remove unreacted monomers and freshly generated byproducts [6-9]. The aim of the research was to synthesize new polymer compounds based on safe (BPA-free), non-toxic components. A method of synthesizing aliphatic-aromatic compounds derived on diphenyl methane has been developed. In this work, twelve new polycarbonates based on diols with DMC monomer were synthesized. Polycarbonates were obtained by polycondensation reaction and their chemical structures were confirmed by means ATR/FTIR. The thermal stability were examined by DSC and TG analyses. The presence of a carbonyl bond on the spectroscopic spectrum confirmed the polycarbonate production. Moreover, GPC analysis was performed to check the molar masses of the obtained polycarbonate. Summary, proposed method applied DMC reagent for introducing carbonate groups. The transesterification reaction DMC with diols in the melt phase was performed, resulting in the formation of PC precursors. In the next step PC compounds are amenable to polymerization reaction. The polycondensation step is carried out under a vacuum condition to remove methanol produced as a recyclable by product.

The synthesis of monomers - diols has been developed at the Department of Polymer Chemistry of the Maria Curie-Skłodowska University. A detailed description of the reagents and procedure has already been published [9]. Three diphenylmethane derivatives were obtained and were named diol M (methylenedi(4,1-phenylene)dimethanol), diol E (2,2'-[methanediylbis(benzene-4,1-diylmethanediylsulfaneyl)]diethanol) and diol H (6,6'-(methanediyl(benzene-4,1-diylmethanediylsulfaneyl))dihexan-1-ol). Polycondensation reactions were carried out with the commercial reagent DMC (dimethyl carbonate). Four organic catalysts were used: zinc acetate, 4-dimethylaminopyridine, benzyltriethylammonium chloride and bis(dibutylchloritin (IV)) oxide.

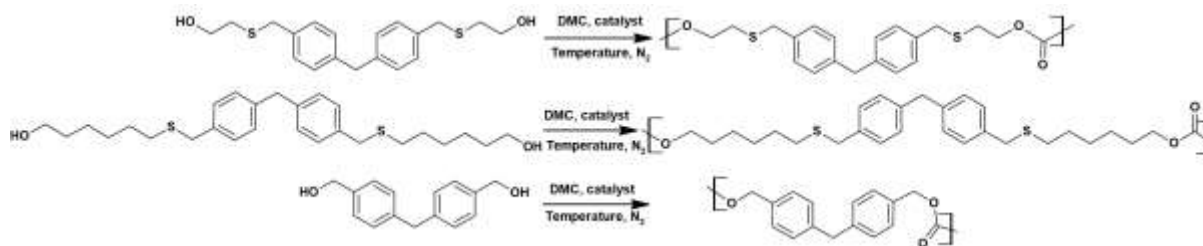


Figure 1. Scheme of diols and DMC reactions.

Short synthesis description: In the three-necked flask equipped with a distillation cooler, gas source and thermometer, Substrates were added in a stoichiometric amount of 0.5:2 (diol:DMC). The catalyst was added in an amount of 0.5 mol%. The reactions were carried out on a heating plate equipped with a magnetic stirrer, in an oil bath, under nitrogen atmosphere for 3 hours after the complete melting of the components. The temperature was kept at 150-170°C. As the reaction proceeded, methanol was released which was fed by a gas to the flask. After two hours, the gas was disconnected. The reactions were carried out for another 2 h under reduced pressure, keeping the temperature at 160°C. The resulting polycarbonates were placed in beakers and quenched with methane dichloride (50 ml) and precipitated with methanol. They were then allowed to evaporate the solvent. In order to completely dry the polycarbonates, they were placed in an oven for 12 hours (50°C).

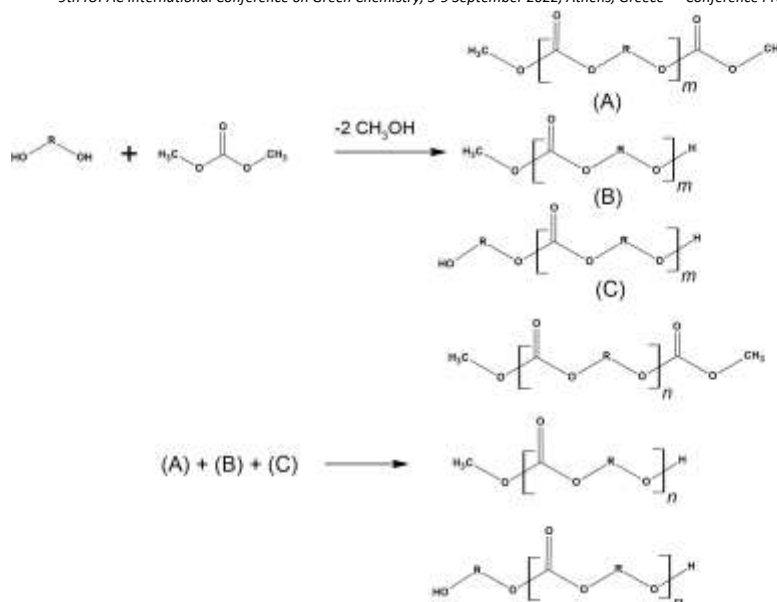


Figure 2. Scheme of transesterification and polycondensation reactions [8-9].

## References

1. A.P. Pêgo, D.W. Grijpma, J. Feijen, *Polymer*, **44** 6495–6505 (2003).
2. W. Kuran, M. Sobczak, T. Listos, C. Debek, Z. Florjanczyk, *Polymer*, **41** 8531–8541 (2000).
3. L. Bottenbruch, in *Engineering Thermoplastics: Polycarbonates, Polyacetals, Polyesters, Cellulose Esters*, ed. L. Bottenbruch, Hanser/Gardner, Cincinnati, Ohio, (1996).
4. X. Shen, S. Liu, Q. Wang, H. Zhang, *Catalyst. Chem. Res. Chinese Universities* **35(4)** 721-728 (2019).
5. T. Geens, L. Goeyens, A. Covaci, *Int J Hyg Environ Health* **214** 339–347 (2011).
6. P.U. Naik, K. Refes, F. Sadaka, C.H. Brachais, G. Boni, J.P. Couvercelle, M. Picquet, L. Plasseraud, *Polym. Chem.*, **3** 1475–1480 (2012).
7. A. Welle, M. Kröger, M. Döring, K. Niederer, E. Pindel, I.S. Chronakis, *Biomaterials*, **28** 2211–2219 (2007).
8. S. Kuckling, D. Kuckling, *Polym. Chem.*, **7** 1642-1649 2016.
9. K. Wnuczek, A. Puszka, B. Podkościelna, *Polymers*, **13(24)** 4437 (2021).

# Amino Acid-Functionalized Metal-Organic Frameworks for Sustainable Asymmetric Catalysis

Kuntal Manna<sup>1\*</sup>, Rajashree Newar<sup>1</sup> and Naved Akhtar<sup>1</sup>

<sup>1</sup>Department of Chemistry, Indian Institute of Technology Delhi, Hauz Khas, New Delhi, 110016, India

\*kmanna@chemistry.iitd.ac.in

## Abstract text:

Active Pharmaceutical Ingredient (API) is the pharmacologically active component of a drug and is responsible for its efficacy. API constitutes about 25% of a drug's retail selling price, and its cost is increasing significantly in recent years. Chiral APIs are essential building blocks to produce pharmaceuticals, agrochemicals and biologically active molecules. The industrial synthesis of chiral compounds typically depends on the solvent-intensive optical resolution or precious late transition metal-based homogeneous catalysts,<sup>[1][2]</sup> primarily because of the lack of efficient heterogeneous earth-abundant metal catalysts.<sup>[3]</sup> Due to the rising demand for chiral compounds and the increasingly strict safety, quality and environmental requirements of bulk scale synthesis, the development of highly active and enantioselective heterogeneous catalysts based on earth-abundant metals and inexpensive chiral feedstock is an open challenge in the pharmaceutical and chemical industries for environment-friendly and economical production of optically active compounds.

We have recently developed a strategy to synthesize novel heterogeneous enantioselective catalysts based on amino acid-functionalized metal-organic frameworks (MOFs) and earth-abundant metals for sustainable asymmetric organic transformations.<sup>[4]</sup> Constructed from metal-cluster secondary building units and organic bridging linkers, MOFs provide a unique platform for the simple preparation of single-site chiral catalysts via site-isolation owing to their porous and crystalline nature as well as modular and tunable properties.<sup>[5][6]</sup> The chiral MOF-iron catalyst was synthesized following a multi-step post-synthetic modifications of easily affordable amine-tagged zirconium UiO-68 MOF having a formula of  $Zr_6O_4(OH)_4(L-NH_2)_6$  ( $L-NH_2 = 2'$ -amino-[1,1':4,1''-terphenyl]-4,4''-dicarboxylate).<sup>[4]</sup> The tandem amide coupling between the amino-group of UiO-68 MOF and the carboxylic acid group of N-Fmoc-protected L-valine in the presence of HBTU and diisopropylethylamine in DMF, and subsequent deprotection of amino-group afforded amino acid-grafted UiO-68-MOF (L-val-UiO). L-val-UiO was further modified by treating with picolinaldehyde at room temperature to give the corresponding pyridylimine-bearing tridentate nitrogen-donor ligand-functionalized MOF (L-valim-UiO). <sup>1</sup>H NMR spectrum of the digested L-valim-UiO displayed the characteristic peaks of the pyridylimine moiety with the evidence of complete functionalization of the amino-groups of L-val-UiO.

The deprotonation of amide NH of L-valim-UiO by *sec*-BuLi followed by the reaction with FeCl<sub>2</sub> in THF afforded the corresponding iron-metalated MOF (L-valim-UiO-FeCl). The crystallinity of MOFs was maintained upon lithiation and metalation as evidenced by the similarity of its PXRD pattern with that of pristine UiO-68-NH<sub>2</sub>. ICP-OES analysis of the digested metallated L-valim-UiO-FeCl revealed the Fe-loading of 27 with respect to the N-donor ligand. L-valim-UiO and L-valim-UiO-FeCl have a BET surface area of 1765 m<sup>2</sup>/g and 987 m<sup>2</sup>/g, respectively. L-valim-UiO-FeCl particles have octahedral morphology, and the average diameter of the particles is 1.0 μm as shown by transmission electron microscopy. The DFT-optimized structure revealed a five-coordinate iron-species of L-valim-FeCl(THF) within the MOF in THF as the ground state. X-ray absorption near edge structure (XANES) analysis indicated that the oxidation state of the iron-center in L-valim-FeCl(THF) is +2. Fitting of the extended X-ray absorption fine structure (EXAFS) regions of L-valim-FeCl at the Fe K-edge revealed the coordination of each Fe<sup>II</sup> center to three nitrogen atoms of a chelating valim-ligand, one chloride and one oxygen atom of a THF in a distorted square pyramidal geometry.

Upon treatment of LiCH<sub>2</sub>SiMe<sub>3</sub> (1.2 equiv with respect to Fe) in THF, chiral L-valim-UiO-Fe became a highly active and enantioselective catalyst for hydrosilylation and hydroboration of a range of aliphatic and aromatic carbonyls to afford the corresponding chiral alcohols with enantiomeric excesses up to 99%. The chemoselectivity and enantioselectivity of chiral MOF-catalysts could be easily optimized by adjusting their pore sizes and post-synthetic modification techniques. At a 0.5 mol % Fe-loading, hydrosilylation of ketones using (OEt)<sub>2</sub>MeSiH was completed within 2 h in THF at 25 °C to afford silyl ethers in excellent yields, and the corresponding secondary alcohols were obtained after hydrolysis with high enantiopurity. Under the standard reaction conditions with 0.5 mol % L-valim-UiO-Fe, acetophenone and several substituted acetophenone bearing methoxy, hydroxy and nitro-functional groups were efficiently reduced to the corresponding alcohols with enantiomeric excesses ranging from 90-99%. Impressively, the MOF-Fe catalyst displayed high turnover numbers of up to 10000 and was recycled and reused more than 15 times without diminishing the enantioselectivity. The enantioselectivities of hydrosilylation reactions were also very high for a range of alkyl aryl ketones, unsymmetric benzophenones and heteroaryl ketones, and aliphatic ketones such as 6-methylhept-5-en-2-one, 2-octanone and cyclopentyl methyl ketone. Alcohols with 99% ee were afforded in quantitative yields from alkyl aryl ketones and unsymmetric benzophenones. The reduction of heteroaryl ketones such as acetyl pyridines and 2-acetyl thiophene generates the corresponding optically active alcohols with 99% and 84% ee, respectively. L-valim-UiO-Fe displayed much

higher activity and enantioselectivity than its homogeneous control catalyst, likely due to the formation of robust single-site catalyst in the MOF through site-isolation.<sup>[4]</sup> The yields of the reactions and % ee were determined by Agilent 7890B gas chromatograph equipped with a mass detector (Agilent 5977B GC/MSD) and HP-5MS Ultra Inert 30 m-250  $\mu\text{m}$ -0.25  $\mu\text{m}$  column for GC-MS and chiral CycloSil-B column 30 m-250  $\mu\text{m}$ -0.25  $\mu\text{m}$  for GC-FID analysis.

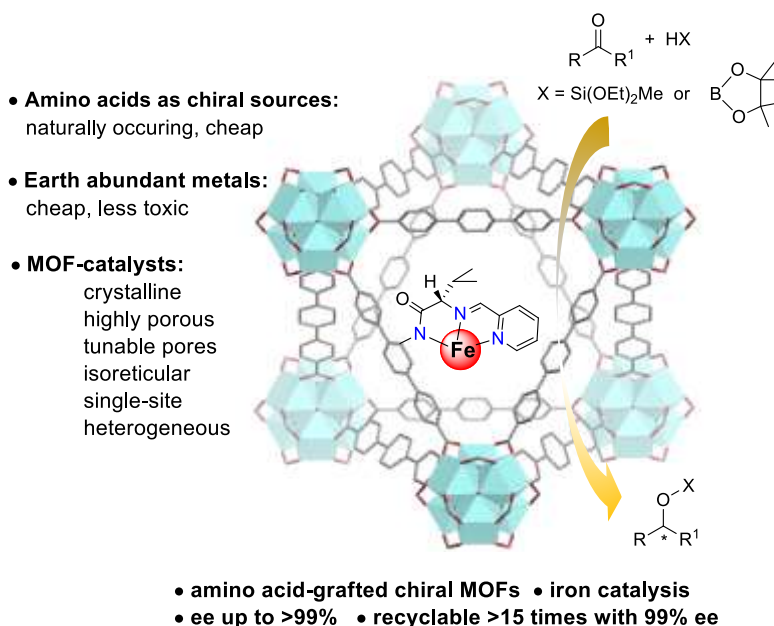


Figure 1. The development of heterogeneous single-site earth-abundant metal catalysts based on amino-acid functionalized MOF for sustainable asymmetric catalysis.

In the case of hydrosilylation reactions, the spectroscopic, kinetic and computational studies suggest iron-silyl as the catalytic species, which undergoes enantioselective 1,2-insertion of carbonyl into Fe–Si bond as the turnover limiting step to give Fe-alkyl intermediate. The subsequent  $\sigma$ -bond metathesis of Fe-alkyl and silane generate the chiral silyl ether products. This work highlights the importance of MOFs as the tunable molecular material for designing chiral solid catalysts based on inexpensive natural feedstocks such as chiral amino acids and abundant metals for the sustainable production of optically active compounds.

## Acknowledgements

This research is supported by the Science and Engineering Research Board (SERB), India (project ECR/2017/001931). The authors acknowledge the Central Research Facility, IIT Delhi, for instrument facilities.

## References

- W. S. Knowles, *Acc. Chem. Res.*, **16** 106 (1983).
- P. Etayo, A. Vidal-Ferran, *Chem. Soc. Rev.*, **42** 728 (2013).
- A. F. Trindade, P. M. P. Gois, C. A. M. Afonso, *Chem. Rev.*, **109** 418 (2009).
- R. Newar, N. Akhtar, N. Antil, A. Kumar, S. Shukla, W. Begum, K. Manna, *Angew. Chem. Int. Ed.*, **60** 10964 (2021).
- H. Furukawa, K. E. Cordova, M. O’Keeffe, O. M. Yaghi, *Science*, **341** No. 1230444 (2013).
- J. S. Seo, D. Whang, H. Lee, S. I. Jun, J. Oh, Y. J. Jeon, K. Kim, *Nature*, **404** 982 (2000).

## Green Synthesis Promoted by Ionic Liquids

Zhimin Liu \*

*Institute of Chemistry, Chinese Academy of Sciences (CAS), Beijing 100190, P. R. China*

*\*e-mail address: liuzm@iccas.ac.cn*

Green synthesis to access chemicals are of significance for the development of green and sustainable chemistry. Our group has been working in this fields with focus on green solvent-mediated approaches [1-8]. At this symposium, I will talk about our recent work on ionic liquids (ILs)-promoted green synthesis. ILs are a kind of molten salts composed of organic cations and inorganic/organic anions, remaining in a liquid state below 100 °C, and there exist multiple interactions among the IL systems, which provide the ILs with unique properties and advantages over traditional molecular solvents and thus wide applications. In chemical reactions, ILs have been employed as solvents, catalysts and additives.

Our group has designed task-specific ILs to realize chemical reactions in green way, and proposed several metal-free approaches to access chemicals over ILs under mild conditions [1-6]. For example, we synthesized CO<sub>2</sub>-reactive ILs that are able to chemically capture and activate CO<sub>2</sub> via forming anion-based carbonate/carbamate intermediates, thus further accomplishing its transformation to a series of heterocycles including quinazoline-2,4(1H,3H)-diones, cyclic carbonates, 2-oxazolidinones, oxazolones and benzimidazolones under metal-free conditions [1,2]. We developed IL-catalyzed approaches to reduce CO<sub>2</sub> with hydrosilanes and amines, in which ILs are capable of activating the Si-H bond in hydrosilanes and the N-H bond in amine substrates via H-bonding, thus achieving the reductive transformation of CO<sub>2</sub> to formamides, benzimidazoles and benzothiazoles via cooperative catalysis. We found that azolate anion-based ILs that can chemically capture CO<sub>2</sub> via formation of carbamate could serve as robust nucleophiles to attack C≡C bond in propargylic alcohols, and could efficiently catalyze the hydration of propargylic alcohols to produce α-hydroxy ketones with the assistance of atmospheric CO<sub>2</sub> gas under metal-free conditions [3].

We proposed cooperative catalysis strategy of hydrogen bond donor and acceptor of ILs for chemical reactions [4,5]. In this protocols, cations of the ILs act as the H-bond donor and anions as the acceptor, forming H-bonds with the reactant molecules, respectively, in opposite ways, which can cooperatively catalyze some reactions. For example, the acidic IL, 1-butylsulfonate-3-methylimidazolium trifluoromethanesulfonate ([SO<sub>3</sub>H-BMIm][OTf]) was found to be capable of efficiently catalyzing the ring-closing C-O/C-O bond metathesis reactions of aliphatic diethers to O-heterocycles [4]. The ILs with cation as H-bond donor and anion as H-bond acceptor, e.g., 1-ethyl hydroxyl-3-methylimidazolium trifluoromethanesulfonate ([HO-EtMIm][OTf]), can also catalyze dehydrative etherification of monohydric alcohols and dehydrative cyclization of diols to ethers under metal-, acid-, solvent-free and mild conditions [5]. [HO-EtMIm][OTf] shows performances even better than sulfuric acid in some cases, and a series of aliphatic ethers, aromatic ethers and cyclic ethers could be obtained in 100% selectivity and high yields. We believe that the above IL-catalyzed metal-free processes and strategies display promising practical applications.

In addition, we also developed some IL-metal catalytic systems, and realized the selective transformation of CO<sub>2</sub> to value-added chemicals. For example, we performed the reduction of CO<sub>2</sub> with amine and H<sub>2</sub> over Pd/C in 1-butyl-3-methylimidazolium tetrafluoroborate, which could realize the selective production of formamides (at 120 °C) or N-methylamines (at 160 °C) in high yields. Moreover, 1,2-bis(N-heterocyclic)ethanes were for the first time obtained from cyclic amines and CO<sub>2</sub>/H<sub>2</sub> via McMurry reaction of formamides coupled with subsequent hydrogenation [6].

Our findings are expected to bring new opportunities in the field of green chemical reactions, which will promote the development of new technology. The ILs-based green processes and strategies may be commercialized for production of value-added chemicals in the future.

### Acknowledgements

The financial from National Natural Science Foundation of China (No. 22121002, 21890761) is appreciated.

### References

1. Y. Zhao, B. Han, Z. Liu, *Acc. Chem. Res.* **54**, 3172 (2021).
2. Y. Zhao, B. Yu, Z. Yang, H. Zhang, L. Hao, Z. Liu, *Angew. Chem. Int. Ed.*, **53**, 5922 (2014).
3. Y. Zhao, Z. Yang, B. Yu, H. Zhang, H. Xu, L. Hao, B. Han, Z. Liu, *Chem. Sci.* **6**, 2297 (2015).
4. H. Wang, Y. Zhao, F. Zhang, Y. Wu, B. Han, Z. Liu, *Angew. Chem. Int. Ed.* **59**, 11850 (2020).
5. H. Wang, Y. Zhao, F. Zhang, Z. Ke, B. Han, Z. Liu, *Sci. Adv.* **7**, eabg0396 (2021).
6. R. Li, Y. Zhao, H. Wang, J. Xiang, Y. Wu, B. Yu, B. Han, Z. Liu, *Chem. Sci.* **10**, 9822 (2019).
7. X. Yu, Z. Yang, B. Qiu, S. Guo, P. Yang, B. Yu, H. Zhang, Y. Zhao, X. Yang, B. Han, Z. Liu, *Angew. Chem. Int. Ed.* **58**, 632 (2019).
8. G. Ji, Z. Yang, F. Zhang, Y. Zhao, B. Yu, Z. Ma, Z. Liu, *Angew. Chem. Int. Ed.* **55**, 9685 (2016).

# Natural Deep Eutectic Solvents as Versatile Tools for the Development of Green Processes

Andromachi Tzani and Anastasia Detsi\*

Laboratory of Organic Chemistry, School of Chemical Engineering, National Technical University of Athens,  
Zografou Campus, 15780 Athens, Greece

\*adetsi@chemeng.ntua.gr

Green chemistry possesses the spirit of sustainable development and is entering as a dynamic force to a constantly increasing number of chemical processes in the 21<sup>st</sup> century. In the chemical world, strategies for increasing sustainability often require the redesign of reactions and modifications of existing chemical processes aiming, among other things, at the prevention of waste, minimization of byproducts, reduction of chemicals used as solvents and auxiliaries in a wide range of laboratory and industrial applications.

Natural Deep Eutectic Solvents (NADES), eutectic mixtures comprised of natural products (primary and secondary metabolites) have been characterized as the green solvents of the 21<sup>st</sup> century. They possess favorable properties and advantages over common organic solvents such as low vapor pressure, high extractive capacity, low production costs, low toxicity, biodegradability as well as etc. The array of potential applications of NADES spans from organic synthesis, enzyme-catalyzed reactions, extraction processes, drug delivery, CO<sub>2</sub> capture and storage, biocompatible nanosystems and many more.

This presentation will emphasize the multifaceted character of NADES showing case studies on their applications as solvents for extraction of valuable phytochemicals from plants and biomass as well as their ability to act as solvents and catalysts for the development of greener synthetic methodologies for bioactive organic compounds. [1-5]

As far as the extraction processes are concerned, the development and optimization of the ultrasound-assisted extraction of phytochemicals from wild rosehip “pseudofruits” and olive leaves will be presented. The process development involves the synthesis, characterization and screening of a variety of NADES possessing different physicochemical properties, which affect the quality of the obtained extracts. The optimization of the process is performed using experimental design, and examines the effect of the most important process parameters such as extraction time, NADES/H<sub>2</sub>O ratio and solvent/dry biomass ratio on the antioxidant activity, the Total Phenolic Content (TPC) and Total Flavonoid Content (TFC) of the extracts.

The application of task-specifically designed NADES in carbon-carbon forming reactions, such as the Knoevenagel and aldol reactions, will be also presented, focusing on the role of the NADES components on the reaction yield and efficiency as well as on the recyclability and reusability of these solvents. The reaction proceed smoothly in the selected NADES and the developed methodologies are very promising especially for the synthesis of small “chemical libraries” of flavonoid analogues.

## Acknowledgements

Funding by the European Union and Greek national funds through the Operational Program Competitiveness, Entrepreneurship and Innovation, under the call RESEARCH-CREATE-INNOVATE, grant number T2EDK-0233, “Green\_Wild\_ROSE.gr” is gratefully acknowledged.

## References

1. M.-A. Karadendrou, I. Kostopoulou, I. V. Kakokefalou, A. Tzani, A. Detsi *Catalysts*, **12** 249 (2022)
2. A. Tzani, S. Kalafateli, G. Tatsis, M. Bairaktari, I. Kostopoulou, A.R.N. Pontillo, A.R.N., A. Detsi, *Sustainable Chemistry*, **2** 576 (2021).
3. D. Skarpalezos, A. Detsi, *Applied Sciences* **9**, 4169 (2019)
4. S. Koutsoukos, T. Tsiaka, A. Tzani, P. Zoumpoulakis, A. Detsi, *Journal of Cleaner Production*, **241**, 118384, (2019)
5. Tzani, A.; Karadendrou, M.A.; Tsiaka, T.; Kritsi, E.; Zoumpoulakis P.; Detsi A. "Deep Eutectic Solvents: Properties, Applications and Toxicity", Chapter 2: Exploring the Role of Natural Deep Eutectic Solvents (NADES) Towards the Valorization of Food Processing Industry Waste. Nova Science Publishers, **2022**, 19-51.

## A New Example of Natural Deep Eutectic Solvents as A Green Approach to the Solubilization and Stabilization of Biomolecules

Lamya Al Fuhaid<sup>1\*</sup>, Arwa Alghuneim<sup>1</sup>, Imed Gallouzi<sup>1</sup>, Young H. Choi<sup>2</sup>, Robert Verpoorte<sup>2</sup>, Geert-Jan Witkamp<sup>1</sup> and Andreia Farinha<sup>1</sup>

<sup>1</sup>King Abdullah University of Science and Technology, Division of Biological and Environmental Science and Engineering, Thuwal, Saudi Arabia

<sup>2</sup>Natural Products Laboratory, Leiden University, Leiden, The Netherlands

\*lamya.fuhaid@kaust.edu.sa

The biocompatible natural deep eutectic solvents (NADES) can solubilize and stabilize various of molecules such as polyphenols, DNA, and proteins <sup>[1]</sup>. This feature of NADES is partly due to their supramolecular network. NADES were shown to dissolve the components of biofilms, providing a green solution for membrane biofouling in reverse osmosis <sup>[2]</sup>. Here we focus on an application of NADES as green solvents for the stabilization one of the least stable macromolecules, RNA.

In order to investigate the stability of RNA in NADES, several NADES were prepared by combining various primary metabolites and mixing them at elevated temperatures. Total RNA was extracted from human HeLa cells. The stability of RNA molecules in NADES was monitored over time by evaluating the RNA quantity and quality through concentration measurements and gel electrophoresis, respectively.

The extracted RNA maintained 100% of its initial concentration when stored in NADES compared to ~90% when stored in water (Figure 1).

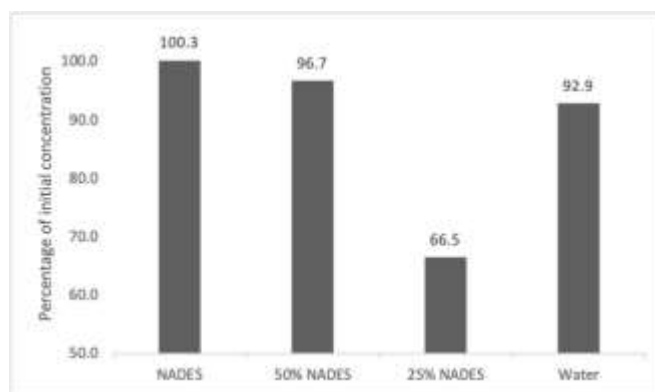


Figure 23. The concentrations of RNA stored for two weeks in different media compared to their initial concentrations.

Our preliminary results show that NADES can maintain the concentration and integrity of RNA. The increased stability of RNA molecules could enhance the robustness and accessibility of mRNA vaccines, facilitating their storage and transport.

### Acknowledgments

The authors thank King Abdullah University of Science and Technology (KAUST) for funding this research.

### References

- [1] Y. H. Choi, J. van Spronsen, Y. Dai, M. Verberne, F. Hollmann, I. W. C. E. Arends, G. J. Witkamp, R. Verpoorte, *Plant Physiol.* **2011**, *156*, 1701–1705.
- [2] M. F. Nava-Ocampo, L. Al Fuhaid, R. Verpoorte, Y. H. Choi, M. C. M. van Loosdrecht, J. S. Vrouwenvelder, G. J. Witkamp, A. S. F. Farinha, S. S. Bucs, *Water Res.* **2021**, *201*, 117323.



## Affordable Ionic Liquids: A Thermal Investigation

Maariyah Y. Suleman<sup>1\*</sup>, C.J. Clarke<sup>2</sup> and A. Brandt-Talbot<sup>1\*</sup>

<sup>1</sup>Department of Chemistry, Imperial College London, White City, London, W12 0BZ, UK

<sup>2</sup>Department of Chemical Engineering, Imperial College London, South Kensington, London, SW7 2AZ, UK

\*Contact E-mail: m.suleman18@ic.ac.uk, agi@imperial.ac.uk

Ionic liquids are liquids composed of a cation and anion, with a melting point at or near room temperature.<sup>1</sup> These ionic liquids have seen great use in several applications, to name a few, biomass extraction, biphasic reactions, catalysis and in CO<sub>2</sub> capture. Understanding the thermal stability of these ionic liquids is vital for implementation of ionic liquids in industrial applications that require elevated temperatures. Currently, a limited number of ionic liquids have been studied for their thermal stability and corresponding degradation mechanisms, and they are often costly with limited industrial applicability.<sup>1,2</sup>

In this research, the ionic liquids employed focus on pairing of the hydrogen sulfate anion, [HSO<sub>4</sub>]<sup>-</sup>. Additionally, a range of cations based on mono/dialkylated imidazole and tri/tetra alkylated amine were studied. To give a thorough comparisons these were studied alongside conventionally popular ionic liquids based on pairings utilizing the following anions: chloride, Cl<sup>-</sup> and acetate, [OAc]<sup>-</sup>. These hydrogen sulfate ionic liquids are of interest as they have recently found application in biomass processing whilst synthesis of these ionic liquids is advantageously simple and of a low-cost.<sup>3,4,5</sup>

In this talk, I will present thermal gravimetric data showing the greater thermal stability of low-cost hydrogen sulfate ionic liquids compared to common analogous ionic liquids. Additionally, thermal differences between two different classifications of ionic liquids; protic and aprotic ionic liquids. The suitability of the current range of techniques used to deduce the thermal stability of protic ionic liquids will also be discussed. Analytical techniques which will be discussed include: thermogravimetric analysis coupled with mass spectroscopy, direct-insertion-probe spectroscopy, simultaneous thermal analysis. Additionally, experimental data will be used to support the investigation of the relative stability and identification of ionic liquid decomposition products at ambient pressure and under vacuum.

Thermogravimetric analysis under ambient pressure showed that protic and aprotic hydrogen sulfate ionic liquids are more stable than the equivalent chloride and acetate ionic liquids. Under vacuum, the molecular cation for the protic imidazolium based ionic liquid was detected, whilst the mass spectrum of the aprotic analogue only showed molecular fragments, suggesting that evaporation of the amine occurs for the protic ionic liquid under vacuum. In order to differentiate between the evaporation and degradation of the protic hydrogen sulfate based ionic liquids, isothermal TGA and STA was carried out for [HC<sub>4</sub>im][HSO<sub>4</sub>], [C<sub>4</sub>C<sub>1</sub>im][HSO<sub>4</sub>] and [N<sub>4110</sub>][HSO<sub>4</sub>] under air, nitrogen, helium and argon.

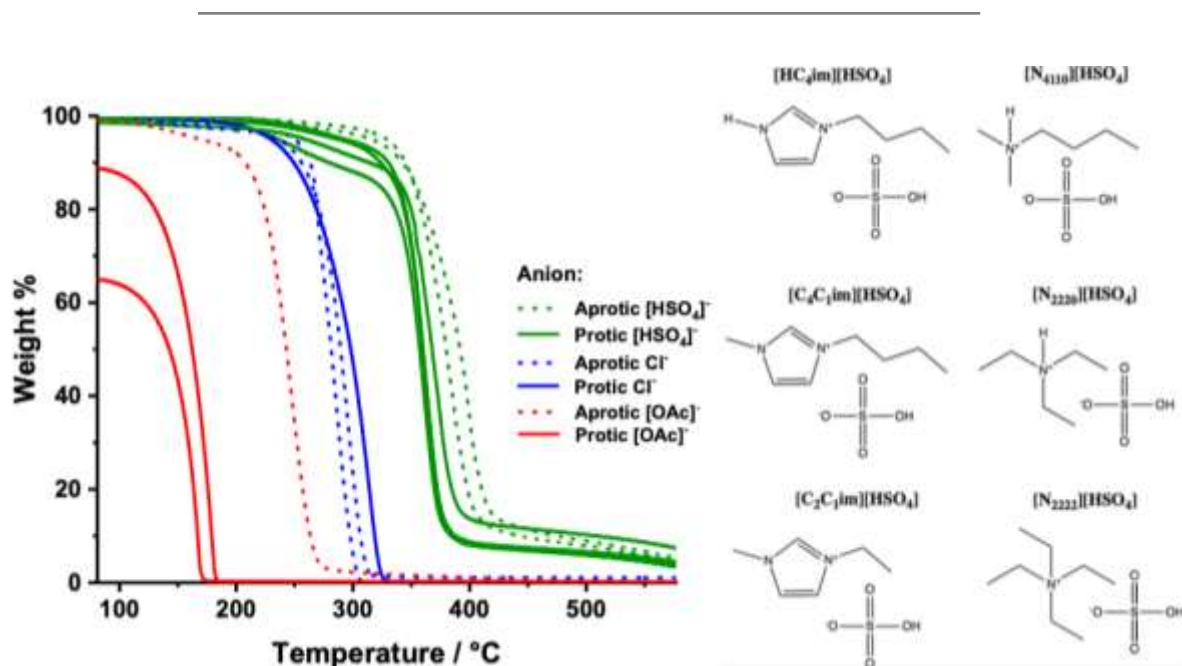


**Figure 1.** TGA thermographs for several imidazolium hydrogen sulfate based PILs (solid green) and AILs (dashed green); Imidazolium chloride PILs (solid blue), imidazolium and ammonium chloride AILs (dashed blue); Imidazolium protic and aprotic acetate ILs (solid and dashed red) and ammonium acetate PILs (solid red). Chemical structures of select protic and aprotic hydrogen sulfate based ionic liquids used throughout this study.

## References

- [1] M.T.Clough, K.Geyer, P.A.Hunt, J.Mertes and T.Welton, *Phys. Chem. Chem. Phys.*, **15**, 20480–20495, (2013).
- [2] T.L.Greaves and C.J.Drummond, *Chem. Rev.*, **108**, 206–237, (2018).
- [3] L.Chen, M.Sharifzadeh, N.M.Dowell, T.Welton, N.Shah & J.P. Hallett, *Green Chem.*, **16**, 3098–3196, (2014).
- [4] A.Brandt-Talbot, F.J.V.Gschwend, P.S.Fennell, T.M.Lammens, B.Tan, J.Weale and J.P.Hallett, *Green Chem.*, **19**, 3078–3102, (2017).
- [5] P.Verdía, A.Brandt-Talbot, J.P.Hallett, M.J.Ray and T.Welton, *Green Chem.*, **16**, 1617–1627, (2014).

**Bio-derived ionic liquids: synthesis and biological activity**

Marina M. Seitkalieva,<sup>1,\*</sup> Anna V. Vavina,<sup>1</sup> Ksenia S. Egorova,<sup>1</sup> Valentine P. Ananikov V.P.<sup>1</sup>

<sup>1</sup> N.D. Zelinsky Institute of Organic Chemistry Russian Academy of Sciences

\* [s\\_marina@ioc.ac.ru](mailto:s_marina@ioc.ac.ru)

In recent years, the field of ionic liquids (ILs) application has expanded significantly. As alternative solvents ILs are used in chemical synthesis, catalysis, biocatalysis, electrochemistry, analytics, for the extraction, and separation of bioactive compounds, etc. ILs have been shown to possess a wide range of biological activities, including cytotoxic, antiviral and antimicrobial properties. [1] Lately, a large study on the mechanisms of cytotoxic action of various classes of commercial ILs was made and guide for designing ILs with targeted biological activity was compiled. [2]

However, widespread use of ILs is hindered by their high cost and toxicity. The rational design of ILs based on the selection of cations, functional groups, linkers, and anions will make it possible to influence the physicochemical and biological properties of the final ILs. It is assumed, that the use of initial reagents obtained from renewable biomaterials will significantly reduce the cost of ILs and their environmental impact. So, various bio-derived ILs were obtained from natural compounds, such as choline, amino acids, carbohydrates and various organic acids and oils.

Earlier, we demonstrated that depending on the position of the biofragment (in the anion or cation) and the substituents in the cationic center, the properties of the final ILs differed significantly. For example, for cinnamate-based ILs, the introduction of cinnamic acid into the cation leads to a more significant increase in cytotoxicity than in the anion. [3] The cytotoxicity of ILs with salicylate-anion was higher than that of imidazolium ILs with cation functionalized with salicylic acid. [4]

Recently, new protic ILs from a bio-derived platform chemical (5 HMF) were obtained, and their physicochemical and biological properties were studied. [5] Novel ILs had a protonated tertiary amino group in the cation and different inorganic anions ( $\text{Cl}^-$ ,  $\text{SO}_4^{2-}$ ,  $\text{H}_2\text{PO}_4^-$ ). Most of them had low (< 88 °C) and were readily soluble in water. Cytotoxicity of several 5-HMF-derived ILs in human fibroblasts was comparable to that of common imidazolium ILs, whereas other ILs were significantly more active. The substituents in the cationic core had a prominent impact on the cytotoxicity of the ILs, whereas the nature of the anion was less important. Bactericidal activity of the ILs against Gram-negative and Gram-positive bacteria was tested. The IL with the sulfate anion demonstrated a cellulose-dissolving ability.

## Acknowledgements

The part of the work was supported by the Russian Science Foundation (RSF Project № 21-73-10262).

## References

1. Vereshchagin A.N., Frolov N.A., Egorova K.S., Seitkalieva M.M., Ananikov V.P., *Int. J. Mol. Sci.*, **22** 6793 (2021).
2. Dzhemileva L.U., D'yakonov V.A., Seitkalieva M.M., Kulikovskaya N.S., Egorova K.S., Ananikov V.P., *Green Chem.*, **23** 6414 (2021).
3. Vavina A.V., Seitkalieva M.M., Posvyatenko A.V., Goedeve E.G., Strukova E.N., Egorova K.S., Ananikov V. P. *J. Mol. Liq.*, 118673 (2022).
4. Egorova K.S., Seitkalieva M.M., Posvyatenko A.V., Khrustalev V.N., Ananikov V.P., *ACS Med. Chem. Lett.*, **6** 1099 (2015).
5. Seitkalieva M.M., Vavina A.V., Posvyatenko A.V., Egorova K.S., Kashin A.S., Gordeev E.G., Strukova E.N., Romashov L.V., Ananikov V.P., *ACS Sustainable Chem. Eng.*, **9** 3552 (2021).

## Optimization of a green extraction method for the recovery of bioactives from cornelian cherry (*Cornus mas* L.) fruits using $\beta$ -cyclodextrin as an extraction enhancer

Anastasia Loukri\*, Anastasia Kyriakoudi, Ioannis Mourtzinis

Laboratory of Food Chemistry and Biochemistry, Department of Food Science and Technology, School of Agriculture, Aristotle University of Thessaloniki, 54124 Thessaloniki, Greece

\* [loukriap@agro.auth.gr](mailto:loukriap@agro.auth.gr)

Cornelian cherry (*Cornus mas* L.) is a plant that mainly grows in Europe and West Asia. Its edible fruits are deep red in color and have oval shape and sour or sweet taste. Their beneficial health effects (e.g. antioxidant, antimicrobial, anti-inflammatory, neuroprotective) have been attributed to the presence of various bioactive compounds such as phenolic acids, flavonoids, anthocyanins, iridoids, vitamin C etc. [1, 2]. Their levels depend on the cultivar, the stage of maturity as well as the cultivation practices. In this view, cornelian cherry fruits as well as their extracts, find applications in the development of novel functional food products including ice creams, beverages, beers, vinegars and meat products [3]. Conventional extraction techniques often involve the use of toxic organic solvents. The last decades, the interest of the scientific community has been focused on alternative green solvents, such as the aqueous solutions of cyclodextrin, that could reduce the negative health and environmental impact. More specifically, cyclodextrins, can be used as extraction enhancers through the formation of inclusion complexes with a variety of bioactives, such as phenolic compounds [4]. Even though cyclodextrins have been already used for the extraction of phenolic compounds from various plant materials, e.g. beetroots [5], coffee pulp [6] and red grape pomace [7], to the best of our knowledge, extremely limited is the information regarding their use for the recovery of phenolic compounds from cornelian cherry fruits [8].

In this frame, the aim of the present study was the optimization of a green extraction approach for the recovery of bioactive compounds from cornelian cherry fruits with the use of aqueous solutions of  $\beta$ -cyclodextrin ( $\beta$ -CD) as extraction enhancers with the aid of Response Surface Methodology.

Fresh cornelian cherry fruits were provided by “Physis Ingredients” (Serres, Greece). Upon arrival at the laboratory, the fruits were destoned, homogenized in a Pulverisette 11 Knife Mill (Fritsch GmbH, Idar-Oberstein, Germany) and then stored at -20 °C until further analysis. An unblocked full factorial central composite design (CCD) was applied to the study of four factors, namely, duration of extraction (min), temperature of extraction (°C), solvent to solid ratio (v/w) and concentration of cyclodextrin (mg/mL). Each of these factors had five equally spaced levels in the design, coded as follows: -a, -1, 0, +1, +a, where  $a = 2n/4$ ,  $n =$  number of variables, and -1, +1 and 0 correspond to the low, high and mid-levels, respectively (Table 1). The CCD had 7 of the factorial points at the center of the design, for a total of thirty one experiments, replicated for the estimation of error. The runs were set using the software Minitab 15.1.20.0 (Minitab, Inc., State College Pennsylvania, USA). Polynomial response surfaces were fitted to the response variables namely, total phenolic content, total monomeric anthocyanins, total flavonoids and antiradical activity. Statistical analysis of the experimental data was performed using the same software. Water or aqueous-alcoholic solutions were also examined for comparison purposes.

Table 1. Levels of factors in actual and coded values used in the experimental design.

Factors	Level				
	Coded values				
	-a	-1	0	+1	+a
	Actual values				
Duration (min)	10	23	35	48	60
Temperature (°C)	40	50	60	70	80
Solvent:solid ratio (v/w)	5	17	28	39	50
Concentration of $\beta$ -cyclodextrin (mg/mL)	0	4.6	9.3	13.9	18.5

Linear, quadratic and interaction effects of the examined factors were found to significantly ( $p < 0.05$ ) influence the recovery of the compounds of interest from cornelian cherry fruits. Cyclodextrin was found to contribute to the recovery of the examined bioactives as extraction enhancer.

Our proposed procedure is suitable for food, pharmaceutical and cosmeceutical applications.

### Acknowledgements

This research has been conducted in the frame of the Regional Operational Programme Central Macedonia 2014-2020 (“Development of natural product with neuroprotective action based on the plant Cornelian cherry”, action

code: KMP6-0079229) that was co-financed by Greek national funds and the European Union (European Regional Development Fund).

## References

1. A. Martinović, I. Cavoski, *Food Chem.*, **318** 126549 (2020).
2. G.E. Pantelidis, M. Vasilakakis, G.A. Manganaris, G. Diamantidis. *Food Chem.*, **102** (2007).
3. M. Parveez Zia, I. Alibas, *Food Chem.*, **364** 130358 (2021).
4. I. Mourtzinou, A. Goula, *Polyphenols in Agricultural Byproducts and Food Waste*. In: *Polyphenols in Plants*. Academic Press (2019).
5. P. Tutunchi, L. Roufegarinejad, H. Hamishehkar, A. Alizadeh, *Food Chem.*, **297** 124994 (2019).
6. A. Loukri, P. Tsitlakidou, A. Goula, A.N. Assimopoulou, K.N. Kontogiannopoulos, I. Mourtzinou, *Appl. Sci.*, **10** (2020).
7. A. Alibante, A. Lakka, E. Bozinou, A. Chatzilazarou, S. Lalas, D.P. Makris, *Beverages*, **7** 59 (2021).
8. B.M. Popović, B. Blagojević, D. Latković, D. Četojević-Simin, A.Z. Kucharska, F. Parisi, G. Lazzara, *Lwt.* **141** (2021).

## Sorption of CO<sub>2</sub> in Composite Cellulose Acetate – Ionic Liquid Membranes

Giannis Kontos, Costas Tsiptsias and Ioannis Tsivintzelis\*

Department of Chemical Engineering, Aristotle University of Thessaloniki, 54124 Thessaloniki, Greece

\*tioannis@cheng.auth.gr

The use of polymer membranes for the separation of CO<sub>2</sub> from natural gas presents several advantages, such as low energy demands, small equipment volume and absence of liquid wastes [1, 2]. For these reasons, such process has been suggested for CO<sub>2</sub> capture from flue gases generated from fossil fuels combustion.

In this study, the sorption of CO<sub>2</sub> in composite polymer membranes, consisting of cellulose acetate, as polymer matrix, and an ionic liquid, as potential absorption promoter, was experimentally studied. Two ionic liquids were selected for investigation, 1-butyl-3-methylimidazolium hydrogen sulfate ( [BMIM<sup>+</sup>][HSO<sub>4</sub><sup>-</sup>] ) and choline glycine ( [Ch<sup>+</sup>][Gly<sup>-</sup>] ), since they present adequate CO<sub>2</sub> dissolution ability, due to the presence of the hydrogen sulfate anion (HSO<sub>4</sub><sup>-</sup>) [3] and the glycine anion (Gly<sup>-</sup>) [4], respectively. Experiments were performed at 35°C and pressures ranging from 50-70 bar.

The composite membranes were prepared through the solvent casting method. In more detail, cellulose acetate was dissolved in acetic acid, up to 5 wt.%, and, subsequently, ionic liquid was added, resulting in solutions containing 0 and 20 wt.% ionic liquid with respect to the polymer weight. The solutions were casted into petri-dishes and remained at room temperature for around 48 hours. Upon solvent evaporation, the films were removed from the petri-dishes and dried under vacuum for 3 days to remove residual solvent. The obtained films were stored in a desiccator before investigation.

Subsequently, the amount of the dissolved CO<sub>2</sub> in the composite polymer matrix was determined using the Mass-Loss-Analysis technique [5]. According to this method, a known mass of the composite polymer matrix is inserted in a high-pressure cell under CO<sub>2</sub> atmosphere of constant temperature and constant (high) pressure. The equilibrium amount of the sorbed CO<sub>2</sub> in the polymer matrix is determined by monitoring the gas desorption after the quick depressurization of the system, assuming the diffusion behavior. The equilibration time was determined through several preliminary experiments.

Some representative results for the sorption of CO<sub>2</sub> in CA – [BMIM<sup>+</sup>][HSO<sub>4</sub><sup>-</sup>] and CA – [Ch<sup>+</sup>][Gly<sup>-</sup>] composite membranes are presented in Figures 1 and 2, respectively.

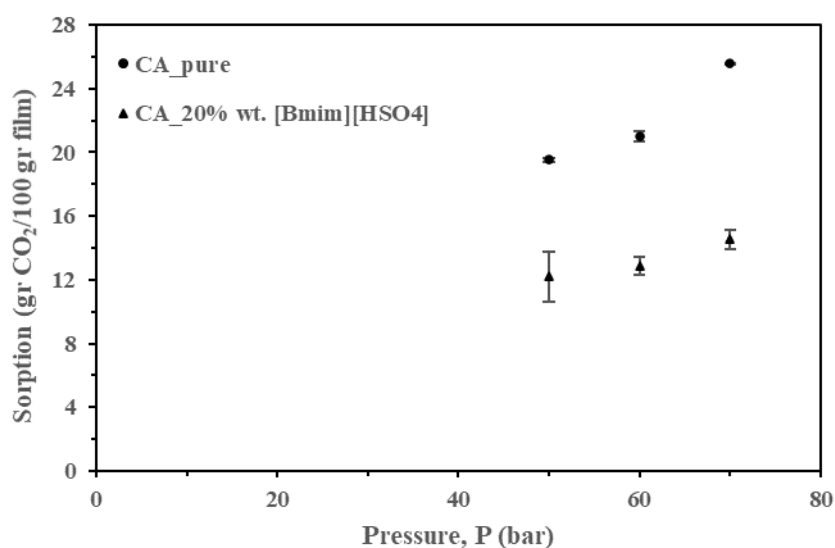


Figure 1. Sorption of CO<sub>2</sub> in CA – [BMIM<sup>+</sup>][HSO<sub>4</sub><sup>-</sup>] composite membranes.

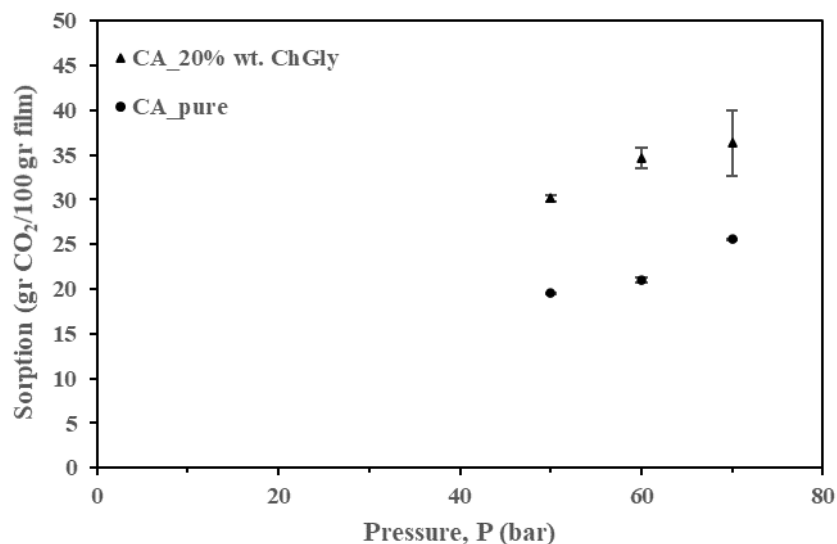


Figure 2. Sorption of CO<sub>2</sub> in CA – [Ch<sup>+</sup>][Gly<sup>-</sup>] composite membranes.

The results reveal that only [Ch<sup>+</sup>][Gly<sup>-</sup>] acted as CO<sub>2</sub> dissolution promoter, since the CO<sub>2</sub> sorption in the composite increases with increasing ionic liquid concentration. This observation can be attributed to the existence of the amine group in the glycine anion that induces the chemical absorption of CO<sub>2</sub> in the [Ch<sup>+</sup>][Gly<sup>-</sup>] containing polymer matrix, contrary to the mainly physical absorption in the [BMIM<sup>+</sup>][HSO<sub>4</sub><sup>-</sup>] containing composite.

### Acknowledgements

The work was co-financed by Greece and EU through the Operational Program “Human Resources Development through PhD studies”, implemented by State Scholarships Foundation (IKY).

### References

1. R.W. Baker, K. Lokhandwala, *Ind. Eng. Chem. Res.* **47(7)** 2109 (2008).
2. R.W. Baker (2000) *Membrane Technology and Applications*, John Wiley & Sons, Ltd.
3. I. Mejía, K. Stanley, R. Canales, J.F. Brennecke, *J. Chem. Eng. Data* **58(9)** 2642 (2013).
4. F. Zhang, C.G. Fang, Y.T. Wu, Y.T. Wang, A.M. Li, Z.B. Zhang, *Chem. Eng. J.* **160(2)** 691 (2010).
5. A. Kumar, R.K. Gupta (1998) *Fundamentals of polymers*, CRC Press.

# Organonitriles as complexing agents for the double metal cyanide-catalyzed synthesis of polyether, polyester, and polycarbonate polyols

Chinh Hoang Tran, Soo Jeong Lee, Su Hyeon Jeon, Il Kim\*

Department of Polymer Science and Engineering, Pusan National University, Busandaehag-ro 63-2, Geumjeong-gu, Busan 46241, Republic of Korea

\*E-mail: ilkim@pusan.ac.kr

Organonitriles play an important role in organometallic chemistry for numerous applications both in organic synthesis and catalysis [1–3]. Herein, various nitriles compounds have been investigated as complexing agents (CAs) for double metal cyanide (DMC) catalysts (Figure 1(a)). The complexation of these CAs within DMC framework was characterized by combining structure-sensitive characterization techniques. The catalytic activity of the resultant DMC catalysts was evaluated via the ring-opening polymerization (ROP) of propylene oxide (PO),  $\epsilon$ -caprolactone (CL), and copolymerization of PO with CO<sub>2</sub> (Figure 1(b–d)).

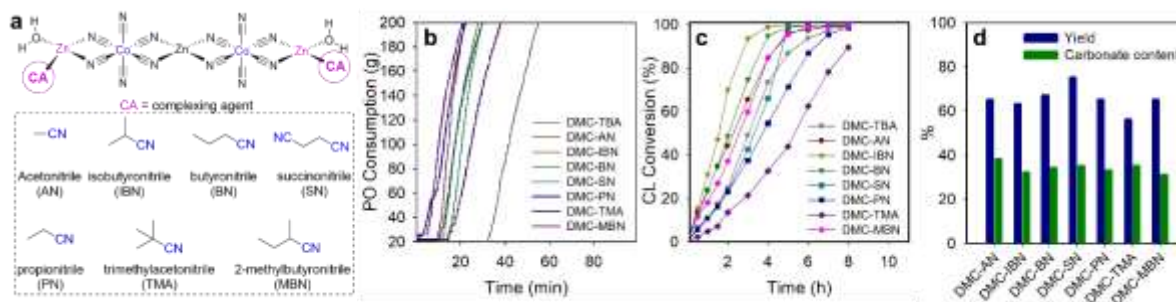


Figure 1. Typical structure of the DMC catalyst bearing various nitrile CAs (a) and catalytic activity of the DMC catalysts for the ROP of propylene oxide (b), ROP of  $\epsilon$ -caprolactone (c), and copolymerization of propylene oxide with CO<sub>2</sub> (d).

Table 1. Summary of the polymerization results.

Catalyst	ROP of PO		ROP of CL		Copolymerization of PO and CO <sub>2</sub>			
	$t_p$ (min)	TOF (min <sup>-1</sup> )	$t_p$ (h)	TOF (h <sup>-1</sup> )	CO <sub>2</sub> (%)	Yield (%)	$M_n$ (g/mol)	PDI
DMC-AN	21	429	5	51	38.04	65	9000	4.76
DMC-IBN	28	327	3	83	32.31	63	2100	2.70
DMC-BN	30	294	4	61	34.04	67	2700	2.20
DMC-SN	30	333	5	57	34.50	75	4200	2.01
DMC-PN	22	381	7	33	33.13	65	3800	2.62
DMC-TMAN	38	221	5	47	34.68	56	2700	2.05
DMC-MBN	20	561	8	37	30.77	65	3500	2.85

The DMC catalysts bearing nitrile CAs exhibit remarkably higher activity than the conventional DMC catalysts using *tert*-butyl alcohol (TBA) as a CA.

DMC-MBN and DMC-IBN showed highest activity for the ROP of PO and CL, respectively, whereas DMC-SN exhibited highest efficiency toward copolymerization of PO and CO<sub>2</sub>.

The resultant polypropylene oxide polyols were characterized by narrow dispersity (1.1–1.2) and low unsaturation level (0.004–0.014). Tunable molecular weight polycaprolactone polyols (500–9,800 g mol<sup>-1</sup>) were successfully synthesized. Polycarbonate polyols with relatively high yield (56–75%) and carbonate content (30–38%) were also achieved.

## Acknowledgements

This work was supported by a National Research Foundation of Korea (NRF) grant funded by the Korean government (MSIT) (2021R1A2C2003685) and was partly supported by the Korea Institute of Energy Technology Evaluation and Planning (KETEP) grant funded by the Korean government (MOTIE) (20208401010080).

## References

1. J.M. Bellerby, M.J. Mays, *J. Chem. Soc., Dalton Trans.*, **13** 1281 (1975).
2. V.Y. Kukushkin, A.J.L. Pombeiro, *Chem. Rev.*, **102** 1771 (2002).
3. S.F. Rach, F.E. Kühn, *Chem. Rev.*, **109** 2061 (2009).



# Nanomaterials & Ionic liquids for advanced applications

## Electroless plating on 3D printed photocurable resin artifacts without the use of chromium and palladium solutions

Antonios Bairamis<sup>1\*</sup>, Katerina Mavronasou<sup>1</sup>, Alexios Grigoropoulos<sup>1</sup>, Evangelos Papaioannou<sup>1</sup>,  
Ioanna Deligkiozi<sup>1</sup> and Alexandros Zoikis Karathanasis<sup>1</sup>  
<sup>1</sup>Creative Nano PC, 4 Leventi Street, Peristeri, 12132 Athens, Greece  
\*a.bairamis@creativenano.gr

### Abstract

Plating on plastics (PoP) is a key process for producing a metallic coating on non-conductive polymeric substrates to enhance their wear and corrosion resistance and to aesthetically improve their appearance. The process can be divided into four main steps whose objectives are: (a) to remove dirt (*degreasing*), (b) increase the hydrophilicity and roughness of the surface (*etching*), (c) seed the surface with nucleation sites (*activation*), and finally (d) create a conductive thin metallic layer (*metallization*). Currently, industrial processes employ toxic and/or expensive chemicals such as chromic acid for the etching and Pd-Sn colloidal solutions for the activation of the polymeric surface before the final electroless deposition step [1]. In the last 20 years, the PoP research community has been investigating greener and less expensive alternative procedures that do not involve the use of Cr<sup>6+</sup> and/or Pd-Sn [2,3,4]. In addition, coupling of PoP with 3D polymer-based printing technologies can lead to the manufacturing of complex, custom-made metallized plastic objects that are used in scientific, industrial, and daily-life applications.

In this study, photocurable resin artifacts were 3D printed via stereolithography (SLA) and then coated via an environmentally benign and cost-effective process that employs potassium hydroxide (KOH) for the etching (instead of Cr<sup>6+</sup> solutions) [5], nickel acetate [Ni(CH<sub>3</sub>COO)<sub>2</sub>] for the activating (instead of Pd-Sn colloidal solutions) [2], sodium borohydride (NaBH<sub>4</sub>) as the reducing agent [2,5], and Ni-P electroless solution for the final metallization step (Table 1) [5,6]. The chemical and morphological properties of the polymeric surface were evaluated by FT-IR spectroscopy, thermogravimetric analysis (TGA), contact angle measurements (CA) and scanning electron microscopy (SEM). Adhesion tests were also used in order to evaluate the adhesion quality of the metallic layer on the plastic substrate. In Figure 1 a graphical representation of the current industrial process and the alternative proposed method is presented.

Table 1. Chemical composition of Ni-P electroless bath.

Compound	Concentration (g/L)
NiSO <sub>4</sub> ·6H <sub>2</sub> O (nickel sulfate hexahydrate)	32
Na <sub>3</sub> C <sub>6</sub> H <sub>5</sub> O <sub>7</sub> (trisodium citrate)	20
NaPO <sub>2</sub> H <sub>2</sub> (sodium hypophosphite)	28
NH <sub>4</sub> Cl (ammonium chloride)	25
NH <sub>4</sub> OH (ammonium hydroxide)	pH = 9 at 45 °C

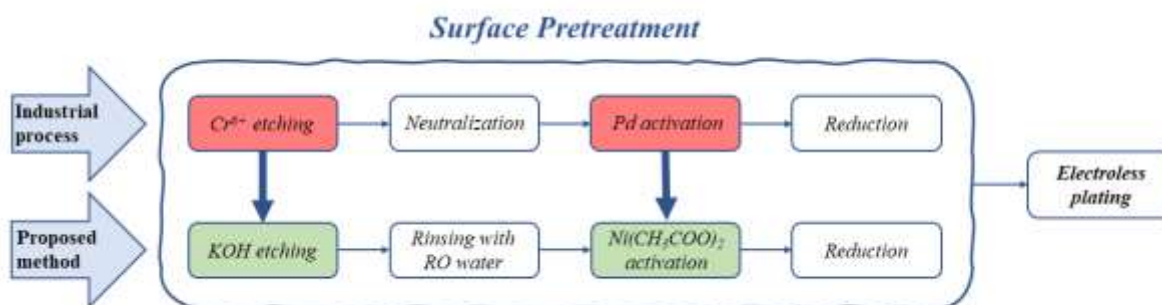


Figure 1. Graphical representation of the current industrial process (top) and the proposed method herein (bottom).

A comparative study was conducted to optimize the etching process by varying the KOH concentration (100 – 200 g/L), immersion time (15 – 120 min) and temperature (25 – 60 °C). The results showed that metallization was successful under specific set of conditions. Room temperature etching required rather long immersion times, greater than one hour, which would make the overall electroless PoP process time-consuming and practically not industrially applicable. An elevated temperature of 45 °C and a KOH concentration of at least 150 g/L were necessary to successfully etch the polymer surface within 30 min, a time period that is reasonable for an industrial process. Higher temperatures led to excessive etching and sample degradation, even for shorter immersion times,

whereas more diluted KOH solutions led to insufficient etching and as a result, metallization was not possible. Similarly, optimization of the activation process by varying the aforementioned factors was also performed. The overall results suggested that electroless PoP of 3D printed resin artifacts was feasible at a temperature of 45 °C and immersion time intervals of 30 min for the etching (200 g/L KOH), activation (5 g/L Ni(CH<sub>3</sub>COO)<sub>2</sub>) and Ni-P metallization steps. In Figure 2 some 3D printed artifacts of complex geometry are presented, before and after their metallization.



Figure 2. 3D printed artifacts of complex geometry before and after their metallization.

### Acknowledgements

This research work has received funding from the **3DPlate** project [7] under the RESEARCH-CREATE-INNOVATE call and will be the starting point for the recently awarded **FreeMe** EC project (HORIZON-CL4-2021-RESILIENCE-01-12).

### References

1. G.A. Krulik, *J. Chem. Educ.*, **55**(6) 361-365 (1978).
2. R. Suman, D. Nandan, A. Haleem, S. Bahl, M. Javaid, *Materials Today: Proceedings*, **28**(3) 1575-1579 (2020).
3. L.M. Luo, Z.L. Lu, X.M. Huang, X.Y. Tan, X.Y. Ding, J.G. Cheng, L. Zhu, Y.C. Wu, *Surf. Coat. Technol.*, **251** 69-73 (2014).
4. L.A.C. Teixeira, M.C. Santini, *J. Mater. Process. Technol.*, **170**(1-2) 37-41 (2005).
5. R. Bernasconi, C. Credi, M. Tironi, M. Levi, L. Magagnin, *J. Electrochem. Soc.*, **164**(5) B3059-B3066 (2017).
6. H. Zhang, L. Shen, J. Chang, *J. Ind. Text.*, **41**(1) 25-40 (2011).
7. <https://www.3dplate.gr/>

## Robust flow synthesis of defect-incorporated ZnO quantum dots and investigation of their structure-property interlink

Sayoni Sarkar<sup>1\*</sup>, Ajit R. Kulkarni<sup>2</sup>, and Rohit Srivastava<sup>3</sup>

<sup>1</sup>Centre for Research in Nanotechnology and Science, <sup>2</sup>Department of Metallurgical Engineering and Materials Science,

<sup>3</sup>Department of Biosciences and Bioengineering, Indian Institute of Technology Bombay, Mumbai, 400076, India

\*Corresponding author: sayoninitt@gmail.com

### Introduction:

In recent years, colloidal zinc oxide quantum dots (ZnO QDs) with dominant defect chemistry have befitting utility in the emerging areas of agriculture, energy, and health care. The novel characteristics of ZnO QDs are primarily accredited to the singly ionized oxygen vacancies ( $V_{O}^{\bullet}$ ) that render them unique size-controlled optical, physiochemical, and biological properties. These intriguing features of ZnO QDs are accomplished through the fabrication methods and process variables adopted. However, recent studies involving conventional batch synthesis of nanomaterials have revealed flawed process control, the discrepancy in scale-up, poor reproducibility and yield, leading to unnecessary energy consumption and material wastage. To combat these challenges, rapidly evolving quantum dots production technologies that tend toward sustainable development have ushered in newer strategies which, in the long run, will be beneficial to meet the increased demand for high-quality ZnO QDs [1] [2]. Thus, in this study, the structure-property interlink has been explored for defective ZnO QDs synthesized by a sustainable continuous flow synthesis platform by certain sophisticated characterization and analytical techniques, including high-angle annular dark field scanning transmission electron microscopy (HAADF-STEM), Fourier transform infrared (FTIR), electron paramagnetic resonance (EPR), and UV-visible spectroscopy. This will promulgate the idea of enhanced functionality of the QDs induced by the confluence of “green chemistry” and flow synthesis, which has the potency to accelerate application based-pristine-quantum dots development.

### Experimental:

Zinc acetate ( $(Zn(CH_3COO)_2)$ ) and lithium hydroxide (LiOH) were procured from Sigma Aldrich (USA). The as-purchased precursors were dissolved in absolute ethanol (99.99%). Synthesis of defect-enriched colloidal ZnO quantum dots ( $Z_d$ -QDs) was performed in the constructed continuous flow platform. This in-house platform consists of a stainless-steel helically coiled reactor positioned inside a water bath held at 75°C and a T-mixer to aid fast mixing and efficient heat transfer. These are essential for accelerated nucleation-growth kinetics that eventually led to monodispersed QDs. Ethanolic solutions of the raw precursors were fed by the peristaltic pumps into the mixing junction via the two separate inlets of the T-mixer. The pumps were calibrated to ensure a constant flowrate of 2.4 ml/min. The strategies for process intensification also involved heating the  $Zn(CH_3COO)_2$  solution (0.1M) to 75°C and maintaining this temperature throughout the synthesis by placing the round bottom flask containing the solution in a heating mantle. However, the LiOH solution (0.1 M) in the beaker was held at room temperature. These ambient synthesis conditions were aimed to enhance the defect-mediated luminescent properties of  $Z_d$ -QDs as well as other properties of nanosystems that rely on homogenous particle sizes. The competency of this designed sustainable flow assembly was validated by HAADF-STEM, HR-TEM, FTIR, EPR and UV-visible spectroscopy for transmittance studies. The HAADF-STEM and HR-TEM images were captured by the Tecnai G2, F30 transmission electron microscope (acceleration voltage of 300 kV). FTIR, UV-visible, and EPR spectroscopic measurements were done in JASCO FT/IR-600, Carry 100 UV-Vis, and JES - FA200, JEOL, Japan, respectively.

### Results and discussion:

The particle size distribution and crystalline nature of quasi-spheroid-shaped  $Z_d$ -QDs were analysed systematically by HAADF-STEM and HR-TEM. Fig. 1a demonstrates the HAADF-STEM image of homogenous sized  $Z_d$ -QDs revealing an average size of 4.5 nm determined from the narrow particle size histogram, denoting enhanced structural attributes. Coupled with this imaging technique, HR-TEM was performed to investigate the internal features of nanostructured  $Z_d$ -QDs. It is apparent from the corresponding image (shown in the inset of Fig. 1a) that the estimated lattice fringe spacing of 2.6 Å can be well correlated to the (101) plane of the wurtzite structure of ZnO. Further, the HR-TEM image corroborated that the “green” continuous flow approach could precisely synthesize phase-pure  $Z_d$ -QDs on a large-scale. Besides, to gain an in-depth understanding of the surface functionality of  $Z_d$ -QDs, FTIR spectroscopy was employed to identify the active functional groups with respect to the peak value in the IR region, as shown in Fig. 1b. The results elucidate the presence of a number of absorption peaks from 1000-4000  $cm^{-1}$ . The symmetric and asymmetric stretches of  $\nu_{C=O}$  (carbonyl group) at 1588 and 1421  $cm^{-1}$  identified the acetate groups attached to the surface of the  $Z_d$ -QDs via chemisorption. The peak in the range of 3000- 3700  $cm^{-1}$  and 1012  $cm^{-1}$  is typically due to  $\nu_{O-H}$  stretching and bending modes of hydroxyl groups. FTIR spectra suggest that these functional groups are present only at the surface of  $Z_d$ -QDs. The absorption peaks due to the interatomic vibrations of  $Z_d$ -QDs are usually present below 1000  $cm^{-1}$  (fingerprint region). The Zn-O

vibrational modes were identified in the near-infrared (NIR) region at  $665\text{ cm}^{-1}$ , designated to the polar stretching and deformation present in the sample, which is evident from Fig. 1b.

The presence of rich intrinsic  $\text{V}_{\text{O}}^{\bullet}$  density in  $\text{Z}_{\text{d}}$ -QDs was investigated by EPR spectroscopy (Fig. 1c). EPR is a powerful non-destructive analytical method for determining the defects that serve as the origin for photoluminescence characteristics in ZnO nanoparticles. Thus, the room temperature measurements recorded the EPR signal related to  $\text{V}_{\text{O}}^{\bullet}$  at approximately  $g \sim 2.003$  in the as-synthesized  $\text{Z}_{\text{d}}$ -QDs [3]. This observation evinced that the reactor's micro-environment heavily supported the promotion of an increased density of surface  $\text{V}_{\text{O}}^{\bullet}$  in  $\text{Z}_{\text{d}}$ -QDs. Hence, these  $\text{V}_{\text{O}}^{\bullet}$ -rich  $\text{Z}_{\text{d}}$ -QDs have a flair for attracting immense attention in biomedicine, optoelectronics, photonics, and beyond. The UV-visible transmittance spectrum of colloidal  $\text{Z}_{\text{d}}$ -QDs was measured within the spectral range (300-700 nm) as depicted in Fig. 1d. that substantiates an intriguing aspect of the optical properties of the synthesized samples. It was discernible from the recorded spectrum that  $\text{Z}_{\text{d}}$ -QDs exhibited an optical transmittance of  $\sim 98.2\%$  in the visible regime 450-700 nm. Further, a distinct increase in the transmittance from 98.2% to almost 100% was observed within the region of 459-365 nm. These UV-visible transmittance studies suggest that  $\text{Z}_{\text{d}}$ -QDs can be a desirable candidate as a transparent active ingredient for healthcare (mainly cosmetics) and in flexible sensor applications.

In summary, the defective ZnO QDs synthesized by the in-house fabricated continuous flow platform exhibited superior structural and optical features driven by the anomalous surface chemistry. The designed synthesis protocol is benign and easily scalable with convenient downstream processes. Thus, this continuous flow assembly can be extrapolated to facilitate the production of colloidal quantum dot systems that harmoniously adapts to the "green chemistry" ideologies and successfully tailor the processing conditions for pilot-scale synthesis. The fabricated  $\text{Z}_{\text{d}}$ -QDs additionally display remarkable transmittance that fuels the potency of these QDs for ubiquitous widespread application in the age of "Industry 4.0".

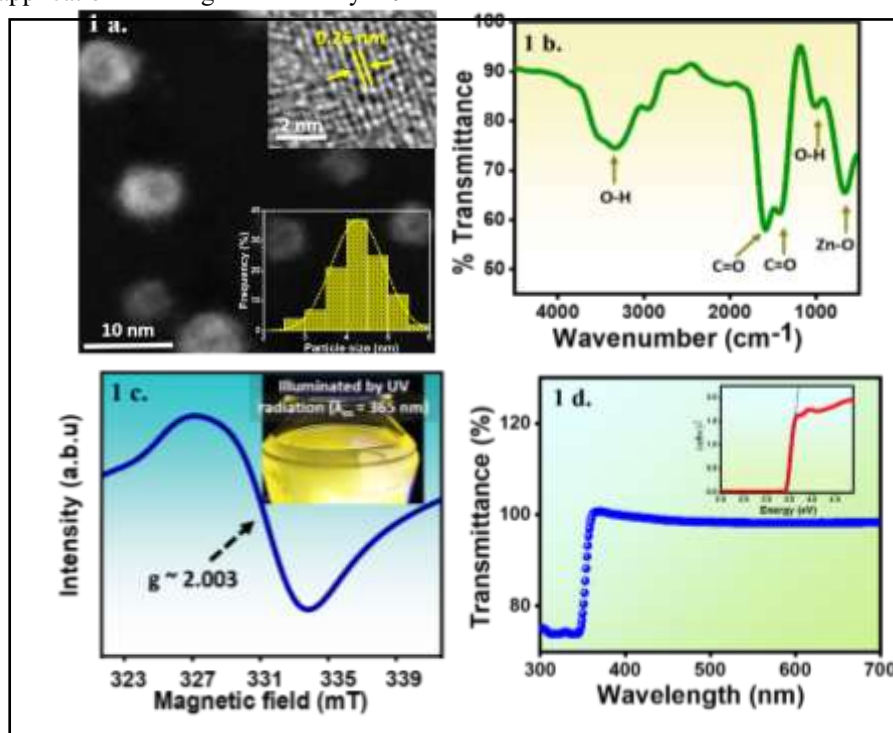


**Fig 1.** a) HAADF-STEM images of as-synthesized  $\text{Z}_{\text{d}}$ -QDs, with bottom inset showing the particle size distribution histogram and the top inset displaying the lattice fringe spacing estimated from HR-TEM image. b) FTIR spectra of  $\text{Z}_{\text{d}}$ -QDs indicating the presence of surface functional groups. c) EPR spectra of  $\text{Z}_{\text{d}}$ -QDs, the inset depicts the as-fabricated colloidal QDs under UV-irradiation. d) UV-vis transmittance spectra of  $\text{Z}_{\text{d}}$ -QDs and the absorption spectra shown at the inset.

#### Acknowledgement:

The authors are thankful to CRNTS, SAIF and the Department of MEMS, IIT Bombay, for the central instrumentation support. SS thanks Mr. Nilesh Marle, technical superintendent, CRNTS, IIT Bombay, for his assistance in EPR studies. SS is grateful for the funding support from the Prime Minister's Research Fellowship scheme (PMRF), the Ministry of Higher Education, Government of India to conduct the detailed measurements.

#### References:

- Choi, C.H., Su, Y.W. and Chang, C.H., *CrystEngComm*, **15**(17) 3326-3333 (2013).
- Hao, N., Zhang, M. and Zhang, J.X., *Biomaterials science*, **8**(7) 1783-1801 (2020).
- Asok, A., Gandhi, M.N. and Kulkarni, A.R., *Nanoscale*, **4**(16) 4943-4946 (2012).

## Development and Application of Chromogenic Ionic Liquid Crystals

Andreia F. M. Santos<sup>1</sup>, Maria H. Godinho<sup>2</sup>, Madalena Dionísio<sup>1</sup>, J. L. Figueirinhas<sup>3</sup> and Luis C. Branco<sup>1\*</sup>

<sup>1</sup>LAQV-REQUIMTE, Department of Chemistry, and <sup>2</sup>i3N/CENIMAT, Department of Materials Science, NOVA School of Science and Technology, NOVA University of Lisbon, Campus de Caparica, 2829-516 Caparica, Portugal; <sup>3</sup>CeFEMA and Department of Physics, Instituto Superior Técnico, University of Lisbon, Av. Rovisco Pais, 1, 1049-001 Lisbon, Portugal.

\*Corresponding author: l.branco@fct.unl.pt

Ionic liquids are low-melting organic salts, conventionally lower than 100 °C, which have a wide range of properties (i.e., high chemical and thermal stability, high ionic conductivity and large electrochemical windows) able to be tuned by varying the constituent ions, determining a wide range of applications. When combined with a suitable cation or anion to exhibit liquid crystalline behavior, the ionic liquid crystal originated comprise the generic properties of both ionic liquids and liquid crystals (dynamic molecular order, anisotropic physical properties, self-assembling ability, among others) [1]. In this work, novel ionic liquids crystals were prepared by sustainable methods, aiming to reduce the reaction time, the solvent usage and to improve their yields, based on pyridinium and 2-, 3- or 4- methylpyridinium cations substituted with a hexyl (C<sub>6</sub>), dodecyl (C<sub>12</sub>) and hexadecyl (C<sub>16</sub>) chains [2]. The combination of these organic cations with task-specific counter-ions are interesting to modulate its mesomorphic behavior and to design new stimuli-responsive materials.

It is known that electroactive species with electrochromic properties and molecules showing a photochemical reversible behavior can be incorporated into an ionic liquid and benefit from the synergy of its properties, increasing their performance as smart materials [3,4]. In this context, the adequate combination of commercially available chromogenic (*photo-*, *thermo-* and *electrochromic*) materials in the most promissory ILCs are tested. Additionally, intrinsically photo- and electrochromic ionic liquid crystals containing methyl orange anion and vanadate anion, respectively, are prepared and applied as stimuli-responsive devices.

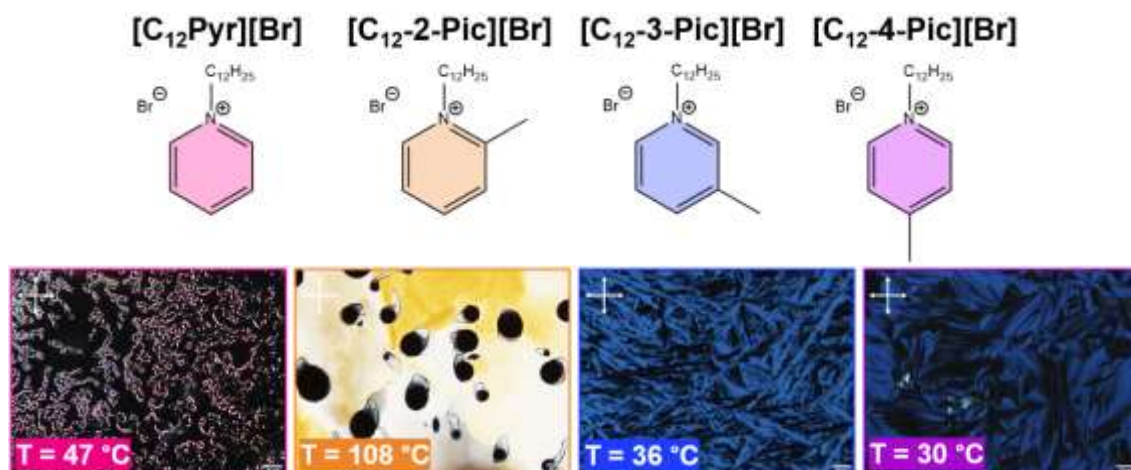


Figure 1. Ionic liquid crystals based on [C<sub>12</sub>Pyr][Br] and [C<sub>12</sub>-*n*-Pic][Br] and their thermotropic mesophases (POM images).

### Acknowledgements:

This work was supported by the Associate Laboratory for Green Chemistry LAQV (UID/QUI/50006/2019), i3N (UID/CTM/50025/2019) and CeFEMAS (UID/CTM/04540/2019), which are financed by national funds from FCT-MCTES and by FEDER funds through the COMPETE 2020 Program. The authors also thank the National Funds through FCT-MCTES and POR Lisboa 2020, under the projects numbers POCI-01-0145-FEDER-007688, PTDC/CTM-REF/30529/2017 (NanoCell2SEC) and Action European Topology Interdisciplinary Action (EUTOPIA CA17139). A. F. M. Santos acknowledges FCT-MCTES for the PhD Grant (SFRH/BD/132551/2017).

### References

1. K. Goossens, K. Lava, C.W. Bielawski, K. Binnemans, *Chem. Rev.*, **116** 1743 (2016).
2. A. F. M. Santos, C. Cruz, M. H. Godinho, M. Dionísio, J. L. Figueirinhas, L. C. Branco, *Liq. Cryst.*, (2022). DOI: 10.1080/02678292.2022.2070783
3. N. Jordão, L. Cabrita, F. Pina, L.C. Branco, *Chem. Eur. J.*, **20** 3982 (2014).
4. N. Jordão, P. Ferreira, H. Cruz, A.J. Parola, L.C. Branco, *ChemPhotoChem*, **3** 525 (2019).

## Ionic Liquids-modified Metal Organic Frameworks: Preparation and Application in Adsorption

Aurelia Visa<sup>1\*</sup>, Bianca Maranescu<sup>1,2</sup> and Lavinia Lupa<sup>3</sup>

<sup>1</sup> "Coriolan Dragulescu" Institute of Chemistry, 24 Mihai Viteazul Blv, 300223 Timisoara, Romania

<sup>2</sup> Department of Biology-Chemistry, Faculty of Chemistry, Biology, Geography, West University Timisoara, 16 Pestalozzi Street, 300115 Timisoara, Romania

<sup>3</sup> Faculty of Industrial Chemistry and Environmental Engineering, Politehnica University Timisoara, 6 Vasile Parvan Blv, 300223 Timisoara, Romania

\*e-mail: apascariu@yahoo.com

The growth of industrial activities considerably increases the delivery of toxic substances and various pollutants to the environment from industrial wastewater. The presence of organic pollutants (OPs) at values higher than the maximum admitted values can affect human health and the environment. Therefore, it is essential to remove the pollutants from wastewater before discharge. In the present study, the adsorption potential of three types of metal organic frameworks (MOFs) based on phosphonate, obtained in the reaction of phosphonoacetic acid (CP), N,N-bis (phosphonomethyl)glycine (Gly) and etidronic acid with divalent metal salts in hydrothermal conditions, has been investigated [1-3]. The obtained phosphonate MOFs were modified with ammonium and imidazolium based ionic liquids (ILs). The study involves batch-type experiments investigating the effects of the solution pH, solid:liquid ratio, initial concentration of OPs and contact time on the adsorption efficiency of the studied materials. In order to determine the maximum adsorption capacity of the studied MOFs and for the interpretation of the results obtained in the equilibrium study, several empirical isotherms were used: Freundlich, Temkin, Langmuir and Dubinin–Radushkevich. The characteristic parameters for each isotherm and correlation coefficient ( $R^2$ ) have been determined. Adsorption kinetics were discovered to follow the pseudo-second-order model. The ILs modification of MOFs increased the adsorption capacities of the materials [4,5].

### Acknowledgements

This work was partially supported by Program no 2, from the "Coriolan Dragulescu" Institute of Chemistry Timisoara, Romania and by a grant of the Romanian National Authority for Scientific Research, CNCS – UEFISCDI, project number PN-III-P4-PCE2021-0089.

### References

1. H.S. Cho, H. Deng, K. Miyasaka, Z. Dong, M. Cho, J.K. Kang, O.M. Yaghi, O. Terasaki, *Nature* **527** 503 (2015)
2. Á. Vílchez-Cózar, E. Armakola, M. Gjika, A. Visa, M. Bazaga-García, P. Olivera-Pastor, D. Choquesillo-Lazarte, D. Marrero-López, A. Cabeza, R.M. P. Colodrero, K.D. Demadis, *ACS Appl. Mater. Interfaces* **14** 11273–11287 (2022)
3. M. Bazaga-García, Á. Vílchez-Cózar, B. Maranescu, P. Olivera-Pastor, M. Marganovici, G. Ilia, A. Cabeza Díaz, A. Visa, R. M. P. Colodrero, *Dalton Transactions*, **50**, 6539-6548 (2021)
4. B. Maranescu, L. Lupa, A. Visa, *Appl. Surf. Sci.* **481**, 83, (2019)
5. B. Maranescu, L. Lupa, A. Visa, *Pure Appl. Chem.* **88**, 979 (2016)

## Bioinspired Dendritic Polymer Composites Combining Adsorption and Catalysis for Water Purification

Michael Arkas<sup>1\*</sup>, Konstantinos Giannakopoulos<sup>1</sup>, Nafsica Mouti<sup>1</sup>, Marina Arvanitopoulou<sup>1</sup>, Rafael Panagiotopoulos<sup>1</sup>, Paraskevi Gkomoza<sup>2</sup>, and Michail Vardavoulias<sup>2</sup>

<sup>1</sup>Institute of Nanoscience Nanotechnology, NCSR "Demokritos", Patriarchou Gregoriou Street, 15310 Athens, Greece

<sup>2</sup>PyroGenesis SA, Technological Park of Lavrion, 1 Athens-Lavrion Ave., 195 00 Lavrion, Greece

\*m.arkas@inn.demokritos.gr

### Introduction

The vast majority of the radially polymerized dendritic polymer applications are based on their coupling with appropriate substrates [1]. Water resources remediation is no exception. A variety of compositions has been employed to produce membrane, film, powder, filter, clay, inorganic carbon, and magnetic composites [2]. The evolution of our initially proposed functionalized derivatives [3] passed through their incorporation into ceramic filters [4] and their merging with cyclodextrins [5] to the physical and chemical binding to the solid host through crosslinking [6]. In the last decade, there is an ever-increasing tendency to deviate from the conventional chemical methods and try to imitate natural-synthetic paths. In this context, we were inspired by the diatom biosilicification process mediated by the proteins called silaffins and used instead hyperbranched poly(ethylene imine) (HPEI) in order to produce its solid support: silica-nanospheres. The resulting composite adsorbed a wide variety of pollutants [7]. The adsorbent cost though, even if standard regeneration methods are taken into account is still prohibitive for large-scale implementations. The solution currently examined by the scientific community is to take advantage of synergistic adsorption and catalytic neutralization of pollutants taking place in dendritic cavities bearing metal nanoparticles (Figure 1) [8]. Adopting this approach and still having biomimicry in mind we emulated biomineralization processes and used HPEI to produce silica-silver nanoparticle catalysts [9]. Still, this method has its drawbacks. Delays due to the diffusion of the reactants into the catalytic core and tedious recovery of the catalyst powder through centrifugation. The solution to the first issue is to alter the silica formation mechanism and insert HPEI molecules bearing metal nanoparticles into the orthosilicic acid gelation. In this way, the catalysts are in direct contact with the reaction solution. The second problem is resolved by immobilization of the gels onto the surface of the reactor. Herein we present an example of coating stainless steel by catalytic silica-HPEI-silver nanoparticle xerogel.

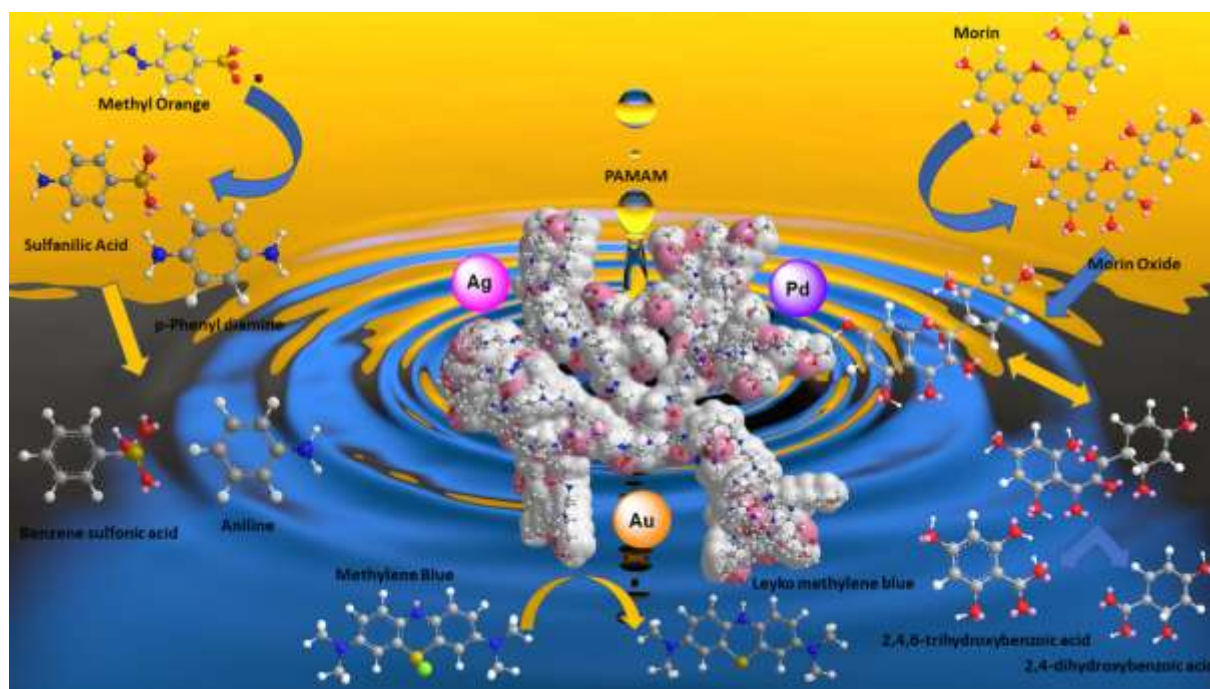


Figure 1. Schematic representation of catalytic decomposition paths of Morin, Methyl Orange, Methylene Blue dyes mediated by metal nanoparticles.

### Synthesis and Characterization

For the formation of silver nanoparticles 12,5 ml of  $\text{AgNO}_3$  (0,1M) were reacted with 50 ml 1mM solutions of HPEIs (Mw 2000, 5000, 25000, or 750000) for 8 days. Then, they were added to 125 ml 1M orthosilicic acid prepared from hydrolysis of tetraethoxysilane by 5mM  $\text{HNO}_3$  and the pH was adjusted to 7.5 with trizma base. Thermal spay treatment with stainless-steel microspheres is adopted in order to induce a microporous network to stainless steel coupons. The latter were immersed into the above gel-forming solution and sonicated for 15 min. The hybrid orthosilicic acid HPEI gel containing the biomimetically reduced silver nanoparticles formed onto the



surface micropores was slowly dried to xerogels at 65°C. When humidity removal was complete and no more weight loss was observed the metal coupons were thoroughly rinsed with deionized water to remove the excess of the xerogel. The nanocomposite coatings were characterized by IR and UV-Visible Spectroscopy, Dynamic Light Scattering, zeta potential and Thermogravimetry. Coating uniformity was established by optical (Figure 2a,b) and Scanning Electron Microscopy (SEM) (Figure c) and Energy Dispersive Spectroscopy (EDS) (Figure 3a). The silver-containing laminates exhibited comparable to much better catalytic properties than silica-silver nanoparticle catalysts towards nitrophenol reduction [9] (Figure 3b) but were able to complete at least 10 catalytic cycles instead of 3.

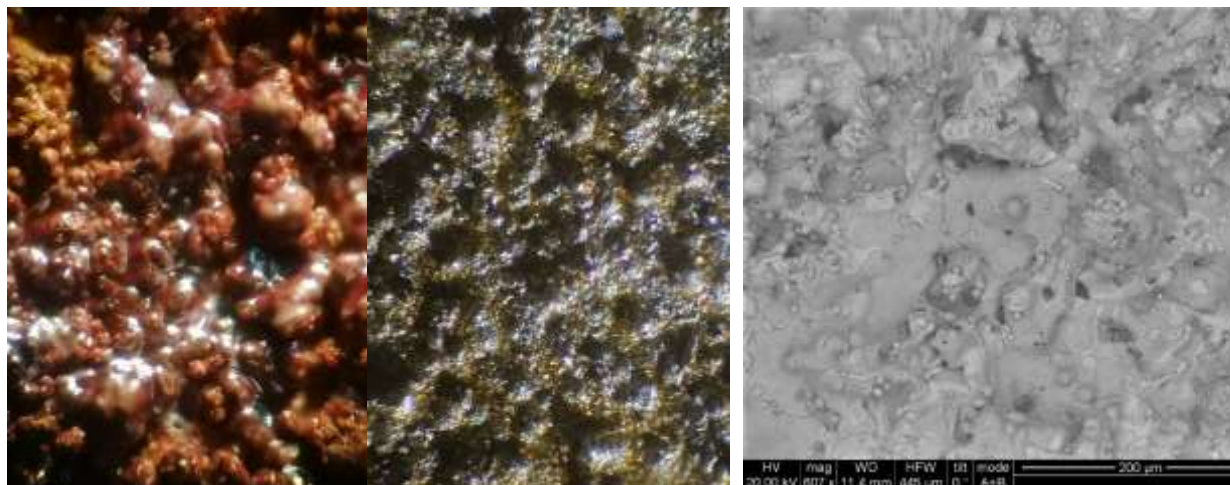


Figure 2. Optical Microscopy of (a) gel formed into the metal micropores (b) dried xerogel coatings onto stainless steel (c) SEM Micrograph of the dried xerogel.

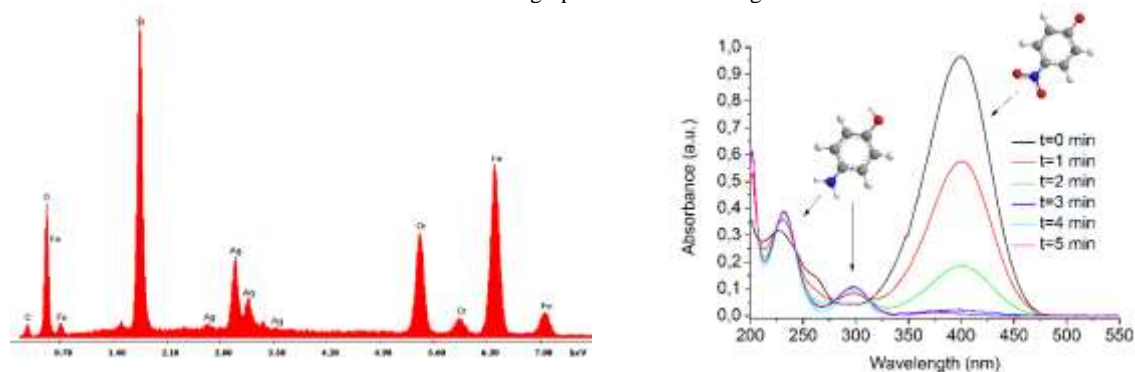


Figure 3. (a) Energy-dispersive X-ray spectroscopy of SiO<sub>2</sub>-PEI-Ag coatings to stainless steel. (b) UV-Vis spectra of 4-nitrophenol reduction.

## Acknowledgements

This work was co-financed by Greece/Greek General Secretariat for Research and Technology and European Union under the frame of EPAnEK 2014-2020 Operational Programme Competitiveness, Entrepreneurship Innovation, project “MEDNANOLEAT” grant number T6YBII-00081.

## References

1. M. Douloudi, E. Nikoli, T. Katsika, M. Vardavoulias, M. Arkas, *Nanomaterials*, **11** 19 (2020).
2. M. Douloudi, E. Nikoli, T. Katsika, M. Arkas Chapter 17: Dendritic polymers for water resources remediation in Book *Novel Materials for Environmental Remediation Applications : Adsorption and Beyond*. Elsevier. In Press.
3. M. Arkas, D. Tsiourvas, C. M. Paleos *Chem. Mater.* **15** 2844 (2003).
4. M. Arkas, D. Tsiourvas, C. M. Paleos *Chem. Mater.* **17** 3439 (2005).
5. M. Arkas, R. Allabashi, D. Tsiourvas, EM Mattausch, R Perfler *Environ. Sci. Technol.* **40** 2771 (2006).
6. R. Allabashi, M. Arkas, G. Hörmann, D. Tsiourvas *Water Res.* **41** 476 (2007).
7. M. Arkas, D. Tsiourvas *J. Hazard. Mater.* **170** 35 (2009).
8. M. Arkas, I. Anastopoulos, D. A. Giannakoudakis, I. Pashalidis, T. Katsika, E. Nikoli, R. Panagiotopoulos, A. Fotopoulou, M. Vardavoulias, M. Douloudi *Nanomaterials* **12** 445 (2022).
9. M Arkas, M Douloudi, E Nikoli, G Karountzou, I Kitsou, E Kavetsou, D Korres, S Vouyiouka, A Tsetsekou, K Giannakopoulos, M Papageorgiou *React. Funct. Polym.* **174**, 105238 (2022).

## Tuning the surface chemistry of nanoporous activated carbons towards diesel fuel desulfurization

Eleni D. Salonikidou<sup>1</sup>, Dimitrios A. Giannakoudakis<sup>1</sup>, Margaritis Kostoglou<sup>1</sup>, Eleni A. Deliyanni<sup>1</sup>, Konstantinos S. Triantafyllidis<sup>1,2</sup>

<sup>1</sup> Department of Chemistry, Aristotle University of Thessaloniki, University Campus, Thessaloniki, Greece

<sup>2</sup> Center for Interdisciplinary Research and Innovation (CIRI-AUTH), Balkan Center, 10th km Thessaloniki-Thermi Rd, P.O. Box 8318, 57001 Thessaloniki, Greece

\*elensalonikidou@gmail.com

During the last decade, the issue of deep desulfurization of liquid transportation fuels has attracted the research interest due to the strict regulations establishing the maximum levels of sulfur to be less than 10 ppmwS, as well as the harmful effects on human health and ecosystem, arising from the combustion of sulfur compounds [1,2]. Among the various methods proposed, adsorptive desulfurization using nanoporous materials, like activated carbons, has been proposed as an effective, low-cost and green-oriented process for the elimination of sulfur-containing molecules from liquid fuels, in order to complete the industrially applied method of hydrodesulfurization [3]. In the present work, numerous commercial metal-free activated carbons with varying physicochemical features were tested for the adsorptive desulfurization of a model, along with the real diesel fuel, under mild conditions. With the intention to investigate in depth which physicochemical properties affect the desulfurization performance of the adsorbents, in addition to tuning their surface chemistry, four activated carbons with different porosity, surface chemistry heterogeneity and desulfurization efficiencies were chemically modified through treatment with HNO<sub>3</sub>. Initially, the adsorptive capacity of the carbons was evaluated for the removal of 4,6-dimethyldibenzothiophene (4,6-DMDBT) from hexadecane, starting from low initial sulfur concentration (20 ppmwS). Aiming at exploring the impact of the co-presence of aromatic compounds in the desulfurization procedure, several model diesel fuels were created, with the addition of benzene and naphthalene with different initial concentrations, as a representative of the mono- and di- aromatics, respectively. The co-presence of an additional sulfur compound, dibenzothiophene (DBT), in the model diesel fuel was also explored.

The results clearly designate that the chemical treatment through HNO<sub>3</sub> had a positive effect on the adsorptive desulfurization efficiency of the activated carbons, implying that tuning the surface chemistry of the carbons via oxidation is an efficient strategy for material's design. Moreover, it was seen that there was a quite complicated correlation among the desulfurization performance of the adsorbents and their principal physicochemical properties, with both porosity and particularly surface chemistry to play a key role. The addition of benzene and naphthalene lowered the amount of sulfur adsorbed, revealing the antagonistic character of the aromatics. Increasing the concentration of the aromatics, mimicking those of the real diesel fuel, led to stronger competition and higher decrement of the performance of the carbons. On the contrary, the employed activated carbons indicated outstanding performance for the ultra-deep desulfurization of model and real diesel fuel (5.7 ppmwS), when higher amount of adsorbent is used, meaning desulfurizing 30 mL fuel/ g adsorbent in comparison to 400 mL fuel/ g adsorbent used in the previous experiments. The results revealed that the remaining sulfur concentration after adsorption in the model fuel was below 0.2 ppmwS and below 1 ppmwS for the real diesel fuel.

### Acknowledgments

This research has been co-financed by the European Regional Development Fund of the European Union and Greek national funds through the Operational Program Competitiveness, Entrepreneurship and Innovation (EPAnEK 2014-2020), under the Action "RESEARCH-CREATE-INNOVATE B' CALL" (Project: DESULFUR, code: T2EAK-01976).

### References

1. E. Svinterikos, I. Zuburtikudis and M. Al-Marzouqi, J. Nanotechnol., DOI:10.1155/2019/2809867.
2. K. S. Triantafyllidis and E. A. Deliyanni, Chem. Eng. J., 2014, 236, 406–414.
3. E. D. Salonikidou, D. A. Giannakoudakis, E. A. Deliyanni and K. S. Triantafyllidis, J. Mol. Liq., 2022, 351, 118661.

## Plant based fabrication of CuO/NiO Nanocomposite: A Green Approach for Low-Level Quantification of Vanillin in Food Samples

Amber R. Solangi<sup>1\*</sup>, Arfana Mallah<sup>2</sup>, Iqleem H. Taqvi<sup>3</sup>

<sup>1</sup>National Centre of Excellence in Analytical Chemistry, University of Sindh, 76080 Jamshoro, Pakistan

<sup>2</sup>M.A.Kazi Institute of Chemistry, University of Sindh, 76080 Jamshoro, Pakistan

<sup>3</sup>Dept. of Chemistry, Govt. College University Hyderabad, Pakistan

\*Email address of Corresponding Author: [ambersolangi@gmail.com](mailto:ambersolangi@gmail.com); [amber.solangi@usindh.edu.pk](mailto:amber.solangi@usindh.edu.pk)

### Abstract

Vanillin is a flavoring substance commonly used in the food and pharmaceutical industry. The rampant use of vanillin has significant implications on human health. In the present experiment, a simple, green, and economic electrochemical sensor is constructed by combining the characteristics of CuO/NiO nanocomposite material. The fabricated nanocomposite was characterized through advanced tools such as XRD, FTIR and TEM which revealed high crystalline structure, surface functionalities and Nano flower like morphology of prepared material. The modified electrode was constructed using CuO/NiO/GCE. For the investigation of conductive nature, the proposed CuO/NiO/GCE was exploited to the primary electrochemical characterization tools e.g. Cyclic voltammetry (CV) and electrochemical impedance spectroscopy (EIS). The CuO/NiO/GCE was utilized as sensitive electrochemical sensor for the determination of vanillin under acceptable linear dynamic range at scan sweep of 100 mV/s. The PBS buffer with pH 7 was optimized for the fluent determination of vanillin. The LOD of proposed sensor was found to be lower than other reported electrochemical sensors. The analytical applicability of CuO/NiO/GCE was tested in different food samples such as ice cream and chocolate. The modified electrochemical sensor manifested acceptable recovery values in real food samples which exhibits the reliability of CuO/NiO/GCE.

# Nanomaterials for energy & environment

# Perovskite BaTaO<sub>2</sub>N: A Promising Candidate for Solar Water Splitting

Mirabbos Hojamberdiev\*

Institut für Chemie, Technische Universität Berlin, 10623 Berlin, Germany

\*Corresponding author: [hmirabbos@gmail.com](mailto:hmirabbos@gmail.com)

Although hydrogen is a zero-emission energy carrier, its current global production still heavily relies on fossil fuels. Current momentum on renewable energy and environmental remediation is unprecedented because of fast climate change. We all know that the world is hurrying up to achieve the United Nations Sustainable Development Goals (SDGs) by 2030 without pausing even during the COVID-19 pandemic. One of the important SDGs is Goal 7: Affordable and Clean Energy. As a replica of natural photosynthesis, a semiconductor-based artificial photosynthetic system is regarded as one of the most economically viable, highly efficient, and environmentally benign chemical processes to generate green hydrogen energy from solar water splitting. However, to harness solar energy efficiently, it is necessary to enhance the visible-light-driven photocatalytic performance of the existing materials and to discover novel visible-light-active materials. Mixed-anion compounds offer new opportunities in this regard [1]. As a 600 nm-class photocatalyst, BaTaO<sub>2</sub>N has received particular attention due to its small bandgap ( $E_g = 1.8$  eV), suitable band edge positions for visible-light-induced water splitting, chemical stability, and nontoxicity [2,3]. BaTaO<sub>2</sub>N is routinely synthesized by a two-step method: (i) the synthesis of a corresponding oxide precursor and (ii) its high-temperature nitridation under an NH<sub>3</sub> atmosphere for a prolonged period. This two-step method leads to the formation of various defects that negatively affect the water splitting performance. Therefore, we have (i) applied an NH<sub>3</sub>-assisted direct flux growth approach to reduce the defect density of BaTaO<sub>2</sub>N, (ii) engineered the bandgap by cation substitution, and (iii) explored the effects of the altered morphology, size, and porosity on the visible-light-induced water oxidation activity and photoelectrochemical performance of BaTaO<sub>2</sub>N. The findings revealed that the photocatalytic activity and photoelectrochemical performance of BaTaO<sub>2</sub>N were significantly influenced by its morphology, size, porosity, substituent type, and substitution concentration. Particularly, the BaTaO<sub>2</sub>N crystal structures obtained by nitridation of oxide precursor without KCl flux exhibited a higher surface area and high anodic photocurrents compared to the BaTaO<sub>2</sub>N crystal structures obtained by nitridation of oxide precursor with KCl flux due to the high number of dangling bonds acted as a nucleation centers for the highly dispersed CoO<sub>x</sub> cocatalyst nanoparticles. Also, an NH<sub>3</sub>-assisted direct flux growth approach reduced the density of intrinsic defects in BaTaO<sub>2</sub>N crystals, leading to the substantial enhancement in water oxidation activity. The Mg-substituted BaTaO<sub>2</sub>N and Al-substituted BaTaO<sub>2</sub>N independently exhibited the highest amounts (in 5 h) of evolved O<sub>2</sub> (503.6 μmol) and H<sub>2</sub> (117.4 μmol), respectively, whereas the Zr-substituted BaTaO<sub>2</sub>N showed the high photocatalytic activities in both O<sub>2</sub> (446.8 μmol) and H<sub>2</sub> (80.4 μmol) half-reactions due to the altered potentials of the valence and conduction bands and an increased density of charge carriers.

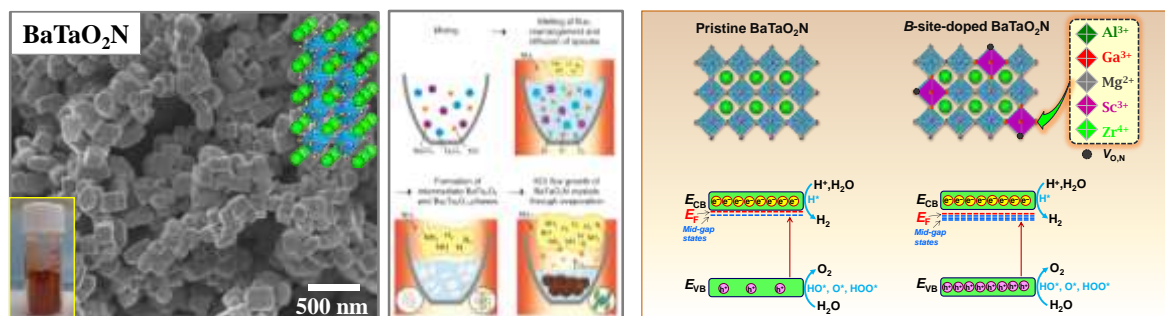


Figure 1. BaTaO<sub>2</sub>N crystals grown by an NH<sub>3</sub>-assisted flux method (left) and band structures of pristine and cation doped BaTaO<sub>2</sub>N (right).

## Acknowledgements

This project received funding from the European Union's Horizon 2020 Research and Innovation Programme under the Marie Skłodowska-Curie grant agreement no. 793882.

## References

1. H. Kageyama, K. Hayashi, K. Maeda, J. P. Attfield, Z. Hiroi, J. M. Rondinelli, K. R. Poeppelmeier, *Nat. Commun.*, **9** 772 (2018).
2. R. Marchand, F. Pors, Y. Laurent, O. Regreny, J. Lostec, J.M. Haussonne, *J. Phys. Colloques*, **47** C1-901 (1986).
3. M. Higashi, R. Abe, K. Teramura, T. Takata, B. Ohtani, K. Domen, *Chem. Phys. Lett.*, **452** 120 (2008).

## Natural mineral lintsite as the base for the new range of functional materials

Galina O. Kalashnikova<sup>1</sup>, Elena S. Zhitova<sup>2</sup>, Ekaterina A. Selivanova<sup>1</sup>, Yakov A. Pakhomovsky<sup>1</sup>, Victor N. Yakovenchuk<sup>1</sup>, Aiiia V. Bazai<sup>1</sup>, Taras L. Panikorovskii, Victor N. Korovin<sup>1</sup>, Maria N. Timofeeva<sup>3,4</sup>, Anatoliy I. Nikolaev<sup>1</sup>

<sup>1</sup>Federal Research Center «Kola Science Center» RAS, 14 Fersman Street, 184209, Apatity, Russian Federation;

<sup>2</sup>Department of Crystallography, Faculty of Geology, St. Petersburg State University, 7–9 University Emb. Street, 199034, St. Petersburg, Russian Federation;

<sup>3</sup>Borsov Institute of Catalysis SB RAS, Prospekt Akad. Lavrentieva 5, 630090, Novosibirsk, Russian Federation;

<sup>4</sup>Novosibirsk State Technical University, Prospekt K. Marksa 20, 630092, Novosibirsk, Russian Federation

\*g.kalashnikova@ksc.ru

### Introduction

The central aim of this work was to investigate natural lintsite family minerals properties, find their interesting and useful sides for engineering, materials and ecology; develop a universal and green method for the synthesis of synthetic counterparts of minerals; use for synthesis end-product waste from regional ore-enrichment and metallurgical plants; reproduce and save the most useful properties of the minerals for their synthetic analogs.

### Experimental

Chemicals used were of reagent or analytical grade quality, obtained from commercial suppliers and used without further purification (Merck and Aldrich). Powder of titanyl sulfate  $(\text{NH}_4)_2\text{TiO}(\text{SO}_4)_2 \cdot \text{H}_2\text{O}$  (STA) was the loparite and sphene treatment product (PJSC «Apatit», PhosAgro company and Kola Science Centre, Russia).

The evaluation of chemical compositions of natural and synthetic samples and their transformed forms, identification their morphology were determined using scanning electron microscope LEO-1450 (Carl Zeiss Microscopy, Oberkochen, Germany) equipped with the QUANTAX 200 energy-dispersion system (Bruker, Ettlingen, Germany) with standardless processing (Geological Institute, Kola Science Centre, Russia) at 20 kV, 500–1000 pA, 1–3 μm spot size. The study was carried out using polished and unpolished samples for synthetic samples. The content of elements in research solutions were studied by AAAnalyst 400 Atomic Absorption Spectrometer and ICP-mass spectrometer system ELAN 9000 DRC-e (PerkinElmer LAS, USA) (Institute of Chemistry, Kola Science Centre, Russia). The synthetic phases and their transformation product were characterized by means of powder X-ray diffraction using a Bruker D2 Phaser diffractometer ( $\text{CuK}\alpha$  radiation, 30 kV/10mA) (XRD Research Center, St. Petersburg State University).

The products after catalytic tests were analyzed by a gas chromatograph (Agilent 7820) equipped with a flame ionization detector and using a HP-5 capillary column, after separation by centrifugation of the catalysts (Borsov Institute of Catalysis SB RAS and Novosibirsk State Technical University, Russia).

### Results and Discussion

Federal Research Center «Kola Science Center» of RAS is situated near the Khibiny Mountains (Kola Peninsula, Murmansk region, Russia) which is one of the place on the Earth with more than 500 types of minerals. For the same reason, the Europe-biggest mining companies: PJSC «Apatit» and «JSC Kola Mining & Metallurgical Company», and some other leading enterprises («KovdorGOK», «Kovdorsluyda», «Oikon», «Lovozerky GOK») are situated in Murmansk region in Arctic zone. These companies producing up to 100% phosphoric raw materials in Russia, 10–12% iron ores, 18–20% Ni, Cu and Co, up to 100% Zr, 80–90% mica, about 35% ceramic raw materials, 70–80% Nb- and Ta-bearing concentrates. Mineral processing at mining all around the world, mining and chemical plants is known to be accompanied by the formation of solid and liquid wastes of both natural and synthetic origin. Stored in tailing dumps, these wastes pose a serious environmental hazard. At the same time, mineral components of the tailings can either be turned into natural geochemical barriers, preventing the dissolved toxic elements from escaping into the environment, or converted into valuable engineering materials [1].

One of the amazing example of these materials is the synthetic analogs of titanosilicates minerals from lintsite family (Fig. 1). We have established that crystal structure of lintsite has interesting property in its transformation. In this work our research interests have been concentrated on the study of unusual single-crystal-to-single-crystal transformation of natural framework titanosilicates of the lintsite family [2] and their synthetic counterpart AM-4 [3]. The transformation occurs in any acidic solution. Protonation of the above mentioned compounds results in the formation of new layered titanosilicates K3 (after kukisvumite), L3 (after lintsite) and SL3 (after AM-4) with new crystal structure. All these compounds have the same composition,  $\text{Ti}_2\text{Si}_4\text{O}_{10}(\text{OH})_4$ , and the similar structure motifs. It was discovered that the crystal structure of the new crystalline titanosilicate is based upon electroneutral titanosilicate blocks that are closely packed together to form a dense layered structure. Blocks are linked by hydrogen bonds [4]. In view of the fact that natural minerals of lintsite group are extremely rare for large scale production, in this work we started to find the new ways to synthesize their analogue AM-4 on the base of inexpensive and additional processing raw materials (titanyl sulfate  $(\text{NH}_4)_2\text{TiO}(\text{SO}_4)_2 \cdot \text{H}_2\text{O}$  (STA)).

Especially pure and, therefore, expensive reagents are often used for the synthesis of titanosilicates, which significantly increases the cost and limits their widespread use. It is possible in laboratory but not in technological

scale. We have developed an innovative technology of lintsite synthesis, which better for terms of technological, environmental and economic importance. Because it is based on the use of available titanium-containing raw materials and modern technological methods that provide high physical and technical properties of the final product.

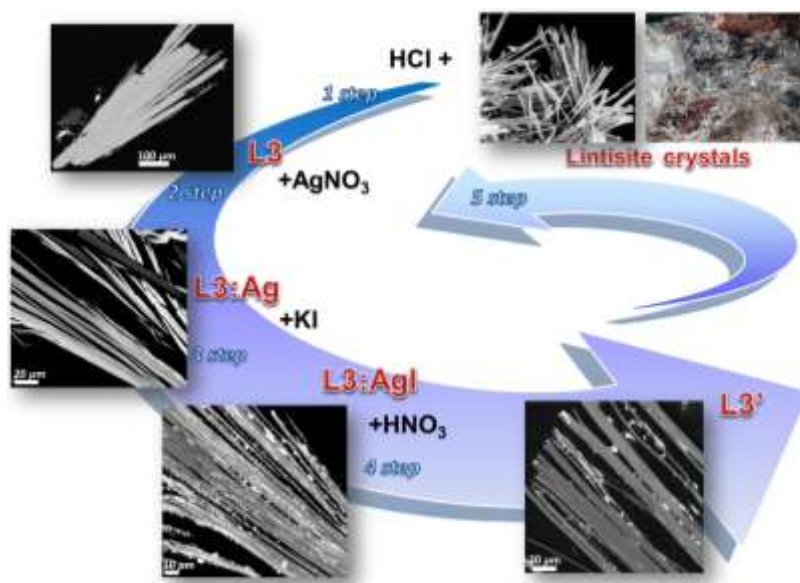


Figure 1. Titanosilicate nanopuzzle L3 operation scheme.

## Conclusions

The perspectives of practical use of synthetic analog lintsite (AM-4) and SL3 include (photo)catalysis, purification of radioactive wastes and energy storage. In particular, this material can be used for the catalytic synthesis of 1.5-benzodiazepine from 1.2-phenylenediamine and acetone, for the synthesis of 1-methoxy-2-propanol (PGME) from methanol and propylene oxide (PO), selective removal of iodine from water solutions, cleaning of industrial electrolytes from noble metals (Ag), and production of self-cleaning building materials.

It is possible to create new compounds on the base of titanosilicate nanopuzzle (L3 or SL3) with predicted properties for different fields of science and technology.

It is important that SL3 material can be used as the recyclable sorbent and not only for one process or cycle (Fig.1). It can help reduce the cost of producing new batches of sorbent and its subsequent disposal.

New titanosilicates useful materials are synthesized on the base of end-product waste from regional ore-enrichment and metallurgical plants that will help to improve more comprehensive processing of these sources and their competent disposal.

## Acknowledgements

This work was conducted within the framework of the budget projects AAAA-A17-117041710082-8 for Boreskov Institute of Catalysis (investigation of the AM-4 and SL3 catalytic properties) and AAAA-A17-117020110035-5 (investigation of the crystal structure of the titanium containing Khibiny minerals) for Nanomaterials Research Centre of the Federal Research Centre «Kola Science Centre» RAS (NMRC KSC RAS), respectively. We are grateful to PhosAgro/UNESCO/IUPAC grant № 4500422248 (synthesis of the lintsite synthetic analogs and granulation of the titanosilicates powders).

## References

1. A.I. Nikolaev, G L.Gerasimova, M.G. Maslova, *Minerals as Advanced Materials II* (Ed. S.V.Krivovichev). Springer-Verlag, Berlin-Heidelberg, (2012).
2. G.O. Kalashnikova, E.S.Zhitova, E.A. Selivanova, et al. *Microporous and Mesoporous Materials*, 313 (2021). DOI: 10.1016/j.micromeso.2020.110787
3. M.S. Dadachov, J. Rocha, A. Ferreira, et al., *Chem. Commun.*, 2371-2372 (1997).
4. Patent 2567314 RU C01G 23/00, C01B 33/20 (2006.01), date of publication 10.11.2015, Bull. № 31.

## Green synthesis of nanosized energy storage electrode materials for lithium-ion batteries

Ahmed M. Hashem\*

*Inorganic Chemistry Department, National Research Centre, 33 El Bohouth St., (former El Tahrir St.), Dokki-Giza 12622, Egypt*

*\*ahmedh242@yahoo.com*

### Abstract

Design a safe and green rechargeable lithium-ion battery (LIBs) with high efficiency, good long life, and high specific capacity plays a critical role in today's world of mobile communications, portable electronics, and electric vehicle. So, the green synthesis and characterization of nanostructural electrode materials that adopt this kind of rechargeable batteries leads to batteries with even high energy densities and allows reduction of size of the battery packs to power the same equipment. Nanosized materials are important for electrochemical energy storage and are expected to improve the performance of lithium batteries. The use of nanosized solid-state materials not only improves the power density but also facilitates Li-ions insertion/extraction in/out of the storage materials, which improves the cycle life of lithium batteries. Nanosized electrode materials used in lithium-ion batteries can offer; large surface area, shorter distance for Li diffusion, good strain relaxation, interface control, continuous electron transport pathway and higher specific capacity and better rate capability than the large size particles. This will provides LIBs with; faster charging and long discharging time, longer battery life, higher power, operation in extreme temperature conditions and ultra-safe characteristics. These advantages candidate lithium-ion batteries to be the best choice for electric vehicles which can decrease the rely on fossil fuel, improve the quality of air and develop the transportation system as they are low- or zero-emission which can be operated by lithium-ion batteries.

Keywords; Nanotechnology; electrode materials; Li-ion batteries; electric vehicles.

### References

1. Hua Wang, Tianyi Li, Ahmed M. Hashem, Ashraf E. Abdel-Ghany, Rasha S. El-Tawil, Hanaa M. Abuzeid, Amanda Coughlin, Kai Chang, Shixiong Zhang, Hazim El-Mounayri, Andres Tovar, Likun Zhu, and Christian M. Julien, Nanostructured Molybdenum-Oxide Anodes for Lithium-Ion Batteries: An Outstanding Increase in Capacity, *Nanomaterials* 2022, 12, 13
2. A.M. Hashem, H. Abuzeid, M. Kaus, S. Indris, H. Ehrenberg, A. Mauger, C.M. Julien, Green synthesis of nanosized manganese dioxide as positive electrode for lithium-ion batteries using lemon juice and citrus peel, *Electrochimica Acta* 262 (2018)74-8.



# Galvanic-Replacement Enabled Synthesis of In(OH)<sub>3</sub>/Au/C Nanocomposite and Its Photocatalytic Degradation of Methylene Blue

P. M. Wong<sup>1</sup>, R. D. Tilley<sup>2</sup>, J. C. Juan<sup>3</sup>, J. C. Lai<sup>4</sup>, T. H. Lim<sup>1\*</sup>,

<sup>1</sup>Faculty of Applied Sciences, Tunku Abdul Rahman University College, 53300, Kuala Lumpur, Malaysia

<sup>2</sup>School of Chemistry, University of New South Wales, Sydney, 2052 Australia

<sup>3</sup>Nanotechnology & Catalysis Research Centre, University of Malaya, 50603, Kuala Lumpur, Malaysia

<sup>4</sup>Biopolymer Research Group, School of Chemical and Energy Engineering, Universiti Teknologi Malaysia, Skudai 81310, Malaysia

\* limth@tarc.edu.my

## Abstract text:

Indium metal nanoparticles (sub-10 nm) stabilized on conductive carbon (In NPs/C) were recently reported to be an excellent reducing platform for the controlled growth of Ag nanoparticles in which excellent size and shape controls were achieved simultaneously by forcing galvanic replacement to occur in a confined space.[1-2] In this paper, we extended the work to gold by reacting In NPs/C with gold chloride in dark in water at room temperature in a galvanic manner to produce a In(OH)<sub>3</sub>/Au/C nanocomposite. The chosen carbon imparted colloidal stability, high surface area and water dispersibility—three features deemed desirable for the efficient photodegradation of dyes in water. The In(OH)<sub>3</sub>/Au/C nanocomposite was characterized using a combination of HRTEM, PXRD and TGA. The galvanic reaction between In NPs and gold chloride was also tracked in real time using UV-Vis spectroscopy to gain insights into the replacement efficiency. The In(OH)<sub>3</sub>/Au/C nanocomposite was tested as a photocatalyst to degrade methylene blue and its performance would be discussed.

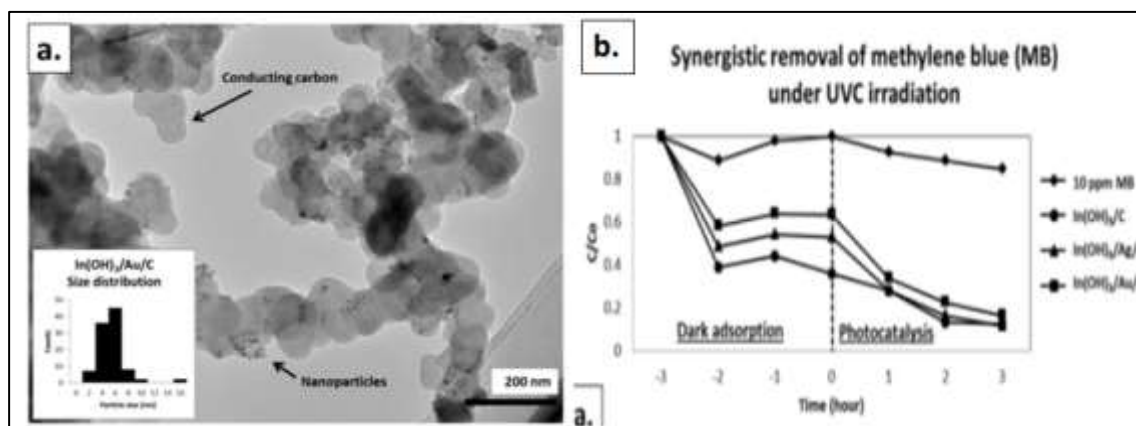


**Figure 1.** (a) Bright field TEM images of In(OH)<sub>3</sub>/Au/C nanocomposite showing In(OH)<sub>3</sub> NPs and Au NPs distributing on carbon substrate with mean particle size of 6.5 ± 2.1 nm; (b) Synergistic removal of methylene blue (MB) under UVC irradiation with 10 ppm MB solution. The removal efficiencies of 10 ppm MB were calculated to be 15 % for blank, 87 % for In(OH)<sub>3</sub>/C, 88 % and 84 % for In(OH)<sub>3</sub>/Au/C nanocomposite;

## Acknowledgements

The authors express their gratitude to the Ministry of Education Malaysia and Tunku Abdul Rahman University College for funding this work through the Fundamental Research Grant Scheme (grant number 4F827) and TARUC Research Grant (project number 86007).

## References

1. P. M. Wong, J. C. Juan, J. C. Lai, T. H. Lim, ACS Omega, 5(23), 13719-13728 (2021).
2. C. Andronesco, J. Masa, R. D. Tilley, J. J. n Gooding, W. Schuhmann, Curr. Opin. Electrochem., 25, 100644 (2021).

**Au-Cu<sub>2-x</sub>Te disk-on-dot Hetero-nanostructure Photoelectrocatalysts**

Suvodeep Sen and Narayan Pradhan\*

School of Materials Sciences, Indian Association for the Cultivation of Science, Kolkata, West Bengal, India

Email: suvodeepsen671@gmail.com

**Abstract**

Plasmonic copper chalcogenide semiconductor nanocrystals coupled with plasmonic Au nanoparticles have been widely studied as photoelectrocatalysts for solar water splitting. Among these, while sulphides and selenides are extensively reported, but heterostructures of copper tellurides have not been explored. This is possibly due to larger size of telluride ion and difficulty in lattice matching for creating the heterojunctions. Herein, plasmonic semiconductor Cu<sub>2-x</sub>Te disks grown on Au particles were explored (**Fig. 1a**) as efficient photoelectrocatalysts for hydrogen evolution reactions (HER). This has been successfully designed by growing Cu<sub>2-x</sub>Te disks on presynthesized Au particles under optimized reaction conditions. Resulting disk-on-dot nanocrystals acted as efficient photoelectrocatalysts for H<sub>2</sub> evolution reaction with low Tafel slope and less cathodic overpotential in presence of light (**Fig. 1b**). Details of their synthesis, characterization, optical properties and electrocatalytic activities are studied in this report.

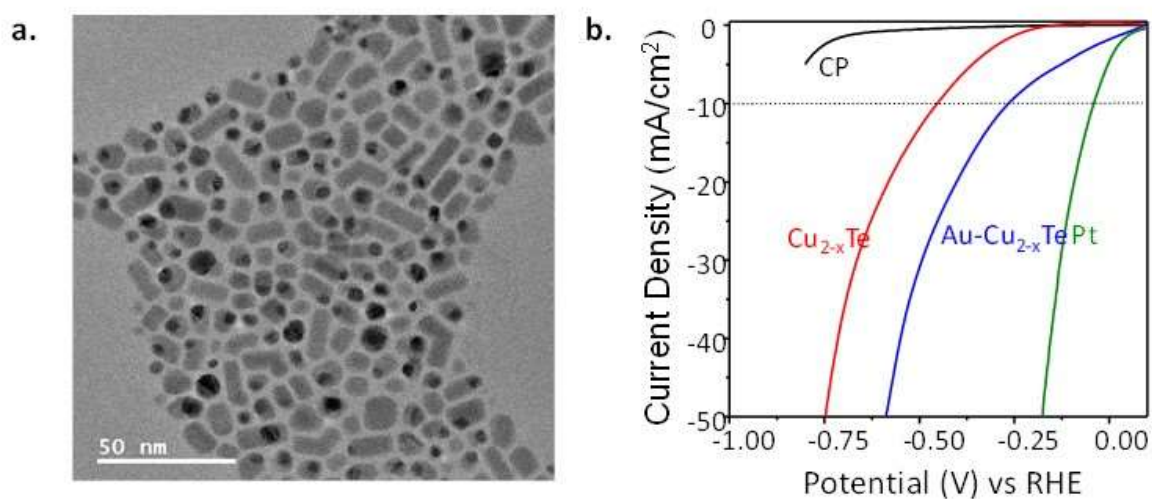


**Fig. 1.** (a) TEM images of Au-Cu<sub>2-x</sub>Te. (b) Polarization plot of Carbon Paper, Cu<sub>2-x</sub>Te, Au-Cu<sub>2-x</sub>Te nanocrystals and Pt wire

**Acknowledgements**

DST-SERB (EMR/2016/001795) of India is acknowledged for funding. Suvodeep Sen acknowledges UGC for fellowship.

**References**

1. S. Linic, P. Christopher, D. B. Ingram, *Nat. Mater.*, **10**, 911-921 (2011).
2. S. K. Dutta, S. K. Mehetor, N Pradhan, *J. Phys. Chem. Lett.*, **6**, 936-944 (2015).

# Plastic waste recycle and valorization

## Chemical recycling of plastic waste towards waxes and lubricants

Jonathan Van Waeyenberg and Bert F. Sels\*

Center for Sustainable Catalysis and Engineering, Faculty of Bioscience Engineering, KU Leuven, Heverlee 3001, Belgium.

\*bert.sels@kuleuven.be

Polyethylene plastics comprises a big part of the growing plastic waste production. This plastic is however hard to recycle, they often end up in landfills or are simply burned. There is a high need for implementing new recycling pathways as a way to increase the conversion towards a circular economy. Recently, researchers have shown increasing interest in polyethylene chemical recycling as it is a promising way to extend the polyethylene life cycle and a potential valuable feedstock for the chemical industry. In this context, the aim of this study is the chemical recycling of polyethylene plastics towards valuable chemicals, specifically the conversion to waxes and lubricants (base oils). The scope of this study is to obtain industrially relevant waxes such as paraffin and microwaxes. In addition, this research focuses on producing high quality base oils for lubricants such as Group III and IV base oils.

The applied methodology for achieving wax and base oil products is structured in three stages: (I) a (mild) pyrolysis step, (II) physical separations (distillation), and (III) catalytic upgrading and refining. (I) In the first step, a conical spouted bed reactor was used, this reactor shows high conversion towards heavier hydrocarbons and minimizes secondary cracking as well as secondary side-reactions. This reactor thus shows to be very suitable for the production of waxes and lubricants [1,2]. The main product of this pyrolysis step is a pyrolysate which is high in olefinicity and has a limited isomer content, its carbon distribution ranges from gaseous to heavy wax products. (II) In a second step, distillation needs to be applied to separate the heavy ( $C_{20+}$ ) fraction from the lighter liquid fraction in the pyrolysate. This heavy fraction can then be used for the optimization towards waxes, the lighter fraction can then be used for the production of base oils. (III) Finally, catalytic upgrading was implemented for tuning these fractions towards waxes and lubricants (base oils). The main focus in the catalytic upgrading step is the use of solid acid catalysts such as zeolites and modified (mesoporous) zeolites. This stage is important as it permits to tune the properties of the isolated pyrolysate fraction. Different catalytic conversion strategies were applied depending of the desired products.

The important parameters for the wax properties are their average molecular weight, the branching quantity (isomer content), amount of branches per isomer (monobranching vs. multibranching) and site of branching (end- to middle-chain). For obtaining the desired isomer content for each wax type, a skeletal isomerization can be implemented. This study focuses on two types of isomerization strategies. One isomerization strategy is the use of the double bonds of the olefinic rich pyrolysate, these are then later removed by hydrogenation catalysis. To our knowledge, this kind of skeletal isomerization, which uses double bonds of long chained olefins, is not studied to a great extent yet. Another strategy is the hydroisomerization, here metals on solid acid catalysts can be used for the isomerization and hydrogenation. A comparison of the different catalytic modifications is of focus in this study. For the production of lubricants (base oils), the liquid fraction of the pyrolysate is used. The applied strategy in this research is the use of solid acid catalysts for a dimerization or oligomerization using the olefinic molecules. In this way longer hydrocarbons can be obtained with long side-chains. After hydrogenation and distillation, these dimers and oligomers can be used as alternative base oils.

To gain more insight in the catalytic steps, a model compound study was used for the wax and base oil products. For the waxes, the branching chemistry was monitored in detail. The dimerization or oligomerization chemistry was monitored for the base oil production. Some findings of the model compound study for the waxes using the skeletal isomerization with the double bonds can be seen in Figure 1. Different selectivities for the mono- and multibranching yields can be acquired with different types of catalysts. A major difference in one-dimensional 10-membered ring (1D-10MR) and three-dimensional 10- or 12-MR ring zeolites can be seen. This reflects the ability of the 1D-10MR ring zeolites for pore-mouth catalysis, resulting in less multibranching. Different selectivities can also be noted for the branching site on the molecule, this reflects again the importance of the choice of isomerization catalyst.

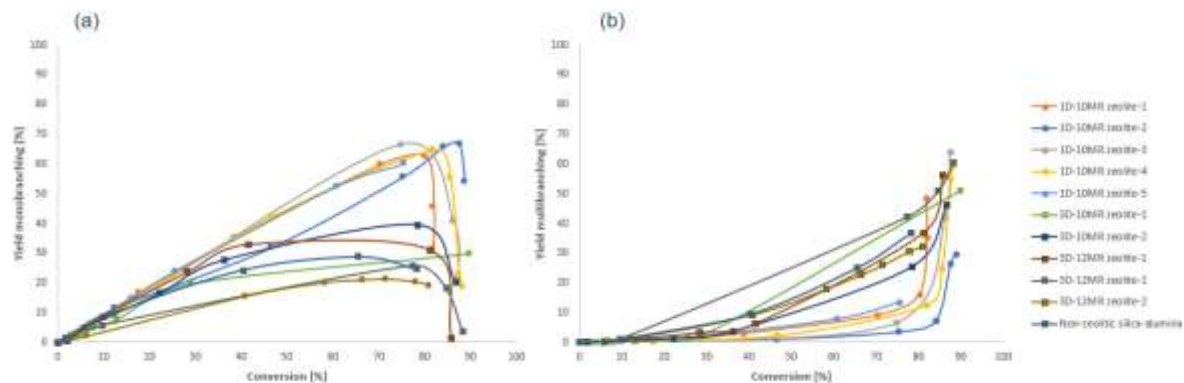


**Figure 1.** Yield of the monobranching (a) and multibranching (b) in function of the overall conversion, using a 1-octadecene model compound that was tested with different solid acid catalysts.

In the lubricant study, some promising catalysts show very fast and high conversions with high dimer/oligomer yields. Different selectivities can be noted for the dimers/oligomers, leading to products with different properties.

### Acknowledgements

This work was supported via the WATCH SBO project (HBC.2019.0001) and F.W.O.-Vlaanderen (G0B7218N).

### References

1. M. Arabiourrutia, G. Elordi, G. Lopez, E. Borsella, J. Bilbao, M. Olazar. *Journal of Applied Pyrolysis*, **94** 230 (2012)
2. M. Arabiourrutia, G. Elordi, M. Olazar, J. Bilbao. *Pyrolysis*, 285 (2017)

## Valorization of Polyhydroxyalkanoates as Circular Carbon Feedstock Beyond Bioplastics

Joel B. Mensah<sup>1\*</sup>, Minka C. Snoek<sup>1</sup>, Pieter C. A. Bruijninx<sup>1\*</sup>

<sup>1</sup>Organic Chemistry and Catalysis, Debye Institute for Nanomaterials Science, Utrecht University, Universiteitsweg 99, 3584 CG Utrecht, The Netherlands

\* [j.b.mensah@uu.nl](mailto:j.b.mensah@uu.nl), \* [p.c.a.bruijninx@uu.nl](mailto:p.c.a.bruijninx@uu.nl)

A sustainable synthesis of chemicals and materials necessitates a paradigm shift, namely our transition from a linear to a circular society. Central to this, will be the implementation of closed carbon loops and reduction of net CO<sub>2</sub> emissions. In the energy sector, this can be tackled by decarbonization of the energy source, *i.e.*, shifting away from burning of fossil feedstocks and expanding wind, solar, hydro, and nuclear technologies for heat and energy generation.[1] On the contrary, decarbonization is not an option for the chemical industry, as most of the products and their properties fundamentally rely on carbon-based structures. Carbon neutrality in the chemical sector can then only be achieved by carbon circularity. This calls for methods that combine recycling with the use of renewable resources as virgin feedstock intake to make up for inevitable recycling losses. In this light, carbon-containing waste streams, in addition to CO<sub>2</sub> and biomass, should be considered an (equitable) resource.

Microorganisms can, for example, be employed to sequester carbon-containing waste streams and provide a reservoir for the production of renewably sourced chemicals. In fact, such microbial conversions are highly versatile and allow the conversion of dilute carbon concentrations into structures of considerable chemical complexity that offer manifold synthetic opportunities to connect to chemical value chains. One promising approach is to convert this carbon microbially to polyhydroxyalkanoate (PHA) biopolymers (Figure 1). The linear, isotactic PHA typically consists of C<sub>3</sub>–C<sub>14</sub> hydroxy acid units, which can be tailored through metabolic engineering, and due to their high biocompatibility and low water-solubility are generally considered as bio-based substitutes for fossil-sourced plastics.[2] With microbial PHA production evolving into a mature technology, we believe that new prospects arise to use these materials beyond application as biopolymers.

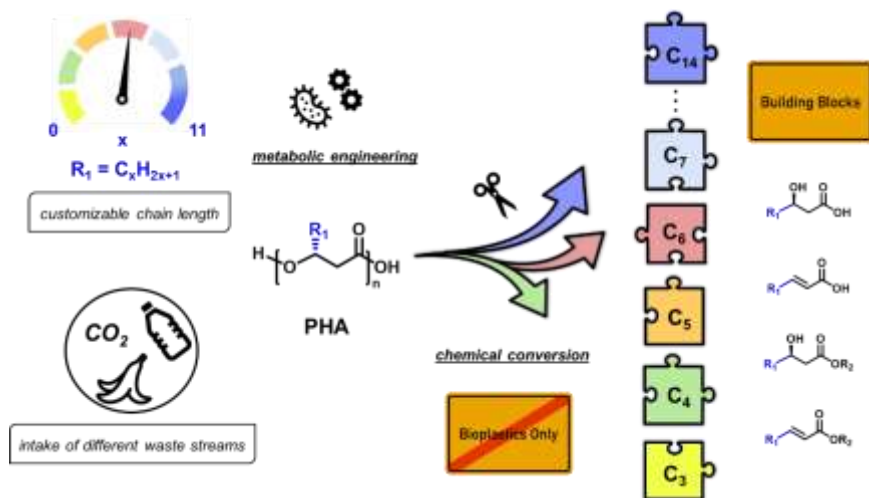


Figure 1. PHA valorization as platform for the conversion into new circular C<sub>3</sub>-C<sub>14</sub> building blocks.

In this work, we report on the emerging opportunities presented by waste-sourced PHAs for valorization as circular feedstock with a focus on poly(3-hydroxybutyrate) (PHB).[3] We propose to view PHB as a sequestered, functionalized reservoir of waste carbon for lower molecular weight C<sub>4</sub> building blocks [4, 5], allowing for a strategy similar, yet complementary to making platform molecules from (hemi)cellulose or lignin.[6] Complementary in the sense that it enables a new path to functionalized C<sub>4</sub>-monoacids which are limited and show a narrower product scope than sugar-based C<sub>3</sub>- and C<sub>5</sub>-platforms.

Furthermore, we have investigated the solvolysis of PHB at different reaction conditions, which gave access to methyl (R)-3-hydroxybutyrate (M3HB) and methyl crotonate (MC) as the principal PHB-derived platform molecules which can indeed be readily further (de)functionalized into various (value-added) compounds. The choice of the reaction conditions (*e.g.*, pressure, temperature, and reaction time) and/or use of solid catalysts (*e.g.*, TiO<sub>2</sub> or zeolites) allowed for steering of the product selectivity towards M3HB or MC respectively (Figure 2).

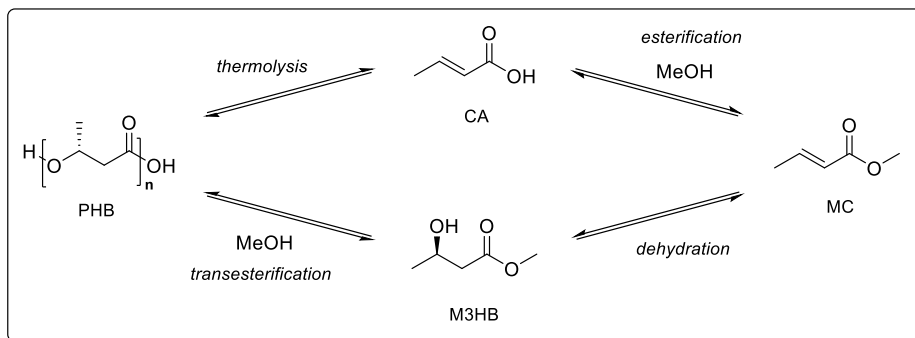


Figure 2. Depolymerization of PHB to M3HB and MC.

## Acknowledgements

J.B.M. gratefully acknowledges funding by the NWO [OCENW.XS21.2.099] and the Franz-Effenberger-Postdoctoral-Fellowship [awarded by the German Chemical Society (GDCh) sponsored by Clariant AG].

## References

1. IRENA, Global energy transformation: A roadmap to 2050, Abu Dhabi (2019).
2. V.C. Kalia, S.K. Singh Patel, R. Shanmugam, J.-K. Lee, *Bioresour. Technol.* **326** 124737 (2021).
3. J.B. Mensah, P.C.A. Bruijninx, *submitted* (2022).
4. H. Ariffin, H. Nishida, Y. Shirai, M.A. Hassan, *Polym. Degrad. Stab.* **95** 1375–1381 (2010).
5. A. Parodi, M. D'Ambrosio, L. Mazzocchetti, G.A. Martinez, C. Samorì, C. Torri, P. Galletti, *ACS Sustain. Chem. Eng.* **9** 12575–12583 (2021).
6. I. Delidovich, K. Leonhard, R. Palkovits, *Energy Environ. Sci.* **7** 2803–2830 (2014).

## Delamination of polyamide/polyolefin multilayer films by selective glycolysis of polyurethane adhesive

G. O'Rourke<sup>1</sup> and D. De Vos<sup>1\*</sup>

<sup>1</sup> Centre for Membrane Separations, Adsorption, Catalysis and Spectroscopy for Sustainable Solutions (cMACS), KU Leuven, 3001 Leuven, Belgium \*dirk.devos@kuleuven.be

### Abstract text:

The persistence of plastic packaging waste is a major environmental issue, which is gaining particular global concern. Since there is an annually growing production and most commercial plastics are non-biodegradable and very diverse in composition, waste management strategies fall short in preventing the accumulation of these plastics in landfills, rivers and oceans. Around 40% of the produced plastics is converted by the packaging industry. Recycling of multilayer packaging is challenging due to the heterogeneity of plastic types that can be comingled by chemical bonding with adhesives. Solvent based recovery allows efficient separation, but lacks fundamental insight to date. For this purpose, delamination of polyamide(PA)/polyolefin (PO) multilayers, glued together by polyurethane (PUR), was investigated. Two strategies were evaluated for recycling of the multilayers. A first method, using solvent targeted dissolution-precipitation (STRAP) for fractionation of the outer plastic layers (PO or PA) gave mixed fractions. (1) Fractionation of the film would be enabled by a solvent that is selective for either the OPA, or for the polyolefin layer. However, such a purely physical dissolution was difficult since covalent links exist between the various layers, e.g. between the corona-treated PP or PE, and the PUR adhesive (figure 1.a). In contrast, specifically targeting the PUR adhesive by glycolysis-depolymerization accomplished highly selective separation. A single processing step at mild temperatures in sustainable solvents based on ethylene glycol oligomers, detached the PA from the PO fraction, leading to split films without impurities (figure 1.b).

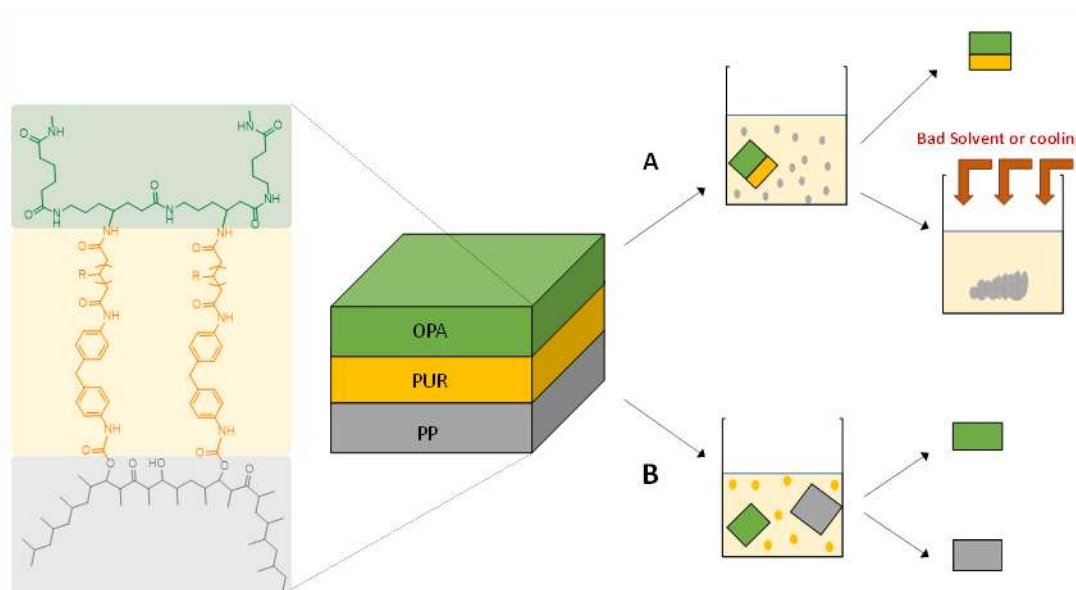


Figure 1. Structure of the investigated PP-based multilayer film and attempted methods for multilayer separation: (A) dissolution-precipitation with PP specific solvents at elevated temperature, (B) delamination by PUR glycolysis in alcohol solvents for detaching the two plastic layers.

Hence, in this work, a sustainable glycolysis-delamination process was developed that is selective for PUR. By employing diol solvents, in combination with ethanol amine (EA) or KOH, complete splicing of multilayer films was accomplished. Mass recovery was complete, demonstrating that diethylene glycol is a highly selective solvent for PUR (figure 2.) . This study is the first in its kind to analyze the chemistry of delamination in depth and introduces a process that could be generally applicable for a multitude of other multilayers that are bonded by PUR adhesives.



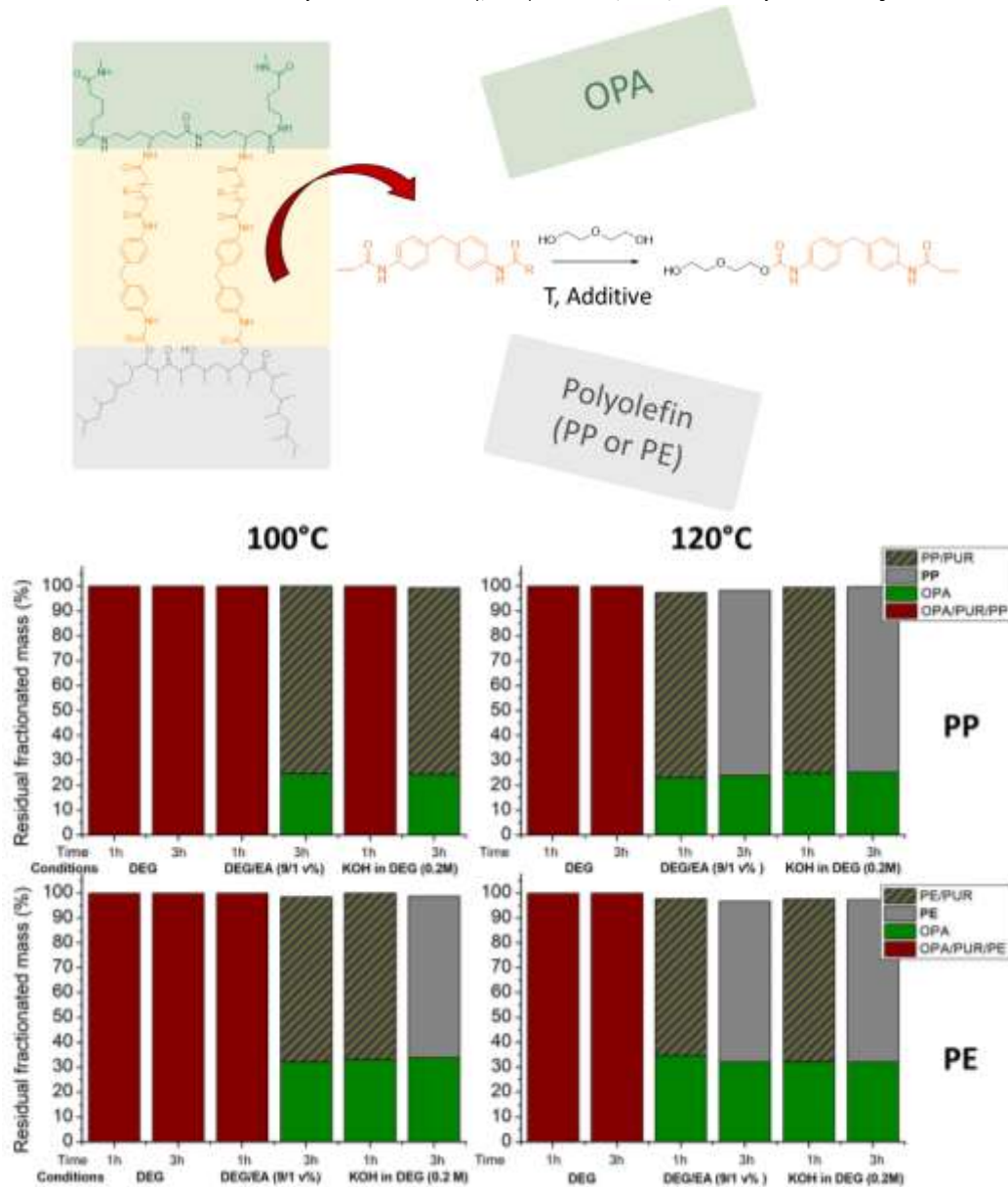


Figure 2. Multilayer delamination by glycolysis of PUR, with DEG with base additives: concept (top), quantified results (bottom). Mass fractions of residual films were determined gravimetrically; purities by ATR FTIR. Red bars: no multilayer separation; shaded bars: impure PP/PUR films; grey bars: pure PP or PE films.

## Acknowledgements

The authors are grateful for the financial support provided by the Catalisti-Moonshot project Multilayer granted by the Vlaams Agentschap Innoveren & Ondernemen (VLAIO). National Institutes of Health grant U12AV123456 (PV, CHO).

## References

1. T. W. Walker, N. Frelka, Z. Shen, A. K. Chew, J. Banick, S. Grey, M. S. Kim, J. A. Dumesic, R. C. Van Lehn, G. W. Huber, Recycling of multilayer plastic packaging materials by solvent-targeted recovery and precipitation. *Sci. Adv.* **6**, 1–10 (2020).

## Back-to-monomer recycling of polycondensation polymers: opportunities for chemicals and enzymes

Shanmugam Thiyagarajan,\* Evelien Maaskant-Reilink, Tom A. Ewing, Mattijs K. Julsing, Jacco van Haveren

Wageningen Food & Biobased Research, Wageningen, P. O. Box 17, 6700 AA, The Netherlands

\*E-mail: [shanmugam.thiyagarajan@wur.nl](mailto:shanmugam.thiyagarajan@wur.nl)

The use of plastics in a wide range of applications has grown substantially over recent decades, resulting in enormous growth in production volumes to meet the demands. Though a wide range of biomass-derived chemicals and materials are available on the market, the production volumes of such renewable alternatives are currently not sufficient to replace their fossil-based analogues due to various factors, performance and cost-effectiveness are in particular.

Hence, the majority of plastics are still industrially produced from fossil-based feedstocks. Moreover, various reports have clearly raised concern about the plastics that are not recycled at their end-of life and instead end up in landfills or the oceans. To avoid further pollution of our planet, it is highly desirable to develop recycling processes that use plastic waste as feedstock. Chemical recycling processes could potentially offer a solution, since they afford monomers from which new polymers can be produced, with the same performance as virgin plastics. In this presentation, the opportunities for using either chemical or biochemical (i.e., enzymatic) approaches in the depolymerization of polycondensation polymers for recycling purposes will be presented. Our aim is to highlight the strategies that have been developed so far to break down plastic waste into monomers, providing the first step in the development of chemical recycling processes for plastic waste, and to create a renewed awareness of the need to valorize plastic waste by efficiently transforming it into virgin plastics.

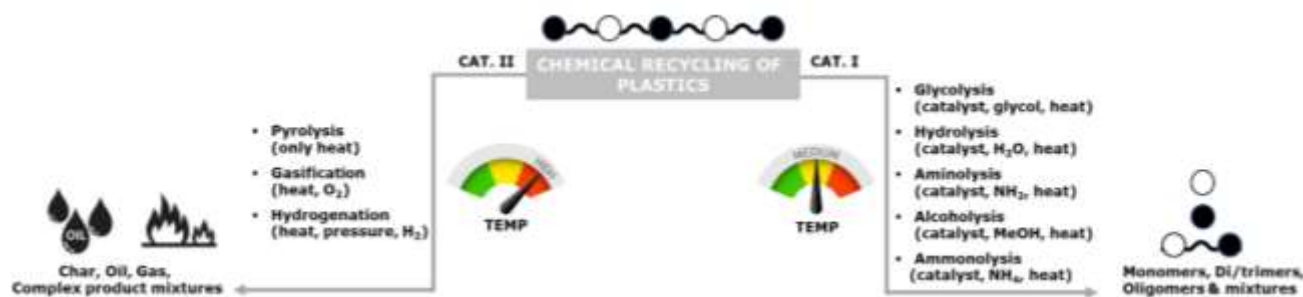


Figure 1. Classification of chemical recycling of plastics

### Acknowledgements

This research was funded by the Knowledge Base programme “Towards a circular and climate neutral society” of Wageningen University & Research (WUR), in the project “Bio-(chemical) recycling of products” (KB-34-011-002).

### References

1. S. Thiyagarajan, E.M. Reilink, T. A. Ewing, M.K. Julsing, J. van Haveren, *RSC Adv.*, **12**, 947-970 (2022).

## Debromination by soxhlet extraction and chemical recycling (pyrolysis) of various plastics collected from waste electric and electronic equipment

Charitopoulou M.A.<sup>1\*</sup> and Achilias D.<sup>1</sup>

<sup>1</sup> Department of Chemistry, Aristotle University of Thessaloniki (AUTH), 54124 Thessaloniki, Greece

\*e-mail address of corresponding author: ccmariia@chem.auth.gr

### Introduction

Nowadays, the amount of waste electric and electronic equipment (WEEE) has increased enormously because of the rapid expansion and consumption of electronic devices and their short lifespan. Recycling of WEEE is challenging, due to the presence of various materials including glass, metals and plastics (20-30%). Among the polymers identified in WEEE, high-impact polystyrene (HIPS), acrylonitrile-butadiene-styrene (ABS), polycarbonate (PC) and blends of PC/ABS, etc. are in larger amounts [1]. Brominated flame retardants (BFR) are often added into plastics in order to reduce their flammability, but they are toxic substances that must be removed. Pyrolysis is an environmentally friendly method, since secondary valuable materials or monomers can be recovered [2]. In the present work various plastic samples originating in WEEE, including televisions, computers, printers and remote controls, were gathered from a recycling plant and from end-of-life household appliances. All samples were subjected to Fourier transform infrared spectroscopy (FTIR) analysis and thermal pyrolysis in order to identify the polymers that were present in each device. Evolved Gas Analysis (EGA) using a pyrolyser was applied in order to investigate the degradation behaviour of the samples. X-ray fluorescence (XRF) analysis took place aiming to find which samples were brominated flame retarded and estimate the total bromine content of each sample. All brominated samples were subjected to soxhlet extraction with butanol with a view to reducing the bromine content, while maintaining the structure of the polymers, enabling their recycling through pyrolysis.

### Experimental

Various plastic materials from WEEE were collected from a recycling plant and from end-of-life household appliances and included eight television samples, three computer samples, two printer samples and three remote control samples. The solvent chosen for the soxhlet extraction was butanol, due to its low toxicity. After their collection, all plastic samples were reduced in size, using hand cutting tools and they were analysed by various techniques. Fourier transform infrared spectroscopy (FTIR) was applied in order to recognise the polymers that were present in each device, since they were unknown. Evolved gas analysis (EGA) was applied in order to receive information about the decomposition temperature range of the samples and for this reason, they were heated within the range of 100–700 °C, applying a rate of 20 °C/min. X-ray fluorescence (XRF) was conducted to all samples in order to identify the possible presence of bromine, in case they were brominated flame retarded. In this case they were subjected to soxhlet extraction in order to reduce bromine. There was used a soxhlet extractor and each time ~1.3 g of each sample was inserted into the thimble in the soxhlet apparatus and the spherical flask was filled with 130 ml of butanol. The extraction time was 6hr. After this pretreatment, samples were again analysed by XRF. Chemical recycling (pyrolysis) of the plastic samples took place before and after the pretreatment for the determination of the derived products and evaluate its effect on the products distribution.

### Results and Discussion

According to the FTIR spectra received (Figure 1), for all samples two strong peaks were formed within the range: 2840-2950 cm<sup>-1</sup> which are due to C-H bond; and are indicative of styrenic polymers, ABS or HIPS. Also, in some cases a peak at ~1750 cm<sup>-1</sup> was observed, which is due to C=O bond that is indicative of polyesters, such as PC. The EGA results showed that the thermal degradation of the samples in most cases followed a one-step mechanism, since one strong peak was observed. However, in some cases two maximum peaks were received; but usually, only the one of them was stronger and was considered as the main degradation peak.

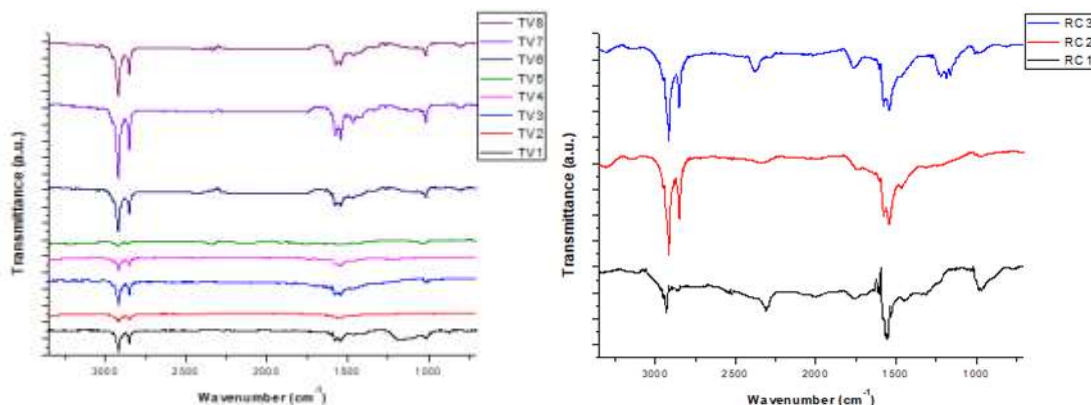


Figure 24. FTIR spectra indicatively for the television samples (left) and the remote control samples (right).

From XRF analysis it was found that 44% of the samples (7 out of 16) comprised bromine. Specifically, 25% (2 out of 8) of the television samples were found to contain bromine, 33% (1 out of 3) of the remote controls comprised bromine, in case of the computer samples 67% (2 out of 3) contained bromine and as regards the printer samples (100%) both of them comprised bromine. Different values of wt. % Br were detected among the different categories of the samples. In Table 1 the exact bromine content of each sample, is presented. All brominated samples were subjected to a 6hr. soxhlet extraction with butanol in order to reduce the bromine content and the results showed that in all cases tested bromine reduction was achieved, proving that soxhlet extraction was an efficient technique for the extraction of BFR from plastics originating in WEEE. However, in all cases examined incomplete removal of the bromine was achieved, since the maximum reduction reached ~35%.

During the thermal pyrolysis of all television samples there were formed various hydrocarbons, such as styrene (monomer) and others, which are indicative of styrenic polymers ABS or HIPS or polystyrene (PS). Nevertheless, in all cases a peak attributed to 1,3-butadiene was observed, excluding the possibility of being PS samples. Taking into account all the products formed and the fact that no nitrogenated compounds were observed in cases of the TV1-TV3 and TV5-TV8 samples, the possibility of being ABS samples was excluded; and so, they were HIPS samples. On the other hand, TV4 was a blend of ABS/PC, due to the formation of nitrogenated and phenolic compounds respectively. Likewise, the rest of the products were found and all plastic samples were identified. For all of them there were received various useful products, such as the monomers (e.g., styrene) and other secondary valuable products (for instance phenolic compounds).

Table 1. Bromine content according to XRF analysis.

Category of samples	Samples' name	wt. % Br measured
Television samples	TV1	0
	TV2	0
	TV3	0
	TV4	0.444
	TV5	5.767
	TV6	0
	TV7	0
	TV8	0
Computer samples	C1	2.59
	C2	0
	C3	0.191
Printer samples	PR1	1.054
	PR2	0.1
Remote control samples	RC1	0
	RC2	0
	RC3	0.627

## Conclusions

The thermal degradation of all samples was investigated by EGA analysis and seemed to follow a one-step mechanism in most cases tested. All samples were analysed by FTIR and were subjected to thermal pyrolysis in order to identify the polymer(s) present in each sample. According to the results obtained, they were either styrenic polymers ABS or HIPS or in some cases they were blends of ABS/PC. XRF analysis was also conducted with the aim of detecting the presence of bromine in the samples, in case they comprised BFR. Results showed that 44% of the samples contained bromine. All brominated samples were subjected to soxhlet extraction with butanol aiming to reduce their bromine content and it was observed that it led to bromine reduction in all cases tested, proving that it can be considered as an efficient technique for the debromination of plastics originating in WEEE.

## Acknowledgements



The research work was supported by the Hellenic Foundation for Research and Innovation (HFRI) under the HFRI PhD Fellowship grant (Fellowship Number: 853...).

## References

1. C. Ma, J. Yu, B. Wang, Z. Song, J. Xiang, S. Hu, S. Su, L. Sun, *Renewable and Sustainable Energy Reviews*, **61** 433–450 (2016).
2. M.A. Charitopoulou, K.G. Kalogiannis, A.A. Lappas, D.S. Achilias, *Environ. Sci. Pollut. Res.* **28** 59190–59213 (2021).

## Pre-treatment to remove additives from plastic waste based on the use of biosolvents

Ana M. Ferreira<sup>1,\*</sup>, Isa Sucena<sup>1</sup>, Mariana I. S. Aguiar<sup>1</sup>, Vanessa Otero<sup>2,3</sup>, Eva Mariasole Angelin<sup>2,4</sup>, Maria João Melo<sup>2</sup> and João A.P. Coutinho<sup>1</sup>

<sup>1</sup>CICECO - Aveiro Institute of Materials, Department of Chemistry, University of Aveiro, 3810-193 Aveiro, Portugal; <sup>2</sup>LAQV-REQUIMTE, Department of Conservation and Restoration, Faculdade de Ciências e Tecnologia, Universidade NOVA de Lisboa, 2829-516 Monte da Caparica, Portugal; <sup>3</sup>VICARTE, Department of Conservation and Restoration, Faculdade de Ciências e Tecnologia, Universidade NOVA de Lisboa, 2829-516 Monte da Caparica, Portugal; <sup>4</sup>Conservation Science Department, Deutsches Museum, Museumsinsel 1, 80538, Munich, Germany.

\*ana.conceicao@ua.pt

Plastics (polymers) are essential in our daily life and packaging is the most common plastic application worldwide. Due to their limited biodegradability, plastics have a high prevalence in the environment, making them one of the most important environmental issues. However, recycling plastics remains a challenge due to the relatively low quality of the recycled material, since many of the recycling processes cannot handle additives present in the plastic matrix. In this work, a pretreatment technique (dissolution/precipitation) using biosolvents investigated to remove additives from plastic packaging waste, contributing to an easier plastic recycling process, while minimizing the environmental impacts of the process. The plastic waste used in this study was packaging of high-density polyethylene (HDPE) with two different colors, i.e., blue and orange. First, we identified the colorants in HDPE, and found that both plastics contained a single pigment. Then, we used limonene, a renewable solvent, to solubilize HDPE, and the common volatile organic compound toluene was also applied for comparison purposes. After the HDPE dissolution a wide range of alcohols (mono-, di-, tri-alcohols) were used as anti-solvent in order to maximize the purity of the polymer recovered. The use of limonene as solvent for the plastic dissolution, in combination with polyalcohols with an intermediate alkyl chain length and a large number of hydroxyl (OH) groups, were found to work best as anti-solvent (1,2,3-propanetriol and 1,2,4-butanetriol), resulting in the removal of up to 94% and 100% of the blue and orange pigment, respectively. Furthermore, the thermal properties of the recovered HDPE, such as decomposition temperature, melting temperature, and heat of fusion, showed similar values to the respective reference polymers. Finally, three extraction cycles were performed, demonstrating that the solvent and anti-solvent could be recovered and reused, assuring the process's economic feasibility and sustainability viability. This pre-treatment provides a secondary source of raw materials and money for the recycling process, potentially improving the quality of recovered polymers and assisting in the development of a cost-effective and sustainable recycling process [1].

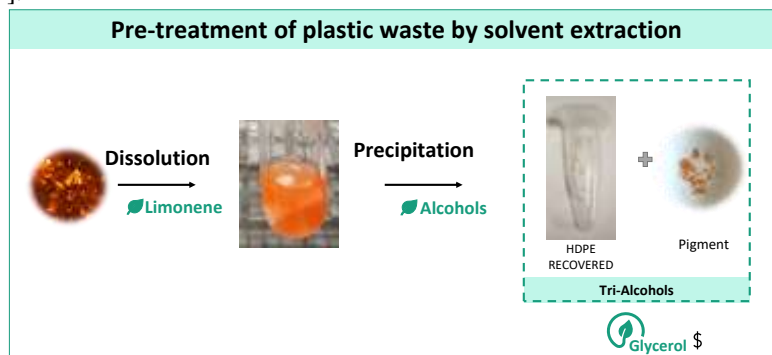


Figure 1. Schematic representation of the pre-treatment process developed to remove orange pigment from HDPE using the dissolution/precipitation technique.

### Acknowledgements

This work was developed within the scope of the project CICECO-Aveiro Institute of Materials, UIDB/50011/2020, UIDP/50011/2020 & LA/P/0006/2020, financed by national funds through the FCT/MEC (PIDDAC). This publication is based upon work from COST Action FUR4Sustain- European network of FURan based chemicals and materials FOR a Sustainable development, CA18220, supported by COST (European Cooperation in Science and Technology). Portuguese Foundation for Science and Technology (FCT-MCTES) for 2020.00647.CEECIND (Vanessa Otero), and Research UnitLAQV-REQUIMTE (UIDB/50006/2020; UIDP/50006/2020).

### References

1. A.M.Ferreira, I. Sucena, V. Otero, E.M. Angelin, M.J. Melo, J.A.P. Coutinho, *Molecules*, **27** 1 (2022).

## Reductive Depolymerization of Polyesters and Polycarbonates with Hydroboranes by Using a Lanthanum(III) Tris(amide) Catalyst

Marie Kobylarski, Jean-Claude Berthet\* and Thibault Cantat\*

LCMCE/IRAMIS/NIMBE/CEA, CNRS, Université Paris-Saclay, CEA Saclay, 91191 Gif-sur-Yvette, France.

\*[jean-claude.berthet@cea.fr](mailto:jean-claude.berthet@cea.fr), [thibault.cantat@cea.fr](mailto:thibault.cantat@cea.fr)

The worldwide massive production of plastics (368 Mt per year) [1] and the poor recycling rate of waste materials make them a scourge for the environment. Waste storage in landfills, their incineration or the mechanical recycling which gradually degrades the physical properties of plastic polymers, are not sustainable solutions. Chemical recycling, which is the depolymerization of materials into valuable monomers or chemicals, seems to be an appealing route for the future.

Currently, well-known solvolysis processes catalyzed by bases, acids and ionic liquids enable the depolymerization of polymers by hydrolysis, aminolysis or transesterification reactions.[2] They offer the recovery of pure monomers useful for the production of new virgin plastics.

Recently, reductive depolymerization processes of oxygenated and nitrogenated materials have appeared. These methods offer alternative approaches to access new value added products from plastics. The routes need to develop catalytic systems (catalyst and reducing agent) that would be able to selectively cut and reduce polarized bonds (carbon-oxygen and/or carbon-nitrogen) of the polymers to obtain the corresponding monomers (alcohols, amines or hydrocarbons).

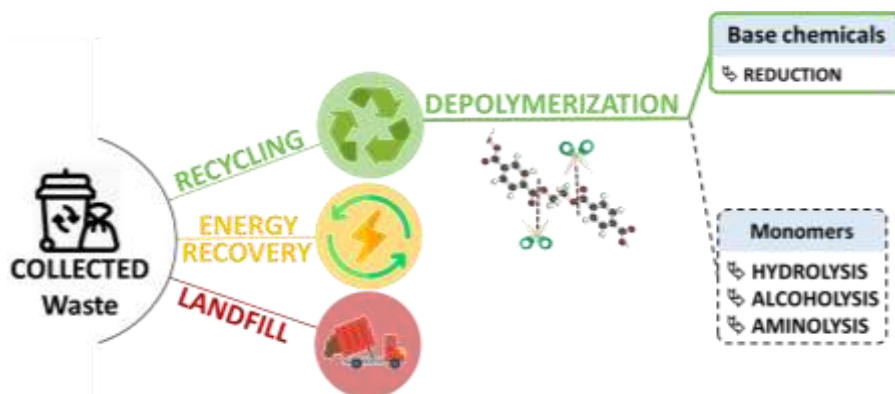


Figure 25. Reductive depolymerization, an alternative approach in plastic recycling

Such reductive deconstruction methods are scarce and are all based on the use of  $H_2$  or hydrosilanes as reductants. The catalytic hydrogenolysis of oxygenated and nitrogenated polymers (polyesters, polyamines and polyurethanes) was reported with Ru(II) and Ir(III) catalysts under high pressures and temperatures, whereas their catalytic hydrosilylations could take place under milder conditions with metal-based catalysts (Ir(III), Zn(II), Mo(VI)) or organocatalysts ( $[Ph_3C][B(C_6F_5)_4]$  and  $B(C_6F_5)_3$ ).[3,4] Hydroboranes as reductants could offer distinct reactivity and selectivity due to their higher hydride donor ability than hydrosilanes and an additional pronounced Lewis acidity.

Inspired by the work of T. J. Marks *et al.*,[5] on the reduction of esters, we considered the trisamide complex  $La[N(SiMe_3)_2]_3$  as a 4f-catalyst and the pinacolborane as a hydride donor, for the reductive depolymerization of a wide range of polyesters and polycarbonates.[6]



Figure 26. Our catalytic system for the reductive depolymerization of polyesters and polycarbonates

## Acknowledgements

For financial support, we acknowledge CEA, CNRS, the University Paris-Saclay, and the European Research Council (ERC Consolidator Grant Agreement no. 818260). T.C. thanks the Fondation Louis D.–Institut de France.

## References

1. PlasticsEurope, *Plastic -The Facts*, Belgium, (2020).
2. C. Jehanno, M. M. Pérez-Madrigal, J. Demarteau, H. Sardon and A.P. Dove, *Polym. Chem.*, **10** 172 (2019).
3. E. Feghali, L. Tauk, P. Ortiz, K. Vanbroekhoven and W. Eevers, *Polymer Degradation and Stability*, **179** 109241 (2020).
4. A. C. Fernandes, *Green Chem.*, **23** 7330 (2021).
5. C. J. Barger, A. Motta, V. L. Weidner, T. L. Lohr and T. J. Marks, *ACS Catal.*, **9** 9015 (2019).
6. M. Kobylarski, J-C. Berthet, T. Cantat, *Chem. Commun.*, Advance article (2022).  
(<https://pubs.rsc.org/en/content/articlepdf/2022/cc/d2cc00184e> on the 28/02/2022)

## Poly(ethyleneterephthalate) and polyethylene targeted solubilization and recovery with green solvents

J. Afonso<sup>1</sup>, S. Aparício and I.M. Marrucho<sup>1,\*</sup>

<sup>1</sup>Centro de Química Estrutural and Departamento de Engenharia Química, Instituto Superior Técnico, Universidade de Lisboa, Avenida Rovisco Pais, 1049-001 Lisboa, Portugal

\*[isabel.marrucho@tecnico.ulisboa.pt](mailto:isabel.marrucho@tecnico.ulisboa.pt)

The recyclability of polymers is of crucial importance in the present days considering the amount of plastic waste that is generated every day. According to the Eurostat Statistics, between 2005 and 2014, EU produced around 15 million tons per year of plastic packaging waste. Usually, this type of waste consists of a mix of different of various polymers and even aluminum foils therefore the recycling of this type of waste is challenging as it has low yield, high energy consumption and CO<sub>2</sub> emissions as lower quality and uneven end product. Thus, a more efficient and greener approach to this problem is needed. The specific solubilization of each polymer in a given solvent that can dissolve a given polymer without solubilizing the remaining ones is a good approach as the yield of this strategy is much higher and both the polymer and solvent can then be recovered by precipitation using an antisolvent. This approach results in the recovery of each polymer with high yield, purity and almost no changes from the original material [1 - 2]. Nevertheless, this strategy still makes use of organic volatile solvents that make the process not environmentally safe, health hazardous and also economically unfavorable due to loss of the solvent.

The process designed for the recycling of water bottles, uses NADES (natural deep eutectic solvents) composed of terpenes (menthol and thymol) as well as terpenes that are liquid at room temperature (limonene) to the target solubilization of PET and PE from water bottles and water bottle cap, respectively. The Hansen solubility parameters were used to screen the best solvents (NADES or biobased solvents) for each one of the polymers. The dissolution of PET is accomplished in about 7 minutes and can then be precipitated using a mixture of water and ethanol which results in a remarkable 99 % recovery of polymer and 99% recovery of the solvent. The recovered PET was analyzed by FTIR, X-ray diffraction and RMN and exhibited almost no changes from the original PET others than a slight increase in crystallinity [3]. The selective dissolution of the PE with high efficiency was already accomplished and the method has already proven to be capable of dissolving only the targeted polymer when a mixture of both polymers. PET and PE are present. The recovered PE will also be analyzed with FTIR, X-ray diffraction and RMN.



Figure 1. Recovered PET and PE as well as the recycled NADES.

### Acknowledgements

Afonso J. gratefully acknowledges the financial support of FCT/MCTES (Portugal) for PhD fellowship 2021.07949.BD and the project PTDC/EAM-AMB/2023/2021.

### References

1. T. W. Walker, N. Frelka, Z. Shen, A. K. Chew, J. Banick, S. Grey, M. S. Kim, J. A. Dumesic, R. C. Van Lehn, G. W. Huber, Recycling of multilayer plastic packaging materials by solvent-targeted recovery and precipitation. *Sci. Adv.* 6, eaba7599 (2020).
2. T. Mumladze, S. Yousef, M. Tatariants, R. Kriūkienė, V. Makarevicius, S. Lukošiuūtė, R. Bendikieneb, G. Denafasa, Sustainable approach to recycling of multilayer flexible packaging using switchable hydrophilicity solvents. *Green Chem.* 15, (2018).
3. S. Pestana, J. Machado, R. D. Pinto, B. D. Ribeiro, I. M. Marrucho, Natural eutectic solvents for sustainable recycling of poly(ethyleneterephthalate): closing the circle. *Green Chem.* 23, (2021).



# Pollution prevention & remediation

## Sustainable Water Purification Processes using Ionic and Porous Materials

Luis C. Branco<sup>1</sup>, K. Zalewska<sup>1</sup>, S. Freitas<sup>1,2</sup>, L. Rodrigues<sup>2</sup>, I. Matos<sup>1</sup>, M. Bernardo<sup>1</sup>, M. J. Nunes<sup>1</sup>, P. Esteves<sup>2</sup>

<sup>1</sup>LAQV-REQUIMTE, Faculdade de Ciências e Tecnologia, Universidade Nova de Lisboa, Campus de Caparica, 2829-516 Caparica, Portugal.

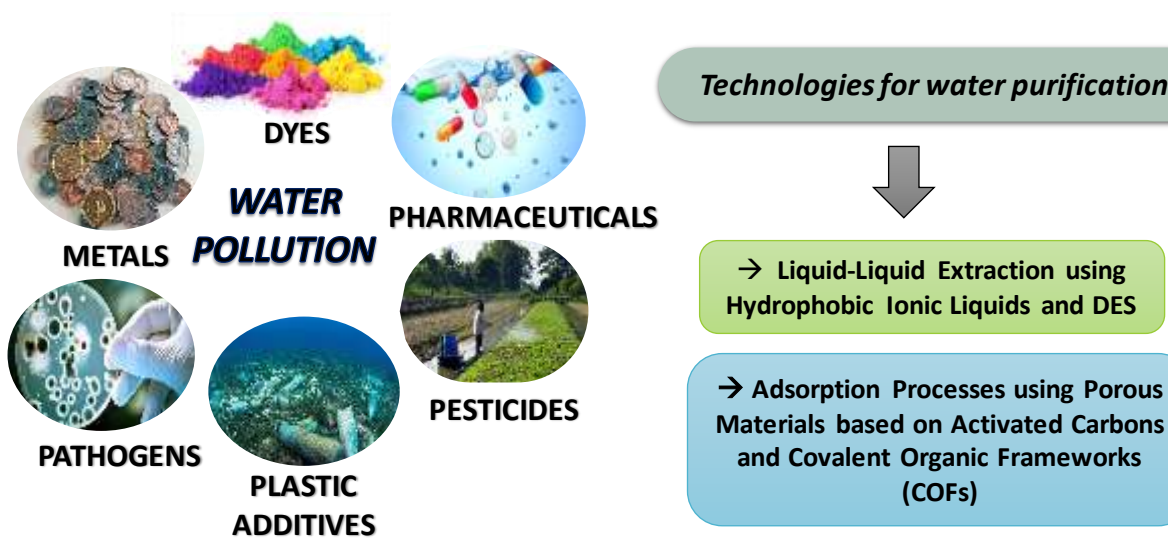
<sup>2</sup>Instituto de Química, Universidade Federal do Rio de Janeiro, Av. Athos da Silveira Ramos, 149, CT, Bl. A-622, Cid. Universitária, Rio de Janeiro, RJ, 21941-909, Brazil.

\*Corresponding author: [lbranco@fct.unl.pt](mailto:lbranco@fct.unl.pt)

Water resources are the main vehicle for the environmental dispersion of chemical pollutants [1]. Nowadays, the discovery of sustainable and efficient processes to promote the purification of the contaminants from water is highly required. The presence of these contaminants in the environment may cause risks to ecosystems and to human since they are designed to have a specific action on the human body and to act in very low concentrations. The application of porous materials such as activated carbons and covalent organic frameworks, ionic liquids (ILs) and deep eutectic solvents (DES) for efficient removal of micropollutants from water streams have been explored. ILs as organic salts with low-melting points possessing peculiar physical and chemical properties and significant interest for extraction and separation applications [2, 3]. Also, DES as innovative materials prepared by suitable combination of hydrogen bond donors (HBD) and acceptors (HBA) have been reported for several applications [4]. Herein, we presented different purification processes using hydrophobic ILs and DES for liquid-liquid extractions [5, 6] as well as porous materials for adsorption systems.

As proof of concept, several organic contaminants based on antibiotics, pesticides and plastic additives as model compounds have been selected for water remediation processes. The optimized analytical methodology involved the quantification of contaminants in water phase by UPLC-DAD and UPLC-MS/MS.

The most promissory porous materials and ionic systems will be tested for effective removal of contaminants from river water samples.



**Acknowledgements:** The authors thank the financial support by FCT – MCTES (UID/QUI/00100/2013, UID/QUI/50006/2013), FCT-CAPES Project, MAR2020 (MAR-02.01.01-FEAMP-0042; INOVA4AQUA project) and Solchemar company.

### References

- [1] P. Kehrein, M. van Loosdrecht, P. Osseweijer, M. Garfí, J. Dewulf, J. Posada, *Environ. Sci.: Water Res. Technol.* 6 (2020) 877.
- [2] M. Patel, R. Kumar, K. Kishor, T. Mlsna, C. U Pittman Jr, D. Mohan, *Chem Rev* 119 (2019), 3510.
- [3] Sónia P. M. Ventura, Francisca A. Silva, Maria V. Quental, Dibyendu Mondal, Mara G. Freire, João A. P. Coutinho, *Chem. Rev.* 117 (2017) 6984.
- [4] C. Florindo, L. C. Branco, I. M. Marrucho, *ChemSusChem* 12 (2019) 1549.
- [5] C. Florindo, F. Lima, L. C. Branco, I. M. Marrucho, *ACS Sustainable Chem. Eng.* 7 (2019) 14739.
- [6] C. Florindo, N. V. Monteiro, B. D. Ribeiro, L. C. Branco, I. M. Marrucho, *J. Mol. Liq.* 297 (2020) 111841.

## Bisphenol A adsorption on Hydrophobic Activated Carbon

Samia M. Al-Madhari, El-Said I. El-Shafey\*

Chemistry Department, College of Science P.O. Box 36, Sultan Qaboos University, PC 123, Muscat, Oman

\*Corresponding Author: [dr\\_el\\_shafey2004@yahoo.co.uk](mailto:dr_el_shafey2004@yahoo.co.uk)

### Abstract

Activated carbon (AC) was prepared from date palm leaflets via phosphoric acid activation. AC was oxidized with nitric acid (OAC) and was functionalized using amide coupling process, n-alkylamines (methyl-, ethyl-, propyl-, butyl-, octyl) to produce hydrophobic activated carbons. AC surface area (425 m<sup>2</sup>/g) was decreased on oxidation and surface functionalization. FTIR and TGA showed that the bonding between n-alkyl amine and the carbon surface is evidently chemical. Bisphenol A, an endocrine disruptor, was tested for its removal from aqueous solution at different initial pH, time, concentration, temperature. Optimum adsorption took place at initial pH = 6.0, thus, kinetic and equilibrium studies were carried out at initial pH of 6.00 using the carbons produced in this work together with a commercial activated carbon (CAC) for comparison. Equilibrium time was found to be ~ 10 hours for HACs, however for AC, CAC and OAC, ~ 30 hours were required for reaching equilibrium. Adsorption data were found to follow the pseudo second order kinetic model. Adsorption rate was found to increase as temperature increases with the activation energy ranging between 4.23-14.0 kJ/mol indicating the physical nature of BPA adsorption. The equilibrium studies show a better fitting to the Langmuir isotherm when compare to the Freundlich isotherm. Equilibrium adsorption was found to increase with the increase in temperature. Hydrophobic activated carbons (HACE, HACP and HACB) show higher adsorption capacity than AC. Thermodynamic parameters show that the removal of BPA is spontaneous and endothermic in nature with physical adsorption dominating their removal from aqueous solution. From this study, HACs, particularly with short immobilized n-alkyl chains, show better performance than activated carbons in terms of kinetics and equilibrium.

## The Influence of the Support and the Synthesis Method on the Activity of Pt-Catalysts for the Hydrogenation of Cl-Pollutants in Water.

Antonio E. Palomares<sup>1\*</sup> and Adrián Pla-Hernández<sup>1</sup>

<sup>1</sup>Instituto de Tecnología Química, Universidad Politécnica de Valencia - Consejo Superior Investigaciones Científicas, Avenida de los Naranjos s/n, 46022, Valencia, España

\*e-mail apalomar@iqn.upv.es

Water is a fundamental resource for the society and it is necessary to guarantee the supply of quality water for population all around the world. One of the most important treatments for water is disinfection and this is usually made with chlorine compounds. However, this process can produce pollutant by-products such as chlorite and chlorate. These by-products have negative effects on health such as oxidative stress or haemoglobin size change and the World Health Organization has set a provisional limit of 0.7 mg L<sup>-1</sup> for both pollutants in drinking water [1, 2, 3].

In this work, a catalytic reduction reaction is used to remove these ions from water streams at room temperature and atmospheric pressure using hydrogen as a reducing agent. This techniques has been successfully used for the removal of other pollutants, as nitrates and bromates, in water phase [4, 5]. The catalysts were prepared by wet impregnation of different platinum salts on different supports (different types of zeolites and metallic oxides) and the activity and the physico-chemical characteristics of the different materials have been studied.

The platinum precursor salt used were PtCl<sub>4</sub>, H<sub>2</sub>PtCl<sub>6</sub>·6H<sub>2</sub>O and Pt(NH<sub>3</sub>)<sub>4</sub>(NO<sub>3</sub>)<sub>2</sub>. After impregnation, the sample was dried at room temperature and the material was calcined at different temperatures. Before reaction the catalyst was activated with hydrogen. The catalysts have 5 wt.% of platinum and in a typical reaction with 1 g of catalyst were added to 600 mL of water containing 50 ppm of chlorate or chlorite. The experiments were performed in a batch stirred tank reactor at room temperature and atmospheric pressure, using hydrogen as reducing agent and ionic chromatography to analyse the reactants and products. The catalysts were characterized with different techniques such as inductively coupled plasma (ICP), X-ray diffraction (XRD), temperature programmed reduction (TPR) and N<sub>2</sub> adsorption.

The characterisation of the samples showed that Pt nanoparticles were generated on the support during the catalyst activation in hydrogen flow at 200 °C and that the Pt or PdH<sub>x</sub> –phase was formed during cooling the samples to room temperature. In general all the catalysts tested enhanced significantly the reaction rate compared to the blank without catalyst and achieved a complete conversion of the ClO<sub>x</sub><sup>-</sup> to Cl<sup>-</sup>. The reaction rate for the hydrogenation of the ions using both Pt catalysts was ClO<sub>3</sub><sup>-</sup> < ClO<sub>2</sub><sup>-</sup> < ClO<sup>-</sup> due to the different stability of the ClO<sub>x</sub><sup>-</sup> anions.

Nevertheless, the activity of the different catalysts depends on the support used and on the catalyst preparation method. In Figure 1 are shown the different results obtained depending on the Pt-precursor salt used (right) and on the calcination temperature (left). As it can be seen the best results are obtained when using the PtCl<sub>4</sub> as the precursor and with the lowest calcination temperature. This can be related with a different dispersion of the Pt sites as the HRFESM characterization of the samples has shown.

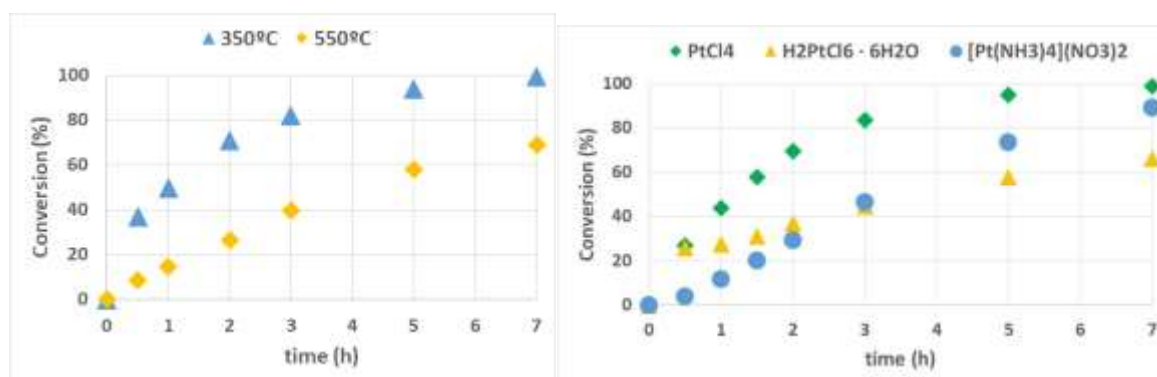


**Figure 1** – Chlorate conversion of 5%Pt catalysts supported on: alumina prepared using different Pt salt precursors (right) and calcined at different temperatures (left).

The other factor influencing the activity of the catalyst in this reaction is the support. The catalytic activity of 5% Pt catalysts supported on different type of zeolites and on aluminium oxide was compared and the results are shown in Figure 2 (left). A laminar MWW zeolite (Si/Al=16), a BEA zeolite (Si/Al= 12), a FAU zeolite (Si/Al=6)

and gamma alumina were used for this comparison. As it can be seen Pt-FAU is the most active catalyst, followed by Pt-Al<sub>2</sub>O<sub>3</sub>, Pt-BEA and Pt-MWW. These results show the influence of the surface acidity and the topology on the catalyst activity, obtaining the best results with the Pt-FAU zeolite that has a highest number of Brönsted acid sites in their surface (lower Si/Al ratio), a 3D structure with large cavities and higher surface area. Those factors influence the metal dispersion and favour the reactants diffusion towards the active sites.

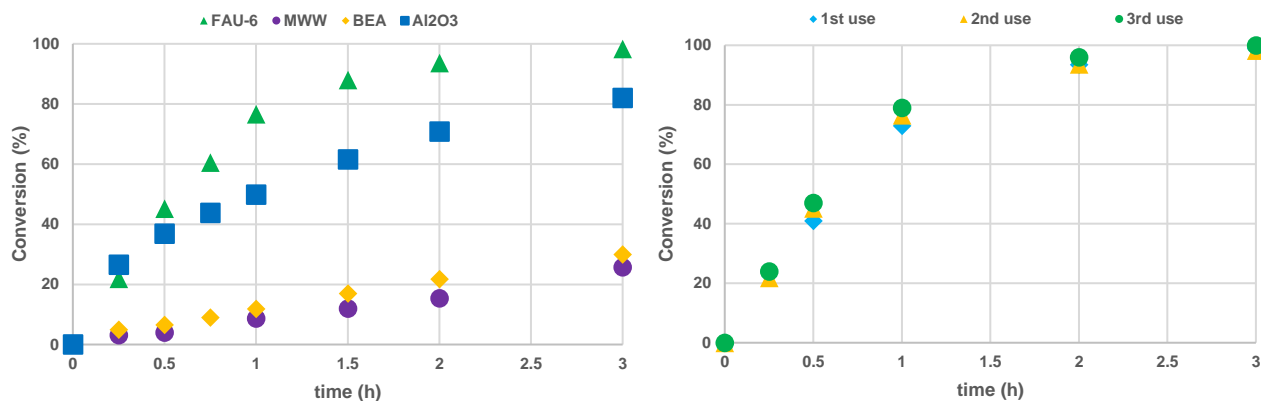


**Figure 2** – Chlorate conversion of 5%Pt catalysts supported on: left: FAU-6, MWW (SI/Al = 16), BEA (SI/Al =12) and gamma alumina (left); FAU with Si/Al = 6 during 3 uses of the same catalyst (right).

A study of the reuse of the catalyst with highest activity (FAU-6) was done and the results are shown in figure 2 (right). As it can be seen this catalyst preserves its activity throughout 3 successive reactions indicating a high stability of the catalyst.

Finally, the influence of the Si/Al ratio on the catalytic activity was studied by using Pt-FAU with different Si/Al ratio (6 and 40). It was observed that the activity of the catalyst with lower Si/Al ratio was much higher than the activity of the catalyst with higher Si/Al ratio. These results show again the enormous influence of the Si/Al ratio on the catalyst activity, that can be related to a better dispersion of Pt on the zeolite with a higher Al content or to an activation of the reactants on the Brönsted acid sites present on the zeolite surface.

The results obtained may conclude that catalytic hydrogenation using Pt-catalysts is an adequate process for the removal of Cl<sup>-</sup> anions in polluted water. It was observed that there is a strong influence of the support on the catalytic activity, obtaining the best results with the catalyst with a higher number of acid centres, with a high surface area and with lower diffusional problems: These characteristics are probably improving the dispersion of platinum on the surface of the support and favouring the interaction of the reactants with the active sites. In this way the best results have been obtained with the catalyst supported on FAU with a Si/Al ratio of 6. This catalyst is an active and stable material that can reduce the chlorates in successive reaction cycles without important deactivation.

## Aknowledgment

This work was supported by Spanish Ministry of Science and Innovation for the pre-doctoral grant PRE2019-088100, associated with the project RTI2018-101784-B-I00 and by the Regional Ministry of Education, Research, Culture and Sport for the grant from the Prometeo programme for research groups of excellence (PROMETEO/2021/077).

## References

- 1.- UNESCO, ONU-Agua, *Informe Mundial de las Naciones Unidas sobre el Desarrollo de los Recursos Hídricos 2020: Agua y Cambio Climático*, UNESCO, París (2020).
- 2.- United Nations Environment Programme, *Disinfectants and Disinfectant By-Products - Environmental Health Criteria 216*, Knowledge Repository - UNEP. UNEP. 2000. Web. 8 Apr 2022 <<https://wedocs.unep.org/20.500.11822/29525>>
- 3.- D. Couri, M. S. Abdel-Rahman & R. J. Bull, *Environmental Health Perspectives*, **46**, 13-17 (1982)
- 4.- J.L. Cerrillo, A.E. Palomares, *Catalysts* **11** (3) 365 (2021)
- 5.- J.L. Cerrillo, C. Wittee, G. Agostini, F. Rey, A.E. Palomares, L. Kiwi-Minsker, *Catalysis Science & Technology* **10** 3646-3653 (2020)

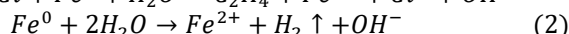
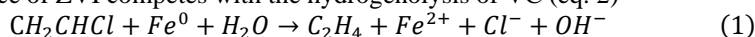
## Nitrogen doped graphene efficiently promotes the reduction of vinyl chloride by nano zero-valent iron

Qiong Ouyang\*, Dominique J. Tobler and Hans Christian Bruun Hansen

Department of Plant and Environmental Sciences, University of Copenhagen, Thorvaldsensvej 40, DK-1871 Frederiksberg C, Denmark

\*qiong@plen.ku.dk

**Introduction:** Vinyl chloride (VC), a known carcinogen, is found in many contaminated soils and groundwaters due to past uncontrolled releases to the environment but also because it forms and accumulates during microbial reductive dechlorination of per- and tri-chloroethylene (PCE, TCE). While TCE and PCE are relatively easily degraded via abiotic and biotic dechlorination processes, VC is more resistant [1]. Zerovalent-iron (ZVI) is one of the most widely used reductive reagents for chlorinated ethylene degradation, however, it reacts slowly with VC [2]. This is because VC is reduced by electrons from ZVI to produce ethylene (eq. 1), but the hydrogen evolution reaction on the surface of ZVI competes with the hydrogenolysis of VC (eq. 2)



Carbonaceous material (CM) such as biochars and activated carbon have been shown to protect ZVI materials from fast anaerobic corrosion [3], and also to enable fast removal of chlorinated ethylenes from the water phase due to their hydrophobic sorption properties. In addition, CM materials have been shown to enable reductive dechlorination by acting as an electron mediator as for example demonstrated for the degradation of TCE in the presence of biochar and the iron(II, III) hydroxide green rust [4]. However, to date there are no studies that assessed the potential beneficial effects of CM materials on VC degradation by ZVI materials. In this study, a range of CM materials were tested for their catalytic properties in reactions between VC and nanoscale ZVI (nZVI).

**Materials and methods:** Among the CMs, except for graphene, which is obtained directly from Sigma (Graphene nanoplatelets, 300 m<sup>2</sup>/g), other CMs are pyrolysed in a muffle furnace (LT3/11, Nabertherm), under the protection of a nitrogen atmosphere throughout the process, using a temperature ramp of 150°C/h until the final temperature, keeping this temperature for 1h, and then cooling to room temperature. Nitrogen amended graphene (N-graphene) is prepared by mixing graphene and urea in a certain proportion followed by pyrolysis. Batch VC dechlorination experiments with nZVI (2 g/L; synthesized using the borohydride reduction method [5]) and CM were set-up under anaerobic conditions using sealed 10 mL headspace vials. Quantitative analysis of VC and reduction products was performed in duplicate using GC-FID/ECD to determine concentration of reactants and products at specific time intervals. Then, the amount of substance (n) of VC that has been reduced in the vial at time t is divided by the initial amount of VC (n<sub>0</sub>) to calculate the adsorption efficiency. The reduction efficiency was calculated similarly, using the percentage of the total amounts of all products in the vial divided by n<sub>0</sub>. Methanol, tert-butanol (TBA), and 1-10 phenanthroline (PHT) were used as scavengers in quenching experiments, since the first two were reported to quench atomic hydrogen, while PHT quenched ferrous ions [6].

**Results:** The reactivity of NG950 was first explored in the nZVI reduction VC system. When the dose of NG950 gradually increased from 1 g/L to 6 g/L, the removal rates of VC after 68 h were 49.0%, 74.8%, 96.3% and 97.9%, respectively (Fig. 1). The production of ethylene followed first-order kinetics, with a reaction rate constants (k) of 0.01592, 0.02583, 0.04414 and 0.07393 h<sup>-1</sup>, respectively. Comparing NG950 with the other 15 CMs, NG950 resulted in the fastest ethylene formation (Fig. 2a). After 8 days of reaction, the reduction efficiency for the NG950 system increased from 8% to about 80% compared with the nZVI alone system. No clear correlation could be found between adsorption and reduction efficiency (Fig. 2b). The effect of pyrolysis temperature in the range of 400-1100 °C on the properties of N-graphene was further explored, and the results showed that more than 80% reduction could be obtained at 600, 800 and 950 °C after reaction for 8 d. However, further kinetic experiments showed that the k values of the products at these three temperatures were 0.02568, 0.02662 and 0.04652, respectively, which indicated that 950 °C was the optimum pyrolysis temperature. The electrons required for the reduction of VC in the nZVI system may come directly from nZVI, or indirectly from Fe<sup>2+</sup>, or from atomic hydrogen generated during anaerobic corrosion. Quenching experiments were used to test the reaction mechanism in the NG950/nZVI system. The experimental results showed that the addition of methanol and PHT had almost no effect on the reactivity of the system, while with the addition of TBA at concentrations of 50 mM and 200 mM, the rates of ethylene formation in the system decreased by 57.0% and 64.3%, respectively. This result will preliminarily rule out the electronic contribution from Fe<sup>2+</sup>. However, when N-graphenes prepared at five different pyrolysis temperatures were used in the nZVI system, there was no significant difference in the production of hydrogen, and the adsorption capacities of the five types of N-graphenes for hydrogen were almost the same. All CMs that have been used in the experiments were characterized, involving C and contents, XRD, BET, and XPS, etc., but none of them had obvious correlation with the catalytic performance. This study shows that the graphene and certain biochars strongly catalyse the hydrogenolysis of VC, by facilitating formation and transfer of atomic hydrogen and by mediating electron exchange from nZVI to VC.

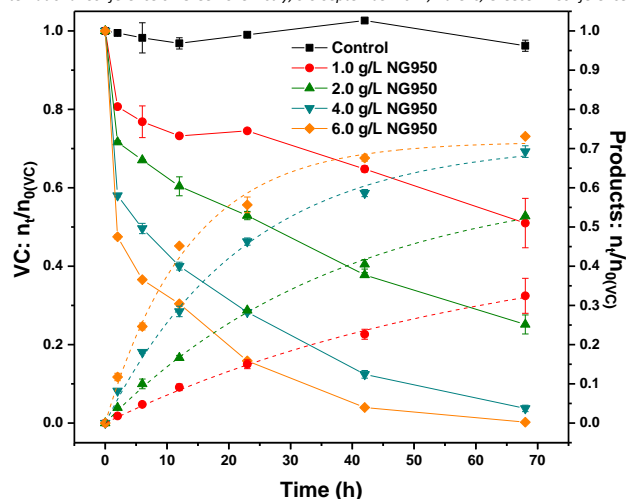


Figure 1. The effect of NG950 dosage on the system.

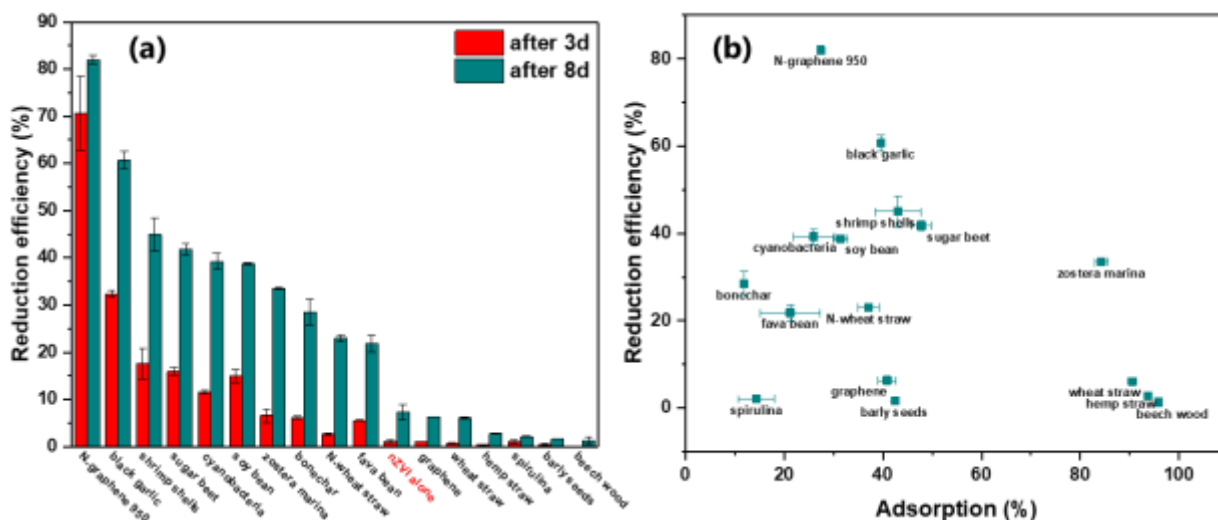


Figure 2. a. Comparison of the reactivity of different CMs; b. correlation between adsorption and reduction of different CMs.

## Acknowledgements

The authors thank the Guangzhou Elite Project (GEP) for financial support to Qiong Ouyang.

## References

1. PM Bradley, FH Chapelle. *Environmental Science & Technology*, 30(6), 2084-2086 (1996).
2. Deng, B., Burris, D. R., & Campbell, T. J. *Environmental Science & Technology*, 33(15), 2651-2656 (1999).
3. Guan, X., Du, X., Liu, M., Qin, H., Qiao, J., & Sun, Y. *Journal of Hazardous Materials*, 394, 122564 (2020).
4. Ai, J., Ma, H., Tobler, D. J., Lu, C., van den Berg, F. W., ... & Bruun Hansen, H. C. *Environmental Science & Technology*, 54(6), 3643-3652 (2020).
5. Fang, Z., Qiu, X., Chen, J., & Qiu, X. *Desalination*, 267(1), 34-41 (2011).
6. Li, J., Lan, H., Liu, H., Zhang, G., An, X., Liu, R., & Qu, J. *ACS applied materials & interfaces*, 11(17), 15709-15717 (2019).

## Photocatalytic removal of methylene blue and thiabendazole by reduced ZnO: influence of oxygen vacancies on adsorption and photocatalytic degradation

Alireza Ranjbari<sup>1,2</sup>, Ju Ho Kim<sup>1</sup>, Jiyun Kim<sup>1</sup>, Jihee Yu<sup>1</sup>, Mireu Park<sup>1</sup>, Nayoung Kim<sup>1</sup>, Kristof Demeestere<sup>2</sup>, Philippe M. Heynderickx<sup>1,2,\*</sup>

<sup>1</sup> Center for Environmental and Energy Research (CEER), Ghent University Global Campus, Songdo, Incheon, South Korea;

<sup>2</sup> Department of Green Chemistry and Technology, Faculty of Bioscience Engineering, Ghent University, Ghent, Belgium

\*Philippe.Heynderickx@Ghent.ac.kr

The application of photocatalysis as a solution for the treatment of water and wastewater has gained great attention in recent years. Semiconductors are the most commonly utilized materials for photocatalysis. Due to its optical and electronic properties, non-toxicity, low cost, and ability to complete mineralization of pollutants, zinc oxide is a popular metal oxide for photocatalytic degradation of organic compounds in water. However, using ZnO also has limitations, such as photo-corrosion, insufficient bandgap for visible light activation, and high rates of electron-hole recombination [1].

Adding surface oxygen vacancies by hydrogen reduction was investigated in order to overcome the aforementioned limitations of the ZnO catalyst. This has been tested under simulated solar light irradiation for the photocatalytic degradation of methylene blue and thiabendazole (typical fungicide).

Commercial ZnO provided by Sigma-Aldrich was used as catalyst in this research. The hydrogen reduction was performed by Autochem II Micromeritics equipment. The catalyst was pretreated at 130°C for 20 minutes with He gas. The gas flow was changed to 10% H<sub>2</sub>/Ar, and the temperature was increased with a rate of 10 K/min. By changing the final reduction temperature and hold time, the optimal conditions for catalyst reduction have been selected.

TPR analysis indicates that several Gaussian peaks can be fitted in the reduction spectrum of ZnO. The corresponding temperature of each peak was used as the reduction temperature of each ZnO sample. In order to understand the role of oxygen vacancies in photocatalyst behavior, FE-SEM, EDS, XPS, XRD, BET surface area and Tauc plot have been used to characterize different temperature reduced samples. XPS analysis reveals that the adsorption and photocatalytic degradation of the selected micropollutants are significantly enhanced when surface oxygen is reduced and when the vacancy-to-lattice oxygen ratio is increased. Analysis by FE-SEM and XRD indicates that the reduction of ZnO did not have a significant impact on the material's surface morphology. In addition, Tauc plot analysis indicates that the optimally reduced ZnO has a narrower bandgap, compared to the commercial ZnO, which allows excitation by a wider wavelength range of visible light.

To gain more insight into the changes that occurred in ZnO by oxygen reduction, our recently published kinetic model [2] was used to describe the reversible adsorption in the dark and photocatalytic degradation under simulated sunlight. Figure 1 shows the degradation rate and adsorption removal of methylene blue at different pHs.

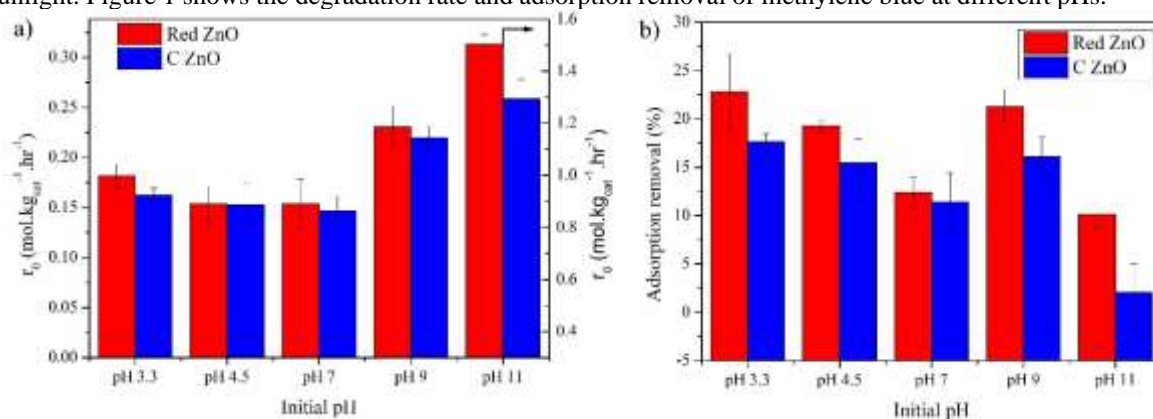


Figure 1. Effect of pH on a) reaction rate, and b) adsorption removal of methylene blue by commercial ZnO (C ZnO) and reduced ZnO at optimum temperature (red ZnO). Methylene blue 10 mg/L, ZnO 500 mg/L.

By increasing the reduction temperature to its optimal value, the adsorption removal and photocatalytic activity of commercial ZnO considerably increases. This is due to an increase in the ratio of vacancy-to-lattice oxygen at the surface of the catalyst. The newly created vacancy oxygen sites can act as an adsorption site and it can provide a way to transfer the excitons to the adsorbed molecules, hereby preventing recombination of electron-holes. By further increasing of reduction temperature, it has been noticed that – in addition to surface oxygen – the bulk oxygen can be reduced. The bulk oxygen vacancy is not in direct contact with the contaminants in solution and, hence, it cannot act as an adsorption site. However, it can act as an electron trap which prevents the transfer of electrons to the contaminants and causes recombination of electron-holes which decreases the degradation rate.



## References

1. S. Deepracha, A. Ayrat, M. Ogawa, *Appl. Catal., B.* 284 (2021) 119705.
2. A. Ranjbari, K. Demeestere, F. Verpoort, K. H. Kim, P. M. Heynderickx, *Chem. Eng. J.* 431 (2022) 133349.

## Landfill leachate treatment by using fixed bed columns packed with WWTP sludge porous carbons

I. Oliveira<sup>1\*</sup>, D. Vicente<sup>1</sup>, M. Bernardo<sup>1</sup>, I. Matos<sup>1</sup>, N. Lapa<sup>1</sup> and I. Fonseca

<sup>1</sup> LAQV/REQUIMTE, Faculdade de Ciências e Tecnologia, Universidade Nova de Lisboa, 2829-516 Caparica, Portugal

\* ifo19529@campus.fct.unl.pt

Solid waste sanitary landfills have been the most common and most important way of dealing with residues across the world [1]. Leachate is the contaminated water that drains from a landfill [2]. A particular and unique treatment that is effective in treating the many variants of leachates has not been found [3] so the present work was developed within the scope of the ongoing study to define new methodologies for the treatment of leachate, namely through adsorption processes, by using activated carbons obtained from WWTP sludge as adsorbents.

The nature of landfill leachate depends on a wide variety of factors. Although each leachate has its own characteristics, they can be classified as young, medium or mature, regarding the age of the landfill [3]. Landfill leachate in the mature (methanogenic) phase, that is the type of leachate in study, is characterized for low concentrations of volatile fatty acids and low BOD<sub>5</sub>/COD ratio, very low concentrations of heavy metals and the dissolved organic carbon is mainly composed by refractory compounds such as fulvic and humic like compounds [4].

In the field of leachate treatment, adsorption with conventional adsorbents, such as activated carbon, is a widely used process with relative success [4]. In the present work, activated carbons were developed from dehydrated WWTP sludge and dehydrated and demineralized sludge, both of which were subjected to physical activation using CO<sub>2</sub>, and chemical activation using K<sub>2</sub>CO<sub>3</sub> and KOH agents. The optimized carbons were subsequently applied in the removal of humic acids (HAs), as they represent a major constituent in leachate from a mature landfill, and these macromolecules correspond to the non-biodegradable organic carbon that contribute to the coloring of the leachate. To analyze the potential of the activated carbons developed, the same tests were carried out with a commercial activated carbon (BDH) identified as suitable for color removal.

The carbons from the sludge that did not undergo demineralization (DS) showed higher activation yields compared to the carbons from demineralized sludge (DSD) and, in turn, the carbons resulting from physical activation with CO<sub>2</sub> showed the highest activation yields. However, the low activation yields of the materials derived from DSD sludge was balanced with high specific surface areas (950 – 1008 m<sup>2</sup>/g), comparable to the surface area of BDH carbon (914 m<sup>2</sup>/g). Regarding surface chemistry, carbons derived from sludge were characterized by high mineral content and alkaline character, while commercial carbon had low ash content and acidic properties.

The adsorption tests were carried out in continuous mode with fixed bed columns packed with 0.05 g of each carbon and by passing 10 ppm of a humic acid solution through the column with a flow rate of 3 ml/min. A leachate sample collected in a sanitary landfill classified as stable, was also passed through the columns.

Figure 1 presents the results of bed height (Z) and mass transfer zone (MTZ) for all the used carbons.

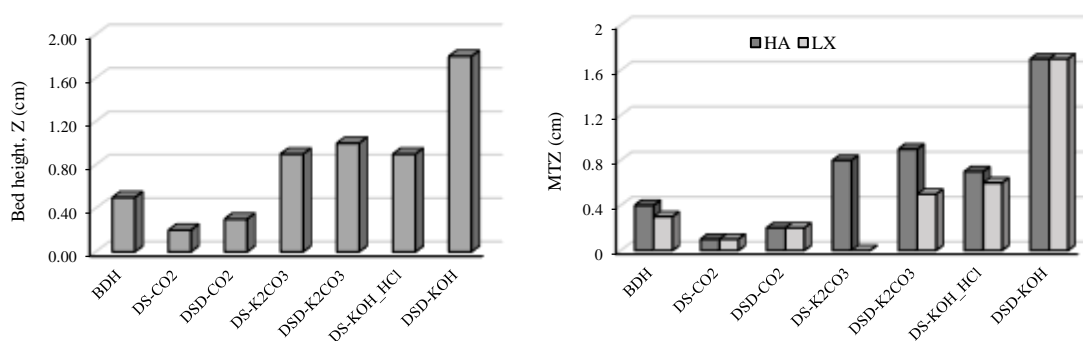


Figure 1. Bed height (left) and MTZ (right) of the humic acids' adsorption columns packed with the carbons. HA -Humic Acids solution; LX - Leachate sample.

The carbons with lower density, thus with higher bed heights (Z), provided higher mass transfer zones (MTZ) and, therefore, greater HAs adsorption capacities (Figure 2). It was also possible to confirm that the carbons with these characteristics, namely DSD- K<sub>2</sub>CO<sub>3</sub> and DSD-KOH samples, had longer saturation times than the others.

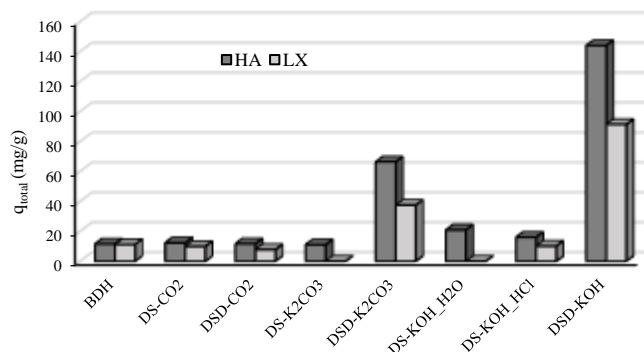


Figure 2. Total adsorption capacities of humic acids of the columns packed with the carbons. HA – Humic Acids solution; LX – Leachate sample.

It was also concluded that the columns performed worse in removing HAs from the leachate sample than from the synthetic HAs solution due to competition of other components present in the leachate.

The application of the Thomas model to the experimental breakthrough curves did not achieve a good fit in some cases due to the very long adsorption kinetics that may be associated with diffusional limitations or the adsorption mechanism itself.

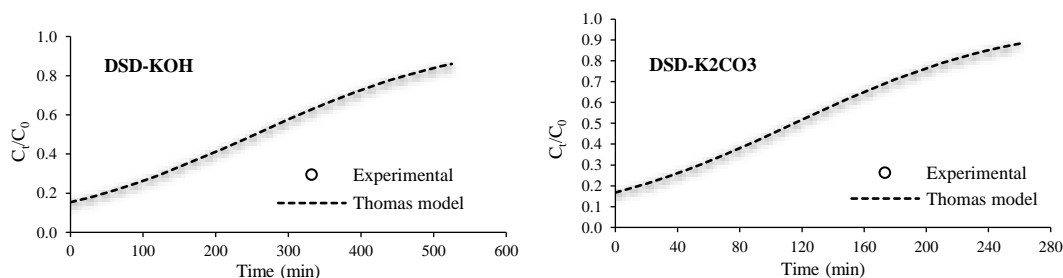


Figure 3. Humic acids breakthrough curves of adsorption columns packed with DSD-KOH (left) and DSD-K<sub>2</sub>CO<sub>3</sub> (right) carbons

The carbons from KOH activation had the highest adsorption capacity of HAs, 91.4 – 144.1 mg/g, with a better performance to that of the commercial carbon.

## Acknowledgements

This work was supported by the Associate Laboratory for Green Chemistry - LAQV which is financed by national funds from FCT/MCTES (UIDB/50006/2020 and UIDP/50006/2020).

## References

- [1] K. Wang, L. Li, F. Tan, and D. Wu, "Treatment of landfill leachate using activated sludge technology: A review," *Archaea*, vol. 2018. Hindawi Limited, 2018. doi: 10.1155/2018/1039453.
- [2] P. Rathnayake, W. A. P. P. Rathnayake, and G. B. B. Herath, "A REVIEW OF LEACHATE TREATMENT TECHNIQUES." [Online]. Available: <https://www.researchgate.net/publication/329915923>
- [3] L. San-Pedro, R. Méndez-Novelo, E. Hernández-Núñez, M. Flota-Bañuelos, J. Medina, and G. Giacomán-Vallejos, "Selection of the activated carbon type for the treatment of landfill leachate by fenton-adsorption process," *Molecules*, vol. 25, no. 13, Jul. 2020, doi: 10.3390/molecules25133023.
- [4] M. A. M. Reshadi, A. Bazargan, and G. McKay, "A review of the application of adsorbents for landfill leachate treatment: Focus on magnetic adsorption," *Science of the Total Environment*, vol. 731. Elsevier B.V., Aug. 20, 2020. doi: 10.1016/j.scitotenv.2020.138863.

## Asymmetric poly(ionic liquid)–ionic liquid membranes for gas separation

Bruna F. Soares<sup>1</sup> and Isabel M. Marrucho<sup>1,\*</sup>

<sup>1</sup>Centro de Química Estrutural and Departamento de Engenharia Química, Instituto Superior Técnico, Universidade de Lisboa, Avenida Rovisco Pais, 1049-001 Lisboa, Portugal

\*Corresponding author: [isabel.marrucho@tecnico.ulisboa.pt](mailto:isabel.marrucho@tecnico.ulisboa.pt)

Non-solvent induced phase separation (NIPS) is one of the most used techniques to produce polymeric membranes from a wide variety of polymers. Nevertheless, this method has never been employed before in the preparation of poly(ionic liquid) (PIL)-based membranes [1-2]. The use of PILs and their derived materials incorporating ionic liquids (PIL–IL) has emerged as a highly promising strategy to design dense membranes with improved CO<sub>2</sub> separation [3-4]. In this context, considering that membrane thickness is a critical parameter for their industrial scale application, this study is a step forward in the preparation of integral asymmetric PIL–IL membranes, with a top dense thin layer and a bottom porous layer. Solutions of poly([Pyr11][NTf2]) PIL and 20 wt% of [C4mpyr][NTf2] IL in acetone/dimethylformamide and acetone/formamide mixtures were prepared. The effect of several parameters of phase inversion process, namely, casting solution concentration and evaporation time, on the morphology (Figure 1) and gas separation performance of the resulting asymmetric PIL–20 IL NTf2 membranes, was evaluated and compared to those of dense PIL–20 IL NTf2 membrane. The results indicate that the choice of the appropriate solvent mixture strongly impacts membrane morphology and gas separation properties.

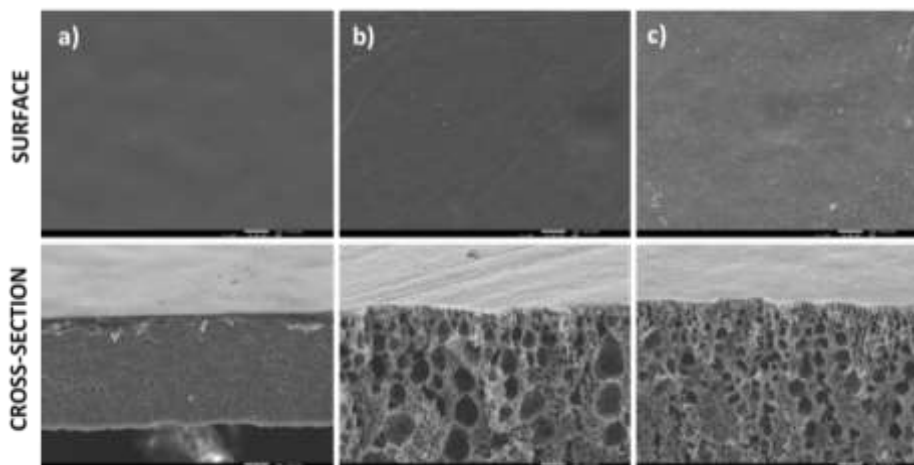


**Figure 1.** SEM images of PIL–20 IL NTf2/acetone: dimethylformamide membranes at solvent ratios of 80:20 and casting evaporation times of (a) 1, (b) 5 and (c) 10 min.

From SEM analysis, it was shown that the type of co-solvent used, dimethylformamide or formamide, as well as, different evaporation times strongly influenced the PIL–20 IL NTf2 membrane morphology. Regarding the CO<sub>2</sub> permeances of the resulting asymmetric PIL–20 IL NTf2 membranes a significant increase was observed. In particular, for PIL–20 IL NTf2/acetone: formamide (85:15) membrane a 10-fold increase in CO<sub>2</sub> permeance was obtained compared with dense membranes, whereas only a small decrease in selectivity was observed.

### Acknowledgements

Bruna F. Soares gratefully acknowledges the financial support of FCT/MCTES (Portugal) for PhD fellowship 2021.05450.BD. This work was financed by CQE project (UIDB/00100/2020).

### References

1. Mazinani, S.; Darvishmanesh, S.; Ehsanzadeh, A.; Van der Bruggen, B., *J. Membr. Sci.* 2017, 526, 301-314.
2. Kahrs, C.; Schwellenbach, J., *Polymer* 2020, 186, 122071.
3. Tomé, L. C.; Gouveia, A. S. L.; Freire, C. S. R.; Mecerreyes, D.; Marrucho, I. M., *J. Membr. Sci.* 2015, 486, 40-48.
4. Tomé, L. C.; Marrucho, I. M., *Chem. Soc. Rev.* 2016, 45, 2785-2824.

## Fast peroxydisulfate oxidation of the antibiotic Norfloxacin catalyzed by cyanobacterial biochar

Chen Wang<sup>1\*</sup>, Hans Christian Bruun Hansen<sup>1</sup>, Mogens Larsen Andersen<sup>2</sup>, Bjarne W. Strobel<sup>1</sup>, Hui Ma<sup>1</sup>, Nadia Dodge<sup>2</sup>, Poul Erik Jensen<sup>2</sup>, Peter E. Holm<sup>1</sup>

<sup>1</sup>Department of Plant and Environmental Sciences, University of Copenhagen, Thorvaldsensvej 40, DK-1871 Frederiksberg C, Denmark

<sup>2</sup>Department of Food Science, University of Copenhagen, Rolighedsvej 26, DK-1958 Frederiksberg C, Denmark

\*Corresponding author (Chen Wang): Email address: [chwa@plen.ku.dk](mailto:chwa@plen.ku.dk)

**Introduction.** Norfloxacin (NOR) is a slowly degrading and frequently detected antibiotic in surface waters at concentrations of ng L<sup>-1</sup> to µg L<sup>-1</sup> levels [1]. Persulfates comprising peroxydisulfate (S<sub>2</sub>O<sub>8</sub><sup>2-</sup>, PDS) and peroxymonosulfate (HSO<sub>5</sub><sup>-</sup>, PMS) are popular advanced oxidation reactants due to their versatility, as well as low storage and transportation costs [2]. Biochar is a low-cost, easily accessible and environmentally friendly carbonaceous material that can be used to activate persulfate for pollutant oxidation [3]. Activation produces highly reactive oxygen species (ROS) that can oxidize and mineralize antibiotics. However, radicals are short-lived and non-selective [4], while non-radical oxidants have a higher selectivity for contaminants [5]. Therefore, it is of interest to explore the conditions that stimulate degradation of antibiotics through non-radical pathways.

**Materials and methods.** In this study, biochar material was prepared by in-situ pyrolysis of N-rich (6.2%) cyanobacterial biomass for peroxydisulfate (PDS) catalysis and NOR degradation. Microalgae powder (2 g) was dried overnight (24 h) at 80 °C, then heated to 200, 500 and 950 °C at a rate of 150 °C/h and then held there for 1 h using a muffle furnace (LT3/11, Nabertherm), under N<sub>2</sub> atmosphere (≥99.9% N<sub>2</sub>) with a flow rate of 0.5 L/min. Cyanobacterial biochars (CBs) pyrolyzed at 200 and 500 °C are categorized as low pyrolysis temperature (PT) CBs, while pyrolysis at 950 °C results in high PT CB. Degradation kinetics and adsorption isotherm data were used to evaluate the performance of CBs. Experiments were conducted using 250 mL Erlenmeyer flasks with 100 mL of 5 mg L<sup>-1</sup> NOR solution under continuous shaking (125 rpm) at 20 °C. The initial solution concentration of NOR for adsorption experiments was set at 5 mg L<sup>-1</sup>, the pH was fixed at about 6.8 using Na<sub>2</sub>HPO<sub>4</sub> - NaH<sub>2</sub>PO<sub>4</sub> buffer (0.2 M), and the dosage of biochar was 100 mg L<sup>-1</sup>. Immediately after completion of the above adsorption reaction, an amount of PDS stock solution was added to the same reaction vessel to ensure an initial PDS concentration of 10 mM. High performance liquid chromatography and Ultra Performance Liquid Chromatography - tandem Mass Spectrometer were used to determine NOR and degradation products. Radical quenching tests, electrochemical measurements, and electron spin resonance (EPR) spectroscopy were used to reveal the reaction mechanism for low and high PT CBs.

**Results.** NOR at an initial concentration of 5 mg L<sup>-1</sup> achieved 100% degradation within 120 min in presence of CB pyrolyzed at 950 °C (CB950). High PT CB exhibited excellent performance compared to low PT CB (Figure 1). CB950 caused 3 times higher NOR degradation compared to low pyrolysis temperature (PT) CBs and other widely used catalysts. CB950 achieved a maximum surface area normalized first-order rate constant  $k_{SA}$  of 4.38×10<sup>-2</sup> min<sup>-1</sup> m<sup>-2</sup> L<sup>-1</sup>. NOR degradation by CBs/PDS was active over a broad pH range (3 - 10), but with increasing rates under alkaline conditions. Reused CB950 was still able to achieve 100% NOR degradation after four times recycling. The EPR data are consistent with the quenching experiments and confirm that both hydroxyl and sulfate radicals are important reactants in the oxidation of NOR in presence of the low PT CBs. EPR showed that Mn<sup>II</sup> further promotes generation of radicals. For the high PT biochar CB950, neither a large number of hydroxyl nor of sulfate radicals was produced thus indicating they were not dominating oxidants in NOR degradation. Linear-sweep voltammetry with CB950 used as working electrode showed a strong current increase from 0.03 to 6 mA when the potential increased from 0.5 to 1.6 V against Ag/AgCl reference electrode, demonstrating that PDS and NOR together promotes an anodic electron exchange reaction. Combined oxidation by electron transfer reactions and radicals dominate in presence of high PT CBs. High PT CB act as an electron mediator to facilitate the acceptance of electrons by PDS from NOR. Dominating metabolites comprise fluoride (80% defluorination) and low molecular compounds. This study demonstrates the possibility of utilizing algal bloom biomass to produce biochar to be used as green and easily fabricated catalysts for the removal of organic contamination from wastewater.

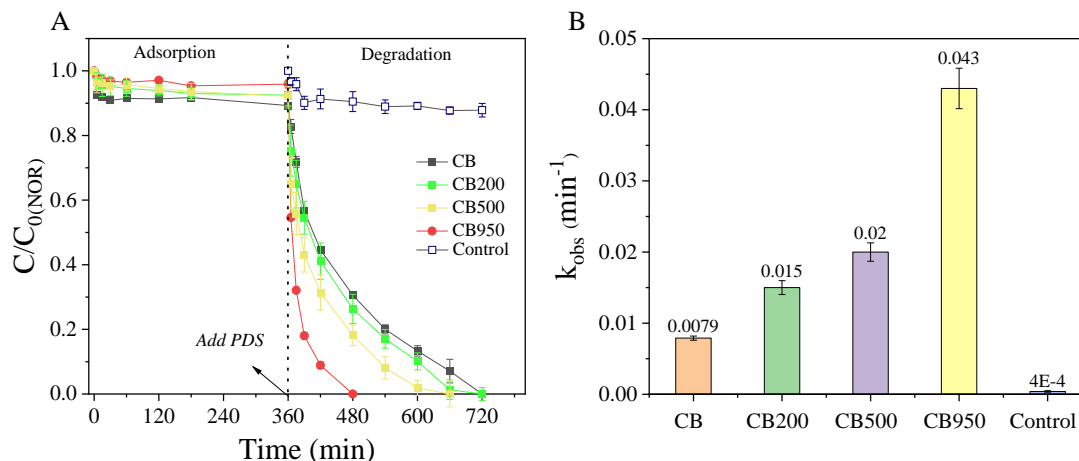


Figure 1. NOR degradation by CBs. (A) NOR degradation by PDS in presence of different CBs and control, (B) Pseudo-first-order kinetic constants for NOR degradation by different CBs. ([PDS] 10 mM; pH 6.8 (0.2 M phosphate buffer) and biochar dosage  $100 \text{ mg L}^{-1}$ ;  $[\text{NOR}]_0 5 \text{ mg L}^{-1}$ ). Error bars represent standard deviation of triplicates.

## Highlights

- Reactivity of cyanobacterial biochar increases with pyrolysis temperature.
- CB pyrolyzed at 950 °C obtains the fastest NOR degradation and can be recycled.
- CBs are active at pH 3-10, with increasing rates under alkaline conditions.
- Organic,  $\cdot\text{OH}$ ,  $\text{SO}_4^{\cdot-}$  radicals and  $\text{Mn}^{\text{II}}$  degrade NOR in presence of low PT CB.
- Combined oxidation by electron transfer and radicals dominates in presence of high PT CB

## References

1. Pan, Y., et al., *Norfloxacin pollution alters species composition and stability of plankton communities*. *J Hazard Mater*, 2020. **385**: p. 121625.
2. Lee, J., U. von Gunten, and J.H. Kim, *Persulfate-Based Advanced Oxidation: Critical Assessment of Opportunities and Roadblocks*. *Environ Sci Technol*, 2020. **54**(6): p. 3064-3081.
3. Shang, Y., et al., *Removal of sulfamethoxazole from water via activation of persulfate by Fe3C@NCNTs including mechanism of radical and nonradical process*. *Chemical Engineering Journal*, 2019. **375**.
4. Zhang, T., et al., *Efficient Peroxydisulfate Activation Process Not Relying on Sulfate Radical Generation for Water Pollutant Degradation*. *Environmental Science & Technology*, 2014. **48**(10): p. 5868-5875.
5. Oh, W.-D. and T.-T. Lim, *Design and application of heterogeneous catalysts as peroxydisulfate activator for organics removal: An overview*. *Chemical Engineering Journal*, 2019. **358**: p. 110-133.

## New biodegradable metal complex for photo-Fenton like processes at neutral pH

P. Prete<sup>1\*</sup>, A. Fiorentino<sup>1</sup>, L. Rizzo<sup>2</sup>, A. Proto<sup>1</sup>, R. Cucciniello<sup>1</sup>

<sup>1</sup> Dep. Chemistry and Biology, University of Salerno, Via Giovanni Paolo II, 132 – 84084 Fisciano (SA), Italy

<sup>2</sup> Dep. Civil Engineering, University of Salerno, Via Giovanni Paolo II, 132 – 84084 Fisciano (SA), Italy

\*pprete@unisa.it

Fenton and photo Fenton processes are among the most effective advanced oxidation processes (AOPs) in industrial wastewater treatment. However, they are still barely feasible for full-scale applications due to the requirement of a strongly acidic pH to ensure the solubility of iron ions [1]. To cope with this limitation, alternative processes have been proposed as (photo) Fenton-like processes, including both heterogeneous and homogeneous catalysed processes [2].

Heterogeneous catalysts involve iron- and non-iron based materials in place of dissolved iron ions typically used in classic Fenton processes. Alternative homogeneous catalysts, instead, involve the use of chelating agents to form with iron or other transition metals, complexes soluble at neutral and circumneutral pH and active in Fenton-type mechanism [3,4].

Thus, following the benign-by-design approach, a new, green, active and fully biodegradable (96% in 28 days) catalyst, ferric iminodisuccinate (FeIII-IDS), able to promote the Fenton-like process will be presented herein for the treatment of a real olive mill wastewater [5].

Fe-IDS supported (photo) Fenton-like processes were performed at circumneutral pH with different catalyst loadings at fixed H<sub>2</sub>O<sub>2</sub> initial concentration. Experiments were performed in dark and under solar and UV-C irradiation to evaluate the effect of radiation source, and compared to other AOPs, namely classic Fenton performed at pH 3, and H<sub>2</sub>O<sub>2</sub> photolysis under both solar and UV-C irradiation. The best results (54% and 49% COD removals for solar and UV-C radiation respectively), were obtained using a [H<sub>2</sub>O<sub>2</sub>]/[Fe-IDS] molar ratio of 250 (H<sub>2</sub>O<sub>2</sub> 58.8 mM, Fe-IDS 0.021 mM).

### Acknowledgements

This work was financially supported by research fund “FARB”, University of Salerno (ORSA193377 and ORSA203722) and PROGEMA project funded through PON “Ricerca e Innovazione” 2014–2020 e FSC.

### References

- [1] L. Clarizia, D. Russo, I. Di Somma, R. Marotta, R. Andreozzi, *Appl. Catal. B Environ.* **209** (2017).
- [2] P. Prete, A. Fiorentino, L. Rizzo, A. Proto, R. Cucciniello, *Curr. Opin. Green Sustain. Chem.* **28** 100451 (2021).
- [3] A. Fiorentino, R. Cucciniello, A. Di Cesare, D. Fontaneto, P. Prete, L. Rizzo, G. Corno, A. Proto, *Water Res.* **146** 206–215 (2018).
- [4] A. Di Cesare, M. De Carluccio, E.M. Eckert, D. Fontaneto, A. Fiorentino, G. Corno, P. Prete, R. Cucciniello, A. Proto, L. Rizzo, *Water Res.* **184** 116194 (2020).
- [5] A. Fiorentino, P. Prete, L. Rizzo, R. Cucciniello, A. Proto, *J. Environ. Chem. Eng.* 106802 (2021).

## Reduce Greenhouse Gas Emissions by optimizing Wastewater Treatment Plants

Maria Cristina Collivignarelli <sup>1,2</sup>, Marco Carnevale Miino <sup>1\*</sup>, Vincenzo Torretta <sup>3</sup>, Elena Cristina Rada <sup>3</sup>, Ioannis A. Katsoyiannis <sup>4</sup>, Lucian-Ionel Cioca <sup>5</sup> and Sabrina Sorlini <sup>6</sup>

<sup>1</sup> Department of Civil Engineering and Architecture, University of Pavia, via Ferrata 3, 27100 Pavia, Italy

<sup>2</sup> Interdepartmental Centre for Water Research, University of Pavia, Via Ferrata 3, 27100 Pavia, Italy

<sup>3</sup> Department of Theoretical and Applied Sciences, Insubria University of Varese, Via G.B. Vico 46, 21100 Varese, Italy

<sup>4</sup> Laboratory of Chemical and Environmental Technology, Department of Chemistry, Aristotle University of Thessaloniki, 54124 Thessaloniki, Greece

<sup>5</sup> Industrial Engineering and Management Department, Faculty of Engineering, Lucian Blaga University of Sibiu, 10 Victoriei Blv., 550024 Sibiu, Romania

<sup>6</sup> Department of Civil, Environmental, Architectural Engineering and Mathematics, University of Brescia, via Branze 43, 25123 Brescia, Italy

\*marco.carnevalemiino01@universitadipavia.it

**Introduction:** Greenhouse gases (GHG) are at the basis of current climate change phenomena [1]. Not only industrial sector but also, wastewater treatment plants (WWTPs) emit GHG during their operation, specifically CO<sub>2</sub>, CH<sub>4</sub>, and N<sub>2</sub>O, and treatments in both water and sludge line are responsible for these emissions. GHG can be emitted directly (e.g., CH<sub>4</sub> lost by the anaerobic digester collection system) or indirectly (e.g., CO<sub>2</sub> emitted due to energy consumption) [2,3]. In previous studies, the positive effect of functionality checks in terms of increase in pollutants removal yields, reduction of energy and reagents consumption have been highlighted [4–6]. In this work the impact of an optimized WWTP has been studied in terms of GHG emission.

**Methods:** A full-scale WWTP which treats both urban and industrial wastewater was used as case study for the analysis. Data collected from the optimized period (after functionality checks and up-grade execution) were compared with data of a control period collected when the WWTP operated in non-optimized conditions. Each period lasted one year. GHG were therefore estimated based on energy and reagents consumption and biological sludge production. Biological and chemical sludge were assumed to be disposed in agriculture and landfill respectively. GHG emission factors were assumed based on existent literature [7–12]. Based on data provided by the water utility, treated flowrates were almost constant in the two periods.

**Results and discussion:** Based on results of previous functionality checks, several improvements (such as the optimization of the reagents dosage, revamping of the air supply system, removal of dead volumes in reactors), have been applied to the WWTP. Therefore, GHG emission were estimated and compared with the non-optimized plant (control case) (Figure 1). Three sectors were considered: energy, sludge disposal and reagents. In all of these sectors, the GHG emitted by the optimized plant was significantly lower than the control case (up to -76 %, in case of reagents use and production). Considering all of these aspects, optimizing WWTP reduce GHG direct and indirect emissions by 46%.

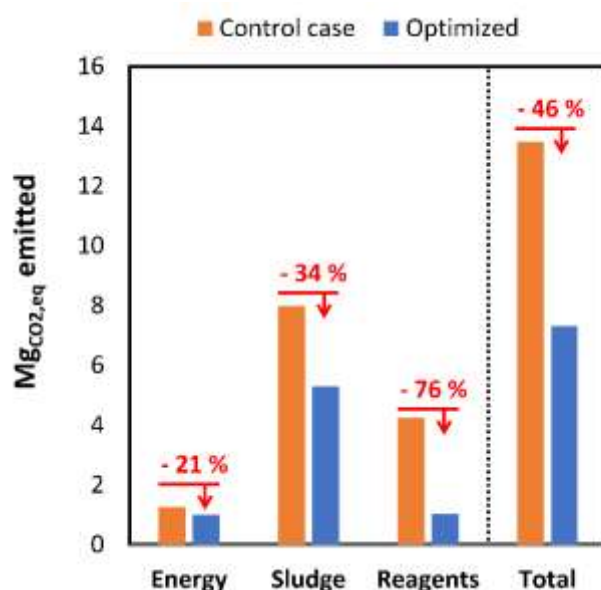


Figure 1. GHG emitted in the optimized period compared with emissions in the control case.

**Conclusions:** This work is focused on the impact of an optimized WWTP in terms of efficiency on GHG emissions. After functionality checks and several improvements, a WWTP was used as reference for estimating



GHG emission. Considering, energy required, reagent use and production and sludge disposal, results highlighted that optimizing the operational efficiency of WWTP can help to reduce GHG emissions up to 46%.

## Acknowledgements

The authors would like to thank ASMia S.r.l. for providing the data necessary for this study.

## References

1. S. Manabe, *Tellus A Dyn. Meteorol. Oceanogr*, **71** 1620078 (2019).
2. R. Gori, L.-M. Jiang, R. Sobhani, D. Rosso, *Water Res.*, **45** 5858–5872 (2011).
3. G. Mannina, T.F. Rebouças, A. Cosenza, K. Chandran, *J. Clean. Prod.*, **217** 244–256 (2019).
4. M. C. Collivignarelli, M. Carnevale Miino, S. Manenti, S. Todeschini, E. Sperone, G. Cavallo, A. Abbà, *Environ. Process.*, **7** 563–578 (2020).
5. S. Manenti, S. Todeschini, M. C. Collivignarelli, A. Abbà, *Environ. Process.*, **5** 23–42 (2018).
6. M. C. Collivignarelli, G. Bertanza, A. Abbà, S. Damiani, *Int. J. Environ. Sci. Technol.*, **16** 3455–3466 (2019).
7. D. Romano, C. Arcarese, A. Bernetti, A. Caputo, M. Cordella, R. De Lauretis, E. Di Cristofaro, A. Gagna, B. Gonella, F. Moricci, G. Pelis, E. Taurino, M. Vitullo, *National Inventory Report 2021*, (2021)
8. G. Zhao, M. Garrido-Baserba, S. Reifsnnyder, J.C. Xu, D. Rosso, *Sci. Total Environ.*, **665** 762–773 (2019).
9. Intergovernmental Panel on Climate Change, Volume 3: Industrial Processes and Product Use, Chapter 2 - Mineral Industry Emissions. In *2006 IPCC Guidelines for National Greenhouse Gas Inventories*, 1–40 (2006).
10. K. P. Law, K. R. Pagilla, *J. Clean. Prod.*, **290** 125874 (2021).
11. D. Kyung, D. Kim, N. Park, W. Lee, *J. Environ. Manage.*, **131** 74–81 (2013).
12. City of Winnipeg, *Emission Factors in kg CO<sub>2</sub>-Equivalent per Unit* (2011).

## Designing of thiourea-functionalized chitosan aerogels for deep cleaning of wastewaters containing heavy metal ions

Claudiu-Augustin Ghiorghita\*, Maria Marinela Lazar, Ioana Victoria Platon, Maria Valentina Dinu  
 "Petru Poni" Institute of Macromolecular Chemistry, Grigore Ghica Vodă Alley, 41A, Iasi 700487, Romania  
 \*e-mail address of corresponding author: [claudiu.ghiorghita@icmpp.ro](mailto:claudiu.ghiorghita@icmpp.ro)

Chitosan-based materials are thoroughly scrutinized for their great potential in removing heavy metal ions from contaminated waters. The chemical versatility of chitosan supports the elaboration of various grafting/cross-linking strategies to design materials with tunable/improved metal ions chelating properties. Among the strategies under investigation, the development of hydrogels with high surface area and grafting of sulphur-bearing functional groups are of particular interest because they allow the fabrication of sorbents featuring fast kinetics and/or selectivity towards specific metal ions [1, 2].

In this contribution a simple one-pot method to prepare chitosan aerogels functionalized with thiourea by formaldehyde cross-linking/grafting using multiple cryostructuring steps is reported. Information on structural, textural, morphological and mechanical features of the aerogels was obtained by FTIR spectroscopy, dynamic water vapor sorption, scanning electron microscopy and uniaxial compression measurements. The performance of prepared aerogels in the removal of Cu(II), Ag(I) and Pb(II) metal ions from wastewaters was investigated as a function of pH, initial metal ion concentration and contact time.

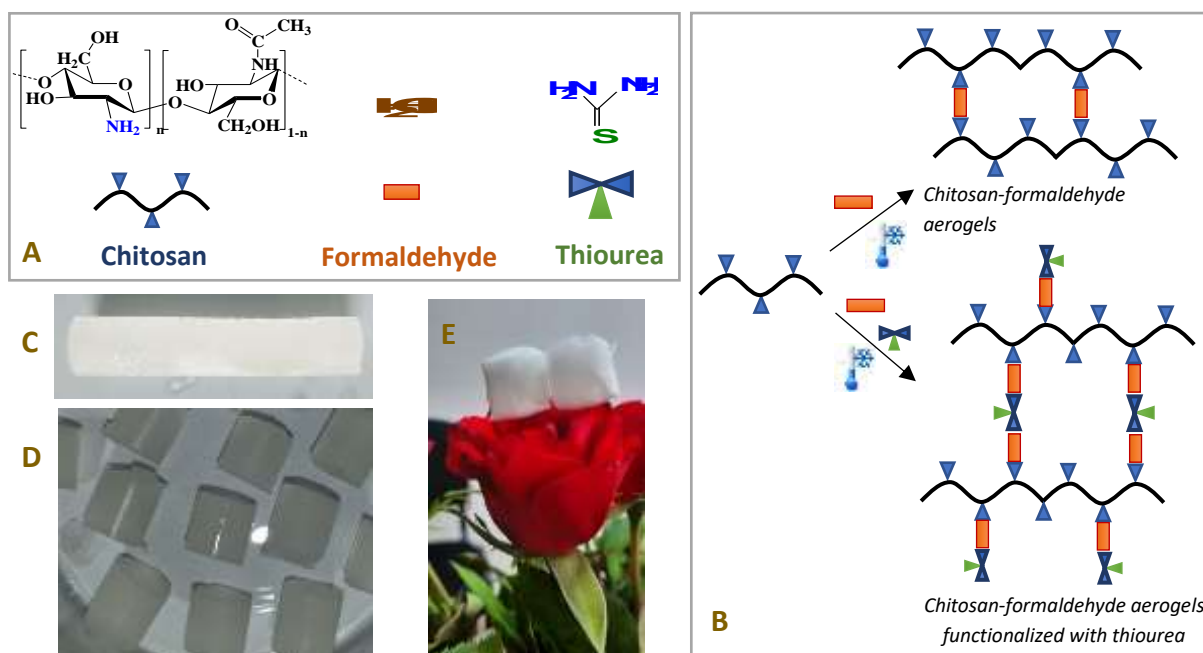


**Figure 1.** (A) Chemical structures of main reagents used in this work. (B) Schematic illustration with the preparation pathway of chitosan and thiourea-chitosan aerogels. Optical images of: (C) monolith-like chitosan aerogels immediately after synthesis, and (D) in cut pieces before washing, as well as (E) of freeze-dried aerogels on top of a rose flower.

### Acknowledgments

This work was supported by grants of the Ministry of Research, Innovation and Digitization, CNCS/CCCDI – UEFISCDI, project number *PN-III-P1-1.1-TE-2021-0771*.

### References

1. P. Sáez, I.A. Dinu, A. Rodríguez, J.M. Gómez, M.M. Lazar, D. Rossini, M.V. Dinu, *Int. J. Biol. Macromol.*, **164** 2432-2449 (2020).
2. J. Guo, X. Fan, Y. Li, S. Yu, Y. Zhang, L. Wang, X. Ren, *J. Hazard. Mater.*, **415** 125641 (2021).

## A potential biotechnological approach to recover technology-critical elements from complex aqueous mixtures

Thainara Viana<sup>1\*</sup>, Bruno Henriques<sup>1</sup>, Nicole Ferreira<sup>1</sup>, João Pinto<sup>1</sup>, Daniela Tavares<sup>1</sup>, João Colónia<sup>1</sup>,  
Jéssica Jacinto<sup>1</sup>, and Eduarda Pereira<sup>1,2</sup>

<sup>1</sup> Department of Chemistry, LAQV-REQUIMTE, University of Aveiro, 3810-193 Aveiro, Portugal

<sup>2</sup> LCA, Department of Chemistry, University of Aveiro, Aveiro, Portugal

\*thainara@ua.pt

### Introduction

Electronic waste (e-waste) is one of the most ascending waste streams, whose management has become a priority to minimize environmental impacts, such as water contamination [1]. This waste is also a rich source of elements with high economic and technological interest (technology-critical elements – TCE), such as cobalt, platinum, and rare earth elements (REEs), which can be recovered and re-introduced into the production cycle [2]. The use of living macroalgae as biosorbent has been highlighted with potential to recover TCE from contaminated waters [3], taking advantage of the potential intracellular accumulation (bioaccumulation) as an additional step to biosorption [4]. Yet most studies focus on the removal of a single element from simple solutions (synthetic water, containing one element or a small specific group of elements). The main objective of the present work was to evaluate and optimize the parameters that influence the efficiency of the biosorption/bioaccumulation process performed by *Ulva lactuca* in a complex mixture of contaminants: simulated lamp industry effluent (Y, Eu, La, Ce, Tb, Gd, Hg, Pb, Zn, Cu, Co, Cd, Pt), at different contamination levels (10, 100 and 190 µg/L). Optimization followed the Response Surface Methodology with a Box-Behnken Design (18 trials). In addition, the behaviour of the elements in solution was evaluated, as well as the allocation of elements in the macroalgae (biosorbed and/or bioaccumulated).

### Experimental

The macroalga *Ulva lactuca* was collected at low tide from the NW coast of Ria de Aveiro, Portugal (40°38'39"N, 8°44'43"W). *U. lactuca* was washed and maintained in aerated aquaria containing filtered seawater, at room temperature and natural photoperiod (12 h light : 12 h dark) until use. Saline water was collected at high tide from the Atlantic Ocean, next to Barra beach, Portugal (salinity 35; 40°64'41"N, 8°74'53"W). The collected water was filtered using Millipore porous filters (0.45 µm) and subsequently diluted to evaluated salinities using ultrapure water.

A known amount of *U. lactuca* (1 to 5 g/L, fresh weight) cut in discs (diameter (Ø) = 5.5 ± 0.1 cm, Figure 1) was exposed for 144 h to 1 L of a complex mixture at different contamination levels (10 to 190 µg/L), at different water salinity (15 to 35). At pre-determined times, aliquots (10 mL) were collected and stored in polystyrene tubes, previously acidified with HNO<sub>3</sub> (65 % v/v) for posterior analysis. Control (simulated effluent without macroalgae) and blank (living macroalgae in clean water) solutions were run in parallel with the exposure assays to guarantee the quality control.

Concentrations of REEs in aqueous solutions and seaweed were measured through Inductively Coupled Plasma associated with optical emission spectroscopy (ICP-OES) on a HORIBA Jobin Yvon, model ACTIVA M, methodology described in [4].

Partitioning of elements between surface (extracellular sorption) and internalized parts (intracellular uptake) of *U. lactuca*. was assessed by i) EDTA 0.001 mol/L in NaCl solution (0.6 mol/L); ii) ultrasound water bath (US) (NaCl 0.6 mol/L); iii) US+EDTA [4], [5]. Macroalgae were characterized by fourier transform infrared (FTIR) and scanning electron microscope (SEM) before and after the exposure and treatment with EDTA.



Figure 1: Discs of *U. lactuca* used in the experiments

## Results and Discussion

In general, *U. lactuca* presented high removal efficiencies for all elements (central point conditions > 75 %) except for Pt and Cd. Results from central point showed a low standard deviation (< 0.99) and a low coefficient of variation (< 1.2 %), which guarantee the reproducibility and feasibility of results. For REEs, at an exposure time of 24 h, the obtained optimal conditions for the evaluated response (removal, %) were: 5 g/L of *U. lactuca* (fresh weight) at salinity 15 (Figure 1B) and at an initial concentration of 10  $\mu\text{g/L}$ , allowing to remove 71 - 87 % of the REEs from the complex solution. Through the cell partitioning of the sorbed elements, via selective extractions with EDTA, it was found that most of them were located on the external surface of *U. lactuca*. Characterization methods, as FTIR (Figure 2b) and SEM analysis, support EDTA results, exposing a clean macroalgae surface post-washing procedure.

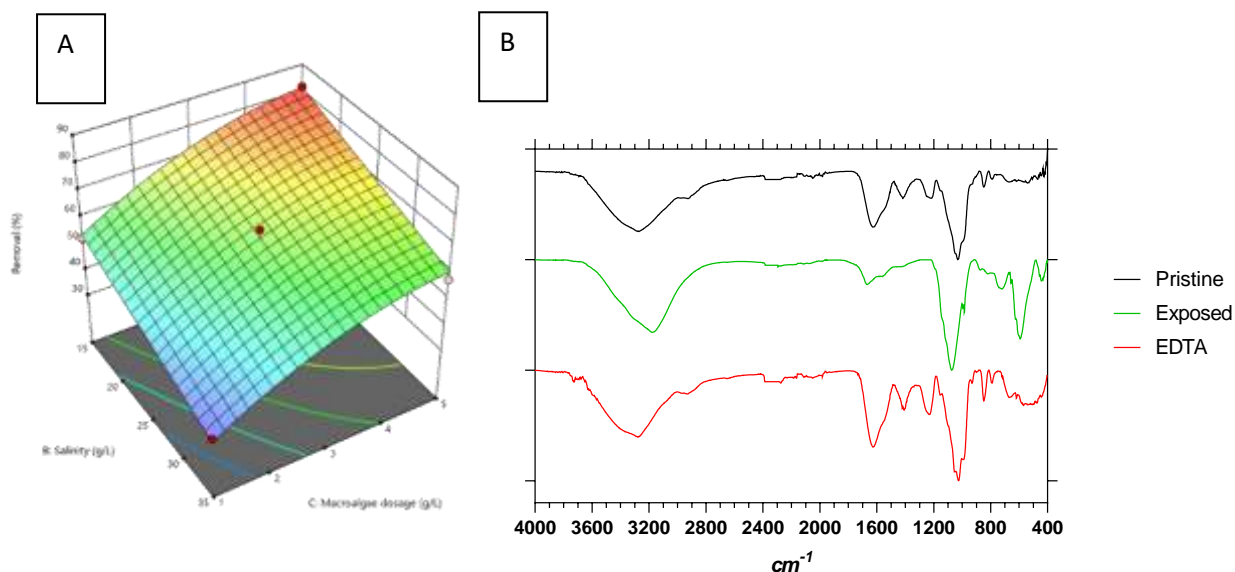


Figure 2. A) 3D-surface response for Eu removal at 24 h of exposure (initial concentration of 100  $\mu\text{g/L}$ ); B) FTIR of *Ulva lactuca* pristine to assays (black line), after exposure (green line) and after EDTA treatment (red line).

## Conclusions

The present study revealed that living marine macroalgae can be the basis of an efficient, greener, and low-cost technology to remediate complex effluents containing potentially toxic elements, rare earth elements, and platinum group metals, that despite being below wastewater discharge limits still reach marine ecosystems, representing a threat.

## Acknowledgements

Bruno Henriques acknowledges FCT for the research contract (CEECIND/03511/2018) under the CEEC Individual 2018, while João Pinto and Jessica Jacinto acknowledge their PhD grant (2020.05323.BD and UI/BD/151290/2021, respectively). Thanks are also due to the financial support to REQUIMTE (UIDB/50006/2020) to FCT/MEC through national funds, and the co-funding by the FEDER, within the PT2020 Partnership Agreement and Compete 2020. This work was supported by the project N<sup>o</sup>46998\_N9ve-REE, co-funded by Portugal 2020 program (PT2020), PO Centro and European Regional Development Fund.

## References

- [1] L. Schweitzer and J. Noblet, "Water Contamination and Pollution," in *Green Chemistry*, Elsevier, 2018, pp. 261–290.
- [2] StEP Initiative, "Annual Report: Five years of the StEP Initiative," 2011.
- [3] N. Ferreira *et al.*, "Assessment of marine macroalgae potential for gadolinium removal from contaminated aquatic systems," *Sci. Total Environ.*, vol. 749, p. 141488, Dec. 2020.
- [4] B. Henriques *et al.*, "Simultaneous removal of trace elements from contaminated waters by living *Ulva lactuca*," *Sci. Total Environ.*, vol. 652, pp. 880–888, 2019.
- [5] E. Noriega-Fernández *et al.*, "Innovative Ultrasound-Assisted Approaches towards Reduction of Heavy Metals and Iodine in Macroalgal Biomass," *Foods*, vol. 10, no. 3, p. 649, Mar. 2021.

## Continuous Adsorption Process for Cr(VI) on Hydrothermally Treated Chitosan/Polyvinyl Alcohol Beads

Eylul Kosoglu<sup>1</sup> and Yasar A. Aydin<sup>1\*</sup>

<sup>1</sup>Marmara University, Faculty of Engineering, Chemical Engineering Dpt., Basibuyuk, 34854 Maltepe, Istanbul, Turkey

\*[yasar.aydin@marmara.edu.tr](mailto:yasar.aydin@marmara.edu.tr)

Pollution of water resources due to the discharge of industrial wastes is an important environmental problem. Industrial wastewater contains large amounts of heavy metal ions and organic pollutants, which endanger human health and the environment. For this reason, many studies have been carried out to remove heavy metals from water. The adsorption process is widely used for the removal of heavy metals from wastewater due to its low cost, applicability and environmental friendliness [1,2]. The efficiency of adsorption is heavily dependent upon the choice of adsorbent. The required qualifications involve many chemical and structural properties such as high mechanical and chemical stability, low cost, ease of regeneration and reuse, high surface area and befitting porous structure and chemical functionality [2]. Chitosan, a cheap and sustainable natural polysaccharide with high density of -NH<sub>2</sub> and -OH functionalities, meets many of these demands with the exception of limited physical stability in mildly acidic environment. Yet, physical and/or chemical modification procedures can be used to alter solubility and improve adsorption capacity. To date, modified forms of chitosan, i.e cross-linked, blended or as a composite component, have been synthesized and used in various adsorbent processes [3].

In this work, chitosan/polyvinyl alcohol blend beads synthesized by hydrothermal method were used in the continuous adsorption process for Cr(VI) ions. In order to evaluate the efficiency and sustainability of the process column and process parameters of bed height, initial concentration and flow rate were studied at different levels. Additionally, the desorption efficiency and reusability of chitosan/polyvinyl alcohol beads were investigated at three consecutive adsorption-desorption cycles.

For this purpose, 4 wt.% chitosan solution prepared in 4 % (v/v) acetic acid was blended with 10 wt.% PVA solution in equal proportions. Gelling was achieved in 1.0 M NaOH solution for 24 hours. Beads were transferred to a stainless-steel autoclave where hydrothermal treatment was performed at 140 °C for 12 hours. After drying the beads were utilized as the fixed bed adsorbent material for continuous Cr (VI) adsorption experiments. The process parameters of flow rate, initial concentration and bed height were varied between 2 -6 mL/min, 25-75 ppm and 2.5-7.5 cm, respectively. Cr (VI) concentration of solutions was analyzed spectrophotometrically at 540 nm. Data were used for the construction of breakthrough curves and modeling studies were conducted using Thomas and Bohart-Adams models. Regeneration was studied in 0.1 M NaOH. All experiments were conducted in triplicates and results were reported as the average. The structural properties of beads were investigated using N<sub>2</sub> adsorption (BET), scanning electron microscopy (SEM), Fourier transform infrared (FT-IR) spectroscopy.

According to the results, highest removal efficiency was achieved at the lowest studied flow rate of 2 mL/min, with 6 cm of bed height and 50 ppm initial Cr(VI) concentration. Both Thomas and Bohart-Adams models were descriptive of the adsorption data with regression coefficients over 90%. The surface area of the blend beads were determined as 2.96 m<sup>2</sup>/g with overall pore volume of 0.35 cm<sup>3</sup>/g.

### Acknowledgements

The study was financially supported by Marmara University Scientific Research Projects Coordination Unit.

### References

1. M.R. Agarwal, K. Singh, *Journal of Water Reuse and Desalination*, 7 387 (2016).
2. D. Chen, L. Wang, Y. Ma, W. Yang, *NPG Asia Materials*, 8 e301 (2016).
3. R. Yi, W. Cai, C. Dang, B. Han, L. Liu, J. Fan, *Chemical Engineering Research and Design*, 156 43 (2020).

## Effect of blending Methanol with Gasoline on the Exhaust Emissions

V. Ibrahim<sup>1\*</sup>, S. Safwat<sup>2</sup>, Manal Amine<sup>1</sup>, Ezis. Awad<sup>1</sup>, and Y. Barakat<sup>1</sup>

<sup>1</sup> Egyptian Petroleum Research Institute, Nasr City, Cairo, Egypt

<sup>2</sup> Faculty of science, Alexandria University, Egypt

\*corresponding author email: [viola\\_ibrahimm@yahoo.com](mailto:viola_ibrahimm@yahoo.com)

### Abstract

Methanol is regarded as a renewable biofuel as it can be produced from biomass. It could be valuable environmentally friendly gasoline additive as it enhances octane number and decreases the exhaust emissions so it is associated with positive impacts on the environment. In the present work, hydrocarbon Gasoline (80 Research Octane Number) was blended with 3, 6, 9, 12, and 15 volume percent of methanol to give five methanol-gasoline blends M3, M6, M9, M12, and M15 respectively. These fuel blends were used to investigate the impact of methanol on the research octane number (RON), the motor octane number (MON) and the exhaust emissions (CO, NO<sub>x</sub>, SO<sub>2</sub>, HC, CO<sub>2</sub> and excess O<sub>2</sub>). RON single stroke test engine was applied for combustion. The experimental results show that the addition of methanol leads to a significant increase in RON and MON (Fig.1). For exhaust emission the results show that it leads to a significant reduction in CO, SO<sub>2</sub> and HC emissions while the addition of methanol up to 15% leads to increase in CO<sub>2</sub> and NO<sub>x</sub> emissions (Fig. 2). The significant decrease in CO could be attributed to the high oxygen content of gasoline methanol blends compared to the base gasoline. This excess in oxygen content improves the combustion of methanol gasoline blends [1-2].

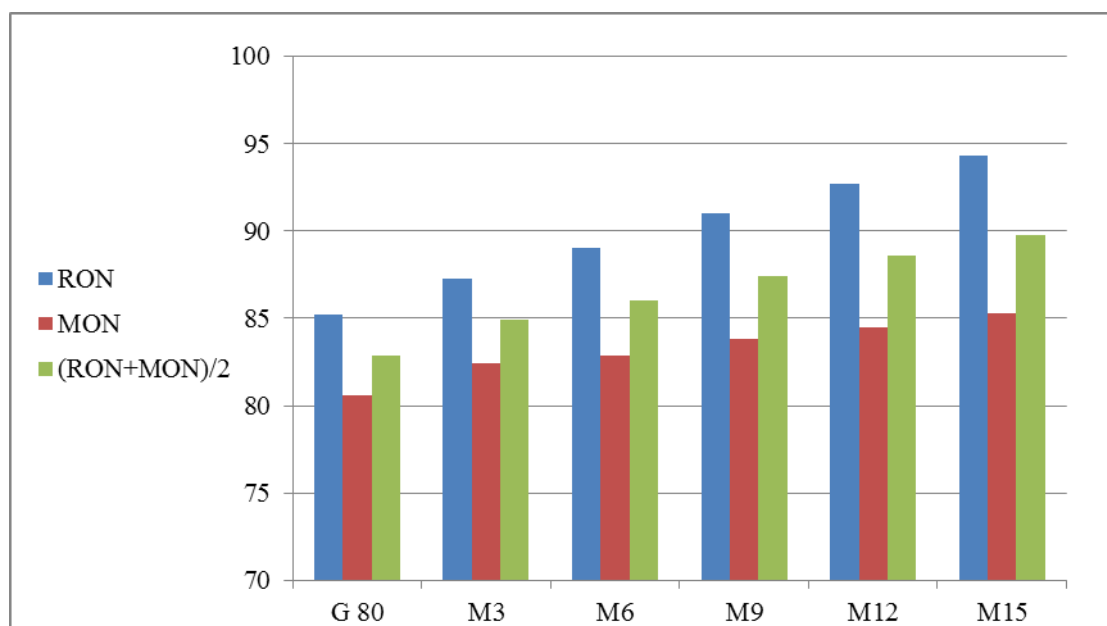


Figure 27: Effect of methanol addition on octane number of hydrocarbon base gasoline 80

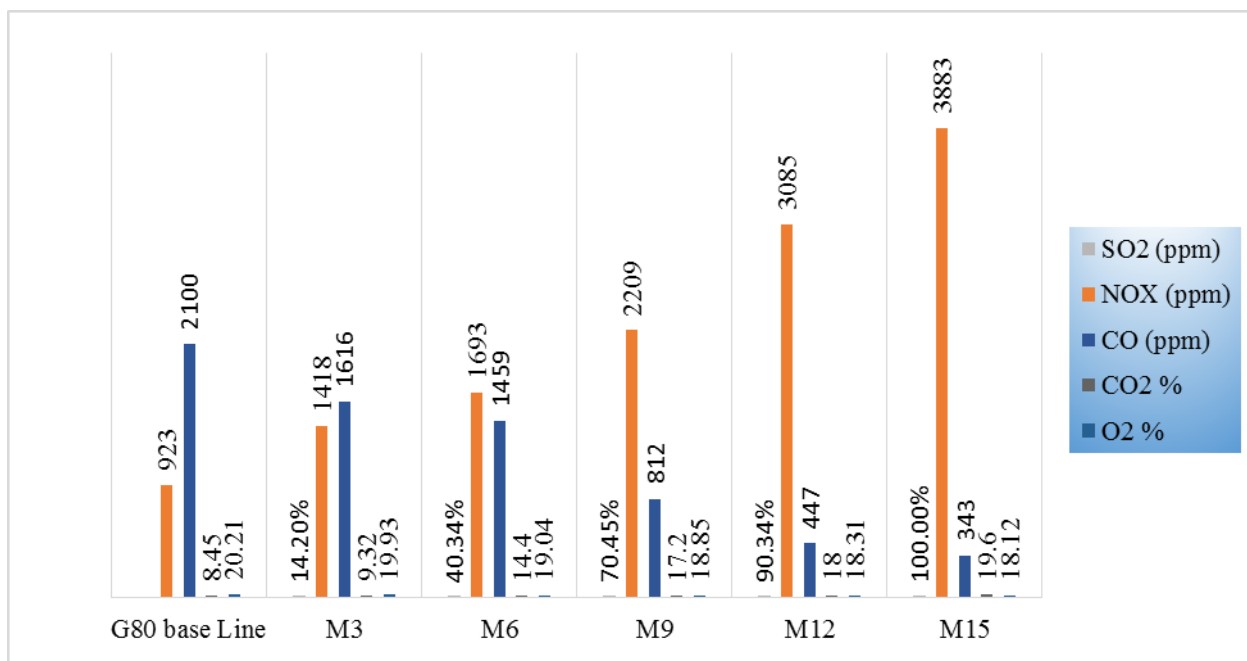


Figure 28: Emissions pollutants against the Increase in Methanol Concentration in the blends

### References

1. A.K. Agarwal, H.K.A. Dhar, , Fuel Processing Technology, **121** 16 (2014).
2. P.Obulesu R. SivaKumar B.Ramanjaneyulu, materialstoday: PROCEEDINGS, 39 Part 1 590 (2021),



# One-pot solvent-free synthesis of renewable plasticizer alcohols/bio-oil from wastewater grown microalgal biomass via. in-situ crystallization of hydroxyapatite

Vivek Suresh Dalvi\*, Farah Naaz, Anushree Malik

Applied Microbiology Lab, Centre for Rural Development and Technology, Indian Institute of Technology, Delhi, 110016

\*dalvi.vivek11@gmail.com

## Abstract text:

Synthesis of industrially important chemicals and materials from renewable sources for a carbon neutral petroleum-free economy is compelling globally. Here we have developed a holistic approach for synthesizing renewable plasticizer alcohols using photosynthetic microalgae reclaiming wastewater dissolved CO<sub>2</sub> and nutrients. To achieve the same, the municipal wastewater grown microalgal biomass polishing nutrients from anaerobically treated municipal wastewater was hydrothermally liquefied (HTL) at subcritical conditions under an inert environment and using K<sub>2</sub>CO<sub>3</sub> as an alkaline catalyst. The biosolids, co-product of HTL, contained in-situ crystallized hydroxyapatite (HTL-HA) with multi-metal (Si, Mg, Na, Fe, Zn, Cu, Cd, Ni, Mn) substitutions, exhibiting weak lattice hydroxyl peak than considerable hydroxyl vacancies (Lewis acid sites), and strong P–OH complex peak (Brønsted acid sites). The in-situ synthesized HTL-HA catalytically upgraded the bio-oil (UBO), and, Interestingly, UBO contained a 90% mass fraction in the direct fuel range with a maximum product yield of C16-C25 compounds. The heterogeneity induced with the system by HTL-HA (acidic) and K<sub>2</sub>CO<sub>3</sub> (basic) selectively yielded 171 gKg<sup>-1</sup> of esters and 70 gKg<sup>-1</sup> of alcohols with a significant fraction of Bis (2-Ethylhexyl) phthalate (131 gKg<sup>-1</sup>) of raw feedstock.

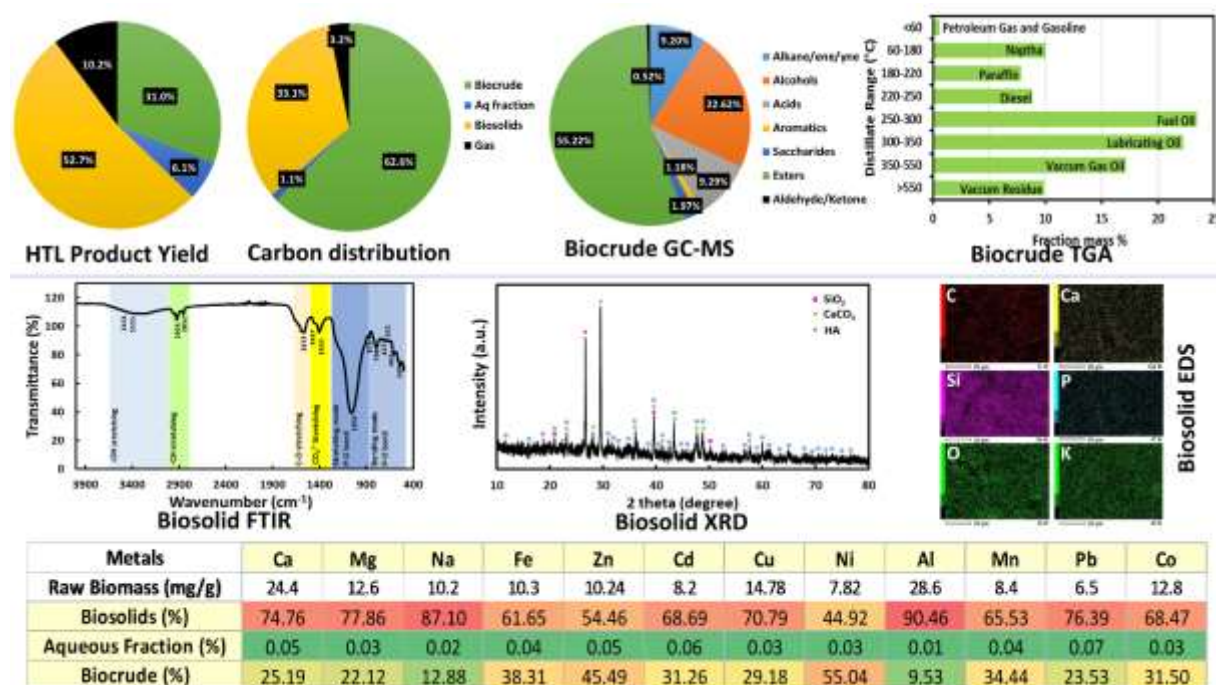


**Figure 1.** Representation of biocrude, biosolid product characterization, and heavy-metal partitioning post hydrothermal liquefaction treatment

Another phthalate with properties of a plasticizer found in the biocrude was dibutyl phthalate [1]. 11% FAMES-methyl octanoate (octanoic acid, methyl ester), methyl decanoate (caprate), methyl laurate, methyl linolenate, methyl behenate, methyl erucate (methyl cis-13-docosanoate), and methyl lignocerate (methyl tetracosanoate) were present in the biocrude. The rest of the valuable compounds in the biocrude had properties of food additives or personal care products. L-arabitol, a low-calorie sugar alcohol, finds its application in the food industry as a sweetener, generally used to regulate the blood sugar level in diabetic patients [2]. Another food additive (used in improving flavor) found in the biocrude was Octanoic acid, methyl ester [3]. Fatty alcohol named 1-hexadecanol, with an area percentage of 4.24%, was also observed in the biocrude. This compound is used in Personal care product industries as a surfactant/emulsifier/thickening agent in shampoos, creams, lotions, etc.

## Summary:

Overall, the efforts signify the applicability of the developed process of recirculation photobioreactor for wastewater resource conservation and recovery integration with subcritical hydrothermal liquefaction. The process creates a novel approach for creating high-value product streams from water reclamation sources that can

significantly impact taxpayer money, generating employability in green chemistry for profit in a traditionally regulated water industry with contributing to biofuels and green catalysis. These findings provide the basis for new frontiers in microalgae-based fuels, chemicals, and bioproducts at both the fundamental and macro commercialization levels.

**Acknowledgement:**

The authors gratefully acknowledge LOTUS-HR project sponsored by the Department of Biotechnology (DBT), Government of India, for financial support (BT/IN/Indo Dutch/19/2016) and MI-FIRP (MI02021G) for partial support of this work.

**References:**

1. Chen, D., Sun, X., Zhang, K., Fan, G., Wang, Y., Li, G., Hu, R., 2017. A Noncontact Dibutyl Phthalate Sensor Based on a Wireless-Electrodeless QCM-D Modified with Nano-Structured Nickel Hydroxide. *Sensors* 17, 1681. <https://doi.org/10.3390/s17071681>
2. Loman, A.A., Islam, S.M.M., Ju, L.K., 2018. Production of arabitol from enzymatic hydrolysate of soybean flour by *Debaryomyces hansenii* fermentation. *Appl. Microbiol. Biotechnol.* 102, 641–653. <https://doi.org/10.1007/s00253-017-8626-5>
3. Wang, L., Dou, G., Guo, H., Zhang, Q., Qin, X., Yu, W., Jiang, C., Xiao, H., 2019. Volatile organic compounds of *Hanseniaspora uvarum* increase strawberry fruit flavor and defense during cold storage. *Food Sci. Nutr.* 7, fsn3.1116. <https://doi.org/10.1002/fsn3.1116>

## Effect of water to biomass ratio of hydrothermal carbonization on the adsorption properties of hydrochar from waste seaweed

Sepideh Soroush<sup>1,2</sup>, Frederik Ronsse<sup>2</sup>, Philippe M. Heynderickx<sup>1,2,\*</sup>

<sup>1</sup> Center for Environmental and Energy Research (CEER) – Engineering of Materials via Catalysis and Characterization, Ghent University Global Campus, 119-5 Songdomunhwa-Ro, Yeonsu-Gu, Incheon, 406-840 South Korea,

<sup>2</sup> Department of Green Chemistry and Technology, Faculty of Bioscience Engineering, Ghent University, 653 Coupure Links, Ghent, B-9000, Belgium,

\* Corresponding author. Tel: +82 32 626 4206, E-mail: [Philippe.Heynderickx@Ghent.ac.kr](mailto:Philippe.Heynderickx@Ghent.ac.kr)

In this study, hydrochar has been produced from waste seaweed (*Sargassum*) at different process temperatures and with different water to biomass ratios. The experiments have been done for fresh seaweed without additional water as far as the moisture content of *Sargassum* was 90% by weight.

The produced hydrochar was applied to adsorb methylene blue dye. The results showed that the produced hydrochar is significantly affected by reaction temperature and water to biomass ratio. The carbon content of hydrochar increased by increasing the temperature, on the other hand adsorption capacity was correlated with the water to biomass ratio.

*Sargassum* as brown algae was used as biomass feedstock and *Sargassum* samples were collected from the coast of Busan, South Korea. The mass yield is a parameter to quantitatively show how much hydrochar can be produced from waste seaweed via hydrothermal carbonization. Figure 29 shows that with increasing reaction temperature, the yield decreased which was linked to escaping volatile compounds from biomass [1].

Hydrochar from fresh seaweed without additional water showed a significantly higher yield in comparison to hydrochar produced from dried biomass.

In the case of water to biomass ratio of 10 after 210°C, the yield increased which was linked to secondary reactions or more specifically, the polymerization of the small intermediate organic molecules into a solid phase.

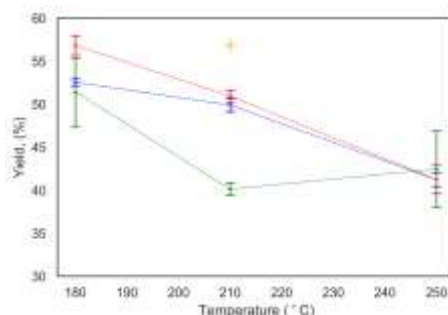


Figure 29. Hydrochar yield (wt.%) as a function of reaction temperature at (—) W:b (water to biomass ratio) =3, (—) W:b =5, (—) W:b =10, (—) fresh seaweed, dashed lines are added to guide the eye

Adsorption experiments were performed using methylene blue (MB) dye. Hydrochar contains oxygen-containing acidic functional groups, such as carboxylic acid groups on the surface of the hydrochar, and can adsorb the cationic MB molecule.

In order to describe the mechanism of adsorption, Langmuir and Freundlich adsorption isotherms (Figure 30 a,b) were fitted to the experimental MB adsorption data. The results showed that by increasing the water to biomass ratio, the adsorption capacity had been decreased. This observation could explain by the amount of oxygen in hydrochar that decreased (Figure 31) so it might conclude that carboxylic functional group has been reduced. By decreasing the carboxylic functional group, the adsorption capacity has been decreased which this result is compatible by the result of FTIR and elemental analysis.

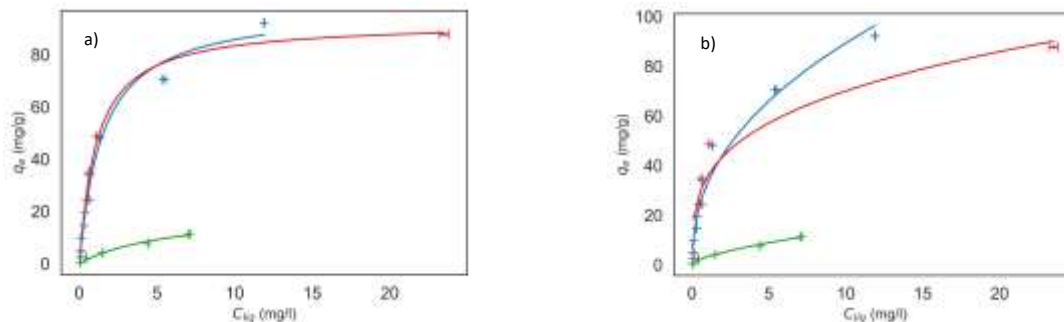


Figure 30. a) Langmuir b) Freundlich adsorption isotherms for hydrochar produced at 210°C, (—) W:b =3, (—) W:b =5, (—) W:b =10.

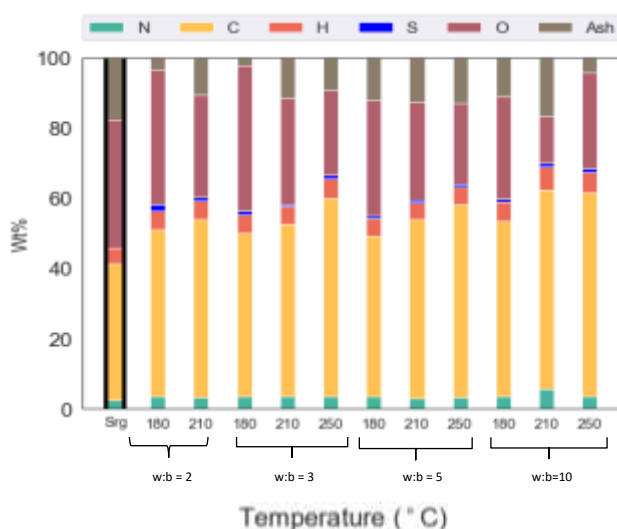


Figure 31. Effect of HTC temperature and water to biomass ratio on hydrochar elemental composition.

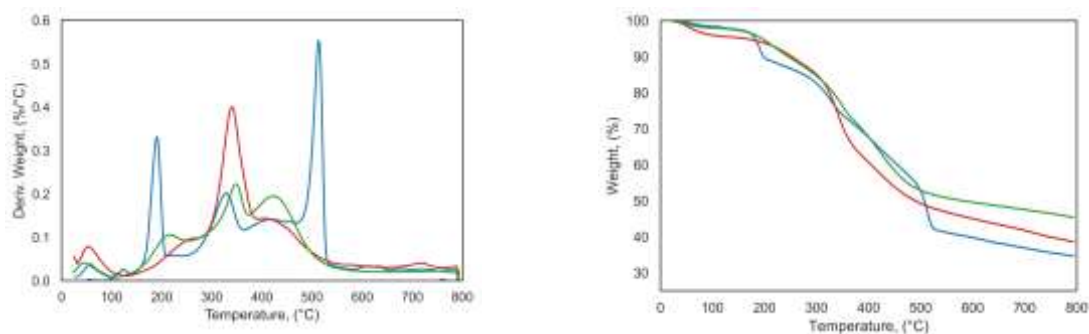


Figure 32. TGA and dTG curves of hydrochar at 210°C, (—) W:b =3, (—) W:b =5, (—) W:b =10

The thermogravimetric (TGA) and differential thermogravimetric (DTG) analyses were used to determine the material's thermal stability and the thermal mass loss of the material. As shown in Figure 32, three stages were observed for thermal decomposition. The weight loss graph, reveals that at 800°C, the highest overall mass loss is related to hydrochar produced at w:b= 3 and by increasing the water to biomass ratio the final mass loss decreased. This observation confirms that the thermal stability of those hydrochars which were produced at higher water to biomass ratio is higher [2, 3].

In conclusion, water to biomass ratio of 5 for *Sargassum* seaweed is found to be optimal, as it results in the highest hydrochar mass yield and it displays the highest maximal adsorption capacity.

## Acknowledgements

This work has been supported by the Research and Development Program of Ghent University Global Campus (GUGC), Korea.

## References

1. Soroush, S., et al., *Production of solid hydrochar from waste seaweed by hydrothermal carbonization: effect of process variables*. Biomass Convers. Biorefin., DOI: 10.1007/s13399-022-02365-9, 2022.

2. Kang, K., et al., *Microwave-assisted hydrothermal carbonization of corn stalk for solid biofuel production: Optimization of process parameters and characterization of hydrochar*. *Energy*, 2019. **186**: p. 115795.
3. Ross, A.B., et al., *Classification of macroalgae as fuel and its thermochemical behaviour*. *Bioresour. Technol.*, 2008. **99**(14): p. 6494-6504.

## Biochemical and antioxidant response modulation by plant growth promoting *Bacillus* spp strains to improve drought tolerance in maize

Sadia Javed<sup>1\*</sup> and Muhammad Azeem<sup>1</sup>

<sup>1</sup>Department of Biochemistry, Government College University, Faisalabad, 38000, Pakistan.

\*[sadiajaved@gcuf.edu.pk](mailto:sadiajaved@gcuf.edu.pk)

Abstract text:

Various technologies including traditional breeding are used to cope with drought stress. However, the interactions between plants and bacteria emerged as an interesting era of knowledge that can be used for novel agriculture practices. The aim of present study is to promote plant growth characteristics include mineral uptake and various phytohormones production by indigenously isolated bacteria from textile industrial wastewater. The polymerase chain reaction and DNA sequencing techniques are used to identify the isolated microorganisms. Nucleotide sequence of 16S rRNA gene of isolated bacterial strains used for comparative analysis through sequencing alignment tool. This compares the sequence of isolated species with already known sequences in the database and conform the bacterial species at the strain level. Isolated strains were able to produce ammonia, auxin, fix atmospheric nitrogen, and solubilized inorganic phosphorus by in-vitro plant growth promoting traits assay. In greenhouse experiment on two maize (*Zea mays* L.) cultivars isolated *Bacillus* spp. strains individually induce a similar drought stress amelioration effect in plant growth under sterile soil conditions. Plant length and biomass was improved 18.6% and 19.5% by bacterial inoculation as compared to control plant. Total chlorophyll, carotenoids and anthocyanin was increased 19.3%, 28.5% and 10.6% as compared to the uninoculated plants respectively. Biochemical attributes including total soluble sugars, total soluble proteins and ascorbic acid was improved 87.1%, 33.1% and 52.7% respectively. Lipid peroxidation (MDA) and hydrogen peroxide (H<sub>2</sub>O<sub>2</sub>) was reduced 50.8% and 41.4% by bacterial inoculation. Activity of antioxidant enzymes catalase (CAT), peroxidase (POD), ascorbate peroxidase (APX) and superoxide dismutase (SOD) was decreased 63.0%, 26.6%, 34.11% and 56.25% as compared to the uninoculated plants respectively. Stress amelioration is dependent on a specific plant-strain interaction evident in the differences in the evaluated biochemical attributes, lipid peroxidation and antioxidant responses. Such bacteria could be used in future for biotic and abiotic conditions having potential for sustainable agricultura [1-4].

Keywords: maize, *Bacillus* spp., antioxidant, growth promotion, drought

1. Azeem, M.; Haider, M.Z.; Javed, S.; Saleem, M.H.; Alatawi, A. Drought Stress Amelioration in Maize (*Zea mays* L.) by Inoculation of *Bacillus* spp. Strains under Sterile Soil Conditions. *Agriculture* **2022**, *12*, 50.
2. Lahlali, R.; Ezrari, S.; Radouane, N.; Belabess, Z.; Jiang, Y.; Mokrini, F.; Tahiri, A.; Peng, G. *Bacillus* spp.-Mediated Drought Stress Tolerance in Plants: Current and Future Prospects. In *Bacilli in Agrobiotechnology: Plant Stress Tolerance, Bioremediation, and Bioprospecting*, Islam, M.T., Rahman, M., Pandey, P., Eds.; Springer International Publishing: Cham, 2022; pp. 487-518.
3. Othibeng, K.; Nephali, L.; Myoli, A.; Buthelezi, N.; Jonker, W.; Huyser, J.; Tugizimana, F. Metabolic Circuits in Sap Extracts Reflect the Effects of a Microbial Biostimulant on Maize Metabolism under Drought Conditions. **2022**, *11*, 510.
4. Moreno-Galván, A.; Romero-Perdomo, F.A.; Estrada-Bonilla, G.; Meneses, C.H.S.G.; Bonilla, R.R.J.M. Dry-caribbean *Bacillus* spp. strains ameliorate drought stress in maize by a strain-specific antioxidant response modulation. **2020**, *8*, 823.

## Poster presentations

Alternative and benign chemical processes (microwaves, ultrasounds, photochemistry, electrochemistry, flow chemistry, etc.)



# Electrochemical synthesis as alternative synthetic strategies for the Manganese phthalocyanine and its graphene quantum dot conjugate

Douaa AlMarzouq<sup>1\*</sup>, Shereen A. Majeed<sup>2</sup>, Ozlem Budak<sup>3</sup> and Atif Koca<sup>3\*</sup>

<sup>1</sup>Department of Environmental Health, College of Health Sciences, The Public Authority of Applied Education and Training, P.O. Box 1428, Faiha 72853, Kuwait

ds.almarzouq@paaet.edu.kw (D. AlMarzouq)<sup>1\*</sup>, and akoca@marmara.edu.tr (A. Koca)<sup>3\*</sup>

## Abstract:

Manganese phthalocyanine (**MnPc**) bearing peripherally substituted octacarbazole moieties was synthesized and characterized by matrix-assisted laser desorption/ionization spectrometry (MALDI), FT-IR, and UV-Vis spectroscopy. The complex was then conjugated to graphene quantum dots (GQDs) via  $\pi$ - $\pi$  stacking and characterized by energy dispersive X-ray spectroscopy (EDX), transmission electron microscopy (TEM), energy dispersive spectroscopy, and X-ray diffraction. Electrochemical synthesis as alternative synthetic strategies provide an effective green route which offers advantageous features such as avoiding the chemical oxidizing and reducing agents used in traditional synthetic methods. Electrochemical performances of **MnPc** and its nanoconjugate were investigated using cyclic voltammetry (CV), square wave voltammetry (SWV) and spectroelectrochemistry (SEC) to determine the influence of the carbazole substituents and graphene quantum dots on the redox mechanism of **MnPc**. Although the carbazole substituents did not significantly influence the reduction processes of **MnPc**, they induced **MnPc** coating onto the electrode surface due to cationic electropolymerization of the carbazole substituents. The composite comprising graphene quantum dots and **MnPc** exhibited redox responses that were comparable to those of **MnPc**.

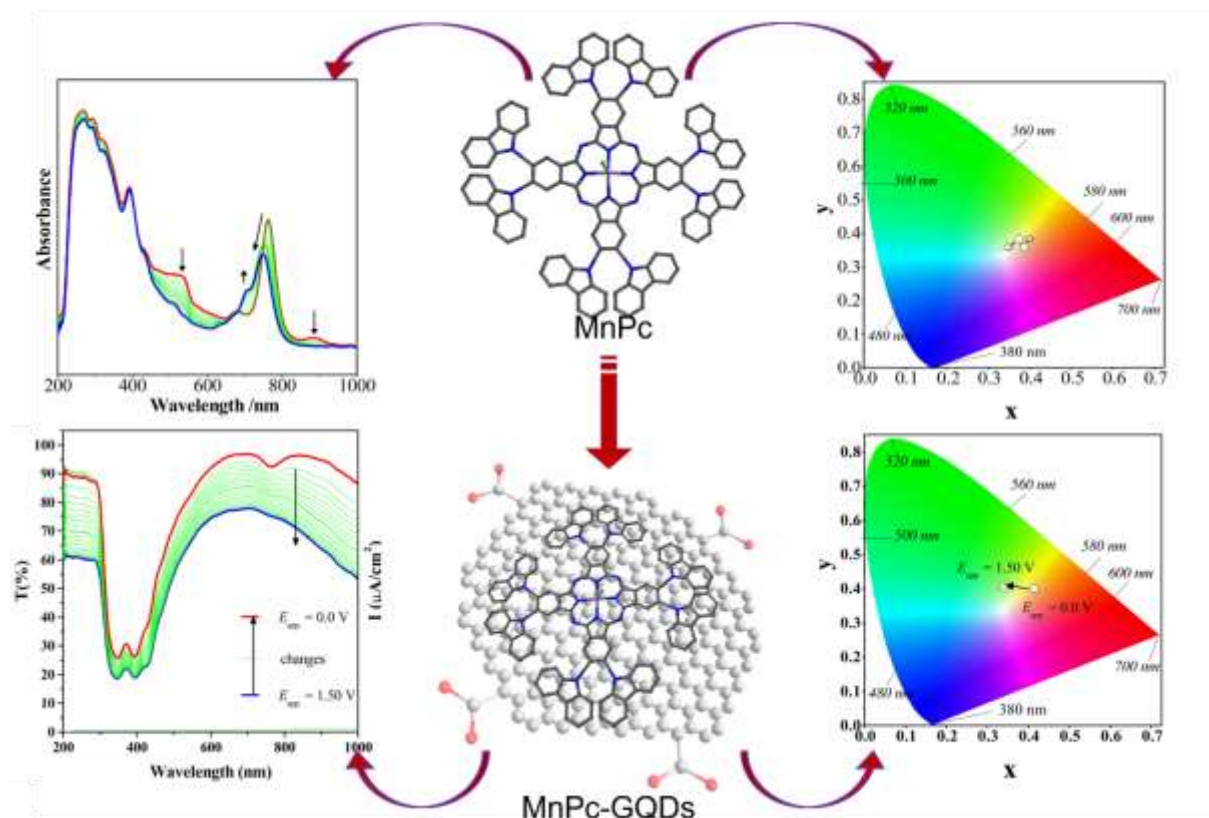


Figure 1. Graphical Abstract – Pictogram for **MnPc** and **MnPc-GQDs** related Electrochromic measurements

## 1. Experimental

### 1.1 Materials

Carbazole **1**, anhydrous manganese chloride, and cesium fluoride salts were obtained from Sigma-Aldrich. 5,6-Dichlorophthalonitrile **2** was purchased from TCI (Toshima, Japan). All solvents were obtained from local commercial suppliers. Compound **3** in this study was synthesized according to a literature procedure [1, 2].

### 1.2 Instrumentation

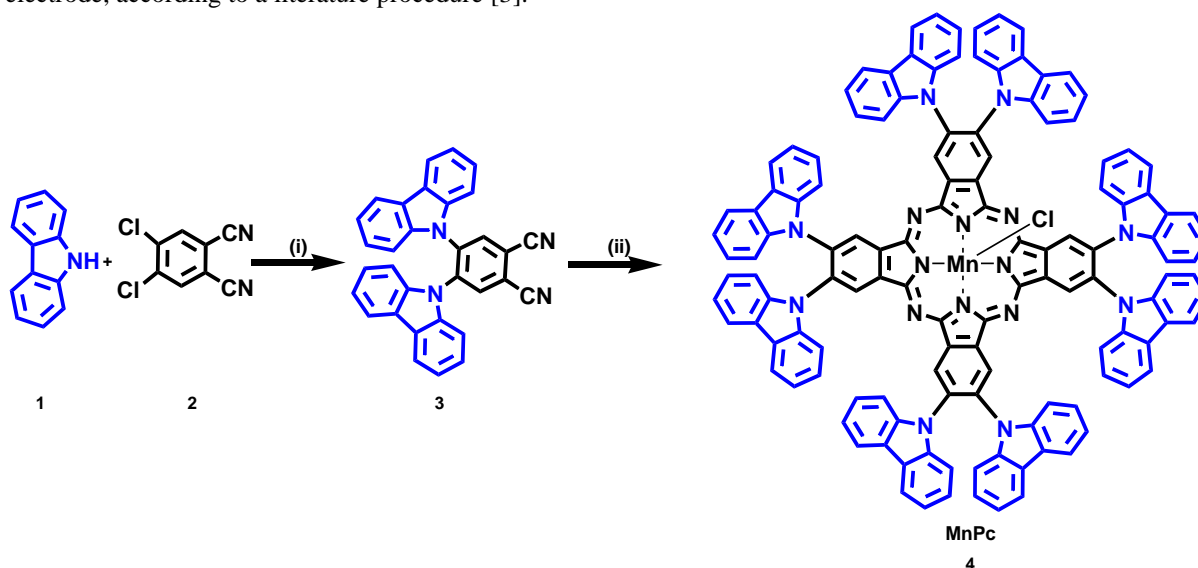
Electronic absorption spectra were measured with a Varian Cary 5 or Shimadzu UV-2600 spectrophotometer. A Zeiss 1210 transmission electron microscope operated at a 100-kV acceleration voltage was used to obtain transmission electron microscopy (TEM) images.

Energy dispersive X-ray spectroscopy (EDX) measurements were performed on a JEOL instrument with EDX attached to a Scanning Electron Microscope Model JSM IT100, functioning with integral SEM-EDX software in ordinary laboratory conditions.

X-ray diffraction (XRD) data were collected over the  $2\theta = 10\text{--}80^\circ$  range, scanning at  $0.010^\circ \text{ min}^{-1}$  and 192 s per step. A zero-background silicon wafer slide was used and the measurements were performed using a Bruker® D8 Discover diffractometer, equipped with a Lynx Eye detector, under Cu  $K\alpha$  radiation ( $\lambda = 1.5405 \text{ \AA}$ ). Elemental analyses were performed using an ElementarVario Micro Cube.

### 1.3 Electrochemical measurements

Cyclic voltammetry (CV), square wave voltammetry (SWV) and in situ spectroelectrochemical (SEC) measurements were performed using a potentiostat (GAMRY Instruments, Reference 600 Potentiostat/Galvanostat/ZRA) coupled with an Ocean Optics QE65000 diode array spectrophotometer according to a literature procedure [3]. In these experiments, a glassy carbon (GCE), Pt wire, and Ag/AgCl electrodes (containing saturated KCl aqueous electrolyte) were used as the working, counter, and reference electrodes, respectively. All measurements were performed in dichloromethane (DCM) / tetrabutylammonium perchlorate (TBAP) electrolyte. In situ UV-Vis spectroelectrochemical and electrocolorimetric measurements were performed in a thin-layer quartz spectroelectrochemical cell with a three-electrode configuration using a Pt tulle working electrode, according to a literature procedure [3].



**Scheme 1.** Synthetic route to **MnPc**. (i) DMF, CsF, 75–85 °C, 24 h; (ii) MnCl<sub>3</sub>, 1-pentanol, 130 °C, 24 h, N<sub>2</sub> gas.

#### Synopsis:

Manganese phthalocyanine bearing peripherally substituted octacarbazole moieties was synthesized and characterized. The complex was then conjugated to GQDs. The effect of the carbazole substituents and nanomaterial conjugation on the electrochemical performances of the complex were investigated.

#### Acknowledgements

The authors acknowledge the Public Authority for Applied Education and Training (PAAET), Kuwait. This research and the findings achieved herein were supported by PAAET project number *HS-19-03*. The authors express their gratitude to the Kuwait University Research Administration-RSP unit general facilities of the Faculty of Science GFS GS 02/01, GS 03/01, GS 01/05), and to Dr. Abdullah Alhendal at the Chemistry Department – Kuwait University, for his support and access to facilities. The authors thank the Turkish Academy of Sciences (TUBA) for the financial support for electrochemical analysis.

#### References

1. S.A. Majeed, B. Ghazal, D.E. Nevonon, P.C. Goff, D.A. Blank, V.N. Nemykin, S. Makhseed, Evaluation of the Intramolecular Charge-Transfer Properties in Solvatochromic and Electrochromic Zinc Octa(carbazolyl)phthalocyanines, *Inorganic Chemistry*, **56** 11640-11653 (2017).
2. S.A. Majeed, B. Ghazal, D.E. Nevonon, V.N. Nemykin, S. Makhseed, Spectroscopic and TDDFT studies on the charge-transfer properties of metallated Octa(carbazolyl)phthalocyanines, *Dyes and Pigments*, **170** 107593 (2019).
3. Ö. Kurt, A. Koca, A. Gül, M.B. Koçak, Synthesis, electrochemistry and in situ spectroelectrochemistry of novel hexadeca-substituted phthalocyanines with three different groups, *Synthetic Metals*, **206** 72-83 (2015).

## Microwave- and ultrasound-promoted greener synthesis of tolperisone derivatives and their biological evaluation

Yelizaveta Belyankova<sup>1,2,\*</sup>, Saniya Tursynbek<sup>1,2</sup>, Anuar Dauletbakov<sup>1,2</sup>, Zhuldyz Bazhikova<sup>1,2</sup>, Assel Ten<sup>1</sup>, Alexey Zazybin<sup>1,2</sup>

<sup>1</sup>Department of Chemical Engineering/Kazakh-British Technical University, 050000, Almaty, Kazakhstan

<sup>2</sup>Institute of Chemical & Biological Technologies/Satbayev University Satbayev University, 050013, Almaty, Kazakhstan

\*belyankovae@gmail.com

Synthesis under alternative conditions consuming less energy as well as investigation of biological activity of new compounds is an integral part of green chemistry.

Tolperisone derivatives were synthesized by N-alkylation reaction of tolperisone base, which was obtained from commercially available hydrochloride, and corresponding halogenalkanes. The synthesis was carried out in acetonitrile with thermal (85°C), microwave (90-250 W) or ultrasound (50-60Hz, 35-42°C) activation. The progress of reactions and purity of products were checked using the TLC method on silica gel plates with iodine vapors development. The separation and purification of substances was carried out by crystallization from appropriate solvents. The higher yields were observed when microwave irradiation was used to promote the reaction.

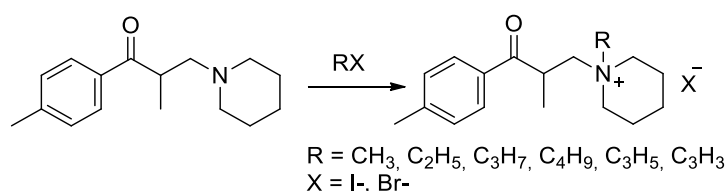


Figure 1. Synthesis of tolperisone's derivatives via N-alkylation reaction

Tolperisone derivatives were evaluated on their myelostimulating activity. In terms of leukopoiesis-stimulating activity, *N*-methyl derivative was slightly inferior to the reference drug methyluracil, however, in terms of erythropoiesis- and thrombocytopoiesis-stimulating activity, it exceeded the activity of the reference drug. *N*-ethyl derivative was not effective in erythropoiesis and thrombopoiesis stimulating, but in terms of leukopoiesis-stimulating activity, it was comparable to the activity of the reference drug.

Local anaesthetic and toxicity assessment of *N*-propyl, *N*-propargyl and *N*-butyl derivatives showed that *N*-butyl tolperisone derivative was 0.84 and 1.36 times more toxic than lidocaine and trimecaine respectively. *N*-butyl derivative's 1% solution showed duration of anaesthetics 0.95 and 1.3 times longer than lidocaine and trimecaine respectively.

Antidiabetic activity was assessed by the inhibition of  $\alpha$ -glucosidase [1] and  $\alpha$ -amylase [2] activity of the synthesized substances. The test compounds did not show inhibitory activity against  $\alpha$ -amylase. Low inhibitory activity against  $\alpha$ -glucosidase was showed by *N*-propyl (16%) and *N*-allyl (11%) derivatives.

Based on the current data of biological activity of tolperisone's derivatives, it could be concluded that myelostimulating activity and local anaesthetic toxicity decrease with the growth of alkyl chain length.

### Acknowledgements

This Research has been funded by the Science Committee of the Ministry of Education and Science of the Republic of Kazakhstan (Grant No. AP08857345).

### References

1. M. Telagari, K. Hullatti, Indian J Pharmacol, 47(4) 425-429 (2015).
2. P. Bernfeld, Academic Press, New York, 149-158 (1955).

## Pre-treatment of beech wood using choline chloride-based deep eutectic solvents

Pierre-Alann Cablé<sup>1\*</sup>, Fabrice Mutelet<sup>1</sup>, Yann Le Brech<sup>1</sup>

<sup>1</sup>Université de Lorraine, Ecole Nationale Supérieure des Industries Chimiques, Laboratoire Reactions et Genie des Procédés (UMR CNRS 7274), 1 rue Grandville, 54000 NANCY, France.

\*pierre-alann.cable@univ-lorraine.fr

One of the main challenges of our decades is to be able to **substitute fossil fuel by green and sustainable energy**. The goal is to design processes to get new fuels and chemicals from renewable resources. Lignocellulosic biomass (wood, herbaceous, agricultural wastes) which is a complex network of macromolecules (cellulose, hemicelluloses, lignin), is the main renewable carbon source on earth. (and aromatic carbons). Furthermore, lignocellulosic biomass can be converted into bio-derived value-added fuels, chemicals and materials. These bio-products are produced by using specific chemical pathways (bio- and thermochemical). Besides, its valorisation in “biorefinery” could lead to climate change mitigation with the production of biofuels and green chemicals with a lower environmental impact than petroleum resources. Indeed, extraction and separation of value-added compounds from lignocellulosic biomass by simple and clean fractionation is a significant dynamic area of research.

Currently, processes require an excessive volume of organic/inorganic solvents or a high-energy consumption (kraft, soda cooking, sulphite). The main goal is to perform biomass fractionation at low temperature (below 150°C) with “green solvents” in order to substitute conventional processes. “Green chemistry” promotes the use of environmentally friendly solvents. Initially, ionic liquids have been used for fractionation and biomass pre-treatments. Due to their high cost and toxicity, a new class of “green solvents” emerged: deep eutectic solvents (DES). DES are formed by hydrogen bonding between a hydrogen bond donor (HBD) and a hydrogen bond acceptor (HBA). A charge delocalization occurs through the hydrogen bond which is mainly responsible for the decrease of the melting point. The latter is lower than the melting point of the individual HBD and HBA. The resulted solvent is liquid at room temperature and behaves like a pure compound. Currently, most of the DESs are based on materials from renewable resources (sugars, amines, carboxylic acids, etc.). They are cheap and usually considered non-toxic and biodegradable. Nevertheless, their toxicity and biodegradability should be investigated case by case.

During the last decade, several studies have shown promising results for the fractionation of lignin using DESs<sup>1-7</sup> on different types of biomass. DESs have the ability to cleave the ether bonds without affecting the C-C linkages in lignin. This cleavage is the main mechanism leading to lignin depolymerisation which further facilitates lignin extraction from the biomass. Delignified biomass could be used for pulp/paper or ethanol production. Isolated lignin can be used directly in different application (i.e polymer) or converted to high-value monomers (phenols) by thermochemical process (i.e. pyrolysis).

This work investigates fractionation of beech wood (very popular in Lorraine, East of France) using choline chloride-based DESs. The studied DESs are selected from previous studies on delignification found in the literature: ChCl:glycerol [1:2], ChCl: Oxalic Acid [1:1], ChCl : Acetic Acid [1:1], ChCl: Ethylene Glycol [1:2].

The experimental results show a significant impact of the HBDs in the prepared DES. The Total Polyphenol Content (TPC) measured by Folin-Ciocalteu test is used as a global indicator for the comparison of different DESs

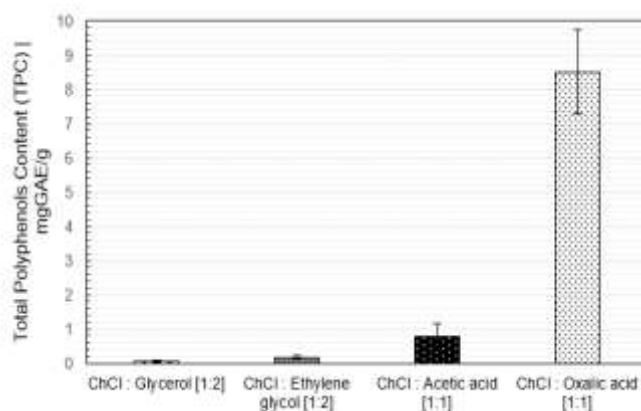


Figure 33. Influence of hydrogen bond donor (HBD) on polyphenols extraction using choline chloride-based deep eutectic solvents

(figure 1) and for the process optimisation (Box-Behnken design). Optimisation is made on temperature, time and wood/DES ratio. In order to give new insights concerning DES delignification mechanisms, several analyses (IR,

liquid state NMR  $^{13}\text{C}$ ,  $^{31}\text{P}$ , HSQC  $^1\text{H}$ - $^{13}\text{C}$ , elemental analysis, XRD, Klason lignin, HPLC-UV-MS) were carried out on extracted lignin, treated wood and liquid DES phase obtained from fractionation process.

## References

1. Mamilla JLK, Novak U, Grilc M, Likozar B. *Biomass Bioenergy*. 2019
2. Jablonsky M, Haz A, Majova V. *Cellulose*. 2019
3. Alvarez-Vasco C, Ma R, Quintero M, et al. *Green Chem*. 2016
4. Wang Y, Kim KH, Jeong K, Kim NK, Yoo CG. *Curr Opin Green Sustain Chem*. 2021
5. Liu Y, Chen W, Xia Q, et al. *ChemSusChem*. 2017
6. Liu Y, Deak N, Wang Z, et al. *Nat Commun*. 2021
7. Pi Q feng, Zhu Y ting, Lü W, Liao Y he, Wang C guang, Ma L long. *J Fuel Chem* 2021

## Cocrystallization through green mechanochemical synthesis: An approach to improve solubility of drugs

Amanda C. de Almeida<sup>1\*</sup>, Patricia O. Ferreira<sup>1</sup>, Giovanna de P. Costa<sup>1</sup>, Laura T. Ferreira<sup>2</sup> and Flávio J. Caires<sup>1,2</sup>

<sup>1</sup> School of Sciences, São Paulo State University, 17033-360, Bauru, Brazil;

<sup>2</sup> Institute of Chemistry, São Paulo State University, 14800-060, Araraquara, Brazil;

\*amanda.cosmo@unesp.br

Solid-state grinding (belonging to mechanochemical methods) is an effective and inherently green method – compared to conventional solution-based methods – that offers a rapid, facile, reproducible, and low or no waste methodology for the preparation of multicomponent solid forms. Besides that, no or only small amounts of solvent are employed during the synthesis process, named as Neat grinding (NG) or Liquid-assisted grinding (LAG), respectively [1,2].

One of the most significant issue faced by the pharmaceutical industry is the poor solubility of drugs that can be improved through multicomponent solid approaches, such as pharmaceutical cocrystals. A cocrystal can be defined as multicomponent crystalline structure composed by an active pharmaceutical ingredient (API) and a pharmaceutically acceptable compound (coformer), in a defined stoichiometric ratio, bounded by non-covalent interactions, mainly hydrogen bonds. In addition, cocrystals can overcome the physicochemical properties without compromising the drug's therapeutic benefit [3–6].

It is estimated that 40% of marketed drugs and 90% of those under development have low aqueous solubility, which affects their bioavailability and, consequently, their efficacy [5,7]. Furthermore, it is related to ADME-Tox (absorption, distribution, metabolism, excretion, and toxicity) properties, and since cocrystals may enable greater solubility, and subsequently absorption, less API is required in the dosage form and side effects are reduced [5,7,8]. In this context, the present work aimed to use mechanochemistry as a green methodology in the synthesis of a soluble cocrystal of ciprofloxacin (CIP) – a broad-spectrum antibiotic that has low aqueous solubility and permeability in biomembranes – with niacin (NCA; vitamin B3) as coformer.

The mechanochemical synthesis (NG and LAG) was performed in a mixer mill, in which equimolar amounts of CIP and NCA were grounded at a frequency of 30 Hz for 30 min. Ethanol was used for LAG synthesis in a ratio of 0.25  $\mu\text{L mg}^{-1}$ , as determined by Friščić et al. [9]. Then, the samples were characterized by differential scanning calorimetry (DSC), infrared spectroscopy (IR), and powder X-ray diffractometry (PXRD). The aqueous solubility studies were assessed by the saturation shake-flask method and the measurements were performed using a UV spectrophotometer at 277 nm.

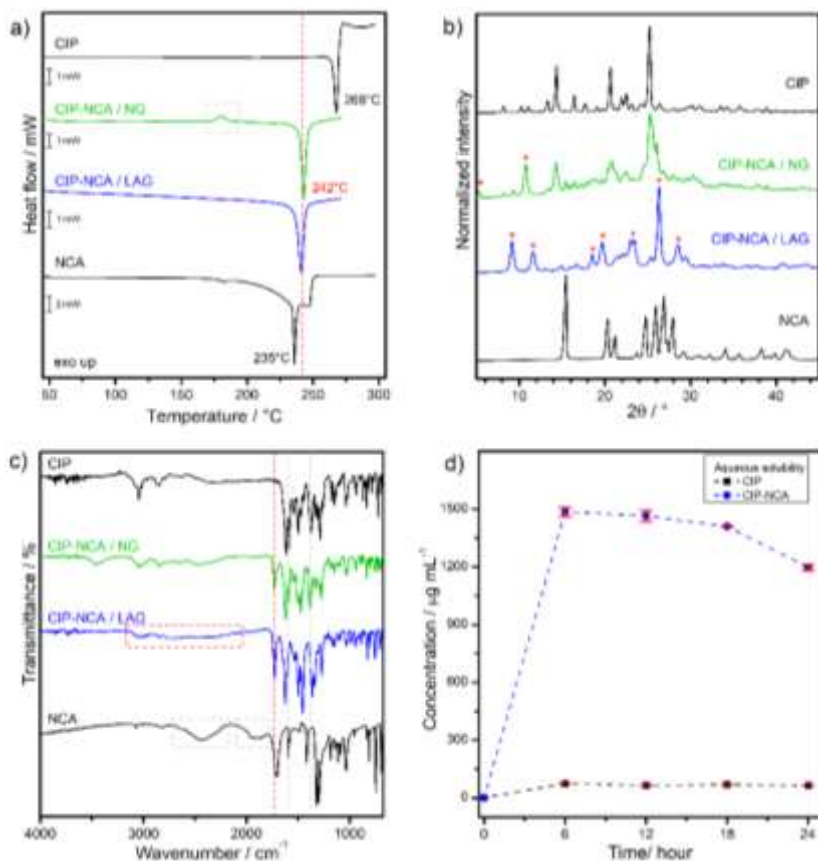


Figure 1. DSC curve (a), PXRD diffractograms (b), IR spectra (c), and solubility evaluation (d) for CIP-NCA cocrystal. The CIP-NCA systems showed distinct thermal behavior, with intermediate melting compared to the precursors (Figure 1a). Regarding PXRD, new diffractometric peaks were observed in Figure 1b (signed with asterisks) indicating that a new crystalline phase was obtained. Along with the IR spectra (Fig. 1c) which showed a shifted carbonyl stretching band, as well as a decrease in the intensities of CIP carboxylate bands and the hydrogen bond O-H...N of the NCA cofomer, confirms the establishment of a new supramolecular synthon and the formation of a new cocrystal. Furthermore, the NG sample presented a small exothermic event at 180°C in DSC curve, that corresponds to cocrystallization on heating, confirmed by PXRD (Fig. 2). In this case, it can be concluded that the LAG synthesis was more efficient, and the small amount of solvent used acted as a catalyst [10].

It is noteworthy that the aqueous solubility of the cocrystallized CIP was improved approximately twenty-fold (Fig. 1d). This behavior of the CIP in cocrystal form throughout the experiment may be linked to supersaturation phenomena similar to amorphous drugs, also known as the “spring and parachute” mechanism [11].

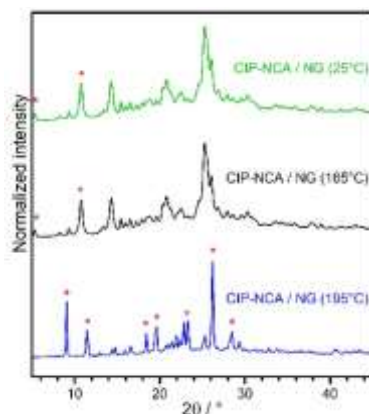


Figure 2. PXRD diffractograms of CIP-NCA / NG cocrystal at 25°C, heated to 165°C and to 195°C.

Finally, we could conclude that the green mechanochemical method was extremely effective in the synthesis of ciprofloxacin cocrystals, where small amounts of solvent were required. The synthetic process was rapid, low energy demand, reproducible, and, as expected, made it possible to produce a multi-component solid form with improved solubility.

## Acknowledgements

This study was possible thanks to the scholarship granted from the Brazilian Federal Agency for Support and Evaluation of Graduate Education (CAPES), in the scope of the Program CAPES-PrInt, process number 88887.310463/2018-00, Mobility number 88887.684961/2022-00. The authors are also thankful for CNPq processes number 317282/2021-2 and 422893/2021-8.

## References

1. D. R. Weyna, T. Shattock, P. Vishweshwar, and M. J. Zaworotko, *Cryst. Growth Des.* **9**, 1106 (2009).
2. M. S. H. Mithu, S. A. Ross, A. P. Hurt, and D. Douroumis, *J. Drug Deliv. Sci. Technol.* **63**, 102508 (2021).
3. A. C. de Almeida, C. Torquetti, P. O. Ferreira, R. P. Fernandes, E. C. dos Santos, A. C. Kogawa, and F. J. Caires, *Thermochim. Acta*, **685**, 178346 (2020).
4. G. Kotbantao and M. Charoenchaitrakool, *J. CO<sub>2</sub> Util.* **17**, 213 (2017).
5. O. N. Kavanagh, D. M. Croker, G. M. Walker, and M. J. Zaworotko, *Drug Discov. Today*, **24**, 796 (2019).
6. N. Shan, M. L. Perry, D. R. Weyna, and M. J. Zaworotko, *Expert Opin. Drug Metab. Toxicol.* **10**, 1255 (2014).
7. P. Kundu, S. Das, and N. Chattopadhyay, *Int. J. Pharm.* **565**, 378 (2019).
8. J. Wang and T. Hou, *Comb. Chem. High Throughput Screen.* **14**, 328 (2011).
9. T. Frišćić, S. L. Childs, S. A. A. Rizvi, and W. Jones, *CrystEngComm*, **11**, 418 (2009).
10. M. Karimi-Jafari, L. Padrela, G. M. Walker, and D. M. Croker, *Cryst. Growth Des.* **18**, 6370 (2018).
11. A. Karagianni, M. Malamataris, and K. Kachrimanis, *Pharmaceutics*, **10**, 1 (2018).

## Steroidal fused pyrroles: an environmentally friendly alternative to the synthesis of plant growth promoters

María G. De los Santos,<sup>1</sup> Esaú Ruiz-Sánchez,<sup>2</sup> Adolfo López-Torres<sup>3</sup> and María A. Fernández-Herrera.<sup>1\*</sup>

<sup>1</sup>Departamento de Física Aplicada, Cinvestav Mérida, 97310, Mérida, Yucatán; México.

<sup>2</sup>Tecnológico Nacional de México, Instituto Tecnológico de Conkal, Avenida Tecnológico s/n, C.P. 97345, Conkal, Yucatán, México.

<sup>3</sup>Instituto de Biotecnología, Universidad Del Papaloapan. Circuito Central Num. 200, Col. Parque Industrial, 68301, Tuxtepec, Oaxaca, México.

\*mfernandez@cinvestav.mx

This work describes the synthesis of norcholestane pyrroles and their evaluation as growth phytohormones in habanero pepper crops (*Capsicum chinense* Jacq) an endemic plant to the Yucatan Peninsula. The synthesis is based on an ecological route based on the potential of superheated water as solvent and the experience of our research group in the modification and study of naturally occurring organic compounds.

The synthesis route was performed in 4 steps (Figure 1). In the first step, the regioselective opening of the diosgenin side chain was carried out by a Lewis acid catalyzed acetolysis ( $\text{BF}_3 \cdot \text{OEt}_2 / \text{Ac}_2\text{O}$ ). Once the 26-hydroxy-22-oxocholestane system was obtained, the C-26 hydroxyl group was oxidated to yield the corresponding aldehyde. The next step was the cleavage of the C-C bond of the aldehyde at C-26 to generate the 27-norcholestane systems corresponding to the desired 1,4-dicarbonyl moiety. For this reaction, superheated water (which is water kept in a liquid state by pressure at a temperature above its natural boiling point (100 °C) and below its critical temperature (374 °C), [1,2]) was used under microwave (MW) conditions, as the physical and chemical properties of water change, that allows to have a higher solubility of organic compounds. [3,4]. Although the reactions of steroids practically do not take place in water due to their poor solubility, those conditions change under superheated water. The 3,4,5-trimethoxyaniline promotes the cleavage of the C-C bond and the reaction proceeds at 160 °C and 10 bar pressure. From the 1,4-dicarbonyl system, pyrroles were synthesized as part of the side chain under MW conditions using the primary amines benzylamine, ethanolamine, propanolamine and *R*-(+)- $\alpha$ -methylbenzylamine. The reaction products were characterized by  $^1\text{H}$  and  $^{13}\text{C}$  NMR, infrared spectroscopy, polarimetry and mass spectrometry.

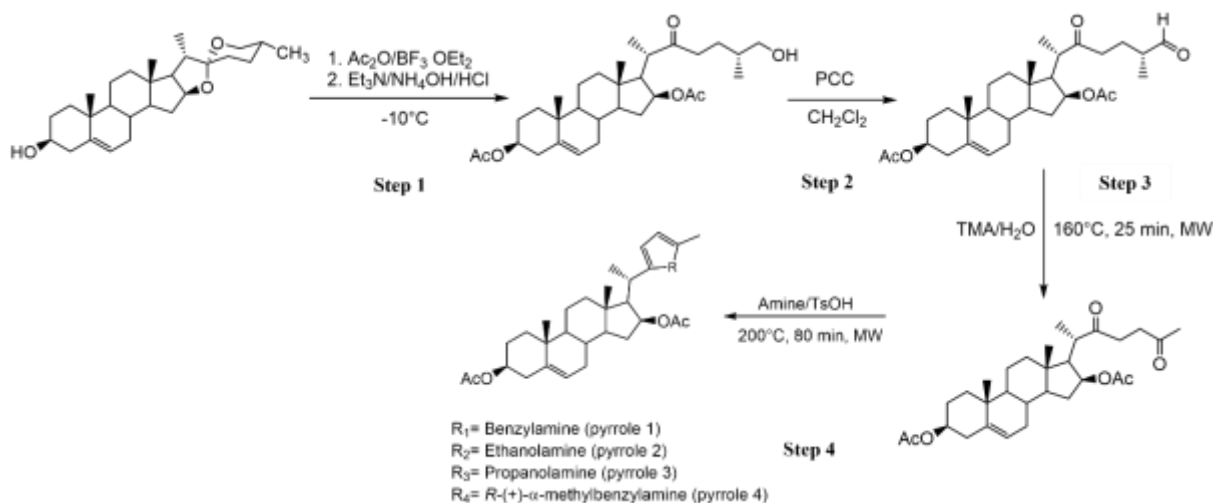


Figure 2. Synthetic pathway of steroidal pyrroles formation.

The plant growth analysis was carried out under greenhouse conditions (25-35 °C, R.H. 55-75%). The vegetative material used was habanero pepper (*Capsicum chinense* Jacq) variety Prime which, 20 days after the plants emerged, were transplanted into 2 L pots containing soil from the region and 10, 17, 21, and 28 days after transplanting into the pots. The application of steroidal compounds was carried out directly on the foliage of the plants. A commercial product based on cytokinin hormone was used as a positive control and water as negative control. Tukey's method was used for an analysis of variance and comparison of means.

The from the 4 steroidal pyrroles are shown in Table 1. The accumulation of biomass can be appreciated, being pyrrole 4 the one that presented the highest values in the variables of dry biomass of leaves and roots.



Table 1. Growth analysis of habanero pepper.

Steroidal pyrroles	Plant height (cm)	Stem diameter (mm)	Number of leaves/planta	Stem dry biomass (gr)	Dry leaf biomass (gr)	Dry root biomass (gr)
<b>1.- Pyrrole 1</b>	23.8±1.69	0.38±0.01	12.0±0.46	0.33±0.04	0.95±0.08 e	0.40±0.04 c
<b>2.- Pyrrole 2</b>	27.6±1.32	0.41±0.01	13.5±0.32	0.46±0.02	1.10±0.03 de	0.43±0.01 bc
<b>3.- Pyrrole 3</b>	26.7±1.30	0.38±0.01	13.2±0.49	0.46±0.01	1.27±0.05 abc	0.40±0.01
<b>4.- Pyrrole 4</b>	27.1±1.54	0.42±0.01	13.6±0.99	0.48±0.04	1.21±0.05 bcd	0.48±0.03 ab

The experimental conditions proposed for the synthetic route to obtain the pyrroles provide a novel ecofriendly procedure to generate compounds with potential application as growth phytohormones in habanero pepper plants complying with at least 6 of the principles of green chemistry.

#### Acknowledgments

This work was supported by a PhosAgro/UNESCO/IUPAC Partnership in Green Chemistry for Life research grant. MGDSL thank Conacyt for the PhD fellowship (852222).

#### References

1. A. R. Katritzky, S. M. Allin, M. Siskin. *Acc. Chem. Res.*, 29 399 (1996).
2. B. Kuhlmann, E. M. Arnett, M. Siskin. *J. Org. Chem.*, **59** 3098 (1994).
3. M. Siskin, A. R. Katritzky, *Chem. Rev.*, **101** 825 (2001).
4. Y. Ikushima, K. Sato, T. Yokoyama, M. Arai, *Angew. Chem. Int.* **38** 2910 (1999)

## The radiation chemistry as a green alternative for the synthesis of graphene-supported gold nanoparticles

Dejan P. Kepić<sup>1\*</sup>, Andjela M. Stefanović<sup>1,2</sup>, Jovana R. Prekodravac<sup>1</sup>, Milica D. Budimir<sup>1</sup>, Vladimir B. Pavlović<sup>3</sup>, and Biljana M. Todorović Marković<sup>1</sup>

<sup>1</sup>Vinča Institute of Nuclear Sciences - National Institute of the Republic of Serbia, University of Belgrade, P.O.B. 522, 11001 Belgrade, Serbia

<sup>2</sup>Faculty of Chemistry, University of Belgrade, Studentski trg 12-16, 11158 Belgrade, Serbia

<sup>3</sup>Faculty of Agriculture, Department of Agricultural Engineering, University of Belgrade, Nemanjina 6, 11080 Belgrade, Serbia

\*e-mail address of corresponding author: d.kepic@vin.bg.ac.rs

### Abstract text:

Conventionally, gold nanoparticles are synthesized via the reduction of chloroauric acid with a suitable reductant at elevated temperatures and with the addition of a stabilizing agent to prevent their aggregation and precipitation. Here, gold nanoparticles were obtained by gamma irradiation at low doses (1-20 kGy) which provides a fast, economical, and green alternative to conventional synthesis because it does not involve harsh chemicals, prolonged reaction time, and the irradiation takes place at room temperature. Gold nanoparticles were obtained using chloroauric acid as a precursor in the presence of two types of graphene material: electrochemically exfoliated graphene from highly oriented pyrolytic graphite and graphene oxide obtained via Hummers' method. Samples were irradiated at four irradiation doses of 1, 5, 10, and 20 kGy with the addition of isopropanol to quench oxidative species generated by the radiolysis of water.

Oxygen-functional groups from graphene surface had an important role in the nucleation and growth of gold nanoparticles thus eliminating the need for an additional stabilizing agent. When electrochemically exfoliated graphene was used as support, synthesized gold nanoparticles had sizes of up to 40 nm, and nearly half of them fit in the 11-20 nm size range. Increasing the irradiation dose resulted in a higher abundance of smaller nanoparticles (up to 10 nm in size). On the other hand, in the presence of graphene oxide, synthesized gold nanoparticles had sizes between 6-10 nm for the lowest irradiation dose, and with the increase in the absorbed dose larger particles of up to 90 nm were obtained. Simultaneously, gamma irradiation causes the reduction of graphene material and partial restoration of graphene's conjugated structure.

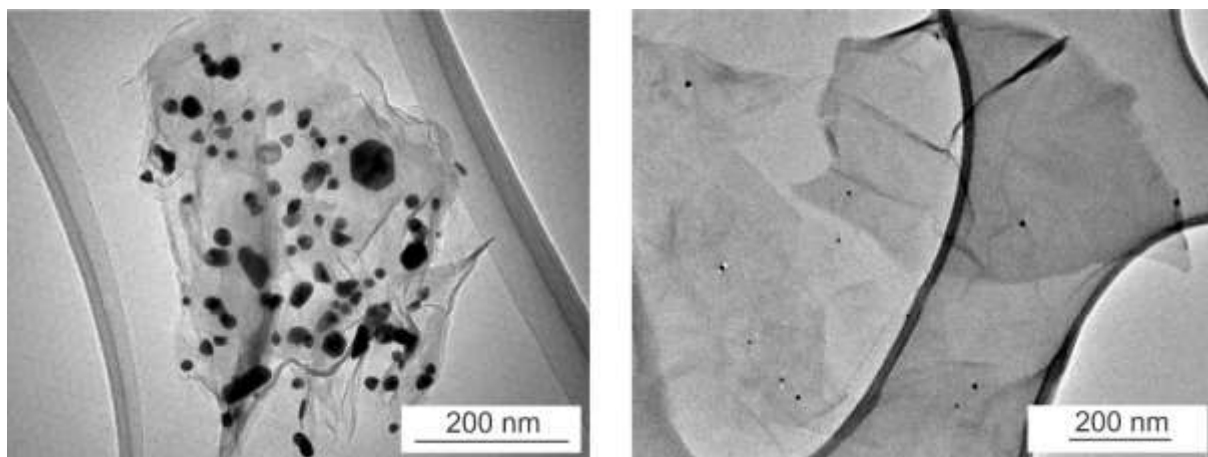


Figure 1. TEM images of gold nanoparticles obtained at the dose of 1 kGy using exfoliated graphene (left) and graphene oxide (right) as support.

### Acknowledgements

The research was supported by the Science Fund of the Republic of Serbia, #7741955, Are photoactive nanoparticles salvation for global inflectional treath? - PHOTOGUN4MICROBES and by the Ministry of Education, Science and Technological Development of the Republic of Serbia, grant number 451-03-68/2022-14/200017. D.K. acknowledges the support from the project of bilateral collaboration between the Republic of Serbia and the People's Republic of China [Project No. 451-02-818/2021-09/12].

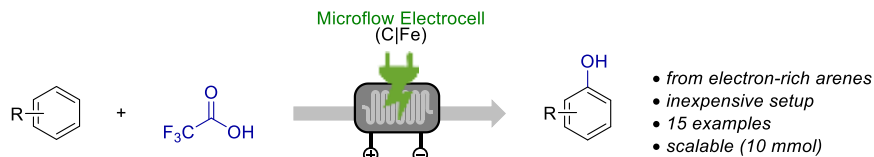
## Electrochemical Synthesis of Aryl Alcohols in Continuous-Flow

Anni Kooli and Maksim Ošeka\*

Tallinn University of Technology, School of Science, Akadeemia tee 15, 12618, Tallinn, Estonia

\*maksim.oseka@taltech.ee

Aryl oxygen products can be found in many bioactive and natural compounds. They are also common building blocks for synthesis in academia and chemical industry. Electrochemical synthesis of aryl alcohols is an environmentally friendly approach, as we can avoid stoichiometric amounts of toxic oxidants and metal-catalysts. Herein, we present a mild and green way to synthesize aryl alcohols electrochemically by using a continuous-flow setup. The continuous-nature of the process allowed us to prevent the decomposition of sensitive products under the electrochemical reaction conditions and therefore expand the reaction scope beyond electron-poor and neutral arenes.



Scheme 1. Electrochemical hydroxylation of arenes with trifluoroacetic acid

We demonstrated the electrochemical hydroxylation of electron-rich arenes with 15 examples, in which trifluoroacetic acid was used as an oxygen source. Also, a successful scale-up experiment (10 mmol scale) was carried out. The developed transformation was carried out in an inexpensive self-made flow microreactor [1].

### Acknowledgements

The authors acknowledge financial support from the European Regional Development Fund through Dora Plus program and the programme Mobilias Plus (Grant No MOBTP180), the Estonian Ministry of Education and Research (Grant No PRG1031) and the Centre of Excellence in Molecular Cell Engineering (2014-2020.4.01.15-0013).

### References

1. A. Kooli, L. Wesenberg, M. Beslać, A. Krech, M. Lopp, T. Noël, M. Ošeka, *Eur. J. Org. Chem.*, e202200011 (2022).

## Direct electrochemical oxidation of abietanes

Inês S. Martins\*, Jaime A. S. Coelho<sup>b</sup>, Carlos A. M. Afonso<sup>a</sup>

<sup>a</sup>Instituto de Investigação do Medicamento (iMed.U LISBOA), Faculty of Pharmacy, University of Lisbon, Av. Prof. Gama Pinto, 1649-003 Lisboa, Portugal. <sup>b</sup>Centro de Química Estrutural, Institute of Molecular Sciences, Faculty of Sciences,

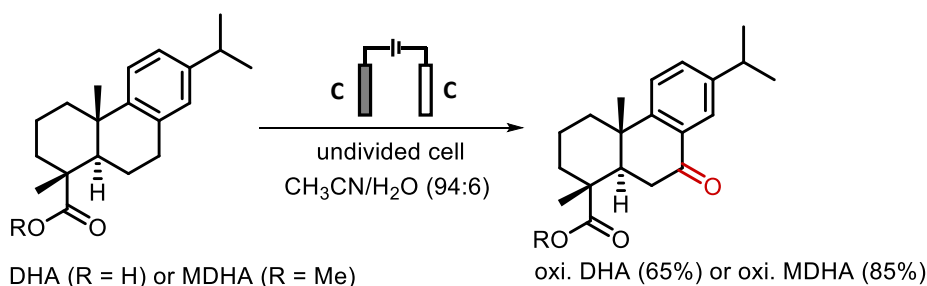
University of Lisbon, Campo Grande, 1749-016 Lisboa, Portugal

\*samartins.ines@gmail.com

Colophony, a natural resin obtained from coniferous trees, is constituted by a group of diterpenes known as abietanes, which, along with its derivatives, has been found to have a wide variety of interesting biological activities, including the antimicrobial, antiviral, antitumoral, and anti-inflammatory activities. Constituents of this resin have a wide range of industrial applications, including synthetic rubbers, adhesives and fragrances. [1,2]

The benzylic oxidation of dehydroabietic acid, an abietane from colophony, and its methyl ester derivative, has been reported using oxidative protocols, such as using Jones reagent [3], Swern oxidation [4] or either using Chromium trioxide in stoichiometric [5] or catalytic quantities. [6] However, these protocols fail in the context of sustainability for several reasons, such as the use of toxic reagents and stoichiometric amounts.

The electrochemistry equipment used in this work were an ElectraSyn 2.0 system by IKA.



Scheme 1: Electrochemical oxidation of dehydroabietic acid (DHA) and its methyl ester derivative (MDHA).

Herein, we report an electrochemical method for the benzylic oxidation of dehydroabietic acid, an alternative greener protocol for the formation of the benzylic ketone in very good yields using modern electrochemical methods. (Scheme 1). Moreover, this method can be applied to the corresponding methyl ester derivative. [7-9]

### Acknowledgements

The project leading to this application has received funding from the European Union's Horizon 2020 research and innovation programme under grant agreement No 951996.

### References

1. M.A. González, J. Correa-Royero, L. Agudelo, A. Mesa, L. Betancur-Galvis, Eur J Med Chem. 2009, 44(6), 2468–2472.
2. G. Eksi, S. Kurbanoglu, S.A. Erdem, Elsevier Inc.. 2020, 313–345 p.
3. E. Alvarez-Manzaneda, R. Chahboun, F. Bentaleb, E. Alvarez, M. A. Escobar, S. Sad-Diki, et al. Tetrahedron. 2007, 63, 11204.
4. R.J. Rafferty, R.W. Hicklin, K.A. Maloof, P.J.Hergenrother. Angew. Chem. Int. Ed. 2014, 53, 220.
5. S.M.C.S. Monteiro, A.J.D. Silvestre, A.M.S. Silva, J.A.S.Cavaleiro, V. Félix, M.G.B.Drew. New J. Chem. 2001, 25, 1091.
6. Z. Zhou, X. Wang, T. Zhou. Russ. J. Gen. Chem. 2019, 89, 819.
7. L. Meng, J. Su, Z. Zha, L. Zhang, Z. Zhang, Z. Wang. Chem. - A Eur. J. 2013, 19, 5542.
8. H. Wang, K. Liang, W. Xiong, S. Samanta, W. Li, A. Lei. Sci. Adv. 2020, 6, eaaz0590.
9. J.A. Marko, A. Durgham, S.L. Bretz, W. Liu. Chem. Commun. 2019, 55, 937.

## Continuous Formation of Bioderived Cyclic Carbonates using Supported Ionic Liquid Based Catalysts and Supercritical Carbon Dioxide (scCO<sub>2</sub>) as Solvent and Reagent

Philipp Mikšovský<sup>1\*</sup>, Elias N. Horn<sup>1</sup>, Michael Schnürch<sup>1</sup> and Katharina Bica-Schröder<sup>1</sup>

<sup>1</sup>TU Wien, Institute of Applied Synthetic Chemistry, Getreidemarkt 9/E163, Austria

\* [philipp.miksovsky@tuwien.ac.at](mailto:philipp.miksovsky@tuwien.ac.at)

The use of bioderived chemicals has attracted increasing attention in the past years in order to reduce the dependence on crude oil as limited feed stock.

In this context, cyclic carbonates with an increasing annual production provoked by applications as electrolytes in lithium ion batteries as well as aprotic polar solvents or monomeric building blocks for polyurethanes are compounds of scientific and industrial interest. One of the most important synthetic strategies for the synthesis of cyclic carbonates is the catalytic coupling of epoxides with carbon dioxide (CO<sub>2</sub>).<sup>[1]</sup> Suitable renewable starting material for cyclic carbonates derived from epoxides and CO<sub>2</sub> are for example oils, fats and fatty acids and terpenes like limonene or carvone.<sup>[2]</sup>

While several catalysts were reported for this purpose, the combination of supercritical carbon dioxide (scCO<sub>2</sub>) and ionic liquids as catalytic system show a particular property of high value. The high solubility of scCO<sub>2</sub> in ionic liquids makes ionic liquids ideal candidates as reaction media in combination with scCO<sub>2</sub> for catalytic processes. In contrast, ionic liquids show extremely low solubility in scCO<sub>2</sub>, thus rendering them attractive for immobilized catalytic phases in heterogeneous catalysis<sup>[3]</sup>, where leaching of the catalyst from the supporting material can be an issue.

For the immobilization of ionic liquids towards continuous flow processes, supported ionic liquid phases (SILPs) are a well-known and widely used concept for catalytic and numerous other applications.<sup>[4]</sup> SILP materials contain of a thin film of ionic liquid on supporting material e.g. mesoporous silica which offers a high surface area that is advantageous for catalytic processes.

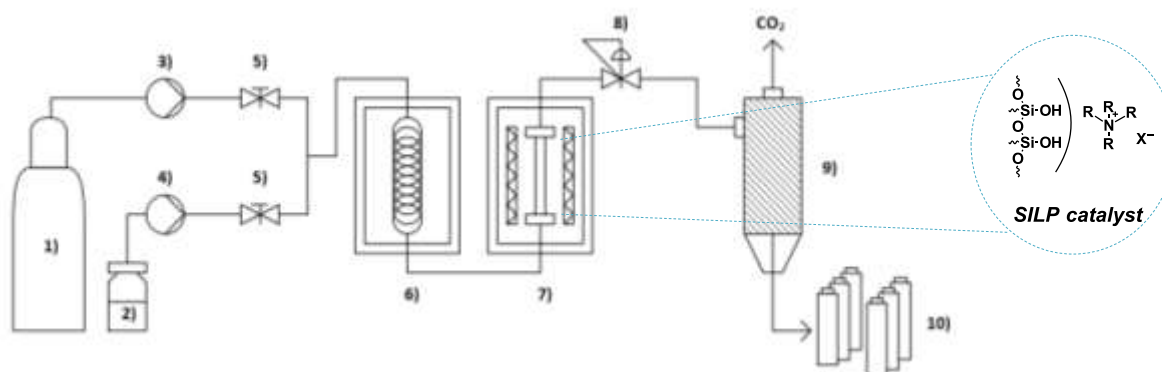


Figure 1: Schematic representation of the scCO<sub>2</sub> flow device; 1) liquid CO<sub>2</sub> supply; 2) substrate supply; 3) CO<sub>2</sub> pump; 4) substrate pump; 5) hand operated valve; 6) oven with preheating coil 7) oven with catalyst cartridge; 8) back-pressure regulator; 9) gas-liquid separator; 10) product collector

We combined the concept of SILP catalysis and scCO<sub>2</sub> for the formation of bioderived limonene carbonates in continuous flow starting from diastereomeric mixtures of limonene oxide and limonene dioxide. During the initial evaluation of various ammonium and imidazolium based ionic liquids as catalytically active species in batch mode, ammonium halides showed promising performance regarding yield and selectivity. For the continuous flow process, the heterogeneous version of this catalyst was prepared *via* physisorption of catalytically active ionic liquid on mesoporous silica.

The continuous flow reactions were performed with a scCO<sub>2</sub> flow device (Figure 1), where mixtures of substrate and scCO<sub>2</sub> get pumped with HPLC pumps through a catalyst cartridge which is filled with the heterogeneous catalyst and placed in a HPLC oven. After CO<sub>2</sub> release *via* a back-pressure regulator and a gas/liquid separator, substance is collected in different fractions.

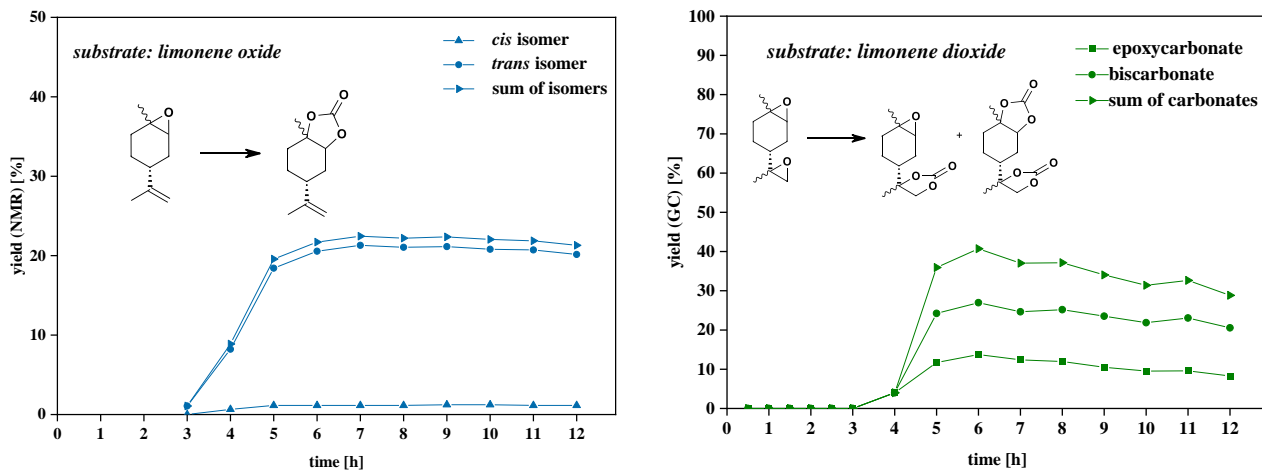


Figure 2: Continuous formation of limonene derived cyclic carbonates starting from limonene oxide (left) and limonene dioxide (right) using ammonium halide based supported ionic liquids (SILPs) as heterogeneous catalysts.

After optimizing the system including screening of temperature, pressure, catalyst loading and flow rates of substrate as well as CO<sub>2</sub>, being used as sole solvent and reagent, a constant production of limonene carbonates as well as epoxycarbonates and biscarbonates was achieved as shown in Figure 2. Additionally, the long-term behavior of the heterogeneous SILP catalysts was investigated in 48 h experiments.

## Acknowledgements

This project has received funding from the European Research Council (ERC) under the European Union's Horizon 2020 research and innovation programme (Grant agreement No. 864991).

## References

- [1] A. J. Kamphuis, F. Picchioni, P. P. Pescarmona, *Green Chemistry* **2019**, *21*, 406-448.
- [2] (a) L. Longwitz, J. Steinbauer, A. Spannenberg, T. Werner, *ACS Catalysis* **2018**, *8*, 665-672; (b) F. de la Cruz-Martínez, M. Martínez de Sarasa Buchaca, J. Martínez, J. Fernández-Baeza, L. F. Sánchez-Barba, A. Rodríguez-Diéguez, J. A. Castro-Osma, A. Lara-Sánchez, *ACS Sustainable Chemistry & Engineering* **2019**, *7*, 20126-20138.
- [3] (a) U. Hintermair, G. Zhao, C. C. Santini, M. J. Muldoon, D. J. Cole-Hamilton, *Chemical Communications* **2007**, 1462-1464; (b) P. Lozano, E. García-Verdugo, R. Piamtongkam, N. Karbass, T. De Diego, M. I. Burguete, S. V. Luis, J. L. Iborra, *Advanced Synthesis & Catalysis* **2007**, *349*, 1077-1084.
- [4] A. Sainz Martínez, C. Hauzenberger, A. R. Sahoo, Z. Csendes, H. Hoffmann, K. Bica, *ACS Sustainable Chemistry & Engineering* **2018**, *6*, 13131-13139.
- [5] L. Maisonneuve, O. Lamarzelle, E. Rix, E. Grau, H. Cramail, *Chemical Reviews* **2015**, *115*, 12407-12439.

## Microwave assisted one-pot synthesis of bridgehead bicyclo[4.4.0]boron heterocycles as DNA visible light photo-interacting molecules with possible theranostic applications

Polinikis Paisidis,<sup>1</sup> George Psomas,<sup>2</sup> Antigoni Kotali<sup>3</sup> and Konstantina C. Fylaktakidou<sup>1\*</sup>

<sup>1</sup>Lab of Organic Chemistry/Aristotle University of Thessaloniki/Chemistry Dept, 54124 Thessaloniki, Greece,

<sup>2</sup>Lab of Inorganic Chemistry/Aristotle University of Thessaloniki/Chemistry Dept, 54124 Thessaloniki, Greece,

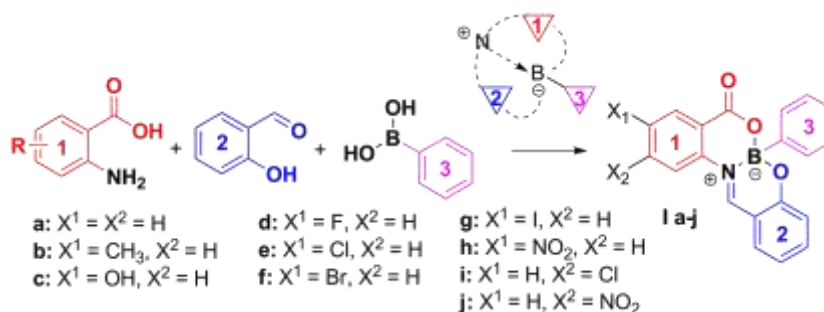
<sup>3</sup>Lab of Organic Chemistry/Aristotle University of Thessaloniki/Dept of Chemical Engineering, 54124 Thessaloniki, Greece  
\*kfyllakta@chem.auth.gr

Multicomponent reactions, especially those that leave no residual byproducts, are important in organic synthesis and medicinal chemistry since, most of the times, there is no need for purification of the final obtained products. In addition, the performance of the reactions under microwave irradiation, that usually require much less time to be completed, offer energy-saving conditions compared to the thermal ones. Thus, more often, those reactions characterize procedures that fulfill green chemistry requirements.

The assembly of compounds bearing N- and O- donors with aryl boronic acids may lead to the synthesis of tetrahedral boron containing compounds that contain the zwitterionic  $^+N \rightarrow B^-$  moiety [1] and provide bicyclic or polycyclic compounds with interesting properties. For example one-pot reaction of anthranilic acids, salicylaldehydes and arylboronic acids provide the tetracyclic compound **I** via an assembly shown in Scheme 1.

It seems to be an interest in such molecules. For example, compound **Ia** has shown luminescence with aggregation-induced emission enhancement [2]. A structure-activity relationship study with variation of substituents on salicylaldehyde molecule has shown that the fluorescence emission was decreased in wavelength maxima when electron-donating groups have been attached or when conjugation has been introduced [2]. More complex structures bearing such main core were found to exhibit photophysical properties for live cell bio-imaging applications [3],[4].

Published syntheses of various derivatives like **I** were performed in MeOH reflux for 12 h and when necessary the products were purified by column chromatography [2]. Other groups were heating all three components in EtOH at 70 °C for 18 h [3],[4], or under MW irradiation for some min in toxic CCl<sub>4</sub> [5]. Although all attempted syntheses gave the products in an efficient way and in high yields, we have tried to improve the conditions in order to obtain compounds **Ia-j**.



**Scheme 1:** One-pot synthesis of bridgehead bicyclo[4.4.0]boron heterocycles **Ia-j**. Reaction conditions: **1+2+3** (1/1/1 equimolar amounts) in toluene containing activated molecular sieves. MW irradiation, 60 min, 180 °C.

From the series of the targeted compounds only **Ia** and **Ie** have been reported in the literature. Our design, within this study, afforded variation initially in anthranilic acid for three reasons: a) we have studied *o*-aminobenzoic derivatives in open-flexible and rigid forms for their photo-excitations and DNA photo-cleavage and we have found that positioning and nature of X<sub>1</sub> and X<sub>2</sub> are important [6],[7]; b) substitution on this part was also essential for obtaining large Stokes Shifts and high fluorescence quantum yields [8]; and c) we envisioned that the existence of the zwitterions on the structures of compounds **I** may enhance DNA affinity and in addition the bathochromic shift to visible light irradiation may allow photodynamic effects to appear to the compounds. This way, combination of fluorescence (bio-imaging) and photodynamic activity (anticancer and /or antimicrobial inactivation) may allow the discovery of novel lead compounds for photo-theranostics.

In our attempted preliminary synthetic protocol, reagents **1** (X<sub>1</sub>= X<sub>2</sub> = H), **2** and **3** were dissolved in toluene and the mixture was refluxed overnight in a Dean-Stark apparatus to give compound **Ia**. The reaction didn't seem to be completed in less hours heating. The same product has been obtained when isolated salicylanthranilimine (**1+2**, Schiff base) has been refluxed with phenylboronic acid (**3**) under the same reaction conditions, thermally. Having secured the synthesis of compound **Ia** we have attempted the one-pot three-component reaction under MW irradiation in toluene containing activated molecular sieves for 60 min, 180 °C. All reactions were giving the products pure, crystallized upon cooling of the toluene solution, in excellent yields. Simple filtration and washing with ethyl acetate or mixture of ethyl acetate and petroleum ether were completing the procedure.

Preliminary DNA photo-cleavage experiments with compound **1f** under UV-A irradiation have shown excellent reactivity. It is interesting to mention that, to the best of our knowledge, besides bio-imaging [3],[4] biological activity of such compounds have not been investigated so far. Nevertheless, derivatives that contained amino acids instead of anthranilic acids exhibited activity against human neutrophil elastase [9].

Thus, we have synthesized compounds **1a-j** in excellent yields and in an improved microwave assisted synthesis using a safer solvent with lower environmental risk [10]. In addition the synthetic protocol gives flexibility for the synthesis of derivatives with hydrolytic stability in human plasma by simply exchanging salicylaldehyde to *o*-OH-benzophenone [4]. These compounds give promise for possible non-invasive photo-theranostic applications.

## References

1. A. Kotali, A. Maniadaki, E. Kotali, P.A. Harris, E. Rózycka-Sokołowska, P. Bałczewski, J.A. Joule, *Tetrahedron*, **58** 512 (2017).
2. S. Guieu, C.I.C. Esteves, J. Rocha, A.M.S. Silva, *Molecules*, **25** 6039 (2020).
3. F.M.F. Santos, J.N. Rosa, N.R. Candeias, C.P. Carvalho, A.I. Matos, A.E. Ventura, H.F. Florindo, L.C.Silva, U. Pischel, P.M.P. Gois, *Chem. Eur. J.*, **22** 1631 (2016).
4. F.M.F. Santos, A.I. Matos, A.E. Ventura, J. Gonçalves, L.F. Veiros, H.F. Florindo, P.M.P. Gois, *Angew. Chem. Int. Ed.*, **56** 9346 (2017).
5. M. Adib, E. Sheikhi, H.R. Bijanzadeh, L.-G. Zhu, *Tetrahedron*, **68** 3377 (2012).
6. A. Panagopoulos, T. Balalas, A. Mitrakas, V. Vrazas, K.R. Katsani, A.E. Koumbis, M.I. Koukourakis, K.E. Litinas, K.C. Fylaktakidou, *Photochem. Photobiol.*, **97** 826 (2021).
7. C. Mikra, M. Bairaktari, M.-T. Petridi, A. Detsi, K.C. Fylaktakidou, *Processes*, **10** 384 (2022).
8. J. Zhou, L. Liu, Y. Pan, Q. Zhu, Y. Lu, J. Wei, K. Luo, Y. Fu, C. Zhong, Y. Peng, Z. Song, *Chem. Eur. J.*, **24** 17897 (2018).
9. F. Montalbano, P.M.S.D. Cal, M.A.B.R. Carvalho, L.M. Gonçalves, S.D. Lucas, R.C. Guedes, L.F. Veiros, R. Moreira, P.M.P. Gois, *Org. Biomol. Chem.*, **11** 4465 (2013).
10. M. Tobiszewski, J. Namieśnika, F. Pena-Pereira, *Green Chem.*, **19** 1034 (2017).



## Advancing flow chemistry through continuous API manufacturing: A Process route towards Celecoxib

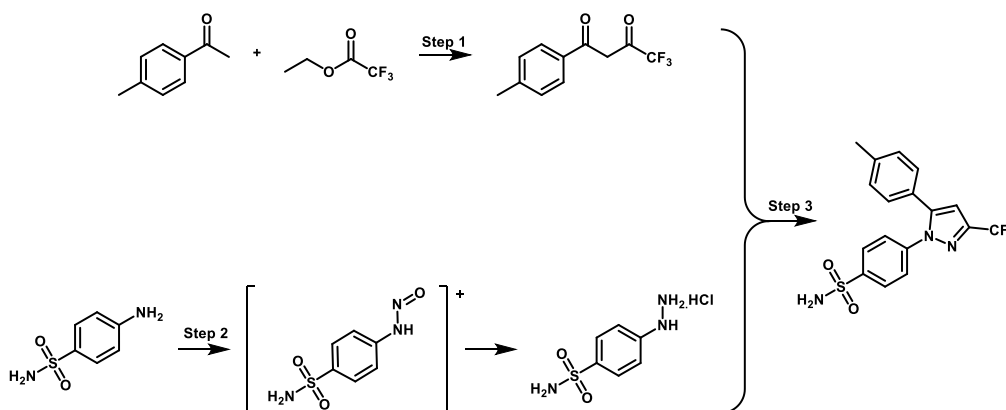
Nicole C Neyt-Galetti<sup>1</sup>, Chris van der Westhuizen<sup>1</sup>, Darren L. Riley and Jenny-Lee Panayides<sup>1\*</sup>

<sup>1</sup>Pharmaceutical Technologies, Council for Scientific and Industrial Research Future Production: Chemicals, Meiring Naudé Road, Pretoria, South Africa, 0184

<sup>2</sup>Department of Chemistry, Natural and Agricultural Sciences, University of Pretoria, Pretoria, 0028, South Africa.

\* jpanayides@csir.co.za, nneyt@csir.co.za

Herein we have reported an improved batch synthesis and alternative flow chemistry route towards Celecoxib, a non-steroidal anti-inflammatory drug. The synthesis of Celecoxib involves a Claisen condensation of methylacetophenone and ethyltrifluoroacetate (step 1) to afford the dione as shown in Scheme 1. This is subsequently reacted with a hydrazine intermediate to finally afford the desired API (Active Pharmaceutical Ingredient), Celecoxib (step 3). The process was validated and optimized under batch conditions and thereafter translated to flow. The final process was achieved in a continuous fashion, telescoping both stages 1 and 2 affording several advantages which include: safer reaction conditions, minimal handling of toxic reagents, faster reaction times, and the use of greener solvents. Similar overall yields were achieved in flow when compared to the batch process, however a significant reduction in overall reaction times were achieved in flow. Furthermore, a full sustainability study was performed with the aid of a green metrics toolkit to analyse the overall sustainability and environmental impact of the process. Additionally, we employed DoE (Design of Experiments) software, and LC (liquid chromatography) traces to aid in our optimization studies increasing the overall reaction efficiency.



**Scheme 1:** Process study towards Celecoxib

### Acknowledgements

Council for Scientific and Industrial Research (Parliamentary Grant), Department of Science and Innovation (FEI Grant)

### References

- (1) Scholtz, Chantal, and Darren L. Riley. *Reaction Chemistry & Engineering*, **2021**, 6, 138-146.
- (2) Gaulier, S.M.; McKay, R. and Swain, N.A. *Tetrahedron Lett.*, **2011**, 52, 6000.
- (3) Singh, S.K.; Reddy, P.G.; Rao, K.S.; Lohray, B.B.; Misra, P.; Rajjak, S.A.; Rao, Y.K. and Venkateswarlu, A. *Bioorg. Med. Chem. Lett.*, **2004**, 14, 499.
- (4) Boschi, D.; Lazzarato, L.; Rolando, B.; Filieri, A.; Cena, C.; Di Stilo, A.; Fruttero, R. and Gasco, A. *Chem. Biodiversity.*, **2009**, 6, 369.
- (5) Desai, D.; Kaushal, N.; Gandhi, U.H.; Arner, R.J.; D'Souza, C.; Chen, G.; Vunta, H.; El-Bayoumy, K.; Amin, S. and Prabhu, K.S. *Chem.-Biol. Interact.*, **2010**, 188, 446.
- (6) Menozzi, G.; Merello, L.; Fossa, P.; Mosti, L.; Piana, A. and Mattioli, F. *Il Farmaco*, **2003**, 58, 795.
- (7) Kuge, Y.; Katada, Y.; Shimonaka, S.; Temma, T.; Kimura, H.; Kiyono, Y.; Yokota, C.; Minematsu, K.; Seki, K.; Tamaki, N.; Ohkura, K. and Saji, H. *Nucl. Med. Biol.*, **2006**, 33, 21.
- (8) Gao, M.; Wang, M.; Miller, K.D.; Hutchins, G.D. and Zheng, Q-H. *Appl. Radiat. Isot.*, **2009**, 67, 2019.

## Chalcones as alkyne surrogates for the synthesis of pyrazoles through sequential mechanochemical (3+2)-cycloaddition with nitrile imines and deacylative oxidation

Greta Utecht-Jarzyńska<sup>1</sup>, Anna Kowalczyk<sup>1,2</sup> and Marcin Jasiński<sup>1\*</sup>

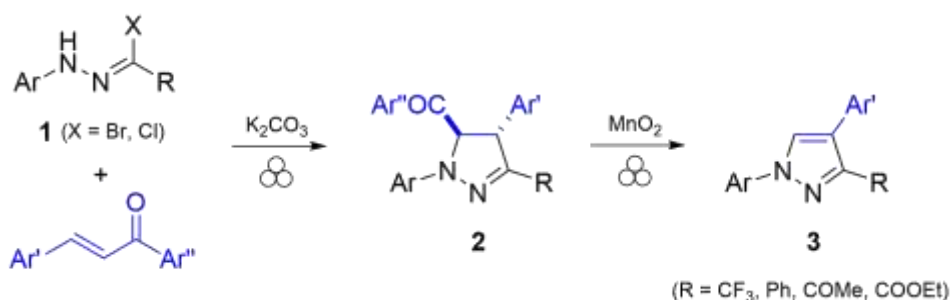
<sup>1</sup>Faculty of Chemistry, University of Lodz, Tamka 12, 91403 Łódź, Poland

<sup>2</sup>The University of Lodz Doctoral School of Exact and Natural Sciences, Banacha 12/16, 90237 Łódź, Poland

\*mjasinski@uni.lodz.pl

In the past two decades, great attention has been focused on fluorinated and non-fluorinated pyrazole ring as relevant structural motif present in various biologically active compounds and advanced materials of special properties [1]. Common synthetic method for the preparation of pyrazole derivatives relies on cyclocondensation of 1,3-dielectrophilic compounds (1,3-dicarbonyls and their equivalents) with hydrazines, whereas another powerful strategy is based on Huisgen reaction, typically employing diazoalkanes as suitable 1,3-dipolar reagents [2]. In a series of recent work we have demonstrated trifluoroacetonitrile imines as convenient building blocks for preparation of various trifluoromethylated *N*- and *S,N*-heterocycles both *via* (3+2)-cycloaddition and (3+3)-annulation reactions [3]. The mentioned electron-deficient 1,3-dipoles can easily be generated *in situ* by base-induced dehydrohalogenation of the respective hydrazonoyl bromides **1** (R = CF<sub>3</sub>) [4], and in the presence of chalcones they smoothly lead to the corresponding *trans*-configured 5-acylpyrazolines in a complete regio- and diastereoselective manner [5]. Notably, the latter (3+2)-cycloadducts can be efficiently oxidized with MnO<sub>2</sub> leading to either fully substituted or 1,4-disubstituted 3-trifluoromethylpyrazoles, depending on the polarity of the solvent used.

In continuation of our study on the synthesis and applications of 5-acylpyrazolines of type **2**, here we report the synthesis of a series of fluorinated and non-fluorinated pyrazoles **3** through environmentally friendly solvent-free mechanochemical approach (Scheme 1). The impact of the devised ball-milling procedure on the reaction times, scope, selectivity of both (3+2)-cycloaddition and subsequent oxidative steps as well as the proposed mechanistic scenario of the observed deacylative aromatization will be discussed.



Scheme 1. Mechanochemical synthesis of fluorinated and non-fluorinated pyrazoles **3**.

### Acknowledgements

This work has been supported by the University of Lodz in the framework of the IDUB program (M.J.; grant no. 3/IDUB/DOS/2021).

### References

1. a) A. Ansari, A. Ali, M. Asif, Shamsuzzaman, *New J. Chem.*, **41** 16 (2017); b) P. K. Mykhailiuk, *Chem. Rev.*, **121** 1670 (2021).
2. S. Fustero, M. Sánchez-Roselló, P. Barrio, A. Simón-Fuentes, *Chem. Rev.*, 111 6984 (2011).
3. a) G. Utecht, A. Fruziński, M. Jasiński, *Org. Biomol. Chem.*, **16** 1252 (2018); b) G. Utecht, G. Młostoń, M. Jasiński, *Synlett*, **29** 1753 (2018); c) P. Grzelak, G. Utecht, M. Jasiński, G. Młostoń, *Synthesis*, **49** 2129 (2017); d) G. Utecht-Jarzyńska, A. Michalak, J. Banaś, G. Młostoń, M. Jasiński, *J. Fluorine Chem.*, **222-223** 8 (2019).
4. G. Młostoń, K. Urbaniak, G. Utecht, D. Lentz, M. Jasiński, *J. Fluorine Chem.*, **192** 147 (2016).
5. A. Kowalczyk, G. Utecht-Jarzyńska, G. Młostoń, M. Jasiński, *Org. Lett.*, doi:10.1021/acs.orglett.2c00521 (2022).

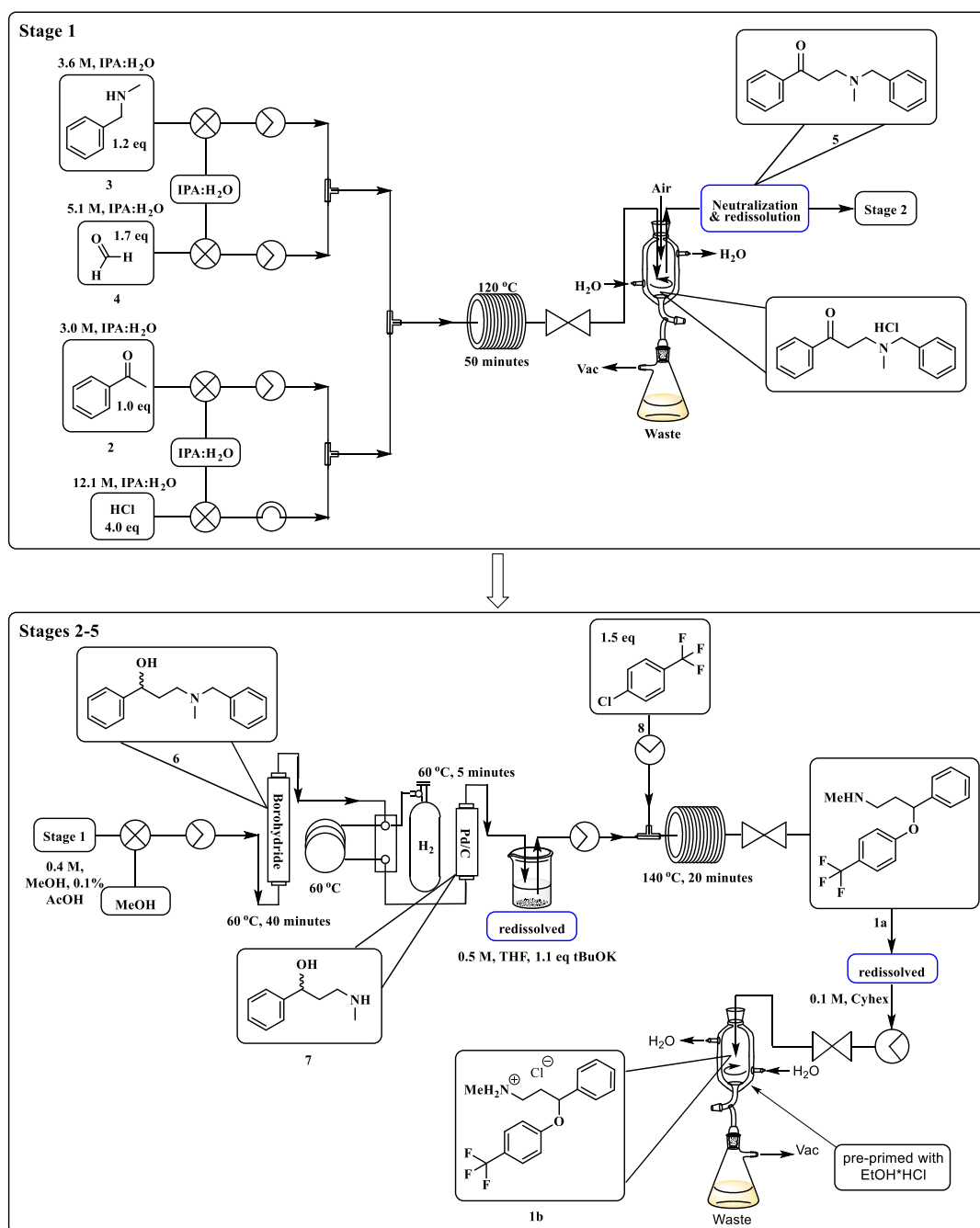
# A multistep microflow process towards Selective Serotonin Reuptake Inhibitor (SSRI), Fluoxetine.

Lorinda T. van Wyk<sup>1</sup> and Darren L. Riley<sup>1\*</sup>

<sup>1</sup>Department Chemistry, University of Pretoria, Pretoria, 0028, South Africa.

\*darren.riley@up.ac.za.

According to a study conducted by the World Health Organization (WHO) in 2017, more than 300 million people are affected by depression globally making it the most common illness worldwide [1]. Fluoxetine **1**; ranking 20<sup>th</sup> in the top 200 prescribed drugs in the US in 2018; is a second-generation SSRI class antidepressant useful in the treatment of depression and other mental disorders [2-4]. In this research project, we focused our attempts on obtaining a greener, safer and more sustainable flow route towards the synthesis of fluoxetine hydrochloride **1b**. The proposed five stage synthetic batch process route towards fluoxetine **1** was translated to a viable flow route which utilises a collection of flow chemistry techniques (**Scheme 1**) [5,6].



**Scheme 1.** Proposed flow synthetic route for the synthesis of Fluoxetine hydrochloride **1b**.

The five-stage synthesis of fluoxetine commences with a three-component Mannich reaction involving acetophenone **2**, *N*-methylbenzylamine **3**, formaldehyde **4** and hydrochloric acid to afford the corresponding 3-(benzyl(methyl)amino)-1-phenylpropan-1-one **5** which is then subjected to polymer-supported borohydride in a reduction step to form the respective racemic alcohol **6**. This is further debenzylated with hydrogen gas and palladium on carbon catalyst to form 3-(methylamino)-1-phenylpropan-1-ol **7**. Subsequent treatment with potassium *tert*-butoxide and 4-chlorobenzotrifluoride **8** affords the desired free base fluoxetine **1a** which is treated with ethanolic hydrogen chloride to yield fluoxetine hydrochloride **1b**.

## Acknowledgements

I would like to thank my supervisor Professor Darren L Riley for his help and guidance during the project, the University of Pretoria for the use of the facilities and lastly both Sasol Ltd and the CSIR for financial support.

## References

1. [WHO], W.H.O., *Depression and Other Common Mental Disorders: Global Health Estimates*. 2017, World Health Organization: Geneva.
2. Rej, R.K., et al., *Chemoenzymatic asymmetric synthesis of fluoxetine, atomoxetine, nisoxetine, and duloxetine*. *Tetrahedron: Asymmetry*, 2013. **24**(15-16): p. 913-918.
3. Welch, J.T. and D.S. Lim, *The synthesis and biological activity of pentafluorosulfanyl analogs of fluoxetine, fenfluramine, and norfenfluramine*. *Bioorganic & Medicinal Chemistry*, 2007. **15**: p. 6659-6666.
4. Fuentes, A.V., M.D. Pineda, and K.C.N. Venkata, *Comprehension of Top 200 Prescribed Drugs in the US as a Resource for Pharmacy Teaching, Training and Practice*. Pharmacy (Basel), 2018. **6**(2).
5. Deadman, B. J., Battilocchio, C., Sliwinski, E. & Ley, S. V., 2013. A prototype device for evaporation in batch and flow chemical processes. *Green Chemistry*, 15(8), pp. 2050-2055.
6. Neyt, N. C. & Riley, D. L., 2018. Batch-flow hybrid synthesis of the antipsychotic Clozapine. *Reaction Chemistry & Engineering*, Volume 3, pp. 17-24.

## Microreactor based on TiO<sub>2</sub> nanotubes for photocatalytic degradation of organic compounds in water

Vasilyev A.S.<sup>1\*</sup>, Morozov A.N.<sup>1</sup>, Gartman T.N.<sup>1</sup>, Pochitalkina I.A.<sup>1</sup> and Sovetin F.S.<sup>1</sup>  
<sup>1</sup>Mendeleev University of Chemical Technology of Russia, 125047, Moscow, Miusskaya square, 9, Russia  
 \* alexandr.s.vasilyev@gmail.com

Prevention of environmental pollution is one of the main directions of green chemistry [1]. Thus, special attention is currently paid to Advanced Oxidation Processes (AOPs) as a promising technology for water treatment from toxic wastes and microorganisms [2]. A special role in these processes is played by photocatalysis, which is a rapidly developing direction and one of the most promising in the field of water purification. Photocatalysis is considered to be an ecologically clean process because it achieves complete mineralization of hard-to-oxidize organic impurities without the formation of secondary pollutants in the presence of light [3]. Particular interest in photocatalysis is caused by the possibility of reducing the purification process energy consumption by using the energy of the sun. Unlike classical catalytic processes, photocatalysis requires continuous irradiation of the catalyst surface with light, which creates significant difficulties when creating photocatalytic reactors. Moreover, in order to achieve complete mineralization of organic compounds, the reactor geometry should ensure sufficiently long contact of reagents with the photocatalyst surface. Microchannel systems allow significant intensification of such processes due to the more effective organization of mass transfer in the reactor as compared to traditional reactors. Therefore, the development of microchannel systems for photocatalytic processes is of current interest for the further improvement of environmental technologies. In this paper, the results of the phenol degradation efficiency studies carried out in the newly developed photocatalytic microchannel reactor with a photoactive layer comprised of highly ordered titanium oxide nanotubes (NTs) are presented.

Microchannels of the photoactive layer of TiO<sub>2</sub> NTs were obtained using an electrolytic method and photolithography. To set the shape and size of the microchannels, a photoresist film was applied to the titanium foil and developed by the original procedure. The photoactive layer of TiO<sub>2</sub> NTs was formed by a titanium anodization procedure, according to the previously developed technique [4]. Then, the photoresist was removed, and the process of thermal crystallization of amorphous TiO<sub>2</sub> NTs was carried out at 450 °C under a stream of air.

The morphology of the photoactive film was studied using a JSM-6510 LV scanning electron microscope (SEM) (JEOL, Japan). The process of photocatalytic degradation of phenol was carried out by circulating 50 ml of aqueous phenol solution at a rate of 0.6 l/h under mixed light irradiation with an intensity of 100 mW/cm<sup>2</sup>. The phenol concentration was determined by gas-liquid chromatography on a Trace 1310 chromatograph (Thermo Scientific, Italy). The initial phenol concentration was 10 mg/l.

Figure 1 shows a digital photograph and SEM image of the obtained TiO<sub>2</sub> NTs microchannel system.

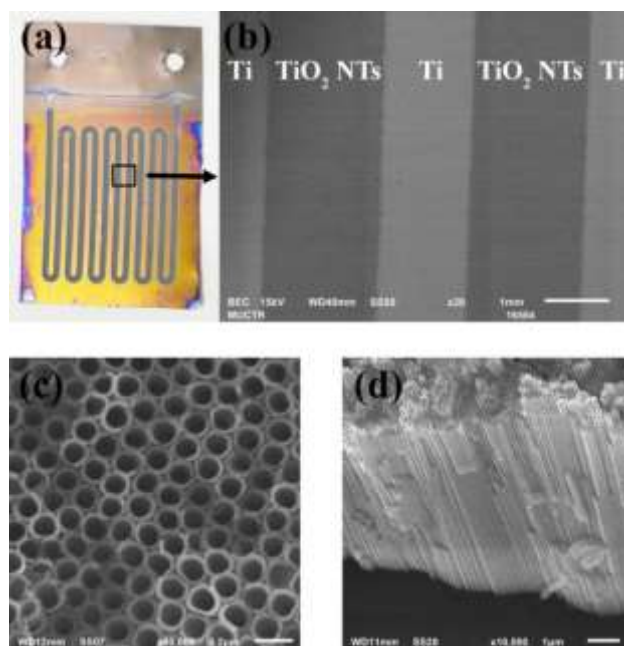


Figure 1. Digital photography (a) and SEM micrographs (b-d) of obtained microchannels from TiO<sub>2</sub> NTs

It can be seen that the obtained microchannel system of TiO<sub>2</sub> NTs is of high quality. The channels are strictly parallel and precisely reflect the geometry specified by the photoresistive mask. The SEM micrograph (Fig. 1b) obtained using reflected electrons shows a clear boundary between metallic titanium and TiO<sub>2</sub> NT microchannels, indicating good isolation of titanium with a film photoresist. The absence of anodic regions on the protected titanium does not lead to the appearance of defects and unevenness on the titanium surface, which is a critical factor in the good sealing of microreactor channels. According to the SEM (Fig. 1c-d), the film consists of TiO<sub>2</sub> NTs, which are located strictly parallel to each other and perpendicular to the titanium substrate and have a narrow size distribution. In the film plane, local self-organization of NTs into hexagonal domains is observed. According to the presented microphotographs, the average inner diameter of the TiO<sub>2</sub> NTs is 110±5 nm, the wall thickness is 12±3 nm, and the length is 9.6±0.3 μm.

The protoreactor has a layered structure. The titanium foil with a photoactive layer is sandwiched between PTFE sheet and quartz glass, which is used to allow catalyst irradiation. A 0.1 mm thick silicone gasket is placed between the titanium foil and the quartz window. Figure 2 shows the kinetic curves of phenol degradation in the developed microreactor.

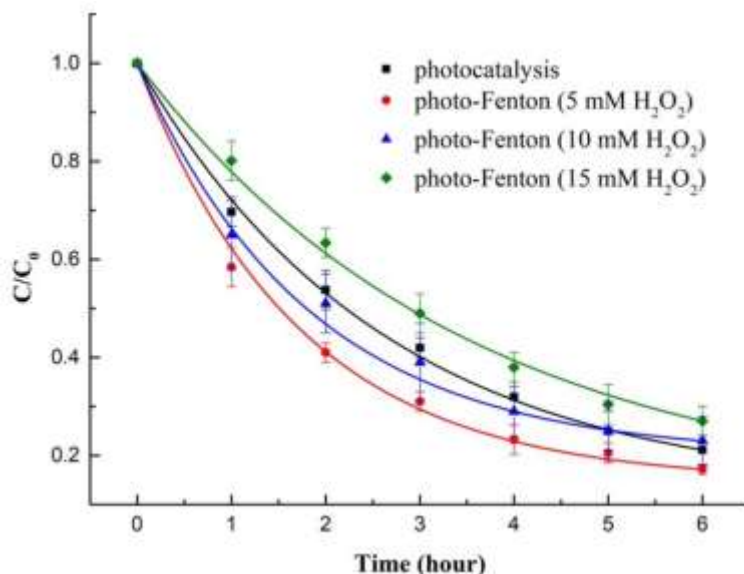


Figure 2. Kinetic curves of photocatalytic degradation of phenol in a microreactor

As can be seen, the function of the phenol degradation degree from the concentration of H<sub>2</sub>O<sub>2</sub> has an extremum. This behavior can be explained by the decomposition of hydrogen peroxide along with the photocatalytic oxidation of phenol. This causes blocking of the active centers on the photocatalytic surface, which are necessary for the oxidation of phenol molecules. Additionally, bubbles released during the process of H<sub>2</sub>O<sub>2</sub> decomposition also block the photocatalytic surface. Thus, as the concentration of H<sub>2</sub>O<sub>2</sub> increases, the blocked surface increases, which negatively affects the rate of phenol degradation. Due to the strong gas contamination of the system, a large deviation of phenol concentrations was observed during parallel studies, which was reflected in the appearance of a large error.

In the course of the study, the main technological possibilities of the created microreactor were determined. It was shown that the developed microreactor system has high photocatalytic activity. When phenol aqueous solution was cycled through the microreactor at a rate of 0.6 l/h, the degree of phenol degradation after 6 hours of the process was 78%. The effect of different geometries of microchannels on the efficiency of phenol degradation in aqueous medium has been determined. It was found that channels with a width of up to 3 mm were most effective in the recirculation mode.

## Acknowledgements

The authors are grateful to the staff of the Center for Collective Use for studying the samples by the SEM.

## References

1. H.C. Erythropel, J.B. Zimmerman, T.M. de Winter et al., *Green Chemistry*, 20 1929 (2018).
2. P.K. Pandis, C. Kalogirou, E. Kanellou et al., *ChemEngineering*, 6 8 (2022).
3. A. Zuliani, C.M. Cova, *Photochem*, 1 147 (2021).
4. A.N. Morozov, A.V. Denisenko, A.I. Mihaylichenko, M.Yu. Chayka, *Nanotechnologies in Russia*, 14, 9-10 444 (2019).

# Alternative fossil fuels and biofuels, green bio-energy

## A Comparison Study of Trace Metal Profiles of Biodiesel and Bioglycerol Produced From Heated and Unheated Canola Oil Using High Performance ICP-MS

Mirella Elkadi<sup>1\*</sup>, Rukayat Bojesomo, Abhijeet Raj, Mohamed Ibrahim and Sasi Stephen

<sup>1</sup> Department of Chemistry, College of Arts and Sciences, Khalifa University, P.O Box: 127788, Abu Dhabi, UAE

\*mirella.elkadi@ku.ac.ae

### Abstract:

The study determines the effect of the heating temperature of cooking oil on its trace metal content as well as on the biodiesel and bioglycerol produced from such oil. Additionally, the impact of the increase in free fatty acids (FFA) in oil on biodiesel yield because of the formation of soap and water is investigated, which requires acid pretreatment when an alkali catalyst is used. For optimum biodiesel yield from oils, a CCD-based RSM analysis and conventional single factor optimization are applied. Trace metal analysis is done utilizing ICP-MS, where Cu and Zn are found in high concentrations. The optimal conditions for the highest biodiesel yield are methanol to oil molar ratio of 12:1, a catalyst concentration of 1.0 wt. %, and a reaction time of 60 minutes. Thermal stress on canola oil was shown to have a significant influence on the yield of biodiesel and its trace metal levels.

### Introduction

The production of biodiesel from waste cooking oil has been of interest lately due to its availability and as a means of solving the disposal problems. This will also reduce the cost of biodiesel production, which has always been the major drawback to its commercialization. However, heating deteriorates the physicochemical properties of vegetable oil for both edible and biofuel uses. The high temperature used in frying creates changes in the physicochemical characteristics of the oil used. This has significant implications for human health as well as the potential use of heated vegetable oil for biodiesel generation [1]. Depending on the heating or frying temperature, the amount of FFA increases while the biodiesel conversion and yield decrease due to the formation of soap and water [2]. Some researchers have employed two-step methods; acid and base-catalyzed esterification and transesterification reactions [3, 4]. Heavy or trace metals are present in the oil feedstock (mainly from the soil) used in biodiesel production and can be transferred to the biodiesel that is produced. They are present in low concentrations, necessitating the use of sensitive methods such as ICP-MS because heavy or trace metal pollution is a serious environmental problem. The major objective of this study was to explore the relationship between operating parameters such as methanol to oil molar ratio, catalyst concentration, and reaction time in order to achieve a unique optimum single-step base-catalyzed transesterification condition for biodiesel production from canola oil heated at different temperatures. Also, the effect of heating temperature on the elemental content of the biodiesel was compared to that of oil feedstock.

### Effects of operating parameters on Biodiesel Yield

All transesterification reactions were carried out at a temperature below the boiling point of methanol (64.7 °C). This is to avoid methanol evaporation that can slow down the reaction and accelerate the saponification of glyceride by the alkali catalyst before the completion of the reaction [2, 4]. According to the statistical analysis results, the methanol to oil molar ratio and catalyst concentration are the most significant operating parameters affecting the biodiesel's percentage yield. The least significant parameter is the reaction time.

Similarly, three moles of alcohol (e.g., methanol) to one mole of oil (triglyceride) is required for transesterification to occur, yielding three moles of methyl ester (biodiesel) and one mole of bioglycerol (crude) as a waste [5]. The increase in the methanol to oil molar ratio from 3 to 12 molar ratio and catalyst concentration from 0.5 wt. % to 1 wt. % subsequently increases biodiesel yield as observed in the RSM and single factor optimization analysis. However, increasing the methanol to oil molar ratio above 12:1 and high catalyst concentration (above 1.0 wt. %) drastically decreases biodiesel yield from 96% to 80% for the biodiesel produced in all the studied cases. The higher molar ratio of methanol alters the separation of bioglycerol from biodiesel due to the high solubility factor. This could also result in the recombination of bioglycerol with monoglyceride (reverse transesterification reaction) [4].

Furthermore, high catalyst concentration leads to saponification reaction (soap formation), which in turn negatively affects the yield of biodiesel. A maximum biodiesel yield was attained at a reaction time of 60 minutes for both the RSM and single-factor analysis. This is similar to the results reported by Patil and Deng [4]. Above the reaction time of 60 minutes, the increase does not more or less influence the biodiesel yield, with a slight decrease in yield being noticed.

### Elemental analysis

Inductively coupled plasma mass spectrometry (ICP-MS) gives a valuable depiction of the integrative elemental concentrations in biofuels processed in a manner such that the total concentration of trace metals and elements in digested aqueous samples is obtained. The analyzed elements are categorized into three groups based on their present concentration: low-concentration, mid-concentration, and high-concentration. The low-concentration elements ranged from 0.44 ppb (Zr) to 602 ppb (Sr), the mid-concentration elements ranged from 94 ppb (Zr) to 2074 ppb (Rb), and the high-concentration elements ranged from 648 ppb (Cu) to 6834 ppb (Zn). Cs were not found in all the canola oil and biodiesel analyzed. In general, the concentration of the analyzed element levels



decreases by a factor of 100 or above as the frying temperature of the canola oil and the resulting biodiesel rises in most of the analyzed elements (Figure 1a).

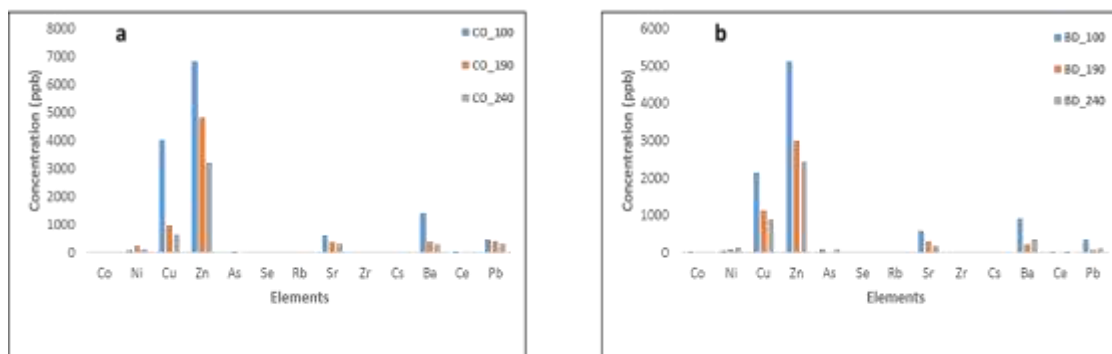


Figure 1: Profile for elements present in (a) canola oil, (b) biodiesel

## Conclusion

The optimum conditions for biodiesel production from both heated and unheated canola are methanol to oil molar ratio of 12:1, catalyst concentration of 1.0 wt. %, and reaction time of 60 minutes. The trace metal analysis reveals Cu and Zn as high-concentration metals and Pb, As, Se, and Zr, among others as low-concentration elements in both unheated and heated oil feedstock and their corresponding biodiesel produced. The innovation of this work doesn't only rely on optimization of the biodiesel yield produced from laboratory-prepared waste canola oil as a reference for public waste cooking or frying oil exposed to different temperatures (100 °C–240 °C) and their trace metal levels, but also the effects of the thermal stress on the trace metal levels of the oil samples and their respective biodiesel produced.

## Acknowledgements

The authors acknowledge the financial support from Khalifa University, UAE, through the CIRA-2020-106 project. The authors would also like to acknowledge Ahmed Nafees for his support on fuel analysis.

## References

1. A.M. Giuffrè, C. Zappia, and M. Capocasale, *Journal of the American Oil Chemists' Society*, **94**(6) 819 (2017).
2. H. Hamze, M. Akia, and F. Yazdani, *Process Safety and Environmental Protection*, **94** 1 (2015).
3. Sahar, et al., *Sustainable Cities and Society*, **41** 220-226 (2018).
4. P.D. Patil and S. Deng, *Fuel*, **88**(7)1302-1306 (2009).
5. M.A. Zahed et al., *Environmental Processes*, **5**(2) 303-312 (2018).

## Pretreatment of nitrogen-rich hydrothermal liquefaction biocrudes by demetallization: Recalcitrant effect of basic nitrogenates and metalloporphyrins

Muhammad Salman Haider<sup>1\*</sup>, Daniele Castello<sup>1</sup>, Thomas Helmer Pedersen<sup>1</sup>, and Lasse Rosendahl<sup>1</sup>

<sup>1</sup> Department of AAU Energy, Aalborg University, Aalborg, Denmark

\*mush@energy.aau.dk

Hydrothermal liquefaction (HTL) is a promising technology and yet, the most exciting scientific and engineering challenge to produce sustainable long haul transportation fuels. During HTL, wet/dry biomass with no lipid content restriction is converted into a high quality biocrude at temperatures between 300-420 °C and pressure above the saturation pressure of water. HTL biocrudes from *Spirulina* algae and sewage sludge were produced in a pilot scale continuous facility with a throughput of up to 100 L/h. Furthermore, high-pressure in line filters (~5 µm) were used for removal of inorganic compounds and mineral solids, from HTL product mixture containing the biocrude and the water by product. Despite its high quality, filtered HTL biocrude contains consistent amounts of inorganics (~0.1-0.4 wt.%) in the form of organometallics along with both basic and non-basic nitrogen containing compounds (NCCs). Therefore, the presence of high level of inorganic (~0.1-0.4 wt.%) in these biocrudes should be addressed, before carrying out catalytic hydrotreatment. The residual and detrimental effect of metals and basic NCCs in the fossil crude are well-established. These contaminants lead to the poisoning and deactivation of the bulk catalyst, leading to reactor plugging. Organometallics and hetero-cyclic NCCs may react at high temperatures with catalyst and form low melting eutectic compositions, which can either block catalytic active sites or sinter high-surface area catalyst support. These undesired pathways reduce catalyst activity and thus lead to high catalyst replacement cost. Moreover, these pathways could limit catalyst selection, process operation, and process development for biocrude upgrading. All these drawbacks suggest addressing the removal of organometallics before catalytic hydrotreatment. The aim of this work is to build knowledge around the demetallization of HTL biocrude by using different acids, and to understand the effect of both basic and non-basic NCCs during the demetallization of highly nitrogenous HTL biocrudes i.e., sludge (~ 4 wt.% N) and *Spirulina* (~ 8 wt.% N). This work will rationalize the importance of demetallization and point out the challenges in the presence of basic and non-basic NCCs.

In this study, an original methodology was explored by using six different organic and inorganic acids (0.1-0.5 M) for the removal of metals from highly nitrogenous HTL biocrudes. After demetallization, the biocrude and extracted acids were characterized through Fourier-transform ion cyclotron resonance mass spectrometry (FT-ICR MS), Inductively coupled plasma optical emission spectroscopy (ICP-OES), ash analysis, elemental analyzer (CHN/O), higher heating value (HHV), GC-MS, total organic carbon (TOC) and total nitrogen (TN).

Acid-washing with 0.1-0.5 M H<sub>2</sub>SO<sub>4</sub> shows drastic reduction of metals (~85 wt.%) from sludge biocrude (~0.07 wt. % to ~0.01 wt.% of inorganics). However, no sign of demetallization was observed in case of *Spirulina* biocrude (contains 0.17 wt.% of inorganics). Further investigation of these biocrudes through GC-MS revealed that the sludge biocrude contains non basic NCCs while, *Spirulina* biocrude mostly contains basic NCCs. FT-ICR MS of *Spirulina* biocrude shows the presence of iron-porphyrins structures. GC MS of extracted water phase after the demetallization of *Spirulina* biocrude indicates the presence of organic salts of basic NCCs. This means, that the demetallization of *Spirulina* biocrude in the presence of acids and basic NCCs underwent undesired protonation because of their high basicity during acid base reaction. Overall, this work rationalizes the importance of demetallization and point out the challenges in the presence of heteroatom N. Finally, this work also proposes the possible layout of the process integration of demetallization at continuous HTL plant.

### Acknowledgements

This work has received funding from European Union's Horizon 2020 research and innovation program under grant no. 818413 (NextGenRoadFuel) and Lowcarbfuels.dk a Danish funded project.

## Hydrodeoxygenation of oleic acid over Ni catalysts supported on Beta zeolite

Georgios Iakovou<sup>1</sup>, Antigoni Margellou<sup>1</sup>, Konstantinos Triantafyllidis<sup>1,2,\*</sup>

<sup>1</sup>Department of Chemistry, Aristotle University of Thessaloniki, Thessaloniki, Greece

<sup>2</sup>Center for Interdisciplinary Research and Innovation (CIRI), AUTH, 57001 Thessaloniki, Greece

\*[ktrianta@chem.auth.gr](mailto:ktrianta@chem.auth.gr)

The global need for greenhouse gases reduction and the in tandem trend for carbon neutrality, has brought on an increased interest in the production and consumption of environmentally sustainable fuels. Edible oils of crops were used in the production of first generation biofuels by means of esterification and transesterification<sup>1</sup>. Second generation biofuels improved the sustainability factor of the fuels by utilizing thermo-chemical or biochemical processing of lignocellulosic biomass and hydrotreatment of vegetable oils, waste cooking oils or animal fats, producing green-fuels directly or by providing platform compounds (bio-crudes) for further processing<sup>2,3</sup>. Algae is a feedstock which shows high potential for green-fuel production due to its high lipid content and has attracted wide global acceptance as energy resource<sup>4</sup>. The hydrodeoxygenation (HDO) process in algae shows a potential yield of liquid hydrocarbons of up to 60% depending on reaction conditions, reactor design the quality of the feedstock and the selected catalyst<sup>5</sup> and has brought on the development of third and fourth generation of biofuels. During biomass-derived fragments or lipid HDO, reactions like hydrogenation, hydrogenolysis, decarbonylation, decarboxylation and dehydration take place, depending in great part on the selected catalyst and the reaction conditions. The most employed catalysts in the HDO process are the common sulfided Ni/Mo or Co/Mo catalysts, (noble-)metal catalysts on various supports such as metal oxides like Al<sub>2</sub>O<sub>3</sub> and Ce<sub>0.6</sub>Zr<sub>0.4</sub>O<sub>2</sub> or zeolites like ZSM-5, H-Beta etc. In addition to the hydrogenation efficiency of the metal, the active sites of the catalyst support play a defining role in the HDO affecting conversion, selectivity and reaction rate. Aiming at cost-reduction, non-noble metal catalysts have gained momentum in recent studies and Ni-based catalysts have been found to give better performance than many noble-metal catalysts<sup>1</sup>. In this work, we investigated the HDO of oleic acid as a model compound using a custom-made Ni/Beta catalyst. Oleic acid is a C18 monounsaturated fatty acid which exists in various animal and vegetable fats and oils and this study aims to identify specific parameters (solvent, temperature, pressure, time) that promote each individual reaction type (hydrogenation, decarbonylation etc.) in order to utilize the results in the study of bio-fuel production from algae.

A custom catalyst has been produced by the method of dry impregnation of an H-Beta zeolite (Si/Al=12.5) with Ni(NO<sub>3</sub>)<sub>2</sub>·6H<sub>2</sub>O aiming to final metal content of 10 wt.%. After the impregnation the catalyst was dried, heat treated at 500°C and reduced with H<sub>2</sub> at 450°C. The catalyst was characterized by X-ray diffraction (XRD) to determine the nickel crystalline phases (and zeolites), by N<sub>2</sub> porosimetry at -96°C to determine the micro/mesoporous characteristics, by FT-IR with in situ pyridine sorption to determine the Brønsted and Lewis acid sites and by x-ray photoelectron spectroscopy (XPS) to determine the oxidation state of nickel and the surface composition of the catalyst.

Catalytic HDO experiments of the oleic acid were carried out in an autoclave high-pressure stirred batch reactor. Hydrogen pressure was set at 50 bar (at room temperature) while commencing each experiment. Temperatures of 220°C and 250°C were studied and reaction time of 60min and 90min. The solvents used were Hexane (supercritical at 250°C), Octane, Dodecane and Hexadecane. Analysis of the products by GC-MS showed that the reaction at a temperature of 250 °C promotes the conversion of oleic acid to aliphatic alkanes and their isomers in the range of hydrocarbons/fuels (gasoline, kerosene, diesel; C5-C16), in percentages of 74-86%. The production of alkanes shows a relative reduction depending on the chain size of the solvent as the use of hexane yields a liquid product with 86% content in alkanes, the use of octane 80% and dodecane 74% at the temperature of 250 °C. The decrease of the concentration of alkanes goes in tandem with a high concentration of acids and esters (methyl-, ethyl-) of stearic acid (C18) which derive from oleic acid after hydrogenation of its double bond and subsequent esterification. Increasing the reaction time to 90 min appears to promote deoxygenation and alkane production with further conversion of stearic acid (decrease from 16% at 60 min to 7% at 90 min, in octane). A graphical summary of the concentration of the liquid products at the above different reaction and solvent conditions is given in Figure 1.

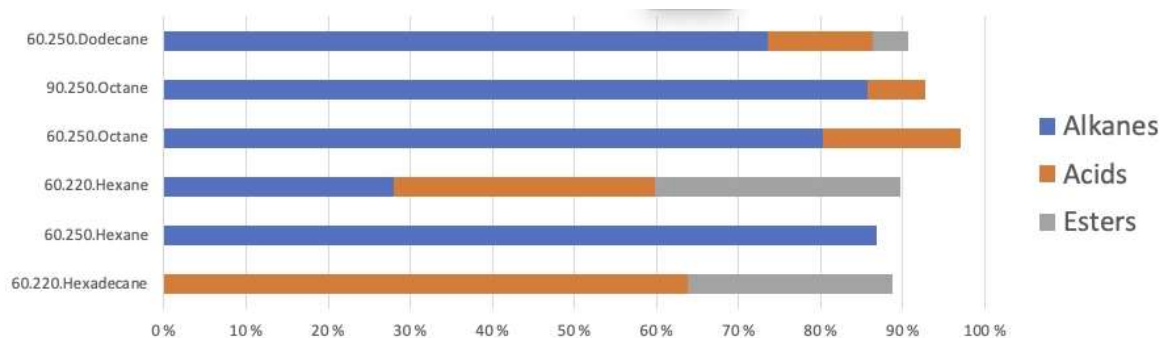


Figure 34. Relative concentrations (GC-MS) of liquid products in the hydrodeoxygenation of oleic acid over 10%Ni/Beta catalyst, at 50 bar H<sub>2</sub> and varying different time and temperature conditions

### Acknowledgements

This research has been co-financed by the European Regional Development Fund of the European Union and Greek national funds through the Operational Program Competitiveness, Entrepreneurship and Innovation (EPAnEK 2014-2020), under the Action “RESEARCH – CREATE – INNOVATE” B’ CALL (ALGAFUELS project, code: T2EDK-00041).

### References

- (1) Hongloi, N.; Prapainainar, P.; Prapainainar, C. Review of Green Diesel Production from Fatty Acid Deoxygenation over Ni-Based Catalysts. *Molecular Catalysis* **2022**, *523*, 111696. <https://doi.org/10.1016/j.mcat.2021.111696>.
- (2) Naik, S. N.; Goud, V. V.; Rout, P. K.; Dalai, A. K. Production of First and Second Generation Biofuels: A Comprehensive Review. *Renewable and Sustainable Energy Reviews* **2010**, *14* (2), 578–597. <https://doi.org/10.1016/j.rser.2009.10.003>.
- (3) Dimitriadis, A.; Natsios, I.; Dimaratos, A.; Katsaounis, D.; Samaras, Z.; Bezergianni, S.; Lehto, K. Evaluation of a Hydrotreated Vegetable Oil (HVO) and Effects on Emissions of a Passenger Car Diesel Engine. *Frontiers in Mechanical Engineering* **2018**, *4*.
- (4) Galadima, A.; Muraza, O. Biodiesel Production from Algae by Using Heterogeneous Catalysts: A Critical Review. *Energy* **2014**, *78*, 72–83. <https://doi.org/10.1016/j.energy.2014.06.018>.
- (5) Brown, R. C. *Thermochemical Processing of Biomass: Conversion into Fuels, Chemicals and Power*; John Wiley & Sons, 2019.

## Bio-based production of hydrogen and CO<sub>2</sub> utilization

Mariamichela Lanzilli<sup>1,\*</sup>, Nunzia Esercizio<sup>1</sup>, Simone Landi<sup>2</sup>, Genoveffa Nuzzo<sup>1</sup>, Carmela Gallo<sup>1</sup>,  
Emiliano Manzo<sup>1</sup>, Angelo Fontana<sup>1,2</sup> and Giuliana d'Ippolito<sup>1</sup>

<sup>1</sup>Institute of Biomolecular Chemistry CNR, Via Campi Flegrei 34, 80078, Pozzuoli, Napoli, Italy.

<sup>2</sup> Department of Biology, University of Naples "Federico II", Via Cinthia, I-80126 Napoli, Italy.

\*e-mail address \*m.lanzilli@icb.cnr.it

### Abstract

Bio-based processes can make the economy more sustainable and lower its dependence on fossil fuels, converting low cost renewable feedstocks and CO<sub>2</sub> into valuable bio-products with the help of microorganisms in bioreactors. *Thermotoga neapolitana* is a marine anaerobic bacterium with an optimal growth temperature of 80°C, suitable for conversion of from sugar-based waste and renewable feedstocks into hydrogen with yields close to theoretical values<sup>1,2</sup>. The fermentation process has shown general robustness, reproducibility and consistency and a low risk of contamination because of the hyperthermophilic conditions. We have recently reported in *T. neapolitana* an unprecedented pathway involved in the recycling of CO<sub>2</sub> through the coupling of acetate and carbon dioxide and the concomitant production of L-lactic acid (95% e.e), without affecting hydrogen production<sup>3,4</sup>. This patented process, called Caphnophilic (CO<sub>2</sub>-requiring) Lactic Fermentation (CLF) may become the cornerstone for economically attractive biotechnological applications based on Carbon Capture Utilization (CCU). In this contribution, we present activities and latest results related to the biochemical cross-talking and metabolic engineering of the pathways related to hydrogen and lactic acid production<sup>5,6,7</sup>. These are crucial aspects to further improve rate and yield of the process for guaranteeing its sustainability.

### References

1. G. d'Ippolito, L. Dipasquale, F. M. Vella, I. Romano, A. Gambacorta, A. Cutignano, A. Fontana. *International Journal of Hydrogen Energy*, **35**, 6 (2010)
2. M. Lanzilli, N. Esercizio, G. Nuzzo, C. Gallo, E. Manzo, A. Fontana and G. d'Ippolito, *International Journal of Molecular Science* **22**, 1: 341 (2021).
3. G. d'Ippolito, L. Dipasquale, A. Fontana, *ChemSusChem*, **7** (9), 2678-2683 (2014).
4. Pradhan N., d'Ippolito G., Dipasquale L., Esposito G., Panico A., Lens P., Fontana A., *Bioresource Technology*, **332**, 125127 (2021).
5. G. d'Ippolito, S. Landi, N. Esercizio, M. Lanzilli, M. Vastano, L. Dipasquale, N. Pradhan, A. Fontana, *Frontiers in Microbiology*, **11**, 171, (2020).
6. N. Esercizio, M. Lanzilli, M. Vastano, Z. Xu, S. Landi, L. Caso, C. Gallo, G. Nuzzo, E. Manzo, A. Fontana and G. d'Ippolito, *Microorganisms*, **9** (8), 1688 (2021).
7. G. d'Ippolito et al., *International Journal of Molecular Science*, *submitted* (2022).

## Spent coffee grounds conversion to bio-crude oil via hydrothermal liquefaction

D. Liakos<sup>1,2</sup>, K. Triantafyllidis<sup>2</sup>, L. Chrysikou<sup>1</sup>, N. Tourlakidis<sup>1</sup>, V.M. Vasdekis<sup>1</sup>, S. Bezergianni<sup>1\*</sup>

<sup>1</sup>Centre for Research & Technology Hellas (CERTH), Chemical Process & Energy Resources Institute (CPERI), Thessaloniki, 6km Charilaou-Thermi, 57001, Greece

<sup>2</sup>Aristotle University of Thessaloniki (AUTH), Department of Chemistry, University Campus, 54124 Thessaloniki, Greece

\* [sbezerg@certh.gr](mailto:sbezerg@certh.gr)

Energy and transportation fuels increased demand, along with the new European regulations, have raised the need to exploit new resources for fuel production. Second generation biofuels will play a major role in coverage of these needs, as they are generated from residues and wastes, and thus appear as very promising candidates for green energy generation[1]. Residual biomass conversion into liquid biofuel intermediates can be accomplished through two main thermochemical processes, pyrolysis, and hydrothermal liquefaction (HTL)[1]. HTL has numerous advantages over pyrolysis such as the absence of the costly drying step of the feedstock before the reactions, the catalytic behaviour of solvent in HTL, and the boosted oil yield and properties. Also, HTL can convert a wide variety of materials, including municipal wastes, algae, forest, and agricultural residues, which are available in decent quantities[1]. Coffee is a largely traded and consumed good. The annual consumption of coffee is estimated at 10 million tonnes (in the last five years), as stated by the international coffee organization[2]. Coffee is a lignocellulosic material and therefore, coffee-derived wastes appear as a sustainable residual feedstock. Thus, exploiting spent coffee grounds via HTL appear as a very promising pathway in the biofuel production chain.

In the present study, spent coffee grounds, in raw and pre-treated (stated as de-oiled coffee) form, were converted to bio-crude oil via HTL. The pre-treatment step of spent coffee grounds included the removal of lipids, antioxidants, and some proteins from the raw feedstock. Coffee is a lignocellulosic material, meaning its structure is consisted of cellulose, hemicellulose, and lignin at most. The structural analysis of the pre-treated biomass is presented in *Table 2*. The aim of the study was to assess the potential production of bio-crude oil via HTL and find the optimal conditions to achieve maximum oil yield. The solvent used in the process was deionized water, while the conditions investigated included temperature (three different sets of temperature 280°- 300°- 320°C) and residence time (15 and 30 min). No catalyst was used during the study, the initial pressure of the reactor was constant at 30 bar and the solid-to-liquid ratio was 1/10 in all sets of conditions. Each set of conditions was applied twice to ensure higher accuracy of the results.

*Table 6: Results of pretreated spent coffee grounds structural analysis*

	<i>Pre-treated spent coffee grounds</i>
<i>Ash (wt%)</i>	1.94
<i>Proteins (wt%)</i>	15.24
<i>Cellulose (wt%)</i>	12.10
<i>Hemicellulose (wt%)</i>	33.53
<i>Lignin (wt%)</i>	31.81

The experiments were conducted in a bench top, high-pressure stirred batch reactor with internal vessel volume of 250 mL (Parr 4576A). The reactor is coupled with a J type thermowell for heating and a U-type cooling coil for rapid temperature drop. During a typical experiment, the vessel was loaded with 10g of feedstock (raw or pre-treated) and 100 mL of deionized water (to set the solid to liquid ratio to 1/10). Then, the reactor was sealed and purged 3 times with nitrogen to remove air (absence of oxygen during the reactions). Finally, the reactor inlets were compressed to 30 bar with nitrogen as compression gas (to keep the water in liquid state during heat up), then heated and kept to the desired temperature according to the set of conditions, before finally cooling to room temperature.

The products of HTL process include solid, liquid and gas streams. Upon decompression of the reactor, a gas product sample was collected in a sample bag and analyzed via GC-FID. The collection of the products after the reactor cooldown was initiated with vacuum filtration of the slurry mix in a Buchner funnel with filter paper. The collected liquid from the flask was the aqueous phase product, and it contained the aquatic solvent and some dissolved organic compounds. Then, the remaining filter cake in the filter paper was washed with 250 – 300 mL of acetone to separate bio-crude oil from solids (hydro-char) and collected it in the flask. The solids were dried in an oven at 105°C overnight and weighted, while the acetone was completely removed in a rotary evaporator at 40°C under reduced pressure to collect the final bio-crude oil product.

While the study is still ongoing, there are some basic results regarding the HTL of pretreated coffee. According to literature, temperature directly affects the liquefaction of biomass as lignin chains start to decompose at 280°C, while on the other hand cellulose and hemicellulose start decomposing in milder conditions (lower

temperature)[3]. Yang et al. studied the effect of temperature and residence time in HTL of raw spent coffee grounds. In the range of 200° – 300°C they noticed an increment in oil yield as the temperature rose to 275°C. At higher temperatures (300°C) they found a lower yield with higher proportions of aqueous and gas products[4]. They justified these results based on the secondary decomposition reactions in more severe conditions which lead to gas and solids formation from liquified organic compounds[4].

In this study though, the bio-crude oil yield increased along with the reaction temperature even at 320°C as presented in *Figure 35*. As the main parameter affecting the optimal temperature is the feedstock structure, raw and pretreated coffee differ in lipid and extractives content. These components are easier to liquefy at mild conditions and therefore lead to higher oil yield at lower temperature. Nevertheless, pretreated coffee grounds consist only of the structural materials such as cellulose, hemicellulose, lignin, and some proteins. Cellulose and hemicellulose require mild conditions to liquefy but most of the products are located at the aqueous phase. So, in this case, the liquid yield is strongly depended on the lignin liquefaction which require severe conditions (over 280°C). With approximately 30 %wt. of structural lignin, high temperature is essential to get most of lignin chains in oil product (22.3%wt. at 320°C). These findings are also confirmed by the reduction of the solids at higher temperatures.

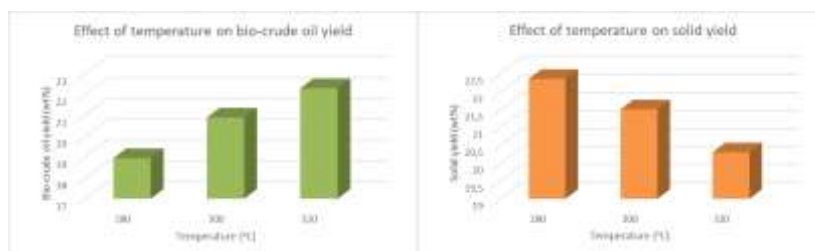


Figure 35: Effect of reaction temperature on bio-crude oil yield

Apart from, the liquid and solid products analysis, this study also focused on distribution of molecules in gas products which is innovative as in most studies the gas is accounted as 100% CO<sub>2</sub>. According to *Table 7*, CO<sub>2</sub> is indeed the main gas product based on decarbonylation and Boudouard reactions, but there are also some other light hydrocarbons present. The secondary decomposition reactions produce ethane (~0.1 v/v%), C<sub>6</sub><sup>+</sup> (~0.2 v/v%) and more importantly methane at significant proportions (~7 v/v%), which confirms that secondary decomposition of biomass is causing loss of useful hydrocarbons in gas.

Table 7: Composition of gas product in HTL of pre-treated spent coffee grounds

Gas molecule	Concentration (v/v%)
Carbon dioxide (CO <sub>2</sub> )	91.0 – 93.0
Hydrocarbons with 6 or more carbon atoms	0.1 – 0.3
Ethane (C <sub>2</sub> H <sub>6</sub> )	0 – 0.12
Methane (CH <sub>4</sub> )	6.5 – 7.3
Hydrogen (H)	0 – 0.5

## Acknowledgements

This research has been co-financed by the European Union and Greek national funds through the Operational Program Competitiveness, Entrepreneurship, and Innovation, under the call RESEARCH – CREATE – INNOVATE (project code: “Brew2Bio”).

## References

- [1] Dimitriadis A, Bezergianni S. Hydrothermal liquefaction of various biomass and waste feedstocks for biocrude production: A state of the art review. *Renewable and Sustainable Energy Reviews* 2017;68:113–25. <https://doi.org/10.1016/j.rser.2016.09.120>.
- [2] International Coffee Organization n.d. <https://www.ico.org/prices/new-consumption-table.pdf> (accessed February 23, 2022).
- [3] Seehar TH, Toor SS, Shah AA, Pedersen TH, Rosendahl LA. Biocrude production from wheat straw at sub and supercritical hydrothermal liquefaction. *Energies (Basel)* 2020;13. <https://doi.org/10.3390/en13123114>.
- [4] Yang L, Nazari L, Yuan Z, Corscadden K, Xu CC, He QS. Hydrothermal liquefaction of spent coffee grounds in water medium for bio-oil production. *Biomass and Bioenergy* 2016;86:191–8. <https://doi.org/10.1016/j.biombioe.2016.02.005>.

## The effect of kaolin and hectorite clay on the Fischer-Tropsch synthesis condensed hydrocarbon products

Agija Stanke<sup>1\*</sup>

<sup>1</sup>Riga Technical University, Institute of Applied Chemistry, Paula Valdena 3, Riga, LV-1048, Latvia

\*agija.stanke@gmail.com

Human emissions of GHG are primary driver of climate change and global warming. Amongst different human activities, transportation makes the largest contribution to the GHG emissions [1]. Liquid hydrocarbon fuels produced from fossil resources are widely used, but environmental problems and the depletion of oil resources are forcing the search for alternative fuels [2]. Fischer-Tropsch synthesis (FTS) provides an opportunity to produce liquid fuels such as gasoline (C<sub>5</sub>–C<sub>11</sub>), and diesel (C<sub>12</sub>–C<sub>20</sub>) from synthesis gas (CO + H<sub>2</sub>). What makes this process attractive is that synthesis gas can be obtained not only from natural gas and coal, but also from alternative and renewable feedstock, such as biomass, and organic, and plastic waste [3].

A wide range of products is usually obtained in the synthesis of FTS, so the control of selectivity is particularly important. It is known, that the FTS product selectivity can be strongly influenced by changing the catalyst parameters, such as physical properties, structure, and composition [4]. In addition, industrial catalysts may differ from those developed in the laboratory. The preparation of technical catalysts (catalysts for industrial scale use) involves structuring of powders with additives into mm-sized bodies. Additives used can influence catalyst in different ways, and thus can influence catalyst performance [5]. Therefore, it is important to investigate the influence of different additives.

Clays are often used as catalyst binders, fillers, and modifiers [5]. In this study, two natural clays – kaolin and hectorite – were used as binders to make Fischer-Tropsch synthesis catalyst granules, and the effect of clays on the condensed hydrocarbon products of FTS was investigated. The synthesis method as well as structural and textural characteristics of a powdered iron based catalyst with the Fe<sub>2</sub>O<sub>3</sub> phase supported on SBA-15 have been published previously [6]. Catalyst granules were made by extruding wet mixture of catalyst powder and clay (2:1 wt%) through syringe needle. After extrusion catalyst granules were dried and calcined in air at 550 °C for 5 h with a 1 °C/min temperature ramping. Depending on the clay used as the binder, the catalyst granules were named Kaolin-Fe<sub>2</sub>O<sub>3</sub>/SBA-15, and Hectorite-Fe<sub>2</sub>O<sub>3</sub>/SBA-15, respectively.

The prepared granules were loaded in the commercial customized micro-activity reactor (*Microactivity-Effi, PID Eng&Tech S.L.*). After catalyst activation *in-situ* at 350 °C using CO, FTS was performed at 280 °C, 20 bar (gauge) using gas mixture consisting of H<sub>2</sub>:CO:N<sub>2</sub> = 4:2:1 with GHSV = 6000 NmL/g<sub>cat</sub>·h. The reaction effluent passed through a series of hot and cold trap to condense products. After 50 h on stream (when a steady state was reached), liquid hydrocarbon products were collected for a period of 24 h and used for the analysis. At this time on stream, CO conversion was approximately 50% for Kaolin-Fe<sub>2</sub>O<sub>3</sub>/SBA-15 and approximately 40% for Hectorite-Fe<sub>2</sub>O<sub>3</sub>/SBA-15 catalyst.

Condensed reaction products were analyzed off-line using Shimadzu Nexis GC-2030 gas chromatograph (GC) equipped with Restek Rtx®-5MS column (30 m, 0.25 mmID, 0.1 μm), flame ionization detector (FID), and Shimadzu GCMS-QP2020 NX mass spectrometer (MS).

Product distribution (fractions of hydrocarbons with *n* carbon atoms in a chain) were calculated from FID chromatograms as:  $y_n = \frac{\sum X_n}{\sum X_{HC}} \cdot 100\%$

where  $\sum X_n$  is the sum of peak areas of hydrocarbons with *n* carbon atoms in a chain, and  $\sum X_{HC}$  is the sum of all hydrocarbon peak areas present.

Average hydrocarbon chain length  $C_a$  was calculated as:  $C_a = \frac{\sum n \cdot X_n}{\sum X_{HC}}$ .

The results showed that clay used as a binder affected liquid hydrocarbon product distribution (Figure 1), and composition (Figure 2). Calculated average liquid hydrocarbon chain length for products obtained using Kaolin-Fe<sub>2</sub>O<sub>3</sub>/SBA-15 was 9.7, whereas for Hectorite-Fe<sub>2</sub>O<sub>3</sub>/SBA-15 catalyst it was 10.2. Liquid hydrocarbon products can be divided into 3 parts relatively corresponding to gasoline range (C<sub>5</sub>–C<sub>11</sub>), diesel range (C<sub>12</sub>–C<sub>20</sub>), and heavier (C<sub>21+</sub>) hydrocarbons. Most of the products were gasoline range (i.e., 76% for Kaolin-Fe<sub>2</sub>O<sub>3</sub>/SBA-15, and 72% for Hectorite-Fe<sub>2</sub>O<sub>3</sub>/SBA-15).



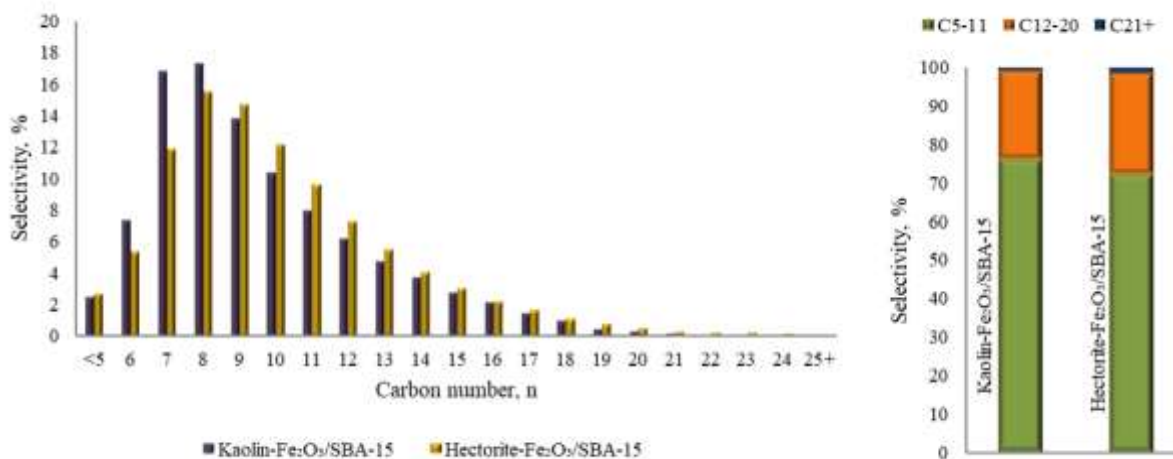


Figure 1. The influence of clay used as catalyst granule binder on the liquid hydrocarbon phase product distribution (GC-FID/MS analysis)

In the GC-MS/FID chromatogram in the C<sub>6</sub>-C<sub>14</sub> range, it was possible to differentiate n-paraffin, 1-olefin, 2-olefin, and n-alcohol peaks and thus it was possible to obtain detailed information on the composition of the area. Kaolin contributed to the formation of branched hydrocarbons and internal olefins, whereas hectorite contributed to the formation of n-paraffins.

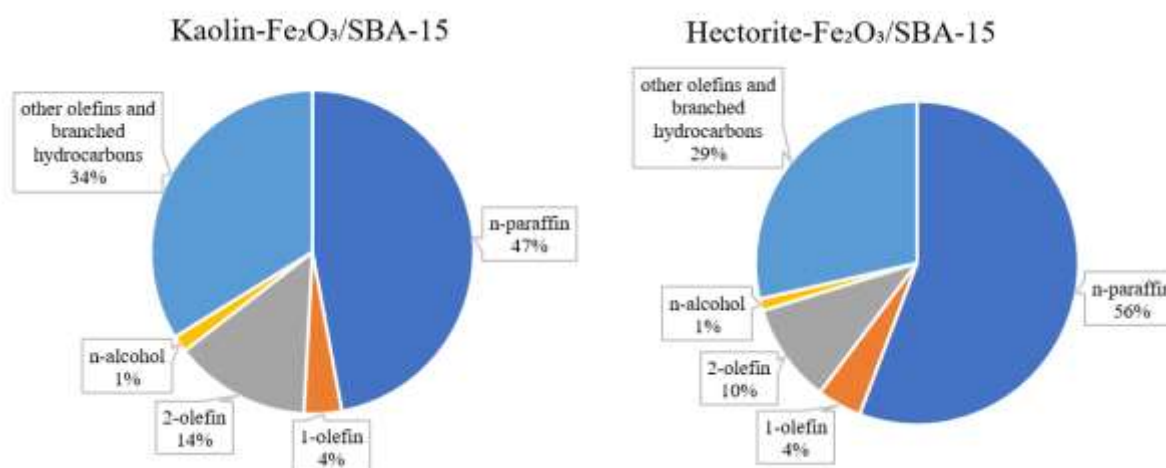


Figure 2. The influence of clay used as catalyst granule binder on the composition of the C<sub>6</sub>-C<sub>14</sub> liquid hydrocarbon phase products (GC-FID/MS analysis)

## Acknowledgements

This work has been supported by the European Social Fund within the Project No 8.2.2.0/20/I/008 «Strengthening of PhD students and academic personnel of Riga Technical University and BA School of Business and Finance in the strategic fields of specialization» of the Specific Objective 8.2.2 «To Strengthen Academic Staff of Higher Education Institutions in Strategic Specialization Areas» of the Operational Programme «Growth and Employment». This research/publication was supported by Riga Technical University's Doctoral Grant programme.

## References

1. Y. Kazancoglu, M. Ozbiltekin-Pala, Y.D. Ozkan-Ozen, *Sustain. Cities Soc.*, **70** 102924 (2021).
2. S.S. Ail, S. Dasappa, *Renew. Sustain. Energy Rev.* **58** 267–286 (2016).
3. H. Mahmoudi, M. Mahmoudi, O. Doustdar, H. Jahangiri, *Biofuels Eng.*, **2** 11–31 (2017).
4. C. Liu, Y. Chen, Y. Zhao, S. Lyu, L. Wei, X. Li, Y. Zhang, *Fuel*, **263** 116619 (2020).
5. S. Mitchell, N.L. Michels, J. Pérez-Ramírez, *Chem. Soc. Rev.*, **42** 6094–6112 (2013).
6. A. Stanke, V. Kampars, O.A. Lazar, M. Enachescu, *Key Eng. Mater.*, **850** 144–150 (2020).

## Photochemical dimerization of volatile conjugated dienes produced photobiologically

Sindhujaa Vajravel, Anup Rana, Leandro Cid Gomes, Henrik Ottosson\*

Department of Chemistry –Ångström Laboratory, Uppsala University, Box 523, 751 20, Uppsala, Sweden

\*e-mail address of the corresponding author: henrik.ottosson@kemi.uu.se

### Abstract text:

Catalyzed oligomerization of fossil-based alkenes into commercial fuels and other chemicals is nowadays routine (1), however, these production processes, apart from not using renewable resources, often involve high temperatures and pressures. Processes that run at ambient temperature and pressure should be more desirable in terms of the energy economy. On the other hand, most biofuels are derived from vegetable oils, sugar, and biomass, sources which also are not sustainable in the long term. Here, we report on the development of fourth-generation biofuel that can help mitigate global warming by utilizing CO<sub>2</sub> and sunlight as, respectively, carbon and energy sources (2). We focused on the photobiological production of volatile hydrocarbons (*e.g.* bioisoprene) from cyanobacteria which at a subsequent step photochemically dimerized into dimers with useful jet fuel properties. A high yield of photosensitized dimerization of isoprene was achieved with di(naphth-1-yl)methanone as a photosensitizer, and the hydrogenated dimers can be utilized as drop-in jet fuels (3). Now we have also investigated the sensitized photodimerization of a series of other dienes using di(naphth-1-yl)methanone. Besides isoprene, the conjugated dienes included are 2,3-dimethyl-1,3-butadiene, penta-1,3-diene, 2,4-hexadiene, cyclohexa-1,3-diene and 1,3-butadiene. Our results show that the highest yield of dimers was obtained from cyclohexa-1,3-diene while the lowest resulted from 2,4-hexadiene and 1,3-butadiene upon irradiation with 365 nm light. The relationship between the photodimerization yield and the structure, substitution, and steric hindrance of the diene will be discussed.

### Acknowledgements

We greatly acknowledge the Swedish Energy Agency for financial support of the present project through grants 44728-1 and 52576-1.

### References

1. C. T. O'Connor and M. Kojima, *Catalysis today*, **6(3)** 329-349 (1990).
2. B. Abdullah, S. A. F. A. S. Muhammad, Z. Shokravi, S. Ismail, K. A. Kassim, A. N. Mahmood, M. M. A. Aziz, *Renewable and sustainable energy reviews*, **107** 37-50 (2019).
3. A. Rana, L.C. Gomes, J. Rodrigues, H. Arrou-Vignod, J.Sjölander, N.P.Vedin, O. El Bakouri, K. Stensjö, P. Lindblad, L. Andersson, and M. Berglund, (2022).

Biomass derived platform & fine  
chemicals, pharmaceuticals, monomers,  
polymers, materials

## Lignin model compounds hydrogenolysis over base metal catalysts

Raphaël Abolivier\* and James A. Sullivan  
 UDC School of Chemistry, Belfield, Dublin 4, Ireland  
 \*raphael.abolivier@ucd.connect.ie

### Introduction

Lignin valorization is a crucial step in the development of efficient and economically valuable biorefineries. Lignin is a complex heterogeneous and robust bio-polymer present within lignocellulosic materials, the backbone of all plants. Lignin's structure is based on three phenol-like building blocks (coumaryl alcohol, coniferyl alcohol and sinapyl alcohol) randomly linked through either ether or carbon-carbon bonds (so-called "linkages").

The cost-effective generation of platform chemicals (*i.e.* feedstocks for the chemical, pharmaceutical and polymer industries generated from biomass) will be a crucial step for the future of the chemical industry. These compounds are expected to partially replace certain feedstocks currently obtained from petroleum-refining processes (unsustainably) [1]. Such molecules could also lead to the emergence of new applications (*e.g.* the synthesis of new active drugs or new thermo-plastics) [2].

Lignin valorization through depolymerization can be performed using different approaches. This project focuses on the heterogeneously-catalyzed hydrogenolysis pathway specifically targeting a class of linkage. This was selected aiming at the conservation of the phenolic backbone of the lignin building blocks within the obtained products and has the potential advantage of catalyst recycling.

A commonly used method to simplify such studies is the use of model compounds as substrates [3]. These are small molecules that contain lignin's most common linkages. The use of these enables the generation of reproducible results which in turn can give insights on lignin-related chemistry.

Within this poster we show the hydrogenolysis of lignin analogues using supported earth-abundant and inexpensive (transition) metal catalysts. The move from the use of critical noble metal catalysts to the use of plentiful transition metal catalysts is one of the major challenges in the field of heterogeneous catalysis and sustainable chemistry in general and is addressed in this project.

### Experimental

A set of nickel (Ni) loaded ZSM-5 catalysts (5 %, 10% and 20 %) have been synthesized through a hydrothermal method (IWI). The catalysts were then reduced in a 3% H<sub>2</sub>/Ar atmosphere for 3 hours at 500 °C. These have been characterized and applied in the hydrogenolysis of lignin model compounds. A comparative study of the effects of different metal catalysts was performed by studying the reactivity of cobalt- and copper-based catalysts at similar metal loadings under similar reaction conditions.

The selected model compounds for this study are diphenyl ether (which contains a 4-O-5 linkage) and 2-Phenylethyl phenyl ether (which contains a β-O-4 linkage) (see Fig. 1).

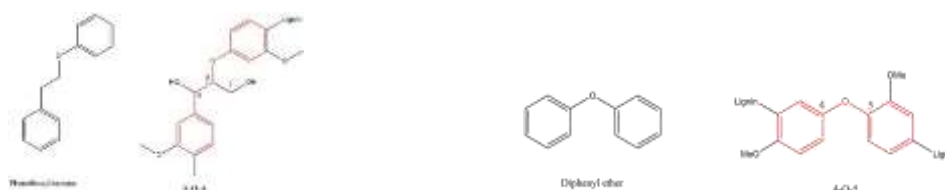


Figure 1. Lignin model compounds, 2-phenylethyl phenyl ether (left) and diphenyl ether (right).

One of the limitations of studies using model compounds is the presence, in native lignin, of different substituents on the carbons surrounding the target ether bond. To address this problem, different model compounds with a range of substituents on the C<sub>α</sub> of the β-O-4 substrate have been studied here (see Fig. 2).

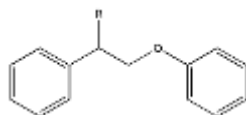


Figure 2. Range of studied model compounds for the b-O-4 linkage (R = H or O or OH).

The generated products were analyzed by Gas Chromatography (GC) and Gas Chromatography-Mass Spectroscopy (GC-MS) for quantitative and qualitative purposes, respectively.

The synthesized catalysts were characterized using: X-ray Diffraction, Scanning Electron Microscopy, Transmission Electron Microscopy, X-ray Photoelectron Spectroscopy and  $N_2$  physisorption.

The reaction conversions and selectivities (towards aromatics and alcohols) were selected as comparable parameters for the assessment of the efficiency of each of the catalysts.

The reactions were performed (in isopropanol) in a stirred, high pressure, Parr reactor under a hydrogen atmosphere (5-10 bar), in a temperature range between 250 °C and 300 °C.

## Results

Preliminary characterization results are shown below.

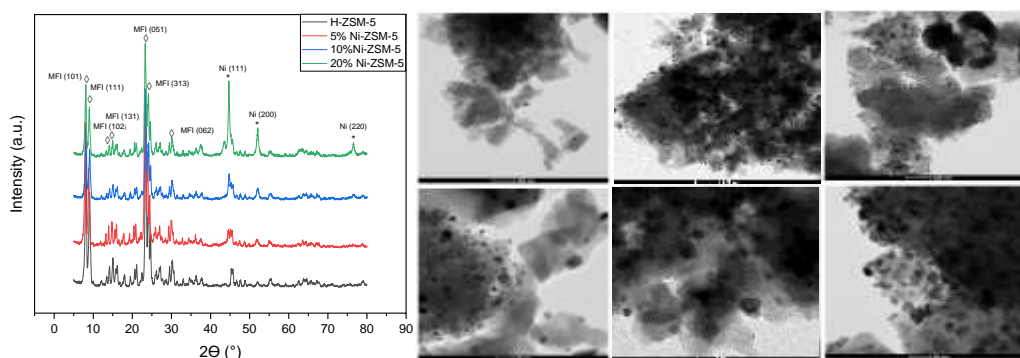


Figure 3. XRD patterns of H-ZSM-5; 5%-; 10%- and 20%-Ni-ZSM-5 (left). TEM images of 5%- (left); 10%- (middle) and 20%-Ni-ZSM-5 (right) at 200 nm scale (top) and 50 nm scale (bottom) (right).

XRD confirms the retention of both the zeolite support structure and the deposition of Ni particles. Typical diffraction peaks of an MFI framework (such as ZSM-5) were observed at  $2\theta$  of 8.07°; 9.02°; 13.98°; 14.97°; 23.29°; 24.05° and 30.28° assigned to the lattice planes of (101); (111); (102); (131); (051); (313) and (062), respectively. The diffraction lines at 44,72°; 52,07° and 76,57° were assigned to the (111); (200) and (220) lattice planes of Ni (0), respectively.

With increasing Ni content, it was observed that the related reflections became more intense with no apparent shift in the Ni peak positions. This confirms that Ni was successfully deposited on the ZSM-5 support. It was also observed that the support structure remained stable during the metal loading process as no significant modification of the ZSM-5 diffraction peaks was seen.

TEM (see Fig 3) shows that dispersed semi-spherical Ni nanoparticles formed on the support's surface for all samples. Average Ni nanoparticle sizes were estimated around 18.1 (n=56); 34.1 (n=65) and 29.8 nm (n=100) for the 5%-; 10%- and 20%-loaded Ni-ZSM-5 catalysts, respectively.

## Acknowledgements

This research was supported by BiOrbic, Bioeconomy SFI Research Centre, which is funded by Ireland's European Structural and Investment Programmes, Science Foundation Ireland (16/RC/ 3889) and the European Regional Development Fund.

## References

- [1] S. Takkellapati, T. Li and M. A. Gonzalez, "An overview of biorefinery-derived platform chemicals from a cellulose and hemicellulose biorefinery," *Clean Technologies and Environmental Policy*, 2018.

- [2] M. Ibrahim, R. Sriprasanthi, S. Shamsudeen, F. Adam and S. Bhawani, "A concise review of the natural existence, synthesis, properties, and applications of syringaldehyde," *Bioresources*, 2012.
- [3] C. W. Lahive, P. C. J. Kamer, C. S. Lancefield and P. J. Deuss, "An Introduction to Model Compounds of Lignin Linking Motifs; Synthesis and Selection Considerations for Reactivity Studies," *ChemSusChem*, 2020.

## Lignin-based benzoxazines: a tunable key-precursor for various applications

A. Adjaoud<sup>1,2</sup>, L. Puchot<sup>1</sup>, P. Verge<sup>1\*</sup>

<sup>1</sup> Luxembourg Institute of Science and Technology, Esch-sur-Alzette, Luxembourg

<sup>2</sup> University of Luxembourg, Esch-sur-Alzette, Luxembourg

\*[pierre.verge@list.lu](mailto:pierre.verge@list.lu)

The meaningful concept of circular economy and tighter environmental legislation to phase out single-use plastics have prompted the scientific community to transform the polymer industry toward bio-based and recyclable materials. Lignin, an earthbound polymer, epitomized the main source of phenolic compounds for the conception of bio-derived materials. Strategies toward lignin valorization flourished as lignin can be incorporated as fillers for composites, depolymerized into high-valued added chemicals, or modified to produce sustainable materials<sup>1</sup>. Polybenzoxazines (PBZs) are mono-component thermosets, and recently emerged as a promising alternative to phenolic and epoxy resins thanks to their superior mechanical properties and thermal stability<sup>2</sup>. The past two decades witnessed the explosive growth of research works on the design of benzoxazine from renewable resources stemming from the exceptional versatility of their chemical structure. As unmodified lignin meets few commercial applications, we have reported a promising green and eco-friendly approach to increase the reactivity of lignin<sup>3</sup>. In this study, a technical soda lignin was esterified in solvent-free condition with phloretic acid, a naturally occurring compound extracted from the leaves of apple trees. This sustainable synthetic route grants technical lignin with ester bonds and an increased number of phenolic reactive sites. Therefore, this enriched platform of *ortho*-free phenolic rings was employed for the catalyst-free design of a series of lignin-based benzoxazines (LBZs). The properties of the bio-based resins can be easily tuned depending on the amine used to close the benzoxazine ring. Bio-based amines synthons such as long-alkyl chain stearylamine confers hydrophobicity to LBZs coatings ( $\theta = 96^\circ$ ), while furfurylamine-based LBZs generate high- $T_g$  ( $T_g = 197^\circ\text{C}$ ) and high thermal stability ( $\text{CR}_{800} = 45.8\%$ ) materials well adapted for fire-retardancy applications. Amino-alcohol derivatives grant recyclability to cross-linked lignin-vitrimer thanks to dynamic transesterification exchanges, joining the recent but growing family of lignin-based vitrimers ( $\tau_{200}^* = 233\text{ s}$ ). This presentation will highlight the versatility of lignin-based benzoxazine in terms of application, by simply tuning the type of amine used to close the oxazine ring (Figure 1).

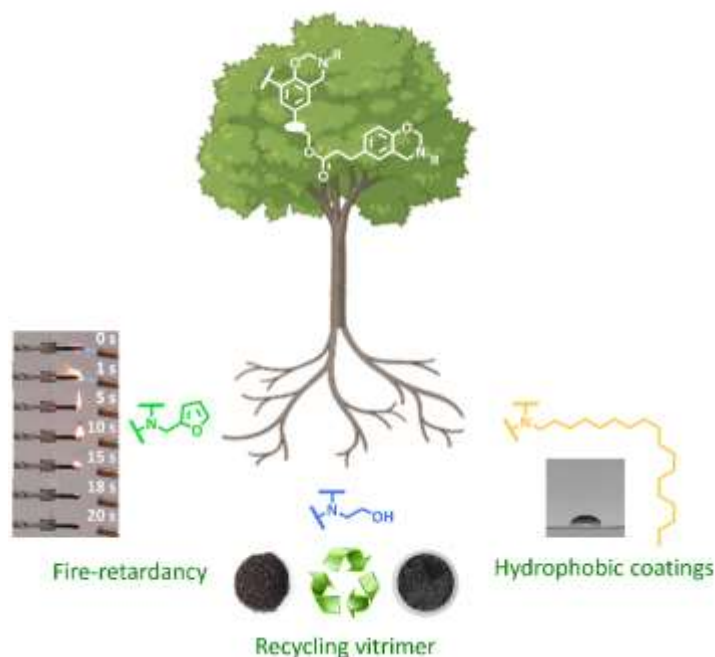


Figure 36 Multi-purpose applications of lignin-based benzoxazines

### Acknowledgements

The authors would like to thank the FNR for the funding of the project LIGNOBENZ (C18/MS/12538602).

### References

1. Kai, D.; Tan, M. J.; Chee, P. L.; Chua, Y. K.; Yap, Y. L.; Loh, X. J., *Green Chem.*, **18** 5 (2016).
2. Ishida, H., *Handbook of Benzoxazine Resins*, Elsevier: Amsterdam (2011).
3. Adjaoud, A.; Dieden, R.; Verge, P., *Polymers* 2021, **13** 4 (2021).

## Comparative analysis of the biological activity of proanthocyanidins from fruit and non-fruit trees and shrubs of Northern Europe

Andersone A.<sup>1\*</sup>, Janceva S.<sup>1</sup>, Lauberte L.<sup>1</sup>, Zaharova N.<sup>1</sup>, Senkovs M.<sup>2</sup>, Ramata-Stunda A.<sup>2</sup>, Telysheva G.<sup>1</sup>, Rieksts G.<sup>1</sup>

<sup>1</sup>Latvian State Institute of Wood Chemistry, Dzerbenes Street 27, LV-1006, Riga, Latvia

<sup>2</sup>Latvia University of Latvia, Faculty of Biology, Jelgavas Street 1, LV-1004, Riga, Latvia

\*anna.andersone@kki.lv

Proanthocyanidins have been the focus of increasing interest in the last years as a result of their high biological activities (antioxidant, antibacterial, anti-inflammatory, anticancer, etc.) [1], which have prompted their use in therapeutic needs, also in food and cosmetic industries. Proanthocyanidins are chemically heterogeneous oligomers of polyhydroxy-flavan-3-ol monomer units linked mainly by C4–C6 or C4–C8 bonds (B-type proanthocyanidins). Less widespread are the A-type proanthocyanidins, characterized by the presence of flavanol units doubly-linked by C4–C8 and C2–O7 or C4–C6 and C2–O7 bonds (Figure 1)[2].

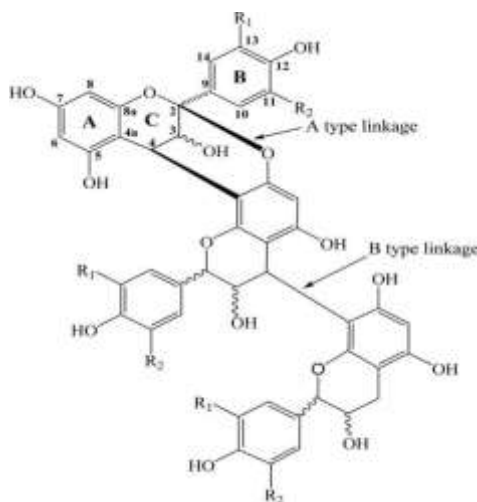


Figure 1. Chemical structure of proanthocyanidins [2].

Proanthocyanidins are found in significant amounts in the bark of various tree and shrub species, which are burned to produce heat without exploiting their potential to produce proanthocyanidins or proanthocyanidins-rich extract. The purpose of the study was a comparative analysis of the biological activity of proanthocyanidins isolated from the biomass (bark and branches) of fruit and non-fruit trees and shrubs of Northern Europe. As a raw material for the isolation of proanthocyanidins, the following was used: grey alder - *Alnus incana*, black alder - *Alnus glutinosa*, willow - *Salix caprea*, sea buckthorn - *Hippophae rhamnoides L.* and black chokeberry - *Aronia melanocarpa*.

The main process for isolating proanthocyanidins from the bark/twigs is the extraction process. The selectivity of the extraction of proanthocyanidins depends not only on the extraction method and the type of solvent used, but also on the temperature, extraction time, solvent to biomass mass ratio, and biomass fineness. The main way to increase the yield of the target product from biomass is to choose an extraction method (single-stage or sequential extraction using solvents of different polarities) and optimize the modes of the selected extraction method. To intensify the targeted extraction of proanthocyanidins, it is necessary to use activating effects. The most promising of the known approaches to the pretreatment of plant raw materials (lignocellulosic biomass) is mechanical activation. Solid-phase mechanochemical processing allows processes to be carried out without the use of solvents, which allows the development of economical and environmentally friendly technologies. Mechanical activation allows you to increase the speed and yield of target products (proanthocyanidins) that are part of the plant material. From the point of view of solid-state chemistry, the main factors for increasing the reactivity of lignocellulose in heterogeneous reactions are an increase in the defectiveness of the polymer structure, including the amorphization of cellulose crystallites.

Hydrophilic extracts were isolated by the convective extraction of biomass at 60 °C for 30 min using the following solvents: distilled water or aqueous ethanol (1:1, v/v). The proanthocyanidin content of the extracts was determined by oxidative depolymerization to anthocyanidins in acid butanol using procyanidin dimer B2 as a reference compound. The purification of proanthocyanidins from non-tannin phenolics and sugar was carried out using a Sephadex LH-20 column with 96% EtOH and 70% (v/v) acetone as the respective purification solvents. In the purification process, low-molecular-weight phenolics were eluted with 96% EtOH, and the PACs were eluted with



70% (v/v) acetone. Purified proanthocyanidins were evaporated using a rotary evaporator prior to being freeze-dried. The obtained results show that 40 % EtOH (w/w) ensures the highest proanthocyanidins yield from the biomass. The yields of proanthocyanidins varied between 12-16 % on dry biomass. The content of proanthocyanidins in fruit shrubs biomass was higher than in non-fruit trees biomass. As a result of mechanochemical treatment of the *Alnus incana* bark in a roller mill, dispersed products with a predominant particle size of  $\leq 20 \mu\text{k}$  was obtained (SEM data). Grinding in a mechanical activator (roller mill) leads to an increase in the specific surface area of the processed material by 3-4 times, a decrease in the average particle size, and an increase in the total pore volume by 4-5 times. The yield of proanthocyanidins of treated *Alnus* bark samples was 1.5 times higher compared to the referent sample (untreated bark). Combining the results of the TOF-MS,  $^{13}\text{C}$ -NMR, and UHPLC-ESI-MS/MS, the analysis indicated that proanthocyanidins from all biomass were procyanidin of type B, where the units of catechin/epicatechin monomer in the oligomers with a degree of polymerization being 2–5 were related to the bond C4-C8 or C4-C6. The all proanthocyanidins isolated revealed high antioxidant activity in tests with stable radicals DPPH $^{\bullet}$  and ABTS $^{+\bullet}$ . Radical scavenging activity determined spectrophotometrically was expressed in terms of IC $_{50}$  (the scavenger concentration required for 50% inhibition of free radicals).

Oxygen radical absorption capacity (ORAC) is one of the most widely used methods that provide information about the antioxidant ability to protect a substratum (fluorescein in this particular case) from oxidation with oxygen peroxy radicals. When compared to Trolox (4.0 (mmol TE) $\cdot\text{g}^{-1}$ ), proanthocyanidins as antioxidants are more efficient (4.8 (mmol TE) $\cdot\text{g}^{-1}$  to 5.3 (mmol TE) $\cdot\text{g}^{-1}$ ) by protecting fluorescein against oxidation. These proanthocyanidins' properties can be valuable not only in the creation of pharmaceuticals on the basis of plant secondary metabolites but also in the food and cosmetics industries to slow down the oxidative processes occurring in raw materials and finished products at different stages of the technological process during storage. The evaluation of the antimicrobial activity of the proanthocyanidins against test cultures of microorganisms was carried out according to the method for determining the sensitivity of microorganisms to antimicrobial drugs. Antimicrobial activity was studied in 96-well plates by the twofold serial broth microdilution method, which allowed the determination of the minimum inhibitory (MIC) and minimum bactericidal/fungicidal concentrations (MBC/MFC). The results show that all proanthocyanidins have high antimicrobial activity against both Gram-positive and Gram-negative bacteria. These results provide the scope of further research on the proanthocyanidins for applications in the prevention and treatment of infectious diseases. At concentrations similar to the MIC values observed in anti-microbial activity tests, no toxic effect was observed, thus confirming the potential for practical use of the proanthocyanidins.

## Acknowledgments

ERDF project nr. Nr.1.1.1.1/19/A/146 “Biorefinery processing of sea buckthorn non-fruit biomass using innovative techniques and comprehensive analytical investigation, for obtaining prospective for Latvian bioeconomy high value-added products, including serotonin” is greatly acknowledged.

## References

1. A. Rauf, M. Imran, T. Abu-Izneid, P.S. Iahtisham-Ul-Haq C.N. Hamelinck, X. Pan, H.A. Rasul Suleria. *Biomedicine & Pharmacotherapy*, **116** 108999 (2019).
2. L. Panzella, A. Napolitano. *J. Agric. Food Chem.*, **70** 3, 751–75 (2022).

## Physicochemical changes of alginate/polyacrylic acid mixture induced by host-guest interactions of the appended units

Ludmila Aricov\*, Anca Leonties, Raluca Visan, Rodica Baratoiu, Elena Hristea, Iulia Matei,

Alexandru Neculae, Sorin Mocanu and Gabriela Ionita

“Ilie Murgulescu” Institute of Physical Chemistry, Romanian Academy, Spl. Independentei 202, 060021 Bucharest, Romania

\*aricov\_ludmila@yahoo.com

### Abstract:

In recent decades, efforts have been made to create complex supramolecular materials and to investigate their applications in environmental remediation, catalysis, nanomedicine, electronic devices, sensors, etc. In this study we analyzed the physicochemical changes of the host-guest based supramolecular assemblies formed between functionalized alginate with  $\beta$ -cyclodextrin ( $\beta$ -CD) units and functionalized polyacrylic acid (PAA) with alkyl chains (Figure 1).

Methods used to describe the behavior of the polymers and their mixture include rheological measurements, FTIR spectroscopy, dynamic light scattering, together with electronic paramagnetic resonance spectroscopy (EPR). The EPR spectroscopy was used to correlate local changes with macroscopic changes in alginate/PAA systems. For this, spin labelled alginate and spin labelled CD functionalized alginate were introduced in the systems. Our previous results evidenced that EPR method is sensitive to host interactions both in solutions and in gel phase [1, 2]. The behavior of alginate/PAA system was investigated both in solutions and in gel state generated by adding divalent cations which chelates the carboxylic groups from alginates and PAA.

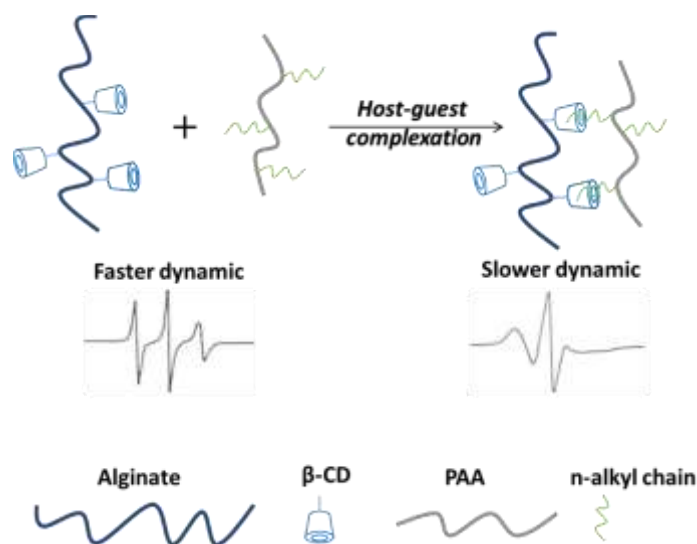


Figure 1. Representation of host-guest interaction between functionalized alginate with  $\beta$ -CD units and functionalized polyacrylic acid (PAA) with alkyl chains.

This work highlighted the changes of the mixture, between functionalized alginate with  $\beta$ -CD units and functionalized PAA with alkyl chains, induced by host-guest interactions of the appended units. The EPR spectroscopy revealed that the  $\beta$ -CD and alkyl chains units to polymers chains can modulate the properties of supramolecular material based on host-guest interactions.

### Acknowledgements

The study was supported by the Romanian National Authority for Scientific Research, CNCS-UEFISCDI, project PN-III-P1-1.1-PD-2021-0169 contract no. PD106/2022 and Romanian Academy within the research programs “Colloids and dispersed systems” and “EPR and fluorescence studies on supramolecular interactions in inhomogeneous systems” of the “Ilie Murgulescu” Institute of Physical Chemistry.

### References

1. G. Ionita, A.M. Ariciu, D.K. Smith, V. Chechik, *Soft Matter* **11** 46 (2015).
2. E.I. Popescu, L. Aricov, S. Mocanu, I. Matei, E. Hristea, R. Baratoiu, A. Leonties, C. Petcu, E. Alexandrescu, G. Ionita, *New J. Chem.* **45** 8083 (2021).

## Development of olive oil and $\alpha$ -tocopherol containing emulsions stabilized by FucoPol: Rheological and textural analyses

Sílvia Baptista<sup>1,2,3,\*</sup>, João R. Pereira<sup>1,2</sup>, Cátia Gil<sup>1,2</sup>, Cristiana A.V. Torres<sup>1,2</sup>, Maria A.M. Reis<sup>1,2</sup>, Filomena Freitas<sup>1,2</sup>

<sup>1</sup> Associate Laboratory i4HB - Institute for Health and Bioeconomy, School of Science and Technology, NOVA University Lisbon, Caparica, Portugal;

<sup>2</sup> UCIBIO – Applied Molecular Biosciences Unit, Department of Chemistry, School of Science and Technology, NOVA University Lisbon, 2819-516 Caparica, Portugal

<sup>3</sup> 73100, Lda. Edifício Arcis, Rua Ivone Silva, 6, 4º piso, 1050-124 Lisboa, Portugal

\*silvia.baptista@73100.pt

Current sustainability concerns demand the utilization of biobased raw materials. In the cosmetic industry, polysaccharides are being incrementally used as rheology modifiers in skin-care products, which can increase the spreading properties of products and enhance their sensorial profile [1,2]. In this study, the bacterial exopolysaccharide FucoPol was used to form and stabilize emulsions at different oil/water (O/W) ratios with four different oils generally used in cosmetic applications. Response surface methodology (RSM) was used for defining the optimal ingredients (FucoPol, olive oil and  $\alpha$ -tocopherol) concentration for emulsion development. The structural and mechanical attributes of the obtained emulsions were assessed using rheo-logical and texture analysis, demonstrating that FucoPol can be used as a natural emulsifier, acting as a potential alternative to other emulsifiers. FucoPol high performance with olive oil was supported by an effective im-pact on the physicochemical and structural characteristics of the emulsions, mainly on their emulsification stability.

### Acknowledgements

This work is financed by national funds from FCT—Fundação para a Ciência e a Tecnologia, I.P., in the scope of the project UIDP/04378/2020 and UIDB/04378/2020 of the Research Unit on Applied Molecular Biosciences—UCIBIO and the project LA/P/0140/2020 of the Associate Laboratory Institute for Health and Bioeconomy—i4HB. The author acknowledges 73100, Lda for funding of PhD program.

### References

1. Baptista, S.; Freitas, F. Bacterial Polysaccharides: Cosmetic Applications; 2021; ISBN 9783030357344.
2. Freitas, F.; Alves, V.; Reis, M.A.M. Bacterial Polysaccharides: Production and Applications in Cosmetic Industry. Polysaccharides 2014, 1–24.

## Cellulose Nanocrystal Modification with Subberin Fatty Acids and Application in Additive Manufacturing Resins Reinforcement

Anda Barkane,<sup>a,\*</sup> Sergejs Gaidukovs<sup>a</sup>

[a] Institute of Polymer Materials, Faculty of Materials Science and Applied Chemistry, Riga Technical University, P. Valdena 3/7, LV-1048 Riga, Latvia  
E-mail: Anda.Barkane@rtu.lv

This report contains information about cellulose nanocrystal (CNC) modification with subbering fatty acids and then incorporation in additive manufacturing bio-based resin for UV-assisted printing. Vegetable oil-based resins show good results for UV-induced curing applications. Unfortunately vegetable oil-based resins still lack in comparison to commercial resins that are petroleum-based.<sup>[1]</sup> CNC can be applied as an enhancer for vegetable oil-based resins.<sup>[2]</sup> CNC was modified to obtain via esterification with subberin fatty acids to obtain hydrophobic CNC then introduced in vegetable oil-based resin as a reinforcement with enhanced compatibility.

CNC modification was verified with Fourier Transformation Infrared spectrometer (FTIR) and modification effect on CNC dimensions as well as thermal stability and wettability was also investigated. Printed samples were tested for matrix interaction with the modified CNC and caused changes in mechanical performance, thermal, and thermomechanical properties.

By modifying CNC thermal stability and wettability can be adjusted without compromising particle dimensions. CNC modification enhanced performance of vegetable oil-based resin. Developed resins with modified CNC could replace petroleum-based resins used in UV-assisted additive manufacturing technologies.

### Acknowledgements

This research was supported by Riga Technical University's Doctoral Grant program.

### References

- [1] Díez-Pascual, A. M.; Rahdar, A., *Macromol*, **2021**, 1 (4), 276-292.
- [2] Barkane, A.; Platnieks, O.; Jurinovs, M.; Gaidukovs, S., *Polymer Degradation and Stability*, **2020**, 181.

**Bioproduction of 2-Phenylethanol by *Acinetobacter soli***

**Ana. R. S. Bernardino**<sup>1,2,3</sup>, **Cristiana A. V. Torres**<sup>1,2\*</sup>, **Filipa Grosso**<sup>4,5</sup>, **Luísa Peixe**<sup>4,5,6</sup>, **Maria A. M. Reis**<sup>1,2</sup>

<sup>1</sup> *Laboratory i4HB - Institute for Health and Bioeconomy, School of Science and Technology, NOVA University Lisbon, Caparica, Portugal*

<sup>2</sup> *UCIBIO – Applied Molecular Biosciences Unit, Department of Chemistry, School of Science and Technology, NOVA University Lisbon, Caparica, Portugal*

<sup>3</sup> *LAQV-REQUIMTE, Chemistry Department, FCT/Universidade NOVA de Lisboa, 2829-516 Caparica, Portugal*

<sup>4</sup> *UCIBIO – Applied Molecular Biosciences Unit, REQUIMTE, Faculty of Pharmacy, Department of Biological Sciences, Laboratory of Microbiology, University of Porto, Porto, Portugal*

<sup>5</sup> *Associate Laboratory i4HB - Institute for Health and Bioeconomy, Faculty of Pharmacy, University of Porto, Porto, Portugal*

<sup>6</sup> *CCP – Culture Collection of Porto-Faculty of Pharmacy, University of Porto, Porto, Portugal*

\*c.torres@fct.unl.pt

2-Phenylethanol (2-PE) is an aromatic alcohol with rose-like scent, one of the most used fragrances applied in cosmetic and home care product industries, but also in food and beverage and pharmaceutical fields. The majority of the commercialized aroma is produced chemically, from chlorobenzene, benzene or styrene oxide in harsh conditions, generating side products that can affect the aroma quality [1,2]. Naturally, it can be obtained by extraction from rose petals and other plant tissues, but due to the complexity of the extraction process and the low concentrations that are found in plants, the costs are more than 250 times higher than the chemically synthesized aroma [2]. However, the demand for natural products is increasing and the natural rose aroma cannot cover the demand. Therefore, biotechnological approaches have been studied as alternative processes, since 2-PE obtained by this way can be considered as natural [2,3]. The use of milder conditions and the possibility of using wastes and industrial byproducts in biotechnological processes, favoring a circular economy, are additional advantages of this approach. Several microorganisms are able to produce 2-PE, but the limitation of the biotechnological production process is the low productivity that can be obtained due to the product toxicity to the producing microorganism. Yeasts, as *Kluyveromyces marxianus* and *Saccharomyces cerevisiae* are the most reported 2-PE producers, achieving product concentrations usually below 4 g/L [3,4]. The bacterial production is less common, reported in concentrations under 152 mg/L for non-engineered bacteria [5-7].

In this work, a bacterium isolated from a river water and identified as *Acinetobacter soli* was found to produce 2-PE in concentrations near 2 g/L from L-phenylalanine (L-Phe), revealing itself a promising platform for the aroma production and standing out from the previously reported bacteria. This work includes the assessment of the best conditions, regarding medium composition and operational conditions, to produce 2-PE.

Experiments to assess the operation conditions more suitable for 2-PE production were carried out in 500 mL baffled shaking flask in an orbital shaker at 200 rpm. Different cultivation media composition supplemented with L-Phe were tested, based on the cultivation media reported in literature for soil bacteria and for *Acinetobacter* species [8-12]. Additionally, to improve the production process, different temperatures, from 23 to 37 °C and, pH from 5 to 8, were tested. All the cultivation media were supplemented with 5 g/L of L-Phe.

A 2 L bioreactor equipped with pH, temperature, stirring, aeration and dissolved oxygen control was used to study the best aeration conditions (1 and 2 vvm), dissolved oxygen concentration (30 and 50%) and L-Phe concentrations (2.5, 5 and 7 g/L). The dissolved oxygen was kept at 30 or 50% by automatic variation of stirring speed (300-1000 rpm). Assays were performed in a batch mode, at pH 7 and 30°C.

2-PE toxicity was also assessed, growing the bacteria in the presence of 0 to 5 g/L of 2-PE.

From the cultivation medium screening, glucose was chosen as carbon source for bacterial growth and L-Phe as 2-PE precursor. Within these experiments a 2-PE production between 1.60 and 1.78 g/L, were achieved. It was found that glucose and yeast extract are crucial for 2-PE production and L-Phe cannot be used as sole carbon and/or nitrogen source, even though it is reported that the use of L-Phe as sole nitrogen source favors the pathway for the aroma production [13].

Regarding the studies of temperature and pH, it was found that higher temperatures and lower pH have a negative effect on the microorganism growth and aroma production. The production is favored at lower temperatures and in a pH range of 7 to 8. The best cellular growth and 2-PE production ( $1.77 \pm 0.02$  g/L) was achieved at 30 °C and pH 7, as it is reported for several *Acinetobacter* species.

As *Acinetobacter soli* is an aerobic microorganism, different oxygen supplementations and dissolved oxygen (DO) percentages were tested. An increase of oxygen flow rate from 1 to 2 vvm, caused a decrease in biomass production and in 2-PE production, while an increase of DO from 30 to 50% resulted in similar kinetic parameters. Thus, 1 vvm and 30 % of dissolved oxygen were the selected conditions to proceed.

In the optimized conditions, runs with different concentrations of L-Phe were performed in bioreactor to assess the precursor concentration that leads to a more favorable process. Using 5 g/L of L-Phe, not all the precursor was consumed, being its consumption faster in the beginning of the run, decreasing throughout the experiment. When a lower concentration was used (2.5 g/L), the precursor was completely consumed by the end of the experiment, but its consumption was slower than for 5 g/L of L-Phe. These results suggest that the production rate increases with the concentration of the precursor. Then, 7 g/L of L-Phe was tested, resulting in a behavior and kinetic parameters similar to the calculated in the run with 5 g/L of L-Phe, but the unconverted amount of the precursor was higher. Therefore, 5 g/L of L-Phe were used for the following assays.

The kinetic parameters obtained for the most favorable conditions for *Acinetobacter soli* growth and production are represented in Table 1.

2-PE seems to have a toxic effect on bacterial growth, affecting *Acinetobacter soli* growth even when 1 g/L of 2-PE was present in the broth, in these conditions after 24 h growth, the biomass concentration was 51 % of the obtained when no 2-PE was present. These results suggest that 5 g/L of 2-PE completely inhibited growth of *Acinetobacter soli*.

Table 1. - Parameters calculated for 2-PE production obtained with the selected conditions at 16 h.

Biomass (g/L)	3.4 ± 1.1
L-Phe <sub>cons</sub> (g/L)	4.00 ± 0.74
2-PE <sub>prod</sub> (g/L)	1.92 ± 0.13
Y(p/s) (g/g)	0.49 ± 0.07
Rp(g/L.h <sup>-1</sup> )	0.12 ± 0.01

*Acinetobacter soli* showed to be a promising 2-PE producer, being able to produce 1.92 g/L of 2-PE from L-Phe. This value was reported only for yeasts, so far. The best conditions for 2-PE production by *Acinetobacter soli* were found to be 1 vvm, 30 °C, pH 7 and higher L-Phe concentrations lead to higher 2-PE production rates. However, 2-PE negatively affects cellular growth at relatively low concentrations, so 2-PE removal from the broth should be an important approach to improve its production.

## Acknowledgements

This work was financed by national funds from FCT - Fundação para a Ciência e a Tecnologia, I.P., in the scope of the project UIDP/04378/2020 and UIDB/04378/2020 of the Research Unit on Applied Molecular Biosciences - UCIBIO and the project LA/P/0140/2020 of the Associate Laboratory Institute for Health and Bioeconomy - i4HB, and by the European Union's Horizon 2020 research and innovation programme through Project Bio Innovation of a Circular Economy for Plastics (BioICEP), under grant agreement No 870292, supported by the National Natural Science Foundation of China (grant numbers: Institute of Microbiology, Chinese Academy of Sciences: 31961133016; Beijing Institute of Technology: 31961133015; Shandong University: 31961133014). This work was recently patented (PT 115777 B, 2021), and partially funded by the project ACINETOBACTER\_POCI-01-0145-FEDER-042759. Ana R. S. Bernardino acknowledge FCT, Portugal, for the PhD Fellow grant SFRH/BD/138011/2018. Filipa Grosso is supported by national funds through FCT in the context of the transitional norm DL57/2016/CP1346/CT0034.

## References

1. A. Vorster, M. S. Smit, D. J. Opperman, *Organic Letters*, **21** 7034 (2019).
2. X. Qian, W. Yan, W. Zhang, W. Dong, J. Ma, K. Ochsenreither, M. Jiang, F. Xin, *Critical Reviews in Biotechnology*, **39**:2 235 (2018).
3. F. Gao, A. J. Daugulis, *Biotechnology and Bioengineering*, **104** 2 332 (2009).
4. C-H. Shu, S-S. Zhou, W. OC. Nirwana, *Journal of Chemical Technology and Biotechnology*, **96** 4 899 (2020).
5. N. Jollivet, M-C. Bézenger, Y. Vayssier, J-M. Belin, *Applied Microbiology and Biotechnology*, **36** 790 (1992).
6. P. Deetae, P. Bonnarme, H. E. Spinnler, S. Helinck, *Applied Microbial and Cell Physiology*, **76** 1161 (2007).
7. H. E. Spinnler, A. Djian, *Applied Microbial and Cell Physiology*, **35** 264 (1991).
8. J. Chen, P. T. Huang, K. Y. Zhang, F. R. Ding, *Journal of Applied Microbiology*, **112** 4 660 (2012).
9. M. Sunitha, P. Ellaiah, R. B. Devi, *African Journal of Microbiology Research*, **4** 4 297 (2010).
10. Z. R. Wang, J.P.Sheng. X. L. Tian, T. T. Wu, W. Z. Liu, L. Shen, *African Journal of Microbiology Research*, **5** 16 2359 (2011)
11. R. Valério, A.R.S. Bernardino, C.A.V. Torres, C. Brazinha, M. L. Tavares, J. G. Crespo, M. A. Reis, *Bioprocess and Biosystems Engineering*, **44** 4 737 (2021).
12. U. Beshay, D. Abd-El-Haleem, H. Moawad, S. Zaki, *Biotechnology Letters*, **24** 1295 (2002).

13. J. J. Rodríguez-Romero, C. A. Aceves-Lara, C. F. Silva, A. Gschaedler, L. Amaya-Delgado, J. Arrizon, *Biotechnology Reports*, **25** (2020)

## Study of the modification of chitosan structure with 2-methoxy-4-vinylphenol for enhanced antioxidant activity

Georgia Michailidou<sup>1\*</sup>, Alexandra Zamboulis<sup>1</sup>, Dimitrios Bikiaris<sup>1\*</sup>

<sup>1</sup> Laboratory of Polymer Chemistry and Technology, Department of Chemistry, Aristotle University of Thessaloniki, GR-541 24 Thessaloniki, Macedonia, Greece

\*Correspondence: [dbic@chem.auth.gr](mailto:dbic@chem.auth.gr), [michailidougeorgia18@gmail.com](mailto:michailidougeorgia18@gmail.com)

Chitosan (CS) is the only cationic natural polysaccharide derived through alkali deacetylation from fungi, arthropods, and crustaceans. It is a non-toxic, biodegradable and biocompatible, material employed in pharmaceutical and biomedical applications [1]. Derivatization of CS with various monomers results in new materials with ameliorated physicochemical properties. 2-methoxy-4-vinylphenol (MVP) is a monomer derived from buckwheat extraction, with antioxidant and anticancer properties [2]. In the present study, modification of CS structure with MVP in different ratios was conducted through free radical polymerization (Figure 1).

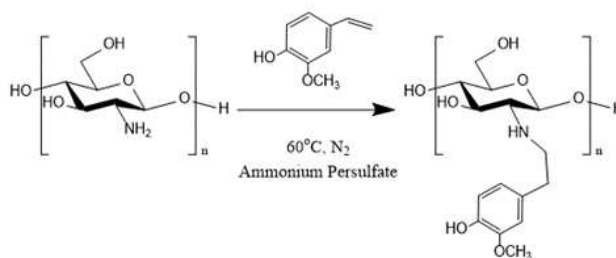


Figure 1. Schematic representation of the CS-MVP reaction

The structure of CS-MVP materials was examined by infra-red and <sup>1</sup>H-NMR measurements. The solubility of the new materials in different pH values was assessed, while through contact angle and swelling measurements the hydrophilicity and swelling ability of the newly formed derivatives were evaluated. Results revealed the successful derivatization of the polysaccharide. The new materials presented appropriate swelling efficacy while their surface hydrophilicity heavily depends on the applied ratio of the MVP. These results render the new CS-MVP materials promising candidates for their further utilization in pharmaceutical applications.

### Acknowledgements

«The implementation of the doctoral dissertation was co-financed by Greece and the European Union (European Social Fund-ESF) through the Operational Program "Human Resources Development, Education and Lifelong Learning", 2014-2020, in the context of the project "Reinforcement of human resources through implementation of doctoral research - Sub-action 2: Program for the award of IKY scholarships to doctoral candidates of Greek universities»

### References

- [1] A. Zamboulis, S. Nanaki, G. Michailidou, I. Koumentakou, M. Lazaridou, N.M. Ainali, E. Xanthopoulou, D.N. Bikiaris, *Polymers (Basel)*. 12 (2020) 9–11.
- [2] D.H. Kim, S.I. Han, B. Go, U.H. Oh, C.S. Kim, Y.H. Jung, J. Lee, J.H. Kim, *Anticancer Res.* 39 (2019) 6685–6691.



## **Degradation and environmental impact of biodegradable plastics.**

Fannie Burgevin<sup>1</sup>

*1 University of Bath, UK*

The persistence of plastic in the environment has become a major issue in the last decades. Biodegradable products are presented by many as part of the solution to this global plastics crisis. However, until now, very little research examining the precise fate and impact in the open environment of biodegradable plastics have been conducted. Many products are not tested with sufficient standards before being put on the market and sold as biodegradable. Moreover, biodegradation tests do not represent well the reality in the open environment. Combination of degradation tests performed in well-controlled conditions in the lab, with tests in the field and biodegradation experiments with respirometer are essential to prove and assess the degradation and biodegradation potential of a material.

This work aims to provide better understanding of the fate of common biodegradable polymers (PLA, PBAT, PBS...) in the environment (marine, soil, air) by monitoring their degradation in the field and in the laboratory under controlled conditions and study the impact of controlled intrinsic properties such as molecular weight and composition to better understand the characteristics required to limit their environmental impact.

# How to Design Single Atom Alloy Catalysts towards High-efficient Biomass Conversion

Guoqing Cui<sup>1\*</sup>, Min Wei<sup>2</sup>, Guiyuan Jiang<sup>1</sup>, Chunming Xu<sup>1</sup>

<sup>1</sup>State Key Laboratory of Heavy Oil Processing/China University of Petroleum, Beijing, China

<sup>2</sup>State Key Laboratory of Chemical Resource Engineering, Beijing University of Chemical Technology, Beijing, China

\*e-mail address of corresponding author (cui@cup.edu.cn)

With the huge consumption of limited reserves fossil fuels and increasing environmental issues, catalytic conversion of biomass-derived platform molecules has recently attracted considerable attention in both fundamental study and industrial application, in which glycerol hydrogenolysis to 1,2-propylene (1,2-PDO) is an essential process in the production of high value-added chemicals. Although an increasing research endeavor has been performed, how to design efficient catalysts to acquire high activity, selectivity and stability simultaneously, still remains a big challenge. Single atom alloy (SAA) catalysts, with advantages of particular geometric and electronic structure, provide unique active centers that exert excellent catalytic performance in a broad scope of reactions. In the hydrogenolysis process, Cu-based catalysts have shown promising selectivity in cleaving C–O bond but suffer from unsatisfactory activity and poor stability. In contrast, Pt-based catalysts exhibit superior activity but are prone to break C–C bond, resulting in a loss of selectivity. Inspired by the above facts, if a bimetallic SAA catalyst is designed by distributing Pt atoms onto Cu nanoparticles to marry the advantages of them, both activity and selectivity can be guaranteed.

A series of elaborate characterizations including AC–HAADF–STEM, *in situ* CO–DRIFTS and *in situ* EXAFS confirm the formation of SAA, where a few Pt atoms are absolutely isolated by Cu atoms. As expected, the PtCu–SAA exhibits extraordinary catalytic performance towards glycerol hydrogenolysis to 1,2-PDO (conversion: 99.6%; selectivity: 99.2%), under mild reaction conditions (200 °C, 2 MPa). Most notably, the TOF value of PtCu–SAA reaches up to  $2.6 \times 10^3 \text{ mol}_{\text{glycerol}} \cdot \text{mol}_{\text{PtCu-SAA}}^{-1} \cdot \text{h}^{-1}$ , calculated on the basis of moles of whole single atom alloy sites (with two atoms) on the surface of PtCu–SAA, which is 8–120 fold larger than that of metal catalysts ever reported. This is to our knowledge the highest reactivity among heterogeneous catalysts under identical reaction conditions. Furthermore, both *in situ* experimental studies (*in situ* glycerol-EXAFS and *in situ* glycerol-DRIFTS) and DFT calculations substantiate that the Pt–Cu interface sites serve as intrinsic active centers: the single Pt atom facilitates the activation adsorption of central C–H bond in glycerol molecule, whilst the terminal C–O bond undergoes dissociation adsorption on adjacent Cu atoms. Consequently, this interfacial synergistic catalysis changes the reaction pathway (with a lower activation energy) in comparison with traditional monometallic catalysts, accounting for the largely boosted activity and selectivity.

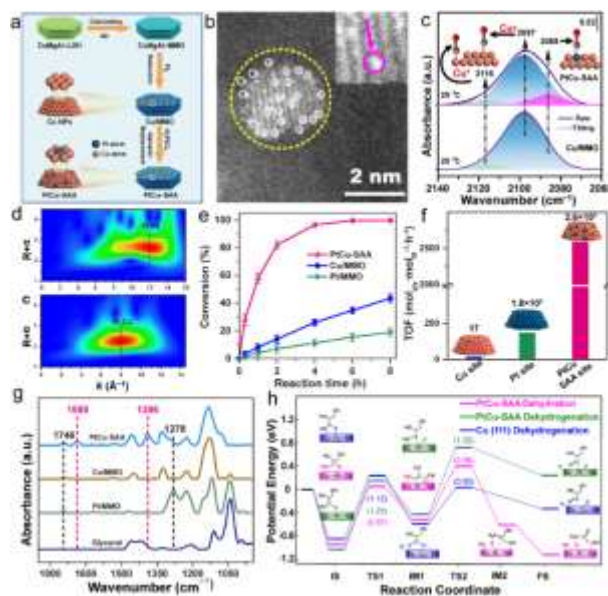


**Figure 1.** Synthesis, characterization and catalytic reaction of PtCu–SAA. a) schematic illustration, b) AC–HAADF–STEM, c) *in situ* CO–DRIFTS, d) *in situ* EXAFS, e) conversion of glycerol versus reaction time, f) the TOF value, g) *in situ* glycerol-DRIFTS, h) DFT study.

## Acknowledgements

This work was supported by the National Natural Science Foundation of China, the National Key Research and Development Program, and the Fundamental Research Funds for the Central Universities.

## Development of Sugar-Derived Bioconjugates: A More Sustainable Alternative to PEGylation

*Emma L. Daniels*<sup>1</sup>, Dr. Antoine P. Buchard<sup>\*1,3</sup>, Dr Hannah S. Leese<sup>\*2,3</sup>, and Prof Steve Parker<sup>1,3</sup>

<sup>1</sup> Department of Chemistry, University of Bath, Claverton Down, Bath, BA2 7AY, UK

<sup>2</sup> Department of Chemical Engineering, University of Bath, Claverton Down, Bath, BA2 7AY, UK

<sup>3</sup> Centre for Sustainable and Circular Technology, CSCT, University of Bath, Claverton Down, Bath, BA2 7AY, UK

\*[apb46@bath.ac.uk](mailto:apb46@bath.ac.uk), [hsl25@bath.ac.uk](mailto:hsl25@bath.ac.uk)

Bioconjugation, the attachment of biomolecules to synthetic polymers, produces novel, hybrid materials that combine the advantageous properties of each component, whilst overcoming their limitations. For example, when in conjugation with polymers, therapeutic proteins show reduced toxicity and immunogenicity and improved in vivo stability [1]. As such, bioconjugates have become valuable healthcare materials – bioconjugates are used as therapeutics, drug delivery systems and in bio-sensing [2,3]. The vast majority of conjugates use poly(ethylene glycol) (PEG) as their synthetic polymer component. However, so called ‘PEGylation’ has several drawbacks. PEG does not biodegrade, so its conjugates can lead to bioaccumulation and toxicity [4]. PEG is also derived from fossil fuels. Therefore, alternative polymer components need to be found. The use of renewably sourced, biodegradable polymers is particularly desirable to alleviate the toxicity and environmental impact of bioconjugate design.

Recently, several renewably-sourced monomers have been developed through the coupling of CO<sub>2</sub> sugar derivatives [5-7]. The corresponding polymers are made by alcohol-initiated ring opening polymerization (ROP). The resulting polymers are degradable by hydrolysis to yield sugar diols and CO<sub>2</sub>, and have potential to be both biodegradable and biocompatible. These properties make them ideal sustainable bioconjugation partners. In this work, we will detail the synthesis and modification of such polymers to enable their employment as the synthetic component of bioconjugates. In particular, the use of a maleimide-functional initiator to produce thiol-reactive polymers derived from D-Mannose will be highlighted (**Figure 1**).

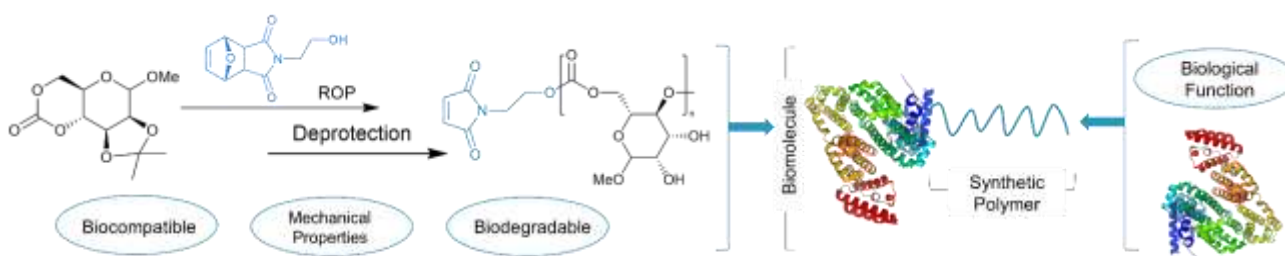


**Figure 1** Bioconjugate design; attachment of a maleimide-functional, mannose-derived polycarbonate with a thiol-containing biomolecule.

The resulting maleimide-functional polymers have been shown to be reactive towards small molecule thiols, such as mercaptoacetic acid and trithiols, via Michael Addition chemistry [8]. Post-polymerisation treatment with aqueous acid enables deprotection of the acetal protecting group. The degree of deprotection can be controlled while minimizing chain decomposition, and results in water-soluble polymers that retain their maleimide functionality. As well as expanding the reactivity of these polymers to water-soluble thiols (such as L-cysteine and glutathione), acetal deprotection is accompanied by an increase in glass transition temperature,  $T_g$ .

To demonstrate bioconjugation, bovine serum albumin (BSA) was chosen as a model protein. Work towards novel bioconjugates of BSA and deprotected mannopyranose-polycarbonates will be discussed and evidenced by LC-MS, SDS-PAGE, and MALDI-ToF mass spectrometry.

### Acknowledgements

This work was supported by the Engineering and Physical Sciences Research Council grant, EP/L016354/1. The authors gratefully acknowledge the Material and Chemical Characterisation Facility (MC<sup>2</sup>) at University of Bath.

## References

1. J. Lutz, H. Börner, *Progress in Polymer Science*, 2008, **33**, 1-39.
2. L. Meng, *Biosensors and Bioelectronics*, 2020, **159**, 11218.
3. O. D. Krishna, *Peptide Science*, 2010, **94**, 32-48
4. Y. Hou and H. Lu, *Bioconjugate Chemistry*, 2019, **30**, 1604-1616
5. G. L. Gregory, L. M. Jenisch, B. Charles, G. Kociok-Köhn, A. Buchard, *Macromolecules*, 2016, **49**, 7165-7169
6. T. M. McGuire, C. Pérale, R. Castaing, G. I. Kociok-Köhn, A. Buchard, *Journal of the American Chemical Society*, 2019, **141**, 13301-13305
7. T. M. McGuire, E. M. López-Vidal, G. L. Gregory, A. Buchard, *Journal of CO<sub>2</sub> Utilization*, 2018, **27**, 283-288.
8. R. J. Pounder, M. J. Stanford, P. Brooks, S. P. Richards, A. P. Dove, *Chemical Communications*, 2008, **41**, 5158-5160

## Durability in Sea Water of 3D Printed Materials based on Polyhydroxyalkanoate / Polybutylene Succinate Blends

Gerda Gaidukova<sup>1\*</sup> and Sergejs Gaidukovs<sup>2</sup>

<sup>1</sup>Latvian Maritime Academy, Flotes 3-7, Riga LV-1016, Latvia

<sup>2</sup>Institute of Polymer Materials, Faculty of Materials Science and Applied Chemistry, Riga Technical University, P. Valdena 3/7, LV-1048 Riga, Latvia

This presentation deals with the FFF 3D printing of biobased Polyhydroxyalkanoate (PHA) / Polybutylene Succinate (PBS) blends, which could be a brilliant alternative to the existing fossil polymers used in FFF 3D printing. Thermoplastic polymers acrylonitrile butadiene styrene (ABS), polylactic acid (PLA), polyamide (PA), and polycarbonate (PC), are commonly used in printing. Their sustainability is limited due to the fossil source of raw components. The high environmental impact of 3D printing process could be decreased using biobased analogs such as PBS and PHA. The application of the present biopolymer materials and printed articles in the Baltic Sea seawater environments was considered in this presentation. The long-term durability of the printed materials was assessed in the water media for at least two months. The results were complemented with the environmental impact assessment through inventory analysis of the technological processes.

The PHA/PBS blends 30/70, 50/50, and 30/70 have been prepared by melt compounding in a twin-screw extruder. In the second stage, the filaments prior to FFF printing were extruded with a 3Devo single screw extruder machine. The diameter of the filaments was 1.75 mm. Then, the obtained compositions have been printed with the delta type printer into double-dog bone shapes. The prepared compositions showed very good printability. The samples were saturated through immersion in modeled conditions by using synthetic seawater and real environments with the use of seawater from the Baltic Sea (Gulf of Riga) and water from river Lielupe. The durability and degradation properties of the proposed biomaterials were evaluated by means of structure control and mechanical durability. The characteristic images of the 3D printed samples used in the durability test are shown in Figure 1.



Figure 1. FFF 3D printed samples used in seawater durability tests.

### Acknowledgments

This research has been supported by the European Regional Development Fund within the Activity 1.1.1.2 “Post-doctoral Research Aid” of the Specific Aid Objective 1.1.1 “To increase the research and innovative capacity of scientific institutions of Latvia and the ability to attract external financing, investing in human resources and infrastructure” of the Operational Programme “Growth and Employment” (No. 1.1.1.2/VIAA/3/19/478).

### References

1. S. Bakradze, E. Arājs, S. Gaidukovs, V.K. Thakur, *Polymers*, **12**(12) (2020).

# Lignocellulose Sustainable Material Preparation Strategy from Biomass Waste

Sergejs Gaidukovs<sup>1\*</sup> and Sergejs Beluns<sup>2</sup>

<sup>1</sup>Institute of Polymer Materials, Faculty of Materials Science and Applied Chemistry, Riga Technical University, P. Valdena 3/7, LV-1048 Riga, Latvia

\* [sergejs.gaidukovs@rtu.lv](mailto:sergejs.gaidukovs@rtu.lv)

The strategy to prepare all lignocellulose sustainable material from biomass waste is presented herein. These materials can be formulated as sustainable composites from lignocellulose and hemicellulose matrices loaded with lignocellulose components. The proposed strategy incorporates the use of only sustainable and biobased raw materials or minimal chemical treatment routes. For example, agricultural and wood industry waste could be used to prepare sustainable biocomposites. Different size fractions of cellulose – nanocrystals, nanofibers could be processed into spatial network structures, while hemicellulose - xylan could act as a modifier providing strength and toughness. Lignin addition to the obtained materials provides enhanced thermal stability. Further modification could be performed including the natural and modified vegetable oils and waxes developing transparent/translucent and hydrophilic/hydrophobic materials.

The processing technology includes the water solution blending and assembly of the components into the bulk materials of the controlled porosity and density. Finally, foams, papers, coatings, and composites could be obtained. The raw natural micro- and nano-components composition adjustment provide broad possibilities to control the exploitation properties of the materials. Durability properties of the prepared materials relate directly to the material composition, formulation process, lignocellulose modification route, and biocomposite processing technology. The rigid, soft, and ductile deformational performance of the materials can be easily controlled to some extent. The lignocellulose components' regulated assembly could be used to control the nanostructure and final performance characteristics of the composites.

Application of the obtained materials includes sustainable films, coatings, packaging, insulation and composites.

## Acknowledgments

This research is funded by the Latvian Council of Science, project RealHLC No. lzp-2019/1- 0390.

## References

1. S. Beluns, O. Platnieks, S. Gaidukovs, O. Starkova, A. Sabalina, L. Grase, V.K. Thakur, G. Gaidukova, *International Journal of Molecular Sciences*, **22** (23), 2939 (2021).
2. S. Beluns, S. Gaidukovs, O. Platnieks, I. Mierina, L. Grase, G. Gaidukova, O. Starkova, P. Brazdausks, V.K. Thakur, *Industrial Crops and Products*, **170**,113780 (2021).

## Biochars and activated carbons obtained from herbs as low-cost and regenerable adsorbents of polymers

Marlena Gęca<sup>1\*</sup>, Małgorzata Wiśniewska<sup>1</sup> and Piotr Nowicki<sup>2</sup>

<sup>1</sup>Department of Radiochemistry and Environmental Chemistry, Institute of Chemical Sciences, Faculty of Chemistry, Maria Curie-Skłodowska University in Lublin, M. Curie-Skłodowska Sq. 3, 20-031 Lublin, Poland,

<sup>2</sup>Department of Applied Chemistry, Faculty of Chemistry, Adam Mickiewicz University in Poznań, Uniwersytetu Poznańskiego 8, 61-614 Poznań, Poland.

\*marlena.geca@wp.pl

Limited reserves of natural resources make it necessary to find new, renewable materials. Plants are materials of natural origin, which grow up after harvesting making them inexhaustible resource. Moreover, because of their seasonal growth, harvesting the herbs will not disturb the balance of the ecosystem. Solids obtained from plant biomass are environmentally friendly and their disposal is not troublesome. Activated carbons prepared from the herbs have large surface area and great amounts of surface oxygen functional groups, which make them very effective adsorbents.

Polymers are synthetic compounds which should not get into the environment. They can disturb the balance of the ecosystem, which can have negative consequences for living organisms. Limitation of the polymer amount in the environment is necessary to keep naturally occurring ecosystems unchanged. Macromolecular compounds could be removed from aqueous solutions by adsorption on biochar and activated carbon surfaces. Polymer desorption possibilities from the solid surface enables multiple application of adsorbents, which may reduce the generation of wastes. In the present study, the carbonaceous adsorbents were prepared from the nettle and sage herbs, and used for the removal of polymers from the aqueous solutions.

For this purpose, the plant materials were fragmented into 1.5-2.0 cm pieces, dried at 100 °C and divided into two parts. One of them was pyrolysed for 60 min at 400 °C under nitrogen atmosphere. The biochars obtained in this way were labelled as NE\_B (in case of nettle herb) and SA\_B (in case of sage herb). The second part of the starting materials was subjected to chemical activation. At the beginning the samples were impregnated with 50% H<sub>3</sub>PO<sub>4</sub> at the weight ratio 1:2. After 24 h the samples were dried at 110 °C and subjected to two stages heat treatment, firstly at 200 °C for 30 min and finally at 500 °C for 30 min. Activated carbon obtained from the nettle herb was marked as NE\_AC and that from the sage herb - as SA\_AC. The textural parameters and the surface oxygen functional groups content for biochars and activated carbons were determined. Obtained materials were used for removal of poly(acrylic acid) and polyethyleneimine from aqueous solution (in single and mixed systems of adsorbates). The mean molecular weight of both polymers was 2 000 Da. Poly(acrylic acid) (PAA) is an anionic polymer containing carboxyl group in its structure, whereas polyethyleneimine (PEI) is polymer with cationic character coming from their amine groups. Adsorbed amounts of macromolecular compounds were determined using static method based on the decrease of the adsorbate concentration in the solution after the adsorption process. The PAA concentration was determined by its reaction with hyamine 1622 resulting in formation of white-coloured complex absorbing light at wavelength 500 nm [1]. On the other hand, the PEI reaction with CuCl<sub>2</sub> resulting in formation of blue-coloured complex absorbing light at wavelength 285 nm [2] was applied. Next, the desorption process was carried out in the examined systems using distilled water. The adsorption-desorption measurements were performed at three pH values, i.e. 3, 6 and 9. Moreover the surface charge density and zeta potential were determined for the suspensions without and in the presence of PAA or PEI and their mixture (PAA+PEI).

Obtained activated carbons are characterized by well-developed surface area and low micropore contribution, which can have positive effect on polymer macromolecules adsorption (Table 1). In turn, the surface area of prepared biochars are very small, however mean pore size is about 10 nm, which may be favorable for the penetration of large PAA and PEI molecules into their interior (Table 2).

Table 1. Textural parameters of activated carbons.

Adsorbent	Surface area [m <sup>2</sup> /g]		Pore volume [cm <sup>3</sup> /g]		Mean pore size [nm]	Micropore contribution
	total	micropore	total	micropore		
NE_AC	801	157	0.847	0.074	4.231	0.087
SA_AC	842	155	0.826	0.074	3.926	0.090

Table 2. Textural parameters of biochars.

Adsorbent	Surface area [m <sup>2</sup> /g]	Pore volume [cm <sup>3</sup> /g]	Mean pore size [nm]
NE_B	2.527	0.006	9.594
SA_B	2.182	0.006	10.555

Data presented in Table 3 indicate that both obtained biochars have greater concentration of the surface oxygen functional groups than the activated carbons. Adsorbents prepared from the nettle herb have greater amounts of surface groups in comparison to the analogous materials obtained from the sage herb. Additionally, both activated carbons show acidic character of the surface. Only NE\_B biochar is characterized by a predominance of basic functional groups. High concentration of functional groups is a very positive feature, because it increases the number of possible interactions with the segments of polymeric chains, the result of which is specific structure of adsorption layer.

Table 3. Acid-base properties of biochars and activated carbons.

Adsorbent	Acidic groups [mmol/g]	Basic groups [mmol/g]	Total amount [mmol/g]
NE_B	1.041	1.753	2.794
NE_AC	0.858	0.272	1.13
SA_B	1.109	1.008	2.197
SA_AC	0.436	0.215	0.651

The analysis of the data presented in Table 4 leads to the conclusion that at pH 3 poly(acrylic acid) is adsorbed in greater amounts than polyethyleneimine, independently on the adsorbent type. This proves that PAA carboxyl groups show greater affinity to the solid surface groups. Moreover more coiled conformation of polyacid macromolecules (PAA functional groups are present in undissociated form in solutions at pH 3) enable not only dense packing of adsorption layer, but also effective entering of polymeric coils into the solid pores.

Table 4. Polymers adsorbed amounts on the surface of activated carbons, initial concentration of both polymers was 100 ppm, pH 3.

Studied system	Adsorbed amount [mg/g]	
	NE_AC	SA_AC
PEI	24.58	25.48
PEI + PAA	30.35	24.53
PAA	99.08	89.67
PAA + PEI	63.55	58.05

The PAA adsorbed amounts are noticeably higher in case of NE\_AC activated carbon. It can be the result of slightly larger pore size of this solid and almost two times higher concentration of its surface groups. The PAA adsorbed amounts are considerably lower in the mixed system of both polymers. Polyethyleneimine adsorption from single solution remains on the similar level on both activated carbons surfaces. The presence of PAA has small effect on its adsorption. In the mixed adsorbate systems the PAA-PEI complexes are formed due to the strong electrostatic attraction between the polymers with opposite charge. They can be adsorbed on the solid surface or can remain in the solution. Such complexes formation has unfavorable influence on PAA removal from mixed adsorbate system.

To sum up, activated carbons obtained via chemical activation of the nettle and sage herbs show good sorption properties towards poly(acrylic acid) and polyethyleneimine, both in relation to single and binary systems of adsorbates. For this reason they can be successfully applied in the ground water and wastewaters purification.

## References

1. W.B. Crummett, R.A. Hummel, *Journal of the American Water Works Association* **1** 209–219 (1963).
2. J. Patkowski, D. Myśliwiec, S. Chibowski, *International Journal of Polymer Analysis and Characterization*, **21** 6 486-494 (2016).



## Enzymatic modification of biopolymers with phenolic antioxidants

Archontoula Giannakopoulou<sup>1</sup>, Renia Fotiadou<sup>1</sup>, Georgia Tsapara<sup>1</sup>, Angeliki C. Polydera<sup>1</sup>, Alexandra V. Chatzikonstantinou<sup>1</sup>, Stamatia Spyrou<sup>1</sup> and Haralambos Stamatis<sup>1\*</sup>

<sup>1</sup>Biotechnology Laboratory, Department of Biological Applications and Technologies, University of Ioannina, 45110 Ioannina, Greece

\*[hstamati@uoi.gr](mailto:hstamati@uoi.gr)

### Abstract

Polymers, such as chitosan (CS) and carboxymethylcellulose (CMC) or hybrids, such as chitosan-gelatin (CS-GEL) are characterized by unique biological properties such as, biocompatibility, biodegradability, nontoxicity, and affinity to proteins [1,2]. Moreover, they contain several reactive amino and hydroxyl groups, susceptible to chemical modifications [3]. The enzymatic targeted modification of polymers has widely attracted the scientific interest for development of innovative biomaterials with enhanced biological properties, such as their antioxidant and antimicrobial activities [4]. The present work describes the application of biocatalytic systems with hydrolytic and redox properties for the targeted crosslinking of various polymers with phenolic bioactive compounds, such as hydroxytyrosol with the ultimate goal of improving their biological and mechanical properties. The successful grafting of the phenolic compounds onto the different polymers was confirmed through various spectroscopic techniques, such as ultraviolet-visible (UV-Vis) spectroscopy. Finally, the modified polymers exhibited strong antimicrobial activity against bacterial populations of *Escherichia coli* BL21DE3 strain as well as an enhancement in their antioxidant activity, suggesting their future potential applications in pharmaceutical and food industry.

### Materials

Chitosan from crab shells (low viscosity), carboxymethyl cellulose, sodium salt, low viscosity (CMC) and laccase from *Agaricus bisporus* (>4 U/mg, lyophilized) were purchased from Sigma-Aldrich (St. Louis, MO, USA). Gelatin from porcine skin was purchased from Fluka (Charlotte, North Carolina, US).

### Methods

#### Enzymatic modification of the polymers

The prepared CS, CS-GEL and CMC solutions were enzymatically modified by laccase from *Agaricus bisporus* with phenolic compounds, such as hydroxytyrosol. Specifically, to a final reaction volume of 20 mL, 1.3% w/v CS or 1.3% w/v CS-GEL or 1.3% w/v CMC solution were mixed with 5 mM hydroxytyrosol solution solubilized in MeOH and 0.086 U/mL (60 µg/mL) laccase from *Agaricus bisporus* were added to initiate the reaction. The reactions were plated on petri dishes and incubated at 30 °C and 80 rpm O/N. At standard time intervals, 1 mL of the reaction was taken in order to monitor the reaction progress through the changes observed in the UV spectra. Finally, the plates were placed open to dry at 45 °C O/N to form films (as shown in Figure 1).



Figure 1. Enzymatic modification of chitosan with phenolic compounds, such as hydroxytyrosol.

#### Antimicrobial properties

Initially, 100 µL of bacterial population was inoculated from stock bacterial populations of *Escherichia coli* BL21DE3 strain, stored in glycerol, in 5 mL of fresh Lysogeny Broth (LB). After incubation at 37 °C, O/N under constant stirring at 180 rpm the pre-culture absorbance was measured at 600 nm and diluted with fresh LB so that the new culture reached an optical density (OD) of about 0.08 absorbance. The new culture was incubated at 37 °C, under stirring at 180 rpm, until the bacterial population present an O.D. of 0.2-0.5. The culture was then centrifuged at 4,000 rpm for 5 minutes, the bacterial precipitate was restored and redissolved in saline (0.9% w/v NaCl). After three successive washes the bacterial pellet was redissolved in an equal volume of the culture. Bacterial population samples of 107 CFU/mL were prepared. Approximately 0.5 mg of each sample was added into an Eppendorf tube containing 100 µL of the bacterial population and it was incubated for 12 hours in a cold chamber. 100µL of bacterial in the absence of sample were used as a control. Then, 25 µL of the bacterial population that interacted with the sample, were inoculated into 225 µL of fresh LB medium in an Elisa microplate well. The microplate was then placed in an incubator chamber at 37 °C and measurements of the O.D. at 600 nm were taken after eight hours.

## Results and Discussion

The laccase catalyzed oxidation of phenolic compounds, such as hydroxytyrosol (HD) to reactive intermediates and their subsequent reaction with the functional groups of chitosan was examined. Ultraviolet-visible (UV-Vis) spectroscopy was applied to monitor the reaction progress. As shown in Figure 2, the reaction spectrum presents a significant increase in the absorption band in the range 450-550 nm over time, followed by its gradual shift to 520 nm, suggesting the successful modification of chitosan with hydroxytyrosol.

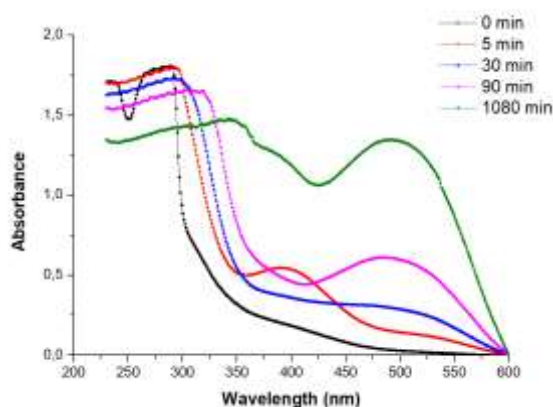


Figure 2. Ultraviolet-visible (UV-Vis) spectrum in the range of 200-600 nm of the reaction progress of the enzymatic functionalization of chitosan (CS) with hydroxytyrosol catalyzed by laccase from *Agaricus bisporus* at standard time intervals.

Also, the antibacterial activity of the enzymatically modified membranes was evaluated and the results are presented on Table 1. Chitosan itself has antimicrobial activity, reducing cell growth to 56% compared to cell growth incubated for 12 hours in the absence of any inhibitory agent. The modified CS almost totally inhibits the bacterial cell growth, as shown in Table 1, suggesting that the enzymatic modification was successful.

Table 1. % Growth of the bacterial cells of strain BL21DE3 after 12 hours in the presence of non-modified and enzymatically modified chitosan membranes with phenolic compounds (the standard deviation was less than 5% in all cases).

Samples	Growth (%)
Control	100
Chitosan	56
Enzymatically Modified Chitosan	8

## Conclusions

The present work demonstrated that a series of various polymers, including chitosan, cellulose and a hybrid chitosan-gelatin polymer were efficiently functionalized with various phenolic compounds through the action of an oxidoreductase enzyme, namely laccase from *Agaricus bisporus*. The efficient cross-link of the biopolymers with the products derived from the laccase-mediated oxidation of phenolics was confirmed through various spectroscopic methods, such as UV-Vis spectroscopy. Finally, the enzymatically modified derivatives were characterized by strong antimicrobial properties, significantly superior to the biological activities that exhibited the non-modified polymers, implying their future potential application in many areas, from food-packaging to pharmaceuticals and cosmetics.

## Acknowledgements

This research has been co-financed by the European Regional Development Fund of the European Union and Greek national funds through the Operational Program Competitiveness, Entrepreneurship, and Innovation, under the call RESEARCH-CREATE-INNOVATE (project code: T2EDK-01410).

## References

1. Wang, W., Xue, C., & Mao, X., *International Journal of Biological Macromolecules*, **164** 4532 (2020).
2. Wu, L.-Q., Embree, H. D., Balgley, B. M., Smith, P. J., & Payne, G. F., *Environmental Science & Technology*, **36** 3446 (2002).
3. Karaki, N., Aljawish, A., Humeau, C., Muniglia, L., & Jasniewski, J., *Enzyme and Microbial Technology*, **90** 1 (2016).
4. Yang, J.; Sun, J.; An, X.; Zheng, M.; Lu, Z.; Lu, F.; Zhang, C., *RSC Advances*, **8** 6759 (2018).

## Taking advantage of side reactions: the example of furfuryl alcohol polymerization

Pierre Delliere<sup>1</sup> Lucie Quinquet<sup>1</sup> and Nathanael Guigo<sup>1\*</sup>

<sup>1</sup>Institut de Chimie de Nice, Université Côte d'Azur, CNRS, UMR 7272, 06108 Nice, France.

\*Nathanael.Guigo@univ-cotedazur.fr

Abstract text:

Furfuryl Alcohol (FA) is a key intermediate building block in the value-chain of furfural (Figure 1). Via acidic initiation, FA polymerizes into Poly(furfuryl alcohol) (PFA) which is a bio-based thermoset capable of showing high-temperature performances. PFA resins are employed in composite applications for binding various type of fibres or fillers. FA can also be impregnated and polymerized within wood to increase its dimensional stability and resistance to e.g. marine borers' attack.[1] The peculiar properties of PFA are associated with its dense network formed by cycloaddition of furanic and dihydrofuranic units.

This communication aims at highlighting how furan ring opening reactions – so far simply considered as side reactions can impact the PFA structure and properties. We have demonstrated that the crosslink density and the glass transition temperature ( $T_g$ ) of the final cross-linked PFA can be modified when FA polymerization is conducted with protic polar solvents.[2] We have recently proposed to use the so-called Degree of Open Structures (DOS) as a quantitative indicator for assessing the ring opening reactions during FA polymerization. As highlighted in Figure 1, ring opening during FA polymerization lead to the formation of carbonyl species –mostly ketonic groups. Therefore, we have adapted a titrimetric method and a quantitative spectroscopic method (i.e. derivatization with a fluorinated phenyl hydrazine followed by <sup>19</sup>F NMR spectroscopy) to quantify the side carbonyls formed during polymerization. The results obtained with both methods are consistent and in agreement with <sup>13</sup>C quantitative solid-state NMR. Interestingly we have shown that the DOS is multiplied by a factor 2 when polymerization is performed in presence of water.[3] Overall, the DOS can reach values as high as 0.15 meaning that about 15 % of the furanic units present in PFA are opened in the final resins.[3] We have also investigated the role of different acidic initiators (i.e. Bronsted and Lewis acidic initiators) and the water content on the DOS values. In general, the presence of water remains the most influencing factor for controlling and increasing the DOS while the type of initiator lead to marginal DOS variations among samples [4]. Finally the presentation will focus on how the presence of such carbonyl species can be fully exploited to generate new macromolecular architectures with tunable properties.

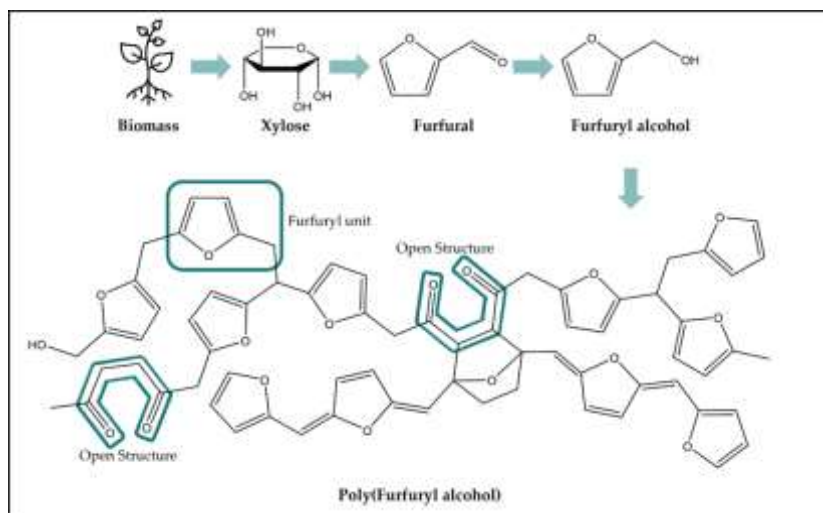


Figure 1. value chain from biomass to PFA and PFA structure with special emphasis on opened rings [adapted from ref. 4].

### Acknowledgements

The authors would like to acknowledge the French Agence Nationale de la Recherche – ANR for funding the project FUTURES (ANR-19-CE06-0005).

### References

1. L. S. Martin, S. Jelavić, S. M. Cragg and L. G. Thygesen, *Green Chem.*, **23**, 8003 (2021).
2. G. Falco, N. Guigo, L. Vincent and N. Sbirrazzuoli, *ChemSusChem*, **11**, 1805 (2018).
3. P. Delliere, N. Guigo, *Macromolecules*, **55**, 1196 (2022).
4. L. Quinquet, P. Delliere, N. Guigo, *Molecules*, **27**, 3212 (2022).

## Exploration of sulphur incorporation within sugar-derived cyclic monomers to predict reactivity and polymer properties

Craig Hardy<sup>1</sup> and Antoine Buchard<sup>1\*</sup>

<sup>1</sup>Centre for Sustainable and Circular Technologies, Department of Chemistry, University of Bath, Bath, BA2 7AY, UK.

\*a.buchard@bath.ac.uk

As part of our ongoing research programme on renewable polymers, we, amongst others, have been investigating the potential of monosaccharides as naturally abundant, structurally diverse and highly functionalisable, renewable alternative to petroleum-based plastics.[1,2] Within the last decade the substrate scope has widely expanded, now encompassing a extensive variety of functional groups, including sulphur-containing monomers such as thio-/thiono-carbonates.[3,4] Whilst similar to their oxygenated counterparts, sulphur-containing polymers can possess altered physical properties as well as new features such as photo-degradability.[3,5]

Starting from tri-O-acetyl-D-glucal (commercial or easily prepared from the natural product D-glucose) we have successfully developed efficient synthetic methodologies towards a novel assembly of bi-cyclic monomers with different sulphur/oxygen configurations within the carbonyl functional group. A detailed structural assessment is reported for each monomer, and we discuss any correlations and the potential influence these have upon the polymerisability and subsequent properties of the resultant polymers. Under previously optimised conditions,[3] organocatalytic ring opening polymerisation (ROP) of the monomers proceeds at room temperature, and results in monomer conversions from 15 to 99 % dependant on structural properties as well as the initial monomer concentration. Number average molar masses were largely dependant upon the polymerisation control, reaching in excess of 7,500 g mol<sup>-1</sup> for the xanthate and thionocarbonate monomers. In comparison, the carbonate and thiocarbonate monomers displayed poor control resulting in lower molecular weights and bimodal polymer distributions. The resultant polymers possess differing microstructures dependant on the sulphur configurations within the carbonate group that were identified and assigned accordingly. In addition the unsaturation of the C6 pyranose sugar ring, demonstrated an increase in ring strain and subsequently polymerisability, resulting in both greater conversion (90 %) and molar masses (>10,000 g mol<sup>-1</sup>).

A strong correlation was observed between both the torsion angle ( $\chi$ ) and the calculated ring strain ( $\Delta H_{iso}$ ) of monomers 1–5 as well as the  $\chi$  and observed monomer concentration demonstrating a direct connection between monomer conversion and the ring strain. This allowed for the influence of sulphur incorporation within the carbonyl functional group to be assessed and polymerisability to be rationalised based upon structural properties of the monomers. Lastly, all polymers were shown to be amorphous, with glass transition temperatures ( $T_g$ ) from 65 to 104 °C dependant on sulphur incorporation, and each have an onset of thermal degradation ( $T_{d5\%}$ ) of around 136 to 215 °C. When increasing the sulphur incorporation a decrease in both  $T_g$  and  $T_{d5\%}$  is observed, showcasing a decrease in thermal stability that may be primarily attributed to the increase the free volume within the polymer structure due to the longer carbon–sulphur bonds (C–S (1.73–1.76 Å) and C=S (1.65 Å)), with electronic effects also likely to have an impact.

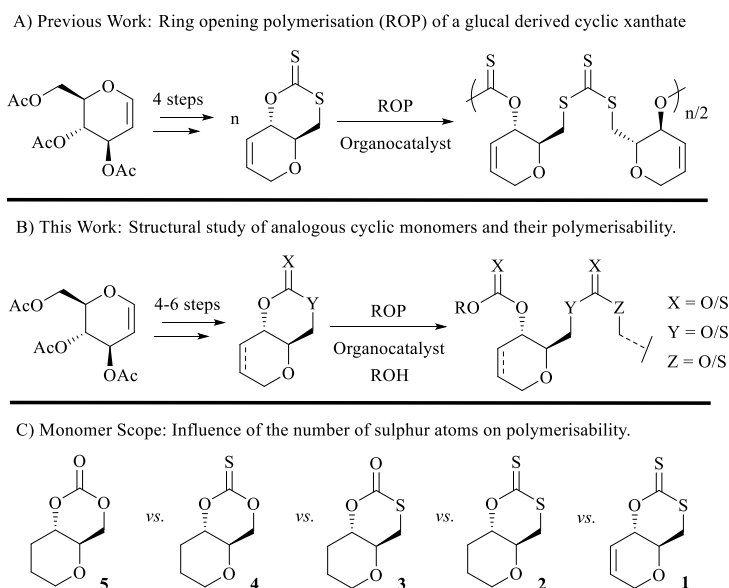


Figure 37. (A) Organocatalysed ring opening polymerisation of a cyclic xanthate; (B) Organocatalysed ring opening polymerisation of novel cyclic monomers and investigation of polymerisability and the properties of resultant polymers; (C) Concept of exploring quantity and arrangement of sulphur atoms within the carbonyl/thiocarbonyl linkage.

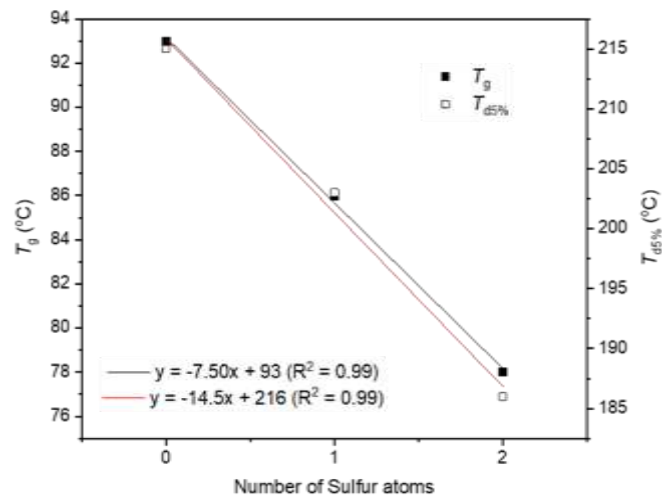


Figure 38. Thermal analysis of both glass transition temperature and degradation temperatures of polymers poly(2–5) versus the quantity of sulphur atoms in their respective monomers. Notable omissions include poly(3) ( $T_g$  = N/A) and poly(5) ( $T_{d5\%}$  = 136 °C).

### Acknowledgements

We thank the Royal Society (UF\160021, fellowship to AB; RGF\EA\201023; RGF\EA\180028, studentship to CH) for research funding.

### References

1. G. L. Gregory, E. M. López-Vidal and A. Buchard, *Chem. Commu.*, 2017, **53**, 2198-2217.
2. S. L. Kristufek, K. T. Wacker, Y.-Y. T. Tsao, L. Su and K. L. Wooley, *Nat. Prod. Rep.*, 2017, **34**, 433-459.
3. C. Hardy, G. Kociok-Köhn and A. Buchard, *Chem. Commu.*, 2022, **58**, 5463-5466.
4. E. M. López-Vidal, G. L. Gregory, G. Kociok-Köhn and A. Buchard, *Polym. Chem.*, 2018, **9**, 1577-1582.
5. U. L. D. I. Kalana, P. P. Datta, R. S. Hewawasam, E. T. Kiesewetter and M. K. Kiesewetter, *Polym. Chem.*, 2021, **12**, 1458-1464.

## Green synthesis and characterization of novel furan-based oligoesters for organogel applications

Ioan Bîtcan<sup>1</sup>, Anamaria Todea<sup>1</sup>, Diana Dreavă<sup>1</sup>, Iulia Păușescu<sup>1\*</sup>, Francisc Peter<sup>1</sup>, Lajos Nagy<sup>2\*</sup> and Sándor Kéki<sup>2</sup>

<sup>1</sup>Politehnica University Timisoara, Faculty of Industrial Chemistry and Environmental Engineering, 6 Vasile Parvan Bvd, 300223, Timisoara, Romania;

\* e-mail: iulia.pausescu@upt.ro

<sup>2</sup>Department of Applied Chemistry, Faculty of Science and Technology, University of Debrecen, H-4032

Egyetem tér 1, 4032 Debrecen, Hungary

\* e-mail: nagy.lajos@science.unideb.hu

The utilization of vegetable oils and their derivatives as raw materials came in the spotlight of green chemistry in the past decades. Their universal availability, low price, and biodegradability place oil derivatives as important biobased sources for polymer synthesis, as well [1]. Castor oil is one of the most studied natural oils due to its high content of ricinoleic acid, a natural hydroxy acid (> 80%). The presence of the double bond in the ricinoleic acid molecule allows additional functionalization by grafting reactions. Copolymers of hydroxy acids have been already synthesized by biocatalysis and have promising applications in several fields [2].

5-Hydroxymethylfurfural (HMF), a biobased platform chemical obtained during biomass pretreatment allows a wide range of chemical modifications, leading to important value added products. Recently, it has been quantitatively oxidized to 5-hydroxymethyl-2-furoic acid (5OH2FA) by *Gluconobacter oxydans* DSM 50049 cells [3]. A combination of vegetable oil and furan derivatives represents a sustainable synthetic way to materials with original properties obtained through simple, green, and efficient processes.

In this study, the polymerization of ricinoleic acid and 5OH2FA was investigated by a green biocatalytic pathway. The reactions were carried out using commercially available native and immobilized lipases as catalysts in organic solvents, ionic liquids, and solvent-free systems, at various molar ratios and temperatures up to 80°C. The lipase from *Pseudomonas stutzeri* showed the highest catalytic efficiency at 50°C in *t*-BuOH. The insertion of 5OH2FA units into the ricinoleic acid estolide backbone was demonstrated by MALDI-TOF MS and 2D NMR analysis. The thermal properties of the oligoester products were evaluated by TG and DSC.

The organogelator ability of the resulted oligoesters in the absence or presence of other components was tested by using several organic solvents with different log P values, at different temperatures. The morphological, and rheological properties of the resulted organogels were evaluated.

### Acknowledgements

This work was supported by a grant of the Romanian Ministry of Education and Research, CNCS - UEFISCDI, project number PN-III-P1-1.1-TE-2019-1573, within PNCDI III, contract number TE 101.

### References

1. A. Todea, I. Bîtcan, D. Aparaschivei, I. Păușescu, V. Badea, F. Peter, V. Gherman, G. Rusu, L. Nagy, S. Kéki, *Polymers* **11**, 9 (2019).
2. A. Todea, D. Aparaschivei, V. Badea, C.G. Boeriu, F. Peter, *Biotechnol. J.* **13**, 6 (2018).
3. M. Sayed, S.-H. Pyo, N. Rehnberg, R. Hatti-Kaul, *ACS Sustainable Chem. Eng.* **7**, 4, 4406 (2019).

## Xylose and hemicellulose sugar streams dehydration to furfural in aqueous and biphasic media

S. P. Ioannidou<sup>1</sup>, A. G. Margellou<sup>1</sup>, and K. S. Triantafyllidis<sup>1,2,\*</sup>

<sup>1</sup> Department of Chemistry, Aristotle University of Thessaloniki, Greece

<sup>2</sup> Center for Interdisciplinary Research and Innovation (CIRI), AUTH, Thessaloniki, Greece

\*e-mail: [ktrianta@chem.auth.gr](mailto:ktrianta@chem.auth.gr)

There is a growing demand to investigate the utilization of renewable sources for fuels, chemicals and materials within the scope of sustainable development by applying the principles of Green Chemistry. Lignocellulosic biomass which is composed of the three biopolymers cellulose, hemicellulose and lignin, constitutes one of the most attractive renewable feedstocks. This study aims to the valorization of the hemicellulose fraction and of its most abundant carbohydrate and respective monomer sugar, i.e. xylan and xylose, towards furfural, which amongst other applications, it can be used as a substrate for producing hydrocarbon based fuels via condensation and hydrodeoxygenation processes.

Pure (model) xylose was utilized to investigate the effect of the dehydration reaction conditions (time, temperature and pressure), medium (water, organic solvent) and catalyst (homogeneous/liquid or solid acid catalysts, concentration etc). Various organic solvents were utilized to form biphasic systems, combined with the use of NaCl to facilitate the in-situ extraction of the formed furfural to the organic phase, while inorganic acids in very low concentrations were used as catalysts (H<sub>2</sub>SO<sub>4</sub>, H<sub>3</sub>PO<sub>4</sub>, HCl). Real hemicellulose aqueous streams, isolated during the dilute acid hydrothermal pretreatment of beechwood sawdust, were also used for the furfural production experiments. The aqueous solution, after the reaction, was analyzed by HPLC while the organic phase in the case of biphasic systems, after separation, was analyzed by GC-MS.

The optimum process conditions for higher furfural yield were 175°C, 15 min and 10 bar N<sub>2</sub>. The reaction temperature, in comparison with the time, is the dominating factor which affects conversion of xylose, reaching the maximum ~100% at about 190°C. On the other hand, selectivity to furfural is higher at moderate temperatures and shorter time due to the commence of degradation/condensation reactions of furfural and higher by-products selectivity at higher temperatures and longer time reactions. The moderate pressure of 10 bar also improves the furfural yield in comparison with the absence of N<sub>2</sub> or at higher pressures. Water and ethanol were tested as reaction solvent with water to be more appropriate for the xylose dehydration reaction. Preliminary experiments in biphasic systems were also conducted with the aim to induce the in-situ extraction of furfural to the organic phase, thus reducing its degradation to humins which occurs mainly in the aqueous phase. The water:THF (1:1) and the higher NaCl concentration led to enhanced furfural recovery and yield via its extraction to the organic phase. In the above optimization, sulphuric acid (H<sub>2</sub>SO<sub>4</sub>) at low concentrations was used as the homogeneous/liquid catalyst. Higher sulphuric acid concentration led to higher conversion of xylose but lower selectivity and yield of furfural due to furfural degradation towards humins. In the case of the real hemicellulose aqueous streams derived from the hydrothermal pretreatment of beechwood sawdust, slightly more intense conditions compared to the model xylose experiments were needed to achieve comparable high sugars conversion and moderate/high furfural selectivity and yield, along with humins formation.

### Acknowledgements

The support via EU-Horizon 2020 and internal funds is gratefully acknowledged. S. Ioannidou would like to acknowledge the financial support through the PhD scholarship program GRACE (Graduate School for Climate and Environment) and HEPTA project of Karlsruhe Institute of Technology.

## Production of value-added furanic compounds via photocatalytic selective oxidation of 5-hydroxymethylfurfural

Zoi-Lina Koutsogianni<sup>1</sup>, Dimitrios A. Giannakoudakis<sup>1,\*</sup>, Kyriazis Rekos<sup>1</sup>, Sofia Tsoumachidou<sup>1</sup>,  
Konstantinos S. Triantafyllidis<sup>1,2,\*</sup>

<sup>1</sup> Department of Chemistry, Aristotle University of Thessaloniki, 54124 Thessaloniki, Greece

<sup>2</sup> Center for Interdisciplinary Research and Innovation (CIRI-AUTH), Balkan Center, 57001 Thessaloniki, Greece

\*e-mail address of corresponding author: [dagchem@gmail.com](mailto:dagchem@gmail.com); [ktrianta@chem.auth.gr](mailto:ktrianta@chem.auth.gr)

### Abstract:

Due to the upcoming limitation of the petroleum based raw materials, production of value-added chemicals through the utilization of abundant biomass is currently a key research objective that concentrates also the industrial attention. 5-hydroxymethyl-furfural (HMF) is among the chemical compounds that can be obtained from cellulosic biomass [1]. HMF, owing to the presence of two functional groups, can undergo facile chemical transformations, resulting to products of high added value. Among them is 2,5-diformyl-furan (DFF) which is widely used for the preparation of urea-furan resins, pharmaceuticals, fungicides, etc. The achievement of the photocatalytic selective oxidation of HMF to DFF, under mild conditions of pressure and temperature and predominately without the use of additional reagents, is an area of great scientific interest. The design and development of novel efficient nano-photo-catalysts plays the most important role. Among a great variety of materials with photocatalytic properties, titanium oxide based materials have shown efficient photoactivity especially in applications such as the unselective oxidative decomposition of organic compounds [2].

In the present work, titanium oxide nanotubes were prepared using two commercial TiO<sub>2</sub> nanomaterial precursors, P25 and P90. In order to limit the formation of aggregations and to achieve better dispersion and activation of the nanoparticles, low-frequency ultrasounds were applied during the synthesis followed by hydrothermal treatment (150 °C) [3]. Physicochemical characterization revealed the existence of significant differences in the physicochemical features, with the nanotubes derived from titania P90 (TiNTbs-90) having smaller average sizes (6-19 nm external diameter) (**Figure 1**) and higher specific surface area (325 m<sup>2</sup>/g) comparing to the nanotubes derived from titania P25 (TiNTbs-25).

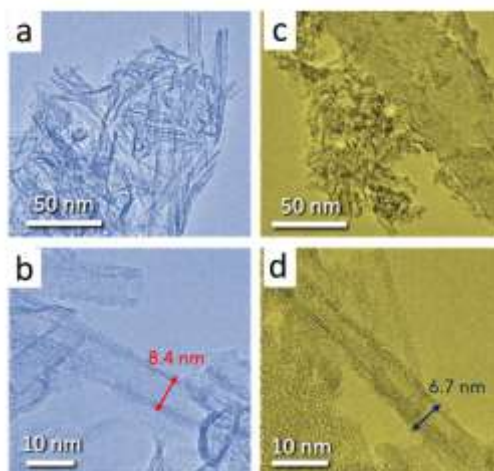


**Figure 39.** TEM and HRTEM images: (a-b) TiNTbs-25 and (c-d) TiNTbs-90.

The photocatalytic activity of the one-dimensional nanomaterials was evaluated by monitoring the partial oxidation of HMF in acetonitrile solution under the influence of low-intensity ultraviolet light (UV) radiation (370 nm) for 1 h. The commercial titania materials showed higher conversion (84–100%) compared to nanotubes (50–77%). However, the selectivity towards DFF was greater for the nanotubes resulting in a better overall performance (**Figure 2**). In particular, P90-derived nanotubes exhibited a four-fold higher DFF selectivity compared to TiO<sub>2</sub> P90 nanoparticles, while P25-derived nanotubes exhibited a more than 50% higher DFF selectivity compared to P25 TiO<sub>2</sub> nanoparticles. The highest yield of 43% was recorder in the case of TiNTbs-90, a value almost two times higher comparing to TiNTbs-25 and more than three times higher comparing to TiO<sub>2</sub> P90 nanoparticles.



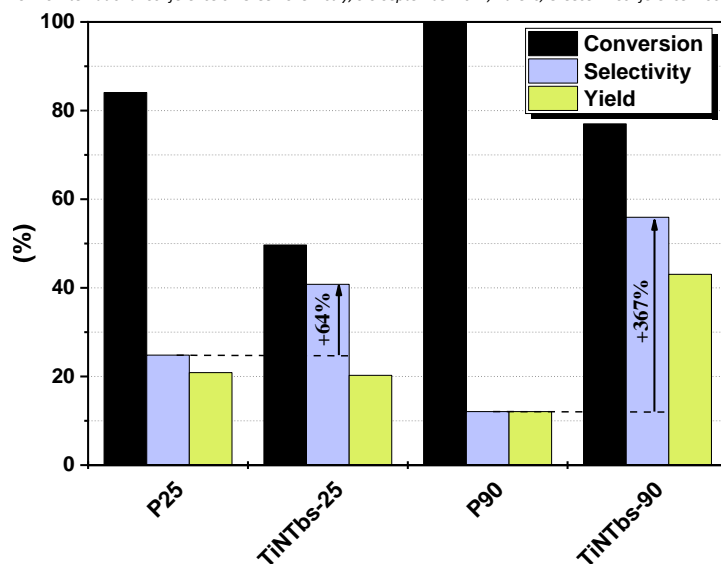


**Figure 2.** Conversion, selectivity and yield of the commercial materials, P25 and P90, and corresponding nanotubes TiNTbs-25 and TiNTbs-90, after one hour of UV exposure ( $\sim 34^{\circ}\text{C}$ , 300 rpm magnetic stirring, 1g/L catalyst concentration, 15 ml stock solution of 1mM HMF in acetonitrile).

### Acknowledgements

This research has been co-financed by the European Regional Development Fund of the European Union and Greek national funds through the Operational Program Competitiveness, Entrepreneurship and Innovation (EPAnEK 2014-2020), under the Action “RESEARCH – CREATE – INNOVATE” B’ CALL (project code: T2EDK-01243).

### References

1. D. A. Giannakoudakis, J. C. Colmenares, D. Tsiplakides, K. S. Triantafyllidis, *ACS Sustainable Chemistry & Engineering*, **9**(5) 1970–1993 (2021).
2. D. A. Giannakoudakis, V. Nair, A. Khan, E. A. Deliyanni, J. C. Colmenares, K. S. Triantafyllidis, *Applied Catalysis B: Environmental*, **25** 117803 (2019)
3. D. A. Giannakoudakis, K. Vikrant, A. P. LaGrow, D. Lisovytskiy, K.-H Kim, T. J. Badosz, J. C. Colmenares, *Chemical Engineering Journal*, **415** 128907 (2021).

## Use of V<sub>2</sub>O<sub>5</sub> Sheets as an Efficient Catalyst for the Hydroxyalkylation Alkylation Reaction for the Production of Biofuel Precursors

Sahil Kumar, Tripti Chhabra, and Venkata Krishnan\*

School of Basic Sciences and Advanced Materials Research Center, Indian Institute of Technology Mandi, Kamand, Mandi 175075, H.P., India. Email: [vk@iitmandi.ac.in](mailto:vk@iitmandi.ac.in)

The demand for fossil fuels increases day by day to meet the world's energy demands because of industrial development, and the rapid increase in population. For now, the entire world using predominantly non-renewable fossil fuels, such as coal, gas, and petrol to meet these energy demands. Due to burning of these fossil fuels, large amount of CO<sub>2</sub> produced which ultimately causes global warming. Also, these energy resources are very limited. So, there is an urgent need to find their replacement. Lignocellulosic biomass is a promising solution to these problems because it can be utilized as a transportation fuel, since it is naturally abundant and environmentally sustainable. Chemicals obtained from lignocellulose only contain a maximum of six carbon atoms for example furfural, methyl furan, 5-hydroxymethyl furan (5-HMF), etc. For the production of biofuel, these chemicals undergo C-C coupling reactions, such as hydroxyalkylation alkylation reaction (HAA) reaction, Heck coupling followed by hydrodeoxygenation (HDO) to give the formation of C<sub>8</sub> to C<sub>22</sub> hydrocarbon (biofuel) [1,2]. In our work, we demonstrated the synthesis of V<sub>2</sub>O<sub>5</sub> sheets by using ammonium mono vanadate and oxalic acid at an ambient ratio, which serves as an active, reusable, and highly stable catalyst for the HAA reaction of 2-methyl furan and furfural.

**Synthesis method:** V<sub>2</sub>O<sub>5</sub> sheets have been synthesized according to a previous procedure with some modifications [3]. In brief, 1.7 g of ammonium mono vanadate and 1.8 g of oxalic acid are added in a round bottom flask. Subsequently, 65 mL of distilled water was added into it and allow the solution to stir for 12 h at room temp. To obtain a solution of dark red color having pH less than 3. Further, this red colored solution was transferred to a 100 mL Teflon lined autoclave and kept in an oven at 180 °C for 24 h. NH<sub>4</sub>V<sub>4</sub>O<sub>10</sub> was obtained by centrifugation was washed with distilled water and dried overnight at 80 °C. The dried compound was then ground in mortar pastille and put into a muffle furnace at 400 °C for 1 h at 5 °C min<sup>-1</sup> ramp rate to obtain V<sub>2</sub>O<sub>5</sub> nanosheets. The as-synthesized catalyst has been characterized by using various techniques, such as PXRD, XPS, TGA, TPD and SEM.

**Characterization of V<sub>2</sub>O<sub>5</sub> sheets:** The PXRD pattern of V<sub>2</sub>O<sub>5</sub> sheets is shown below in Fig. 1(a). The PXRD reveal the the formation of an orthorhombic phase of V<sub>2</sub>O<sub>5</sub> having great crystallinity. The XPS spectra of V<sub>2</sub>O<sub>5</sub> is shown in Fig.1(b). The peaks at 525.07 eV and 517.47 eV arise due to the spin-orbit coupling of the component corresponding to V<sup>5+</sup> 2p<sub>1/2</sub> and V<sup>5+</sup> 2p<sub>3/2</sub>. The peaks at 523.57 eV and 516.25 eV corresponds to V<sup>4+</sup> 2p<sub>1/2</sub> and V<sup>4+</sup> 2p<sub>3/2</sub>, indicating the formation low oxidation state vanadium. SEM images of V<sub>2</sub>O<sub>5</sub> reveals the sheet-like morphology as shown in Fig. 1(c,d).

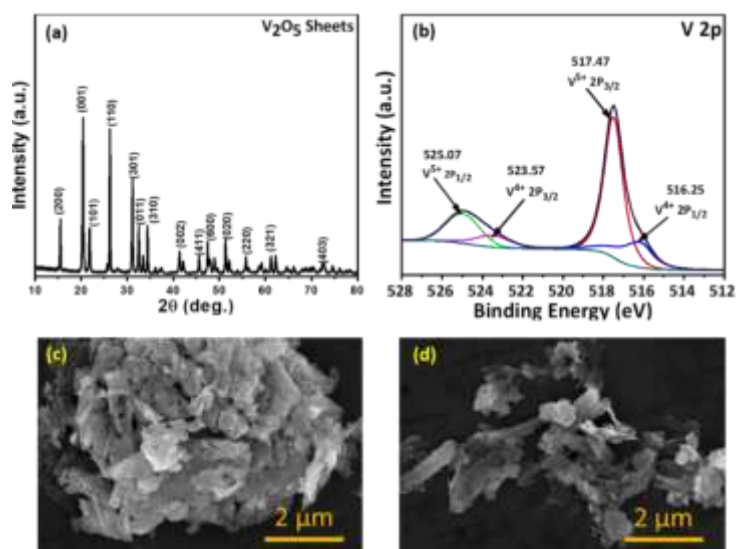
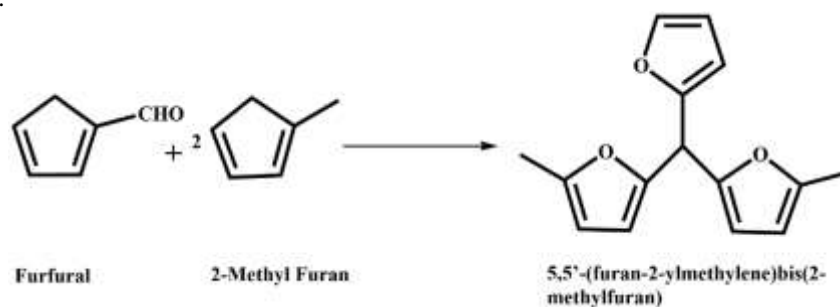


**Fig. 1** (a) PXRD plot of V<sub>2</sub>O<sub>5</sub>, (b) XPS spectra of V 2p, (c,d) SEM images of V<sub>2</sub>O<sub>5</sub> sheets.

**Catalytic activity study:** Catalytic reaction performed in this study is schematically shown in Scheme 1. In brief, it was performed in a 5 mL glass vial, which include a rice magnetic bead. The temperature of the reaction was controlled by using an oil bath. In a typical reaction, 1 mmol of furfural, 2 mmol of 2-methyl furan, and 100 mg of catalyst was added to the glass vial. Close the glass vial and sealed it with help of teflon and kept it in the oil bath when its temperature reaches to 55 °C. The reaction mixture was stirred at 55 °C for 24 h. The catalyst is

separated by centrifugation after the addition of ethyl acetate. The product was purified and isolated using column chromatography.



**Scheme 1.** HAA catalytic reaction for the production of biofuel precursor.

Further studies on substrate scope, mechanism and stability of the catalyst are in progress. Nevertheless, the currently obtained results clearly demonstrates the feasibility of using  $V_2O_5$  nanosheets as an efficient heterogenous catalyst.

### References

1. Chhabra, T.; Dwivedi, P.; Krishnan, V., *Green Chemistry*, , **24**, 898-910, (2022).
2. Raguindin, R. Q.; Gebresillase, M. N.; Han, S. J.; Seo, J. G., *Sustainable Energy & Fuels*, **4** (6), 3018-3028, (2020).
3. Song, H.; Zhang, C.; Liu, Y.; Liu, C.; Nan, X.; Cao, G., . *Journal of Power Sources*, **294**, 1-7, (2015).

## Metabolic engineering of *Methyloviumicrobium alcaliphilum* 20Z for production of ectoine from methane and lignocellulosic sugars

Eun Yeol Lee\*, Diep Ngoc Pham

Department of Chemical Engineering, Kyung Hee University, Yongin-si,  
Gyeonggi-do 17104, South Korea

\*Correspondence to: [eunylee@khu.ac.kr](mailto:eunylee@khu.ac.kr)

Bioconversion of renewable sources to value-added products has emerged as an attractive strategy for industrial biomanufacturing. In this study, we engineered *Methyloviumicrobium alcaliphilum* 20Z to metabolize lignocellulose-derived sugars, including glucose and xylose, together with methane. Xylose was used to supply more ribulose 5-phosphate, which is subsequently condensed with formaldehyde to operate the ribulose monophosphate (RuMP) cycle. Glucose was supplied for strengthening the carbon flux through the Embden-Meyerhof-Parnas (EMP) pathway. RNA-seq data of engineered strain grown on three substrates (methane, xylose, glucose) revealed the up-regulation of the aspartate metabolism pathway, which involves the production of ectoine. Ectoine is an osmotic protective agent that has been widely applied in biotechnology, cosmetics, and medicine. Engineered strain grown on three substrates generated a 1.7-fold higher productivity of ectoine (26.43 mg/g-DCW) compared to methane solely (15.65 mg/g-DCW). The ectoine biosynthesis-transcription repressor gene (*ectRI*) was knocked out to improve the biosynthesis of ectoine. As a result, the mutant strain produced ectoine productivity of 37.93 mg/g-DCW, which is higher than the initial condition by 2.4-fold. The co-cultivation of three substrates presented in this study provided a novel strategy for enhancing ectoine production in methanotrophic bacteria without using a high-salt medium.

**Keywords:** methane, xylose, glucose, ectoine, methanotrophic bacteria.

### References

- I.I. Mustakhimov, A.S. Reshetnikov, A.S. Glukhov, V.N. Khmelenina, M.G. Kalyuzhnaya, and Y.A. Trotsenko, *J. Bacteriol.* 192(2), 410-417 (2010).
- A.D. Nguyen, T.H.T. Chau, E.Y. Lee, *Chem. Eng. J.* 420, 127632 (2020).
- J. E. Gonzalez and M. R. Antoniewicz, *Curr. Opin. Biotechnol.* 43, 86-95 (2017).

## Laccase immobilization onto polymeric supports for synthetic dyes degradation

Anca Leonties\*<sup>1</sup>, Ludmila Aricov<sup>1</sup>, Raluca Visan<sup>1</sup>, Aurica Precupas<sup>1</sup>, Alexandru Neculae<sup>1</sup>, Catalina Gifu<sup>2</sup>, Adina Raducan<sup>3</sup>

<sup>1</sup> Department of Colloid Chemistry, "Ilie Murgulescu" Institute of Physical Chemistry, Romanian Academy, Spl. Independentei 202, 060021 Bucharest, Romania;

<sup>2</sup> Department of Polymer, National Institute for Research and Development in Chemistry and Petrochemistry - ICECHIM, Spl. Independentei 202, 060021 Bucharest, Romania;

<sup>3</sup> Department of Physical Chemistry, Faculty of Chemistry, University of Bucharest, Bd. Elisabeta 4-12, 030018, Bucharest, Romania.

\*[ancaleonties@gmail.com](mailto:ancaleonties@gmail.com)

Synthetic dyes are hazardous contaminants found in aqueous environments that hinder efforts to obtain safe and readily available water. Counteracting the side effects of synthetic dyes by selective decontamination of aqueous media may be achieved under optimal conditions using enzymes. However, these natural catalysts are unstable due to the protein structure, which is easily distorted by unfavorable chemical and physical factors. Therefore, the current study was designed to improve the resistance of the *Trametes versicolor* Laccase against pH, temperature and long-term storage by using solid support immobilization. For this, the laccase was immobilized on supports made from pure chitosan or polyacrylic acid-chitosan mixture, while glutaraldehyde was used as crosslinking agent. The kinetic characterization was performed to understand how the polymeric mixture stabilizes and improves the catalytic properties of the enzyme. Furthermore, it was investigated whether the laccase is protected from both thermoinactivation and unwanted effect of long-term storage. In the applicative part, the immobilized enzyme was tested against two azo dyes in terms of discoloration efficiency and compared with the free enzyme.

Materials: Chitosan with low molecular weight (CS), laccase (Lc, EC 1.10.3.2, from *Trametes versicolor*), polyacrylic acid (PAA), glutaraldehyde (Ga), 2,2'-Azino-bis (3-ethylbenzothiazoline-6-sulfonic acid) diammonium salt (ABTS) were all supplied by Sigma-Aldrich Chemical Co. and used without further purification.

Methods: The CS and CSPAA (2:1 wt.) microspheres were obtained by the precipitation of the polymeric solutions in sodium hydroxide solution [1, 2]. The laccase was covalently immobilized onto glutaraldehyde activated polymeric microspheres and the total protein content evaluated by the modified Bradford assay [1]. The final products were noted CSGaLc and CSPAAGaLc and further analyzed. The laccase assay conditions were chosen so that proper spectrophotometric monitoring of ABTS consumption, good time scale for the kinetic experiments and the detection of Lc thermal inactivation were ensured. The extended kinetic curves of the substrate decomposition in the presence of Lc were measured for 10 minutes at  $\lambda = 420$  nm ( $\epsilon = 36000$  M<sup>-1</sup> cm<sup>-1</sup>) and converted in substrate concentration in time curve. The linear portions of the extended curves were linearly fitted and used to obtain initial reaction rates ( $r^0_R$ ). The Michaelis-Menten method was used to investigate the effect of substrate concentration on free and immobilized Lc while the overall inactivation rates were estimated using the Selwyn test [1].

Depending on the chosen support, the laccase had different activity patterns. The differences generated due to the immobilization supports were revealed by the Selwyn test and data are illustrated in **Figure 1**. The results proved that the CSGaLc was inactivated at large substrate conversions while for the CSPAAGaLc this phenomenon was diminished.

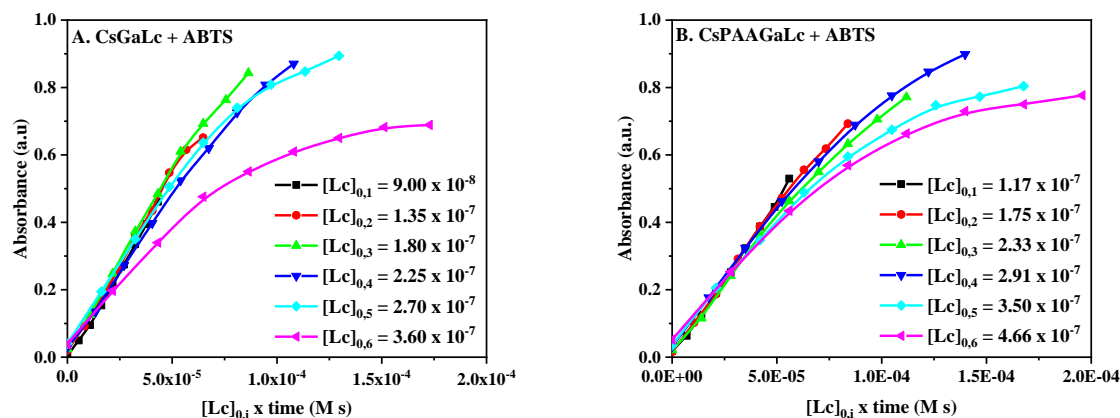


Figure 1. Selwyn test representation for inactivation of immobilized Lc at different initial concentrations -  $[Lc]_{0,i}$  by ABTS. (A. CsGaLc and B. CsPAAGaLc).

The overall operational stability of immobilized laccase was strongly influenced by the microspheres composition, the PAA content playing a leading role. The CSPAAGaLc had the highest reaction rate, the highest amount of active enzyme and the best operational profile. The results underline the fact that both the support and the enzyme immobilization technique could be implemented in the pollutant removal protocols from real wastewater samples.

### Acknowledgements

This work was supported by project TE 68/2022-PN-III-P1-1.1-TE-2021-0418 and by the Romanian Academy within the research program 'Colloids and dispersed systems' of the 'Ilie Murgulescu' Institute of Physical Chemistry.

### References

1. L. Aricov, A. R. Leonties, I. C. Gifu, D. Preda, A. Raducan, D.F. Anghel, *J. Env. Manag.* **276** 111326 (2020).
2. A. R. Leonties, A. Răducan, D. C. Culiță, E. Alexandrescu, A. Moroșan, D. E. Mihaiescu, L. Aricov, *Chem. I Eng. J.* **439** 135654 (2022).

## Tailored pretreatment/fractionation of forest and agricultural biomass towards selective isolation of lignin, hemicellulose and cellulose

Antigoni G. Margellou\*, Eleni A. Psochia, Stylianos Torofias and Konstantinos S. Triantafyllidis

<sup>1</sup>Department of Chemistry, Aristotle University of Thessaloniki (AUTH), Thessaloniki, Greece

\*amargel@chem.auth.gr

Biorefinery schemes aim to the valorization of the whole lignocellulosic biomass. The most important step is the pretreatment/fractionation of the biomass components which can enhance the downstream valorization towards value added chemicals and fuels. Within this context, this work aims to the efficient isolation of cellulose, hemicellulose and lignin from a wide variety of forest and agricultural residues, i.e. beech wood sawdust, poplar and olive tree prunings, etc. The fractionation of the lignocellulosic biomass is based in one or two step pretreatments.

Hydrothermal pretreatment in neat water under relatively intense conditions (220 °C, 15 min) enhances the hemicellulose removal (65-96%) in the liquid fraction, in the form of xylose monomers and degradation products (organic acids, HMF, furfural, etc.) [1-2]. In the solid fraction, the “surface lignin” can be extracted by “green” and easily recoverable solvents (ethanol, acetone, etc.) [3]. Delignification of the hydrothermally pretreated samples is in the range of 44-57%, depending on the biomass nature. Biomass loss, i.e. not being recovered in the form of useful sugars, furans or acids, due to humins formation can be prevented by the addition of dilute acid as catalyst during the pretreatment which allowed milder (temperature, time) conditions leading to enhanced recovery of xylose monomers at high degrees of hemicellulose removal (40-80%).

Alternatively, organosolv pretreatment with ethanol-water as solvent mixtures can be applied. During organosolv pretreatment, hemicellulose is removed in the liquid fraction (43-59%) while lignin is recovered as solid (delignification: 33-61%), depending on the type of biomass. Both hemicellulose removal and delignification can be increased to 48-90% and 51-86%, after the addition of dilute sulfuric acid as catalysts during the organosolv pretreatment. Finally, combination of the hydrothermal pretreatment in aqueous dilute acid with subsequent organosolv pretreatment can led to efficient recovery of each component, especially via providing a clean monomeric sugar stream in the first step and a clean lignin fraction in the second step. The biomass remained after the recovery of hemicellulose and lignin can be converted to pure highly crystalline cellulose via bleaching process using NaClO<sub>2</sub>/CH<sub>3</sub>COOH media. Cellulose recovery can be as high as 66-99% on initial cellulose content in parent biomass and is strongly depended on the pretreatment/fractionation process and biomass type.

### Acknowledgements

This research has been co-financed by the European Regional Development Fund of the European Union and Greek national funds through the Operational Program Competitiveness, Entrepreneurship and Innovation (EPAnEK 2014-2020), under «Special Actions "Aquaculture" - "Industrial Materials" - "Open Innovation In Culture"» (project code: T6YBII-00341).

### References

1. C.K. Nitsos, K.A Matis & K.S. Triantafyllidis, *ChemSusChem*, **6(1)** 110 (2013).
2. C. K. Nitsos, T. Choli-Papadopoulou, K.A. Matis & K.S. Triantafyllidis, *ACS Sustainable Chemistry & Engineering*, **4(9)** 4529 (2016)
3. C. Nitsos, P. Lazaridis, A. Mach-Aigner, K. Matis & K. Triantafyllidis, *ChemSusChem*, **12** 179 (2019).

## Solid-catalyst assisted OxiOrganosolv pre-treatment of wheat straw for enzymatic and microbial conversion to bioactive food additives

Stefanidis S.D.<sup>1</sup>, Kalogiannis K.G.<sup>1</sup>, Karakoulia S.A.<sup>1</sup>, Marianou A.<sup>1</sup>, Staikos S.<sup>2</sup>, Karnaouri A.<sup>2</sup>, Topakas E.<sup>2</sup> and Lappas A.A.<sup>1\*</sup>

<sup>1</sup>Chemical Process and Energy Resources Institute, Centre for Research and Technology Hellas, 57001 Thessaloniki, Greece

<sup>2</sup>Industrial Biotechnology & Biocatalysis Group, Biotechnology Laboratory, School of Chemical Engineering, National Technical University of Athens, 15780 Athens, Greece

\* angel@cperi.certh.gr

### Introduction

Wheat straw is an abundant lignocellulosic agricultural residue that is typically underutilized as low-value animal feed, presenting great potential for utilisation as a renewable feedstock for the production of high added value products. In this work, we investigated the valorisation of wheat straw into nutraceuticals, and more specifically, omega-3 fatty acids. Wheat straw was first fractionated employing an acid-free oxidative organosolv process (OxiOrganosolv) to produce mainly a cellulose-rich solid fraction (pulp). Non-toxic metal oxides and zeolites were used as catalysts to facilitate the fractionation of the feedstock at low temperature. Sugar monomers were obtained from the cellulose-rich pulp via enzymatic hydrolysis using suitable commercial enzyme cocktails. Subsequently, the sugar monomers were used as carbon source for the growth of the heterotrophic marine microalgae *Cryptocodinium cohnii* (*C. cohnii*), and the production of the omega-3 fatty acids. The innovative aspect of this work is the use of the solid catalysts for the fractionation to reduce the severity of the reaction conditions.

### Experimental

The wheat straw feedstock was a soft wheat straw composed of 15.5 wt% extractives, 16.6 wt% lignin, 39.9 wt% cellulose, 22.9 wt% hemicellulose and 3.1 wt% ash. The catalysts that were screened for the catalytic OxiOrganosolv pre-treatment included Fe and Cu pure or mixed metal oxides. The Cu metal oxide was prepared via the thermal decomposition of copper (II) nitrate trihydrate (CuO) at 500 °C for 3 h under air flow at a heating rate of 5 °C/min. The Fe-Cu mixed metal oxide was synthesized via the controlled co-precipitation method, followed by calcination at 500 °C (Cu<sub>2</sub>FeO). A microporous Y zeolite catalyst with a SiO<sub>2</sub>/Al<sub>2</sub>O<sub>3</sub> molar ratio of 5 (Y SAR 5) was also tested. The Y zeolite was purchased from Zeolyst in the NH<sub>4</sub><sup>+</sup>-form and was converted to the H<sup>+</sup>-form by calcination at 550 °C for 4 h under air flow at a heating rate of 5 °C/min. The surface, pore and acidic properties of all catalysts tested are shown in Table 1.

Table 8. Properties of the catalysts used for the catalytic OxiOrganosolv pre-treatment of wheat straw.

Catalyst	BET surface area (m <sup>2</sup> /g)	Micropore surface area (m <sup>2</sup> /g)	External surface area (m <sup>2</sup> /g)	Micropore volume (cm <sup>3</sup> /g)	Total pore volume (cm <sup>3</sup> /g)	Brønsted acid sites (μmol/g)	Lewis acid sites (μmol/g)
Cu <sub>2</sub> FeO	24	0	24	0	0.160	n.d.	n.d.
CuO	1	0	1	0	0.000	n.d.	n.d.
Y SAR 5	918	882	36	0.333	0.378	385	146

The wheat straw biomass was pre-treated via OxiOrganosolv [1] in a 50:50 water:acetone or a 50:50 water:ethanol co-solvent system. The pre-treatment was carried out in a stirred autoclave reactor in pure oxygen atmosphere at 16 bar pressure and at a temperature of 150-160-175 °C for 120 min, without the addition of any soluble acid catalyst. For the catalytic OxiOrganosolv runs, the solid catalyst was added in the reactor at a 1:10 catalyst:feedstock ratio. The pre-treatment produced a cellulose-rich solid fraction (pulp) and a liquid fraction containing sugar monomers and oligomers, as well as precipitated lignin after evaporation of the organic solvent from the liquid fraction. The cellulose-rich pulp from the pre-treatment of wheat straw was enzymatically hydrolysed to obtain sugar monomers using commercial enzyme cocktails, Cellic® CTec2 and Cellic® HTec2, respectively. The sugar monomers were subsequently used as a carbon source for the growth of the heterotrophic marine microalga *C. cohnii*, according to previously described procedures [2], for the production of fatty acids.

### Results and discussion

The pretreatment achieved high lignin removal from wheat straw, up to 88%, as well as close to 100% recovery of the wheat straw cellulose in the produced pulp. The maximum pulp cellulose content achieved was 83%. The most optimum reaction temperature was 175 °C in either acetone or EtOH water mixtures (Figure 1). When using a solid catalyst, the delignification of wheat straw at 150 °C in EtOH:water increased from 42% to up to 63%. The cellulose recovery in the produced pulp remained high, close to 90%, while the cellulose content of the pulp also increased slightly, from 56% to 59% (Figure 2). Cellulose conversion to glucose via enzymatic hydrolysis (Figure 3) increased significantly compared to the untreated wheat straw, attributed to the removal of the protective lignin and the opening of the cellulose structure to the action of the enzymes (Figure 3). The Cu<sub>2</sub>FeO and CuO catalysts produced pulps that exhibited higher hydrolysability (62% and 70%, respectively), compared to the corresponding non-catalytic pre-treatment at 150 °C with EtOH (49%). Finally, regarding the production of the fatty acids, the



OxiOrganosolv pulps proved to be excellent carbon sources for the growth of *C. cohnii*, both compared to sugars derived from untreated wheat straw, and to a model glucose solution. The sugars derived from wheat straw pulps pre-treated with the Cu<sub>2</sub>FeO and CuO catalysts exhibited comparatively poor performance; this was attributed to the presence of Cu ions in the hydrolysates that were leached from the catalysts and inhibited the growth of the microalgae. Future work will focus on more stable metal oxides and other types of acidic zeolites.

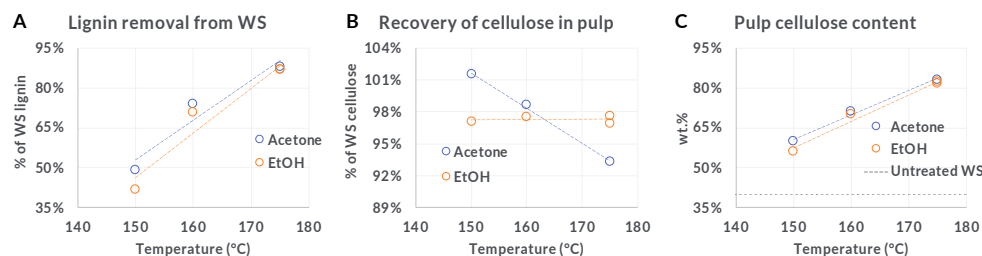


Figure 40. Results from the non-catalytic OxiOrganosolv pre-treatment of wheat straw.

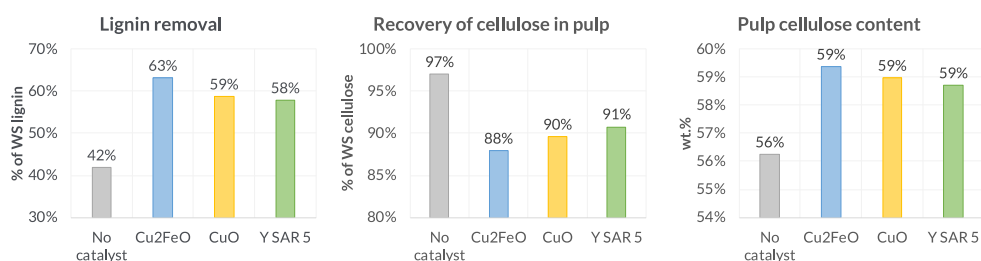


Figure 41. Results from the catalytic OxiOrganosolv pre-treatment of wheat straw (150 °C, EtOH).

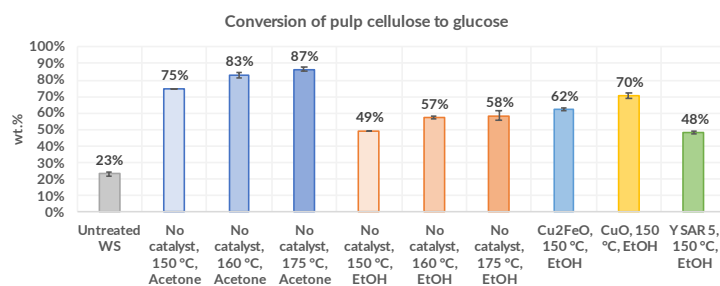


Figure 42. Conversion of pulp cellulose to glucose via enzymatic hydrolysis.

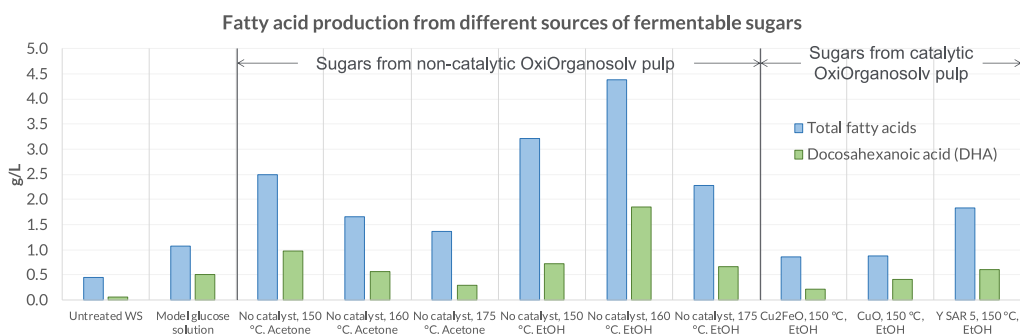


Figure 43. Production of total fatty acids and docosahexanoic acid from the microbial conversion of pulp-derived sugars.

## Acknowledgements

This research was co-financed by the European Regional Development Fund of the European Union and Greek national funds through the Operational Program Competitiveness, Entrepreneurship and Innovation, under the call RESEARCH – CREATE – INNOVATE (project code: T2EDK-00468).



## References

1. K.G. Kalogiannis, A. Karnaouri, C. Michailof, et al. *Bioresource Technol.* **313** 123599 (2020).
2. A. Chalima, A. Hatzidaki, A. Karnaouri, E. Topakas. *Appl Energ.* **241** 130 (2019).

## Production of bio-based gluconic acid from agro-industrial residues: Experimental analysis, process design and techno-economic evaluation

Marianou A., Kaldis S., Michailof C., Lappas A., Karakoulia S.\*

<sup>1</sup>Chemical Process and Energy Resources Institute, Centre for Research and Technology Hellas, Thessaloniki, 6th km. Charilaou – Themi Road, GR-570 01 Themi, Greece

\*matoula@certh.gr

The current work addresses the production of gluconic acid from agro-industrial residues rich in cellulose and/or starch, such as potato peels. The feedstock is converted through a cascade process into pure bio-based gluconic acid, classified in the list of the top 12 ‘hot’ bio-based chemicals due to its numerous applications in the pharmaceutical, metallurgical and polymer industries [1]. Gluconic acid is produced by the oxidation of glucose, which may be performed either biotechnologically or via chemo-catalysis. On an industrial level, due to the lack of efficient heterogeneous catalysts, the synthesis of gluconic acid is currently performed by fermentation, accounting for its small-scale production and increased price. Furthermore, the isolation and purification of the final product is a multi-step process involving different techniques such as centrifugation, adsorption, evaporation, crystallization and ion-exchange. Hence, the cost-effective and eco-friendly production of high purity gluconic acid is remaining a challenge for the chemicals industry. [2]. Thus, the current study proposes a feasible, experimentally developed cascade chemocatalytic process for the production of gluconic acid from potato peels, validated via process modeling and techno-economic analysis.

The catalytic experiments were conducted, in a high-pressure autoclave C-276 stirred reactor by Parr Instruments (USA) with controllable temperature and stirring and continuous monitoring of the temperature. Ion chromatography ICS-5000 (Dionex, USA) was used for the analysis of the liquid samples. The chromatographic method developed allows the simultaneous qualitative and quantitative analysis of 11 sugars, 13 organic acids (including gluconic acid) and 5-HMF.

Based on the experimental results, the process for the production of the desired acid from biomass rich in cellulose and/or starch is modelled in detail using ASPEN PLUS™, a market-leading chemical process optimization software. The process modeling of gluconic acid production is described starting from the biomass feedstock until the production of the biochemicals. Firstly, pretreated or raw biomass rich in cellulose and/or starch undergoes a hydrolysis step, in H<sub>2</sub>O with 1.0 % maleic acid as a catalyst, towards glucose. Afterwards, the glucose-rich solution is submitted to oxidation, over 0.3Au/SiO<sub>2</sub> in a basic aqueous solution of NaOH (pH8) using H<sub>2</sub>O<sub>2</sub> as an oxidant [3] resulting in gluconic acid. The unreacted biomass from all the processes (bio-tar) is retrieved for energy utilization.

Optimized simulation for the process is performed by applying the experimental results of the project and upscaling them at an industrial scale. After the modeling of the process (Figure 1), a cost analysis was held. From the data derived from the simulations regarding equipment design characteristics, estimation of equipment costs and capital investment calculations were performed, based on established techniques [4]. Furthermore, the operational costs of the processes were also calculated. Via cash flow analysis, the minimum selling price- production cost of the corresponding end product of the process was calculated. Moreover, several parameters that have an impact on the production cost of the biochemicals were investigated through sensitivity analysis.

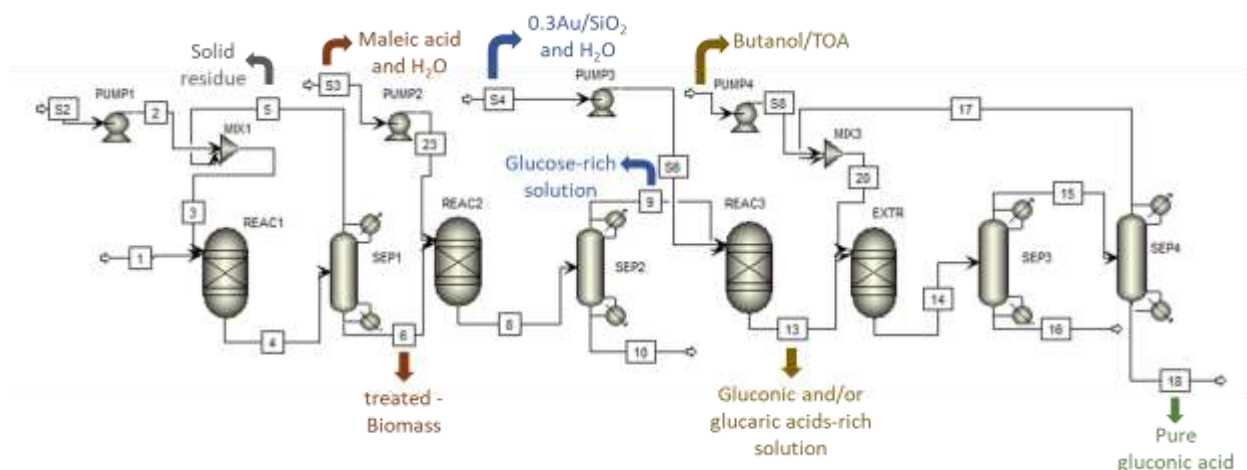


Figure 1. Overview of gluconic acid production process from biomass rich in cellulose and/or starch.

As was confirmed, following the proposed process configuration and parameters, considerable production rates of gluconic acid can be obtained rendering the process plan promising, according to the results of the techno-economic analysis.

### Acknowledgements

This project has received funding from the Hellenic Foundation for Research and Innovation (HFRI) and the General Secretariat for Research and Technology (GSRT), under grant agreement No 287-128035/I2.

### References

1. T. Mehtio, M. Toivari, M. G. Wiebe, A. Harlin, M. Penttila, A. Koivula, *Crit Rev Biotechnol*, **36** 904 (2016).
2. P. Parimal, K. Ramesh, B. Subhamay, *Chemical Engineering and Processing: Process Intensification*, **104** 160 (2016).
3. S.A. Karakoulia, A.A. Marianou, C.M. Michailof, A.A. Lappas, *Catal. Today* (2022) submitted.
4. M. S. Peters, K. D. Timmerhaus, R. E. West, *Plant design and economics for chemical engineers (5th ed.)*, McGraw-Hill (2002).

## Depolymerisation of lignin in sugarcane bagasse by hydrothermal liquefaction to optimize catechol formation

Kwanele B. Mazibuko<sup>1</sup>, Nirmala Deenadayalu<sup>1</sup> and Lethiwe D. Mthembu<sup>1</sup>

<sup>1</sup>Durban University of Technology, PO Box 1334, Durban, 4000, South Africa

\*21409480@dut4life.ac.za

### Abstract

In order to establish suitable conditions to produce catechol from a renewable source, a liquefaction process of lignin obtained from sugarcane bagasse (SB) was investigated. Figure 1 illustrate the catechol production from lignin extracted from biomass. The effect of temperature (100–250 °C), reaction time (60–240 min), and potassium hydroxide (KOH) concentration (1–10 %) were assessed using response surface methodology (RSM) based on the Box-Behnken design (BBD). The screening experiments were performed in a 100 ml batch Parr reactor, equipped with a type J thermocouple (iron-constantan), a magnetic stirrer and polytetrafluoroethylene (PTFE) liner. The liquid and solid fractions was washed with water. The solid and liquid fractions were separated by vacuum filtration [1] [2]. The lignin fragment was quantified using high performance liquid chromatography (HPLC) and characterized using Fourier transform infrared spectroscopy (FTIR). The optimum conditions were found to be 175 °C, 240 min, and 10 % of KOH concentration, which yielded 79.11 ppm of catechol from sugarcane bagasse. The analysis of variance (ANOVA) indicated that the design model was significant at the 95% confidence level.

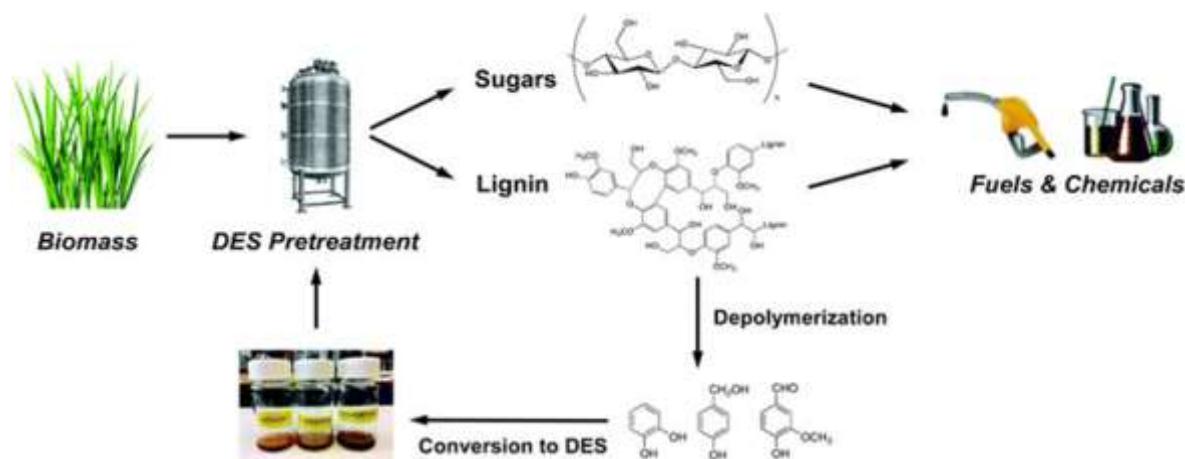


Figure 1. Catechol production from lignin derived.

### Acknowledgements

The authors would like to thank the National Research Foundation (South Africa), Durban University of Technology for the financial support and Sugar Milling Research Institute (Durban, South Africa) for bagasse provision.

### References

1. T. Mkhize, L.D. Mthembu, R. Gupta, A. Kaur, R.C. Kuhad, P. Reddy, N. Deenadayalu. Enzymatic saccharification of acid/alkali pre-treated, mill-run, and depithed sugarcane bagasse. *BioResources*, **11**, 6267-6285 (2016).
2. C.S. Goh, K.T. Lee, S. Bhatia, Hot compressed water pretreatment of oil palm fronds to enhance glucose recovery for production of second-generation bioethanol. *Bioresour Technol*, **101**, 7362-7367 (2010).

## Synthesis and color reduction of Lignin nanoparticles encapsulating CeO<sub>2</sub> for safe, anti-oxidant and high SPF sunscreen

Sadaf Mearaj<sup>1</sup> and Joon Weon Choi<sup>2\*</sup>

<sup>1</sup>Seoul National University, GSIAT, South Korea

\*cju@snu.ac.kr

Abstract text:

The prolonged exposure of human skin to sunlight causes harmful consequences. Sunscreens are commonly used for protecting the skin from UV radiations. However, they contain active ingredients such as Organic chemical filters (OCFs), Physical mineral filters (PMFs) and UV boosters. Recent studies have reported that these active ingredients in sunscreen formulations have harmful effect on marine organisms [1]. Lignin one of the most abundant biopolymer in nature has attracted worldwide attention. Large amount of lignin is produced as a by-product of paper and pulp industry. It contains phenyl propane units and abundant phenolic hydroxyl groups that provides it with UV-shielding properties. These properties enables the use of lignin as an eco-friendly sunscreen additive [2]. However, the dark colour of industrial lignin hinders the applicability of lignin-based sunscreen. TiO<sub>2</sub> and ZnO are the widely used UV-absorbers but these have poor dispersibility and photocatalytic activity affecting the performance of sunscreen. Cerium oxide (CeO<sub>2</sub>) a rare earth metal has tremendous biomedical application and is also reported to have UV- shielding and antioxidant properties [3]. However, there is no research based on lignin/CeO<sub>2</sub> for sunscreen formulations. In this study lignin nanoparticles (LNPs) encapsulating cerium oxide (CeO<sub>2</sub>) were utilized to fabricate a novel light colored and broad spectrum sunscreen.

Kraft lignin was lightened by methanol fractionation, acetylation and acetylation of methanol fractionated lignin. The obtained lignins were synthesized into lignin nanoparticles (LNPs) by dialysis method. The LNPs were analysed by zeta-sizer, NMR, 2DHSQC and L&W brightness colour test to investigate the differences. The LNPs were encapsulated with CeO<sub>2</sub>. LNPs encapsulating CeO<sub>2</sub> were mixed with pure NIVEA cream in different ratios (1%, 2%, 4%, 6%, 8%, 10%) to develop a light-coloured lignin-based sunscreen. The sunscreen performance was evaluated by UV-transmittance, SPF measurement and anti-oxidant test. The safety of the developed sunscreen was further evaluated by cyto-toxicity test.

A visible reduction in colour was seen after fractionation and follow up acetylation. After synthesizing into lignin nanoparticles, the colour was further reduced. Based on the analysis mentioned above, acetylated-methanol fractionated lignin showed better properties as compared to the other two kinds of lignin. Thus, methanol-acetylated LNPs was chosen to encapsulate CeO<sub>2</sub>. After mixing with a cream, the colour was completely reduced with no staining on the skin. Under an amount of 6% of LNPs-CeO<sub>2</sub> addition into the cream, the SPF of lignin-based sunscreen reached 70.27 which is best enough to meet the daily needs and it showed almost no staining on the skin. The anti-oxidant performance increased with the increased concentration of LNPs-CeO<sub>2</sub>. Cytotoxicity test indicated safety and biocompatibility of the lignin-based sunscreen.

This work demonstrates the applicability of lignin for sunscreen formulations and also addresses the issue of lignin colour. A simple and economical approach was used the lighten the colour of lignin. Moreover, this study utilizes a novel approach of encapsulating CeO<sub>2</sub> with lignin for sunscreen applications which has not been reported before. This novel Lignin nanoparticle based CeO<sub>2</sub> anti-oxidant sunscreen has good potential in high-end and natural skincare products.

### Acknowledgements

This research was funded by the Basic Science Research Program (NRF-2019R1A2C2086328) of the National Research Foundation funded by the Ministry of Science and ICT.

### References

- [1] D. Sánchez-Quiles, A. Tovar-Sánchez, Are sunscreens a new environmental risk associated with coastal tourism?, *Environ. Int.* 83 (2015) 158–170. <https://doi.org/10.1016/J.ENVINT.2015.06.007>.
- [2] X. Qiu, Y. Li, Y. Qian, J. Wang, S. Zhu, Long-Acting and Safe Sunscreens with Ultrahigh Sun Protection Factor via Natural Lignin Encapsulation and Synergy, *ACS Appl. Bio Mater.* 1 (2018) 1276–1285. <https://doi.org/10.1021/acsabm.8b00138>.
- [3] C. Xu, X. Qu, Cerium oxide nanoparticle: A remarkably versatile rare earth nanomaterial for biological applications, *NPG Asia Mater.* 6 (2014). <https://doi.org/10.1038/am.2013.88>.

# Hydrothermal upgradation and mineralization strategies for synthesis of platform chemicals, pharmaceuticals and biomaterials-The ultimate wastewater grown algal biorefinery approach

Farah Naaz<sup>1</sup>, Arghya Bhattacharya<sup>1</sup>, Kamal Kishore Pant<sup>2</sup>, Anushree Malik<sup>1</sup>,

<sup>1</sup>Applied Microbiology Laboratory, Centre for Rural Development and Technology, IIT Delhi, Delhi-110016, India

<sup>2</sup>Catalytic Reaction Engineering Laboratory, Department of Chemical Engineering, IIT Delhi, Delhi- 110016, India

Corresponding author email: [farahnz25@gmail.com](mailto:farahnz25@gmail.com), [farah.naaz@rdat.iitd.ac.in](mailto:farah.naaz@rdat.iitd.ac.in)

## Abstract

Waste valorization, especially the development of biorefineries out of waste resources are the prime steps towards attaining a circular bioeconomy [1]. Integration of wastewater bioremediation using microalgae and a green processing technique like hydrothermal liquefaction (HTL) to valorize this microalgal biomass shows potential of developing a sustainable waste biorefinery. Lately, the focus of researchers working on HTL has been on the biocrude as a fuel value product [2]. However, using strategic hydrothermal upgradation of biocrude and hydrothermal mineralization of the aqueous fraction, platform chemicals, pharmaceuticals and biomaterials can be synthesized, which have a promising potential of developing a sustainable biorefinery.

HTL conditions for high biocrude yield (43±3%, dry biomass basis) were optimized. The HTL products; biocrude, aqueous fraction and solids were characterized using GC-MS analysis, LC-MS analysis, CHN analysis, MPAES analysis. The HTL biocrude yield was appreciable but it comprised of high nitrogen and oxygen content (that decreased its fuel value/calorific value) and hence, it required upgradation (deoxygenation and denitrogenation). Furthermore, the GC-MS analysis of the biocrude showed the presence of high value industrially relevant compounds that required enrichment. Efforts were made to improve the quality (upgradation/enrichment) of the HTL products by varying the solvent (methanol or butanol)/catalyst (ZSM-5 or KOH)/reaction gas (CO<sub>2</sub>) during the HTL reactions, keeping all other HTL conditions same as that of the optimized reaction. On the other hand, the LCMS analysis of aqueous fraction showed the presence of highly valuable pharmaceuticals (minoxidil and ethosuximide), that were quantified for the first time in the current study. Additionally, this calcium and phosphorus rich aqueous fraction was hydrothermally mineralized to produce hydroxyapatite, a bone mineralizer (synthetic bone).



*This work targets 6 sustainable development goals, critical to the survival of earth.*

## Acknowledgements

The financial support by Department of Biotechnology, Ministry of science and technology, India (grant number DBT/IC-2/Indo-Brazil/2016-19/06) and Multi-Institutional Faculty Interdisciplinary Research Projects (MFIRP) scheme of the Industrial Research & Development (IRD) Unit of IIT-Delhi, India (grant no. IITD/IRD/MI02021/MFIRP) are greatly appreciated.

## References

1. Mohan, S. V., Nikhil, G. N., Chiranjeevi, P., Reddy, C. N., Rohit, M. V., Kumar, A. N., & Sarkar, O. (2016). Waste biorefinery models towards sustainable circular bioeconomy: critical review and future perspectives. *Bioresource technology*, 215, 2-12.
2. Ratha, S. K., Renuka, N., Abunama, T., Rawat, I., & Bux, F. (2022). Hydrothermal liquefaction of algal feedstocks: The effect of biomass characteristics and extraction solvents. *Renewable and Sustainable Energy Reviews*, 156, 111973.

# Hybridization of chemically modified cellulose and hydroxyapatite applicable to tough biomass materials

Kohei Okuda\* and Tadashi Mizutani

Graduate School Science and Engineering, Doshisha University

\*cyjf1703@mail4.doshisha.ac.jp

Abstract text:

We synthesized the coprecipitated nanocomposites of carboxymethyl cellulose (CMC) and hydroxyapatite (HAP) by imitating biomineralization of bones in order to develop tough biomass materials. The CMC-HAP composite with a degree of substitution of 0.5 had the most controlled HAP crystal growth and the highest bending strength (101 MPa) and elastic modulus (10.5 GPa). These results indicate that the interaction between the organic-inorganic interface of carboxy groups of CMC improve the mechanical properties. Despite its low load on people and environment, these composites have the higher bending strength and the elastic modulus than those of polyamide 6 (92 MPa) and polyamide 6 with 40 wt % glass fibers ( $5.5 \pm 1.2$  GPa), so they can be expected to be used in new biomass materials alternative to petroleum-derived engineering plastics

## 1. Introduction

In this research, we synthesized the coprecipitated nanocomposites of carboxymethyl cellulose (CMC) and hydroxyapatite (HAP:  $\text{Ca}_{10}(\text{PO}_4)_6(\text{OH})_2$ ) by imitating biomineralization of bones in order to develop tough biomass materials.

In recent years, the problems of global warming, oil depletion, and marine plastic waste have become more serious, and materials that are environmentally friendly and have excellent mechanical properties are emphasized. Therefore, we focused on the bones produced by biomineralization. Bones are organic-inorganic composites consisting of collagen fibers and HAP. Since the crystal growth of HAP is controlled by the hydroxy groups and carboxy groups on the surface of the collagen fibers, bones have the “brick-and-mortar” structure in which the organic phase and the inorganic phase are regularly arranged and bonded [1]. Therefore, although bones are produced under extremely mild conditions, they have both the flexibility of organic polymers and the rigidity of inorganic crystals, and exhibit high toughness comparable to the bending strength of iron [2]. Like collagen, CMC is fibrous and has many carboxy groups that can interact with HAP, so they can bind and orient with HAP [3-5]. In addition, CMC and HAP are obtained in large quantities from the abundant forest and mineral resources of the earth. If the composites having a function comparable to or higher than that of bone can be synthesized from CMC and HAP, it can be expected to be used as a new tough biomass material to replace the conventional petroleum-derived engineering plastics and ceramic materials. In this study, we clarified the optimum degree of carboxymethylation of CMC that improves the mechanical properties of the CMC-HAP composite.

## 2. Experimental section

### Carboxymethylation of cellulose

Cellulose powder was stirred in 2-propanol/2 M NaOH mixed solution (9/1, v/v) at 60 °C for 30 minutes. Sodium chloroacetate powder was added with feed degree of substitutions (the number of carboxymethyl groups introduced in the three hydroxy groups in the glucose unit of cellulose) was 0.1, 0.3, and 0.5, and the mixture was stirred at 60 °C for 3 hours. After completions of the reaction, the mixture was neutralized with 1 M HCl aqueous solution until the pH reached 7, followed by addition of methanol, and the precipitates were collected by suction filtration. After washed with water and methanol (1/1, v/v), the precipitate was dehydrated by adding methanol[6]. The obtained powder was vacuum dried at 80 °C for 2 hours.

### Hybridization of CMC and HAP by coprecipitation

As shown in Fig. 1, CMC powder with feed degree of substitution of 0.1, 0.3, 0.5, or unmodified cellulose powder (i.e., degree of substitution 0) was stirred in an aqueous solution prepared by mixing  $\text{Na}_2\text{HPO}_4$  and NaOH at 70 °C for 30 minutes. Aqueous  $\text{CaCl}_2$  was added at a rate of 0.06 mL/s at 70 °C. After completion of the addition, the mixture was stirred at the same temperature for 1 h. The feed CMC/HAP weight ratio was 30/70. After being cooled to room temperature, to the mixture was added water–acetone (1:1, v/v). The white precipitates were suction filtered, and washed with water–acetone (1:1, v/v). Finally, the powder was dehydrated by adding a large excess of acetone and then suction filtered. The obtained powder on filter paper was vacuum dried at 80 °C for 2 hours.

The inorganic contents of the obtained coprecipitated composites powders were assessed by thermogravimetric analysis. The crystallite sizes on *c*-axis direction of HAP were determined by X-ray diffraction. Also, the composite powders were placed in a mold with a rectangular slot with dimensions of 4 mm × 13 mm, and they were uniaxially pressed at 300 MPa at 120 °C for 5 min to obtain prism-shaped test blocks of 4 mm × 13 mm × 1.5–1.7 mm. The bending strengths and elastic moduli were evaluated by a three-point bending test.

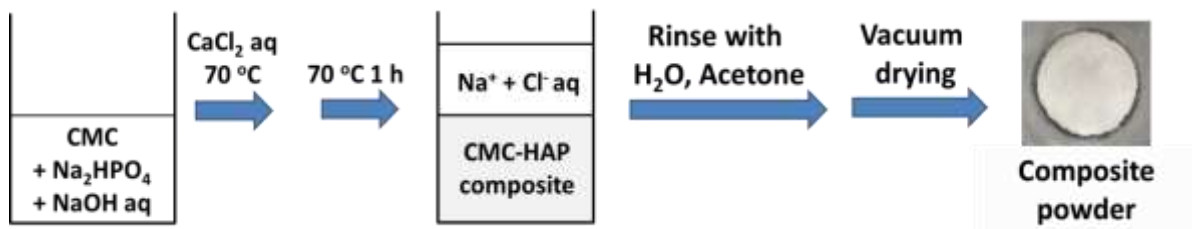


Fig. 1. Synthesis of the composites of CMC and HAP by coprecipitation.

### 3. Results and discussion

The inorganic contents of the obtained coprecipitated composite powders were 62 to 64 wt%, which were close to the feed value of 70 wt%, regardless of the degree of substitution of carboxymethyl groups.

Fig. 2 shows that the higher the degree of substitution of CMC, the smaller the crystallite size of HAP in the *c*-axis direction. Since the *a*-plane of the crystallite of HAP is positively charged, the anionic carboxy groups bind to the *a*-plane of HAP [7]. Therefore, a high density of the carboxymethyl groups on cellulose would retard the crystal growth of HAP. Also, the higher the degree of substitution of CMC and the more controlled the crystal growth of HAP, the higher the bending strength of the composites. These results indicate that the interaction between the carboxy group of CMC and the *a*-plane of HAP formed the “brick-and-mortar” structure of CMC and HAP as shown in Fig. 3, which improved the mechanical properties of the composites.

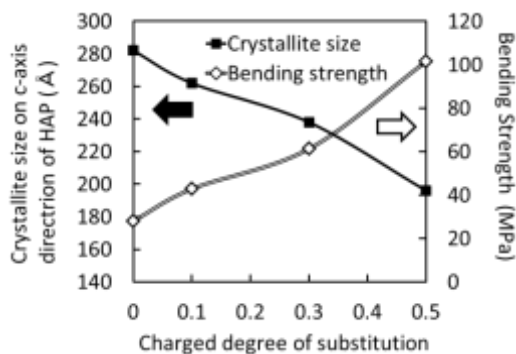


Fig. 2. Effects of the degree of substitution on the crystallite size on *c* axis direction of HAP and the bending strengths of the composites

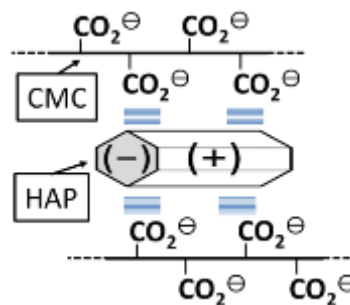


Fig. 3. Schematic representation of the brick-and-mortar structure of CMC-HAP

Despite that CMC and HAP are obtained in large quantities from the abundant forest and mineral resources on the earth and have a low burden on humans and the environment, the composite of HAP and CMC with a charged substitution degree of 0.5 has a bending strength comparable to that of polyamide 6 (92 MPa) [8]. Moreover, its elastic modulus was 10.5 GPa, higher than that of polyamide 6 with 40 wt % glass fibers ( $5.5 \pm 1.2$  GPa) [9]. These findings indicate that they can contribute to Sustainable Development Goals (SDGs) as a new tough biomass composite materials that can replace the petroleum-derived engineering plastics used in car and airplane bodies.

### Acknowledgements

This work was supported by JST SPRING, Grant Number JPMJSP2129. We thank Professor Ken Hirota for his kind advices of the molding process

### References

1. L.C. Palmer, C.J. Newcomb, S.R. Kaltz, E.D. Spoerke, S.I. Stupp, *Chem. Rev.* **108** 4754 (2008).
2. J. Ma, J. Wang, X. Ai, S. Zhang, *Biotech. Adv.* **32** 744 (2014).
3. K. Okuda, T. Mizutani, K. Hirota, T. Hayashi, K. Zinno, *ACS Sustainable Chem. Eng.* **9** 158 (2021).
4. K. Okuda, K. Hirota, T. Mizutani, Y. Numamoto, *Mater. Adv.* **2** 5691 (2021).
5. K. Okuda, R. Shigemasa, K. Hirota, T. Mizutani, *ACS Omega* **7** 12127 (2022).
6. T. Heinze, K. Pfeiffer, *Die Angewandte Makromolekulare Chemie* **266** 37 (1999)
7. T. Kawasaki, M. Niikura, Y. Kobayashi, *J. Chromatography* **515** 125 (1990).



8. Z.G. Hernández, Z.N.M. Teran, P.G. Morones, R.Y. Macías, S.G.S Rosales, G.Y.Romero, I.S. Nieves, E.H. Hernández, *J. Appl. Polym. Sci.* **138** 50857 (2021)
9. M. Nagakura, Y. Tanimoto, N. Nishiyama, *Dent. Mater. J.* **36** 415–421 (2017)

## Synthesis and Characterization of Unsaturated Polyester Resins Based on Adipic Acid

L. Papadopoulos<sup>1,\*</sup>, Alexandra Zamboulis<sup>1</sup>, Christina Kyriakou-Tziamtzi<sup>2</sup>, S. Tsompanidis<sup>3</sup>, N. Athanasopoulos<sup>3</sup>, Electra Papadopoulou<sup>4</sup>, Konstantinos Chrissafis<sup>2</sup> and Dimitrios N. Bikiaris<sup>1,\*</sup>

<sup>1</sup>Laboratory of Organic Chemical Technology, Department of Chemistry, Aristotle University of Thessaloniki, GR-54124, Thessaloniki, Greece

<sup>2</sup>Solid State Physics Section, Physics Department, Aristotle University of Thessaloniki, GR-541 24 Thessaloniki, Greece

<sup>3</sup>Phee, 17 Kolokotroni Str., Rio, Patras, GR-26504, Tel : 2613023239, www.phee.gr

<sup>4</sup>CHIMAR HELLAS SA, 15km National Road Thessaloniki-Polygyros, GR-57001 Thessaloniki, Greece

\*lazaros.geo.papadopoulos@gmail.com, dbic@chem.auth.gr

### **Abstract**

Management of plastics has grown into a challenge for our society. On one hand, single use plastics have contributed substantially to the accumulation of waste in landfills and oceans, poisoning the environment through microplastics formation. On the other hand, crude oil, the primary raw material for plastics production, is a nonrenewable resource whose price has been fluctuating along with its projected availability. Therefore, the need for the development of polymers from renewable resources, the so-called bio-based polymers, has emerged.

Among others, unsaturated polyester resins (UPRs) are one of the most used polymer classes today. They are linear polycondensation products which contain unsaturated double bonds in the polymer backbone. They are then combined with unsaturated monomers, called reactive diluents, to create three dimensional networks via radical polymerization, which can be thermally or UV induced. The aim of this work is the production of novel UPRs based on adipic acid, a biobased monomer with a huge market and environmental potential. Several characterization methods were utilized to examine the physicochemical properties of the materials.

**Keywords:** *unsaturated polyester resins, adipic acid, biobased polymers*

### **Acknowledgements**

This research has been co-funded by the European Regional Development Fund (ERDF) and Greek national funds through the Operational Program "Competitiveness, Entrepreneurship and Innovation", EPAnEK 2014-2020, under the call "Aquaculture"- "Industrial materials"- "Open innovation in culture" as well as by private funds (project T6YBP-00006).

## Exploring the potential of itaconic acid based unsaturated polyester resins as high performance green materials for UV 3D printing applications

Lazaros Papadopoulos<sup>1</sup>, Tobias Robert<sup>2</sup> and Dimitrios Bikiaris<sup>1\*</sup>

<sup>1</sup>Department of Chemistry, Aristotle University of Thessaloniki, GR-541 24 Thessaloniki, Greece

<sup>2</sup>Fraunhofer Institute for Wood Research—Wilhelm-Klauditz-Institut WKI, Bienroder Weg 54E, 38108 Braunschweig, Germany

\*dbic@chem.auth.gr

### Abstract

Additive manufacturing (AM), also known as three-dimensional (3D) printing, is a production technique for products of high customization regarding their size, shape, and design. Guided by Computer Aided Design (CAD) software, objects are printed layer by layer, achieving accuracy and significantly less waste material compared to traditional processing techniques.

AM can employ different types of polymers, depending on the specifications of the 3D printer. One of the most used polymers are UV curable resins, mainly comprised from acrylic acid based polyesters and polyurethanes. However, acrylic acid based materials can possess allergenic and irritation potential, can be volatile and toxic, especially at low molecular weights, while also not being produced from renewable resources. Therefore, alternative biobased monomers and resins are of high interest.

In this work, we developed unsaturated polyester resins, of high biobased content, and studied their properties and printability with a DLP 3D printer. To this end, monomers from renewable resources were utilized for the synthesis of the polyesters, like itaconic acid, succinic acid and 1,3 propane diol. The produced resins were evaluated regarding their physicochemical properties and the materials produced via 3D printing were characterized as to their thermomechanical properties.

**Keywords:** DLP 3D printing, biobased polymers, itaconic acid.

### Acknowledgements



The research work was supported by the Hellenic Foundation for Research and Innovation (HFRI) under the 3rd Call for HFRI PhD Fellowships (Fellowship Number: 6186).

## Bio-based P-F resins for wood-based panels by substituting phenol and formaldehyde with biomass-derived phenolics and furfural

Christina P. Pappa<sup>1,2</sup>, Stylianos A. Torofias<sup>1,2</sup>, Antigoni G. Margellou<sup>1,2</sup>, Electra Papadopoulou<sup>3</sup>,  
Paschalis Tsirogiannis<sup>3</sup>, Themistoklis Sevastiadis<sup>3</sup>, Konstantinos S. Triantafyllidis<sup>1,2,\*</sup>

<sup>1</sup> Department of Chemistry, Aristotle University of Thessaloniki (AUTH), 54124 Thessaloniki, Greece

<sup>2</sup> Center for Interdisciplinary Research and Innovation (CIRI-AUTH), Balkan Center, 10th km Thessaloniki-Thermi Rd,  
P.O. Box 8318, 57001 Thessaloniki, Greece

<sup>3</sup> CHIMAR HELLAS SA, 15km NR Thessaloniki-Polygyros, 57001 Thermi, Thessaloniki, Greece

\*e-mail address of corresponding author: [ktrianta@chem.auth.gr](mailto:ktrianta@chem.auth.gr)

In recent decades, concerns about the environment, sustainability of materials and products, as well as long-term petrochemical supply security has created a significant need to shift focus towards alternative sources of energy, chemicals and materials. In particular, intense focus has been placed on the partial or complete replacement of petroleum based raw materials/chemicals used in the production of Phenol-Formaldehyde (PF) resins, i.e., phenol and formaldehyde [1]. PF resins/binders are major components in construction and furniture industry and thus, investigating alternative green chemicals to be utilized in the production of bio-based PF-type resins and their wood-based composites, is of paramount importance. In addition, minimization of the use of formaldehyde, would lead to reduced problems owing to its emissions from wood-based panels.

Lignocellulosic biomass, obtained from agricultural/forestry residues, food industry processes and so on, is considered as one of the most promising sources of raw materials as it is a natural and sustainable alternative to petroleum [2]. Lignin is one of the three main components of biomass and is the most abundant natural source of phenolics. Lignin has been already studied for replacing phenol in PF resins and wood composites with success, in percentages as high as 50 wt% [3]. In addition, lignin can be depolymerized to highly reactive phenolic monomers and low molecular weight oligomers, such as phenol, guaiacol, creosol etc., with appropriate processes like fast pyrolysis. The lignin bio-oils composition can be tailored, depending on the use or not of catalysts, in order to contain reactive alkoxy/alkyl phenols and aromatics [4]. Furthermore, by utilizing integrated biorefinery processes that aim towards the holistic utilization of biomass, furanic monomers like furfural can be obtained from hemicellulose-derived xylose and be further utilized as sustainable green alternative to formaldehyde.

In this work, we studied the reactivity of phenolic monomers found in lignin fast pyrolysis bio-oils (replacing phenol) as well as the reactivity of furfural (replacing formaldehyde) in the condensation reactions taking place during the synthesis of PF resins. The lignin bio-oils were derived from fast pyrolysis experiments of organosolv lignin isolated from agricultural and wood residues, mainly olive tree prunings and commercial beechwood sawdust organosolv lignins. The composition of the bio-oils was determined by GC-MS, GC-FID, and NMR (by AUTH). Representative phenolics included in the bio-oils were 2-methylphenol, 2,4-dimethylphenol, guaiacol, syringol, creosol and 2-methoxy-4-propylphenol. The reactivity and crosslinking ability of individual phenolics with formaldehyde or furfural was studied with the aim to identify the reaction mechanisms involved. Based on these data, model bio-oil mixtures were prepared at necessary quantities to synthesize PF resins. The level of replacement of phenol or formaldehyde in the produced resins was 20 wt.%. The new bio-based PF resins were synthesized and tested for their bonding capacity in plywood panels production by CHIMAR. The plywood panels were manufactured in dimensions of 50x50cm and were evaluated for their physical and mechanical properties according to European standards EN 314-1:2004 and EN 314-2:1993 while formaldehyde emissions were determined by the Gas analysis method (EN ISO 12460-3:2015).

The results showed that the use of such biomass derived chemicals/monomers for the replacement of petrochemical phenol and formaldehyde is possible and the respective resins have promising performance.

### Acknowledgements

This research has been co-financed by the European Regional Development Fund of the European Union and Greek national funds through the Operational Program Competitiveness, Entrepreneurship and Innovation (EPAnEK 2014-2020), under the Action "RESEARCH – CREATE – INNOVATE" B' CALL (project code: T2EDK-01243).

### References

1. B. Kumar, P. Verma, *Fuel* **288** 119622 (2021).
2. P.R. Sarika, P. Nancarrow, A. Khansaheb, T. Ibrahim. *Polymers*, **12** (2020)
3. E. Papadopoulou, S. Kountouras, K. Chrissafis, M. Kirpluks, U. Cabulis, P. Svirglerova, B. Benjelloum-Mlayah, *Tappi Journal*, **16** (2017)
4. A.G Margellou, P.A Lazaridis., I.D. Charisteidis, C.K. Nitsos, C.P. Pappa, A.P. Fotopoulos, S. Van den Bosch, B.F. Sels, K.S. Triantafyllidis, *Appl. Catal. A Gen.*, **623** (2021)

## Development of an engineered methanotroph-based platform for methane-to-indole 3-acetic acid bioconversion for sustainable agriculture

Diep Ngoc Pham<sup>1</sup>, Dung Hoang Anh Mai<sup>1</sup>, Anh Duc Nguyen<sup>1</sup>, Tin Hoang Trung Chau<sup>1</sup> and Eun Yeol Lee<sup>1,\*</sup>

<sup>1</sup>Department of Chemical Engineering, Kyung Hee University, Yongin-si, Gyeonggi-do 17104, South Korea

\*Correspondence to: [eunylee@khu.ac.kr](mailto:eunylee@khu.ac.kr)

Methane is the second most abundant greenhouse gas and is a potential factor causing global warming [1]. Recently, methane-based biorefineries have got much attractive, owing to the vast resource, inexpensive cost of this C1 gas, and a sustainable solution for mitigating atmospheric methane [1, 2]. In nature, methanotrophic bacteria are a unique microbial group capable of using methane as food in ambient conditions [3]. Methanotrophs, therefore, have been utilized to convert methane to value-added products. A better understanding of C1-assimilation pathways opened more opportunities to take advantage of methanotrophs for the efficient production of target chemicals [4]. With high carbon fluxes passing through, the non-oxidative ribulose monophosphate (RuMP) pathway is a potential starting point for metabolic engineering type I methanotrophs [5, 6]. Among anthropogenic sources, agriculture practices contribute to a large portion of methane emissions [1]. As a consequence of rising temperatures and shifts in climate patterns, the already limited arable lands would be adversely affected, posing a huge threat to human global food security in the future [7]. To face this problem, plant-growth-promoting bacteria (PGPB), which are capable of synthesizing phytohormones, are applied and promoted as a promising and sustainable approach to enhance the productivity of crops and reduce the use of chemical fertilizers without damaging the natural environment [8]. Extensive literature concerning this topic has revealed that, as the main biological sink of methane, methanotrophic bacteria are responsible for mitigating methane emissions from paddy fields [9]. However, no clear evidence for the ecological roles of this bacterial group in the paddies has been found. In the current study, we aimed to overproduce L-tryptophan (tryptophan), an aromatic amino acid generated from non-oxidative RuMP, from methane using *Methylovimicrobium alcaliphilum* 20Z. From the possibility of tryptophan overproduction, we continued engineering the biosynthesis pathway of indole 3-acetic acid (IAA), a phytohormone derived from tryptophan. By applying targeted metabolic engineering approaches, the titer of auxin was significantly improved. Moreover, this novel platform could extremely stimulate wheat growth *in vitro* with higher germination rate, shoot and root length. This study provides a novel platform for “waste-to-value” process and a proof-of-concept on the development of methanotroph to become PGPB, a first step to realize a novel sustainable process: plant growth-promoting platform coupled with methane emission mitigation.

Recombinant plasmids were constructed by using Gibson Assembly. The recombinant plasmids were transferred to methanotrophic cells via electroporation as described in the previous study [10]. Recombinant methanotrophs were cultivated in the 500-mL baffled flasks containing 50 mL of nitrate mineral salt (NMS) medium supplemented with 5  $\mu$ M of tungsten to support growth and sealed by screw caps [11]. Methane (50%, v/v) was supplied to the culture flasks by using a gas-tight syringe. The gas-fulfilled culture flasks were then placed in shaking incubators set to 30°C and 230 rpm. The air was refreshed, and methane was injected every 24 h. All chemicals used in this study were purchased from Sigma Aldrich Inc. (Germany) and Daejung Chemicals and Metals Co. (Korea). Tryptophan was analyzed from both supernatant and cell extracts by a spectrophotometric method described by Nagaraja et al. with a slight modification [12]. Tryptophan reacts with p-phenylenediamine dihydrochloride in a solution of sulfuric acid with an absorbance maximum of 520 nm. IAA was analyzed by a chemical method using a Salkowski reagent composed of 0.5 M ferric chloride and 35% perchloric acid [13]. The absorption of the resulting pink product was measured at a wavelength of 520 nm using a NanoPhotometer. The wheat seeds (*Triticum aestivum* L.) used in this experiment were purchased from a local market in Korea. The seed germination study was performed as described by Meena et al. [14].

The feedback-resistant genes AroG<sup>fbr(D146N)</sup> and TrpE<sup>fbr(S40F)</sup> originated from *E. coli* were expressed under P<sub>tac</sub> promoter in *M. alcaliphilum* 20Z<sup>X</sup>, an engineered strain capable of utilizing xylose as a co-substrate to support growth and methane assimilation from RuMP pathway. The resultant strain, RS00, produced tryptophan from methane with a titer of 39.6 mg/L (6.60 mg/L/d), which was 5.2-fold higher than that of 20Z<sup>X</sup> (7.2 mg/L (1.27 mg/L/d)). Co-expression of feedback-resistant genes and *aro8* and *aro10* from *S. cerevisiae* along with *aldH* from *E. coli* in 20Z<sup>X</sup> led to 10.5 mg/L of IAA in RS01 strain after 144 h of cultivation. Moreover, using xylose, a lignocellulosic biomass-derived sugar, as co-substrate could enhance the titers of tryptophan and IAA in RS00 and RS01 strains by 60% and 82%, respectively (Table 1).

Table 1. Production yield of products in parental strain and engineered strains.

Strain	Product	Carbon source	Product titer (mg/L)	Yield (mg/g DCW)
20Z <sup>X</sup>	Tryptophan	Methane	7.6 ± 1.9	6.0 ± 1.9
RS00	Tryptophan	Methane	39.6 ± 2.3	35.1 ± 0.4
RS00	Tryptophan	Methane + Xylose	63.3 ± 2.5	31.5 ± 0.1
RS01	IAA	Methane	10.5 ± 0.8	9.0 ± 0.6
RS01	IAA	Methane + Xylose	19.1 ± 0.2	10.0 ± 1.2

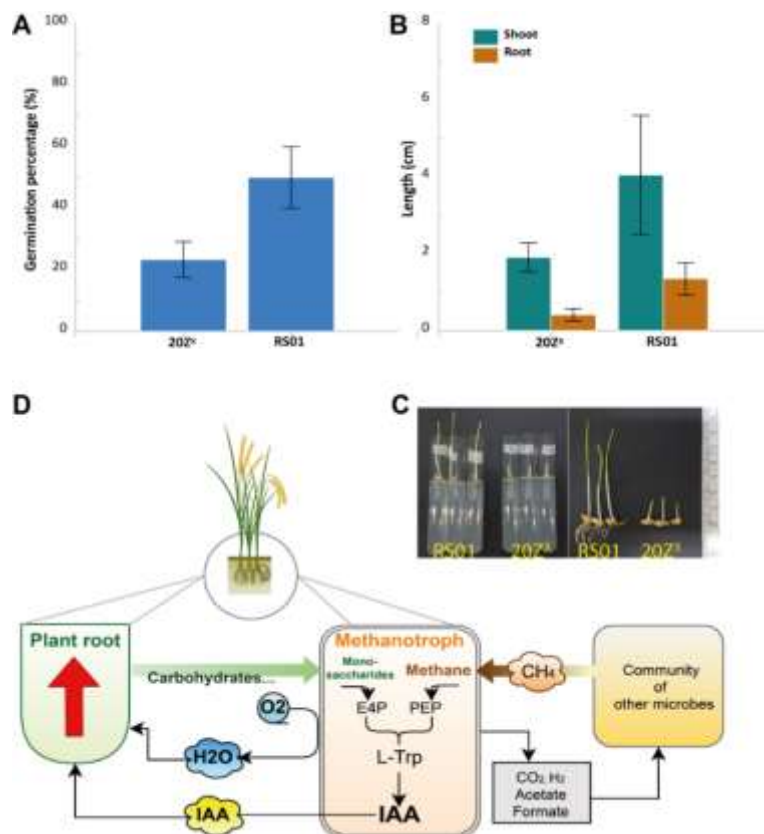


Figure 1. Stimulation of plant growth at early-stage by engineered IAA-producing strain RS01. (A-C) Effect of methanotrophic suspension on germination percentage (A); root and shoot length (B, C) of wheat seeds under high saline-alkaline condition. All data are presented as average ± standard deviation (n=5); (D) Possible interaction between engineered methanotroph with plant root and other microbes in soil.

In this study, under saline-alkaline conditions, the germination percentage and elongation of the shoots and roots of wheat seeds treated with the IAA-producing strain were significantly improved, being 114%, 199% and 362% higher than those of control treatments, respectively (Fig. 1).

## Acknowledgements

This research was supported by the C1 Gas Refinery Program through the National Research Foundation of Korea (NRF) funded by the Ministry of Science and ICT (2015M3D3A1A01064882).

## References

1. M. Saunio, et al., *Earth System Science Data Discussions*, 1-136 (2019).
2. R.B. Jackson, S. Abernethy, J.G. Canadell, M. Cargnello, S.J. Davis, S. Féron, S. Fuss, A.J. Heyer, C. Hong, C.D. Jones, H. Damon Matthews, *Philos. Trans. Royal Soc. A*, **379(2210)** p.20200454 (2021).
3. R.S. Hanson and T.E. Hanson, *Microbiol. Rev.* **60(2)** 439-471 (1996).
4. E.Y. Lee, Springer Nature 2019.
5. Y. Fu, L. He, J. Reeve, D.A. Beck, M.E. Lidstrom, *MBio*, **10(2)** (2019).
6. A.D. Nguyen, J.Y. Park, I.Y. Hwang, R. Hamilton, M.G. Kalyuzhnaya, D. Kim, E.Y. Lee, *Metab. Eng.*, **57** 1-12 (2020).
7. T. Wheeler, J. Von Braun, *Science* **341(6145)** 508-513 (2013).
8. A.N. Yadav, P. Verma, B. Singh, V. Chauhan, A. Suman, A.K. Saxena, *Adv. Biotechnol. Microbiol.*, **5(5)** 1-16 (2017).
9. V. Davamani, E. Parameswari, S. Arulmani, *Sci. Total Environ.*, **726** 138570 (2020).

10. A.D. Nguyen, I.Y. Hwang, O.K. Lee, D. Kim, M.G. Kalyuzhnaya, R. Mariyana, S. Hadiyati, M.S. Kim, E.Y. Lee, *Metab. Eng.* **47** 323-333 (2018).
11. D.S. Ojala, D.A. Beck, M.G. Kalyuzhnaya, *Methods Enzymol.* **495** 99-118 (2011).
12. P. Nagaraja, H.S. Yathirajan, R.A. Vasantha, *Anal. Biochem.*, **312(2)** 157-161 (2003).
13. E. Glickmann, Y. Dessaux, *Appl. Environ. Microbiol.*, **61(2)** 793-796 (1995).
14. K.K. Meena, M. Kumar, M.G. Kalyuzhnaya, M.S. Yandigeri, D.P. Singh, A.K. Saxena, D.K. Arora, *Antonie Van Leeuwenhoek* **101(4)** 777-786 (2012).

## The effect of organic acids on the degradation of PLA/PBAT blends

Marta Pinero\*<sup>3</sup>, Luís P. C. Gonçalves<sup>1</sup>, Rafael Rebelo<sup>1</sup>, Ana C. Fonseca<sup>1</sup>, Josefa Fonseca<sup>2</sup>, Manuel Rola<sup>2</sup>, Jorge F. J. Coelho<sup>1</sup>, Filipe Rola<sup>2</sup>, Arménio C. Serra\*

<sup>1</sup> CEMMPRE, Department of Chemical Engineering, University of Coimbra, Rua Sílvio Lima-Pólo II, 3030-790 Coimbra, Portugal

<sup>2</sup> SICOR-Sociedade Industrial de Cordoaria, S.A., Rua 13 de Maio 1533, Ap.10, 3889-852 Cortegaça, Portugal

<sup>3</sup> Chemistry Department, University of Coimbra, Rua Larga, 3030-790 Coimbra, Portugal

\*pineiromarta@gmail.com

The degradation of PLA/PBAT in natural environment has already been studied [1]. These tests have the disadvantage of requiring several years to be representative [2]. For certain uses like agriculture a rapid degradation is needed accordingly to the production cycles. In this case the materials in film or yarn form need to lose mechanical properties quickly.

In this work, the degradability of a commercial PLA/PBAT blend (Bio-Flex®) was studied with the addition of chloroacetic acids (tri-TCA and di-DCA) as strong organic acids. TCA is used in agriculture and DCA is used in pharmaceuticals.[3] The work also studied the substitution of acid by esters (E1,E2,E3) in order to get more stable additives and less aggressive to the mechanical processing parts. Samples were subjected to accelerated degradation tests for outdoor performance (OP) simulation.

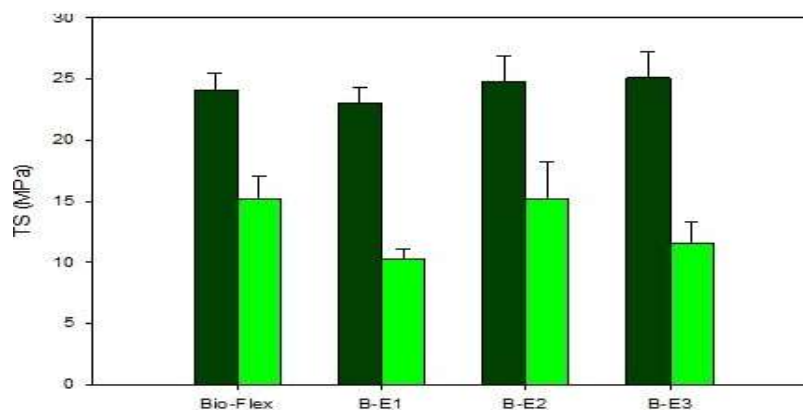


Figure 1. Tensile tests of the after outdoor performance tests (200 hours) of mixtures of Bio-flex and DCA esters additives. Before (dark green) and after (light green) OP test.

The presence of DCA and TCA enhance the hydrolysis of the polyester bonds, accelerating the degradation of the (Bio-Flex®). The samples of Bio-Flex® blended with esters were characterized before and after the degradation tests, basically by thermal, mechanical, and microscopic properties. SEM, thermal (DSC and TGA) and mechanical properties show that the additives do not significantly change the properties of Bio-Flex® during hot blending. After the degradation tests, SEM shows holes and cracks in the samples, a loss of Tg and a decrease in PLA crystallinity by DSC, and a decline of the mechanical properties.

Conclusion: Chloroacetic acids and esters were used to improve the degradation of PLA/PBAT blends. Their suitability for increasing the degradation ratio of PLA/PBAT blends was successfully demonstrated by microscopy and loss of thermal and mechanical properties as well as chromatography.

### Acknowledgements

The authors thank the financial support from Greenfil (POCI-01-0247-FEDER-033146).

### References

1. Y. Weng, Y. Jin, Q. Meng, L. Wang, M. Zhang, Y. Wang, Biodegradation behavior of poly(butylene adipate-co-terephthalate)(PBAT), poly(lactic acid)(PLA), and their blend under soil conditions. *Polymer Testing* **918** 32 (2013).
2. J. Napper, R. Thompson, Environment Deterioration of Biodegradable, Oxo-biodegradable, Compostable, and Conventional Plastic Carrier Bags in the Sea, Soil, Open-Air over a 3Year Period. *Environ. Sci. Technol.* 4775 53 (2019).
3. G. Koenig, E. Lohmar, N. Rupprich, M. Lison, A. Gnass, Chloroacetic acids. *Ullmann's Encyclopedia of Industrial Chemistry* (Ed. 7th) 2012



## Cellulose micro/nanoparticles as green polymer reinforcing agents

Eleni Psochia<sup>1</sup>, Dimitra Brenda<sup>1</sup> and Konstantinos S. Triantafyllidis<sup>1,2\*</sup>

<sup>1</sup>Department of Chemistry, Aristotle University of Thessaloniki, 54214 Thessaloniki, Greece

<sup>2</sup>Center for Interdisciplinary Research and Innovation (CIRI-AUTH), Balkan Center, 10th km Thessaloniki-Thermi Rd, P.O. Box 8318, 57001 Thessaloniki, Greece

\* ktrianta@chem.auth.gr

Biomass-derived materials are in the spotlight of scientific interest offering a great alternative to petroleum-based products. Their renewable and biodegradable nature, along with the interesting features that they exhibit, are recently attracting attention and are being used in a broad range of applications. Polysaccharides, lipids, or proteins are being employed to synthesize green and sustainable polymer nanocomposites. Cellulose, the most abundant natural polymer, is distinguished for its exceptional properties and is widely used in different applications, from packaging, textile and paper industry to adhesives, coatings or drug delivery systems and tissue engineering [1]. Special focus is placed on nanocellulose, which depending on the process used, can be in the form of cellulose nanofibers (CNFs) or cellulose nanocrystals (CNCs). Large surface area, high aspect ratio, low density, as well as high crystallinity and tensile strength, are some of the most important features that render nanocellulose an appealing candidate for polymer reinforcement [2] [3].

In this work, cellulose micro/nano particles of various morphologies and sizes were produced following different green synthetic pathways. Namely, CNFs were produced using three different mechanical processes, which included planetary milling, ultrasonication and high shear blending. Planetary milling was used as a pretreatment step prior to sonication and blending process to facilitate the particles' size reduction. For the synthesis of CNCs, a typical sulfuric acid hydrolysis procedure was employed. All cellulose nanoparticles were characterized as to their size by Dynamic Light Scattering (DLS) or Particle Size Analyzer (PSD), their structure and crystallinity by means of Fourier Transform Infrared Spectroscopy (FT-IR) and X-Ray Diffraction (XRD), respectively, while their thermal stability was assessed with Thermogravimetric Analysis (TGA). Their specific surface area was measured using the Brunauer–Emmett–Teller (BET) method, whereas their morphological characteristics were observed by Scanning Electron Microscopy (SEM), Transmission Electron Microscopy (TEM) and Atomic Force Microscopy (AFM). The results demonstrate the successful production of various nanocellulosic particles with promising properties, highlighting their dynamic potential as biobased reinforcing agents in polymeric substrates.

### Acknowledgements

This research has been co-financed by the European Regional Development Fund of the European Union and Greek national funds through the Operational Program Competitiveness, Entrepreneurship and Innovation (EPAnEK 2014-2020), under «Special Actions "Aquaculture" - "Industrial Materials" - "Open Innovation In Culture"» (project code: T6YBII-00341).

### References

- [1] H. Kargarzadeh *et al.*, “Recent developments on nanocellulose reinforced polymer nanocomposites: A review,” *Polymer (Guildf)*, vol. 132, pp. 368–393, 2017, doi: 10.1016/j.polymer.2017.09.043.
- [2] D. Trache *et al.*, *Nanocellulose: From Fundamentals to Advanced Applications*, vol. 8, no. May. 2020.
- [3] C. Zinge and B. Kandasubramanian, “Nanocellulose based biodegradable polymers,” *Eur. Polym. J.*, vol. 133, no. May, p. 109758, 2020, doi: 10.1016/j.eurpolymj.2020.109758.

## Glucose hydrogenation/hydrogenolysis towards sugar alcohols over Pt/Ru catalysts supported on micro/mesoporous activated carbon

Kyriazis C. Rekos<sup>1</sup>, Antigoni G. Margellou<sup>1</sup> and Konstantinos S. Triantafyllidis<sup>1,2\*</sup>

<sup>1</sup>Department of Chemistry, Aristotle University of Thessaloniki (AUTH), Thessaloniki, Greece

<sup>2</sup>Center for Interdisciplinary Research and Innovation (CIRI), AUTH, Thessaloniki, Greece

\*Corresponding author: [ktrianta@chem.auth.gr](mailto:ktrianta@chem.auth.gr)

Most chemicals and fuels are produced from nonrenewable fossil, petroleum and carbon resources. Their intensive use leads to progressive decrease of their availability, higher cost of the derived end-products and serious environmental pollution. The use of renewable and abundant natural resources, such as lignocellulosic biomass, is a promising alternative that has been put forward over the last decades. To this end, sustainable and efficient (bio)chemical processes need to be developed for a cost-competitive valorization of biomass and its fractions, i.e. carbohydrates (from cellulose and hemicellulose) and phenolics (from lignin). The hydrogenation/hydrogenolysis of glucose towards C2-C6 sugar alcohols has been recognized as one of the most promising biomass valorization routes to produce high added-value chemicals, such as sorbitol, 1,2-propanediol, glycerol, etc.

The global sugar alcohol market was estimated at \$3,360 million in 2019 and is expected to reach \$4,800 million by 2027. Sorbitol accounted for the highest sugar alcohol market share in 2019. Sorbitol has a broad spectrum of applications such as a low-calorie sweetener (food processing industry), a substrate for producing vitamin C, and also in the pharmaceutical and cosmetic industry or as a starting substrate that can further be transformed into downstream products (e.g., ethylene glycol [EG], 1,2-propanediol, and glycerol) used in the polymers industry.

The hydrogenation/hydrogenolysis of glucose to sugar alcohols is based on catalytic reactions with the use of various types of catalysts, such as metals, e.g. Pt, Ru, Ni, etc. supported on activated carbons. In this work, we studied the performance of Ru and Pt catalysts supported on micro/mesoporous activated carbon, in the hydrogenation and hydrogenolysis of glucose, in neat water, at a range of temperatures (120 – 180°C), at relatively low hydrogen pressure of 3 MPa and at a range of reaction time (1 – 5h). The impact of metal loading (1–5 wt.%), on glucose conversion and selectivity to the various products was also systematically addressed.

It was shown that Pt is significantly more selective towards hexitols (sorbitol and mannitol) compared to Ru, in glucose-rich reaction media. For example, the 5wt% Pt/AC catalyst afforded hexitols yield of 84.2 wt.% (at 98.9% conversion) compared to 63.1 wt.% (at 97.6% wt.% conversion) obtained by the corresponding Ru catalyst, the latter being also selective towards glycerol and propane-1,2-diol (propylene glycol). Optimization of the time/temperature conditions, resulted to even higher sorbitol selectivity/yield of ca. 90 wt.% (at 100% conversion). Both Pt and Ru exhibited relatively high glucose hydrogenation activity towards hexitols, versus retro-aldol reactions that lead directly to smaller C2–C4 compounds, while the difference in the final product yields between the two metals was attributed to the higher hexitols hydrogenolysis (C-C cleavage) reactivity of Ru.

### Acknowledgements

This project has received funding from the European Union's Horizon 2020 research and innovation programme under Grant Agreement No. 952941.

### References

1. P. A. Lazaridis, S. Karakoulia, A. Delimitis, S. M. Coman, V. I. Parvulescu, K. S. Triantafyllidis, *Catl. Today*, **257** 281-290 (2015).
2. P.A. Lazaridis, S.A. Karakoulia, C. Teodorescu, N. Apostol, D. Macovei, A. Panteli, A. Delimitis, S.M. Coman, V.I. Parvulescu, K.S. Triantafyllidis, *Appl. Catal. B: Env.*, **214** 1-14 (2017)

## Synthesis and closed-loop recycling of plant oil-based polyamides

Maximilian Rist<sup>1</sup> and Andreas Greiner<sup>1\*</sup>

<sup>1</sup>Macromolecular Chemistry and Bavarian Polymer Institute, University of Bayreuth, Universitaetsstrasse 30, 95440 Bayreuth, Germany

\*greiner@uni-bayreuth.de

Abstract text:

Polyamides are widely applied in high demanding applications like automotive and electronics because of their desirable properties including high mechanical strength and durability. Bio-based polyamides although known since the 1950s are still almost exclusively sourced from castor oil. This causes a high dependency on growth and cultivation of castor beans, limiting availability and supply.[1]

In this study we targeted this problem by synthesizing high performance polyamides from plant oil-based oleic acid. By the use of oleic acid virtually any vegetable oil or animal fat can be used as a resource for the synthesis of these bio-based polyamides, resulting in a higher diversification of the feedstock. Microalgae-strains like *Chlorella vulgaris* can also be used to produce oleic acid in a fast and sustainable way without competing the food industry. As these microalgae can be cultivated on non-arable land, have a high reproduction rate and also capture CO<sub>2</sub> from the environment, they are a truly sustainable resource for bio-based polyamides.[2]

We were able to synthesize an oleic-acid based diacid with 100% atom-efficiency in high yields and polycondensation purity. Different polyamides were then synthesized by melt polycondensation of the bio-based monomer together with linear diamines in different chain-lengths. The synthesized polyamides have a carbon-based bio-content of at least 55% and their molecular weight is in the range of typical commercial polyamides. All polyamides showed a high thermal stability and melting points of >170 °C. They also showed high crystallinity of ~50% and mainly  $\alpha$ -phase structures. The polyamides also show a lower water absorption than conventional bio-based polyamides, resulting in a better dimensional stability and better processability. They also show high elasticity and good mechanical strength, which makes them desirable materials for the use as fibers and automotive parts.

Recovery of the monomer in high purity after microwave-assisted depolymerization of the polyamides was also successful with a 99% recovery rate. The recovered monomer could be successfully used to synthesize recycled polyamide, which was not distinguishable from the virgin polymer.

### Acknowledgements

The authors are indebted for financial support by the German Federal Ministry of Education and Research

### References

1. F. Stempfle, P. Ortmann, S. Mecking, *Chemical Reviews*, 116, 4597–4641 (2016).
2. T. an Phung Hai, N. Neelakantan, M. Tessman, S. D. Sherman, G. Griffin, R. Pomeroy, S. P. Mayfield, M. D. Burkart, *Green Chem.*, **22**, 3088–3094 (2020).

## Use of tosylated glycerol carbonate for the preparation of new functionalized pyrazole compounds

Inesa Zagorskytė<sup>1</sup>, Eglė Arbačiauskienė<sup>1</sup>, Aurimas Bieliauskas<sup>2</sup>, Patrick Rollin<sup>3</sup> and Algirdas Šačkus<sup>1,2\*</sup>

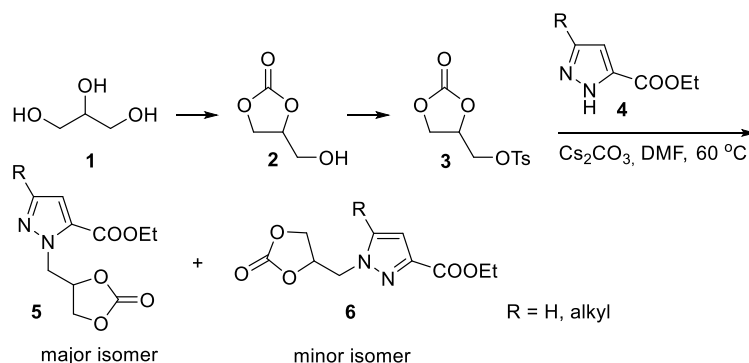
<sup>1</sup>Department of Organic Chemistry, Kaunas University of Technology, Radvilėnų pl. 19, LT-50254 Kaunas, Lithuania

<sup>2</sup>Institute of Synthetic Chemistry, Kaunas University of Technology, K. Baršausko g. 59, Kaunas LT-51423, Lithuania

<sup>3</sup>Université d'Orléans et CNRS, ICOA-UMR 7311, BP 6759, F-45067 Orléans, France

\*algirdas.sackus@ktu.lt

Glycerol carbonate (GC) is an industrial biosourced chemical with great potential for use in a wide range of applications, from solvents to heterocyclic compounds [1]. GC-derived synthons have been introduced through conversion into *O*-sulfonylated forms – either mesylate or tosylate – as versatile bis-electrophilic reagents for fine chemistry [2,3]. In continuation of our interest in using *O*-sulfonylated glycerol carbonates for heterocyclic compounds [4], we report here the *N*-glycerylation of functionalized 1*H*-pyrazoles using tosylated glycerol carbonate (TGC).



Scheme 1. Synthesis of *N*-glycerylated 1*H*-pyrazole carboxylates.

The reaction of ethyl 3-substituted-1*H*-pyrazole-5-carboxylates **4** with TGC **3** was carried out in DMF in the presence of Cs<sub>2</sub>CO<sub>3</sub> to produce 1-[(2-oxo-1,3-dioxolan-4-yl)methyl]-1*H*-pyrazole-5- and -3-carboxylates as regioisomeric pyrazole derivatives **5** and **6**, respectively (Scheme 1). The discrimination between regioisomeric compounds **5** and **6** was based on data from <sup>1</sup>H-<sup>13</sup>C HMBC, <sup>1</sup>H-<sup>15</sup>N HMBC, and <sup>1</sup>H-<sup>1</sup>H NOESY experiments. In order to evaluate the synthetic potential of *N*-glycerylated hybrids as building blocks to obtain more complex structures, the reactivity of carbonate compounds **5** and **6** with various nucleophilic species such as alcohols, thiols and amines was investigated. The structures of the novel functionalized pyrazoles were confirmed by <sup>1</sup>H, <sup>13</sup>C, and <sup>15</sup>N NMR spectroscopy and HRMS investigation.

### References

1. P. Rollin, L.K. Soares, A.M. Barcellos, D.R. Araujo, E.J. Lenardao, R.G. Jacob, G. Perin, *Appl. Sci.* **11**, 5024 (2021).
2. A.-C. Simão, B. Lynikaite-Pukleviciene, C. Rousseau, A. Tatibouët, S. Cassel, A. Šačkus, A.P. Rauter, P. Rollin, *Lett. Org. Chem.* **3**, 744 (2006).
3. J. Rousseau, C. Rousseau, B. Lynikaitė, A. Šačkus, C. De Leon, P. Rollin, A. Tatibouët, A. *Tetrahedron* **65**, 8571 (2009).
4. G. Vilkauskaitė, S. Krikštolaitytė, O. Paliulis, P. Rollin, A. Tatibouët, A. Šačkus, *Tetrahedron* **69**, 3721 (2013).

**Enzyme-induced crosslinking to tailor chitosan/gelatin-based encapsulation carriers**

Danillo Y. Namba<sup>1,2</sup>, Samara C. Silva<sup>1</sup>, Eliane Colla<sup>3</sup>, Pricila Marin<sup>2</sup>, Maria-Filomena Barreiro<sup>1,\*</sup>,  
Arantzazu Santamaria-Echart<sup>1,\*</sup>

<sup>1</sup>*Centro de Investigação de Montanha (CIMO), Campus de Santa Apolónia, Instituto Politécnico de Bragança, 5300-253 Bragança, Portugal*

<sup>2</sup>*Universidade Tecnológica Federal do Paraná, Av. Dos Pioneiros, 3131-Jardim Morumbi, Londrina 86036-370, Brazil*

<sup>3</sup>*Departamento Acadêmico de Alimentos (DAALM) – Programa de Pós-graduação em Tecnologia de Alimentos (PPGTA) – Universidade Tecnológica Federal do Paraná, Câmpus Medianeira, 85884-000, Paraná, Brazil*  
 \*barreiro@ipb.pt (M-F.B.), asantamaria@ipb.pt (A.S-E.)

The development of encapsulation carriers based on biopolymers are evolving to sustainable methodologies avoiding the use of hazardous chemicals, generally associated with environmental impacts and adverse effects on human's health. In this context, enzymes are becoming an attractive alternative to traditional chemicals to perform crosslinking approaches in protein-polysaccharide-based systems [1]. This type of formulations is of high interest for edible food and nutraceutical applications, also due to the nutritional properties conferred by the proteins and the biological attributes provided by the polysaccharide [2].

The objective of the work is focused on developing chitosan-gelatin particles through the emerging enzyme-induced crosslinking approach using transglutaminase (TGase). This approach was also complemented with the physical crosslinking strategy using tripolyphosphate (TPP). Aiming to validate their potential as carriers, a design of experiments approach (central composite rotatable design, CCRD) was applied to tailor the swelling degree of the particles in simulated digestion conditions.

Chitosan brand 90/200/A1 was provided from Biotechnologie GmbH (deacetylation degree of 91.9%) and gelatin from porcine skin, Type A (gel strength 90-110 Bloom; average molecular weight 20000–25000), from Sigma Aldrich and Transglutaminase (ACTIVA WM 110 active units/g) from Ajinomoto Foods Europe S.A.S. were employed. The particles were prepared by two steps comprising the consolidation of the particles' conformation by an external crosslinking with TPP, followed by an internal covalent crosslinking induced by TGase. In the first stage, chitosan/gelatin acidic solution at 3 wt% (w/v) was prepared and added with the TGase. The solution was dropped by the dripping technique in a 5% TPP coagulation bath. The obtained particles were filtered and transferred to a water bath at 50 °C to perform the TGase covalent crosslinking. Finally, the particles were recovered by filtration and freeze-dried. The gelatin content ( $x_1$ , % wt), TGase concentration relative to gelatin ( $x_2$ , U/ggel) and crosslinking time at 50 °C ( $x_3$ , min) were set by the CCRD experimental design including three replicates at the central point (17 assays). As responses the swelling degree (SD) at pH 3 for 2 h ( $Y_3$ , % wt) and at pH 3 and 7 for 2 h and 6 h, respectively ( $Y_{3+7}$ , % wt) were analyzed [3,4]. Table 1, summarizes the used conditions and responses for the assays.

Table 1 - Coded levels (and real values) of the experimental design (Gelatin content ( $x_1$ , % wt), TGase concentration ( $x_2$ , U/ggel), and bath time at 50° C ( $x_3$ , min)) and the obtained SD responses (at pH 3 ( $Y_3$ , % wt) and at pH 3 and 7 ( $Y_{3+7}$ , % wt))

Assay	Coded levels (real values)			Responses	
	$x_1$ (% wt)	$x_2$ (U/ggel)	$x_3$ (min)	$Y_3$ (% wt)	$Y_{3+7}$ (% wt)
1	-1 (14.1)	-1(24)	-1(48)	239.85	270.28
2	1(41)	-1(24)	-1(48)	350.14	286.54
3	-1(14.1)	1(36)	-1(48)	265.82	329.76
4	1(41)	1(36)	-1(48)	281.51	319.25
5	-1(14.1)	-1(24)	1(72)	207.02	212.04
6	1(41)	-1(24)	1(72)	247.95	249.40
7	-1(14.1)	1(36)	1(72)	335.87	295.08
8	1(41)	1(36)	1(72)	273.08	270.79
9	-1.68(5)	0(30)	0(60)	280.66	278.92
10	1.68(50)	0(30)	0(60)	294.89	284.81
11	0(27.5)	-1.68(20)	0(60)	267.64	275.77
12	0(27.5)	1.68(40)	0(60)	322.24	327.89
13	0(27.5)	0(30)	-1.68(40)	307.04	311.61
14	0(27.5)	0(30)	1.68(80)	295.54	230.49
15	0(27.5)	0(30)	0(60)	308.71	287.73
16	0(27.5)	0(30)	0(60)	298.78	281.95
17	0(27.5)	0(30)	0(60)	319.64	286.45

A statistical analysis of the obtained results was performed and some of the parameters are summarized in Table 2. Considering the  $F_{Cal}$  values higher in comparison to  $F_{Tab}$  the predicted models were established, in general, considering the influence of the coefficients with p-value < 0.05 as significant.

Table 2. Predicted models and  $R^2$ ,  $F_{Cal}$  and  $F_{Tab}$  of the SD responses at pH 3 and pH 3 and 7.

Response	Predicted models			
	Adjusted model	$R^2$	$F_{Cal}$	$F_{Tab}$
SD at pH 3	$Y = 301.45 + 9.37x_1 + 14.88x_2 - 9.62x_1^2 - 7.09x_2^2 - 24.79x_1x_2 - 18.48x_1x_3 + 24.58x_2x_3$	86.30	8.101	3.293
SD at pH 3 + 7	$Y = 282.53 + 20.82x_2 - 26.06x_3 + 5.29x_2^2 - 5.59x_3^2 - 11.05x_1x_2$	95.46	46.269	3.204

Aiming to validate the predictive models to tailor the SD of the particles based on the enzyme-induced crosslinking reaction, an optimized formulation was selected and prepared by triplicate. Considering the final application of the particles as bioactive carriers, a formulation with potential to preserve the compounds during the digestion process (pH 3 for 2 h) and release in the intestine (pH 3 for 2 h and pH 7 for 6 h) was defined. The optimized formulation included the  $x_1$ ,  $x_2$ , and  $x_3$  coded values of -1.68, 1, and 0 (corresponding to 5 %wt, 36 U/ggel and 60 min uncoded values).

Table 3. SD at pH<sub>3</sub> and PH<sub>3+7</sub> responses corresponding to the predictive model and experimental results and relative deviation between them.

Responses	Predictive	Experimental	Relative deviation
SD at pH 3	307.95 ± 0.00	160.14 ± 8.29	92.02
SD at pH 3 + 7	327.20 ± 0.00	319.91 ± 1.02	2.28

The results evidenced the suitable capability of the models to predict the desired objectives (minimize  $Y_3$  and maximize  $Y_{3+7}$ ). Relative deviations lower than 20% are considered adequate to validate the models [5], fact observed in  $Y_{3+7}$  response. The relative deviation  $Y_{3+7}$  of 92.02% exceeded the defined value, nevertheless, it was verified no divergent relative deviation between the experimental values and predictive responses for all the models for each of the CCRD runs, demonstrating their suitable predictive capability within the studied experimental range. To highlight that the experimental value in  $Y_3$ , resulted lower in comparison to the corresponding predicted value, indicating that values calculated through the predictive model would correspond to lower values when prepared experimentally.

## Acknowledgements

This work was partially funded by the Portuguese Foundation for Science and Technology (FCT, Portugal) and FEDER under the PT2020 program - financial support to CIMO (UIDB / 00690/2020). National funding by FCT, P.I., through the institutional scientific employment program-contract for Arantzazu Santamaria-Echart, and through the individual research grant SFRH/BD/148281/2019 for Samara C. Silva.

## References

1. N. Pilipenko, O.H. Gonçalves, E. Bona, I.P. Fernandes, J.A. Pinto, G.D. Sorita, F.V. Leimann, M.F. Barreiro, *Carbohydrate Polymers*, **223** 115035 (2019).
2. C. Tan, D.J. McClements, *Foods*, **10** 821 (2021).
3. M.A. Malana, J.D. Bukhari, R. Zohra, *Designed Monomers and Polymers*, **17** 266 (2013).
4. X. Li, R. Guo, X. Wu, X. Liu, X., L. Ai, Y. Sheng, Y. Wu, *Carbohydrate Polymers*, **239** 116194 (2020).
5. M.I. Rodrigues, A. F. Iemma, *CRC Press*, Boca Raton, FL (2014).

## Degradation Studies of PLA/PBAT Blends in Simulated Marine Environments

Maria Elisa Serra<sup>\*3</sup>, Rafael Rebelo<sup>1</sup>, Luís P. C. Gonçalves<sup>1</sup>, Ana C. Fonseca<sup>1</sup>, Josefa Fonseca<sup>2</sup>, Manuel Rola<sup>2</sup>, Jorge F. J. Coelho<sup>1</sup>, Filipe Rola<sup>2</sup>, Arménio C. Serra<sup>1</sup>

<sup>1</sup>CEMPRE, Department of Chemical Engineering, University of Coimbra, Rua Sílvio Lima-Pólo II, 3030-790 Coimbra, Portugal

<sup>2</sup>SICOR-Sociedade Industrial de Cordoaria, S.A., Rua 13 de Maio 1533, Ap.10, 3889-852 Cortegaça, Portugal

<sup>3</sup>CQC and Chemistry Department, University of Coimbra, Rua Larga, 3030-790 Coimbra, Portugal

\*melisa@ci.uc.pt

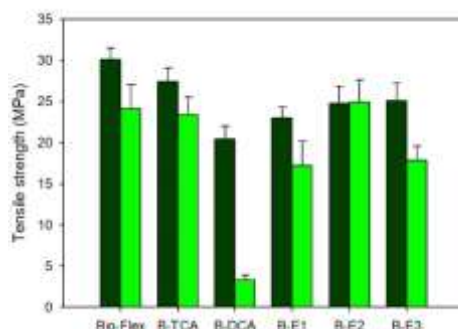
Poly(butylene adipate-co-terephthalate) (PBAT) is a polymer with good compostability properties. It is an aliphatic-aromatic copolyester[1] that presents good ductile mechanical properties[2] and when blended with the more rigid PLA its properties may improve. Blends of PLA/PBAT are already commercialized (e.g.: Bio-Flex<sup>®</sup> - FKUR & Ecovio<sup>®</sup> - BASF) and have the compostability seal (according to EN 13432 standard).

In certain circumstances, like in fishing or agricultural activities, these materials could substitute polyethylene/propylene, particularly in the case of ropes or fishing nets[3]. In both cases control of the degradation process is desirable. The development of plastic formulations which deteriorate faster causing fewer impacts to environment is a defined situation.[4]

In this work, the control of the degradability of a commercial blend of PLA/PBAT (Bio-Flex<sup>®</sup>) by adding small amounts of strong acids, namely, trichloroacetic (TCA), dichloroacetic (DCA) or its esters (E<sub>1</sub>,E<sub>2</sub>,E<sub>3</sub>) in order to control degradation, is studied. Additionally, the addition of commercial antioxidants was tested in order to slow down the degradation process.

The PLA/PBAT samples blended with different additives were subjected to accelerated degrading tests in simulated marine environments. Two kinds of situations were tested. The samples were immersed in saline water or samples were put in dry environments, only in contact with small amounts of saline water. In both situations a UV/V lamp simulates solar irradiation.

The samples were characterized before and after degradation tests by Fourier-Transform Infrared Spectroscopy (FTIR), Differential Scanning Calorimetry (DSC), Scanning Electron Microscopy (SEM), and Mechanical performance. Also, Size-exclusion Chromatography (SEC) and contact angle were evaluated. Acids were found to be highly effective in increasing the degradation of the PLA/PBAT blend. As expected, DCA esters showed less activity and could be used to control the degradation process. The addition of commercial antioxidants reverts the degradation process.



The analysis of the tensile strength of the samples showed that among the tested additives, DCA causes higher degradation of the material subject to saline water environment (dark green, initial samples and light green, after tests). Analysis of other properties of the tested materials will be provided in this work.

### Acknowledgements

The authors are thankful for financial support from Greenfil (POCI-01-0247-FEDER-033146).

### References

1. T. Kijchavengkul, R. Auras, M. Rubino, S. Selke, M. Ngouajio, and R. T. Fernandez, *Polym. Degrad. Stab.*, 95, 2641 (2010).
2. Musioł, W. Sikorska, H. Janeczek, W. Walach, W. Walach, A. Hercog, B. Johnston, J. Rydz, *Waste Manag.*, 77, 447 (2018)

3. M. Deroiné, A. Le Duigou, Y. M. Corre, P. Y. LeGac, P. Davies, G. César, S. Bruzaud, *Polym. Degrad. Stab.*, **108**, 319 (2014).
4. I. E. Napper and R. C. Thompson , *Environ. Sci. Technol.*, **53** (2019).



## Flow chemistry synthesis of a potential new class of biorenewable monomers, fuel oxygenates and bio-based lubricants

Martin Ravutsov,<sup>1</sup> Miroslav Dangelov,<sup>1</sup> Maya Marinova<sup>1</sup> and Svilen Simeonov<sup>1\*</sup>

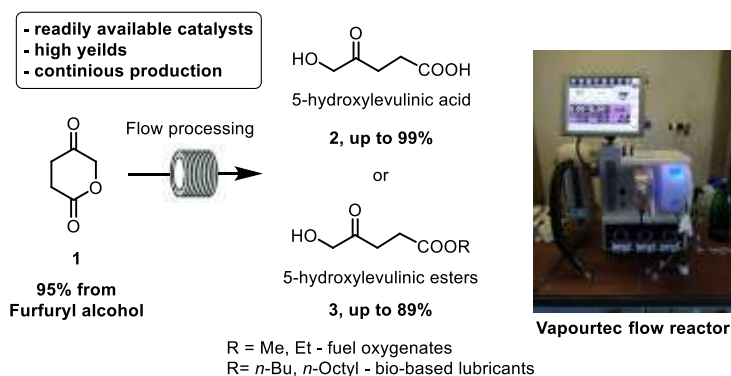
<sup>1</sup> Institute of Organic Chemistry with Centre of Phytochemistry, Bulgarian Academy of Sciences, Acad. G Bonchev str. Block 9, 1113 Sofia, Bulgaria  
svilen@orgchm.bas.bg

Levulinic acid is a biorenewable chemical largely available from lignocellulosic biomass that finds a variety of applications in the production of important chemical commodities.<sup>1</sup> The esters of levulinic acid attracted a considerable interest due to their application as bio-fuels and fuel additives.<sup>2</sup> Furthermore, the esters with long-chain alcohols are used as bio-based lubricants.<sup>3</sup>

Furfuryl alcohol is another major derivative arising from lignocellulosic biomass and its production is a notable example of an industrialized process. Encouraged by our previous investigations on the use of Achmatowicz rearrangement of furfuryl alcohol as a key step in the production of important polyols,<sup>4</sup> herein we report the synthesis of 5-hydroxylevulinic acid **2** and its esters **3** as a potential new class of biorenewable fuel additives and bio-based lubricants.

Through this investigation we subjected the readily available from furfuryl alcohol lactone **1** to hydrolysis or acloholysis under flow conditions (Scheme 1). We have undertaken an intensive screening of various acidic heterogeneous catalysts and found about that the readily available Amberlyst 15<sup>®</sup> provided up to 99% yield of 4-ketovalerolactone (**2**), which is used as a monomer for the synthesis of the biodegradable polymer poly(4-ketovalerolactone) (PKVL).

By taking advantage of the natural reactivity of **1** we then completed the synthesis of various ester derivatives **3** in good yields without extensive use of highly acidic catalysts usually required for the production of the analogous Levulinic acid esters. In contrast, mild basic condition provided the desired esters in excellent yields.



**Scheme 1.** Synthesis of 5-hydroxylevulinic acid and its esters

In summary, we reported the first use of the readily available from furfural alcohol lactone **1** in the synthesis of new biorenewable chemical commodities. The corresponding levulinate-analogues were achieved in excellent yields under flow conditions in the presence of readily available and cheap catalysts.

### Acknowledgements

The authors acknowledge National Science Fund of Bulgaria (grant KP-06-OPR-01/2).

The project leading to this application has received funding from the European Union's Horizon 2020 research and innovation programme under grant agreement no. 951996.

### References

- W.P. Xu, X.F. Chen, H.J. Guo, H.L. Li, H.R. Zhang, L. Xiong, X.D. Chen, *J. Chem. Technol. Biotechnol.*, **96** 3009 (2021).
- D. Di Menno Di Bucchianico, Y. Wang, J.C. Buvat, Y. Pan, V.C. Morenob, S. Leveneur, *Green Chem.*, **24** 614 (2022).
- K.Y. Nandiwale, S.K. Yadava, V.V. Bokade, *J. Energy Chem.*, **23** 535 (2014).
- S. P. Simeonov, M. A. Ravutsov and M. D. Mihovilovic, *ChemSusChem*, **12**, 2748 (2019).

## A biorefinery approach for integrated recovery of anthocyanins and pectin from blueberry pomace

Kusumika Sinha Roy<sup>1,2,3\*</sup>, Amit Arora<sup>1,3</sup>, Antonio F. Patti<sup>2</sup>, Kellie Tuck<sup>2</sup>

<sup>1</sup>IITB – Monash Research Academy, Indian Institute of Technology, Bombay, Powai, Mumbai 400076, India; <sup>2</sup>School of Chemistry, Monash University, Clayton, Victoria 3800, Australia ; <sup>3</sup>Centre for Technology Alternatives for Rural Areas (CTARA), Indian Institute of Technology, Bombay, Powai, Mumbai 400076

\*[kusumika.sinharoy@monash.edu](mailto:kusumika.sinharoy@monash.edu)

**Background** - A biorefinery utilizes biomass instead of petroleum to generate fuels and chemicals through an integrated process [1]. Fruit and vegetable waste is one of the biggest classes of food loss waste and valorization of these waste into high value products through a biorefinery approach might be an effective way for disposal of these waste [2]. Fruit peel waste is a good choice of feedstock for biorefineries as they are a source of chemicals, like cellulose, hemicellulose, anti-oxidants and enzymes [3].

**Rationale** - With the growing consumer awareness and preference towards all natural products, natural colorants extracted from plant sources are competing with synthetic colorants in the food processing industry [4]. Blueberries are a source of a natural food color, called anthocyanin, that is capable of imparting red, blue, or green color to food depending on its pH [5]. Additionally, anthocyanins find applications in nutraceutical industries due to their antioxidant activity, and their role in prevention of cardiovascular diseases and degeneration of the eye [6,7]. Blueberries are also a good source of pectin, a natural plant-based polysaccharide that finds extensive use in food industries due to its gel forming properties [8]. Blueberries are cultivated across the world, but are prone to post harvest losses due to the high respiratory rate of the fruit [9]. This makes them an ideal choice for the biorefinery approach. This work focuses on valorization of blueberry waste to produce high valued chemicals like anthocyanins and pectin from blueberry pomace.

**Experimental** - Extraction of anthocyanins and pectin was performed with distilled water using probe sonicator from Fisher Scientific. Fig 1 represents the flowchart for the overall biorefinery process. All the membrane-based filtration was done using a dead-end membrane filtration unit from HP 4750 stirred cell, Sterlitech Corporation. The composition of the purified pectin was analysed, and further analysis was done with ATR-FTIR (Attenuated Total Reflection Fourier Transform Infrared) spectrometer and GPC (Gel Permeation Chromatography). The anthocyanins were quantified spectrophotometrically and analysed by a HPLC-DAD (High Pressure Liquid Chromatography, with a Diode Array Detector) at 520 nm.

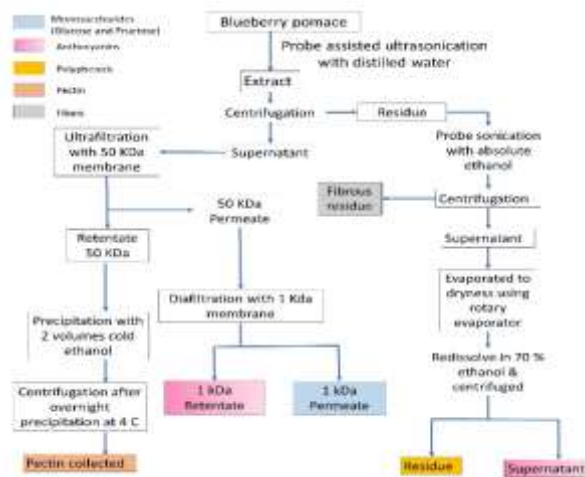


Fig 1: Process flowchart for recovery and purification of compounds

**Results** – The optimum parameters for extraction of anthocyanin from blueberry pomace was 30 minutes and 60 % amplitude reading of the instrument (Fig 2 a,b). Pectin was co-extracted in the water extract and purification yielded 37.1 mg/g dw (dry weight) with 55.6 % galactouronic acid content and 9.5 % bound anthocyanins (Fig 2 c). FTIR analysis revealed the presence of -COOH and -COCH<sub>3</sub> groups in the purified pectin (Fig 2 d). From purification of the remaining filtrate with 1 kDa membrane, 24.2 % of 3.7 mg/g anthocyanin was recovered which was at par with the food industry standard for natural colorants. The residual biomass when extracted with 90 % ethanol yielded 1 mg/g dw of 75.9 % pure anthocyanins. The higher purity anthocyanins in ethanolic extract can serve as high value nutraceutical in food industry.

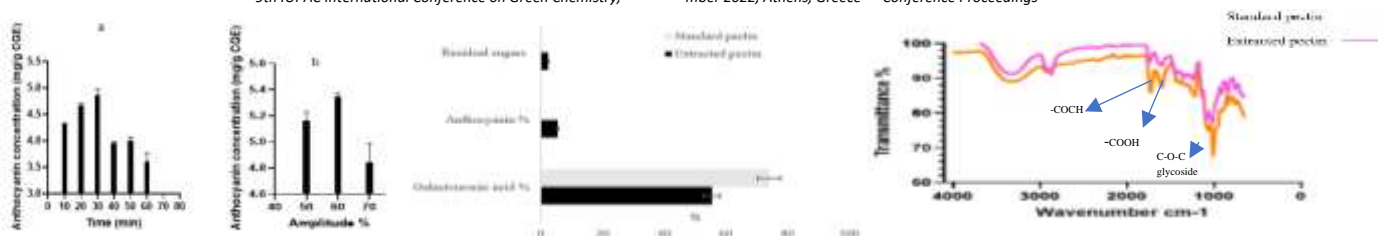


Fig 2: a. Optimization of time for extraction of anthocyanin using distilled water b. Optimization of amplitude % for extraction of anthocyanin using distilled water c. Composition analysis of purified pectin d. FTIR analysis of purified pectin

**Acknowledgements-** Authors would like to express their gratitude towards Department of Biotechnology, Government of India for funding this work.

#### References-

- O'Callaghan, K. Technologies for the utilisation of biogenic waste in the bioeconomy. In *Food Chemistry* (Vol. 198, pp. 2–11). Elsevier Ltd. (2016) <https://doi.org/10.1016/j.foodchem.2015.11.030>.
- Esparza, I., Jiménez-Moreno, N., Bimbela, F., Ancín-Azpilicueta, C., & Gandía, L. M. Fruit and vegetable waste management: Conventional and emerging approaches. In *Journal of Environmental Management* (Vol. 265). Academic Press. (2020). <https://doi.org/10.1016/j.jenvman.2020.110510>.
- Joglekar, S. N., Pathak, P. D., Mandavgane, S. A., & Kulkarni, B. D. Process of fruit peel waste biorefinery: a case study of citrus waste biorefinery, its environmental impacts and recommendations. *Environmental Science and Pollution Research*, 26(34), 34713–34722. (2019). <https://doi.org/10.1007/s11356-019-04196-0>.
- Martins, N., Roriz, C. L., Morales, P., Barros, L., & Ferreira, I. C. F. R. Food colorants: Challenges, opportunities and current desires of agro-industries to ensure consumer expectations and regulatory practices. In *Trends in Food Science and Technology* (Vol. 52, pp. 1–15). Elsevier Ltd. (2016). <https://doi.org/10.1016/j.tifs.2016.03.009>
- Kalt, W., Cassidy, A., Howard, L. R., Krikorian, R., Stull, A. J., Tremblay, F., & Zamora-Ros, R. Recent Research on the Health Benefits of Blueberries and Their Anthocyanins. In *Advances in Nutrition* (Vol. 11, Issue 2, pp. 224–236). Oxford University Press. (2020) <https://doi.org/10.1093/advances/nmz065>
- Xu, L., Tian, Z., Chen, H., Zhao, Y., & Yang, Y. Anthocyanins, Anthocyanin-Rich Berries, and Cardiovascular Risks: Systematic Review and Meta-Analysis of 44 Randomized Controlled Trials and 15 Prospective Cohort Studies. In *Frontiers in Nutrition* (Vol. 8). Frontiers Media S.A. (2021). <https://doi.org/10.3389/fnut.2021.747884>
- Khoo, H. E., Ng, H. S., Yap, W. S., Goh, H. J. H., & Yim, H. S. Nutrients for prevention of macular degeneration and eye-related diseases. In *Antioxidants* (Vol. 8, Issue 4). MDPI. (2019). <https://doi.org/10.3390/antiox8040085>
- Hotchkiss, A. T., Chau, H. K., Strahan, G. D., Nuñez, A., Simon, S., White, A. K., Dieng, S., Heuberger, E. R., Yadav, M. P., & Hirsch, J. Structure and composition of blueberry fiber pectin and xyloglucan that bind anthocyanins during fruit puree processing. *Food Hydrocolloids*, 116. (2021). <https://doi.org/10.1016/j.foodhyd.2020.106572>
- Bof, M. J. et al. 'Bio-Packaging Material Impact on Blueberries Quality Attributes under Transport and Marketing Conditions', *Polymers*. doi: 10.3390/polym13040481. (2021)

## Enzymatic modification of a polysaccharides-rich extract from green marine macroalgae *Ulva* sp. for the enrichment of its biological activity

Stamatia Spyrou<sup>1</sup>, Alexandra V. Chatzikonstantinou<sup>1</sup>, Renia Fotiadou<sup>1</sup>, Archontoula Giannakopoulou<sup>1</sup>, Petros Katapodis<sup>1</sup>, Epaminondas Voutsas<sup>2</sup>, Haralambos Stamatis<sup>1\*</sup>

<sup>1</sup>Laboratory of Biotechnology, Department of Biological Applications and Technologies, University of Ioannina, 45110 Ioannina, Greece

<sup>2</sup>Thermodynamics and Transport Phenomena Laboratory, Department of Chemical Engineering - Section II, National Technical University of Athens, Heroon Polytechniou 9, Zographos, 15780 Athens, Greece

\*Corresponding author: [hstamati@uoi.gr](mailto:hstamati@uoi.gr)

### Abstract

Marine macroalgae represent a rich source of bioactive compounds that can be used in various food, cosmetic and pharmaceutical products for health improvement. More specifically, *Ulva* sp. has been proven to contain bioactive compounds, such as polyphenols, polysaccharides, carotenoids, and  $\omega$ -3 fatty acids that possess significant bioactivity<sup>1</sup>. It is typical that *Ulva* sp. has a rich content of sulfated polysaccharides that possess anti-viral, anti-tumour, anti-coagulant, hepatoprotective, immuno-stimulating, anti-depressant and anti-anxiolytic activities and are increasingly requested for pharmaceutical and food applications<sup>2</sup>. Alongside, biocatalysis is widely used for the targeted modification of natural compounds in order to enhance their biological activity, among many properties<sup>3</sup>.

In the present work, an aqueous extract, rich in polysaccharides, was prepared from *Ulva* sp., a green macroalgae collected from Epirus coast. The prepared extract was assessed for its plenty of carbohydrates with Phenol-Sulfuric acid assay. A method for its enzymatic modification with a carbohydrase mixture, commercially available as “Viscozyme”, was developed, in order to be produced mono- and oligosaccharides from the mother, polysaccharides-rich extract. Both natural and enzymatically modified extracts were assessed for their antioxidant activity with DPPH and FRAP methods, their antimicrobial activity against a gram positive and a gram negative bacteria and their enzyme inhibitory activity against dermal aging enzymes such as elastase, lipoxigenase and collagenase. The results indicated the rich content of carbohydrates in the prepared extract as well as its successful enzymatic treatment with the carbohydrase mixture. As far as the biological activities of natural and modified extract are concerned, the enhancement of mother extract’s bioactivity after the enzymatic treatment is clear, highlighting the importance of the produced oligo- and monosaccharides.

### Materials-Methods

*Ulva* sp. was collected from Epirus coast in March 2019 and an aqueous extract, rich in polysaccharides, was prepared from its dry batch<sup>4</sup>. More specifically, five grams of dry ulva flakes were soaked in 100 mL d.d. H<sub>2</sub>O at 90°C for 30 min. The resulting extract was filtered and subjected to lyophilization. The extract was assessed for the presence of carbohydrates by Phenol-Sulfuric acid method<sup>4</sup> and was enzymatically modified with a carbohydrase mixture, commercially available as “Viscozyme”, for different reaction times<sup>5</sup>. Each sample was tested for the presence of reducing sugars with DNSA method. The reaction conditions that led to the highest reducing sugar content were chosen as the most appropriate and were further exploited for the enzymatic modification of the extract. The aqueous extract was modified with the carbohydrase mixture and lyophilized for further usage.

Both natural and modified extracts were assessed for different biological activities. More specifically, DPPH and FRAP methods were conducted in order to be assessed different aspects of extracts’ antioxidant activity. Additionally, extracts were tested for their antimicrobial activity against a Gram negative (*Escherichia coli*) and a Gram positive (*Corynebacterium glutamicum*) bacteria and for their enzyme inhibitory activity against dermal aging enzymes e.g. lipoxigenase, elastase and collagenase. The enzymes that were used for inhibition assays are highly homologous with the human ones. All reagents were of analytical grade and purchased from reliable sources.

### Results

The most important findings of this work are presented on the below Figure. The enzymatic treatment of the aqueous extract with a commercially available carbohydrase mixture, led to a new chemical profile, consisting of oligo- and monosaccharides in place of mother polysaccharides. As it was anticipated, the resulting products possessed different bioactivities compared to the corresponding ones before enzymatic treatment. More specifically, enhancement of extract’s antimicrobial, enzyme inhibitory and antioxidant activity was observed in most cases, results which are very crucial and are reported for first time for *Ulva* sp. macroalgae, highlighting the importance of reaction’s products and arousing the interest for further investigation of the chemical nature of the resulting products.

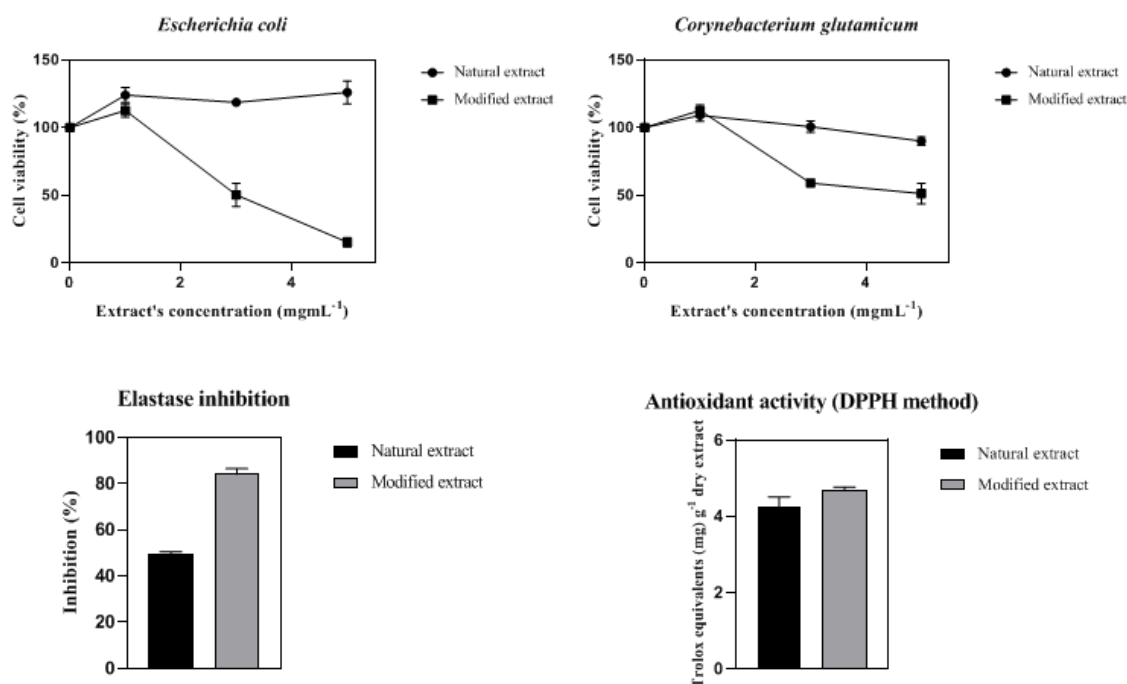


**Figure 1.** The most important findings, as far as the biological activities of natural and modified extracts are concerned, are presented. Charts for their antimicrobial activity against *Escherichia coli* and *Corynebacterium glutamicum* strains at different tested concentrations, for their elastase inhibitory activity at the concentration of 5 mgmL<sup>-1</sup> and for their antioxidant activity expressed as Trolox equivalents (mg) g<sup>-1</sup> dry extract, are given.

## Acknowledgements

This research was co-financed by the European Regional Development Fund of the European Union and Greek national funds through the Operational Program Competitiveness, Entrepreneurship and Innovation, under the call 'Aquaculture'-'Industrial Materials'-'Open Innovation In Culture'(project:Biomalga, project code: T6YBII-00033).

## References

1. A.M. Cikoš, S. Jokić, D. Šubarić, I. Jerković, *Mar. Drugs*, **16** 348 (2018).
2. H. Dominguez, E.P. Loret, *Mar. Drugs*, **17** 357 (2019).
3. I. Antonopoulou, S. Varriale, E. Topakas, U. Rova, P. Christakopoulos, V. Faraco, *Appl. Microbiol. Biotechnol.*, **100** 6519–43 (2016).
4. R.T. Neto, C. Marçal, A.S. Queirós, H. Abreu, A.M.S. Silva, S.M. Cardoso, *Int. J. Mol. Sci.*, **19** 2987 (2018).
5. N. Trivedi, V. Gupta, C.R.K. Reddy, B. Jha, *Bioresour. Technol.*, **150** 106-112 (2013).

## Synthesis of profluorescent nitroxide-alginate bioconjugate for biocompatible scavenging and detection of ROS in bone tissue culture

Nattawut Decha<sup>1</sup>, Jirut Meesane<sup>2</sup> and Chittreya Tansakul<sup>1\*</sup>

<sup>1</sup>Division of Physical Science and Center of Excellence for Innovation in Chemistry, Prince of Songkla University  
15 Kanchanavanich Road, Hat Yai, Songkhla 90110, Thailand

<sup>2</sup>Institute of Biomedical Engineering, Faculty of Medicine, Prince of Songkla University  
15 Kanchanavanich Road, Hat Yai, Songkhla 90110, Thailand

\*chittreya.t@psu.ac.th

Reactive oxygen species (ROS), such as hydroxyl radical, superoxide anion and hydrogen peroxide, is usually produced in all eukaryotic cells for signal transduction and neurotransmission, etc. These molecules are unstable compounds or radical moieties. Therefore, overproduction of ROS provides an imbalance between oxidants and antioxidants called oxidative stress. The imbalance of ROS can cause lipid, protein, DNA or cell membrane damages. These implicated coronary artery disease, diabetes, Alzheimer and osteoporosis [1]. Osteoporosis is commonly found in people of all ages, especially old and middle-ages. Bone tissue engineering using scaffold can be used to treat these patients after the cartilage surgery [2]. Microbial biomass, alginate, is known for its biocompatibility as well as biodegradability, and displays an important role in cell growth as bio-based scaffold for bone tissue culture [3]. Detection and scavenging of ROS in bone tissue culture is crucial, however ROS is difficult to be directly detected due to its instability. Nitroxide probe is one of reported detectors, which can indirectly detect ROS [4]. Nitroxide bearing fluorophore commonly known as profluorescent nitroxide is non-fluorescent resulting from transferring of excited electrons from a fluorophore to an unpaired-electron of nitroxide. Indirect detection of ROS is depicted in **Figure 1**. For example, interaction between hydroxyl radical and dimethyl sulfoxide (DMSO) would afford methyl radical which are trapped by profluorescent nitroxide probe **1**, and consequently fluorescent compound **2** is generated [5].

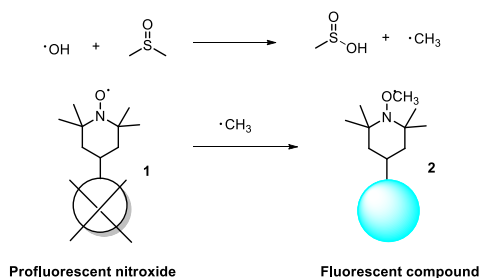


**Figure 1.** Reaction between hydroxyl radical and DMSO as well as reaction between profluorescent nitroxide **1** and methyl radical to construct fluorescent methoxyamine **2**

In this study, for the purpose of ROS scavenging and detection in bone tissue culture, profluorescent nitroxide-alginate bioconjugate **3** consisting of alginate for naturally derived-biomass scaffold, nitroxide quencher and fluorophore was designed (**Figure 2**). Bone tissue culture containing nitroxide-alginate conjugate **3** without DMSO should be non-fluorescent. After an addition of DMSO, interaction between DMSO and produced ROS would provide sulfoxyl or methyl radicals. Then **3** would be trapped either by sulfoxyl radical or methyl radical to form fluorescent methoxyamine **4a**, methanesulfinamide **4b** or methanesulfonamide **4c**.

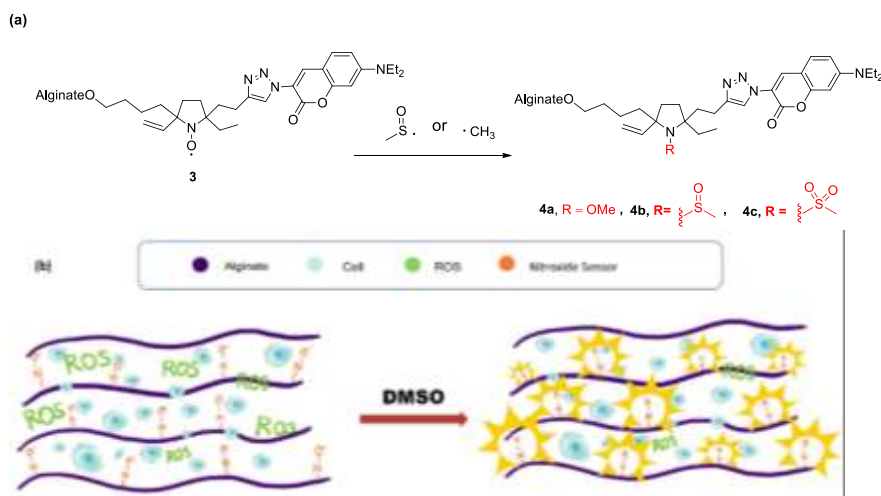
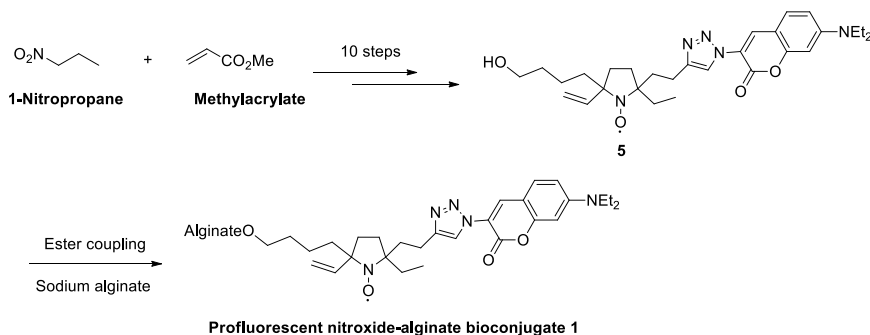


**Figure 2. (a)** Restoration of fluorescence by interaction between profluorescent nitroxide-alginate bioconjugate **3** and sulfoxyl radical or methyl radical to form fluorescent compounds **4**, **(b)** illustration of indirect scavenging and detection of ROS in bone tissue culture

Synthesis of profluorescent nitroxide probe was briefly described in **Scheme 1**. 1-Nitropropane and methyl acrylate were used as starting materials to achieve the profluorescent nitroxide probe **5** in 10 steps. Alginate and **5** was assembled via ester coupling reaction to achieve profluorescent nitroxide-alginate bioconjugate **1** [6]. All synthesized compounds were purified by column chromatography, and characterized by  $^1\text{H}$  and  $^{13}\text{C}$  NMR and IR spectroscopies as well as high-resolution mass spectrometry. Noted that bioconjugate **1** was purified by dialysis.



**Scheme 1.** Synthesis of profluorescent nitroxide-alginate bioconjugate **1**

In this research, profluorescent nitroxide-alginate bioconjugate **1** was successfully synthesized in 11 steps. For detection of ROS, this probe will be utilized in bone tissue culture in PBS buffer treated with cold atmospheric plasma for a minute under argon atmosphere to accelerate the generation of ROS. The 100% plasma-treated PBS (pPBS) will further diluted in PBS to final concentrations of 12.5%, 25%, 37.5%, 50%, 62.5% pPBS, which was then directly added in a 1/6 dilution in the media to the cells. The calibration curve of fluorescence intensities versus concentrations of ROS will be obtained for quantitative analysis.

## Acknowledgements

The Royal Golden Jubilee Doctoral Scholarship  
Center of Excellence for Innovation in Chemistry (PERCH-CIC)  
Division of Physical Science, Faculty of Science, Prince of Songkla University

## References

1. M. Sleiman, H. Destailats, L.A. Gundel, *Talanta*, **116** 1033 (2013).
2. J.J. Green, J.H. Elisseeff, *Nature*, **540** 386 (2016).
3. J. Venkatesan, I. Bhatnagar, P. Manivasagan, K-H. Kang, S-K. Kim, *Int. J. Biol. Macromol.*, **72** 269 (2015).
4. B. Miljevic, K.E. Fairfull-Smith, S.E. Bottle, Z.D. Ristovski, *Atmos. Environ.*, **44** 2224 (2010).
5. X-F. Yang, X-Q. Guo, *Analyst*, **126** 1800 (2001).
6. A. Bernkop-Schnurch, C.E. Kast, M.F. Richer, *J. Control. Release*, **71** 277 (2001).

**European Sustainable BIO-based nanoMaterials Community (BIOMAC)**Zoe Terzopoulou<sup>1</sup>, Konstantinos S. Triantafyllidis<sup>1</sup>, Dimitrios Bikiaris<sup>1</sup><sup>1</sup>Department of Chemistry, Aristotle University of Thessaloniki (AUTH), Thessaloniki, Greece\*Corresponding author: [ktrianta@chem.auth.gr](mailto:ktrianta@chem.auth.gr); [dbic@chem.auth.gr](mailto:dbic@chem.auth.gr)

The successful implementation of the European Circular Bio-Economy relies on the development of benign technologies for the sustainable production of chemicals, fuels and materials derived from the utilization of waste biomass. A wider adoption of such products can solve several problems linked to solid waste disposal, as they could be further re-used at the end of their life cycle, ensuring full circularity. Nanostructured bio-based materials (NBM) are the answer to many challenges faced by our society, embracing several applications in the fields of packaging, automotive, printed electronics, agriculture, and construction. Due to their small size, nanomaterials have peculiar physical, mechanical, chemical, and electrical properties which could expand the range of revolutionary applications.

NBMs can be based on polymers derived from biomass fractions or synthesized from biomass-originated monomers, being further reinforced with nanomaterials/nanoadditives also derived from biomass, such as nanocellulose, nanolignin or nano-porous biochar. In general, bio-based polymers have recently gained increasing interest as an alternative to fossil-based polymers. Their annual production growth is estimated by around 15-20% using renewable sources, thus reducing CO<sub>2</sub> emissions by 60-80% and the needs for non-renewable energy use at about 70%. However, many technical, economical, and regulatory barriers still hinder the full deployment of bio-based polymers and related nanomaterials in the market and limit the implementation of solutions based on such materials. The Horizon2020 project BIOMAC aims at reducing these barriers and fostering the European Bioeconomy. It is one of the biggest EC-funded projects with 33 partners (academia, institutions, and companies) from 12 European countries. BIOMAC establishes a self-sustainable Open Innovation Test Bed (OITB) capable of upscaling the production of NBMs and facilitating the market-readiness of the related technologies and products. SMEs will be granted access to the services and facilities of the BIOMAC ecosystem after an initial validation phase, where practical applications of NBM will be demonstrated.

The BIOMAC ecosystem will function as a cluster of parallel activities taking the form of 17 Pilot lines (PLs) covering the whole value chain, from biomass fractionation and intermediate chemicals to final bio-based polymers and composites. The PLs are grouped in 3 clusters and their activities will enable the realization of 5 concrete outputs (Test Cases), demonstrating the validity of BIOMAC's approach and the high value of NBM applications. Below is the list of the Test Cases (TeCs):

*TeC1: Automotive*

Bio-based resins reinforced with NBMs will be used in the fabrication of interior car parts and components for the automotive industry. These will be succinate-based polyesters and isocyanate-free polyurethane resins with exceptional physical properties including toughness, flexibility, and resistance to abrasion and temperature.

*TeC2: Agricultural applications*

The use of different biomaterials and NBMs will be validated in agricultural applications. Succinic and lactic acid will be derived from biomass and will be used as monomers in the development of completely biodegradable succinate and PLA biopolymers. Both biopolymers will be nano-reinforced with nanolignin, biochar, nanocellulose, etc., to create materials with enhanced mechanical properties and decreased water vapor transmission rates, as well as with antioxidant/optical properties and UV/thermal resistance appropriate for mulch films, injection-molded clips, thermoformed/injection molded pots, seeds coating, coating for controlled-release fertilization etc., to be used in agriculture. Biopolymers and nano additives will contribute to soil amendment and remediation after biodegradation of bioplastics in soil, to improve technical performances while increasing soil health and quality.

*TeC3: Food packaging*

Vacuum thermoforming will be post-utilized to produce bio compostable and biodegradable food containers, using bio-based PLA foils. These will be reinforced with bacterial nanocellulose and nanolignin to enhance the mechanical and antibacterial properties of flexible packaging materials. Two additional techniques will be applied on PLA film i.e., coating with NBMs to improve its permeability to gaseous compounds (water and oxygen), and specific micro/nano textured geometries will be designed, fabricated and replicated using nanoimprint lithography. This will further enhance the antimicrobial and antifungal properties of the film's surface, leading to improved food maintenance/conservation and safety.

*TeC4: Construction*

Bio-based polymer and composites will be tested in the construction industry. A footbridge module made from isocyanate free TPU biopolymers reinforce



d with nanolignin, biochar and nano fibrillated cellulose will be constructed with 3D printing technology. Fused filament fabrication (FFF) filaments prepared by melt extrusion will be used, and simple printing tests of the bio-filament will be performed using conventional fused deposition modelling equipment. The final product is expected to have high UV and fire resistance, anti-fouling & easy-cleaning capability.

#### *TeC5: Printed Electronics*

The main objective will be to develop stretchable conductive layers embedded into textiles (sock with integrated conductors) using a bio-based stretchable substrate, an ink and adhesives with printed electronic processes. Bio-based inks will be reinforced with bio-resins. TPU produced by REX and bio-based succinate polyesters will be used as flexible substrates, and nano-copper for stretchable electrical prints will be integrated directly into textiles as stretchable circuitry between sensors and electronics. To achieve this, nano biochar will be modified by nano-copper and silver to enhance their electrical conductivity.

#### *The Open Call and after-life sustainability*

After the successful demonstration of the five TeCs, BIOMAC will launch an Open Call aiming to select 5 new TeCs by companies and research bodies interested to access the ecosystem services. The BIOMAC ecosystem will offer them services for upscaling biomaterial concepts through the Pilot Lines and cover the assessment of regulation, safety, sustainability, circularity, and market potential. It will provide open services and solutions, accessible to SMEs or other Industries from a single-entry point. Through the Pilot lines, technologies that have been developed up to TRL 4-5 will be upscaled and validated up to TRL 7. This same procedure will be extended after the project's official duration, granting innovators and researchers access to the ecosystem's services at fair conditions and cost beyond 2024.

### **Acknowledgements**

This project has received funding from the European Union's Horizon 2020 Research and Innovation Programme under Grant Agreement No. 952941

## The study of a natural antioxidant interaction with a biomaterial substrate

Raluca M. Visan<sup>1\*</sup>, Anca R. Leonties<sup>1</sup>, Ludmila Aricov<sup>1</sup>, Mihai Anastasescu<sup>1</sup> and Daniel G. Angelescu<sup>1</sup>

<sup>1</sup>"Ilie Murgulescu" Institute of Physical Chemistry, Romanian Academy, 202 Splaiul Independentei st., 060021, Bucharest  
\*rvisan@icf.ro

Nowadays, potential biological effects of natural antioxidant substances are extensively investigated for understanding the mechanism of interaction with the human tissues. Flavonoids and their derivatives are considered to be a representative class of polyphenolic compounds. Quercetin (QE) is a dietary yellow powder, widely known for valuable medicinal purposes like antitumor and anti-inflammatory activities. Despite this fact, its poor solubility in aqueous medium constitutes the main reason of restricted applications. Chitosan (CT) is a natural versatile polysaccharide, which can be shaped in nanoparticles, thin films or microspheres for enzyme immobilization on support materials [1]. Moreover, CT is able to carry various hydrophilic and hydrophobic drugs. Its macromolecular architecture can be crosslinked by small anion molecules like polyphosphates to finally achieve stable materials [2]. In this work, it has been designed an experimental and computational model, in order to explore the quercetin interaction behavior with a biopolymer gel formed by chitosan (CT) and phytic acid (PA). The experimental procedure involves obtaining a biomaterial substrate loaded with QE, formed through a very gentle synthesis method (ionotropic gelation). QE powder was solubilized in ethanol 99% followed by evaporation of the solvent. A PA solution was added drop-wise using a sterile syringe to an aqueous medium consists of polymer and antioxidant. The encapsulated nanoparticles were formed spontaneously and further washed, purified and analysed. Morphological features were evaluated and investigated by AFM, DLS, fluorescence, FT-IR and UV-Vis spectroscopy. Molecular dynamics simulations were performed using GROMACS 4.5.4. software. The starting geometry of the CT chain was generated using the Avogadro package. QE associations with CT chains mediated by PA molecules were analysed.

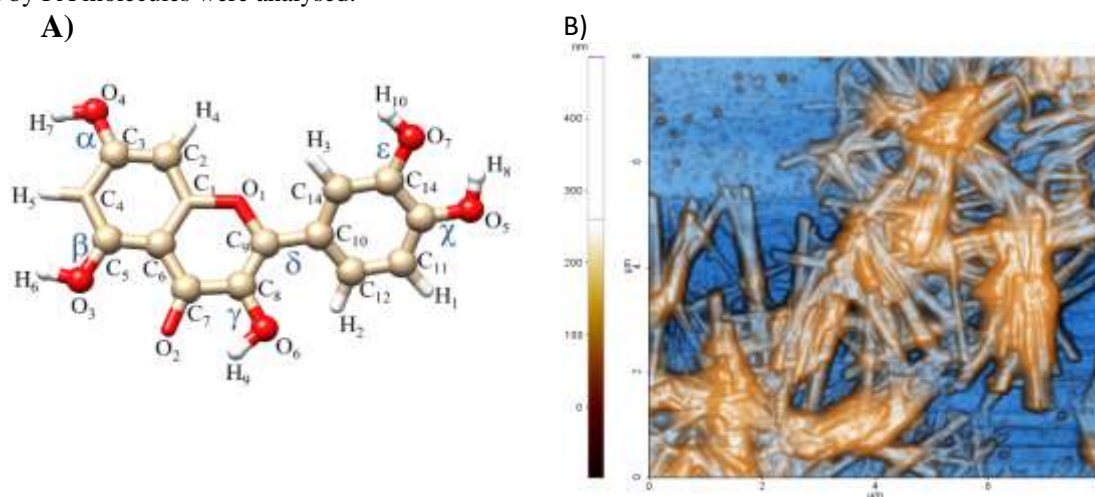


Figure 1. A) Structure of QE ; B) Representative AFM image of the QE loaded CT-PA

QE loaded-nanomaterials were successfully synthesized and investigated through experimental and computational methods. The QE molecules were entrapped in the CT-PA network through hydrogen-bonding interactions. As it can be seen in the Figure 1, outstanding fibrillar shapes of loaded CT-PA nanosystems were obtained at a specific concentration of CT. Moreover, the geometry, atom name and dihedral angle labelling for QE are represented above.

**Acknowledgements:** This work was supported by the Romanian Academy within the research program "Colloids and dispersed systems of the "Ilie Murgulescu" Institute of Physical Chemistry and by the UEFISCDI government project TE 68/2022-PN-III-P1-1.1-TE-2021-0418.

### References

- R.M. Visan, A.R. Leonties, L. Aricov, V. Chihaiia and D.G. Angelescu, *Phys. Chem. Chem. Phys.*, **23** 22601-22612 (2021).
- A.R. Leonties, A. Răducan, D.C.Culiță, E. Alexandrescu, A. Moroșan, D.E. Mihaescu, L. Aricov, *Chem. Eng. J.*, **439** 135654 (2022).

## Towards sustainability: Exploring the properties of novel vanillic acid-based polyesters

Eleftheria Xanthopoulou<sup>1,2</sup>, Alexandra Zamboulis<sup>2</sup>, Zoi Terzopoulou<sup>1,2</sup>, Dimitrios N. Bikiaris<sup>2,\*</sup> and George Z. Papageorgiou<sup>1,4\*</sup>

<sup>1</sup> Department of Chemistry, University of Ioannina, P.O. Box 1186, GR-45110 Ioannina, Greece

<sup>2</sup> Laboratory of Polymer Chemistry and Technology, Department of Chemistry, Aristotle University of Thessaloniki, GR-54124 Thessaloniki, Greece

<sup>3</sup> Digital Manufacturing and Materials Characterization Laboratory, School of Science and Technology, International Hellenic University, 14km Thessaloniki, 57001 N. Moudania, Greece

<sup>4</sup> Institute of Materials Science and Computing, University Research Center of Ioannina (URCI), GR-45110, Ioannina, Greece

[\\*elefthxanthopoulou@gmail.com](mailto:*elefthxanthopoulou@gmail.com)

As global energy and resources have faced enormous challenges over the years, conventional petroleum-based polymers are considered as one of the most important environmental threats. The continuous growth of waste accumulation after their short-term use, along with their contribution to greenhouse gases' emissions, have intensified the public awareness over the quest of alternative routes towards the production of polymeric materials. Thus, different approaches for the transition from a petrochemically-dependent society to a bioeconomy have been proposed, both by academic and industrial communities. One of the most prevalent routes is the exploitation of renewable resources towards the production of sustainable monomers, polymers, and chemicals. Within this context, , One of the most promising monomers derived from lignin biomass is vanillic acid (VA), which constitutes an oxidation product of vanillin, the most produced aroma chemical and appears as a great alternative building block for thermoplastic polyesters. Herein, the properties of novel VA-based polyesters were investigated. Specifically, the structural features were measured using multiple techniques, such as Fourier-transformed Infrared spectroscopy (FTIR) and Nuclear Magnetic Resonance spectroscopy (NMR), while the thermal transitions were evaluated via Differential Scanning Calorimetry (DSC). Finally, the mechanical properties were investigated as they affect the final application of the materials.

### Acknowledgements

This work is based upon COST Action FUR4Sustain, CA18220, supported by COST (European Cooperation in Science and Technology).

## FDCA-based copolyesters modulate the properties of PLA-based blends

Zoi Terzopoulou<sup>a,b</sup>, Alexandra Zamboulis<sup>a\*</sup>, Lazaros Papadopoulos<sup>a</sup>, Dimitrios N. Bikiaris<sup>a</sup>, George Z. Papageorgiou<sup>b</sup>

[a] Laboratory of Chemistry and Technology of Polymers and Dyes, Department of Chemistry, Aristotle University of Thessaloniki, GR-541 24 Thessaloniki, Greece

[b] Department of Chemistry, University of Ioannina, P.O. Box 1186, GR-45110 Ioannina, Greece

\*azamboulis@gmail.com

Poly(lactic acid) (PLA) is currently the most frequently used biobased thermoplastic polyester. It is compostable, processable but also brittle. The properties of polymers often need tuning to obtain final products with the desirable characteristics for specific applications. Polymer blending has attracted considerable interest as an easy and cost-effective method of fabricating materials for a wide range of applications. Therefore, PLA blends with both biodegradable and non-biodegradable polymers have been investigated for many applications. Biobased polymers derived from 2,5-furan dicarboxylic acid (2,5-FDCA), a promising monomer produced by the oxidation of hydroxymethylfurfural, are in the forefront of both academic and industrial research towards this goal.<sup>[1]</sup> In this work, biobased and biodegradable copolymers poly(butylene 2,5-furan dicarboxylate-co-adipate) (PBF-co-PBAd) with different comonomer ratios were synthesized and blended with PLA, to produce fully biobased blends and examine their physicochemical properties.

PBF, PBAd and PBF-co-PBAd copolymers were synthesized with the transesterification and melt polycondensation method with Titanium(IV) butoxide catalyst. The copolymers were prepared in three different molar ratios; 25/75, 50/50 and 75/25. Afterwards, each homopolymer and copolymer was blended with 70 wt% PLA by melt compounding at 190 °C and 35 rpm for 5 min. Intrinsic viscosity  $[\eta]$  was measured with an Ubbelohde viscometer. The chemical structures and comonomer ratios were confirmed with NMR spectroscopy. Thermal transitions and thermal stability were examined with Differential Scanning Calorimetry (DSC) and Thermogravimetric Analysis (TGA), respectively. Mechanical properties were studied with nanoindentation. The compatibility of the blends was evaluated with Scanning Electron Microscopy (SEM) and DSC. Finally, reactive blending was tested as a means to improve the compatibility of the polymer blends.

### Acknowledgements

This research is based upon work from COST Action FUR4Sustain, CA18220, supported by COST (European Cooperation in Science and Technology) and is co-financed by Greece and the European Union (European Social Fund- ESF) through the Operational Programme «Human Resources Development, Education and Lifelong Learning» in the context of the project “Reinforcement of Postdoctoral Researchers - 2nd Cycle” (MIS-5033021), implemented by the State Scholarships Foundation (IKY).



### References

[1] Terzopoulou, Z., Papadopoulos, L., Zamboulis, A., Papageorgiou, D. G., Papageorgiou, G. Z., & Bikiaris, D. N., *Polymers*, 12(6) 1209 (2020).

## Synthesis and properties of poly(glycerol pimelate), a hyperbranched polyester for ocular drug delivery

Eirini Nakiou<sup>1</sup>, Alexandra Zamboulis<sup>1</sup> and Dimitrios Bikiaris<sup>1\*</sup>

<sup>1</sup>Laboratory of Polymer Chemistry & Technology, Department of Chemistry, Aristotle University of Thessaloniki, Greece

\*dbic@chem.auth.gr

Aliphatic polyesters are widely used for biomedical, pharmaceutical and environmental applications due to their high biodegradability and low-cost production. They can undergo hydrolysis within a reasonable time frame, which is a necessary property for biomedical applications. Besides linear polyesters, star and hyperbranched polyesters based on glycerol and  $\omega$ -fatty diacids have gained considerable interest for the development of novel biodegradable and biocompatible materials.

Pimelic acid is a seven-carbon aliphatic dicarboxylic acid with the chemical formula  $\text{HOOC}(\text{CH}_2)_5\text{COOH}$ . Both glycerol, which can be converted to glucose through a series of chemical transformations in the liver, and pimelic acid are generally regarded as safe materials according to the US Food and Drug Administration (FDA), and thus have been approved to be used in products for medical and tissue engineering applications [1].

Ocular drug delivery is one of the most challenging tasks faced by pharmaceutical researchers due to the anatomy, biochemistry and physiology of the eye and it is a great challenge for the formulator to pass through the protective barriers of the eye without causing any tissue damage [2]. In this context, we have investigated the synthesis of poly(glycerol pimelate) (PGP) as a promising candidate for ocular biocompatible materials, and we will present the synthesis and characterization of PGP polyesters. The synthesis of PGP was performed in two stages: (a) a one-step non-catalyzed polycondensation leading to the pre-polymer (oligoesters) and (b) thermal crosslinking. A series of pre-polymers with different properties were produced by changing the reaction parameters: the molar ratio of the reactants and the reaction time and temperature (160 - 180 °C), while the determination of acid values was used to monitor the conversion. Crosslinking was carried out at 120 °C under vacuum for 24 - 48 h to obtain the final elastomeric products. Pre-polymers and final polymers were characterized by infra-red and nuclear magnetic spectroscopies, differential scanning calorimetry and X-ray diffraction. The optimal polyesters were further used as contact lenses for the delivery of the ophthalmic drug liftegrast for the dry eye disease treatment.

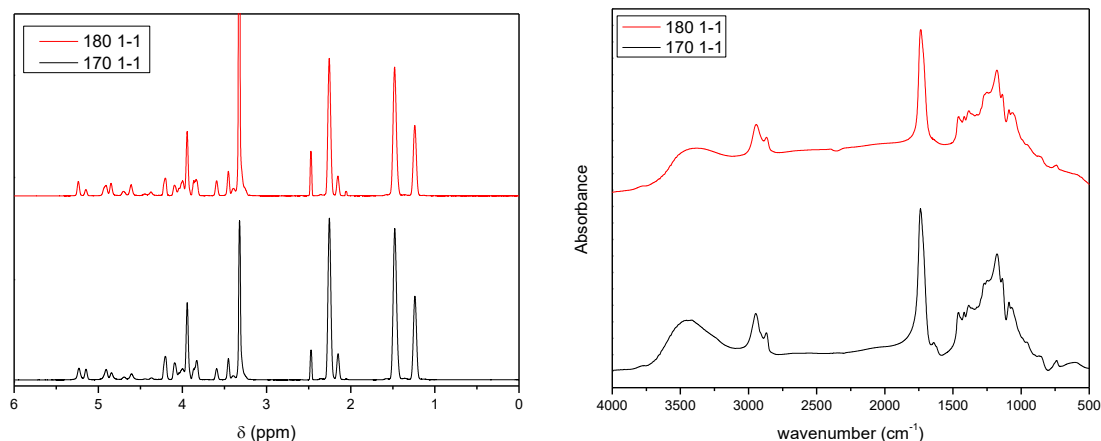


Figure 1. <sup>1</sup>H NMR and IR spectra of two PGP pre-polymers.

### References

1. H. Kimura, Y. Ogura, *Ophthalmica*, **215** 143 (2001).
1. A. Zamboulis, E. Nakiou, E. Christodoulou, D. N. Bikiaris, E. Kontonasaki, L. Liverani, A. R. Boccacini, *Int. J. Mol. Sci.*, **20** 6210 (2019).

# Synthesis and analysis of bio-based epoxy resin from native lignin derived oligomers

Yingtuan Zhang<sup>1</sup> and Bert F. Sels<sup>2\*</sup>

<sup>1</sup>Center for Sustainable Catalysis and Engineering, Faculty of Bioscience Engineering, KU Leuven, Heverlee 3001, Belgium.

\*bert.sels@kuleuven.be

## 1. Introduction

Lignin is the most abundant natural source of renewable aromatic molecules on earth [1]. Based on the difference in molecular weight, it can be further divided into several groups—lignin monomers, lignin oligomers and lignin macromolecules [2]. Among them, lignin oligomers has becoming a new focus of study due to its wide existence, underestimated value and unique functionality [3]. In the recent developed reductive catalytic fractionation (RCF) process under the ‘lignin-first’ biorefinery concept, a considerable amount of phenolic lignin oligomers is generated through a sustainable way [4, 5]. From some structural elucidating studies, it has been proved that these RCF oligomers has a relatively low molecular weight, compared to lignin oligomers from other sources [6]. Also, they possess a high amount and  $\gamma$ -OH substituted propyl end-chain, which brings them an impressively high amount of aliphatic hydroxyl groups content [7]. Until now, possible conversion and valorization of these RCF oligomers has been investigated, which lifted the veil of their huge potential in serving as green building blocks for fine chemicals, polymers, and other high-value products [8]. Here, we report a novel bio-based epoxy resin with clear structure and high functionality. Several parameters during RCF were studied and their effects on the final produced lignin oligomers were compared. The oligomers with the lowest molecular weight and highest hydroxyl groups content were selected as the best candidates for the synthesis of epoxy resin. Meanwhile, the glycidylation process of lignin molecules was thoroughly studied using both lignin model compounds and lignin oligomers, which later provided us a bio-based epoxy resin with clear structural information as well as good properties.

## 2. Results and discussion

Multiple RCF parameters including catalyst, solvent, additive, as well as hydrogen pressure, temperature and time were investigated. Starting from a conventional Ru-Methanol system, and ending in some new combination such as Ni-Ethylene glycol system, it was discovered that different catalyst-solvent-additive combination had significant effect on the lignin oligomers’ structure—molecular weight and hydroxyl groups content. On the other hand, the changing in the numbers of hydrogen pressure, temperature and time had direct relation to the reaction’s severeness, which consequently influenced mainly the lignin oligomer’s yield. Three candidates with either the lowest molecular weight, the high aliphatic hydroxyl groups content or the high phenolic hydroxyl groups content were selected from the results in Figure 1, as well as a counter reference with exactly the opposite properties.

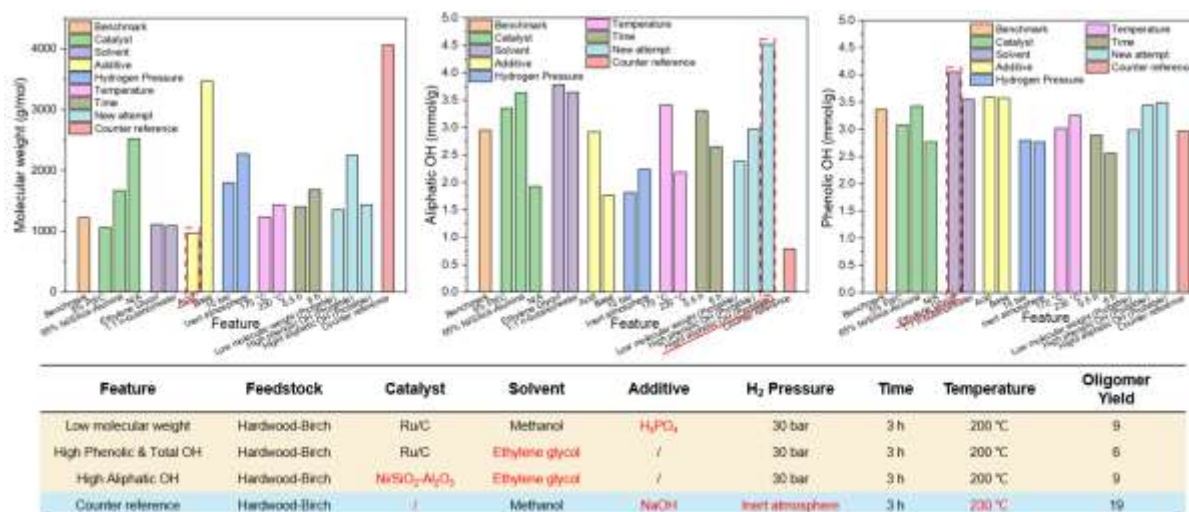
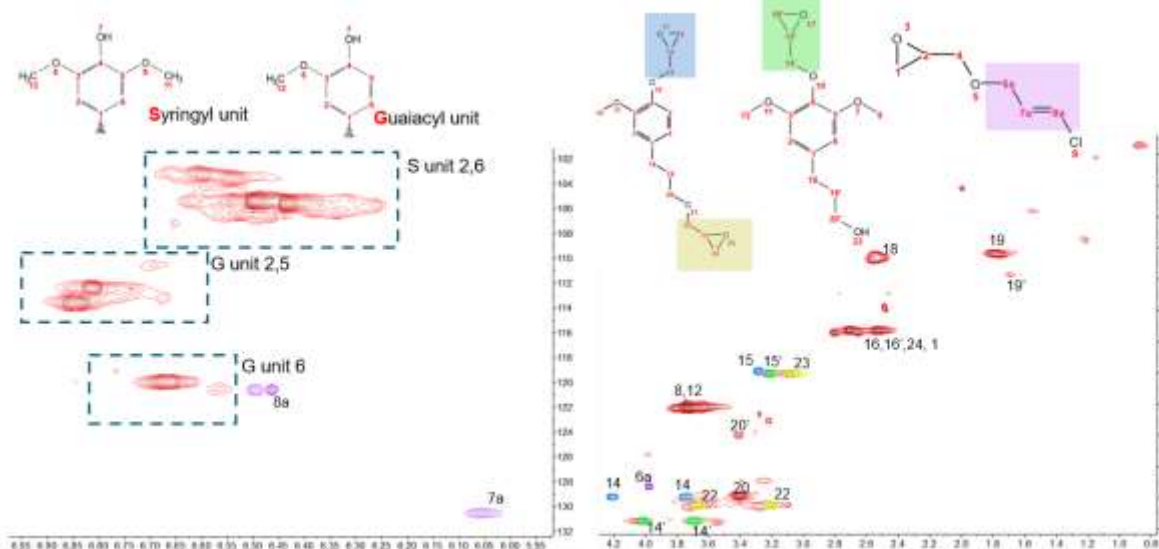


Figure 1. The screening results from different RCF parameters.

A model compounds group consisting of dihydroconiferyl alcohol, dihydrosinapyl alcohol and 5-(3-hydroxy-2-phenylpropyl)-2-methoxyphenol were used as substrates for studying the glycidylation process in lignin molecules. Under the effect of epichlorohydrin and NaOH, the phenolic hydroxyl groups were well converted to epoxy rings, but such conversion was not observed in the aliphatic hydroxyl groups. This is due to lower reactivity of aliphatic hydroxyl groups, especially their less vulnerability to be deprotonized. When a stronger based—NaH was applied, the aliphatic conversion improved significantly to almost one hundred percent, which further confirmed the necessity of strong base in the glycidylation of less active hydroxyl groups. The similar pattern was then discovered

in the glycidylation of lignin oligomers from RCF. Seeing from Figure 2, the epoxy rings at different positions—aliphatic end-chain, phenolic Syringyl units and phenolic Guaiacyl units were clearly distinguished in the 2D HSQC NMR spectrum. Using NaH as the base catalyst, an aliphatic conversion as high as ninety eight percent was achieved, which took a great advantage of the considerably high amount of aliphatic hydroxyl groups in the RCF lignin oligomers. Together with the phenolic positions, a total of 103.2 epoxy rings was discovered in per 100 aromatic units, which later brought good thermal and mechanical properties.



**Figure 2.** The 2D HSQC NMR spectrum and the assignments of the glycidylated RCF lignin oligomer.

## References

- Bertella, S. and J.S. Luterbacher, *Lignin Functionalization for the Production of Novel Materials*. Trends in Chemistry, 2020. **2**(5): p. 440-453.
- Prothmann, J., et al., *Identification of lignin oligomers in Kraft lignin using ultra-high-performance liquid chromatography/high-resolution multiple-stage tandem mass spectrometry (UHPLC/HRMS(n))*. Anal Bioanal Chem, 2018. **410**(29): p. 7803-7814.
- Crestini, C., et al., *Milled wood lignin: a linear oligomer*. Biomacromolecules, 2011. **12**(11): p. 3928-35.
- Van den Bosch, S., et al., *Tuning the lignin oil OH-content with Ru and Pd catalysts during lignin hydrogenolysis on birch wood*. Chem Commun (Camb), 2015. **51**(67): p. 13158-61.
- Van den Bosch, S., et al., *Reductive lignocellulose fractionation into soluble lignin-derived phenolic monomers and dimers and processable carbohydrate pulps*. Energy & Environmental Science, 2015. **8**(6): p. 1748-1763.
- Liao, Y.H., et al., *A sustainable wood biorefinery for low-carbon footprint chemicals production*. Science, 2020. **367**(6484): p. 1385-+.
- Van Aelst, K., et al., *Reductive catalytic fractionation of pine wood: elucidating and quantifying the molecular structures in the lignin oil*. Chemical Science, 2020. **11**(42): p. 11498-11508.
- Van Aelst, K., et al., *Low molecular weight and highly functional RCF lignin products as a full bisphenol a replacer in bio-based epoxy resins*. Chem Commun (Camb), 2021. **57**(46): p. 5642-5645.

# Catalytic processes (homogeneous, heterogeneous and bio-catalysis)



## Design of noble-metal-free molecular catalysts and photosensitizers for photocatalytic hydrogen production

Dimitra Gioftsidou,<sup>1</sup> Charikleia Tzatzia,<sup>1</sup> Georgios Landrou,<sup>2</sup> Antonios Hatzidimitriou,<sup>1</sup> Athanasios G. Coutsoulelos,<sup>2</sup> and Panagiotis A. Angaridis<sup>1\*</sup>

<sup>1</sup>Aristotle University of Thessaloniki, Department of Chemistry, Thessaloniki, Greece

<sup>2</sup>University of Crete, Department of Chemistry, Heraklion, Crete, Greece

\*panosangaridis@chem.auth.gr

The increasing global energy demand makes the need for a sufficient and sustainable energy supply one of the biggest challenges of the 21st century. Among the various types of renewable energy sources currently in use, solar energy appears to be a viable choice; however, the available methods for storing it are costly and inefficient. A practical solution involves storage of solar energy by converting it into chemical energy, using photochemical water splitting and generation of H<sub>2</sub>, a solar fuel, which can be stored for use at any point. Inspired by nature, a smart and attractive approach for H<sub>2</sub> production via photochemical water splitting is artificial photosynthesis, in which light is absorbed by a photosensitizer, initiates a series of electron transfers to appropriate catalysts that oxidize H<sub>2</sub>O to O<sub>2</sub> (water oxidation catalyst, WOC) and reduce the released H<sup>+</sup> to H<sub>2</sub> (hydrogen evolving catalyst, HEC).[1] The most successful photocatalytic systems that have been utilized for H<sub>2</sub> production rely on heavy and precious transition metals.[2] In this respect, the development of novel systems which are based on low cost and earth abundant 3d metals is of special interest.[3]

In this work, we synthesized a series of homoleptic and heteroleptic Ni(II) and Co(III) complexes bearing chelating heterocyclic thioamidate ligands for utilization as HECs.[4] The hemi-lability of the ligands and the presence of H<sup>+</sup> binding sites in the complexes, as well as their ability for electrocatalytic H<sub>2</sub> production from H<sub>2</sub>O (as found by cyclic voltammetry studies), renders them suitable candidates as molecular catalysts for H<sub>2</sub> production under photocatalytic conditions. Indeed, by combining these complexes either with molecular photosensitizers, such as photoluminescent Cu(I) complexes, or with nano-sized photosensitizers, such as N-doped carbon quantum dots (NCdots),[5] we obtained efficient noble-metal-free photocatalytic systems capable of reducing H<sup>+</sup> from H<sub>2</sub>O to H<sub>2</sub>, using visible light as the only energy source. Systematic structural variations of the catalysts allowed tuning of the photocatalytic activity and the investigation of structure-activity relationships. Spectroscopic studies and DFT calculations are in progress to get a better understanding of the catalytic mechanism. Finally, we immobilized the molecular catalysts on appropriate solid supports to get stable and recyclable materials for heterogeneous photocatalytic H<sub>2</sub> production.

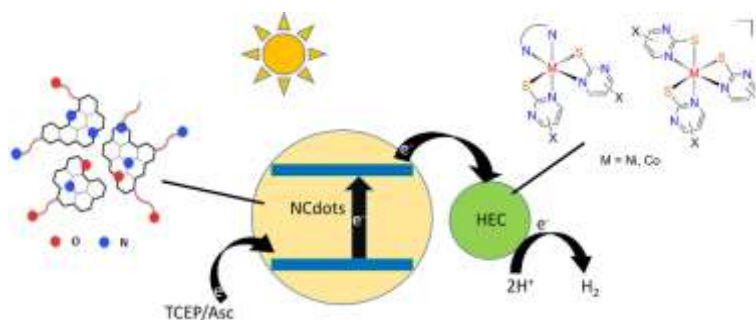


Figure 1. Schematic representation of the photocatalytic H<sub>2</sub> production system used in this study.

### References

1. N.S. Lewis, D.G. Nocera, *PNAS*, **104** 15729 (2007).
2. E.D. Cline, S.E. Adamson, S. Bernard, *Inorg. Chem.*, **47** 10378 (2008).
3. P. Du, R. Eisenberg, *Energy Environ. Sci.*, **5** 6012 (2012).
4. Z. Han, W.R. McNamara, M.S. Eum, P. Holland, R. Eisenberg, *Angew. Chem. Int. Ed.*, **51** 1667 (2012).
5. C. Hu, M. Li, J. Qiu, Y.P. Sun, *Chem. Soc. Rev.*, **48** 2315 (2019).

## Aluminum metal–organic framework-supported single-site nickel-catalyst for heterogeneous chemoselective hydrogenation of nitro and nitrile compounds

Neha Antil<sup>1</sup> and Kuntal Manna<sup>1\*</sup>

<sup>1</sup>Department of Chemistry, Indian Institute of Technology, Delhi, India

\*kmanna@chemistry.iitd.ac.in

Primary and secondary amines, including anilines, are key intermediates in synthesizing agrochemicals, pharmaceuticals, fine chemicals, and industrial materials.[1-3] Developing chemoselective and heterogeneous earth-abundant metal catalysts is essential for environment-friendly chemical synthesis. Despite significant progress with non-noble metal nanoparticles in recent years,[4-7] developing single-site, well-defined heterogeneous and chemoselective earth-abundant metal catalysts with excellent tolerance of various functional groups under mild reaction conditions is challenging. To circumvent such difficulties, the design and synthesis of single-site heterogeneous catalysts based on the inorganic metal-oxo-nodes of metal–organic frameworks (MOF) have drawn considerable interest. The secondary building units (SBUs) of many MOFs has functional OH groups to mimic metal oxides/hydroxides. Due to the tunable pores, high chemical and thermal stability, presence of highly dispersed and uniform OH groups at the nodes, and predictable structures, MOFs offer a unique platform to develop robust single-site nickel-hydride catalysts.[8, 9] We have reported a highly efficient, chemoselective and reusable single-site nickel(II) hydride catalyst based on robust and porous aluminum metal–organic frameworks (MOFs) (DUT-5) for hydrogenation of nitro and nitrile compounds to the corresponding amines at 1 bar H<sub>2</sub> pressure.

DUT-5 MOF having the formula of Al( $\mu_2$ -OH)(bpdc) is constructed from aluminumoxide as SBUs and biphenyldicarboxylate (bpdc) as organic linkers via a solvothermal reaction of AlCl<sub>3</sub>.6H<sub>2</sub>O with bpdc in DMF at 120 °C. Deprotonation of  $\mu_2$ -OH with *n*-BuLi followed by post-synthetic metalation of lithiated DUT-5 with NiBr<sub>2</sub> resulted in the bond formation of nickel with  $\mu_2$ -O to afford Al( $\mu_3$ -ONiBr)(bpdc). The treatment of DUT-5-NiBr with NaEt<sub>3</sub>BH resulted in formation of nickel hydride species, DUT-5-NiH. Synthesized MOF catalyst was characterized using PXRD, BET and TEM. Oxidation state and coordination environment of Ni in DUT-5-NiBr and DUT-5-NiH was investigated by XNAES and EXAFS. DUT-5-NiH was highly effective for the hydrogenation of nitro and nitrile compounds. All the catalysis were performed using 50 mL Parr pressure vessels (4793 (VGR)-T-SS-3000-DVD). Aromatic nitro compounds bearing electron-withdrawing and electron-donating functional groups were successfully hydrogenated to the corresponding amines with excellent yields and selectivity upto 99% using DUT-5-NiH (1 mol% Ni) catalyst in *p*-xylene as the solvent under 1 bar H<sub>2</sub> at 90-130 °C in 6-30 h. DUT-5-NiH was also highly chemoselective in the hydrogenation of nitroarene-bearing groups sensitive to reduction such as iodo, aldehyde, keto, nitrile, and thio. Interestingly, under identical reaction conditions, heterocyclic nitro arenes such as 4-nitropyridine and 5-nitroindole were also hydrogenated to their corresponding amines. The conversions were analyzed using gas chromatography (GC) equipped with a mass detector (Agilent 5977B GC/MSD). Pure products were simply isolated via simple removal of catalysts by centrifugation followed by evaporation of solvent *in vacuo*.

Interestingly, hydrogenation of nitriles selectively afforded either primary or secondary amines depending on the reaction conditions. At a 1.0 mol % Ni loading, dibenzylamine was obtained quantitatively from the hydrogenation of benzonitrile at 90 °C under 1 bar of H<sub>2</sub>. In contrast, benzylamine was afforded quantitatively when the same catalytic reaction was carried out at 130 °C in the presence of 1.1 equiv of di-*tert*-butyl dicarbonate (Boc<sub>2</sub>O) or acetic anhydride (Ac<sub>2</sub>O) with respect to benzonitrile under 1 bar of H<sub>2</sub> followed by acid hydrolysis. Nitriles bearing various functional groups such as alkyl, halo, methoxy, and amino functional groups were fully converted to the corresponding substituted symmetric dibenzyl amines at 90 °C in 90–100% yields. At a 1.0 mol % Ni loading, DUT-5-NiH also gave complete conversion of various substituted nitriles at 130 °C in the presence of Boc<sub>2</sub>O to give the corresponding N-Boc-benzylamines within 6 h, and the corresponding primary amines were isolated as HCl salts after carbamate hydrolysis in acidic conditions. Heterocyclic nitriles, dinitrile and aliphatic nitriles were also reduced to corresponding amines in excellent yields. We found that the hydrogenation of substituted aryl nitriles in the presence of benzylic primary amines under identical reaction conditions gave unsymmetric secondary amines by the reaction of benzylic primary amines and the arylmethanimine intermediate.

The mechanism for the hydrogenation of nitriles was investigated by experimental and computational studies. The plot of initial rates versus substrate concentration showed saturation in high substrate concentrations. Saturation kinetics implies reversible nitrile coordination to nickel followed by the turnover-limiting step. In addition, the initial substrate conversion rates had first-order rate dependence on nickel concentrations and zeroth-order dependence on the pressure of H<sub>2</sub>. Our kinetic data indicated that a substrate molecule and the nickel catalyst were involved in the turnover-limiting state of the catalytic cycle in the hydrogenation of aryl nitriles. To further study the mechanism of DUT-5-NiH-catalyzed hydrogenation of nitriles, we performed DFT calculations using the method (B3LYP) and a basis set of 6-311G(d,p) using the Gaussian 09 software suite, and the calculated energy profile will be discussed in details.

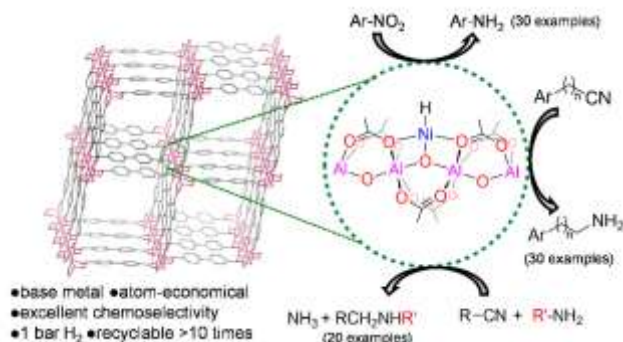


Figure 1. Illustrating the single site Nickel-hydride catalyst supported on DUT-5 metal-organic framework (DUT-5-NiH) for the synthesis of primary and secondary amines.[10]

DUT-5-NiH has a broad substrate scope with excellent functional group tolerance in the hydrogenation of aromatic and aliphatic nitro and nitrile compounds under 1 bar  $H_2$ . Moreover, it could be recycled and reused at least 10 times. Interestingly, pharmaceutical compounds bearing cyanide and nitro groups were hydrogenated to their corresponding amines. Symmetric or unsymmetric secondary amines were also synthesized selectively by changing the reaction conditions of the nitrile hydrogenation. This work has demonstrated that DUT-5 node-ligated single-site base-metal hydrides are promising catalysts in hydrogenation reactions for sustainable synthesis of chemical feedstocks owing to their low cost, excellent stability and reactivity, and usage of cheap and atom-economic reductant hydrogen. In the presentation, importance and benefits of DUT-NiH over other heterogeneous catalysts along with its synthesis and characterization will be discussed in details. The substrate scope (80 examples) for hydrogenation reactions will be illustrated, and the reaction mechanism for hydrogenation of nitriles with its energy profile diagram will also be discussed.

## Acknowledgements

This research is supported by the Science and Engineering Research Board (SERB), India (project ECR/2017/001931). Prof. B. Jayram is gratefully thanked for providing access to his supercomputing facility. Authors acknowledge the Central Research Facility, IIT Delhi, for instrument facilities.

## References

1. R.S. Downing, P.J. Kunkeler, H. van Bekkum, *Catal. Today*, **37** 121 (1997).
2. J. Marquez, D. Pletcher, *J. Appl. Electrochem.*, **10** 567 (1980).
3. A. Cyr, P. Huot, J.-F. Marcoux, G. Belot, E. Laviron, J. Lessard, *Electrochimica Acta*, **34** 439 (1989).
4. P.J. Cossar, L. Hizartidis, M.I. Simone, A. McCluskey, C.P. Gordon, *Org. Biomol. Chem.*, **13** 7119 (2015).
5. P. Zhou, L. Jiang, F. Wang, K. Deng, K. Lv, K. Z. Zhang, *Sci. Adv.*, **3** e1601945 (2017).
6. P. Zhou, L. Jiang, S. Wang, X. Hu, H. Wang, Z. Yuan, Z. Zhang, *ACS Catal.*, **9** (2019).
7. J. Wang, Q. Tang, S. Jin, Y. Wang, Z. Yuan, Q. Chi, Z. Zhang, *New J. Chem.*, **44** 549 (2020).
8. K. Manna, P. Ji, Z. Lin, F.X. Greene, A. Urban, N.C. Thacker, W. Lin, *Nat. Commun.*, **7** 12610 (2016).
9. P. Ji, K. Manna, Z. Lin, X. Feng, A. Urban, Y. Song, W. Lin, *J. Am. Chem. Soc.*, **139** 7004 (2017).
10. N. Antil, A. Kumar, R. Newar, N. Akhtar, W. Begum, A. Dwivedi, K. Manna, *ACS Catal.*, **11** 3943 (2021).

## Feruloyl esterase-catalyzed synthesis of a bioactive sugar ester based on phenolic compounds derived from the halophyte *Salicornia* spp.

Io Antonopoulou\*, Ulrika Rova, Paul Christakopoulos

Biochemical Process Engineering, Division of Chemical Engineering, Department of Civil, Environmental and Natural Resources Engineering, Luleå University of Technology, SE-97187 Luleå, Sweden

\* e-mail address of corresponding author: [io.antonopoulou@ltu.se](mailto:io.antonopoulou@ltu.se)

*Salicornia* is a genus of succulent halophyte flowering plants that frequently occur in saline areas and comprise the most salt-tolerant land plant. The valuable properties of *Salicornia* species have been long known with displayed applications in folk medicine for treatment of bronchitis, hepatitis and diarrhea [1]. The important biological properties of *Salicornia* are owed to the numerous bioactive phenolic compounds found in their extracts. Among them, hydroxycinnamic acids (HCAs), such as ferulic acid (FA), sinapic acid (SA), p-coumaric acid (p-CA) and caffeic acid (CA) are detected in high amounts [2]. This class of naturally occurring compounds shows strong antioxidant activity together with anti-aging, skin regenerative, anti-inflammatory, antimicrobial, antiviral and skin whitening properties among others and has great potential for application in formulation of bioactive products, such as functional feed, food and cosmetics [3][4].

However, a significant limitation for the application of HCAs and thus plant extracts containing HCAs is often their low solubility in both aqueous and oil media. A common strategy to overcome this issue is to stabilize HCAs by a (trans)esterification reaction. Feruloyl esterases (FAEs, EC 3.1.1.73) are an interesting esterase subclass that, in nature, catalyze the hydrolysis of the ester bond between  $\alpha$ -L-arabinofuranose and FA or other hydroxycinnamic acids, present in lignocellulose. They have been identified as a promising biocatalytic tool for performing (trans)esterification reactions in the past years. However, this approach requires low water content by employing organic solvents as reaction medium in order to avoid the naturally occurring side-hydrolysis reaction. Although FAEs are not so stable in low water content media as the well-known lipases, their ability as biocatalytic tools for (trans)esterification has been demonstrated [5]. Their major advantage over lipases is the specificity towards HCAs, allowing acylation of FA with a wide range of hydrophilic or lipophilic substitutions, such as alcohols, polyols or sugars. Enzymatic stabilization offers a green and sustainable alternative to classic esterification methods that involve use of strong acids or expensive and toxic reagents as catalysts, high temperatures (150-250°C), long reaction times, low yields and process limitations owed to heat sensitivity and oxidation susceptibility of FA [6]. The approach could enable the application of HCAs and thus *Salicornia* extracts in a variety of bioactive products offering exceptional selectivity and no need for deodorization and bleaching of final products, that is observed during conventional (trans)esterification.

Aim of this study is to efficiently synthesize the stabilized ester of FA, raffinose ferulate, by employing the commercial multi-enzymatic preparation Depol 740L® (Biocatalysts Ltd.). Raffinose ferulate has been previously synthesized, however, the followed approach included a direct esterification reaction and low water content (3%) offering low yields and long incubation times (11.9%, 3.57 mM, after 6 days) [7]. This ester has been shown to have comparable antioxidant activity as FA, while it is a more hydrophilic compound that allows application in water-based formulations. In our approach we synthesized the ester by a transesterification reaction using an activated donor (vinyl ferulate or methyl ferulate). Since raffinose as acceptor is water soluble, it has to be introduced in a soluble form in the reaction as part of an aqueous phase including the enzyme and buffer. As such, a compromising ratio between the aqueous phase containing the acceptor and the organic phase containing the donor has to be achieved, in order to acquire high transesterification yields and selectivity over hydrolysis. In this work, we optimized the reaction conditions for the synthesis of raffinose ferulate by investigating the effect of medium, water content, donor and acceptor concentration, pH, temperature and time on the yield and selectivity. Using vinyl ferulate as donor, an estimated total product concentration of 42.2 mM corresponding to a 35.2% donor conversion was observed, at only 24 hours of incubation. Three distinct peaks (one major and two minor) were identified as transesterification products during HPLC analysis, while there is strong indication of di-feruloylation of raffinose.

The pharmacokinetic properties of the synthesized compound were predicted and compared to FA. More specifically, SwissADME (<http://www.swissadme.ch/index.php>) was used to obtain data on the physicochemical properties, lipophilicity, water solubility, pharmacokinetics, druglikeness and medicinal chemistry of compounds. A free online tool provided by Molsoft (<http://molsoft.com/mprop/>) was also utilized to calculate molecular properties and overall druglikeness of the compounds. The toxicity of the compound was predicted through the freely available webserver ProTox II ([https://tox-new.charite.de/protox\\_II/index.php?site=compound\\_input](https://tox-new.charite.de/protox_II/index.php?site=compound_input)), which calculated the median lethal dose (LD50) and provides an estimation of acute toxicity, hepatotoxicity, carcinogenicity, immunotoxicity, mutagenicity, cytotoxicity, Tox21 Nuclear receptor signaling pathways and Tox21 Stress response pathways. *In vitro* assays were employed in order to investigate the anti-inflammatory and antiviral effect of raffinose ferulate. Raffinose ferulate has potential as promising stabilized derivative towards application as a bioactive agent to boost immunity and potentially have significant health benefits if used to supplement formulations within the feed, food and cosmetics industry.

### Acknowledgements

This work is supported by the Horizon 2020-funded project AQUACOMBINE- Integrated on-farm Aquaponics systems for co-production of fish, halophyte vegetables, bioactive compounds, and bioenergy (Grant agreement ID: 862834).

### References

1. R. Giordano, Z. Saii, M. Fredsgaard, L.S.S. Hulkko, T.B.G. Poulsen, M.E. Thomsen, N. Henneberg, S.M. Zucolotto, L. Arendt-Nielsen, J. Papenbrock, M.H. Thomsen, A. Stensballe. *Molecules*, **26** 3140 (2021).
2. S. Kim, E.Y. Lee, P.F. Hillman, J. Ko, I. Yang, S.J. Nam. *Molecules*, **26** 2252 (2021).
3. A.R Lima, V. Castañeda-Loaiza, M. Salazar, C. Nunes, C. Quintas, F. Gama, M. Pestana, P.J. Correia, T. Santos, J. Varela, L. Barreira. *Food Chemistry*, **33** 127525 (2020).
4. R. Giordano, G.E. Aliotta, A.S. Johannesen, D. Voetmann-Jensen, F.H. Laustsen, L.A. Andersen, A. Rezai, M. Fredsgaard, S.L. Vecchio, L. Arendt-Nielsen, M.H. Thomsen, A. Stensballe. *Pharmaceuticals*, **15** 150 (2022).
5. I. Antonopoulou, S. Varriale, E. Topakas, U. Rova, P. Christakopoulos, V. Faraco. *Applied Microbiology and Biotechnology*, **100** 6519-6543 (2016).
6. N.G. Li, Z.H. Shi, Y.P. Tang, B.Q. Li, J.A. Duan. *Molecules*, **14** 2118-2126 (2009).
7. J. Couto, R. St-Louis, S. Karboune. *Journal of Molecular Catalysis B: Enzymatic*, **73** 53-62 (2011).

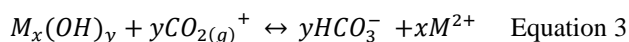
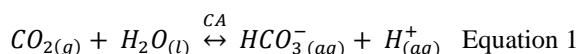
## Utilization of industrial residues as co-capturing agents for enzyme-accelerated CO<sub>2</sub> capture

Ayanne De Oliveira Maciel, Paul Christakopoulos, Ulrika Rova, Io Antonopoulou\*

Biochemical Process Engineering, Division of Chemical Engineering, Department of Civil, Environmental and Natural Resources Engineering, Luleå University of Technology, SE-97187 Luleå, Sweden

\* e-mail address of corresponding author: [io.antonopoulou@ltu.se](mailto:io.antonopoulou@ltu.se)

Natural weathering of rocks is an important sink for atmospheric CO<sub>2</sub> [1]. Inspired by nature, the application of this concept utilizing materials rich in carbonates, silicates and oxides and supplying CO<sub>2</sub> at higher concentrations than the atmospheric, shows potential of utilizing enhanced weathering as new method for carbon sequestration [2]. The mechanism involved in the chemical weathering comprises normally of two main steps: CO<sub>2</sub> hydration into formation of bicarbonate (Equation 1) and mineral dissolution (Equation 2 for carbonates and Equation 3 for hydroxides). However, the conversion of CO<sub>2</sub> to bicarbonate is a limiting reaction step. Paths to accelerate rock dissolution via the employment of biotechnological routes has received increasing attention [3]. Carbonic anhydrase (CA) is one of the fastest enzymes in nature, catalyzing the hydration of CO<sub>2</sub> to bicarbonate, which is the limiting step of CO<sub>2</sub> absorption [4][5]. The enzyme has been reported to increase mineral weathering by enhancing the dissolution rate in minerals, such as dolomite and limestone [6][7]. Exploiting a bio-based accelerated weathering route is a novel approach in CCUS (Carbon Capture Utilization and Capture), and it can have great use in the context of geological CO<sub>2</sub> storage, which up to date is focused on the injection of gaseous CO<sub>2</sub> to the bedrock. The utilization of aqueous solutions rich in bicarbonates as temporary storage form of CO<sub>2</sub>, as obtained in the accelerated weathering, could reduce safety concerns related to gas leakage and promote faster *in-situ* mineralization for permanent CO<sub>2</sub> geological storage [8]. Besides, the use of CA enables a more sustainable capture process since the enzymatic reaction does not require high temperatures and/or high pressures. Finally, the repurposing of industrial residues as co-capturing agents in post-combustion absorption is a meaningful strategy towards cleaner CO<sub>2</sub> capture processes, which traditionally has relied on amine-based solvents.



Aim of the study is to investigate the extent of acceleration of the CO<sub>2</sub> capture step in a CCS concept by applying CA during weathering of industrial residues. In this study, two different residue materials from the paper and pulp industry were assessed as co-capturing agents by utilizing a biochemical accelerated weathering approach. The effect of CA in enhancing the CO<sub>2</sub> capture and carbonate dissolution was evaluated.

An evolved thermostable CA from *Desulfovibrio vulgaris* (DvCA8.0) was overexpressed in *E. coli*. Lime mud and green liquor sludge were tested as co-capturing agents in CO<sub>2</sub> capture experiments. The amount of calcite (CaCO<sub>3</sub>) in the residues was approximately 95% w/w and 50% w/w for each material, respectively, as assessed by XRD. Green liquor sludge contained about 8.5% w/w of Mg(OH)<sub>2</sub> – which can also present co-capturing properties. Experiments were carried out in a glass reactor coupled to a heater/stirrer. Gas (20% v/v CO<sub>2</sub>) was fed to the reactor containing the material suspension and CA, by sparging. A reaction control was performed using buffer instead of enzyme. The pH of the solution was measured over time as an indication of the CO<sub>2</sub> absorption in the mixture. At the end of the reaction, the total amount of bicarbonate formed was quantified through a precipitation step forming calcium carbonate, by utilizing an adapted method from Mirjafari et al. [9]. The concentration of Ca<sup>+2</sup> ions in the solution was determined by spectrophotometry (Spectroquant), in order to quantify the extent of mineral dissolution owed to calcite.

Application of CA showed a significant improvement in bicarbonate formation and calcite dissolution. When CA was coupled with lime mud, a 3-fold increase in the bicarbonate yield and a 2-fold increase in the yield of calcium ions was observed, compared to the non-catalyzed reaction involving only lime mud. Similarly, when CA was coupled with green liquor sludge, a 2.5-fold increase in bicarbonate yield and a 2.3-fold increase in calcium ions yield was shown. CA accelerated the CO<sub>2</sub> hydration, leading to a faster drop in the pH value of the solution by the formation of H<sup>+</sup>. At more acidic environments, the mineral dissolution was favored. For lime mud, the pH dropped from an initial value of 10-10.5 to 7.1 in 55 minutes, while when CA was added, the time was significantly reduced by 27%. For green liquor sludge, the drop of pH value to 7.1 took more time, approaching 120 minutes for the CA-accelerated reaction. The non-catalyzed reaction did not reach a pH of 7.1 within the experiment time.

For further assessments, variables such as temperature of reaction, CO<sub>2</sub> flow rate, residue concentration, and enzyme load will be evaluated to understand their influence in CO<sub>2</sub> capture rate and mineral dissolution. As

conclusion, CA had a relevant effect in promoting accelerated weathering, demonstrating viability to be coupled in mineral systems rich in carbonates. The findings open the path towards application of CA in CCS processes, while co-use of industrial residues and CO<sub>2</sub> from industrial emissions in such process may be a driving force for establishing *in situ* CCS processes near industrial emitters. This could eliminate the need of material transportation for storage. The paper and pulp industry may be a good candidate for establishing a carbon neutral production cycle and promoting waste recycling and the establishment of a circular economy.

### Acknowledgements

This work is supported by the Swedish Energy Agency project INSURANCE (grant number ID: 2020-019943). BillerudKorsnäs Karlsborg (Sweden) is acknowledged for providing materials.

### References

- [1] J. Hartmann and S. Kempe, "What is the maximum potential for CO<sub>2</sub> sequestration by 'stimulated' weathering on the global scale?," *Naturwissenschaften*, vol. 95, no. 12, pp. 1159–1164, 2008, doi: 10.1007/s00114-008-0434-4.
- [2] R. D. Schuiling and P. Krijgsman, "Enhanced weathering: An effective and cheap tool to sequester CO<sub>2</sub>," *Clim. Change*, vol. 74, no. 1–3, pp. 349–354, 2006, doi: 10.1007/s10584-005-3485-y.
- [3] T. Shen, W. Li, W. Pan, S. Lin, M. Zhu, and L. Yu, "Role of bacterial carbonic anhydrase during CO<sub>2</sub> capture in the CO<sub>2</sub>-H<sub>2</sub>O-carbonate system," *Biochem. Eng. J.*, vol. 123, pp. 66–74, Jul. 2017, doi: 10.1016/J.BEJ.2017.04.003.
- [4] M. Sjöblom *et al.*, "Enzyme-Assisted CO<sub>2</sub> Absorption in Aqueous Amino Acid Ionic Liquid Amine Blends," *ACS Sustain. Chem. Eng.*, vol. 8, no. 36, pp. 13672–13682, 2020, doi: 10.1021/acssuschemeng.0c03497.
- [5] A. de Oliveira Maciel, P. Christakopoulos, U. Rova, and I. Antonopoulou, "Carbonic anhydrase to boost CO<sub>2</sub> sequestration: Improving carbon capture utilization and storage (CCUS)," *Chemosphere*, p. 134419, 2022, doi: <https://doi.org/10.1016/j.chemosphere.2022.134419>.(Accepted)
- [6] I. M. Power, A. L. Harrison, G. M. Dipple, and G. Southam, "Carbon sequestration via carbonic anhydrase facilitated magnesium carbonate precipitation," *Int. J. Greenh. Gas Control*, vol. 16, pp. 145–155, Aug. 2013, doi: 10.1016/j.ijggc.2013.03.011.
- [7] I. M. Power, A. L. Harrison, and G. M. Dipple, "Accelerating Mineral Carbonation Using Carbonic Anhydrase," *Environ. Sci. Technol.*, vol. 50, no. 5, pp. 2610–2618, 2016, doi: 10.1021/acs.est.5b04779.
- [8] K. Mortezaei, A. Amirlatifi, E. Ghazanfari, and F. Vahedifard, "Potential CO<sub>2</sub> leakage from geological storage sites: advances and challenges," *Environ. Geotech.*, vol. 8, no. 1, pp. 3–27, 2021, doi: 10.1680/jenge.18.00041.
- [9] P. Mirjafari, K. Asghari, and N. Mahinpey, "Investigating the application of enzyme carbonic anhydrase for CO<sub>2</sub> sequestration purposes," *Ind. Eng. Chem. Res.*, vol. 46, no. 3, pp. 921–926, 2007, doi: 10.1021/ie060287u.

# Mono-Phosphine Metal-Organic Framework- Supported Cobalt Catalyst for Efficient Borylation Reactions

Wahida Begum<sup>1</sup> and Kuntal Manna<sup>1\*</sup>

<sup>1</sup>Department of Chemistry, Indian Institute of Technology, New Delhi, India

\*[Kuntal.Manna@chemistry.iitd.ac.in](mailto:Kuntal.Manna@chemistry.iitd.ac.in)

The use of phosphine ligands for synthesising various types of transition metal catalysts have always been of immense importance owing to their unique feature of allowing convenient change of electronic effect without undergoing much change in steric effects.<sup>1</sup> This property of phosphine ligands has always attracted researchers for their use in carrying out various transformations in organic synthesis as can be evident by the synthesis of sterically hindered biaryl-phosphines by Buchwald for stabilizing the R<sub>3</sub>P-Pd complexes.<sup>2</sup> In particular, Mono-phosphine ligands are easy to use because of their flexible structures and excellent catalytic activity. The synthesis of monoligated phosphine base metal complexes is challenging because of their tendency to undergo ligand exchange reactions.<sup>3</sup> The site isolation in metal-organic frameworks (MOFs) could be employed in order to prevent such ligand exchange reactions and also to stabilize the mono-phosphine R<sub>3</sub>P-M intermediate species formed during the reaction cycle.<sup>4</sup> MOFs are porous molecular materials which are used for developing active and chemoselective heterogeneous base metal catalysts.<sup>5,6</sup> They are highly tunable materials that allow for development of single-site solid catalysts.<sup>7</sup>

Here, we have developed a heterogeneous metal-organic framework (MOF) supported monoligated phosphine-cobalt complex that could be used as an active catalyst for carrying out aromatic C-H bond borylation reactions and also hydroboration reactions in various types of alkenes. The cobalt mono-phosphine based MOF was synthesised by using Zr-oxo-hydroxo as SBUs and 4',4''',4''''-phosphanetriyltris([1,1'-biphenyl]-4-carboxylate) [P(ArCO<sub>2</sub>)<sub>3</sub>] as the organic linkers via a solvothermal reaction of ZrCl<sub>4</sub> with P(ArCO<sub>2</sub>H)<sub>3</sub> having benzoic acid as the modulator in DMF at 90 °C for 5 days. The MOF was metalated with CoCl<sub>2</sub> in THF post-synthetically and afforded the cobalt functionalized mono-phosphine MOF (MOF-P-CoCl<sub>2</sub>). The synthesized MOF was characterized by using BET, PXRD and IR. Further, the MOF-P-COCl<sub>2</sub> was treated with NaEt<sub>3</sub>BH<sub>4</sub> to obtain the active catalyst MOF-P-Co.

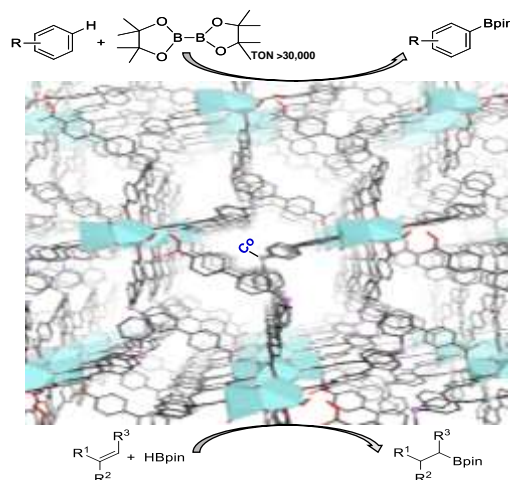


**Figure 1.** Design of amino alcohol-functionalized metal-organic frameworks to develop robust single-site earth-abundant metal catalysts for heterogeneous asymmetric catalysis.

Metal loading ICP-OES data of Co-functionalized MOF were obtained with an Agilent 5110 ICP-OES and analysed using Dichroic Spectral Combiner (DSC). The conversions of the reactions were analysed by gas chromatography (GC) using Agilent 7890B gas chromatograph equipped with mass detector (Agilent 5977B GC/MSD). The catalyst showcased a TON of 30,000. The MOF showcased recyclability and reusability upto 13 times for C-H borylation. The oxidation state of the Co centre within the MOF was established to be +2 by XPS. XPS was recorded on an X-ray photoelectron spectrometer, PHI 5000 Versa Probe III using Al-K $\alpha$  (h $\nu$ =1486.6eV) X-ray source. 307 m<sup>2</sup>/g of BET surface area was observed for MOF-P-COCl<sub>2</sub>. Surface area was measured with a BELLSORP MAX II-high performance gas and vapor adsorption system with three microporous ports. Further, the mechanistic pathway was also investigated for the C-H borylation reactions of arenes and simultaneously DFT calculations were also done for the same using DFT method (B3LYP) and a basis set of 6-311G (d,p) on Gaussian 09 software.



At a 0.5 mol% Co-loading, MOF-P-Co acts as a robust and active catalyst for aromatic C-H borylation and has a wide substrate scope involving various functionalised arenes and heterocycles. The monoligated phosphine cobalt species is not accessible in solution due to the lack of steric protection around the cobalt centre to prevent intermolecular interaction.

### Acknowledgements

This research is funded by CSIR-HRDG [01(3040)/21/EMR-II] and IRD, IIT Delhi (MI02099). Authors acknowledge the Central Research Facility, IIT Delhi, for instrument facilities.

### References

1. A.L. Clevenger, R.M. Stolley, J. Aderibigbe, J. Louie, *Chem. Rev.*, **120**, 6124 (2020).
2. R. Martin, S.L. Buchwald, *Acc. Chem. Res.*, **41**, 1461(2008).
3. T. Sawano, Z. Lin, D. Boures, B. An, C. Wang, W. Lin, *J. Am. Chem. Soc.*, **138**, 9783 (2016).
4. T. Drake, P. Ji, W. Lin, *Acc. Chem. Res.*, **51**, 2129 (2018).
5. Q. Han, C. He, M. Zhao, B. Qi, J. Niu, C. Duan, *J. Am. Chem. Soc.*, **135**, 10186 (2013).
6. M. Liu, J. Wu, H. Hou, *Chem. Eur. J.*, **25**, 2935 (2019).
7. D.T. Genna, A.G. Wong-Foy, A.J. Matzger, M.S. Sanford, *J. Am. Chem. Soc.*, **135**, 10586 (2013).

## Use of Magnetic Cross-Linked Tyrosinase Aggregates for Biocatalytic Processes in Deep Eutectic Solvents

Bellou G. M., Fotiadou R., Giannakopoulou A., Polydera C. A., Stamatis H.\*

Laboratory of Biotechnology, Department of Biological Applications and Technologies, University of Ioannina, Ioannina, Greece

\* Corresponding author: [hstamati@uoi.gr](mailto:hstamati@uoi.gr)

### Abstract

As the need for the usage of “greener” and sustainable practices in biochemical processes arises, neoteric solvents, such as Deep Eutectic Solvents (DESs) have emerged as environmentally-friendly alternatives to conventional petrochemical solvents [1]. A DES is formed by mixing at least two compounds, one of which is a hydrogen bond acceptor (HBA) and the other is a hydrogen bond donor (HBD). When both compounds are derived from nature, DESs are called Natural DESs (NADESs). This type of solvent possesses exceptional features, such as biodegradability, biocompatibility, non-volatility, stability, inexpensive and energy-efficient synthesis. DESs are implemented in biocatalysis, acting as co-solvents or replacing chemical solvents in which various enzymatic reactions can take place [2, 3].

In this work, tyrosinase extracted from fresh mushrooms was immobilized through cross-linking in the presence of magnetic nanoparticles and the resulting biocatalyst (magnetic Cross-Linked Enzyme Aggregates, mCLEAs) was studied in terms of its biochemical characteristics in various DESs-aqueous solutions. Additionally, tyrosinase mCLEAs were used in the homogeneous modification of the polymer chitosan (CS) with caffeic acid in the presence of a DES acting as plasticizer [4]. It is well-known that the graft of phenolic compounds on chitosan offer improved physical properties such as antioxidant properties [5,6] and that the employment of DESs in chitosan films lead to a significant increase in the plasticity of the films [7]. Results indicated that the type and the concentration of the DES play a major role in the catalytic function and stability of the oxidoreductase. Furthermore, the biocatalyst demonstrated great ability in the simultaneous functionalization of chitosan in the presence of DES, enhancing its antioxidant activity and plasticity. Moreover, mCLEAs could be obtained from the reaction medium by implementing magnetic field and reused, thus serving a purpose of bioeconomy.

### Experimental

Deep Eutectic solvents ChCl:U (1:2), ChCl:Gly (1:2), ChCl:EG (1:2), ChCl:PG (1:2), ChCl:BG (1:2), ChCl:BG (1:4), ChCl:Fru:H<sub>2</sub>O (5:2:5), ChCl:U:Gly (1:1:1), ChCl:U:EG (1:1:1), ChCl:Gly:EG (1:1:1), EAC:U (1:1.5), EAC:Gly (1:1.5), EAC:EG (1:1.5), Bet:Gly (1:2), Bet:Gly (1:3), Bet:EG (1:3), Chol DHP:Gly (1:3), Chol DHP:EG (1:3) (Abbreviations: ChCl: Choline Chloride, EAC: Ethylammonium Chloride, Bet: Betaine, Chol DHP: Choline Dihydrogen Phosphate, U:Urea, Gly:Glycerol, EG:Ethylene Glycol, PG:Propylene Glycol, BG:Butylene Glycol, Fru:Fructose) were prepared by mixing the corresponding compounds in a specific molar ratio and mixtures were incubated and stirred. For the preparation of tyrosinase mCLEAs, fresh mushrooms were cut, homogenized in buffer, centrifuged and magnetic nanoparticles and ammonium sulfate were added to the solution. Afterwards, glutaraldehyde solution was added and the mixture was stirred in room temperature, centrifuged at the end and mCLEAs were washed with buffer. The activity of free tyrosinase from mushrooms and mCLEAs in the presence and absence of various %v/v concentrations of DESs was measured spectrophotometrically by measuring the oxidation of L-Dopa. For the homogeneous modification of chitosan with caffeic acid in the absence and in the presence of DES, neat chitosan solution or 10% v/v Bet:Gly (1:3)-containing chitosan solution and caffeic acid solution were mixed and tyrosinase mCLEAs were added. At the end of the reaction, mCLEAs were removed by using a magnet and the solutions were left to dry until the creation of films. The oxidation of caffeic acid by tyrosinase mCLEAs and the operational stability of the biocatalyst in this reaction was monitored through HPLC, by observing the consumption of caffeic acid. The presence of the oxidized caffeic acid in the chitosan films was observed by dissolving specific amounts of films in 1% v/v acetic acid and measuring the solutions spectroscopically. The antioxidant activity of the unmodified and modified chitosan films was determined by the ABTS assay as described elsewhere [8], with a slight modification.

### Results

The activities of tyrosinase mCLEAs and free tyrosinase were studied at the concentration of 10% v/v of all DESs and at increasing concentrations (20, 50 and 70 % v/v) of certain ones (Figure 1). Results showed that the activity of both free tyrosinase and tyrosinase mCLEAs depended on the type and the concentration of the DES. Comparing free and immobilized tyrosinase, mCLEAs displayed better activity in most DESs and presented better stability in the increased concentrations of most DESs. However, in both cases, the activity of tyrosinase decreased with the rise in DESs' concentration.

Tyrosinase mCLEAs and the DES Bet:Gly (1:3) were further used in the modification of the polymer chitosan. Essentially, for the first time, tyrosinase mCLEAs were used in the oxidation of caffeic acid in the presence of the DES-containing chitosan solution, for the simultaneous functionalization of the polymer with the caffeic acid derivative and the enhancement of its plasticity. Tyrosinase mCLEAs showed decent operational stability at the modification of caffeic acid, as at the 10<sup>th</sup> cycle the biocatalyst preserved around 50% and 40% of its catalytic activity in the absence and in the presence of the DES, respectively. Concerning the modification of



## Suitability of volcanic materials as green catalysts for environmental purposes

María Emma Borges Chinae<sup>1\*</sup>, Héctor de Paz Carmona<sup>1</sup> and Pedro Esparza Ferrera<sup>2</sup>

<sup>1</sup> Chemical Engineering Department, University of La Laguna, Tenerife, Canary Islands 38200, Spain

<sup>2</sup> Chemistry Department, University of La Laguna, Tenerife, Canary Islands 38200, Spain

\*eborges@ull.edu.es

Environmental protection is considered a current priority of the European Union Commission. In this context, the advanced oxidation processes (AOPs) for environmental decontamination purposes have received much attention during the last years [1,2]. AOPs have great advantages for the treatment of pollutants, even in low concentration, enabling complete mineralization or decomposition of most organic materials. Photocatalytic oxidation is a highly effective novel method speeding up the oxidation process and can be combined with ultraviolet-visible irradiation to offer a powerful treatment of wastewater. This AOP has been demonstrated as a promising approach for wastewater cleaning due to its high efficiency and low costs when solar radiation can be used to activate the photocatalytic material [3,4]. Metal-transition oxides as  $\text{TiO}_2$ ,  $\text{WO}_3$  or  $\text{V}_2\text{O}_5$  are probed photocatalysts with high efficiencies for pollutant degradations, chemical stability, and non-toxic properties [5].

Nevertheless, natural materials such as volcanic materials (ashes, sand, etc.) have shown significant photocatalyst activity for wastewater decontamination using artificial UV/visible light and natural sunlight. This work builds on our previous research [6-8] by studying natural materials as suitable green photocatalysts for pollutants photodegradation. The objective of this research work is to study natural materials acting as photocatalyst for the decontamination of aqueous media and air. It is intended to evaluate the properties and characteristics of natural materials economically favorable due to its high presence in large natural environments of volcanic origin. For this purpose, several volcanic materials were characterized and its photoactivity was tested under several conditions using sun irradiation to constitute an energetically sustainable process for water/air decontamination.

For the characterization of the photocatalyst, the following techniques were used: nitrogen physisorption, mercury porosimetry, scanning electron microscopy for determine the structural characteristics; X-ray diffraction and spectroscopy X-ray photoelectron to determine its composition and UV-Visible spectroscopy of diffuse reflectance to determine its potential as a photocatalyst (band-gap). To study the photocatalytic activity of the material, two configurations of different photoreactors were used.

Photocatalytic tests were carried out using artificial UV/visible light and natural sunlight in a slurry-type reactor and pilot plant scale photoreactors equipped with a parabolic sunlight collector. According to the material characterization, one of the natural volcanic materials tested (volcanic black sand) seems to have significant potential as a photocatalyst, showing a bandgap (Figure 1) corresponding to 3 eV (UV-radiation at 450 nm).

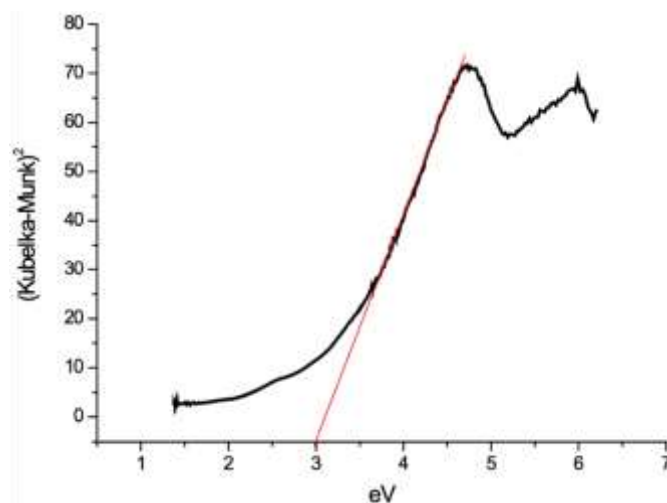


Figure 1. UV-vis spectra in Kubelka-Munk units vs. photonic energy (eV) for natural material tested as photocatalyst.

The photocatalytic activity was determined in terms of adsorption and photocatalytic properties. The pollutant is adsorbed on the material surface in the absence of a light source, decreasing its content (> 80%). On the other hand, a good photocatalytic activity has been observed achieving approximately a 100 % wastewater decontamination when sunlight was used as energy source, and about 80 % when visible and ultraviolet light were used (Figure 2).

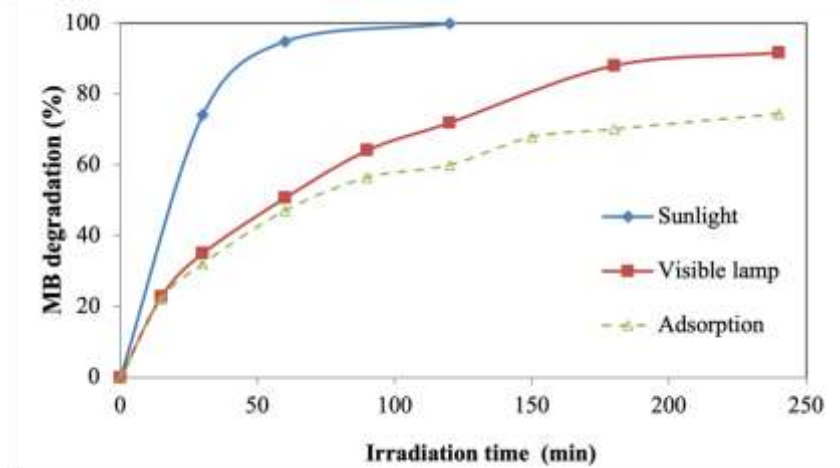


Figure 2. Pollutant degradation in wastewater by photocatalysis using sunlight

Our results describe the viability of using natural materials as photocatalyst for wastewater treatment at laboratory and pilot plant scales. Checking the photocatalytic activity of the natural volcanic material tested, through spectroscopy infrared of its surface, its photocatalytic capacity has been further highlighted against the adsorption phenomenon since the contaminant has been completely degraded not only from the water to be treated, but also that adsorbed on the surface of the photocatalytic material.

### Acknowledgements

- CONVOCATORIA DE LAS AYUDAS PARA LA RECUALIFICACIÓN DEL SISTEMA UNIVERSITARIO ESPAÑOL 2021-2023 (B.O.C. 140, de 9 de julio de 2021), convocatoria financiada por subvención directa concedida a la Universidad de La Laguna por Orden UNI/551/2021, de 26 de mayo, del Ministerio de Universidades. Financiación por la Unión Europea - Fondos Next Generation EU.
- Proyecto: PDC2021-121131-C22 del Programa Estatal de I+D+i Orientada a los Retos de la Sociedad.

### References

1. I.A. Ike, T. Karanfil, J. Cho, J. Hur, *Water Res.*, **164**(1) 114929 (2019).
2. M. Gągól, A. Przyjazny, G. Boczkaj, *Chem. Eng. J.*, **338** 599 (2018).
3. T. Bui, P. Bansal, B. Lee, T. Mahvelati-Shamsabadi, T. Soltani, *Appl. Surf. Sci.*, **506** 144184 (2020).
4. Y. Song, Y. Peng, N. Long, Z. Huang, Y. Yang, *Appl. Surf. Sci.*, **542** 148584 (2021).
5. A. Piątkowska, M. Janus, K. Szymański, S. Mozia, *Catalysts*, **11**(1) 1-56 (2021).
6. M.E. Borges, M. Sierra, P. Esparza, *Clean Techn. Environ. Policy*, **19**(4) 1239-1245 (2017).
7. M.E. Borges, M. Sierra, E. Cuevas, R.D. García, P. Esparza, *Sol. Energy*, **135** 527-535 (2016).
8. M.E. Borges, M. Sierra, J. Méndez-Ramos, P. Acosta-Mora, J.C. Ruiz-Morales, P. Esparza, *Sol. Energ. Mat. Sol. C.*, **155** 194-201 (2016).

# Green Chemicals From Dehydration and Partial Dehydrogenation of Sugar Cane Fusel Oil

Livia Padilha de Lima, Gustavo Metzker, Mauricio Boscolo\*

Sao Paulo State University (UNESP), Sao Jose do Rio Preto, SP, Brazil

\*mauricio.boscolo@unesp.br

Fusel oil is a by-product formed during alcoholic fermentation, and it is composed by a mixture of insoluble organics obtained from the distillation of fuel ethanol, along with isoamyl alcohol, isobutanol and other minorities [1]. In general, for every 1000 liters of distilled fuel ethanol, 2.5 liters of fusel oil are produced [2]. As around 30 billion liters of ethanol are produced in Brazil per year, 80 million liters of fusel oil are generated.

So, our goal is to carry out the partial dehydrogenation of the sugarcane fusel oil to be a source of renewable chemicals having layered double hydroxides (LDH) hydrotalcite-like materials ( $Mg_6Al_2CO_3(OH)_{16}\cdot 4H_2O$ ) as precursor of the metal mixed oxides (MMO) used as catalysts. the establishment of a technically and economically viable methodology for the transformation of Fusion Oil will yield an extra source of financial resources for this agribusiness sector.

Dehydrogenation and dehydration area catalytic and endothermic processes and for that there is an excess of energy available in many Brazilian sugarcane mills making this process self-sustainable.

Hydrotalcite-based catalyst was synthesized replacing 20 % of  $Mg^{2+}$  by  $Zn^{2+}$  ( $Zn_{20}LDH$ ) and its respective oxide ( $Zn_{20}MMO$ ). X-ray diffraction (XRD) patterns exhibit sharp reflection with high intensity with characteristic basal spacing at  $10-25^\circ$  (Miller index 003; 006 and 113), and broad and asymmetric peaks at  $34-66^\circ$  (Miller index 012, 015 and 018) for  $Zn_{20}LDH$ . Surface area analysis (BET) indicated  $154,3 \pm 2,1 \text{ m}^2\text{g}^{-1}$  for  $Zn_{20}MMO$ .

At atmospheric pressure, the catalytic reactions were carried out in a stainless still bed reactor packed with the catalyst powder dispersed in silica gel 100 mesh. The feed flux was 0.1 and 0.2  $\text{mL min}^{-1}$  and temperatures of 500 and 600°C, generating a mixture of products which can highlight aldehydes, olefins, esters, ethers and aromatic compounds (Fig. 1), showing the versatility of this methodology for obtaining important organic compounds for the fine chemicals industry.

No products of aldol condensation were observed in any conditions tested, contrarily we expected, but the direct dehydration to form di-isoamyl ether as well as the first dehydrogenation of the isoamyl alcohol to form isoamyl aldehyde occurred in all conditions.

Interesting, when the reactor is operated with a flow of 0.1  $\text{mL min}^{-1}$  at 600°C, do not form aromatic and phenolic compounds.

The subsequent analysis of the catalysts used in the reactions by thermogravimetric analysis (TGA) indicated that the primary source of deactivation of these materials was the deposition of carbon on the surface. Other catalytic systems and reaction conditions are under study to determine the main factor to turn the process more selective.

## Acknowledgements

The São Paulo Research Foundation, FAPESP (2020/02471-4)

## References

- Patil, Avinash & Koolwal, S.M. & Butala, H.D.. *International Sugar Journal*. **104**. 51-58+63. (2002).

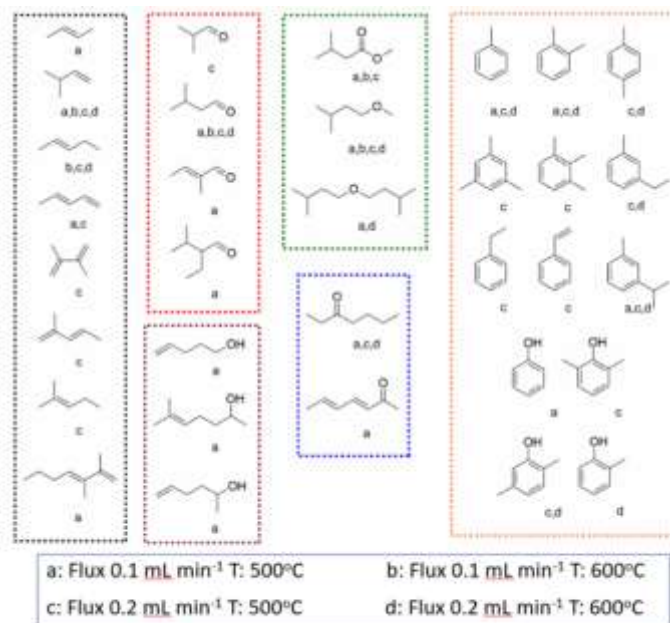


Fig. 1. Chemicals from the catalytic dehydrogenation and dehydration process of the fusel oil

2. Marcela C. Ferreira, Antonio J. A. Meirelles, and Eduardo A. C. Batista. *Industrial & Engineering Chemistry Research* **52** (6), 2336-2351 (2013).
3. Wiyantoko, Bayu & Kurniawati, Puji & Purbaningtias, Tri & Fatimah, Is. Synthesis and Characterization of Hydrotalcite at Different Mg/Al Molar Ratios. *Procedia Chemistry*. (2014).

## Optimization of furan-based oligoester enzymatic synthesis by design of experiments

Diana Maria Dreavă<sup>1</sup>, Ioan Bîțcan<sup>1</sup>, Andreea Petrovici<sup>1</sup>, Iulia Păușescu<sup>1\*</sup>, Francisc Peter<sup>1</sup>, Anamaria Todea<sup>1</sup>

<sup>1</sup>Politehnica University Timisoara, Faculty of Industrial Chemistry and Environmental Engineering, 6 Vasile Parvan Bvd, 300223, Timisoara, Romania

\* e-mail: iulia.pausescu@upt.ro

In an effort to minimize the resource depletion and the environmental problems due to petroleum-based monomers used for polymer production, nowadays various platform chemicals and polymeric materials are obtained from biomass processing [1]. 5-Hydroxymethylfurfural is a platform chemical from which many valuable compounds such as 5-hydroxymethyl-2-furoic acid (5OH2FA) can be obtained and used subsequently as monomers for the production of bio-based polyesters. In order to improve the properties of furan-based polyesters, in particular their biodegradability, monomers with furan units are mixed with biodegradable co-monomers [2].

The enzymatic synthesis of biopolymers represents currently an alternative method for chemical polymerization due to the biodegradability and natural origin of enzymes, efficient catalytic activity in mild reaction conditions and low impact on the environment. The most efficient enzymes used for polyester synthesis are lipases mainly the lipase B from *Candida Antarctica*. The polyesters obtained through enzymatic polymerization are important for their applicability in food industry, medical and pharmaceutical fields.

One biodegradable compound that can be used as monomer for furan-based polyester synthesis is ricinoleic acid which is a natural unsaturated hydroxy-fatty acid that can be obtained through hydrolyzation in alkaline media from castor oil, a non-edible bio-based oil. Due to its structure (double bond, hydroxyl and ester groups), ricinoleic acid is an important resource for obtaining functional polymers with various applications [3].

In order to optimize the oligoester synthesis based on 5-hydroxymethyl-2-furoic acid (5OH2FA) and ricinoleic acid (RCA) in this study the statistical technique Design of Experiments (DoE) was used. Box-Behnken design from Unscrambler software package was used for the optimization of oligoesters. Three parameters were selected (temperature, biocatalyst concentration reported to the amount of monomers, molar ratio between monomers) and their influence on the average molecular weights and relative content of the reaction products was studied. The temperature varied between 60 and 80°C, the proportion of the biocatalyst in relation to the monomers between 10 and 30%, and the molar ratio RCA: 5OH2FA from 1:1 to 5:1 were investigated. Based on the MALDI-TOF MS spectra and GPC analysis of each sample, the average molecular weights ( $M_n$ ,  $M_w$ ), and the relative composition of the reaction product (homopolymers and copolymers) were calculated and used as response variables. The optimal reaction conditions were determined based on DOE results and statistical analysis. The structure of the copolymer was demonstrated by NMR analysis. Although the polymerization degree is modest the obtained products could be useful in pharmaceutical, food, or medical applications.

### Acknowledgements

This work was supported by a grant of the Romanian Ministry of Education and Research, CNCS - UEFISCDI, project number PN-III-P1-1.1-TE-2019-1573, within PNCDI III, contract number TE 101.

### References

1. A. Todea, D.M. Dreavă, I.C. Benea, I. Bîțcan, F. Peter, C.G. Boeriu, *Processes* 9, 646 (2021).
2. A. Todea, D. Aparaschivei, V. Badea, C.G. Boeriu, F. Peter, *Biotechnol. J.* 13, 6 (2018).
3. S.F. Feng, P. Zhang, P. Jiang, Z. Zhang, J. Deng, Z. Cao, *Eur. Polym. J.* 169, 111125 (2022).



## Catalytic dehydration of 1,3-Butanediol into 1,3-Butadiene

G. Fayad , E.V. Makshina , B. Lagrain , B.F. Sels \*

Center for Sustainable Catalysis and Engineering (CSCE), KU Leuven, Celestijnenlaan 200F,  
3001, Leuven-Belgium  
e-mail: [bert.sels@kuleuven.be](mailto:bert.sels@kuleuven.be)

1,3-Butadiene (BD) the most basic and important conjugated diene is a key derivative of the petrochemical industry and an intermediate of many industrial products <sup>1</sup>. It is widely used as a raw material for the manufacture of a diversity of synthetic rubbers, elastomers and polymeric resins <sup>2</sup>. BD is mainly produced as a by-product of the steam cracking process for ethylene and propylene production or from oxidative dehydrogenation of n-butane and n-butene <sup>3</sup>. However, the depletion of these non-renewable feedstocks, closely related to the rapid growth in world population, increases the demand towards BD production from a greener and more sustainable routes using biomass-derived renewable materials <sup>4</sup>. Butanediol isomers (i.e. 1,3-, 1,4- and 2,3-BDOs) are produced in high yields from the biomass fermentation process, therefore, the acid-catalyzed dehydration of such C<sub>4</sub> alcohols can be regarded as an alternative potential route towards BD <sup>2</sup>.

Our work aims to stably produce BD with a very high yield from the catalytic dehydration of 1,3-BDO in the gaseous phase. To realize this goal, the catalytic behavior of several acidic commercial zeolites with different topologies were tested at 300 °C under atmospheric pressure in a fixed-bed flow reactor. Results revealed that the framework structure of zeolites plays a crucial role in governing butadiene selectivity. In addition to topology, active site accessibility, acid strength and acid site density can have a prominent impact on conversion rate, selectivity as well as stability in such dehydration reactions. While better sites accessibility may lead to shorter diffusion paths in the catalyst particle and lower cokes formation, hence, higher conversion and higher butadiene selectivity may be achieved; weak acid sites might decrease propylene formation by hindering carbon-carbon catalytic cracking as well as formation of undesirable side products (e.g. oligomerization of butadiene). To tackle these properties, new dehydration catalysts such as mesoporous, nanosized, layered as well as Boron-incorporated zeolites were synthesized by several groups and their catalytic activity were studied. Consequently, taking into consideration all these crucial properties, there is a potential of surpassing 80% in butadiene yield from the direct dehydration of 1,3-BDO.

### Acknowledgments:

Moonshot project, CSCE-KU Leuven, UGent-INCAT.

### References:

1. F. Jing, B. Katryniok, M. Araque, R. Wojcieszak, M. Capron, S. Paul, M. Daturi, J.-M. Clacens, F. De Campo, A. Liebens, F. Dumeignil, M. Pera-Titus, *Catal. Sci. Technol.*, **6** 5830-5840 (2016).
2. A.C. Rodriguez, M.S. Sad, H. Cruchade, L. Pinard, C.L. Padró, *Microporous Mesoporous Mat.*, **320** 111066 (2021).
3. F. Jing, B. Katryniok, S. Paul, L. Fang, A. Liebens, M. Shen, B. Hu, F. Dumeignil, M. Pera-Titus, *ChemCatChem.*, **9** 258-262 (2017).
4. J.H. Lee, S.B. Hong, *Appl. Catal. B: Environ.*, **280** 119446 (2021).

## Boosting Bicyclic-Aziridines Potential Through Enzymatic Kinetic Resolution in Flow

Milene A. G. Fortunato<sup>1</sup>, João R. Vale<sup>1</sup>, Filipa Siopa<sup>1\*</sup> and Carlos A. M. Afonso<sup>1\*</sup>

<sup>1</sup>The Research Institute for Medicines (iMed.Ulisboa), Faculty of Pharmacy, University of Lisbon, Av. Prof. Gama Pinto, 1649-003, Lisboa, Portugal

\*[filipasiopa@ff.ulisboa.pt](mailto:filipasiopa@ff.ulisboa.pt); [carlosafonso@ff.ulisboa.pt](mailto:carlosafonso@ff.ulisboa.pt)

The demand for enantiomerically pure compounds in the pharmaceutical industry increases the complexity of the synthetic routes. Among the methodologies to obtain enantiopure compounds, lipase mediated kinetic resolution offers a green process, with a well-established route, distinct advantages of high activity, selectivity, and mild operating conditions. [1]

$\alpha$ -hydroxycyclopenteno-aziridines (bicyclic-aziridines) are an intermediary to achieve molecules with biological properties such as functionalized aminocyclopentitols (e.g., peramivir, ticagrelor, neplanocin A and trehazolin).[2] The bicyclic-aziridines are obtained in a racemic mixture through a photochemical transformation of pyridinium salts, for which we developed a flow reactor for gram-scale preparation. [3] These bicyclic-aziridines have a free secondary alcohol in their structure, allowing for an enzymatic kinetic resolution, which could be achieved by using Novozym 435, an immobilized lipase, CAL B. The obtention of enantiopure bicyclic-aziridines unlocks synthetic routes to complex chiral structures.

We herein disclose the enzymatic kinetic resolution of two bicyclic-aziridines: allyl bicyclic-aziridine and butyl bicyclic-aziridine, from early batch studies to flow (Figure 1 (B,D) and (C, E)).

We successfully obtained with short residence times (*S*)-allyl bicyclic-aziridine 98% enantiomeric excess (*ee*) and 46% isolated yield (Figure 1(C)), as well the obtention of (*R*)-butyl bicyclic-aziridine acetate in 95% *ee* and 20% isolated yield (Figure 1(B)).

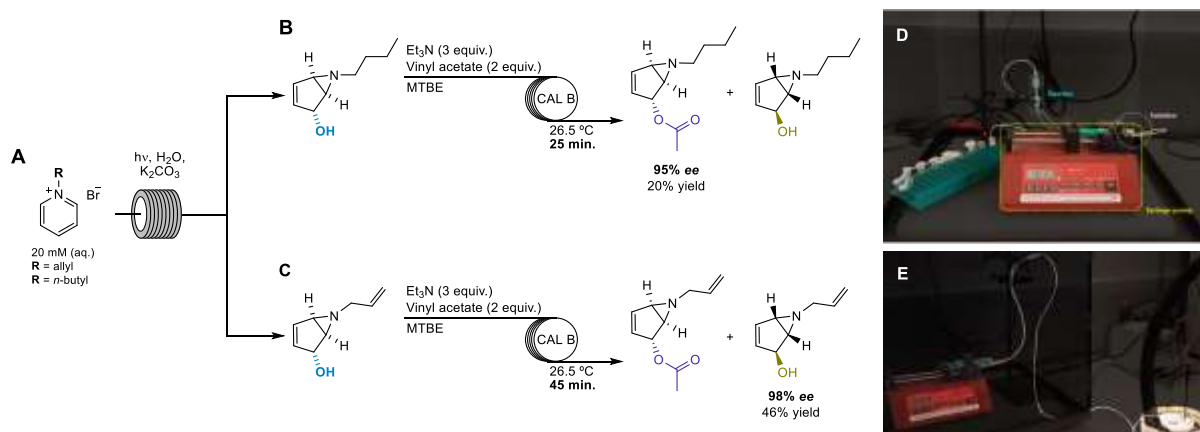


Figure 1. Obtention of enantiomeric pure bicyclic-aziridines: (A) Photochemical transformation of pyridinium salts in flow; Enzymatic kinetic resolution of (B) butyl-bicyclic-aziridine and (C) allyl-bicyclic-aziridine. Flow setup of enzymatic kinetic resolution (D) and (E).

### Acknowledgements

The authors acknowledge Fundação para a Ciência e Tecnologia (FCT) for financial support (2021.06598.BD, PTDC/QUI-QOR/32008/2017, UIDB/04138/2020 and UIDP/04138/2020). The project leading to this application has received funding from the European Union's Horizon 2020 research and innovation programme under grant agreement No 951996.

### References

- Z.S. Seddigi, M.S. Malik, S.A. Ahmed, A.O. Babalghith, A. Kamal, *Coord. Chem. Rev.*, **348** 54 (2017).
- a) U. Kořak, M. Hrast, D. Knez, N. Marař, M. Črnugelj, S. Gobec, *Tetrahedron Lett.* **56** 529 (2015). b) J. Zou, P.S. Mariano, *Photoch. Photobio. Sci.* **7** 393 (2008). c) R. Ash, R. M. Barrer, C.G. Pope, *Proc. R. Soc. London, Ser. A*, **271** 19 (1963).
- a) L. Kaplan, J.W. Pavlik, K.E. Wilzbach, *J. Am. Chem. Soc.* **94** 3283 (1972). b) F. Siopa, J.P.M. Ant3nio, C.A.M. Afonso, *Org. Process Res. Dev.* **22** 551 (2018). c) M.A.G. Fortunato, C.-P. Ly, F. Siopa, C.A.M. Afonso, *Methods Protoc.* **2** 67 (2019).

## Effect of Aqueous Choline Chloride-Based DES Solutions on the Biocatalytic Performance of Immobilized Hydrolases

Renia Fotiadou, Myrto G. Bellou, Elena Gkantzou, Angeliki C. Polydera and Haralambos Stamatis\*.  
Laboratory of Biotechnology, Department of Biological Applications and Technologies, University of Ioannina, Ioannina, Greece

\*Corresponding author: [hstamati@uoi.gr](mailto:hstamati@uoi.gr)

### Abstract

Hydrolases such as  $\beta$ -glucosidases (BGLs) and proteases (trypsin) are among the most significant industrial enzymes. They belong to the ubiquitous enzyme family of hydrolases. More specifically, BGLs catalyze the cleavage of  $\beta$ -1-4 glycosidic bonds, whereas in specific conditions can mediate the transglycosylation of glucose derivatives. Numerous industrial processes require the exploitation of BGLs e.g., for the production of biofuels, flavour and juice clarification, and pharmaceuticals synthesis<sup>1</sup>. On the other hand trypsin is a serine protease, found in the digestive system of many vertebrates, where it hydrolyzes proteins, mainly at the carboxyl side of the amino acids lysine or arginine. It is used for numerous biotechnological processes and proteomic analysis. However, limitations regarding low stability and insufficient reusability of soluble enzymes hamper their application. Hence, immobilization of enzymes is a promising prospect which enhances the utilization of biocatalysts in biotechnologically related applications. Green nanoparticles deriving from agricultural wastes are gaining ground for enzymes immobilization. Moreover, Deep Eutectic Solvents (DESs) are a type of green solvents which are employed in many biocatalytic reactions owing to their benign features and beneficial effect on enzymes performance<sup>2</sup>.

In this regard,  $\beta$ -glucosidase from the hyperthermophilic bacterium *Thermotoga maritima* (Tm) and trypsin from bovine pancreas were immobilized on the functionalized surface of green magnetic nanoparticles occurred from an olive leaf extract. The immobilization yield, specific activity, and enzymatic performance on DESs binary systems were investigated. The aim of this work was to assess the activity of the immobilized enzyme on different aqueous choline chloride DESs solutions. The effect of DESs as co-solvents on the enzymatic hydrolysis of substrates and the apparent kinetic constants of immobilized enzymes were also evaluated.

The results of this study demonstrated that green nanoparticles are robust and environmental-friendly nanocarriers for the effective immobilization of hydrolases. The new nanobiocatalytic systems (immobilized enzymes) were able to perform enzymatic reactions in aqueous DESs solutions. In particular, immobilized Tm's activity was screened on different choline chloride-based DESs solutions with substantial observations. The hydrogen bond donor and the % DESs concentration (v/v) seemed to affect the hydrolytic activity of immobilized Tm. ChCl:BG had a profound impact on the enzymatic performance of immobilized enzymes and so, it is considered a promising co-solvent for biotechnological reactions of interest. However, in the cases of salicin and esculin hydrolysis (phenolic glucosides), reaction rates were decreased with choline chloride-based DESs as co-solvents.

### Materials

$\beta$ -Glucosidase from *Thermotoga maritima* (BGL) was obtained from Megazyme (E-BGOSTM). Trypsin from bovine pancreas was obtained from Sigma. Choline chloride (ChCl, Sigma), urea (U, Fluka), glycerol (0.5% max water, Gly, Fisher Scientific), butylene glycol (BG, TCI), D(-)-fructose (Fru, Sigma) were of analytical grade. Acetonitrile and water were for liquid chromatography. Buffers and aqueous solutions were prepared in double distilled water (ddH<sub>2</sub>O).

A hydrogen bond acceptor (HBA) and a hydrogen bond donor (HBD) were mixed in specific molar ratios as described before<sup>3</sup>.

Immobilization of hydrolases on green hybrid zinc oxide-iron oxide nanoparticles was proceeded through covalent bonding using EDC/NHS, as described before by Chatzikonstantinou et al., with minor modifications<sup>4</sup>.

Hydrolysis reactions of phenolic glucosides or peptides were monitored and quantified by high performance liquid chromatography (HPLC) equipped with a  $\mu$ Bondapack C18 reversed-phase column (particle size 10  $\mu$ m, length 300 mm, diameter 3.9 mm) and a diode array UV detector.

### Results

Some key results are presented in Figure 1 and Table 1. Choline chloride-based DES have been used extensively as co-solvents in different enzyme mediated reactions. In with work, a variety of ChCl-based DES with different hydrogen bond donors were prepared in order to evaluate the catalytic activity of immobilized Tm. As shown in Figure 1, the hydrolysis of *p*-NPG was used as the model reaction and specific DESs were applied as co-solvents at different concentrations (v/v). At lower concentrations of DESs, a favorable effect on the immobilized enzyme activity was observed. More specifically, HBDS with hydroxyl groups enhanced remarkably the enzymatic

performance in some cases. The apparent kinetic constants were also affected with the inclusion of DESs. In particular, it was observed that  $K_m$  and  $V_{max}$  values were increased in any case.

Regarding the hydrolysis of phenolic glucosides, immobilized Tm was able to catalyze the cleavage of  $\beta$ -1-4-glucosidic bond in different aqueous DES solutions (10% v/v) (Table 1). However, reaction rates were substantially affected. A possible explanation is that in aqueous DES solutions occur mass transfer limitation issues.

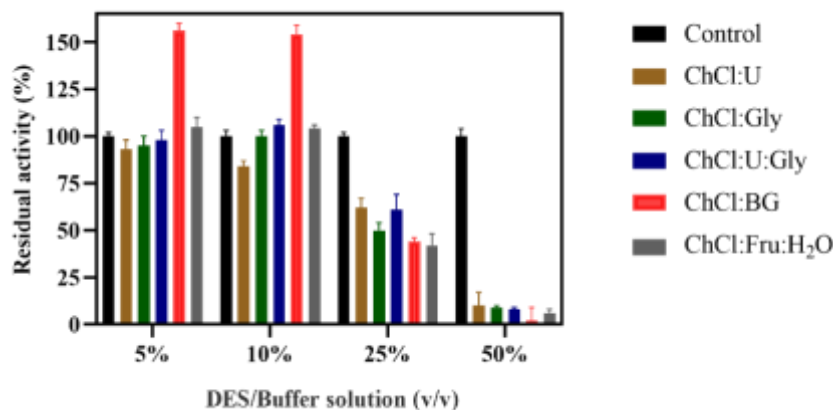


**Figure 44.** Hydrolytic activity of immobilized Tm at different concentrations of DES/buffer solutions (v.v). *p*-NPG was used as model substrate.

**Table 1.** Reaction rates of the hydrolysis of phenolic glucosides catalyzed by 0.050 mg mL<sup>-1</sup> immobilized enzyme at 50 °C.

	Esculin hydrolysis	Salicin Hydrolysis
	Reaction Rate ( $\mu\text{M min}^{-1} \text{mg}^{-1}$ nanobiocatalyst)	
Buffer	433	710
ChCl:U	263.6	247.4
ChCl:Gly	325.8	269.2
ChCl:Gly:U	273	272
ChCl:BG	318.4	303.6
ChCl:Fru:H <sub>2</sub> O	335.2	307.4

In conclusion, the immobilization of hydrolases on green hybrid zinc oxide-iron oxide nanoparticles stabilizes the enzymes. The new nanobiocatalysts (immobilized hydrolases) were able to effectively perform hydrolytic reactions in aqueous DES solutions

## Acknowledgements

This research has been co-financed by the European Regional Development Fund of the European Union and Greek national funds through the Operational Program Competitiveness, Entrepreneurship and Innovation, under the call RESEARCH—CREATE—INNOVATE (project code: T2EDK-03599).

## References

- G. Singh, A. K. Verma, V. Kumar., 3 Biotech, 6 3 (2016).
- H. Vanda, Y. Dai, E. G. Wilson, R. Verpoorte, Y. H. Choi., *Comptes Rendus Chim*, **21** 628 (2018).
- A. E. Delorme, J.-M. Andanson, V. Verney., *Int. J. Biol. Macromol*, **163** 919 (2020).
- A. V. Chatzikonstantinou, A. C. Polydera, E. Thomou, N. Chalmpes, T. N. Baroud, A. Enotiadis, L. Estevez, M. Patila, M. A. Hummami, K. Spyrou, E. P. Giannelis, A. G. Tzakos, D. Gournis, H. Stamatis., *Bioresource Technology Reports* **9** 100372 (2020).

## Dry Reforming of Methane over Fe-Co Based Alumina Supported Catalysts

Sholpan S. Itkulova<sup>1,2\*</sup>, Yerzhan A. Boleubayev<sup>1</sup>, Kirill A. Valishevskiy<sup>1</sup>, Alexander R. Brodsky<sup>1,2</sup>,  
Nurlygul K. Orazova<sup>2</sup>, and Perizat I. Komekbayeva<sup>2</sup>

<sup>1</sup> D.V.Sokolsky Institute of Fuel, Catalysis, and Electrochemistry, 142, Kunaev str., Almaty, 050010, Republic of Kazakhstan;

<sup>2</sup> Kazakh-British Technical University, 59, Tole bi, Almaty, 050000, Republic of Kazakhstan

\* e-mail: [sholpan.itkulova@gmail.com](mailto:sholpan.itkulova@gmail.com), [s.itkulova@ifce.kz](mailto:s.itkulova@ifce.kz)

**Abstract:** The Fe-Co-based alumina supported catalysts with or without additive of Pt were tested in the dry reforming of methane (DRM). Their activity was compared under atmospheric pressure and varying the process temperature within 400-800°C. The 5-20% Co-Fe-Pt/Al<sub>2</sub>O<sub>3</sub> catalyst exhibits the high activity and selectivity in the syngas production by DRM. Methane is almost completely converted at 800°C. Adding small amount of Pt (0.25 wt.%) slightly increases in activity, promotes the reverse water gas shift reaction, and prevents coke formation. The catalysts have been characterized by a number of physico-chemical methods (BET, XRD, TEM, SEM, H<sub>2</sub>-TPR, and Messbauer spectroscopy). By Messbauer spectroscopy, the formation of bi- and trimetallic clusters of Fe-Co, Fe-Pt, and Fe-Co-Pt have been observed.

There are several technologies for methane reforming to produce syngas. Among them dry reforming of methane (DRM) (Eq.1) is an attractive way to utilize the main greenhouse gases (Eq. 1). More importantly, the biogas mainly composed of carbon dioxide and methane is a cheap renewable source for DRM. Besides, some reservoirs of natural gas can contain comparable concentrations of CO<sub>2</sub> and methane, which makes the reaction more desirable for commercialization.



Despite its considerable environmental potentials, DRM is not considered an industrially mature process. The principal reason for this is the carbon-forming reaction, which quickly deactivates conventional reforming catalysts if used without the presence of steam. Ni-based catalysts are commonly used ones and widely investigated. Nevertheless, no effective commercial catalyst to date exists which operates without carbon formation.

In the present work, the performance of Fe-Co based catalysts used in DRM is discussed. The effect of amount of metals and Pt additive on the catalyst behavior has been investigated.

The polymetallic Fe-Co-containing catalysts were prepared by impregnating alumina with an aqueous solution of Fe, Co, and Pt compounds followed by thermal treatment. Total content of Fe and Co was varied within 5-20 wt.%. The mass ratio of Fe:Co was kept as 1:1. The trimetallic catalysts were synthesized by adding of 0.25 wt.% of Pt to the Fe-Co/Al<sub>2</sub>O<sub>3</sub>.

The physicochemical properties of the catalysts were studied using TEM, SEM, BET, TPR-H<sub>2</sub>, Mossbauer spectroscopy, and XRD.

The process of dry reforming of methane (DRM) was carried out in a laboratory flow quartz reactor supplied with programmed heating and a controlled feeding velocity. The gas hourly space velocity (GHSV) was 1000 h<sup>-1</sup> and process was operated under the atmospheric pressure. The temperature was varied within 400-800°C. The initial and final reaction products were on-line analyzed using the GC's.

The catalysts activity was tested in the dry reforming of methane. The effect of temperature on methane and carbon dioxide conversion over the new polymetallic supported catalysts was studied. Also, the influence of the content of metals was examined.

At 800°C, methane is almost completely converted over the synthesized catalysts: X(CH<sub>4</sub>) is > 99.0%, while carbon dioxide conversion degree is lower and reaches 90-92%.

Syngas is the only product of CO<sub>2</sub> reforming of methane over the catalysts. The ratio of the H<sub>2</sub>/CO in the synthesis gas is < 1 and is varied within 0.90-0.94.

By Messbauer spectroscopy, the formation of the bimetallic Fe-Co, Fe-Pt, and possibly trimetallic Fe-Co-Pt clusters were shown. The bi- and trimetallic Fe-Co catalysts are much higher active than the monometallic Co- and Fe-supported catalysts.

The results obtained show that the new multicomponent catalysts based on Fe and Co with additive of noble metal and supported on alumina have the high activity and stability in the dry reforming of methane.

### Acknowledgements

This research was funded by the Science Committee of the Ministry of Education and Science of the Republic of Kazakhstan, Grant No AP08855848.

## Catalytic properties of Ni-Cu mixed oxides deposited on stainless steel meshes by plasma jet sputtering

Květa Jirátová<sup>1\*</sup>, Petr Soukal<sup>2</sup>, Timur Babii<sup>3</sup>, Jana Balabánová<sup>1</sup>, Martin Koštejn<sup>1</sup>, Martin Čada<sup>2</sup>, Jaroslav Maixner<sup>4</sup>, Pavel Topka<sup>1</sup>, Zdeněk Hubička<sup>2</sup>, František Kovanda<sup>3</sup>

<sup>1</sup>Institute of Chemical Process Fundamentals of the Czech Academy of Sciences, Prague, Czech Republic; \*jiratova@icpf.cas.cz

<sup>2</sup>Institute of Physics, Academy of Sciences of the Czech Republic, Prague, Czech Republic

<sup>3</sup>Department of Solid State Chemistry, University of Chemistry and Technology, Prague, Czech Republic

<sup>4</sup>Central Laboratories, University of Chemistry and Technology, Prague, Czech Republic

Plasma jet sputtering is a convenient method for preparing catalysts supported on stainless steel meshes. Such catalysts are particularly suitable for processes carried out at high space velocities [1]. One of them is the catalytic total oxidation of volatile organic compounds (VOC), an economically feasible and environmentally friendly method of reducing VOC emissions. Mixed oxides are efficient catalysts in oxidation of VOC. Cobalt oxide-based catalysts in combination with Mn oxides are particularly active [2]. However, cobalt compounds are among the strategic materials and are expensive. Therefore, we have attempted to investigate new oxidation catalysts based on nickel oxide in combination with other transition metal oxides. In this contribution, we have decided to study properties and oxidation activity of Ni-Cu mixed oxides prepared by hollow cathode plasma jet sputtering, as both metals are easily accessible and plasma jet sputtering can be realized on a large scale.

Hollow cathode plasma jet sputtering of Ni, Cu and Ni+Cu mixtures in an Ar+O<sub>2</sub> oxidizing atmosphere has been used to create thin oxide coatings on stainless steel meshes. The prepared samples differ in molar ratios of both components and are labeled as Cu, NiCu14, NiCu11, NiCu41 and Ni (numbers denotes Ni:Cu molar ratios, e.g., the NiCu14 sample contains Ni and Cu in molar ratio of 1:4). The properties of the supported catalysts were characterized by EDX, powder XRD, SEM, temperature programmed reduction (H<sub>2</sub>-TPR), Raman spectroscopy, and XPS. The catalytic activity was examined in the deep oxidation of ethanol and toluene, which were used as model VOCs. The activity of the catalysts in the oxidation of ethanol and toluene was evaluated as specific activity (amount of reactant converted per unit mass of metal oxides per hour) at chosen reaction temperatures. All properties of the prepared catalysts were compared with grained catalysts obtained by calcination (500 °C in air) of coprecipitated precursors with corresponding compositions.

The catalysts prepared by Ni and/or Cu sputtering on stainless steel meshes had very low content of Ni-Cu oxides (~0.3 wt.%). Molar ratios of Ni and Cu determined by EDX were very close to the demanded values (Table 1). Powder XRD patterns of sputtered Ni and Cu catalysts revealed presence of NiO (bunsenite) or CuO (tenorite). When both elements were deposited simultaneously, a mixture of NiO and CuO was formed. Evaluation of lattice parameters and crystallite size was very difficult due to the few distinguishable peaks present. In addition, a diffraction peak at ~51.1° corresponding to the stainless steel support overlapped the most intense NiO peak at ~50.7°. For these reasons, the calculated D values (the sizes of the NiO coherent domains in Table 1) are less accurate. Powder XRD patterns of the oxide samples obtained from the coprecipitated precursors showed the same oxides (NiO, CuO or their mixtures). SEM images of the meshes revealed uniform distribution of Cu, Ni, and Ni-Cu oxide particles on the meshes, not differing from each other.

Table 1 also summarizes the surface areas (S<sub>BET</sub>) of the oxides deposited on the meshes. The deposited Ni oxide showed the largest surface area (5.2 m<sup>2</sup> g<sup>-1</sup>), while the Cu one showed substantially lower surface area (1.8 m<sup>2</sup> g<sup>-1</sup>). Surface area of the deposited Ni-Cu oxide catalysts varied from 0.8 to 3.0 m<sup>2</sup> g<sup>-1</sup>. Surface area of the grained catalysts obtained from coprecipitated precursors varied from 3.3 m<sup>2</sup>g<sup>-1</sup> (the NiCu14 sample) to 17.8 m<sup>2</sup>g<sup>-1</sup> measured for the Ni catalyst; thus, they surface areas of the Ni-Cu oxide catalysts prepared by different ways were very similar.

Table 1. Properties of Ni-Cu oxide catalysts sputtered over stainless steel meshes and those from coprecipitated precursors

Sample	Meshes							Grains					
	Ni/(Ni+Cu) Expected mol mol <sup>-1</sup>	Ni/(Ni+Cu) EDX mol mol <sup>-1</sup>	Ni/(Ni+Cu) XPS mol mol <sup>-1</sup>	XPS/ EDX	MeO <sub>x</sub> <sup>a</sup> wt.%	D <sub>NiO</sub> nm	S <sub>BET</sub> m <sup>2</sup> g <sub>oxides</sub> <sup>-1</sup>	Ni/(Ni+Cu) AAS mol mol <sup>-1</sup>	Ni/(Ni+Cu) XPS mol mol <sup>-1</sup>	XPS/ AAS	D <sub>NiO</sub> nm	S <sub>BET</sub> m <sup>2</sup> g <sub>oxides</sub> <sup>-1</sup>	
Cu	0	0.00	0		0.21	-	9.4	0	0.01		-	7	
NiCu14	0.2	0.14	0.43	3.1	0.30	12.1	3.3	0.21	0.43	2.0	12.1	22	
NiCu11	0.5	0.49	0.58	1.2	0.30	13.7	10.1	0.53	0.72	1.4	13.1	28	
NiCu41	0.8	0.74	0.61	0.8	0.29	11.7	10.2	0.80	0.71	0.9	18.5	33	
Ni	1	0.98	1	1	0.17	9.0	17.8	1	1	1.0	33.1	14	

<sup>a</sup> Ni+Cu oxides content (determined by weighing the stainless steel meshes before and after the Ni and Cu sputtering)

Reducibility of the obtained Ni-Cu oxides was examined by H<sub>2</sub>-temperature programmed reduction. The positions of T<sub>max</sub> in TPR patterns are presented in Table 2. The reduction profile of the sputtered Cu catalyst is rather complex with a broad reduction feature ranging from 200 °C to 400 °C with maximum at 277 °C. Small peak was also observed at 337 °C. As the powder XRD of Cu catalyst confirmed the presence of CuO in this catalyst, this

reduction feature was ascribed to the reduction of  $\text{Cu}^{2+}$  species to  $\text{Cu}^0$ . The Ni catalyst exhibited one reduction peak with a maximum at 404 °C. The peak included the reduction of  $\text{Ni}^{2+}$  to  $\text{Ni}^0$ . The Ni-Cu oxide catalysts from coprecipitated precursors were reduced at lower temperatures compared to the Ni and Cu samples (Table 2). The reduction maxima observed at 257, 270, and 270 °C for the NiCu14, NiCu11, and NiCu41 catalysts, respectively, were shifted to lower temperatures with increasing copper content in the catalysts, as precipitated Ni catalyst was reduced mainly at 367 °C. Reduction of sputtered Ni-rich catalysts was slightly worse than that from the coprecipitated precursors.

Raman spectra of the examined catalysts revealed several (Table 2). The Cu catalysts of both types showed identical main band at 298  $\text{cm}^{-1}$  along with two minor bands at 344 and 628  $\text{cm}^{-1}$ . The Ni-containing catalysts showed a broad band at 535  $\text{cm}^{-1}$  for the precipitated catalysts, which shifted slightly to higher values for sputtered catalyst. The shift of Ni-O band can be attributed to the smaller particles formed during the precipitation of the catalysts precursors. The grained Ni catalyst revealed a broad band even at 488  $\text{cm}^{-1}$ .

Table 2. Positions of the reduction maxima during TPR measurements and observed Raman bands of the Ni-Cu oxide catalysts

Sample	$T_{\text{max}}$ observed during TPR, °C		Raman bands, $\text{cm}^{-1}$	
	Meshes	Grains	Meshes	Grains
Cu	277; 337	265; 281	298; 348; 628	296; 344; 628
NiCu14	295; 354	257	299; 348; 552broad; 628sh	296; 344; 535
NiCu11	303; 340	270	299; 347; 548; 628sh	296; 344; 535
NiCu41	309	219sh; 270	299; 543broad	535broad
Ni	404	300sh; 367		200; 387sh; 488broad

The XPS measurements proved presence of NiO and CuO on the surface of all catalysts. The surface Ni concentration was higher than the bulk concentration for both types of catalysts, with the sputtered NiCu14 catalyst being almost 1.5 times higher than in the grained ones. The ratio of surface to bulk concentration close to 1 was approximately the same for the other catalysts (Table 1).

The activity of sputtered catalysts with different Ni-Cu molar ratios in the oxidation of ethanol and toluene is shown in Figure 1, left. In the ethanol oxidation, the activity increased significantly with increasing Ni:Cu molar ratio, with the Ni catalyst being the most active. In the toluene oxidation, the maximum activity was observed for the NiCu11 catalyst. Toluene oxidation took place at temperatures about 130 °C higher than the ethanol oxidation. The grained catalysts showed (Figure 1, right) the highest activity in ethanol oxidation over the NiCu14 and NiCu41 catalysts. In the oxidation of toluene, the NiCu11 catalyst showed the maximum activity. As expected, the activity of the grained catalysts obtained from coprecipitated precursors was higher than that of the pelletized coprecipitated catalyst (NiCu11<sub>pell</sub>, 4x3 mm pellets) due to the internal diffusion of the reactants.

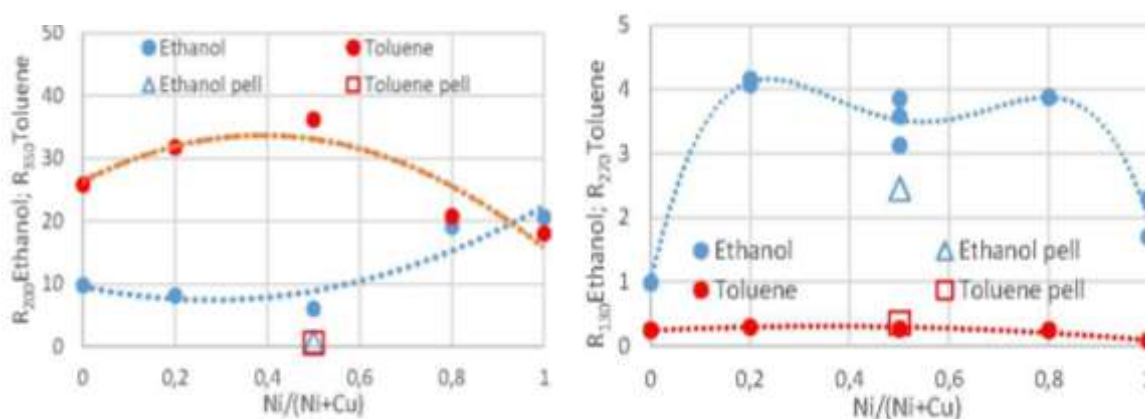


Figure 1. Comparison of catalytic activity of sputtered (left) and grained (right) Ni-Cu oxide catalysts (GHSV=20  $\text{l g}^{-1} \text{h}^{-1}$ , 800 ppm of VOC)

Comparing the activity of the sputtered catalysts (Fig. 1 left) with that of calcined coprecipitated NiCu11 in the form of pellets (NiCu11<sub>pell</sub>), the activity of the sputtered catalysts was ~10 times higher for ethanol oxidation and almost 40 times higher for toluene oxidation, although the amount of active components in the sputtered catalysts was almost 30 times lower.

## Acknowledgements

The work was supported by Czech Science Foundation (project No. 21-04477S).

## References

1. A. Cybulski, J.A. Moulijn, Structured Catalysts and Reactors, CRC Press, Taylor and Francis (2006).

2. P. Topka, K. Jirátová, M. Dvořáková, J. Balabánová, M. Koštejn, F. Kovanda, *Environ. Sci. Pollut. Res.* (2021), <https://link.springer.com/article/10.1007/s11356-021-15906-y>



## Bioconversion of daidzin and genistin in seed and roots extracts of Korean wild soybean into daidzein and genistein by $\beta$ -galactosidase from *Thermoproteus uzoniensis*

Kyung-Chul Shin<sup>1</sup>, Su-Hwan Kang<sup>2</sup>, Deok-Kun Oh<sup>2</sup>, Dae Wook Kim<sup>3</sup>, Sae Hyun Kim<sup>3</sup>, Chae Sun Na<sup>3,\*</sup> and Yeong-Su Kim<sup>3,\*</sup>

<sup>1</sup>Department of Integrative Bioscience and Biotechnology, Konkuk University, Seoul 05029, Republic of Korea

<sup>2</sup>Department of Bioscience and Biotechnology, Konkuk University, Seoul 05029, Republic of Korea

<sup>3</sup>Department of Wild Plants and Seeds Conservation, Baekdudaegan National Arboretum, Bonghwa 36209, Republic of Korea

\* Correspondence: [yskim@koagi.or.kr](mailto:yskim@koagi.or.kr)

Abstract text:

A putative  $\beta$ -galactosidase from the extreme thermophile *Thermoproteus uzoniensis* ( $\beta$ -Gal<sub>Tu</sub>) was cloned and expressed in *Escherichia coli* for potential application in isoflavone conversion. Isoflavones have attracted attention because of their biological activities against cancer, heart disease, symptoms of menopause, and osteoporosis, which can be improved by deglycosylation of isoflavones into aglycones that are quickly absorbed in human body because of their lower molecular weight and better hydrophobicity than those isoflavones. In this study, we investigated that production of daidzein and genistein from Korean wild soybean (*glycine soja*) using  $\beta$ -Gal<sub>Tu</sub>.  $\beta$ -Gal<sub>Tu</sub> was purified by His-trap affinity chromatography with a specific activity of 1,103  $\mu$ mol/min/mg, and exists as a homodimer of 113 kDa. Biochemical properties of  $\beta$ -Gal<sub>Tu</sub> such as effects of pH and temperature, thermostability, and substrate specificities.  $\beta$ -Gal<sub>Tu</sub> showed the highest activity for *p*-nitrophenyl (*p*NP)- $\beta$ -D-galactopyranoside among aryl glycosides, and its hydrolase activities for isoflavone glycosides followed the order genistin > daidzin > ononin > glycitin at pH 5.0 and 90 °C.  $\beta$ -Gal<sub>Tu</sub> completely hydrolyzed daidzin and genistin in the seed extract of wild soybean into 2.77 mM daidzein after 80 min with a productivity of 1.86 mM/h; and 3.85 mM genistein after 70 min with a productivity of 3.30 mM/h. Moreover, daidzin and genistin in the root extract of wild soybean were completely converted to 9.89 mM daidzein and 1.67 mM genistein for 180 min and 30 min with the productivities of 3.30 mM/h and 3.36 mM/h, respectively, which showed the highest productivities compared to other glycosidases. This is the first report on the production of isoflavone aglycones (daidzein and genistein) from isoflavone glycosides (daidzin and genistin) in wild soybeans. This study will be helpful for industrial production of isoflavone aglycone using wild soybean.

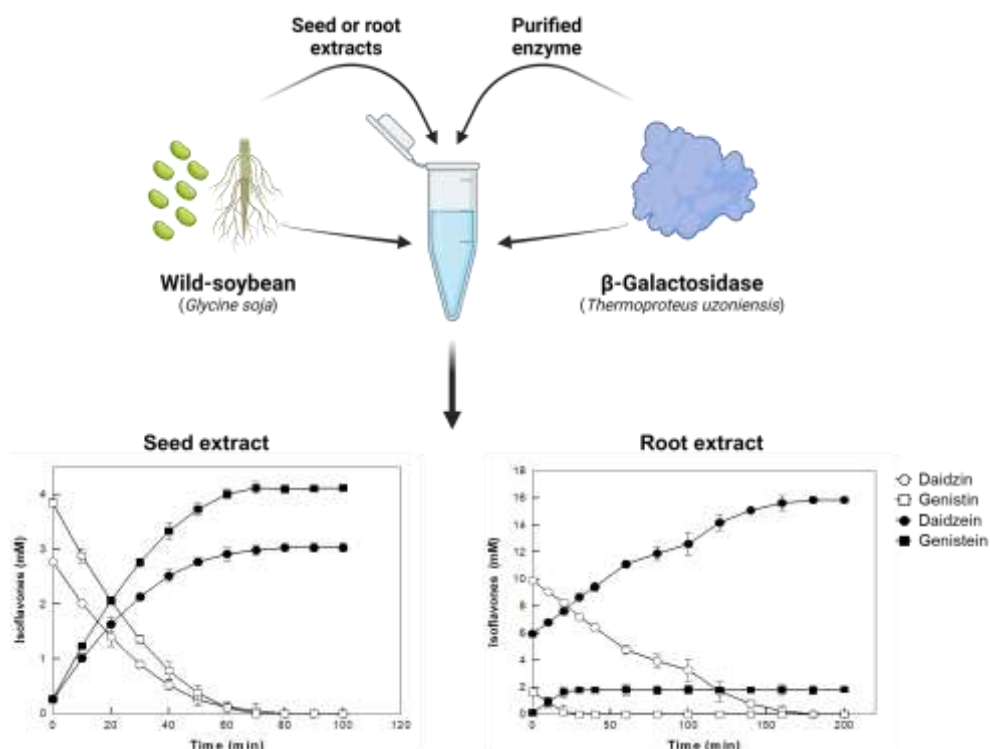


Figure 1. Production of daidzein and genistein from daidzin and genistin in the seed and root extracts of wild soybean by thermostable  $\beta$ -galactosidase from *Thermoproteus uzoniensis*

### Acknowledgements

This work was supported by the Basic Science Research Program through the National Research Foundation of Korea (NRF) funded by the Ministry of Education (NRF-2020R111A1A01063145)

## Cobalt-copper oxide catalysts and their performance in total oxidation of ethanol

Květa Kupková<sup>1</sup>, Jana Balabánová<sup>2</sup>, Květa Jirátová<sup>2</sup>, Jean-Marc Giraudon<sup>3</sup>, Jean-Francois Lamonier<sup>3</sup>,  
František Kovanda<sup>1\*</sup>

<sup>1</sup>Department of Solid State Chemistry, University of Chemistry and Technology, Prague,  
Technická 5, 166 28 Prague, Czech Republic

<sup>2</sup>Institute of Chemical Process Fundamentals of the CAS, Rozvojová 135, 165 02 Prague, Czech Republic

<sup>3</sup>University of Lille, Unité de Catalyse et Chimie du Solide, UMR CNRS 8181, Cité Scientifique, Bâtiment C3,  
59650 Villeneuve d'Ascq Cedex, France

\*Frantisek.Kovanda@vscht.cz

Volatile organic compounds (VOC) in industrial gases represent a serious environmental problem; they contribute to ozone/smog formation and some of them exhibit toxic, narcotic or carcinogenic properties. Concentration of these pollutants in air can be reduced applying the catalytic total oxidation to carbon dioxide and water as the final products; this process is markedly energy saving compared to the elimination of VOC by thermal combustion. Besides the rather expensive noble metals-containing catalysts, cheaper transition metal oxides are also used as catalysts in this process. Both cobalt and copper are active components in oxide catalysts used for VOC removal and their combination can be beneficial due to the synergistic effect [1,2].

The oxide catalysts were obtained by heating of precursors, prepared by coprecipitation of nitrate solutions containing Co and Cu in various molar ratios (4:1, 1:1, and 1:4). The single-component precursors containing only Co and Cu were precipitated as well. The dried and powdered products were formed into pellets and calcined for 4 h at 500 °C in air. After cooling, the pellets were crushed and sieved to obtain the fraction with particle size of 0.160-0.315 mm, which was used in catalytic experiments. The samples were labeled by acronyms with cation composition, i.e., Co, CoCu41, CoCu11, CoCu14, and Cu. The prepared oxide catalysts were characterized by elemental analysis (AAS), surface analysis (XPS), powder XRD, Raman spectroscopy, nitrogen adsorption, and temperature programmed reduction (H<sub>2</sub>-TPR). The catalytic performance was examined in the deep oxidation of ethanol, which was used as a model VOC. The catalytic reaction was carried out in a fixed bed reactor (5.0 mm i.d.) in the temperature range from 80 to 400 °C and temperature ramp of 2.0 °C min<sup>-1</sup>. The inlet ethanol concentration in air was 750 ppm at GHSV of 20 l g<sub>cat</sub><sup>-1</sup> h<sup>-1</sup>. The T<sub>50</sub> and T<sub>90</sub>(CO<sub>2</sub>) temperatures (the temperatures needed to achieve 50% ethanol conversion and 90% conversion of all organic compounds to CO<sub>2</sub>, respectively) were chosen as a measure of the catalysts activity. Selectivity in ethanol oxidation to formation of acetaldehyde and carbon monoxide was described by maximum concentrations of both compounds occurrence at corresponding temperatures.

The metals contents in the catalysts are presented in Table 1; the determined Co:Cu molar ratios are close to those adjusted in nitrate solutions used in the precursors coprecipitation. The catalysts contained also small amount of sodium cations remaining in the prepared products after washing. The XPS analysis showed strong enrichment of the surface with Cu in the CoCu41 catalyst, while surface of the CoCu11 and CoCu14 catalysts was enriched with Co. Powder XRD pattern of the Cu catalysts corresponded to CuO (tenorite) and the Co catalyst contained only Co<sub>3</sub>O<sub>4</sub> with a spinel structure. Powder XRD patterns of the Co-Cu oxide catalysts showed diffraction peaks corresponding to both CuO and Co<sub>3</sub>O<sub>4</sub>; it indicated formation of a mixture of spinel-type Co<sub>3</sub>O<sub>4</sub> and CuO during heating of coprecipitated Co-Cu precursors. Part of copper cations can also occupy sites in the spinel lattice. It is difficult to determine from XRD patterns, whether the spinel structure corresponds to Co<sub>3</sub>O<sub>4</sub> or Cu<sub>x</sub>Co<sub>3-x</sub>O<sub>4</sub>; these oxides have very similar positions of diffraction lines with only small shifts caused by small difference in the Co and Cu cation sizes. Evaluation of powder XRD data showed that the spinel lattice parameters in Co-Cu samples were slightly larger (about 8.089 Å) compared to the Co sample (8.084 Å). The XRD coherent domains (often considered as approximate crystallite sizes) were calculated from the broadening of diffraction peaks; they reflected structure ordering of the prepared oxides. The crystallite sizes of spinel-type oxides in all Co-Cu samples were very similar (about 30 nm). The CuO crystallite sizes increased with increasing copper content in the samples, from 16 nm in the CoCu41 sample to 33 nm in the Cu one (Table 1). The Raman spectra of Co-Cu oxide catalysts also showed a simple superposition of the bands characteristic for single-component Co and Cu oxides, i.e., Co<sub>3</sub>O<sub>4</sub> and CuO; relative intensities of the bands corresponded to the Co and Cu contents in the samples. A shift in the positions of Raman bands did not prove clearly the formation of Co-Cu mixed oxides as the band positions could be affected by shape and size of the crystallites. Both powder XRD patterns and Raman spectra of the Co-Cu catalysts indicated that mixtures of Co<sub>3</sub>O<sub>4</sub> and CuO rather than Co-Cu mixed oxides were formed during heating of the coprecipitated precursors. The measured N<sub>2</sub> adsorption isotherms were classified as type II isotherms corresponding to non-porous or macroporous materials. A small adsorption at low relative pressures (maximum 6 cm<sup>3</sup> g<sup>-1</sup>) was found and, therefore, no micropores were likely present in the catalysts. The determined values of surface area (S<sub>BET</sub>), mesopore volume (V<sub>meso</sub>), and average pore size decreased with increasing Cu content in the catalysts (Table 1). The hydrogen consumptions during TPR measurements are summarized in Table 2. The Co catalyst exhibited two reduction peaks: a smaller peak with a maximum at 292 °C and a larger one with a maximum at 378 °C. The TPR profile of Co catalyst was characteristic for Co<sub>3</sub>O<sub>4</sub> reduction; the first reduction peak was

ascribed to reduction of  $\text{Co}^{3+}$  to  $\text{Co}^{2+}$  and the larger peak to the reduction of  $\text{Co}^{2+}$ . The TPR profile of Cu catalyst was more complex with a broad reduction feature ranging from 200 °C to 450 °C with maximum at 414 °C; it might be ascribed to the reduction of  $\text{Cu}^{2+}$  species to metallic copper. The Co-Cu catalysts were reduced at lower temperatures compared to the Co and Cu samples. The reduction maxima were observed at 313, 271, and 253 °C for the CoCu14, CoCu11, and CoCu41 catalysts, respectively; a shift to lower temperatures with increasing cobalt content in the catalysts was found (Table 2).

Table 1. Characteristics of the prepared Co-Cu oxide catalysts: Content of Co and Cu components, crystallite sizes determined from XRD data, and textural properties determined from nitrogen adsorption

Sample	Metal content (wt. %)			Co:Cu ratio		Crystallite size (nm)		$S_{\text{BET}}$ ( $\text{m}^2 \text{g}^{-1}$ )	$V_{\text{meso}}$ ( $\text{cm}^3 \text{g}^{-1}$ )	Pore size (nm)
	Co	Cu	Na	AAS	XPS	spinel	CuO			
Co	66.3	-	1.75	1:0	-	26	-	27	0.23	32
CoCu41	56.7	15.0	0.17	4:0.98	2.29:1	30	16	21	0.18	32
CoCu11	35.3	37.2	0.34	1:0.98	1.30:1	26	28	19	0.09	18
CoCu14	14.3	59.3	0.57	1:3.84	2.55:4	33	28	18	0.08	16
Cu	-	75.1	0.77	0:1	-	-	33	5	0.02	14

Results obtained during testing of the Co-Cu oxide catalysts in the ethanol oxidation are summarized in Table 2. The low  $T_{50}$  temperature (90 °C) indicated high activity of the CoCu41 catalyst, while the Cu catalyst showed the highest  $T_{50}$  value (186 °C). Acetaldehyde and carbon monoxide were detected as the main by-products of ethanol oxidation over the examined catalysts. The most active catalyst, CoCu41, showed relatively high acetaldehyde formation (444 ppm); the highest concentration of acetaldehyde (629 ppm) was found on the Cu catalyst. The amount of carbon monoxide produced during the reaction was low; maximum concentrations ranged between 5 and 14 ppm, with an exception of the Co catalyst, which showed 131 ppm of CO. The  $T_{90}(\text{CO}_2)$  temperature is an important parameter for the VOC total oxidation. The lowest  $T_{90}(\text{CO}_2)$  temperature (159 °C) was found for the CoCu41 catalyst, while much higher temperatures were found for the Cu-rich CoCu14 (197 °C) and Cu (259 °C) catalysts. The Co catalyst was active ( $T_{50}$  temperature 105 °C) but exhibited a relatively high  $T_{90}(\text{CO}_2)$  temperature (202 °C). For all copper-containing catalysts, a linear correlation between the temperature of the main reduction peak in TPR profiles and their activity in ethanol oxidation ( $T_{50}$  temperatures) was observed; only the copper-free Co catalyst clearly deviated from this dependence.

Table 2. TPR results and performance of the Co-Cu oxide catalysts in the ethanol deep oxidation

Sample	Hydrogen consumption ( $\text{mmol g}^{-1}$ )	$T_{\text{max}}$ (TPR) (°C)	$T_{50}$ (°C)	$T_{90}(\text{CO}_2)$ (°C)	Acetaldehyde formation* (ppm / °C)	CO formation* (ppm / °C)
Co	16.8	292; 378	105	202	544 / 137	131 / 202
CoCu41	18.1	214; 253	90	159	444 / 134	7 / 170
CoCu11	16.7	271	99	172	428 / 141	7 / 171
CoCu14	12.5	260; 313	131	197	340 / 164	12 / 199
Cu	12.6	375; 414	186	259	541 / 212	9 / 216

\* Maximum concentration during the catalytic experiment and temperature, at which it was detected

The Co-Cu oxide catalysts prepared from coprecipitated precursors contained a mixture of  $\text{Co}_3\text{O}_4$  and CuO (detected by powder XRD and Raman spectroscopy). The TPR results indicated that CuO present in the samples promoted reduction of  $\text{Co}_3\text{O}_4$ . The most active CoCu41 catalyst was reduced at the lowest temperature, likely due to the high dispersion of CuO on the surface of  $\text{Co}_3\text{O}_4$  particles. In contrast, the surface area of the Co-Cu oxide catalysts was not critical for their performance in deep oxidation of ethanol. A synergistic effect of Co and Cu components in the catalysts was observed for CoCu41 and CoCu11 samples. The CoCu41 catalysts showed the highest activity and selectivity, achieving 90% conversion to  $\text{CO}_2$  at 159 °C (compared to 202 and 259 °C observed for the Co and Cu catalysts, respectively).

## Acknowledgements

Authors thank the Czech Science Foundation for financial support (project 21-04477S).

## References

1. A.M. Carrillo, J.G. Carriazo, *Appl. Catal. B*, 164 443 (2015).
2. S. Li, H. Wang, W. Li, X. Wu, W. Tang, Y. Chen, *Appl. Catal. B*, **166-167** 260 (2015).

## Photocatalytic Degradation of Ceftazidime in Wastewaters and Landfill Leachate using Manganese Oxides Supported on TiO<sub>2</sub>-Graphene Nanocomposite Catalysts

Eleni Evgenidou<sup>1,2</sup>, Panagiotis Pavlidis<sup>1</sup>, Efthymia Ioannidou<sup>3</sup>, Dimitrios Trikkaliotis<sup>3</sup>, Christina Nannou<sup>1,2</sup>, George Kyzas<sup>3</sup>, Dimitris Bikiaris<sup>4</sup>, Dimitra Lambropoulou<sup>1,2</sup>

<sup>1</sup> Department of Chemistry, Aristotle University of Thessaloniki, GR 54124, Thessaloniki, Greece

<sup>2</sup> Centre for Interdisciplinary Research and Innovation (CIRI-AUTH), Balkan Center, Thessaloniki, 10<sup>th</sup> km Thessaloniki-Thermi Rd, GR 57001, Greece, dlambro@chem.auth.gr

<sup>3</sup> Department of Chemistry, International Hellenic University, Kavala, Greece, kyzas@chem.ihu.gr

<sup>4</sup> Laboratory of Polymer Chemistry and Technology, Department of Chemistry, Aristotle University of Thessaloniki, GR-541 24 Thessaloniki, Greece, dbic@chem.auth.gr

In the present study the photocatalytic treatment of ceftazidime (CEF), a third-generation cephalosporin, has been investigated using manganese oxides supported on graphene oxide (GO)- titania (TiO<sub>2</sub>) nanocomposites. GO-TiO<sub>2</sub> nanocomposites were prepared by using a mild ultrasonically assisted synthetic route with different mass ratios of graphene (1–5 % wt %). With the MnO<sub>x</sub> active component loaded by means of ultrasonic impregnation. The characterization of the catalysts and the determination of their physicochemical properties was conducted employing Fourier transform infrared spectroscopy (FTIR), scanning electron microscopy (SEM), BET analysis and X-Rays Diffraction (XRD). The degradation kinetics followed the first-order kinetic law. The synthesized composite with 1% GO and 5% MnO appeared to be the most effective catalyst. Tests were performed using a secondary effluent from a wastewater treatment plant and a landfill leachate. The nearly complete removal of the target compound could be achieved after 1 h at low concentration to 6h at high concentration in leachate matrix. Moreover, the kinetic effects of catalyst dosage, contaminant concentration, chemical oxidants (H<sub>2</sub>O<sub>2</sub>, S<sub>2</sub>O<sub>8</sub><sup>2-</sup>) and solution pH on CEF degradation were studied, and the transformation products were identified by liquid chromatography–High Resolution mass spectrometry (LC-HRMS) to propose the possible transformation pathways.

### Acknowledgments

This research has been co-financed by the European Union and Greek national funds through the Operational Program Competitiveness, Entrepreneurship, and Innovation, under the call RESEARCH – CREATE – INNOVATE (2<sup>nd</sup> Cycle) (Project acronym: PROMoTE; Project code: T2EDK-04066).



Με τη συγχρηματοδότηση της Ελλάδας και της Ευρωπαϊκής Ένωσης

## Alternative and greener microwave assisted alkyl levulinate production.

Susana O. Ribeiro<sup>1</sup>, Andreia F. Peixoto<sup>1</sup>, Andreia Leite<sup>1\*</sup>

<sup>1</sup>REQUIMTE-LAQV, Department of Chemistry and Biochemistry, University of Porto, 4169-007 Porto, Portugal

\*acleite@fc.up.pt

In this work, microwave irradiation (MW) was used as hybrid process to extract silica from rice husks and to prepare bio-based SBA-15 mesoporous silica. SBA-15 was synthesized using both hydrothermal methodology in a MW heated reactor and using an autoclave. The MW\_SBA-15 was post-functionalized with SO<sub>3</sub>H- groups. The structural and chemical composition of the prepared materials were characterized by several techniques such as elemental analysis, XPS, FT-IR, XRD, SEM and N<sub>2</sub> adsorption/desorption isotherms confirming the successful preparation of the materials. SBA-15 functionalized with the organosilane CSPTMS was applied as catalyst in the production of fuel additives such as alkyl levulinate using the biomass-derived platform molecule 5-hydroxymethylfurfural (5-HMF). Different types of reactors (conventional, MW and high-pressure batch reactor) were used to compare their efficiency to convert 5-HMF. The results showed that MW reactor allowed the best activity and selectivity. The effects of temperature reaction and use of different alcohols simultaneously as solvent and reagent, were evaluated and showed that higher temperature favors the production of ethyl levulinate and that the increase in the alcohol carbon chain promoted the production of heavy organic compounds. The ability of SBA15@CSPTMS to be reusable were evaluated and it is noteworthy to mention that no significant loss of activity was observed during four catalytic cycles.

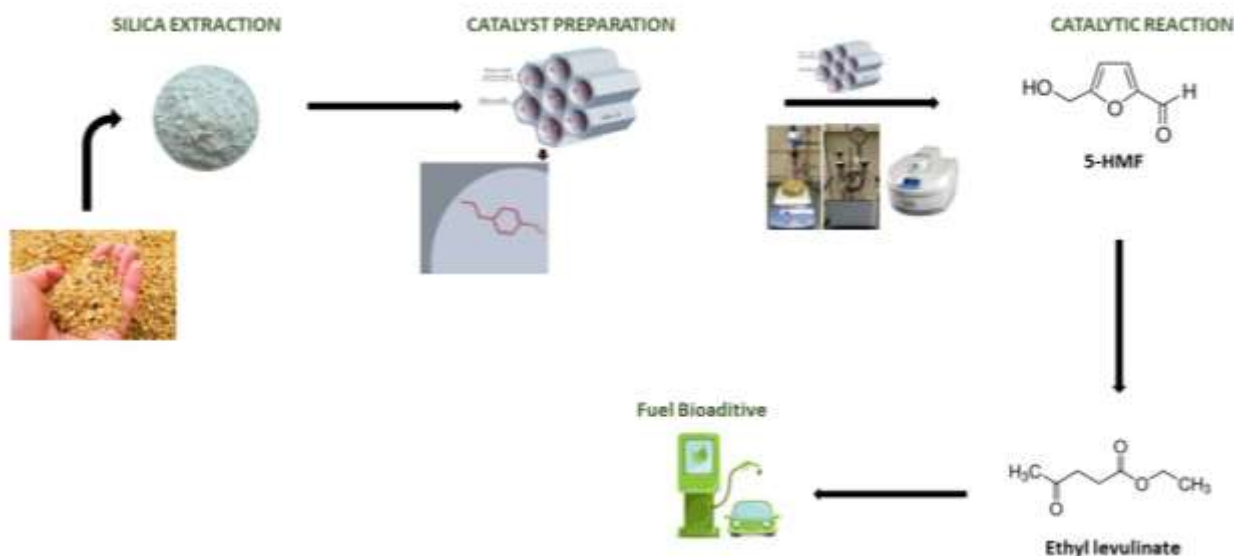


Figure 1. Representative scheme of the described work.

### Acknowledgements.

This work received financial support from National Funds (FCT/MCTES, Fundação para a Ciência e Tecnologia and Ministério da Ciência), under the Partnership Agreement PT2020 through project PTDC/QUI-QIN/28142/2017. Additionally, the research team would like to thank the projects NORTE-07-0162-FEDER-000048, UIDB /50006/2020, UIDP/50006/2020. A. Leite thank FCT for funding through program DL 57/2016 – Norma transitória.

## Towards an artificial metalloprotein-controlled enantioselective allylic substitution reaction

Maria Logotheti<sup>1</sup>, Paul Hünemörder<sup>2</sup>, Esteban Meija<sup>2\*</sup>, Matthias Höhne<sup>1\*</sup>

1. Institute for Biochemistry, University of Greifswald, Felix-Hausdorff-Straße 4, 17487 Greifswald, Germany

2. Leibniz Institute for Catalysis, Albert-Einstein-Straße 29A, 18059 Rostock, Germany

\*. matthias.hoehne@uni-greifswald.de, \*esteban.meija@catalysis.de

### Transferring a metal-photoactivated allylic substitution reaction into a protein host to improve reaction efficiency and achieve enantioselectivity in aqueous conditions.

In this study we are aspiring to transfer an efficient copper-photoactivated allylic-C-H alkynylation reaction into aqueous conditions and aiming to induce enantioselectivity, via the use of a suitable protein scaffold [1].

To this purpose, we have chosen *LmrR*, a dimeric protein, which has been already used efficiently as a protein host for metal-catalysed reactions in aqueous conditions [2-5].

The reaction of interest leads to the efficient formation of 1,4-enyne compounds at room temperature in organic solvent, using a copper(I) terpyridyl complex as photo-initiator.

We have shown that the protein's dimeric cavity has a good affinity for the copper-terpyridyl complex. Thus, the copper catalyst can be trapped via non-covalent interactions inside the cavity.

We have determined the factors that are necessary for compatibility between protein and the reaction-components and are working further via reaction-engineering on overcoming the compatibility barrier.

Our next step is to enhance reaction efficiency in the aqueous environment further and induce enantioselectivity.

### References

1. A.A. Almasalma, E. Mejía, *Synthesis*, **52**, 04 (2019).
2. Z. Zhou, G. Roelfes, *ACSCatal.* **2021**, **11**, 15 (2021).
3. Z. Zhou, G. Roelfes, *NatCatal*, **3** (2020).
4. I. Drienovská, A.S. Remkes, C. Gutiérrez de Souza, G. Roelfes, *ChemBioChem*, **21**, 21 (2020).
5. J. Bos, W.R. Browne, A.J.M. Driessen, G. Roelfes, *J.Am.Chem.Soc.* **2015**, 137 (2015).

## Turning Green Ideas into Industrial Success

Nikki Man, Fritz Schoenberg, Alexandre Vieira Silva, Raphael Fritsche, Henriette Nowothnick, Sonja Jost

*DUDE CHEM GmbH, Köpenicker Str. 325, 12555 Berlin, Germany  
man@dudechem.com*

DUDE CHEM is a Green Chemistry start-up with its roots in the German Cluster of Excellence in Catalysis at the University of Technology Berlin. As a high-tech virtual manufacturer, we facilitate greener outsourcing of pharmaceuticals and their intermediates in order to transform the current pharma-chemical industry towards into an environmentally benign sector. Our multi-disciplinary team combines expertise in both green chemistry and digitization.

The use of quantum chemical methods allows for accelerating development time for specific challenges like solvent screenings or extraction problems by the use of tailor made applications, e.g. for catalyst reuse in homogeneous solvent systems:

A Suzuki coupling reaction of an important API class will be shown, that is used for the treatment of hypertension. In this case the expensive Pd catalyst could be reused up to 4 times while salts and product could be easily removed and isolated in one step.

In another case study we will show how the change of synthesis design towards an API led to a much greener process in which toxic solvents were replaced. By direct comparison of the old industrial process with the new one one clearly sees that the number of synthesis steps were shorten and a more atom efficient route was established. By calculating the PMI (Process mass index) and the E-factor of both processes it is shown that the PMI was improved for the new process by a factor of ~3 and the E-factor by 4.

## Manganese-Catalyzed Hydrogenation of Sclareolide to Ambradiol

Nadja E. Niggli<sup>1</sup>, Viktoriia Zubar<sup>1</sup>, Niels Lichtenberger<sup>1</sup>, Mathias Schelwies<sup>2</sup>, Thomas Oeser<sup>3</sup>, A. Stephen K. Hashmi<sup>1,3</sup>, and Thomas Schaub\*<sup>1,2</sup>

<sup>1</sup>Catalysis Research Laboratory (CaRLa), Im Neuenheimer Feld 584, 69120 Heidelberg, Germany

<sup>2</sup>BASF SE, Carl-Bosch-Straße 38, 67056 Ludwigshafen, Germany

<sup>3</sup>Organisch-Chemisches Institut, University of Heidelberg, Im Neuenheimer Feld 270, 69120 Heidelberg, Germany

\* thomas.schaub@basf.com

The most established synthetic route towards (–)-Ambrox, a fragrance compound of industrial interest, is a three-step procedure starting from the diterpene (–)-Sclareol.<sup>[1]</sup> The traditional approach in this sequence suffers from the reduction-step from (+)-Sclareolide to (–)-Ambradiol, which is usually performed using the expensive and difficult to handle KBH<sub>4</sub>, red-Al, or LiAlH<sub>4</sub>.<sup>[2]</sup> In addition, super-stoichiometric waste is thereby generated which renders this approach in general disadvantageous for larger scale applications. These limitations were previously addressed with the transition-metal catalyzed hydrogenation of (+)-Sclareolide avoiding such reagents by the use of highly active but expensive noble metal catalysts<sup>[3]</sup> or less reactive earth-abundant metals<sup>[4]</sup>, both in combination with relatively large amounts of base. In order to make this process even more economically interesting, we report a high yielding Mn-catalyzed hydrogenation of (+)-Sclareolide to (–)-Ambradiol employing a new bench-stable Mn-PNN complex under relatively mild reaction conditions at low manganese and base loadings (Figure 1).<sup>[5]</sup> This complex can be synthesized from a commercially available manganese precursor as well as an air stable and readily available PNN-pincer ligand. Its easy synthesis along with the good activity and chemoselectivity observed, make this new catalyst a cost-effective alternative to the frequently used Ru-catalysts.

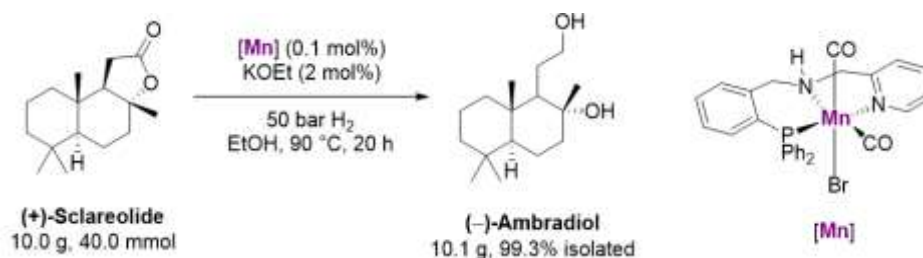


Figure 1. Efficient hydrogenation of (+)-Sclareolide using the newly developed Mn-PNN complex.

### Acknowledgements

CaRLa is being co-financed by the Ruprecht-Karls University of Heidelberg and BASF SE, Ludwigshafen, Germany.

### References

- [1] S. Yang, H. Tian, B. Sun, Y. Liu, Y. Hao, Y. Lv, *Sci. Rep.* **2016**, *6*, 32650.
- [2] e.g. A. F. Barrero, E. J. Alvarez-Manzaneda, R. Chahboun, A. F. Arteaga, *Synth. Commun.* **2011**, *34*, 3631–3643.
- [3] P. Dupau, L. Bonomo, L. Kermorvan, M. Haldimann Sanchez (Firmenich SA), WO 2019/175158A1, **2019**. M. Schelwies, J. Schwaben, R. Paciello (BASF SE), WO 2021/001240 A1, **2021**.
- [4] M. B. Widegren, M. L. Clarke, *Org. Lett.* **2018**, *20*, 2654–2658.
- [5] V. Zubar, N. Lichtenberger, M. Schelwies, T. Oeser, A. S. K. Hashmi, T. Schaub, *ChemCatChem* **2022**, *14*, e202101443.



# Hydrogenative Depolymerization of Polyurethanes Catalyzed by a Manganese Pincer Complex

Edward Ocansey<sup>1</sup>, Viktoriia Zubar<sup>1</sup>, Andreas T. Haedler<sup>2</sup>, Markus Schütte<sup>3</sup>, Stephen K. Hashmi<sup>1,4</sup>, Thomas Schaub<sup>1,2</sup>

<sup>1</sup>Catalysis Research Laboratory (CaRLa), University of Heidelberg, Heidelberg, Germany

<sup>2</sup>BASF SE, Carl-Bosch-Straße 38, 67056 Ludwigshafen, Germany

<sup>3</sup>BASF Polyurethanes GmbH, Elastogranstr. 60, 49448 Lemfoerde, Germany

<sup>4</sup>Organisch-Chemisches Institut, Heidelberg University, Im Neuenheimer Feld 270, 69120 Heidelberg, Germany

\*thomas.schaub@basf.com

Chemical recycling, in particular hydrogenative depolymerization, offers a promising way to utilize plastic waste.<sup>[1-3]</sup> This is an important avenue for dealing with the pollution caused by plastic waste and also to limit the use of fossil feedstocks as a source of monomers for the production of various polymeric plastic materials.<sup>[4,5]</sup> This report highlights the manganese-catalyzed hydrogenation of polyurethane materials to the corresponding monomeric units (Figure 1). The key to success is a Mn pincer complex as a potent hydrogenation catalyst in combination with elevated temperatures (up to 200 °C) and suitable solvents to ensure sufficient solubility of the polymers. A wide array of polyurethane compounds of varying polyol and isocyanate compositions, some of which contain significant amounts of urea functionalities, are depolymerized, resulting in polyetherols and diaminotoluene (TDA) in yields of up to 89 % and 76 %, respectively.

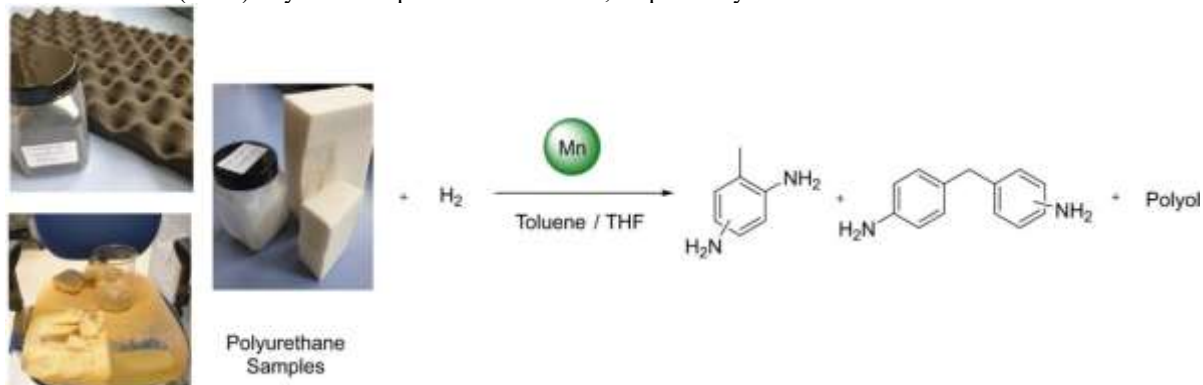


Figure 1: Hydrogenation of polyurethane model

## Acknowledgements

CaRLa is being co-financed by the Ruprecht-Karls University of Heidelberg and BASF SE, Ludwigshafen, Germany

## References

- [1] E. M. Krall, T. W. Klein, R. J. Andersen, A. J. Nett, R. W. Glasgow, D. S. Reader, B. C. Dauphinais, S. P. Mc Ilrath, A. A. Fischer, M. J. Carney, D. J. Hudson, N. J. Robertson, *Chem. Commun.* 2014, 50, 4884–4887
- [2] J. A. Fuentes, S. M. Smith, M. T. Scharbert, I. Carpenter, D. B. Cordes, A. M. Slawin, M. L. Clarke, *Chem. Eur. J.* 2015, 21, 10851–10860
- [3] S. Westhues, J. Idel, J. Klankermayer, *Sci. Adv.* 2018, 4, eaat9669
- [4] Viktoriia Zubar, Andreas Haedler, Markus Schütte, A. Stephen K. Hashmi, Thomas Schaub, *ChemSusChem*, 2021, DOI: 10.1002/cssc.202101606
- [5] Wei Zhou, Paul Neumann, Mona Al Batal, Frank Rominger, A. Stephen K. Hashmi, Thomas Schaub, *ChemSusChem*, 2020, DOI: 10.1002/cssc.202002465

## Diffusion and Adsorption Effects in TS-1/SAC Composites Catalysts for the Green Epoxidation of Methyl Oleate with H<sub>2</sub>O<sub>2</sub>

Adrián Osorio, Michael Goepel, David Poppitz, Muslim Dvoyashkin and Roger Gläser\*

Institute of Chemical Technology, Universität Leipzig, Linnéstr. 3, 04103 Leipzig, Germany

\*roger.glaeser@uni-leipzig.de

### Introduction

In the last decade, interest has been focused on the development of efficient and green processes for the transformation of renewable resources into value-added chemicals. One prominent example is of fatty acid methyl esters (FAMES), which are produced via the Prilezhaev reaction with several disadvantages such as the highly production of corrosive waste and leads to undesirable epoxy-ring opening [1-2]. In contrast, epoxidation of FAME using hydrogen peroxide is one of the most attractive sustainable options to produce renewable epoxides since it is easy to use and water is the only by-product (Figure 1). For the latter process titanium silicalite-1 (TS-1) has gained considerable attention as a promising catalyst in recent research [3]. With et al. [4] reported a hybrid concept in which the catalytically active component TS-1 is combined with a sorptive functionality of a polymer-based spherical activated carbon (SAC). This new composite material shows higher catalytic activity (based on Ti-sites) than pure TS-1. However, the exact role of the carbon in the TS-1-catalyzed epoxidation is not clear. Therefore, in the present work, TS-1 and two TS-1/SAC composite catalysts (called Composite\_A and Composite\_B based on the composition of both components) were investigated regarding their catalytic activity and selectivity to understand whether the additional adsorption capacity of SAC affects the epoxidation of methyl oleate (MO) to epoxy methyl oleate (eMO) using these composite catalysts. Furthermore, the effect of the addition of the TS-1 on the diffusion behavior of the reactants inside the composite catalyst is investigated.

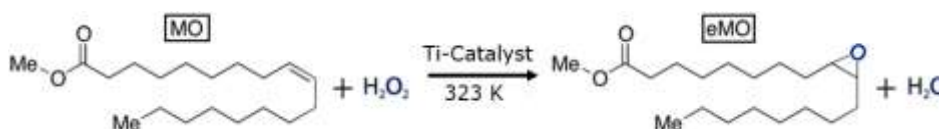


Figure 1. Epoxidation of methyl oleate using hydrogen peroxide using a Ti-catalyst.

### Experimental Part

The syntheses of TS-1 and TS-1/SAC composites (spherical carbon supports supplied by Blücher GmbH) were carried out according to the method proposed by With et al. [4]. Diffusion experiments were conducted by <sup>1</sup>H NMR using a wide bore 9.4 Bruker BioSpin spectrometer following the experimental methodology from Dvoyashkin et al. [5]. Catalytic experiments were conducted in the liquid-phase using a two-neck round-bottom flask (V = 25 mL) containing a magnetic stirrer and connected to a reflux condenser at 323 K. In a typical experiment, 10 mL of acetonitrile (99.9%, VWR) were added with 90 mg of MO (≥ 99%, Sigma-Aldrich) and 150 mg of the catalyst. The reaction mixture including the catalyst was stirred (stirring speed = 600 min<sup>-1</sup>) for 5 h at 323K before starting the reaction. Samples were taken at 0, 0.5, 1.5, 3 and 5 h intervals before starting the reaction via H<sub>2</sub>O<sub>2</sub> addition to investigate adsorption effects. After 5 h, 140 mg of H<sub>2</sub>O<sub>2</sub> (30 wt.-% aqueous solution, Sigma-Aldrich) were added to initiate the reaction and samples were taken after 5.5, 6.5, 8 and 10 h. A defined amount of the sample (0.1 mL) was diluted in 0.5 mL of acetonitrile and analyzed by gas chromatography (Shimadzu GC 2010 equipped with a flame ionization detector). The turnover number ( $n_{eMO,t=5} n_{Ti}^{-1}$ ) of MO conversion was calculated as moles of epoxy methyl oleate produced per mole of titanium sites present in the catalyst.

### Results and Discussion

SEM images suggest the formation of TS-1 crystals on the surface of the SAC. The presence of MFI-type crystals was confirmed by the characteristic peaks at  $2\theta = 7.9^\circ, 8.9^\circ, 23.1^\circ, 23.9^\circ$  and  $24.4^\circ$  observed by XRD. Weight fractions of TS-1 and SAC in the synthesized composites as determined by thermo-gravimetric analysis (TGA) were 26 and 74 wt.-% in Composite\_A and 56 and 44 wt.-% in Composite\_B, respectively. Figure 2 shows an illustration of the three assumed MO diffusion regimes and their associated Diffusion coefficients in a TS-1/SAC composite particle as determined by PFG-NMR. Bulk diffusion ( $D_1$ ), diffusion in the inter-crystalline spaces formed by the aggregation of TS-1 crystals ( $D_2$ ) and diffusion within the pores of the SAC ( $D_3$ ). Furthermore, MO diffusion is not expected to be observed into the TS-1 micropores (0.54 nm) as the molecular size of the MO is too large to access them (approx. 2.5 nm along the C-C segments, 0.5 nm for the cross section). With increasing TS-1 content in the composite, the probability of finding MO molecules with the  $D_2$  diffusion coefficient increases, i.e. the population of molecules diffusing between the intercrystalline spaces of TS-1 increases. Furthermore, the probability of finding a MO molecule in the SAC pores decreases notably with the increase of the TS-1 content. This is explained by the TS-1 crystals blocking part of the pore system of the SAC. This was also confirmed by characterization via nitrogen sorption, mercury intrusion porosimetry and SEM images (not shown here).

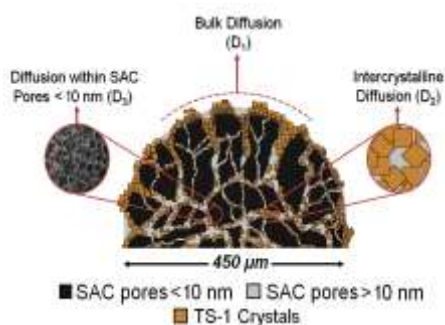


**Figure 2.** Illustration of the three types of MO diffusion into a composite particle of TS-1 and SAC followed by PFG-NMR spectroscopy.

Adsorption of the reactant MO needs to be taken into account when assessing the activity of the composite catalysts (Figure 3 (left)). A reduction of MO concentration in the liquid phase with no epoxy methyl oleate (eMO) formation was observed. This indicates a significant adsorption of the reactant molecules on the solid materials without a chemical reaction occurring. The term apparent conversion was thus used to express the reduction of reactant concentration in the liquid phase ( $1 - (n_{MO,t} n_{MO,0}^{-1})$ ). A reduction in observed reactant concentration is thus caused by the interplay of reaction and (unreactive) adsorption on the catalyst surface. The TS-1/SAC composites are nearly four and six times more active for the conversion of MO with  $H_2O_2$  in the liquid phase than a commercial TS-1 catalyst with an epoxide selectivity of 81 % and 96 % (Figure 3 (right)). The higher conversion for the composites with respect to TS-1 may be attributed to an adsorptive enrichment of the reactants on the catalyst surface in the vicinity of the catalytically active sites of the TS-1.

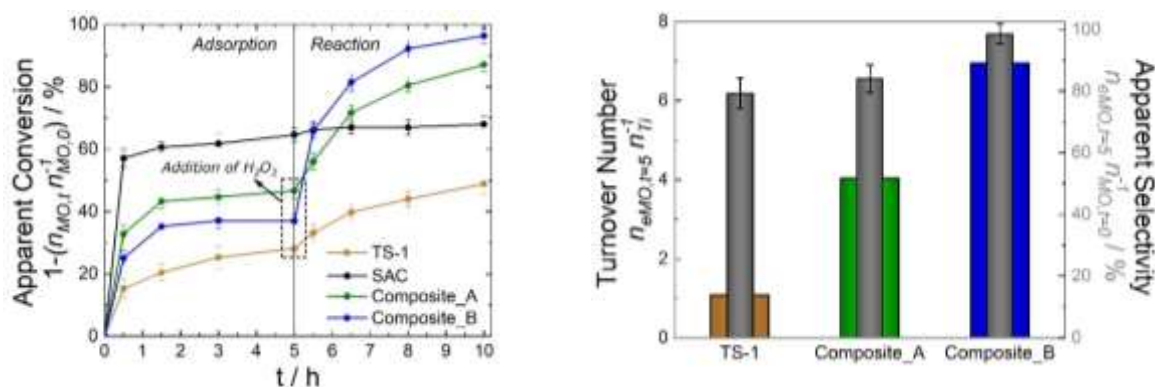


**Figure 3.** (Left): Apparent conversion expressed as  $1 - (n_{MO,t} n_{MO,0}^{-1})$  in the MO epoxidation with  $H_2O_2$  initiation. (Right): Turnover number ( $n_{eMO,t=5} n_{Ti}^{-1}$ ) and relative molar amount of eMO (apparent selectivity) expressed as  $n_{eMO,t=5} n_{MO,t=0}^{-1}$  after 5 h of reaction over TS-1, Composite\_A and Composite\_B.

## Conclusions

Composites of TS-1 and spherical activated carbon are up to six times more active (normalized by molar Ti-content) than a commercial TS-1 with comparable epoxide selectivity of ca. 80%. Experiments with physical mixtures (not shown) indicate a true synergistic effect with composite formation. An increase in eMO selectivity (82 vs. 96%) for the Composite\_B over the Composite\_A indicates a decrease in the irreversible adsorption of the reaction product (eMO), possibly caused by less unfavorable adsorption occurring inside the SAC pores, which are more likely to be blocked by TS-1 at higher TS-1 loadings. Addition of a strong adsorbent to the catalytically active species may lead to an overestimation of conversion due to removal of the reactant from the liquid phase (through adsorption). Moreover, the overall conversion and apparent selectivity are reduced due to irreversible (under reaction conditions) adsorption of reactants and products, respectively. Furthermore, increasing the TS-1 content in the composite material increases the Ti-content normalized activity despite the overall mass-transfer being slower in the composite with higher TS-1 loading. This counterintuitive finding can be explained with the partial blockage of the smaller SAC pores by TS-1 preventing the unwanted diffusion and adsorption of reactants in these pores. Also, this could be caused by the increased probability of finding reactant molecules within the inter-crystalline space between agglomerated TS-1 crystals.

## Acknowledgements

The authors are grateful to DAAD for financing of the research project and to Blücher GmbH for providing the polymer based spherical activated carbon.

## References

1. M. de Torres, I.W.C.E. Arends, J.A. Mayoral, E. Pires, G. Jiménez-Osés, *Appl. Catal., A* **425** 91-96 (2012).
2. S.-C. Chua, X. Xu, Z. Guo, *Process Biochem. (Oxford, U. K.)* **47** 1439-1451 (2012).
3. N. Wilde, J. Přeck, M. Pelz, M. Kubů, J. Čejka, R. Gläser, *Catal. Sci. Technol.* **6** 7280-7288 (2016).
4. P.C. With, N. Wilde, A. Modrow, B. Böhringer, R. Gläser, *Chem. Eng. Technol.* **38** 1671-1676 (2015).
5. M. Dvoyashkin, N. Wilde, J. Haase, R. Gläser, *RSC Adv.* **8** (2018) 38941-38944.

## Photocatalytic degradation of RB5 with modified graphitic carbon nitride (g-C<sub>3</sub>N<sub>4</sub>) as catalyst.

Papamichail P.,<sup>1\*</sup> Deliyanni E.<sup>1</sup>

<sup>1</sup>Laboratory of Chemical and Environmental Technology, Department of Chemistry, Aristotle University of Thessaloniki, 54124, Greece

\*e-mail address of corresponding author: [polypapamich@gmail.com](mailto:polypapamich@gmail.com)

### Abstract

Graphitic carbon nitride (g-C<sub>3</sub>N<sub>4</sub>), a metal-free catalyst, has been widely used in recent years as a photocatalyst mainly due to its ability to provide a large number of catalytic reaction sites <sup>[1]</sup>, decomposing this way organic and inorganic substances under UV and visible light <sup>[4]</sup>.

In the present study, four heterogeneous graphitic carbon nitride samples were prepared after the surface modification of the pristine sample g-C<sub>3</sub>N<sub>4</sub>, i.e. a) by recalcination and b) by oxidation of the of the pristine sample of the photocatalyst. The pure photocatalyst was prepared from melamine, and urea as precursors.

The recalcination was performed at 550 °C for 4 hours for both precursors.

For the oxidation surface modification, an amount of the pristine photocatalyst, prepared either from melamine or urea as precursors, was added to an equimolar mixture of 40 mL H<sub>2</sub>SO<sub>4</sub> / HNO<sub>3</sub>, for 5 hours under ambient conditions. <sup>[1]</sup>.

The characterization of the photocatalysts was performed with XRD, SEM, BET, FTIR, XPS, UV-reflectance while the pH-point of zero charge was also measured <sup>[2]</sup>. The results of X-ray diffraction and SEM showed that the samples prepared with melamine as a precursor showed a greater crystallinity than the samples prepared with urea as a precursor, while the BET results revealed that the samples prepared after recalcination presented larger specific surface area than the samples prepared after oxidation.

Accordingly, the results of the photocatalytic activity showed that the samples prepared with urea as precursor presented higher degree of RB5 degradation with the sample prepared after recalcination to have the highest yield. Similar trend was observed for the samples prepared with melamine as precursor.

The mechanism of the degradation process was investigated in the presence of different scavengers (methanol, potassium iodide, inert nitrogen atmosphere) in order to investigate the formation of holes (h<sup>+</sup>), superoxide anion radicals (•O<sup>2-</sup>) and hydroxyl radicals (•OH) during the photocatalytic process. Among these, •O<sup>2-</sup> appear to have a favorable role in the photodissociation of RB5. In conclusion, surface modification of the photocatalyst leads to increased degradability of RB5 dye under UV and sunlight.

### References

- 1.Choudhary, P., et al. (2020). Oxidized graphitic carbon nitride as a sustainable metal-free catalyst for hydrogen transfer reactions under mild conditions. *Green Chemistry*.
- 2.Dorraji, M., et al. (2017). Photocatalytic activity of g-C<sub>3</sub>N<sub>4</sub>: An empirical kinetic model, optimization by neuro-genetic approach and identification of intermediates. *Chemical Engineering Research and Design*, 113-175.
- 3.Saroyan, H., et al. (2019). Reactive Black 5 Degradation on Manganese Oxides Supported on Sodium Hydroxide Modified Graphene Oxide. *Applied Sciences* 9, (10), 2167.
- 4.Zhang, Q., et al. (2021). Advancing Graphitic Carbon Nitride-Based Photocatalysts toward Broadband Solar Energy Harvesting. *ACS Materials Letters*, 3(6), 663–697.

## A comparative study of the CO<sub>2</sub> methanation efficiency of dispersed Rh, Ru and Ir nanoparticles: Effect of metal nature and supporting material

Georgia Botzolaki, Anatoli Rontogianni, Grammatiki Goula, Ersi Nikolaraki, Sotiris Fanourgiakis, Ioannis V. Yentekakis\*

Laboratory of Physical Chemistry & Chemical Processes ([www.pccplab.tuc.gr](http://www.pccplab.tuc.gr)), School of Chemical & Environmental Engineering, Technical University of Crete, 73100 Chania, Crete, Greece.

\*Corresponding Author ([yentek@isc.tuc.gr](mailto:yentek@isc.tuc.gr))

### ABSTRACT

Energy needs of modern life inevitably keep high and unluckily increasing fossil fuels (coal, oil, and natural gas) utilization in order to address those. Among others, this leads to the emission of enormous quantities of CO<sub>2</sub> in the atmosphere. However, CO<sub>2</sub> is a greenhouse gas and its high and continuously increasing concentration in the atmosphere renders it as the determinant cause of global warming and the concomitant climate change. Therefore, control of CO<sub>2</sub> emissions is an urgent environmental need. Besides the direct efforts for partial -or even complete- replacement of carbon-based fuels with renewable energy sources, CO<sub>2</sub> capture and storage (CCS) and CO<sub>2</sub> utilization/recycling through its conversion to added-value products and fuels (e.g. methane, methanol) technologies are nowadays among the approaches that receive intense research and technological interest. Here we report on the CO<sub>2</sub> methanation efficiency of Rh, Ru and Ir, dispersed on a variety of mixed oxide supports with the characteristic of different oxygen storage capacity and mobility, namely  $\gamma$ -Al<sub>2</sub>O<sub>3</sub> (AL), Al<sub>2</sub>O<sub>3</sub>-CeO<sub>2</sub>-ZrO<sub>2</sub> (ACZ) and CeO<sub>2</sub>-ZrO<sub>2</sub> (CZ). The effect of the active metal nature as well as of the oxygen storage capacity (OSC) of the supporting material on CO<sub>2</sub> conversion efficiency and methane production selectivity are comparatively addressed. It has been found that the activity of the noble metals investigated under the titled reaction follows the same order Ir<Rh<Ru on all the supports used. However, for each active phase supported on different supports a significant but non monotonic influence of the OSC of the support on CO<sub>2</sub> methanation output characteristics occurred; the support with intermediate value of OSC was found to be optimal for promoting CO<sub>2</sub> methanation on Ir, Rh and Ru, independently of the nature of the active phase. Tuning this characteristic of the supporting materials we might lead to the design of more efficient CO<sub>2</sub> hydrogenation towards methane catalytic formulations.

**Acknowledgements:** The present work was co-funded by the European Union and Greek national funds through the Operational Program "Competitiveness, Entrepreneurship and Innovation", under the call "RESEARCH-CREATE-INNOVATE" (project code: T2EAK-00955).



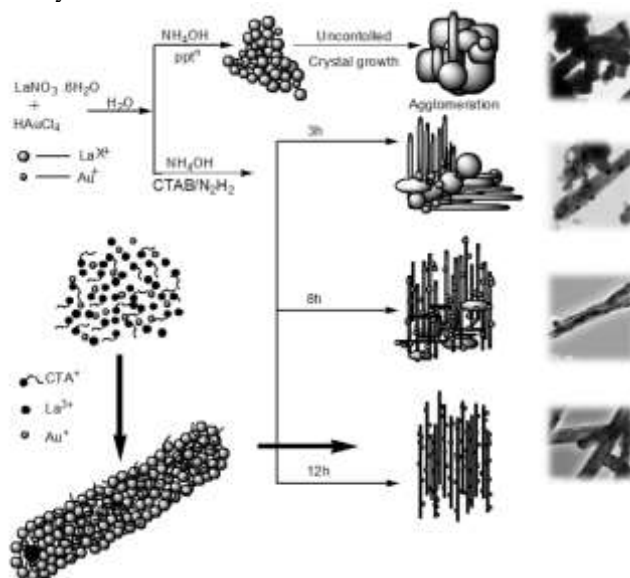
# Fabrication of Au nanoparticles supported on one-dimensional (1D) La<sub>2</sub>O<sub>3</sub> nanorods for selective Esterification of Methacrolein to Methyl Methacrylate with Molecular Oxygen

Bappi Paul<sup>1</sup>

<sup>1</sup>National Institute of Technology Nagaland Dimapur, Nagaland India 797103  
e-mail:bappipaulnits@gmail.com

**Keywords:** Esterification; Methyl methacrylate; Nanorod; High selectivity.

Here we demonstrate a simple and cost effective synthetic route for selective esterification of aldehydes with high productivity in the presence of molecular oxygen (O<sub>2</sub>) on gold supported lanthanum oxide (Au/La<sub>2</sub>O<sub>3</sub>) nanoparticle catalyst. Au nanoparticles with sizes of 2–7 nm supported on 1D La<sub>2</sub>O<sub>3</sub> nanorods with diameters between 20 and 50 nm was synthesized by room-temperature surfactant-assisted single-step preparation method. The as-synthesized catalyst was thoroughly characterized by powder XRD, SEM, HR-TEM, H<sub>2</sub>-TPR, XPS, TGA/DTA, FTIR, BET, EXAFS and UV-visible spectroscopy. This prepared nanostructured catalyst was found to be highly effective in liquid phase production of methyl methacrylate through direct oxidative esterification of methacrolein with high turnover number of ~1136. The effect of various reaction controlling parameters like reaction temperature, pressure and time of reaction were investigated and was studied. High methacrolein conversion of 89% and with high methyl methacrylate selectivity of 98% was attained without the use of any external additives. The synergistic effect between the surface Au NPs and La<sub>2</sub>O<sub>3</sub> nanorods plays an important role towards the activity of the catalyst.



## References

(1) Li, Y.; Zheng, Y.; Wang, L.; Fu, Z. Oxidative esterification of methacrolein to methyl methacrylate over supported gold catalysts prepared by colloid deposition. *ChemCatChem* **2017**, *9*, 1960–1968, DOI 10.1002/cctc.201601688.

## TiO<sub>2</sub>-ZrO<sub>2</sub> as supports of metal particles for the oxidation or reduction of pollutants in the Water

Gustavo Rangel-Porras<sup>1\*</sup>; Adán Quiroga-Almaguer<sup>1</sup>; Cristina Moncada-Sánchez<sup>2</sup>; Raúl Miranda-Avilés<sup>2</sup>; Mercedes Salazar-Hernández<sup>2</sup>; Aurelio Ramírez Hernández<sup>3</sup>.

<sup>1</sup>University of Guanajuato, Chemistry Department, Noria Alta s/n, Guanajuato, Guanajuato, México.

<sup>2</sup>University of Guanajuato, Mines, Metallurgy and Geology Department, Guanajuato, Guanajuato, México.

<sup>3</sup>University of Papaloapan, Chemistry Department, Tuxtepec, Oaxaca, México.

\*e-mail address: rangel\_porrasgustavo@hotmail.com

### Abstract:

Catalytic processes application have been one of the many methods proposed for the water treatment, were wide application had have in the oxidation of organic pollutants by ultraviolet or visible radiation assistance in presence of heterogeneous catalysts. The advantage of the solid as catalysts is due by the easier separation of the medium. In addition, these catalysts have been also used in reduction reaction of chemical species in waste water. One of the studied reactions is the reduction of nitroarene compounds which have been reported as pollutant in industrial water. Many solids are actually researched with the purpose to know the mechanisms over the surface and finding the better materials for these applications. In this work, we studied the application of TiO<sub>2</sub>-ZrO<sub>2</sub>-based mixed oxide modified with the impregnation of copper and silver particles for the reduction and oxidation of nitroarene compounds with the purpose to determine the most adequate application of these materials for the water treatment.

The catalytic materials were prepared by impregnation of copper and silver particles on TiO<sub>2</sub>-ZrO<sub>2</sub>. The support of mixed oxide was synthesized by sol-gel route from alcoxide precursors in ethanol medium. The catalysts were used in the reduction of nitroarenes in presence of sodium borohydride, following the reaction by ultraviolet-visible spectroscopy. In addition, the synthesized solids were also tested in the photooxidation of nitroarenes in presence of hydrogen peroxide.

The Figure 1 shows the spectra of nitrophenol during the reduction reaction to aminophenol. The TiO<sub>2</sub>-ZrO<sub>2</sub> materials did not show activity in the reduction of this compound; however, once the copper or silver were supported on the solid, the reaction was carried out in a short time. Slight differences were observed depending on the impregnation method as well as the metal supported.

On the other hand, the photooxidation of nitrophenol occurred in presence of the unmodified mixed oxide of TiO<sub>2</sub>-ZrO<sub>2</sub>; nevertheless, the activity changed with the copper and silver incorporation over the mixed oxide surface. The oxidation reaction depended on of pH of aquatic system.

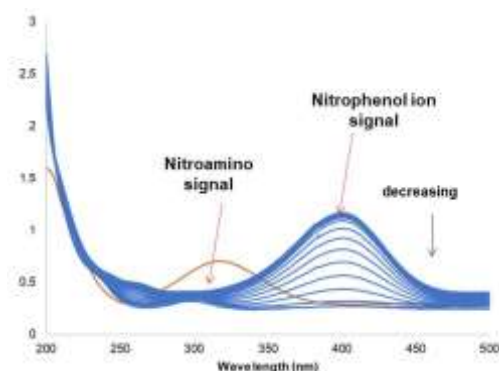


Figure 1. Uv-vis spectra of nitrophenol reduction.

The results showed interesting aspect about the difference in the catalytic activity of materials with copper and silver, as well as the contribution of the both metals in the bimetallic catalysts.

### Acknowledgements

The authors thank to the University of Guanajuato in Mexico for the facilities and financial supports for this research.

### References

1. C.N. Hamelinck, A.P.C. Faaij, H. Den Uil, H. Boerrigter, *Energy*, 29 1743 (2004).
2. R. Ash, R. M. Barrer, C.G. Pope, *Proc. R. Soc. London, Ser. A*, **271** 19 (1963).

## Sustainable N-doped basic carbon catalysts for the synthesis of nitrogen heterocycles

Marina Godino-Ojer<sup>1</sup>, Vanessa Ripoll Morales<sup>1</sup>, Luisa M. Pastrana-Martínez<sup>2</sup>, Francisco J. Maldonado-Hódar<sup>2</sup>, Elena Pérez-Mayoral<sup>3\*</sup>

<sup>1</sup>Facultad de Ciencias Experimentales, Universidad Francisco de Vitoria, UFV, Ctra. Pozuelo-Majadahonda km 1.800, 28223 Pozuelo de Alarcón, Madrid, Spain

<sup>2</sup>Departamento de Química Inorgánica, Facultad de Ciencias, Universidad de Granada, Avenida de Fuente Nueva, 18071 Granada, Spain

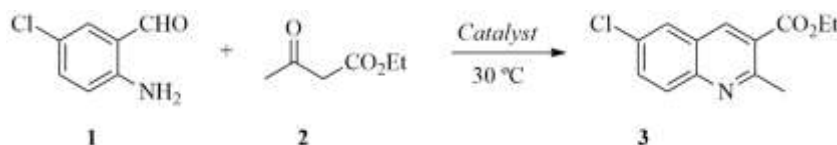
<sup>3</sup>Departamento de Química Inorgánica y Química Técnica, Universidad Nacional de Educación a Distancia, UNED, Urbanización Monte Rozas, Avenida Esparta s/n, Ctra. de Las Rozas al Escorial Km 5, 28232 Las Rozas-Madrid, Spain  
\*eperez@ccia.uned.es

The management of non-renewable plastic wastes has become one of the most concerning environmental issue that affects human health, wildlife, and water quality. Moreover, COVID-19 pandemic has dramatically impacted on plastic pollution due to the massive increasing of single-use personal protective equipment and disposable plastic packaging. Since the beginning of the pandemic, plastic use was increased by 40% for medical purposes and 17% for other applications across the world [1]. In the frame of the 2030 Agenda, reduce, re-use, and recycling waste plastic is a great challenge for societies to address the Sustainable Development Goals (SDGs). In this context, the development of eco-friendly green chemistry processes opens new opportunities to give a second life to plastic wastes. Specifically, the waste polyethylene terephthalate (PET) is an attractive raw material to design catalytic active carbon materials [2, 3].

Quinolines are nitrogen-containing heterocycles with biological activity, which make them interesting target compounds in medicine [4]. In addition, quinolines also present a wide range of applications in food, dye, materials, refineries and electronics industries. In the present work, it is presented an efficient methodology for green synthesis of quinolines by the Friedländer condensation catalyzed by N-doped basic-carbon materials derived from waste plastic.

Carbon materials were prepared based on plastic bottles made from up to 90% recycled PET [5]. Chemical activation using K<sub>2</sub>CO<sub>3</sub> and urea as N-compound was performed by adapting the experimental protocol previously reported by Arenillas et al. [6]. Four different homogeneous PET/K/Urea mixtures were prepared by mixing the components at varying the PET/K/urea ratio: 1:0.5:0, 1:0.5:0.25, 1:0.5:0.5 and 1:0.5:1, respectively. The composition and the textural characteristics of the samples were determined from N<sub>2</sub> adsorption/desorption isotherms, thermogravimetric and elemental analyses.

Catalytic performance was assessed in the Friedländer condensation reaction from 2-amino-5-chlorobenzaldehyde (0.5 mmol) and ethyl acetoacetate (5 mmol), under solvent-free conditions, at 30 °C, using 25 mg of catalyst. (scheme 1). The reactions were performed in a three-necked vessel of 10 mL volume under atmospheric pressure by using a multiexperiment work station StarFish (Radley's Discovery Technologies UK); each vessel was provided with a reflux condenser, thermometer, and magnetic stirrer. Evolution of the reaction was analyzed by collecting samples at different times 5, 10, 15, 30, 60, 90, and 120 min and diluted with dichloromethane (0.5 mL). Afterwards, the catalyst was separated by filtration, and the solvent evaporated in vacuo. Samples were analyzed by <sup>1</sup>H NMR spectroscopy using a Bruker AVANCE DPX-300 spectrometer (300 MHz for <sup>1</sup>H). <sup>1</sup>H chemical shifts (δ) in [D<sub>6</sub>]DMSO are referenced to internal tetramethylsilane.



Scheme 1. Synthesis of quinolines **3** from 2-amino-5-chlorobenzaldehyde **1** and ethyl acetoacetate **2** catalyzed by N-doped basic carbon catalysts

Carbon materials present low specific surface area ( $S_{\text{BET}}$ ) ranging 10-20 m<sup>2</sup>/g and increased N loading, depending on the used urea proportion, which increases from PET/K/Urea 1:0.5:0.25 to PET/K/Urea 1:0.5:1, as expected. The FTIR-ATR spectra of samples show characteristic bands of nitrogen at ca. 1650 cm<sup>-1</sup> and 1500 cm<sup>-1</sup> corresponding to C-N and C=N bonds. Moreover, both samples PET/K/Urea 1:0.5:0.25 to PET/K/Urea 1:0.5:0.5 show a broad band above 3000 cm<sup>-1</sup> associated to C-OH groups. Figure 1 shows the evolution of the conversion and selectivity values with the time.



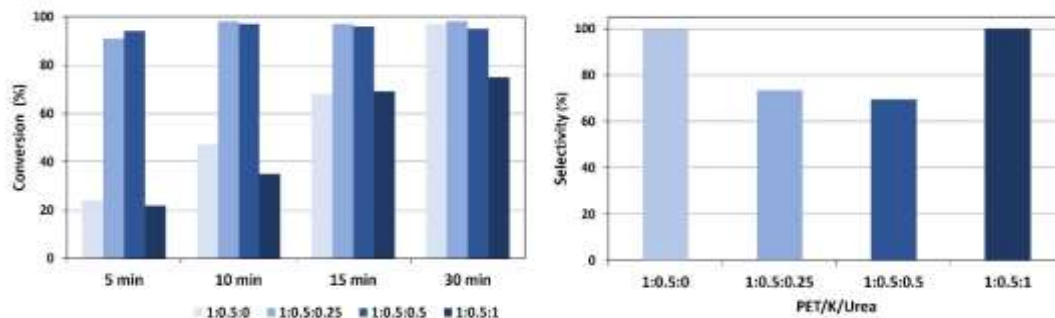


Figure 1. (a) Conversion vs time and (b) selectivity values for the synthesis of quinolines after 30 min, catalyzed by *N*-doped basic-carbon materials derived from waste plastic.

As it can be observed from Figure 1a, all investigated carbon catalysts were active in the reaction yielding high conversion values after only 30 min of reaction time. It is noteworthy that both catalysts PET/K/Urea 1:0.5:0 and PET/K/Urea 1:0.5:1, without and with the highest urea proportion, respectively, selectively led to quinoline **3** in 97 and 75% (30 min), respectively. At the shortest reaction time, differences regarding reactivity have been observed for both catalysts probably due to the distinct active phases and, therefore, the basicity of the samples.

On the other hand, PET/K/Urea 1:0.5:0.25 and PET/K/Urea 1:0.5:0.5 reached conversion values up to 90% after only 5 min, although with decreased selectivity (up to 77%) in comparison with PET/K/Urea 1:0.5:0 and PET/K/Urea 1:0.5:1, while observing the appearance of a stable intermediate compound whose NMR signals could be assigned to the corresponding aldol resulting of the first and rate-limiting step of the reaction (Figure 1b). In both cases, selectivity to **1** is increased with the time, being superior to 82% after 120 min in the presence of PET/K/Urea 1:0.5:0.5 sample, as a typical behavior of the processes taking place through reactions in cascade. These preliminary results strongly suggest that an optimal N content for the investigated catalysts is required. It is interesting to highlight that the obtained results show a great potential from a mechanistic point of view for the design of new strategies for the generation of future, efficient and environmentally sustainable carbon catalysts.

In summary, we report herein a new family of eco-friendly *N*-doped carbon catalysts derived from plastic wastes, easily prepared, highly efficient and selective for the quinoline synthesis under solvent-free and mild reaction conditions.

## Acknowledgements

This work has been supported by Francisco de Vitoria University (Project Ref. UFV2021-21) and by the Project ref. RTI2018-099224-B-I00, MICIN/ AEI/ 10. 13039/ 501100011033/FEDER “Una manera de hacer Europa”. L.M.P.-M. acknowledges to MICIN the RYC-2016-19347 contract.

## References

1. S.K. Mallick, M. Pramanik, B. Maity, P. Das, M. Sahana, *Sci. Total Environ.*, 796 148951 (2021).
2. M. Godino-Ojer, A.J. López-Peinado, R.M. Martín-Aranda, J. Przepiórski, E. Pérez-Mayoral, E. Soriano, *ChemCatChem*, **6-12** 3440 (2014).
3. D. González-Rodal, J. Przepiórski, A.J. López Peinado, E. Pérez-Mayoral, *Chem. Eng. J.*, **382** 122795 (2020).
4. A. Weyesa, E. Mulugeta, *RSC Adv.*, **10**, 20784 (2020).
5. <https://www.bezoya.es/compromiso-bezoya/>
6. A. Arenillas, F. Rubiera, J.B. Parra, C.O. Ania, J.J. Pis, *Appl. Surf. Sci.*, **252** 619 (2005).

# New Strategies for the Conversion of Biobased Furanics into High-value Added Synthons

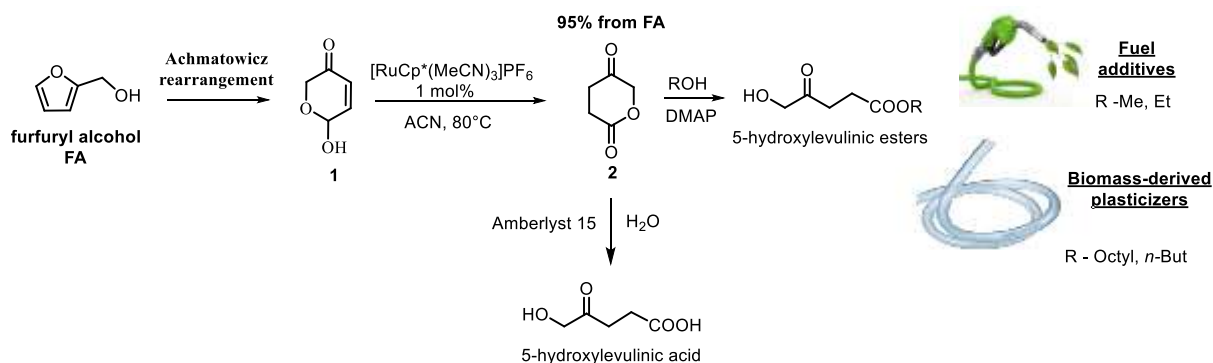
Ekaterina Vakareslka, Martin Ravutsov,<sup>1</sup> Miroslav Dangelov,<sup>1</sup> Maya Marinova<sup>1</sup> and Svilen Simeonov<sup>1\*</sup>

<sup>1</sup> Institute of Organic Chemistry with Centre of Phytochemistry, Bulgarian Academy of Sciences, Acad. G Bonchev str. B19, Bulgaria  
svilen@orgchm.bas.bg

Among other primary biorenewable building blocks, furfural is an important intermediate available from carbohydrates such as xylose and arabinose. Moreover, its production from lignocellulosic biomass is one of the few examples of an industrialized biorefinery process. [1] Furfuryl alcohol is a major derivative arising from the hydrogenation of furfural and finds many applications in the production of resins, fragrances and biofuels. A very interesting transformation of furfuryl alcohols was reported in the early 70s by Osman Achmatowicz who demonstrated the formation of 6-hydroxy-(2H)-pyran-3(6H)-one **1** from furfuryl alcohol (Scheme 1). Latter this reaction was named Achmatowicz rearrangement and proved to be an efficient synthetic tool that produce structurally complex derivatives from simple furans. This transformation holds its unique place in the synthesis of natural products and in the diversity oriented organic synthesis. [2] Recently our group showcased its potential as a key step in the biorefinery towards the production of biorenewable C5-alcohols.[3]

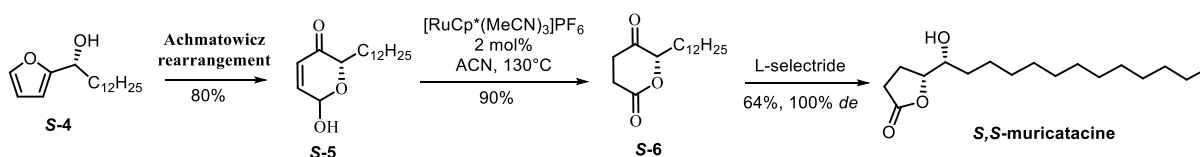
Encouraged by our previous investigations herein we report an efficient redox-neutral  $[\text{RuCp}^*(\text{CH}_3\text{CN})_3][\text{PF}_6]$  catalyzed allylic alcohol isomerization of Achmatowicz rearrangement products that provide access to structurally complex lactones from biogenic furans. Furthermore, we applied our findings in biorefinery and the synthesis of natural Acetogenins.

Initially we focused our efforts towards the synthesis of 5-hydroxylevulinic acid and its esters (Scheme 1) as a potential new class of biorenewable fuel additives. 5-hydroxylevulinic acid is a derivative of the biorenewable Levulinic acid whose esters attracted considerable interest due to their application as bio-fuels and fuel additives.[4] To our delight we achieved the synthesis of 5-hydroxylevulinic acid in very high yields via lactone **2**. Furthermore, by taking advantage of the natural reactivity of **2** we successfully completed the synthesis of various ester derivatives in good yields without extensive use of highly acidic catalysts required for preparation of the analogous Levulinic acid esters.



**Scheme 1.** Synthesis of 5-hydroxylevulinic acid and its esters

When considering the incorporation of the biorefinery into the chemical industry, apart from the synthesis of bulk chemical commodities a facile entry into high-value added functionalized products and synthons from renewable resources is required. To this end we used our findings in the synthesis of biologically active acetogenin muricatacine isolated from the seeds of *Annona muricata*. We started our synthesis from the reported asymmetric furfuryl alcohol *S*-4 and achieved the asymmetric synthesis of *S,S*-muricatacine in 3 steps wherein the key step was the diastereoselective tandem reduction/isomerization of intermediate *S*-6 to give the desired product in 100% *de* 9 (Scheme 2).



**Scheme 2.** Synthesis of *S,S*-muricatacine

In summary we reported the first Ru-catalyzed allylic alcohol isomerization of Achmatowicz rearrangement products. The process is characterized by low catalyst loadings, mild reaction conditions, high yields and is redox neutral thus avoiding the extensive use of oxidants or reductants. Our strategy was explored in the synthesis of a potentially new class of biorenewable fuel additives and biologically active natural Acetogenins.

### Acknowledgements

The authors acknowledge National Science Fund of Bulgaria (grant KP-06-OPR-01/2) and the National Scientific Program "VIHREN" (grant KP-06-DV-1).

The project leading to this application has received funding from the European Union's Horizon 2020 research and innovation programme under grant agreement no. 951996.

### References

1. J.-P. Lange, E. van der Heide, J. van Buijtenen, R. Price, *ChemSusChem*, **5**, 150 (2012)
2. A.K. Gosh, M. Brindisi, *RSC Adv.*, **6**, 111564 (2016)
3. S. P. Simeonov, M. A. Ravutsov and M. D. Mihovilovic, *ChemSusChem*, **12**, 2748 (2019)
4. W. Xu, X. Chen, H. Guo, H. Li, H. Zhang, L. Xiong, X. Chen *J. Chem. Technol. Biotechnol.*, **96**, 3009 (2021)
5. M. Rieser, J. Kozlowski, K. Wood, J. McLaughlin, *Tetrahedron Lett.*, **23**, 1137 (1991)

# Development of Transition-Metal-Free Lewis Acid-Initiated Double Arylation of Aldehyde: A Sustainable Approach Towards the Total Synthesis of Anti-breast Cancer Agent

Sanjay Singh<sup>1</sup> and Chinmoy Kumar Hazra<sup>1\*</sup>

<sup>1</sup>Department of Chemistry, Indian Institute of Technology, Delhi, India

\* chinmoy@chemistry.iitd.ac.in

With a wide variety of commercially available drugs having unsymmetrical di and triaryl methane pharmacophore, the synthesis of such molecules from common feedstock are considered a useful synthetic task. Though various metal-catalyzed cross-coupling methods are known to achieve the task, reported concerns with the use of such costly and toxic metal catalysts limit the usefulness of such protocols. [1-3] The title work describes a sustainable and robust metal-free double hydroarylation strategy for the synthesis of symmetrical /unsymmetrical diaryl- and triarylmethanes in excellent yields using Lambert salt (0.2-1.0 mol%) as the catalyst. Despite the anticipated challenges associated with controlling selective product formation, unsymmetrical diaryl- and triarylmethanes products are obtained unprecedentedly. A highly efficient gram-scale reaction has also been reported (TON for symmetrical product = 475 and for unsymmetrical product = 390). The synthetic utility of the methodology is demonstrated by the preparation of several unexplored diaryl- and triarylmethanes-based biological relevant molecules, such as arundine, vibrindole A, turbomycin B, anti-inflammatory agent. A total synthesis of phenanthrene based anti-breast cancer agent is also demonstrated in one pot. [1] Further, control experiments, Hammett analysis, HRMS and GC-MS studies reveal the reaction intermediates and reaction mechanism.[4]

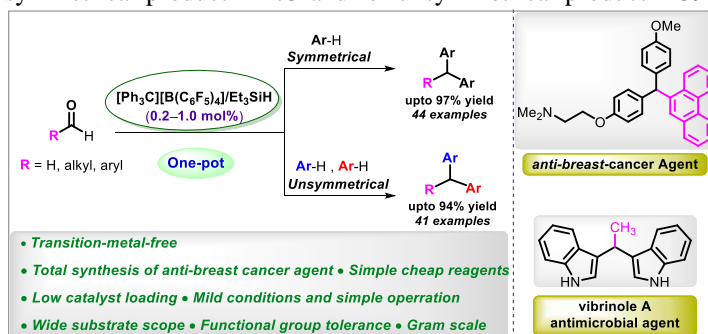


Figure 1. Lewis-acid initiated Brønsted acid-catalyzed Friedel-Crafts hydroarylation reactions of aldehydes.

The triarylmethane motif is a privileged structure in functional materials including organic dyes, fluorescent probes for bioimaging, and sensors for metal ions and demonstrates a huge range of biological activities. [5] The last couple of decades has witnessed an incredible development in the advancement of catalytic creation of diaryl- and triarylmethanes motifs. However, these protocols have one or more innate drawbacks, such as harsh conditions, hazardous and toxic chemicals, corrosive acids, expensive transition metal catalyst, pre-functionalized starting materials with relatively low yields and limited substrate scope, poor selectivity often being detrimental to the sustainable approach. Therefore, a sustainable protocol to synthesize both symmetrical as well as unsymmetrical diaryl- and triarylmethanes (TRAMs) in an atom economic fashion are highly desirable. Hence, we envisaged a unique methodology, whether reactions could be carried out between aldehydes and electron-rich arenes to give the corresponding diaryl- and triarylmethanes *via* transition-metal-free approach under ambient conditions. From our recent findings, we have established that it is indeed feasible and herein we present an attractive and sustainable alternative method for the synthesis of triarylmethane derivatives using *in-situ* generated Lambert salt **1a**. [6]

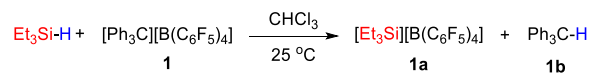


Figure 2. Si-H bond activation by using trityl salt (**1**).

Lambert salt **1a**, [Et<sub>3</sub>Si][B(C<sub>6</sub>F<sub>5</sub>)<sub>4</sub>] was generated (Figure 1) by the *In-situ* activation of Si-H bond of Et<sub>3</sub>SiH with trityl borate (**1**, [Ph<sub>3</sub>C][B(C<sub>6</sub>F<sub>5</sub>)<sub>4</sub>]) that was confirmed by the detection of **1b** by GC-MS data (Figure 2). Interestingly, Friedel-Crafts arylation of aldehydes selectively afforded either symmetrical or unsymmetrical di- and trisubstituted methanes depending on the reaction conditions. In a dry Schlenk tube, the catalyst [Ph<sub>3</sub>C][B(C<sub>6</sub>F<sub>5</sub>)<sub>4</sub>] (**1**, 1.00 mol%, 1.84 mg) was taken followed by N<sub>2</sub> purging using a balloon. Further, Et<sub>3</sub>SiH (3.0 mol%, 1.0 μl) was added to the above solution for *in-situ* generations of the [Et<sub>3</sub>Si][B(C<sub>6</sub>F<sub>5</sub>)<sub>4</sub>] (**1a**). After that the substrate aldehydes (0.2 mmol) was added to the solution followed by the addition of aromatic nucleophile (2.1 equiv., 0.42 mmol) for symmetrical products and the reaction mixture was charged with two different aryl nucleophiles (1.1 equiv.) each for unsymmetrical products. Aldehydes bearing various functional groups such as alkyl, halo, nitro, cyano, and, methoxy functional groups were fully converted to the corresponding polysubstituted methanes at 25 °C in excellent yields with TON = 475 for symmetrical and 390 for unsymmetrical products. It is worth mentioning that this protocol provides excellent results using only 0.2 to 1.0 mol% of catalyst, one of the lowest catalyst loading used till to date. Further, we have explored this methodology for the construction of several pharmaceutical molecules and a facile approach for the total synthesis of *anti-breast-cancer* agent. We have also performed some control experiments and Hammett correlation study to investigate the reaction mechanism and also by the analysis of HRMS and GC-MS data for the detection of the reaction intermediates. A possible catalytic

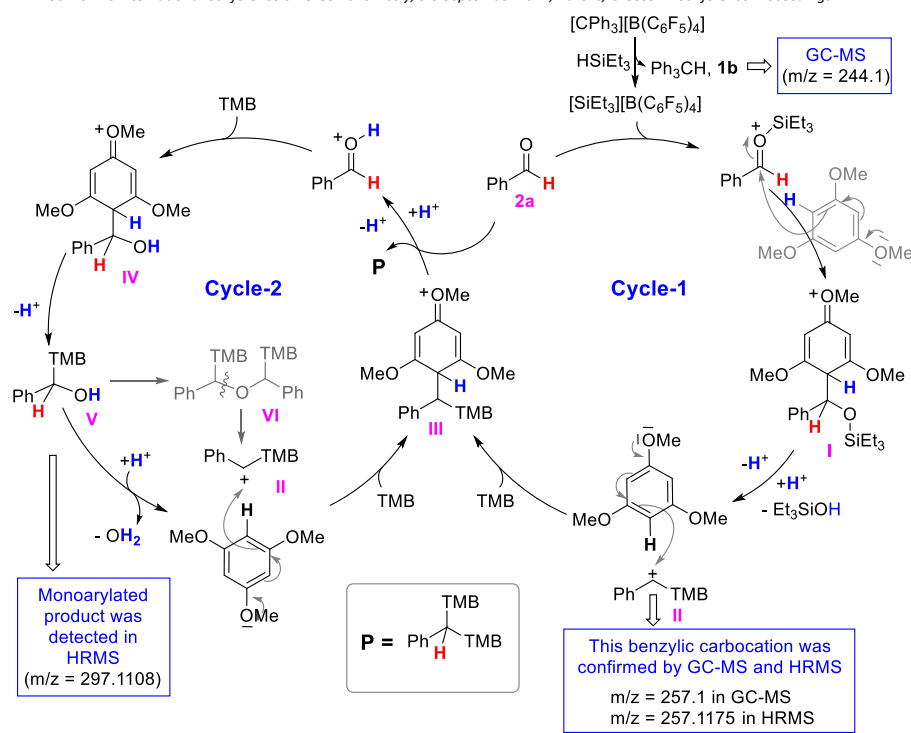


Figure 3. Catalytic cycle for the synthesis of triarylmethane. Counter anion [B(C<sub>6</sub>F<sub>5</sub>)<sub>4</sub>]<sup>-</sup> is omitted for better clarification. TMB = 1,3,5-Trimethoxybenzene.

cycle is proposed in which a stable carbocation is formed by the action of *in-situ* generated a three coordinate silylium ion as an initiator. [7] Based on these findings, the reaction was found to follow a Lewis acid-initiated and Brønsted acid-catalyzed pathway Figure 3.

We have described a variety of diaryl- and triarylmethanes (TRAMs) can be synthesized unprecedentedly by a one-pot transition-metal-free and sustainable methodology using as low as 0.2 mol% of catalyst, one of the lowest catalyst loading used till to date. This approach affords a convenient synthesis of symmetrical and unsymmetrical triarylmethanes/diarylmethanes starting from readily available aldehydes and electron-rich arenes. The synthetic utility of this approach towards the efficient synthesis of triarylmethanes/diarylmethanes-based unexplored medicinally active molecules initiated by *in-situ* generated Lambert salt. A highly efficient gram-scale reaction has also been reported (TON for symmetrical product = 475 and for unsymmetrical product = 390). The substrate scope (85 examples) for hydroarylation has been illustrated, and the reaction mechanism for the Friedel-Crafts reactions of aldehydes with control experiments and the Hammett correlation study has been discussed.

## Acknowledgement

This research is supported by the Science and Engineering Research Board (SERB), India (project SRG/2019/000213). Authors acknowledge the Central Research Facility, IIT Delhi, for instrument facilities.

## References

1. B. Wei, Q. Ren, T. Bein, P. Knochel, *Angew. Chem., Int. Ed.* **2021**, *60*, 10409–10414.
2. M. Nambo, C. M. Crudden, *Angew. Chem., Int. Ed.* **2014**, *53*, 742–746; *Angew. Chem.* **2014**, *126*, 761–765.
3. O. Allemann, S. Duttwyler, P. Romanato, K. K. Baldrige, J. S. Siegel, *Science* **2011**, *332*, 574–577.
4. (a) C. K. Hazra, J. Jeong, H. Kim, M.-H. Baik, S. Park, S. Chang, *Angew. Chem. Int. Ed.* **2018**, *57*, 2692; (b) M. M. Guru, P. R. Thorve, B. Maji, *J. Org. Chem.* **2020**, *85*, 806–819.
5. (a) D. F. Duxbury, *Chem. Rev.* **1993**, *93*, 381; (b) M. S. Shchepinov, V. A. Korshun, *Chem. Soc. Rev.* **2003**, *32*, 170; (c) G. C. Welch, R. R. San Juan, J. D. Masuda, D. W. Stephan, *Science* **2006**, *314*, 1124–1126.
6. (a) H. F. T. Klare, L. Albers, L. Süsse, S. Keess, T. Müller, M. Oestreich, *Chem. Rev.* **2021**, *121*, 5889–5985; (b) J. B. Lambert, J. A. McConnell, W. J. Schulz, Jr. *J. Am. Chem. Soc.* **1986**, *108*, 2482–2484; (c) Q. Wu, E. Irran, R. Müller, M. Kaupp, H. F. T. Klare, M. Oestreich, *Science* **2019**, *365*, 168–172.
7. S. Singh, R. Mahato, P. Sharma, N. Yadav, N. Vodnala, C. Kumar Hazra, *Chem. Eur. J.* **2022**, *28*, e202104545.

## Catalytic Activity of Cobalt Schiff-Base Complexes in Hydrosilylation of Alkynes

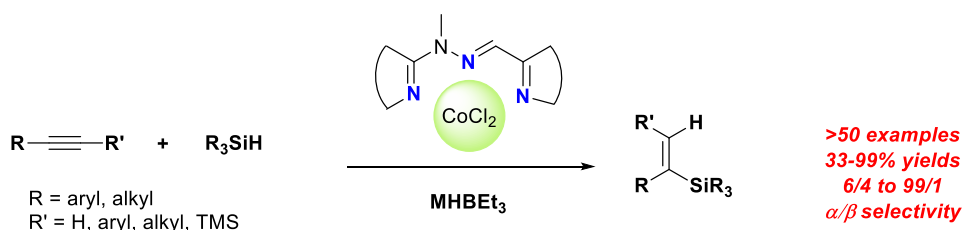
Skrodzki Maciej,<sup>1,2</sup> Ortega Garrido Victor,<sup>2,3</sup> Csáky Aurelio G.,<sup>3</sup> Patroniak Violetta,<sup>2</sup> Pawluć Piotr<sup>1,2</sup>

Faculty of Chemistry, Uniwersytetu Poznańskiego 8, 61-614 Poznań,  
Adam Mickiewicz University in Poznań, Poland

<sup>2</sup> Center for Advanced Technology, Uniwersytetu Poznańskiego 10,  
61-614 Poznań, Adam Mickiewicz University in Poznań, Poland

<sup>3</sup> Catedrático de Química Orgánica, Grupo de Síntesis Orgánica y Bioevaluación, Instituto Pluridisciplinar  
Universidad Complutense, Paseo de Juan XXIII, 1, 28040-Madrid  
e-mail: Maciej.skrodzki@amu.edu.pl

Hydrosilylation is one of the most important catalytic reactions used in a large industrial scale for the synthesis and modification of silicon compounds.<sup>[1]</sup> The commonly used catalysts in this process are platinum compounds, however, high price of platinum and impossibility of its reuse in technological processes, have prompted scientists to search for alternative cheaper solutions, based on other elements, but of similar effectiveness. From the environmental and economic point of view, compounds based on earth abundant metals are more desirable as catalysts than those based on noble metals. On the other hand, in the era of molecular-heavy and complex ligands, it is essential to develop a rational and sustainable coordination environment.



**Scheme 1:** Scope, general catalyst structure and yields of reactions

In the communication we present a bench-stable cobalt(II) complex, with 3N-donor socket-type benzimidazole-imine-2H-imidazole ligand as a precatalyst for regioselective hydrosilylation of terminal alkynes. Both aromatic and aliphatic alkynes could be effectively hydrosilylated with primary, secondary, and tertiary silane to give  $\alpha$ -vinylsilanes in high yields with excellent Markovnikov selectivity and extensive functional-group tolerance. Catalyst loading varies within 0.5 – 0.05 mol %, which is one of the most efficient reported so far in the literature on cobalt-catalyzed alkyne hydrosilylation.

**Acknowledgement:** The work was supported by grant no. POWR.03.02.00-00-I026/16 co-financed by the European Union through the European Social Fund under the Operational Program Knowledge Education Development.

### References

- [1] Hydrosilylation - A Comprehensive Review on Recent Advances (ed. B. Marciniec) Springer **2009**.
- [2] M. Skrodzki, V. Patroniak, P. Pawluć, *Org. Lett.* **2021**, 23, 3, 663–667.
- [3] M. Skrodzki, V. Ortega Garrido, A. G. Csáky, P. Pawluć, *J. Catal.*, **2022**, 411, 116-121.

## A study on the multicycle redox characteristic of La-Fe-oxide for chemical looping CO<sub>2</sub> conversion to CO

Hyun Seok Kang<sup>1</sup>, Seung Hun Baek<sup>2</sup>, Roosee Lee<sup>2</sup>, Jong Heon Chong<sup>2</sup>, Young Soo Ko<sup>3</sup>, Jung Min Sohn<sup>1, 2, \*</sup>

<sup>1</sup> Department of Energy Storage & Conversion Engineering, Jeonbuk National University, Jeonju, Jeollabuk-do, 54896, Republic of Korea

<sup>2</sup> Department of Mineral Resources & Energy Engineering, Jeonbuk National University, Jeonju, Jeollabuk-do, 54896, Republic of Korea

<sup>3</sup> Department of Chemical Engineering, Kongju National University, 1223-24 Cheonan-daero, Seobuk-gu, Cheonan 31080, Korea

\*jmsohn@jbnu.ac.kr

### Abstract:

Fossil fuel consumption has gradually risen on a global scale [1,2]. It has caused an increase in CO<sub>2</sub> emissions, which is accelerating global warming. Efforts to convert the emitted CO<sub>2</sub> into a usable gas are ongoing [3,4]. Reverse Water Gas Shift-Chemical Looping(RWGS-CL) has drawn the attention of researchers as a method to convert CO<sub>2</sub> into CO [5]. This study was investigated to determine the optimal La-Fe-oxide ratio for an oxygen carrier in the reverse water gas shift chemical looping.

La-Fe-oxides were synthesized with four different molar ratios (La<sub>2</sub>O<sub>3</sub>: Fe<sub>2</sub>O<sub>3</sub> = 1:5, 1:10, 1:15, 1:20) by solid state reaction. La<sub>2</sub>O<sub>3</sub> and Fe<sub>2</sub>O<sub>3</sub> were mixed and grounded well and then calcined. The furnace was heated up to 1200 °C at a rate of 5 °C/min and remained at 1200 °C for 3 h in the atmosphere. TGA, XRD, SEM, TPO-CO<sub>2</sub>, and GC analyses were performed.

It was observed that 1:10 La-Fe-oxide was most appropriate when using 15% CO<sub>2</sub>/N<sub>2</sub>, while 1:5 La-Fe-oxide was most suitable for 99.9% CO<sub>2</sub> when CO<sub>2</sub> was introduced as oxidizing agent instead of oxygen or air. In order to confirm the oxidation of oxide by CO<sub>2</sub>, the production of CO was investigated with GC. The GC analysis confirmed that CO production for 1:5 La-Fe-oxide was 9.3 mmol/g and 12.233 mmol/g for 1:10. It was claimed that La-Fe-oxide can be used, and CO<sub>2</sub> can be a promising oxidizing agent for reverse water gas shift chemical looping process.

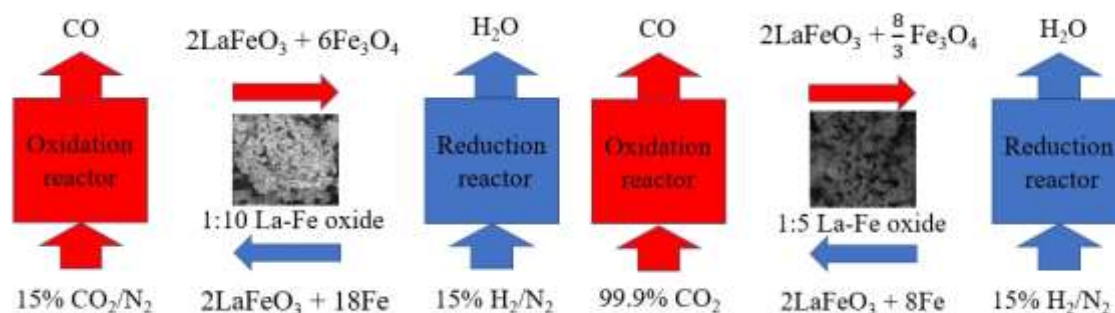


Figure 1. Schematic diagram of RWGS-CL with La-Fe mixed oxide

### Acknowledgements

This work was supported by the National Research Foundation of Korea(NRF) grant funded by the Korea government(MSIT) (No. 2021R1A2C2013129).

### References

1. J.H. Hwang, E.N. Son, R. Lee, S.H. Kim, J.I. Baek, H.J. Ryu, K.T. Lee, J.M. Sohn, *Catal. Today* **303** 13 (2018).
2. J.H. Hwang, K.-T. Lee, *J. Ceram. Process. Res.* **19** 372 (2018).
3. M. Reli, P. Huo, M. Šihor, N. Ambrozova, I. Troppová, L. Matejova, J. Lang, L. Svoboda, P. Kuśtrowski, M. Ritz, *J. Phys. Chem. A* **120** 8564 (2016).
4. W. Shin, S.H. Lee, J.W. Shin, S.P. Lee, Y. Kim, *J. Am. Chem. Soc.* **125** 14688 (2003).
5. M. González-Castaño, B. Dorneanu, H. Arellano-García, *Reaction Chemistry & Engineering*, **6** 954 (2021).

## Co-Ce supported SiO<sub>2</sub> for preferential CO oxidation in hydrogen rich gases -influence of the preparation method

Silviya Zh. Todorova<sup>1\*</sup>, Bozhidar K. Grahovski, Diana G. Filkova, Iliyana Hristova, Hristo G. Kolev, Daniela B. Karashanova<sup>2</sup>

<sup>1</sup> Institute of Catalysis, Bulgarian Academy of Sciences, Acad. G. Bonchev St., Bldg. 11, 1113 Sofia, Bulgaria

<sup>2</sup> Institute of Optical Materials and Technologies "Acad. Jordan Malinowski", Bulgarian Academy of Sciences, Acad. G. Bonchev St., Bldg. 109, 1113 Sofia, Bulgaria  
todorova@ic.bas.bg

It is well known that H<sub>2</sub>-polymer electrolyte membrane fuel cells (PEMFCs) are promising devices for the replacement of conventional electricity generators due to the expectations of a significantly higher efficiency, low emission of pollutants and low operating temperature. PEMFCs have been specifically targeted for automotive applications because of their high-power density and low operating temperatures. Since the PEMFCs are operated at relatively low temperatures (80°C), their Pt-anode catalyst is extremely sensitive to CO contaminant (1%) in reformed gases, which poisons the catalyst and diminishes the performance. The carbon monoxide concentration has to be reduced to below 10 ppm. Since the PROX reaction can operate at low temperatures and atmospheric pressure, it is a simple, efficient, and economic method for CO removal from hydrogen rich streams in comparison with other methods as membrane separation or pressure swing methods. Catalysts for PROX process should possess high CO conversion ability (about 99.9%) in order to achieve <10 ppm in the reaction mixture in wide temperature interval (50-150°C) and good resistance to the presence of CO<sub>2</sub> and H<sub>2</sub>O.

Catalysts so far proposed for the PROX process are based mainly on noble metals, such as Pt, Rh, and Ru, deposited on different supports with or without any promoters. Due to high price of precious metals, non-precious metal catalysts have been considered as a potential alternative for the CO PROX reaction. Co-based catalysts have shown promising catalytic performance for the CO PROX reaction. The main drawback of the bulk cobalt oxide appears to be the reduction to the metallic Co under the excess H<sub>2</sub>, which lead to deactivation [1]. Different studies indicate that a highly oxidized form of cobalt that exhibits strong interaction with a support allows CO activation that could lead to high activity for the preferential oxidation of CO in excess H<sub>2</sub> [2].

Two series of Co-Ce/SiO<sub>2</sub> catalysts were prepared by impregnation. The Ce was introduced first and after calcination the Co was deposited in the first series. In the second one the samples were obtained from a mixed aqueous solution of Co(NO<sub>3</sub>)<sub>2</sub>·6H<sub>2</sub>O and Ce(NO<sub>3</sub>)<sub>2</sub>·6H<sub>2</sub>O (samples denoted (xCo/yCe)/SiO<sub>2</sub>). All samples were calcined 3 h at 450 C. The as prepared samples were characterized by X-ray diffraction (XRD), BET, X-ray photoelectron spectroscopy (XPS), temperature programmed reduction (TPR), HRTEM.

Samples prepared by successive impregnation showed very low catalytic activity. Significantly higher activity was shown by the samples obtained by impregnation from a mixed solution of nitrates.

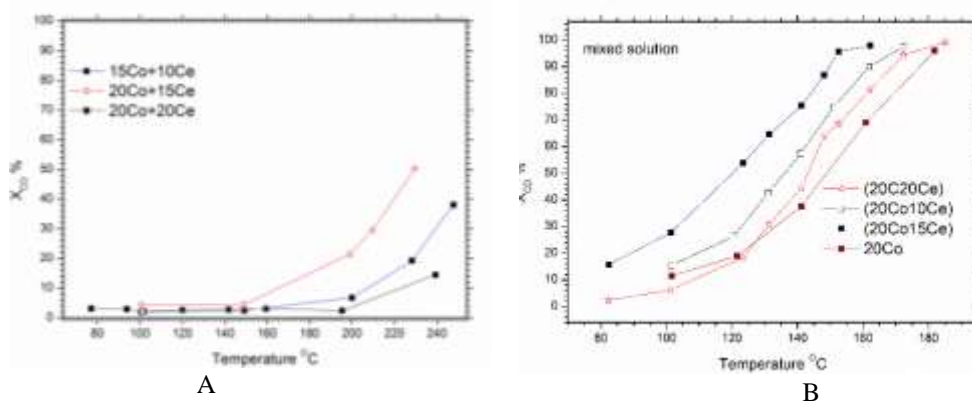


Figure 1. CO conversion to CO<sub>2</sub> on A) catalysts prepared by consecutive deposition of Ce and Co and B) catalysts prepared from mixed solution

According to XRD data, the two-component catalysts clearly exhibit two crystalline phases after calcinations at 450 C: Co<sub>3</sub>O<sub>4</sub> with spinel structure and CeO<sub>2</sub> with fluorite structure (data not presented here). No mixed phase between cobalt and cerium oxides was observed. The mean particles sizes of Co<sub>3</sub>O<sub>4</sub> for all bi-component samples have comparable mean particles size (about 35 nm), which means that the sequence of impregnation with Co and Ce salts has a little effect on Co<sub>3</sub>O<sub>4</sub> dispersion.



The presence of ceria in the two-component samples gives rise to an increase in the reduction temperature of cobalt oxide. These shifts to higher temperature are probably due to some supply of oxygen from  $\text{CeO}_2$ .

The analysis of studied fresh most active catalyst samples performed by high resolution TEM identified  $\text{CeO}_2$  cerianite, cubic,  $a = 5.41100 \text{ \AA}$ , (COD # 96-900-9009) and  $\text{Co}_3\text{O}_4$ , cubic,  $a = 8.16910 \text{ \AA}$ , (COD # 96-900-5901). analysis of different regions of  $(\text{CeCo})/\text{SiO}_2$  samples indicated homogeneous distribution of Co and Ce on the support. As can be seen from HRTEM cobalt oxides and  $\text{CeO}_2$  are homogeneously distributed on the support, and both oxide phases are in strong contact.

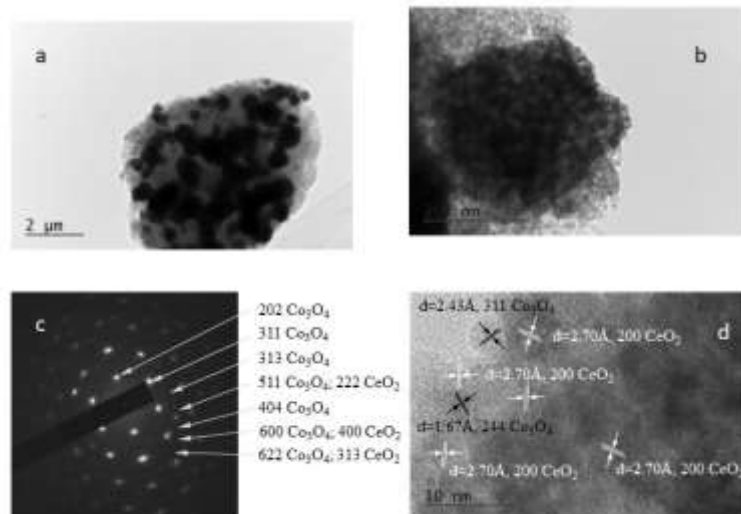


Figure 2. TEM image of  $(20\text{Co}15\text{Ce})/\text{SiO}_2$  sample (a) and (b), the corresponding SAED patterns with phase identification (c), HRTEM image of the marked in (b) area (d).

Catalytic tests showed that cerium modified the catalytic behavior of cobalt in preferential CO oxidation in hydrogen rich gases.

The homogeneous distribution of  $\text{Co}_3\text{O}_4$  and  $\text{CeO}_2$  and good contact between them are key factors controlling the activity since the main active phase in PROX process is cobalt oxide. Because of close interaction between  $\text{Co}_3\text{O}_4$  and  $\text{CeO}_2$  in the catalyst prepared with common solution of Co- and Ce nitrates, more surface oxygen species are provided to the cobalt oxide.

### Acknowledgements

The authors kindly acknowledge the financial support of project № BG05M2OP001-1.002-0014 „Center of competence HITMOBIL – Technologies and systems for generation, storage and consumption of clean energy”, funded by Operational Programme “Science and Education For Smart Growth” 2014-2020, co-funded by the EU from European Regional Development Fund

### References

1. Z. K Zhao, X.L. Lin, R.H. Jin, Y.T. Dai, G.R. Wang, *Cat. Sci. Technol.* **2**, 554 (2012).
2. K. Omata, Y. Kobayashi, M. Yamada, *Catal. Commun.* **6**, 563 (2005)

## Polyethylene Biodegradation by *Bacillus* Species from a Landfill Site

Seung-Do Yun<sup>1</sup>, Min-Ju Seo<sup>2</sup> and Soo-Jin Yeom<sup>1,2\*</sup>

<sup>1</sup> School of Biological Sciences and Biotechnology, Graduate School, Chonnam National University, Yongbong-ro 77, Gwangju 61186, South Korea

<sup>2</sup> School of Biological Sciences and Technology, Chonnam National University, Yongbong-ro 77, Gwangju 61186, South Korea

\*soojin258@jnu.ac.kr

Polyethylene (PE) is the most abundant synthetic polymer that has been indispensable in all aspects of modern life because of its various applications [1]. The PE is extremely recalcitrant to natural biodegradation processes, resulting in massive accumulation in the environment [2]. Therefore, decomposition of PE using microorganisms should be investigated for development of environment-friendly process. To obtain potential microorganisms for PE degradation, we took a landfill sample and screened. *Bacillus* species successfully isolated from a landfill that specifically enriched in non-carbonaceous nutrient medium, with PE powder as the only carbon source. Among the screened *Bacillus* species, *B. thuringiensis* JNU01 has the highest cell growth levels in media with PE powder, and microbe treated PE has new chemical functional groups such as hydroxyl, carboxyl, and amide groups in the inert hydrocarbon. *B. thuringiensis* JNU01 treated PE film showed defective external sites and relatively high hydrophilicity by scanning electron microscope and contact angle analysis. Moreover, obtained PE powder after cultivation with *B. thuringiensis* JNU01 were analyzed by GC-MS. Interestingly, various alkane derivatives as potential renewable resources were detected, indicating that *B. thuringiensis* JNU01 biodegrades PE and provides significant insights into the discovery of novel functions of *Bacillus* species as well as their potential as the PE decomposers.

### Acknowledgements

This work was supported by the National Research Foundation of Korea (NRF) grant funded by the Korea government (MSIT) (No. 2020R1C1C1004178, 2022R1C1C2003774).

### References

1. Harshvardhan, K. and B. Jha, *Polymers (Basel)*. 12(1), 123 (2020).
2. Chamas, A. *et al.*, *ACS Sustainable Chemistry & Engineering*. 8(9), 3494 (2020).

## Biodegradation of polystyrene by bacteria from the soil in common environments

Ye-Bin Kim<sup>1</sup>, Min-Ju Seo<sup>1</sup> and Soo-Jin Yeom<sup>1,2\*</sup>

<sup>1</sup> School of Biological Sciences and Biotechnology, Graduate School, Chonnam National University, Yongbong-ro 77, Gwangju 61186, South Korea

<sup>2</sup> School of Biological Sciences and Technology, Chonnam National University, Yongbong-ro 77, Gwangju 61186, South Korea

\*soojin258@jnu.ac.kr

Plastics, synthetic organic polymers, have been indiscriminately used because of its some advantages such as inexpensive, lightweight, strong, durable, and corrosion-resistant materials with high thermal and electrical insulation properties [1]. However, plastics cause environmental pollution. Among the plastics, polystyrene (PS), the sixth type of commercially distributed plastic, is difficult to biodegrade due to its unique chemical structure that comprises phenyl moieties attached to long linear alkanes [2]. In this study, we investigated the biodegradation of PS by mesophilic bacterial cultures obtained from various soils in common environments. Two novel strains, *Pseudomonas lini* JNU01 and *Acinetobacter johnsonii* JNU01, were specifically enriched in non-carbonaceous nutrient medium, with PS as the only carbon source. Their growth rates after culturing in basal media increased more than 3-fold in the presence of PS. To confirm changes of chemical structures in PS, obtained PS samples after cultivation with *P. lini* JNU01 and *A. johnsonii* JNU01 were analyzed by fourier transform infrared spectroscopy. Obtained PS showed an increase in the amount of oxidized PS indicating that *P. lini* JNU01 and *A. johnsonii* JNU01 have some biocatalysts for biodegradation of PS. Moreover, field emission scanning electron microscopy analysis confirmed PS biodegradation by biofilms of the screened microbes. Water contact angle measurement additionally offered insights into the increased hydrophilic characteristics of PS films. Furthermore, *A. johnsonii* JNU01 showed higher PS degradation activity than *P. lini* JNU01. Thus, we chose *A. johnsonii* JNU01 for candidate to find a potential enzyme for PS degradation using bioinformatics and transcriptional analyses. We found alkane-1-monooxygenase (AlkB) in *A. johnsonii* to be involved in PS biodegradation, which was confirmed by the hydroxylation of PS using recombinant AlkB. These results provide significant insights into the discovery of novel functions of *Pseudomonas* sp. and *Acinetobacter* sp., as well as their potential as PS decomposers.

### Acknowledgements

This work was supported by the National Research Foundation of Korea (NRF) grant funded by the Korea government (MSIT) (No. 2020R1C1C1004178, 2022R1C1C2003774).

### References

1. Thompson, R.C., et al., *Philos Trans R Soc Lond B Biol Sci*, 2009. **364**(1526).
2. Ho, B.T., T.K. Roberts, and S. Lucas, *Critical Reviews in Biotechnology*, 2018. **38**(2).

## Catalytic oxidation of propane and *n*-hexane over cobalt loaded hierarchical ZSM-5 zeolite

Bozhidar K. Grahovski<sup>1</sup>, Ralitsa G. Velinova<sup>2</sup>, Iliyana D. Yordanova<sup>1\*</sup>, Hristo G. Kolev<sup>1</sup>, Anton B. Naydenov<sup>2</sup>, Silviya Zh. Todorova<sup>1</sup>

<sup>1</sup> Institute of Catalysis, Bulgarian Academy of Sciences, Acad. G. Bonchev St., Bldg. 11, 1113 Sofia, Bulgaria

<sup>2</sup> Institute of General and Inorganic Chemistry, Bulgarian Academy of Sciences, Acad. G. Bonchev St., Bldg. 11, 1113 Sofia, Bulgaria

\*e-mail: yordanova@ic.bas.bg

In recent years, the attention of scientists has focused on the use of zeolites as catalysts supports due to their thermal and acid stability and moisture resistance. They have high specific surface area which is a prerequisite for the creation of active catalytic systems. Metals and metal oxides can be deposited on them as highly dispersed nanoparticles and thus create active catalytic systems in which a large number of active centers are accessible to the reagents in the catalytic processes. One of the best adsorbents and supports for catalytic systems used for the degradation of VOCs are zeolite aluminosilicates, thanks to their adjustable surface properties, their controllable hydrophobicity and the ability to deposit metals and metal oxides.

Zeolite ZSM-5 is a well-known high silicon crystalline aluminosilicate with wide area of applications as catalyst and sorbent. Although belonging to the group of medium porous zeolites, ZSM-5 has a relatively high resistance to coke formation. Due to the combination of high hydrothermal structural stability and large surface mass to volume ratio, this zeolite is widely used in reactions that rely on chemical and physical interactions occurring on the crystalline surface [1, 2]. During catalytic reactions on porous materials an often occurring serious problem is the constrained diffusion of the reactants and products, and relatively rapid deactivation of the zeolite catalyst because of limited access to the active sites due to the formation of coke. There are two approaches to solve these problems: 1) by drastically reducing the crystallite size, which increases the active surface area of the material and 2) through post-synthetic treatments forming additional micro- and/or meso-pores on the crystal surface to improve access to the active sites [3]. The treatment of the zeolites with HF acid in combination with NH<sub>4</sub>F is an easily controllable chemical approach to creating hierarchical zeolites. In our previous investigations we found that cobalt supported on the zeolite ZSM-5 with different Si/Al ratios 100, 40 and 23 is promising catalysts for the reaction of complete oxidation of propane, butane and *n*-hexane.

In this work we present the VOC oxidation of cobalt modified ZSM-5 after fluoride etching post-synthetic treatment. Post-synthetic treatments were performed with hydrofluoric acid in combination with ammonium fluoride to form some additional porosity without changing considerably the Si/Al ratio of the zeolite framework. In our previous investigations we found that cobalt supported on the zeolite ZSM-5 with different Si/Al ratios 100, 40 and 23 is promising catalysts for the reaction of complete oxidation of propane, butane and *n*-hexane.

In this work we present the VOC oxidation of cobalt modified ZSM-5 after fluoride etching post-synthetic treatment. Post-synthetic treatments were performed with hydrofluoric acid in combination with ammonium fluoride to form some additional porosity without changing considerably the Si/Al ratio of the zeolite framework.

The starting ZSM-5 materials having different Si/Al ratios were kindly provided by SUD-CHEMIE AG (H-MFI-90, Si/Al = 50) and ALSIPENTA zeolite GmbH (SH-27, Si/Al = 23), respectively. The ZSM-5 sample of Si/Al = 40 ratio was synthesized according to [4]. The ZSM-5 zeolites were modified by etching using an aqueous solution of 0,25M HF hydrofluoric acid and ammonium fluoride. Cobalt was incorporated from Co(CH<sub>3</sub>COO)<sub>2</sub>·4H<sub>2</sub>O by incipient wetness impregnation technique followed by drying and calcinations. The obtained materials were characterized by BET, XRD, UV-vis, XPS, TPR and tested in complete oxidation of *n*-hexane and propane.

The X-ray pattern for the starting sample contains all signals corresponding to the ZSM-5 phase with a high degree of crystallinity. According to the XRD data the crystallinity and structural of the acidic treated zeolite show that the characteristics are preserved in hierarchical samples. No cobalt oxide diffraction lines in the XRD spectra of Co modified samples were observed, indicating fine dispersion of cobalt oxides. The results of nitrogen adsorption/desorption isotherms were used to obtain the specific surface areas and pore sizes of the initial and modified catalysts (Table 1).

Table 1. Texture parameters of ZSM-5 before and after acidic treatment

Sample	S <sub>BET</sub> m <sup>2</sup> g <sup>-1</sup>		Total pore volume, cm <sup>3</sup> g <sup>-1</sup>		Average pore diameter, nm		V <sub>micro</sub> cm <sup>3</sup> g <sup>-1</sup>	
	Starting zeolite	After treatment	Starting zeolite	After treatment	Starting zeolite	After treatment	Starting zeolite	After treatment
Si/Al=23	349	340	0,20	0,22	2,34	3,00	0,16	0,14
Si/Al=40	331	391	0,25	0,24	2,98	3,00	0,16	0,15
Si/Al=50	444	422	0,34	0,51	3,10	5,60	0,14	0,14

After the etching process, changes in the textural properties (specific surface area and pore volume) of the treated sample were observed. As a result of the applied acidic treatment, decreasing of the specific surface area and micropore volume was observed, while the total volume of the pores increased, and this is more noticeable for the sample Si/Al=50. The formation of different cobalt oxide species would be suggested from TPR data: extra framework Co<sub>3</sub>O<sub>4</sub>; CoO strongly interacting with zeolite framework and framework cobalt or some other types of cobalt silicate (Fig. 1a). UV-vis spectra give additional information about cobalt species present in Co-ZSM-5 catalyst (Fig. 1b). The presence of Co<sub>3</sub>O<sub>4</sub> in all investigated samples is evidenced by the appearance of bands at 408 nm in and 770 nm (Figure 1b). Bands at 510, 593 and 650 nm are ascribed to the Co<sup>2+</sup> ions located at the intersections of straight and sinusoidal channels ( $\beta$  site).

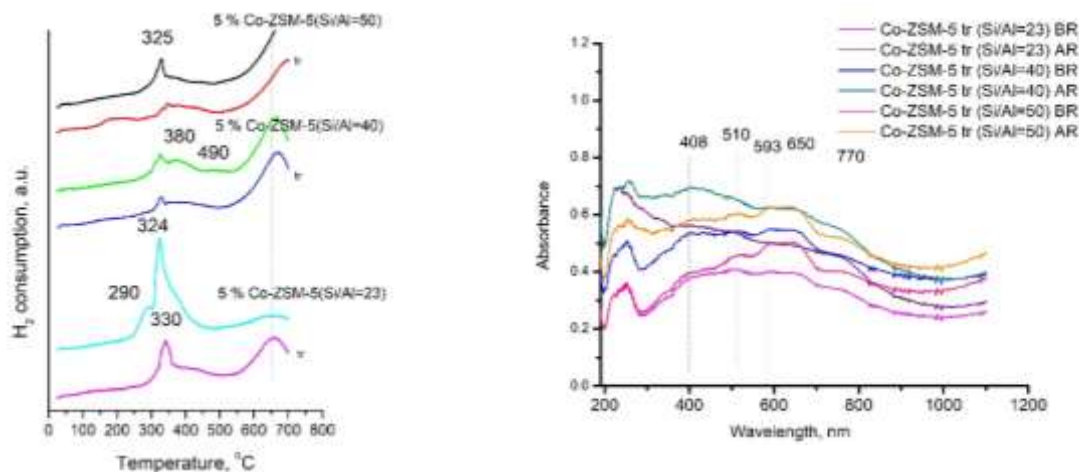
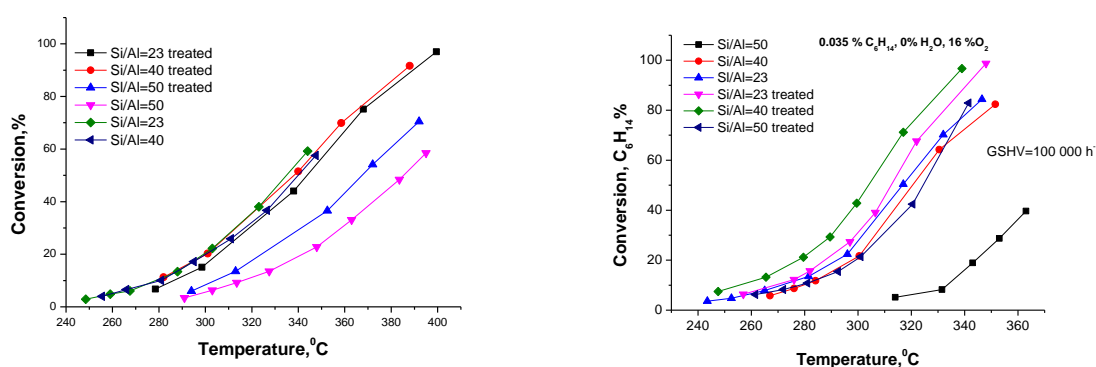


Figure 1. a) TPR data of studied samples; b) UV-vis of Co-ZSM-5 before and after reaction



Catalytic tests of complete oxidation of propane and n-hexane were carried out on samples of Co-ZSM-5 with different ratios of Si/Al=23, Si/Al=40 and Si/Al=50 after treatment with a hydrofluoric acid buffer solution and ammonium fluoride. The data are presented in Figure 2a, b.

The results show that the treatment with a buffer solution of hydrofluoric acid and ammonium fluoride does not affect the catalytic activity in the case of propane for the samples with the ratio Si/Al=23 and Si/Al=40, in contrast to the sample Si/Al=50 where an improvement in activity is observed. The studies regarding n-hexane show that

the treatment improves the catalytic activity in all the investigated cases, and the most noticeable effect is observed in the sample with a ratio of Si/Al=50. The sample with Si/Al=50 ratio showed good thermal stability.

### Acknowledgements

The authors express their gratitude to the National Science Fund of Bulgaria for the financial support under the Contract KII-06-H49/4.

### References

1. H. Sato, N. Ishii, K. Hirose, S. Nakamura, in: *Studies in Surface Science and Catalysis*, A.I. Y. Murakami, J.W. Ward (Eds.), Elsevier 755 (1986).
2. Q. Zhou, Y.-Z. Wang, C. Tang, Y.-H. Zhang, *Polymer Degradation and Stability* **80** 23 (2003).
3. T. Todorova, Yu. Kalvachev, H. Lazarova, M. Popova, *Compt. rend. Acad. bulg. Sci.*, **69** (10) 1283 (2016).
4. T Hardenberg, L Martens, P Mesman, H Muller, C Nicolaidis, *Zeolites* **12**: 685(1992).

## Catalytic hydrodeoxygenation (HDO) of lignin-derived phenolic compounds over zeolite-supported nickel catalysts

Foteini F. Zormpa<sup>1</sup>, Antigoni G. Margellou<sup>1</sup>, Vasileia-Loukia Yfanti<sup>1,2</sup> and Konstantinos S. Triantafyllidis<sup>1,3\*</sup>

<sup>1</sup>Department of Chemistry, Aristotle University of Thessaloniki (AUTH), Thessaloniki, Greece

<sup>1</sup>Department of Chemical Engineering, Aristotle University of Thessaloniki (AUTH), Thessaloniki, Greece

<sup>3</sup>Center for Interdisciplinary Research and Innovation (CIRI), AUTH, Thessaloniki, Greece

\*Corresponding author: [ktrianta@chem.auth.gr](mailto:ktrianta@chem.auth.gr)

The upcoming depletion of fossil fuels has already resulted in the need of finding alternative feedstocks for fuel and chemicals production [1]. Lignin is one of the three main structural components of lignocellulosic biomass and is considered as the most abundant natural source of aromatic/phenolic compounds. According to different degradation processes, such as pyrolysis, high value-added bio-oils enriched in alkoxy/alkyl-phenols can be obtained from lignin [2]. Lignin derived bio-oils can be further upgraded to cycloalkanes via down-stream hydrodeoxygenation (HDO) and can be utilized as drop-in jet bio-fuels [3].

This work focuses on the catalytic HDO of lignin/phenolic monomers, derived via fast pyrolysis, by the use of zeolite-supported nickel catalysts under mild conditions (T=140-250 °C, 0.5-2 h, 0-70 bar H<sub>2</sub>). In order to identify the reaction mechanisms involved, model aromatic/phenolic compounds with different side chains and functional groups were studied, i.e. alkoxy/alkyl phenols, alkoxy-aromatics, aromatic aldehydes, etc. Nickel catalysts supported on Beta and ZSM-5 zeolites led to high conversion (>95%) and enhanced cyclohexane yields. The activity and the deoxygenation capacity can be correlated with the acidic and the micro/mesoporous properties of the zeolitic supports as well as the complexity of the model compound.

### Acknowledgements

The support via EU-Horizon 2020 and internal funds is gratefully acknowledged.

### References

1. H. Li, A. Riisager, S. Saravanamurugan, A. Pandey, R.S. Sangwan, S. Yang, R. Luque, ACS Catal., 8(1) 148-187 (2018).
2. A.G. Margellou, P.A. Lazaridis, I.D. Charisteidis, C.K. Nitsos, C.P. Pappa, A.P. Fotopoulos, K.S. Triantafyllidis, *Appl. Catal. A: Gen.*, **623** 118298 (2021).
3. F. Cheng, C.E. Brewer, *Renew. Sust. Energ. Rev.*, **72** 673-722 (2017).

# CO<sub>2</sub> utilization



# The effect of reaction conditions on CO<sub>2</sub> Hydrogenation with Cu/ZnO/SBA-15 catalyst

Zane Abelniece<sup>1</sup>

<sup>1</sup>Riga Technical University, Institute of Applied Chemistry, Paula Valdena Str. 3, Riga LV-1048, Latvia

\*zane.abelniece@rtu.lv

## Introduction

As the amount of CO<sub>2</sub> in the atmosphere increases, the negative effects on the environment also significantly increase. CO<sub>2</sub> catalytic conversion is effective way to minimize emissions. CO<sub>2</sub> combined with hydrogen from renewable sources, can be used for the production of methanol, what can be used as renewable fuel or as an intermediate to produce valuable chemicals [1].

While research for developing more effective catalyst continues, Cu-based catalysts has been considered as most active for methanol production. In our previous studies Cu/ZnO/SBA-15 catalyst showed good activity and selectivity for methanol producing.

In this work the effect of reaction conditions - H<sub>2</sub> to CO<sub>2</sub> molar ratio and reaction pressure- on CO<sub>2</sub> hydrogenation reaction in a fixed-bed tubular micro-activity reactor (Microactivity-Effi, PID Eng&Tech S.L.) at 250 °C has been studied.

## Materials and Methods

### Catalyst preparation

The preparation of catalysts: An aqueous solution (15 ml) of appropriate amount of Cu(NO<sub>3</sub>)<sub>2</sub>·2.5H<sub>2</sub>O and Zn(NO<sub>3</sub>)<sub>2</sub>·6H<sub>2</sub>O was prepared and then an aqueous solution (15 ml) of glycine was added to the first to obtain the “impregnation solution” as in [2]. The “impregnation solution” was added dropwise to of SBA-15 (ACS Material LLC) and water was allowed to evaporate into the air by stirring at the room temperature. The viscous blue gel obtained after evaporation was treated for 15 min in an ultrasonic bath, and then calcined at 350 °C for 4 h. Metal loadings of Cu and Zn calculated were 30 wt.% and 5 wt.%, respectively.

### Catalyst testing

The CO<sub>2</sub> hydrogenation was carried out in a Microactivity-Effi, PID Eng&Tech S.L. fixed-bed tubular micro-activity reactor. The catalyst mass for reaction used was 0.2 g, and it was diluted with quartz until volume of 3 ml. Reaction temperature was 250 °C and time on the stream 50 hours. A flow of CO<sub>2</sub> and N<sub>2</sub> was 10 mL min<sup>-1</sup> and H<sub>2</sub> was 40 mL min<sup>-1</sup> or 30 mL min<sup>-1</sup>, respectively. The synthesized catalysts were reduced before the reaction under a flow of H<sub>2</sub> (50 mL min<sup>-1</sup>) at 300 °C temperature for 4 h.

The effluent gas from the reactor passed through cold trap (T=5 °C) to condense the products. The reactor outlet gases were analyzed by on-line gas chromatograph (Shimadzu Nexis GC-2030) equipped with four columns, flame ionization detector and thermal conductivity detector. Helium was used as a carrier gas. 250 μL of sample was injected using sample loop. Multicolumn chromatography system consisting of two Restek Porapak Q 80/100 (6 ft, 2 mmID) and Restek Molesieve 5A 60/80 (6 ft, 2 mmID) columns and thermal conductivity detector was used for the analysis of gases.

The space time yield of methanol (STY) is calculated as follows:

$$STY_{CH_3OH} = (m_{prod} \cdot X_{CH_3OH}) / (t \cdot m_{cat}) \quad (1)$$

where m<sub>prod</sub> represents the total mass of methanol and water formed (g), X<sub>CH<sub>3</sub>OH</sub> is the mass fraction of methanol, t indicates the time of reaction (h), m is the mass of the catalyst (g). Methanol content in the condensed products were determined by IR spectra, recorded using UATR Accessory on Perkin Elmer equipment and methanol content were measured at 1015 cm<sup>-1</sup> (baseline 975-1055 cm<sup>-1</sup>) based on calibration measurements.

## Results and Conclusion

As can be seen in Figure 1, increase of reaction pressure enlarged STY of reaction in the range of studied pressure. Also higher H<sub>2</sub> to CO<sub>2</sub> molar ratio allowed to obtain higher amount of methanol. By using H<sub>2</sub> to CO<sub>2</sub> molar ratio 4:1 and 20 bar pressure at 250 °C temperature, the CO<sub>2</sub> conversion of reaction increased reaching 124.5 mg CH<sub>3</sub>OH h<sup>-1</sup>gcat<sup>-1</sup>.

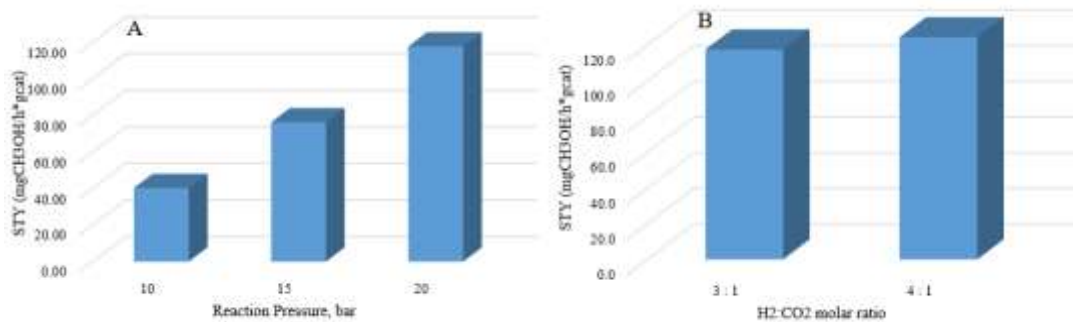


Figure 1. Catalytic activity reported as STY A. Influence of reaction pressure at H<sub>2</sub>:CO<sub>2</sub> molar ratio 3:1; B. Influence of H<sub>2</sub>:CO<sub>2</sub> molar ratio at 20 bar reaction pressure.

## Acknowledgements

This work has been supported by the European Regional Development Fund within the Activity 1.1.1.2 “Post-doctoral Research Aid” of the Specific Aid Objective 1.1.1 “To increase the research and innovative capacity of scientific institutions of Latvia and the ability to attract external financing, investing in human resources and infrastructure” of the Operational Programme “Growth and Employment” (No.1.1.1.2/VIAA/3/19/396).

## References

- [1] I. U. Din, M. S. Shaharun, M. A. Alotaibi, A. I. Alharthi, A. Naeem, *J. CO<sub>2</sub> Util.*, **34**, 20–33, (2019).
- [2] M. Mureddu, F. Ferrara, A. Pettinau, *Appl. Catal. B Environ.*, **258**, 117941 (2019).

**Cu||Ag tandem-operation for highly efficient CO<sub>2</sub> conversion toward C<sub>2</sub>-3 products**Joo Yeon Kim<sup>1</sup> and Hyun S. Ahn<sup>1\*</sup><sup>1</sup>Department of Chemistry, YONSEI University, Seoul, 50 Yonsei-ro, Seodaemun-gu, Seoul, Republic of Korea

\*ahnhs@yonsei.ac.kr

## Abstract text:

To overcome hurdles left in electrochemical CO<sub>2</sub> conversion including complex reaction mechanism and competitive hydrogen evolution reaction (HER), we introduced Cu-Ag bi-potentiostatic system controlling each bias independently. Considering that the generally adopted Cu-Ag bimetallic systems have failed to elucidate the interplay between Cu-Ag (electrodes) was nearly impossible, the research suggested a custom-made flow cell enabling fine control of various reaction circumstances. We suggested significant clues for enlightening C<sub>2</sub><sup>+</sup>-related interplay mechanism. Interestingly, we have succeeded in not merely demonstrating the sequential interplay between Cu and Ag, but achieving a 67% of C<sub>2</sub><sup>+</sup> selectivity even including a considerable amount of 1-PrOH generation at 6.5%.

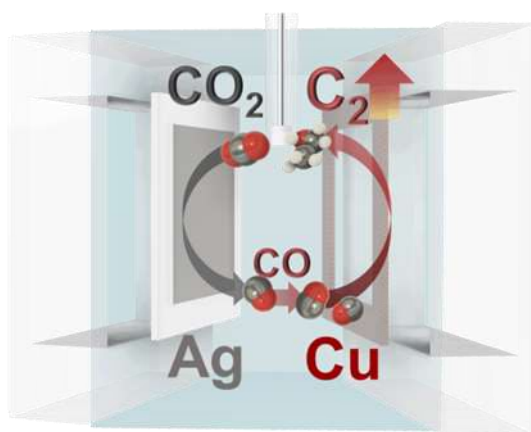


Figure 1. Schematic illustration of the experiment

In addition to achieving successful CO interplay investigation, we strive to elucidate these sequential reactions by varying multi-components; array, form, gap, metal species, and applied potential of the electrodes. Also, we attempt to figure out factors determining the pathway between methane and C<sub>2</sub><sup>+</sup> chemicals, by the hydrogen-producing electrode incorporation with the Cu.

# Electrochemical *In-situ* Analysis of CO<sub>2</sub> Reduction Reaction on Gold Grain Boundary

Yunwoo Nam and Hyun S. Ahn\*

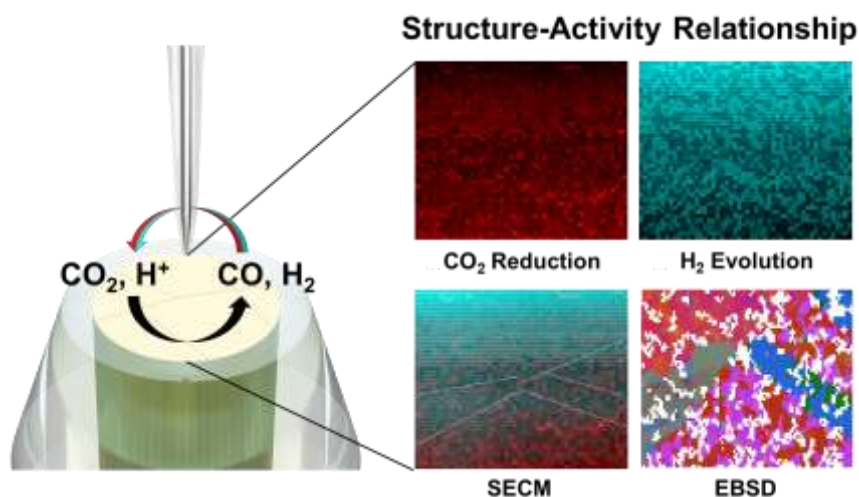
Department of Chemistry, Yonsei University, 50 Yonsei-ro, Seodaemun-gu, Seoul, Republic of Korea

\*ahnhs@yonsei.ac.kr

## Abstract

Understanding the relationship between structure and activity is critical in catalyst engineering to enhance the selectivity and efficiency of electrochemical catalysts. A grain boundary, which is an interface between two grains with different orientations, is well-known for increasing the selectivity of electrochemical carbon dioxide reduction reaction (CO<sub>2</sub>RR) in contrast to competitive hydrogen evolution reaction.[1] However, direct evidence of the correlation between grain boundary density and highly selective CO<sub>2</sub>RR is still absent. Here, we observed polycrystalline gold surface *in-situ* where the reactions are taking place with scanning electrochemical microscopy (SECM). The relationship between surface structure and catalytic activity was elucidated by a specially designed voltammetry sequence which enables selective product collection. Simultaneous catalytic reactions visualized individually via SECM will provide a basis for understanding an overall CO<sub>2</sub>RR.

## Table of Contents



## References

1. R.G. Mariano, K. McKelvey, H.S. White, M.W. Kanan, *Science*, **358**, 1187 (2017).

# Nanosheets of lithium silicate with excellent CO<sub>2</sub> capture kinetics and extraordinary stability at high temperatures

Rajesh Belgamwar and Vivek Polshettiwar\*

Department of Chemical Sciences, Tata Institute of Fundamental Research

email\_rajesh.belgamwar@tifr.res.in, vivekpol@tifr.res.in

## Abstract:

An excessive amount of CO<sub>2</sub> is the leading cause of climate change, and hence, its reduction in the Earth's atmosphere is critical to stop further degradation of the environment. [1] While a lot of research has been done on post-combustion low-temperature CO<sub>2</sub> capture, there are very few high temperature pre-combustion CO<sub>2</sub> capture processes. As one of the best-known high-temperature CO<sub>2</sub> capture sorbents, lithium silicate (Li<sub>4</sub>SiO<sub>4</sub>) faces two challenges: moderate sorption kinetics and poor sorbent stability. In this work, we have designed and synthesized lithium silicate nanosheets (LSNs), [2-5] which showed high CO<sub>2</sub> capture capacity (35.3 wt% CO<sub>2</sub> capture using 60% CO<sub>2</sub> feed gas, close to the theoretical value) with ultra-fast kinetics and enhanced stability at 650 °C. Because of the nanosheet morphology of the LSNs, they provided an excellent external surface for CO<sub>2</sub> adsorption at each Li site, yielding excellent CO<sub>2</sub> capture capacity. The nanosheet morphology of the LSNs allowed efficient CO<sub>2</sub> diffusion to ensure reaction with the entire sheet as well as providing extremely fast CO<sub>2</sub> capture kinetics (0.22 g<sup>-1</sup> min<sup>-1</sup>). As is known, conventional lithium silicates rapidly lose their capture capacity and kinetics within the first few cycles due to the formation of thick carbonate shells and also due to the sintering of sorbent particles; however, the LSNs were stable for at least 200 cycles without losing their capture capacity or kinetics. The LSNs neither formed a carbonate shell nor underwent sintering, allowing efficient adsorption-desorption cycling. We also proposed a new mechanism, a mixed-phase model, to explain the unique CO<sub>2</sub> capture behavior of the LSNs, using detailed (i) kinetics experiments for both adsorption and desorption steps, (ii) in situ diffuse reflectance infrared Fourier transform (DRIFT) spectroscopy measurements, (iii) depth-profiling X-ray photoelectron spectroscopy (XPS) of the sorbent after CO<sub>2</sub> capture.

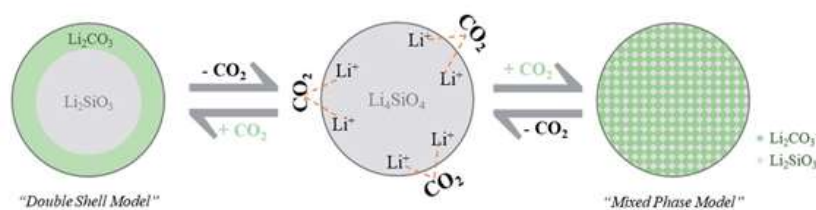


Figure 1. Proposed mixed-phase vs. double shell model for CO<sub>2</sub> adsorption-desorption.

LSNs show high capture capacity, fast kinetics and cycling stability for more than 200 cycles of a CO<sub>2</sub> sorbent. We perform various kinetics and spectroscopic studies (XPD depth profiling and in situ DRIFT) to prove the proposed mechanism of the mixed phase model.

## Acknowledgements

This work was supported by the Department of Atomic Energy (DAE), Government of India (under project no. R&D-TIFRRTI4003). We acknowledge the use of the EM and XRD facilities of TIFR, Mumbai.

## References

1. J. G. Vitillo, B. Smit and L. Gagliardi, Introduction: Carbon capture and separation, *Chem. Rev.*, **2017**, 117, 9521–9523.
2. A. Maity, R. Belgamwar, V. Polshettiwar. Facile Synthesis Protocol to Tune Size, Textural Properties & Fiber Density of Dendritic Fibrous Nanosilica (DFNS): Applications in Catalysis and CO<sub>2</sub> Capture. *Nature Protocols* **2019**, 14, 2177–2204.
3. A. Maity, S. Chaudhari, J. J. Titman and V. Polshettiwar, Nanosponges of acidic amorphous aluminosilicate for catalysis, plastic degradation and CO<sub>2</sub> to fuel conversion, *Nat. Commun.*, **2020**, 11, 3828.
4. A. K. Mishra, R. Belgamwar, R. Jana, A. Datta and V. Polshettiwar, Defects in nanosilica catalytically convert CO<sub>2</sub> to methane without any metal and ligand, *Proc. Natl. Acad. Sci. U.S.A.*, **2020**, 117, 6383–6390.
5. R. Belgamwar, A. Maity, T. Das, S. Chakraborty, C. P. Vinod, V. Polshettiwar, Lithium silicate nanosheets with excellent capture capacity and kinetics with unprecedented stability for high-temperature CO<sub>2</sub> capture, *Chem. Sci.*, **2021**, 12, 4825.

# CO<sub>2</sub> valorization by sorption-enhanced reverse water-gas shift reaction for low-temperature CO synthesis: a kinetic study of the reaction and water adsorption

Alex Desgagnés and Maria-Cornélia Iliuta\*

Université Laval, Département de génie chimique, 2325 Rue de l'Université, Québec, QC, Canada

\*[maria-cornelia.iliuta@gch.ulaval.ca](mailto:maria-cornelia.iliuta@gch.ulaval.ca)

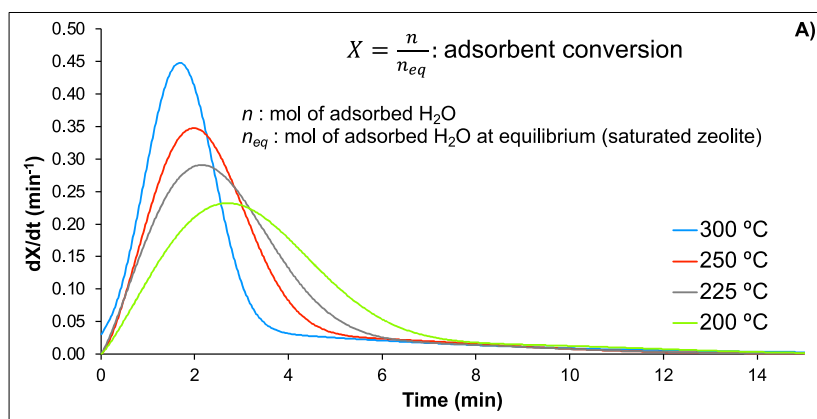
## Introduction

Carbon capture and conversion represents an interesting strategy for reducing CO<sub>2</sub> emissions that has economic potential through the generation of value-added products. CO<sub>2</sub> valorization through catalytic hydrogenation reactions are promising ways to produce highly versatile chemicals such as carbon monoxide. The conversion of CO<sub>2</sub> to CO via the reverse water-gas shift (RWGS) reaction represents the starting point of all CO<sub>2</sub> hydrogenation processes [1-4] since the mixture of CO and H<sub>2</sub>, known as syngas, can be used as a feedstock for the synthesis of useful chemicals or alternative fuels. However, the RWGS reaction is limited by constraining thermodynamic barriers, which drastically limits the CO<sub>2</sub> conversion of the reaction below 600 °C (< 40 %). Considering this evidence, water, the main by-product of the reaction, can be removed from the reaction media using hydrophilic adsorbents. This technique, known as sorption-enhanced reaction process (SERP), represents an innovative strategy to overcome the limits imposed by thermodynamics by shifting the equilibrium according to Le Chatelier's principle. The operation of the SERP applied to the RWGS reaction allows notably i) to increase considerably the CO<sub>2</sub> conversion ii) to lower the operating temperature of the reactor and thus the energy costs, and finally 3) to decrease the sintering and deactivation of the catalyst [4]. In the present work, this intensified RWGS process was investigated using a new copper-promoted metallurgical residue as a catalyst and a 13X-based adsorbent known for its high adsorption capacity and selectivity for water at high temperatures [5]. The study focused on the development of kinetic models to accurately describe the experimentally measured (i) intrinsic reaction rate of RWGS and (ii) rate of water adsorption on the adsorbents. Understanding the kinetics of these two interrelated processes (reaction and water adsorption) is essential before modeling a SE-RWGS reactor, which is a key step in the design of a process prior to its scale-up.

## Experimental

For conventional RWGS experiments (without adsorbent), the catalyst was prepared by a deposition-precipitation method. Briefly, UGSO, the metallurgical residue used as a catalyst support, was suspended in distilled water under stirring at 65°C. Simultaneously, a solution containing the copper precursor (Cu(NO<sub>3</sub>)<sub>2</sub>·3H<sub>2</sub>O, 99 %, Acros Organics) and another containing a basic precipitating agent (NH<sub>4</sub>HCO<sub>3</sub>, 99 %, Acros Organics) were added dropwise to the initial water-UGSO mixture. The whole was stirred for 30 minutes at constant temperature, then the resulting solid was recovered by vacuum filtration. The catalyst was then dried and calcined at 400°C for 3h. For the sorption-enhanced (SE) RWGS tests, 13X zeolite was used as received from the manufacturer (Particle size < 10 µm, Advanced Speciality Gas Equipment, Part No: MS-1328) and mechanically mixed with the catalyst dispersed in an aqueous solution. The water adsorption study was performed in an intelligent gravimetric analyzer (IGA-003, Hiden Isochema) equipped with a microbalance capable of accurately measuring (±0.1 µg) the sample mass over time. Gas flow rates, temperature and humidity in the reaction chamber were adjusted to the desired conditions. Conventional and intensified RWGS reaction tests were performed in a 40 cm long fixed bed reactor where the temperature and reactant flow rates were respectively adjusted by a temperature controller and mass flow meters. The kinetic study of water adsorption and RWGS reaction was conducted between 200 and 300 °C, where the reaction intensification effect is most easily observed. A Langmuir-Hinshelwood-Hougen-Watson heterogeneous kinetics method based on the packed-bed reactor model was used to investigate the reaction rates, while an empirical model (double stretched exponential) was able to properly portray the water adsorption data [6].

## Results preview



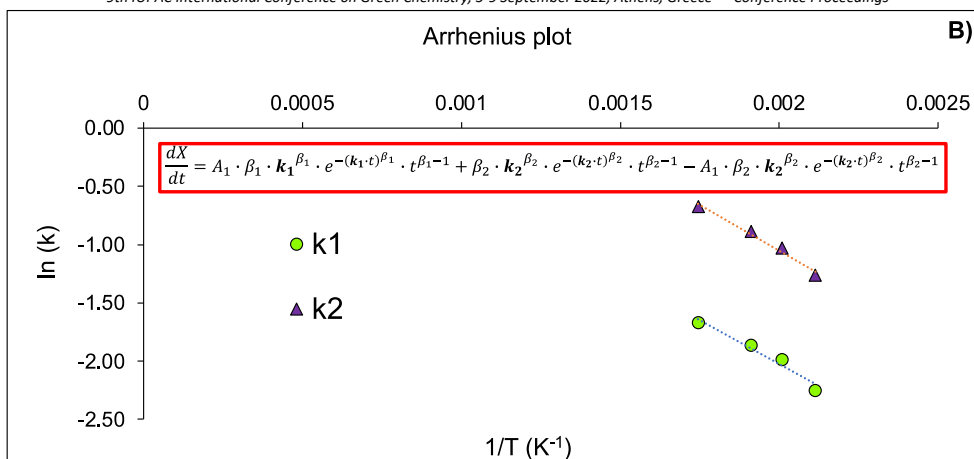


Figure 1. A) Conversion rate of the adsorbent (at  $X = 0$ , the adsorbent is free of water, at  $X = 1$ , the equilibrium adsorption capacity is reached) as a function of time in the temperature range studied ( $P_{\text{H}_2\text{O}} = 9.64$  kPa,  $P = 101.325$  kPa). B) Rate constant of water adsorption following an Arrhenius law

The findings of this study have allowed the identification of kinetic parameters that accurately describe the behavior of the adsorbent under RWGS reaction conditions, as well as that of the studied catalyst in the investigated temperature range. As expected, an increase in temperature boosts the adsorbent conversion rate (as can be seen on Figure 1. A) and that of the RWGS reaction, but the water adsorption capacities diminish. In the analyzed temperature range, we note that a temperature of 250°C is optimal to observe the reaction intensification effect. Lower than this value, the reaction rate is largely decreased, while higher, the water adsorption becomes more negligible. These results can be used to model a reactor operating the innovative SE-RWGS process for the conversion of  $\text{CO}_2$  into  $\text{CO}$ , a value-added product.

### Acknowledgements

Funding from the National Science and Engineering Research Council of Canada (NSERC) is gratefully acknowledged, as is funding from the Centre for Innovation and Research on Carbon Utilization in Industrial Technologies (CIRCUIT) program.

### References

- [1] W. Benzinger, E. Daymo, M. Hettel, L. Maier, C. Antinori, P. Pfeifer, O. Deutschmann, Reverse water gas shift (RWGS) over Ni – Spatially-resolved measurements and simulations, *Chemical Engineering Journal* 362 (2019) 430-441. <https://doi.org/10.1016/j.cej.2019.01.038>.
- [2] Y.A. Daza, J.N. Kuhn,  $\text{CO}_2$  conversion by reverse water gas shift catalysis: comparison of catalysts, mechanisms and their consequences for  $\text{CO}_2$  conversion to liquid fuels, *RSC Advances* 6(55) (2016) 49675-49691. <https://doi.org/10.1039/c6ra05414e>.
- [3] M.D. Porosoff, B. Yan, J.G. Chen, Catalytic reduction of  $\text{CO}_2$  by  $\text{H}_2$  for synthesis of  $\text{CO}$ , methanol and hydrocarbons: challenges and opportunities, *Energy & Environmental Science* 9(1) (2016) 62-73. <https://doi.org/10.1039/c5ee02657a>.
- [4] T.T.N. Vu, A. Desgagnés, M.C. Iliuta, Efficient approaches to overcome challenges in material development for conventional and intensified  $\text{CO}_2$  catalytic hydrogenation to  $\text{CO}$ , methanol, and DME, *Applied Catalysis A: General* 617 (2021). <https://doi.org/10.1016/j.apcata.2021.118119>.
- [5] V.R. Mollo-Varillas, F. Bougie, M.C. Iliuta, Selective adsorption of water vapor in the presence of carbon dioxide on hydrophilic zeolites at high temperatures, *Separation and Purification Technology* 282 (2022) 120008. <https://doi.org/https://doi.org/10.1016/j.seppur.2021.120008>.
- [6] M. Ghodhbene, F. Bougie, P. Fongarland, M.C. Iliuta, Hydrophilic zeolite sorbents for In-situ water removal in high temperature processes, *The Canadian Journal of Chemical Engineering* 95(10) (2017) 1842-1849. <https://doi.org/10.1002/cjce.22877>.

## Nickel-NHC-complexes for CO<sub>2</sub> Photoreduction using the Cooperative Effect of Ionic Liquids

Lisa Eisele<sup>1\*</sup>, Dominik Eder<sup>2</sup> and Katharina Bica-Schröder<sup>1</sup>

<sup>1</sup>TU Wien, Institute for Applied Synthetic Chemistry, Getreidemarkt 9/163, 1060 Vienna, Austria

<sup>2</sup>TU Wien, Institute of Materials Chemistry, Getreidemarkt 9/163, 1060 Vienna, Austria

\*[lisa.eisele@tuwien.ac.at](mailto:lisa.eisele@tuwien.ac.at)

Caused by current climate challenges and continuously growing emissions of carbon dioxide, the development of methodologies for carbon capture and valorisation is more imperative than ever.<sup>[1]</sup> Carbon dioxide (CO<sub>2</sub>) is an abundant, inert and renewable source of carbon and thus interesting for further conversion to fuels and feedstock chemicals; therefore the development of processes utilising CO<sub>2</sub> has been of significant interest in the last decade.<sup>[2]</sup> To develop an efficient process, the high thermodynamic and kinetic barrier for CO<sub>2</sub> reduction needs to be overcome. Eventually, photocatalytic generation of carbon monoxide (CO) from CO<sub>2</sub> allows for *in-situ* carbonylation towards feedstock chemicals using CO<sub>2</sub> as a resource and thereby offers the potential for safer and greener carbonylation chemistry on industrial scale.

Besides commonly used ruthenium and rhenium photocatalysts, newly developed systems based on iridium- and nickel-*N*-heterocyclic carbene-complexes (NHC-complexes) show desirable results in the reduction of CO<sub>2</sub>.<sup>[3]</sup> Apart from the high selectivity for CO as main product, this system enables photocatalytic reduction under visible light. Additionally, using nickel as catalyst material comes with the benefit of cheap and earth abundant catalytic components.

We have thus developed a novel reaction protocol for Ni-NHC photocatalysts, allowing for a fast and facile synthesis in high yields. The Ir-Ni-NHC-photocatalytic system is further supported by ionic liquids that show considerable potential as cooperative media in CO<sub>2</sub> photoreduction, as they can solubilise and activate large concentrations of CO<sub>2</sub>. Detailed studies on the impact of various ionic liquids in photocatalytic CO<sub>2</sub> reduction are currently ongoing.

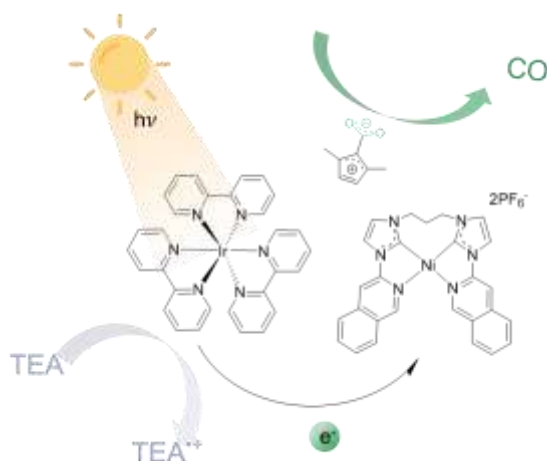


Figure 1: Ir-Ni-NHC-photocatalytic system in ionic liquids

### Acknowledgements

This project has received funding from the European Research Council (ERC) under the European Union's Horizon 2020 research and innovation programme (Grant agreement No. 864991).

### References

- [1] Q. Liu, L. Wu, R. Jackstell, M. Beller, *Nat. Commun.* **2015**, *6*, 5933.
- [2] A. Sainz Martinez, C. Hauzenberger, A. R. Sahoo, Z. Csendes, H. Hoffmann, K. Bica, *ACS Sustain. Chem. Eng.* **2018**, *6*, 13131–13139.
- [3] V. S. Thoi, N. Kornienko, C. G. Margarit, P. Yang, C. J. Chang, *J. Am. Chem. Soc.* **2013**, *135*, 14413–14424.



## New photocatalytic materials for carbon dioxide valorization in carbonylation chemistry using the cooperative effect of ionic liquids

Bletë Hulaj<sup>1\*</sup>, Lisa Eisele<sup>1</sup> and Katharina Bica-Schröder<sup>1</sup>  
<sup>1</sup>Technische Universität Wien, Getreidemarkt 9/163, 1060 Vienna, Austria  
 \*blete.hulaj@tuwien.ac.at

The replacement of hazardous carbon monoxide with more benign surrogates is highly desirable, and recent ideas focus on the valorization of carbon dioxide as an abundant, non-toxic and renewable carbon source. To achieve this, the high thermodynamic and kinetic barrier for the reduction of carbon dioxide to carbon monoxide needs to be overcome [1].

Photocatalytic systems consisting of a photosensitizer and a photocatalyst such as Ru and Re showed high selectivity for carbon monoxide formation with a turnover number above 50, allowing for visible light photocatalyzed reduction of carbon dioxide [2]. Ionic liquids show considerable potential as cooperative media as they can solubilize large concentrations of carbon dioxide, and are also able to activate carbon dioxide.

Materials that combine both photocatalyst and ionic liquid are thus highly desirable for a photocatalytic carbon dioxide reduction to generate carbon monoxide and the *in situ* conversion into carbonyl compounds. Immobilization of the photocatalyst is favourable, facilitating catalyst handling and recovery, and enables the use in continuous processes.

Consequently, we have developed different ionic liquid-photocatalyst polymers by copolymerization of the ionic liquid 1-butyl-3-vinylimidazolium chloride and photocatalytically active Re- and Ru-complexes bearing vinyl groups. The synthesis of the polymer systems was conducted *via* radical polymerization utilizing varying ratios of photocatalytic materials with vinyl functionalized ligand system and ionic liquids affording high yields of the desired material. Analysis of the synthesized materials with UV-Vis spectroscopy showed high correlation with reported values for vinyl group monomers; the spectra were minimally shifted from 455 nm for the vinyl modified Ru monomer to 480 nm for the Ru-IL-polymer as shown in figure 2 [3].

The obtained novel polymers synthesized from the copolymerisation of ionic liquids and photocatalysts, will be further studied for the visible-light photoreduction of carbon dioxide, aiming for a continuous production of carbon monoxide under benign conditions.

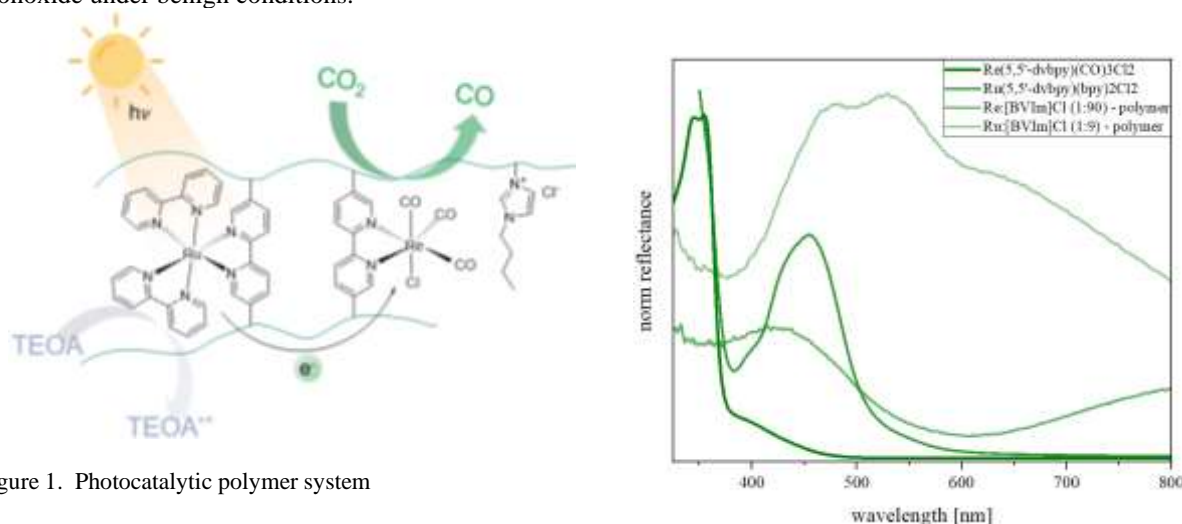


Figure 1. Photocatalytic polymer system

### Acknowledgements

This project has received funding from the European Research Council (ERC) under the European Union's Horizon 2020 research and innovation programme (Grant agreement No. 864991).

### References

1. B.A. Rosen, A. Salehi-Khojin, M.R. Thorson, W. Zhu, D.T. Whipple, P.J.A. Kenis, R.I. Masel, *Science* 334 (2011) 643–644.
2. Y. Kuramochi, O. Ishitani, H. Ishida, *Coordination Chemistry Reviews* 373 (2018) 333–356.
3. H.J. Nie, J.Y. Shao, J. Wu, J. Yao, Y.W. Zhong, *Organometallics* 31 (2012) 6952–6959.

## Syngas Production by Carbon Dioxide Conversion of Methane over Co-based Catalyst with High Stable Activity

Sholpan S. Itkulova<sup>\*</sup>, Yerzhan A. Boleubayev<sup>1</sup>, Kirill A. Valishevskiy<sup>1</sup>, Akbope K. Borangazieva<sup>1</sup>, and Zhuldyz U. Ibraimova<sup>1</sup>

<sup>1</sup> D.V.Sokolsky Institute of Fuel, Catalysis, and Electrochemistry, 142, Kunaev str., Almaty, 050010, Republic of Kazakhstan;

\* e-mail: [sholpan.itkulova@gmail.com](mailto:sholpan.itkulova@gmail.com), [s.itkulova@ifce.kz](mailto:s.itkulova@ifce.kz)

Climate change and the depletion of oil resources are the main problems facing the entire world community. In the interests of sustainable development, a search is being made for new alternative cheap and renewable sources of energy, petrochemistry, and environmental protection. In the long term, carbon dioxide can serve as a source of renewable raw materials. In recent years, carbon dioxide reforming of methane, also called as dry methane reforming (DRM), has generated a lot of interest because it can convert two major greenhouse gases (CO<sub>2</sub> and CH<sub>4</sub>) to syngas (CO+H<sub>2</sub>).

This work deals with the production of synthesis gas by dry reforming of methane over the Co-based catalysts supported on a matrix composed of alumina modified with zirconia and rare-earth metal oxides. Also, the effect of steam on DRM over the catalysts has been studied. The multicomponent 5%Co-M/Al<sub>2</sub>O<sub>3</sub>-ZrO<sub>2</sub>-R catalysts showed the high stable activity during its long-term continuous testing for 400 hours. The catalysts were characterized by a number of physico-chemical methods.

### Experimental

The multicomponent 5%Co-M/Al<sub>2</sub>O<sub>3</sub>-ZrO<sub>2</sub>-R catalysts, where M is a noble metal (Pt) and R is Ce or/and La oxides were synthesized by impregnation and tested in dry and steam reforming of methane. The processes were carried out in a quartz flow reactor supplied with programmed heating, controlled feed velocity, a programmable syringe pump, and GCs. Stainless steel reactor with catalyst volume – 100 mL was used in order to carry out the long-term tests. The dry (DRM) and bireforming (combined steam-dry – BRM) reforming of methane have been studied under atmospheric pressure, varying gas hourly space velocity (GHSV) within 1000-3000 h<sup>-1</sup> with using a feed with a ratio of CH<sub>4</sub>/CO<sub>2</sub>=1:1 and varying temperature within 300-800°C. The 0.5-2.0 vol. parts of steam has been added to a feed to provide bireforming of methane. To elucidate the stability the 5%Co-M/Al<sub>2</sub>O<sub>3</sub>-ZrO<sub>2</sub>-CeO<sub>2</sub>-La<sub>2</sub>O<sub>3</sub> catalyst was continuously tested for a long-term period: 400 hours in DRM and 100 hours bireforming of methane. The catalysts were characterised by BET, XRD, SEM, TEM, and TPR methods.

### Results/Discussion

The catalysts perform a high activity in both dry and steam reforming of methane. Methane is almost completely converted at 750-800°C depending on the catalyst composition and process type. Adding steam in amount 0.1-1 volume parts to a feed of carbon dioxide + methane always leads to decrease in temperature of methane complete conversion and enriching syngas with hydrogen over the synthesized catalysts.

The 5%Co-Pt/Al<sub>2</sub>O<sub>3</sub>-ZrO<sub>2</sub>-CeO<sub>2</sub>-La<sub>2</sub>O<sub>3</sub> catalyst showed a high stable activity for all period of testing in both processes: 400 hours in DRM and 100 hours in byreforming of methane.

Under conditions  $t=700^{\circ}\text{C}$ ,  $P=1\text{ atm}$ ,  $\text{GHSV}=1000\text{ h}^{-1}$ ,  $\text{CH}_4:\text{CO}_2=1:1$ , methane conversion was varied within 96.0-96.6%, while the extent of carbon dioxide conversion was insignificantly less and varied within 90.4-92.3% (Figure 1).

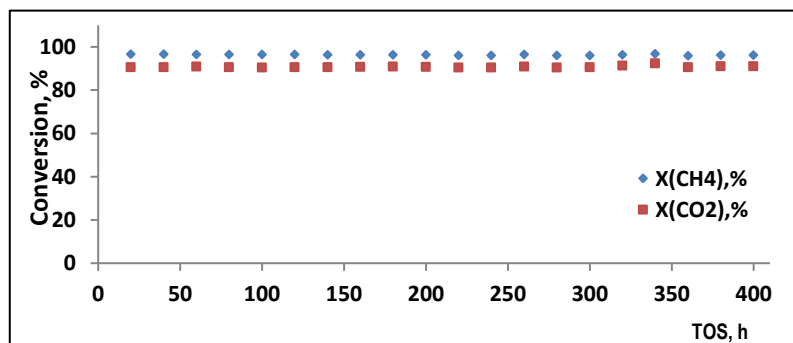


Figure 1. Dependence of conversion of CO<sub>2</sub> and CH<sub>4</sub> on process duration over the 5%Co-Pt/Al<sub>2</sub>O<sub>3</sub>-ZrO<sub>2</sub>-CeO<sub>2</sub>-La<sub>2</sub>O<sub>3</sub> ( $t=700^{\circ}\text{C}$ ,  $P=1\text{ atm}$ ,  $\text{GHSV}=1000\text{ h}^{-1}$ ,  $\text{CH}_4/\text{CO}_2=1:1$ )

The ratio of H<sub>2</sub>/CO in the syngas formed in DRM was 0.9.

In combined steam-dry reforming of methane (CH<sub>4</sub>:CO<sub>2</sub>:H<sub>2</sub>O=1:1:1), H<sub>2</sub>/CO ratio was increased to 1.3 under the same conditions.

A high dispersed state of metals was observed by TEM. The effect of the second metal on reducibility of Co was revealed by TPR method.

### **Conclusion**

The 5%Co-M/Al<sub>2</sub>O<sub>3</sub>-ZrO<sub>2</sub>-R catalysts developed performs the extremely high activity and stability in syngas production carbon dioxide reforming of methane.

The synthesis gas composition can be controlled by adjusting the composition of the feed.

### **Acknowledgements**

This research was funded by the Science Committee of the Ministry of Education and Science of the Republic of Kazakhstan, Grant No AP08855848.

## Upgrading biogas, produced from the anaerobic digestion of municipal wastewater treatment sludge, to biomethane by applying membrane gas separation

Chrysovalantou Koutsiantzi<sup>\*1</sup>, Anastasios Zouboulis<sup>2</sup>, Manassis Mitrakas<sup>1</sup>, Eustathios S. Kikkinides<sup>1</sup>

<sup>1</sup> Department of Chemical Engineering, Aristotle University of Thessaloniki

<sup>2</sup> Department of Chemistry, Aristotle University of Thessaloniki

\* Correspondence: vkoutsiantzi@gmail.com

### Abstract

Biogas is considered as an alternative renewable fuel, which due to its nature can potentially help reduce the global climate change, while at the same time can lead to the reduction of treated wastes. It is mainly produced by the anaerobic digestion (AD) of carbon-containing waste materials (e.g., sludge from the wastewater treatment plants, from manure, from landfills etc.) [1,2]. However, as the biogas even after pretreatment for the removal of minor constituents (e.g., moisture, NH<sub>3</sub> and H<sub>2</sub>S), still contains significant amounts of CO<sub>2</sub>, it is considered of particular importance to upgrade it, by removing most of carbon dioxide content, and capturing this for potential further reuse.

In the current study, a membrane process investigated for the efficient CO<sub>2</sub> separation from CH<sub>4</sub>, which are the major constituents of biogas, and leading to biogas upgrade towards biomethane, aiming to meet the requirements for effective energy use (e.g., by connecting the CH<sub>4</sub>-rich gaseous into the natural gas grid). Therefore, the main goal is the production of high purity biomethane (>95%) from biogas with the simultaneous CO<sub>2</sub> capture.

The mass flow of inlet gas mixture, consisting of CO<sub>2</sub> and CH<sub>4</sub> and simulating biogas, was controlled by a mass controller between 1000-3000 mL/min and the feed pressure was controlled by a back pressure regulator (BPR) in a range between 5-10 bars. The gas streams were analyzed directly, applying a specific gas analyzer for the CH<sub>4</sub> and CO<sub>2</sub> content. The examined membrane is the polyimide hollow fiber UBE UMS-B2 module.

A series of laboratory tests carried out for the evaluation of this membrane module, regarding the CO<sub>2</sub> removal, the typical results are presented in Fig. 1. The biogas upgrade membrane assembly in continuous flow designed to operate under the optimal defined separation conditions. The laboratory research results are respectively validated and verified also via a pilot-scale biogas upgrading system, where the reactor is fed with real pre-treated biogas from the anaerobic digestion of Thessaloniki's Wastewater Treatment Plant, under continuous flow.

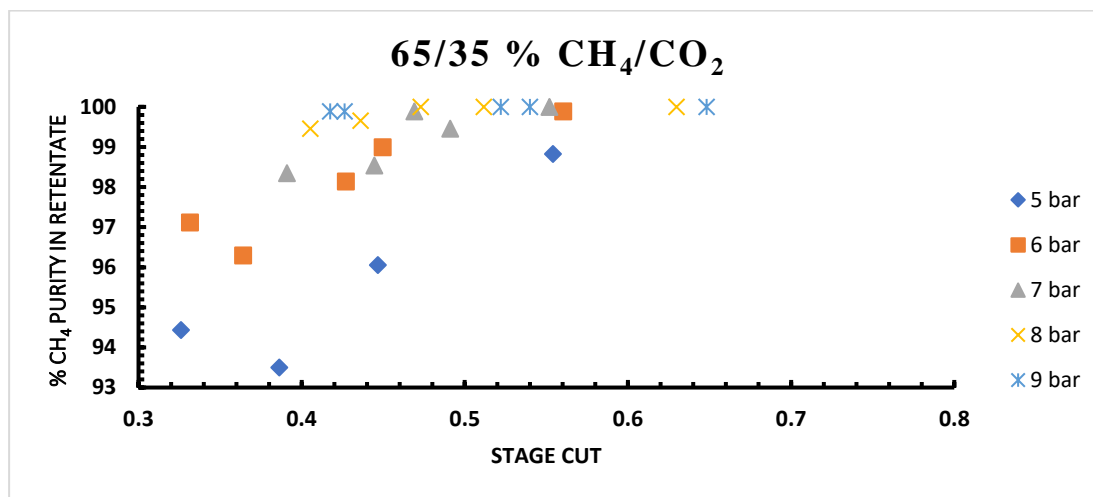


Figure 1. Mixed gas separation performance according to the applied pressure for the typical CH<sub>4</sub>/CO<sub>2</sub> biogas mixture at 20°

C; CH<sub>4</sub> purity in the retentate stream for various back pressure values (5-9 bar).

### Acknowledgements

This research has been co-financed by the European Union and Greek national funds through the Operational Program Competitiveness, Entrepreneurship, and Innovation, under the call RESEARCH-CREATE-INNOVATE (project code: T2EDK-01293).

## References (selected)

- [1] T. A. Seadi *et al.*, *Biogas Handbook*. University of Southern Denmark Esbjerg, 2008. [Online]. Available: <https://books.google.gr/books?id=znSAmAEACAAJ>
- [2] A. Janusz-Cygan, J. Jaschik, and M. Tańczyk, “Upgrading Biogas from Small Agricultural Sources into Biomethane by Membrane Separation,” *Membranes*, vol. 11, no. 12, p. 938, 2021, doi: 10.3390/membranes11120938.



European Union  
European Regional  
Development Fund



## Dynamic simulation of biogenic CO<sub>2</sub> methanation in fixed and structured catalytic reactors for decentralized Power-to-Gas applications

Dimitrios Mertzis<sup>1\*</sup>, Grigorios Koltzakis<sup>1</sup> and Zissis Samaras<sup>1</sup>

<sup>1</sup>Lab of Applied Thermodynamics, Faculty of Engineering, Mech. Eng. Dpt., Aristotle University of Thessaloniki

\*jimmer@auth.gr

Power-to-Gas (PtG) processes are a recent research field focused on the seasonal storage of renewable electricity surplus through the generation of synthetic natural gas (SNG). Especially, through the utilisation of biogenic CO<sub>2</sub> sources (biogas, biomass combustion/gasification/pyrolysis), the opportunity to produce decentralized “Green” methane arises even more reducing the carbon footprint of renewable energy storage as existing natural gas infrastructure is exploited. In the PtG concept, renewable electricity surplus produces H<sub>2</sub> through electrolysis which is fed in a Sabatier reactor along with captured CO<sub>2</sub> at temperatures around 300-350°C to produce methane. Due to the intermittent nature of renewables such as solar and wind energy, reliable operation of the methanation reactor under transient and dynamic conditions is necessary.

Packed bed reactors are the most common type of methanation reactor available but in general temperature control is challenging and requires several intercooled reactors in series or catalyst distribution [1] increasing reactor size and complexity. The methanation reaction is highly exothermic. Due to the large reaction heat and the high activity of the catalysts towards methane, hot spots usually occur at the reactor inlet. These hot spots must be kept below 500°C to avoid catalyst degradation and optimize methane yield [2]. Monolithic structured reactors on the other hand present low pressure drop, high heat transfer and cross flow area making them easier to control especially under dynamic inlet conditions. Several models have been developed for the fixed bed reactor and only a few for honeycomb methanation reactors. The most important parameters affecting the performance of the reactor are reaction kinetics and heat transfer. The kinetics for the methanation reactor have been thoroughly researched, mainly to study the methane reforming reaction which is the reverse reaction. Indirect reaction schemes (CO methanation + water-gas shift reaction) have been investigated by Xu and Froment [3] while direct CO<sub>2</sub> methanation reaction schemes of the Langmuir-Hinshelwood (LHHW) type have been recently published by Koschany et al. [4]. Both kinetic studies are widely adopted by the scientific community either for steady state or transient models. On the other hand, catalyst thermal properties such as conductivity and capacity are largely affected by device geometry, substrate and catalyst loading [5] and properties. Since the majority of methanation models published are axial, pseudo-homogeneous and steady state, they are not suitable for thermal performance evaluation in the PtG context.

In this study, a 2D/3D heterogeneous dynamic model has been developed for the simulation of packed bed and monolithic methanation reactors. Exothermia suite (ES), a software package developed by Exothermia SA, an Aristotle University of Thessaloniki spin-off company, was used for the simulations. ES was originally developed for exhaust after-treatment modelling applications where honeycomb catalysts are common. Basic model inputs are reactor geometry, material properties, reaction schemes and a reactor cooling sub-model. Industrial reactor oil-cooling methodology is adopted through the modeling of a hydraulic system in which heat transfer between the reactor wall and coolant is calculated using a surface-calibrated thermal resistivity factor. Reactor properties and boundary conditions are fully customizable and are read in tabularized format in the form of “\*.csv” files. The model has been calibrated through widely cited publications both for fixed bed and structured reactors. Detailed sensitivity analysis has been performed to determine the cooling model parameters and their effect on heat transfer and reactor performance. A parametric analysis was performed with literature-accepted kinetic parameters modifying several catalyst attributes (tortuosity, thermal capacity/conductivity, diffusion parameters, heat and mass transfer coefficients).

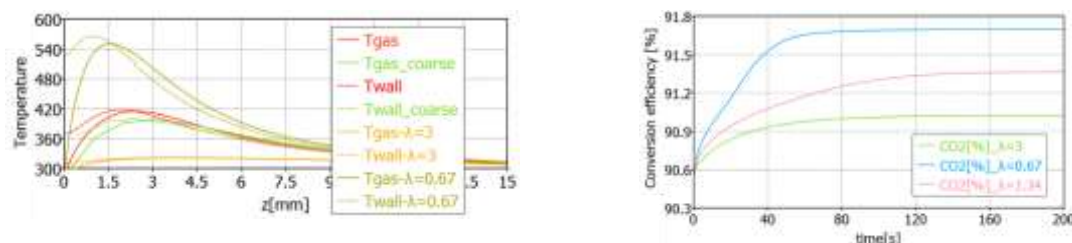


Figure 1. Packed bed model axial temperature profile for different catalyst thermal conductivity and axial discretization scenarios (left) and CO<sub>2</sub> conversion efficiency for different catalyst thermal conductivity scenarios (right)

Preliminary model runs showed a direct effect of catalyst temperature on CH<sub>4</sub> yield and CO<sub>2</sub> consumption as at elevated temperatures CH<sub>4</sub> formation is inhibited. Catalyst porosity/tortuosity and thermal conductivity significantly affect catalyst temperature however it does not have a crucial effect on CH<sub>4</sub> yield and CO<sub>2</sub> conversion efficiency but mainly on hotspot location. Reduced porosity leads to lower peak temperatures and shifts the axial

temperature peak further into the reactor as seen in literature [5]. The two reactor types are compared and combined in a dynamic inlet PtG scenario of biogas/syngas upgrading for SNG production. The analysis shows that higher space velocities are achievable in honeycombs without risking temperature increase allowing for larger tube diameters and lower construction costs. Solid and gas peak temperatures are observed in different axial locations due to the high effect of thermal conductivity present in the structured honeycomb catalyst. Three different case studies were simulated a) Oxy-Gasification of solid digestate (a by-product of biogas plants) and mixing of the produced syngas with H<sub>2</sub> from electrolysis, b) Methanation of CO<sub>2</sub> originating from biogas upgrade with H<sub>2</sub> from electrolysis and c) biogas methanation with H<sub>2</sub> from electrolysis. Seven different scenarios were compared to account for feed gas composition, load and inlet composition fluctuation and a shut-down and hot start-up scenario. The simulations show that the proposed two-stage reactor with intermediate water removal can achieve very high CH<sub>4</sub> yields (>90% in all cases tested) without compromising catalyst durability. Fast start-up times and optimization through cooling temperature control are also findings that highlight the concept's flexibility and robustness.

### Acknowledgements

The implementation of the postdoctoral research/work is co-financed by Greece and the European Union (European Social Fund) through the Operational Program "Development of Human Resources, Education and Lifelong Learning", in the context of the Action "SUPPORTING POST-DOCTORAL RESEARCHERS - Cycle B' (MIS 5033021) which implements the State Scholarship Foundation (IKY)

### References

1. M. Götz, J. Lefebvre, F. Mörs, A. McDaniel Koch, F. Graf, S. Bajohr, R. Reimert, T. Kolb, *Renew Energ*, **85** 1371–1390 (2016)
2. S. Rönsch, J. Köchermann, J. Schneider, S. Matthischke, *Chem EngTechnol* **39** 2 208–218 (2016).
3. J. Xu, G. F. Froment, *AIChE*, **35** 1 88-96(1989)
4. F. Koschany, D. Schlereth, O. Hinrichsen, *Appl Catal B-Environ*, **181** 504-516 (2016)
5. B. Kreitz, G. D. Wehinger, T. Turek, *Chem Eng Sci*, **195** 541-552 (2019)

## Coupling Reaction of CO<sub>2</sub> with Epoxides by Highly Nucleophile 4-Aminopyridines

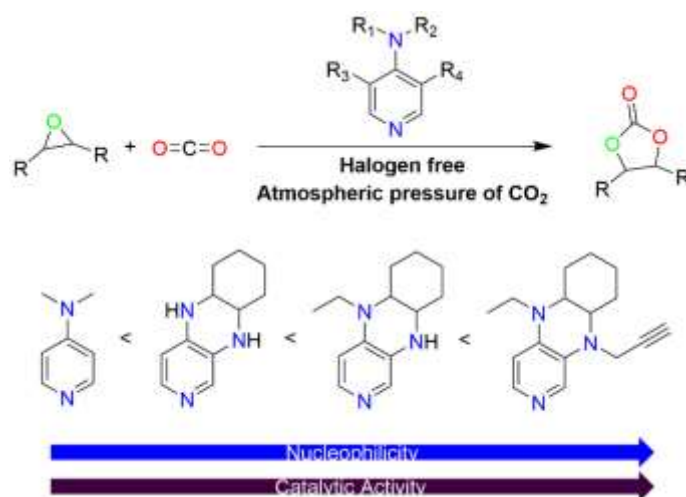
Wuttichai Natongchai,<sup>1</sup> Jesús Antonio Luque-Urrutia,<sup>2</sup> Chalida Phungpanya,<sup>1</sup> Miquel Solà,<sup>2</sup> Valerio D'Elia,<sup>1\*</sup> Albert Poater,<sup>2\*</sup> and Hendrik Zipse<sup>3</sup>

<sup>1</sup>Department of Materials Science and Engineering, School of Molecular Science and Engineering, Vidyasirimedhi Institute of Science and Technology (VISTEC), 555 Moo 1, 21210, Payupnai, WangChan, Rayong, Thailand.

<sup>2</sup>Institut de Química Computacional i Catàlisi and Departament de Química, Universitat de Girona, C/M. Aurèlia Capmany, 69, 17003 Girona, Catalonia, Spain.

<sup>3</sup>Department Chemie, Ludwig-Maximilians-Universität München, Butenandtstraße 5-13, Haus F, 81377 München, Germany.  
\*e-mail: [Wuttichai.n\\_sl6@vistec.ac.th](mailto:Wuttichai.n_sl6@vistec.ac.th)

Cyclic organic carbonates have a wide range of amazing uses, including as solvents and chemical intermediates in the manufacture of fine chemicals and polymers. Importantly, the widely desired potential to recycle CO<sub>2</sub> as a C1 source for the synthesis of common compounds under benign conditions is provided by the synthesis of cyclic carbonates via the coupling reaction of CO<sub>2</sub> with epoxides and the development of single-component halogen-free organocatalysts in the highly investigated for the coupling reaction of CO<sub>2</sub> with epoxides is sought-after to improve the sustainability of the process and lower costs. In this study, highly nucleophilic 3,4-diaminopyridine derivatives were prepared and used as catalyst for the coupling reaction of CO<sub>2</sub> and epoxides. From predictive calculations of epoxide-specific carbon basicities suggested that highly nucleophilic 3,4-diaminopyridines possess suitable basicity to serve as active single-component catalysts for the coupling reaction. Indeed, experimentally, the most active compounds of this class performed efficiently for the conversion of epoxides to carbonates under atmospheric pressure outperforming the catalytic activity of traditional N-nucleophiles. Importantly, the 3,4-diaminopyridino scaffold could be easily supported on polystyrene resin and used as a recyclable heterogeneous catalyst under atmospheric CO<sub>2</sub> pressure. Finally, the mechanism of the coupling reaction, which was catalyzed by several N-nucleophiles, was examined. This highlighted the significance of the nucleophilicity of 3,4-diaminopyridine in successfully promoting the critical initial step of epoxide ring-opening without the addition of nucleophiles or hydrogen bond donors.



### References

1. W. Natongchai, J.A. Luque-Urrutia, C. Phungpanya, M. Solà, V. D'Elia, A. Poater, H. Zipse, *Org. Chem. Front.*, **8**(3) 613-627 (2021).
2. W. Natongchai, S. Posada-Pérez, C. Phungpanya, J.A. Luque-Urrutia, M. Solà, V. D'Elia, A. Poater, *J. Org. Chem.*, **87**(5) 2873-2886 (2022).



## Development of Cu<sub>2</sub>O/BiVO<sub>4</sub> heterojunction photocatalysts for sustainable artificial photosynthesis.

Eva Naughton\*, James A. Sullivan, and Ravindranathan Thampi.

*UCD School of Chemistry, Belfield, Dublin 4, Ireland.*

*eva.naughton@ucdconnect.ie*

### Introduction

Since the industrial revolution fossil fuels have driven economic growth and now, approximately 85% of global energy generation comes from combustion of coal, oil, and natural gas. [1]. However, temperature increases due to rising CO<sub>2</sub> levels are projected to have many negative impacts, such as rising sea levels and loss of biodiversity, and therefore scientists are looking for methods to tackle this increase in atmospheric CO<sub>2</sub> levels.

In nature, photosynthesis in plants occurs through a z-scheme mechanism that involves a two-step photoexcitation. First, electrons in photosystem (PS) II and PS I are excited to their respective LUMOs following visible light absorption. Next, the electrons in the LUMO of PS II are transferred to the HOMO of PS I through an electron mediator, neutralising the photogenerated holes therein. The remaining photogenerated electrons (used to reduce CO<sub>2</sub>) and holes (used to oxidise H<sub>2</sub>O) are left in the LUMO of PS I and the HOMO of PS II, respectively [2]. There is much potential to mimic this process artificially. Therefore, artificial photosynthesis (AP) using two distinct light absorbing species is an important area of research as a successful system would mean that waste CO<sub>2</sub> and free solar radiation can create fuels and valuable chemicals using abundant visible light as an energy provider.

“Z-scheme” is the term used to explain the observed efficient electron/hole separation mechanism obtained through the use of two co-located semiconductors [3]. These systems involve the use of a semiconductor with a high energy conduction band (CB) and a medium energy valence band (VB) (the reduction photocatalyst), and one with a low energy VB and medium energy CB (the oxidation photocatalyst). Following photon absorption and electron excitation, the electrons in the CB of the oxidation photocatalyst combine with the holes in the VB of the reduction photocatalyst. This leads to retention of strong reduction and oxidation abilities in the two semiconductors, spatial separation of charge carriers, and an extended light harvesting range (albeit with a necessarily decreased photon-to-exciton efficiency) [4].

The intent of this work is to investigate various heterogeneous direct z-scheme photocatalytic systems synthesised *via* facile hydrothermal methods, characterise these using a range of techniques and then test them in the AP reaction under visible light irradiation. The physical, optical, electronic, and photocatalytic properties of the different materials produced are examined and compared.

### Experimental

Cu<sub>2</sub>O/BiVO<sub>4</sub> is prepared in this study as a surface-decorated z-scheme system where BiVO<sub>4</sub> is the oxidation photocatalyst (and the support), and Cu<sub>2</sub>O is the reduction photocatalyst (and decorated on the surface). This geometry was achieved using deposition-precipitation methods. BiVO<sub>4</sub> serves as a substrate to provide surface sites that allow for nucleation and growth of Cu<sub>2</sub>O [4]. In this work, a hydrothermal method was used to synthesise monoclinic BiVO<sub>4</sub> using Bi(NO<sub>3</sub>)<sub>3</sub> and NH<sub>4</sub>VO<sub>3</sub> [5]. Cu<sub>2</sub>O was then grown on the surface of the BiVO<sub>4</sub> using Cu(CH<sub>3</sub>COO)<sub>2</sub> and an ethylene glycol reduction. BiVO<sub>4</sub>, Cu<sub>2</sub>O and Cu<sub>2</sub>O/BiVO<sub>4</sub> composites with molar ratios of 1:7, 1:3, and 1:1 were prepared and characterised using XRD, XPS, FTIR, UV-Vis DRS, SEM/EDX, and CO<sub>2</sub> TPD experiments.

### Results and Discussion

XRD (see figure 1 a)) gave confirmation of the phase of the materials and the sharp peaks indicated that they are highly crystalline. Furthermore, it is evident that Cu<sub>2</sub>O is present in the composite materials, and therefore the possibility for the formation of a heterojunction exists. These results also show that the incorporation of Cu<sub>2</sub>O onto the BiVO<sub>4</sub> surface does not affect the crystallinity of either component.

XPS (see figure 1 b)) confirmed the existence of Cu<sub>2</sub>O (and CuO – following Cu<sub>2</sub>O oxidation in the atmosphere) in the composite materials. As the percentage of copper present in the composite increases, we see an increase in the binding energy of Cu<sup>+</sup> derived electrons. These values are 932.3, 932.4, and 932.7 eV for the Cu<sub>2</sub>O/BiVO<sub>4</sub> 1:7, 1:3, and 1:1 samples, respectively. This trend is as expected for z-scheme systems and, therefore, may indicate band bending in the composite, providing evidence for the formation of a heterojunction.

FTIR spectroscopy (see figure 1 c)) gave information about the surfaces of the materials and shows that each can adsorb both H<sub>2</sub>O and CO<sub>2</sub>, the AP reactants. Furthermore, several characteristic vibrations can be observed, for example a large broad band in all spectra of the BiVO<sub>4</sub>-containing materials between 700 – 900 cm<sup>-1</sup> can be attributed to V-O bends and stretches [6], and, in the spectrum of the Cu<sub>2</sub>O sample, a band at 632 cm<sup>-1</sup> resulting from a Cu-O bend [7].

UV-Vis DRS spectra (see figure 1 d)) indicate that all the as-synthesized materials possess strong absorption in UV and visible-light regions, with absorbance across the visible region being proportional to the  $\text{Cu}_2\text{O}$  loading.  $\text{CO}_2$  TPD experiments (see figure 1 e)) show that  $\text{BiVO}_4$  is not a good  $\text{CO}_2$  adsorbent, while  $\text{Cu}_2\text{O}$  is. This should be beneficial as, according to the proposed reaction mechanism,  $\text{CO}_2$  reduction using  $\text{Cu}_2\text{O}/\text{BiVO}_4$  composites should occur on the  $\text{Cu}_2\text{O}$  semiconductor surface. Having said this, the  $\text{CO}_2$  adsorbed on  $\text{Cu}_2\text{O}$  is relatively stable (as shown by its  $T_{\text{des}}$ ) and this may affect the rates of  $\text{CO}_2$  reduction steps.

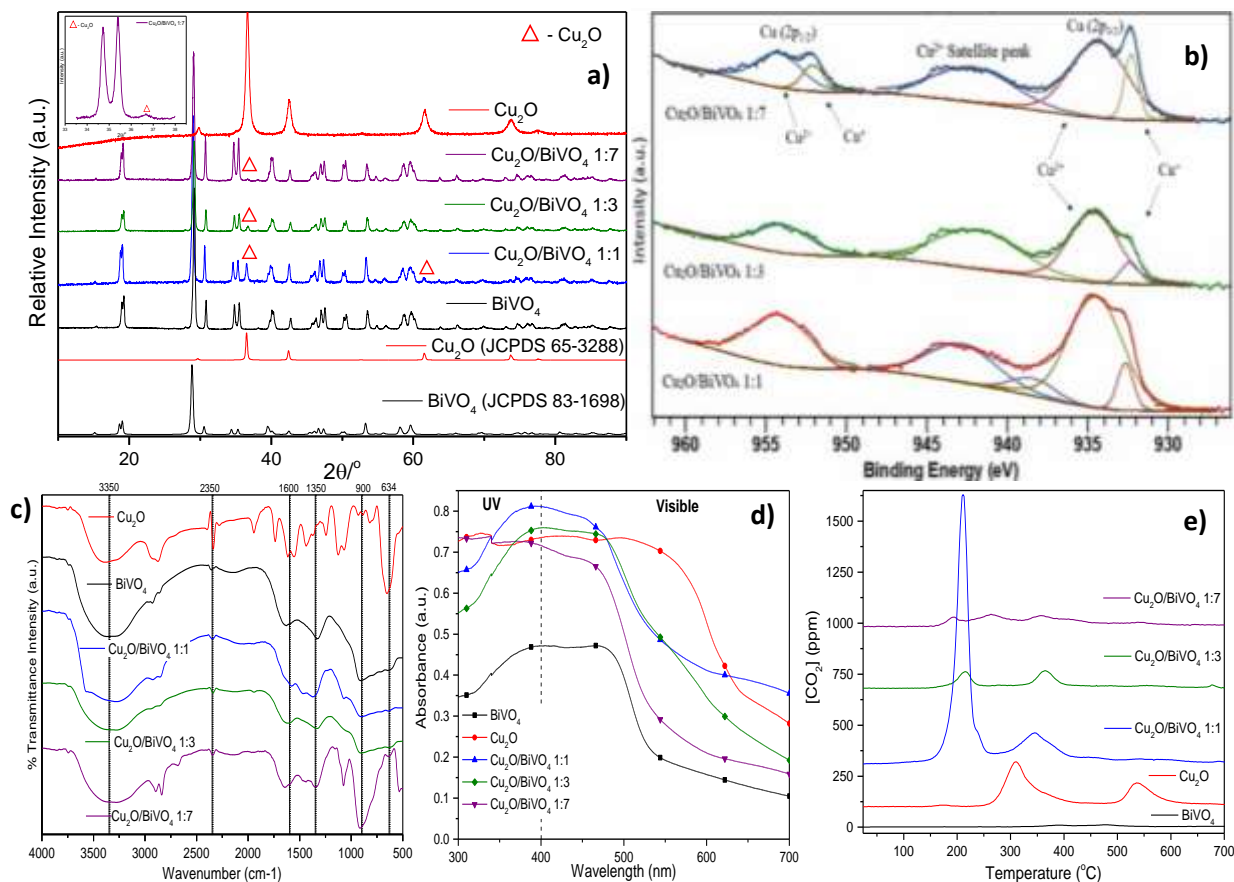


Figure 1. XRD (a), XPS (b), FTIR (c), and UV-Vis DRS (d) spectra, and  $\text{CO}_2$ -TPD (e) from all the prepared materials.

## Conclusions

By decorating a  $\text{BiVO}_4$  surface with  $\text{Cu}_2\text{O}$ , both the extent of visible light absorption and the concentration of  $\text{CO}_2$  that can be adsorbed increase. These characteristics are potentially beneficial to the material's reactivity in promoting artificial photosynthesis and, hence, the composites should demonstrate enhanced reactivity in the AP reaction compared to  $\text{BiVO}_4$ . The presentation will also cover the photoluminescent properties of these materials (where it would be expected that z-scheme materials will have retarded radiative decay processes), the SEM/EDX characterisations (which provide information on the morphology and composition of the particles) and the reactivity of the materials in the AP reaction under batch conditions.

## Acknowledgements

This submission has been supported in part by funding from Science Foundation Ireland (SFI) under grant number 16/RC/3889 and is co-funded under the European Regional Development Fund and by BiOrbic industry partners.

## References

- Zhang, B., Sun, L., Kemi, KTH 2019, *Chemical Society Reviews*, **vol. 48**, no. 7, pp. 2216-2264.
- Zhou, P., Yu, J. & Jaroniec, M. 2014, *Advanced Materials (Weinheim)*, **vol. 26**, no. 29, pp. 4920-4935.
- Natarajan, T.S., Thampi, K.R. & Tayade, R.J. 2018, *Applied Catalysis. B, Environmental*, **vol. 227**, pp. 296-311
- Xu, Q., Zhang, L., Yu, J., Wageh, S., Al-Ghamdi, A.A. & Jaroniec, M. 2018, *Materials Today (Kidlington, England)*, **vol. 21**, no. 10, pp. 1042-1063.
- Chen, Q., Zhou, M., Ma, D. & Jing, D. 2012, *Journal of Nanomaterials*, **vol. 2012**, pp 1-6.
- Zhang, X., Zhang, Y., Wang, D. & Qu, F. 2014, *Journal of Nanomaterials*, **vol. 2014**, pp. 1-6.
- Bai, S., Han, J., Zhao, Y., Chu, H., Wei, S., Sun, J., Sun, L., Luo, R., Li, D. & Chen, A. 2020, *Renewable Energy*, **vol. 148**, pp. 380-387.

## Effect of Interaction between Ru and N dopant in N-doped Titanium Oxide supported Heterogeneous catalyst over CO<sub>2</sub> Hydrogenation to Formate

Kwangho Park

Clean Energy Research Center, Korea Institute of Science and Technology  
5, Hwarang-ro 14-gil, Seongbuk-gu, Seoul, 02792, Republic of Korea

\*kwangho@kist.re.kr

### Abstract text:

Transition of energy sources from the fossil-fuel into renewable energy in the fields of energy and chemical engineering sectors has been urged by the global commitment to mitigate the abrupt climate change caused by global warming. However, due to the intermittency of the natural energy sources and low-efficiency for the long-distance transportation of renewable energy, high-energy and cost effective energy carrier has been explored for decades. In this regard, formic acid is a highly promising hydrogen carrier, which produced from the water electrolysis by renewable electricity, by the virtue of the high gravimetric hydrogen capacity, equal to 53 g·L<sup>-1</sup> and 4.4 wt%, and high volumetric energy density of 7.5 MJ·L<sup>-1</sup>. [1-3] However, the step of H<sub>2</sub> storage, i.e., CO<sub>2</sub> hydrogenation to FA, is lagging because conversion of gaseous CO<sub>2</sub> and H<sub>2</sub> to formic acid is thermodynamically unfavorable. Over the several years, remarkable reaction systems for hydrogenation of CO<sub>2</sub> to FA have been proposed by the electrocatalytic, photocatalytic, and thermocatalytic ways. [4-6] Among them, thermocatalytic hydrogenation by using transition metal-based catalysis has been widely investigated method, by the virtue of high feasibility of scale-up production processes and viability of the reversible conversion of CO<sub>2</sub> and H<sub>2</sub> to FA, and vice versa using the existing industrial infrastructures.

Here, we present a novel heterogeneous Ru single atoms catalysts supported on the N-doped titanium oxide supports for thermocatalytic hydrogenation of CO<sub>2</sub> to formate. The heterogeneous Ru SAC catalysts have been comprehensively characterized through the experimental analysis such as XPS, NEXAFS, EXAFS, and so on. The description on the nature of the catalyst and catalytic performances on the hydrogenation will be considered on on-site presentation. In particular, the effect of the chemical structure of N dopant sites on the catalyst stability will be investigated in-depth based on the experimental results combined with DFT calculation.

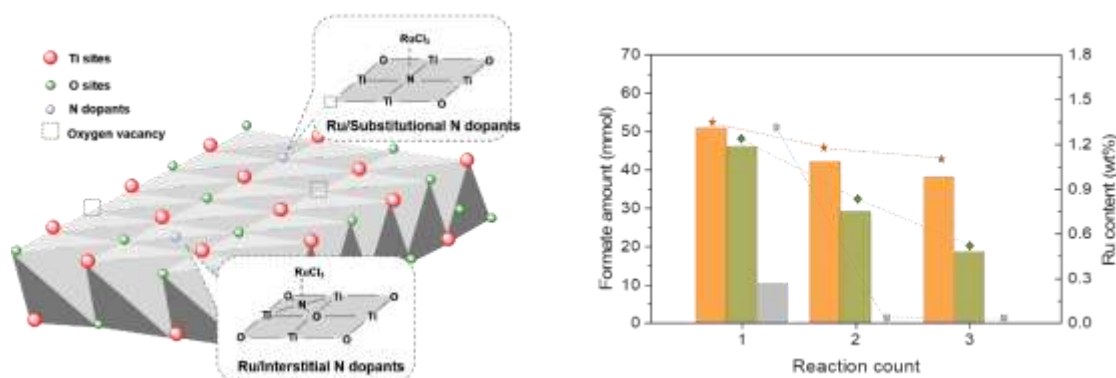


Figure. Schematic representation of the Ru SAC supported on N-doped TiO<sub>2</sub> support and experimental results of catalyst recyclability assessments.

### References

1. S. E. Hosseini and M. A. Wahid, *Renewable Sustainable Energy Rev.*, 2016, 57, 850–866.
2. M. R. Shaner, H. A. Atwater, N. S. Lewis and E. W. McFarland, *Energy Environ. Sci.*, 2016, 9, 2354–2371.
3. P. Häussinger, R. Lohmüller and A. M. Watson, *Ullmann's Encyclopedia of Industrial Chemistry*, 2011.
4. D. Mellmann, P. Sponholz, H. Junge and M. Beller, *Chem. Soc. Rev.*, 2016, 45, 3954–3988.
5. B. Loges, A. Boddien, F. Gärtner, H. Junge and M. Beller, *Top. Catal.*, 2010, 53, 902–914.
6. K. Sordakis, C. Tang, L. K. Vogt, H. Junge, P. J. Dyson, M. Beller and G. Laurenczy, *Chem. Rev.*, 2017, 118, 372–433.

## Design and application of catalytically active hollow-fiber membrane reactors

Julia A. Piotrowska<sup>1\*</sup>, Katharina Bica-Schröder<sup>1\*\*</sup> and Michael Harasek<sup>2</sup>

<sup>1</sup> Technische Universität Wien, Institute for Applied Synthetic Chemistry, Getreidemarkt 9/E163, Austria

<sup>2</sup> Technische Universität Wien, Institute of Chemical, Environmental and Bioscience Engineering, Getreidemarkt 9/E166, Austria

\* julia.kalarus@tuwien.ac.at

\*\* katharina.schroeder@tuwien.ac.at

In order to mitigate deleterious anthropogenic effects of emitted carbon dioxide (CO<sub>2</sub>), various systems for CO<sub>2</sub> capture and storage (CSS) have been developed. Among a wide range of methods such as adsorption, absorption or cryogenic distillation, membrane-based separation processes have attracted a significant interest, due to their mild operating conditions, easy scale-up and low energy consumption [1].

Apart from CO<sub>2</sub> separation, utilization of CO<sub>2</sub> and its conversion into value-added products can be considered as a promising way to reduce the CO<sub>2</sub> level in the atmosphere [2]. Thus, combining the catalytic CO<sub>2</sub> conversion together with the membrane-based separation process, appears as the most comprehensive strategy towards the independence from fossil raw materials and energy sources.

There are several types of membrane modules available, namely plate- and frame- module, spiral wound module, tubular module and hollow fiber module. The most relevant advantage of the hollow fiber module is the possibility of having a very large surface area. Commonly, polymeric hollow fiber membranes are fabricated in the process called non-solvent induced separation (NIPS). NIPS is a well-established method, which allows for the development of fibers with the desired properties, tailored to the specific application. A wide spectrum of polymeric materials can be utilized for the formation of a membrane [3]. Coating of a membrane is one of the most prominent ways to enhance its gas separation performance. Moreover, it is beneficial not only in terms of the gas separation, but the coating may serve also as the immobilization medium for the catalyst [4].

The overall goal of our research is the development of polymeric hollow fiber membranes, followed by their functionalization with catalytically active species for CO<sub>2</sub> conversion. Subsequently, the modified membranes may be applied in the membrane-based reactors, where both separation and catalyzed CO<sub>2</sub> conversion take place simultaneously. In such systems, the equilibrium restrictions can be overcome, resulting in the higher yield of the reaction.

In our experiments we prepared hollow fiber membranes under various spinning conditions. For the polymer dope polyethersulfone (PES) was chosen due to its superior capability for CO<sub>2</sub> separation. Hollow fiber membranes were coated with a solution of Pebax 1657, a block copolymer which is commonly known to improve the separation performance of the membrane. Moreover, the effect of the addition of various ionic liquids to the coating solutions was tested, since they are known to promote the gas separation performance of membranes [5].

Ultimately, morphologies of the coated membranes were characterized by scanning electron microscopy (SEM). Gas separation properties were investigated by the single gas permeation tests. For the reference, the flat sheet membranes have been coated with the analogous coating solutions.

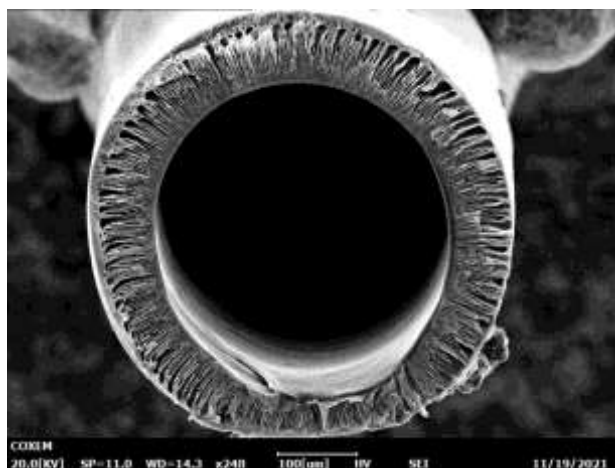


Figure 1. SEM image of the spun PES hollow fiber, coated with Pebax.

## Acknowledgements

Polyethersulfone of different polymerization grades was provided by Sumitomo Chemical Company, whereas the polyethersulfone flat sheet membranes were provided by 3M Deutschland GmbH. The support of the aforementioned companies is gratefully acknowledged. This project has received funding from the European Research Council (ERC) under the European Union's Horizon 2020 research and innovation programme (Grant agreement No. 864991).

## References

1. R.S.K. Valappil, N. Ghasem, M. Al-Marzouqi, *J. Ind. Eng. Chem.*, **2021**, 98, 103-129.
2. A.A. Khan, M. Tahir, *J. CO<sub>2</sub> Util.*, **2019**, 29, 205-239.
3. N. Peng, N. Widjojo, P. Sukitpaneenit, M.M. Teoh, G.G. Lipscomb, T.S. Chung, J.Y. Lai, *Prog. Polym. Sci.*, **2012**, 3(10), 1401-1424.
4. M. Baniamer, A. Aroujalian, S. Sharifnia, *Int. J. Energy Res*, **2020**, 45(2), 2353-2366
5. M. Zia ul Mustafa, H. bin Mukhtar, N.A.H. Md Nordin, H.A. Mannan, R. Nasir, N. Fazil, *Chem Eng Technol*, **2019**, 42(12), 2580-2593

## Conversion of glycidol to glycerol carbonate using Halogen-free bio-based organic salts

Jitpisut Poolwong<sup>1</sup>, Vatcharaporn Aomchad<sup>1</sup>, Silvano Del Gobbo<sup>1</sup>, Arjan W. Kleij<sup>2,3\*</sup> and Valerio D'Elia<sup>1\*</sup>

<sup>1</sup>Department of Materials Science and Engineering, School of Molecular Science and Engineering, Vidyasirimedhi Institute of Science and Technology (VISTEC), 555 Moo 1, 21210, Payupnai, Wangchan, Rayong, Thailand.

<sup>2</sup>Institute of Chemical Research of Catalonia (ICIQ), Barcelona Institute of Science & Technology (BIST), Av. Països Catalans 16, 43007 - Tarragona (Spain).

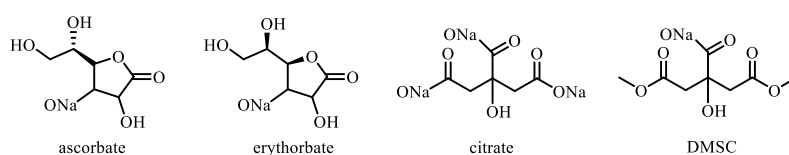
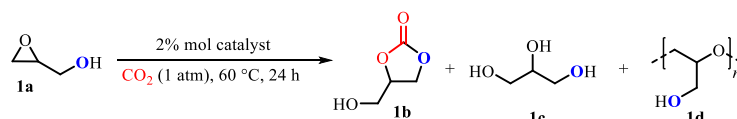
<sup>3</sup>Catalan Institute for Research and Advanced Studies (ICREA), Pg. Lluís Companys 23, 08010 - Barcelona (Spain)

\*valerio.delia@vistec.ac.th, akleij@iciq.es

Nowadays, glycerol carbonate (GC) or 2,4-hydroxymethyl-2-oxo-1,3-dioxolane has obtained much interest due to its several properties such as specific reactivity, biodegradability, lack of toxicity or flammability, solubility in water and low vapor pressure. GC has found a wide range of applications, especially as a building block for the production of chemicals and polymers, organic solvent, a liquid carrier electrolytes in lithium batteries and an additive in cosmetics.<sup>1-3</sup> GC can be synthesized by several routes such as glycerol reacts with dimethyl carbonate<sup>4</sup> and cycloaddition of CO<sub>2</sub>. In this work, we are interested in utilization of CO<sub>2</sub> to glycidol to produce glycerol carbonate under mild and neat condition by using bio-based materials as a catalyst<sup>5</sup>.

Chemicals and method: Sodium ascorbate was purchased from TCI. Sodium citrate and sodium erythorbate were purchased from Krungthepchemi Co., Ltd. Carbon dioxide (>99.995%) was purchased from Bangkok industrial gas (BIG). All reagents were stored under ambient conditions. NMR spectra were measured on an automated "Bruker" 600 MHz for <sup>1</sup>H (125 MHz for <sup>13</sup>C). Reactions under ambient pressure (CO<sub>2</sub> balloon): the glycidol 1a (25 mmol) was charged in a 50 mL round bottom Schlenk and equipped with a magnetic stirrer, followed by the addition of the suitable amount of catalyst. A rubber balloon containing about 2 L CO<sub>2</sub> was connected to the Schlenk flask and part of the CO<sub>2</sub> was used to flush the flask in order to replace the air and stirred for 24 h. After this period, an aliquot of the reaction mixture was analyzed by <sup>1</sup>H NMR spectroscopy in DMSO-d<sub>6</sub> or CDCl<sub>3</sub> to determine glycidol conversion and 1b selectivity after the addition of a known amount of 1,3,5-trimethylbenzene as a standard. Reactions performed in an autoclave: the same reaction mixture as described above was prepared in a 120 mL stainless steel autoclave equipped with magnetic stirrer, after which CO<sub>2</sub> gas from a cylinder was added into the autoclave at the desired pressure. The mixture in the autoclave was stirred for 24 h at the temperature of choice. Hereafter, the excess of CO<sub>2</sub> in the reactor was carefully vented and an aliquot of the reaction mixture was analyzed by <sup>1</sup>H NMR spectroscopy in DMSO-d<sub>6</sub> or CDCl<sub>3</sub> to determine glycidol conversion and 1b selectivity after the addition of 1,3,5-trimethylbenzene as a standard<sup>5</sup>.

Table 1. Screening of biobased homogeneous catalysts for the cycloaddition of CO<sub>2</sub> to glycidol 1a under atmospheric pressure conditions.<sup>a</sup>



Entry	Catalyst	Solubility	Glycidol source	1a Conversion (%) <sup>b</sup>	1b Selectivity (%) <sup>b</sup>	pK <sub>b</sub> of anion
1	Na-ascorbate	soluble	commercial	100	64±5	9.8
2	Na-erythorbate	soluble	commercial	100	79±1	9.96
3	Na <sub>3</sub> -citrate	partial	commercial	100	90±3	7.6 <sup>c</sup>
4 <sup>d</sup>	DMSC	soluble	commercial	100	26±2	10.87 <sup>e</sup>

<sup>a</sup> Glycidol (25 mmol), catalyst (2 mol%), 60°C, 1 bar CO<sub>2</sub> (balloon), 24 h. <sup>b</sup> Determined by <sup>1</sup>H NMR using 1,3,5-trimethylbenzene as a standard. <sup>c</sup> pK<sub>b1</sub> of the citrate anion. <sup>d</sup> 1,5-dimethyl mono-sodium citrate (DMSC) was used. <sup>e</sup> Value based on the pK<sub>b3</sub> of the citrate anion.

The catalytic performance of various bio-based salts as homogeneous catalysts. These catalysts were tested through the CO<sub>2</sub> fixation reaction. We selected this kind of catalysts due to its inexpensiveness, nontoxicity and being renewable. The

selected bio-based homogeneous catalysts were screened for catalytic activity using the cycloaddition of CO<sub>2</sub> to glycidol (**1a**) as a benchmark reaction (Table 1). The reaction was carried out under ambient conditions (60 °C, CO<sub>2</sub> balloon). Among of these catalysts, sodium citrate exhibits the best catalytic conversion of glycidol (**1a**) with the highest selectivity to yield glycerol carbonate (**2b**) as a major product. From the catalytic performance result of sodium citrate. We choose sodium citrate to study the conversion of other epoxy alcohols (Table 2). The cycloaddition of other epoxy alcohols was studied under more demanding reaction conditions than **1a**.

Table 2. Optimization conditions of sodium citrate homogeneous catalysts for the cycloaddition of CO<sub>2</sub> to differently substituted epoxy alcohol.<sup>a</sup>

Entry	Substrates	Conversion (%)	Selectivity b (%)	Selectivity c (%)	Selectivity d (%)
1	4a	>99.9	10	77	13
2	5a	76	31	69	-
3 <sup>b</sup>	6a	77	70	30	-
5 <sup>c</sup>	7a	22	37	63	-

<sup>a</sup> Substrates (25 mmol), catalyst (4 mol%), 60°C, 10 bar CO<sub>2</sub>, 24 h. <sup>b</sup> At 80°C. <sup>c</sup> At 30 bar, 72 h.

Substrate **4a** was used to study, the result shows sodium citrate can catalyze this reaction with fully conversion of **4a** to produce two carbonate products **4b** and **4c**, and a triol **4d**. In the case of substrates **5a** and **6a** were used to probe the catalytic performance of sodium citrate. The results exhibit good conversion 76 and 77%, respectively. The products mixture of two isomers of cyclic carbonate (**6b** and **6c**) were observed. Finally, sodium citrate was used to test catalytic performance with the challenging sterical substrate **7a**, which required harsher condition with 30 bar CO<sub>2</sub> and 72 h. Under this condition, 22% conversion of **7a** was observed. These results are in good agreement that biobased sodium citrate catalyst shows the performance for the conversion of other epoxy alcohol without any halide additives.

## Acknowledgements

V. D. E. thanks the National Research Council of Thailand (grants N41A640170 and N42A650196) for supporting this research. A. W. K. is grateful to the Cerca program/Generalitat de Catalunya, ICREA, Ministerio de Ciencia e Innovación (PID2020-112684GB-100 and Severo Ochoa Excellence Accreditation 2020–2023 CEX2019-000925-S).

## References

- Z. Wang, R. Gérardy, G. Gauron, C. Dambon and J.-C. M. Monbaliu, *Reaction Chemistry & Engineering*, 2019, **4**, 17-26.
- M. O. Sonnati, S. Amigoni, E. P. Taffin de Givenchy, T. Darmanin, O. Choulet and F. Guittard, *Green Chemistry*, 2013, **15**, 283-306.
- N. Yadav, F. Seidi, D. Crespy and V. D'Elia, *ChemSusChem*, 2019, **12**, 724-754.
- L. T. Thanh, K. Okitsu, L. V. Boi and Y. Maeda, *Catalysts*, 2012, **2**.
- J. Poolwong, V. Aomchad, S. Del Gobbo, A. W. Kleij and V. D'Elia, *ChemSusChem*, 2022, **n/a**.

## Preparation of CO<sub>2</sub> sorption pellets from polyaniline using microwave heating

Milena Šetka<sup>1\*</sup>, Albert Behner<sup>1</sup> and Miroslav Šooš<sup>1</sup>

<sup>1</sup> Department of Chemical Engineering, University of Chemistry and Technology, Technická 3, 166 28 Prague 6 – Dejvice, Czech Republic

\*setkam@vscht.cz

The porous nitrogen-doped carbons (N—C) have been intensively studied and exploited in various applications such as gas sorption and separation, energy storage, catalysis, etc (1). The common synthesis procedure for the N—C is based on the annealing treatment of carbon precursor at a high temperature (>500 °C) for a long period (from one to tens of hours). The energy consumption of 170–200 kWh is roughly estimated for the preparation of 1 ton of N—C resulting in the emission of 127.5–150 kg of CO<sub>2</sub> (2). The entire synthesis procedure of the N—C has a negative environmental impact. Therefore, employing alternative energy sources such as microwave irradiation can reduce energy usage and ensure a more environmentally sustainable and economically viable synthesis approach for the widely applicable materials such as N—C. This procedure requires the use of non-transparent materials to electromagnetic waves that can convert microwave energy into heat and simultaneously enable the carbonization of the starting material (2). In this work, we compared the preparation of the N—C derived from polyaniline (PANI) using thermal and microwave heating and tested the properties of these materials as a CO<sub>2</sub> sorbent. PANI was selected due to two reasons: (i) it has been demonstrated that N—C made of PANI showed good CO<sub>2</sub> adsorption capacity (3) and (ii) PANI is a good microwave adsorption material with the loss tangent ( $\tan \delta = \varepsilon'' / \varepsilon'$ ) value of 0.15, where  $\varepsilon''$  and  $\varepsilon'$  are dielectric constant and dielectric loss, respectively.

The chemical oxidative polymerization at a low temperature (4 °C) was used for the synthesis of PANI using the modified synthesis procedure from the literature (4). Aniline (7.5 ml) was dissolved in the solution of hydrochloric acid (75 ml of 1M HCl) and stirred for 30 min. In the next step, the solution of ammonium persulfate (292.5 ml with a concentration of 0.28 mol/L) was added with a speed rate of 5 ml/min, and the reaction mixture was stirred (500 RPM) for 4 hours. The suspension of PANI aggregates was left for overnight precipitation. The final PANI material in the form of the pellets was formed using vacuum filtration and later dried at 80 °C and pressure of 200 mbar for 24 hours. The PANI pellets with a mass of 10 g were produced in a batch containing 375 ml in total volume (see **Figure 1a**). The diameter, shape and thickness of the PANI pellet were influenced by the dimensions of the filtration funnel and the total volume of synthesized polymer solutions, respectively. This production method of PANI pellets is considered a simple and scalable procedure in comparison to the state-of-art approaches (3).

In order to form N—C, the PANI pellets were carbonized using both thermal and microwave heating (samples further called N—C\_PANI). In case of thermal heating, the PANI pellets were placed in the ceramic annealing crucibles with the lid and carbonized at a temperature range of 500-800 °C in the air environment. The heat rate of 10°C/min was used and the samples were kept at the target temperature for 1 min. After the heating was switched off, the samples were left in the oven till the temperature dropped under 150 °C. For the microwave heating, the carbonization of PANI pellets was performed in the microwave oven (SAMSUNG MS23F301TAS/EO), where different power (300, 450 and 800 W) and times (70, 140 and 210 s) of carbonization were investigated. The cooling time was 2 min after the microwave heating.

The aim of this work was to determine the influence of the thermal and microwave carbonization on the morphology, chemical composition and absorption properties of the N—C\_PANI samples. The transformation in the morphology was noticed in the N—C\_PANI in comparison with the PANI (Figure 1B) samples after both thermal (Figure 1C) and microwave (Figure 1D) carbonization. Also, the chemical changes were confirmed by Fourier-transform infrared spectroscopy (FTIR) where several new features were displayed in the FTIR spectra of N—C\_PANI. These modifications were connected with the breaking of PANI bonds and their cross-linking that resulted in the formation of carbon networks doped with nitrogen, as was early reported in the work of Rozlívková et.al (5). The highest similarities in chemical composition were observed for the samples carbonized thermally at 800 °C (N—C\_PANI\_800°C) and under microwave irradiation with the power of 450 W and time of 140 s (N—C\_PANI\_450W\_140s). Both samples showed three characteristic absorbance bands in the FTIR spectra (see **Figure 2**). The band around 3430 cm<sup>-1</sup> is described as the resonance of —O—H band or —NH— stretching vibration of secondary amine groups. The bands occurring in the range of 1589-1608 cm<sup>-1</sup> and 1250-1261 cm<sup>-1</sup> are related to quinoid ring stretching and sp<sup>3</sup> carbon that is complementary with sp<sup>2</sup> G and D-bands in Raman spectra with the contribution of C=N and C—N groups, respectively (5). The samples of N—C\_PANI\_800°C and N—C\_PANI\_450W\_140s showed a similar CO<sub>2</sub> capacity performance reaching the values of 3.8 and 4 mmol g<sup>-1</sup> at the pressure of 1 bar and temperature of 0°C, respectively.

This work demonstrated the possibility of the preparation of PANI pellets with a mass of hundreds of grams by the simple approach of vacuum filtration. The successful production of N—C from PANI was achieved using microwave carbonization as a simplified approach with a low energy utilization and exceptionally rapid processing times. The material prepared by microwave heating showed similar properties to the thermal one in terms of morphology, chemical composition and CO<sub>2</sub> sorption capacity. Therefore, these results suggested the possibility for thermal carbonization substitution with more environmentally sustainable approach of the microwave heating.



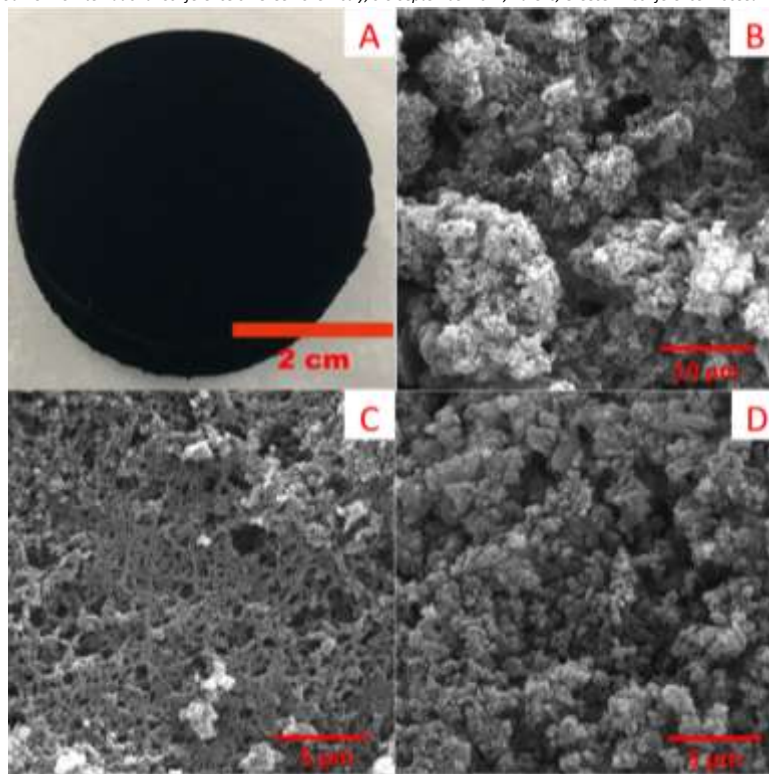


Figure 1. The photography of PANI monolith prepared by vacuum filtration (A). Scanning Electron Microscopy images of the PANI (B) and N—C\_PANI after thermal carbonization at 800°C (C) and microwave carbonization at 450W for 140s (D).

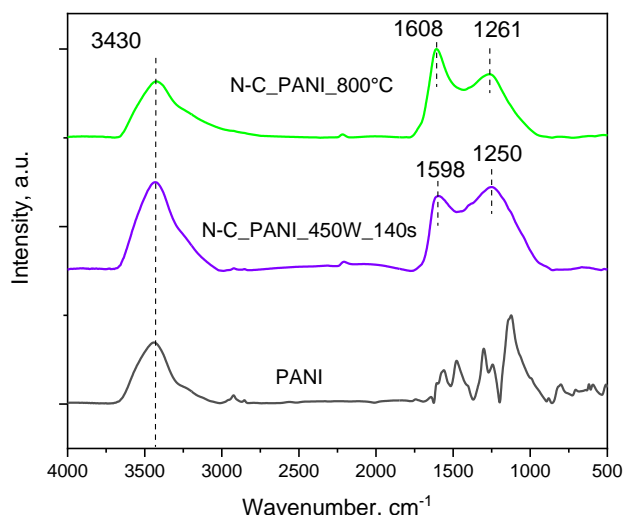


Figure 2. Comparison of FTIR spectra for PANI and carbonized PANI during thermal heating at 800 °C for 1 min with the heating ramp of 10°C/min (N—C\_PANI\_800°C) and microwave heating at 450 W for 140 s (N—C\_PANI\_450W\_140s).

## Acknowledgments

This work was supported by the Technology Agency of the Czech Republic (TAČR), via Grant No. TO01000329, and Junior Grand of UCT Prague, via Grant No. 409 85 2221.

## References

1. Inagaki M, Toyoda M, Soneda Y, Morishita T., Nitrogen-doped carbon materials, *Carbon*, **132** (2018).
2. Glowniak S, Szczesniak B, Choma J, Jaroniec M., Advances in Microwave Synthesis of Nanoporous Materials, *Adv Mater*, **33** (2021).
3. Kutorglo EM, Kovacovic J, Trunov D, Hassouna F, Fucikova A, Kopecky D, et al., Preparation of carbon-based monolithic CO<sub>2</sub> adsorbents with hierarchical pore structure, *Chemical Engineering Journal*, **388** 12 (2020).
4. Liu S, Zhang Z, Huang F, Liu Y, Feng L, Jiang J, et al., Carbonized polyaniline activated peroxymonosulfate (PMS) for phenol degradation: Role of PMS adsorption and singlet oxygen generation, *Applied Catalysis B: Environmental*, **286** (2021).
5. Rozlívková Z, Trchová M, Exnerová M, Stejskal J., The carbonization of granular polyaniline to produce nitrogen-containing carbon. *Synth Met*, **161** 11 (2011).

## Utilization of CO/CO<sub>2</sub>-containing industrial process gas into valuable polyurethane building blocks

Deepika Tyagi<sup>a</sup>, Suresh Raju<sup>a</sup>, Martin R. Machat,<sup>\*ab</sup> Christoph Guertler,<sup>\*ab</sup> Walter Leitner<sup>\*ac</sup>

<sup>a</sup>RWTH-Aachen University, CAT Catalytic Center, Worringer Weg 2, 52074 Aachen, Germany

<sup>b</sup>Covestro Deutschland AG, Kaiser-Wilhelm-Allee 60, 51368 Leverkusen, Germany.

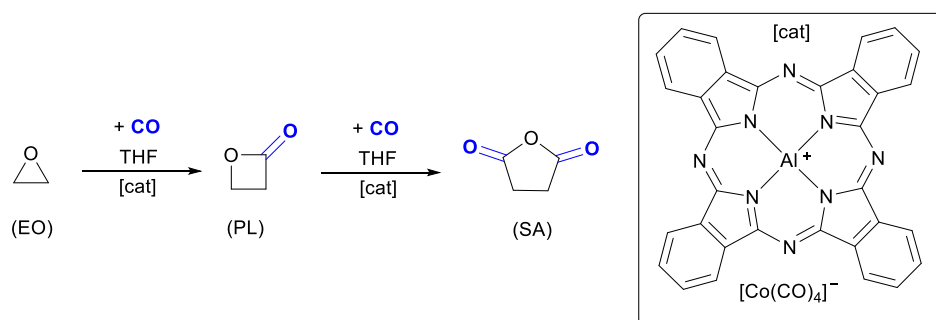
<sup>c</sup>Max-Planck-Institut für Chemische Energiekonversion,

Stiftstraße 34-36, 45470 Mülheim an der Ruhr, Germany

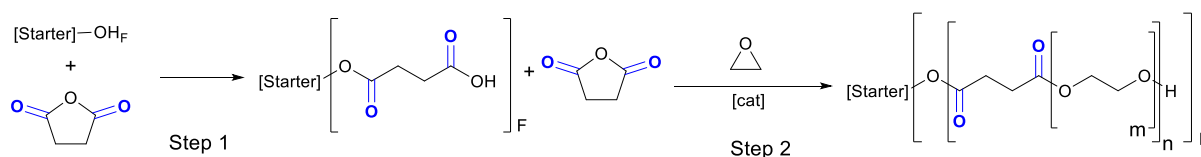
\*martin.machat@covestro.com, deepika.tyagi@catalyticcenter.rwth-aachen.de

### Abstract

The current goal of the chemical industries is to become less dependent on fossils as a source of carbon and rely more on renewable carbon resources. At the same time, it is important to reduce the greenhouse gas emissions by decarbonization. In this regard, the EU-funded Carbon4PUR project [1] aimed to utilize CO/CO<sub>2</sub>-containing industrial process gas (blast furnace gas) from the steel industry to produce valuable building blocks for the polyurethane (PUR) industry. The chemical process to utilize this mixed CO/CO<sub>2</sub>-containing gas stream is built up by a sequence of consecutive technologies starting with Covestro's industrially established CO<sub>2</sub>-technology that facilitates the catalytic conversion of CO<sub>2</sub> with propylene oxide to produce polyether-carbonate polyols along with a CO<sub>2</sub>-depleted gas stream [2, 3]. In the second step, selective CO conversion takes place with this stream realizing a catalytic ring-expansion carbonylation of epoxides to lactones and cyclic anhydrides.<sup>3</sup> These diacid derivatives in the presence of starter molecules are used as building blocks for polyether ester polyols, which are essential components for the formation of rigid construction foams. This work demonstrates the first proof of concept of the individual chemical conversion steps of the Carbon4PUR process from lab to technical scale with a particular focus on the final industrial applicability [1-3].



Scheme 1. Carbonylation of ethylene oxide (EO) with CO to  $\beta$ -propiolactone (BPL) and succinic anhydride (SA) in two steps using  $[Pc-Al][Co(CO)_4]$  as a carbonylation catalyst.



Scheme 2. <sup>tert</sup>Amine-catalyzed co-polymerization of SA and EO to yield a polyether ester polyol. Ring-opening reaction of SA with the OH functionalized starter molecule occurs already in the absence of a catalyst forming a Brønsted acid in step 1. Upon addition of EO, copolymerization of SA and EO takes place, both autocatalytic and amine-catalyzed in step 2.



Figure 1. Rigid PIR-foams on lab-scale utilizing Carbon4PUR polyol made from CO-derived SA produced by carbonylation and commercially obtained SA.

Herein we report: (a) The synthesis of epoxide double carbonylation catalysts and the chemical conversion of CO<sub>2</sub> by adapting Covestro's industrially established CO<sub>2</sub>-technology on mixed CO/CO<sub>2</sub>-containing gas streams. (b) Utilization of CO as feedstock for a carbonylation process to selectively convert epoxides to cyclic lactones and anhydrides as intermediates for the polymer industry. (c) Utilization of cyclic anhydrides for the production of sustainable polyester polyols for PUR applications like rigid construction foam or wood coatings (Figure 1).

### Acknowledgements

This project has received funding from the European Union's Horizon 2020 research and innovation program under grant agreement no. 768919. The authors would like to thank all colleagues and partners those have been involved in the project.

### References

1. Horizon 2020, Carbon4PUR Project: <https://www.carbon4pur.eu/>
2. J. Langanke, A. Wolf, J. Hofmann, K. Böhm, M. A. Subhani, T. E. Müller, W. Leitner and C. Gürtler, *Green Chem.*, **16**, 1865 (2014).
3. M. R. Machat, J. Marbach, H. Schumacher, S. Raju, M. Lansing, L. C. Over, L. Adler, J. Langanke, A. Wolf, W. Leitner and C. Gürtler, *React. Chem. Eng.*, **7**, 580 (2022).

## Carbon Nanostructures Obtained through CO<sub>2</sub> Utilization

Michail Vagenas<sup>1,2\*</sup>, Niki Plakantonaki<sup>1</sup>, Tatiana Giannakopoulou<sup>1</sup>, Nadia Todorova<sup>1</sup>, Ilias Papailias<sup>1</sup>, Christos Argirusis<sup>2</sup> and Christos Trapalis<sup>1</sup>

<sup>1</sup>*Institute of Nanoscience and Nanotechnology, National Centre for Scientific Research "Demokritos", Patriarkou Grigoriou E & Neapoleos 9, 15341, Attika, Greece*

<sup>2</sup>*School of Chemical Engineering, National Technical University of Athens, Heroon Polytechniou 9, 15773 Zografou, Greece*

\**m.vagenas@inn.demokritos.gr*

Anthropogenic carbon dioxide (CO<sub>2</sub>) emissions threaten the preservation of our everyday life conditions as we know them. Conversion of CO<sub>2</sub> into value-added products poses a powerful alternative towards a low-carbon economy. Progress has been made through the recent decades to obtain functional chemicals utilizing CO<sub>2</sub>. On the other hand, demand for nanocarbon materials (NCMs) in industries is highly accelerating due to their long-term stable life cycle, as well as large surface area, high electrical conductivity, low production cost, and superior chemical, thermal and mechanical stability. NCMs fabricated through CO<sub>2</sub> conversion is a new promising technology offering products with physicochemical properties suitable for a wide range of applications [1]. Alkali and alkaline-earth reducers have been utilized towards this direction. Magnesiothermal technology, evaluating CO<sub>2</sub> as a feedstock is emerging, mainly due to the low cost of Mg, its high availability and the lowest free energy of reduction reaction Mg exhibiting among the other alkaline earth metals [2-3]. Moreover, no extreme pressure needs to be applied, thus making the process facile and scalable.

Low-dimensional carbon materials, as for example graphene, carbon nanofibers (CNFs) and carbon nanotubes (CNTs) derived from CO<sub>2</sub> reduction is a promising and economically viable way towards a CO<sub>2</sub> utilization. In this study, we investigate the impact of reduction duration on the yield and the physicochemical properties of nanocarbon products. Experiments were conducted in quartz tube furnace, heating Mg at 675 °C under constant CO<sub>2</sub> flow. The resultant products' physicochemical properties were characterized, both before and after by-product removal, by X-Ray diffraction (XRD) analysis, scanning electron microscopy (SEM) and Raman spectroscopy. Changing the exposure time of Mg to CO<sub>2</sub> from 10 to 60 mins, NCMs with different shape and morphology were obtained during the reduction reaction.

### Acknowledgements

The authors appreciate the financial support from the project "T1EDK-01729 CARBONGREEN" (MIS 5848538) co-financed by the European Union and Greek national funds through the Operational Program Competitiveness, Entrepreneurship and Innovation, under the call RESEARCH-CREATE-INNOVATE.

### References

1. T. Giannakopoulou, G. Pilatos, N. Todorova, N. Boukos, T. Vaimakis, I. Karatasios, C. Trapalis, *Materials Today Chemistry*, **19** 100388 (2021).
2. H. Zhang, X. Zhang, X. Sun, Y. Ma, *Sci Rep*, **3** 3534 (2013).
3. A. Dabrowska, A. Huczko, S. Dyjak, *Physica Status Solidi B*, **249** 2373 (2012).

## Hybrid energy storage based on CO<sub>2</sub> capture and renewable energy sources (RES); Construction and operation of a novel flue gas storage and supply system

Petros Gkotsis<sup>1</sup>, Manassis Mitrakas<sup>2</sup> and Anastasios Zouboulis<sup>1,\*</sup>

<sup>1</sup>Laboratory of Chemical and Environmental Technology, Department of Chemistry, Faculty of Sciences, Aristotle University of Thessaloniki, 54124, Thessaloniki, Greece; [petgk@chem.auth.gr](mailto:petgk@chem.auth.gr); [zoubouli@chem.auth.gr](mailto:zoubouli@chem.auth.gr)

<sup>2</sup>Analytic Chemistry Laboratory, Department of Chemical Engineering, School of Engineering, Aristotle University of Thessaloniki, 54124, Thessaloniki, Greece; [mmitraka@cheng.auth.gr](mailto:mmitraka@cheng.auth.gr)

\*Correspondence: [zoubouli@chem.auth.gr](mailto:zoubouli@chem.auth.gr)

### Abstract:

The present work is part of a circular economy LIFE project (acronym: CO<sub>2</sub>toCH<sub>4</sub>), aiming to develop and demonstrate an innovative hybrid energy storage unit, based on renewable energy sources (RES) and the Capture, Sequestration and re-Utilization of carbon dioxide (CCSU) from typical power plant flue/waste gases, burning fossil fuels (in this case: lignite). This prototype pilot unit will consist of four sub-units: (1) an electrolyser for the production of green hydrogen from water electrolysis, by using preferentially RES, (2) a specially designed process for the initial sequestration/storage and the subsequent supply of the flue gases, as directly received from the chimney, (3) a flue gas purification sub-unit for the effective separation of CO<sub>2</sub> from the flue gases, leading to a CO<sub>2</sub>-rich gaseous stream, and (4) an ex-situ bio-methanation unit for the conversion of CO<sub>2</sub> to methane, with the use of appropriate microorganisms and after its reaction with the H<sub>2</sub> obtained from the electrolyser.

The present work focuses mainly on the construction, installation and operation of the second integral sub-unit of the aforementioned prototype pilot unit, which aims at the initial storage and supply of the flue gases from the power plant of Public Power Corporation (PPC), located near the region of Agios Dimitrios (Kozani, N.-W. Greece). This sub-unit will be composed mainly from the following sub-parts: (i) a washing water column, for the initial cooling of flue gases and the partial removal of moisture and Suspended Solids (SS), (ii) an air cooling (refrigeration) unit, to remove the remaining moisture, (iii) a vacuum pump, for pumping the flue gases from the previous units, (iv) an air compressor, for the compression of the flue gases to up to 5 bars, and v) the final CO<sub>2</sub> storage tank. An appropriate electrical control and automation system will be also utilized in order to allow the remote monitoring and control of all equipment with reduced human intervention. With this novel flue gas storage and supply system, it is expected that at least 400 m<sup>3</sup> of flue gases will be collected and stored per month for further utilization in the bio-methanation unit, corresponding to the low flow rate of 0.5-0.6 m<sup>3</sup>/h, as compared with the total flue gases flow rate in the chimney, which is approximately 1,200,000 m<sup>3</sup>/h.

### Keywords

CO<sub>2</sub> Capture, Sequestration and re-Utilization (CCSU); flue gases storage and cleaning system; circular economy

### Acknowledgements

The “Demonstration of a mobile unit for hybrid energy storage based on CO<sub>2</sub> capture and renewable energy sources (LIFE CO<sub>2</sub>toCH<sub>4</sub>)” project has received funding from the LIFE Programme of the European Union.



# Computational Chemistry towards greener chemical processes

## Betanidin zwitterionic and nonionic dimer conformers towards DSSCs application: A DFT investigation to optoelectronic and charge transfer properties

Rene Costa\*<sup>1,2,3</sup> Ohoud S. Al-Qurashi<sup>4</sup> Nuha Wazzan<sup>5</sup> Alexander Pogrebnoi<sup>1</sup> Tatiana Pogrebnyaya<sup>1</sup>

<sup>1</sup>Department of Materials and Energy Science and Engineering, School of Materials, Energy, Water and Environmental Sciences, The Nelson Mandela African Institution of Science and Technology, P. O. Box 447 Arusha, Tanzania

<sup>2</sup>Department of Physical and Environmental Sciences, Faculty of Science, Technology and Environmental Studies, The Open University of Tanzania, P. O. Box 23409 Dar es Salaam, Tanzania

<sup>3</sup>Tabora Regional Centre, The Open University of Tanzania, P. O. Box 1204 Tabora, Tanzania

<sup>4</sup>Department of Chemistry, Faculty of Science, University of Jeddah, Jeddah 21959, Saudi Arabia

<sup>5</sup>Department of Chemistry, Faculty of Science, King Abdulaziz University, Jeddah 21589, Saudi Arabia

\*Corresponding email: [renec@nm-aist.ac.tz](mailto:renec@nm-aist.ac.tz) / [costarene9@gmail.com](mailto:costarene9@gmail.com)

### Abstract

Betanidin structural conformers contain zwitterionic and nonionic moieties. The isolated and cluster systems of dye dimer conformers are investigated using density functional theory (DFT). Conformers enable the evaluation of their unique characteristics, which may be advantageous in future dye-sensitised solar cells (DSSCs). We examined the properties of the isomerisation reaction that predominates in equilibrium vapour between conformers. The spectro-electrochemical, optoelectronic, and thermodynamic properties of betacyanin dimers using betanidin as the building block are determined using molecular simulation and modelling. This ongoing effort addresses three critical issues regarding betacyanin dimer materials and their use as dimer conformers in DSSCs. To begin, how do zwitterionic and nonionic betacyanin dimers differ structurally? Second, which of the materials is more zwitterionic or nonionic toward the betacyanin dimer? Third, which of the materials is a zwitterionic or nonionic betacyanin dimer, indicating the possibility of aligning energy levels? Diverse conformer dimer architectures enable the realisation of a broad range of desired properties and necessitate a greater understanding of zwitterionic and nonionic betacyanin dimer materials to establish design concepts applicable to DSSCs. Additionally, the design concepts derived from these simulation studies were used to build the DSSCs application. Our work provides a rational insight into the logical design of required conforming moieties compared to betacyanin monomer.

**Keywords:** betacyanin dimer; zwitterionic betanidin dimer; nonionic betanidin dimer

## Development of bioplastic disposable food packaging from starch and cellulose

Lidya Hailu<sup>1</sup>, Ramesh Duraisamy<sup>2</sup>, Masood Akhtar Khan<sup>2</sup> and Belete Yilma<sup>2</sup>

<sup>1</sup>Department of chemistry, Debre Tabor University, Ethiopia

<sup>2</sup>Department of chemistry, Arba Minch University, Ethiopia

\*Corresponding author: E-mail: lidiyahailu1@gmail.com

Tel.: +251920917248

### Abstract

**Introduction:** Disposable food packaging is a single-use plastics that can include any disposable plastic item which could be designed and use only once. Waste is also increasing rapidly with the increasing mass consumption of products with a short life span. Researchers focused towards developing bioplastic, however, mostly used natural recourses are edible food such as corn, rice and potato which can create the problem of food security.

**Objective:** This study aimed to prepare and evaluate bioplastic food packaging material from avocado seed starch and sugarcane bagasse cellulose.

**Methodology:** Bioplastic food packaging material was prepared from avocado seed starch and sugarcane bagasse cellulose (0, 5, 10, 15w/w%) and glycerol as a plasticizer with various amount of 3, 4, 5mL through solution casting technique. Physico-mechanical, structural, thermal properties, and biodegradability characterization of prepared bioplastic was performed using the universal tensile testing machine, FTIR, UV - V is spectroscopy, and SEM.

**Results:** Results have shown that an increasing amount of glycerol resulted in increases in water absorption, density, water vapor permeability, and elongation at break of prepared bioplastic. However, it causes decreases in %transmittance, the tensile strength of prepared bioplastic. Likewise, the addition of cellulose fiber (0-15%) increases %transmittance ranged ( $91.34 \pm 0.12 - 63.03 \pm 0.05\%$ ), density ( $0.93 \pm 0.04 - 1.27 \pm 0.02 \text{g/cm}^3$ ), tensile strength ( $2.91 \pm 6.18 - 4.21 \pm 6.713 \text{MPa}$ ) of prepared bioplastic. On the other hand, it causes decreases in water absorption ( $14.4 \pm 0.25 - 9.40 \pm 0.007\%$ ), water vapor permeability ( $9.306 \times 10^{-12} \pm 0.3 - 3.57 \times 10^{-12} \pm 0.15 \text{g} \cdot \text{s}^{-1} \cdot \text{m}^{-1} \cdot \text{Pa}^{-1}$ ) and elongation at break ( $34.46 \pm 3.37 - 27.63 \pm 5.67\%$ ) of prepared bioplastic. All prepared bioplastic films completely degraded within 15 days under open soil atmosphere.

**Conclusion:** Studied results showed starch bioplastic reinforced with 15 % cellulose plasticized with 3 mL of glycerol had improved results than other combinations of glycerol and cellulose with avocado seed starch. Thus, biodegradable disposable food packaging materials have been successfully produced by employing avocado seed starch and sugarcane bagasse cellulose.

**Key Words:** Avocado seed; Bioplastic; Cellulose; Food packaging; Glycerol.



## Physiological Regulation of Antifungal Properties of Agaricomycetes Mushroom *Schizophyllum commune*

Tamar Khardziani\*, Violeta Berikashvili, Eka Metreveli, Aza Kobakhidze, Eva Kachlishvili, Vladimir Elisashvili, Mikheil Asatiani

The Institute of Microbial Biotechnology, Agricultural University of Georgia, Tbilisi, Georgia

\*e-mail address of corresponding author: [t.khardziani@agruni.edu.ge](mailto:t.khardziani@agruni.edu.ge)

Keywords: higher basidiomycetes, plant pathogenic fungi, antifungal properties, submerged fermentation

### Abstract text:

Nowadays, the search for natural sources of novel and effective antifungal substances became necessary, which is caused by intensive application of synthetic fungicides. It has been proven that synthetic fungicides caused considerable concern, primarily due to the environmental pollution, toxicity and carcinogenic effect of synthetic compounds found in food after fungicide application. In the present study, twenty two higher basidiomycetes isolated from various ecological niches of Georgia and belonging to different taxonomic groups were screened for their activities against phytopathogenic fungi such as *Aspergillus niger* and *Fusarium oxysporum*. For cultivation of tested mushroom species and for expression of antifungal potential submerged (SF) fermentation of different plant raw materials were performed and various approaches and strategies have been exploited. During screening program, among all tested mushroom species Agaricomycete mushroom *Schizophyllum commune* demonstrate most promising antifungal activity grown on glucose contained synthetic medium (50% and 36% respectively). The study of physiological factors that enhance antifungal activity was provided. For this reason different carbon sources (in concentration 4%) such as maltose, glucose, xylose and mannitol were tested. It should be noted that almost all tested carbon sources demonstrate similar antifungal activities and varied from 45% to 50% against *A. niger* and from 54% to 57% against *F. oxysporum*. Different lignocellulosic wastes such as, mandarin juice productin waste (MJPW), wheat straw (WS), banana peels (BP) corn cobs (CC), ethanol production waste (EPR), and wheat bran (WB) were tested. It was shown, that 4% of appeared as a best substrate and demonstrate increase of antifungal activity (57% and 45% respectively). Beside this optimal concentration of MJPW was determined. The presence of 6% MJPW in nutrient medium demonstrate 69% and 73% of antifungal activity. Moreover, 6% of peptone appeared as a best nitrogen source. The presence of yeast extract in concentration 6% were most appropriate source for antifungal properties of *Sch. commune*. The results obtained show that *Sch. commune* can be considered as a promising source of antifungal bioactive substances. The antifungal activity of mushrooms strongly depends on physiological factors of growth and successfully can be regulated by selection of appropriate compounds of nutrient medium.

### Acknowledgements

The work was implemented with financial support of the project FR-19-3719 by the Shota Rustaveli National Science Foundation of Georgia.

# New bismuth titanates based photocatalysts: a comprehensive DFT and experimental insight

Aleksei G. Krasnov<sup>1\*</sup>, Mariia S. Koroleva<sup>1</sup>, Igor R. Shein<sup>2</sup>, Irina V. Piir<sup>1</sup>

<sup>1</sup>Institute of Chemistry, Federal Research Center Komi Science Center UB RAS, 48 Pervomaiskaya st., Syktyvkar, 167982, Russia.

<sup>2</sup>Institute of Solid State Chemistry, UB RAS, 91 Pervomaiskaya st., Ekaterinburg, 620990, Russia.  
alexey-krasnov@rambler.ru

The heterogeneous photocatalysis process with semiconductors is one of the preferable purification methods. The possibility of applying natural and renewable solar energy to purify water, air, and surfaces from organic pollutants (including drugs) makes photocatalysis environmentally friendly and economical cost. Bismuth titanates with various structural types are stated to be perspective photocatalysts [1-2]. Several strategies are known to enhance the photocatalytic activity of the single material photocatalysts in visible light, *e.g.*, the optimization of crystal structure, surface area, and morphology; the manipulation of native defects; doping to adjust the optoelectronic properties. In the present work, combined *ab initio* and experimental investigations of Al-, Sc-, Ga-, Y-, In-, La-doped bismuth titanates with the pyrochlore and layered perovskite structures were performed.

All calculations were performed by means of the density functional theory (DFT) using the PAW method as implemented in the VASP package. The GGA-PBE formalism was used to describe exchange-correlation effects during geometry optimization. We employed the screened Coulomb hybrid exchange-correlation functionals to accurately calculate the optoelectronic properties. The group-III elements doped pyrochlore photocatalysts were synthesized by a coprecipitation method<sup>2</sup>. Characterization of the properties by a complex of physicochemical methods (XRD, SEM-EDX, TEM, DSC, dynamic light scattering method, low-temperature physical method nitrogen sorption, diffuse scattering spectroscopy) was carried out. We carefully detected phase formation temperature of the samples. The SEM analysis of each sample revealed only one phase, in which element ratios were close to the initial ones. The estimated crystallite size by Sherrer's equation is 30–50 nm with noticeable agglomerates of about 100–500 nm according to SEM and with the formation of the particles (200–600 nm) in the aqueous medium. The isoelectric points of the nanopowders seem to be shifted to the strongly acidic region, resulting in the formation of negative surface particle charges at pH in distilled water.

The excellent agreement between DFT calculated and experimental structural parameters of the doped bismuth titanates is found (Figure 1). Single-phase doped bismuth titanates are wide-gap semiconductors with the strong abilities to be active photocatalysts under Vis irradiation. The optical  $E_g$  values for direct/indirect transitions are in good agreement with DFT predicted values and are in the visible light. The calculated low effective masses of the charge carriers and suitable band edges positions confirm the ability of the doped bismuth titanates to act as Vis-photocatalysts. The photocatalytic activity is evaluated through the decomposition of the rhodamine B and paracetamol water solutions under Vis irradiation.

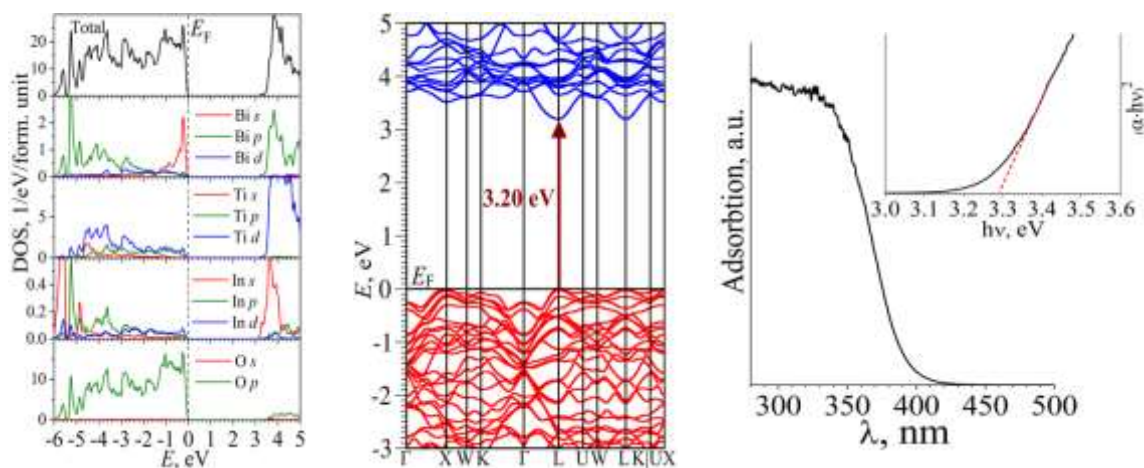


Figure 1. Electronic structure (HSE03 level) and experimental absorption spectrum of the  $\text{Bi}_{1.5}\text{In}_{0.5}\text{Ti}_2\text{O}_7$  pyrochlore.

## Acknowledgements

The research was done using the equipment of Center for Collective Use «Khimiya» of Russian Academy of Sciences Ural Branch Federal Research Center Komi Science Center Institute of Chemistry; Center for Collective Use of IMM UrB RAS "Supercomputer Center URAN IMM UrB RAS." This work was supported by the Council on grants of the President of the Russian Federation (MK-310.2021.1.3).

## References

1. D. Noureldine, S. Lardhi, A. Ziani, M. Harb, L. Cavallo, and K. Takanebe, *J. Mater. Chem. C*, **3** 12032 (2015).
2. A. G. Krasnov, M. S. Napalkov, M. I. Vlasov, M. S. Koroleva, I. R. Shein, and I. V. Piir, *Inorg. Chem.*, **59** 12385 (2020).

## Pd-catalyzed allylic substitution between C-based nucleophiles and Bicyclic Aziridines

João Oliveira\*<sup>1,2</sup>, Gredy Kiala<sup>2</sup>, Filipa Siopa<sup>1,2</sup>, Carlos Afonso<sup>2</sup>, Julie Oble<sup>2</sup>, and Giovanni Poli<sup>2</sup>.

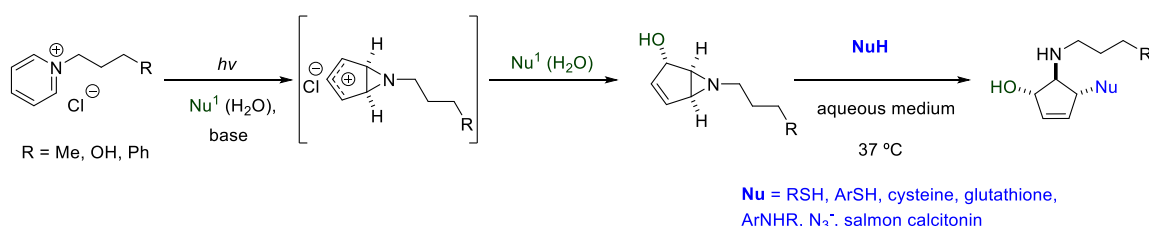
<sup>1</sup>Research Institute for Medicines (iMed.Ulisboa), Faculty of Pharmacy, Universidade de Lisboa, Av. Prof. Gama Pinto, 1649-003 Lisbon, Portugal.

<sup>2</sup>Sorbonne Université, Faculté des Sciences et Ingénierie, CNRS, Institut Parisien de Chimie Moléculaire (IPCM), 4 place Jussieu 75252 Paris Cedex 05 France.

\*jaco@campus.ul.pt

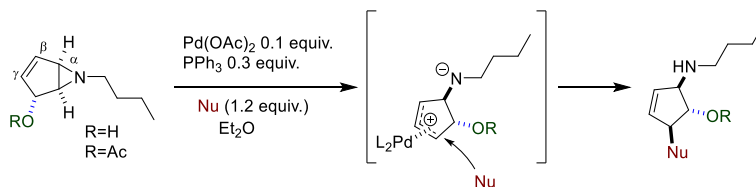
Aziridines are highly reactive three-membered heterocycles. They are well known to organic chemists for their great potential as building blocks for the synthesis of carbocycles with significant biological activity, such as aminocyclopentitols and beta-lactams.<sup>[1]</sup>

A short route for the synthesis of these structures is the photochemical transformation of pyridinium salts to bicyclic-aziridines. The photochemical rearrangement forms a *cis*-fused cyclopenteno-aziridine allylic cation which reacts stereospecifically with poor nucleophiles/solvent devising a stable bicyclic-aziridine containing a new C-Nu bond in *trans*-position (Scheme 1).<sup>[2]</sup> In 2016, We reported the ring opening of these aziridines structures by performing a S<sub>N</sub>2 reaction with nucleophiles such as azides, anilines, and thiols, forming new carbon-heteroatom bonds (Scheme 1).<sup>[3]</sup>



Scheme 5. Photochemical transformation of pyridinium salt and an example of ring opening.

Considering the peculiar structure of the above described  $\alpha$ -oxycyclopenten-aziridines in connection with our long-standing interest in Pd-catalyzed allylations, we were intrigued by the thought of investigating the behaviour of such cyclic substrates against soft carbon-based pro-nucleophiles under Pd(0) catalysis. Within this framework, we recently developed a palladium-catalyzed ring opening of vinyl aziridines. This process proceeds takes place through  $\eta^3$ -allylpalladium complex formation via aziridine cleavage, and  $\gamma$ -reactivity of carbon-based nucleophiles leading to new carbon-carbon bonds (Scheme 2).<sup>[4]</sup> In this line, will be described recent efforts on the enantioselective opening of the aziridine via Pd catalysis.



Scheme 6. Palladium catalysis followed by nucleophilic attack.

**Acknowledgements:** This project has received funding from the European Union's Horizon 2020 research and innovation programme under grant agreement No 951996 *Biomass4Synthons*. We also thank the Fundação para a Ciência e Tecnologia for financial support (PhD grant 2020.04589.BD) and project (PTDC/QUI-QOR/32008/2017 and PESSOA 2018/2019 (Proc. 441.00 França and PHC PESSOA 2018 No 40875QJ)

### Acknowledgements

This project has received funding from the European Union's Horizon 2020 research and innovation programme under grant agreement No 951996 *Biomass4Synthons*. We also thank the Fundação para a Ciência e Tecnologia for financial support (PhD grant 2020.04589.BD) and project (PTDC/QUI-QOR/32008/2017 and PESSOA 2018/2019 (Proc. 441.00 França and PHC PESSOA 2018 No 40875QJ)) A short introduction can be placed here.

### References

1. S. Vandekerckhove, M. D'hooghe, *Bioorg. Med. Chem.* **21** 643 (2013).
2. L. Kaplan, J. W. Pavlik, K.E. Wilzbach, *J. Am. Chem. Soc.* **94** 3283 (1972).
3. J.R. Vale, F. Siopa, P.S. Branco, C.A.M. Afonso, *Eur. J. Org. Chem.* 2048–2053 (2016).
4. J.A.C. Oliveira, G. Kiala, F. Siopa, A. Bernard, G. Gontard, J. Oble, C.A.M. Afonso, G. Poli *Tetrahedron* **51** 121182 (2020).R.

## Characterization of Giant Reed as a Potential Feedstock for Fast Catalytic Pyrolysis

Manqoba S.<sup>1</sup>, Sammy L.K.<sup>2</sup> and Yusuf M.I.<sup>3</sup>

<sup>1</sup>Durban University of Technology, 121 Steve Biko Rd., Musgrave, Berea, Durban, 4001

<sup>2</sup>Vaal University of Technology, Andries Potgieter Blvd, Vanderbijlpark, 1900

<sup>3</sup>University of Witwatersrand, Jorissen St., Braamfontein, 2050

The application of lignocellulosic biomass to produce biofuels via pyrolysis process has attracted considerable attention worldwide. Biomass materials exhibit different behaviours when subjected to thermal degradation processes due to their diverse nature and wide range of properties. Characterization step for the biomass is a critical step prior to pyrolysis process initiation. This step consist of techniques that are excellent tools for exploring biomass structure and its chemical properties [1]. The characterization results can be utilized to optimize the performance of the chosen biomass based on required product distribution for the pyrolysis process [2]. The most prominent properties that determine quality of the biofuel are heating values, ash content, proximate analysis (ash, moisture, volatile and fixed carbon content), and ultimate analysis (C, H, N, S and O compositions).

### Giant Reed Characterization

The current study focuses on physical and chemical characterization of Giant Reed which is readily available in South Africa and highly invasive. Adopted characterization techniques for studying physical structure of Giant Reed were Scanning Electron Microscopy (SEM) and Brunauer-Emmett-Teller (BET). X-ray diffraction (XRD) was used as a technique to investigate the crystal structure of Giant Reed. In order to determine functional groups and elemental composition of Giant Reed, Fourier Transform Infrared Spectroscopy (FTIR) and Energy-Dispersion X-ray Spectroscopy (EDS) were employed respectively. In order to determine optimum temperature of thermal degradation behaviour of Giant Reed, Thermogravimetric Analysis (TGA) was used. The knowledge of biomass properties allows the prediction of environmental impacts and technicality of pyrolysis process. Hence, thermal degradation behaviour is a result of the feedstock physical and chemical properties. This also provide valuable information with regards to understanding the reactions that occur during the pyrolysis process.

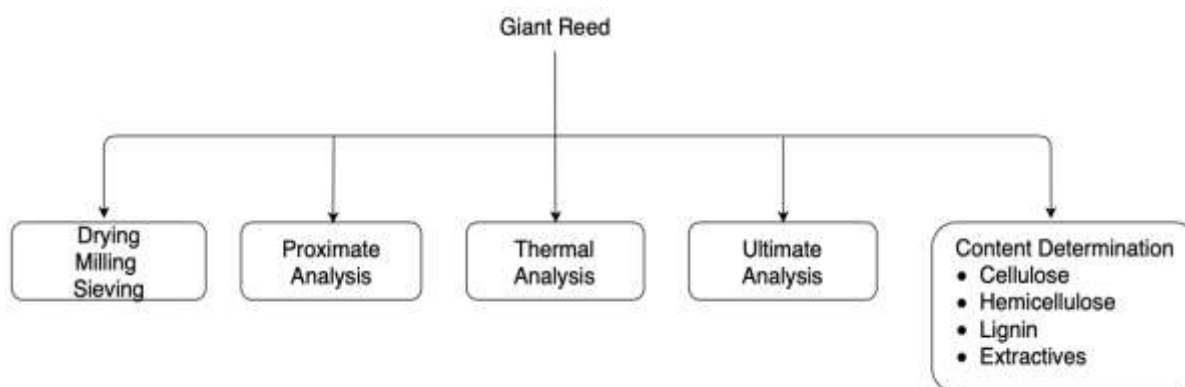


Figure 1: Analyses for characterization of Giant Reed

- Giant Reed mowed in spring for the current study has been harvested in Ladysmith, Kwa-Zulu Natal province, South Africa.
- The culm of the Giant Reed was considered in the current study.
- The culm was cut into short pieces and then be dried for 24 h at 105 °C to reduce the moisture below 10 wt%.
- The oven-dried Giant Reed was grinded followed by sieving to a particle size range of 0.5 – 2 mm.

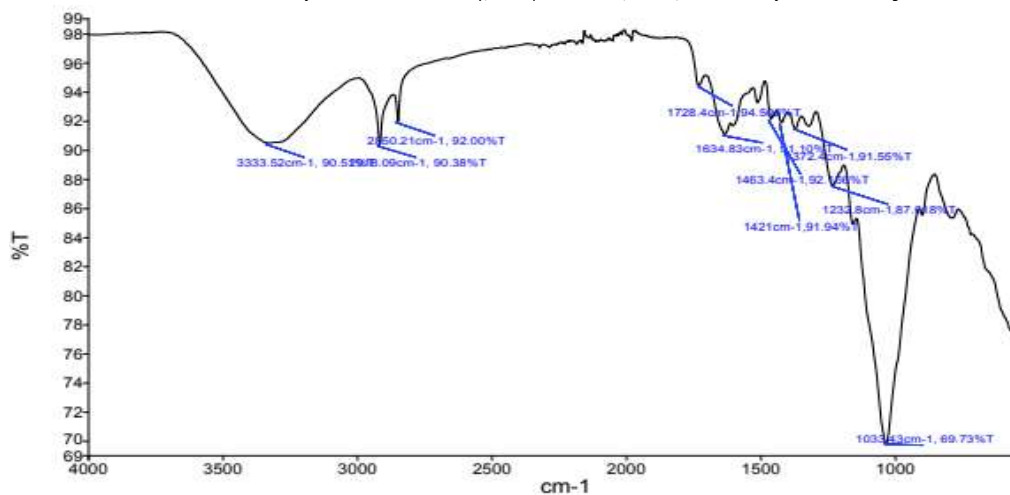


Figure 1: FTIR spectra of natural Giant Reed

The region between 3300 and 3000  $\text{cm}^{-1}$  relate to hydroxyl stretches in several compounds, and amines and amides in amino acids. This band is broad as seen in figure 2 because of the high number and large density of hydrogen bonds, mainly hydroxyl radicals.

Table 1: SEM elemental distribution for natural Giant Reed

All results in weight%					
Spectrum	C	O	Si	K	Total
<b>Spectrum 1</b>	53,78	44,71	1,44	0,07	100
<b>Spectrum 2</b>	59,4	40,01	0,5	0,08	100
<b>Spectrum 3</b>	61,87	37,78	0,35	0	100
<b>Spectrum 4</b>	53,15	45,42	1,33	0,09	100
<b>Spectrum 5</b>	52,77	45,57	1,51	0,15	100
<b>Mean</b>	56,2	42,7	1,03	0,08	100
<b>Std. deviation</b>	4,16	3,58	0,55	0,05	
<b>Max.</b>	61,87	45,57	1,51	0,15	
<b>Min.</b>	52,77	37,78	0,35	0	

From table 1, it can be observed that the carbon element is main element present in natural Giant Reed with an average of 56.2wt%. The mean values of oxygen and silicon present in natural Giant Reed were 42.7 and 1.03wt%, respectively.

### Acknowledgements

The authors are indebted to the National Research Foundation (NRF) for the financial support given to this research.

### References

- [1] R. K. Singh, T. Patil, and A. N. Sawarkar, "Pyrolysis of garlic husk biomass: physico-chemical characterization, thermodynamic and kinetic analyses," *Bioresource Technology Reports*, vol. 12, p. 100558, 2020.
- [2] M. A. Shah, M. Khan, and V. Kumar, "Biomass residue characterization for their potential application as biofuels," *Journal of Thermal Analysis and Calorimetry*, vol. 134, no. 3, pp. 2137-2145, 2018.

## Synthesis of new class dual functionalized ionic liquids and their performance for effective CO<sub>2</sub> capture: Properties and interaction mechanism analysis

Surya Chandra Tiwari<sup>1</sup>, Sreedevi Upadhyayula<sup>1</sup> and K. K. Pant<sup>1</sup>  
*<sup>1</sup> Indian Institute of Technology, India*

### Abstract:

CO<sub>2</sub> capture using benign cost-effective solvents is an essential unit operation not only in the process industry for CO<sub>2</sub> separation and recovery from industrial off-gas streams but also for direct capture from air to clean the environment. Several solvents are identified, by researchers, with high CO<sub>2</sub> capture efficiency due to their favorable chemical and physical properties, interaction mechanism with CO<sub>2</sub>, and low regeneration energy cost. However, alkanolamines are the most frequently used solvent for CO<sub>2</sub> captures, such as monoethanolamine (MEA), diethanolamine (DEA), and Methyldiethanolamine (MDEA). These solvents have several issues, such as low thermal stability, heat-stable salt formation, and being highly degradable. Therefore, a new class solvent needs to be developed to overcome these issues. Dual functionalized ionic liquids (FILs) have the potential to overcome these limitations. Hence, this work synthesized a new class of dual functionalized ionic liquids (DFILs) by the acid-base neutralization reaction using polyamine triethylenetetramine (TETA) as cation and cyclic amines as anions. The complete protonation of cation was confirmed by <sup>1</sup>H NMR and ATR- FTIR spectroscopy analysis. Further, chemical properties such as thermal stability of DFILs were analyzed, and the results demonstrated that the strength of the ionic bond of DFILs was similar strength of raw chemicals. Therefore, the stability of DFILs is good enough for the application of CO<sub>2</sub> capture. Additionally, viscosity and alkalinity of aqueous DFILs were evaluated, and results revealed that triazole-based DFILs showed comparatively high viscosity and lower alkalinity. Further CO<sub>2</sub> loading experiment was confirmed that CO<sub>2</sub> loading more than 1.5 (mol CO<sub>2</sub>/mol DFILs) for all DFILs and the loading decreased with increasing temperature. The <sup>13</sup>C NMR analysis of CO<sub>2</sub>-loaded aqueous DFILs suggests that a high amount of carbamate and bicarbonate is formed in the aqueous DFILs- CO<sub>2</sub> system. Overall, these DFILs showed good potential for effective CO<sub>2</sub> capture.

**Key words:** CO<sub>2</sub> Capture, Viscosity, Interaction Mechanism, Ionic Liquids

# Education and societal awareness – UN Sustainable Developments Goals



## Green Chemistry for high school: methoxylation of alpha-pinene over ionic resins

Madalena Frade<sup>1</sup>, PA. Mourão<sup>1</sup>, I. Cansado<sup>1,2</sup> and José E. Castanheiro<sup>1\*</sup>

<sup>1</sup>MED, Departamento de Química e Bioquímica, Escola de Ciências e Tecnologia, Universidade de Évora/, Portugal  
<sup>2</sup>LAQV-REQUIMTE, Departamento de Química e Bioquímica, Escola de Ciências e Tecnologia, Universidade de Évora/, Portugal

\*jefc@uevora.pt

The twelve principles of green chemistry as introduced by Anastas and Warner [1] can be summarized as follows: 1. Limit the production of residues to avoid treatments; 2. Maximize the incorporation of all materials used into the final product; 3. Use and manufacture little or no toxic products; 4. Replace toxic solvents as well as the intermediaries of syntheses; 5. Limit the energy expenditure; 6. Use renewable resources; 7. Use catalytic processes; 8. Reduce the quantity of derivative products; 9. Conceive biodegradable substances; 10. Catalytic reagents are superior to stoichiometric reagents; 11. Analyze in real-time to prevent the accidents by developing a sourer fundamental chemistry; 12. Minimize the potential for chemical accidents, including releases, explosions, and fires. The principles of green chemistry make it possible to produce by minimizing waste, by reducing the use of toxic products and by using fast and effective reactions.

$\alpha$ -Pinene is a renewable raw material usually obtained from pine gum or as a waste from the Kraft process [2]. Its acid catalysed methoxylation yields a complex mixture of monoterpenic ethers, being  $\alpha$ -terpinyl methyl ether the main product. The  $\alpha$ -terpinyl methyl ether smells grapefruit-like and might be used as flavour and fragrance for perfume and cosmetic products, as additive for pharmaceuticals as well as in food industry. Figure 1 shows the methoxylation of alpha-pinene.

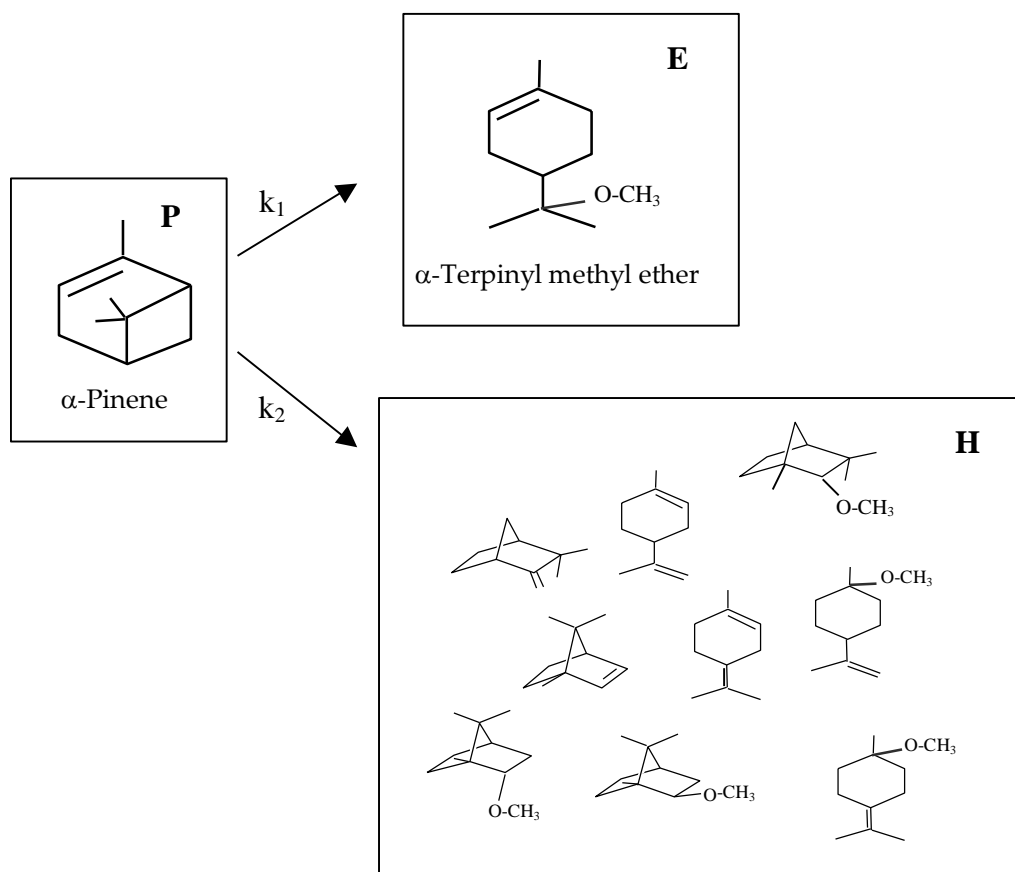


Figure 1. Scheme of alpha-pinene methoxylation

Strong homogeneous acid catalysts, e.g sulphuric acid, have been used, but the effluent disposal leads to environmental problems and economical inconveniences. These problems can be overcome using solid acid catalysts. Beta zeolite [3] heteropolyacids supported on silica [4] and mesoporous silicas functionalized with sulfonic acid groups [5] have been used for the  $\alpha$ -pinene alkoxylation.

The aim of this work is to study the alpha-pinene methoxylation over Dowex resin. This work is an experiment carried out with students of Homogenous and heterogenous course (Master of Chemistry). Different reaction

parameters such as, amount of catalyst, concentration of alpha-pinene were studied and optimized. Also, a kinetic model was proposed. With this work the Green Chemistry Thematic is introduced in the classroom, through heterogeneous catalysis (principle 10) and the use of renewable raw material (principle 6), as a necessary tool for sustainable development.

Figure 2 shows the results of alpha-pinene methoxylation in the presence of a Dowex resin. The solid lines represent the model fitted to the data points.

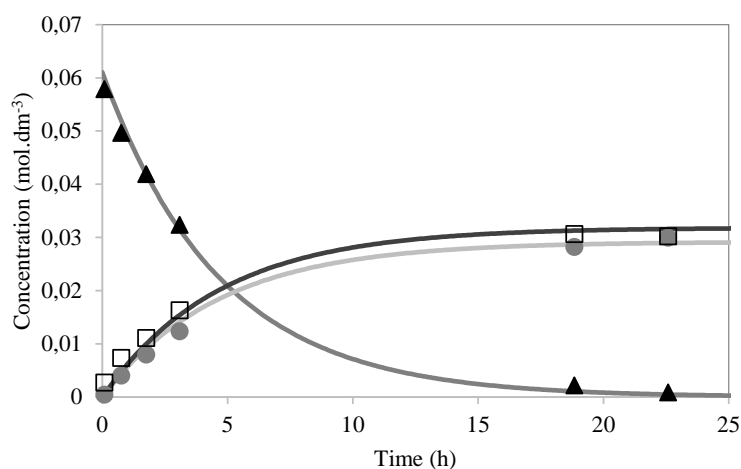


Figure 2. Methoxylation of alpha-pinene in the presence of a Dowex resin. Concentration *versus* time. (▲) $\alpha$ -pinene; (●)  $\alpha$ -terpinyl methyl ether; (□) H-lumps all the minor components. The solid lines represent the model fitted to the data points. Reaction conditions: initial concentration of  $\alpha$ -pinene = 0.061 mol.dm<sup>-3</sup>; Temperature=60°C; catalyst loading =0.2 g.

## References

1. Paul T. Anastas and John C. Warner, *Green Chemistry: Theory and Practice* (Oxford University Press: New York), 1998.
2. R.M. Traynor, et al., in D.F. Zinkel and J. Russels (Editors), *Naval Stores*, Pulp Chemical Association, New York, 1989, Chap.12, p. 479.
3. K. Hensen, C. Mahaim, W.F. Hölderich, *Appl. Catal. A:Gen.*, **149** 311. (1997).
4. D.S. Pito, I. Matos, I.M. Fonseca, A.M. Ramos, J. Vital, J.E. Castanheiro, *Appl. Catal. A: Gen.*, **373** 140 (2010).
5. J.E. Castanheiro, L. Guerreiro, I.M. Fonseca, A.M. Ramos, J. Vital, *Stud. Surf. Sci. Catal.*, **174** 1319 (2008).

## How green chemistry education can empower chemistry students to be promoters of sustainable substances-handling practices in their communities

Liliana Mammino\*

\*University of Venda, University Road, Thohoyandou 0950, South Africa

\*sasdestria@yahoo.com

Pursuing sustainability entails a large number of components. Some of them are related to everyday practices, i.e., to the behaviors of individual persons. The handling of substances and materials is one of the major aspects having great impact on sustainability. One of the most impressive example in recent time is the case of plastic and microplastic pollution. Preventing this pollution would not require the elimination of plastics (what would likely be unrealistic in the current economical stage), but it would require that all plastic objects, after they cease being useful, are disposed in a way that does not allow them to enter the environment. This, in turn, requires conveying the message to citizen in all communities, including the poorest ones. Reaching all individuals in the needed capillary way is not easy if left only to designated official bodies. Furthermore, human beings tend to adopt certain behavior patterns more willingly if they are convinced of their importance than if they are simply instructed to implement them. The proposition of alternative options is likely to be more convincing if it is based on transmission of knowledge, expressing the relevant knowledge in a way that is accessible to the group involved at a given moment. Students taking chemistry courses and getting acquainted with green chemistry are likely to be in an ideal position to find the most suitable ways to transmit knowledge about the appropriate uses and final disposal of substances and materials to their communities.

The content of the presentation is based on the presenter's direct experience at introducing green chemistry to third year chemistry students (with great attention to students' responses), and on observations highlighting the needs for dissemination of information about the handling on substances and materials in a rural area in South Africa. Many of the green chemistry principles [1] can also be related to everyday practices, from waste prevention and reutilization of items whenever possible to energy saving and resources' saving. These aspects are particularly suitable for students to identify and explore them actively, within interactive sessions or independently as homework. Independent search has proven to favor attention to details and good internalization of relevant ideas [2]. Underpinning chemistry concepts need to be adequately emphasized, including the routes leading to undesirable effects on human health and the environment. Particular attention is advisable for substances and materials of common use, such as household chemicals or plastics, and for chemicals used extensively in a given context (e.g., agrochemicals in rural areas).

Students often show particular interest in the implications of the green chemistry principles for everyday life, up to the point that, on more than one occasion, they have spontaneously proposed outreach initiatives towards secondary schools or communities [3]. Years ago, a group of students at the University of Venda had taken the initiative of organizing a refuse recycling activity, managing it in an entrepreneurial way and successfully convincing communities to participate in it. Regrettably, it did not continue with subsequent students' cohorts after the initial organizers graduated and moved elsewhere, what indicated that the entrepreneurial skills needed to organize a rather large-scale separate refuse collection may be difficult to maintain through successive cohorts of students in an institution, if handled mostly by students. On the other hand, it also highlighted the effectiveness with which students can communicate with communities on something about whose importance they are convinced. Initiatives aimed at the dissemination of information about crucial sustainability aspects are affordable for any groups of students and can play crucial roles. The information may include the appropriate handling of substances and materials, such as the precautions to be taken with potentially harmful substances (including, e.g., agrochemicals), the need to avoid using excess amounts, the need to avoid dispersing things in the environment, the importance of replacing open-air burning of vegetable materials with more sustainable practices, and others that may be relevant for specific contexts. Students are in a position to better identify the most suitable terms to propose behavior-patterns shifts in their communities. On the other hand, deep and complete understanding of the underlying chemistry concepts is a necessary pre-requisite for the design of explanations expressed in simple terms. The teacher's guidance is essential in the process of acquisition of adequate conceptual understanding and can offer valuable inputs or serve as verification reference in the design of simplified (even highly simplified) and convincing messages.

The effectiveness of the outlined approaches may be enhanced through exchanges of information among different departments in the same institutions (e.g., chemistry and agriculture), among institutions operating in analogous contexts (e.g., rural areas), and among tertiary and secondary educational institutions in the same area. The efficiency of the approaches can be progressively enhanced through recursion-type optimization of their details across subsequent editions of each initiative-type.

## References

1. P.T. Anastas, J.C. Warner, *Green Chemistry: Theory and Practice*. New York: Oxford University Press, (1998).
2. C.M. Kgoetlana, H.F. Makhubele, *et al.*, in L. Mammino, J. Apotheker (Eds), *Research in Chemistry Education*. Cham (Switzerland): Springer (2021), pp. 169-175.
3. L. Mammino. In V. Gomes Zuin, L. Mammino (Eds), *Worldwide Trends in Green Chemistry Education*. Royal Society of Chemistry, (2015), pp. 1–15.

# Green analytical chemistry

## Determination of air pollutants in confined crowded places

Chrystalla Kaikiti, Marinos Stylianou, Agapios Agapiou\*

*Department of Chemistry, University of Cyprus, P.O.Box 20537, 1678 Nicosia, Cyprus*

*\*E-mail: agapiou.agapios@ucy.ac.cy, Tel.: +357-22-895432, Fax: +357-22-895088*

In the last decade, indoor air pollution in confined places like houses, crowded premises, and workplaces is considered worrying both to humans and exposed workers. According to global health organizations, the daily exposure to Volatile Organic Compounds (VOCs) and Particulate Matters (PMs) air pollutants can cause hazardous effects to the individual's health. The aim of this study was the analysis of ambient air in various confined premises (e.g. institutes of personal care, and specifically in hair and nail salons in which various chemical products are used for different daily actions, as well and in other high congestion places such as shopping malls and schools). The indoor air analysis was performed by monitoring the emitted VOCs, as well as the PMs, inside the respective sampling environments. The sampling of VOCs entailed the use of passive, active, and dynamic headspace (DH) techniques on coating cartridges of Tenax TA sorbent tube, and the subsequent analysis using thermal desorption coupled with gas chromatography/mass spectrometry (TD-GC/MS). Simultaneously with the VOCs' sampling, PMs of different aerodynamic diameters 1, 2.5, 4, and 10  $\mu\text{m}$  ( $\text{PM}_{10}$ ,  $\text{PM}_4$ ,  $\text{PM}_{2.5}$ ,  $\text{PM}_1$ ), were measured. The obtained results showed that ubiquitous and infrequent VOCs are emitted in the low ppb<sub>v</sub> levels, including the BTEX, along with benzaldehyde, styrene, mesitylene, phenol, ethyl acetate, chlorinated compounds, siloxanes, etc. PMs measurements also revealed elevated values in all examined places, indicating the need for better ventilation and use of greener chemical products.

## Impact of UV-B Exposure on Physicochemical Properties of Poly(ethylene terephthalate): On the way to microplastics formation

Nina Maria Ainali<sup>1,2</sup>, Dimitrios N. Bikiaris<sup>1\*</sup>, Dimitra A. Lambropoulou<sup>2,3</sup>

<sup>1</sup>Department of Chemistry, Laboratory of Polymer Chemistry and Technology, Aristotle University of Thessaloniki, GR-541 24 Thessaloniki, Greece; [ainali.nina@gmail.com](mailto:ainali.nina@gmail.com)

<sup>2</sup>Laboratory of Environmental Pollution Control, Department of Chemistry, Aristotle University of Thessaloniki, GR-541 24 Thessaloniki, Greece

<sup>3</sup>Center for Interdisciplinary Research and Innovation (CIRI-AUTH), Balkan Center, Thessaloniki, GR-57001, Greece  
\* [ainali.nina@gmail.com](mailto:ainali.nina@gmail.com); [dbic@chem.auth.gr](mailto:dbic@chem.auth.gr)

Nowadays, the low degradability of the widely used synthetic polymers in the natural environment, combined with the inadequate waste management, provokes their accumulation in the environment, notably in the marine environment, provoking severe environmental pollution. In fact, approximately 13 Mts of these plastics per year end up in oceans, where they are further fragmented to microplastics (MPs, plastic items with diameters  $\leq 5$ mm) under the effect of several environmental stresses. These formed microplastics pose threat to aquatic and land-living organisms, whereas the effects of their consumption via drinking water and the trophic chain, are still under investigation for human health. Despite the effect of the several physicochemical mechanisms in the natural habitat is characterized as the main path of plastics fragmentation, the research in the field of the weathering features of plastics and the mechanism of microplastics' formation is still limited. In the light of the above, with the purpose to improve the evaluation of plastic degradation and the aforementioned research gaps, the present study aims to characterize and understand the physicochemical changes of poly(ethylene terephthalate) (PET) induced by UV exposure. In more detail, PET, which is widely used in plentiful applications covering from packaging to textile applications owing to its numerous merits, in the form of thin films was exposed to UV-B irradiation for specific intervals. The photodamage was initially examined by several methods throughout the examined intervals, such as Fourier-transform infrared spectroscopy (FTIR) which proved the formation of new oxidized products during UV exposure, while X-Ray diffraction (XRD) and differential scanning calorimetry (DSC) measurements boosted the obvious effect of UV irradiation in their crystalline and thermal properties. Scanning Electron Microscopy (SEM) exemplified also the important morphological alterations in the irradiated samples, while mechanical properties deterioration was proved as a significant indication that UV irradiation leads to a drop in plastics properties and their gradual fragility, potentially leading to microplastic formation. The mechanism of plastic deterioration properties of PET before and after UV exposure was also investigated by Py-GC/MS demonstrating the alterations of the ratio between the low molecular weight compounds and the relatively higher molecular weight hydrocarbons throughout UV exposure, proposing significant proposals and problematic areas for the quantification of PET microplastics in real environmental samples with the aid of a Py-GC/MS instrumentation.

### Acknowledgements



The research work was supported by the Hellenic Foundation for Research and Innovation (HFRI) under the 3rd Call for HFRI PhD Fellowships (Fellowship Number: 6567).

## A novel device for on-line determination of ammonia/ammonium in ambient air

Lukas Alexa\* and Pavel Mikuska

Department of Environmental Analytical Chemistry, Institute of Analytical Chemistry of the Czech Academy of Sciences, Brno, 60200, Czech Republic

\*alexa@iach.cz

Ammonia ( $\text{NH}_3$ ) is a significant gaseous pollutant present in the atmosphere. As a neutralizing agent of acidic species,  $\text{NH}_3$  forms particle-phase ammonium ( $\text{NH}_4^+$ ) salts and contributes thus to the formation of secondary atmospheric aerosols [1].

Knowledge of the sources, distribution, and chemistry of  $\text{NH}_3/\text{NH}_4^+$  in the atmosphere is limited by the availability of reliable techniques that enable measurement in real time at low concentrations. Determination of atmospheric  $\text{NH}_3$  is also difficult due to dynamic equilibrium with particulate  $\text{NH}_4^+$ , which may cause artifacts.

A sensitive and fast method for simultaneous determination of  $\text{NH}_3/\text{NH}_4^+$  in ambient air is presented [2].  $\text{NH}_3$  is continuously sampled by a Cylindrical Wet Effluent Diffusion Denuder (CWEDD) into deionized water and on-line analysed by continuous flow system with fluorescence detector (FLD) while  $\text{NH}_4^+$  is sampled by a Condensation Growth Unit – Aerosol Counterflow Two-Jets Unit (CGU-ACTJU) sampler into water and analysed with another FLD (Fig. 1). The very sensitive fluorescence detection of  $\text{NH}_4^+$  in solution is based on its reaction with ortho-phthalaldehyde and sulphite to form isoindol-1-sulphonate.

The results obtained by the developed method were compared with a reference method based on sampling of pollutants on filters and “dry” diffusion denuders (DDPs) coated by  $\text{H}_3\text{PO}_4$ .

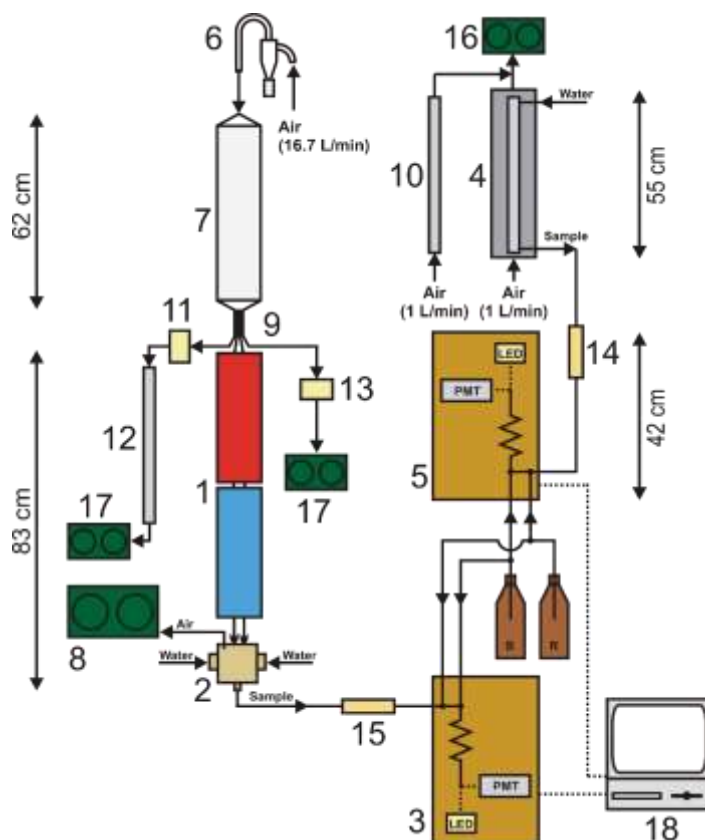


Figure 1. Scheme of the apparatus: 1, CGU; 2, ACTJU; 3,5, FLDs with photomultiplier tubes (PMTs), light-emitting diode (LED), reagent solution (R), and buffer solution (B); 4, CWEDD; 6, cyclone inlet PM2; 5, 7, annular diffusion denuder; 8, 16, 17, membrane pumps; 9, flow splitter; 10, 12, DDPs; 11, 13, NILU filter units; 14, 15, anion-exchange columns; 18, computer.

The optimized method was used for the determination of  $\text{NH}_3/\text{NH}_4^+$  in urban air in Brno in two campaigns: from 8<sup>th</sup> to 16<sup>th</sup> February 2018 and from 17<sup>th</sup> to 25<sup>th</sup> September 2018 (Fig. 2). The calibration curve of  $\text{NH}_4^+$  in solution is linear in the concentration range  $5 \times 10^{-9} - 2 \times 10^{-6}$  M. Limit of detection (LOD = 3 s/n) of  $\text{NH}_3$  is  $3.52 \text{ ng m}^{-3}$  (5.05 ppt), resp.  $1.04 \text{ ng m}^{-3}$  for  $\text{NH}_4^+$ . The developed method enables on-line measuring of distribution of  $\text{NH}_3/\text{NH}_4^+$  in ambient air with time resolution of 1 s.



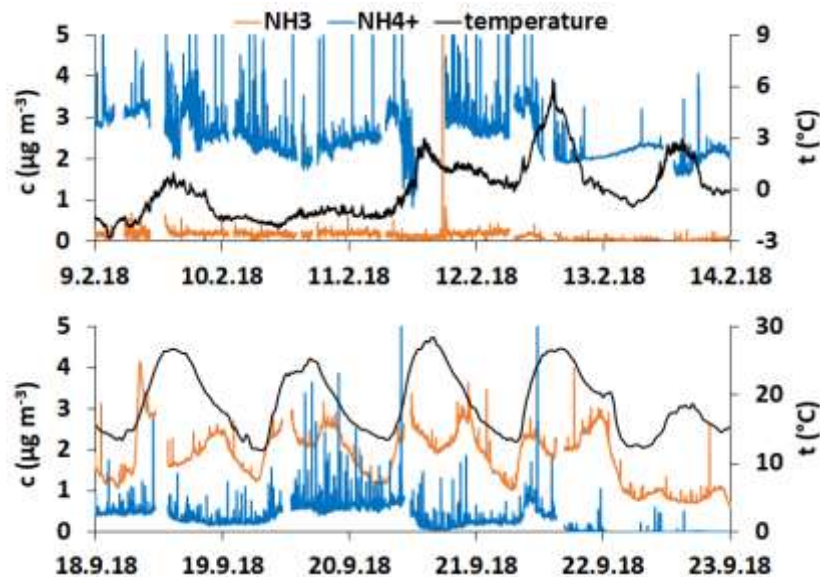


Figure 2. Determination of  $\text{NH}_3/\text{NH}_4^+$  in urban air in Brno.

The described method can be used for monitoring of fast concentration changes and transformation of  $\text{NH}_3/\text{NH}_4^+$  in ambient air. The main advantages include automated online analysis with fast data recording, elimination of sampling artifacts, especially evaporation and degradation of analytes on filters, and overall reduced costs. Because of the high sensitivity and short time resolution, the method might be applied to the study of new particle formation.

### Acknowledgements

This work was supported by Grant Agency of the Czech Republic under project No. 503/20/02203S.

### References

1. R. Harrison, M. Jones, *Sci. Total Environ.* **168** 195 (1995).
2. L. Alexa, P. Mikuska, *Anal. Chem.* **92**, 15827 (2020).

## Application of green solvents and procedures for analysis of pharmaceuticals in environmental samples

Vasil Andruch<sup>1\*</sup>, Elena Kupcová<sup>2</sup>, and Barbora Benická<sup>2</sup>

<sup>1</sup>Department of Analytical Chemistry, Institute of Chemistry, Faculty of Science, P. J. Safarik University, Kosice, Slovakia

<sup>2</sup>Department of Chemistry, Faculty of Natural Sciences, Matej Bel University, Banska Bystrica, Slovakia

\*vasil.andruch@upjs.sk

The current period is marked by an increase in the use of various pharmaceuticals in the treatment of diseases. However, in addition to the positive effect of pharmaceuticals, we must also think about the possible pollution of the environment. Therefore, monitoring the concentration of pharmaceuticals and their metabolites in the environment, especially in groundwater and wastewater, is an important task for analytical chemists. The principles of green chemistry [1,2] were extended to the field of analytical chemistry [3,4]. At the beginning of our century, so-called deep eutectic solvents were designed [5,6], which very quickly attracted researchers from various fields, especially in the field of materials research. This is due to the interesting properties of these solvents, in particular the tunability of their physical properties as well as that they can be considered more environmentally friendly compared to conventional solvents. The use of these solvents in analytical chemistry began only recently, around the middle of the last decade [7]. Another way to ensure the greenness of analytical procedures is to use so-called microextraction procedures. The combination of microextraction procedures and deep eutectic solvents can provide interesting solutions that meet the requirements of green analytical chemistry. We would like to present our vision of the current state of the use of green solvents and procedures in the analysis of environmental samples.

### Acknowledgements

This work was supported by the Scientific Grant Agency of the Ministry of Education, Science, Research and Sport of the Slovak Republic (VEGA 1/0220/21).

### References

1. P.T. Anastas, M.M. Kirchhoff, *Acc. Chem. Res.*, **35** 686 (2002).
2. P. Anastas, N. Eghbali, *Chem. Soc. Rev.*, **39** 301 (2010).
3. A. Gałuszka, Z.M. Migaszewski, P. Konieczka, J. Namieśnik, *TrAC - Trends Anal. Chem.*, **37** 61 (2012).
4. A. Gałuszka, Z. Migaszewski, J. Namieśnik, *TrAC - Trends Anal. Chem.*, **50** 78 (2013).
5. A.P. Abbott, G. Capper, D.L. Davies, H.L. Munro, R.K. Rasheed, V. Tambyrajah, *Chem. Commun.*, 2010 (2001).
6. A.P. Abbott, D. Boothby, G. Capper, D.L. Davies, R.K. Rasheed, *J. Am. Chem. Soc.*, **126** 9142 (2004).
7. A. Shishov, A. Bulatov, M. Locatelli, S. Carradori, V. Andruch, *Microchem. J.*, **135** 33 (2017).

## **Green Analytical method for the assay of some selected drugs**

Safwan Fraihat

*The univarsity of Jordan, Jordan*

A green method for the determination of Gentamicin and neomycin antibiotics in drug formulations were developed. The method is based on selective oxidation of the drugs using iodate oxidizing agent in the presence of iodide ion, then the resultant iodine was determined spectrophotometrically as iodine-starch complex. All the variables affecting the reaction were studied and optimized. The developed method was applied in the determination of the drugs in some pharmaceutical formulations.

## Activity-Guided Isolation and Identification of Metabolites from Endophytic Fungus using HPLC-DAD, Mass Spectrometry and Multidimensional NMR Spectroscopy

Nazifi S. Ibrahim<sup>1,2</sup>, Craig P. Butts<sup>2</sup>, Ahmed A. Yakasai<sup>1\*</sup>

<sup>1</sup>Department of Pure and Industrial Chemistry, Bayero University, P.M.B. 3011, Kano, Nigeria.

<sup>2</sup>School of Chemistry, University of Bristol, BS8, ITS, Bristol, United Kingdom.

nsibrahim.chm@buk.edu.ng

Abstract text:

Endophytic fungi *Cladosporium spp.* isolated from healthy leaves of *Psidium guajava* was cultured in potato dextrose broth (PDB), tenellin production medium (TPM) and Rice medium (RM). The antioxidant activity of the crude ethyl acetate extracts was observed in DPPH and ABTS followed by further fractionation on C18 column (water acetonitrile gradient). Activity-guided purification and HPLC-DAD analysis of the active fractions revealed the presence of three pairs of alkaloids as the major constituents. The structure of the isolated metabolites was determined by various spectroscopic techniques, including NMR, UV, and MS. The results of the 1D and 2D (including <sup>15</sup>N) NMR spectra as well as MS fragmentations, phenazine alkaloids were identified as; phenazine-1-ol (1), phenazine-1-carboxylic acid (2) and phenazine-1-carboxamide (3). The 15N and HMBC experiments provided fast resolution of the aromatic proton assignments and the type of phenazine derivatives isolated. This study reveals the first-time isolation of these metabolites from *Cladosporium spp.*, an endophytic fungus obtained from the leaves of an ethnomedicinal plant *Psidium guajava*. Gene tracking and modification will enable bulk isolation of these major constituent for further bioactive study.

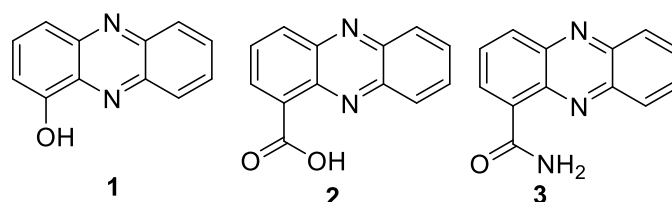


Figure 1: Phenazine derivatives isolated from *Cladosporium spp.*

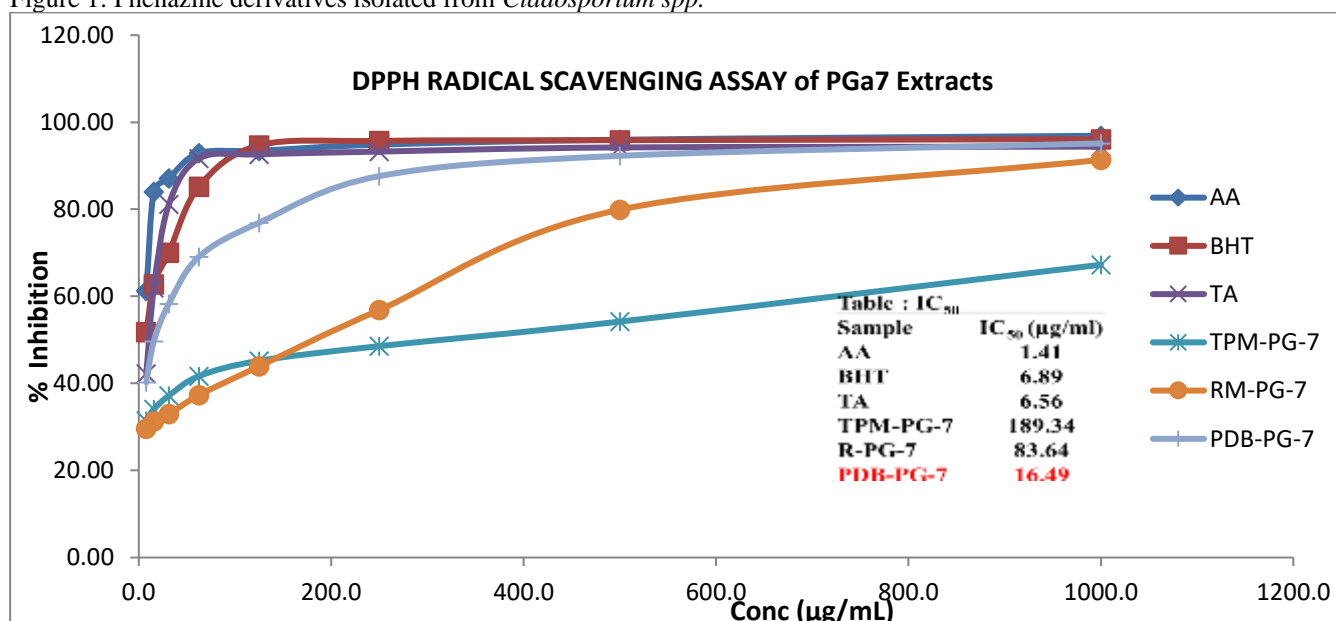
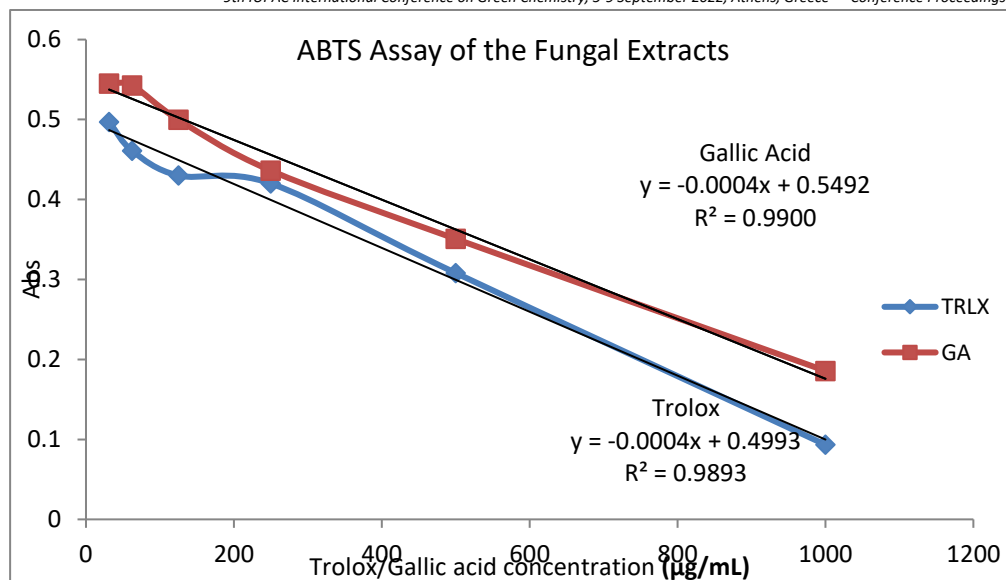


Figure 2: % Inhibition and IC<sub>50</sub> of DPPH radical scavenging Assay of the Extracts

Table 1: Antioxidant activity by ABTS methods of the extracts (1mg/mL) expressed as Trolox and gallic acid equivalent mg/mg. Values are the mean of three replicates ± standard deviation

Extract	Trolox Equivalents (mg TE/g)	Gallic Acid Equivalents (mg GAE/g)
PDB	0.4969 ± 0.003	0.5452 ± 0.0006
TPM	0.0934 ± 0.021	0.1857 ± 0.016
RM	0.0246 ± 0.0003	0.0274 ± 0.004



### Acknowledgements

The authors are thankful to Bayero University and University of Bristol for providing all the necessary resources needed and funding for the research.

### References

1. K. M. VanderMolen, H. A. Raja, T. El-Elimat and N. H Oberlies, *AMB Express*, **3** 71-78 (2013)
2. A.A. Yakasai, *Uni. of Bristol*, 2011.
3. Y. Pang, S. Ahmed, Y. Xu, T. Beta, Z. Zhu, Y. Shao, J. Bao, *Food Chem.* 2018 **240** 212–221 (2018).
4. A. Evidente, A. Cimmino, Z. Bahmani, S. Castaldi, M. Masi, R. Istatico, J. Abdollahzadeh, J. Amini . *J. Agric. Food Chem.*, **69** 12143–12147 (2021)
5. Z. Xiang, L. Junkai, and W. Qinglai, *Chinese J. Org. Chem.* **39(10)** 2744–58 (2019).

## Biochar as a green modifier for the development of electrochemical biosensors

Cristiane Kalinke<sup>1,3\*</sup>, Paulo R. de Oliveira<sup>2</sup>, Luiz H. Marcolino-Junior<sup>3</sup> and Márcio F. Bergamini<sup>3</sup>

<sup>1</sup>Institute of Chemistry, University of Campinas (Unicamp), 13083-859, Campinas, São Paulo, Brazil.

<sup>2</sup>Federal University of São Carlos (UFSCar), 13600-970, Araras, São Paulo, Brazil

<sup>3</sup>Department of Chemistry, Federal University of Paraná (UFPR), 81531-980, Curitiba, Paraná, Brazil.

\*cristiane.kalinke@gmail.com

Biochar is a carbon-based material obtained from the pyrolysis of biomass in a low amount of oxygen. The material has a porous surface, and high functionalization, allowing a high capacity for sorption and interaction with other species [1, 2]. Biochar can be produced from different types of biomasses, mainly industrial and agricultural waste, making it a sustainable and low-cost material [3]. In this work, the biochar was obtained from castor bean waste from castor oil and biodiesel manufacturing industries. To improve the sorbent capacity of the biochar, the material was subjected to chemical activation treatment using nitric acid in a reflux system. Biochar samples were used as modifiers for the construction of simple, low-cost carbon paste electrodes (50 wt% graphite powder, 25 wt% mineral oil and 25 wt% activated biochar), as summarized in Figure 1.

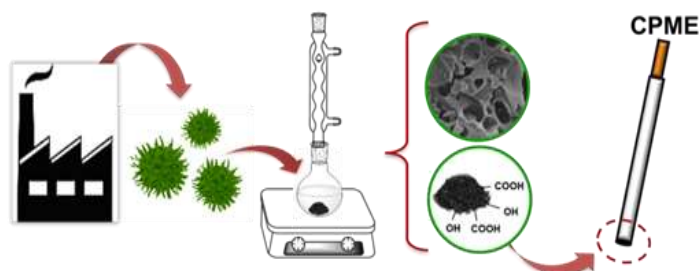


Figure 1. Production, activation, characterization and application of castor bean biochar for the development of biosensors.

The analytical performance of the sensors was evaluated using the redissolution technique, by the spontaneous preconcentration of Fe(III) ions on the carbon paste electrode modified with biochar and subsequent electrochemical synthesis of iron hexacyanoferrate (Prussian Blue, PB) in presence of potassium ferricyanide. Then, glucose oxidase enzyme (GOx) was immobilized on the electrode by using the EDC/NHS pair for glucose determination. In this configuration, the enzyme chemically interacts with glucose in solution, oxidizing it to gluconic acid and hydrogen peroxide, which is monitored by the reaction with Prussian white (PW) (Figure 2). Activated biochar stood out for presenting an increase in surface area, porosity, number of defects and insertion of oxygenated functional groups, as shown in the results of Table 1.

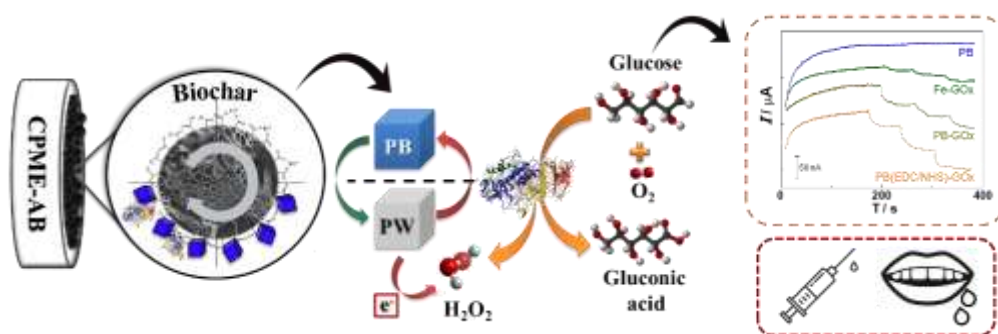


Figure 2. Anchoring of iron for the synthesis of Prussian blue used for the catalyze and electro-oxidation of glucose.

Table 1. Characterization results obtained with castor bean biomass, pristine (untreated) and activated biochar [4].

Material	Procedure	Surface area (m <sup>2</sup> g <sup>-1</sup> )	I <sub>b</sub> /I <sub>c</sub>	Functional groups (mmol g <sup>-1</sup> )
Pristine biochar	Pyrolysis (400 °C, 5 °C min <sup>-1</sup> , 60 min)	4.80±0.28	1.05	4.98±0.29
Activated biochar	Chemical activation (50 vol% HNO <sub>3</sub> , 60 °C, 3 h)	6.15±0.40	1.30	7.87±0.16

The proposed sensor was applied for the enzymatic detection of glucose. The analytical performance of the biosensor was evaluated by amperometric measurements in the presence of glucose, presenting a linear region between 50 and 5000  $\mu\text{mol L}^{-1}$ , and a limit of detection of 0.938  $\mu\text{mol L}^{-1}$ . The analytical performance of the proposed device was comparable to other biosensors containing PB and GOx for the enzymatic detection of glucose. The biosensor also showed good enzyme-substrate affinity by the Michaelis-Menten apparent kinetic constant ( $K_M^{app} = 4.16 \text{ mmol L}^{-1}$ ), which is essential for subsequent reactions for glucose determination.

The method showed good repeatability (RSD = 2.51%), reproducibility (RSD = 6.21%) and stability, and was effectively applied for glucose determination in real samples of human saliva and blood serum at levels commonly reported in the literature for these biological samples (0.326 and 2.20  $\text{mmol L}^{-1}$ , respectively). Good recovery values (90.7–105%) were also obtained for the determination of glucose in spiked samples. Thus, it is possible to evidence the application of activated biochar as an electrode modifier, obtained from residual biomass from industrial processes, which presents biocompatibility for the biomolecules anchoring aiming the development of environmentally friendly biosensors.

### Acknowledgements

CK, PRO, LHMJ and MFB would like to thank to the Brazilian Coordination of Improvement of Higher Education Personnel (Capes, Brazil. Financial code 001) and National Council for Scientific and Technological Development (CNPq, Brazil).

### References

1. J. Lehmann, S. Joseph. *Biochar for environmental management: science and technology*, Routledge, 2012.
2. L. Dai, Y. et al. *Renewable and Sustainable Energy Reviews*, **107**, 20-36 (2019).
3. C. Kalinke et al. *Green Chemistry*, **23**, 5272 (2021).
4. C. Kalinke et al. *J. Braz. Chem. Soc.*, **51**(5), 941-952 (2019).

## A protein-based free-standing transparent elastomer and its potential applications

Ramesh Nandi and Nadav Amdursky

Schulich Faculty of Chemistry, Technion – Israel Institute of Technology, Haifa, 3200003, Israel

E-mail: [nandi.ramesh@campus.technion.ac.il](mailto:nandi.ramesh@campus.technion.ac.il)

A most important endeavor in modern materials research is the current shift toward green environmental and sustainable materials. Natural resources are one of the attractive building blocks for making environmentally friendly materials. In most cases, however, the performance of nature-derived materials is inferior to the carefully designed synthetic materials. The performance issue is pronounced for conductive polymers. Conductive polymers are a special class of materials having potential for a wide range of applications (such as solar cells and bioelectronics). Like many common polymers, conductive polymers are derived from petrochemicals and are not biodegradable, hence creating tons of waste over time. To overcome this issue, here, we adopted a synthetic strategy to make a proton conductive, biodegradable, free-standing transparent elastomeric polymer out of bovine serum albumin (BSA). This polymerization process is spontaneous, relies on the reshuffling of disulfide crosslinking present in the protein structure, and is an energy-efficient one-pot synthesis. The protein used in this process is one of the most affordable proteins, resulting in the ability to create large-scale inexpensive materials, having an estimated price tag of \$0.01 per cm<sup>2</sup>. Inherent biodegradability and biocompatibility of the elastomer make it potent for different applications. Here we focus on two applications; the first one is a solid-state electrode for sensing electrophysiological signals utilizing its conductive property. The second one is not related to the conductivity; instead, we take advantage of the BSA protein and its natural ability to bind various organic chromophores to explore the polymer as a platform for molecular doping. Following molecular doping, we focus on studying excitonic energy transfer across five chromophores. Lastly, we demonstrate the molecular doping capability of the polymer to create a coating for the light-emitting diode (LED) to replace toxic conventional inorganic phosphor/quantum dot-based materials for white light generation.



Figure: An image of a 15 × 15 cm BSA polymer.

### Acknowledgement

Gutwirth fellowship for financial support.

### References

1. R. Nandi, Y. Agam, and N. Amdursky, A protein-based free-standing proton-conducting transparent elastomer for large-scale sensing applications, *Adv. Mater.*, *33*, 2101208, 2021.
2. R. Nandi, and N. Amdursky, A protein-based polymer matrix as a versatile platform for long-range energy transfer and organic down-converting material for bio-LED application, (Unpublished)



## Beeswax-based waterproof paper as a sustainable substrate for electrochemical sensing platforms

Paulo R. de Oliveira<sup>1\*</sup>, Alejandro G.M. Ferrari<sup>2</sup>, Cristiane Kalinke<sup>3</sup>, Juliano A. Bonacin<sup>3</sup>, Craig E. Banks<sup>2</sup> and Bruno C. Janegitz<sup>1</sup>

<sup>1</sup>Federal University of São Carlos (UFSCar), 13600-970, Araras, São Paulo, Brazil.

<sup>2</sup>Manchester Metropolitan University (MMU), Manchester, M1 5GD, United Kingdom.

<sup>3</sup>Institute of Chemistry, University of Campinas (Unicamp), 13083-859, Campinas, São Paulo, Brazil.

\*paulo.oliveira@ufscar.br

With the appearance of the COVID 19 pandemic, the limitation of access to fast analysis devices for monitoring viral disease became evident in many countries, especially in economically developing countries. This led to a dash to search for new monitoring devices, mainly for the SARS-CoV-2 virus, in terms of accuracy, simplicity, and low cost [1]. However, after the measurement these devices can become unworkable for a second application, thus being discarded after use, which also conducts to an environmental problem. Taking this into account, the development of new, more sustainable analytical platforms becomes another challenge.

From an electrochemical point of view, most monitoring devices are based on screen-printed electrodes (SPEs) and mainly on the development of alternative conductive inks with low environmental impact [2]. However, this work focuses its efforts on the development of a low-cost, biodegradable substrate for the disposition of the conductive ink and the insulator. More precisely, this work aims to evaluate the construction of a biodegradable and impermeable substrate for the manufacture of SPEs.

For this proposal, commercial photographic paper without any surface chemical treatment (matte finish) was used, and beeswax (BW) dispersed in hexane was applied on the paper surface. The device configuration (Figure 1A) consists of the arrangement of three electrodes (conductive ink) and an electrical insulator-based electrode area delimiter, both deposited by using an automatized screen-printer and commercial inks [3].

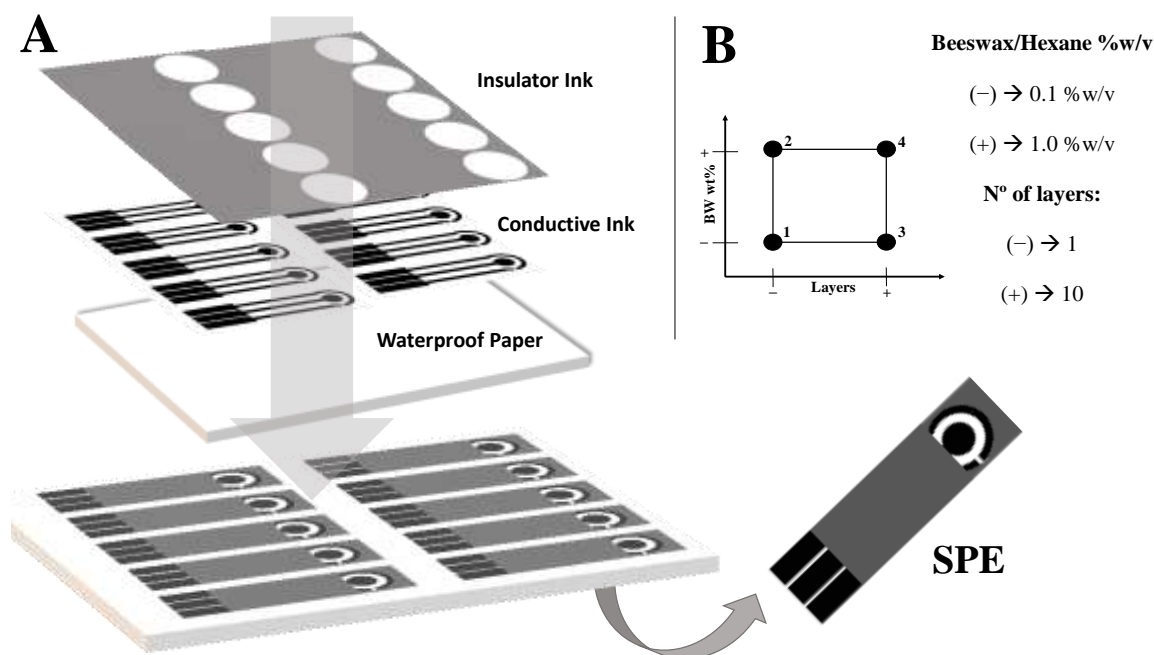


Figure 1. (A) Scheme of Screen-printed electrodes building with waterproof paper, electrode structures (conductive inks), and the insulator ink; (B)  $2^2$  exploratory factorial design (without central point) used for the composite waterproof paper substrate optimization. Evaluated factors: Beeswax %w/v and number of layers.

In this step of the work, the influence of the amount of BW on the properties of the SPEs was evaluated, varying the percentage of BW in the dispersion and the number of layers applied (by brushing). This evaluation was performed using a multivariate analysis strategy (Figure 1B), in which the response was evaluated in terms of hydrophobicity by the water contact angle, using a lab-made goniometer [4], heterogeneous electron transfer rate constant ( $K^0$ ), and effective surface area, both by cyclic voltammetry analysis, using a Metrohm Eco Chemie PGSTAT30 Potentiostat/Galvanostat. A direct dependence was observed between the amount of BW applied on the paper in the responses (Table 1). However, a small amount of BW, about  $40 \mu\text{g}$  per electrode as observed in test 3, was able to considerably increase the hydrophobicity of the paper (higher water contact angle), which allows electrochemical measurements in an aqueous medium. Hence, the proposed electrode has shown similar properties

in comparison to the results obtained with SPEs building using a commercial polymer matrix, commonly used. This fact allows the proposed waterproof paper to be used as a cheaper and environmentally friendly alternative to commonly used substrates. In a second step, this electrode will be applied as an electrochemical sensor for the determination of SARS-CoV-2 in human biological samples.

Table 1. Electrochemical and water contact angle performance comparison between the electrodes with different substrate platforms obtained from multivariate analysis. Complete data can be found in the references.

Substrate	Beeswax wt%	Number of layers	$K^0$ (cm s <sup>-1</sup> )	Surface area (cm <sup>2</sup> )	Water contact angle (°)
Paper	-	-	0.0091±0.0001	0.0620±0.0003	96.80±0.70
Test 1	0.1 (-)	1 (-)	0.0110±0.0005	0.0636±0.0006	105.42±0.65
Test 2	1.0 (+)	1 (-)	0.0115±0.0003	0.0640±0.0008	122.76±5.49
Test 3	0.1 (-)	10 (+)	0.0118±0.0001	0.0646±0.0011	126.57±7.63
Test 4	1.0 (+)	10 (+)	0.0122±0.0001	0.0650±0.0006	126.36±4.26

### Acknowledgements

CK, PRO, BCJ and JAB would like to thank to São Paulo Research Foundation (FAPESP, Brazil. Grants# 2021/07989-4, 2019/00473-2, 2019/01844-4, 2017/21097-3, and 2013/22127-2) and Coordination of Improvement of Higher Education Personnel (Capes, Brazil. Finance Code 001, and 88887.504861/2020-00).

### References

1. Brazaca, L. C., Dos Santos, P. L., de Oliveira, P. R., Rocha, D. P., Stefano, J. S., Kalinke, C., Muñoz, R. A. A., Bonacin, J. A., Janegitz, B. C., Carrilho, E. Biosensing strategies for the electrochemical detection of viruses and viral diseases—A review. *Analytica Chimica Acta*, 1159, 338384, 2021.
2. Camargo, J. R., Orzari, L. O., Araujo, D. A. G., de Oliveira, P. R., Kalinke, C., Rocha, D. P., Santos, A. L., Takeuchi, R. M., Munoz, R. A. A., Bonacin, J. A., Janegitz, B. C. Development of conductive inks for electrochemical sensors and biosensors. *Microchemical Journal*, 164, 105998, 2021.
3. Foster, C. W., Metters, J. P., Kampouris, D. K., Banks, C. E. Ultraflexible screen-printed graphitic electroanalytical sensing platforms. *Electroanalysis*, 26(2), 262-274, 2014.
4. Stalder, A. F., Kulik, G., Sage, D., Barbieri, L., Hoffmann, P. A snake-based approach to accurate determination of both contact points and contact angles. *Colloids and surfaces A: physicochemical and engineering aspects*, 286(1-3), 92-103, 2006.

## Application of the SPA analytical method for the determination of tar in pyrolytic gases in the tyres pyrolysis process

Sergejs D. Osipovs<sup>1\*</sup> and Aleksandrs I. Pučkīns<sup>2</sup>

<sup>1</sup>Department of Applied Chemistry, Daugavpils University, Parādes 1A street, Daugavpils, Latvia

\*sergejs.osipovs@du.lv

Converting waste to energy is now gaining additional importance for solving economic and environmental problems. Globally, the disposal of polluted tyres is becoming a major environmental issue; the main causes of this problem are population growth, an increase in the number of vehicles and rapid industrialization.

Approximately 1.5 billion used tyres are discarded every year. They will eventually end up in the waste stream, leading to serious potential waste and environmental problems. The 75–80% of used tyres survive in the environment as waste. The service life of a used tyre is 80–100 years in landfills because of the thermostatic polymer structure, which does not melt and is not distributed into its chemical constituents. Waste tyres are bulky and landfill causes fire and toxicity due to the accumulation of harmful gases or the habitat of disease vectors, flies and rodents. As a result, waste and tyre disposal is viewed as a serious environmental pollution problem. In tyres, rubber has a high calorific value, making it an ideal raw material for fuel protection. Recovery of energy and materials is considered an efficient way to use waste.

Pyrolysis is a thermochemical recycling method in which organic polymers are converted to liquid oil at high temperatures (400–600°C) in the absence of oxygen (O<sub>2</sub>). Pyrolysis dissolves waste and also produces useful by-products. In this case, gas, liquid and solid phases are formed.

The solid product of pyrolysis, known as biochar, consists mostly of carbon but also contains ash originating from biomass. Biochar, which represents 12–15 wt% of the products of pyrolysis, can be used as boiler fuel but more intriguing applications include soil amendment, carbon sequestration agent, and activated carbon. The pyrolysis oil from waste tyres has characteristics similar to those of diesel fuel. Non-condensable gases from pyrolysis, yielding 13–25 wt%, are a flammable mixture of carbon monoxide, hydrogen, carbon dioxide, and light hydrocarbons suitable for generating process heat. Pyrolytic gases have a high calorific value, about 30–40 MJ Nm<sup>-3</sup>. The energy obtained during the combustion of pyrolytic gas is sufficient for the pyrolysis process, and it can be used for other purposes. In addition, pyrolytic gas contains ash particles, volatile alkali metals and tar.

Tar is a complex mixture of acids, aldehydes, ketones, alcohols, phenols, and aromatic hydrocarbons. Its composition depends upon the conditions of gasification. Tar is an undesirable by-product of pyrolysis due to a number of problems, like its condensation and formation of tar aerosols.

Traditional methods for tar sampling are based on cold solvent-trapping coupled with solvent absorption in impingers. Collected solvents are analysed by different methods. A normal cold-trapping method samples and quantifies biomass tar in the concentration range from 1 mg m<sup>-3</sup> to 300 g m<sup>-3</sup> (on naphthalene basis). This method involves a long sampling time (about 1 h as a function of tar concentration), possible sample losses, and analytes segregation resulting from aerosol formation.

In the present work, SPA method for determining the concentration of tar compounds was chosen. The SPA method was developed by The Royal Institute of Technology in Sweden [1] to measure tar compounds ranging in molecular weight from benzene to coronene. According to this method, tar is sampled by collecting it on a column with a small amount of amino-phase sorbent. For each sample, 100 mL of gas is withdrawn from a sampling line using a syringe or a pump. The sampling line is kept between 250–300°C to minimize tar condensation. The original SPA method does not allow for determining such volatile organic compounds as benzene, toluene, and xylenes, some of which, because of their high concentration in tar, will not collect on the amino-phase sorbent. In the previous paper [2–4], an improved system of sampling was suggested and described, whereby one more adsorbent cartridge loaded with another sorbent is added. The best results were obtained while using activated coconut charcoal as the second sorbent. In this study, a modified sampling device consisting of 500 mg of amino-phase sorbent and 100 mg of activated coconut charcoal was chosen as optimal for sampling tar (including its volatile organic compounds) in non-condensable gas produced in tyres pyrolysis.

For research in a real-life context was chosen technology, that is based on the principle of a quick heating of fine-grained oil shale by the solid heat carrier (hot ash) in the rotary drum reactor followed by its thermal decomposition. The pyrolysis experiments were performed in a fixed-bed reactor situated in eastern Latvia (Daugavpils). The plant is based on the globally recognized horizontal rotating drum technology with a capacity of 9 t of shale per day. The stainless-steel reactor has an inner diameter of 2.24 m with an 8 m tall. The main characteristics of the reactor are as follows: operating mode of the unit – cyclical; speed of rotation,  $\omega$  s<sup>-1</sup> – 0.15;

oil shale feed,  $G_f$  ( $\text{kg s}^{-1}$ , dry basis) – 5.26; heat carrier feed,  $G_a$  ( $\text{kg s}^{-1}$ ) – 10.46; working temperatures of pyrolysis – 350–480°C (depending on type of raw material); fuel oil performance, % for tyre/PP/ABS/PS/PE – 44/92/60/80/85; dry carbon residue capacity, % for tyre/PP/ABS/PS – 30/3/25/10; steel cord performance, % for tyre – 12; own fuel consumption for heating in pyrolysis mode and production of own gas,  $\text{L t}^{-1}$  of raw materials. This unit allow obtaining a high-calorific liquid fuel with a calorific value of 38–40  $\text{MJ kg}^{-1}$  and gaseous fuel with a calorific value of 41–42  $\text{MJ kg}^{-1}$ .

A tar sampling device consisting of two consecutively joined columns with adsorbents was made particularly for the present research. The first column was a 3 mL single fritted reservoir with 500 mg of loosely packed aminopropyl-bonded silica adsorbent (the exchange capacity was about 0.6 meq  $\text{g}^{-1}$ , the particle size was 50  $\mu\text{m}$ , the average pore size was 60 Å). The second column was a 1 mL single fritted reservoir with 100 mg of activated coconut charcoal (the surface area was 1070  $\text{m}^2 \text{g}^{-1}$ , the particle size was 20/40 mesh, 420–840  $\mu\text{m}$ ) packed loosely.

Tar was sampled at the pyrolytic gas temperature of 250°C. It was drawn through the adsorbent cartridges at the flow rate of 100  $\text{mL min}^{-1}$  for various periods of time, namely 1, 2, and 3 minutes, resulting in 100, 200, and 300 mL of the pyrolytic gas being drawn through the adsorbents respectively.

Then both sorbents were analysed separately. All heavy compounds of the tar are completely adsorbed on amino-phase adsorbent, and light compounds of the tar, such as benzene and toluene, are partially adsorbed on this amino-phase adsorbent, and partially on activated coconut charcoal. The total amounts of each compound were calculated, as well as the tar on both sorbents. The results were converted to normal cubic meters of pyrolytic gas. The dependence of the concentration of the total tar and some of its compounds on both sorbents on the volume of the pyrolytic gas passed through them has been investigated. It was concluded that the volume of pyrolytic gas had little or no effect on the total amount of tar found on both adsorbents. For example, when 100 mL of pyrolytic gas was passed through the adsorbents, the total tar concentration was  $7348 \pm 228 \text{ mg m}^{-3}$ ; when 200 mL was collected, the concentration was  $7412 \pm 302 \text{ mg m}^{-3}$ ; and at 300 mL the concentration was  $7395 \pm 269 \text{ mg m}^{-3}$  (Table 1).

Table 1. Compound speciation with respect to volume of sampled pyrolytic gas

Compounds	Mass Percentage		
	100 mL	200 mL	300 mL
Benzene	54.87	54.03	53.26
Toluene	13.11	12.99	12.81
Indene	1.10	1.08	1.06
Naphthalene	1.86	1.82	1.81
Acenaphthylene	0.02	0.02	0.02
Fluorene	0.01	0.01	0.01
Phenanthrene	0.02	0.02	0.02

The number of compounds collected on the amino-phase adsorbent also depends on the volume of pyrolytic gas drawn through both of them. In other words, when 100 mL of pyrolytic gas was drawn through the adsorbents, only 28 compounds were detected and identified on the amino-phase one, 200 mL of pyrolytic gas yielded 37 compounds, and 300 mL of pyrolytic gas gave 42 compounds. A growth of the number of compounds detected and identified on amino-phase sorbent results from the increase of the pyrolytic gas volume drawn through the adsorbents from 100 to 200 mL. A further increase of the volume of the sampled pyrolytic gas also leads to a growth in the number of compounds detected and identified, albeit not a sharp one. It is worth mentioning that those 9 compounds that were additionally detected and identified when the volume of pyrolytic gas rose from 100 to 200 mL make up only 0.45% of the tar mass found on both adsorbents, and the 5 compounds additionally revealed when the volume of pyrolytic gas rose from 200 to 300 mL make only 0.23% of the tar mass.

## References

1. C. Brage, Q. Yu, G. Chen, K. Sjöström, *Fuel*, **76** 137–142 (1997).
2. S. Osipovs, *Anal. Bioanal. Chem.*, **391** 1409–1417 (2008).
3. S. Osipovs, *Fuel*, **103** 387–392 (2013).
4. S. Osipovs, *Int. J. Environ. Anal. Chem.*, **89** 871–880 (2009).

## A new environmentally friendly method for the determination of mercury

Andrea Gajdošová<sup>1</sup>, Jana Šandrejová<sup>1\*</sup>, Vasil Andruch<sup>1</sup>

<sup>1</sup>Department of Analytical Chemistry, Institute of Chemistry, Faculty of Science, P. J. Šafárik University in Košice, Moyzesova 11, SK-041 54 Košice, Slovakia

\*jana.sandrejova@upjs.sk

We present a simple, rapid and environmentally friendly method for the determination of mercury. The method is based on the formation of a specific ion association complex between Hg(II) and the polymethine dye Astra Phloxine in the presence of iodide ions. The analytical wavelength was chosen in the region of an intense narrow band with maximum at 600 nm that bathochromically shifted related to the band of the aggregated dye. The calibration graph was linear over the concentration range of 0.04–0.4 mg/L Hg. An automated flow-based system coupled with spectral pipette for detection was used to reducing of reagents consumption. In addition, we examined the possibility of cloud point extraction (CPE) procedure for the preconcentration of traces of mercury before its spectrophotometric determination. CPE procedure and automated flow based system are complies with the Green Analytical Chemistry principles.

### Acknowledgements

This work was the result of the research project No. 1/0124/20 financed by the Scientific Grant Agency of the Ministry of Education of the Slovak Republic and the Slovak Academy of Sciences.

# Green Chemistry & UN Sustainable Developments Goals

## **Chemistry in the question of human survival**

Marcos Aurelio Gomes da Silva

*Department of Chemistry, Federal University of Juiz de Fora, Brazil*

When comparing the human species with other mammals, differences are observed in the forms and performance of biological “equipment”. It is well-known that the “son of man” is one of the mammals that for the longest time depends on its fellow creatures to acquire the minimum conditions for survival. It takes, for example, about a year to develop the ability to walk alone, whereas in the case of felines, this time is a few days.

However, in the fight for survival, the human being could count on an intellectual “equipment” that determined differences in relation to other animals. Water, food, clothing, shelter and energy were and are minimum requirements for individual and group biological survival, under the conditions imposed by the environment.

In the last two hundred years, the enormous expansion of chemical and physical knowledge has given materials an irremediable social and economic value. Associated with medicine and poison, well-being and doping, energy that heats and feeds, pollution, contamination and the purity of air, food, environments, fuel production, energy that heats and feeds, chemistry marked the historical evolution of the world and men.

The role of chemistry in health preservation, in applications in hygiene, cleaning, water treatment, environment preservation, food production and preservation, among other examples, as well as in medicine, in solutions to ensure longer life and quality of life for people.

Another point to be highlighted is the role of chemistry in environmental preservation, its importance in the treatment and preservation of water and soil, in the control of air quality, among others.

The first signs of familiarity with chemical processes in Brazil occurred with indigenous peoples. They extracted the dye from the plant’s annatto.

Chemistry is present in fundamental phenomena for the functioning of the human body, such as breathing and digestion. Furthermore, it is essential to generate technological innovation and economic development.

# Green Chemistry and entrepreneurship – Sustainable industrial processes



## Effect of NaCl concentration on protein production by submerged cultivation of *Pleurotus ostreatus*

Georgios Bakratsas, Elena Gkantzou, Michaela Patila, Angeliki C. Polydera, Petros Katapodis\*, Haralambos Stamatis\*

Biotechnology Laboratory, Department of Biological Applications and Technologies, University of Ioannina, 45110 Ioannina, Greece

\*Corresponding authors E-mail: hstamati@uoi.gr, Tel +30 26510 07116, pkatapo@uoi.gr Tel +30-2651007212

In the last decades, submerged cultivation of mushrooms has attracted great interest due to rapid and safe biomass production. Bioreactors contribute maximum to this because of the control of cultivation conditions that provide. Mycelium fungi have shown high content of proteins in their biomass, and with the concentration of essential amino acids to dominate, they are considered reliable vegan protein sources. Different conditions could affect protein production by mushroom mycelia such as carbon or nitrogen sources and micronutrients[1]. The effect of salt stress on protein production by submerged cultivation of fungi is something that is not been extensively studied until now[2].

In this study, *Pleurotus ostreatus* strain has been cultivated in different NaCl concentrations (from 0 to 10g/l) in Erlenmeyer flask with a glucose-based medium for biomass and protein production. Samples were withdrawn from the cultures at specific time intervals and measurements of biomass production, sugars consumption, and protein production were executed.

From the main results we can conclude that a concentration of 4g/l NaCl favors most the biomass and protein production of *Pleurotus ostreatus*,  $15.5 \pm 0.3$  g/l and  $2.7 \pm 0.4$  g/l respectively, while the addition of NaCl seems to positively affect the cultivation compared to control cultivation, 0g/l NaCl (Fig.1&2). Protein content seems to be favored by large concentrations of NaCl, with the maximum value being  $19.3 \pm 1.1$  % on the 6<sup>th</sup> day of cultivation (Fig.8). From the sugar consumption, we can conclude that in high NaCl concentrations (>6g/l NaCl) fungus seems to be soaked and delay glucose consumption (Fig. 6,7&8)

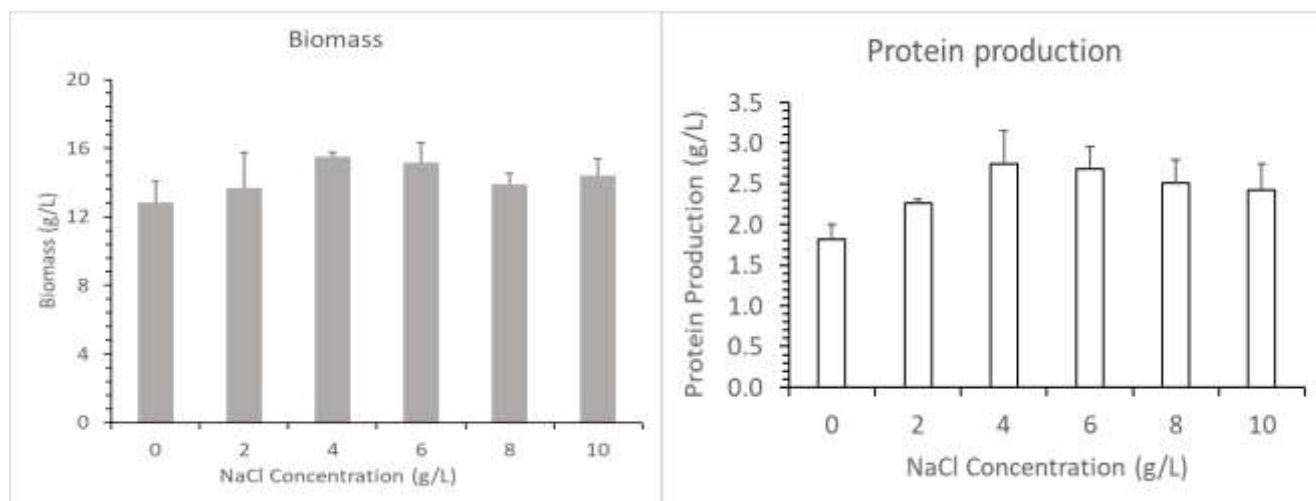


Figure 1. Bar plots of maximum biomass production in

Figure 2. Bar plots of maximum protein production in different NaCl concentrations

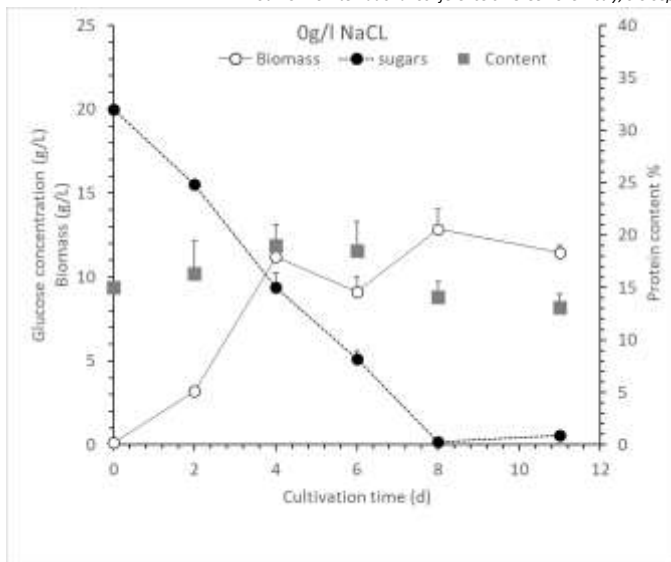


Figure 3. Biomass production, sugars consumption and protein content of *Pleurotus ostreatus* cultivation with 0g/l NaCl

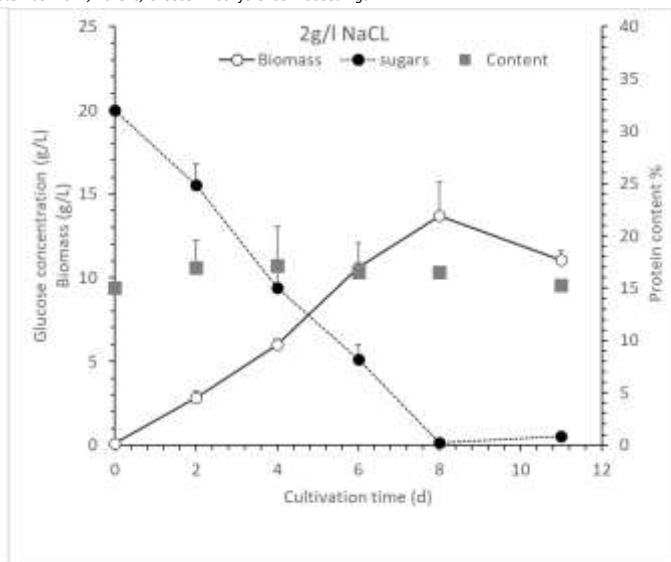


Figure 4. Biomass production, sugars consumption and protein content of *Pleurotus ostreatus* cultivation with 2g/l NaCl

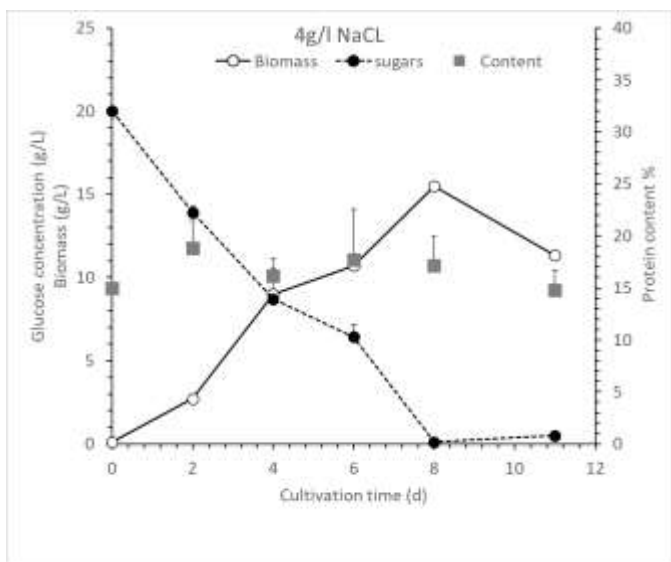


Figure 5. Biomass production, sugars consumption and protein content of *Pleurotus ostreatus* cultivation with 4g/l NaCl

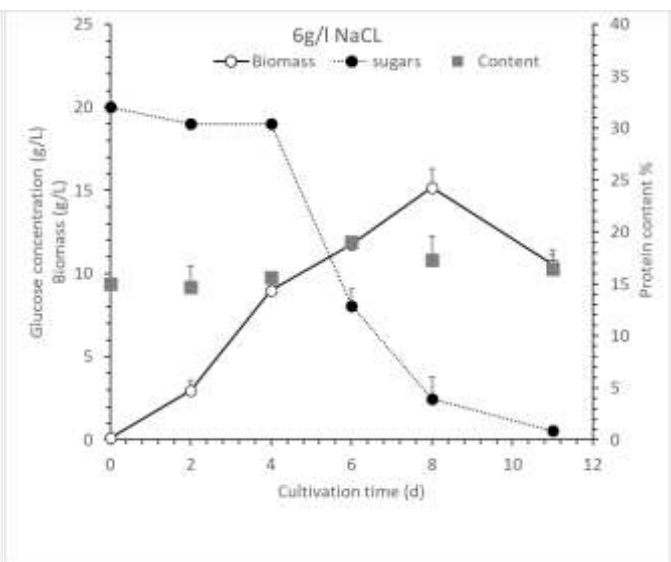


Figure 6. Biomass production, sugars consumption and protein content of *Pleurotus ostreatus* cultivation with 6g/l NaCl

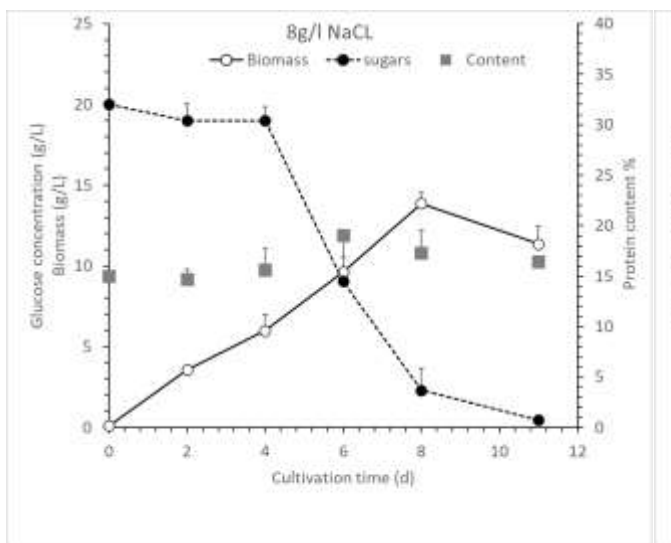


Figure 7. Biomass production, sugars consumption and protein content of *Pleurotus ostreatus* cultivation with 8g/l NaCl

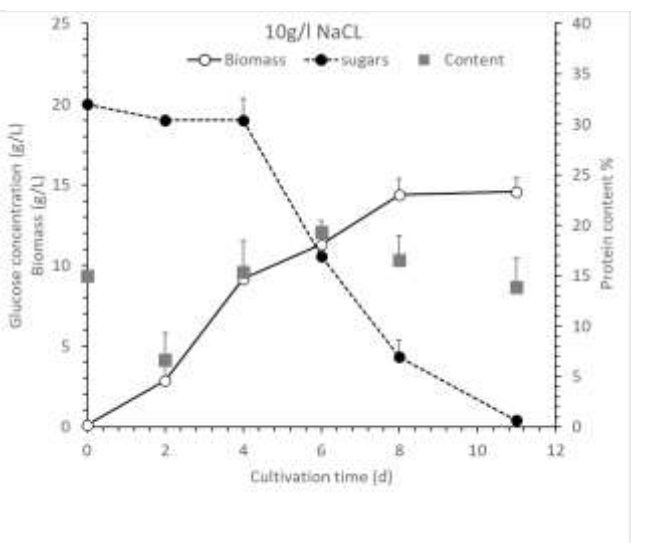


Figure 8. Biomass production, sugars consumption and protein content of *Pleurotus ostreatus* cultivation with 10g/l NaCl

## Acknowledgements

«Co-financed by the European Regional Development Fund of the European Union and Greek national funds through the Operational Program Competitiveness, Entrepreneurship and Innovation, under the call RESEARCH – CREATE - INNOVATE (project code:T2EDK- 02830)»

## References

1. G. Bakratsas, A. Polydera, P. Katapodis, H. Stamatis, *Future Foods*, **4**, 100086 (2021)
2. C. Venâncio, R. Pereira, A.C. Freitas, T.A.P. Rocha-Santos, J.P. da Costa, A.C. Duarte, I. Lopes *Environmental Pollution*, **231**, 1633–1641. (2017)

## A novel device for the carbonate determination, as carbon dioxide, during petroleum and natural gas exploration

Sofia Mylona<sup>1</sup> and Vasilios Koulos<sup>1</sup>

<sup>1</sup>BD INVENTIONS PC, Giannitson 31,54627 Thessaloniki

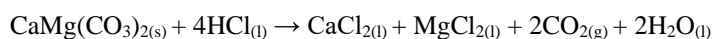
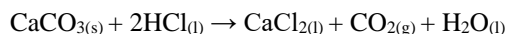
\*e-mail:vasilios.koulos@bd-inventions.com

Abstract text:

In the literature there are lots of research in the area of the carbonate reservoirs. It is estimated that around the 50-60 % of the world's petroleum is going to be found in the carbonate reservoirs. Calcite (calcium carbonate) and dolomite (calcium magnesium carbonate) which are formed during burial at several kilometers' depth are determined during the exploration of the potential new sources of oil reservoirs [1] [2] [3].

In the current work a new instrument is suggested for the determination of the carbonate content during the petroleum reservoirs investigation. The FOGL-MAL, Mud Logging Analyser from BD Inventions is an accurate, fast and low-cost portable and laboratory instrument that conforms with the EN ISO 10693:2013, ASTM D4373-02(2007), and ASTM D1756-02(2007) for the calculation of the carbonated in soil samples in the form of the carbon dioxide.

1.000g of the dried drilling sample is carefully treated with 6N HCl in an enclosed reaction bottle. From the reaction between the specimen and the Hydrochloric acid a pressure is built from the CO<sub>2</sub> formation as can be seen in the equations below.



The reaction of the calcite with the hydrochloric acid is rapid and a pressure rise is detected in the first second after the mixing. Then a slower between the dolomite and the hydrochloric acid can take several minutes until the total CO<sub>2</sub> amount is recorded. Figure 1 shows the stages of the pressure rise during the calcite and dolomite reaction.

The percentage of CaCO<sub>3</sub> and CaMg(CO<sub>3</sub>)<sub>2</sub> in the soil sample can be calculated from the combination of the pressure readings and the above balance equations of the carbonates.

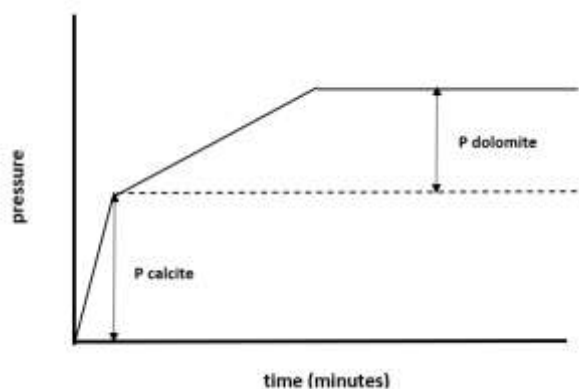


Figure 1. Total content of the Carbonates

### References

- [1] W. S. Donovan, «What Causes Mudlogging Mud Gas Response to Vary?,» de American Association of Drilling Engineers, Denver, Colorado, 2019.
- [2] C. I. C. O. J. C. F. Lamas, «election of the most appropriate method to determine the carbonate content for engineering purposes with particular regard to marls,» Engineering Geology, vol. 81, n° 1, pp. 32-41, 2005.
- [3] T. P. Burchette, «Carbonate rocks and petroleum reservoirs: a geological perspective from the industry,» Geological Society of London, p. 370, 2010.

## Renewable Reagents for Nucleophilic Fluorination

Griša Prinčič<sup>1</sup>, Jan Jelen<sup>2</sup>, Evelin Gruden, Jan Hočevar<sup>1</sup>, Blaž Omahen<sup>1</sup>, Gašper Tavčar<sup>2</sup>, Jernej Iskra\*<sup>1</sup>

<sup>1</sup>Faculty of Chemistry and Chemical Technology, University of Ljubljana Večna pot 113, 1000 Ljubljana <sup>2</sup>Department of Inorganic Chemistry and Technology, Jožef Stefan Institute, Jamova 39, 1000, Ljubljana, Slovenia

\*jernej.iskra@fkt.uni-lj.si

Unique properties of organo-fluorine compounds continue to establish them as an invaluable group of chemicals in industry, petro chemistry, pharmaceuticals and medicine (<sup>18</sup>F PET tracers) [1]. This is supported by the fact that, in 2018 only, more than 31 % of all FDA approved drugs contained fluorine atom(s). This staggering percentage further exemplifies the ever-growing need for new, more efficient, renewable and green approaches in organo-fluorine chemistry [2]. Nucleophilic fluorination presents a straight forward path towards organo-fluorine compounds. However, application of metal fluorides and early organosoluble fluorides (tetrabutylammonium fluoride, ...) presents problems with their solubility and stability [3]. Herein we report the use of two newly developed [4] nitrogen heterocycle-based fluorination reagents with [H<sub>2</sub>F<sub>3</sub>]<sup>-</sup> anion as an active fluorination species (Figure 1, **1** and **2**).

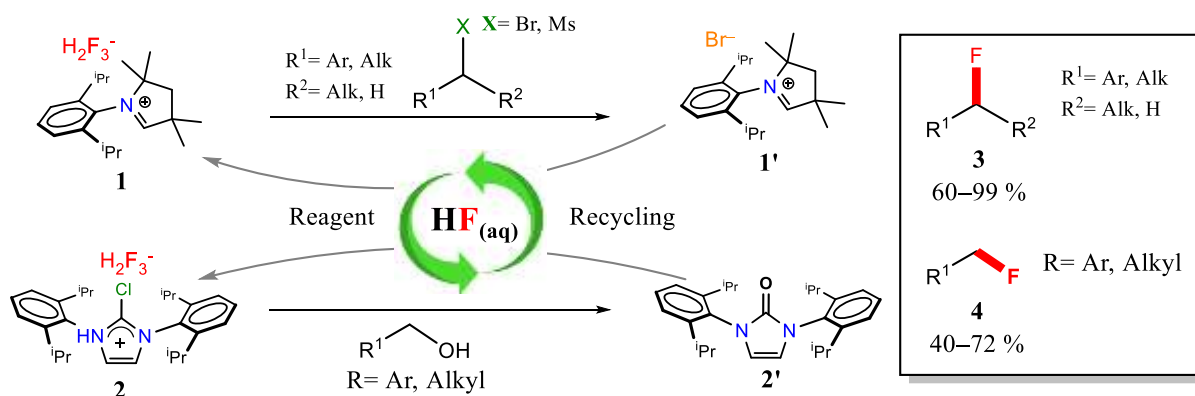


Figure 45. Fluorination with **1** and **2** and their recycle potential.

Reagent **1** is highly specific for nucleophilic fluorination of benzyl bromides to benzyl fluorides **3** with quantitative yields over wide range of substituents as well as for fluorination of <sup>o</sup>1 and <sup>o</sup>2 bromides and mesylates with good to excellent yields. **1** is a useful reagent for fluorination of silicon chlorides ( $R_3SiCl$ ), acid and sulphonyl chlorides as well as  $S_NAr$  of aromatic  $-NO_2$ . Reagent **2** is more specific for fluorination of alcohols and can convert benzyl alcohols to benzyl fluorides **4** with good yields. **1** reacts through a simple  $S_N2$  mechanism where good leaving groups like  $Br^-$  or  $OMs^-$  are replaced with a fluorine atom. The mechanism of **2** is, however, more complex and involves an imidazolium intermediate where oxygen is then transferred to the organic backbone to form imidazolone **2'**.

Both reagents can be recovered after fluorination with precipitation of bromide salts **1'** in the case of **1** and imidazolone **2'** in the case of **2** with petroleum ether and can be converted back to their respected fluorides with aqueous or anhydrous hydrofluoric acid with up to 80 % yield without any loss of activity.

### Acknowledgements

We would like to thank Slovenian research agency (ARRS) for financial support.

### References

1. T. Liang, C.N. Neumann, T. Ritter, *Angew. Chem. Int. Ed.*, **52** 8214 (2013).
2. A. Mullard, 2018 FDA drug approvals. *Nat. Revs. Drug Disc.*, **18** 85 (2019).
3. B. Langlois, L. Gilbert, G. Forat, *In Industrial Chemistry Library, Desmurs*, **8** 244 (1996).
4. B. Alič, J. Petrovčič, J. Jelen, G. Tavčar, J. Iskra, *J. Org. Chem.*, **87** 5987 (2022).

## Curcumin solid dispersion particles as novel Pickering stabilizers

Larissa C. Ghirro<sup>1,2</sup>, Stephany C. de Rezende<sup>1,3,4</sup>, Andreia S. Ribeiro<sup>3,4</sup>, Bogdan Demczuk, Jr.<sup>2</sup>, Maria Filomena Barreiro<sup>1\*</sup> and Arantzazu Santamaria-Echart<sup>1\*</sup>

<sup>1</sup>Centro de Investigação de Montanha (CIMO), Instituto Politécnico de Bragança, Campus de Santa Apolónia, 5300-253 Bragança, Portugal

<sup>2</sup>Campus Campo Mourão, Universidade Tecnológica Federal do Paraná (UTFPR), P.O. Box 271, Campo Mourao 87301-899, Brazil

<sup>3</sup>LSRE-LCM - Laboratory of Separation and Reaction Engineering - Laboratory of Catalysis and Materials Faculdade de Engenharia, Universidade do Porto, Rua Dr. Roberto Frias, 4200-465 Porto, Portugal

<sup>4</sup>ALiCE - Associate Laboratory in Chemical Engineering Faculdade de Engenharia, Universidade do Porto, Rua Dr. Roberto Frias, 4200-465 Porto, Portugal

\*barreiro@ipb.pt, asantamaria@ipb.pt

Although conventional emulsions are extensively used and disseminated in several industrial segments, emulsions stabilized by surface-active colloidal particles, defined as "Pickering emulsions", provide an alternative for producing more stable systems and even transfer their intrinsic properties to the new products [1]. The physical barrier produced by the particles at the oil-water interface allows outstanding stability compared to typical emulsions, maintaining the properties over time. Additionally, following a trend for natural-based products, there is an increase in the demand for novel functional Pickering particles produced with natural materials [2]. Within this context, solid dispersion can be a promising and novel technique to produce Pickering particles. The methodology promotes molecular interactions between a hydrophobic compound, such as curcumin, and a hydrophilic polymeric matrix, improving the wettability of the final particles. In this sense, wettability can be also modulated depending on the SD composition and used polymer.

This work proposes curcumin-based solid dispersion particles to be used as Pickering emulsion stabilizers by using K-carrageenan as the natural polymer. The particles preparation comprised an adapted procedure as follows [3]: an aqueous solution (100 mL of citric acid/sodium citrate aqueous buffer solution (pH 4.5 and 3.58) composed of 0.4g K-carrageenan and Tween 80 (15 and 24.19wt%, polymer-basis) was spilled into ethanol (50 mL) including curcumin (65% purity, 15 and 8.88wt%, polymer-basis). The mixture was sonicated (70% of potency) during 10 min (30 s on/10 s off) and spray-dried in an inert atmosphere. Two formulations were produced, named KC1 and KC2, respectively. For emulsion production, particles were dispersed in distilled water and the oil was slowly added under constant stirring. Then, the mixture was emulsified using an Ultra-Turrax homogenizer at 13,500 rpm for 7 min. Three emulsions were developed using the particles KC1 (water contact angle of  $34.97 \pm 1.21$ ) and KC2 (water contact angle of  $23.78 \pm 1.72$ ). The samples were coded as X  $\phi$  Y (Z), following the precepts where "X" refers the used particle formulation, " $\phi$  Y" the oil fraction and "Z" corresponds to the particle's concentration.

Figure 1 contains the images corresponding to the characterization of the produced Pickering emulsions, namely creaming index, optical and confocal microscopy.

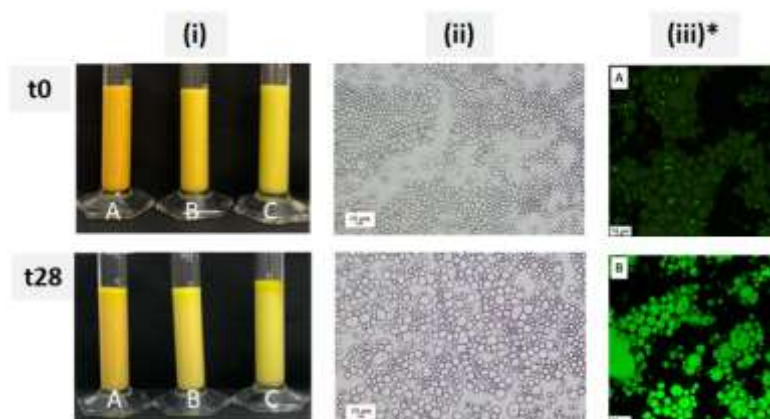


Figure 1. (i) Creaming index of the three emulsions in times 0 (t0) and 28 (t28) days; (ii) Optical microscopy of the emulsion KC1  $\phi$  0.4 (4.7%) in 0 and 28 days; (iii) Confocal microscopy images natural fluorescence of curcumin involved in the KC1 particles of KC1  $\phi$  0.4 (4.7%) sample (A) and the fluorescence of the oil phase stained with Nile red of the sample KC1  $\phi$  0.4 (4.7%) (B). \*The confocal images were acquired at t0, i.e., right after emulsion preparation.

Figure 1 (i) represents the three emulsions and the visual stability over 28 days. For the samples KC1  $\phi$  0.4 (4.7%) (A) and KC2  $\phi$  0.4 (4.7%) (B), no serum phase was observed, and the CI was 0. The behavior was slightly different for the KC1  $\phi$  0.6 (4.0%) (C), where it is noticeable a small oil accumulation at the top of the emulsion. The results obtained through optical microscopy indicated a smaller droplet size for the formulations containing a lower oil

fraction, as well higher amount of particles, maintaining these systems' stability over the evaluated time. These results are according to the literature, where authors reported that this fact is associated with the largest area to be stabilized when a higher oil fraction is presented, making difficult the coverage the entire interfacial area when the concentration of the particles is low [4]. Additionally, confocal microscopy was carried out to verify the successful role of the particles as Pickering stabilizers. The analysis allowed to observe the tight attachment of the particles containing curcumin to the dispersed phase, corroborating the effectiveness of these emulsion stabilizers.

### Acknowledgements

The authors are grateful to the Foundation for Science and Technology (FCT, Portugal) and FEDER under Programme PT2020 for financial support to CIMO (UIDB/00690/2020), LSRE-LCM (UIDB/50020/2020) and ALiCE (LA/P/0045/2020). National funding by FCT, P.I., for the institutional scientific employment program-contract for Arantzazu Santamaria-Echart. FCT for the Research grant SFRH/BD/147326/2019 of Stephany C. de Rezende.

### References

1. M. Keramat, N. Kheydoor, M.T. Golmakani. Oxidative stability of Pickering emulsions. *Food Chemistry X*, **14** 100279 (2022).
2. S. Peito, D. Peixoto, I. Ferreira-Faria, A.M. Martins, H. M. Ribeiro, F. Veiga, J. Marto, A. C. Paiva-Santos. Nano- and microparticle-stabilized Pickering emulsions designed for topical therapeutics and cosmetic applications. *International Journal of Pharmaceutics*, **615** 121455 (2022).
3. F.V. Leimann, O.H. Gonçalves, G.D. Sorita, S. Rezende, E. Bona, I.P.M. Fernandes, I.C.F.R. Ferreira, M.F. Barreiro. Heat and pH stable curcumin-based hydrophilic colorants obtained by the solid dispersion technology assisted by spray-drying. *Chemical Engineering Science*. **205** 248-258 (2019).
4. L. Chen, F. Ao, X. Ge, W. Shen. Food-grade pickering emulsions: Preparation, stabilization and applications. *Molecules*. **25** 3202 (2020).

# Green solvents – Safe reagents and chemicals – Sustainable organic synthesis



## Development of a biographene-polylactic acid hybrid material as support for enzyme immobilization

Gkantzou E.<sup>1</sup>, Alatzoglou Ch.<sup>1</sup>, Patila M.<sup>1</sup>, Polydera A.C.<sup>1</sup>, Spyrou K.<sup>2</sup>, Gournis D.<sup>2</sup>, Stamatis H.<sup>1\*</sup>

<sup>1</sup>Laboratory of Biotechnology, Department of Biological Applications and Technologies, University of Ioannina, Ioannina, Greece

<sup>2</sup>Department of Materials Science and Engineering, University of Ioannina, Ioannina, Greece

\*Corresponding author: [hstamati@uoi.gr](mailto:hstamati@uoi.gr)

### Abstract

The combination of biomolecules with graphene-based materials has been reported as a promising method to fabricate novel graphene–biomolecule hybrid nanomaterials with unique functions in different fields of study, from biology and medicine to nanotechnology and materials science [1]. However, the application of graphene in bio-related sectors requires hydrophilic and biocompatible graphene structures. The exfoliation of graphite to pristine graphene using biological agents, such as bovine serum albumin (BSA) was reported for the first time in 2015 [2]. The adsorbed protein was suggested to inhibit restacking of the graphene sheets and contribute to the material stability. In this sense, we prepared a few-layered biographene (BG) in an aqueous phase via ultrasonication, to exfoliate the graphite flakes, and intercalation of BSA between the flakes, to promote stability of the prepared material. The proposed technique provides BG with functional groups that make the material suitable support for enzyme immobilization. Different hydrolytic and oxidoreductive enzymes were successfully immobilized on the bG surface showing the potential of the system for diverse biocatalytic applications.

One step further, the prepared BG was deposited on the surface of 3D-printed polylactic acid (PLA) structures for the development of a new hybrid material. PLA is a biocompatible and biodegradable polyester made from feedstock, while its large range of mechanical and physical properties allows its engineering to suit different applications. Furthermore, 3D printing offers the capability to design complex microstructured devices, with high reproducibility in a convenient and cost-effective way. PLA-graphene hybrid materials have been reported as promising candidates for biosensor design, combining the biocompatibility of PLA with the excellent conductivity of graphene. In this work, we present a PLA-biographene material for the immobilization of different enzymes, suitable in biocatalytic processes. The prepared material was characterized by a combination of spectroscopic and microscopic techniques and enzyme immobilization was verified with different biochemical techniques.

### Methods

For the synthesis of bio-graphene (BG) 100 mg of graphite were added to 20 mL of ultra-pure water (final graphite concentration 5 mg mL<sup>-1</sup>). The sample was ultra-sonicated for one hour, BSA (final concentration 4 mg mL<sup>-1</sup>) was then added and the solution was allowed to stir for one hour. The sample was centrifuged at 2500 rpm and the supernatant, containing the BG, was selected and collected.

Glucose Oxidase from *Aspergillus niger* was covalently immobilized on both BG and PLA-B-G by using glutaraldehyde as the cross-linker.

### Results

BG was synthesized by following the procedure that is presented in Figure 1. The synthesis involves the exfoliation of graphite in water, in the presence of BSA, producing a water-stable graphene-derivative. This bio-based nanomaterial was further combined with PLA to fabricate a matrix for the immobilization of GOx.

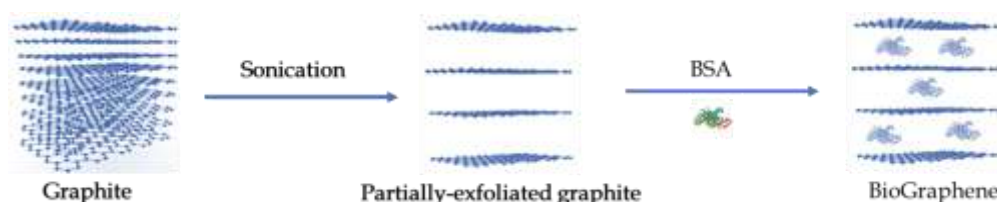


Figure 46. Production of BG via a green exfoliation method.

In the next step, GOx was covalently immobilized in PLA-BG material. The immobilized nanobiocatalyst was tested for its catalytic activity. The immobilized enzyme was found to be effectively used for the oxidation of glucose, indicating that this immobilization matrix could be used for the design of novel glucose biosensors.

## **Acknowledgements**

This research has been co-financed by the European Regional Development Fund of the European Union and Greek national funds through the Operational Program Competitiveness, Entrepreneurship and Innovation, under the call RESEARCH – CREATE - INNOVATE (project code:T2EDK-02171).

## **References**

- [1] Li, D. et al. *When. Nanoscale* 8, 19491–19509 (2016).
- [2] Pattammattel, A. & Kumar, C. V. *Kitchen Chemistry* 101, *Adv. Funct. Mater.* 25, 7088–7098 (2015).

## Dimethyl isosorbide via dimethyl carbonate chemistry: scaling-up, purification and concurrent reaction pathways

Mattia Annatelli,<sup>a\*</sup> Davide Dalla Torre,<sup>a</sup> Fabio Aricò<sup>a</sup>

<sup>a</sup> Department of Environmental Science, Informatics and Statistics, Ca' Foscari University of Venice (IT).

\*e-mail: [mattia.annatelli@unive.it](mailto:mattia.annatelli@unive.it)

**ABSTRACT:** Dimethyl isosorbide (**DMI**) is a well-known bio-based solvent that can be used as green alternative for conventional dipolar media (dimethyl sulfoxide, dimethylformamide). [1] The synthetic procedures to **DMI** reported in the literature are based on the methylation of isosorbide in presence of basic or acid catalysts and employing different alkylating agents. [2] Among them, dimethyl carbonate (**DMC**) - a well-known green reagent and solvent - is considered one of the most promising for its good biodegradability and low toxicity. [3]

In this work, we report a comprehensive investigation on methylation of isosorbide via **DMC** chemistry promoted by basic (nitrogen organocatalysts) or acidic (ion exchange resins) catalysts. In both cases, reaction conditions were optimized and then efficiently applied for the methylation of isosorbide epimers, isoidide and isomannide, and for some preliminary scale-up tests (up to 10 grams of isosorbide). For the first time, all seven methyl and methoxycarbonyl intermediates observed in the etherification of isosorbide were isolated and fully characterized. [4] This has provided an insight on the concurrent reaction pathways leading to **DMI** and on the role played by catalysts in the methylation of isosorbide. As a result, a reaction mechanism for the conversion of isosorbide into **DMI** via **DMC** chemistry has been proposed both in acid and basic conditions.

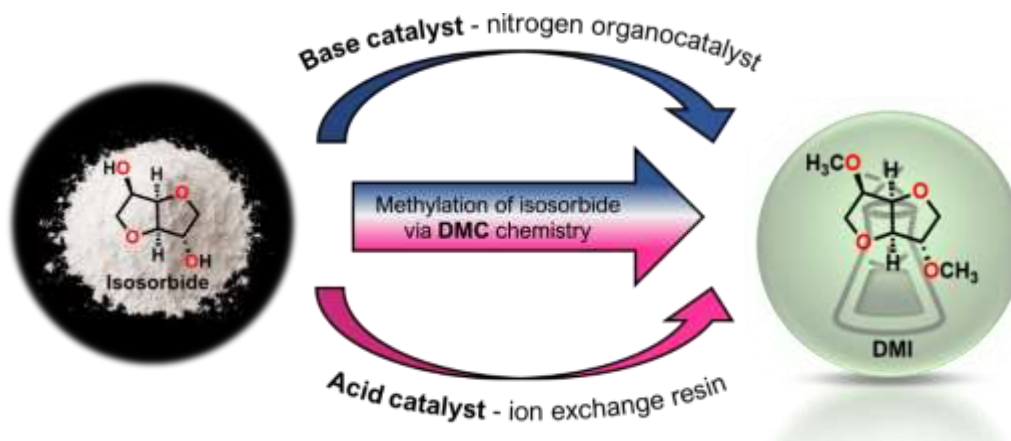


**Figure 1.** Acid and base catalyzed synthesis of dimethyl isosorbide via dimethyl carbonate chemistry.

### References

- [1] (a) F. Gao *et al.*, *Green Chem.*, **2020**, *22*, 6240-6257; (b) J. Sherwood *et al.*, *Chem. Commun.*, **2014**, *50*, 9650-9652; (c) F. Aricò, *Curr. Opin. Green Sustain. Chem.*, **2020**, *21*, 82-88.
- [2] (a) P. Fuertes *et al.*, *WO 2007/096511 A1*, **2007**; (b) A. East *et al.*, *US2008/0021209 A1*, **2008**; (c) S. Chatti *et al.*, *Tetrahedron*, **2001**, *57*, 4365-4370; (d) S. Chatti *et al.*, *Tetrahedron Lett.*, **2001**, *41*, 3367-3370.
- [3] P. Tundo, M. Musolino and F. Aricò, *Green Chem.*, **2018**, *20*, 28-85.
- [4] M. Annatelli, D. Dalla Torre, M. Musolino, F. Aricò, *Catal. Sci. Technol.*, **2021**, *11*, 3411-3421.

## Acidic deep eutectic solvents-based efficient oxidative extractive desulfurization of fuel oil

Boyeon Bae<sup>1</sup>, Seulgi Kang<sup>1</sup>, Ke Li<sup>1</sup>, Yua Kang<sup>1</sup>, Danbi Won<sup>1</sup>, Jeongmi Lee<sup>1\*</sup>

<sup>1</sup>School of Pharmacy, Sungkyunkwan University, Suwon, 16419, Republic of Korea

\*Corresponding authors: jlee0610@skku.edu

### Abstract text:

Fuel oil generates pollutants including NO<sub>x</sub>, SO<sub>x</sub>, and CO. In particular, sulfur compounds in fuel is tightly regulated to prevent environmental pollution such as air pollution and acid rain. Hydrodesulfurization (HDS) is the most common method for removal of sulfur compounds. It operates under high temperature and high pressure and therefore requests high costs and significant energy consumption. In addition, it has limited removal efficiency for several atomic sulfur compounds including benzothiophene (BT), dibenzothiophene (DBT), and their derivatives. For these reasons, alternative or complementary methods to HDS are essential. In recent years, a number of alternative approaches including biodesulfurization (BDS), extractive desulfurization (EDS), and adsorptive desulfurization (ADS) have been suggested. Oxidative extractive desulfurization (OEDS) is a promising alternative approach due to its mild operating conditions and high desulfurization capabilities compared to the others. Performance of OEDS is greatly affected by the type of solvents used. Ionic liquids (ILs) were used, but they have several issues such as high cost, low biodegradability, and toxicity. Deep eutectic solvents (DESs) were also used, and their acidity was suggested as an important parameter in OEDS. In this study, effects of DES acidity on OEDS using H<sub>2</sub>O<sub>2</sub> as a green oxidizing agent were investigated. To this, a series of DESs were designed and synthesized by changing the type of hydrogen bond donors (HBDs) or acids and their molar ratio to hydrogen bond acceptor (HBA). Acidity of DESs was measured using the Hammett method and pH meter, and the desulfurization efficiency was evaluated using gas chromatography-mass spectrometry (GC-MS). The results indicate that acidity and viscosity of DES are important factors in OEDS. Currently, the most efficient OEDS conditions are under optimization with consideration of cost, solubility, and desulfurization efficiency using central composite design-based response surface methodology.

### Acknowledgements

This study received financial support from a research grant from the National Research Foundation of Korea (No. 2020R1A2C1014006).

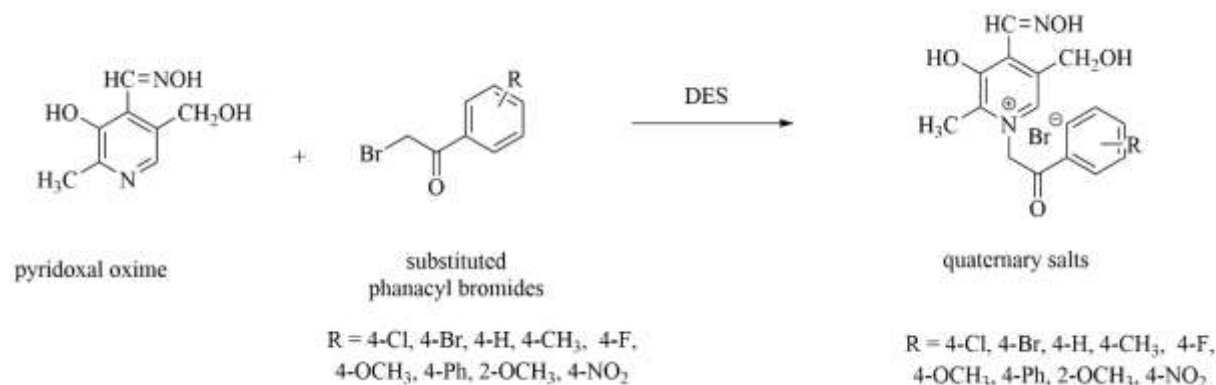
# An Eco-Friendly Preparations of Pyridoxal Oxime Quaternary Salts in Deep Eutectic Solvents

Valentina Bušić, Dajana Gašo-Sokač, Mario Komar and Maja Molnar

Faculty of Food Technology Osijek, Franje Kuhača 18, 31000 Osijek, Josip Juraj Strossmayer University of Osijek, Croatia  
\*e-mail: valentina.busic@pfos.hr

Quaternization of pyridine with alkyl halides or related compounds is an example of the Menshutkin reaction, the most common route to create quaternary salts. The most organic solvents used in conventional synthesis of pyridinium quaternary salts are volatile, hazardous, toxic like anhydrous benzene [1], acetonitrile and acetone [2-3]. Also, a lots of these solvents are considered a hazardous waste when are discarded. Reducing toxicity is one of the most challenging aspects of designing chemical syntheses. Deep eutectic solvents (DESs) have emerged recently as new and green solvents in organic synthesis.

After we successfully quaternized pyridine derivatives in DESs in our previous study Bušić et al. [4], we continue to perform syntheses of pyridoxal oxime quaternary salts in eutectic solvents. In this study it was performed quaternization reaction of pyridoxal oxime and substituted phenacyl bromides in 16 choline chloride-based DESs by three synthetic approaches: conventional, microwave and ultrasound (Scheme). The purpose of this work was to investigate which eutectic solvent is most effective for the quaternization reaction.



Scheme. Quaternization reaction of pyridoxal oxime and substituted phenacyl bromides

After the performed syntheses, the results show that the conventional method, with a long reaction time, generally gave low product yields in eutectic solvents. In the conventional method, the most effective eutectic solvents were: choline chloride: thiourea, choline chloride: oxalic acid, and choline chloride: levulinic acid. The highest yields of reactions in DESs were obtained using microwave irradiation where the most effective eutectic solvents were: choline chloride: oxalic and choline chloride: levulinic. Choline chloride: malic acid, choline chloride: malonic and choline chloride: *trans*-cinnamic acid gave approximately equal yields. In the ultrasound method the most effective eutectic solvents for the quaternization of pyridoxal oxime with substituted phenacyl bromides were choline chloride: oxalic, choline chloride: levulinic and choline chloride: *trans*-cinnamic acid and reactions were carried out with yields higher than those in the conventional method.

The obtained results for quaternization reaction of pyridoxal oxime show that the methods under the influence of microwave and ultrasound irradiation were the most effective for quaternization in eutectic solvents.

## Acknowledgements

This work was supported by Croatian Science Foundation and the Green Technologies in Synthesis of Heterocyclic Compounds Project UIP-2017-05-6593.

## References

1. N. Pidlypnyi, S. Kaul, S. Wolf, M.H.H. Drafz, A. Schmidt, *Naturforsch.*, **69b** 605 (2014).
2. S.K. Kim, *JKCS*, **48** 254 (2004).
3. J. Marek, D. Malinak, R. Dolezal, O. Soukup, M. Pasdiorova, M. Dolezal and K. Kuca, *Molecules*, **20** 368 (2015).
4. V. Bušić, S. Roca, D. Vikić-Topić, K. Vrandečić, J. Ćosić, M. Molnar, D. Gašo-Sokač, *Environ. Chem. Lett.* **18(3)** 889 (2020).

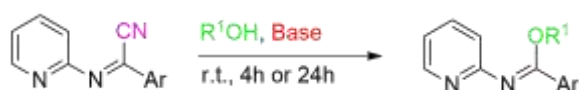
## Green Synthetic Transformation of Benzimidoyl-cyanides to the Valuable Intermediates Alkyl-*N*-pyridin-2-yl-benzimidates

Andriani G. Chaidali and Ioannis N. Lykakis\*

Department of Chemistry, Aristotle University of Thessaloniki, Thessaloniki, Greece

\* [chaidali.and@gmail.com](mailto:chaidali.and@gmail.com); [lykakis@chem.auth.gr](mailto:lykakis@chem.auth.gr)

In this study, the facile transformation of a series of benzimidoyl-cyanides to the corresponding alkyl-*N*-pyridin-2-ylbenzimidates was performed under Green Conditions. The main aim is to develop an one-pot synthetic methodology in the field of sustainable chemistry, in the absence of metals and in the presence only of a base in alcoholic media. From the mechanistic point of view alcoholic media plays a dual role, the solvent, and the nucleophile reagents. Under the evaluation conditions, Cs<sub>2</sub>CO<sub>3</sub> and DBU were selected as the appropriate bases and methanol, ethanol and propanol as the best alcoholic media, at room temperature. Further studies show that amines or thiols can react successfully leading to the corresponding *N*- and *S*-imidates without the requirement of a catalyst or metal, as presented until since now in the literature. [1],[2]. The future goal is to generalize this methodology, by finding the structural boundaries, and the synthesis of compounds with several nucleophilic groups with possible biological activation.



### References

1. Guanjie Wang, Chenlong Wei, Xianfang Hong, Zhenqian Fu, Wei Huang, *Green Chem.*, **22**, 6819-6826 (2020)
2. David J. Birch, Allen J. Guildford, Margaret A. Tometzki., Ralph W. Turner , *J. Org. Chem.*, **47**, 3548-3550 (1982)

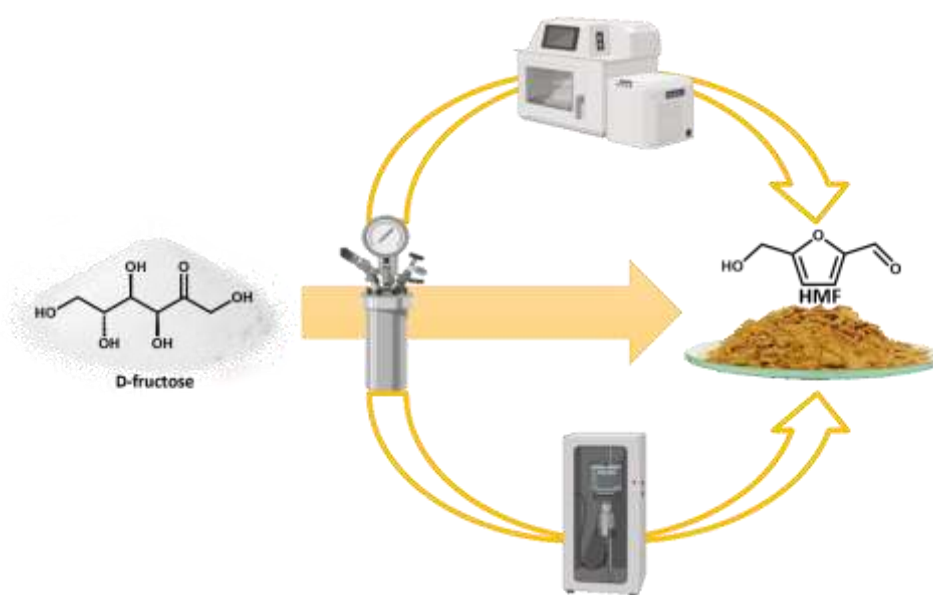
## Multi gram scale synthesis of HMF and comparative environmental evaluation

Beatriz Chicharo\*, Giacomo Trapasso, Mattia Annatelli, Davide Dalla Torre, Giovanna Mazzi, Fabio Aricò

*1Department of Environmental Science, Informatics and Statistics/Ca' Foscari University, Venice*

*\*b.chicharo@campus.fct.unl.pt*

5-Hydroxymethylfurfural (HMF) is a bio-based platform chemical that can be used as building block to produce complex and useful compounds with diverse applicability, in particular, bio-based polymers, materials and fuels [1], [2]. Even though HMF synthesis holds promise for a greener future, with the current state of technology the high production cost limits its competitiveness at an industrial scale[1]. In this project our main goal is to develop an optimized procedure for the synthesis of HMF that will allow us to perform scale-up reactions with competitive yields with a green mindset. The synthesis of HMF from the dehydration of D-fructose, already investigated by our research group[2], was performed with a heterogeneous acid catalyst using various conditions in different settings: autoclave, sonicator and microwave oven. The best results were obtained employing a stainless-steel autoclave which allowed a large scale HMF production using up to forty grams of D-fructose as starting material. The final product was recovered from the crude mixture and purified by a custom-made crystallization procedure. Finally, green metrics were used to evaluate the greenness of the reaction in comparison with previously reported works[3].



### References

- [1] R. Luque, "Chem Soc Rev Recent catalytic routes for the preparation and the upgrading of biomass derived furfural," pp. 4273–4306, 2020, doi: 10.1039/D0CS00041H.
- [2] F. A. Manuele Musolino, John Andraos, "An Easy Scalable Approach to HMF Employing DMC as Reaction Media : Reaction Optimization and Comparative Environmental Assessment," no. Dmc, pp. 2359–2365, 2018, doi: 10.1002/slct.201800198.
- [3] J. Andraos, D. M. Road, O. Mb, and A. Hent, "Simplified Application of Material Efficiency Green Metrics to Synthesis Plans: Pedagogical Case Studies Selected from Organic Syntheses," 2015, doi: 10.1021/acs.jchemed.5b00058.

## Nanoarchitectonics of phosphorylated graphitic carbon nitride for sustainable, selective and metal-free synthesis of primary amides

Priyanka Choudhary, Ajay Kumar and Venkata Krishnan\*

School of Basic Sciences and Advanced Materials Research Center, Indian Institute of Technology Mandi, Kamand, Mandi 175075, H.P., India. Email: [vkkn@iitmandi.ac.in](mailto:vkkn@iitmandi.ac.in)

Amides are well known to be one of the most important class of organic compounds due to their wide spread use in natural, synthetic and biological chemistry [1-3]. Amides form the elemental backbone of biologically active molecules and plays crucial role as intermediates in the synthesis of peptides and proteins [4]. In addition, amides are also used in the synthesis of heterocyclic compounds, pharmaceuticals, natural products, agrochemicals, lubricants, pigments, anti-block reagents, polymers, etc. [5, 6]. The conventional methods of amide synthesis involves reaction of carboxylic acid derivatives, such as aldehydes, ketones, anhydrides, acid chlorides and esters with amine derivatives [7, 8]. Other commonly utilized procedures for the synthesis of amides include Beckmann rearrangement, Staudinger reaction, Aube-Schmidt rearrangement, hydration of nitriles, C-H oxidative amidation and transamidation [2, 9, 10]. However, these methods involve the use of hazardous reactants, stoichiometric reagents, harsh reaction conditions, low atom economy and poor reaction efficiency due to formation of equimolar side products. Hence, the development of sustainable, environment friendly, economic protocols for the formation of amide bond is utmost desired.

For the synthesis of amides, alcohols and aldehydes are considered to be desirable reactants due to their ease of availability, low-cost and non-toxic nature. In addition the expected byproducts for the reaction of alcohols and aldehydes with amine derivatives is only water and hydrogen [9]. However, the direct synthesis of amides from alcohols and aldehydes is a very challenging process because the hemiaminal intermediate formed during the process readily undergoes dehydration rather than dehydrogenation [11]. Hence, a highly effective and selective catalyst is required to catalyze the reaction through dehydrogenation process in order to avoid the formation of nitriles as the side products of the reaction. In the drive toward sustainable and green chemistry, the use of toxic solvents and high energy consumption should be minimized [12]. The use of harmful solvents can cause detrimental impact on human health and increases waste generation in a chemical process [13]. This can be taken care by using environmentally benign reaction medium and optimum conditions of temperature and pressure. The use environmentally benign solvents can reduce environmental-factor and subsequently increase the atom economy of a reaction. The synthesis of amides from aldehydes generally makes use of toxic solvents and requires high temperature and pressure conditions which is not a sustainable process for a large scale industrial process.

In this work, a green, sustainable, ecofriendly and highly selective protocol for synthesis of primary amides from aldehydes using a highly efficient heterogenous, metal-free phosphorylated graphitic carbon nitride (P-GCN) catalyst is demonstrated. The P-GCN catalyst was synthesized via Arbuzov reaction and was thoroughly characterized using several techniques like PXRD, FTIR, TGA, SEM, TEM, XPS, BET and TPD. The reactions were conducted under ambient conditions of temperature and pressure in environmentally benign solvents. The detailed optimization of reaction conditions was carried out in order to achieve high product yield with high catalytic efficacy. The reactions performed at optimized reaction conditions resulted in high yields and high turnover numbers (TON). The P-GCN catalyst exhibited excellent recyclability and the developed protocol can be used for a wide range of substrates demonstrating its wide applicability. In addition, an atom economy of 98% and E-factor of 0.05 was calculated for the developed protocol which is highly desirable in terms of green and sustainable chemistry. The current protocol provide a sustainable approach for the synthesis of amides in a clean atom-economical manner which can pave the way for the development of green organic processes using metal-free catalysts.

**Table 1.** Optimization of reaction conditions for amidation of benzaldehyde using P-GCN catalyst [14].

Entry	Catalyst	Nitrogen source	Temp. (°C)	Solvent	Time (min)	Conversion (%)	Yield (%)
1	P-GCN (10 mg)	NH <sub>4</sub> OAc	RT	EtOH	60	40	36
2	P-GCN (10 mg)	30 % NH <sub>3</sub>	RT	EtOH	60	63	60
3	P-GCN (10 mg)	(NH <sub>4</sub> ) <sub>2</sub> CO <sub>3</sub>	RT	EtOH	60	60	56
4	P-GCN (10 mg)	NH <sub>4</sub> HCO <sub>2</sub>	RT	EtOH	60	52	48
5	P-GCN (10 mg)	(NH <sub>4</sub> ) <sub>2</sub> H <sub>2</sub> PO <sub>4</sub>	RT	EtOH	60	48	45
6	P-GCN (10 mg)	NH <sub>4</sub> Cl	RT	EtOH	60	34	30



7	P-GCN (20 mg)	30 % NH <sub>3</sub>	RT	EtOH	60	73	70
8	P-GCN (30 mg)	30 % NH <sub>3</sub>	RT	EtOH	60	87	83
9	P-GCN (40 mg)	30 % NH <sub>3</sub>	RT	EtOH	60	90	85
10	P-GCN (30 mg)	30 % NH <sub>3</sub>	50 °C	EtOH	60	92	88
11	P-GCN (30 mg)	30 % NH <sub>3</sub>	50 °C	EtOH	90	99	95
12	P-GCN (30 mg)	30 % NH <sub>3</sub>	50 °C	H <sub>2</sub> O	90	69	65
13	P-GCN (30 mg)	30 % NH <sub>3</sub>	50 °C	IPA	90	65	62
14	P-GCN (30 mg)	30 % NH <sub>3</sub>	50 °C	t-BuOH	90	63	58
15	P-GCN (30 mg)	30 % NH <sub>3</sub>	50 °C	DMC	90	40	36
16	P-GCN (30 mg)	30 % NH <sub>3</sub>	50 °C	DMSO	90	45	42
17	P-GCN (30 mg)	30 % NH <sub>3</sub>	50 °C	ACN	90	48	45
18	P-GCN (30 mg)	30 % NH <sub>3</sub>	50 °C	DCM	90	52	48
19	GCN (30 mg)	30 % NH <sub>3</sub>	50 °C	EtOH	90	35	32
20	No Catalyst	30 % NH <sub>3</sub>	50 °C	EtOH	360	0	No reaction

<sup>a</sup>Reaction conditions: solvent (5 mL), benzaldehyde (1 mmol), nitrogen source (3 mmol), RT= 25 °C, <sup>b</sup>isolated yields.

In summary, a highly selective, efficient, green protocol is developed for the amidation of aldehydes using P-GCN nanosheets as the catalyst. The P-GCN catalyst was synthesized by successive phosphorylation of GCN nanosheets which results in the generation of Brønsted acidic sites on the GCN nanosheets which plays crucial role in the amidation reaction. The as-synthesized catalyst exhibited high catalytic performance at optimal conditions of time and temperature in environmentally benign solvents. The developed protocol resulted in high product yields and TON values demonstrating its wide potential for large scale synthesis. In addition, the P-GCN catalysts shows excellent recyclability and reusability. Hence, the developed protocol for the amidation reactions using metal-free P-GCN catalyst can effectively replace the expensive metal based catalysts available in the market which can pave a way towards sustainable and greener future.

## References

- [1] V.R. Pattabiraman, J.W. Bode, *Nature*, **480** 471 (2011).
- [2] V. Polshettiwar, R.S. Varma, *Chem. Eur. J.*, **15** 1582 (2009) -1586.
- [3] P. Sudarsanam, B. Hillary, M.H. Amin, S.B. Abd Hamid, S.K. Bhargava, *Appl. Catal. B.*, **185** 213 (2016).
- [4] S. Mahesh, K.-C. Tang, M. Raj, *Molecules*, **23** 2615 (2018).
- [5] B.L. Bray, *Nat. Rev. Drug Discov.*, **2**, 587 (2003).
- [6] E. Valeur, *Chem. Soc. Rev.*, **38** 606 (2009).
- [7] A. Khalafi-Nezhad, A. Parhami, M.N.S. Rad, A. Zarea, *Tetrahedron Lett.*, **46** 6879 (2005).
- [8] R.S. Mane, B.M. Bhanage, *RSC adv.*, **5** 76122 (2015) -76127.
- [9] K. Yamaguchi, H. Kobayashi, T. Oishi, N. Mizuno, *Angew. Chem. Int. Ed.*, **51** 544 (2012).
- [10] J. Chen, Y. Xia, S. Lee, *Org. Lett.*, **22** 3504 (2020).
- [11] S. Shang, P.-P. Chen, L. Wang, Y. Lv, W.-X. Li, S. Gao, *ACS Catal.*, **8** 9936 (2018).
- [12] D. Dallinger, C.O. Kappe, *Chem. Rev.*, **107** 2563 (2007).
- [13] P. Choudhary, A. Kumar, A. Bahuguna, V. Krishnan, *Emerging Carbon-Based Nanocomposites for Environmental Applications* 71 (2020).
- [14] P. Choudhary, A. Kumar, V. Krishnan, *Chem. Eng. J.*, 431 133695 (2022).

## A greener approach towards coumarin analogues via Natural Deep Eutectic Solvent-mediated Suzuki-Miyaura coupling

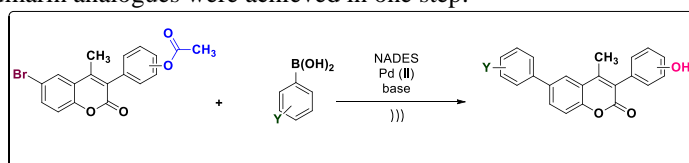
Annita Katopodi<sup>1</sup> and Anastasia Detsi<sup>1\*</sup>

<sup>1</sup>Laboratory of Organic Chemistry, School of Chemical Engineering, National Technical University of Athens, Zografou Campus, Athens, Greece

\*adetsi@chemeng.ntua.gr

Green chemistry is a rapidly developing research field due to the growing environmental awareness and the urge to reduce the use and release of hazardous chemicals in the environment [1]. Green tools are introduced to chemical synthetic procedures which include the use of alternative energy sources (e.g. ultrasound and microwave irradiation) and greener reaction media, such as deep eutectic solvents [2]. Deep eutectic solvents (DES) are liquid eutectic mixtures of at least two components, a hydrogen bond donor (HBD), and a hydrogen bond acceptor (HBA), in appropriate molar ratios, which are capable of forming intermolecular interactions. DES have emerged as a promising alternative to conventional organic solvents, finding application in various scientific fields such as extraction and catalysis [3]. The Suzuki–Miyaura coupling is the most commonly used carbon–carbon bond forming reaction in the pharmaceutical industry. It is the reaction between an aryl boronic acid with an aryl halide in the presence of a palladium catalyst (sometimes partnered with a ligand that stabilises the species and facilitates reaction) and aqueous base in a suitable solvent, such as toluene and dioxane [4].

Coumarins constitute a large class of naturally or synthetically occurring heterocyclic compounds, which belong to the benzopyrone family and possess a wide array of biological activities including antioxidant, anti-inflammatory, neuroprotective and anticancer [5]. In an effort to develop small “chemical libraries” of coumarin derivatives bearing various substituents on the benzopyrone scaffold, we set out to synthesize aryl-substituted coumarins via the Suzuki-Miyaura coupling reaction. The 6-bromo-coumarin scaffold was selected as a substrate, along with a palladium catalyst and an inorganic base. In order to develop a green approach to the desired products, natural deep eutectic solvents (NADES) were applied as solvents combined with a high energy technique (ultrasound). The optimization of the reaction conditions was achieved using a model reaction between the synthetically prepared 3-(4-acetyloxy-phenyl)- 6-bromo-4-methyl-coumarin and phenyl boronic acid. Three different NADES and several inorganic bases were used and conventional as well as ultrasound heating were employed. We were gratified to find that the reaction proceeded smoothly in 20min under ultrasound irradiation producing the desired product in satisfactory yields and that it is applicable to a aryl-boronic acids bearing various substituents. Interestingly, when a coumarin bearing an acetyloxy moiety was used, a concomitant removal of the acetyl group was succeeded under the reaction conditions. Thus, the carbon–carbon bond formation and the deacetylation of the coumarin analogues were achieved in one step.



The developed green methodology produced the desired coumarin analogues in satisfactory yields and purity whereas the recyclability and reusability of the NADES were succeeded for 4 times without compromising the yield and efficiency of the reaction.

### Acknowledgements

A. K. gratefully acknowledges State Scholarships Foundation (IKY). This research is co-financed by Greece and the European Union (ESF) through the Operational Programme (Human Resources Development, Education and Lifelong Learning) in the context of the project “Strengthening Human Resources Research Potential via Doctorate Research” (MIS-5000432), implemented by the State Scholarships Foundation (IKY).

### References

1. A. Tzani, M.A. Karadendrou, T. Tsiaka, E. Kritsi, P. Zoumpoulakis, A. Detsi, Deep Eutectic Solvents: Properties, Applications and Toxicity, Chapter 2: Exploring the Role of Natural Deep Eutectic Solvents (NADES) Towards the Valorization of Food Processing Industry Waste. Nova Science Publishers, 19-51 (2022).
2. S. Gulati, R. Singh, S. Sangwan, *RSC Advances*, **11** 29130 (2021).
3. M.A. Karadendrou, I. Kostopoulou, V. Kakokefalou, A. Tzani, A. Detsi, *Catalysts*, **12** 249 (2022).
4. D. Blakemore, P. Doyle, Y. Fobian, Synthetic Methods in Drug Discovery: Volume 1, Chapter 1: Suzuki–Miyaura Coupling. Royal Society of Chemistry, 1-69 (2015).
5. A. Katopodi, E. Tsotsou, T. Iliou, G.E. Deligiannidou, E. Pontiki, C. Kontogiorgis, F. Tsopeles, A. Detsi, *Molecules*, **26** 5999 (2021).

## Development of bioactive chitosan-based hydrogels using Natural Deep Eutectic Solvents (NADES) as dissolution and gelating agents

Pitterou I.<sup>1</sup>, Ntirogianni A.<sup>1</sup>, Tzani A.<sup>1</sup>, Tsiantas K.<sup>2</sup>, Batrinou A.<sup>2</sup>, Zoumpoulakis P.<sup>2</sup>, Detsi A.<sup>1\*</sup>

<sup>1</sup>Laboratory of Organic Chemistry, School of Chemical Engineering, National Technical University of Athens, Zografou Campus, 15780, Athens, Greece

<sup>2</sup>Laboratory of Chemistry, Analysis and Design of Food Processes, Department of Food Science and Technology, University of West Attica, Ag. Spyridonos, 12243 Egaleo, Athens, Greece

\*adetsi@chemeng.ntua.gr

Hydrogels are 3D hydrophilic polymeric networks that do not dissolve but can swell, in water. In the last few years, there is increasing interest in these materials thanks to their solid and liquid-like properties, high biocompatibility, easy preparation, and versatile applications.

Chitosan is a unique cationic polysaccharide, with well-known antioxidant, lipid-lowering and antimicrobial activities. The cationic nature of chitosan leads, under acidic conditions, to the development of various forms, such as nano/micro-particles, emulsions, fibers, hydrogels, films and membranes [1].

The formation of chitosan hydrogels is usually a two-step process involving polymer dissolution and physical or chemical cross-linking [2]. The formation of physical (or reversible) hydrogels is based on the development of hydrogen and/or Van der Waals bonds as well as electrostatic interactions between the cationic polymer and the cross-linker.

Deep Eutectic Solvents (DES) are mixtures of two or more components, a hydrogen bond acceptor and a hydrogen bond donor, with a low-temperature eutectic point. When the components of the DES are naturally occurring compounds, the solvents are characterised as Natural Deep Eutectic Solvents (NADES). Due to their high biodegradability potential, NADES have emerged in research towards greener processes development, and a wide variety of applications have been reported (extraction solvents, catalysts and solvents for organic synthesis, plasticizers in the production of films etc) [1-5].

In the present work, a greener approach towards the formation of chitosan hydrogels is presented. The ability of Choline Chloride/Lactic Acid (1:2) NADES to act as a dissolution agent for chitosan and simultaneously as a gelator for the formation of a hydrogel was investigated. The components of the NADES were selected on the basis of their safety regarding pharmaceutical and food applications as well as on the basis that, when dissolved in water, the NADES results to an acidic solution (pH 1.62), which is an indispensable requirement for chitosan dissolution.

Swelling ratio and water retention ratio were measured in the obtained hydrogel in a hydrochloric acid solution at pH=1.2. The water retention ratio remained over 90%, after keeping the swollen sample in the HCl solution for 2 hours, showing the maximum value at 5 minutes. Furthermore, the chitosan-based hydrogel achieved a water swelling ratio of 136% after 5 minutes.

In an effort to investigate the ability of a plant extract, obtained using NADES as the extraction and storage medium, we performed an extraction of olive leaves using two different NADES, namely Choline Chloride/Lactic Acid (1:2) and Glucose/Lactic acid (1:5). The as-obtained extracts, rich in phenolic antioxidants, were successfully applied to the developed process to form hydrogels.

The prepared hydrogels were evaluated for their bioactivity, regarding their antioxidant activity (evaluation of their ability to scavenge the stable free radical DPPH and their ability to inhibit lipid peroxidation induced by the thermal free radical initiator AAPH). In addition, antimicrobial activity was assessed on gram negative *Escherichia coli* ATCC 259 and *Salmonella* Typhimurium ATCC 14028 as well as on gram positive *Listeria monocytogenes* ATCC 35152 and *Staphylococcus aureus* ATCC 6538.

### References

1. Detsi, A., Kavetsou, E., Kostopoulou, I., Pitterou, I., Pontillo, A.R.N., Tzani, A., Christodoulou, P., Siliachli, A., Zoumpoulakis, P., *Pharmaceutics*, **12** 669 (2020).
2. Maddaloni, M., Vassalini, I., Alessandri, I., *Sustain. Chem*, **1** 325-344 (2020).
3. Tzani, A., Kalafateli, S., Tatsis, G., Bairaktari, M., Kostopoulou, I., Pontillo, A.R.N., Detsi, A., *Sustain. Chem*, **2** 576-599 (2021).
4. Pontillo, A. R. N., Koutsoukos, S., Welton, T., Detsi, A., *Materials Advances*, **2** 3954-3964 (2021).
5. Tzani, A.; Karadendrou, M.A.; Tsiaka, T.; Kritsi, E.; Zoumpoulakis P.; Detsi A. Chapter 2: Exploring the Role of Natural Deep Eutectic Solvents (NADES) Towards the Valorization of Food Processing Industry Waste. Nova Science Publishers, 19-51 (2022)

## Natural Deep Eutectic Solvents (NADES) as green alternative solvents for the extraction of bioactive compounds from Greek wild rose (*Rosa canina* L.) rosehip shells (hypanthia)

Tzani A.<sup>1</sup>, Kalafateli S.<sup>1</sup>, Karadendrou M.A.<sup>1</sup>, Katopodi A.<sup>1</sup>, Kostopoulou I.<sup>1</sup>, Bobolou D.<sup>1</sup>, Bon A.<sup>1</sup>, Nanou D.<sup>1</sup>, Kalantzi S.<sup>2</sup>, Lemoni, Z.<sup>2</sup>, Mamma D.<sup>2</sup>, Maloupa E.<sup>3</sup>, Papanastasi K.<sup>3</sup>, Grigoriadou K.<sup>3</sup>, Krigas N.<sup>3</sup>, Papadopoulou A.<sup>4</sup>, Kletsas D.<sup>4</sup>, Samanidis I.<sup>5</sup>, Aggeli K.<sup>5</sup>, Stavropoulos G.<sup>5</sup>, Detsi A.<sup>1\*</sup>

<sup>1</sup>Laboratory of Organic Chemistry, School of Chemical Engineering, National Technical University of Athens, Zografou Campus, 15780 Athens, Greece

<sup>2</sup> Biotechnology Laboratory, School of Chemical Engineering, National Technical University of Athens, Zografou Campus, 15780 Athens, Greece

<sup>3</sup> Institute of Plant Breeding and Genetic Resources, Balkan Botanic Garden of Kroussia, HAO-DEMETER, Leoforos Georgikis Sxolis, 570 01, Thessaloniki, Greece

<sup>4</sup> Laboratory of Cell Proliferation and Ageing, Institute of Biosciences and Applications, National Centre for Scientific Research "Demokritos", 15341 Athens, Greece

<sup>5</sup> KORRES SA-NATURAL PRODUCTS, 57<sup>th</sup> Km Athens- Lamia Road, Oinofita Viotia

\*adetsi@chemeng.ntua.gr

*Rosa canina* L. (dog rose or wild rose) is a native shrub of Europe and the Mediterranean region. The 9shell (hypanthium) of its "pseudofruit" (rosehip) consists of a rich source of bioactive phytochemicals such as phenols, flavonoids, tannins, carotenoids, sugars, organic acids (including vitamin C), amino acids and essential oils. Dried rosehips have been traditionally used for the preparation of herbal teas but also to treat cough and cold influenza symptoms [1-3]. Due to the antioxidant and anti-inflammatory activity of rosehip extracts, they are commonly used in the food and cosmetic industries.

For the extraction process, traditional methods are implemented (such as Soxhlet, percolation, maceration etc.) using common organic and, in many cases, volatile solvents. The main disadvantages and limitations of these methods are the relatively long extraction times (ranging from hours to days), the high temperatures and the use of large amounts of costly and often hazardous organic solvents needed. The use of green solvents in plant extraction processes has recently emerged as a sustainable solution. Natural Deep Eutectic Solvents (NADES) are considered as promising solvents for extraction [4-7] due to the formation of strong hydrogen bonds between their components and the targeted extraction compounds which are responsible for the increased extraction yields, the stabilization of the obtained extracts and the protection of the extracted compounds, thus extending their shelf-life [6]. To the best of our knowledge, rosehip extraction using NADES has not yet been studied.

Using an authorized special collection permit of the Institute of Plant Breeding and Phylogenetic Resources (IPBGR) of the Hellenic Agricultural Organization Demeter (Permit 82336/879 of 18/5/2019 & 26895/1527 of 21/4/2021 issued yearly by the Greek Ministry of Environment and Energy), several botanical expeditions were organized in Northern Greece to collect wild-growing *ex-situ* propagation materials with vigorous growth and strong fruiting potential in the wild habitats; these wild materials were taxonomically identified, genetically authenticated, asexually propagated and *ex-situ* cultivated at the premises of the BBGK-IPBGR [8].

In the present study, 5 NADES were task-specifically designed and prepared using the heating and stirring method for the extraction of bioactive compounds from the shells (hypanthia) of the *ex-situ* cultivated rosehips of the BBGK-IPBGR. The NADES components were selected in terms of biocompatibility as the aim was the extracts to be used "as obtained" without further purification or isolation steps in end-products (Figure 1). All the NADES were structurally characterized using NMR and FT-IR spectroscopy. Moreover, two of the most important parameters for the extraction process were determined, namely the pH and the polarity of the NADES and the NADES-water systems.

### Methodology for Rosehip Shells (Hyanthia) Extraction

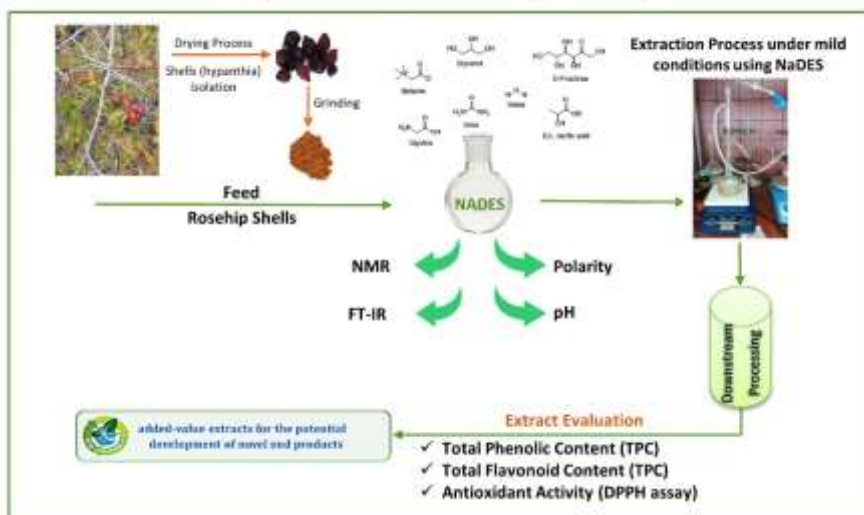


Figure 1. Methodology for rosehip shells (hypanthia) extraction using task-specifically designed NADES sourced from Greek native dogroses in *ex-situ* conservation.

The shells (hypanthia) of rosehips from Greek native dogroses in *ex-situ* conservation were firstly grinded and suspended in selected volumes of each NADES or NADES-water system and were extracted at 40°C. Regarding the extraction parameters, various extraction times (30-360 min), rosehip-to-solvent (5-167 mg/g) and water-to-NADES (0-75%) ratios were studied for each solvent. After extraction, the samples were centrifuged and the supernatants were collected and stored in the dark at 4°C. The total phenolic and total flavonoid content of the obtained extracts were evaluated using the Folin–Ciocalteu and the AlCl<sub>3</sub> complexation colorimetric method, respectively. The antioxidant activity of the extracts was determined by evaluating their radical scavenging ability using the stable DPPH radical [6]. The experimental results were compared to those derived from the conventional extraction of rosehip shells (hypanthia) using water and ethanol/water system as extraction media.

The as-obtained NADES extracts showed similar or, in most of the cases, increased total phenolic and flavonoid contents as well as DPPH radical scavenging ability compared to the corresponding extracts derived from the conventional extraction media. Therefore, the proposed methodology can be considered as a promising and competitive alternative to the conventional extraction of rosehips' shells (hypanthia).

### Acknowledgements

This research was co-funded by the European Union and Greek national funds through the Operational Program Competitiveness, Entrepreneurship and Innovation, under the call RESEARCH-CREATE-INNOVATE, grant number T2EDK-0233, "Green\_Wild\_ROSE.gr".

### References

1. N. Koczka, É. Stefanovits-Bányai, A. Ombódi, *Medicines*, **5** 84 (2018)
2. I. Mármol, C. Sánchez-de-Diego, N. Jiménez-Moreno, C. Ancín-Azpilicueta, M.J. Rodríguez-Yoldi, *Int. J. Mol. Sci.*, **18** 1137 (2017)
3. V.T. Tumbas, J.M. Čanadanović-Brunet, D.D. Četojević-Simin, G.S. Četković, S.M. Đilas, L. Gille, *J. Sci. Food Agric.*, **92** 1273-1281 (2012)
4. A. Tzani, M.A. Karadendrou, T. Tsiaka, E. Kritsi, P. Zoumpoulakis, A. Detsi, Chapter 2: Exploring the Role of Natural Deep Eutectic Solvents (NADES) Towards the Valorization of Food Processing Industry Waste. Nova Science Publishers, 19-51 (2022)
5. D. Skarpalezos, A. Detsi, *Appl. Sci.*, **9** 4169 (2019)
6. A. Tzani, S. Kalafateli, G. Tatsis, M. Bairaktari, I. Kostopoulou, A.R. Pontillo, A. Detsi, *Sustain. Chem.*, **2** 576-598 (2021)
7. S. Koutsoukos, T. Tsiaka, A. Tzani, P. Zoumpoulakis, A. Detsi, *J. Clean. Prod.* **241** 118384 (2019).
8. E. Maloupa, E. Karapatzak, I. Ganopoulos, A. Karydas, K. Papanastasi, D. Kyrkas, P. Yfanti, N. Nikisianis, A. Zahariadis, I.S. Kosma, A.V. Badeka, G. Patakioutas, D. Fotakis, N. Krigas, *Plants* **10** 2634 (2021)

## Bioactive chemical space exploration via greener multicomponent reactions

Mariana Ingold<sup>1</sup>, Victoria de la Sovera<sup>1,2</sup>, Rosina Dapuzo<sup>3</sup>, Paola Hernández<sup>4</sup>, Williams Porcal<sup>1,2\*</sup>, Gloria V. López<sup>1,2\*</sup>.

<sup>1</sup>Laboratorio de Desarrollo de Fármacos y Biología Vascular, Institut Pasteur Montevideo, Mataojo 2020, 11400, Montevideo, Uruguay. <sup>2</sup>Departamento de Química Orgánica, Facultad de Química, Universidad de la República, Av. General Flores 2124, 11800, Montevideo, Uruguay. <sup>3</sup>I+D Biomédico, Centro Uruguayo de Imagenología Molecular, Montevideo, Uruguay. <sup>4</sup>Departamento de Genética, Instituto de Investigaciones Biológicas Clemente Estable, Montevideo, Uruguay.

\* wporcal@fq.edu.uy; vlopez@fq.edu.uy.

Cancer is one of the main causes of death worldwide, accounting for nearly 10 million deaths in 2020 [1]. Currently one of the key objectives in medicinal chemistry is the drug discovery and drug development following the Green Chemistry guidelines [2,3]. In this context, our group has dedicated the last years to the development of compounds with antitumoral activity via efficient and more environmentally friendly methodologies. A synthetic tool explored by our group are multicomponent reactions (MCR) where the product is formed from three or more reagents in a single reaction step with high atomic efficiency [4]. MCRs are a green strategy in which a collection of molecules with a great diversity are generated with a minimum of synthetic effort, time and by-products formation. In this sense, we have previously described green processes for the synthesis of bioactive compounds via Passerini and Ugi MCR and their antiproliferative activity [5,6]. Nearly all compounds displayed potent antiproliferative activities against a panel of six human solid tumor cell lines. Particularly the compound **8a**, a furoxan derivative obtained by Ugi MCR (Figure 1, Route A), exhibited the strongest activity on the SW1573 lung cell line ( $GI_{50} = 21$  nM) with a selectivity index of 470. Preliminary mechanistic studies suggested a relationship between nitric oxide release and antiproliferative activity [6].

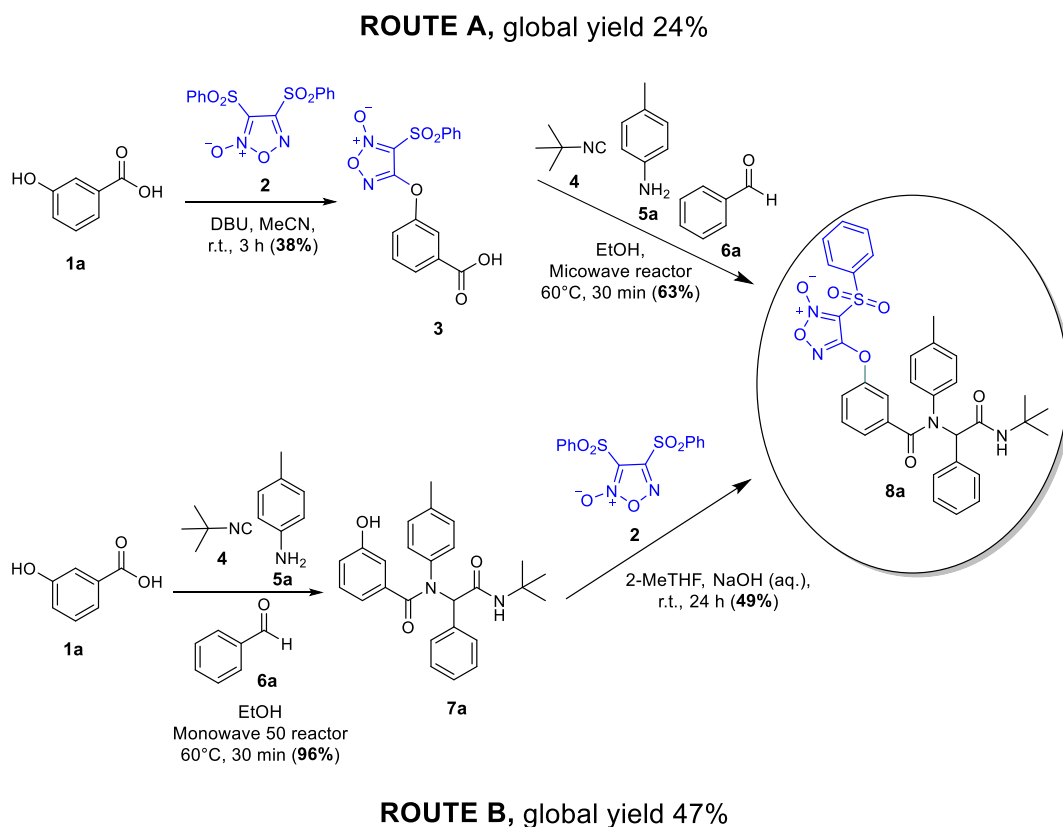


Figure 1. Explored routes for the synthesis of **8a**. Route A, previously reported. Route B, new greener route.

In the present work, we report the synthesis of the lead compound **8a** via a greener synthetic pathway (Figure 1, Route B). The new reaction route for obtaining compound **8a**, in addition to being more eco-friendly, also allowed to obtain it with twice the overall yield. With the optimized conditions, we varied the different components of the reaction to generate new derivatives and expand the chemical space studied. To this end, we not only employed Ugi MCR but also Groebke–Blackburn–Bienaymé (GBB) multicomponent reaction (Figure 2). We studied both MCRs under efficient, safe, and ecofriendly conditions, using green solvents (EtOH and Me-THF) and a conventionally heated sealed-vessel reactor (Monowave 50) to accelerate reactions. This technology mimics many features common to modern single-mode microwave reactors with reduced complexity and at a lower cost. Herein,

we describe the synthesis of a small collection of 12 nitric oxide-releasing molecules, using the furoxan system as a pharmacophore. Biological evaluation as antiproliferative agents in bladder and prostate cancer cells indicated that almost all compounds displayed antiproliferative activity against both cancer cell lines.

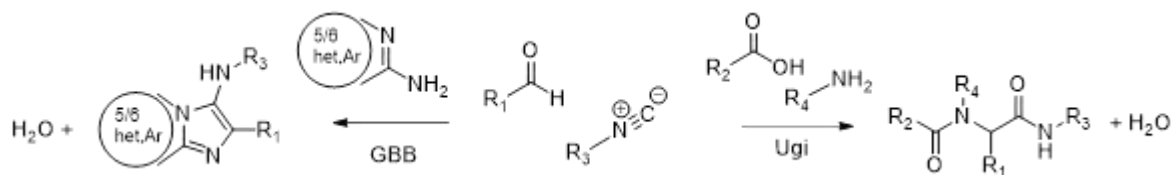


Figure 2. Ugi and GBB multicomponent reactions

## Acknowledgements

This research was funded by CSIC, Udelar, and PEDECIBA-Química, Uruguay

## References

1. World Health Organization (WHO). Available online: <https://www.who.int/news-room/factsheets/detail/cancer> (accessed on 25 April 2022).
2. G. Wu, T. Zhao, D. Khang, et al. *J. Med. Chem.* 62, 9375–9414 (2019).
3. M.C. Bryan, B. Dillon, L.G. Hamann, et al. *J. Med. Chem.* 56, 6007–6021 (2013).
4. T. Zarganes-Tzitzikas, A.L. Chandgude, A. Dömling. *Chem. Rec.* 15, 981–996 (2015).
5. M. Ingold, R. Daputo, S. Victoria, et al. *Eur. J. Med. Chem.* 143, 1888–1902 (2018).
6. M. Ingold, L. Colella, P. Hernández, et al. *ChemMedChem.* 14, 1669–1683 (2019).

## Synthesis of new succinimide derivatives with potential anticonvulsant activity

Szymon Jarzyński<sup>1</sup>, Anna Rapacz<sup>2</sup>, Elżbieta Pękała<sup>2</sup>, Bogna Rudolf<sup>1\*</sup>

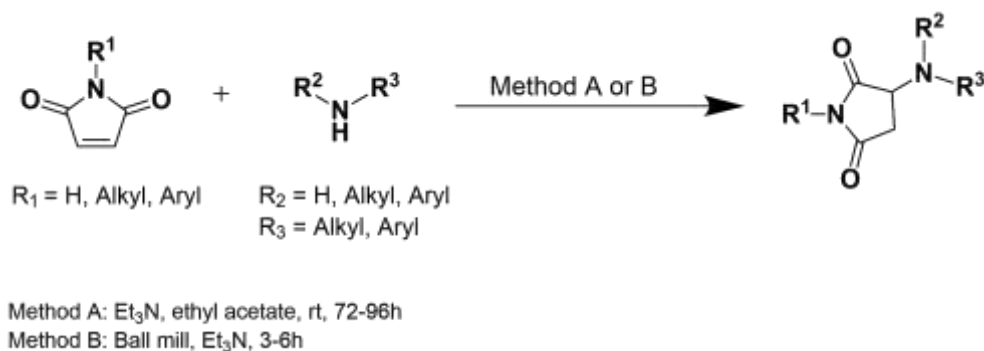
<sup>1</sup>Faculty of Chemistry, University of Lodz, Tamka 12, 91403 Łódź, Poland

<sup>2</sup>Faculty of Pharmacy, Jagiellonian University, Medyczna 9, 30688 Kraków, Poland

\*bogna.rudolf@chemia.uni.lodz.pl

Today people suffer from many diseases of the central nervous system such as epilepsy and depression, which constitute a significant health, social and economic problem. In most cases, pharmacological treatment gives positive results, but still there are many of drug-resistant people for whom the only hope is new antiepileptic drugs. Succinimides are well recognized heterocyclic compounds in drug discovery due to the presence of hydrogen-bond acceptor or donor fragments, as well as the easy possibility of substituting the ring positions 1 and 3. Such systems are key structural molecular bases for compounds that have various effects on the central nervous system. There are many examples of modifying the pyrrolidine-2,5-dione ring in the literature, because it is an integral part of the structure of compounds with antidepressant [1], antibacterial [2], antimutagenic [3] or anticancer properties [4].

The main goal of presented research was to develop procedures for the synthesis of new functionalized succinimide derivatives. The compounds obtained can interact with neurotransmitters and receptors, which play an essential role in proper functioning of the central nervous system. *N*-nonsubstituted and *N*-substituted maleimides were selected as key starting materials for the preparation of succinimide derivatives which were prepared by the aza-Michael reaction with primary and secondary amines in the presence of Et<sub>3</sub>N. During the research, two variants of synthesis were tested, the classical method in organic solvents and with the use of mechanochemistry. Reactions under solvent-free conditions in a ball mill led to products with good yields.



Scheme 1. Mechanochemical synthesis of *N*-nonsubstituted and *N*-substituted succinimides.

### Acknowledgements

This work has been supported by the University of Lodz in the framework of the IDUB program (S.J.; grant no. 23/IDUB/MLOD/2021)

### References

1. M. Z. Wróbel, A. Chodkowski, F. Herold, A. Gomółka, J. Kleps, A. P. Mazurek, F. Pluciński, A. Mazurek, G. Nowak, A. Siwek, K. Stachowicz, A. Sławińska, M. Wolak, B. Szewczyk, G. Satała, A. J. Bojarski, J. Turło, *Eur. J. Med. Chem.* **63** 484 (2013).
2. K. Karthikeyan, P.M. Sivakumar, M. Doble, P.T. Perumal, *Eur. J. Med. Chem.* **45** 3446 (2010).
3. E. Pękała, P. Liana, P. Kubowicz, B. Powroźnik, J. Obniska, I. Chlebek, A. Węgrzyn, G. Węgrzyn, *Mutat. Res.* **758** 18 (2013).
4. M. Cieślak, M. Napiórkowska, J. Kaźmierczak-Barańska, K. Królewska-Golińska, A. Hawrył, I. Wybrańska, B. Nawrot, *Int. J. Mol. Sci.* **22** 4318 (2021).



# DMAP-catalyzed synthesis of quinazolidione and derivatives via *alpha* chloroaldoxime *O*-methanesulfonates and 2-(benzylamino)benzoic acids

Kaewman W.<sup>1</sup>, Kaeobamrung J.<sup>2\*</sup>

Division of Physical Science and Center of Excellence for Innovation in Chemistry, Prince of Songkla University, 15 Kanjanavanit Road, Kohong, Hat-Yai, Songkhla 90112, Thailand

\* Corresponding Author: juthanat.k@psu.ac.th

Quinazolidiones have been shown pharmacologically interesting properties, for example, anti-hypertensive [1], anticonvulsant [2], a promising agent for the treatment of asthma [3], a potential immune-suppressive and anti-inflammatory agent [4]. Due to their interesting properties, a number of quinazolidione syntheses have been therefore developed in recent years.

Alternatively, a reaction of 2-(benzylamino) benzoic acids **1** and *alpha*-chloroaldoxime *O*-methanesulfonates **2** could provide quinazolidione derivatives **3** in the presence of 4-dimethylaminopyridine (DMAP) as a catalyst under mild and friendly environmental conditions. The spectroscopy techniques such as <sup>1</sup>H, <sup>13</sup>C NMR and high resolution mass spectrometry were used to characterize quinazolidione products. This method offers the advantages of low costs, green solvent and metal-free process. The *alpha*-chloroaldoxime *O*-methanesulfonates having both electron donating and withdrawing substituents were applicable to the reaction resulting in 40-90% yields of products (**Figure 1**). Key chemical transformations were nucleophilic substitution, Tiemann rearrangement and cyclic urea formation.

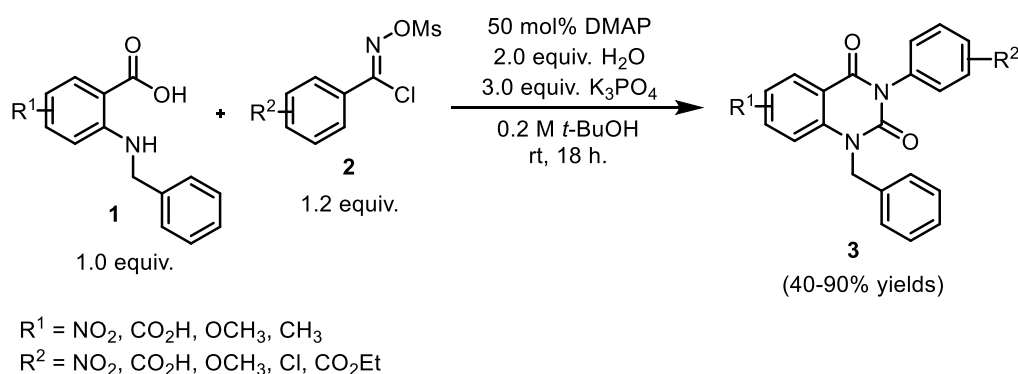


**Figure 1.** DMAP-catalyzed the synthesis of quinazolidiones.

**Keywords:** organocatalysis, Tiemann rearrangement, urea formation, amide formation

## Acknowledgements

Development and Promotion for Science and Technology talents project (DPST scholarship)  
 Division of Physical Science, Faculty of Science, Prince of Songkla University

## Selected References

1. I. A. Rivero, K. Espinoza, R. Somanathan, *Molecules*, **9**(7) 609-616 (2004).
2. M. K. Prashanth, M. Madaiah, H. D. Revanasiddappa, B. Veeresh, *Molecular and Biomolecular Spectroscopy*, **110** 324-332 (2013).
3. V. Dal Piaz, M. P. Giovannoni, *European Journal of Medicinal Chemistry*, **35**(5) 463-480 (2000).
4. G. M. Buckley, N. Davies, H. J. Dyke, P. J. Gilbert, D. R. Hannah, A. F. Haughan, S. C. Williams, *Bioorganic & Medicinal Chemistry Letters*, **15**(3) 751-754 (2005).

## Novel phosphate-containing imidazoles as potential green biologically active substrates

Valentina K. Yu<sup>1</sup>, Altynay B. Kaldybayeva<sup>1,2\*</sup>, Aigul Ye. Malmakova<sup>1</sup>, Kaldybai D. Praliyev<sup>1</sup>, Malika D. Khaitova<sup>3</sup>

<sup>1</sup>JSC «A.B. Bekturov Institute of Chemical Sciences», 106 Ualikhanov St., Almaty, Kazakhstan

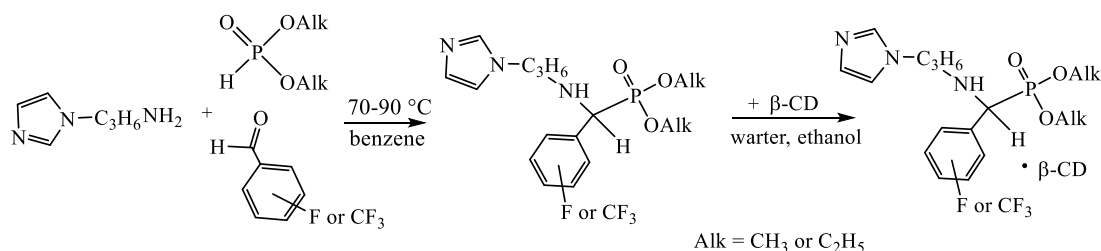
<sup>2</sup>Al-Farabi Kazakh National University, 71 al-Farabi Ave, Almaty, Kazakhstan

<sup>3</sup>C.D.Asfendiyarov Kazakh National Medical University; 94 Tole Bi St., Almaty, Kazakhstan  
altin\_28.94@mail.ru

In crop production, the need for novel environmentally friendly fertilizers is due not only to the fact that when they are introduced, plant productivity increases, but their impact on the soil is accompanied by the reproduction of soil fertility, an increase in its main features (humus, nutrients, effective microorganisms). Ways to increase the efficiency of fertilizers include their modification with plant growth regulators. The problem of fertilizer modifiers, which not only stimulate the growth and development of plants, but enhance their protective functions to natural and technogenic stressful situations (adaptogens for plants), is multifaceted and its solution requires the efforts of many specialists. The chemical aspect of this problem involves the synthetic design of novel molecules with the above properties.

Several reasons served as the basis for realization the Research: in particular, the activity of the imidazole-containing bispidins synthesized by us [1]; biological potential of fluorimidazole derivatives [2]; the practical value of both biologically active substances and highly selective ligands in complexes with copper (II) and nickel (II) ions, structures containing fragments of imidazole and phosphonate [3].

In this work, in order to obtain green plant growth regulators - fertilizer modifiers, we carried out a synthetic design of new imidazole derivatives combined with phosphonate and fluorine fragments under the conditions of a three-component "one-pot" Kabachnik-Fields reaction.



The interaction of 1-(3-aminopropyl)imidazole with di(methyl- or ethyl-)phosphite and the carbonyl component – *o*-, *m*- or *p*-(fluoro- or trifluoromethyl)-benzaldehyde is carried out by boiling in benzene using a Dean-Stark nozzle to remove from the reaction zone of the obtained water as azeotrope with benzene. The yield of target  $\alpha$ -aminophosphonates as viscous oils is 19-91%. In the IR spectra, the bands at 1047-1238 cm<sup>-1</sup> are attributed to the absorption of P=O. In spectra <sup>13</sup>C NMR the signal of the tertiary carbon atom (CHP) is observed in the region of 58.2-71.7 ppm. The signals of carbon atoms of the imidazole ring are observed in the region of 119.8-137.6 ppm.

To study the bioactivity, complexes of aminophosphonates with  $\beta$ -cyclodextrin (1:1) were obtained.

As expected, among the synthesized aminophosphonates, samples were identified that stimulate seed germination, growth and development of 3 Kazakhstan wheat varieties under normal and drought conditions. But, unexpectedly, it turned out that cyclodextrin complexes cause local pain relief on models of infiltration and conduction anesthesia at the level of used local anesthetics - lidocaine and trimecaine in terms of anesthesia index and duration of action. Acute toxicity (LD<sub>50</sub> = 1125 mg/kg) was 3-5 times less than the used anesthetics.

Thus, the expediency of combining fragments of imidazole and phosphonate in one molecule, which has a pronounced biological effect with low toxicity, has been experimentally confirmed.

### Acknowledgements

Funding for this Research was financially supported by the Grant AP 08856051 from Committee of Science of the Ministry of Education and Science of the Republic of Kazakhstan.

### References

1. E.V. Neborak, A.B. Kaldybayeva, L. Bey, A.Y. Malmakova, A.S. Tveritinova, A. Hilal, V.K. Yu, M.V. Ploskonos, M.V. Komarova, E. Agostinelli, D.D. Zhdanov. *Molecules*, **27**, 3872 (2022).
2. G.N. Lipunova, E.V. Nosova, V.N. Charushin. *Chem. Heterocycl. Compd.*, **49**, 1691–1714 (2014).
3. E. Rani, M. Rani. *J. Appl. Chem.*, **7**, 12, 23-33 (2014).

## Solubility of *Moringa oleifera* L. seed in SFE-CO<sub>2</sub>: a response surface methodology analysis

Júlia C. Kessler<sup>1,2,3</sup>, Isabel M. Martins<sup>1,2</sup>, Yaidelin A. Manrique<sup>1,2</sup>, Alírio E. Rodrigues<sup>1,2</sup>, Maria Filomena Barreiro<sup>3</sup>, Madalena M. Dias<sup>1,2\*</sup>

<sup>1</sup> LSRE-LCM - Laboratory of Separation and Reaction Engineering - Laboratory of Catalysis and Materials  
Faculdade de Engenharia, Universidade do Porto, Rua Dr. Roberto Frias, 4200-465 Porto, Portugal

<sup>2</sup> ALiCE - Associate Laboratory in Chemical Engineering Faculdade de Engenharia, Universidade do Porto, Rua Dr. Roberto Frias, 4200-465 Porto, Portugal

<sup>3</sup> Centro de Investigação de Montanha (CIMO), Instituto Politécnico de Bragança, Campus de Santa Apolónia, 5300-253 Bragança, Portugal  
[\\*dias@fe.up.pt](mailto:*dias@fe.up.pt)

The angiosperm *Moringa oleifera* L. (Mo) tree, also denominated tree of life, has been listed as one of the richest plant bioactive sources [1]. Mo seeds' high saturated and monounsaturated fatty acid content (e.g., C<sub>22:0</sub>, C<sub>16:0</sub>, C<sub>18:0</sub>, C<sub>20:0</sub>, C<sub>18:1</sub>) improves the thermal stability of its oil and confers antioxidant activity [2]. Furthermore, the anti-inflammatory and antimicrobial biofunctions of fatty acids, in synergy with sterols, saponins, phenolic acids, tocopherols, tannins, phytates, and alkaloid molecules, have been reported [1, 3]. This desirable composition and respective bioactivity encompass a natural alternative to enhance fine chemistry formulations, which, in turn, requires attention regarding the used extraction methods.

Solvent-free extracts are a trademark of carbon dioxide supercritical extraction (SFE-CO<sub>2</sub>) [4]. This technology is identified as non-toxic, non-inflammable, and readily available. In addition, SFE-CO<sub>2</sub> has GRAS characteristics, and the recovered products are obtained at higher selectivity and natural content composition than conventional techniques. However, this improvement in quality is often accompanied by lower extraction yields [5]. To maximise the extracted content, a response surface methodology (RSM) was applied.

The experimental procedures were conducted with Mo seeds, supplied by Moringa del Sur (Malaga, Spain, [moringadelsur.com](http://moringadelsur.com)), using a bench-scale SFE-CO<sub>2</sub> equipment developed by Manrique [6]. The samples were previously dried at room temperature, ground, and carefully sieved (D-42781, Retsch, Germany) to achieve a particle size between 0.50 mm and 0.70 mm. The process was performed in continuous mode using CO<sub>2</sub> food grade (CAS 124-38-9, 99.9%, Air Liquid) at a flow rate of 4 mL/min for 120 min; 10 g of sample were used in each extraction. The applied design of the experiments (2<sup>2</sup> + 2 central points, 2 blocks) and respective results are shown in Table 1.

The highest extraction yields were obtained for pressures above 195 bar and temperatures below 55 °C, varying from  $\eta=1.81\%$  (10) to 3.38% (7). A proportional increase was observed in the respective solubility values, achieving 786  $\mu\text{g}_{\text{ext}}/\text{g}_{\text{CO}_2}$ , mainly due to the significant contribution of pressure revealed by the ANOVA test ( $\alpha = 0.05$ , data not shown). Moreover, the temperature ( $p \leq 0.05$ ) influences the balance between the CO<sub>2</sub> density and the solute vapour pressure [5, 7]. However, according to the results, no crossover behaviour was observed, which suggests a solubility dominance in the solvation power of the SFE-CO<sub>2</sub> towards the Mo seeds. Literature results support the conclusions on the pressure range applied in this work [5, 7, 8].

Table 1. SFE-CO<sub>2</sub> yield (%) screening of *Moringa oleifera* L. seeds.

N	Block	Pressure, <i>P</i> (bar)	Temperature, <i>T</i> (°C)	$\rho_{\text{CO}_2}$ * (kg/m <sup>3</sup> )	Yield, $\eta$ (%)	Yield, $\eta_{\text{RSM}}$ (%)	Solubility ( $\mu\text{g}_{\text{ext}}/\text{g}_{\text{CO}_2}$ )
1	1	140	45	720	0.18	0.71	41
2	1	140	65	506	0.12	0.59	29
3	1	250	45	857	3.19	3.63	742
4	1	250	65	762	2.10	2.48	491
5 (PC1)	1	195	55	747	1.94	2.15	452
6	2	117	55	480	0.10	0.12	24
7	2	273	55	831	3.38	3.53	786
8	2	195	41	830	2.29	2.33	452
9	2	195	69	656	1.31	1.44	308
10 (PC2)	2	195	55	747	1.81	2.15	422
Proof	-	120	45	658	0.06	0.04	14

\*NIST Online database.

From the SFE-CO<sub>2</sub> optimisation study, Figure 1a represents the RSM analysis ( $R^2 = 0.99046$ ), corroborating the significant influence of pressure and temperature on the extracts' solubility.

$$\eta_{RSM}(\%) = -11.80 + 6.84 \times 10^{-2} \cdot P - 5.32 \times 10^{-5} \cdot P^2 + 2.09 \times 10^{-1} \cdot T - 1.35 \times 10^{-3} \cdot T^2 - 4.71 \times 10^{-4} \cdot P \cdot T + 1.34 \times 10^{-1} \quad (1)$$

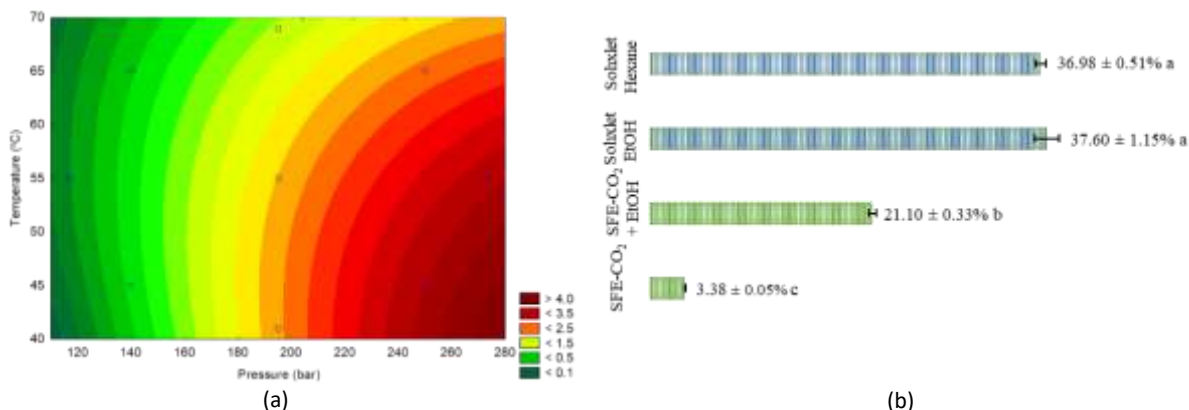


Figure 1. (a) RSM: SFE-CO<sub>2</sub> yield (%) of *Moringa oleifera* L. seeds; (b) Comparison of yield extractions: green and conventional methodologies. Averages with different letters indicate a significant difference with  $\alpha = 0.05$ .

An additional experiment was performed in duplicate using a co-solvent (CO<sub>2</sub>:ethanol (EtOH); 4:1), while maintaining the determined optimized processing conditions. The results were statistically compared to Soxhlet extracts by the Tukey test with  $\alpha = 0.05$  (Statistica StatSoft, version 14, USA). This conventional methodology was carried out with 5 g of sample for 240 min, using 150 mL of EtOH (CAS 64-17-5, absolute) and hexane (CAS 110-54-3, 95%) as extraction solvents, respectively, both obtained from Sigma Aldrich (Madrid, Spain).

An improvement of the CO<sub>2</sub> solubility was obtained using 20% of the co-solvent at 273 bar and 55 °C, resulting in  $\eta=21.20\%$  (Figure 1b). EtOH has a triple effect on the SFE-CO<sub>2</sub> extraction: (i) generally, it enhances the CO<sub>2</sub> density, (ii) increases the extraction of polar compounds, and (iii) improves the mass transfer coefficient in the solid phase [7]. Finally, a significant difference ( $\alpha = 0.05$ ) was obtained for Soxhlet experiments, with  $37.60 \pm 1.15\%$  and  $36.98 \pm 0.51\%$  of extraction yields using EtOH and hexane as solvents, respectively, similarly to the 37.50% hexane oil reported by Nguyen et al. [9].

A lower extraction yield was expected from the SFE methodology due to the selectivity promoted by the CO<sub>2</sub> solvent, especially under low pressures. Usually, chemical composition variations are observed in the extracts obtained by SFE and conventional Soxhlet, indicating increased oil stability, and it has been reported that SFE-CO<sub>2</sub> seed products have sterol and tocopherol at higher contents than the Soxhlet extracts [4]. On the other hand, studies have shown that no significant differences were found in the fatty acids' composition [4, 5, 9].

In spite of extensive reported literature data, studies on Mo seed's bioactive composition, extraction methodologies and applications remain underexploited. Although SFE-CO<sub>2</sub> has been established as a safe and green alternative method, there is still a need to develop a database to seek target compounds optimization. Therefore, the improvement in the extraction yield promoted by the EtOH co-solvent may be a key strategy to enhance the richness of unsaturated fatty acids, such as behenic oil [9, 10].

## Acknowledgements

This work was financially supported by LA/P/0045/2020 (ALiCE), UIDB/50020/2020, UIDP/50020/2020 (LSRE-LCM), and UIDB/00690/2020 (CIMO) funded by national funds through FCT/MCTES (PIDDAC). The authors are thankful for the samples provided by Moringa del Sur (Malaga, Spain), and Júlia Cristiê Kessler acknowledges her PhD. scholarship (ref. 2020.06656.BD) by Fundação para a Ciência e Tecnologia (Portugal).

## References

1. C. K. O. Dzuovor, S. Pan, C. Amanze, P. Amuzu, C. Asakiya, F. Kubi. *C. Rev. Biotechnol.*, 1-23 (2021).
2. P. R. Bhutada, A. J. Jadhav, D. V. Pinjari, P. R. Nemade, R. D. Jain, *Ind. Crops Prod.*, **82** 74-80 (2016).
3. S. Saucedo-Pompa, J. A. Torres-Castillo, C. Castro-Lopez, R. Rojas, E. J. Sanchez-Alejo, M. Ngangyo-Heya, G. C. G. Martinez-Avila, *Food Res. Int.*, **111** 438-450 (2018).
4. K. Ruttarattanamongkol, S. Siebenhandl-Ehn, M. Schreiner, A. M. Petrasch. *Ind. Crops Prod.* **58** 68-77 (2014).
5. S. Zhao, D. Zhang. *Sep. Purif. Technol.*, **113** 9-17 (2013).
6. Y. J. A. Manrique. Supercritical fluid extraction and fractionation of bioactive natural products from cork. PhD Thesis. *Faculty of Engineering of the University of Porto*, 131 (2017).
7. A. Rai, B. Mohanty, R. Bhargava, *Chem. Eng. Commun.*, **204** 957-964 (2017).
8. S. Zhao, D. Zhang, *J. Food Eng.*, **138** 1-10 (2014).

9. H. N. Nguyen, P. D. Gaspillo, J. B. Maridable, R. M. Malaluan, H. Hinode, C. Salim, H. K. P. Huynh, *Chem. Eng. Process.: Process Intensif.*, **50** 1207-1213 (2011).
10. B. Guan, Z. Liu, B. Han, H. Yan, *J. Supercrit. Fluids*, **14** 213-218 (1999).

## Aerobic and Catalyst-free Oxidation of Aldehydes to Acids Promoted by Sunlight or UVA-light

Charikleia S. Batsika,<sup>1</sup> Charalampos Koutsilieris,<sup>1</sup> Giorgos S. Koutouligenis,<sup>1</sup> Maroula G. Kokotou,<sup>2</sup> Christoforos G. Kokotos<sup>1</sup> and George Kokotos<sup>1\*</sup>

<sup>1</sup>Department of Chemistry, National and Kapodistrian University of Athens, Panepistimiopolis, Athens 15771, Greece

<sup>2</sup>Department of Food Science and Human Nutrition, Agricultural University of Athens, Iera Odos 75, Athens 11855, Greece  
\*gkokotos@chem.uoa.gr

Synthetic photochemistry is an alternative green and sustainable approach, offering the possibility for the discovery of novel reactivities. Although applications of solar irradiation for organic synthesis have been demonstrated from the beginning of the 20th century, only in the 21st century visible light-mediated organic synthesis has attracted special attention [1,2]. Many photochemical reactions are unique, because provide access to products which are not accessible by conventional methods. On the other hand, aerobic oxidations are recognized as highly attractive oxidative processes for various applications in organic chemistry, due to their low cost and environmental friendliness [3,4].

The oxidation of aldehydes to the corresponding carboxylic acids is a fundamental and popular oxidative organic transformation, which has attracted high academic interest [5]. However, the aerobic oxidation of aldehydes into the corresponding carboxylic acids is also an industrial process and millions of tons of aliphatic carboxylic acids, (for example, 2-ethylhexanoic acid), are produced per year by such an approach [6].

It is known that aldehydes are prone to oxidation, however synthetic methods for their oxidation to carboxylic acids under green and mild conditions are still scarce. The aerobic oxidation of aldehydes is usually carried out in the presence of metal catalysts [7,8]. In 2019, a metal-free-catalyzed oxidation of aldehydes was reported. *N*-hydroxyphthalimide was used as the catalyst for the aerobic oxidation of aldehydes either in acetonitrile or water and the mechanism of this oxidation was thoroughly investigated [9,10].

The aim of our work was to merge aerobic oxidation with light irradiation and to develop an efficient sunlight or UVA-light promoted oxidation of aldehydes to carboxylic acids under aerobic conditions, without the use of any photocatalyst.

Benzaldehyde and dodecanal were studied as model substrates for the optimization of the reaction conditions. Exploring various light sources (sunlight, common house lamps, LED lamps of different wavelengths) and various solvents, we concluded that the optimum conditions were: LED 370 nm or sunlight as the irradiation source and a mixture of acetone and water as the reaction medium. Under these conditions, aliphatic aldehydes are converted into acids within 3 hours, while aromatic aldehydes require longer reaction time.

The mechanism of the reaction was studied by direct infusion-high resolution mass spectrometry (DI-HRMS). These studies indicate the formation of Griegee intermediates and a mechanism involving a solvent-assisted oxidative transformation.



Figure 1. Light-mediated aerobic oxidation of aldehydes to carboxylic acids.

In conclusion, we have developed a green, sustainable and operationally simple, under very mild conditions, method for the conversion of aldehydes to carboxylic acids. The transformation is light-promoted by either sunlight or LED 370 nm irradiation, without the use of a catalyst, utilizing atmospheric oxygen as the sole oxidant. The most effective solvent medium was proved to be a mixture of acetone and water. Various aliphatic or aromatic aldehydes were successfully employed and the corresponding carboxylic acids were obtained in high to excellent yields.

### Acknowledgements

The research presented was carried out within the framework of a Stavros Niarchos Foundation grant to the National and Kapodistrian University of Athens.

## References

1. M. Oelgemöller, *Chem. Rev.*, **116** 9664–9682 (2016).
2. S. Reischauer, B. Pieber, *iScience*, **24** 102209 (2021).
3. X. Zhang, K.P. Rakesh, L. Ravindar, H.-L. Qin, *Green Chem.*, **20** 4790-4733 (2018).
4. C.A. Hone, O.C. Kappe, *Top. Curr. Chem.*, **377** 2 (2019).
5. M.B. Smith, J. March, *March's Advanced Organic Chemistry: Reactions, Mechanisms, and Structure*, 6th ed., Wiley, Hoboken (2007).
6. J. Kubitschke, H. Lange, H. Strutz, H., *Carboxylic Acids, Aliphatic*. Ullmann's Encyclopedia of Industrial Chemistry (2014).
7. M. Liu, C.-J. Li, *Angew. Chem. Int. Ed.*, **55** 10806 (2016).
8. H. Yu, S. Ru, G. Dai, Y. Zhai, H. Lin, S. Han, Y. Wei, *Angew. Chem. Int. Ed.*, **56** 3867 (2017).
9. P.-F. Dai, J.-P. Qu, Y.-B. Kang, *Org. Lett.*, **21** 1393 (2019).
10. L. Vanoye, M. Abdelaal, K. Grundhauser, B. Guicheret, P. Fongarland, C. De Bellefon, A. Favre-Réguillon, *Org. Lett.*, **21** 10134 (2019).

## Natural product derivatives through organic synthesis as enhanced antioxidant agents

Matsia S.<sup>1\*</sup> Hatzidimitriou A.<sup>2</sup> Salifoglou A.<sup>1</sup>

<sup>1</sup>Laboratory of Inorganic Chemistry and Advanced Materials, School of Chemical Engineering, Aristotle University of Thessaloniki, Thessaloniki 54124, Greece

<sup>2</sup>Laboratory of Inorganic Chemistry, Department of Chemistry, Aristotle University of Thessaloniki, Thessaloniki 54124, Greece

\*E-mail: srmatsia@cheng.auth.gr

### Abstract

Flavonoids are a family of low molecular weight natural products, found plentifully in the plant kingdom. Their diversity goes along with their physiological roles in the specific species of their origin. Flavonoids are now considered as an indispensable component in a variety of nutraceutical, pharmaceutical, medicinal, and cosmetic applications [1]. To date, there exist are no sufficient data about the mechanisms through which such molecules affect human metabolism. However, it is well-known that the antioxidant properties of flavonoids are unique in their nature and application(s) for each plant (parts and products), thereby affecting human nutrition, dietetic habits and cellular protection at the molecular level. To that end, the possibility was explored that appropriate derivatization of a select group of such molecules could be modified in vitro so as to exhibit new or enhanced properties associated with their antioxidant-therapeutic potential [2]. In relevance to such an effort, the basic core structure of flavonoids is shown in **Figure 1**.

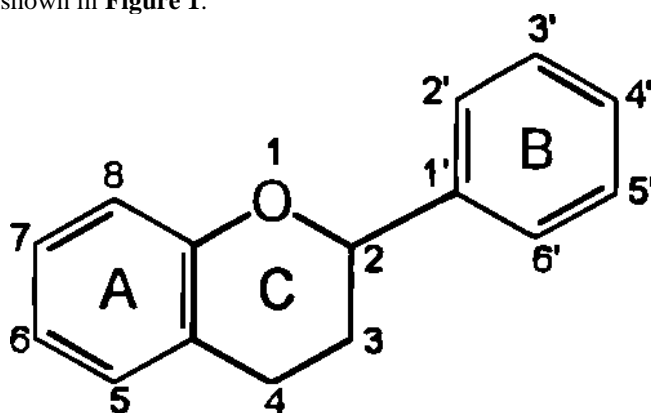


**Figure 1:** Structure of flavonoids

In this work, a select group of such flavonoids was chosen for experimentation, essentially targeting improvement of their antioxidant potential through derivatization. The chosen flavonoids were the following: quercetin, naringin, chrysin, and naringenin [3]. The specific polyphenolic compounds underwent chemical modifications of their substituents, peripheral to the A and C rings, thereby inducing new functional modalities capable of exerting influence over their function in bacterial physiology. The derived products, mainly involving ether and oxime moieties, were subsequently employed in microbiological studies, seeking to evaluate their antimicrobial properties and the extent of their antioxidant potential.

### Materials and methods used in this research

All chemicals were purchased from the following sources and were used without further purification. Naringin 99% was supplied from TCI. Naringenin 98% was purchased from Alfa Aesar. Methanol, Ethanol, dimethylsulfoxide and diamines were purchased from Sigma Aldrich. All manipulations were carried out under aerobic conditions. All analytical methods for the physicochemical characterization of the new derivatives were used according to well-known protocols. FT-IR spectra were recorded on a ThermoFinnigan FT-Infra Red spectrometer, using KBr pellets. A ThermoFinnigan Flash EA 1112 CHNS elemental analyser was used for the simultaneous determination of carbon, hydrogen, and nitrogen (%) at 1800°C. Solution <sup>1</sup>H-, and <sup>13</sup>C-NMR as well as 2D NMR experiments were carried out on a Varian 600 MHz spectrometer. The sample concentration was ~10 mM in methanol and DMSO. Electrospray ionization mass spectrometry (ESI-MS) infusion experiments were carried out on a ThermoFisher Scientific model LTQ Orbitrap Discovery MS (Bremen, Germany), in methanol and introduced into the ESI source of the MS at a flow rate of 5 μL/min, using an integrated syringe pump in a positive ionization mode. Source operating conditions included a 3.7 kV spray voltage and a 320°C heated capillary temperature.

### Synthesis

Briefly, hydroxylamine hydrochloride and sodium oxalate were mixed and dissolved in methanol. To that, an amount of flavonoid was added and the reaction mixture was refluxed for 24 h. The solid yellow powder was isolated by filtration in dried in open air. Recrystallization of the powder was done in methanol using 4-hydroxybenzoic acid. The reaction of the naringenin oxime was shown in **Figure 2**.



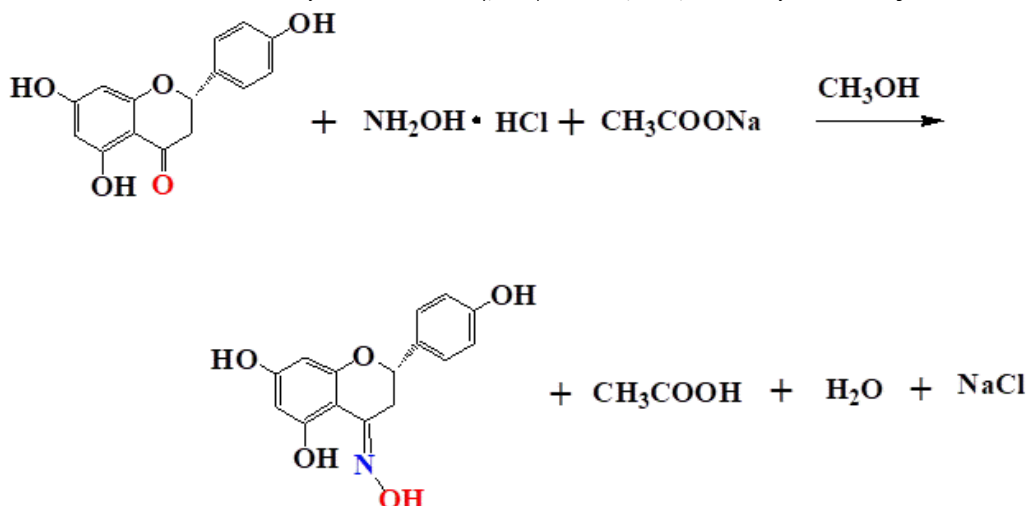


**Figure 1:** Organic synthesis of Naringenin oxime derivative

The comparative spectra of FT-IR between Naringenin and Naringenin oxime are shown in **Figure 3**, depicting the synthesis of a new derivative.

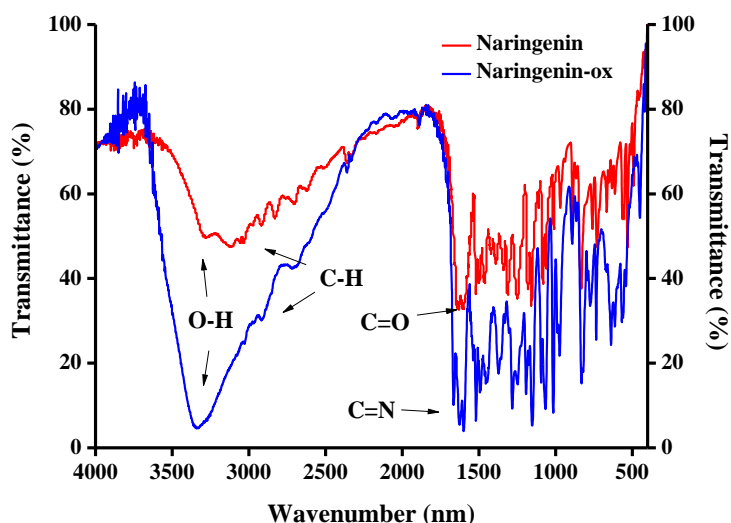


**Figure 3:** FT-IR comparative spectra

All nine derivatives of naringin and naringenin flavonoids are characterized in the solid-state and in solution, through elemental analysis, FT-IR, UV-Visible,  $^1\text{H}$ -,  $^{13}\text{C}$ -, 2D (homonuclear and heteronuclear) NMR, and ESI-MS. Their 3D structure was delineated through X-ray crystallography. The results of the study set the stage for the development of new hybrid flavonoids and derivatives thereof, so as to enhance the antimicrobial arsenal of options, when bacterial insurgents find their way into a) nutritional resources, traditionally used in human diet or products destined for human consumption, and b) humans, thereby affecting their health.

### Acknowledgements

This research is supported by the Operational Program "Human Resources Development, Education and Lifelong Learning" (NSRF 2014-2020), Act: "Strengthening the Human Research Resources through the Implementation of Doctoral Research" - MIS 5000432

### References

1. A.N. Panche, A.D. Diwan, S.R. Chandra, *J. Nutr. Sci.*, 5 e47 (2016).
2. B. Salehi, A. Venditti, Sharifi, M. Rad, D. Kregiel, J. Sharifi-Rad, A. Durazzo, M. Lucarini, A. Santini, E.B. Souto, E. Novellino, H. Antolak, E. Azzini, W.N. Setzer, N. Martins, *Int. J. Mol. Sci.*, 20(6) 1305 (2019).
3. H. Manman, C. Weilan, L. Zhimin, P. Liang, H. Lixia, C. Min, *J. Inorg. Biochem.*, **195** 13-19 (2019)

## A Comprehensive Screening Investigation on using Group Contribution Models for Estimation of the Critical Properties of Deep Eutectic Solvents

Reza Haghbakhsh<sup>1,2</sup>, Mohammad Reza Izadi<sup>3</sup>, Ana Rita C. Duarte<sup>2</sup> and Sona Raeissi<sup>3\*</sup>

<sup>1</sup> Department of Chemical Engineering, Faculty of Engineering, University of Isfahan, 81746-73441, Isfahan, Iran

<sup>2</sup> LAQV, REQUIMTE, Departamento de Química da Faculdade de Ciências e Tecnologia, Universidade Nova de Lisboa, 2829-516 Caparica, Portugal

<sup>3</sup> School of Chemical and Petroleum Engineering, Shiraz University, Shiraz 71345-51154, Iran

\*raeissi@shirazu.ac.ir

The Deep Eutectic Solvents (DES) is a most recent class of green solvents, having been introduced in 2003 by Abbott et al. [1]. However, researchers only initiated serious fundamental investigations on this family of green solvents since 2010. In the past decade, although researchers have unveiled much on their basic and fundamental knowledge, still a long path remains to be taken for the appropriate understanding of these interesting green solvents. Most DESs, similar to ionic liquids, have high melting points, and thus, high critical temperatures. In fact, the critical temperatures often cannot be reached as the DES decomposes before reaching such high temperatures. Therefore, measuring the critical properties by experimental procedures is impossible for most DESs. At the same time, information on the critical properties is essential for many thermodynamic models, such as equations of state. One of the solutions to this problem is the use of thermodynamic models for the estimation of critical properties. Group Contribution (GC) models are among the efficient models which have been used quite successfully for ionic liquids [2,3]. For DESs, researchers carried out the same procedure. However, in almost all of the published studies requiring the critical properties of DESs, the well-known GC model of modified Lydersen-Joback-Reid [2,3], as proposed by Valderrama et al. for ionic liquids was used. This model was combined with the Lee-Kesler mixing rules as proposed by Knapp et al [4]. However, no studies have checked and validated the above method for DESs. In this study, for the first time in literature, a comprehensive study is carried out by comparing different GC models, including the above-mentioned popular model for a large number of DESs (113 DESs). The critical properties including critical temperature, critical pressure, critical volume, and also acentric factors of the investigated DESs are calculated, and by using an indirect method and relating the critical properties to the experimental property of surface tension, the reliability of each group contribution model is investigated. The results showed that the calculated critical temperature and critical volume by almost all of the investigated GC models are in the same order, with low deviations with respect to one another, however, they produce very different values and orders for critical pressure and acentric factor. The results of this study open a new door to thermodynamic researchers of green chemistry to use the most suitable GC model for DESs in thermodynamic modeling, especially by equations of state.

### Acknowledgements

The authors are grateful to Shiraz University, the University of Isfahan, and Universidade Nova de Lisboa for providing facilities. This project has received funding from the European Union's Horizon 2020 - European Research Council (ERC) - under grant agreement No ERC-2016-CoG 725034.

### References

1. A.P. Abbott, G. Capper, D.L. Davies, R.K. Rasheed, V. Tambyrajah, *Chem. Commun.* 70–71 (2003).
2. J. O. Valderrama, P. A. Robles, *I&ECR* **46** 1338-1344 (2007).
3. J. O. Valderrama, W. W. Sanga, J. A. Lazzus, *I&ECR* **47** 1318-1330 (2008)
4. H. Knapp, R. Doring, L. Oellrich, U. Plocker, J.M. Prausnitz, *Chem. Data Ser. VI* (1982)

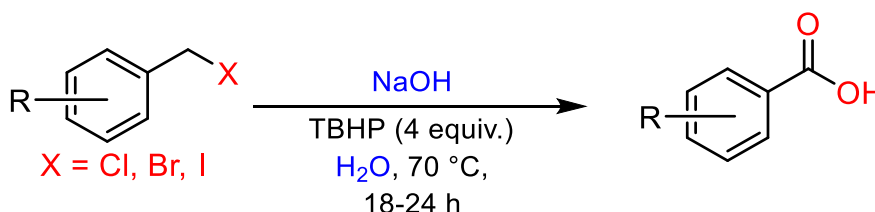
## ***In situ* generated chloride, bromide and iodide as catalysts for the oxidation of benzyl halides to benzoic acids in alkaline water using TBHP as oxidant**

Parul Saini<sup>1</sup> and Anil J Elias<sup>1</sup> \*

<sup>1</sup>Department of Chemistry, Indian Institute of Technology, Delhi, Hauz Khas, New Delhi, 110016, India.  
e-mail: eliasanil@gmail.com

Aromatic carboxylic acids, especially benzoic acid and its derivatives, find extensive use both in academia and industry. Traditionally, carboxylic acids are synthesized by the oxidation of alcohols/aldehydes, and also by the oxidative cracking of unsaturated compounds such as olefins and alkynes. Although a variety of catalytic methods based on transition metals and main group based metal-free catalysts have been developed for oxidation reactions of alcohols, most of these methods suffer from drawbacks, such as the requirement of precious metals, expensive ligands, high temperature, volatile and environmentally unfriendly organic solvents, as well as expensive and toxic additives. Recently, both in industry and academia, there are many reactions being reported of organic synthesis where traditional organic solvents are being replaced by water as a green, inexpensive and safe solvent [1]. However, the development of suitable methods that can help to efficiently isolate the desired compound from the reaction mixture is also an essential part of green chemistry. We have reported the oxidation of benzyl alcohols to benzoic acids using I<sub>2</sub> as well as NaCl as catalysts in the aqueous medium [2-3]. It is well known that industrially, benzaldehydes and benzyl alcohols are prepared from benzyl chlorides and bromides by heating them with stoichiometric excess of aqueous solutions of oxides, hydroxides, or carbonates of the alkali or alkaline earth metals [4]. Therefore, direct oxidation of benzyl halides to benzoic acids by a one-pot method using environmentally friendly reagents, catalysts and solvents will be of immense benefit from the synthetic perspective. Benzyl halide conversion to benzyl alcohol generates halide ions as the side product, which normally are of no utility. Herein, utilizing this halide ion as an *in-situ* generated catalyst, we for the first time report a tandem reaction converting benzyl halides to benzoic acids [5].

**General procedure for oxidation of benzyl halide:** A 10 ml single necked round bottom flask was charged with a magnetic bead, benzyl halide, NaOH, TBHP, and water. This reaction mixture was kept stirring at 70 °C for 18-24 h on a magnetic stirrer. Afterwards, the reaction mixture was made alkaline by aq. NaOH and was extracted with EtOAc. The aqueous layer was neutralized by aq. HCl and extracted with EtOAc. The organic layer was dried over anhydrous Na<sub>2</sub>SO<sub>4</sub>, and after evaporation of the solvent, analytically pure carboxylic acids were obtained.



We have developed an efficient and external catalyst-free one-pot oxidation method for the conversion of benzyl halides to the corresponding benzoic acids using only alkaline water and an oxidant, TBHP. The halide ions generated during the conversion of benzyl halides to benzyl alcohols have been found to act as *in situ* catalysts for this oxidation reaction. The use of water as an inexpensive and green solvent, and a green oxidant TBHP makes this protocol economical, environmentally benign and potentially suitable for commercial and academic applications. By controlling the amount of base required, the yields of the carboxylic acids from benzyl chlorides, bromides and iodides have been maximized and scaled up to gram scale reactions. A series of carboxylic acids were prepared from benzyl halides in high yields under mild reaction conditions. The present method does not require any inert atmosphere protection or purification of products by chromatographic techniques, which makes this an operationally simple and green process. As an industrial application, the synthesis of a key monomer used for the synthesis of polyethylene terephthalate (PET), i. e., terephthalic acid (PTA), has also been accomplished in good yields.

### **Acknowledgements**

This research is supported by SERB DST, India and CSIR, India for financial assistance in the form of research grants to A. J. E [CRG 2019/000013] and [01(2982)/19/EMR-II]. Authors acknowledge the Indian Institute of Technology, Delhi for instrument facilities.

## References

1. S. Handa, G. Fabrice, B. H. Lipshutz, *Science*, **349** 1087 (2015).
2. S. Hazra, M. Deb, A. J. Elias, *Green Chem.*, **19** 5548 (2017).
3. S. Hazra, A. K. Kushawaha, D. Yadav, P. Dolui, M. Deb, A. J. Elias, *Green Chem.*, **21** 1929 (2019).
4. F. Bruhne, E. Wright, *Ullmann's Encyclopedia of Industrial Chemistry*, Wiley-VCH, Weinheim, (2000).
5. P. Saini, A. Krishnan, D. Yadav, S. Hazra, A.J. Elias, *Asian J. Org. Chem.*, **10** 2355 (2021).

## Nickel Phosphide Supported on Graphitic Carbon Nitride as Non-Noble Metal Catalyst for Reductive Amination of Carbonyl Compounds by Transfer Hydrogenation

Devendra Sharma, Priyanka Choudhary and Venkata Krishnan\*

School of Basic Sciences and Advanced Materials Research Center, Indian Institute of Technology Mandi, Kamand, Mandi 175075, H.P., India. Email: [vkkn@iitmandi.ac.in](mailto:vkkn@iitmandi.ac.in)

The development of metal-based heterogeneous catalysts for organic transformation reaction has limited practical application because they exhibit pyrophoricity, require harsh conditions, and generally have low activity. Supported metal nanoparticles have been proposed as a solution to these problems. However, pyrophoricity affects these heterogeneous catalysts, necessitating pretreatment before each catalytic cycle to generate an active metallic state in the catalysts. Combining metal with a non-metal element is promising approach for developing a new class of catalysts. In this context, metal phosphide nanoalloy catalysts, have attracted attention toward organic transformation reactions. This “P-alloying” is the key strategy to developing highly active and stable metal phosphide that can replace conventional sponge metal catalysts for valuable synthesis. The incorporation of inorganic phosphorous into metal nanoparticles has not been studied much more in the field of organic transformation reactions. The addition of P-atom in the metals has several merits in organic transformations reactions such as these metal phosphides are present in the metallic state in the air (stabilizing effect), second is the introduction of P-atom in a metal can modulate the electronic structure of metals species (ligand effect). Density functional theory (DFT) studies reveal that P-atom increases the d-electron density of metals near the Fermi level, facilitating hydrogenation reactions and facilitates the precise creation of well-defined catalytic active sites in metal phosphide catalysts for the selective organic transformation reactions [1,2]. In our work, we synthesized nickel phosphide nanoparticles supported on graphitic carbon nitride (Ni<sub>2</sub>P/GCN), which serves as a highly active, reusable, and high stable heterogeneous catalyst for the reductive amination of carbonyl compounds by using formic acid as reductant.

**Synthesis method:** The Ni<sub>2</sub>P nanoparticles have been synthesized according to previously reported method [3,4]. In brief, NiCl<sub>2</sub>·6H<sub>2</sub>O (1 mM) and NaH<sub>2</sub>PO<sub>2</sub>·H<sub>2</sub>O (5 mM) are added to a beaker with 10 mL deionized (DI) water. The mixture was stirred for 1 h then heated at 100 °C for the evaporation of DI water and left overnight. Then the compound was annealed under Ar atmosphere for 1 h at 200 °C (heating rate 5° min<sup>-1</sup>). After cooling, the product was washed with ethanol and DI water and then dried at 70 °C overnight to form Ni<sub>2</sub>P. To form a composite of Ni<sub>2</sub>P with GCN, 10 mg of Ni<sub>2</sub>P was added to 10 mL of methanol and sonicated for 2 h then 90 mg GCN was added to the solution of Ni<sub>2</sub>P and stirred for 2 h, then again sonicated for 2 h. Finally, drying of the solvent was done using a vacuum rota-evaporator and the obtained product was dried at 70 °C to obtain Ni<sub>2</sub>P/GCN composite. The synthesized catalyst has been characterized by using various techniques such as PXRD, XPS, SEM, TEM, TGA, and TPD.

### Characterization of nickel phosphide

The PXRD patterns of Ni<sub>2</sub>P and Ni<sub>2</sub>P/GCN composite are shown in **Fig 1**. PXRD confirm the formation of hexagonal structure of Ni<sub>2</sub>P and Ni<sub>2</sub>P/GCN composite. The PXRD pattern of Ni<sub>2</sub>P shows a diffraction peak at 40.8°, 44.7°, 47.5°, 54.4°, 54.8° corresponds to (111), (201), (210), (300), (211) crystalline phase. The XRD pattern of Ni<sub>2</sub>P/GCN shows a additional diffraction peaks of GCN at 13.17°, 27.62° corresponds to (100) and (002) crystallite phase, which originate because of interplanar structural packing of the motif and carbon nitride interlayer stacking reflections [3,4].

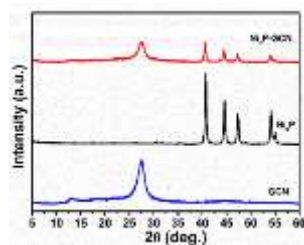


**Figure 1.** PXRD plots of GCN, Ni<sub>2</sub>P, and Ni<sub>2</sub>P/GCN.

The chemical state of Ni and P in the Ni<sub>2</sub>P were examined by XPS technique. **Fig 2b,c**, shows the XPS spectra of Ni 2p and P 2p regions for Ni<sub>2</sub>P. **Fig. 2b** shows two peaks around 853 eV and 870.2 eV, which are similar to metallic Ni 2p<sub>3/2</sub> (852.8 eV) and Ni 2p<sub>1/2</sub> (870.0 eV) binding energy peaks. The P 2p spectra revealed two peaks, showing the presence of phosphorus atoms with distinct electronic states (**Fig. 2c**). The first peak, at 129.5 eV, was close to P<sup>0</sup> (130.0 eV), while second peak at 133.2 eV was assigned to unreduced phosphate species PO<sub>4</sub><sup>-3</sup> resulting from the surface oxidation of Ni<sub>2</sub>P nanoparticles [2].

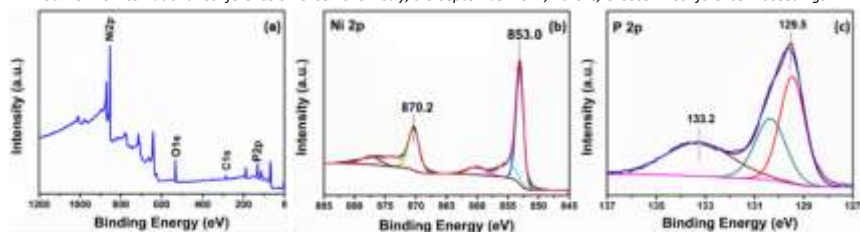
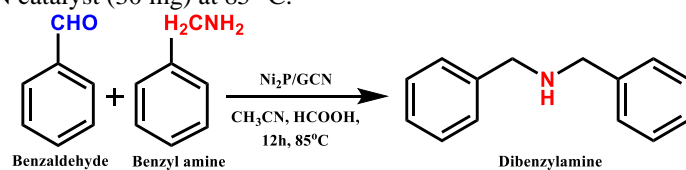


**Figure 2.** (a) Survey XPS spectrum

of Ni<sub>2</sub>P, (b, c) deconvoluted XPS spectra of Ni-2p and P-2p of Ni<sub>2</sub>P.

### Catalytic activity studies

The catalytic activity of the as-synthesized heterogeneous catalyst, Ni<sub>2</sub>P/GCN composite, was investigated for the reductive amination of the carbonyl compounds by using formic acid as reductant. Herein, we developed a simple protocol under ambient catalytic reaction conditions for the transfer hydrogenation of carbonyl compounds with a catalytic amount Ni<sub>2</sub>P/GCN at optimal reaction time using formic acid as a hydrogen source. The catalytic hydrogen transfer reaction was performed using benzaldehyde and benzyl amine as model substrates under the optimized reaction conditions, *viz.*, benzaldehyde (1 mmol), benzyl amine (1 mmol), CH<sub>3</sub>CN (2 mL), formic acid (2 mmol) and Ni<sub>2</sub>P/GCN catalyst (30 mg) at 85 °C.



Further studies on substrate scope, mechanism and stability of the catalyst are underway. Nevertheless, the currently obtained results serves clearly demonstrates the feasibility of using Ni<sub>2</sub>P/GCN as an economical and efficient heterogenous catalyst for reductive amination reactions.

### Acknowledgements

We are thankful to the Advanced Materials Research Centre (AMRC), IIT Mandi, for laboratory and characterization facilities. Devendra Sharma acknowledges the doctoral scholarship from the Ministry of Education (MoE), India.

### References

1. Fujita, Shu, Sho Yamaguchi, Jun Yamasaki, Kiyotaka Nakajima, Seiji Yamazoe, Tomoo Mizugaki, and Takato Mitsudome, *Chemistry—A European Journal*, **27** 4439-4446 (2021).
2. Fujita, Shu, Kiyotaka Nakajima, Jun Yamasaki, Tomoo Mizugaki, Koichiro Jitsukawa, and Takato Mitsudome, *ACS Catalysis* **10**, 4261-4267 (2020).
3. Uekert, Taylor, Hatice Kasap, and Erwin Reisner, *Journal of the American Chemical Society*, **14** 15201-15210 (2019).
4. Indra, A., Acharjya, A., Menezes, P.W., Merschjann, C., Hollmann, D., Schwarze, M., Aktas, M., Friedrich, A., Lochbrunner, S., Thomas, A. and Driess, M., *Angewandte Chemie International Edition* **56** 1653-1657 (2017).

## CO<sub>2</sub>/CH<sub>4</sub> selective hollow fiber and flat sheet membranes based on green solvent

George V. Theodorakopoulos<sup>1,2,\*</sup>, Dionysios S. Karoussos<sup>1</sup>, Andreas A. Sapolidis<sup>1</sup> and Evangelos P. Favvas<sup>1</sup>

<sup>1</sup>Institute of Nanoscience and Nanotechnology, National Center for Scientific Research "Demokritos", Aghia Paraskevi 15341, Athens, Greece

<sup>2</sup>School of Chemical Engineering, National Technical University of Athens, 9 Iroon Polytechniou street, 15780 Zografou, Athens, Greece

\*e-mail address of corresponding author: g.theodorakopoulos@inn.demokritos.gr

### Abstract text:

Polymeric membranes have been regarded as a promising technology for gas separation over the last decades mainly due to their easy fabrication, low and capital and operation cost and small footprint [1]. The most used technique for polymeric membranes fabrication is based on the phase inversion process and the most common used solvent is n-methyl-2-pyrrolidone (NMP) due to its high boiling point (202-204°C) and strong dissolving power. But its toxic and hazardous nature [2] requires special treatment during labor use and before its disposal as waste. Upon the green chemistry guidelines and directives, the reduction or complete elimination of hazardous substances would be mostly favored. Subsequently, in this work, NMP was completely substituted by  $\gamma$ -butyrolactone (GBL), a non-toxic and environmentally friendly solvent with similar characteristics with NMP, both in dope solution and bore liquid. The successful polymeric (co-polyimide, P84) hollow fiber (HF) and flat sheet (FS) membranes fabrication was based on Hansen solubility parameters and cloud point data from the ternary polyimide/solvent/non-solvent diagrams evaluation abetted by complete viscosity study. In this context, in order to have a spinnable dope, the sufficient viscosity of the dope solution is one of the most key parameters [3]. The appropriate viscosity is determined from the molecular concentration and weight of the polymer leading to polymer extrusion and spinning possibility without HF's disruption and discontinuity [4]. Hence, the viscosities of P84/GBL solutions of various concentrations (15-28 wt.%) were measured employing a cone-shaped spindle of a viscometer at three controlled temperatures (30, 40 and 50°C) by a heating circulator and at various shear rates. The critical polymer concentration was determined as the point from where the polymer's viscosity starts to increase exponentially regarding to polymer concentration and the optimum polymer concentration (dope solution) refers to this point or marginally above it. The critical concentration is defined as the intercept of the two extrapolated (tangent) lines of the corresponding linear parts of the viscosity curve [5].

As can be seen from Figure 1a, a significant increase is observed at a critical concentration of about 25 wt.% and this value (or little above) was chosen for the formulation of the spinning dope with GBL solvent. It could be mentioned that at the critical concentration, significant chain entanglement occurs in the spinning dope and the respective fibers show thin skin layers and minimum surface porosity. Indeed, if the concentration of polymer coils is increased beyond this critical value, the coils can no longer remain discrete and become prone to entanglement, as the polymer chains become closely packed enough to form entanglements, which might alter polymer's form from fluid-like to more solid-like. Finally, Figure 1b presents the relationship curve between the viscosity and temperature depicting that the viscosity of polymer solution exhibited strong temperature sensitivity.

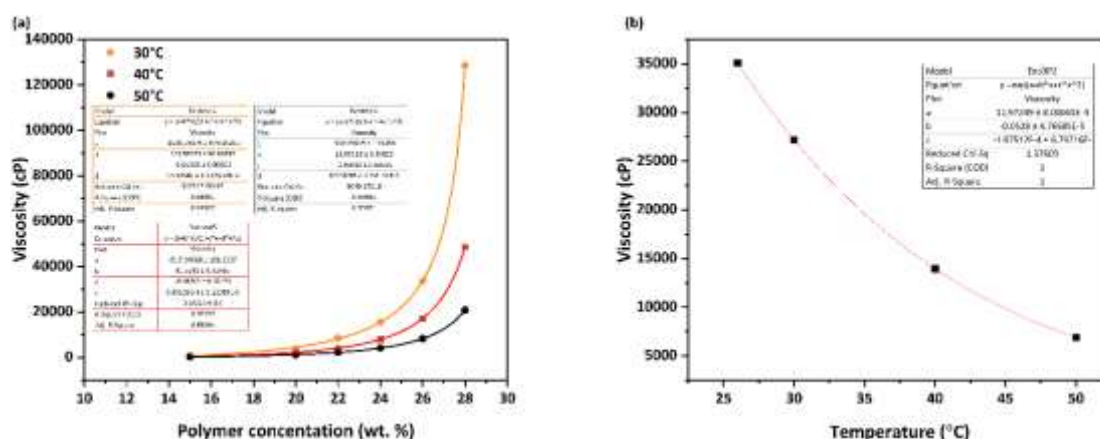


Figure 1. (a) Effect of polymer (P84) concentration on dope viscosity at 30, 40 and 50°C; (b) Temperature-viscosity curve of polymer solution.

The developed HF's were prepared by the dry-wet phase inversion process, which is based on the spinodal decomposition principle, in a spinning set-up, which has been described in previous work [6], whereas dense FS membranes were prepared by the casting method. The derived membranes were characterized by SEM and their mechanical properties were evaluated. The high dope viscosity due to the tighter conformation of the polymer molecule based on the weak nature of GBL solvent and slow diffusion coefficients hampered the rapid water

intrusion into the nascent membrane structure and thus eradicated the tendency of local surface instability for the macrovoid formation resulting in a sponge-like P84 structure (Figure 2).

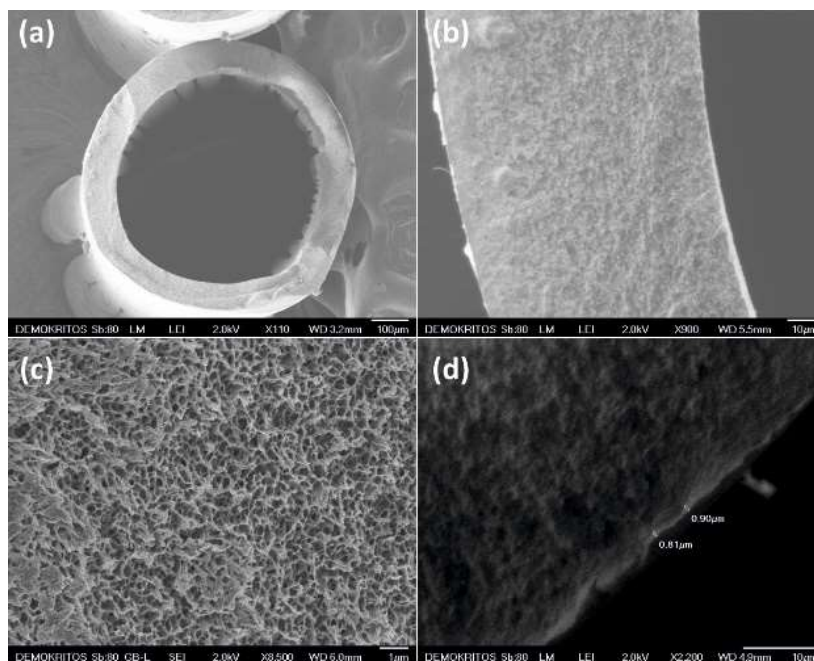


Figure 2. Images of HF membrane: cross section illustrating its morphology and dimension (a); wall (b) and higher magnification displaying its sponge-like structure (c); separation layer thickness (d).

For the first time, preliminary CO<sub>2</sub>/CH<sub>4</sub> separation measurements under continuous flow were performed in order to evaluate their efficiency in real binary CO<sub>2</sub>/CH<sub>4</sub> (10/90 vol.%) mixture separation under elevated pressure conditions. Furthermore, pressurization-depressurization cycle was applied in order to conceive the stability and the possible reversibility of the membranes' structure change by the pressure application. The developed green HF and FS membranes exhibited comparable results to membranes prepared using highly toxic solvents making them promising candidates for CO<sub>2</sub>/CH<sub>4</sub> separation. Specifically, a separation factor of 27.3 and 75.4 of HF and FS membranes, respectively, were achieved. Overall, this work might render primary guidelines for the fabrication of membranes for gas separations in the context of green chemistry and sustainability employing ecofriendly and less hazardous solvents.

### Acknowledgements

The projects entitled "CO<sub>2</sub> separation by using mixed matrix, based on nano-carbon materials membranes (GG-CO<sub>2</sub>)", implemented under the "Action for the Strategic Cooperation between Greek and German Academia and Industry", funded by the Operational Programme "Competitiveness, Entrepreneurship and Innovation" (NSRF 2014–2020) and co-financed by Greece and the European Union (European Regional Development Fund) and "Intelligent Water Treatment for water preservation combined with simultaneous energy production and material recovery in energy intensive industries (intelWATT)" funded from the European Union's Horizon 2020 Research and Innovation Programme under grant agreement No 958454 are acknowledged.

### References

1. P. Salehian, W.F. Yong, T.-S. Chung, Development of high performance carboxylated PIM-1/P84 blend membranes for pervaporation dehydration of isopropanol and CO<sub>2</sub>/CH<sub>4</sub> separation, *J. Mem. Sci.*, **518** 110-119 (2016).
2. Y. Alqaheem, A. Alomair, A. Alhendi, S. Alkandari, N. Tanoli, N. Alnajdi, A. Quesada-Peréz, Preparation of polyetherimide membrane from non-toxic solvents for the separation of hydrogen from methane, *Chem. Centr. J.*, **12** 80 (2018).
3. M. Etxeberria-Benavides, O. Karvan, F. Kapteijn, J. Gascon, O. David, Fabrication of defect-free P84® polyimide hollow fiber for gas separation: pathway to formation of optimized structure, *Membranes*, **10** 4 (2020).
4. T. Hu, G. Dong, H. Li, V. Chen, Effect of PEG and PEO-PDMS copolymer additives on the structure and performance of Matrimid® hollow fibers for CO<sub>2</sub> separation, *J. Mem. Sci.*, **468** 107-117 (2014).
5. N. Peng, T.-S. Chung, K.Y. Wang, Macrovoid evolution and critical factors to form macrovoid-free hollow fiber membranes, *J. Mem. Sci.*, **318** 363-372 (2008).
6. E.K. Chatzidaki, E.P. Favvas, S.K. Papageorgiou, N.K. Kanellopoulos, N.V. Theophilou, New polyimide-polyaniline hollow fibers: synthesis, characterization and behavior in gas separation, *Eur. Polym. J.*, **43** 5010-5016 (2007).



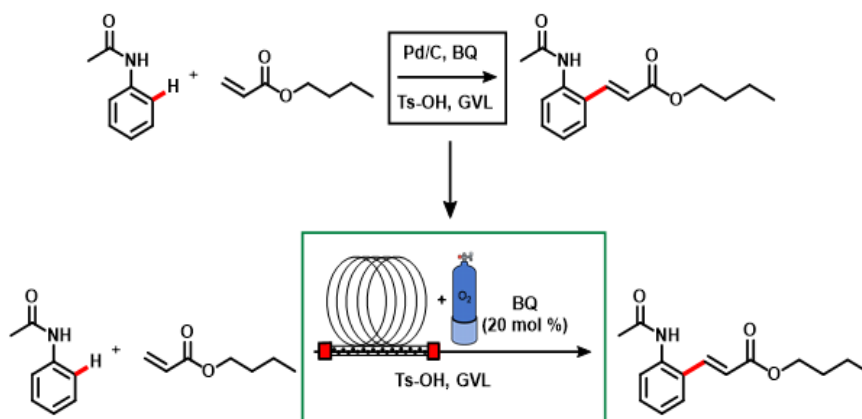
## Aerobic waste-minimized Pd-catalysed C–H alkenylation in GVL using a tube-in-tube heterogeneous flow reactor

Luigi Carpisassi<sup>1</sup>, Francesco Ferlin, Ioannis Anastasiou and Luigi Vaccaro\*

<sup>1</sup>Laboratory of Green Synthetic Organic Chemistry (Green S.O.C.) Department of Chemistry, Biology and Biotechnology  
Università Degli Studi di Perugia, Via Elce Di Sotto 8 06123-Perugia, Italy

\*luigi.vaccaro@unipg.it

Herein we report an innovative flow process for a C–H palladium-catalyzed alkenylation reaction. By carefully analyzing the literature previously exposed, it is evident that despite the flow chemistry has already been adapted to various needs such as the use of heterogeneous catalysts and the use of gas, to date, the coupling of these two technologies remains totally unexplored. The purpose of this work is therefore the implementation of a technological apparatus that can allow the use of gas in flow in the presence of a heterogeneous catalyst for a palladium-catalyzed alkenylation of acetanilides [1] with a view to sustainable development for C–H activation reactions. The aim is to replace the common organic oxidants exploited for this process through the use of molecular oxygen as a sacrificial oxidant.



Scheme 7. tube-in-tube flow reactor representative scheme

At the same time, the use of heterogeneous catalysts in flow guarantees the possibility of efficiently reusing the catalytic system, increasing its efficiency and duration over time. The heterogeneous catalysis applied in flow chemistry results also in a greater stability of the catalytic system and at the same time the prospect of significantly reducing metal leaching in the reaction mixture. Similarly, the use of molecular gas in flow brings various benefits as it is used to ensure the efficiency of the catalyst by reducing or eliminating the addition of additives (oxidants) and therefore intrinsically reducing the production of waste [2], [3]

### Acknowledgements

This study received funding from the NMBP-01-2016 Programme of the European Union's Horizon 2020 Framework Programme H2020/2014-2020/under grant agreement no. [720996]. The Università degli Studi di Perugia and MIUR are acknowledged for financial support to the project AMIS, through the program "Dipartimenti di Eccellenza – 2018-2022".

### References

1. F. Ferlin, S. Santoro, L. Ackermann and L. Vaccaro, *Green Chem.*, **19**, 2510–2514 (2017)
2. Ferlin, F., Van Der Hulst, M. K., Santoro, S., Lanari, D., Vaccaro, L., *Green Chem.*, **21**, 5298-5305 (2019)
3. Trombettoni, V., Sciosci, D., Bracciale, M. P., Campana, F., Santarelli, M. L., Marrocchi, A., Vaccaro, L., *Green Chem.*, **20**, 3222-3231 (2018).

## Waste Minimized $\beta$ -Azidation reaction of $\alpha,\beta$ -unsaturated carbonyl compounds catalyzed by POLITAG-M-F in azeotrope $\text{CH}_3\text{CN}:\text{H}_2\text{O}$ under batch and continuous flow condition.

Gabriele Rossini<sup>1</sup> Giulia Brufani,<sup>1</sup> Federica Valentini,<sup>1</sup> Lucia Rosignoli<sup>1</sup> Luigi Vaccaro\*<sup>1</sup>

Laboratory of Green Synthetic Organic Chemistry (Green SOC), Università degli Studi di Perugia, Dipartimento di Chimica, Biologia e Biotecnologie, Via Elce di Sotto 8, 06123 Perugia (PG), Italia

\*luigi.vaccaro@unipg.it

We report herein a waste minimization protocol for the  $\beta$ -azidation of  $\alpha,\beta$ -unsaturated carbonyl compounds catalyzed by our novel heterogeneous organocatalytic system fluoride based, POLITAG-M-F. Organic azides are known as a well-established class of chemical compounds and valuable synthons in organic chemistry. [1-3] Furthermore, aliphatic azides are common structural units found in a variety of biologically active pharmaceutical ingredients (API) besides being a useful building blocks for the synthesis of a variety of nitrogen-based scaffolds. [4]  $\beta$ -azidation of  $\alpha,\beta$ -unsaturated carbonyl compounds represents a key tool for the introduction of the azido group. By analyzing the literature  $\beta$ -azido carbonyl compounds are obtained using unfavorable conditions for the safety of the process. [5, 6] There is an urgent need in the development of innovative and environmentally friendly chemical methods to produce libraries of complex aliphatic azides of special importance. For these reasons many efforts have been done by our research group for the development of alternative environmentally synthetic strategies for  $\beta$ -azidation processes.[7] The purpose of this work is the development of a new environmentally friendly protocol for the synthesis of  $\beta$ -azido carbonyl by combining the use of a new heterogeneous source of fluoride ion developed by our research group (POLITAG-M-F) and the use of a recoverable reaction medium such as the azeotrope  $\text{CH}_3\text{CN}:\text{H}_2\text{O}$  drastically decreasing the E-Factor value of the protocol compared to the other protocols available in literature. The study has been also directed toward the definition of a continuous-flow protocol aiming at minimizing the environmental footprint of the  $\beta$ -azidation process and increasing the catalytic efficiency of the POLITAG-M-F. Finally, the study has been completed with a comprehensive evaluation of the environmental performance of the developed protocols by considering the principal mass green metrics: E-factor, process mass intensity (PMI), atom economy (AE), reaction mass efficiency (RME).

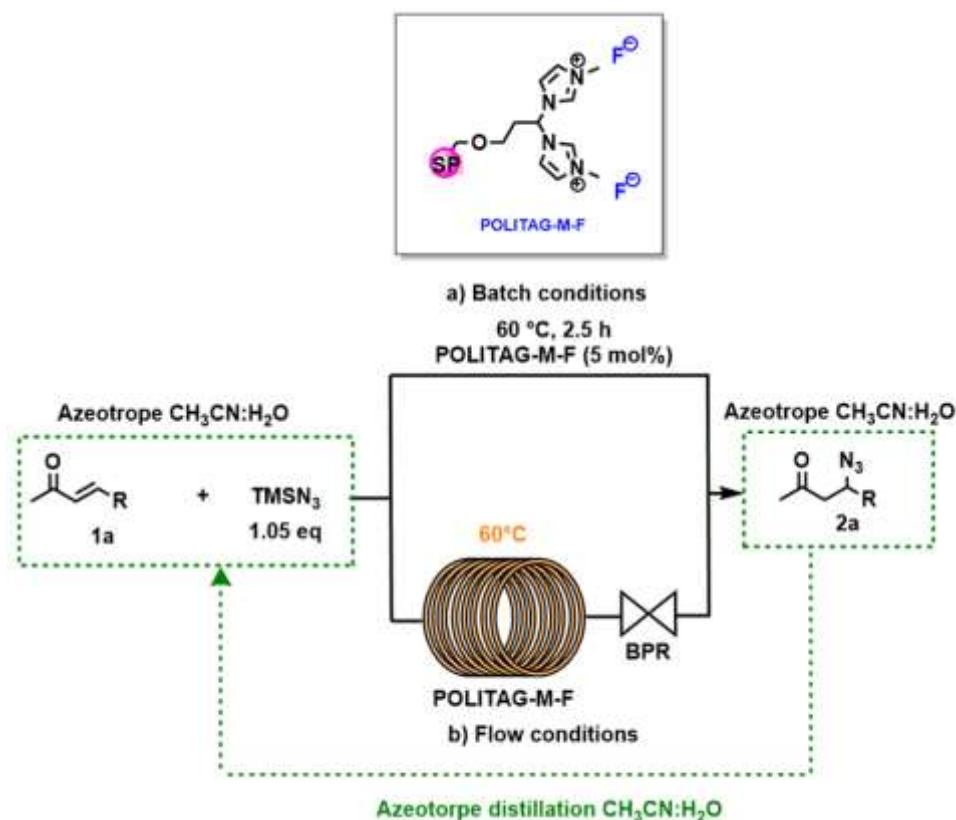


Figure 1.  $\beta$ -azidation of  $\alpha,\beta$ -unsaturated carbonyl compounds in batch and flow conditions using POLITAG-M-F

## Acknowledgements

The Università degli Studi di Perugia and MIUR are acknowledged for financial support for the project AMIS through the program “Dipartimenti di Eccellenza 2018-2022.”

## References

1. Chiba, S. (2012). Application of organic azides for the synthesis of nitrogen-containing molecules. *Synlett*, 1, 21–44. <https://doi.org/10.1055/s-0031-1290108>
2. Waser, J., Carreira, E. M. (2010) Organic Azides: Syntheses and Applications. (Eds: S. Brase, K. Banert, Wiley-VCH: Weinheim, 95-111.
3. Brase, S., Gil, C., Knepper, K. (2005) Zimmermann, V. Organic Azides: An Exploding Diversity of a Unique Class of Compounds. *Angew. Chem. Int.* 44, 5188-5240.
4. Sivaguru, P., Ning, Y., & Bi, X. (2021). New Strategies for the Synthesis of Aliphatic Azides. In *Chemical Reviews* (Vol. 121, Issue 7, pp. 4253–4307). American Chemical Society. <https://doi.org/10.1021/acs.chemrev.0c01124>
5. Taylor, M. S., Zalatan, D. N., Lerchner, A. M., & Jacobsen, E. N. (2005). Highly enantioselective conjugate additions to  $\alpha,\beta$ -unsaturated ketones catalyzed by a (salen)Al complex. *Journal of the American Chemical Society*, 127(4), 1313–1317. <https://doi.org/10.1021/ja044999s>
6. Xu, L. W., Li, L., Xia, C. G., Zhou, S. L., & Li, J. W. (2004). The first ionic liquids promoted conjugate addition of azide ion to  $\alpha,\beta$ -unsaturated carbonyl compounds. *Tetrahedron Letters*, 45(6), 1219–1221. <https://doi.org/10.1016/j.tetlet.2003.11.129>
7. a) Lanari, D., Piermatti, O., Morozzi, C., Santoro, S., Vaccaro, L. (2017) Recent Applications of Solid-Supported Ammonium Fluorides in Organic Synthesis. *Synthesis*, 49, 973-980. b) Ballerini, E., Curini, M., Gelman, D., Lanari, D., Piermatti, O., Pizzo, F., Santoro, S., Vaccaro, L. (2015) Waste Minimized Multistep Preparation in Flow of  $\beta$ -Amino Acids Starting from  $\alpha,\beta$ -Unsaturated Carboxylic Acids. *ACS Sustainable Chem.* 3, 1221–1226; c) Angelini, T., Lanari, D., Maggi, R., Pizzo, F., Sartori, G., Vaccaro, L. (2012) Preparation and Use of Polystyryl-DABCOF2: An Efficient Recoverable and Reusable Catalyst for  $\beta$ -Azidation of  $\alpha,\beta$ -Unsaturated Ketones in Water. *Adv. Synth. Catal.*, 354, 908–916. d) Angelini, T., Bonollo, S., Lanari, D., Pizzo, F., Vaccaro, L. (2012) A Protocol for Accessing the  $\beta$ -Azidation of  $\alpha,\beta$ -Unsaturated Carboxylic Acids. *Org. Lett.*, 14, 4610–4613. e) Fringuelli, F., Lanari, D., Pizzo, F., Vaccaro, L. (2008) Amberlite IRA900F as a Solid Fluoride Source for a Variety of Organic Transformations under Solvent-Free Conditions. *Eur. J. Org. Chem.*, 3928–3932. f) Castrica, L., Fringuelli, F., Gregoli, L., F. Pizzo, Vaccaro, L (2006) Amberlite IRA900N3 as a New Catalyst for the Azidation of  $\alpha,\beta$ -Unsaturated Ketones under Solvent-Free Conditions *J. Org. Chem.*, 71, 9536-9539.

## Density and Refractive Index of Binary Ionic Liquid Mixtures with Common Cations/Anions: Measurement and Modelling

G. Reza Vakili-Nezhaad<sup>1\*</sup>, M. Mohammadzaheri<sup>2,3</sup>, F. Mohammadi<sup>4</sup>, and Mohammed Humaid<sup>1</sup>

<sup>1</sup>Petroleum & Chemical Engineering Department, College of Engineering, Sultan Qaboos University, Muscat 123, Oman

<sup>2</sup>Department of Mechanical & Industrial Engineering, College of Engineering, Sultan Qaboos University, Muscat 123, Oman

<sup>3</sup>Birmingham City University, Birmingham, United Kingdom

<sup>4</sup>School of Health, Isfahan University of Medical Sciences (MUI), Isfahan, Iran

\*e-mail: Vakili@dqu.edu.om

Ionic liquids have many interesting properties, as they share the properties of molten salts as well as organic liquids, such as low volatility, thermal stability, electrical conductivity, non-flammability and much more. Ionic liquids are known to be good solvents for many polar and nonpolar solutes. Combined with their special properties, ionic liquids are good replacements for the conventional toxic and volatile organic solvents. Each ionic liquid has different properties than others. In order to alter, tune and enhance the properties of ionic liquids, sometimes it is necessary to mix different ionic liquids to achieve the desired properties arises. However, using mixtures of ionic liquids in chemical processes requires reliable estimations of the mixtures physical properties such as refractive index and density [1-2].

The ionic liquids used in this work are 1-butyl-3-methylimidazolium thiocyanate ([BMIM][SCN]), 1-butyl-3-methylimidazolium tetrafluoroborate ([BMIM][BF<sub>4</sub>]), 1-hexyl-3-methylimidazolium tetrafluoroborate ([HMIM][BF<sub>4</sub>]), and 1-hexyl-3-methylimidazolium hexafluorophosphate ([HMIM][PF<sub>6</sub>]). These ionic liquids were supplied by Io-li-tec, and used as received. However, new measurements for the density and refractive index were taken for the pure ionic liquids to be used as reference.

In the present work densities and refractive indices of four different binary mixtures of ionic liquids with common cations and/or anions have been measured at various compositions and room conditions. The accuracy of different empirical mixing rules for calculation of the mixtures refractive indices was also studied. It was found that the overall absolute average percentage deviation from ideal solution in calculation of molar volume of the examined binary mixtures is 0.78%. Furthermore, all of the examined mixing rules for calculation of refractive indices of the mixtures were found to be accurate. However, the most accurate empirical formula was found to be Heller's relation with an average percentage error of 0.24%. Finally, some Machine Learning algorithms were also used for our modelling and calculations, which showed very promising results for the prediction of the properties of ionic liquids and their mixtures.

### Acknowledgements

The authors are thankful to Sultan Qaboos University for the financial support through the internal grant project number IG/ENG/PCED/22/02.

### References

1. A. Mokhtaria, H. Bagheri, M. Ghazvini, S. Ghader, *Chemical Engineering Research and Design*, **177** 331 (2022).
2. W. Zheng, X. Liu, J. Zhang, Y. Cheng, W. Wang, *International Journal of Heat and Mass Transfer*, **182** 121983 (2022).

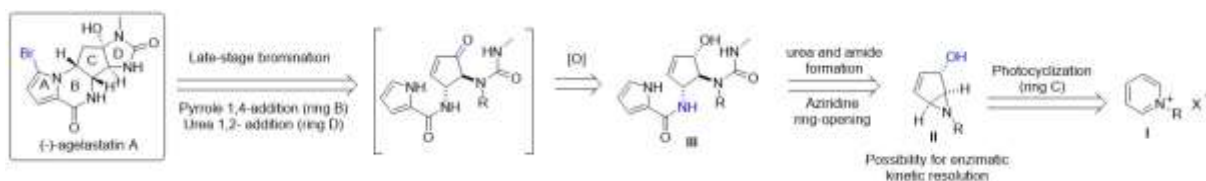
## Total synthesis of (-)-agelastatin A via photochemical transformation of pyridinium salt and early-stage enzymatic resolution

João R. Vale<sup>1,2\*</sup>, Milene Fortunato<sup>1</sup>, Filipa Siopa<sup>1</sup> and Carlos A. M. Afonso<sup>1</sup>

<sup>1</sup>Med.U.Lisboa, Faculty of Pharmacy, University of Lisbon, Av. Prof. Gama Pinto, 1649-003 Lisbon, Portugal; <sup>2</sup>Faculty of Engineering and Natural Sciences, Tampere University, Korkeakoulunkatu 8, 33101 Tampere, Finland

\*jvale@campus.ul.pt

Agelastatin alkaloids have attracted scientific interest since the isolation of (-)-agelastatin A (AgIA) from the sponge *Agelas dendromorpha* by Pietra et al. in 1993.[1] AgIA shows remarkable cytotoxicity against a variety of tumor cells[2] and strong inhibition of osteopontin-mediated neoplastic transformation and metastasis.[3] Additionally, it displays high brine shrimp toxicity and insecticidal properties.[4] Since large quantities of AgIA are problematic to obtain via natural sources, its total synthesis is highly desirable. Asymmetric synthesis is very challenging and reported procedures typically require laborious steps and protecting groups to construct the four contiguous stereocenters of the cyclopentane C-ring.[5] We have developed a new strategy (Scheme 1) that involves an early-stage photochemical transformation of pyridinium salts to bicyclic vinyl aziridines that originate, in one step, the AgIA's C-ring core with the desired functionality and relative configuration. This process allowed the total synthesis of (-)-agelastatin A in only 12 steps with 4% overall yield, with the use of a single protective group.



Scheme 8: Retrosynthetic analysis of agelastatin A.

### Acknowledgements

This project has received funding from the European Union's Horizon 2020 research and innovation programme under grant agreement No 951996. Fundação para a Ciência e Tecnologia (FCT) is acknowledged for financial support to J. Vale (SFRH/BD/120119/2016).

### References

1. M. D'Ambrosio, A. Guerriero, C. Debitus, O. Ribes, J. Pusset, S. Leroy and F. Pietra, *J. Chem. Soc. Chem. Commun.*, 1305 (1993).
2. M. D'Ambrosio, A. Guerriero, M. Ripamonti, C. Debitus, J. Waikedre and F. Pietra, *Helv. Chim. Acta*, **79**, 727 (1996).
3. C. K. Mason, S. McFarlane, P. G. Johnston, P. Crowe, P. J. Erwin, M. M. Domostoj, F. C. Campbell, S. Manaviyar, K. J. Hale and M. El-Tanani, *Mol. Cancer Ther.*, **7**, 548 (2008).
4. T. W. Hong, D. R. Jimenez and T. F. Molinski, *J. Nat. Prod.*, **61**, 158 (1998).
5. S. W. M. Crossley and R. A. Shenvi, *Chem. Rev.*, **115**, 9465 (2015).
6. C.N. Hamelinck, A.P.C. Faaij, H. Den Uil, H. Boerrigter, *Energy*, **29** 1743 (2004).
7. R. Ash, R. M. Barrer, C.G. Pope, *Proc. R. Soc. London, Ser. A*, **271** 19 (1963).

## 'On-Water' directing groups assisted C–H bond functionalization of ferrocene derivatives

Ashutosh Verma<sup>1</sup> and Anil J. Elias<sup>1\*</sup>

<sup>1</sup>Department of Chemistry, Indian Institute of Technology Delhi, Hauz Khas, New Delhi, India

\*eliasanil@gmail.com

Water is the solvent of choice by nature for most of its chemical and biological reactions. It is the cleanest, safest, most economical, non-toxic, and most environmentally benign solvent available in nature [1-2]. However, chemists often prefer to use organic solvents for better solubility and stability of the reagents, intermediates, and catalysts to gain maximum conversion in a reaction. The use and prolonged exposure to organic solvents can cause adverse effects on human beings as well as the environment, mainly when they are used in large quantities [3]. Therefore, greener, atom economical, and environmentally benign synthetic methodologies that use non-toxic, low-cost, and sustainable reaction media such as water are highly desirable [4, 5]. In general, reactions involving organometallic substrates and reagents are almost always performed in organic solvents. It is assumed that metal-carbon bonds are likely to hydrolyze in an aqueous medium. Interestingly, due to this mental block, many reactions involving organometallic substrates have rarely been attempted in water.

During the last two decades, the 'in-water' and 'on-water' reactions came into prominence and both methods are becoming popular among synthetic chemists. In both these methodologies, the solubilities of all the substrates involved in an aqueous medium are not necessary. Recently, using the concept of 'in water' reactions, Ackermann et al. developed a method for mono C-H bond functionalization of ferrocene using *t*-butyl thioetone as a monodentate directing group and TPGS-750M/H<sub>2</sub>O (DL- $\alpha$ -Tocopherol methoxy polyethylene glycol succinate solution) as a designer surfactant [6]. However, 'on-water' reactions for the C-H bond functionalization of ferrocene or similar organometallic substrates have not been reported so far.

The directing group assisted C-H bond activation, and functionalization of ferrocene derivatives, especially of alkyl, aryl, and other functional groups, have been reported mainly using palladium as the catalyst [7, 8]. These reactions were carried out using organic solvents such as *tert*-amyl alcohol, toluene, *N*-methyl pyrrolidone or dichloromethane as the reaction medium. Inspired by Ackermann's report, to develop a robust and greener methodology for C-H bond functionalization of ferrocene derivatives, we decided to relook at C-H activation of the cyclopentadienyl ring of ferrocene using bidentate directing groups under 'in-water' and 'on-water' reaction conditions.

The C-H bond functionalization under the 'on-water' condition was carried out using ferrocene having an 8-aminoquinoline (8-AQ) directing group (1) with 4-iodoanisole (e) as an arylating agent. The substrates, ferrocene 8-aminoquinoline carboxamide, was synthesized by the reaction of acid chloride of ferrocene carboxylic acid with 8-aminoquinoline and ferrocene-picolinamide was synthesized starting from aminomethyl ferrocene and its reaction with picolinoyl chloride by following reported procedure. For the reaction, a 5.0 ml screw-capped vial charged with a magnetic bead and 0.25 mmol of ferrocene with 8-aminoquinoline or picolinamide directing group was used and 5 mol% of Pd(OAc)<sub>2</sub> and 0.5 mmol of K<sub>2</sub>CO<sub>3</sub> were added. Afterwards, 0.75 mmol of aryl iodide and 0.5-1.0 ml of deionized water were added to the reaction mixture. The reaction vial was closed tightly, and it was heated at 80-100 °C. The reaction mixture was worked up using ethyl acetate (2 times) and water. The organic layer was collected and dried over anhydrous Na<sub>2</sub>SO<sub>4</sub>, and afterwards, the solvent was evaporated. The crude product was purified by silica gel column chromatography using hexane and ethyl acetate as the eluent (80:20).

Various iodobenzene derivatives with electron-donating and electron-withdrawing groups at the ortho, meta, and para positions on the aryl ring were screened under the 'on-water' reaction conditions, and 55-98% isolated yield of the respective target products were obtained.

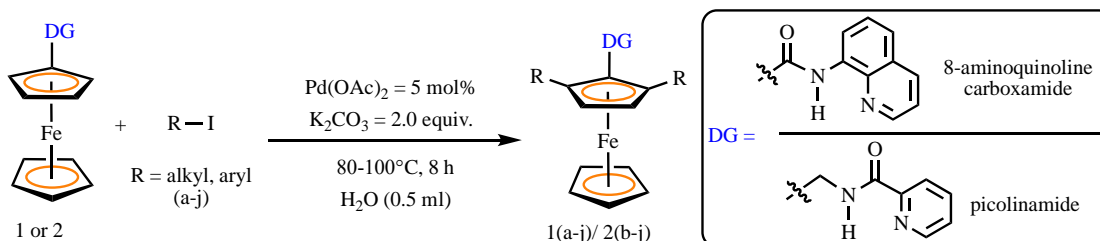


Figure 1. 'On water' C–H functionalization on ferrocene 8-aminoquinoline carboxamides and picolinamides

In this work, we have reported an 'on-water' methodology for the selective synthesis of bis C-H bond functionalized ferrocene derivatives under relatively mild reaction conditions. 8-aminoquinoline and picolinamide were used as selective, inexpensive, and easily removable bidentate directing groups on ferrocene and the reactions were performed exclusively in water. The reaction of ferrocene 8-aminoquinoline carboxamide with various aryl/alkyl iodides using 5 mol% of Pd(OAc)<sub>2</sub> and water as the solvent resulted in 61-93% isolated yield of the cyclopentadienyl bis-arylated products. Similarly, using ferrocene-picolinamide as the substrate with aryl iodides, 55-98% yield of the cyclopentadienyl substituted ferrocene derivatives were obtained. The heterogeneity and stability of substrates, catalysts, and products under 'on-water' reaction conditions enabled us to explore the suitability of the solvent, i.e., water and the catalyst's reusability. Control experiments confirmed the *in situ* formation of palladacycles during the reaction.

### Acknowledgements

The research is financially assisted by SERB DST, India, as well as CSIR, India, to A.J.E. [CRG 2019/000013], [01(2982)/19/EMR-II] and are gratefully acknowledged. A.V. thanks DST Inspire for the fellowship. Authors thank the Indian Institute of Technology Delhi for the instrument facilities.

### References

1. P. Ball, *Proc. Natl. Acad. Sci.* **114** 13327 (2017).
2. S.D. Colson, T.H. Dunning Jr., *Science* **265** 43 (1994).
3. N. Winterton, *Clean Techn. Environ Policy* **23** 2499 (2021).
4. B.H. Lipshutz, *Curr. Opin. Green Sustain. Chem.* **11** 1 (2018).
5. J.G.-Alvarez, E. Hevia, V. Capriati, *Eur. J. Org. Chem.* **2015** 6779 (2015).
6. S.R. Yetra, T. Rogge, S. Warratz, J. Struwe, W. Peng, P. Vana, L. Ackermann, *Angew. Chem. Int. Ed.* **58** 7490 (2019).
7. J. Singh, M. Deb, A.J. Elias, *Organometallics*. **34** 4946 (2015).
8. S. Hazra, M. Deb, J. Singh, A.J. Elias. *Organometallics* **36** 1784 (2017).

## A novel approach towards expanding the utility of Deep eutectic solvents as a biocompatible co-solvent for $\alpha$ -chymotrypsin.

Niketa Yadav, Pannuru Venkatesu\*

Department of Chemistry, University of Delhi, Delhi, India.  
niketayadav2208@gmail.com, venkatesup@hotmail.com\*

Deep eutectic solvents (DES) have raised much attention due to a variety of attractive features. DESs are prepared by mixing a hydrogen bond acceptor and a hydrogen bond donor with simultaneous heating and stirring until a liquid is formed at room temperature. A growing number of studies describe DESs as environmentally acceptable or better alternatives to established reaction solvents in biotransformations.[1] Very recently, these solvents have been the center of attention for researchers in biotechnology, biomedicine and various scientific applications. These environmentally benign solvents have a close analogy with ionic liquids (ILs); however, they offer certain unique merits over traditional ILs. DESs display remarkable properties such as easy preparation, tunable composition, biodegradability, recyclability, inherently low toxicity, sustainability and biocompatibility; these special features validate DESs as new potential solvents/co-solvents for biomolecules.[2,3] We expand on this concept to introduce the idea of forming eutectic reaction media as a biocompatible co-solvent for protein folding/unfolding studies.

Herein, we report the synthesis and characterization of two DESs namely choline chloride-urea (DES-1) and choline chloride-glycerol (DES-2). Along with this a comprehensive biophysical analysis by employing various techniques such as circular dichroism (CD), UV-visible, steady state, and thermal fluorescence spectroscopy of  $\alpha$ -chymotrypsin (CT) in presence of varying concentrations of DES-1 and DES-2 was carried out. This study describes the utility of DES as a stabilizing co-solvent for CT, with enhanced thermal stability along with preservation of its enzymatic activity. Interestingly, DES-1 successfully counteracts the deleterious effect of urea on CT along with protecting the secondary structure of protein.

Overall, both the DESs can be described as potential biocompatible, sustainable, and promising cosolvents for CT with enhanced structural and thermal stability along with preservation of its activity. Thus, present study establishes DES as a relevant alternative to conventional organic/in-organic chemicals with lower environmental footprint.

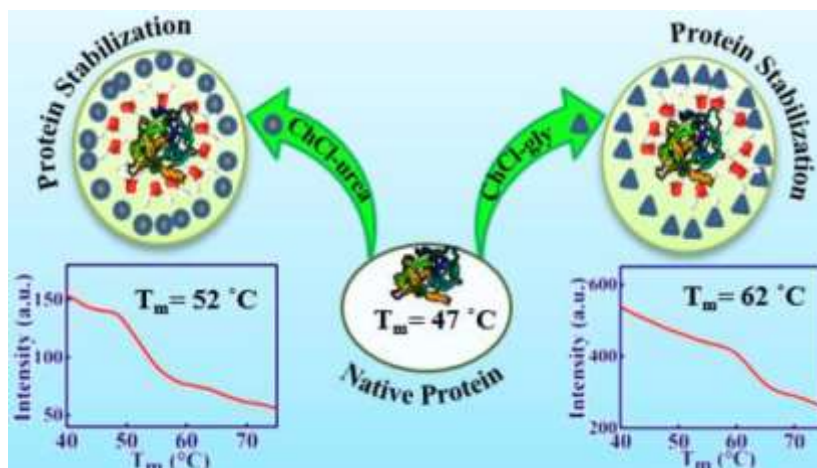


Figure: Protein stabilization of DESs towards protein

This study brings forward a novel application of DESs, i.e., as cosolvents for protein stability. Altogether, the results validate that the aqueous solutions of DESs preserve the stability and activity of enzyme CT. By introducing DESs cosolvents, the thermal stability of CT was enhanced which reflects the suitability of ChCl-urea and ChCl-gly as preserving media for CT against high temperature.

### Acknowledgements

We gratefully acknowledge the Council of Scientific and Industrial Research (CSIR), New Delhi, India, through Grant No. 01/2871/17/EMR-II, for their financial support. N.Y. is grateful to UGC (University Grants Commission), India, for providing a Senior Research Fellowship.



## References

1. T. Welton, *Chem. Rev.*, **99**, 2071–2084 (1999).
2. F. Niknaddaf, S. S. Shahangian, A. Heydari, S. Hosseinkhani and R. H. Sajedi, *Chemistry Select*, **3**, 10603–10607 (2018).
3. J. A. Kist, M. T. Henzl, J. L. Ban˜uelos and G. A. Baker, *ACS Sustainable Chem. Eng.*, **7**, 12682–12687 (2019).

# Nano-materials for energy and environmental applications

## Ecological Treatment Processes for Leathers Intended for Medical Applications

Ariadne Athanasiou<sup>1#</sup>, Konstantinos Giannakopoulos<sup>2</sup>, Nafsica Mouti<sup>2</sup>, Marina Arvanitopoulou<sup>2</sup>, Michael Arkas<sup>2</sup> Sara M. Soto<sup>3</sup> and Georgia Kythreoti<sup>1\*</sup>

<sup>1</sup>Institute of Biosciences and Applications, NCSR "Demokritos", Patriarchou Gregoriou Street, 15310 Athens, Greece

<sup>2</sup>Institute of Nanoscience Nanotechnology, NCSR "Demokritos", Patriarchou Gregoriou Street, 15310 Athens, Greece

<sup>3</sup>ISGlobal, Hospital Clinic - Universitat de Barcelona, 08036 Barcelona, Spain

# Current address: School of Liberal Arts and Sciences, The American College of Greece, 6 Gravias Street, 15342 Athens, Greece

\*geokyth@bio.demokritos.gr

### Introduction

Raw leather is chemically treated, in a process called tanning, providing permanent antiseptic properties with high, long-term resistance to bacteria & fungi. The dry leather then undergoes the finishing process, where special coatings are applied to its surface rendering it resistant to abrasion. We aim to develop an alternative method. Hybrid nanocomposites, composed of silica and hyperbranched poly(ethylene imine) (PEI) are employed as coatings - active ingredient carriers in the medical leather processing technology. The desired properties include antimicrobial, anti-allergic protection, abrasion resistance, and water vapor permeability. The preparation method is environmentally friendly, based on two biomimetic reactions. Silica gelation and spontaneous silver nanoparticle formation that protects from microorganisms [1] are both mediated by the dendritic polymer.

### Synthesis of silver nanoparticle/silica-PEI coatings on leather substrates

To 50 ml of 1mM solutions of hyperbranched poly(ethylene imines) PEI (Mw 2000, 5000, 25000, 750000) corresponding to about 40 mM in primary and secondary amino groups 12,5 ml of AgNO<sub>3</sub> (0,1M) were added. After 1h a change in color of the mixtures, from colorless to light yellow, was observed indicating the beginning of the silver nanoparticle formation. The solutions were allowed to react for 6 days and their color turned into deep orange-brown. The formation of silver nanoparticles was confirmed by visible spectroscopy from the peak at 420 nm which is characteristic of the surface plasmon vibrations of metallic silver nanoparticles. A 100 ml 1M orthosilicic acid solution was prepared from hydrolysis of tetraethoxysilane by 5mM HNO<sub>3</sub> under stirring for 15 min. 50 ml silver-hyperbranched polyethylene imine solutions were added and the pH was adjusted to 7.5 with trizma base. The resulting solution was in turn slowly drop-wise added onto the surface of the leather substrate. The formation of a solid layer due to gelation was observed in about 1 hour. Then the coated leather was dried overnight in an oven at 60°C to transform hydrogel into a xerogel. The coating procedure may be repeated as many times as needed.

### Characterization

The formation of precursor hydrogels was monitored by dynamic light scattering (DLS) and ζ-potential. Xerogels' interactions with the active ingredients and release properties were characterized by spectroscopy (FTIR, visible). Their chemical composition was assessed by thermogravimetry (TG) and Energy-dispersive X-ray spectroscopy while the uniformity of the coatings was established by optical and scanning electron microscopy (SEM) toxicity was evaluated using the *Caenorhabditis elegans* model. The antibacterial activity was tested towards *Escherichia coli*, *Pseudomonas aeruginosa*, and *Staphylococcus aureus*. The antifungal potential was assessed against *Candida parapsilosis* while antiviral action was checked against Covid-19.

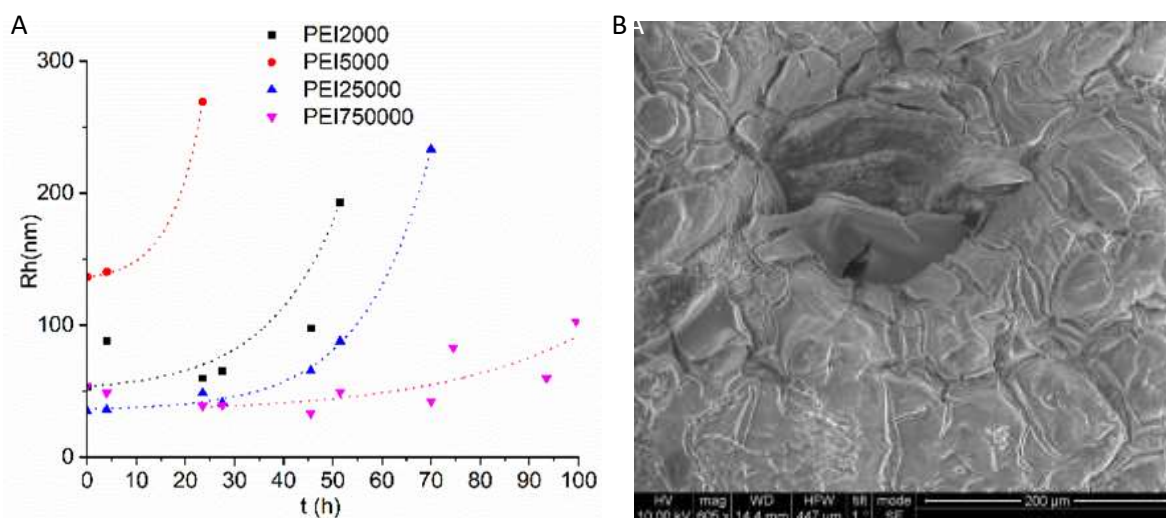


**Figure 1** A. Size of agglomerates formed during the gelation in different Mw PEI solutions-Ag Nanoparticles-Si(OH)<sub>4</sub> as a function of time. B. SEM micrograph indicating the penetration of the xerogel coating into the leather pores

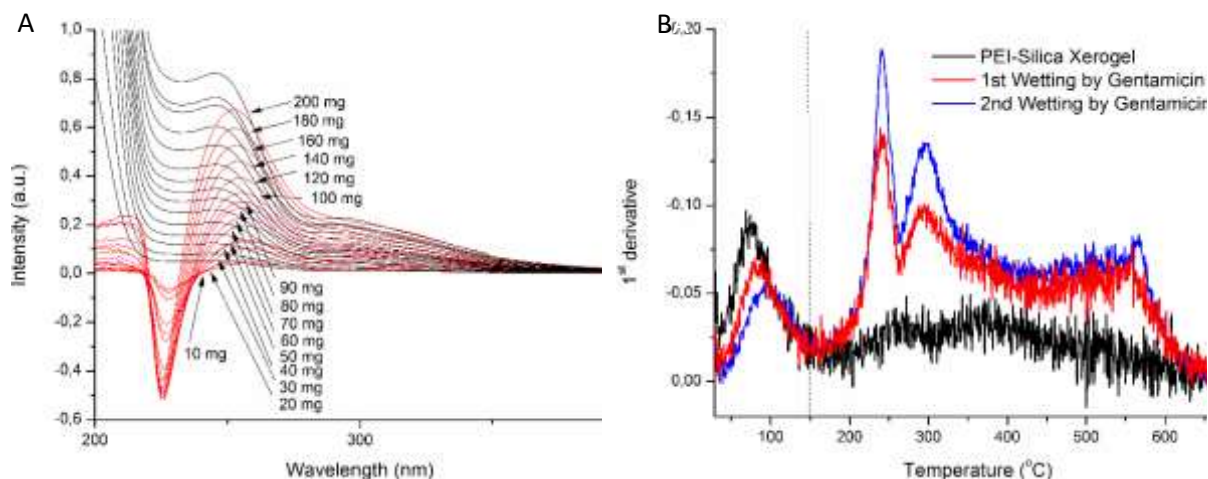


**Figure 2** Monitoring of active ingredient (gentamicin) incorporation. A. UV-visible spectroscopy of gentamicin + PEI complexes at increasing gentamicin concentrations using ultra-pure water (black lines) or 0,1mM PEI as reference (red lines). B. 1<sup>st</sup> derivative of the silica/PEI xerogel thermogravimetric profile before and after 2 gentamicin wetting steps.

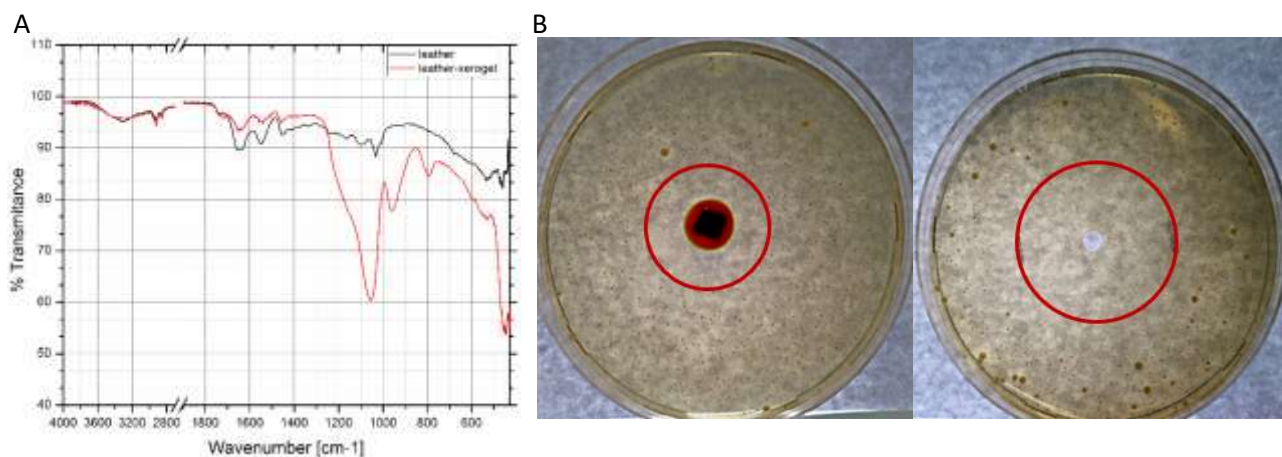


**Figure 3** A. IR spectra of untreated (black) and xerogel coated leather (red) depicting the characteristic silica bands. B. Antibacterial activity determination via disk-diffusion. *Escherichia coli* ATCC 25922 cultures ( $1 \times 10^6$  CFU/ml) in LB-Agar (0.8% w/v) incubated with leather samples coated with Silica Xerogels-PEI-Ag Nanoparticles (0.5 x 0.5 cm; left) and ampicillin (50 mg/ml; right) as a control. Red circles depict halo formation diameters.

## Conclusions

Silica-dendritic PEI composites with silver nanoparticles bearing additional active ingredients (for instance antibiotics) provided antibacterial, antibiofilm, antiviral, and antifungal activity. Apart from the disclosed coating method xerogels may form aqueous dispersions and be introduced to leathers by spraying. Titania (TiO<sub>2</sub>) and Zinc Oxide (ZnO) may also be employed as the suspension base (substrate) to induce or enhance antiallergic properties. Gelation of the PEI-SiO<sub>2</sub> composites may be performed in their pores. The resulting materials may be sprayed on the leather as above. All these combinations are very useful for the production of leathers employed in medical applications such as examination beds, leather medical shoes, ICU beds, surgical beds, leather anti-decubitus pillows, leather wheelchair lining, and leather hospital chairs.

## Acknowledgments

This work was financed by Greece/Greek General Secretariat for Research and Technology and European Union under the frame of EPAnEK 2014-2020 Operational Programme Competitiveness, Entrepreneurship Innovation, project "MEDNANOLEAT" grant number T6YBII-00081.

Ariadne Athanassiou's participation in the congress is funded by the American College of Greece, 6 Gravias Street GR-153 42 Aghia Paraskevi Athens, Greece.

## References

1. M. Arkas, G. Kithreoti, N. Boukos, I. Kitsou, F. Petrakli, K. Panagiotaki, *Nano-Structures and Nano-Objects* **14** 138 (2018).

## Mixed metal oxide nanoparticles for organic solar cell applications

Manar Mostafa<sup>1</sup>, Fathy El-Shahat<sup>2</sup>, Moritz Riede<sup>3</sup> and Ghada Bassioni<sup>1\*</sup>

<sup>1</sup>Chemistry Division, Faculty of Engineering, Ain shams University, Cairo, Egypt

<sup>2</sup>Chemistry Department, Faculty of Science, Ain shams University, Cairo, Egypt

<sup>3</sup>Department of Physics, University of Oxford, Oxford, OX13PU, UK

\*Corresponding author, [ghada\\_bassioni@eng.asu.edu.eg](mailto:ghada_bassioni@eng.asu.edu.eg); Tel: +201001832728

### Abstract

Organic solar cells have great potential for providing inexpensive and more flexible energy options [1]. Recently, metal oxide nanoparticles have attracted great attention as the electron transporting layer (ETL) for Organic solar cells due to their superior electrical properties and excellent chemical stability. Several reports have shown the usage of doped metal oxide nanoparticles such as ZnO [2,3] and TiO<sub>x</sub> [4] layers as efficient electron transport layers in organic solar cells.

We chose to work with doped mixed metal oxide nanoparticles particularly barium titanate doped with cerium. The metal oxide prepared by sol-gel process using titanium isopropoxide (Ti[OCH(CH<sub>3</sub>)<sub>2</sub>]<sub>4</sub>, 98%, Aldrich), barium acetate (Ba(CH<sub>3</sub>COO)<sub>2</sub>, 99%, Aldrich) and cerium acetate (Ce(CH<sub>3</sub>CO<sub>2</sub>)<sub>3</sub>, 99.9%, Aldrich) as starting materials. X-ray diffraction spectroscopy (XRD) used to identify the type of material as well as its phase and crystalline properties. Both scanning electron microscope (SEM) and Transmission electron microscope (TEM) give us important information about the material surface. Diffuse Reflectance Spectroscopy (DRS) shows that barium acetate doped with cerium have suitable band gap to work as ETL in organic solar cell. Different spectroscopic tools like PL give more information about impurity levels and defect detection and consequently possible applications.

Our data give insight on the efficiency of organic solar cells by using doped barium acetate nanoparticles as electron transporting layer between the active layer and the electrode.

### Acknowledgements

The authors would like to thank Mohamed Abel Hay, Nabil El-Faramawy and Ayman Ayoub of the Faculty of Science, Ain Shams University for fruitful discussions and assistance in data analysis.

### References

1. M. Abdelaal, M. H. Abdellatif, M. Riede, G. Bassioni, *Materials*, **14** 1733 (2021).
2. M. Thambidurai, J. Y. Kim, J. Song, Y. Ko, N. Muthukumarasamy, D. Velauthapillai, C. Lee, *Solar Energy*, **106** 95 (2014).
3. M. Thambidurai, J. Y. Kim, C. Kang, N. Muthukumarasamy, H. Song, J. Song, Y. Ko, D. Velauthapillai, C. Lee, *Renewable Energy*, **66** 433 (2014).
4. A. Ranjitha, M. Thambidurai, F. Shini, N. Muthukumarasamy, D. Velauthapillai, **2** 385 (2019).

**Green synthesis of tin sulfide films and effect of annealing**A. Bronusiene<sup>1</sup>, I. Barauskiene<sup>1</sup>, A. Popov<sup>2</sup> and I. Ancutiene<sup>1</sup><sup>1</sup> Department of Physical and Inorganic Chemistry, Kaunas University of Technology, Radvilenu str. 19, LT-50254 Kaunas, Lithuania<sup>2</sup> NanoTechnas – Center of Nanotechnology and Materials Science, Faculty of Chemistry and Geosciences, Vilnius University, Naugarduko st. 24, LT-03225, Vilnius, Lithuania

\*astbak@ktu.lt

Environmentally friendly synthesis of nanoparticles has been attracting a lot of interest during the past few decades all over the world. Elimination of high temperatures and/or high pressures during fabrication of various active materials leads to direct energy saving [1]. Moreover, the application of non-toxic, abundant components allows to reduce energy consumption indirectly through a simpler waste treatment or more efficient processing of raw materials with less CO<sub>2</sub>. SILAR (successive ionic layer adsorption and reaction), as a technique belonging to the eco-friendly synthesis, does not require any energy-intensive tools, such as vacuum, high temperatures and etc. SILAR is also less time-consuming, less expensive and applicable of large area coatings. This technique usually employs aqueous solutions, and is particularly suitable for the formation of metal sulfides [2]. As a group of semiconductors, metal sulfides demonstrate electrical and optical properties that are valuable in many devices, such as current controllers, switching devices or photoconducting cells. Among all metal sulfides, tin sulfide (SnS) receives most attention due to its high optical adsorption coefficient, p-type conductivity and optimal band gap [3]. In addition to this well-known application, SnS exhibits good electrochemical performance due to its layered structure which is favourable for the intercalation of ions. Therefore, SnS is increasingly being considered as an alternative electrode material for electrochemical supercapacitors [4] (ECs). ECs devices fill the gap between conventional electrostatic capacitors and batteries by combining high power density with high energy density as well as shorter charging time (~0.6 s), longer cycle life (~10<sup>6</sup>) and shelf life [5]. Based on the energy storing mechanism, electrochemical supercapacitors are grouped into electric double layer capacitors (EDLCs) and pseudocapacitors. EDLCs, which are usually represented by carbon materials, collect and store energy through an electrostatic charge development between the electrode/electrolyte interfaces [5]. Meanwhile, pseudocapacitors, in which electrochemical Faradaic reactions decide their performance, cover a significantly wider group of active materials, including SnS.

In this work, we have synthesized ascorbate stabilized tin sulfide on the fluorine doped tin oxide (FTO) glass slides by an eco-friendly and low-waste SILAR process. The principle of the process is to immerse the substrate into two separately placed precursor solutions, then wash with distilled water to dispose loosely ions. This is a gentle reaction route when tin(II) and sulfide ions in aqueous solutions react at a low temperature (40 °C). There are no organic solvents, only aqueous solutions were used. In order to improve the solubility of tin(II) chloride in distilled water, environmentally-safe L-ascorbic acid as a reducing and capping agent is used [6]. This reagent is biodegradable, safe and a soft reducing agent. The composition, optical and electrochemical properties of tin sulfides were explored by changing the number (20 or 30) of SILAR cycles and the amount of L-ascorbic acid (0.8 or 1.0 g).

Figure 1 shows the X-Ray diffraction patterns of prepared and annealed samples obtained using 20 or 30 SILAR cycles. Obtained results agree with the typically reported tin sulfide with orthorhombic crystal structure – herzenbergite (JCPDS card number 39-0354). This mineral has his own peaks at  $2\theta=26.38; 37.63; 51.40; 54.43; 65.53^\circ$ . The most intensive peak at  $2\theta=37.63^\circ$  is assigned for herzenbergite, too. It could be seen that when the quantity of L-ascorbic acid increases, the intensity of SnS peaks also increases. Peaks at  $2\theta=33.56$  and  $61.50^\circ$  mark the presence of SnO<sub>2</sub> (JCPDS card number 46-1088). This compound is on the top of the substrate and the background of FTO reflection is not hidden. Results of our previous study showed the presence of a secondary phase Sn<sub>2</sub>S<sub>3</sub> (JCPDS card number 72-31) at  $2\theta=30.8^\circ$  [6]. This time, a negligible noise-like peak for the unannealed samples could also be seen. This peak disappears after annealing of samples in the inert (N<sub>2</sub>) atmosphere at 250°C. It can be noted, that after annealing, the XRD patterns are almost the same, proving that the peaks of the main phase of tin sulfide were unchanged. Also, patterns of the annealed samples are more crystalline and the peaks of herzenbergite are higher.

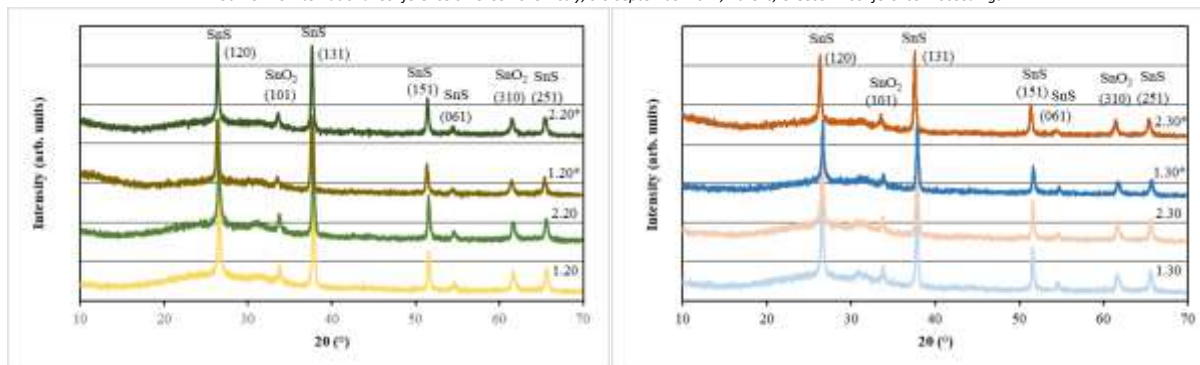


Figure 1. X-Ray diffraction patterns of prepared and annealed\* samples obtained using 20 (left) or 30 (right) SILAR cycles. Amount of used L-ascorbic acid in g: 1 – 0.8; 2 – 1.0.

Results of X-Ray diffraction were used to calculate the size of crystallites through the Scherrer's equation. This proves that particles are of nanometer size between 9-15 nm for prepared samples and 30-38 nm for annealed samples.

Furthermore, Raman analysis strongly agrees with obtained XRD results. This measurement detected characteristic peaks and allowed the identification of herzenbergite. However, Raman investigations revealed local variations in the spectra that are assigned to a secondary phase  $\text{Sn}_2\text{S}_3$  for samples, before annealing.

Bandgap values also confirm the existence of tin sulfide. Calculated results are very close to the theory of herzenbergite. The band gap values of prepared tin sulfides films were 1.1-1.4 eV. After annealing these values decreased and were 1.0-1.2 eV.

Considering the incorporation of the formed coatings into energy storing systems, the initial electrochemical testing was performed. This included cyclic voltammetry (CV) and galvanostatic charge-discharge (GCD) cycling. The shapes of both CV and GCD scans signify about the capacitive behaviour of coatings throughout the Faradaic redox reactions occurring on the surface as well as in the bulk. A comparison of the energetic parameters of the films, especially specific capacitance, calculated from GCD results highlighted the advantage of 30 SILAR cycles over 20 cycles.

In this current work, we described a facile, eco-friendly technique to synthesize L-ascorbate acid stabilized tin sulfide nanoparticles. This material is fairly cheap, environmentally clean and has interesting properties. Tin sulfide was characterized using phasic, optical and electrochemical methods. The XRD analysis showed the major diffraction peaks of herzenbergite with orthorhombic crystal structure and the Raman analysis verifies this. The films annealed at 250 °C exhibited a pure SnS phase, without secondary phases. Obtained results exhibited that the SnS thin films after annealing demonstrate a possibility for usage in electrochemical capacitors.

## References

- [1] J. Singh, T. Dutta, K. H. Kim, M. Rawat, P. Samddar, and P. Kumar, *Journal of Nanobiotechnology*, **16** 1 (2018).
- [2] B. R. Sankapal, R. S. Mane, and C. D. Lokhande, *Materials Research Bulletin*, **35** 2027 (2000).
- [3] J. A. Andrade-Arvizu, M. Courel-Piedrahita, and O. Vigil-Galán, *Journal of Materials Science: Materials in Electronics*, **26** 4541 (2015)
- [4] B. P. Reddy, M. C. Sekhar, S. V. P. Vattikuti, Y. Suh, and S. H. Park, *Materials Research Bulletin*, **103** 13 (2018).
- [5] R. Kötz and M. Carlen *Electrochimica Acta*, **45** 2483 (2000).
- [6] A. Bronusiene, A. Popov, I. Barauskiene, and I. Ancutiene, *Surfaces and Interfaces*, **25** 101275 (2021).



## Surface functionality role in the conductivity of microwave synthesized CQDs thin films

Jovana R Prekodravac<sup>1\*</sup>, Milica Budimir<sup>1\*</sup>, Bojana R Vasiljević<sup>1</sup>, Dejan Kepić<sup>1</sup>, and Biljana Todorović Marković<sup>1</sup>

<sup>1</sup> Institute of the Nuclear Sciences Vinča – National Institute of the Republic of Serbia, University of Belgrade, P.O.B. 522, Belgrade, Serbia

\* [prekodravac@vin.bg.ac.rs](mailto:prekodravac@vin.bg.ac.rs), [budimir@vin.bg.ac.rs](mailto:budimir@vin.bg.ac.rs)

Carbon quantum dots (CQDs) as 0D carbon nanomaterials with extraordinary physicochemical properties have a broad range of applications [1]. Some of the most intriguing are in the form of a thin film for electronic devices and membrane nanofiltration. Solid-state CQDs applications usually involve conjugation and nanocomposite preparation with polymeric matrix in the form of a CQDs thin film deposited on the polymer surface, incorporated into the polymer, or as a sandwich between polymer matrices. In recent years, different CQDs have found universal applications as a membrane system for nanofiltration, water desalination, and osmotic power production among others [2,3]. The CQDs features, as well as their ease of processing, add value to their potential use in biomedicine as well, particularly as antibacterial and antibiofouling coatings. Here we present the surface chemistry effect on morphological and electronic features of N-CQD and FeN-CQD thin films deposited on Mica discs and silicon (Si) wafers applying spin-coating and drop-casting deposition methods.

For N-CQD and FeN-CQD sample preparation, the microwave-assisted method was applied. The reaction conditions were set at a microwave power of 100 W for a one-minute reaction [4]. The N-CQD and FeN-CQD were made from glucose water solution as a carbon source and in the presence of a nitrogen and iron precursor. Samples of N-CQD and FeN-CQD at the concentration of 0.5 mg ml<sup>-1</sup> were deposited on Mica discs applying the spin-coating method at 3 500 rpm spreading 20, 40 or 60 µl of sample to deposit 1 to 3 layers of N-CQD and FeN-CQD samples on a surface of 1 cm<sup>2</sup>. Because of the tremendous centrifugal force upon spin, the sample deposition on the Si-wafer surface was performed using the drop-casting approach as it was more suitable.

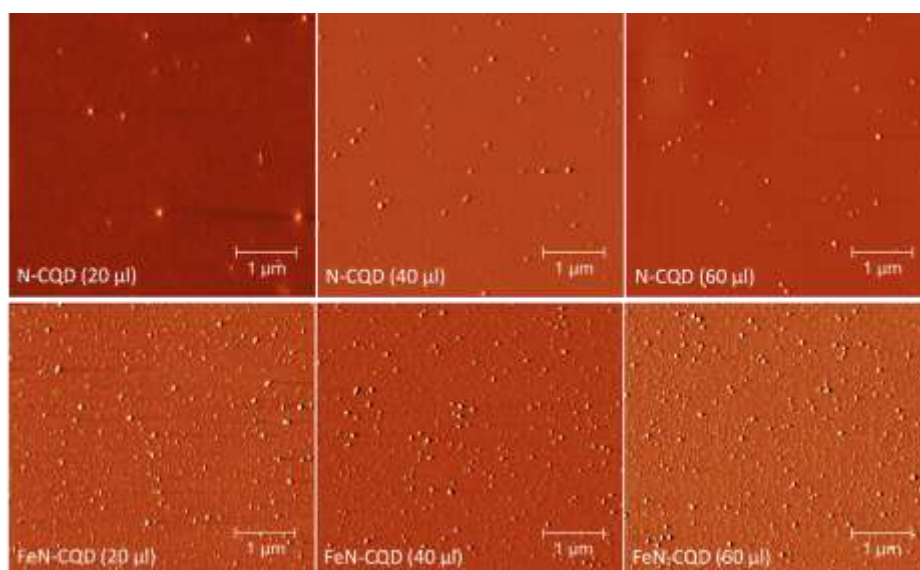


Figure 1. Schematic illustration of the thin film formation on Mica-discs applying the: (A) drop-casting and (B) spin-coating deposition method

Examining the morphological properties, we concluded that regardless of the type or amount of deposited materials on Mica discs by the spin-coating technique, the preparation of homogeneous thin films was achieved. By increasing the volume of deposited material more dense and homogeneous thin films were produced. Due to the more hydrophobic properties of the Si substrate, the drop-casting approach was more appropriate for thin film deposition on the Si wafer surface, revealing the material aggregation at greater concentrations of deposited CQDs, impacting the resulting thin film RMS (Figure 1). The x-CQD thin film morphology was significantly influenced by film thickness, which can be adjusted by the concentration of the depositing solution. Both thin film samples demonstrated good conductivity, continuously rising with the applied current (Figure 2).

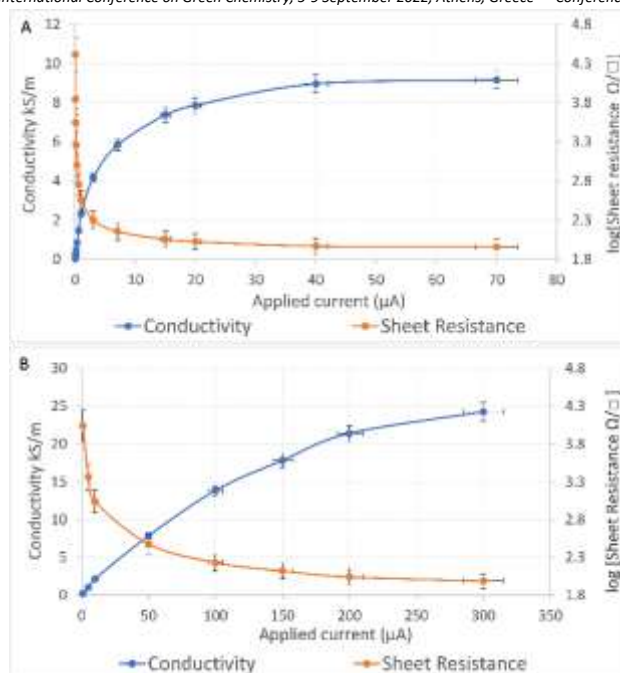


Figure 2. Sheet resistance and conductivity of 60  $\mu$ l x-CQDs deposited thin films on Si substrate: (A) N-CQD/Si and (B) FeN-CQD/Si thin films.

### Acknowledgements

The research was supported by the Science Fund of the Republic of Serbia, #7741955, Are photoactive nanoparticles salvation for global infectious treatment? - PHOTOGUN4MICROBES and by the Ministry of Education, Science and Technological Development of the Republic of Serbia grant number 451-03-68/2022-14/200017.

### References

- [1] X. Xu, R. Ray, Y. Gu, H.J. Ploehn, L. Gearheart, K. Raker, W.A. Scrivens, *J. Am. Chem. Soc.*, **126** 12736 (2004).
- [2] D.L. Zhao, T.-S. Chung, *Water Res.*, **147** 43 (2018).
- [3] Z.M. Marković, M. Kováčová, P. Humpolíček, M.D. Budimir, J. Vajdák, P. Kubát, M. Mičušík, H. Švajdlenková, M. Danko, Z. Capáková, M. Lehocký, B.M. Todorović Marković, Z. Špitalský, *Photodiagnosis Photodyn. Ther.*, **26** 342 (2019).
- [4] J. Prekodravac, B. Vasiljević, Z. Marković, D. Jovanović, D. Kleut, Z. Špitalský, M. Mičušík, M. Danko, D. Bajuk–Bogdanović, B. Todorović–Marković, *Ceram. Int.*, **45** 17006 (2019).

## Effect of Surface Functionalization and Doping of Graphitic Carbon Nitrides on Carbon Dioxide Fixation to Cyclic Carbonates at Atmospheric pressure under Solvent-Free Conditions

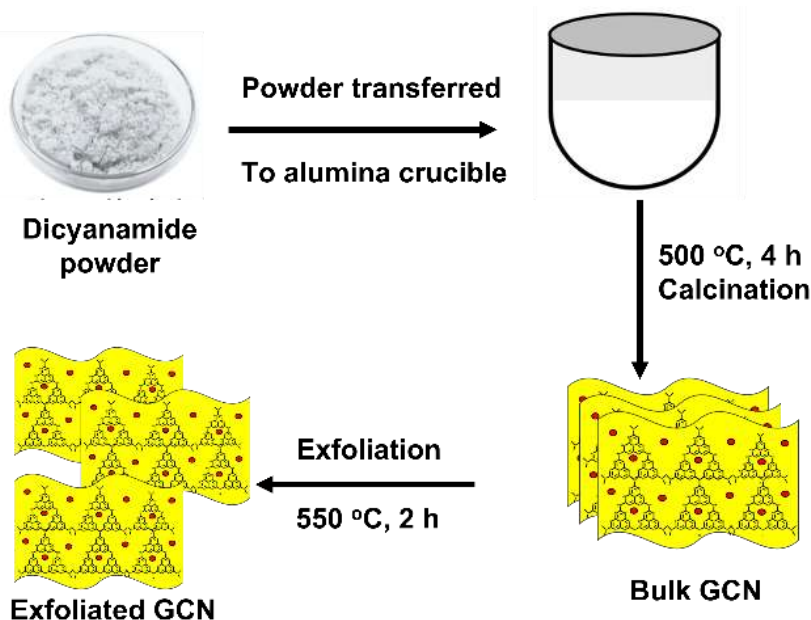
Hushan Chand and Venkata Krishnan\*

School of Basic Sciences and Advanced Materials Research Center,  
Indian Institute of Technology Mandi, Kamand, Mandi 175005, Himachal Pradesh, India.  
Email: [ykn@iitmandi.ac.in](mailto:ykn@iitmandi.ac.in)

### Abstract

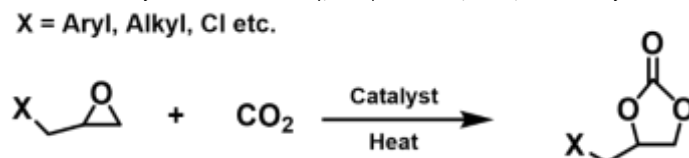
The steadily increasing CO<sub>2</sub> concentration in the atmosphere has resulted in notorious environmental changes in association with global warming, a rise in sea level, species extinction and endangered human health and normal life. To date, numerous processes have been developed for efficient conversion of CO<sub>2</sub> to valuable chemicals at ambient conditions [1]. The cycloaddition of CO<sub>2</sub> and epoxides to yield cyclic carbonates under solvent-free conditions is an eco-friendly way to utilize CO<sub>2</sub> in environmental. For cycloaddition of CO<sub>2</sub> and epoxides, the basic requirement is that a catalyst should possess acid-base dual nature, so that both the reactants can be activated together. Therefore, the development of a metal-free heterogeneous catalyst with acid-base dual functionality could be a better choice for fixation CO<sub>2</sub> to cyclic carbonates.

In this regard, the graphitic carbon nitride could be an effective material for fixation of CO<sub>2</sub> to cyclic carbonates at atmospheric pressure. Further, surface functionalization and doping of graphitic carbon nitride (GCN) can enhance the activity of these materials. The developed catalyst possesses acid-base dual functionality as active sites, which activates both epoxides as well as CO<sub>2</sub> simultaneously to carry out the cycloaddition reaction. The catalytic activity of functionalized GCN, with the sulphonic group, phosphoric group, nitro group, and amino group could be compared for CO<sub>2</sub> fixation to cyclic carbonates. Similarly, the activity could be compared for doped GCN. The different dopants utilized are B, P and S. Specifically, the catalysts have been synthesized using a previously reported calcination method [2], wherein 5 g of the precursor was added in an alumina crucible and heated at 500 °C for 4 h in a muffle furnace with a ramp rate of 5 °C min<sup>-1</sup>. The resultant yellow product (bulk GCN) was ground to a fine powder using pestle mortar. The bulk GCN powder was then thermally exfoliated at 550 °C with a ramp rate of 5 °C min<sup>-1</sup> for 2 h. Scheme 1 shows the graphical representation of synthesis procedure for GCN. Further, the procedure was slightly modified for the synthesis of functionalized and doped GCN accordingly. The synthesis of catalysts have been characterized using XRD, FTIR, Raman, SEM, TEM, etc. Acidic as well as basic sites have been calculated by using temperature-programmed desorption (TPD) measurements.

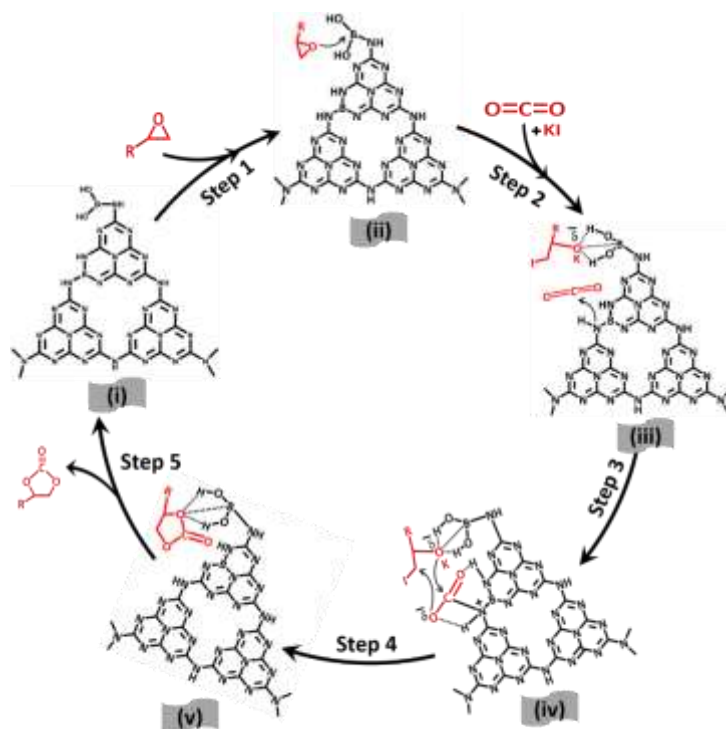


**Scheme 1.** Schematic showing the synthesis of GCN nanosheets.

The procedure for catalytic activity is as follows, 20 mmol epoxide, 100 mg catalyst was mixed in 25 mL round bottom flask (RBF). The RBF was equipped with an adapter through which CO<sub>2</sub> gas was introduced into the reaction mixture. The reaction mixture was heated at 100 °C with continuous stirring (500 rpm) in an oil bath for specific time intervals. Scheme 2 shows the generic reaction for CO<sub>2</sub> fixation to cyclic carbonates using epoxides as a reactant. The acid-base duality induced by different functionalized and doped GCN enables the co-activation of CO<sub>2</sub> and epoxide.



**Scheme 2.** Generic reaction showing  $\text{CO}_2$  fixation to cyclic carbonates.



**Scheme 3.** Schematic representation of the proposed mechanism for for a representative catalyst (B-doped GCN along with KI as cocatalyst) for cycloaddition of  $\text{CO}_2$  into cyclic epoxides.

A mechanism based on acid-base duality has been proposed as shown in Scheme 3, where  $\text{CO}_2$  is activated on the basic sites and epoxide is on the acidic sites through a hydrogen bonding. The co-activated  $\text{CO}_2$  and epoxide react with each other to yield the cyclic carbonates [3]. This work paves way for the rational design and development of suitable catalysts for  $\text{CO}_2$  conversion in a sustainable and environment-friendly way.

#### References:

- [1] T. Biswas, V. Mahalingam, Efficient  $\text{CO}_2$  fixation under ambient pressure using poly (ionic liquid)-based heterogeneous catalysts, *Sustainable Energy & Fuels*, 3 (2019) 935-941.
- [2] H. Chand, P. Choudhary, A. Kumar, A. Kumar, V. Krishnan, Atmospheric pressure conversion of carbon dioxide to cyclic carbonates using a metal-free Lewis acid-base bifunctional heterogeneous catalyst, *Journal of  $\text{CO}_2$  Utilization*, 51 (2021) 101646.
- [3] J. Zhu, T. Diao, W. Wang, X. Xu, X. Sun, S.A. Carabineiro, Z. Zhao, Boron doped graphitic carbon nitride with acid-base duality for cycloaddition of carbon dioxide to epoxide under solvent-free condition, *Applied Catalysis B: Environmental*, 219 (2017) 92-100.

## Portable paper sensing platform using novel histidine-stabilized gold nanoclusters for fast naked-eye detection of Fe ions from water

Markus Zetes<sup>1,2</sup>, Alexandru-Milentie Hada<sup>1,2</sup>, Monica Focsan<sup>1</sup>, Simion Aștilean<sup>1,2</sup>, Ana-Maria Craciun<sup>1,\*</sup>

<sup>1</sup> Nanobiophotonics and Laser Microspectroscopy Center, Interdisciplinary Research Institute in Bio-Nano-Sciences, Babes-Bolyai University, 42 T. Laurian Str., 400271, Cluj-Napoca, Romania

<sup>2</sup> Faculty of Physics, Babes-Bolyai University, 1 M. Kogalniceanu str., 400084, Cluj-Napoca, Romania

\*ana.gabudean@ubbcluj.ro

Nowadays, the pollution generated by toxic chemicals, including heavy metal ions, represents a great concern for the environment, ecosystem and human health. Despite the considerable efforts made by multiple international organizations, many such harmful substances are continuously reaching the environment through different channels such as water and soil [1]. Thus, the development of fast and portable sensing devices for the on-site detection of chemical compounds from real samples, represents a constant challenge of striking necessity. Iron (Fe), for example, is an indispensable micronutrient that participates in many physiological and pathological processes. However, in high concentrations, it can be extremely harmful to not only for humans but also for aquatic and terrestrial life [2].

Therefore, we fabricated here a cheap, fast and ready-to-use paper-based sensing platform using novel photoluminescent histidine stabilized gold nanoclusters (His-AuNCs) for the selective and sensitive naked-eye detection of Fe ions from water, under UV light, *via* photoluminescence (PL) quenching effect. First, we successfully synthesized photoluminescent His-AuNCs using a novel microwave assisted-approach. The intrinsic PL signal exhibited by His-AuNCs at 471 nm ( $\lambda_{ex}$ = 380 nm) was found to be stable under continuous irradiation and over time. The specificity tests performed in solution with His-AuNCs revealed a high selectivity towards Fe ions. Additionally, we found a great dependence between Fe<sup>2+</sup> concentration and the AuNCs' PL quenching, obtaining a linear dynamic range from 0.022 to 4.400 mM with a great correlation coefficient. The limit of detection (LOD) was found to be 0.2  $\mu$ M, a value much lower than the limit of Fe admitted by the World Health Organization in drinking water (35  $\mu$ M). Afterwards, the His-AuNCs were incorporated into Whatmann filter paper substrate in order to achieve an easier-to-use, more efficient and accessible portable sensing platform for low-volume water samples. The obtained His-AuNCs-incorporated Whatman filter paper-based portable sensor was successfully employed for the fast naked-eye detection of Fe levels from water, under UV light excitation, based on the visual detection of PL quenching. The plot of the average blue intensity value of the His-AuNCs-paper spots versus [Fe<sup>2+</sup>] in the 0-123  $\mu$ M range is presented in Figure 1.

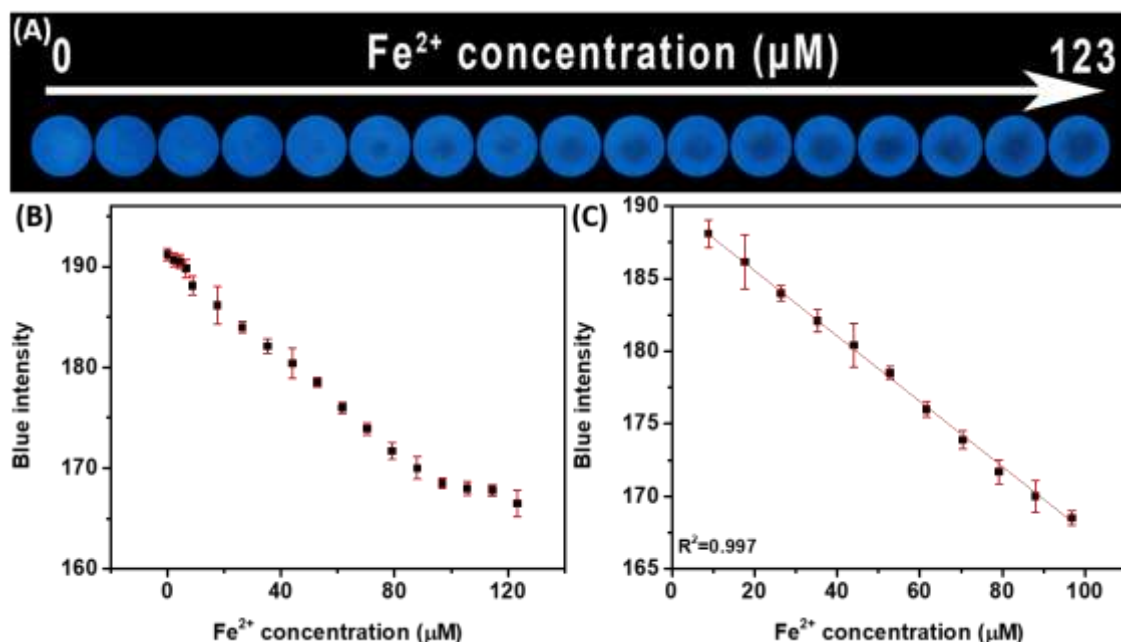


Figure 1. (A) Photographic image of His-AuNCs-paper-based sensor. The images were acquired under UV light excitation, 15 minutes after a solution containing different concentrations of Fe<sup>2+</sup> (0-123  $\mu$ M) was added over the His-AuNCs-paper spots which were previously dried for 24h. (B) Plot of the average blue intensity value of His-AuNCs-paper spot versus [Fe<sup>2+</sup>] in the 0-123  $\mu$ M range. (C) Linear dynamic range from 9 to 97  $\mu$ M.

The LOD of the newly-proposed sensor was found to be 3.2  $\mu\text{M}$ . Finally, the sensing platform was validated for the detection of  $\text{Fe}^{2+}$  from spiked (35  $\mu\text{M}$ ) real water samples with recoveries ranging between 95.2% and 110.3%, proving the great accuracy of our portable sensor. Up to our knowledge, this is the first AuNCs-paper-based sensing platform able to quantify dangerous levels of  $\text{Fe}^{2+}$  from real water-samples, representing thus a promising candidate as a lab-on-a-chip device for environmental sensing applications. Moreover, in view of future applicability, we believe that the photographic images of the portable sensor could be taken by anyone using a smartphone camera and a pocket UV lamp and send to environmental water-monitoring organizations for periodic evaluation of water sources simplifying time-consuming and sophisticated procedures.

### Acknowledgements

This research was funded by the Romanian National Authority for Scientific Research, CNCSIS-UEFISCDI, project PN-III-P1-1.1-TE-2019-0700.

### References

1. R. Naidu et. al., *Environment International*, **156** 106616 (2021).
2. World Health Organization (WHO), Guidelines for drinking-water quality. Vol. 2, Health criteria and other supporting information: addendum, in: Guidelines for Drinking-Water Quality. **Vol. 2**, Health Criteria and Other Supporting Information: Addendum (1998).

## Nature-inspired nanocomposites with exceptional isotropic mechanical and magneto-responsive properties

Artur Feld<sup>1,2,\*</sup>, Axel Dreyer<sup>3</sup>, Agnes Weimer<sup>1,2</sup>, Andreas Kornowski<sup>1</sup>, Rieke Koll<sup>1</sup>, Heshmat Noei<sup>4</sup>, Tobias Krekeler<sup>5</sup>, Lisa Sarah Fruhner<sup>6</sup>, Andreas Stierle<sup>4,7</sup>, Volker Abetz<sup>1,8</sup>, Horst Weller<sup>1,2,9</sup> and Gerold A. Schneider<sup>3</sup>

<sup>1</sup>Institute of Physical Chemistry, Hamburg University, Grindelallee 117, D-20146 Hamburg, Germany

<sup>2</sup>The Hamburg Center for Ultrafast Imaging, University of Hamburg, Luruper Chaussee 149, 22761 Hamburg, Germany

<sup>3</sup>Institute of Advanced Ceramics, Hamburg University of Technology, Denickestrasse 15, D-21073 Hamburg, Germany

<sup>4</sup>DESY NanoLab, Deutsches Elektronensynchrotron DESY, Notkestrasse 85, D-22607 Hamburg, Germany

<sup>5</sup>Electron Microscopy Unit, Hamburg University of Technology, Eißendorfer Str. 42, D-21073 Hamburg

<sup>6</sup>JCNS-1 and ICS-1, Forschungszentrum Jülich GmbH, Leo-Brandt-Straße, 52425 Jülich, Germany

<sup>7</sup>Physics Department, Hamburg University, Jungiusstrasse 11, D-20355 Hamburg, Germany

<sup>8</sup>Institute of Polymer Research, Helmholtz-Zentrum Geesthacht, Max-Planck-Strasse 1, 21502 Geesthacht, Germany

<sup>9</sup>Center for Applied Nanotechnology, Grindelallee 117, D-20146 Hamburg

\*artur.feld@chemie.uni-hamburg.de

Inspired by nature, one of the most promising and challenging approaches is to synthesize nanocomposites, which consist of a combination of soft organic and hard ceramic materials. (1–3) Iron oxide such as magnetite is very suitable for the synthesis of nanocomposite, because magnetite nanoparticles are extensively studied regarding their size and shape-controlled synthesis (4), and also nature makes use of iron oxide as an ultra-hard material in chiton radular teeth. (5) Usually, it was only possible to achieve good mechanical strength with high aspect ratio layered structures of minerals. Approaches with the use of monodispersed nanoparticle supercrystals results in weak mechanical properties in these composites.

We present the successful manufacturing of a nanocomposite consisting of natural fatty acid - oleic acid - coated spherical iron oxide nanocrystals (NC) with exceptional isotropic mechanical properties (Figure 1). (6) We developed a concept to link iron oxide nanoparticles in a well-ordered superstructure by oleic acid molecules during a thermal process. The exceptional mechanical properties - bending modulus of 114 GPa, hardness of up to 4 GPa and strength of up to 630 MPa - are dominated by the covalent backbone of the linked organic molecules.

To our knowledge these are the highest combined values of elastic modulus, strength and nanohardness ever reported for a **synthetic bioinspired organic/inorganic nanocomposite**. Due to the similarity of the nanocomposite to natural hard tissues, medical and environmental applications are conceivable.

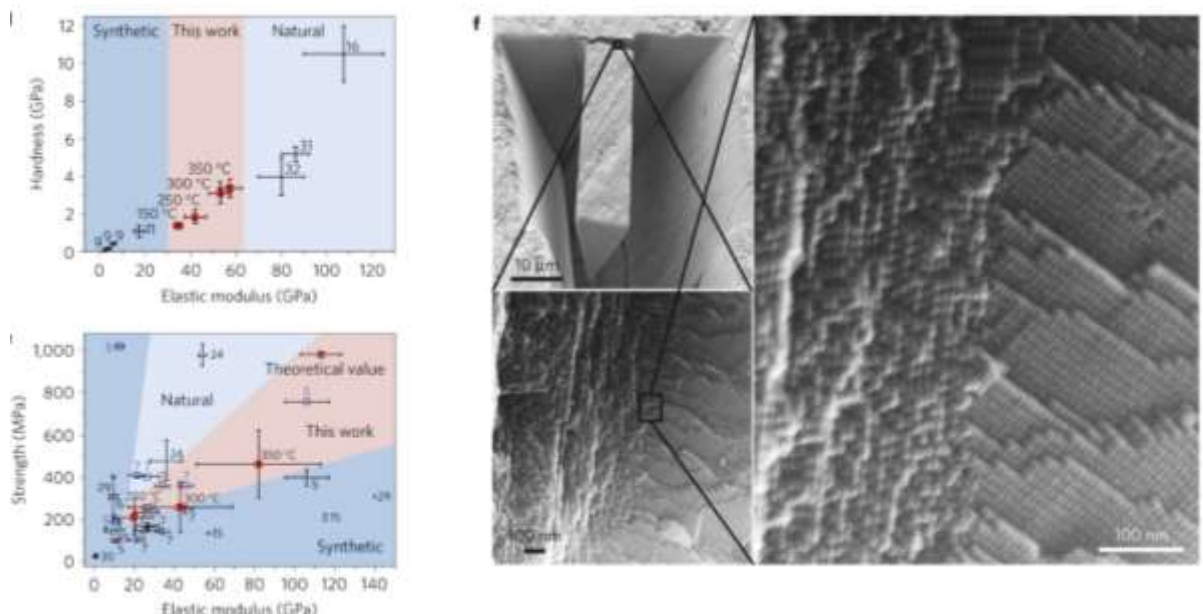


Figure 1. Mechanical characterization of the nanocomposite. Comparison of our results, shown as mean  $\pm$  s.d. ( $3 \leq n \leq 5$ ), with literature values from nanoparticle supercrystals (7), synthetic polymer/ceramic nanocomposites (8–10), enamel (11), nacre (12), and chiton teeth (13). It can be seen that the mechanical properties of our supercrystals surpass by far all other synthetic supercrystals.

We also present a synthesis method for multifunctional nanocomposites with magneto-responsive properties.<sup>(14)</sup> In particular, responsive polymeric nanocomposites that are able to adapt to different surrounding environments are playing an increasingly important role. These materials, per definition, show a built-in ability to respond to physical or chemical stimuli via controlled molecular design.

The challenge for the synthesis of homogeneous polymer-NC nanocomposites is the dispersion of the NC into the polymer

matrix, because of the immiscibility of the inorganic NC with an organic phase. In our work, we applied the diblock copolymer encapsulation<sup>(15)</sup> for the preparation of nanocomposites and focused on the homogeneous dispersion of monodisperse SPIONs in a polymer matrix.<sup>(14)</sup> We present an extensive step-by-step characterization during the different stages of preparation by small-angle X-ray scattering (SAXS) and transmission electron microscopy (TEM), with both methods perfectly complementing each other.

In the first step of the synthesis (Figure 2.), the native oleic acid ligands of the NC were exchanged with PI-DETA in an equilibrium process in *n*-hexane as solvent. PI-DETA is polyisoprene equipped with a 2,2'-diaminodiethylamine headgroup. Then, the SPIONs, PI-*b*-PEO, and 2,2'-azobis(2-methylpropionitrile) were mixed and phase transferred into water. PI-*b*-PEO acted as emulsifying agent and served as shell material. Finally, the double bonds of the PI shell were cross-linked at 80 °C in a radical reaction with AIBN as radical initiator. Empty micelles were removed by means of a magnetic column. The encapsulated NCs, dispersed in water, were mixed with an aqueous PEO solution, lyophilized, and melted at 60 °C.

The combination of advanced synthesis and encapsulation techniques using different diblock copolymers and the thiol-ene click reaction for cross-linking the polymeric shell results in uniform hybrid SPIONs homogeneously dispersed in a poly(ethylene oxide) matrix.

## Acknowledgements

This work was supported by SFB 986 (M3) and SPP 1681 (project 3929/2-1) of the German Research Foundation (DFG).

## References

1. P. Fratzl, R. Weinkamer, *Prog. Mater. Sci.* **52**, 1263–1334 (2007).
2. A. Sellinger *et al.*, *Nature*. **394**, 256–260 (1998).
3. Z. Tang, N. a Kotov, S. Magonov, B. Ozturk, *Nat. Mater.* **2**, 413–418 (2003).
4. A. Feld *et al.*, *ACS Nano*. **13**, 152–162 (2018).
5. J. C. Weaver *et al.*, *Mater. Today*. **13**, 42–52 (2010).
6. A. Dreyer *et al.*, *Nat. Mater.* **15**, 522–528 (2016).
7. P. Podsiadlo *et al.*, *J. Am. Chem. Soc.* **132**, 8953–8960 (2010).
8. P. Podsiadlo *et al.*, *Science (80-. )*. **318**, 80–83 (2007).
9. L. J. Bonderer, A. R. Studart, L. J. Gauckler, *Science (80-. )*. **319**, 1069–1073 (2008).
10. K. Hu, M. K. Gupta, D. D. Kulkarni, V. V Tsukruk, *Adv. Mater.* **25**, 2301–2307 (2013).
11. S. Bechtle *et al.*, *J. R. Soc. Interface*. **9**, 1265–1274 (2012).
12. X. Li, W. C. Chang, Y. J. Chao, R. Wang, M. Chang, *Nano Lett.* **4**, 613–617 (2004).
13. J. C. Weaver *et al.*, *Mater. Today*. **13**, 42–52 (2010).
14. A. Feld *et al.*, *ACS Nano*. **11**, 3767–3775 (2017).
15. C. Schmidtke *et al.*, *Nanoscale*. **5**, 7433–7444 (2013).

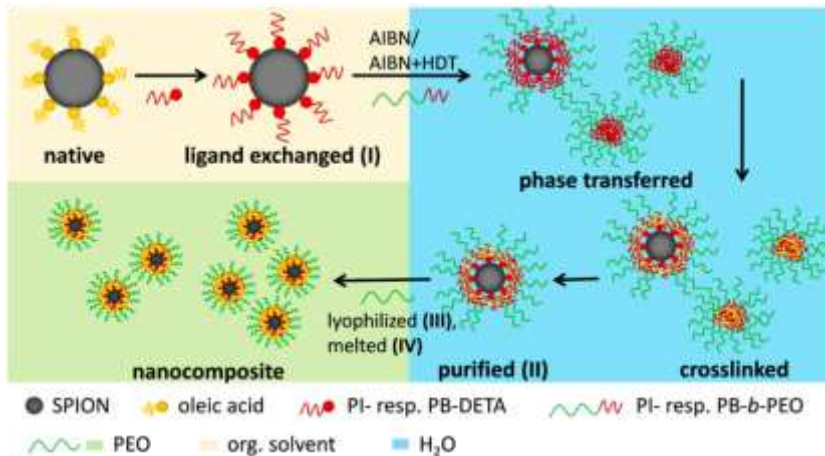


Figure 2. Schematic Illustration of the Preparation of Nanocomposites.



## Metabolic response of Murine Fibroblast cells exposed to Green synthesis mediated Silver Nanoparticles

Isha Gupta<sup>1,2</sup>, Sonia Gandhi<sup>1,\*</sup>, Abhishek Kumar<sup>1</sup>, Vijayakumar Chinnadurai<sup>1</sup>, Anant Narayan Bhatt<sup>1</sup>, Sameer Sapra<sup>2</sup>

<sup>1</sup>Institute of Nuclear Medicine and Allied Sciences (INMAS), Defence Research and Development Organization (DRDO), Delhi, India

<sup>2</sup>Department of Chemistry, Indian Institute of Technology Delhi (IITD), India

\*sonia.inmas@gov.in

### Introduction

Metal nanoparticles have fascinated the entire world due to their unique and peculiar properties. Silver nanoparticles (Ag NPs) have been explored in different fields such as medicine, health care products, wound healing therapies, drug delivery, sensors, diagnostics, and textiles. The eco-friendly green synthesis route of Ag NPs is preferred over chemical synthesis due to its no or low toxicity and simplicity [1]. Still, studies on the metabolic responses of cells or animal models upon exposure to Ag NPs are limited [2]. Here, pharmacometabonomics would provide an insight into the drug-induced metabolic changes in cell lines, ultimately speeding up the drug discovery process [3]. Murine fibroblast (L929) cells were chosen due to their close similarity to dermal fibroblast [4]. The present work highlights the role of NMR-based metabolomics in dose-related concerns of green synthesis mediated Ag NPs.

### Aims and objectives

To study the green synthesis mediated Ag NPs response in murine cells through NMR-based metabolomics.

### Materials and methods

For the green synthesis of Ag NPs, *Ocimum sanctum* (tulsi) extract was added to the silver nitrate solution and kept for heating till the solution changed to reddish-brown. In Transmission electron microscopy (TEM) analysis, particles of around 30 nm were found. Cell viability was evaluated through 3-(4,5-dimethylthiazol-2-yl)-2,5-diphenyltetrazolium bromide (MTT) assay and used for selecting the exposure doses. For pharmacometabonomics, the cells were allowed to grow till they reached 90% confluency (density of 2-3 million cells) on 60 mm Petri dishes. Then, the medium of the cells was replaced by the fresh medium containing Ag NPs at a concentration of 1 and 5 µg/mL (D1 and D2, respectively). Fresh medium without Ag NPs was added to the control cells (C). After 24 h of incubation, medium and cell extracts were collected. Six and nine replicates were prepared for control and Ag NPs exposed cells, respectively. The medium samples were collected separately for exometabolites. The cells were collected separately, extracted for aqueous endometabolites using dual-phase separation, and further evaluated by 1H Nuclear Magnetic Resonance (NMR) spectroscopy. Lyophilised cell extract samples were reconstituted in 550 µL phosphate buffer (pH 7.4) containing 0.5 mM TSP for spectral acquisition. 1H NMR spectra with water suppression (NOESYPR1D) were acquired by the 600 MHz Bruker Avance III spectrometer at 298K with 64 transients collected into 32K data points with a relaxation delay of 2s, flip angle of 90° and a mixing period of 100 ms. After correcting the spectra, twenty-eight metabolites were identified with the help of the Human Metabolome Database (HMDB) and the Chenomx NMR Suite software (Chenomx, Edmonton, Canada). The statistical analysis using Principal component analysis (PCA), partial least squares discriminant analysis (PLS-DA) and one-way Analysis of Variance (ANOVA) followed by Fischer's least significant difference method (Fischer's LSD), was performed to study the similarities or dissimilarities of metabolic profiles of samples using Metaboanalyst 5.

### Results and Discussions

The alterations in cell phenotype upon exposure to green synthesis mediated Ag NPs were evaluated by 1H NMR-based metabolomics (Figure 1). For endometabolites, PCA and PLS-DA showed clustering between control and 1 µg/mL exposed cells. On further increasing the concentration of Ag NPs to 5 µg/mL, slight separation between control and D2 exposed cells was noticed. ANOVA followed by Fischer's LSD reported that seven (lactate, myo-inositol, lysine, threonine, taurine, alanine, and glucose) out of twenty-eight metabolites were altered significantly upon exposure to a higher dose (D2) of biocompatible Ag NPs. For exometabolites, PCA and PLS-DA showed no clear separations among control, D1 and D2, were found. The lower dose (1 µg/mL) was safer than the higher dose (5 µg/mL) of green synthesis mediated Ag NPs due to minimal variation in the systemic metabolic profile of the cells.

## Conclusion

NMR-based metabolic profiling affirmed the biocompatible nature of the lower dose of green synthesis mediated Ag NPs. Green synthesis mediated nanoparticles can help achieve sustainable development by reducing the over-dependency on synthetic routes. Pharmaco-metabonomics is an upcoming "omics" field that can accelerate the drug development process by providing the metabolic profiles on drug exposure and predicting the drug response at different doses.

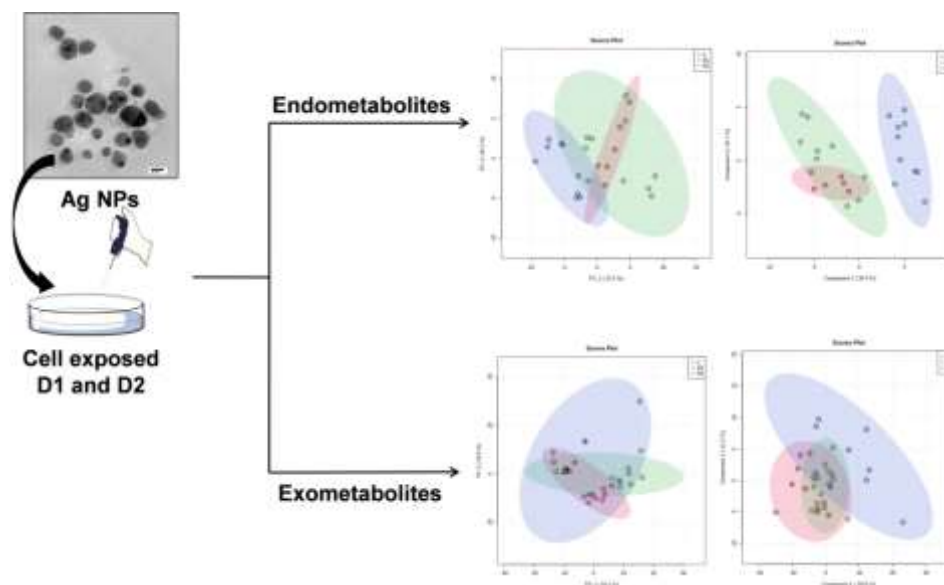


Figure 1. Graphical representation of the metabolic response of murine fibroblast cells exposed to green synthesis mediated silver nanoparticles

## Acknowledgements

The work was supported by Director, Institute of Nuclear Medicine and Allied Sciences (INMAS), Defence Research and Development Organization (DRDO), Delhi, and Indian Institute of Technology Delhi (IITD), India. Isha Gupta was supported by University Grants Commission, India.

## References

1. C. A. Dos Santos, M. M. Seckler, A. P. Ingle, I. Gupta, S. Galdiero, M. Galdiero, A. Gade, and M. Rai, *J. Pharm. Sci.* **103**, 1931 (2014).
2. J. Carrola, V. Bastos, J. M. P. Ferreira de Oliveira, H. Oliveira, C. Santos, A. M. Gil, and I. F. Duarte, *Arch. Biochem. Biophys.* **589**, 53 (2016).
3. T. Burt and S. Nandal, *Clin. Transl. Sci.* **9**, 128 (2016).
4. K. Theerakittayakorn and T. Bunprasert, *World Acad. Sci. Eng. Technol.* **50**, 373 (2011).

## Biomass derived nanoporous carbons for diesel deep desulfurization

Dimitrios A. Giannakoudakis<sup>1</sup>, Eleni D. Salonikidou<sup>1</sup>, Eleni A. Deliyanni<sup>1</sup>, Svetlana Bashkova<sup>2</sup>,  
Konstantinos S. Triantafyllidis<sup>1,3</sup>

<sup>1</sup> Department of Chemistry, Aristotle University of Thessaloniki, University Campus, Thessaloniki, Greece

<sup>2</sup> Department of Chemistry, Biochemistry, and Physics, Fairleigh Dickinson University, Madison, NJ 07940, USA

<sup>3</sup> Center for Interdisciplinary Research and Innovation (CIRI-AUTH), Balkan Center, 10th km Thessaloniki-Thermi Rd, P.O. Box 8318, 57001 Thessaloniki, Greece

\*dagchem@gmail.com

In the past decades, adsorptive desulfurization of liquid transportation fuels has gained attention as an emerging, low-cost and efficient alternative technique to hydrodesulfurization, especially considering the recent strict environmental restrictions of sulfur in liquid fuels [1,2]. So, the research has been focused on the synthesis and fabrication of nanoporous adsorbent materials, like activated carbons, as effective desulfurization adsorbents for the removal of aromatic sulfur compounds [3,4]. In the present study, several biomass-derived activated carbons, produced from cashew nut shells as raw material, were evaluated as desulfurization adsorbents. The chemical activation was performed with the use of phosphoric acid and the carbonization at four different temperatures (400-700°C), in order to tailor the effect of carbonization/activation on the physicochemical properties of the carbons. The desulfurization capability of the obtained biomass materials was tested under mild batch conditions using a model diesel fuel, consisting of 4,6-dimethyldibenzothiophene (4,6-DMDBT, 20 ppmwS), dibenzothiophene (DBT, 20 ppmwS), benzene (801 ppmw) as a mono-aromatic and naphthalene (7323 ppmw) as a di-aromatic component, dissolved in hexadecane, and low amount of adsorbent (400 mL fuel/g). Several simpler model fuels were also studied in order to examine the impact of the presence of aromatic compounds on the adsorptive desulfurization procedure.

It was detected that the production of the activated carbons at various carbonization temperatures led to materials with different physicochemical properties, indicating the importance of the synthesis process. The increment of pyrolysis temperature had a positive impact on the textural properties of the carbons up to 600 °C, and a negative effect on the density of the surface functional groups, especially of the acidic ones. Moreover, a particular trend/correlation among the adsorption capacities of the four activated carbons and the pyrolysis temperature was not observed, mostly due to the alteration of the size and volume of pores and the density of the surface functional groups.

The activated carbon synthesized at 600°C, which contains the highest number of carboxylic surface groups, presented the greatest adsorptive removal of the two thiophenic compounds (DBT and 4,6-DMDBT), exhibiting a rather complex interaction between the carbonization temperature, physicochemical characteristics and adsorption efficiencies. The co-presence of aromatic components in the model fuel, reduced the removal of 4,6-DMDBT from 52.5% in pure hexadecane to 46.1%, revealing the competitive character of the aromatics. The co-existence of DBT in the model diesel fuel dropped the removal of 4,6-DMDBT to 37.3%, suggesting that up to a certain extend the two organosulfur molecules compete with each other in the adsorption on the available active sites of the carbon.

### Acknowledgments

This research has been co-financed by the European Regional Development Fund of the European Union and Greek national funds through the Operational Program Competitiveness, Entrepreneurship and Innovation (EPAnEK 2014-2020), under the Action “RESEARCH-CREATE-INNOVATE B’ CALL” (Project: DESULFUR, code: T2EAK-01976)

### References

1. K. S. Triantafyllidis and E. A. Deliyanni, *Chem. Eng. J.*, **236**, 406–414 (2014)
2. A. Geczo, D. A. Giannakoudakis, K. Triantafyllidis, M. R. Elshaer, E. Rodríguez-Aguado and S. Bashkova, *Environ. Sci. Pollut. Res.* (2020)
3. E. D. Salonikidou, D. A. Giannakoudakis, E. A. Deliyanni and K. S. Triantafyllidis, *J. Mol. Liq.*, **351**, 118661 (2022)
4. B. Saha, S. Vedachalam and A. K. Dalai, *Fuel Process. Technol.*, **214**, 106685 (2021)

## Synthesis and Applications of Cu<sub>2</sub>O Nanoparticle Functionalized TiO<sub>2</sub> for Photocatalyzed Glaser Coupling

Geniece L. Hallett-Tapley<sup>1\*</sup> and Elvin Girineza

<sup>1</sup>Department of Chemistry, Saint Francis Xavier University, PO Box 5000, B2G 2W5, Antigonish, Nova Scotia Canada

\*ghallett@stfx.ca

Glaser coupling involves the oxidative homocoupling of terminal alkynes to form symmetrical 1,3-diynes and is the most widely used procedure to form such molecules [1]. These compounds have a wide variety of applications in the field of biology and material science including the synthesis of polymers and biologically active molecules [2]. In the past, expensive palladium catalysts were the classical way to catalyze such reactions. Currently, the use of copper salts in the presence of a base and an oxidant serves as an alternative method to mitigate expenses, although not without its own drawbacks such as the use of higher temperatures and long reaction times [3]. However, the use of heterogenous copper nanoparticle functionalized semiconductors as a photocatalyst in Glaser coupling remains largely unexplored.

For cuprous oxide nanoparticle synthesis, a simple and safe in-situ synthesis method was adopted from previously published results [4] using the addition of economic and environmentally friendly TiO<sub>2</sub> (Figure 1) as the supporting semiconductor. Furthermore, the photocatalytic capability of these Cu<sub>2</sub>O nanoparticles in the Glaser coupling of phenylacetylene was found to be highly efficient at 10 mM concentrations in the presence of a strong base of equal concentration and methanol solvent. The reaction times ranged from 15 minutes to 2 hours at ambient temperatures – much lower than literature values. By investigating the homocoupling efficiency at a variety of reaction conditions, it was determined that the reaction proceeds through a photooxidative mechanism reliant on the strength of the base used. In addition, the heterogeneous photocatalyst exhibits remarkable recyclability (Figure 2) at moderate light intensities – of note given the known oxophilic nature of the Cu nanoparticle. The reaction performance with TiO<sub>2</sub> as a supporting semiconductor is on-par or better than other supports which were tested including KNbO<sub>3</sub>, KNb<sub>3</sub>O<sub>8</sub>, and optical-grade Nb<sub>2</sub>O<sub>5</sub>.

The promising nature of these results paves the way for a new environmentally friendly, economic, and highly efficient standard by which Glaser coupling is carried out in the future.

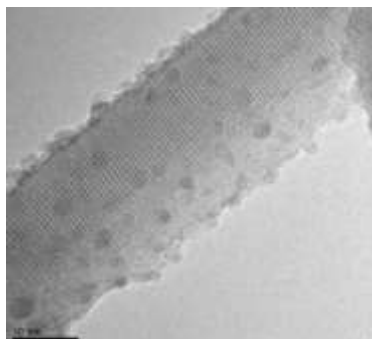


Figure 1. TEM image illustrating monodisperse Cu<sub>2</sub>O nanoparticle functionalization of TiO<sub>2</sub>.

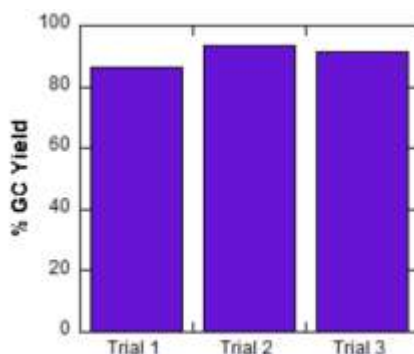


Figure 2. Recyclability of Cu<sub>2</sub>O functionalized TiO<sub>2</sub> in the Glaser coupling of phenylacetylene.

## Acknowledgements

We gratefully acknowledge the Natural Sciences and Engineering Research Council of Canada (GHT- Discovery Grants Program; DAS – Canada Graduate Scholarship, EG – Undergraduate Student Research Award), the Canada Foundation for Innovation and Saint Francis Xavier University University Council for Research for financial support of this work.

## References

1. Sindhu, K. *et al.* *RSC Adv.* **2014**, *4*, 27867–27887.
2. Zhang, S. *et al.* *Adv. Synth. Catal.* **2011**, *353*, 1463-1466.
3. van Gelderen, L. *et al.* *Appl. Organometal. Chem.* **2013**, *27*, 23-27.
4. Januário, E. R. *et al.* *J. Braz. Chem. Soc.* **2018**, *29*, 1527-1537.

## Synthesis and effect of calcination temperature on the physicochemical properties of porous clay heterostructures (PCH) material

Muhammad Kashif<sup>1,2</sup>, JeongMin Kim<sup>1,2</sup>, Soyeon Back<sup>1,2</sup>, Yoo Hyun Song<sup>1,2</sup>, Jaehyun Koo<sup>1,2</sup>, Philippe M. Heynderickx<sup>1,2\*</sup>

<sup>1</sup>Center for Environmental and Energy Research (CEER) – Engineering of Materials via Catalysis and Characterization, Ghent University Global Campus, 119-5 Songdo munhwa-Ro, Yeonsu-Gu, Incheon, 406-840 South Korea.

<sup>2</sup>Department of Green Chemistry and Technology, Faculty of Bioscience Engineering, Ghent University, 653 Coupure Links, Ghent, B-9000, Belgium.

\*Philippe.Heynderickx@Ghent.ac.kr (Philippe M. Heynderickx)

### Abstract

In this study, the porous clay heterostructures material was synthesized via ion exchange by using montmorillonite as host clay. For the first time, the series of PCH samples were prepared at different calcination temperatures (200°C, 400°C, 600°C, and 800°C) under a closed N<sub>2</sub> atmosphere. The montmorillonite, PCH samples with and without calcination were characterized by XRD, N<sub>2</sub>-physisorption, SEM, EDS, and FTIR for investigation of the effect of calcination temperature. Based on the synthesis of PCH and characterization results, we observed that the exact nature of the structural changes of clay material depends on many factors, for example the specific heating rate, holding time and temperature, oxidizing or reducing atmosphere, and cooling rate. Calcination of PCH at the exact temperature is very important because it affects the formation of important active phases, catalytic activity, strength, and durability of clay material. It is of practical importance that these synthesis effects are mapped with respect to applications for adsorption in the framework of pollutant mitigation purposes.

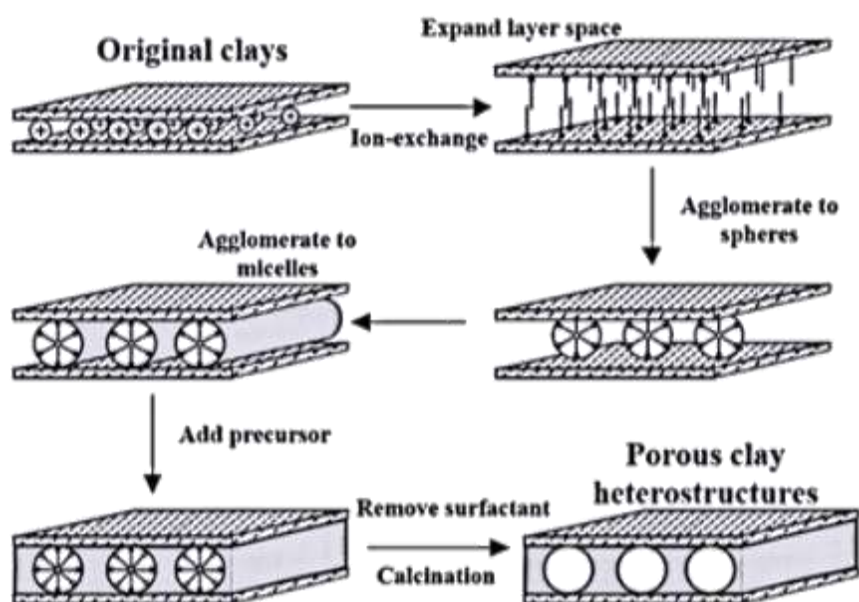


**Fig. 1** Synthesis protocol of porous clay heterostructures (PCH) material.

### Short introduction

Natural minerals e.g. clay and clay-supported catalysts specifically have attracted more attention because of their high abundance and low cost. The swelling capacity, sorption characteristic, acidic nature, ion exchange quality, and textural properties make clays attractive for several applications like adsorption and catalysis. Additionally, clays material is considered as green catalytic materials as they are abundantly available in nature and could be used after minor processing. Clay supported catalysts are non-corrosive solid materials that can be fabricated into the required shape and size for usage inside the reactor tube, could easily be separated from the product stream, and are also easily disposable relatively after using without effect to the surrounding environment [1, 2].

Porous clay heterostructures (PCH) are a new type of modified clay material with micro-mesoporous structure. The synthesis of porous clay heterostructures (PCH) material is based on lamellar aluminosilicate clay with high cation exchange capacity (CEC) as raw material. Through ion exchange, the cationic surfactant is placed between the clay layers, and the organosilicon source is introduced into, and finally, the ordered porous material is obtained with microporous and mesoporous structures by removing the templating agent at the right calcination temperature [1]. The two-dimensional pores between the layers are consistent and orderly. The SiO<sub>2</sub> pore walls are strong and

stable and have the advantages of hydrophobicity and high thermal stability [1]. It has great research values and application potential for different applications [2-8].

## Results and discussion

Results proved that calcination at different temperatures had the main effect on the crystallinity of PCH material and which could also influence the catalytic activity of this material. However, the combustion of the organic carbon chain could also release a large amount of heat and affect the interlayer structure of PCH. The templating agent that is not fully burned may also be carbonized at high temperatures, causing the blockage of the inner channel [2].

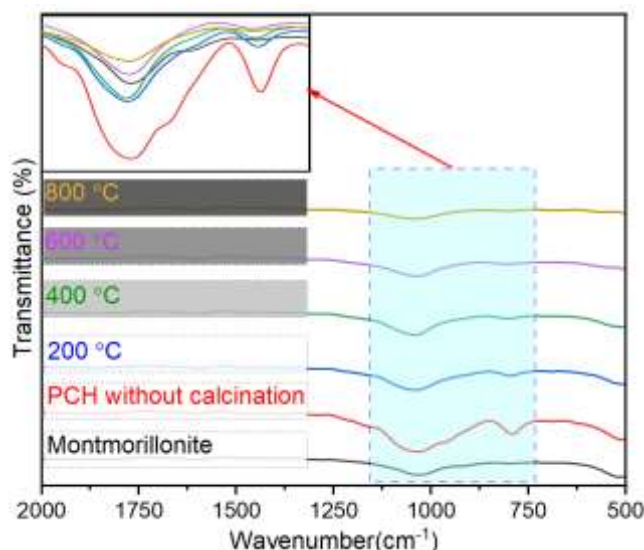


Fig. 2 FTIR analysis of host and modified PCH clay at different calcination temperatures.

## Acknowledgments

This work was supported by the Research and Development Program of Ghent University Global Campus (GUGC), Korea.

## References

- Galarneau, A., A. Barodawalla, and T.J. Pinnavaia, Porous clay heterostructures formed by gallery-templated synthesis. *Nature*, 1995. 374(6522): p. 529-531.
- Cecilia, J., et al., Synthesis, characterization, uses and applications of porous clays heterostructures: a review. *The Chemical Record*, 2018. 18(7-8): p. 1085-1104.
- Kashif, M., et al., Fully selective catalytic oxidation of NO to NO<sub>2</sub> over most active Ga-PCH catalyst. *Journal of Environmental Chemical Engineering*, 2020. 8(2): p. 103524.
- Kashif, M., et al., Most efficient mesoporous Mn/Ga-PCH catalyst for low-temperature selective catalytic reduction of NO with C<sub>3</sub>H<sub>6</sub>. *Vacuum*, 2022: p. 110879.
- Kashif, M., et al., Gallium oxide impregnated on porous clay heterostructures material for selective catalytic reduction of nitrogen oxide with C<sub>3</sub>H<sub>6</sub>. *Journal of Environmental Chemical Engineering*, 2020. 8(4): p. 103943.
- Qu, F., L. Zhu, and K. Yang, Adsorption behaviors of volatile organic compounds (VOCs) on porous clay heterostructures (PCH). *Journal of Hazardous Materials*, 2009. 170(1): p. 7-12.
- Essih, S., et al., Synthesis of Porous Clay Heterostructures Modified with SiO<sub>2</sub>-ZrO<sub>2</sub> Nanoparticles for the Valorization of Furfural in One-Pot Process. *Advanced Sustainable Systems*, 2022: p. 2100453.
- Sanchis, R., et al., Porous clays heterostructures as supports of iron oxide for environmental catalysis. *Chemical Engineering Journal*, 2018. 334: p. 1159-1168.

## The Role of Morphology on the Controlled Crazing of Biopolymer Systems

Ramin Hosseinneshad<sup>1</sup>, Iurii Vozniak<sup>1</sup>, and Andrzej Galeski<sup>1</sup>

<sup>1</sup>Centre of Molecular and Macromolecular Studies, Polish Academy of Sciences, Lodz, Poland

\*ramin.h@cbmm.lodz.pl

Deformation of biopolymeric systems is today one of the most important scientific and technical problems because of the very wide range of applications of biopolymers and continuously growing interest in modified biopolymeric materials by modern technology. This study reveals the influence of biopolymeric nanocomposites' morphological structure on the plastic deformation of bio-based polymeric matrix in air [1-3].

The effect of droplet or fibrillar morphology of dispersed biopolymers within another biopolymer on the deformation process and related structural transformations was studied. The main methods of characterization, namely microscopy (SEM), DSC, WAXS, SAXS, mechanical tests were employed to study the dry crazing mechanism of neat and modified biopolymers in air. Detailed structural studies using microscopy, X-ray, and spectroscopic techniques were aimed at finding the relationship between the structure of the modified biopolymer and the deformation behaviour [4-5].

We found that the introduction of flexible minor biopolymer phase such as poly (butylene adipate-co-succinate-co-glutarate-co-terephthalate), poly (butylene adipate-co-terephthalate), polyhydroxyalkanoate or Polybutylene succinate into the polylactide matrix determines its brittle to ductile transition, which is associated with a change in the mechanism of plastic deformation of the matrix from crazing to shear banding. In detail, the crazing-shear banding transition involves two stages: intensified crazing (observed at a low content of the minor biopolymer phase of about 3 wt.%) and the simultaneous development of crazing and the shear bands (at higher content of the minor phase, about 6 wt.%). At high concentrations of minor phase (above 10 wt.%), shear banding becomes the main mechanism of plastic deformation of the matrix. It should be noted that neat amorphous polylactide demonstrates a quite brittle fracture with craze nucleation before the yielding and subsequent rapid craze-crack transition (Fig. 1).

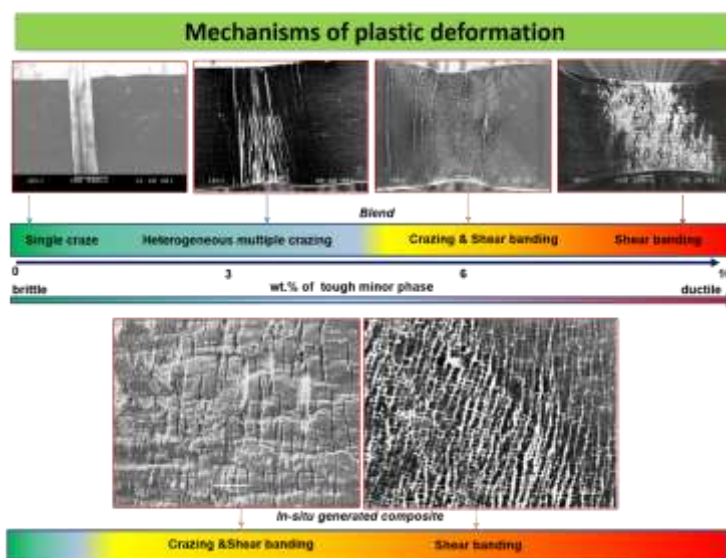


Figure 1. Mechanisms of plastic deformation for polylactide-based biopolymer blends and modified composites.

The transition from droplets/matrix to fibers/matrix morphology determines a more rapid change in the main mechanism of plastic deformation. This is because the flexible minor polymer phase nanofibers additionally span matrix craze surfaces and at large strain, when the craze tufts get broken they bridge the craze gaps increasing both strength and plasticity. Even at 3 wt.% of polymer fibers, intensive crazing is accompanied by the evolution of the shear bands. In the case of 6 and 10 wt.% of fibers, the shear banding becomes the main mechanism of deformation. It was also shown that in the case of droplets/matrix morphology, extensive fragmentation of the crystalline lamellae took place, while limited fragmentation occurs for composite with fibers/matrix morphology (Fig. 2). The limited fragmentation causes a relatively easy plastic deformation by transferring the locally concentrated stresses through matrix lamellae. Fibers/matrix morphology are found to be responsible for altering the character of lamellae fragmentation process.



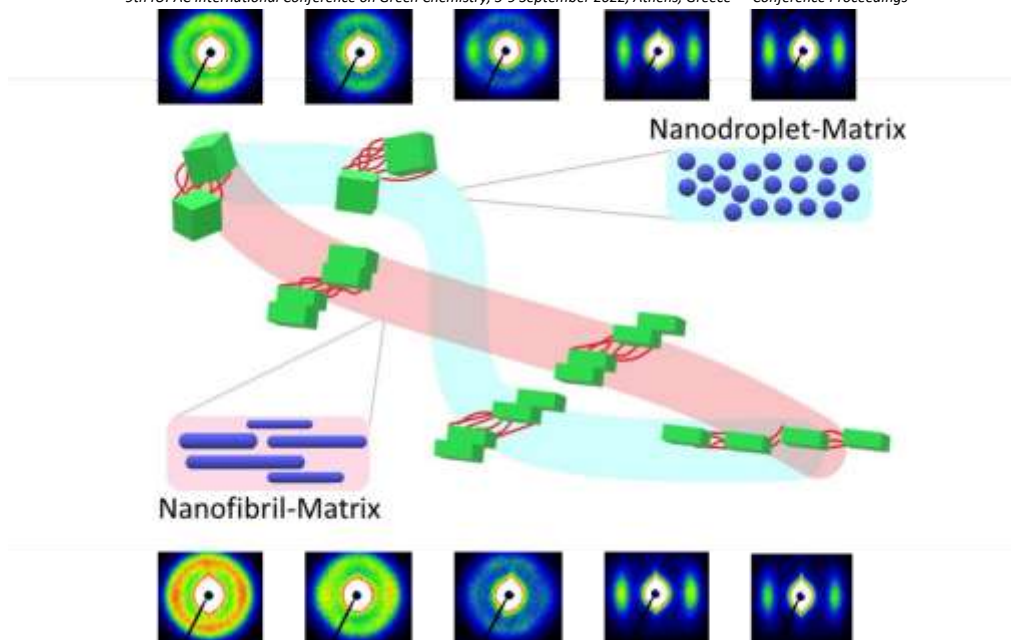


Figure 2. The effect of morphology on the microstructural evolution of biopolymer system reinforced with polyhydroxyalkanoate.

### Acknowledgements

The project was financed from funds of the National Science Centre (Poland) on the basis of the decisions number DEC-2021/41/N/ST5/03389.

### References

1. A. Yarysheva, E. Rukhlya, T. Grokhovskaya, A. Dolgova, O. V. Arzhakova, *J Appl Polym Sci*, **137**, 48567 (2020).
2. A. K. Saad, H. A. Abdulhussain, F. P. C. Gomes, J. Vlachopoulos, M. R. Thompson, *Polymer*, **191** 122278 (2020).
3. O. V. Arzhakova, A. Yu Kopnov, A. I. Nazarov, A. A. Dolgova, A. L. Volynskii, *Polymer*, **186** 122020 (2020).
4. R. Hosseinezhad, I. Vozniak, J. Morawiec, et al., *RSC Adv.* **9**, 30370 (2019).
5. R. Hosseinezhad, I. Vozniak, J. Morawiec, A. Galeski, *Polymers*, **12** 2587 (2020).

## Bimetallic sulfides derived from bi-metal–organic frameworks as sodium anode material with long-term cycling stability

Jiajia Wang<sup>1</sup>, Abuliti Abudula<sup>1</sup>, and Guoqing Guan<sup>1,2\*</sup>

<sup>1</sup>Graduate School of Science and Technology, Hirosaki University, 1-Bunkyocho, Hirosaki 036-8560, Japan

<sup>2</sup>Institute of Regional Innovation (IRI), Hirosaki University, 3 bunkyo-cho, Hirosaki, Aomori 036-8560, Japan

\*e-mail address of corresponding author: guan@hirosaki-u.ac.jp.

### Abstract:

Transition metal sulfides (TMSs) have been widely regarded as the appealing anode candidates for sodium ion batteries (SIBs) because of their prominent theoretical reversible capacities, high electrical conductivity, rich redox reactions, good mechanical and thermal stability<sup>1,2</sup>. However, poor cycling stability and gradient performance for sodium ion batteries limit their applications. In this regard, metal-organic frameworks (MOFs)-derived metal sulfides as the anode material could result in excellent electrochemical performance. In this study, a mixed TMS named as NiS/ZnS-15min was prepared using bimetal-organic frameworks (Ni/Zn MOFs) as the precursor through a facile solid sulfidation way following acid treating process and investigated as the anode for SIBs.

### Experimental Method:

A series of NiS/ZnS was synthesized through a solvothermal method combining a solid sulfidation and acid treating process. Firstly, 150 mg of Ni(NO<sub>3</sub>)<sub>2</sub>·6H<sub>2</sub>O and 150 mg Zn(NO<sub>3</sub>)<sub>2</sub>·6H<sub>2</sub>O was dispersed in 15 mL of ethylene glycol and 90 mg of p-benzenedicarboxylic acid (H<sub>2</sub>BDC) was dispersed in 24 mL of N, N-dimethylformamide (DMF) through the ultrasonication. The above solutions were then mixed and stirred at room temperature for 1 h. Thereafter, the mixture was transferred into a 50 ml Teflon-lined sealed autoclave and heated at 150 °C for 6 h. The Ni/Zn MOF product was collected by centrifugation and washed several times using DMF and ethanol followed by drying at 60 °C in a vacuum oven for 12 h. Then, the Ni/Zn MOFs was heated with thioacetamide (TAA) at a mass ratio of 2:3 in argon atmosphere at 500 °C for 2 h to obtain the NiS/ZnS product. Finally, NiS/ZnS was put into 13 ml 1 M H<sub>2</sub>SO<sub>4</sub> solution containing 0.5 M FeCl<sub>3</sub> and stirred at 60 °C for 15 min or 20 min. After washed by distilled water and CS<sub>2</sub> for several times and dried at 60 °C in a vacuum oven overnight, the resultant product was obtained and labelled as NiS/ZnS-15min or NiS/ZnS-20min, respectively.

For the preparation of the working electrode, 80 wt % active material was mixed with 10 wt% super P and 10 wt% polyvinylidene fluoride (PVDF) in N-methyl-pyrrolidinone (NMP) solvent to form a homogeneous slurry, which was pasted onto a Cu foil, and then dried in a vacuum oven at 80 °C overnight. The electrolyte was 1 M NaSO<sub>3</sub>CF<sub>3</sub> with diglyme (DGM). Charge/discharge measurements were carried out at various current densities over a voltage range of 0.3-3.0 V.

### Results and Discussion:

Figure 1 shows XRD patterns of NiS/ZnS, NiS/ZnS-15min and NiS/ZnS-20min. For the NiS/ZnS sample, it is clearly found that the several typical diffraction peaks located at 2θ=30.09°, 2θ=34.86°, 2θ=46.23°, 2θ=53.62°, 2θ=61.28°, 2θ=65.52° and 2θ=73.55° agree well with the (100), (101), (102), (110), (103), (201) and (202) crystal planes of hexagonal α-NiS (JCPDS No. 02-1280), respectively. Other sharp diffraction peaks with the 2θ values of 28.52°, 47.47° and 56.41° are indexed to the (111), (220) and (311) planes of ZnS (JCPDS No. 05-0566), respectively. There exist the characteristic diffraction peaks of both NiS and ZnS in the NiS/ZnS-15min sample, but the peak intensity of ZnS is weaker than that of the NiS/ZnS sample, indicating the partial removal of ZnS through acid treating. Additionally, all the diffraction peaks of NiS/ZnS-20min match well with the standard NiS and the peaks of ZnS are disappeared, which can infer that ZnS in the NiS/ZnS-20min sample are completely removed.

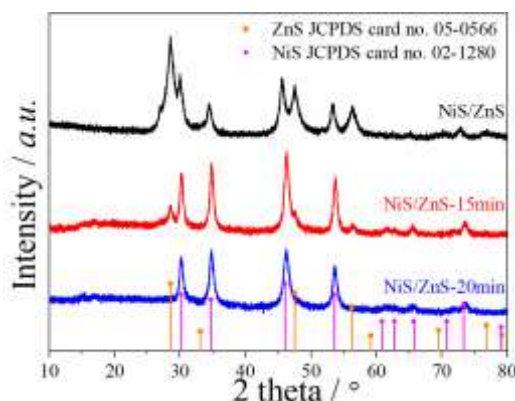


Figure 1. The XRD of NiS/ZnS, NiS/ZnS-15min and NiS/ZnS-20min.

Figure 2 shows the rate capabilities of the NiS/ZnS, NiS/ZnS-15min, and NiS/ZnS-20min based electrodes for SIBs. As seen, the NiS/ZnS-15min based electrode demonstrates the average discharge reversible capacities of

485.1, 453.9, 430.4, 418.2, 405.3, and 381.3 mA h g<sup>-1</sup> at the current densities of 0.1, 0.2, 0.5, 1, 2, and 5 A g<sup>-1</sup>, respectively. More excitingly, an average discharge capacity of 415.5 mA h g<sup>-1</sup> could be achieved when the current density is set back to 0.2 A g<sup>-1</sup>. Furthermore, the rate performance of NiS/ZnS-15min based electrode is much higher than those of NiS/ZnS, and NiS/ZnS-20min based electrodes, which further indicates the fast reaction kinetic and robust integrity of NiS/ZnS-15min electrode.

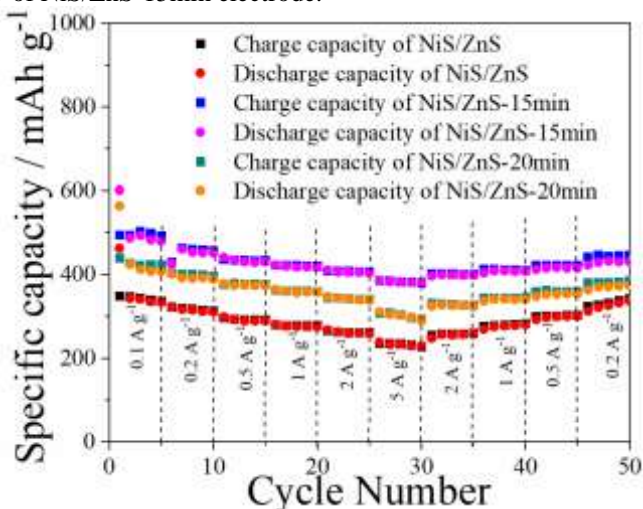


Figure 2. The XRD of NiS/ZnS, NiS/ZnS-15min and NiS/ZnS-20min. Rate capabilities of the NiS/ZnS, NiS/ZnS-15min and NiS/ZnS-20min based anodes at different current densities from 0.1 A g<sup>-1</sup> to 5 A g<sup>-1</sup>.

### Acknowledgements

This work is supported by ZiQoo Chemical Co. Ltd.

### References

1. Lim, Yew Von, Xue Liang Li, Hui Ying Yang, *Advanced Functional Materials*, **31** 10 (2021).
2. Zhang, Long, Qiuping Wei, Junjie An, Li Ma, Kechao Zhou, Wentao Ye, Zhiming Yu, Xueping Gan, Cheng-Te Lin, Jingting Luo, *Chemical Engineering Journal*, 380 (2020).

## Iron-based catalytic materials as energy carriers for carbon dioxide valorization

Alexandra Bakratsa<sup>1</sup>, Georgia Kastrinaki<sup>2</sup>, Vasiliki Zacharopoulou<sup>2</sup>, Maria Karani<sup>2\*</sup>, George Karagiannakis<sup>2</sup> and Vasilis Zaspalis<sup>1, 2</sup>

<sup>1</sup> Department of Chemical Engineering, Aristotle University of Thessaloniki, University campus, Thessaloniki, 54124, Greece

<sup>2</sup> Chemical Process & Energy Resources Institute, CERTH, 6th km. Harilaou-Thermi Rd, Thessaloniki, 57001, Greece

\*mkarani@certh.gr

Up to this day, excessive carbon dioxide (CO<sub>2</sub>) emissions remain a challenge for the global scientific community. Carbon dioxide emissions are linked with greenhouse effects and adverse climate changes. Thus, effective carbon dioxide valorization is of high importance. Recently, carbon dioxide conversion into high added-value products (e.g., methane, C<sub>1</sub>-C<sub>3</sub> deoxygenated products) has attracted considerable attention. Specifically, conversion of CO<sub>2</sub> to gasoline-range (C<sub>5</sub> - C<sub>11</sub>) products is an emerging and promising approach as, if proven technically and financially viable, it will contribute to mitigating current levels of CO<sub>2</sub> emissions in the global atmosphere. Through the Reverse Water-Shift (RWGS) reaction, CO<sub>2</sub> is converted into CO which is subsequently hydrogenated into hydrocarbons via Fischer – Tropsch (FTS) like reactions. The composition and properties of the employed catalysts is crucial for the tandem reaction to proceed; the nature of the catalytic substrate, the reduction of the active metal, the formation of mixed phases, the dispersion of the active phase, the particle size and the porosity of the catalyst are factors that are key to the hydrogenation of CO<sub>2</sub> to CO and can improve the efficiency of the RWGS catalytic reaction [1], [2]. Iron-based catalysts are preferred due to their excellent ability to catalyze RWGS and FTS reactions and also due to the high olefinic nature of the obtained products [3]. Recent studies show that the magnetite surface satisfactorily activates CO<sub>2</sub> [3]. Typically, iron catalysts require the use of alkaline additives to achieve the preferred activity and distribution of desired products [3]. Hence, this work focuses on the synthesis of supported and unsupported iron-based nanoparticles. As a first important step, the synthesized powders are characterized with respect to their morphological and catalytic properties employing various methods (e.g. XRD, FT-IR, BET, DLS, PSD, SEM, TPD-NH<sub>3</sub>).

Magnetite nanoparticles, doped with alkalis, such as Na and K, have been synthesized through co-precipitation, using a mixture of FeCl<sub>2</sub>·4H<sub>2</sub>O and FeCl<sub>3</sub>·6H<sub>2</sub>O as precursor. Sodium (Na) and Potassium (K) have been added to the precursor's solution at a ratio of 1:1 and 1:2. The produced catalytic materials have been dispersed on alumina, high surface area MgO, and HZSM-5 in order to attain multifunctional properties that will catalyze the tandem reaction. Indicative characterization results are presented below. The specific surface area of the catalytic materials was determined by BET analysis and the results showed that magnetite nanoparticles have lower surface (~145.0 m<sup>2</sup>/g) than HZSM-5 (~409.0 m<sup>2</sup>/g) (Table 1). XRD patterns confirm the crystalline structure of the magnetite nanoparticles, while the identified phases are magnetite (Fe<sub>3</sub>O<sub>4</sub>) and hydrous iron oxide (Fe<sub>2</sub>O<sub>3</sub>·H<sub>2</sub>O/β Fe<sub>2</sub>O<sub>3</sub>·H<sub>2</sub>O). According to calculations using the Scherrer equation, the crystallite size of the oxides was determined, which coincides with the particle size and thus particles are monocrystalline (Table 1). A small shift of the NaFe<sub>3</sub>O<sub>4</sub> (1: 1) and KFe<sub>3</sub>O<sub>4</sub> (1: 1) peaks is observed on the corresponding diffractograms, confirming the presence of K and Na ions in the crystal lattice of the magnetite nanoparticles. According to the FT-IR spectrum of Fe<sub>3</sub>O<sub>4</sub> nanoparticles two absorption bands were exhibited at 400 cm<sup>-1</sup> and 551 cm<sup>-1</sup>. The first one is due to Fe-O stretching of octahedral sites and the second one due to Fe-O stretching of the tetrahedral and octahedral sites. Absorbance bands at 420 cm<sup>-1</sup> and 691 cm<sup>-1</sup> are attributed to maghemite. Absorbance peaks at 807 cm<sup>-1</sup> and 907 cm<sup>-1</sup> are assigned to c-OH and d-OH stretching vibrations of goethite form, respectively. A slight shift at the peaks of NaFe<sub>3</sub>O<sub>4</sub> (1: 1) and KFe<sub>3</sub>O<sub>4</sub> (1: 1) is also observed (presence of K and Na ions) (Fig. 1). According to TPD NH<sub>3</sub> analysis, HZSM-5 presented weak and relatively strong acid sites, while NaFe<sub>3</sub>O<sub>4</sub> presented weak acid sites only (Fig. 2.A). The presence of both weak and medium acid sites was identified on the supported magnetite nanoparticles (i.e. Fe<sub>3</sub>O<sub>4</sub>/HZSM-5, NaFe<sub>3</sub>O<sub>4</sub>/HZSM-5, KFe<sub>3</sub>O<sub>4</sub>/HZSM-5), thereby indicating that the observed acidity is mainly attributed to HZSM-5. Stronger acid sites were observed on the KFe<sub>3</sub>O<sub>4</sub>/HZSM-5 catalyst.

Table 9. Physicochemical properties.

Catalytic Material	Surface BET (m <sup>2</sup> /g)	Pore Volume (cm <sup>3</sup> /g)	Pore Size (nm)	Crystallite Size (nm)	Oxides Phases (XRD)
Fe <sub>3</sub> O <sub>4</sub>	145.6	0.498	13.7	12.4	Fe <sub>3</sub> O <sub>4</sub> / Fe <sub>2</sub> O <sub>3</sub> ·H <sub>2</sub> O β Fe <sub>2</sub> O <sub>3</sub> ·H <sub>2</sub> O
NaFe <sub>3</sub> O <sub>4</sub>	145.2	1.916	52.8	13.0	Fe <sub>3</sub> O <sub>4</sub> / Fe <sub>2</sub> O <sub>3</sub> ·H <sub>2</sub> O β Fe <sub>2</sub> O <sub>3</sub> ·H <sub>2</sub> O
KFe <sub>3</sub> O <sub>4</sub>	148.3	0.430	11.6	9.8	Fe <sub>3</sub> O <sub>4</sub> / Fe <sub>2</sub> O <sub>3</sub> ·H <sub>2</sub> O β Fe <sub>2</sub> O <sub>3</sub> ·H <sub>2</sub> O
HZSM-5	409.4	0.372	3.6	-	Al <sub>2</sub> O <sub>3</sub> ·54SiO <sub>2</sub> ZSM-5

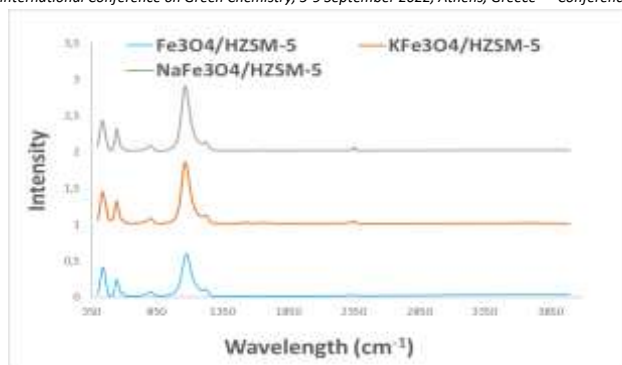
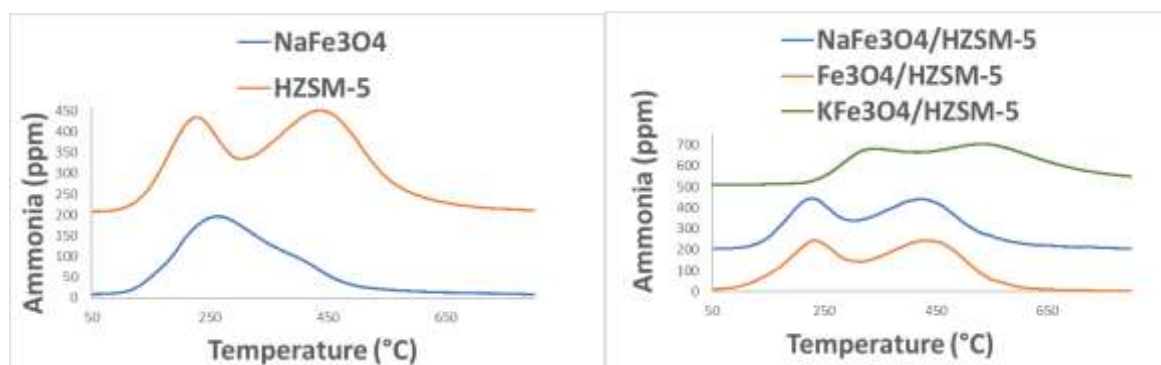


Figure 47. FTIR spectra of magnetite nanoparticles dispersed on HZSM-5.

Figure 48. TPD-NH<sub>3</sub> analysis of A) NaFe<sub>3</sub>O<sub>4</sub> and HZSM-5 without reduction, and B) magnetite nanoparticles dispersed on HZSM-5 upon reduction.Table 10. Desorbed ammonia (TPD-NH<sub>3</sub>)

Catalytic Material	mmol NH <sub>3</sub> /g <sub>cat</sub>
NaFe <sub>3</sub> O <sub>4</sub>	0.385
HZSM-5	0.718
Fe <sub>3</sub> O <sub>4</sub> /HZSM-5	0.673
NaFe <sub>3</sub> O <sub>4</sub> /HZSM-5	0.684
KFe <sub>3</sub> O <sub>4</sub> /HZSM-5	0.634

TPD-NH<sub>3</sub> measurements took place upon reduction of samples at 350°C, for 4h, under hydrogen flow. Preliminary experiments are currently in progress, in a continuous flow reactor (3 MPa, 320°C, H<sub>2</sub>/CO<sub>2</sub> (3:1)), in order to evaluate the performance of the synthesized catalysts and ultimately correlate the latter with the physicochemical properties attained as a result of the synthesis procedure.

## Acknowledgments

We acknowledge the support of this work by the project “PROMETHEUS: A Research Infrastructure for the Integrated Energy Chain” (MIS 5002704) which is implemented under the Action “Reinforcement of the Research and Innovation Infrastructure”, funded by the Operational Programme “Competitiveness, Entrepreneurship and Innovation” (NSRF 2014-2020) and co-financed by Greece and the European Union (European Regional Development Fund).

## References

1. S.C. Lee, J.H. Jang, B.Y. Lee., M.C. Kang, M. Kang, S.J. Choung, *Appl.Catal. A. Gen.* **253** 293 (2003).
2. M. Liu, Y. Yi, L. Wang, H. Guo, A. Bogaerts, *Catal.* **9** 275 (2019).
3. J.Weï, Q. Ge, R. Yao, Z. Wen, C. Fang, L. Guo, H. Xu, J. Sun, *Nat. Commun.***8** 16170 (2017).

## Lignocellulose-based membranes for lithium-ion battery separators

Huishi Li<sup>1</sup>, Kunshan Yu<sup>1</sup>, Sadegh Askari<sup>1</sup>, Artem Kulachenko<sup>3</sup>, Mikael E. Lindström<sup>1</sup>, Olena Sevastyanova<sup>1,2</sup>

<sup>1</sup>KTH-Royal Institute of Technology, Department of Fibre and Polymer Technology, Teknikringen 56-58, Stockholm, Sweden

<sup>2</sup>Wallenberg Wood Science Center – WWSC, Department of Fibre and Polymer Technology, Teknikringen 56-58, Stockholm, Sweden

<sup>3</sup> KTH-Royal Institute of Technology, Department of Solid Mechanics, SE-100 44 Stockholm, Sweden

\*huishi@kth.se

### Introduction

Lithium-ion batteries (LIBs) have aroused interest worldwide due to their high energy density and excellent cycling performance, achieving broad applications in different fields, including electric vehicles and portable electronics. [1] Separators are vital parts of lithium-ion batteries located between the cathode and anode to prevent short circuits, meanwhile, permitting ion transfer within the batteries. Commercial separators account for around 20% of the total cost of batteries. [2] Furthermore, conventional separators are fabricated from synthetic polymers which are not eco-friendly and suffer from issues such as low thermal stability and deficient interfacial contact with electrodes. Herein, separators fabricated from abundant and sustainable wood-based biopolymers are optimized for LIBs separators using lignocellulose fibers fabricated from unbleached Kraft pulps. The effect of residual lignin in LCMFs on improving the mechanical properties and regulating the electrolyte uptake will be investigated in this study.

### Experiment

Pure microfibrillated cellulose fibers (CMF) and lignin-containing microfibrillated cellulose fibers (LCMF) were fabricated from fully-bleached and unbleached softwood pulps and were used as the starting materials for the fabrication of LIBs separators. The lignin content of LCMF is around 10.9% gravimetrically determined by Klason lignin. Detailed characterizations of the physical and chemical properties of films fabricated from CMF and LCMF have been carried out, including morphology characterization using SEM, thermal stability by TGA and mechanical properties. The electrolyte wettability, ionic conductivity and electrochemical properties of CMF and LCMF films as separators will also be tested. Specifically, the effect of residual lignin on the electrochemical properties will be discussed. The properties of CMF and LCMF separators will be compared with the commercial Celgard separator.

### Results and Discussion

The surface morphology of CMF and LCMF films is shown in Figure 1. More condensed structures were formed with the presence of residual lignin in cellulose fibres. Table 1 exhibits the mechanical properties of CMF and LCMF separators. Residual lignin in the cellulose fibers can drastically enhance the mechanical properties of cellulose fibers which is practically important for the LIBs when it comes to resisting the exterior mechanical loading, particularly, during impact and collisions.

Table 1. Mechanical properties of CMF and LCMF films.

Sample	Mean Thickness (μm)	Mean Density (g/cm <sup>3</sup> )	Young's Modulus (GPa)	Ultimate tensile strength (Mpa)	Tensile strain (%) at break
CMF	22.82	1.46	9.98 ± 0.33	254 ± 12	11.6 ± 0.73
LCMF	25.50	1.42	10.65 ± 0.19	300 ± 13	11.0 ± 0.85

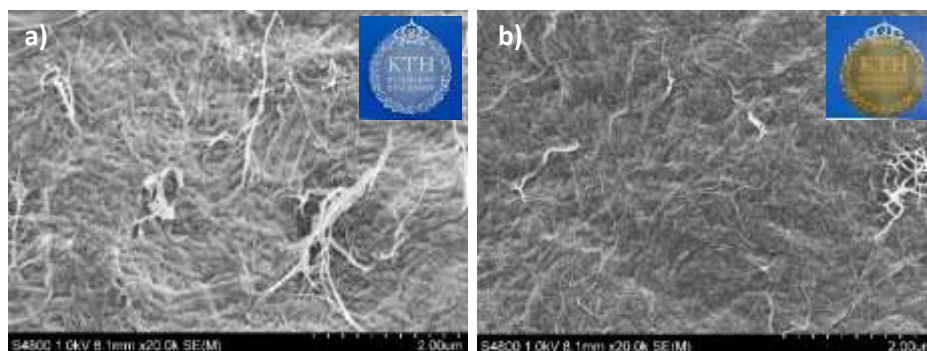


Figure 1. SEM images of film surface fabricated from a) CMF suspensions and b) LCMF suspensions.

## Acknowledgements

China Scholarship Council and Wood and Pulping Chemistry Research Network (WPCRN) are acknowledged for providing financial support.

## References

1. Li, M., Lu, J., Chen, Z., & Amine, K. (2018). *Advanced Materials*, 30(33), 1800561.
2. Huang, X. (2011). *Journal of Solid State Electrochemistry*, 15(4), 649-662.

## Synthesis, Characterization and UVC-activated Photocatalytic Activity of Superparamagnetic Iron Oxide Decorated Indium Hydroxide Nanocomposite

C.Y. Chong<sup>1</sup>, J.C. Juan<sup>2</sup>, Mohd Rafie Johan<sup>2</sup>, C.F. Loke<sup>1</sup>, K.H. Ng<sup>1</sup>, Y. F. Ngeow<sup>3</sup>, T.H. Lim<sup>1\*</sup>

<sup>1</sup>Department of Physical Science, Faculty of Applied Sciences, Tunku Abdul Rahman University College, Kuala Lumpur 53300, Malaysia.

<sup>2</sup>Nanotechnology & Catalysis Research Centre, Institute of Advanced Studies, University of Malaya, Jalan Universiti, Kuala Lumpur 50603, Malaysia.

<sup>3</sup>Centre for Research on Communicable Diseases (CRCD), Faculty of Medicine and Health Sciences, University Tunku Abdul Rahman, Jalan Sungai Long, 43000, Kajang, Selangor, Malaysia.

\*[limth@tarc.edu.my](mailto:limth@tarc.edu.my) (Corresponding author's email)

### Abstract

In this work, a superparamagnetic composite consisting of Fe<sub>3</sub>O<sub>4</sub> nanoparticles decorated In(OH)<sub>3</sub> nanorods ("SPIDIN") was successfully prepared at room temperature via a green method using water as solvent and biocompatible polyvinylpyrrolidone (PVP) as surfactant/stabilizing agent. SPIDIN's performance under UVC as a photocatalyst employed to degrade persisting dyes was investigated. SPIDIN produced was characterized collectively using PXRD, FESEM, HRTEM, EDS, UV-Vis spectroscopy and zeta potential measurement. The In(OH)<sub>3</sub> nanorod moiety prepared was found to possess a direct band gap of 4.4 eV. To better match the band gap, a UVC excitation source with a corresponding photon energy quantized at 4.8 eV was selected for the photodegradation study. Chemical structure wise, SPIDIN was confirmed to be comprised of spherical Fe<sub>3</sub>O<sub>4</sub> nanoparticles (4-5nm) resided on the surface of In(OH)<sub>3</sub> nanorods which have a mean width of 33nm and average aspect ratio of 2-3. SPIDIN exhibited a magnetic susceptibility measured at 1.30 x10<sup>-5</sup>cm<sup>3</sup>g<sup>-1</sup>. Under a 254nm UVC light, SPIDIN was able to degrade 95% of methylene blue and malachite green dyes respectively within 1 hr. The presence of superparamagnetic Fe<sub>3</sub>O<sub>4</sub> moiety chemically bonded to the In(OH)<sub>3</sub> allowed magnetic recovery of the SPIDIN after photodegradation, thus eliminating the need of energy demanding vacuum filtration, and the magnetically isolated SPIDIN could be readily be reused for the next degradation cycle without further drying.



# Phosphonated Polyetheramine-Coated Magnetic Nanoparticles: A Sustainable Approach for Oilfield scale Management

Ali H. Alkaraly<sup>1</sup> and Mohamed F. Mady<sup>1\*</sup>

<sup>1</sup>Department of Chemistry, Bioscience and Environmental Engineering, Faculty of Science and Technology, University of Stavanger, N-4036 Stavanger, Norway

\*mohamed.mady@uis.no

## Abstract

Scale formation is the process of inorganic salt deposition from the aqueous phase because of salt supersaturation. Scale formation can occur in the upstream oil industry and cause problems in the flow assurance. Scale can deposit on almost any surface. Once a scale layer is first formed, it will continue to become thicker unless treated. Most types of oilfield scales are calcium carbonate ( $\text{CaCO}_3$ ) and sulfates of group II elements, for example, strontium (celestite,  $\text{SrSO}_4$ ), calcium (gypsum,  $\text{CaSO}_4 \cdot 2\text{H}_2\text{O}$ ), and barium (barite,  $\text{BaSO}_4$ ) [1,2].

Several attempts have been reported to develop environmentally friendly chemicals-based scale inhibitors (SIs) for oilfield applications. Scale inhibitors (SIs) are a branch of specialty water-soluble chemicals used to prevent or slow scale formation in water systems. In the last 10 years, our Green and Sustainable Chemistry research group at the University of Stavanger has developed many biodegradable and non-toxic phosphonated SIs for oilfield applications. However, so far chemicals that are greener suffer from low performance, high cost, and various incompatibilities with the production system [3,4].

This project aims to investigate for the first time the use of revolutionary magnetic nanoparticles to prevent scale formation under oilfield conditions, using a simple, cost-effective method by attaching environmentally acceptable chemicals to superparamagnetic iron oxide nanoparticles (SPIONs), allowing a facile magnetic removal, along with reuse and/or recycling. In this work, we report the synthesis of SPIONs functionalized with biocompatible trisodium citrate (TSC) as a stabilizer agent to avoid crystal grain growth SPIONs using a coprecipitation approach. The resultant SPIONs@TSC was further functionalized with a partially linear phosphonated polyetheramine (PPEA), as a green scale inhibitor (SI), affording highly monodisperse SPIONs@TSC@PPEA-SI (Figure 1).

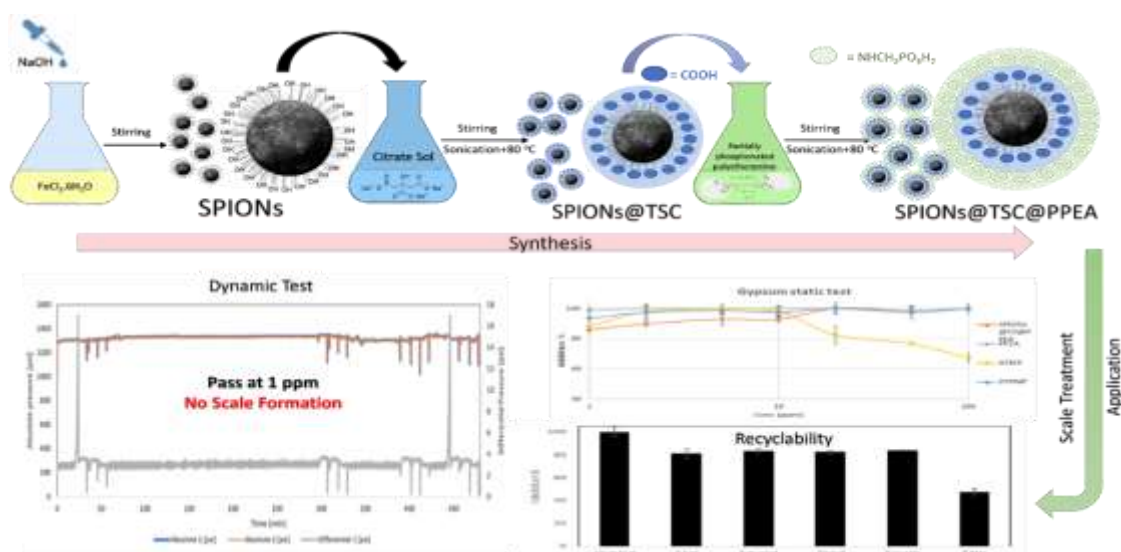


**Figure 1.** Schematic diagram of the synthesis of magnetic nanoparticles coated phosphonated polyetheramine (SPIONs@TSC@PPEA) as oilfield scale inhibitor.

The obtained magnetic nanoparticles were characterized by their surface chemistry, surface charge, size, crystallinity, morphology, and thermal behavior using Zetasizer, DLS (Dynamic Light Scattering), Xray, SEM (Scanning Electron Microscope), TEM (Transmission Electron Microscope), and TGA (Thermogravimetric Analysis), respectively. Furthermore, the inhibition performance of the magnetic core-shell (SPIONs@TSC@PPEA-SI) was evaluated for several oilfield scales, e.g., calcium sulfate scale (gypsum,  $\text{CaSO}_4 \cdot 2\text{H}_2\text{O}$ ) under static and dynamic oilfield conditions according to the Heidrun oilfield, Norwegian Sea, Norway.

The results show that the gypsum scale inhibition efficiency of SPIONs@TSC@PPEA-SI achieved 86% and 90% at low concentrations of inhibitor 1 and 2 ppm, respectively. In addition, the inhibition efficiency of the

recycled **SPIONs@TSC@PPEA-SI** was tested up to 5 times against the gypsum scale. It was found that the recycled **SPIONs@TSC@PPEA-SI** gave a similar performance to the non-recycled magnetic core-shell inhibitor. For the first time, this study has provided the validation of the proof of concept of recovering and recycling SPIONs-based oilfield scale inhibitors.

## References

1. Mady, M. F. Oilfield Scale Inhibitors: Synthetic and Performance Aspects. *Water-Formed Deposits* 2022, 325–352. <https://doi.org/10.1016/b978-0-12-822896-8.00033-9>.
2. Frenier, W. W.; Ziauddin, M., Formation, removal, and inhibition of inorganic scale in the oilfield environment. Society of Petroleum Engineers Richardson, TX: 2008.
3. Mady, M. F.; Kelland, M. A. Review of Nanotechnology Impacts on Oilfield Scale Management. *ACS Applied Nano Materials* 2020, 3 (8), 7343–7364. <https://doi.org/10.1021/acsanm.0c01391>.
4. Mady, M. F.; Kelland, M. A. Overview of the Synthesis of Salts of Organophosphonic Acids and Their Application to the Management of Oilfield Scale. *Energy & Fuels* 2017, 31 (5), 4603–4615. <https://doi.org/10.1021/acs.energyfuels.7b00708>.

# Recyclable Magnetic Nanoparticles Coated-Poly(4-styrenesulfonic acid-co-maleic acid) for Oilfield Scale Control

Abdelrahman Abdelaal<sup>1</sup> and Mohamed F. Mady<sup>1\*</sup>

<sup>1</sup>Department of Chemistry, Bioscience and Environmental Engineering, Faculty of Science and Technology, University of Stavanger, N-4036 Stavanger, Norway

\*mohamed.mady@uis.no

## Abstract

In the upstream petroleum industry, inorganic salts have been formed and deposited in the wells, pipelines, and processing equipment. These mineral salts are called scales and are considered one of the main flow assurance issues in oil and gas productions [1]. The most common mineral scales associated with oilfield applications are calcium carbonate (calcite,  $\text{CaCO}_3$ ) and sulfate salts of calcium (gypsum,  $\text{CaSO}_4$ ), strontium (celestite,  $\text{SrSO}_4$ ), and barium (barite,  $\text{BaSO}_4$ ). Scales hinder the flow of fluid, reduce water conveyance capacity, and lead to accidents [2]. Once the scale is formed, it would be hard to treat it, so it was vital to prevent scale formation from the beginning.

Scale inhibitors (SIs) are the commonest technique for preventing scale deposition in the oil and gas industry. It was well known that most conventional SIs for oilfield scales are organic-chemical-based phosphonates ( $-\text{PO}_3\text{H}_2$ ), sulfonate ( $-\text{SO}_3\text{H}$ ), and carboxylate ( $-\text{COOH}$ ) groups. However, most of these conventional SIs have certain drawbacks, such as low biodegradability and incompatibilities with high calcium brines. So, many commercial SIs are banned for offshore deployment in several oilfields (for example, the U.K. and Scandinavia). So, there were several demands for developing green scale inhibitors with biocompatibility, biodegradability, low toxicity, excellent calcium compatibility, and more thermal stability.

Nanomaterials show great potential in addressing technology challenges in the upstream petroleum industry. A recent hot area for studying nanotechnology has been oilfield scale management [3]. Magnetite ( $\text{Fe}_3\text{O}_4$ ) is a common magnetic iron oxide. It has a cubic inverse spinel structure with oxygen forming an FCC closed packing and Fe cations occupying the interstitial tetrahedral sites and octahedral sites. Superparamagnetic iron nanoparticles (Magnetite) have been widely studied because of their massive aspects and applications. For example, hyperthermia, targeted drug delivery, cell separation, magnetic resonance imaging (MRI) in ultrahigh density magnetic storage media, biological labeling, tracking, imaging, detection, separations, and ferrofluids. It is well known that magnetic nanoparticles are non-toxic and safe for the environment.

In this work, we report for the first time the use of recyclable magnetic nanoparticles as non-toxic scale inhibitors based on typical oilfield conditions in the Norwegian Sea. Our new technique will propose the removal of chemicals-based scale inhibitors from the produced fluids by attaching the chemicals to magnetic nanoparticles ( $\text{Fe}_3\text{O}_4$ ), allowing a facile magnetic removal, along with reuse and/or recycling. Herein, we first synthesized magnetite nanoparticles ( $\text{Fe}_3\text{O}_4$ ) using the co-precipitation method and then coated the resultant magnetite with poly(4-styrenesulfonic acid-co-maleic acid) (PSS-MA), affording  $\text{Fe}_3\text{O}_4@\text{PSS-MA-SI}$  as a new oilfield SI (Figure 1).

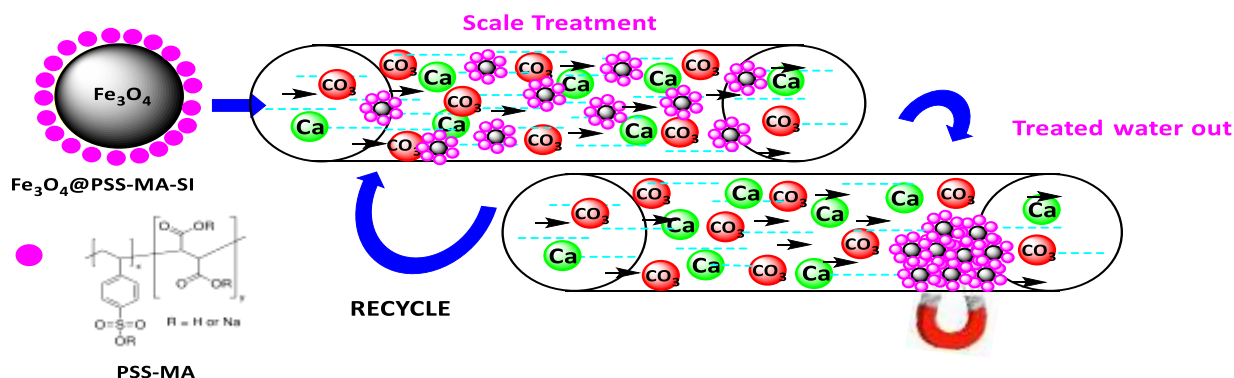


**Figure 1.** Schematic illustration of recyclable magnetic nanoparticles ( $\text{Fe}_3\text{O}_4$ ) coated poly(4-styrenesulfonic acid-co-maleic acid) as scale inhibitor for oilfield applications

The physical and chemical properties of magnetic composite nanoparticles were determined by Transmission Electron Microscopy (TEM), Fourier Transform Infrared (FT-IR), X-ray Diffraction (XRD), and Scanning Electron Microscopy (SEM). In addition, the magnetic properties of the obtained core-shell inhibitor were measured using vibrating sample magnetometry (VSM) to confirm recyclability properties. Moreover,  $\text{Fe}_3\text{O}_4@\text{PSS-MA-SI}$  was evaluated for calcite, gypsum, and barite scale inhibition and compared to commercial sulfonated SI according to the Heidrun oilfield, Norway using a high-pressure dynamic tube blocking rig at approximately 80 bar and 100 °C.

The obtained results showed that the nontoxic  $\text{Fe}_3\text{O}_4@\text{PSS-MA-SI}$  afforded excellent scale inhibition performance against all tested oilfield scales. In addition, the recycled  $\text{Fe}_3\text{O}_4@\text{PSS-MA-SI}$  was successfully

recovered and reused up to 4 cycles, affording a reasonable inhibition performance in comparison with fresh core-shell scale inhibitor **Fe<sub>3</sub>O<sub>4</sub>@PSS-MA-SI**.

### References

1. Mady, M.F., *Chapter 16 - Oilfield scale inhibitors: Synthetic and performance aspects*, in *Water-Formed Deposits*, Z. Amjad and K.D. Demadis, Editors. 2022, Elsevier. p. 325-352.
2. Zhang, Z.-j., et al., *Fluorescent-tagged hyper-branched polyester for inhibition of CaSO<sub>4</sub> scale and the scale inhibition mechanism*. *Materials Today Communications*, 2020. **25**: p. 101359.
3. Mady, M.F. and M.A. Kelland, *Review of Nanotechnology Impacts on Oilfield Scale Management*. *ACS Applied Nano Materials*, 2020. **3**(8): p. 7343-7364.

## Synthesis and characterization of Metal-organic framework of Zn (II) modified by magnetic nanoparticles and multi-walls carbon nanotubes for dispersive solid phase extraction of some benzophenones in water samples

Shereen A. Majeed<sup>1\*</sup> and Douaa AlMarzouq<sup>2\*</sup>

<sup>1</sup>Department of Chemistry, Kuwait University, P.O. Box 5969, Safat 13060, Kuwait

<sup>2</sup>Department of Environmental Health, College of Health Sciences, The Public Authority of Applied Education and Training, P.O. Box 1428, Faiha 72853, Kuwait

\*sh.sh.a.majeed@gmail.com

### Abstract

Benzophenone (BP) derivatives are used as UV-filters in personal care products to protect skin from UV light [1] in its both form of UVA (320–400 nm) and UVB (290–320 nm) [2]. They also can prevent polymers photolysis in plastics and food packaging [3]. BPs are toxic and un-degradable and have been detected in wastewater [4], river water [5], sewage sludge [6] and fishes [7]. Nanotechnology has been known for its potential environmental implementations, including pollutants sensors, water treatment and remediation. Herein a zinc (II) metal-organic framework (Zn-MOF) of 1,2,4,5-benzenetetracarboxylic acid ligand was synthesized. The MOF material was further modified with magnetic nanoparticles (MNPs) and multi-wall carbon nanotubes (MW-CNTs). The nanohybrid synthesis was confirmed by using a variety of characterization techniques such as FT-IR, scanning electron microscopy (SEM), transmission electron microscope (TEM) and X-ray diffraction (XRD) patterns. The nanohybrid was tested to extract and detect some benzophenone (BP) derivatives in water samples via dispersive solid-phase extraction (d-SPE) coupled with gas chromatography-mass detector (GC-MS).

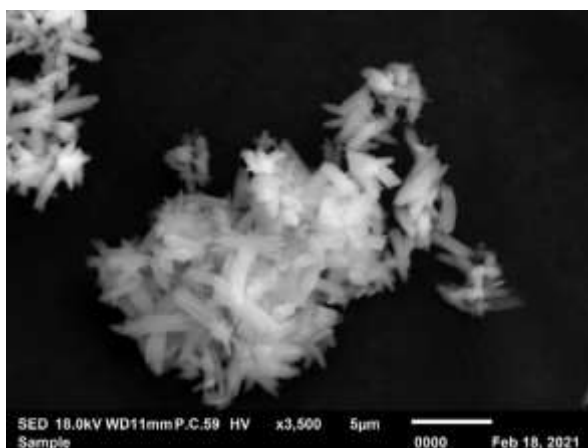


Figure 1. SEM of MOF shows the morphology of MOF.



Figure 2. The magnetic behavior of the synthesized materials.

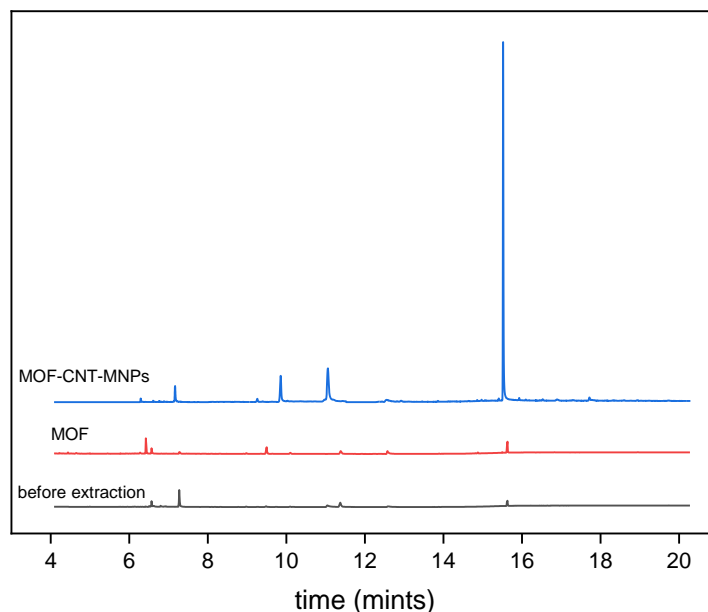


Figure 3. Chromatograms of BPs before extraction and after extraction by MOF and MOF-CNT-MNPs hybrid.

### Acknowledgements

The authors acknowledge the Public Authority for Applied Education and Training (PAAET), Kuwait. . The authors express their gratitude to the Kuwait University Research Administration RSP unit general facilities of the Faculty of Science GFS (GS 02/01, GS 03/01, GS 01/05), and the National Unit for Environmental Research and Services (NUERS) at Kuwait University (SRUL 01/13).

### References

1. Y. Watanabe, H. Kojima, S. Takeuchi, N. Uramaru, S. Sanoh, K. Sugihara, S. Kitamura and S. Ohta, *Toxicology and Applied Pharmacology*, 2015, 282, 119-128.
2. M. Kawaguchi, R. Ito, H. Honda, N. Endo, N. Okanouchi, K. Saito, Y. Seto and H. Nakazawa, *Journal of Chromatography A*, 2008, 1200, 260-263.
3. C. Liao and K. Kannan, *Science of The Total Environment*, 2019, 653, 168-175.
4. C. Almeida, A. Stepkowska, A. Alegre and J. M. F. Nogueira, *Journal of Chromatography A*, 2013, 1311, 1-10.
5. J.-W. Wu, H.-C. Chen and W.-H. Ding, *Journal of Chromatography A*, 2013, 1302, 20-27.
6. F. J. Camino-Sánchez, A. Zafra-Gómez, N. Dorival-García, B. Juárez-Jiménez and J. L. Vilchez, *Talanta*, 2016, 150, 415-424.
7. M. E. Balmer, H.-R. Buser, M. D. Müller and T. Poiger, *Environmental Science & Technology*, 2005, 39, 953-962.

# An Electrochemical Oxidation of Wastewaters through Graphene Oxide Coated Electrode

Dominika Marcin Behunová<sup>1\*</sup> and Miroslava Václavíková<sup>1</sup>

<sup>1</sup>Institute of Geotechnics, Slovak Academy of Sciences, Watsonova 45, 040 01 Kosice, Slovakia

\*behunova@saske.sk

## Introduction

The modification of electrodes is widely implemented to try and improve the active surface area and increase surface interactions that increase the efficiency of electrochemical oxidation. Currently, the research is focused on graphene-based material because of its reported extraordinary physical, chemical, mechanical and electrical properties. Graphene oxide (GO) is a single atomic layer of  $sp^2$  carbon atoms functionalized with many different functional groups (mainly oxygen) [1]. In the past GO was used predominately as a precursor for graphene synthesis. Currently, GO is an attractive material for technological and environmental areas, such as electrochemistry, energy storage devices, application as membrane material, anti-corrosion material etc. [2].

The electrochemical oxidation technique is a relatively new approach in wastewater treatment polluted by azo dyes with promising results. It is a simple and effective method for the treatment of various wastewaters. Oxidants are produced during the process directly at the electrode surface or indirectly from chemical compounds in the treated water. After a few minutes, it provides complete decolouration under a wide range of pH, short retention time and no sludge production [3]. Recent studies confirmed that graphene-based composites show strong binding with many pollutant species. The advantage of graphene material is based on the amphiphilic character which allows removing inorganic and organic molecules at the nanoscale dimension [4]. The large specific surface area and abundant functional groups make GO a strong candidate for wastewater treatment.

## Material and Methods

GO nanosheets were synthesized from graphite powder by the Tour method [1], followed by exfoliated sonification. GO architecture was easily and effectively synthesized by electrophoretic deposition [5]. Electrolysis of Reactive Black 5 (RB5) solution worked under galvanostatic conditions in an electrolytic cell. The synthetic aqueous solution of RB5 was prepared by dissolving  $300 \text{ mg} \cdot \text{L}^{-1}$  of commercial azo dye in NaCl electrolyte. The colour was measured by UV-VIS spectrometer (HITACHI V-2000).

## Results and discussion

The reaction of RB5 in an electrochemical cell with a new GO anode and NaCl as a supporting electrolyte caused discolouration of the solution. Fig. 1 indicated the colour disappearance during the electrochemical and chemical reactions of solution RB5. Almost complete colour removal was achieved within 2 minutes of electrolysis, and RB5 was under the detection limit. The initial dye compounds were degraded to smaller and more polar compounds.

The stability of the electrode was investigated. The electrode was stable without breakouts for 6 minutes; afterwards, the part of the GO film dissolved in the electrolyte. The corrosion of the stainless steel appeared due to an anodic connection. The anode creates the oxygen in consequence the anodic environment is strongly oxidized and very corrosive. The corrosion and gradual destruction of metal started immediately at the disconnection of GO deposition on stainless steel. The mechanism of corrosion produced flacking (surface holes). On the lasting GO deposition, the inclusion was not observed.

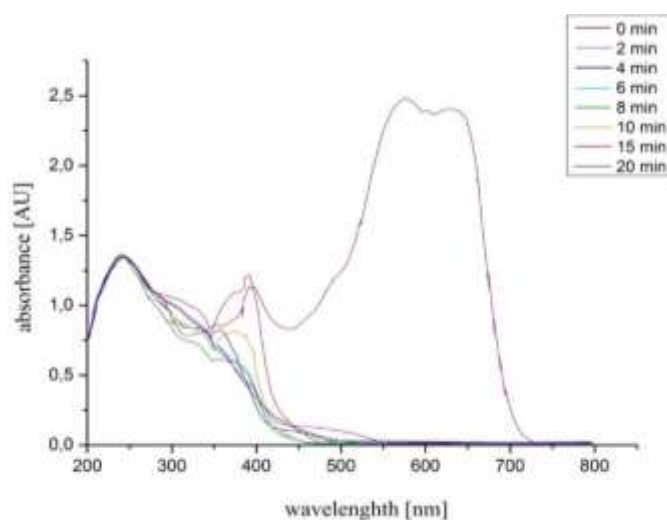


Fig. 1 UV-VIS measurement of RB5 during electrolysis (0, 2, 4, 6, 8, 10, 15 and 20 minutes).

## Conclusion

Graphene oxide-based composites are potentially applicable in environmental applications. The multi-layered graphene film can be continuously grown across the metal grain boundaries of stainless steel and significantly enhance its corrosion resistance [5]. The new electrode can dispose of azo dye in the first two minutes of electro-oxidation. The stability of GO deposition is not sufficient yet. Part of the GO layers was dissolved in the electrolyte and as a consequence process of corrosion was observed. Despite that, the newest research shows, that removal of hazardous chemical materials with GO composite is a prospective alternative for various wastewater treatments. The new electrode is efficient and has a perspective; however, it is necessary to improve stability and repeatability.

## Acknowledgements

This work has been supported by the Marie Curie Programme FP7-People- 2013-IAAPWaSClean project No 612250, H2020-MSCA-RISE-2016-NANOMED project No 734641, APVV-19-0302 and VEGA project No. 2/0156/19.

## References

1. MARCANO, D.C., KOSYNKIN D.V., BERLIN, J.M., SINITSKII, A., SUN, Z., SLESAREV, A., et.al.: Improved synthesis of graphene oxide. *ACS Nano* (2010); 4(8):4806–4814.
2. BROWNSON, D. A. C., SMITH, G. C., BANKS, C. E. (2017) Graphene oxide electrochemistry: the electro-chemistry of graphene oxide modified electrodes reveals coverage dependent beneficial electrocatalysis. *R. Soc. open sci.* 4: 171128.
3. JAGER, D., KUPKA, D., VAČLAVIKOVA, M., IVANICOVA, L., GALLIOS, G. Degradation of Reactive Black 5 by electrochemical oxidation. *Chemosphere* 190 (2018) 405e416
4. PENDOLINO, F., ARMATA, N., (2017): Graphene Oxide in Environmental Remediation Process. In *Springer Briefs in Applied Sciences and Technology*, ISBN 978-3-319-60429-9.
5. MARCIN BEHUNOVA, D., GALLIOS, G., GIRMAN, V., KOLEV, H., KAŇUCHOVÁ, M., DOLINSKÁ, S., & VÁČLAVIKOVÁ, M. (2021). Electrophoretic Deposition of Graphene Oxide on Stainless Steel Substrate. *Nanomaterials*, 11(7), 1779.



## Green Nanopesticides: An approach for the control of Tea pest, *Oligonychus coffeae*

\*Mansi Mishra<sup>a</sup>, Kavya Dashora<sup>a</sup>, Somnath Roy<sup>b</sup>, Zoya Javed<sup>a</sup>, Gyan Datta Tripathi<sup>a</sup>, Meghana Gattupalli<sup>a</sup>

<sup>a</sup>Centre for Rural Development & Technology, Indian Institute of Technology Delhi, New Delhi.

<sup>b</sup>Entomology Department, Tocklai Tea Research Institute, Jorhat, Assam.

\*mansi.mishra@rdat.iitd.ac.in

### Abstract

Tea, *Camellia sinensis*, is a perennial monoculture crop. It is a natural beverage prepared from tender leaves, including a shoot and bud. For different tea pests, it offers a consistent microclimate. *Oligonychus coffeae*, also called Red spider mite (RSM), a sucking pest that causes a dark or reddish-brown stain on the top surface of tea leaves, is among the main tea pests. Crop damage due to the infestation is significant. As a result of the hazardous effects of the acaricide residues on the processed tea leaves, several chemical acaricides are being utilized for the pest control. Investigating alternative pest control methods is urgently necessary. One alternative for the management of RSM might be biosynthesized nanopesticides. Biosynthesized nanopesticides have a high surface-to-volume ratio and regulated, precise distribution, which lowers the environmental risks and consequences. This work investigated the acaricidal efficacy and toxicity of biologically produced nanopesticides to control *Oligonychus coffeae* on tea leaves, which might be a novel approach to improve productivity and biosafety.

**Keywords:** Tea, Red spider mite, Pest management, Nanopesticides, Biosafety.

## Environmentally friendly, electrically conductive, and versatile emulsion-based ink of carbon nanotubes and silver flakes for distributed tactile sensing

M. Najafi<sup>1,2</sup>, M. Safarpour<sup>1,2</sup>, L. Ceseracciu<sup>3</sup>, L. Bertolacci<sup>1</sup>, A. Athanassiou<sup>1</sup>, I. Bayer<sup>1</sup>

<sup>1</sup> Smart Materials, Istituto Italiano di Tecnologia, Via Morego 30, Genova 16163, Italy

<sup>2</sup> DIBRIS, University of Genoa, via Opera Pia 13, Genoa, Italy

<sup>3</sup> Materials Characterization Facility, Istituto Italiano di Tecnologia, Via Morego 30, Genova 16163, Italy

### Abstract

To deal with the effects of electronic waste, the use of polylactic acid (PLA) in green flexible electronics has gotten a lot of interest as a synthetic renewable and biodegradable material. Unfortunately, the development of PLA-based electrical devices is limited by the fact that they can survive three years at sea or in the soil [1]. PLA is highly vulnerable to hydrolytic and enzymatic breakdown in the amorphous area because water may easily infiltrate it, when PLA is mixed with other polymer matrices, phase separation occurs, enhancing water absorption. Aside from that, utilizing a bio-based binder made of a blend of polylactic acid and water-borne polyurethane improves the brittleness of PLA, making it suitable for tactile applications [2, 3].

The fabricated sensor shows an encouraging electrical conductivity of  $1004.1 \pm 2.6$  S/m. Using hybrid conductive micro and nano fillers cause to lowers the percolation threshold and reduces manufacturing costs while keeping the ink's exceptional electrical characteristics [4]. Moreover, CNTs employed as conductivity fillers could bridge the neighboring silver flakes to accelerate electron transport [5]. The large-scale strain sensors have excellent performance over an extensive working range (up to 45% strain), and, as expected, the micro-pressure sensor indicates high-pressure sensitivity ( $0.3\text{kPa}^{-1}$ ) and operation range (0.1-450kPa). Furthermore, the coated ink is biodegradable in marine environments, reducing its accumulation in the ecosystem over time.

### References

1. Wang, J., et al., Biodegradable, flexible, and transparent conducting silver nanowires/polylactide film with high performance for optoelectronic devices. *Polymers*, 2020. 12(3): p. 604.
2. Pyo, S., et al., Recent Progress in Flexible Tactile Sensors for Human-Interactive Systems: From Sensors to Advanced Applications. *Advanced Materials*, 2021: p. 2005902.
3. Lochab, A., et al., Recent advances in carbon based nanomaterials as electrochemical sensor for toxic metal ions in environmental applications. *Materials Today: Proceedings*, 2021.
4. Ambrosetti, G., et al., Solution of the tunneling-percolation problem in the nanocomposite regime. *Physical Review B*, 2010. 81(15): p. 155434.
5. Luo, J., et al., Electrically conductive adhesives based on thermoplastic polyurethane filled with silver flakes and carbon nanotubes. *Composites science and technology*, 2016. 129: p. 191-197.

## Investigating the growth profile of different microalgae strains in nanoemulsion based growth media

Harshita Nigam<sup>1\*</sup>, Anushree Malik<sup>1</sup>, Vikram Singh<sup>2</sup>

<sup>1</sup>Applied Microbiology Laboratory, Centre for Rural Development and Technology, <sup>2</sup>Department of Chemical Engineering, Indian Institute of Technology Delhi, New Delhi, India

\* Corresponding author. Mob: +91 9354721436, E-mail: harshitanigam31@gmail.com

### Abstract:

Microalgal biomass has a wide range of commercial applications. However, the limited biomass productivity using commercially accessible growth mediums obstructs its mass scale productivity. In the present study, previously developed high growth nanoemulsion-based media has been tested for the cultivation of four different microalgae strains. The selected microalgae strains were *Chlorella minutissima*, *Synechocystis pevalekii*, PA4 consortia, and *Navicula* sp. During the 12 days growth period, chlorophyll-a estimation suggested that PA4 consortia showed the highest synthesis of pigment ( $12.7 \mu\text{g ml}^{-1}$ ), followed by *Chlorella minutissima* ( $11.2 \mu\text{g ml}^{-1}$ ), *Synechocystis pevalekii* ( $6.6 \mu\text{g ml}^{-1}$ ), and *Navicula* ( $2.4 \mu\text{g ml}^{-1}$ ) sp. Interestingly, all the four microalgae strains gave higher biomass growth and pigment synthesis (Chl-a) compared to the conventional growth media. The biomass yield obtained was ~1.3 folds in *Chlorella minutissima*, ~2 folds in PA4, 1.3 folds in *S. pevalekii*, and 1.5 folds in *Navicula* sp. in comparison to the control. The cell viability evaluation by MTT assay and total cell counts analysis also confirmed the findings of biomass yield and pigment synthesis. On average, about ~30% more viable cells were obtained in nanoemulsion based media as compared to their control counterparts. Based on the above results, it could be interpreted that the nanoemulsion based media is universal growth promoter for all microalgae strains and could help to solve a significant challenge in microalgae domain. Additionally, the utilization of nanoemulsion growth media promotes biological carbon sequestration and adds a step towards carbon neutrality.

**Keywords:** Nanoemulsion, microalgae, biomass, biofuel, bio-valuable

## A novel Green-Chemistry-inspired approach for lignin-based model compounds valorization by exploiting photocatalytic-microflow reactor

Swaraj R. Pradhan<sup>1\*</sup>, Lisovytskiy Dmytro<sup>1</sup> and Juan C. Colmenares<sup>1\*</sup>

<sup>1</sup> Institute of Physical Chemistry, Polish Academy of Sciences, Kasprzaka 44/52, 01-224 Warsaw, Poland

\* [spradhan@ichf.edu.pl](mailto:spradhan@ichf.edu.pl), \* [jcarloscolmenares@ichf.edu.pl](mailto:jcarloscolmenares@ichf.edu.pl)

### Abstract:

The development of a photocatalytic system for lignin valorization, a significant by-product from paper and pulp industries and bio-refineries, is a challenge because of the high variability in its composition [1]. Microreactor is a superior approach towards photocatalysis because of advantages like improved irradiation profile, sizeable surface-to-volume ratio, enhanced mass transfer characteristics, on-site/on-demand production, higher spatial illumination homogeneity, and better light penetration through the entire reactor depth compared to conventional batch [2]. Recently, the photocatalytic conversion of lignin model compounds especially aromatic alcohol, into its aldehyde has attracted considerable attention due to its fundamental interest and potential applications [3]. Benzyl alcohol oxidation to benzaldehyde is an important reaction, as the aldehyde product finds extensive application in the food, pharmaceutical, perfume, and agrochemical industries. In addition, fluoropolymer-based microreactors have been shown to be a better option in designing the photo-microreactor due to its excellent light transmission and high chemical stability [4].

The current work focuses on the selective photocatalytic oxidation of the lignin-based model compound (benzyl, coniferyl, cinnamyl and vanillin alcohol) in a catalyst deposited polymer-based (Perfluoroalkoxy alkane, PFA) microfluidic photoreactor. Photocatalysis-based selective oxidation of aromatic alcohol has been carried out using commercially available, sol-gel synthesized TiO<sub>2</sub>, monometallic TiO<sub>2</sub>, and bimetallic (e.g., Au/Fe) TiO<sub>2</sub> photocatalysts.

A PFA microtube (microcapillary of 0.8 mm ID), pure from the market, after a cleaning process used for catalyst deposition. An ultrasonic bath (Sonorex-digital RC, 37 kHz, 100% amplitude) was used in sweep mode. The tube was placed in the ultrasonic bath. The catalyst suspension was passed through a cleaned PFA microtube under the influence of ultrasound using a syringe pump (Figure 1). Evaluation of the photocatalytic activity of these micro capillaries carried out for selective conversion of aromatic alcohol to its aldehyde under UV light (375 nm wavelength) [5,6]. The sol-gel synthesized catalysts were analyzed by X-ray diffraction (XRD), UV-Vis DRS, Scanning Electron Microscopy (SEM), and nitrogen physisorption. Some of the important properties of synthesized metal doped catalysts are discussed in table 1.

Table 1. Textural and structural properties of synthesized catalysts.

Photocatalyst	Anatase:Rutile:Brookite phases (%)	Specific Surface Area (m <sup>2</sup> / g)	Bandgap (eV)	Average crystallite size D (nm)
SolT	69:0:31	284	3.3	3.7
CuT	-	577	3.4	-
CoT	-	566	3.4	-
FeT	66:0:34	161	3.1	5.9

\*Sol-gel synthesized TiO<sub>2</sub> (SOLT), 0.5 at% Cu-TiO<sub>2</sub> (CuT), 0.25 at% Co-TiO<sub>2</sub> (CoT), and 0.5 at% Fe-TiO<sub>2</sub> (FeT)

Among all monometallic TiO<sub>2</sub> catalysts, 0.5 at% Fe-TiO<sub>2</sub> showed better BnOH conversion. Though the surface area was increased, crystallinity loss was observed by modifying the catalysts with monometals (Cu, Co).

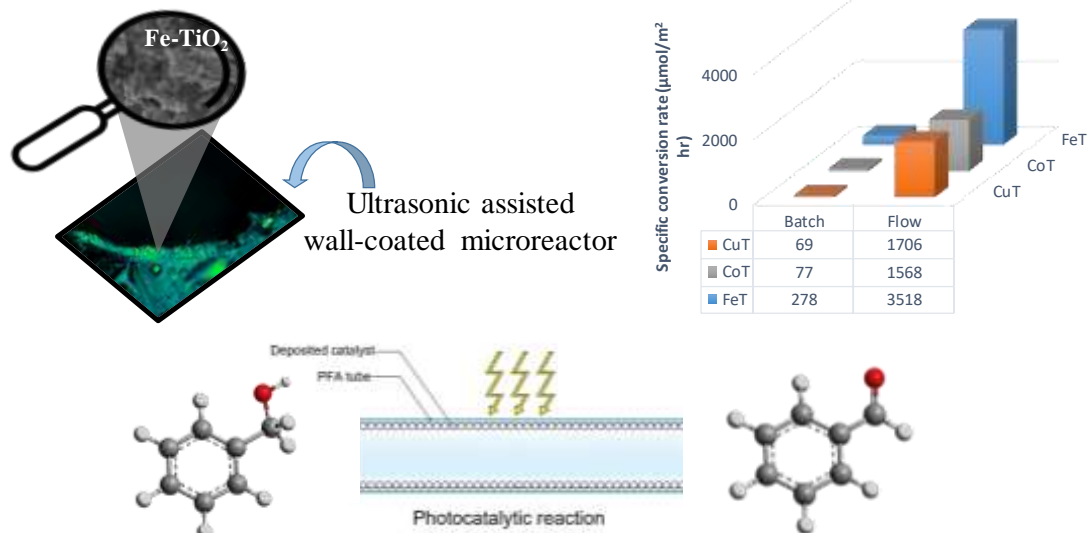


Figure 1. Catalyst deposited PFA microtube and photocatalytic activity of the catalysts. (Sol-gel synthesized TiO<sub>2</sub> (SOLT), 0.5 at% Cu-TiO<sub>2</sub> (CuT), 0.25 at% Co-TiO<sub>2</sub> (CoT), and 0.5 at% Fe-TiO<sub>2</sub> (FeT))

The metal-containing TiO<sub>2</sub> showed higher photocatalytic activity under UV irradiation than the synthesized TiO<sub>2</sub> in the batch system. Among all the metal-containing TiO<sub>2</sub> samples, the 0.5 at% Fe-TiO<sub>2</sub> (both iron and titanium, as cheap, safe, and abundant metals) photocatalyst exhibited the highest BnOH conversion (29%) compared to other catalysts under visible light (515 nm) in a microflow system. This could be explained by the higher crystallite size observed in XRD analysis, high porosity, and flake-like morphology. The utilization of ultrasonication (US) during the deposition process plays a vital role, which leads to an enhanced mass deposition.

The utilization of nano-engineered microreactors as an additive-free system makes it an eco-friendly approach for the selective oxidation of biomass-derived compounds.

### Acknowledgements

This work is supported by the National Science Centre in Poland within SonataBis 5 Project No.2015/18/E/ST5/00306 (<https://photo-catalysis.org/view.php?id=917>).

### References

- E. Gnansounou, A. Pandey, *Life-cycle Assessment of Biorefineries*, 1–39 (2017).  
 T. Noël, J. R. Naber, R. L. Hartman, J. P. McMullen, K. F. Jensen, S. L. Buchwald, *Chem. Sci.*, **2** 287 (2011).  
 X. Yao, Y. Zhang, L. Du, J. Liu, J. Yao, *Renew. Sustain. Energy Rev.*, **47** 519 (2015).  
 B. Ramos, S. Ookawara, Y. Matsushita, and S. Yoshikawa, *J. Environ. Chem. Eng.*, **2** 1487–1494 (2014).  
 C. Zheng, G. He, X. Xiao, M. Lu, H. Zhong, X. Zuo, J. Nan, *Applied Catalysis B: Environmental*, **205** 201 (2017).  
 S. R. Pradhan, V. Nair, D. Giannakoudakis, D. Lisovytskiy, J. C. Colmenares, *Mol. Catal.*, **486** 110884 (2020).  
 S. R. Pradhan, D. Lisovytskiy, J. C. Colmenares, *Catal. Commun.*, **162** 106375 (2022).

## Surface chemistry of new CQDs produced using a microwave-assisted approach as an effective organic pollution removal agent in water medium

Jovana R Prekodravac<sup>1\*</sup>, Bojana R Vasiljević<sup>1</sup>, Dejan Kepić<sup>1</sup>, Milica Budimir<sup>1</sup> and Biljana Todorović Marković<sup>1</sup>

<sup>1</sup> Institute of the Nuclear Sciences Vinča – National Institute of the Republic of Serbia, University of Belgrade, P.O.B. 522, Belgrade, Serbia

\*prekodravac@vin.bg.ac.rs

The pursuit of appropriate photocatalytic material for the treatment of colored industrial discharges, as a major environmental problem, continues in the modern age [1]. The zero-dimensional carbon nanostructures (carbon quantum dots–CQD) with exceptional physicochemical characteristics have a wide range of potential uses, including photocatalytic remediation of organic water contaminants [2]. Here we present nitrogen (N-CQD) and iron/nitrogen co-doped (Fe/N-CQD) quantum dot nanomaterials produced by a microwave-assisted approach as a one-step, environmentally friendly, and cost-effective method. The photoactivity of produced materials on a case study of a specific water pollutant reduction was investigated by exploring the synergistic effect of light source illuminations and the surface chemistry of the materials.

The N-CQD and Fe/N-CQD were synthesized by the simple microwave-assisted method starting from glucose water solution. The reaction mixture containing carbon, nitrogen and/or iron source was heated in a microwave reactor for 1 minute at a fixed temperature (100 °C), followed by cooling down to room temperature [3].

Detailed AFM characterization of produced nanomaterials showed the formation of spherical like shapes with average real particle diameter between 15 and 40 nm. From the EDS results, obtained CQD had a high content of C (64–66 at%) and O (21–24 at%), while XPS analysis showed the presence of N in the form of pyridinic, pyrrolic and graphitic-N, and Fe as Fe<sup>2+</sup>/Fe<sup>3+</sup> (Table 1). Photocatalytic experiments were performed in batch reaction conditions using two light irradiation sources, applying the commercially available lamp (*L*) source (470 nm, 10W) and a closed cylindrical reactor (*R*) with six LEDs (370 nm, 6W) made in our team.

Table 1. The XPS elemental analysis of the N-CQD and Fe/N-CQD samples.

Sample	Elemental analysis			
	C	O	N	Fe
N-CQD	66.4 at%	23.5 at%	10.1 at%	/
Fe/N-CQD	63.8 at%	27.5 at%	6.7 at%	2.0 at%

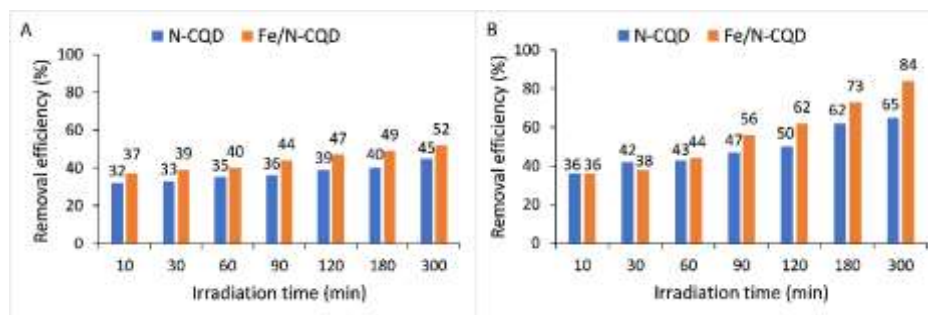


Figure 1. The histograms represent the photoactivity of N-CQD and Fe/N-CQD under (A) the *L* and (B) the *R* as irradiation sources.

When comparing the home-made *R* type irradiation source to a commercially available *L* source, the obtained results showed that the *R* source was more efficient in MB degradation regardless of the photocatalyst's surface chemistry (Figure 1). The *L* source as a free-standing lamp provokes more light scattering than the *R* source. In comparison, the *R* design, which consisted of a closed cylindrical tube with a particular *LED* configuration, allowed for more homogenous light dispersion. The Fe/N-CQD showed improved photoactivity in MB degradation compared to the N-CQD. When Fe/N coordination bonds occur, the electron density on the N atoms decreases, which is believed to be due to electron transfer from the N to the Fe atoms. Consequently, the Fe/N dopants

improve CQD electron-accepting and electron-donating properties, as well as their conductivity, which is advantageous to the entire electron-transfer process and, enhances material's photocatalytic capacity.

### Acknowledgements

The research was supported by the Science Fund of the Republic of Serbia, #7741955, Are photoactive nanoparticles salvation for global infectious disease? - PHOTOGUN4MICROBES and by the Ministry of Education, Science and Technological Development of the Republic of Serbia grant number 451-03-68/2022-14/200017.

### References

- [1] M. Ismail, K. Akhtar, M.I. Khan, T. Kamal, M.A. Khan, A. M. Asiri, J. Seo, S.B. Khan, *Current Pharmaceutical Design*, **25** 3645 (2019).
- [2] T. Teymoorian, N. Hashemi, M.H. Mousazadeh, Z. Entezarian, *SN Applied Sciences*, **3** 305 (2021).
- [3] J. Prekodravac, B. Vasiljević, Z. Marković, D. Jovanović, D. Kleut, Z. Špitalský, M. Mičušík, M. Danko, D. Bajuk-Bogdanović, B. Todorović-Marković, *Ceramics International*, **45** 17006 (2019).

## Synthesis of zinc oxide nanoparticles using Japanese knotweed extract

Miha Ravbar<sup>a,\*</sup>, Andraž Šuligoj<sup>a,b</sup>

<sup>a</sup> Faculty of chemistry and chemical technology, University of Ljubljana, Večna pot 113, 1000 Ljubljana, Slovenia

<sup>b</sup> National institute of chemistry, Hajdrihova 19, 1001 Ljubljana, Slovenia

\*e-mail: miha.ravbar@fkkt.uni-lj.si

Due to ever increasing environmental concerns, a lot of research is being done on the topic of photocatalytic degradation of organic pollutants in water<sup>1</sup>. While titanium dioxide is still the most popular of these photocatalysts, increasing amount of research is being directed toward others, such as zinc oxide, which has comparable electronic, physical and chemical properties and a more facile synthesis<sup>2</sup>. Although green synthesis of ZnO nanoparticles (NPs) using different plant extracts has been reported extensively, the attention is usually given to the synthesis route and antimicrobial and photocatalytic properties of NPs<sup>3</sup>. The effect of plant extracts on morphological and electronical properties, and the role plant extracts play in these changes is seldomly reported.

Herein, we synthesized ZnO nanoparticles (NPs) via a facile synthesis using ethanolic extracts from roots of Japanese knotweed (lat. *Fallopia japonica*). Such NPs were characterized by slower and more controllable crystallite growth upon thermal annealing at 450 °C as well as comparable long-term photocatalytic activity for the degradation of ciprofloxacin. In addition, the modified synthesis route using plant extracts resulted in better antimicrobial activity against both Gram-positive bacteria e.g., *Staphylococcus aureus* and Gram-negative bacteria e.g., *Escherichia coli* and *Campylobacter jejuni*. The materials were further tested for their antimicrobial activity against *S. aureus* under UV-illumination where, again, the photocatalyst prepared with plant extracts was proven to be superior. The main culprit for the observed differences was identified to be the leftovers of plant extract molecules on the surface of the catalyst and was studied extensively by means of thermal gravimetry coupled with mass spectrometry.

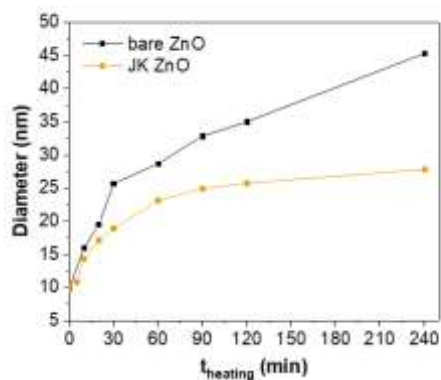


Figure 1: Growth of particles with respect to their annealing time

### References

1. Y. Zhao, Y. Li, L. Sun, *Chemosphere*, **276**, 130201 (2021).
2. S. Murgolo, C. De Ceglie, C. Di Iaconi, G. Mascolo, *Curr. Opin. Green Sustain. Chem.*, **30**, 100473 (2021).
3. P. Basnet, T. Inakhunbi Chanu, D. Samanta, S. Chatterjee, *J. Photochem. Photobiol. B Biol.*, **183**, 201 (2018).



## Synthesis of Ag/Ag<sub>2</sub>O nanoparticles on cellulose paper and cotton fabric using *Eucalyptus globulus* leaf extracts: toward the clarification of formation mechanism

Pablo Salgado<sup>1\*</sup>, Luis Bustamante<sup>2</sup>, Danilo J. Carmona<sup>3</sup>, Manuel Melendrez<sup>4</sup>, Olga Rubilar<sup>5</sup>, Claudio Salazar<sup>1</sup>, Andy J. Pérez<sup>2</sup> and Gladys Vidal<sup>6</sup>

<sup>1</sup>Departamento de Ingeniería Civil, Facultad de Ingeniería, Universidad Católica de la Santísima Concepción, Concepción, Chile

<sup>2</sup>Departamento de Análisis Instrumental, Facultad de Farmacia, Universidad de Concepción, Chile

<sup>3</sup>Departamento de Química Orgánica y Fisicoquímica, Facultad de Ciencias Químicas y Farmacéuticas, Universidad de Chile, Independencia, Santiago, Chile

<sup>4</sup>Department of Materials Engineering (DIMAT), Faculty of Engineering, University of Concepcion, Concepcion, Chile

<sup>5</sup>Centro de Excelencia en Investigación Biotecnológica Aplicada al Medio Ambiente (CIBAMA-BIOREN), Facultad de Ingeniería y Ciencias, Universidad de La Frontera, Chile

<sup>6</sup>Grupo de Ingeniería y Biotecnología Ambiental, Facultad de Ciencias Ambientales y Centro EULA-Chile, Universidad de Concepción, Concepción.

\*psalgado@ucsc.cl

The silver nanoparticles (AgNP) have aroused wide attention in the field of wastewater remediation, especially because its antibacterial activity. Additionally, the green synthesis of nanoparticles is gaining much attention due to its low costs and the use of environmentally friendly chemical compounds derived from plant extracts[1]. However, our understanding of the role of phytochemicals in plant extracts as reducing and capping agents is still not entirely clear. The present study reports the use of *Eucalyptus globulus* leaf extracts and AgNO<sub>3</sub> in obtaining AgNP synthesized on paper and fabric supports with or without addition of NaOH.

The AgNPs were characterized in their morphology and structure by SEM-EDS, TEM-SAED, XRD and UV-Vis diffuse reflectance. To know the mechanism involved in the formation of AgNP, FTIR, UV-Visible spectrophotometry and UHPLC-QTOF-MS analyzes were carried out of *E. globulus* extracts before and after the synthesis of AgNP. Figure 1 shows the visual appearance of the supports with silver nanoparticles and the SEM images of these.

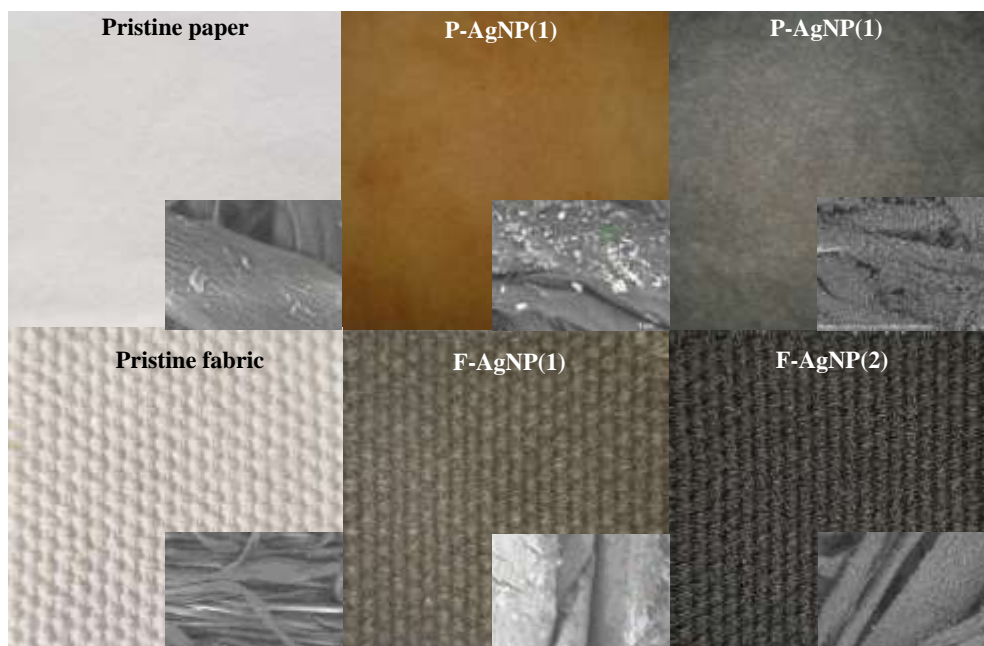


Figure 1. Photographic images of supports and AgNPs supported. Inset figures are SEM images

The results indicate the formation of Ag and Ag<sub>2</sub>O nanoparticles depending on the influence of NaOH in the reaction system (Table 1).

Table 1. Diffraction planes and peaks in P-AgNP(1), P-AgNP(2), F-AgNP(1) and F-AgNP(2) obtained from XRD analysis.

Silver nanoparticle	Diffraction planes	2 $\theta$ (°)			
		P-AgNP(1)	P-AgNP(2)	F-AgNP(1)	F-AgNP(2)
Ag	(111)	38.44	38.17	38.09	37.97
	(200)	44.35	44.31	44.29	44.09
	(220)	64.88	64.52	64.44	64.34
	(311)	78.82	77.45	77.34	77.25
Ag <sub>2</sub> O	(110)	27.81	n.d.	27.73	n.d.
	(111)	32.26	n.d.	32.12	n.d.
	(200)	38.44	n.d.	38.09	n.d.
	(211)	46.22	n.d.	46.15	n.d.
	(220)	54.89	n.d.	54.77	n.d.
	(221)	57.46	n.d.	57.36	n.d.
	(311)	65.80	n.d.	n.d.	n.d.
	(222)	67.77	n.d.	67.31	n.d.

It was also possible to find the presence of phenolic compounds, reducing sugars and proteins in extracts. Phenolic compounds, and to a lesser extent reducing sugars mainly participate as reducing agents in the formation of AgNP, while phenolic compounds would participate as stabilizing agents.

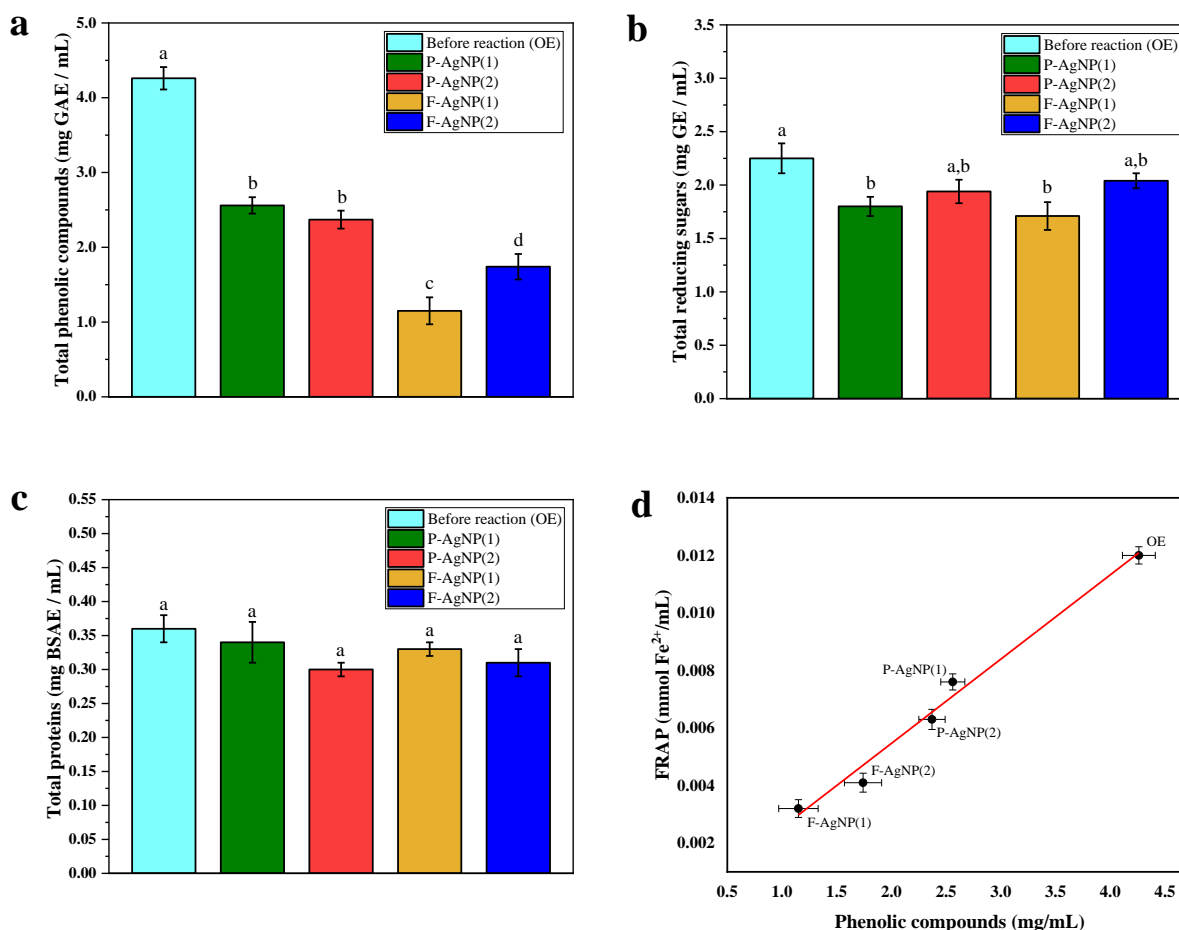


Figure 2. a) Spectrophotometric analysis of phenolic compounds, b) reducing sugars and c) proteins in the original extract (OE) of *E. globulus* before and after the synthesis of AgNP; and d) relation between FRAP and phenolic compounds in *E. globulus* extracts before (OE) and after synthesis of AgNP. Inset legend represents samples. Data are expressed as mean  $\pm$ SD. Different letters on bars indicates significant difference ( $p < 0.05$ ). Differences among groups were compared by ANOVA with Tukey post-hoc analysis.

Furthermore, the supported AgNPs showed considerable antibacterial activity against *E. coli* K12 and photocatalytic activity at visible light.

This study provides evidence of a simple process to support AgNP on cellulose and also providing key information towards the definitive clarification of the mechanism of formation of AgNP by green synthesis.

## **Acknowledgements**

This research was funded by ANID/FONDAP/15130015 and ANID Convocatoria Nacional Subvención a Instalación en la Academia convocatoria año 2019 Folio PAI77190082. Authors would like to acknowledge FONDEQUIP EQM170023 for facilitating UHPLC-QTOF-MS analysis.

## **References**

1. Swilam, N., Nematallah, K.A., 2020. Polyphenols profile of pomegranate leaves and their role in green synthesis of silver nanoparticles. *Scientific Reports* 10(1), 14851.

## Investigation of photocatalytic properties of titanium dioxide nanoparticles onto ceramic roof tiles

M. Kouroutzi<sup>1</sup>, A. K. Stratidakis<sup>2</sup>, M. Kermenidou<sup>1,3</sup>, S. P. Karakitsios<sup>1,3</sup>, D. A. Sarigiannis<sup>1,2,3\*</sup>

<sup>1</sup>Aristotle University of Thessaloniki, Department of Chemical Engineering, University Campus, 54124 Thessaloniki, Greece

<sup>2</sup>Environmental Health Engineering, Institute for Advanced Study IUSS, Pavia, Italy

<sup>3</sup>HERACLES Research Center on the Exposome and Health, Center for Interdisciplinary Research and Innovation, Balkan Center, Bldg. B, 10th km Thessaloniki-Thermi Road, 57001, Greece

\* sarigiannis@cheng.auth.gr

Environmental conditions of the modern era prove that the need for the development of a new bioclimatic product which could improve our living environment is crucial. Based on this, the idea of a “cool roof” comes up with the purpose to improve the microclimate of one or several buildings in an extended urban area, by introducing cool roof tiles with photocatalytic activity.

Titanium dioxide (TiO<sub>2</sub>) is a widely available material, well-known for its photocatalytic ability while being non-toxic and non-hazardous to environmental and human health. To date, applications of TiO<sub>2</sub> nanoparticles include photocatalytic water splitting [1, 2], purification of pollutants [3, 4, 5, 6], photocatalytic self-cleaning [4], photocatalytic antibacterial [7,8,4,5], photo-induced super hydrophilicity [3,8,4,] as well as in photovoltaics [3, 9,10,11] and photosynthesis [12].

Amphiphilic polymeric materials including Polyethylene Glycol (PEG) and Pluronic F-127 have been used in this project aiming to enhance the photocatalytic performance of the TiO<sub>2</sub> nanoparticles. Suspensions of TiO<sub>2</sub> nanoparticles with and without the addition of PEG and Pluronic F-127 were developed after mixing with deionized water under magnetic stirring and ultrasonic action. Part of the suspensions was applied onto the surface of roof tiles and part of it was dried at different temperatures for the characterization of the novel nanoparticles. TiO<sub>2</sub>/PEG nanoparticles were dried at 100°C and 290°C and TiO<sub>2</sub>/Pluronic F-127 were dried at 100°C and 350°C. 290°C and 350°C were selected as temperatures at which PEG and Pluronic F-127 are being degraded, respectively. TiO<sub>2</sub> aqueous suspensions were dried at the same temperatures and used as control samples.

Characterization techniques including Scanning Electron Microscopy (SEM) and the BET (Brunauer-Emmett-Teller) Method were used for the examination of the distribution of nanoparticles onto the surface of the tiles and for the estimation of their specific surface areas. The band gap of all examined samples was estimated by a UV-Vis spectrophotometer between 270 and 800 nm.

An experimental photocatalytic set-up was designed by the research team, composed by the reactor, an ultra-violet source, a target gas pollutant (NO) supply, flow rate valves and a photocatalytic chart station. NO gas with synthetic air were inserted into the layout, into the chamber where the prepared coated tiles were placed and subsequently irradiated with ultraviolet light. The decrease in concentration of pollutants was recorded at predetermined time intervals.

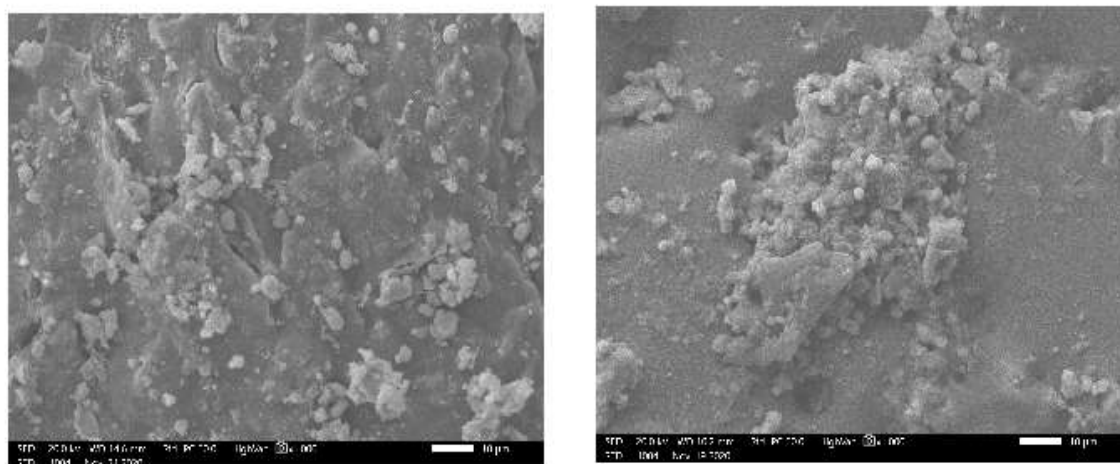


Figure 49: (A) SEM image of TiO<sub>2</sub>/PEG nanoparticles dried at 290 °C; (B) SEM image of TiO<sub>2</sub>/PEG nanoparticles dried at 100 °C

Table 11: Specific Surface Area results and Band Gap of the examined samples

Sample	Description of the sample	Specific Surface Area (m <sup>2</sup> /g)	Band Gap (eV)
#1	TiO <sub>2</sub> /PEG	75.65	3.80
#2	TiO <sub>2</sub>	61.73	3.85
#3	TiO <sub>2</sub> /Pluronic-F127	71.80	4.05

Scanning Electron Microscopy (SEM) images of TiO<sub>2</sub>/PEG nanoparticles dried at 100°C and 290°C are presented in Figure 1A and 1B, respectively, exhibiting the dispersion of both types of nanoparticles onto the surface of the roof tiles.

The results obtained from the characterisation techniques for three types of samples dried at 100°C, are presented in Table 1, aiming to highlight the correlation between the specific surface area of the novel nanoparticles and their band gap. The sample with the highest specific surface area (TiO<sub>2</sub>/PEG), is more possible to exhibit better photocatalytic activity, due to its greater specific surface area (75.65 m<sup>2</sup>/g) and its lower band gap (3.80 eV). As already known, the lower band gap has a positive effect on the photocatalytic activity as lower energy is needed to arouse a photocatalytic reaction [13].

Based on the characterisation results of the studied samples obtained from BET and UV-Vis experiments, nanoparticles of TiO<sub>2</sub> with PEG will potentially exhibit the highest photocatalytic activity among all studied samples. According to preliminary results obtained from the photocatalytic experiments, it was shown that TiO<sub>2</sub>/PEG photocatalytic coating samples exhibited high photocatalytic activity. Additional experiments on the photocatalytic activity of all samples will be conducted for the verification of the present results.

### Acknowledgements

This research was conducted as part of the research project “Green Tile Development-KERAMI” in collaboration with “KEBE-Northern Greece Ceramics” and was funded by the Operational Programme Competitiveness, Entrepreneurship and Innovation 2014-2020 (EPAnEK) of the Hellenic Ministry of Economy and Development.

### References

- O'regan, B., & Grätzel, M. (1991). A low-cost, high-efficiency solar cell based on dye-sensitized colloidal TiO<sub>2</sub> films. *nature*, 353(6346), 737-740.
- Ni, M. (2007). Leung DYC and Sumathy K Renew. *Sust. Energ. Rev.*, 11, 401.
- Carp, O., Huisman, C., & Reller, A. (2004). Environmental toxicity and antimicrobial efficiency of titanium dioxide nanoparticles in suspension. *Progress Solid State Chemical*, 32, 33-38.
- Hashimoto, K., Irie, H., & Fujishima, A. (2005). Invited Review Papers-TiO<sub>2</sub> Photocatalysis: A Historical Overview and Future Prospects. *Japanese Journal of Applied Physics-Part 1 Regular Papers and Short Notes*, 44(12), 8269-8285.
- Murphy, R., & Strongin, D. R. (2009). Surface reactivity of pyrite and related sulfides. *Surface Science Reports*, 64(1), 1-45.
- Sunley, G. J., & Watson, D. J. (2000). High productivity methanol carbonylation catalysis using iridium: the Cativa™ process for the manufacture of acetic acid. *Catalysis Today*, 58(4), 293-307.
- Blake, D. M., Maness, P.-C., Huang, Z., Wolfrum, E. J., Huang, J., & Jacoby, W. A. (1999). Application of the photocatalytic chemistry of titanium dioxide to disinfection and the killing of cancer cells. *Separation and purification methods*, 28(1), 1-50.
- Fujishima, A., Rao, T., & Tryk, D. (2000). P-Doped titania xerogels as efficient UV-visible photocatalysts. *J. Photochem. Photobiol., C*, 1, 1-21.
- Grätzel, M. (2001). Solar water splitting cells. *nature*, 414, 338-344.
- Grätzel, M. (2004). Conversion of sunlight to electric power by nanocrystalline dye-sensitized solar cells. *Journal of Photochemistry and Photobiology A: Chemistry*, 164(1-3), 3-14.
- Laschewsky, A. (2003). Polymerized micelles with compartments. *Current opinion in colloid & interface science*, 8(3), 274-281.
- Carp, O., Huisman, C., & Reller, A. (2004). Environmental toxicity and antimicrobial efficiency of titanium dioxide nanoparticles in suspension. *Progress Solid State Chemical*, 32, 33-38.
- Liao, D., & Liao, B. (2007). Shape, size and photocatalytic activity control of TiO<sub>2</sub> nanoparticles with surfactants. *Journal of Photochemistry and Photobiology A: Chemistry*, 187(2-3), 363-369.

## Harvesting of hot holes and hot electrons generated on plasmonic nanostructures for amine photooxidation reaction

Swathi Swaminathan<sup>1\*</sup>, Vishal Govind Rao<sup>1</sup>, Jitendra K. Bera<sup>1</sup>, Manabendra Chandra<sup>1</sup>

<sup>1</sup>Department of Chemistry, Indian Institute of Technology, Kanpur, Uttar Pradesh-208016, India

\*swathis@iitk.ac.in

Abstract text:

The hot charge carriers (electrons-holes) created as a result of visible light excitation of Au NP has been simultaneously extracted and utilized for driving oxidative coupling of benzylamine to N-benzylidenebenzylamine. The potential energy of the charge carriers can be tuned relative to the redox potential of the reactant molecules demonstrating a wavelength dependence in the catalytic product conversion. The reaction intermediates and products were captured using *in situ* Raman, NMR spectroscopy and a plausible reaction mechanism has been proposed.

Solar light driven photocatalytic materials continue to attract keen interest due to its ability to harvest light efficiently and its capability to reduce the high energy cost of common industrial chemical processes. Plasmonic metal nanoparticles and semiconductor based photocatalysts are widely used in such applications. Semiconductors have wider band gaps compared to metals. Albeit the extensive adoption of semiconductor-based catalysts in practice, wide band gaps and absorption in the ultraviolet region reduce the efficiency in the catalytic processes. The portion of solar radiation attributable to the visible and ultraviolet light are 42% and 4%, respectively. Catalysts active in the visible spectrum of the solar radiation are thus expected to be efficient in comparison with those active in the UV region. Therefore, studies have attempted to discover numerous new materials and develop new strategies in order to efficiently utilise visible light to carry out catalysis. Surface plasmon resonance fosters excellent absorption of the visible light by plasmonic metal nanoparticles (Au, Ag and Cu). Due to their inherent LSPR property they possess broadly tunable optical properties coupled with catalytically active sites that offer unique opportunity for photocatalysis.

We demonstrate the visible-light-driven amine oxidation reaction with the use of gold nanoparticles.<sup>1</sup> These nanostructures, which were synthesised and characterised in our laboratory, serve as water soluble photocatalysts. These chemical transformations occur under ambient laboratory conditions, powered only by a visible light source, utilising the atmospheric oxygen to carry out the reaction. The reaction was monitored through SERS and NMR techniques. We establish a clear wavelength dependence on the enhancement of the product formation. Additionally, the mechanistic studies provide unambiguous evidence for the involvement of both hot electrons and holes in photoinitiation of the substrate. Formation of these hot carriers is a result of the charge separation following the plasmonic non radiative relaxation, which enhances the conversion by 30-40 fold relative to controls. This leads to the formation of an intermediate radical species facilitating a radical pathway. Optimisation of the nanostructure allows for oxidative coupling of several substituted amines as a function of their oxidative potential. We further observed that the amine oxidation reaction is highly selective due to its operation at a low temperature and using a low intensity of visible irradiation. The catalyst achieved a high turnover number through its effective use in low concentrations. These results have important implications for plasmon hot carrier photocatalysis.

### Acknowledgements

S.S. acknowledges support from Ministry of Electronics & Information Technology, Government of India, for a Senior Research Fellowship under the Visvesvaraya PhD Scheme.

### References

1. S. Swaminathan, V. G. Rao, J. K. Bera, M. Chandra, *Angew. Chem. Int. Ed.*, 60, 22, 12532 (2021).

## Versatile synthesis of graphene materials for the removal of copper ions from aqueous solutions

Dimitrios G. Trikkaliotis<sup>1</sup>, Dimitra A. Lambropoulou<sup>2,3</sup>, Athanasios C. Mitropoulos<sup>1</sup>, George Z. Kyzas<sup>1\*</sup>

<sup>1</sup>Department of Chemistry, International Hellenic University, Kavala, Greece

<sup>2</sup>Laboratory of Environmental Pollution Control, Department of Chemistry, Aristotle University of Thessaloniki, GR-541 24 Thessaloniki, Greece,

\*Correspondence: [kyzas@chem.ihu.gr](mailto:kyzas@chem.ihu.gr)

### Abstract

Graphene materials are extensively used in many fields and applications [1]. Here, we present the versatility of graphene oxide (GO) as composite with two multifunctional green polymers chitosan (CS) and poly(vinyl alcohol) (PVA) in wastewater treatment [2]. In the first section we demonstrate a low cost environmental friendly path for the synthesis of GO and reduced GO (rGO thermally processed). The second section is devoted to the synthesis of composite materials in bead and film form. The removal of copper ions from aqueous solutions was studied as a function of solutions temperature, pH and contact time. Pseudo-second kinetic model and Langmuir isotherm fitted the experimental data sufficiently; and thermodynamic studies indicated that the process was spontaneous and endothermic. All raw materials and composites were characterized with AFM, XRD, SEM, EDX, FTIR and BET. Indicative photos of the laboratory products, which are suitable candidates for industrial-scale applications, are displayed.

### Materials and Methods

#### i) GO synthesis

All materials were used as received. Graphite flakes (75 % over 150  $\mu\text{m}$ , 332461), sulfuric acid (98 %), potassium permanganate (99 %) and hydrogen peroxide (30 %) were supplied from Merck Ltd. A simplified Hummers method, without the use of sodium nitrate, was followed for the synthesis of GO, which is then thermally reduced under vacuum.

Briefly, graphite flakes (10 g) were stirred in 230 mL of concentrated  $\text{H}_2\text{SO}_4$  (temperature of solution was  $\sim 0^\circ\text{C}$ ). Then,  $\text{KMnO}_4$  (30 g) was slowly added to the suspension. The rate of addition was controlled to prevent the rapid rise in the temperature of the suspension, which should be less than  $20^\circ\text{C}$ . The reaction mixture was then cooled to  $2^\circ\text{C}$ . After the removal of the ice-bath, the mixture was stirred at room temperature for 30 min. Double distilled water (230 mL,  $\sim 1.5 \mu\text{S}/\text{cm}$ ) was slowly added to the reaction vessel, keeping the solution temperature less than  $98^\circ\text{C}$ . The diluted suspension was stirred for additional 15 min, was further diluted with 1400 mL of double distilled water and then 100 mL of a 30 wt.% solution of  $\text{H}_2\text{O}_2$  was added. The mixture was left overnight. GO particles that settled at the bottom were separated from the excess liquid by decantation. Then, the wet form of GO was separated by centrifugation and washed with deionized water ( $5\text{--}8 \mu\text{S}/\text{cm}$ ) till reach pH  $\sim 6$ . The gel-like material was freeze dried and the GO was obtained (Fig.1A). The rapid heating of GO at  $250^\circ\text{C}$  under vacuum resulted in simultaneous reduction-exfoliation and production of low-oxidized GO.

#### ii) Beads & Films synthesis

The reagents were used as received. Chitosan (310–375 kDa, DDA > 75 %), poly(vinyl alcohol) (MW 13000–23000, 87–89 % hydrolyzed), glutaraldehyde (abbreviated as GLA, 50 % in  $\text{H}_2\text{O}$ ) and sodium tripolyphosphate (abbreviated as TPP, 98 %) were purchased from Sigma-Aldrich.

Briefly, the GO/CS/PVA blend was stirred at  $50^\circ\text{C}$  to form homogenous solution. Although the physical H-bonding in CS/PVA blends results to network with thermal stability and reduced solubility in acidic solutions, suitable cross-linking leads to highly insoluble composites. GLA and TPP were the cross-linking agents and their concentrations were selected in relation to CS amino groups. The aim is to prepare a material that presented high adsorption capacity, which means to have free functional groups (able to bind the copper ions) as well as high durability which means it has to be strongly crosslinked with reagents (i.e. GLA and TPP) so as to render the extreme conditions of effluents. The latter means that the addition of GLA will immediately bind the free functional groups of chitosan. So, it was mandatory to find a balance (optimum ratio) between the added quantity of cross-linker over the whole quantity of the final material. This was the reason that we followed the suggestion of Filipkowska et al. for the bare minimum amount of GLA and TPP as the degree of deacetylation is in close proximity [3]. So, chitosan cross-linked with a homobifunctional aldehyde (GLA) is described by a simplified imine formation with primary amines originating from chitosan. Considering this mechanism, the theoretical stoichiometric ratio for a complete conversion would be 0.5 mol GLA per 1.0 mol of primary amine. The amount of primary amines is calculated (Eq. (1)) by using the degree of deacetylation (DD), and the molecular weight of glucosamine is used as the structural repeating unit (SRU).

$$n_{(\text{primary amine})} = \left( \frac{m_{\text{CS}}}{m_{\text{SRU}}} \right) \cdot \frac{\text{DD}}{100} \quad (1)$$

Then, the mixture was added dropwise to double-distilled water and left for 24 h in gentle stirring at room temperature. The hydrogel beads were washed with deionized water several times till the removal of the residual reagents and dried at  $40^\circ\text{C}$  (Fig.1D). A special discussion can be done for the reason of selecting at least two different cross-linking agents. Chitosan presents high swelling degree in aqueous solutions. Especially in a

powdered form, swells considerably and crumble easily, thus not behaving ideally in packed column configurations common to pump-and-treat adsorption processes, usually leading to plugging of the column. For pure chitosan swelling degrees as high as 2000 % have been reported. In order to overcome this problem chitosan could be crosslinked either covalently, by glutaraldehyde (GLA) or ionically, by a polyanion such as tripolyphosphate (TPP).

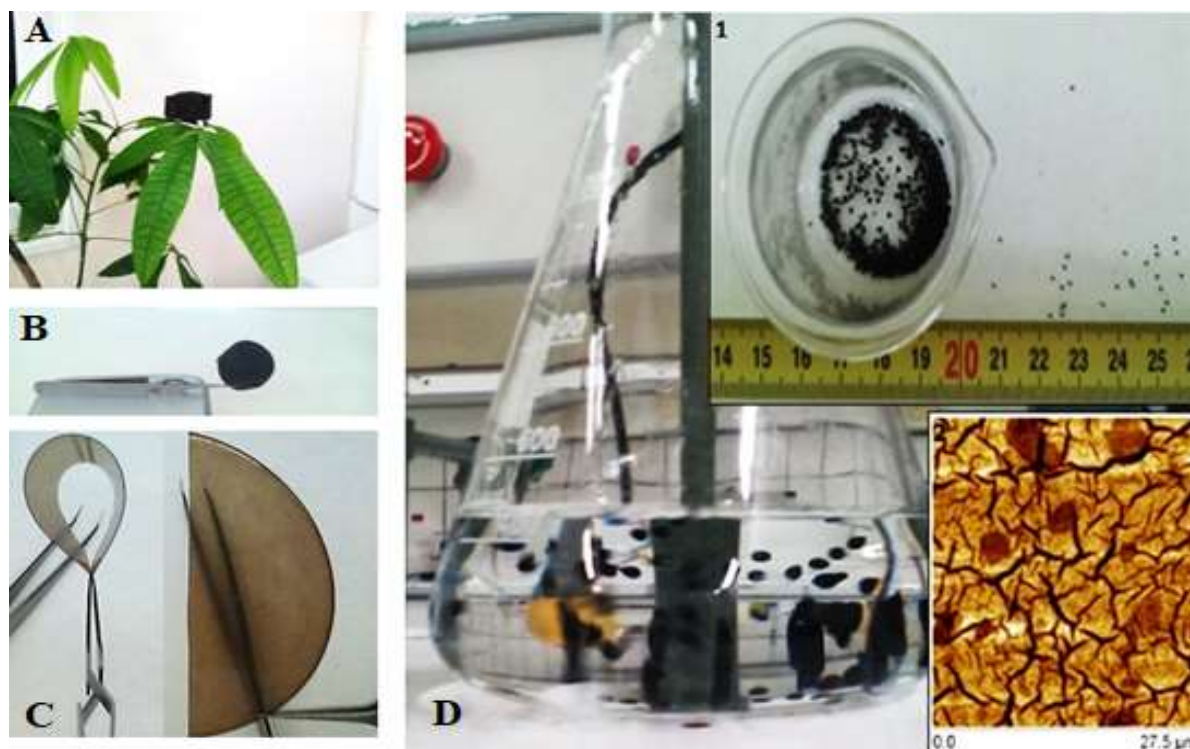


Fig.1. (A) GO aerogel, (B) GO paper, (C) GO/CS/PVA film, (D) GO/CS/PVA adsorbent for water decontamination, (inset1) micro-beads  $\sim 800\mu\text{m}$  and (inset2) visualization of GO sheet dispersion into the polymeric matrix using AFM.

## Results

### i) GO & rGO

The successful synthesis of GO was confirmed through XRD and FTIR characterization techniques and supported with SEM-EDX, UV-Vis, BET and AFM (Fig.2).



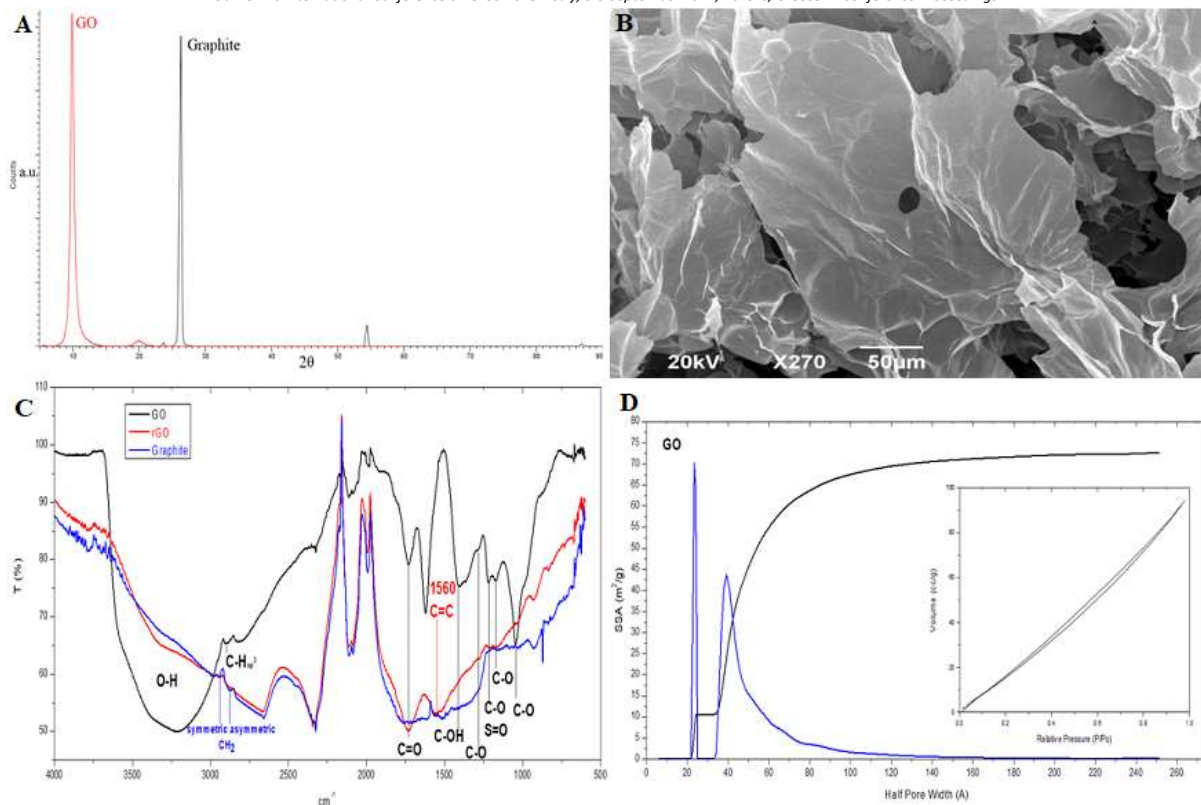


Fig.2. (A) XRD of graphite and GO, (B) SEM of GO, (C) FTIR of graphite, GO and rGO, (D) BET of GO.

Table 1. XRD properties of graphite, GO and rGO

Material	C (%)	d (nm)	S (nm)	Layers/Crystallite
Graphite	92.0	0.339	23.10	68 - 69
GO	70.3	0.929	12.11	13 - 14
rGO	45.1	0.675	2.18	3 - 4

C: crystallinity; d: interlayer distance; S: crystallite size

## ii) Beads & Films

The same raw materials were utilized for the synthesis of beads and films. XRD, FTIR, SEM-EDX and AFM illuminated the composites' structure while the UV-Vis characterization technique was applied to evaluate the copper ions adsorption (Fig.3).

In this study, Cs/PVA/GO blends in bead and film form were used as novel adsorbents for Cu(II) ions removal from aqueous solutions. The selection of copper ions as model pollutant in the present is based on the fact that  $\text{Cu}^{2+}$  can be found in high concentrations because it is usually used in many industrial sectors like metal finishing, electroplating, plastics, and etching. It is recognized as one of the most widespread heavy metal contaminants in the environment. Water contaminated with copper must be treated before being discharged into the environment because of its toxic properties, even at low concentrations. The influence of pH, temperature, contact time and initial copper ion concentration were studied. The effect of initial copper concentration on equilibrium was investigated by carrying out adsorption experiments with the following conditions ( $m=0.03$  g,  $V=30$  mL,  $T=25, 35, 45$  °C,  $N=125$  rpm,  $\text{pH}=5$ ,  $t=24$  h,  $C_0=10-200$  mg/L). Adsorption data were fitted by Langmuir, Freundlich, Langmuir-Freundlich, Temkin, Redlich, and Dubinin-Radushkevich isotherm models. Pseudo-1st, pseudo-2nd order and intra-particle diffusion model were applied to analyze the adsorption kinetic mechanism of Cu(II) onto the beads. Pseudo-second kinetic model and Langmuir isotherm fitted the experimental data sufficiently; and thermodynamic studies indicated that the process was spontaneous and endothermic.

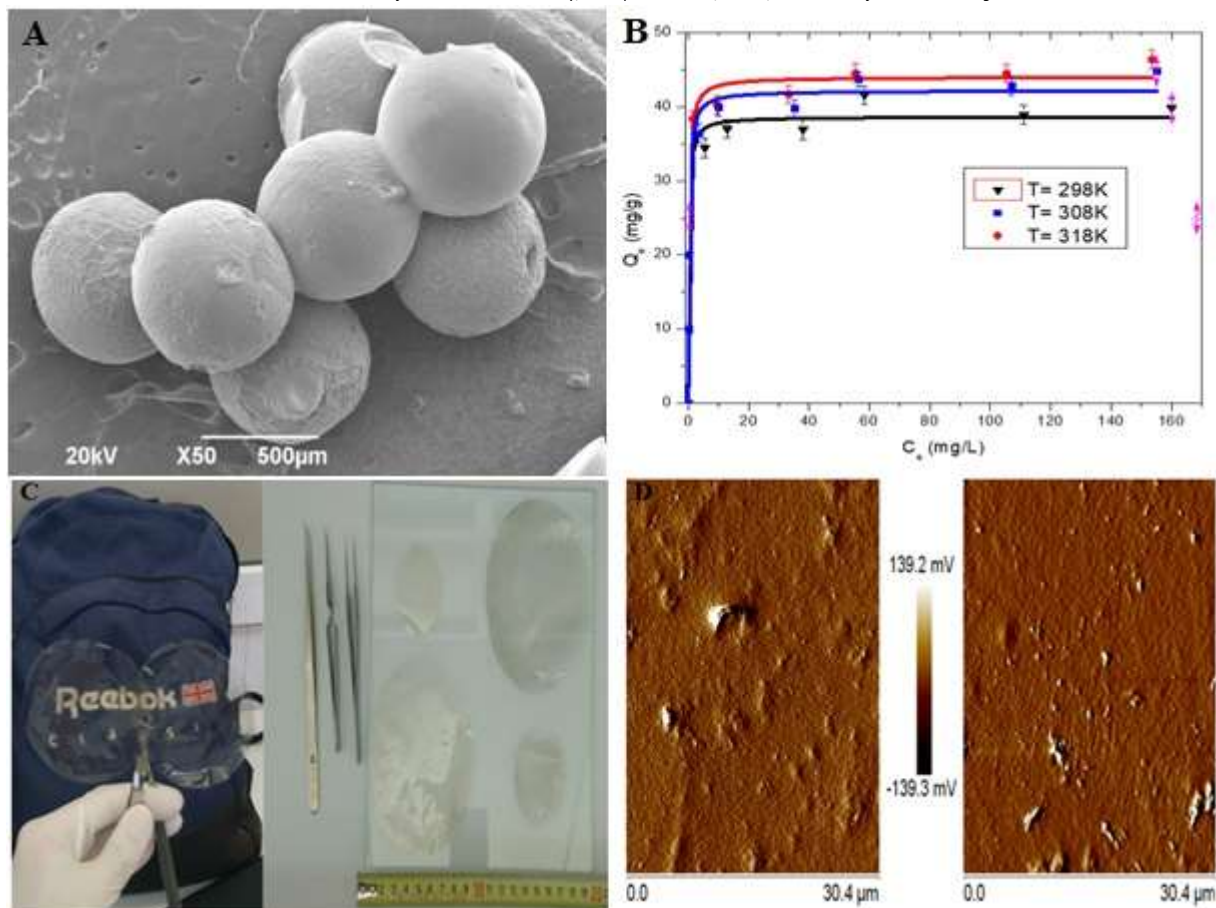


Fig.3. (A) SEM of GO/CS/PVA beads, (B) Adsorption evaluation (Langmuir isotherms), (C) CS/PVA/GO and rGO films, (D) AFM topography of the films.

Table 2. Film roughness

Film CS/PVA-	Roughness (nm)	
	Rq	Ra
GO 0.05%	22.3	14.1
rGO 0.05%	25.9	17
GO 0.1%	29.1	17.8
rGO 0.1%	32.3	21.1
GO 0.3%	62	49.2
rGO 0.3%	79	67.7
GO 0.6%	111	83.3
rGO 0.6%	155	111

## Acknowledgements

This research was funded by the Greek Ministry of Development and Investments (General Secretariat for Research and Technology) through the research project “Intergovernmental International Scientific and Technological Innovation-Cooperation. Joint declaration of Science and Technology Cooperation between China and Greece”, with the topic “Development of monitoring and removal strategies of emerging micro-pollutants in wastewaters” (Grant no: T7DKI-00220).

## References

1. Kostarelos, K.; Novoselov, K. S., Graphene devices for life. In *Nature Nanotechnology*, 2014; Vol. 9, pp 744-745.
2. Kyzas, G. Z.; Deliyanni, E. A.; Matis, K. A., Graphene oxide and its application as an adsorbent for wastewater treatment. In *J Chem Technol Biotechnol* 2013; Vol. 89, pp 196–205.
3. Filipkowska, U.; Zadrozna, M. K.; Jozwiak, T.; Szymczyk, P.; Nierobisz, M., IMPACT OF CHITOSAN CROSS-LINKING ON RB 5 DYE ADSORPTION EFFICIENCY. In *Progress on Chemistry and Application of Chitin and its Derivatives*, 2016; Vol. 21.

## Synthesis and characterization of modified TiO<sub>2</sub> nanoparticles with enhanced visible-light photocatalytic properties

P. Tzevelekidis<sup>1</sup>, E. Charalampous<sup>1</sup> and C. A. Mitsopoulou<sup>1\*</sup>

<sup>1</sup>Laboratory of Inorganic Chemistry, Department of Chemistry, National and Kapodistrian University of Athens, Panepistimiopolis, Zografou 15771, Greece.

\*email: cmitsop@chem.uoa.gr

The industry has focused on nano-technological materials and production systems because of their environmentally friendly properties. Among them, titanium dioxide nanoparticles (TiO<sub>2</sub>) have attracted major interest, mostly due to their chemical stability, low toxicity, low manufacturing cost, and their photocatalytic applications [1]. However, their major drawback originates from their limited ability to absorb the visible spectrum, overcoming which has become the subject of scientific research. One of the most promising methods that have been reported so far, is introducing impurities in the crystal lattice of TiO<sub>2</sub> which leads to the narrowing of the relatively large bandgap of the anatase TiO<sub>2</sub> (~3.2eV) [2]. The combination of copper and titanium oxide nanostructures shows improved photocatalytic performance under visible light [3, 4].

Herein, we report the green synthesis of water-dispersible copper-doped TiO<sub>2</sub> nanoparticles with enhanced absorbance in the visible spectrum through carefully tailoring the synthetic parameters and amount of copper dopant [5,6]. A wide range of analytical techniques, such as FT-IR, UV-Vis, Raman spectroscopy, XRD, TEM, and SEM-EDX, have been employed for the characterization of the doped titanium oxide nanoparticles. The photocatalytic activity of the synthesized nanoparticles was assessed through the degradation of organic pollutants, such as Methylene Blue, under the irradiation of eco-friendly LED and Xenon lamps. In addition, their efficiency as photosensitizers has been addressed through the photochemical splitting of water for hydrogen evolution, employing a novel heteroleptic Ni(II) complex [7,8].

### Acknowledgements

This research is co-funded by the Special Research Account of NKUA and by Greece and the European Union (European Social Fund-ESF) through the Operational Programme «Human Resources Development, Education and Lifelong Learning 2014-2020» in the context of the project “Innovative Titanium Nanoparticles for Development of autocleaning and Auto antibacterial Application” (MIS 5131364).

### References

1. X. Kang, S. Liu, Z. Dai, Y. He, X. Song, Z. Tan, *Catalysts*, **9** 191 (2019).
2. M. Khairy, W. Zakaria, *Egypt. J. Pet.*, **23** 4 (2014).
3. S. Mathew, P. Ganguly, S. Rhatigan, V. Kumaravel, C. Byrne, S.J. Hinder, J. Bartlett, M. Nolan, S.C. Pillai, *SN Appl. Sci.* **8** 2067 (2018).
4. C. Karunakaran, G. Abiramasundari, P. Gomathisankar, G. Manikandan, V. Anandi, *J. Colloid Interface Sci.* **352** 68–74 (2010).
5. B. Choudhury, A. Choudhury, D. Borah, *J. Alloys Compd.*, **646** (2015).
6. C. Liao, Y. Li, S. C. Tjong, *J. Nanomater.* **10** 124 (2020).
7. F. Kamatsos, K. Bethanis, C.A. Mitsopoulou, *Catalysts* **11** 401 (2021).
8. F. Kamatsos, M. Drosou, C.A. Mitsopoulou, *Int. J. Hydrog. Energy* **46** 19705 (2021).

## Engineering of Au/p-C<sub>3</sub>N<sub>4</sub> nanosheets with Enhanced Charge Separation for Photocatalytic Hydrogen Evolution

Hung Giap Van<sup>1,2</sup>, Shuoping Ding<sup>1</sup>, Mai Nguyen Thi Tuyet<sup>2</sup>, Norbert Steinfeldt<sup>1\*</sup>

<sup>1</sup>Leibniz Institute for Catalysis e.V., Albert-Einstein-Straße 29a, 18059 Rostock, Germany

<sup>2</sup>Hanoi University of Science and Technology, 100000 Hanoi, Vietnam

### Introduction

Photocatalytic hydrogen generation is increasingly perceived as a potential alternative to traditional hydrogen production method [1]. Polymeric carbon nitride (p-C<sub>3</sub>N<sub>4</sub>) has been considered as a promising photocatalyst candidate due to its low cost, chemical stability, and visible light reactivity. However, the performance of pure p-C<sub>3</sub>N<sub>4</sub> is limited due to the rapid recombination of photoinduced electron-hole pairs. Therefore, a lot of methods were explored to improve the activity of p-C<sub>3</sub>N<sub>4</sub>. In this work, p-C<sub>3</sub>N<sub>4</sub> was prepared in different atmospheres, treated with H<sub>2</sub>O<sub>2</sub> or ultrasound, and then investigated with Au deposition to optimize its photocatalytic performance. The synthesized materials showed improved charge separation efficiency and H<sub>2</sub> evolution performance.

### Experimental

p-C<sub>3</sub>N<sub>4</sub> samples were prepared by thermal polymerization of urea (550°C, 2h) in the presence of air or argon atmosphere. Prior to Au loading, portions of the synthesized p-C<sub>3</sub>N<sub>4</sub> were treated with H<sub>2</sub>O<sub>2</sub> or ultrasound. Various methods were used to deposit the Au on the p-C<sub>3</sub>N<sub>4</sub> surface, e.g., photo-deposition, adsorption of pre-formed Au nanoparticles, and chemical reduction of HAuCl<sub>4</sub> with NaBH<sub>4</sub> in presence or absence of sodium citrate. Before testing in hydrogen evolution reaction (HER) with triethanolamine (TEOA) as sacrificial agent, the materials were characterized by X-ray diffraction (XRD), X-ray photoelectron spectroscopy (XPS), infrared spectroscopy (FTIR), UV-vis diffuse reflectance spectroscopy (DRS), thermal gravity analysis (TGA), elemental analysis (EA), and photoluminescence spectroscopy (PL). A Zahner workstation was used for the electrochemical characterization. Photocatalytic experiments ( $m_{\text{cat}} = 25$  mg) were performed in a small batch reactor at 25°C under irradiation with white or visible light. The solvent (50 mL) was a mixture of TEOA and water (10v/90v). The amount of hydrogen formed was determined by GC analysis (Agilent 6890) using an Ar stream flowing through the reactor (see also Figure 1).

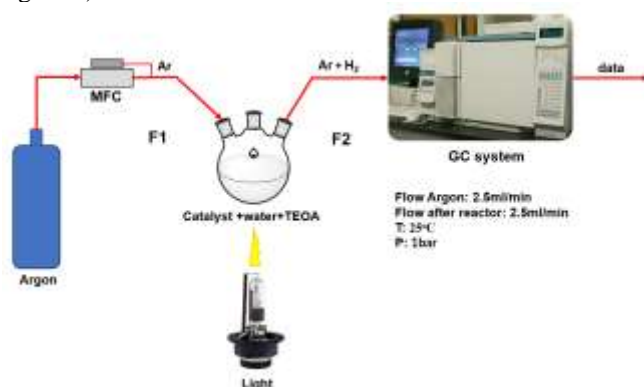
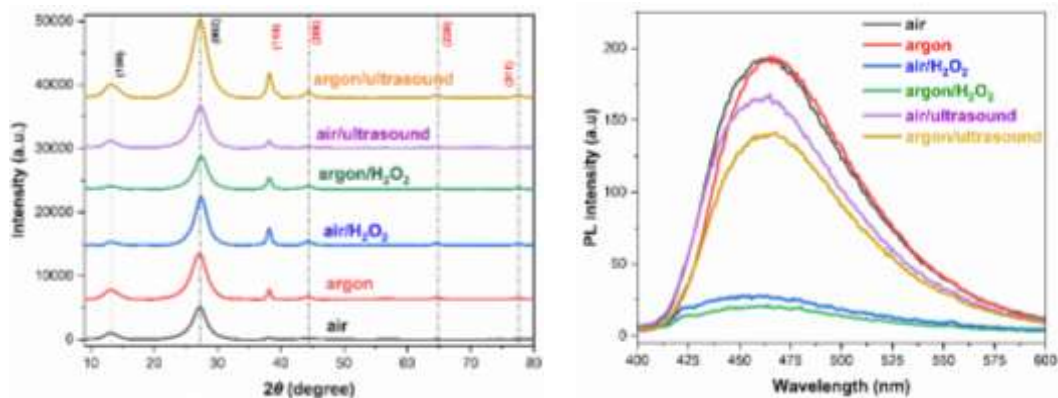


Figure 50. Scheme of the experimental set-up used for study of HER reaction with Au/p-C<sub>3</sub>N<sub>4</sub> catalysts

### Results

XRD powder patterns and PL spectra of 2wt.% Au/p-C<sub>3</sub>N<sub>4</sub> samples synthesized by an identical Au photo-deposition method are shown in Figure 2. All samples show reflections of p-C<sub>3</sub>N<sub>4</sub> at about 13.1 and 27.3 degree and those of metallic Au. The treatment with H<sub>2</sub>O<sub>2</sub> leads to a loss of intensity of the p-C<sub>3</sub>N<sub>4</sub> (100) reflection compared to samples without H<sub>2</sub>O<sub>2</sub> treatment. The different intensity and linewidth of the Au reflections indicate that the size of the deposited Au crystallites is affected by the surface structure of the C<sub>3</sub>N<sub>4</sub> support. Ultrasound treatment resulted in a moderate decrease in PL intensity compared to the untreated material, indicating improved separation of photoexcited electrons and holes in these samples. Almost complete suppression of PL was observed when the p-C<sub>3</sub>N<sub>4</sub> was treated with H<sub>2</sub>O<sub>2</sub> prior to Au deposition.



**Figure 51.** XRD powder patterns (left) and photoluminescence spectra (right) of different 2 wt.% Au/p-C<sub>3</sub>N<sub>4</sub> catalysts.

Photocatalytic results of these samples are presented in Figure 3. The highest hydrogen evolution was observed for the p-C<sub>3</sub>N<sub>4</sub> treated by ultrasound. The ultrasound treatment was previously applied for exfoliation of p-C<sub>3</sub>N<sub>4</sub> sheets [2]. Reasons for the higher activity of the ultrasound treated sample might be a lower distance of the charge carriers traveling to the surface in combination with a reduced charge carrier recombination.

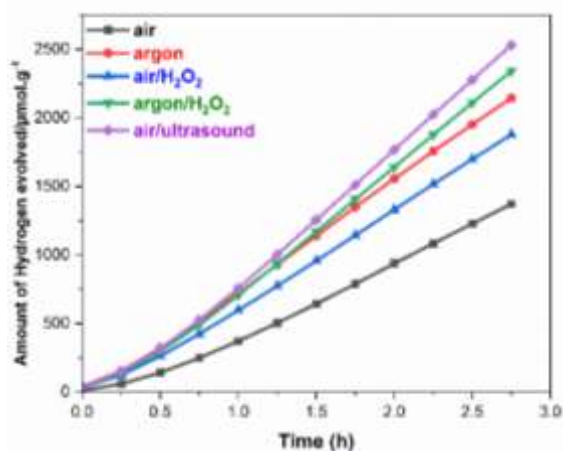


**Figure 52.** Photocatalytic hydrogen evolution under irradiation with white light for various 2wt% Au/p-C<sub>3</sub>N<sub>4</sub> catalysts (the same photo-deposition method of Au was used for all samples).

Besides the particular p-C<sub>3</sub>N<sub>4</sub> structure, the influence of the deposited Au amount, and that of the deposition method on hydrogen evolution was also investigated. With the used Au deposition method (Figure 3), an Au loading of 8% showed the highest hydrogen evolution (3.2 mmol·g<sub>cat</sub><sup>-1</sup> after 3 h). Comparing different deposition methods at an Au loading of 2wt-%, the sample prepared by chemical reduction of HAuCl<sub>4</sub> showed the highest hydrogen production (3.7 mmol·g<sub>cat</sub><sup>-1</sup>). The results clearly show that the photocatalytic performance of the Au/p-C<sub>3</sub>N<sub>4</sub> catalyst in hydrogen evolution are strongly affected by the p-C<sub>3</sub>N<sub>4</sub> surface structure as well the structure and amount of the formed Au nanoparticles.

#### Acknowledgements

This work has been supported by the RoHan Project funded by the German Academic Exchange Service (DAAD, No. 57315854) and the Federal Ministry for Economic Cooperation and Development (BMZ) inside the framework "SDG Bilateral Graduate school programme".

#### References

1. Li, X., Yu, J., et al. *Chemical Society Reviews*, **45** (2016), 2603-2636.
2. Yang, S., et al. *Advanced Materials*, **25** (2013), 2452.

## Synthesis of film Cu,F-TiO<sub>2</sub> NTs photocatalysts with a highly ordered structure for wastewater treatment

Vasil'ev A.S.<sup>1\*</sup>, Morozov A.N.<sup>1</sup>, Gartman T.N.<sup>1</sup>, Pochitalkina I.A.<sup>1</sup> and Sovetin F.S.<sup>1</sup>  
<sup>1</sup>Mendeleev University of Chemical Technology of Russia, 125047, Moscow, Miusskaya square, 9, Russia  
 \* alexandr.s.vasilyev@gmail.com

Contamination of water resources by highly toxic organic compounds present in the effluents of various industries is a significant problem faced by modern mankind. Existing separation treatment technologies do not correspond to modern ideas about the sustainable development of water resources and the closed-cycle economy. In this regard, the task of the development of new effective and environmentally safe methods of wastewater treatment from organic compounds should be considered as an urgent one. To date, Advanced Oxidation Processes (AOPs) are intensively researched and considered as an alternative to the separation methods for removing toxic organic substances from water [1]. Among the methods of water purification from organic pollutants using AOPs, heterogeneous catalytic processes in the presence of H<sub>2</sub>O<sub>2</sub> are the most effective and versatile [2]. Photocatalysis is considered to be an environmentally friendly process due to its ability to achieve full mineralization of hard-to-oxidize organic pollutants without the formation of secondary impurities. At the same time, to create an energy-efficient and energy-saving technology of photocatalytic water purification, it is necessary to develop new immobilized photocatalysts. Recently, the photocatalytic properties of film materials based on TiO<sub>2</sub> nanotubes (NTs) obtained by anodizing metallic titanium have been intensively studied [3]. Increased attention to this object is primarily due to its unique spatially ordered nanostructure and the ability to control the size of TiO<sub>2</sub> NTs over a wide range, which opens up the prospect of obtaining materials with desired properties and functions. The efficiency of photocatalysis depends not only on the morphology of the photocatalyst, but also on its ability to create electron-hole pairs under the action of light [4]. The main way to improve the quantum efficiency of TiO<sub>2</sub> is by doping (co-doping) which is the introduction of two or more impurities of cationic, anionic or mixed type into TiO<sub>2</sub> [5]. According to the literature, one of the most available and promising doping components of TiO<sub>2</sub> is copper [6]. Modification of the crystal lattice of TiO<sub>2</sub> by copper ions leads to the appearance of additional levels in the band gap that increase the frequency of interband electron transitions and shift the absorption boundary to the visible region, which, in turn, improves the photocatalytic activity of TiO<sub>2</sub>. This work is devoted to the preparation of spatially ordered TiO<sub>2</sub> NTs films doped with copper and fluorine using electrolytic and solvothermal methods as well as to the study of their structure and electronic properties.

The initial films made from fluorine-doped TiO<sub>2</sub> NTs (F-TiO<sub>2</sub> NTs) were obtained by anodic oxidation of VT1-00 metallic titanium wafers in a potentiostatic regime at 60 V and constant temperature of the anodizing solution of 25°C [3]. The copper doping of F-TiO<sub>2</sub> NTs samples (Cu, F-TiO<sub>2</sub> NTs) was performed by the solvothermal method in an autoclave equipped with a 5 mL fluoroplastic insert. The doping process was conducted in a 0.25 M solution of copper (II) acetate in ethylene glycol at temperatures from 80 to 180°C for 15 to 180 min. The synthesized films were crystallized by heat-treatment in a Nabertherm R 100G750G13-1 (Nabertherm, Germany) tubular furnace at 450°C in an flow of air with constant rate of heating and cooling of 5 °C/min. The heat-treatment at a constant temperature of 450°C lasted for 1 h.

Figure 1 shows microphotographs of typical morphology of F-TiO<sub>2</sub> NTs and Cu,F-TiO<sub>2</sub> NTs samples obtained by doping at 160°C for 1 hour.

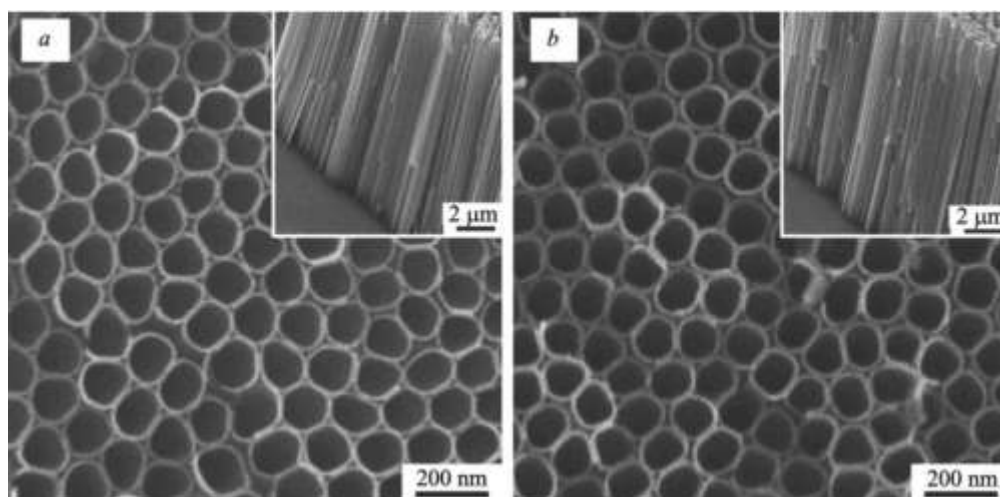


Figure 1. SEM photomicrograph of sections of the surface and cleavage (inset) of the obtained samples: a) F-TiO<sub>2</sub> NTs; b) Cu, F-TiO<sub>2</sub> NTs

Comparing the presented microphotographs, we can see that the solvothermal approach of NTs F-TiO<sub>2</sub> doping with copper ions does not lead to a change in the initial nanotube structure of the films. According to SEM data (Fig. 1b), the obtained films consist of densely packed NTs, which have an open porous structure with local hexagonal self-organization, a smooth outer surface and a narrow size distribution. The inner diameter of the NTs was found to be  $115 \pm 10$  nm, the wall thickness -  $10 \pm 2$  nm, and the length -  $17.2 \pm 1.1$   $\mu$ m. According to the images of the film cleavage, the NTs are parallel to each other and are absolutely homogeneous throughout the entire film thickness. The upper part of the TiO<sub>2</sub> NTs is open, while the lower side the tubes has a closed hemispherical bottom, by which they are attached to the substrate surface.

Figure 2 shows the dependences of Cu content in Cu,F-TiO<sub>2</sub> NTs samples on the duration of the solvothermal doping process at different temperatures.

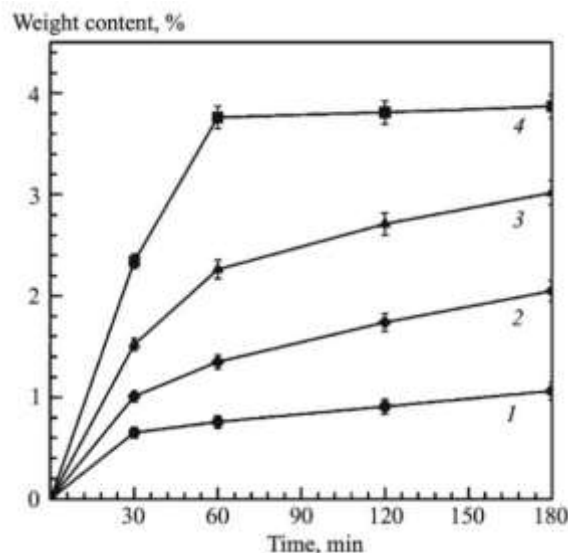


Figure 2. Copper content in Cu, F-TiO<sub>2</sub> samples versus the duration of the solvothermal doping process at different temperatures: 1) 80°C; 2) 120°C; 3) 160°C; 4) 180°C

As can be seen, with an increase in the synthesis temperature, an increase in the rate of F-TiO<sub>2</sub> NTs doping with copper is observed, and for all studied temperatures, the time dependences of the copper content in the samples exhibit the same nonlinear behavior. For each temperature, the maximum rate of F-TiO<sub>2</sub> NTs copper doping is observed in the interval from the start of the process to 1 hour, when the concentration of copper ions in the solution reaches its maximum. A further increase in the duration of the solvothermal process leads to a decrease in the doping rate, which is caused by a decrease in the concentration of copper in the solution. From the data presented in Fig. 2, we can conclude that by changing the duration and temperature of the solvothermal doping process, it is possible to control the copper content in Cu,F-TiO<sub>2</sub> NTs samples in the range from 0 to  $3.87 \pm 0.19\%$ .

Using the absorption spectra of the samples obtained by diffuse reflectance spectroscopy in the wavelength range from 190 to 700 nm, the value of the band gap width ( $E_g$ ) of Cu,F-TiO<sub>2</sub> NTs was estimated. The value of  $E_g$  was estimated by the value of energy of indirect interband electron transitions, which was determined by the well-known graphical method [7]. The performed analysis showed that for all the studied samples the band gap is  $3.20 \pm 0.05$  eV, which coincides with the literature data for crystalline titanium dioxide with the anatase structure. Thus, it has been established that TiO<sub>2</sub> NTs copper doping does not lead to a change in the band gap of TiO<sub>2</sub>, and the appearance of absorption bands in the visible part of the spectrum is probably associated with the formation of surface electronic levels in the band gap of TiO<sub>2</sub> and d-d transitions of Cu atoms.

## Acknowledgements

The authors are grateful to the staff of the Center for Collective Use for studying the samples by the SEM.

## References

1. .K. Pandis, C. Kalogirou, E. Kanellou et al., *ChemEngineering*, **6** 8 (2022).
2. A. Zuliani, C.M. Cova, *Photochem*, **1** 147 (2021).
3. A.N. Morozov, A.V. Denisenko, A.I. Mihaylichenko, M.Yu. Chayka, *Nanotechnologies in Russia*, **14**, 9-10 444 (2019).
4. A.I. Mikhailichenko, A.N. Morozov, A.V. Denisenko, *Theoretical Foundations of Chemical Engineering*, **53**, 4, 632 (2019).
5. C.Di. Valentin, G. Pacchioni, *Catalysis Today*, **206**, 12 (2013).

6. Ozge Kerkez-Kuyumcu, Efgan Kibar, Kubra Dayıoglu, *Journal of Photochemistry and Photobiology A: Chemistry*, **311**, 1. 176 (2015).
7. P. Makula, M. Pacia, W. Macyk, *J. Phys. Chem. Lett.*, **9**, 6814 (2018).



## Size and shape-controlled synthesis of well-defined iron oxide nanocrystals by investigation of the reaction path mechanism

Agnes Weimer<sup>\*†,∞</sup>, Artur Feld,<sup>†,∞</sup>, Andreas Kornowski<sup>†</sup>, Naomi Winckelmans<sup>||</sup>, Jan-Philip Merkl<sup>†,∞</sup>, Hauke Kloust<sup>†</sup>, Robert Zierold<sup>⊥</sup>, Christian Schmidtke<sup>†</sup>, Theo Schotten<sup>∇</sup>, Maria Riedner<sup>#</sup>, Sara Bals<sup>||</sup> and Horst Weller,<sup>†,∞,∇,§</sup>

<sup>†</sup> Institute of Physical Chemistry, Hamburg University, Grindelallee 117, D-20146 Hamburg, Germany.

<sup>∞</sup> The Hamburg Center for Ultrafast Imaging, Hamburg University, Luruper Chaussee 149, D-22761 Hamburg, Germany.

<sup>∇</sup> Fraunhofer-CAN, Grindelallee 117, D-20146 Hamburg, Germany.

<sup>§</sup> Department of Chemistry, Faculty of Science, King Abdulaziz University, P.O BOX 80203 Jeddah 21589, Saudi Arabia.

<sup>#</sup> Department of Chemistry, Hamburg University, Martin-Luther-King-Platz 6, D-20146 Hamburg, Germany.

<sup>||</sup> Electron Microscopy for Materials Science (EMAT), Department Physics, University of Antwerp, Groenenborgerlaan 171, B-2020 Antwerp, Belgium.

<sup>⊥</sup> Center for Hybrid Nanostructures, University Hamburg, Luruper Chaussee 149, 22761 Hamburg, Germany.

<sup>\*</sup>corresponding author: agnes.weimer@chemie.uni-hamburg.de

Magnetic nanoparticles are of significant interest and immense importance for research as well as technological application. These nanoparticles exhibit fascinating magnetic properties, including blocking temperature, coercivity, saturation magnetization, magnetic domain size, and exchange coupling effects, which are affected by size, shape, and crystal structure. [1-3]

For these outcomes, a new synthetic route was developed<sup>[4]</sup>, based on the thermal decomposition of iron oleate. The oleate was synthesized by use of a novel precursor system - Fe(II)CO<sub>3</sub> and Fe<sub>2</sub>(III)(CO<sub>3</sub>)<sub>3</sub>. The method allows the synthesis of highly monodisperse nanocrystals (NC) in various well-defined sizes and morphologies on a gram scale. Furthermore, the elaborated synthetic route accomplished a strict kinetic separation of the formation of iron oleate from the generation of reactive pyrolysis products and the subsequent nucleation during the synthesis.

Size and shape control was achieved by varying the concentration of the ligand oleic acid and the non-coordinating solvent 1-octadecene, the temperature and reaction time, so that octapod-shaped NC in a size range of 20-80 nm and cubic NC with sizes from 20-60 nm could be synthesized. With dilution, the size of the nanoparticles decreases significantly, while at higher concentrations, they become larger, as shown in figure 1.

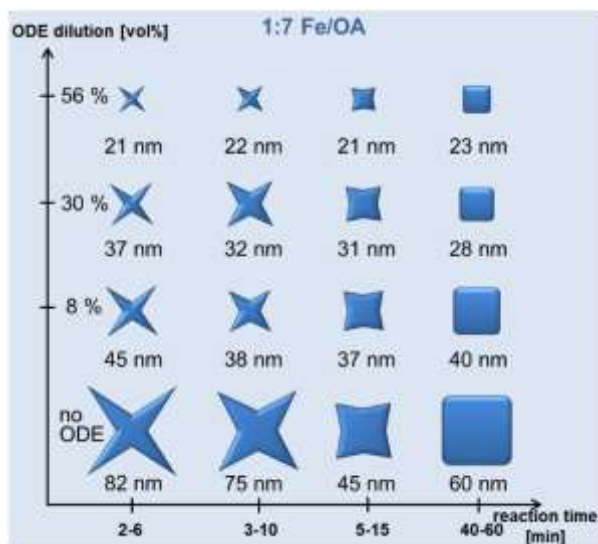


Figure 1. Schematic representation of the influence of reaction time (after nucleation) and factor of dilution on the size and shape of the resulting NC.

The octapod star-shaped morphology, formed shortly after nucleation as a kinetically favored product, could be characterized by a comprehensive structure analysis using transmission electron microscopy (TEM) and electron energy loss spectroscopy tomography (EELS-tomography). As a result of thermodynamic control they transformed into cube-shaped structures due to metamorphosis in 4 phases.

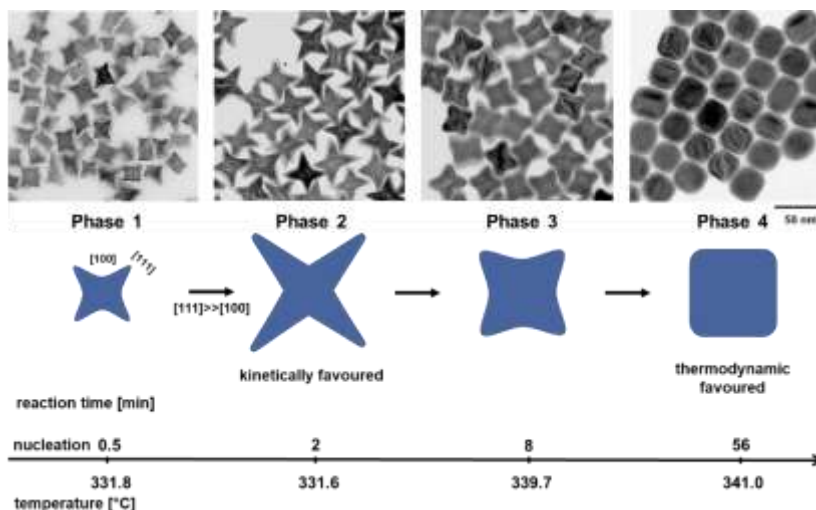


Figure 2. metamorphosis during 1 h of reaction (TEM images of particle size and shape formation) and a corresponding scheme of the different development stages (Fe/OA = 1:7; 1-octadecene = 8 vol %)

Figure 3 illustrates a short overview of possible sizes and shapes that can be synthesized using this approach.

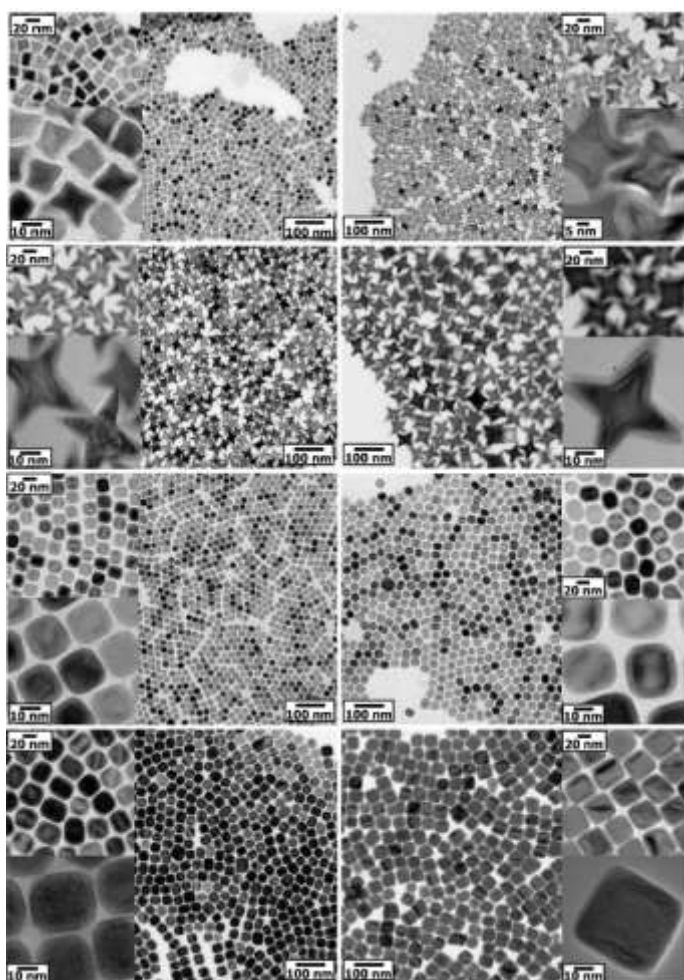


Figure 3. Short overview of TEM images of star-shaped and cubic nanocrystals, which can be synthesized with this approach.

Furthermore, the hydrophobic NCs were transferred into water and encapsulated with a polystyrene shell, based on the seeded emulsion polymerization technique<sup>[5]</sup>, providing biocompatibility and water solubility. This enables the way for a broad spectrum of applications.

Especially iron oxide nanocrystals can be used to effectively remove micro polystyrene particles via adsorption from water showing potential advantages of this particles for removing environmental pollutants by an environmental-friendly procedure.<sup>[6]</sup>

Finally, the goal is to optimize this synthetic approach so that it is biobased and sustainable. One way to do this would be to use bacteria<sup>[7]</sup> to produce particles via biomechanisms. However, such production methods using bacteria allow poor control of shape and size, so in the future, it would be purposeful to adapt the method presented here to a biologically synthesized strategy.

## References

- [1] S.-W. L. Yejin Heo, Eun-Hee Lee, *Chemosphere*. **307**, 135672 (2022).
- [2] S. Chikazumi *et al.*, *J. Magn. Magn. Mater.* **65**, 245–251 (1987).
- [3] M. Hofmann-amtenbrink *et al.*, *Nanostructured Materials for Biomedical Applications* (Transworld Research Network, Kerala, India, 2009), vol. 661.
- [4] A. Weimer *et al.*, *ACS Nano*. **13**, 152–162 (2019).
- [5] A. Feld *et al.*, *ACS Nano*. **11**, 3767–3775 (2017).
- [6] S.-W. L. Yejin Heo, Eun-Hee Lee, *Chemosphere*. **307**, 135672 (2022).
- [7] A. A. Bharde *et al.*, *Langmuir*. **24**, 5787–5794 (2008)

## Investigating the structural and mechanical properties of innovative polypropylene/nanoadditive composites for heating/cooling pipe systems

Eleftheria Xanthopoulou<sup>1</sup>, Evangelia Delli<sup>2</sup>, Dimitrios Gkiliopoulos<sup>3</sup>, Dimitra Kourtidou<sup>2</sup>,  
Konstantinos Chrissafis<sup>2</sup> and Dimitrios N. Bikiaris<sup>1</sup>

<sup>1</sup> *Laboratory of Polymer Chemistry and Technology, Department of Chemistry, Aristotle University of Thessaloniki, Greece*

<sup>2</sup> *School of Physics, Laboratory of Advanced Materials and Devices, Aristotle University of Thessaloniki, GR-541 24, Thessaloniki, Greece*

<sup>3</sup> *Laboratory of Chemical and Environmental Technology, Department of Chemistry, Aristotle University of Thessaloniki, Greece*

*\*[elefthxanthopoulou@gmail.com](mailto:elefthxanthopoulou@gmail.com)*

Polymer-matrix based composite materials performing improved mechanical and thermal properties are of utmost technological importance for a wide variety of applications, including aerospace and structural engineering. Within this context, polypropylene random copolymer (PPR), copolymerized by propylene and ethylene monomers, has attracted the interest of both academic and industrial communities thanks to the higher impact strength, excellent thermal stability, and mechanical properties. Nevertheless, PPR is contaminated easily under appropriate temperature and humidity condition. Thus, the addition of nanoadditives is an effective method to provide the functionality and further enhance physical and mechanical properties of the final materials. Herein, five polypropylene (PPR112)/SiO<sub>2</sub> composites using different filler concentrations (from 1-15 %wt.) were prepared via melt-mixing extrusion process and roughly investigated. Furthermore, the structural features of the composites were examined with the implementation of multiple techniques, such as Fourier-transform Infra-red spectroscopy (FTIR), X-ray Diffractometry (XRD) and Scanning Electron Microscopy (SEM), while Tensile strength and Impact strength were measured to evaluate the mechanical behavior of the synthesized polymeric materials, as they strongly affect their final applications.

### Acknowledgements

This research has been co-funded by European Union-European Regional Development Fund and Greek Ministry of Education, Research and Religions/EYDE-ETAK through program EPANEK 2014-2020/Action "RESEARCH-CREATE-INNOVATE" (project T1EAK-02575).

# Catalyst nanoparticles stabilization and/or redispersion: A new anti-sintering strategy based on the effect of the $O^{\delta-}$ electric double layer account of metal-support interactions.

Ioannis V. Yentekakis<sup>1,\*</sup>

<sup>1</sup>Laboratory of Physical Chemistry & Chemical Processes ([www.pccplab.tuc.gr](http://www.pccplab.tuc.gr)), School of Environmental Engineering, Technical University of Crete, 73100 Chania, Crete, Greece; \* [yentek@isc.tuc.gr](mailto:yentek@isc.tuc.gr) (I. V. Yentekakis)

## Introduction

Effective promotion of catalytic reactions performance is always a grand challenge for heterogeneous catalysis [1-5]. Nevertheless, catalyst nanoparticle stabilization (anti-sintering behaviour) at the typically elevated operation temperatures of catalysis is at least of equivalent, unless of much more importance. Sintering of catalyst nanoparticles is inevitably a leading cause of the degradation of industrial catalysts used for energy and environmental applications as well as for large-scale synthesis of commodity chemicals with obvious economic drawbacks; this justifies the intense research interest on the topic [6-7]. Nanoparticles sintering in supported catalysts implicates two main mechanisms [7, 8]: the so-called Particle Migration and Coalescence (PMC), which concerns the coordinated motion of multiple atoms clusters on the support surface with subsequent coalescence leading to particles growth, and Ostwald ripening (OR), which refers to atomic particles migration from smaller to larger nanoparticles, driven by differences in free energy and local adatom concentrations on the support surface. Since all heterogeneous catalysts are inevitably subjected to sintering during operation and/or catalyst regeneration procedures [6], regardless of what sintering mechanism dominates, the effect poses a grand challenge for the development of sinter-resistant catalysts [8-11].

We have found that the *effective-double-layer*,  $[O^{\delta-}, \delta^+]$  -spontaneously created on the catalyst nanoparticle surfaces via metal-support interactions due to thermally-driven lattice oxygen spillover from supports with substantial oxygen ion lability onto the nanoparticle surfaces [4,5]- can play a key role not only on the intrinsic catalytic activity of the particles [1-3], but also on their sintering behavior [9-11]. This oxygen ions  $O^{\delta-}$  electric layer on the surface of catalyst particles can effectively stabilize their nano-structure even at extreme (high temperature) oxidative sintering conditions, an effect of great importance in heterogeneous catalysis and especially in the cases of catalysts that are prone to sintering or used in high temperature processes. We have developed a mechanistic model which convincingly explains the anti-sintering (anti-PMC and anti-Ostwald ripening) induced by the  $O^{\delta-}$  layer and is schematically shown in Fig. 1.

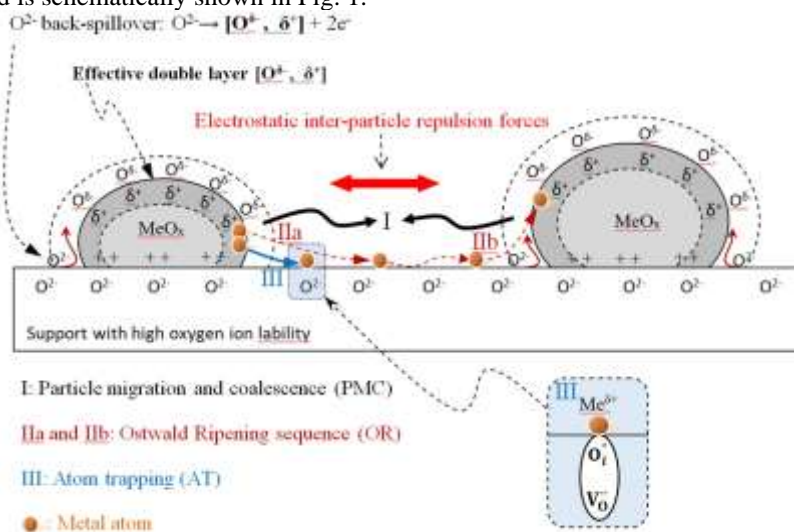


Figure 1. Model for anti-sintering behavior (anti-PMC and anti-OR) and redispersion induced by the simultaneous action of interparticle repulsion forces arising from the  $O^{\delta-}$  layer and atom trapping at oxygen ion vacancies.

In brief, the  $O^{\delta-}$  layer created on catalyst particles interfaced with supports with high oxygen ions lability endows the particle with a net negative charge at its gas-exposed surface, leading to inter-particle repulsion at short range, thus preventing particle-particle encounters followed by coalescence (anti-PMC). At the same time, the  $O^{\delta-}$  modifies surface barrier present on large catalyst particles increasing the activation energies for detachment and reattachment of metal entities whose transport would otherwise lead to continuous growth of large particles at the expense of smaller particles according to the OR model (anti-OR). In addition, atomic trapping by surface oxygen vacancies ( $V_O$ ) [2] existing on supports with high oxygen ions lability acts as a contributing factor in the anti-OR mechanism or even better can lead to re-dispersion [9].

Here, we report results on the resistance, or lack of resistance, to sintering and even the in situ redispersion at high-temperature oxidative conditions of Ir and Rh nanoparticles dispersed on supports encompassing a wide range of lattice oxygen ion lability.

## Experimental

Commercial or laboratory made (via co-precipitation)  $\gamma$ -Al<sub>2</sub>O<sub>3</sub>, ACZ (80wt% Al<sub>2</sub>O<sub>3</sub>-20wt% Ce<sub>0.5</sub>Zr<sub>0.5</sub>O<sub>2- $\delta$</sub> ), CZ (Ce<sub>0.5</sub>Zr<sub>0.5</sub>O<sub>2- $\delta$</sub> ), GDC (10mol% Gd<sub>2</sub>O<sub>3</sub>-CeO<sub>2</sub>) and YSZ (8mol% Y<sub>2</sub>O<sub>3</sub>-ZrO<sub>2</sub>) oxide supports were used for the deposition of Ir and Rh nanoparticles, via wet impregnation, at a nominal metal loading of ~1wt%. Textural, structural and morphological characterizations of the as-produced catalysts were performed by using BET, H<sub>2</sub>-chemisorption, H<sub>2</sub>-TPR, XRD and TEM techniques, among others.

## Results and Discussion

Figure 2 shows the sintering behavior of Ir (Fig. 2a) and Rh (Fig. 2b) nanoparticles under high temperature oxidative treatment (see figure caption for details) when dispersed on supports with different OSC. A strong correlation is evident in both cases. Independent of the nature of metal particles, supports with low or zero OSC (Al<sub>2</sub>O<sub>3</sub> or YSZ) do not prevent particle growth; the opposite is true for supports with high OSC. For Rh particles, in particular, dispersed on supports with high OSC the sintering treatment can cause even re-dispersion

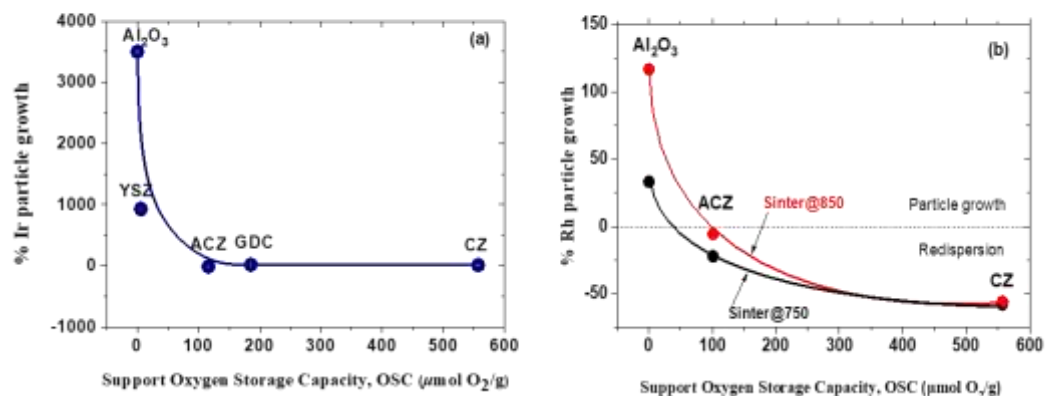


Figure 2. Percentage Iridium (a) and Rhodium (b) particle growth (positive values) or redispersion (negative values) as a function of the oxygen storage capacity (OSC) of the support for Ir catalysts sintered at 750°C for 2h and Rh catalysts sintered at 750°C for 2 h (sinter@750) or at 750°C for 2h + 850°C for 2h (sinter@850) at oxidative atmosphere (air).

## Conclusions

Supports with negligible OSC (e.g.  $\gamma$ -Al<sub>2</sub>O<sub>3</sub>, YSZ) provided no or little resistance to sintering of catalyst nanoparticles. In striking contrast, high resistance to sintering and even redispersion of catalyst nanoparticles resulted on supports characterized by moderate and high OSC values (ACZ, GDC and CZ, respectively). These findings provide a new methodology for sintering prevention or even in situ controlled redispersion of metal catalyst particles. A model has been developed convincingly explains the obtained results. The new methodology of catalyst nanostructure stabilization and/or particle redispersion is of significant fundamental and practical importance for energy and environmental applications (such an implementation is included in the full paper).

## Acknowledgements

This research has been co-financed by the European Union and Greek national funds through the Operational Program “Competitiveness, Entrepreneurship and Innovation”, under the call “RESEARCH-CREATE-INNOVATE” (project code: T2EDK-00955).

## References

1. I.V. Yentekakis, P. Vernoux, G. Goula, A. Caravaca, *Catalysts* **9**, 157 (2019).
2. C.G. Vayenas, S. Bebelis, I.V. Yentekakis, H.-G. Lintz, *Catal. Today*, **111**, 303 (1992).
3. I.R. Harkness, C. Hardacre, R.M. Lambert, I.V. Yentekakis, C.G. Vayenas, *J. Catal.*, 160 19 (1996).
4. C.A. Pliangos, I.V. Yentekakis, V.G Papadakis, C.G. Vayenas, X.E. Verykios, *Appl. Catal. B*, **14** 161 (1997).
5. J. Nicole, D. Tsiplakides, C. Pliangos, X.E Verykios, Ch. Comninelis, C.G Vayenas, *J. Catal.* **204**, 23 (2001).
6. M.D. Argyle, C.H. Baetholomew, *Catalysts*, **5**, 145 (2015).
7. Y. Dai, P. Lu, Z. Cao, C.T. Campbell, Y. Xia, *Chem. Soc. Rev.* **47**, 1740 (2018).
8. T.W. Hansen, A.T. DeLaRiva, S.R. Challa, A.K. Datye, *Acc. Chem. Res.* **46**, 1720 (2013).
9. G. Goula, G. Botzolaki, A. Osatiashtiani, C.M.A. Parlett, G. Kyriakou, R.M. Lambert, I.V. Yentekakis, *Catalysts*, **9**, 541 (2019).
10. I.V. Yentekakis, G. Goula, S. Kampouri, I. Betsi-Argyropoulou, P. Panagiotopoulou, M.J. Taylor, G. Kyriakou, R.M. Lambert, *Catal. Lett.* **148**, 341 (2018).
11. I.V. Yentekakis, G. Goula, P. Panagiotopoulou, S. Kampouri, M.J. Taylor, G. Kyriakou, R.M. Lambert, *Appl. Catal. B.* **192**, 357 (2016).

## Cobalt-manganese catalysts supported on ion exchanged clinoptilolite for n-hexane oxidation

Iliyana D. Yordanova\*, Stanislav D. Hristov and Silviya Zh. Todorova

Institute of Catalysis Bulgarian Academy of Sciences, Acad. G. Bonchev St., Bldg. 11, Sofia 1113, Bulgaria

\* e-mail address of corresponding author: yordanova@ic.bas.bg

### Introduction

VOCs are major air pollutants and their elimination must be strictly regulated. One of the most effective ways to eliminate them is catalytic oxidation. Zeolite based materials are widely used last years in ecofriendly technologies as exhaust gas purification and greenhouse gas adsorption [1]. Zeolites have many applications. In terms of catalysis, they have good properties. Pore size directly determine the absorption and catalytic performance of the specific type of zeolite [2]. Their specific surface area, ordered pore size and structure, thermal stability, shape selectivity, hydrothermal stability, mobility of their cations to act as a catalyst, makes them very suitable as catalyst carriers. Catalysts based on Co-Mn are one of the most effective and economically advantageous in VOCs removal. Their activity is expected to be higher than that of monoxides. The combination of mixed cobalt-manganese oxides deposited over clinoptilolite is expected to have high catalytic activity.

Catalytic activity was examined in the reaction of total oxidation of n-hexane. In the atmosphere, n-hexane participates in radical reactions, which are involved in the formation of photochemical smog. European Directive 2008/50/EU recommends measurement of n-hexane pollutions.

### Experimental Methods

The zeolite used in this work was obtained from a deposit located near Beli Plast village, Eastern Rhodope Mountains, Bulgaria. The analyzed as clinoptilolite material was crushed and sieved into a fraction 0.63–0.80 mm and collected for further studies as “raw clinoptilolite”. It was modified into H-form by ion exchange with 1M  $\text{NH}_4\text{NO}_3$  solution.

Ion exchange was performed in three consecutive cycles in order to obtain complete exchange of interfering cations. The ion exchanged clinoptilolite was filtered, washed to neutral pH, dried for 24 hours at 110 °C, and then calcined for 3 hours at 350 °C. Co-Mn catalysts on ion exchanged zeolite were prepared by the method of wet impregnation from aqueous solutions of ( $\text{Co}(\text{NO}_3)_2 \cdot 6\text{H}_2\text{O}$ ,  $\text{Mn}(\text{NO}_3)_2 \cdot 4\text{H}_2\text{O}$ ). The calculated amounts of diluted salts correspond to 20% by weight as oxides in the final product. The obtained samples were calcined 3 h at 500 °C. The synthesized catalysts were designated depending on the percentage of the metal ion.

The properties of raw clinoptilolite were characterized with AAE-ICP and XRD. The properties of prepared catalysts were characterized with powder XRD, BET, TPR, XPS and in the reaction of total oxidation of n-hexane.

### Results and Discussion

The composition of “raw clinoptilolite” and ion exchanged clinoptilolite was obtained by AES-ICP method. The results are summarized in Table 1.

Table 1. Chemical content of clinoptilolite determined by AES-ICP.

Sample	SiO <sub>2</sub>	Al <sub>2</sub> O <sub>3</sub>	CaO	K <sub>2</sub> O	MgO	Fe <sub>2</sub> O <sub>3</sub>	TiO <sub>2</sub>	MnO	Na <sub>2</sub> O	P <sub>2</sub> O <sub>5</sub>
Raw clinoptilolite	71.45	11.56	3.02	2.60	0.91	0.70	0.12	0.03	<0.01	<0.01
Ion exchanged clinoptilolite	77.10	10.80	0.3	0.60	0.72	0.70	0.09	0.02	<0.01	0.04

The powder XRD analysis showed that the natural material contains 89 wt.% clinoptilolite and opal cristobalite ~ 8 wt.%. The main structure of the ion exchanged carrier is clinoptilolite. In all investigated catalyst samples XRD analysis (Fig. 1a) revealed the existence of mixed metal oxide  $\text{CoMnO}_3$  phase. In 15Co5Mn sample in addition  $\text{Co}_3\text{O}_4$  was determined whereas for 5Co15Mn sample the additional phase was  $\text{MnO}_2$ . So, the cobalt exists in  $\text{Co}^{2+}$  and  $\text{Co}^{3+}$  oxidation states and the manganese is represented in  $\text{Mn}^{3+}$  and  $\text{Mn}^{4+}$  oxidation states on the surface of the samples determined by XPS methods. The obtained phases of mixed Co-Mn oxides are highly dispersed and easily reducible.

All investigated samples demonstrated catalytic activity in total oxidation of n-hexane (Fig. 1b). The conversion attained 100% in the temperature interval 340–360 °C. The sole reaction products were  $\text{CO}_2$  and  $\text{H}_2\text{O}$ . The raw of the catalytic activity in the reaction of total oxidation of n-hexane is 15Co5Mn > 5Co15Mn > 10Co10Mn. The best activity of 15Co5Mn sample is explained with co-existence of  $\text{Co}_3\text{O}_4$  phase together with mixed oxidation states of Co and Mn with ratio Co:Mn close to 1:1 on the surface, determined by XPS.

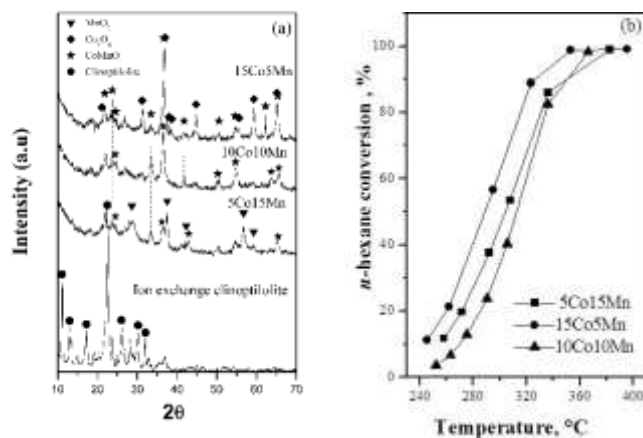


Figure 1(a) XRD patterns of ion exchange clinoptilolite and Co-Mn catalysts and catalytic curves (b) on all Co-Mn investigated samples.

Natural Bulgarian zeolite clinoptilolite demonstrated good properties as support for catalysts applicable in oxidation reaction for environmental protection.

### Acknowledgements

The authors are gratefully acknowledged to the National Science Fund programme 'Competition for financial support for projects of junior basic researchers and postdocs – 2020', for the financial support of project KII-06-M49/2.

### References

1. C. Megías-Sayago, R. Bingre, L. Huang, G. Lutzweiler, Q. Wang, B. Louis, *Frontiers in Chemistry*, **7**, 551 (2019).
2. M. V. Chandak, Y. S. Lin, W. Ji, R. J. Higgins, *Journal of Membrane Science*, **133**, 231 (1997).

## Photocatalytic removal of persistent organic pollutants using immobilized titanium dioxide

Boštjan Žener<sup>1\*</sup>, Lev Matoh<sup>1</sup> and Urška Lavrenčič Štangar<sup>1</sup>

<sup>1</sup> Faculty of Chemistry and Chemical Technology, University of Ljubljana, Večna pot 113, 1000 Ljubljana, Slovenia,

\* [bostjan.zener@fkt.uni-lj.si](mailto:bostjan.zener@fkt.uni-lj.si)

Access to clean and drinkable water has become of increasing concern in the last years due to exponential growth of population, industrialization and water irrigation. Almost half of the world's population lives in regions where demand for water is greater than the ability of supply aquifers to recharge, and because of this imbalance water reuse is crucial. Because of this, it is crucial to develop efficient, non-destructible and sustainable methods for wastewater reuse. [1] Advanced oxidation processes (AOP) and particularly heterogeneous photocatalysis represent a possible solution to this problem because of its ability to degrade organic molecules to non-hazardous products – CO<sub>2</sub>, H<sub>2</sub>O and other inorganic substances. [2]

The aim of this study was the development of a packed bed photoreactor system, to be used for photocatalytic treatment of contaminants in wastewater. To achieve this, a suspension of commercially available TiO<sub>2</sub> (P25) was deposited onto glass beads (diameter ~3 mm) using the dip-coating method. These beads were then packed into a tube (diameter ~10 mm) with a volume of 50 mL. Photocatalytic efficiency of our system under real conditions was tested by observing the degradation rate of various persistent organic pollutants (organic dyes, selection of pharmaceuticals, ...) dissolved in distilled water, bioreactor effluent and central wastewater treatment plant effluent under UV light. Results show that the reactions are expectedly slower in wastewater than in deionized H<sub>2</sub>O, nevertheless, it is shown that removal of the compounds from water is still possible even when other organic molecules are present. [3]

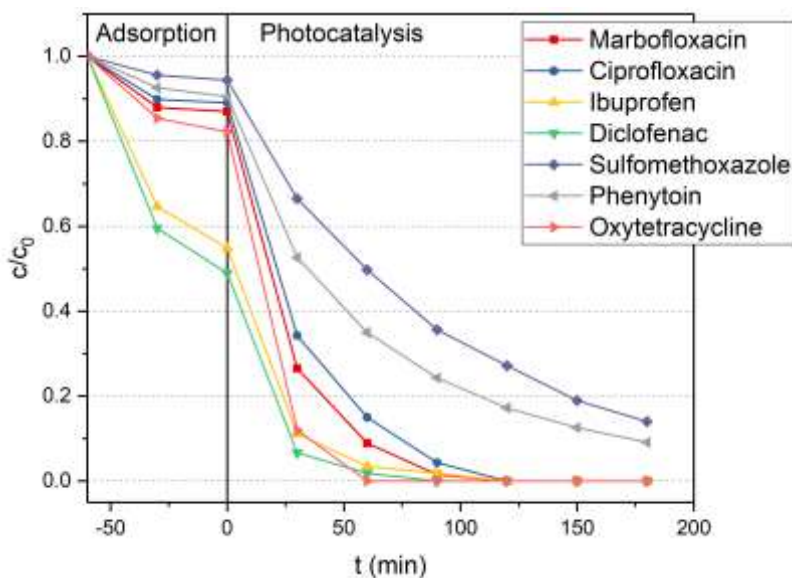


Figure 53: Photocatalytic degradation of pharmaceuticals in distilled water.

### Acknowledgements

The authors acknowledge the financial support from the Slovenian Research Agency (research core funding No. P1-0134 and project No. L7-1848).

### References

1. G. Crini, E. Lichtfouse, Environ. Chem. Lett. **17** (2019) 145–155.
2. M.R. Al-Mamun, S. Kader, M.S. Islam, M.Z.H. Khan, J. Environ. Chem. Eng. **7** (2019) 1-17.
3. B. Žener, L. Matoh, P. Rodič, D. Škufca, E. Heath, U. Lavrenčič Štangar, J. Environ. Chem. Eng. **9** (2021) 1-9.



# Pollution prevention and remediation

## Fatty acids-based Eutectic Solvents Liquid Membranes for Removal of Sodium Diclofenac from Water

J. Afonso<sup>1</sup> and I.M. Marrucho<sup>1,\*</sup>

<sup>1</sup>Centro de Química Estrutural and Departamento de Engenharia Química, Instituto Superior Técnico, Universidade de Lisboa, Avenida Rovisco Pais, 1049-001 Lisboa, Portugal

\*isabel.marrucho@tecnico.ulisboa.pt

Pharmaceuticals have a main role on health and life quality of humans and animals. Nevertheless 30% to 90% of all oral administrated drugs are excreted as active compounds [1], leading the worldwide occurrence of these active compounds and their metabolites in water sources, soils, and biota. As these compounds are designed to have a biological response to small dosages, they are an important threat to public health and ecosystem stability even at low concentration [1]. Additionally, their relative high stability is even more concerning, as the continuous ingestion of small doses can lead to accumulation since the degradation rate is slower than the up taking. On the other hand, conventional wastewater treatment plants (WWTP) are not designed to remove these compounds that enter the environment. Despite the report of diverse cases of life-threatening biological effects of these drugs on wildlife, about 88% of all pharmaceuticals do not have environmental toxicity data [2].

Although the use of eutectic solvents (ES) provides a cheap and efficient solution for the removal of APIs micropollutants [3 - 4], the toxicity of some of the used compounds and their leaching are drawbacks that need to be overcome to develop a fully sustainable system. The use of all natural compounds like sugars, amino acids, organic acids, choline and urea that exhibit low toxicity and have a high biocompatibility might be the answer for this problem.

In this work, ES based on fatty acids were impregnated on porous membranes by soaking and use to remove sodium diclofenac from water using UV-Vis spectroscopy to quantify the extraction efficiency of the membranes. Experimental parameters such as contact time, number of membranes, pH and initial concentration of pharmaceutical were optimized to achieve a remarkable extraction efficiency 97%. These membranes were re-used over 9 more cycles of extraction without decreasing the efficiency.



Figure 1. PVDF membranes impregnated with NADE.

### Acknowledgements

Afonso J. gratefully acknowledges the financial support of FCT/MCTES (Portugal) for PhD fellowship 2021.07949.BD and the CQE project PTDC/EAM-AMB/2023/2021.

### References

1. M. Ibáñez, L. Bijlsma, E. Pitarc, F. J. López, and F. Hernández, Occurrence of pharmaceutical metabolites and transformation products in the aquatic environment of the Mediterranean area, *Trends in Environmental Analytical Chemistry*, vol. 29, p. e00118, 2021. doi: 10.1016/J.TEAC.2021.E00118.
2. OECD, *Pharmaceutical Residues in Freshwater: Hazards and Policy Responses, Studies on Water*. Paris: OECD Publishing, 2019. doi: 10.1787/c936f42d-en.
3. C. Florindo, N. V. Monteiro, B. D. Ribeiro, L.C. Branco, I.M. Marrucho, Hydrophobic deep eutectic solvents for purification of water contaminated with Bisphenol-A, *Journal of Molecular Liquids*, vol 297, 111841, 2020. doi: 10.1016/j.molliq.2019.111841.
4. C. Florindo, L.C. Branco, I.M. Marrucho, Development of hydrophobic deep eutectic solvents for extraction of pesticides from aqueous environments, *Fluid Phase Equilibria*, vol 448, 2017. doi: 10.1016/j.fluid.2017.04.002.

## Energy Balance of a Thermophilic Biological Fluidized Bed Reactor During Exothermic Reactions of Sludge Minimization

Maria Cristina Collivignarelli <sup>1,2</sup>, Marco Carnevale Miino <sup>1\*</sup>, Giacomo Cillari <sup>3</sup>, Stefano Bellazzi <sup>1</sup>,  
Francesca Maria Caccamo <sup>1</sup>, Alessandro Abbà <sup>4</sup> and Giorgio Bertanza <sup>4</sup>

<sup>1</sup> Department of Civil Engineering and Architecture, University of Pavia, via Ferrata 3, 27100 Pavia, Italy

<sup>2</sup> Interdepartmental Centre for Water Research, University of Pavia, Via Ferrata 3, 27100 Pavia, Italy

<sup>3</sup> Department of Energy, Systems, Territory and Constructions Engineering, University of Pisa, Largo Lucio Lazzarino, 56122 Pisa, Italy

<sup>4</sup> Department of Civil, Environmental, Architectural Engineering and Mathematics, University of Brescia, via Branze 43, 25123 Brescia, Italy

\* marco.carnevalemiino01@universitadipavia.it

**Introduction:** Thermophilic biological fluidized bed reactor (TBFBR) proved to be effective for sewage sludge minimization [1,2]. Reactions of organic matter degradation that occur in thermophilic conditions are generally exothermic. Therefore, this work aims to evaluate the amount of energy produced by the degradation of the sewage sludge taking into consideration organic matter removal, external apports of energy and heat losses.

**Materials and methods:** Tests were conducted in a pilot-scale TBFBR (1 m<sup>3</sup>). The energy balance in Eq. 1 takes into account the heat loss from the main tank envelop ( $Q_{\text{maintank}}$ ), the boiler tank ( $Q_{\text{tank}}$ ), the pipes ( $Q_{\text{pipes}}$ ) and the share due to the evaporation ( $Q_{\text{evap.}}$ ) flow rate and convection ( $Q_{\text{conv.}}$ ) from the free surface of the reactor. Finally, the energy from the exothermic reaction, Eq. 2, has been evaluated as a difference between total heat loss ( $Q_{\text{TOT}}$ ) and the energy provided by the boiler to keep reactor temperature ( $Q_{\text{boiler}}$ ):

$$Q_{\text{TOT}} = Q_{\text{maintank}} + Q_{\text{tank}} + Q_{\text{pipes}} + Q_{\text{conv.}} + Q_{\text{evap.}} \quad [1]$$

$$Q_{\text{eso}} = Q_{\text{TOT}} - Q_{\text{boiler}} \quad [2]$$

The monitoring activity has been carried out for one month during winter period to evaluate the energy balance in worst external conditions. The heat loss through the reactor, the boiler tank and the pipes involved common conduction heat transfer. For the evaluation of the heat loss from the free surface of the sludge, the energy loss through evaporation has been determined with the evaporation flow rate based on the formula proposed by Asdrubali [3]. In the calculation, as the fluid is mainly made up of water, the relative enthalpy of vaporization  $I_{\text{water}}$  has been assumed. The energy loss through convection between free surface of the sludge and the environment has been modelled adopting the following Eq. 3:

$$Q_{\text{conv.}} = h \cdot A \cdot (T_p - T_a) \quad [3]$$

where the convection heat transfer coefficient has been hourly determined as follows (Eq. 4):

$$h = 0.22 \cdot (T_p - T_a)^{1/3} \quad [4]$$

**Results and discussion:** More than 80% of COD fed were removed by the TBFBR (Figure 2). After about 30 days, stable conditions were achieved. Considering the period selected in the analysis, the specific removal rate of organic matter was almost 1.4-3.4 kg<sub>COD</sub>/m<sup>3</sup> d. Results of energy balance showed an energy production of 1705 kWh for the month of December. The trend, dominated by the conduction through the apparatus envelop, is almost flat, with an average heat loss through the envelop around 5 kWh, and a loss through conduction and evaporation of 0.008 kWh (Figure 3).

**Conclusions:** In conclusion, TBFBR application for sewage sludge minimization allows to produce a surplus of energy thanks to high energetic exothermal reactions of organic matter degradation. This model helps to quantify the specific amount of energy produced associated to exothermic processes.

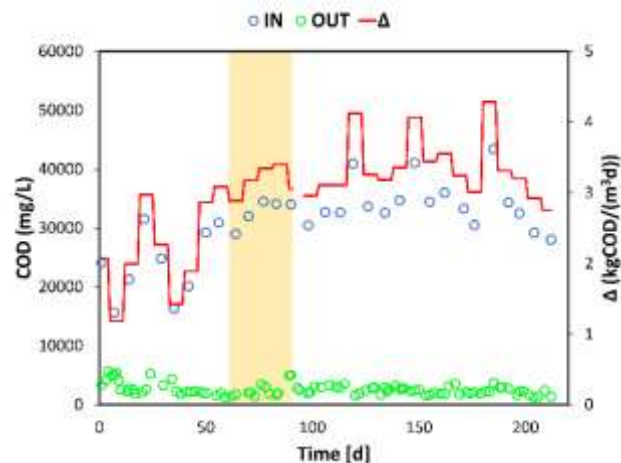


Figure 54. Concentration of COD in and out the TBFBR, and difference of organic matter load between the two streams ( $\Delta$ ). Yellow area represents the selected period (stable and cold conditions) in which the energy balance has been evaluated.

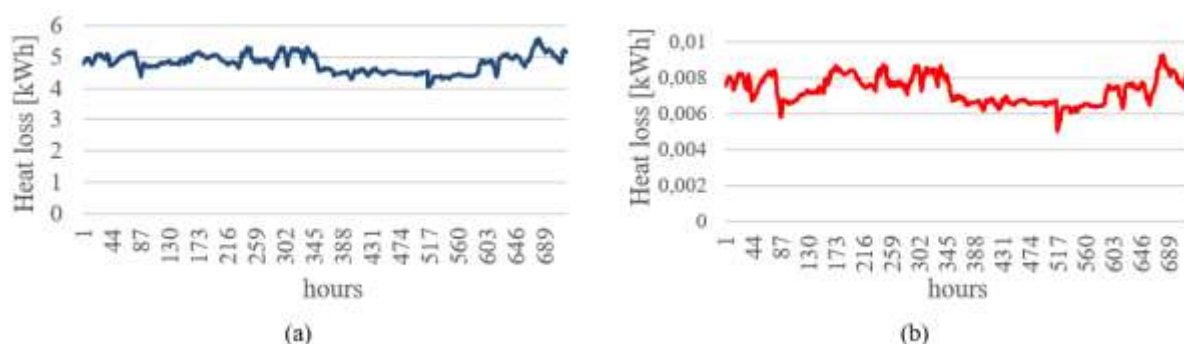


Figure 3. Heat loss through the system envelop (a) and via convection and evaporation from free surface (b)

## Acknowledgements

The authors would like to thank ASM Pavia S.p.a., Pavia Acque S.c.a.r.l., and DTA S.r.l. for the support during the first experimental phase.

## References

1. M.C. Collivignarelli, A. Abbà, F.M. Caccamo, M. Carnevale Miino, A. Durante, S. Bellazzi, M. Baldi, G. Bertanza, *Membranes*, **11** 977 (2021)
2. M.C. Collivignarelli, A. Abbà, M. Carnevale Miino, F.M. Caccamo, S. Argiolas, S. Bellazzi, M. Baldi, G. Bertanza, *Process Saf. Environ. Prot.* **155** 262–276 (2021)
3. F. Asdrubali, *Energy Build.* **41** 311–319 (2009)

## Removal of pharmaceuticals on functionalized activated carbons

El-Said I. El-Shafey, Syeda N. F. Ali

*Chemistry Department, College of Science, Sultan Qaboos University, PC 123, Muscat, Oman*

### Abstract

Activated carbon (AC) was prepared from date palm leaflets via KOH activation. Oxidized activated carbon (OAC) was produced via nitric acid treatment. OAC was converted to basic and hydrophobic activated carbons via surface functionalization using different amine and diamine surfactants (ethylene diamine, propylenediamine, ethylamine and aniline). Surface area of activated carbon (835 m<sup>2</sup>/g) has decreased on oxidation and surface functionalization. Acidic drugs (ibuprofen) and basic drugs (chlorpheniramine and diphenhydramine) were tested for their adsorption on acidic, basic and hydrophobic activated carbons. Drug adsorption was found to be faster on hydrophobic activated carbons than other carbons with data fitting the pseudo second order kinetic model. Activation energies were found to be in the range of physical adsorption. Langmuir adsorption model was found to fit well the sorption of methylene blue. Rising the temperature has shown better performance for drug removal with better performance for ethylamine functionalized activated carbon. Thermodynamic parameters were also calculated.

## Effect of competing anions on chromate and arsenate adsorption by polyethylenimine functionalized silica-based material

Maria Xanthopoulou, Dimitrios Gkiliopoulos, Konstantinos Triantafyllidis, Margaritis Kostoglou, and Ioannis A. Katsoyiannis\*

Laboratory of Chemical and Environmental Technology, Department of Chemistry,  
Aristotle University of Thessaloniki, Box 116, 54124 Thessaloniki, Greece

\*e-mail: katsogia@chem.auth.gr

Arsenic and chromium contamination of groundwaters has triggered worldwide attention due to their toxicity and carcinogenicity. Arsenic and chromium usually coexist in natural waters, which are released through natural causes such as soil corrosion and anthropogenic activity such as mining and alloys industries [1]. In natural water, arsenic is primarily present in inorganic forms and exists in two predominant species, arsenate [As(V)] and arsenite [As(III)]. As(V) is the major arsenic species in surface water, while As(III) is the dominant arsenic in groundwater since it is favored under reducing conditions. As(III) is more toxic to biological systems than As(V). Chromium is found in the environment as both trivalent, Cr(III) and hexavalent, Cr(VI), although the toxicity of the hexavalent form is higher than that of the trivalent form. In aqueous media, arsenic and chromium can exist in several anionic species, mainly as chromate ( $\text{CrO}_4^{2-}$  or  $\text{Cr}_2\text{O}_7^{2-}$ ) and arsenate ( $\text{HAsO}_4^{2-}$  or  $\text{AsO}_4^{3-}$ ) [1, 2]. Adsorption is an important treatment approach as it is easily operated with high efficiency and low cost [2] and there is an increased need for development of adsorbents, which could remove multiple contaminants from waters. In this direction, in our study, we prepared and used a silica-based material functionalized with polyethylenimine ( $\text{SiO}_2$ -PEI) as an adsorbent, which has been proved efficient in removing arsenate and chromate and cases are reported to be simultaneously present in waters. Coexisting anions in natural waters such as phosphates, sulfates and nitrates, might compete with arsenic and chromium oxyanions for active adsorption sites and significantly reduce their removal performance by the adsorbents [3].

In our study we examined the effect of phosphate, sulfate and nitrate anions on chromium and arsenic adsorption by  $\text{SiO}_2$ -PEI. The maximum uptake of arsenic and chromium on  $\text{SiO}_2$ -PEI, in the presence of the other anions at different pH values were studied. Also, the effect of different concentrations of the anions and the effect of the increasing concentration of the adsorbent material were studied. The experiments were performed using a rotary stirrer. Total chromium and arsenic were determined by graphite furnace atomic absorption. Hexavalent chromium was determined by diphenyl-carbazide method, a colorimetric determination where the absorbance of the samples is measured on a spectrophotometer. Phosphates, sulphates and nitrates were determined by test kits.

Initial results of the study on the effect of phosphate ions on Cr(VI) adsorption are presented in Figure 1. The removal rate of hexavalent chromium is over 90% with the presence of 4 mg/L of phosphate anions, for the initial Cr(VI) concentrations over 40  $\mu\text{g/L}$  at pH 7 and a dose of 100 mg/L of the adsorbent,  $\text{SiO}_2$ -PEI. At lower initial chromium concentrations, under 40  $\mu\text{g/L}$ , the presence of phosphate anions had an adverse effect decreasing Cr(VI) removal efficiency.

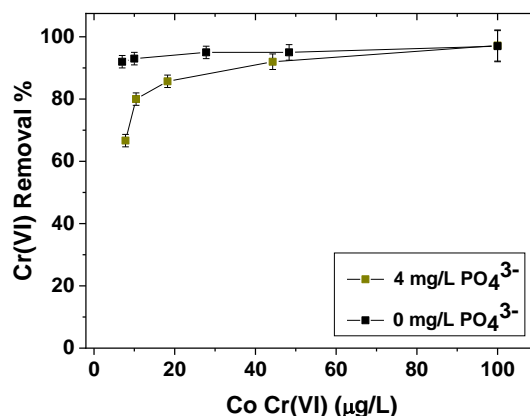


Figure 1. Effect of the presence of phosphate anions on hexavalent chromium adsorption by  $\text{SiO}_2$ -PEI (Adsorbent dose 100 mg/L, pH=7, T=22°C)

## Acknowledgements

The authors are grateful to funding received from the Prefecture of Central Macedonia under the project “Selection of research directions and accreditation of parameters and methods of the chemical and biological sector of the Environmental Control and Research laboratory of the Prefecture of Central Macedonia, Greece”.

## References

1. Mohammed, A.S., Kapri, A., Goel, R. (2011). Heavy Metal Pollution: Source, Impact, and Remedies. In: Khan, M., Zaidi, A., Goel, R., Musarrat, J. (eds) *Biomangement of Metal-Contaminated Soils*. Environmental Pollution, vol 20. Springer, Dordrecht.
2. Chai, W.S., Cheun, J.Y., Kumar, P.S., Mubashir, M., Majeed, Z., Banat, F., Ho, S.H., Show P.L. (2021). A review on conventional and novel materials towards heavy metal adsorption in wastewater treatment application, *Journal of Cleaner Production* 296.
3. John, Y., David, V.E., Mmereki, D. (2018). A Comparative Study on Removal of Hazardous Anions from Water by Adsorption: A Review, *International Journal of Chemical Engineering*, vol. 2018, Article ID 3975948, 21 pages.

## Oxidation and removal of As(III) and organic contaminants from wastewaters and groundwaters using nano-modified biochar

Ioannis Katsoyiannis\*, Stella Chatzimichailidou, Margaritis Kostoglou, Georgios Kizas, Dimitris Giannakoudakis, Konstantinos Triantafyllididis

Department of Chemistry/Aristotle University of Thessaloniki/Thessaloniki/54124/Greece

\*sdchatzim@chem.auth.gr

### Abstract text:

The present study aims to investigate the use of advanced oxidation processes based on sulfate radicals production for oxidation of arsenic (III) to arsenic (V) and removal from water. As a solid matrix for the production of radicals will be biochar, produced by rice husk from the area of Thessaloniki. The ability of biochars to form radicals when the water is spiked with some persulfate salts will be investigated. Initially, the oxidative capacity of plain biochar and persulfate radicals, will be studied, against arsenic [1], in order to study the oxidative pathways of arsenic(III) and evaluate the efficiency of the technology under different conditions (i.e., pH, temperature, catalysts, initial concentrations, water matrix composition). Then, the oxidation methods will be optimized by modifying the oxidation conditions for each experimental route, and by synthesizing new oxidizing methods, such as biochar with properly modified surface area to generate persulfate radicals [4].

The results of this study are expected to be of particular interest in the treatment of water, the quality of which is of great importance for the environment, which constantly receives large loads of pollutants due to human activity.

### Chemicals & Materials:

- Rice straw biomass derived from Chalastra, Thessaloniki, Greece
- GFX
- KOH
- HCl
- Na<sub>2</sub>HAsO<sub>4</sub>\*7H<sub>2</sub>O

### Experimental procedure:

Different biochars were synthesized in different pyrolysis temperatures (300,400,500 °C) under N<sub>2</sub> atmosphere with a hold time of 1 h, and a heating rate of 5 °C/min. The products were sieved using a mortar and a pestle. The biochars underwent acidic, alkali, GFX or montmorillonite modification. After the modification the characteristics of our materials were studied using their FT-IR spectras, SEM micrographs, porosity measurement and their surface elemental composition. Thereinafter the ability of each one of the 12 biochar samples to oxidize different concentrations of arsenic, under different conditions, was tested and compared. Samples were extracted in different time intervals to study the kinetics of the reactions. Arsenic concentration in water was measured by Atomic Absorption Spectroscopy (AFS) coupled with Graphite Furnace.

### References

1. I. Katsoyiannis, A. Zouboulis, *Water Research*, 36 5141-5155 (2002)
2. H. Wang et. al, *Chemical Engineering Journal*, 429 (2022)
3. Z. Jiang et. al, *Environmental Research*, 184 (2020)
4. E. Agrafioti, D. Kalderis, E. Diamadopoulos, *Journal of Environmental Management*, 133 309-314 (2014).



## Pilot scale continuous photocatalytic reactor for removal of emerging contaminants from leachates

Panagiotis Kouvatsis<sup>1,2</sup>, Eleni Evgenidou<sup>1,2</sup>, Christina Nannou<sup>1,2</sup>, Dimitris Bikiaris<sup>3</sup>, Dimitra Lambropoulou<sup>1,2</sup>

*1Department of Chemistry, Aristotle University of Thessaloniki, GR 54124, Thessaloniki, Greece*

*2Centre for Interdisciplinary Research and Innovation (CIRI-AUTH), Balkan Center, Thessaloniki, 10th km Thessaloniki-Thermi Rd, GR 57001, Greece*

*3Laboratory of Polymer Chemistry and Technology, Department of Chemistry, Aristotle University of Thessaloniki, GR-54124 Thessaloniki, Greece*

Landfills are the final repository for a heterogeneous mixture of waste coming from urban, industrial, and commercial sources. Therefore, they possibly generate complex structure and variable content leachates containing thousands of contaminants of emerging concern, being thus one of the most difficult aqueous matrices to treat. Advanced oxidations processes (AOPs) are an effective process to treat this matrix. To this end, a novel, automated photocatalytic pilot-scale plant has been designed and evaluated. The plant has a maximum capacity of 100 L, maximum flow rate of 12 L/min of treated water, and 160 W of UV-C power, serving for heterogeneous photocatalysis employing dispersed TiO<sub>2</sub> nanoparticles with UV irradiation. Pilot tests with different matrix of leachates under continuous operation were carried out for the assessment of the pilot unit performance. Different operating parameters and conditions were tested for the removal of emerging contaminants in leachates using benzotriazole (BZT), as a model contaminant molecule. Namely, the flow rate of the reactor (1, 5 and 10 L/min), the concentration of the model compound, the TiO<sub>2</sub> loading and the UV-C irradiation dose were assessed to define the optimum parameters of the plant performance for both the degradation of BZT and TOC mineralization. According to the results, the removal of BZT was affected by the catalyst loading while the flow rate had rather a negligible effect. The identification of transformation products formed during the photocatalytic process was performed by using an Orbitrap Q Exactive Focus™ high-resolution mass spectrometry system. Thanks to the Compound Discoverer software (version 3.1), more than 12 TPs were identified with the view to untangle the possible reaction pathways involved with BTZ mineralization.

### **Acknowledgments**

This research has been co-financed by the European Union and Greek national funds through the Operational Program Competitiveness, Entrepreneurship, and Innovation, under the call RESEARCH – CREATE – INNOVATE (2<sup>nd</sup> Cycle) (Project acronym: UV-LEACH; Project code: T2EDK-00137).

## Novel diketopyrrolopyrrole-rhodamine conjugates with sensing ability

Andreia Leite,<sup>1</sup> Carla Queirós,<sup>1</sup> Vítor A. S. Almodôvar,<sup>2</sup> Fábio Martins,<sup>1</sup> Augusto C. Tomé,<sup>2</sup> Ana M. G. Silva<sup>1\*</sup>

<sup>1</sup>REQUIMTE-LAQV, Department of Chemistry and Biochemistry, University of Porto, 4169-007 Porto, Portugal

<sup>2</sup>REQUIMTE-LAQV, Department of Chemistry, University of Aveiro, 3810-193 Aveiro, Portugal

\*ana.silva@fc.up.pt

The search for advanced and sensitive methods for sensing chemical substances, namely cations and anions, is urgent and widely sought due to the enormous impact that these substances have on human health and on the environment. Here we offer an efficient solution for the colorimetric and fluorescent detection of  $\text{Li}^+$  and  $\text{CN}^-$  ions based on the displacement mechanism using two new  $\text{Cu}^{2+}$ -chemosensor complexes. For this purpose, two novel photoactive diketopyrrolopyrrole-rhodamine conjugates, chemosensors **1** and **2**, were synthesised through the condensation of diketopyrrolopyrrole-dicarbaldehyde with one and two rhodamine B hydrazide moieties, respectively. The obtained chemosensors **1** and **2** were characterized by  $^1\text{H}$ ,  $^{13}\text{C}$  NMR and high-resolution mass spectrometry, and their photophysical and ion-responsive behaviour were investigated by UV-Vis absorption and fluorescence measurements. Both chemosensors **1** and **2** display a rapid colorimetric response with a remarkable increase in the absorbance and fluorescence intensities upon addition of  $\text{Cu}^{2+}$ , while other metal ions caused no significant effect. Moreover, the resulting  $\text{Cu}^{2+}$ -chemosensor complexes can be used to detect  $\text{CN}^-$  and  $\text{Li}^+$ , with reversibility and low detection limits. The recognition ability of the chemosensors was investigated by adsorption and fluorescence titrations, Job's plot and competitive studies.

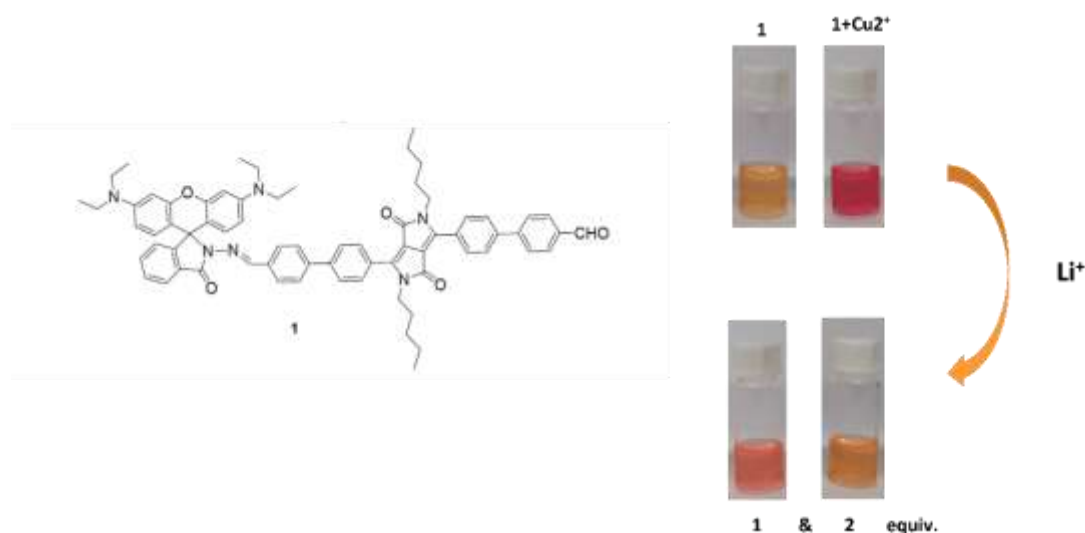


Figure 1. Structure of chemosensor **1** (left) and colorimetric response (right) of chemosensor **1** upon addition of  $\text{Cu}^{2+}$  (top) [ $\text{Cu}^{2+}$ -chemosensor **1** complex] upon addition of  $\text{Li}^+$  1 and 2 equivalents (bottom).

### Acknowledgements

This work received financial support from National Funds (FCT/MCTES, Fundação para a Ciência e Tecnologia and Ministério da Ciência), under the Partnership Agreement PT2020 through project PTDC/QUI- PTDC/QUI-QOR/29426/2017, QIN/28142/2017 and EXPL/QUI-OUT/1554/2021. Additionally, the research team would like to thank the projects NORTE-07-0162-FEDER-000048, UIDB /50006/2020, UIDP/50006/2020. A. Leite and A.M.G. Silva thank FCT for funding through program DL 57/2016 – Norma transitória.

## Visible light-driven degradation Trichloroethylene in aqueous phase with Vanadium-doped TiO<sub>2</sub> photocatalysts

Duc Manh Nguyen<sup>1,2</sup>, Thi Thuong Nghiem<sup>2</sup>, Van Anh Nguyen<sup>2\*</sup> and Esteban Mejía<sup>1\*</sup>

<sup>1</sup>Leibniz Institute for Catalysis (LIKAT), Albert-Einstein-Str. 29a, 18059, Rostock, Germany

<sup>2</sup>School of Chemical Engineering, Hanoi University of Science and Technology, No.1 Dai Co Viet Hanoi, Vietnam

\*Esteban.Mejia@catalysis.de

Trichloroethylene (TCE) is a volatile chlorinated organic compound (VCOC) commonly used as an industrial solvent. Wastewaters contaminated with TCE come from automotive, metal, finishing, and textile industries. It is a pollutant of serious concern in groundwaters, as it is harmful to aquatic and surface ecosystems and to the human health. For instance, results of epidemiological research have shown a causal relationship for TCE overexposure and human organs cancer. There are various reported methods for the degradation of TCE in aqueous media, including the “air stripping method”, where the volatilization is often incomplete, and consequently a residual amount of TCE can still be found in the treated water. Moreover, gas-phase degradation of TCE produces toxic by-products such as phosgene and dichloroacetyl chloride [1].

Photocatalytic degradation of VCOCs in the aqueous phase using semiconductors such as TiO<sub>2</sub> is well known and offers a promising alternative [2]. However, pure TiO<sub>2</sub> can only absorb UV light, which accounts for only 2 ÷ 5% of the solar spectrum, thus restricting its practical application. In the present work, vanadium-doped TiO<sub>2</sub> nanoparticles with enhanced optical properties were prepared via a one-step hydrothermal method. These semiconductors display good catalytic activities in the photodegradation of TCE under visible-light irradiation (Figure 1) [3].

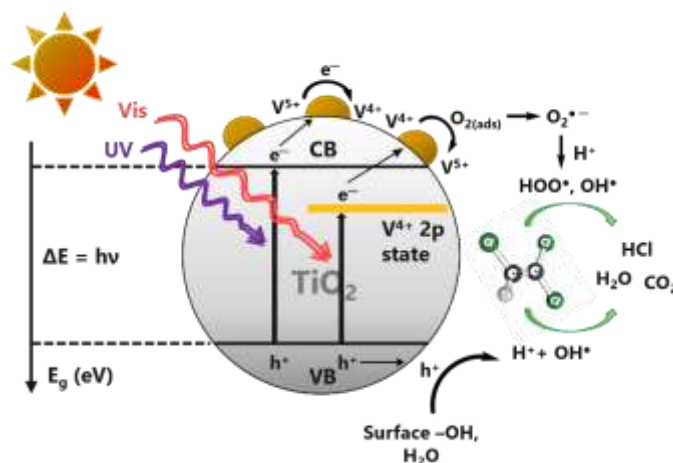


**Figure 1.** Proposed mechanism of photodegradation of TCE over Vanadium-doped TiO<sub>2</sub> photocatalysts

The catalysts were prepared by hydrothermal treatment (190 °C for 9.5 hours) of acidic NH<sub>4</sub>VO<sub>3</sub> aqueous solutions (2.1 × 10<sup>-4</sup> g.mL<sup>-1</sup>) mixed with a certain amount of TiCl<sub>4</sub> (to achieve V/Ti ratios of 0%, 5%, 10%, 15%). The resulting precipitates were washed with water and ethanol and dried at 80 °C for 12 hours. The samples are respectively labeled as: **Undoped TiO<sub>2</sub>**, **0.05V-TiO<sub>2</sub>**, **0.10V-TiO<sub>2</sub>**, and **0.15V-TiO<sub>2</sub>**. The catalysts were thoroughly characterized (Table 1) using powder XRD (Bruker D8 Advance, Cu K $\alpha$  radiation), ICP-OES (715-ES ICP emissions spectrometer), BET surface area (Micromeritics ASAP 2020), XPS (Multilab 2000, Thermal Fisher, Al K $\alpha$  radiation), UV-VIS DRS (Cary-5000, Agilent, BaSO<sub>4</sub> used as a reference material), FT-IR ATR (Nicolet 330), and SEM EDX (Hitachi TM 4000 Plus).

**Table 1.** Physicochemical properties and the total V/Ti molar ratio of as prepared TiO<sub>2</sub> samples

Sample	Aver. crystal size (nm)			Phase content (%)			S <sub>BET</sub> (m <sup>2</sup> .g <sup>-1</sup> )	Pore volume (cm <sup>3</sup> .g <sup>-1</sup> )	Pore size (nm)	ICP-OES (V / Ti)
	A	R	B	A	R	B				
<b>Undoped TiO<sub>2</sub></b>	6.61	6.66	8.30	75.11	4.57	20.32	154.5	0.229	4.8	-
<b>0.05V-TiO<sub>2</sub></b>	6.19	7.27	7.69	76.82	10.54	12.64	-	-	-	0.055
<b>0.10V-TiO<sub>2</sub></b>	5.69	9.10	7.78	76.20	15.46	8.34	155.9	0.153	4.1	0.097
<b>0.15V-TiO<sub>2</sub></b>	5.82	10.40	6.24	74.93	16.74	8.33	-	-	-	0.141

The hydrothermal process in the acid medium (pH = 3) tends to form the anatase phase TiO<sub>2</sub>, where HCl acts as an inhibitor preventing coalescence of the nanocrystallites to form larger particles, and increases the free energy of rutile and brookite phases [4]. With increasing dopant contents, the presence of lattice defects increases as Ti-O bonds in the anatase or brookite structures are broken, allowing rearrangement of the Ti-O octahedra that causes the phase transformation from others to rutile. The existence of intermediate energy states due to the incorporation

of V species into TiO<sub>2</sub> lattice results in a clear redshift to the visible light as well as narrowing the bandgap of doped TiO<sub>2</sub> samples (Figure 2) [5].

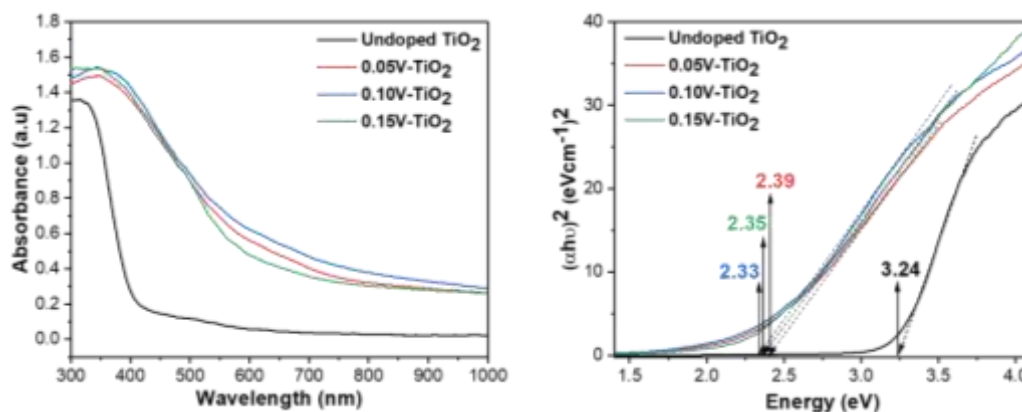


**Figure 2.** UV-Vis DRS (left) and the Tauc plot (right) of as prepared TiO<sub>2</sub> samples

Photocatalytic experiments were carried out under continuous magnetic agitation by mixing an aqueous solution of TCE (1000 ppm) with the catalyst (2 g.L<sup>-1</sup>) in a quartz tube under UV light ( $\lambda = 390$  nm) or in a glass photoreactor under visible light ( $\lambda = 422 \div 700$  nm) under oxygen atmosphere at room temperature (20 to 23 °C). Before and during illumination, samples were withdrawn from the reactor at certain intervals, filtered, extracted with CDCl<sub>3</sub> and the amount of TCE was quantified by <sup>1</sup>H-NMR spectroscopy (Bruker 400 MHz).

In general, doped TiO<sub>2</sub> samples show higher photocatalytic activities than **undoped TiO<sub>2</sub>**. Under the UV irradiation, catalyst **0.10V-TiO<sub>2</sub>** present the optimal activity for degradation of TCE, while the fastest degradation of TCE was obtained over **0.15V-TiO<sub>2</sub>** under the visible irradiation (Figure 3).

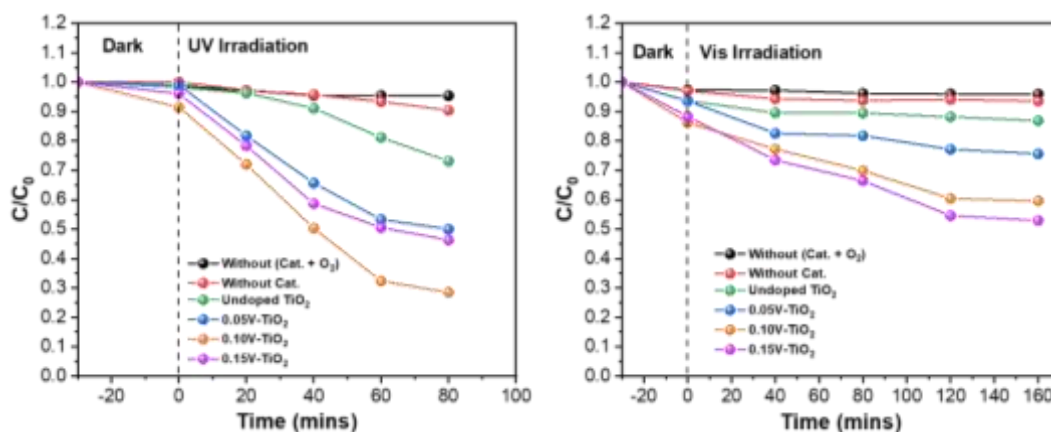


**Figure 3.** Photocatalytic degradation of TCE in the solution with prepared TiO<sub>2</sub> samples

In summary, Vanadium-doped TiO<sub>2</sub> nanoparticles with enhanced optical properties were prepared via a one-step hydrothermal method. The prepared samples show a promising performance for photocatalytic degradation of Trichloroethylene in aqueous phase under both UV light and visible light. This method represents a more sustainable alternative to other existing technologies for the remediation of waters polluted with VCOCs, as it can be performed under visible light and very mild reaction conditions.

## Acknowledgements

This work was supported by the RoHan Project funded by the German Academic Exchange Service (DAAD No. 57315854) and the Federal Ministry for Economic Cooperation and Development (BMZ) inside the framework “SDG Bilateral Graduate School Programme”.

## References

- [1]. Agency for Toxic Substances and Disease Registry, U.S. Department of Health and Human Services, (2019)
- [2]. Y.-C. Hsu, S.-H. Chang, W.-C. Chung and M.-B. Chang, *Environmental Science and Pollution Research*, **26** 26276 (2019).
- [3]. J. Liu, R. Han, Y. Zhao, H. Wang, W. Lu, T. Yu and Y. Zhang, *The Journal of Physical Chemistry C*, **115** 4507 (2011).
- [4]. A. Barnard, P. Zapol and L. A. Curtiss, *J. Chem. Theory Comput.*, **1** 107 (2005).
- [5]. X. Pan, M.-Q. Yang, X. Fu, N. Zhang and Y.-J. Xu, *Nanoscale*, **5** 3601 (2013).

## Absorption of Pollutants by CsPbBr<sub>3</sub> Perovskite

G. Roini<sup>1\*</sup>, M. Maddaloni<sup>2,3</sup>, I. Vassalini<sup>1,3,4</sup>, A. Vinattieri<sup>5,6,7</sup> and I. Alessandri<sup>1,3,4</sup>

<sup>1</sup> Department of Information Engineering, University of Brescia, via Branze 38, 25123, Brescia, Italy.

<sup>2</sup> Chemistry for Technologies Laboratory, Department of Mechanical and Industrial Engineering, University of Brescia, via Branze 38, 25123, Brescia, Italy.

<sup>3</sup> National Interuniversity Consortium of Materials Science and Technology (INSTM), Florence, Italy, , University of Brescia, via Branze 38, 25123, Brescia, Italy.

<sup>4</sup> National Institute of Optics-Italian National Research Council (CNR-INO), University of Brescia, via Branze 38, 25123, Brescia, Italy.

<sup>5</sup> Department of Physics and Astronomy, University of Florence, via G. Sansone 1, Sesto F.no, Italy.

<sup>6</sup> INFN-Firenze, via G. Sansone 1, Sesto F.no, Italy

<sup>7</sup> LENS, via N.Carrara 1, Sesto F.no, Italy

\*E-mail: [g.roini@unibs.it](mailto:g.roini@unibs.it)

### Introduction:

Climate change and environmental sustainability ask for a more efficient and circular waste management. In parallel, water and air purification is another major goal that challenges the scientific community to develop new materials, techniques and strategies. Moreover, there is a growing interest to produce green energy with low-cost materials. In particular, in the last decade, halide perovskites have received considerable interest from the communities of physicists of matter, chemists and materials scientists for the many possible applications to replace the classic semiconductors for photovoltaics, optoelectronics and sensors [1, 2].

Perovskites are a large class of compounds characterized by the formula  $ABX_3$ , having the same structure as  $CaTiO_3$ . The inorganic halide perovskites (HP) are constituted by a halogen (X), a divalent metal (B), and a monovalent metal (A). The main physical properties that make both organic and inorganic halide perovskites excellent materials for devices are: the high mobility of the charge carriers, the high absorption coefficient being direct band-gap semiconductors and the small cross section of the defects (mainly halogen vacancies). In particular,  $CsPbX_3$  (X=Cl, Br, I) is deeply investigated because the bandgap energy  $E_g$  can be finely tuned to cover the whole visible range, when alloying different halides. Typically,  $CsPbBr_3$  is studied for optoelectronic devices like lasers, light amplification system (resonators and waveguides) and other photonic devices.

This research will show how halide perovskites can also be used as substrates for the absorption and catalysts for the photodegradation of pollutants. As an example, Methylene Blue (MB), a typical pollutant that can be found in water as waste of textile industry, has been considered. The final idea is the possibility to circularly reuse perovskites recovered from other applications, such as photovoltaics [3], and exploit their pollutant absorption properties. In this way it is possible to create a double advantage for the environment: reduce the amount of solid waste and improve water quality.

### Materials and methods:

This research is focused on the use of  $CsPbBr_3$  as absorbers of  $10^{-5}M$  aqueous solutions of MB, which simulates a typical range of concentration of organic dye pollutants in textile industry effluents. The  $CsPbBr_3$  was synthesized in powder form according to the following procedure: the precursor salts  $PbBr_2$  (0.17M) and  $CsBr$  (0.035M) were dissolved in DMF (Dymethylformamide) and Methanol (MeOH), respectively. Under magnetic stirring, the  $PbBr_2$  was mixed with  $CsBr$  and the solvents were allowed to evaporate. Once the powdered perovskite was obtained, it was cleaned in 2-propanol, in order to eliminate any solvent residue.

Four different molar ratios of  $PbBr_2/CsBr$  salt precursors, namely 1; 1.9; 2.9 and 3.9, were investigated, leading to the systems called PVK 1, PVK 1.9, PVK 2.9 and PVK 3.9. The XRD analysis of the obtained powders confirmed the presence in all cases of the  $CsPbBr_3$  phase, with a significant percentage of spurious phases for higher molar ratios.

The analysis for the absorption of the MB and its photodegradation was carried out using a UV-VIS spectrometer and illumination was performed by a solar simulator. The study was carried out analyzing the percentage of MB absorbed by the  $CsPbBr_3$  nanopowders (NPs) as a function of time.

In addition, to facilitate the manipulation of the  $CsPbBr_3$  NPs and reduce any eventual Pb release in water during their employment as adsorbents/catalysts, they were incorporated into millimeter-sized hydrogel bubbles made of chitosan (CH), a biopolymer extracted from the shell of waste shrimps. MB absorption experiments were also conducted for this hybrid hydrogel composites, and compared with the absorption of analogous systems made of chitosan alone.

## Results and discussions:

In order to investigate the capabilities of the different  $\text{CsPbBr}_3$  samples (PVK 1, PVK 1.9, PVK 2.9 and PVK 3.9) concerning the pollutant absorption, the synthesized powders were simply put in contact with a MB solution ( $10^{-5}$  M). Two different adsorbent loadings were investigated: 1% and 10%. As shown in **Figure 1**, a very reduced contact time between the MB and perovskite NPs is needed to obtain significant MB absorption. In general, higher absorption is obtained when the perovskite powder loading is 10%. The absorption was confirmed both by the visual analysis, and by the UV-VIS analysis conducted through the spectrophotometer. The samples prepared with a molar ratio of 1:1 between the precursor salts show a greater MB absorption capability than the other ratios. In particular, a complete absorption of the MB can be obtained in only five minute when the PVK system is composed of pure  $\text{CsPbBr}_3$ .

When  $\text{CsPbBr}_3$  is incorporated inside chitosan bubbles (CH-B), the adsorption capability of the system is reduced, as enlightened by the fact that complete MB removal cannot be obtained even after 5 hours. Anyway, it is noteworthy that the incorporation of the perovskite NPs enables to enhance the absorption capabilities of bubbles made of pure chitosan. **Figure 2** shows MB absorption data related to various chitosan-perovskite bubbles, obtained by incorporating the different perovskite powders at 1%. In contrast to what occurs in the case of powders, the hydrogel systems that show best adsorption capabilities (removal of 70% of MB after overnight contact) are those containing perovskite systems 1.9 and 2.9 (**Fig. 2**). Furthermore, unlike the absorption of MB by bare  $\text{CsPbBr}_3$  NPs, the absorption is greater and faster with a reduced percentage of perovskite inside the CH-B (best results in the case of PVK loading equal to 1%).

These results open the way to the use of halide perovskite material as adsorbers for different pollutants in water. Interestingly, the use of chitosan allows to solve the already known stabilization problems of these materials in water [4].

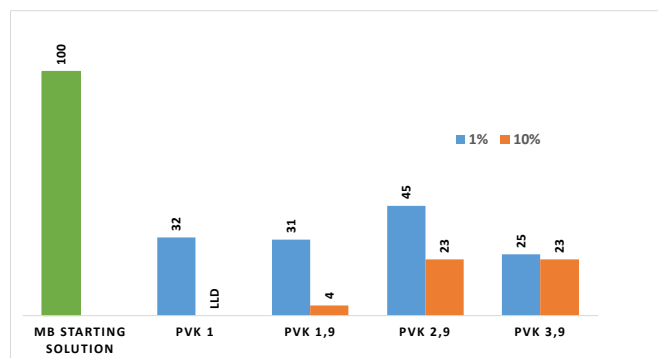


Figure 55: Percentage of MB absorbed by perovskite grains after 5 min.

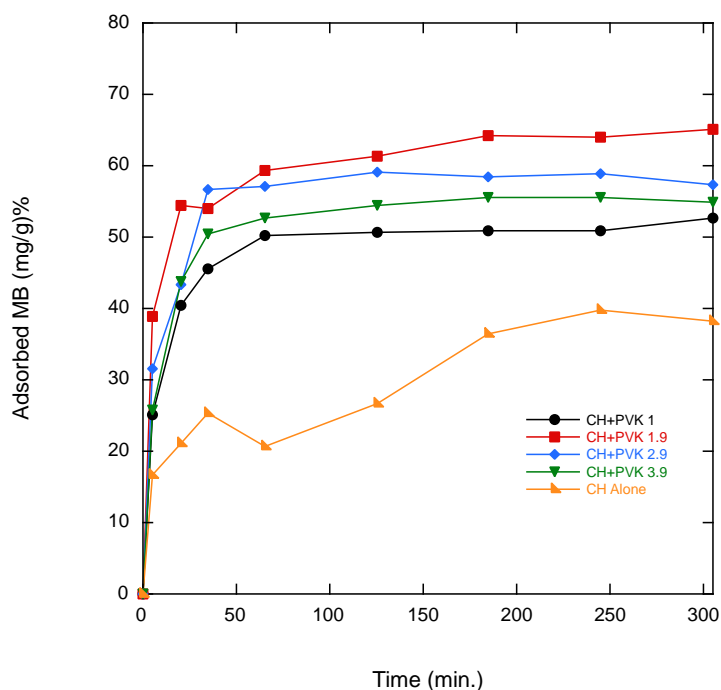


Figure 56: Adsorption curve of MB by bubbles of CH+PVK (1% w/v).

### Acknowledgement:

G. R. research activity is supported by DII, in the framework of “Dipartimento di Eccellenza 2018-2022” program. M. M. acknowledges ENEA for partially supporting her PhD scholarship in the framework of the program “Smart agriculture for the sustainability of the agro-food system”.

I. V.'s research activity was partially funded by the Italian Ministry of University and Research (MUR) through the PRIN project NOMEN (2017MP7F8F).

### References

1. A. K. Jena, A. Kulkarni, and T. Miyasaka: *Halide Perovskite Photovoltaics: Background, Status, and Future Prospects*; Chem. Rev. **119**, 5, 3036 (2019).
2. Yongping Fu et al.: *Metal halide perovskite nanostructures for optoelectronic applications and the study of physical properties*; Nature Reviews Materials **219**, 4, 169.
3. Sol Laura Gutierrez Alvarez et al.: *Morphology-Dependent One- and Two-Photon Absorption Properties in Blue Emitting CsPbBr<sub>3</sub> Nanocrystals*; The Journal of Physical Chemistry Letters **2022** 13 (22), 4897-4904.
4. Guan J, Shen Y et al.: *Internal–External Stabilization Strategies Enable Ultrastable and Highly Luminescent CsPbBr<sub>3</sub> Perovskite Nanocrystals for Aqueous Fe<sup>3+</sup> Detection and Information Encryption*; Advanced Materials Interfaces (**2021**) 8(19).

## Investigation of the degradation of trace substances by combined oxidative-enzymatic wastewater treatment

A. Schmiemann<sup>1,2\*</sup>, L. Hohenschon<sup>1</sup>, J. Grey<sup>1</sup>, I. Bartels<sup>1,2</sup>, J. Schneider<sup>3</sup>, K. Opwis<sup>3</sup>, M. Jaeger<sup>1</sup>, A. Cordes<sup>4</sup>, F. Zhang<sup>5</sup>, G. Müller-Czygan<sup>6</sup>, J.S. Gutmann<sup>2,3</sup> and K. Hoffmann-Jacobsen<sup>1</sup>

<sup>1</sup>Hochschule Niederrhein, Adlerstr. 32, 47798 Krefeld, Germany

<sup>2</sup>Universitaet Duisburg-Essen, Universitaetsstr. 1, 45141 Essen, Germany

<sup>3</sup>Deutsches Textilforschungszentrum Nord-West gGmbH (DTNW), Adlerstr. 1, 47798 Krefeld, Germany

<sup>4</sup>ASA Spezialenzyme GmbH, Am Exer 19 C, 38302 Wolfenbuettel, Germany

<sup>5</sup>HST Systemtechnik GmbH & Co. KG, Heinrichthaler Str. 8, 59872 Meschede, Germany

<sup>6</sup>Hochschule Hof, Alfons-Goppel-Platz 1, 95028 Hof, Germany

\*dorothee.schmiemann@hs-niederrhein.de

Micropollutants proliferation in the aquatic environment is increasingly challenging for the water management industry. As analytical methods for trace substances are continuously developed, the extent of the distribution of xenobiotics in European waters becomes more evident. One of the most important entry pathways of anthropogenic trace substances are municipal wastewater treatment plants, which are unable to completely remove such substances from wastewater [1]. Therefore, research on a fourth purification stage for wastewater treatment plants has been conducted for several years and is still being realized. One of the focuses are oxidative processes that enable the trace substances to be degraded as effectively as possible [2]. Nevertheless, oxidative processes, such as ozonation, may generate transformation products that are more toxic than their parent substance themselves, which suggests the development of post-treatment of these is essential [3].

In nature, oxidative degradation processes take place by oxidoreductases, including laccases. These enzymes oxidize various aromatic and non-aromatic compounds by a radical reaction mechanism using molecular oxygen (Figure 1) [4]. It has already been shown that laccases are able to degrade a wide variety of trace substances [5]. Therefore, laccases could be used as a biological alternative for oxidation processes. In the present study, the toxicity of chemical oxidation by ozonation as well as biological ozonation by laccase is investigated by means of the toxicity test with *A. fischeri* using diclofenac and acetaminophen as model compounds.

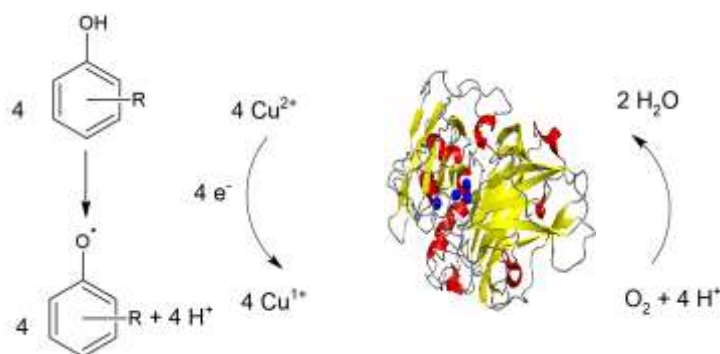


Figure. 1 Reaction mechanism laccase

Ozonation of diclofenac (20 mg/L) resp. acetaminophen (20 mg/L) was performed in a 0.5 L batch-reactor with an oxygen flow of 25 L/h and a generator power of 2.8% for 60 min at room temperature. Degradation of diclofenac and acetaminophen by laccase *T. versicolor* was performed over a period of 48 h under continuous stirring. The toxicity test with *A. fischeri* in accordance with DIN EN ISO 11348, but the bioluminescence was measured in 24-well plates in Tecan Reader Spark 10 M. Degradation kinetics and transformation product formation were analyzed with the Accurate-Mass Q-TOF LC/MS 6530 from Agilent Technologies and the MassHunter Workstation Software Qualitative Analysis Version B.06.00 was used for the evaluation. All investigations were performed in *ddH*<sub>2</sub>O at 20 °C.

Figures 2 and 3 show, respectively, the inhibitory effect (H15) during the degradation of diclofenac and acetaminophen by ozonation (A) and by the laccase *T. versicolor* (B). In addition, the formation and degradation of the transformation products during ozonation are shown. Significantly more toxic products are formed during ozonation than during the degradation by laccase. In both treatments, acetaminophen degradation leads to greater inhibitory effects than diclofenac. After an ozonation time of 10 min, the inhibitory effect of treated acetaminophen is above 90% while for diclofenac it is ca. 50%. In the ozonation of diclofenac, the formation of several transformation products seems to cause an increase in toxicity, whereas for acetaminophen, the formation or degradation of the product with [M+H]<sup>+</sup> 168 (C<sub>8</sub>H<sub>9</sub>NO<sub>3</sub>) correlates with the course of toxicity. During the degradation of these compounds with laccase, the polymerization of diclofenac and acetaminophen were the major



degradation products. Due to the lower toxicity of the degradation with laccase, this can be used as a possible post-treatment for trace substances in wastewater.

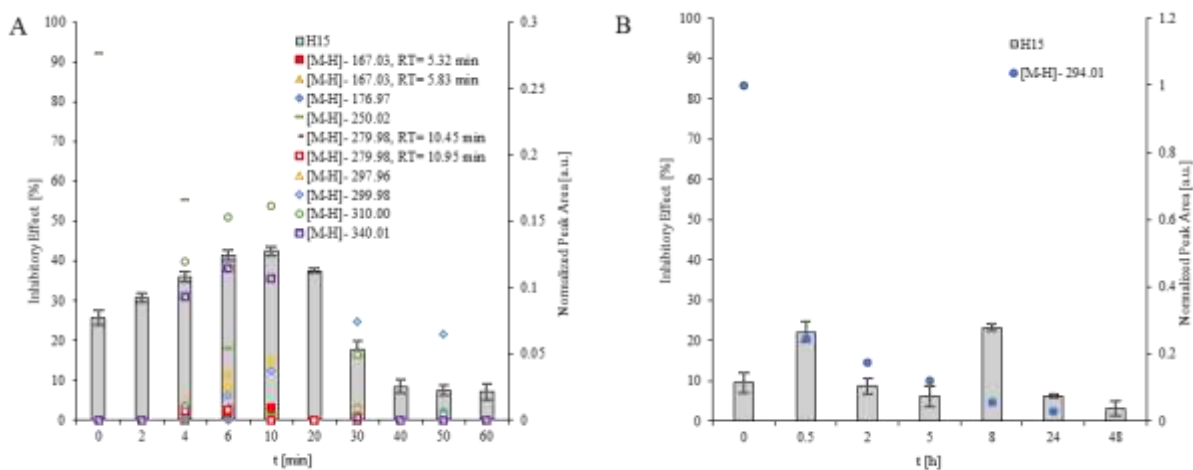


Figure. 2 Degradation of diclofenac through ozonation (A) and laccase digestion (B).

(A) Relative evolution of the normalized peak areas of the ozonation by-products ([M-H]<sup>-</sup>) during ozonation of diclofenac analyzed by LC-MS. (B) Relative evolution of the normalized area of diclofenac ([M-H]<sup>-</sup> 294.01, blue dots) during the degradation of laccase. Acute toxicity evolution after 15 minutes contact time with *A. fischeri* (H15 grey bars)

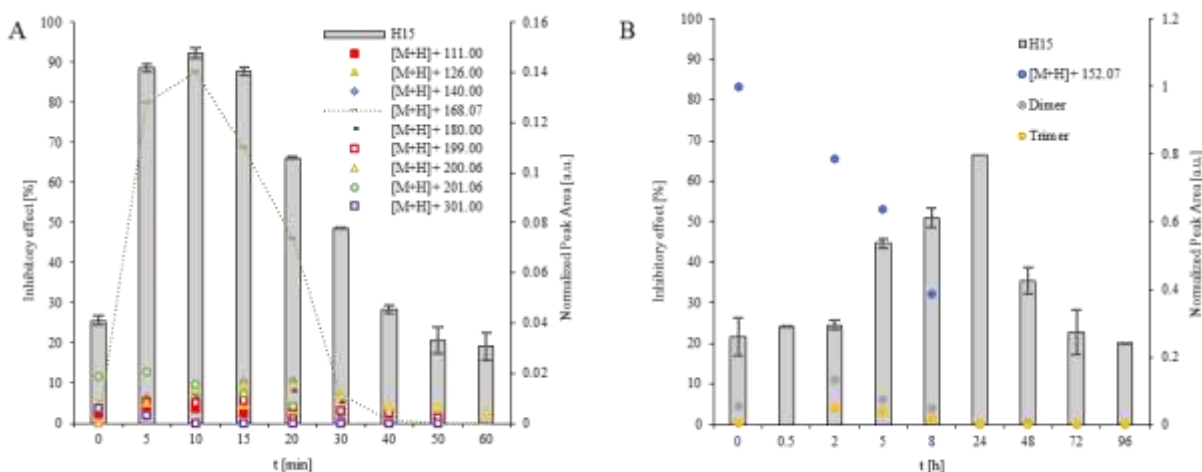


Figure. Degradation of acetaminophen through ozonation (A) and laccase digestion (B).

(A) Relative evolution of the normalized peak areas of the ozonation by-products ([M+H]<sup>+</sup>) during ozonation of acetaminophen analyzed by LC-MS. (B) Relative evolution of the normalized area of acetaminophen ([M+H]<sup>+</sup> 152.07, blue dots) and formation of dimer/trimer during the degradation of laccase. Acute toxicity evolution after 15 minutes contact time with *A. fischeri* (H15 grey bars)

## Acknowledgements

This work was supported by the European Union and the German state of North Rhine-Westphalia in the framework of EFRE-NRW and the project “Enz4Water”, grant 0801523.

## References

- [1] J. Margot, L. Rossi, D. A. Barry, C. Holliger, *WIREs Water* 2015, 2, 457.
- [2] M. Voigt, A. Wirtz, K. Hoffmann-Jacobsen, M. Jaeger, *AIMS Environmental Science* 2020, 7, 69.
- [3] M. Voigt, I. Bartels, D. Schmiemann, L. Votel, K. Hoffmann-Jacobsen, M. Jaeger, *Molecules (Basel, Switzerland)* 2021, 26.
- [4] a) J.-R. Jeon, P. Baldrian, K. Murugesan, Y.-S. Chang, *Microbial biotechnology* 2012, 5, 318; b) M. Chen, M. G. Waigi, S. Li, K. Sun, Y. Si, *Water research* 2019, 166, 115040.
- [5] N. H. Tran, T. Urase, O. Kusakabe, *J. of Wat. & Envir. Tech.* 2010, 8, 125.

## Poly(ionic liquid)s as efficient adsorbents for dyes removal from water streams

Bruna F. Soares<sup>1</sup> and Isabel M. Marrucho<sup>1,\*</sup>

<sup>1</sup>Centro de Química Estrutural and Departamento de Engenharia Química, Instituto Superior Técnico, Universidade de Lisboa, Avenida Rovisco Pais, 1049-001 Lisboa, Portugal

\*Corresponding author: [isabel.marrucho@tecnico.ulisboa.pt](mailto:isabel.marrucho@tecnico.ulisboa.pt)

Dyes are believed to be used since the Neanderthals, when they were extracted from plants, Nowadays, more than 1 million tons of dyes are annually industrially produced and used mainly by textile industries [1]. One of the major problems concerning the use of dyes is that 10 to 15% are discharged to the environment [2]. Polymeric Ionic Liquids (PILs) have already been tested for the extraction of acid, basic and azo dyes such as bromo phenyl blue, methyl blue, orange II, sunset yellow or amaranth, mainly through the use of imidazolium based PILs [3-4]. This work aims to further evaluate the real potential of PILs as sorbent materials for removal of dyes, direct red 80 and reactive blue 5, from aqueous solutions. For that purpose, poly(diallyldimethylammonium TFSI) was synthesized and subsequently tested as dye adsorbent. The experimental parameters were optimized so maximize the extraction efficiency. Several geometries such as coated stir bar, solid phase extraction cartridge or dispersed powder were explored. The results of the adsorptions are very promising (Figure 1) with extraction efficiencies reaching values higher than 90%.



Figure 1 –Schematics of the adsorption experiments, where the initial and final aspect of the PIL and the aqueous dye solution can be observed.

### Acknowledgements

Bruna F. Soares gratefully acknowledges the financial support of FCT/MCTES (Portugal) for PhD fellowship 2021.05450.BD. This work was financed by CQE project (UIDB/00100/2020).

### References

1. B. Okutucu, A. Akkaya and N. K. Pazarlioglu, *Prep. Biochem. Biotechnol.*, 2010, 40, 366–376.
2. V. K. Gupta and Suhas, *J. Environ. Manage.*, 2009, 90, 2313–2342.
3. H. Mi, Z. Jiang and J. Kong, *Polymers (Basel)*, 2013, 5, 1203–1214.
4. A. M. Ferreira, J. A. P. Coutinho, A. M. Fernandes and M. G. Freire, *Sep. Purif. Technol.*, 2014, **128**, 58–66.

## Removing Sulfur Dioxide (SO<sub>2</sub>) by Nanoparticle Piperine Extracted From Piper Nigrum L.

Ceren Tabag<sup>1</sup> and Emir Yıldırım<sup>2</sup>

<sup>1,2</sup>Hisar School, Istanbul, Turkey

E-mail: [ceren.tabag@hisarschool.k12.tr](mailto:ceren.tabag@hisarschool.k12.tr)

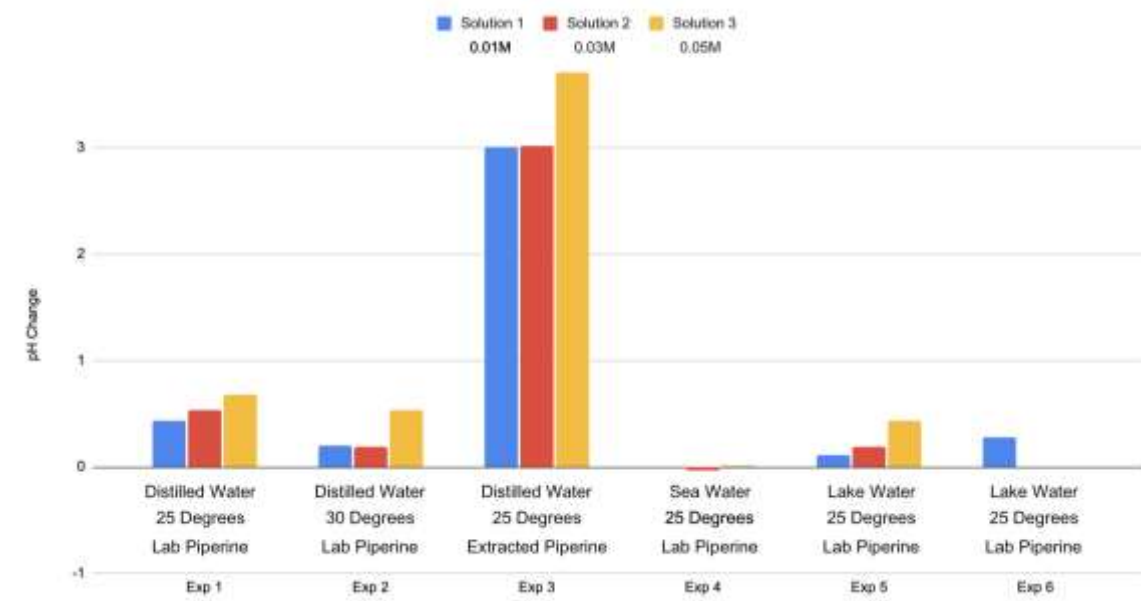
### **Abstract**

This research project aims to remove the sulfuric acid ( $H_2SO_3$ ), which is formed as a result of the reaction of sulfur dioxide gas passing from the atmosphere to the water, from fresh and salty water. Sulfuric acid is the main component of acid rain that is known for its detrimental effect to aquatic life [2]. This study is significant in terms of its contribution to the literature on removing the side effects of sulfur dioxide to the hydrosphere. For this purpose, a chemical molecule named *piperonal piperidine* (piperine) was extracted from *piper nigrum L.*, and used to start a synthetic reaction inside various aqueous mediums. Piperine is the alkaloid responsible for the pungency of black pepper and long pepper [1]. It is an organic compound and the primary alkaloid of *Piper nigrum L.* (Piperaceae) (black pepper) and *Piper longum L.* [3]. The hypothesis was “The effect of sulfur dioxide gas passing from the atmosphere to surface water resources can be purified by using the active ingredient piperine in black pepper”. For this reason, different solutions of different molarity containing basic piperonal piperidine ( $C_{17}H_{19}NO_3$ ) extracted from black pepper, got into acid-base reactions, where pH change is an indicator of. There were four steps in the experiment which were: extraction of piperine from black pepper, obtaining sulfur dioxide, preparing piperine solutions with different concentrations and measuring the pH, and mixing piperine solutions and sulfur dioxide containing solutions to observe pH difference. The extraction of piperine can be made by using a wide variety of solvents such as diethyl ether, alcohol based solvents, and ionic-based solvents [1]. This research utilized ethanol and potassium hydroxide in order to extract piperine from black pepper. The equipment used for measurements were a pH sensor, electronic thermometer, electronic balance and wide range pressure sensor. In total, 16 solutions and 6 iterative experiments were designed in either distilled, fresh, or salty water resources. The first three experiments were made in distilled water, to distinguish the influence of temperature and molarity. The fourth experiment was made in seawater and the final two experiments were in lake water. The reaction that was observed is  $C_{17}H_{19}NO_3(aq) + H_2SO_3(aq) \rightarrow C_{17}H_{19}NO_3H^+(aq) + HSO_3^-(aq)$ . The expected result of the experiment could not be seen in seawater since the pH change was measured as zero. (*Henderson Hasselbalch Equation was used to prove it*). However, the results were as expected in the trials with lake water. These differences are the concrete results of the neutralization reaction as more  $H_2SO_3$  decreased with  $C_{17}H_{19}NO_3$  and evidence that the water was purified.

**Keywords:**

*Piper Nigrum L., Piperine, Sulfur Dioxide, Henderson Hasselbalch Equation, Neutralization, pH Change*

Graph 1: The average pH changes of the six experiments



### References:

1. Gorgani, L., Mohammadi, M., Najafpour, G. D., & Nikzad, M. (2017). Piperine—the bioactive compound of black pepper: from isolation to medicinal formulations. *Comprehensive Reviews in Food Science and Food Safety*, 16(1), 124-140.
2. Lackey, J. B. (1939). Aquatic life in waters polluted by acid mine waste. *Public Health Reports (1896-1970)*, 740-746.
3. Meghwal, M., & Goswami, T. K. (2013). Piper nigrum and piperine: an update. *Phytotherapy Research*, 27(8), 1121-1130.

## Methane combustion over Pd-MeOx/Al<sub>2</sub>O<sub>3</sub> (Me= Co, Ni or Ce) catalysts

Silviya Zh. Todorova<sup>1\*</sup>, Anton Il. Naydenov<sup>2</sup>, Ralitsa G. Velinova<sup>2</sup>, Yordanka G. Karakirova<sup>1</sup>, Hristo G. Kolev<sup>1</sup>

<sup>1</sup> Institute of Catalysis, Bulgarian Academy of Sciences, Acad. G. Bonchev St., Block 11, 1113 Sofia, Bulgaria

<sup>2</sup> Institute of General and Inorganic Chemistry, Bulgarian Academy of Sciences, Acad. G. Bonchev St., Block 11, 1113 Sofia, Bulgaria  
todorova@ic.bas.bg

Catalytic combustion of methane has been extensively investigated for emission control and power generation during the last decades. The alumina-supported palladium catalyst is widely accepted as the most active catalysts for catalytic combustion of methane. The activity of Pd/Al<sub>2</sub>O<sub>3</sub> decreases during time on stream, especially under water vapor. The following order of activity in the reaction of complete oxidation of methane was established: Co<sub>3</sub>O<sub>4</sub> > CuO > NiO > Mn<sub>2</sub>O<sub>3</sub> > Cr<sub>2</sub>O<sub>3</sub> [1]. It may be expected that the combination between Pd and these oxides could lead to the promising catalysts in reaction of complete methane.

In the present work, we investigate the activity of Pd/Al<sub>2</sub>O<sub>3</sub> catalysts promoted with other metal oxides (MOx; M= Ni, Co, Ce). The Pd-based catalysts modified by metal oxide were prepared by sequential impregnation of Al<sub>2</sub>O<sub>3</sub> with aqueous solutions of Me(NO<sub>3</sub>)<sub>2</sub>·6H<sub>2</sub>O and Pd(NO<sub>3</sub>)<sub>2</sub>·2H<sub>2</sub>O and next calcination. All samples were characterized by XRD (X-ray diffraction), TPR (temperature-programmed reduction), EPR (electron paramagnetic resonance) and XPS (X-ray photoelectron spectroscopy). An improvement of activity was observed after modification with different oxides.

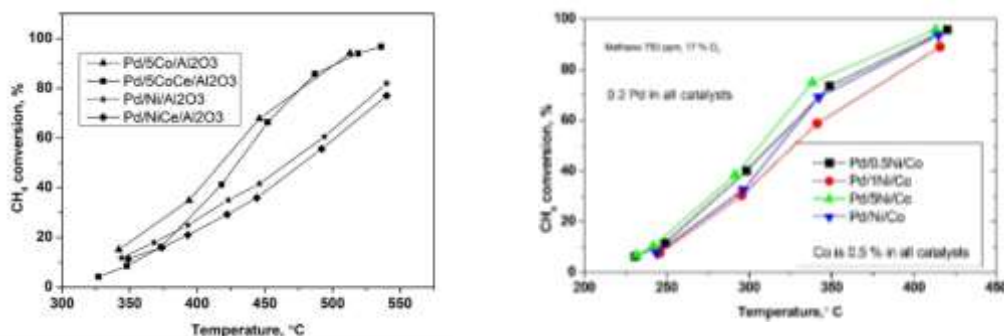


Figure 1. Temperature dependencies of the methane combustion over the different catalysts.

The results demonstrate that the Pd/Al<sub>2</sub>O<sub>3</sub> catalysts modified with Co exhibit the most promising catalytic activity for methane oxidation. According to the XRD data finely dispersed palladium particles were formed on the surface of all samples. XPS analysis shows the presence of both Pd<sup>2+</sup> and Pd<sup>4+</sup> on the surface of the fresh catalysts modified with Co and Ni only, while the modification with Ce before Co or Ni increases the Pd<sup>0</sup> on the surface. The EPR data also suggest the presence of Pd<sup>+</sup> or Pd<sup>3+</sup> forms on the surface of the monocomponent Pd/Al<sub>2</sub>O<sub>3</sub>.

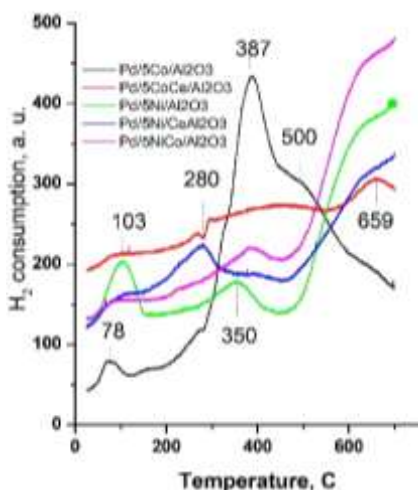


Figure 2. TPR profile of studied samples before catalytic reaction

The reduction behavior of the synthesized catalysts was investigated by means of TPR (Figure 2). Several reduction maxima were observed. The hydrogen consumption in the interval 70-103 °C is attributed to the reduction of PdO [2]. The peak at 350 °C in Ni modified catalyst is ascribed to the reduction of finely divided NiO

particles [2]. The modification with Ce shifts this peak to the low temperature. The reduction peaks at 387 and 500 °C in Pd/Co/Al<sub>2</sub>O<sub>3</sub> catalysts are ascribed to the two-step reduction of Co<sub>3</sub>O<sub>4</sub>. The hydrogen consumption above 500 °C in all samples is attributed to the reduction of Ni-Al or Co-Al oxide phases [2, 3].

The results from different physicochemical characterization indicate the present of cobalt as Co-Al spinel like phase on the catalyst surface. We suggest that occurrence of Co-Al phase plays a significant role for the stabilization of the palladium as PdO, leading to high activity and stability in methane combustion.

It is very likely that, Ce is deposited before the Co deposition, the formation of cobalt surface phase is hindered as well as the further stabilization of PdO phase. The Pd+CoO<sub>x</sub>/Al<sub>2</sub>O<sub>3</sub> sample demonstrates remarkable stability after ageing.

**Acknowledgement.** The authors are gratefully acknowledged to the National Science Fund of Bulgaria, Grant No КП-06-Русия 22.

Research equipment of distributed research infrastructure INFRAMAT (part of Bulgarian National roadmap for research infrastructures) supported by Bulgarian Ministry of Education and Science was used in this investigation.

#### References:

1. J.G. McCarthy, Y.-F. Chang, V.L. Wong, M.E. Johansson, Div. Petrol.Chem. **42** 158 (1997).
2. M. V. Gabrovska, R. M. Edreva-Kardjieva, D. D. Crişan, K. K. Tenchev, D. A. Nikolova, M. Crişan, Bulg. Chem. Comm. **45** 617 (2013)
3. P. Arnoldy and J.A. Moulijn, *J. Catal.* **93**, 38 (1985)

## Commercial photocatalytic paints for environmental remediation

Zouzelka, R., Martiniakova, I., Muzikova, B, Mikyskova, E, Rathousky, J

*Center for Innovation in the field of Nanomaterials and Nanotechnologies, J. Heyrovsky Institute of Physical Chemistry of the CAS, Dolejskova 3, Prague 18223, Czech Republic*

### **Abstract:**

Up to now, the research has been mostly devoted to the photocatalytic removal of individual pollutants. As in real situations, the pollutants are always presented in a mixture, it is crucial to know whether there is some sort of interference, which can influence the efficiency of the whole photocatalytic degradation process. Here, we investigated the ability of two commercial coatings (binder-containing FN NANO®2 and binder-free AEROXIDE® TiO<sub>2</sub> P25) to abate ozone, nitric oxide, and acetaldehyde separately and in their mixtures. Both photocatalysts effectively removed the pollutants present separately in the air stream, achieving conversions of 30–60 % (at an inlet concentration of 0.1 ppmv), even at the UV-A irradiation intensity as low as 0.05 mW cm<sup>-2</sup>. Furthermore, the use of binder-containing coating provided stable ozone conversions (30–40 %) in the full range of relative humidity, which is extraordinary in comparison with published data. The kinetic analysis indicates that the degradation mechanisms of nitric oxide, acetaldehyde, and ozone considerably differed. While for nitric oxide the reaction in the adsorbed state played a crucial role, for acetaldehyde and ozone that was marginal. Importantly, owing to the differences in degradation mechanisms, no mutual interference occurred when pollutant mixtures were treated. This finding is of major importance for the application of photocatalysis as environmental technology.

**Keywords:** photocatalysis; TiO<sub>2</sub>; NO<sub>x</sub>; acetaldehyde; ozone; mixtures

# Toxicology and Ecotoxicology of Chemicals and Products



## Inventory of pesticides used by farmers on paddy fields in peatland area: A case study in Indonesia

Indra Purnama<sup>1,4\*</sup>, Syafrani<sup>1</sup>, Amalia<sup>2</sup>, Anisa Mutamima<sup>3,4</sup>

<sup>1</sup>Universitas Lancang Kuning, Department of Agrotechnology, Faculty of Agriculture, Pekanbaru, Indonesia

<sup>2</sup>Universitas Lancang Kuning, Department of Agribusiness, Faculty of Agriculture, Pekanbaru, Indonesia

<sup>3</sup>Universitas Riau, Department of Chemical Engineering, Faculty of Engineering, Pekanbaru, Indonesia

<sup>4</sup>Research Center of Sustainable Indonesia, Pekanbaru, Indonesia

\*e-mail address of corresponding author: indra.purnama@unilak.ac.id

### Abstract text:

Food safety is a priority in one aspect of sustainable agriculture. However, this is difficult to achieve in practice, especially in developing countries, including Indonesia. The agricultural sector tends to only think about profit without caring about social aspects and the environment. Globally, there is a maximum residue limit (MR) allowed to be in food, including rice [1]. Many countries apply residue limits in their territory because of the impact of pesticide residues still in food when consumed by humans, which can cause poisoning on human health effects [2][3] to become carcinogenic [4-6]. This study aimed to reveal the active ingredients of pesticides used by farmers in a food center in Riau, Indonesia. In this study, the data collection method used was a questionnaire, which was used to record the types of pesticides used by 63 farmers from 250 farmers in Buantan Lestari Village, Riau, Indonesia, for one year; and reviewed the literature. This study revealed that in the last year, various pesticides had been used with 33 active ingredients categorized from extremely hazardous, viz. abamectin (8.2%), to not included in the list based on WHO categories [7], such as 2,4-D dimethylamine, dimehypo, and thiophanate-methyl with the total 7.8%. A preliminary study (unpublished) found that rice from paddy fields grown according to Good Agricultural Practices (GAP) did not contain more than 500 active ingredients of pesticides. On the contrary, rice from paddy fields that used excessive pesticides found seven active ingredients of pesticides, i.e., propiconazole, chlorpyrifos, bifenthrin, azoxystrobin, tebuconazole, tricyclazole, and difenoconazole), which are two pesticides, tricyclazole and propiconazole, were detected exceeding the globally established maximum residue limits two times higher. Surprisingly, there were two active ingredients of pesticides that were not included in the 33 active ingredients of pesticides used by farmers in the past year, bifenthrin and tebuconazole. The rice that contains both active ingredients of pesticides might come from the farmers' rice fields, which were dominated by peatlands. Various parties can use the results of this study in making decisions regarding commitments to realize sustainable agriculture in Indonesia, especially in peatlands.

### Acknowledgements

This work was supported by the Ministry of Education, Culture, Research, and Technology of Republic of Indonesia [grant numbers 001/LL10/PG.AK-2/2022, 2022].

### References

1. WHO/FAO, In *Principles and Methods for the Risk Assessment of Chemicals in Food* (p. 29) (2009).
2. C. Bolognesi, F.D. Merlo, *Encyclopedia of Environmental Health*, 118–132 (2019).
3. W. Boedeker, M. Watts, P. Clausing, E. Marquez, *BMC Public Health*, **20**, 1875 (2020).
4. J. George, Y. Shukla, *Journal of Proteomics*, **74** 12, 2713-2722 (2011).
5. G.M. Rocha, C.K. Grisolia, *Developing World Bioethics*, **19** 3, 148-154, (2018).
6. A. Nath, S.E. Vendan, Priyanka, J.K. Singh, C.K. Singh, S. Kumar, *Current Trends in Biotechnology and Chemical Research*, **3** 1, 1-7, (2013).
7. WHO, In *World Health Organization*, (2020).

# Valorization of renewable and natural resources

## Synthesis and characterization of polysaccharide- and protein-based edible films and modification with zein bilayer coatings

Evmorfia Athanasopoulou<sup>1\*</sup>, Francesco Bigi<sup>2</sup>, Enrico Maurizzi<sup>3</sup>, Andrea Quartieri<sup>2</sup>, Theofania Tsironi<sup>1</sup>

<sup>1</sup>Department of Food Science and Human Nutrition, Agricultural University of Athens, Iera Odos 75, Athens 11855, Greece

<sup>2</sup>Packin, Via Del Chionso, 14/I Reggio Emilia (RE), 42122, Italy

<sup>3</sup>Department of Life Sciences, University of Modena and Reggio Emilia, Via John Fitzgerald Kennedy 17/I, Reggio Emilia (RE), Italy

\*[efiatha@aua.gr](mailto:efiatha@aua.gr)

### Abstract

The rising packaging industry combined with global demand for sustainable production has increased the interest towards the development of biodegradable packaging materials. Biopolymers like polysaccharides, proteins and lipids can replace the use of petroleum-based plastics as a green solution. Food-grade components can be used for the development of edible packaging materials. Plastic wastage is growing at an annual rate of 9%. In 2020, in Europe, 40.5% of plastic waste was referred to the packaging field [1].

Among biopolymers, pectin, gelatin and hydroxypropyl methylcellulose (HPMC) have been reported as effective raw materials for food packaging products due to their non-toxic, sustainable, biocompatible, and biodegradable properties. Pectin is a structural polysaccharide from representing one of the main constituents of the cell walls of plants. Pectin is extracted from citrus peel and is water-soluble but insoluble in organic solvents. The main structural compound of pectin is galacturonic acid (70%). The main chain of pectin is a linear anionic backbone with no side parts and regions with non-anionic parts. Pectin has also free carboxyl groups in its structure which give in pectin solutions acidic pH. In the food packaging industry, pectin is used for films mainly because it is compatible with other natural polysaccharides, proteins or lipids [2].

Edible films made from gelatin have already been tested in the literature for food preservation and shelf-life extension. Gelatin is considered as an alternative biopolymer that can be used for food packaging to improve the functionality of the products. Gelatin is a water-soluble protein that comes from partial hydrolysis of collagen. Due to the hydroscopic properties of gelatin, the produced films have the tendency to dissolve when coming in contact with moisture. The properties of gelatin films depend on molecular weight distribution and amino acid synthesis. These two characteristics depend on different sources and the conditions of gelatin extraction [3].

Cellulose is the most common polysaccharide which is used in the food industry and specifically in food packaging, to replace plastics derived from petroleum. HPMC is produced by modification of cellulose in alkali treatments. Sodium hydroxide solution at a concentration of 18% is used in purified wood pulp to obtain HPMC. Methyl and hydroxypropyl ether groups get into the cellulose, as alkali cellulose reacts with methyl chloride and propylene oxide, respectively. HPMC is odorless and tasteless and HPMC-based films exhibit neutral sensory properties (aroma and taste) [4].

Zein is the main storage protein of corn and consists of 80% of the whole protein of corn. Inside the zein, the endosperm tissue of corn can be found. Materials based on plasticized zein or blended with zein have good mechanical properties and the ability to form films. More than 50% of amino acids in zein structure are hydrophobic. However, glutamine, which is a hydrophilic amino acid, is in a percentage of around 25%. Zein is not soluble in water but it is soluble in alcohol and it has been already widely tested in edible films and coatings [5].

The aim of the study was to synthesize edible films using pectin, gelatin and HPMC. Each biopolymer was at a percentage of 2% and films were produced by solvent casting method. The solutions were mixed in proportions of 1:1, and three additional types of films were produced: pectin – gelatin, HPMC – pectin, and HPMC – gelatin. All six types of films were tested for their mechanical properties, water permeability, optical properties and UVA barriers. Zein solution was incorporated onto the surface of the developed films in order to reduce their water permeability, by spraying in a proportion of 1:2 zein:hydrocolloid solution.

The water vapor transmission rate (WVTR) is an important property of films, as food packaging may be used to control the exchange of humidity between the environment and the food. WVTR was determined gravimetrically, according to ASTM E96 method with slight modification. Films were sealed on top of glass vials. Vials contained 2 g anhydrous CaCl<sub>2</sub> in order to achieve 0% RH and were placed into a desiccator with BaCl<sub>2</sub> (90% RH). Desiccator was isothermally stored at 40 °C for 10 days. WVTR was calculated according to the equation:  $WVTR = \frac{\Delta W}{\Delta t} * A$ , where  $\frac{\Delta W}{\Delta t}$  is the measuring weight of the vials per day (g/day) and A is the surface of the film (m<sup>2</sup>). The units of WVTR are  $\frac{g}{day} * m^2$ . An average of 5 measurements of each film were used.

The bilayer coatings with zein exhibited lower WVTR, because of its hydrophobic nature of zein (Table 1).

Table 1. Water Vapor Transmission Rate of the films based on pectin, gelatin HPMC, with and without zein-based coating.

	Water Vapor Transmission Rate ( $\frac{g}{day} * m^2$ )	
	Without Zein coating	With Zein coating
Pectin Control	4307.28 ± 382.22	3762.21 ± 81.33
Gelatin Control	3064.33 ± 437.36	2866.24 ± 602.45
HPMC Control	3671.72 ± 1153.65	2752.02 ± 137.59
HPMC – pectin	3778.03 ± 506.11	3208.15 ± 227.52
HPMC – gelatin	3659.66 ± 731.83	2296.31 ± 533.10
Pectin – gelatin	5439.86 ± 763.48	2955.41 ± 972.69

The color parameters ( $L$ ,  $a$ ,  $b$ ) were defined by CR-400 Minolta colorimeter (Minolta Camera, Co., Ltd., Osaka, Japan) with D65 illuminant and 10° observer angle. Calibration of the instrument was executed with white standard ( $L^* = 99.36$ ,  $a = -0.12$  and  $b = -0.06$ ). The total color variation ( $\Delta E$ ) of all films was calculated according to:  $\Delta E = \sqrt{\Delta L^2 + \Delta a^2 + \Delta b^2}$  where  $\Delta L$ ,  $\Delta a$  and  $\Delta b$  are the differences between the value of the film and the white standard. An average of 12 measurements of each film were used. Lightness is represented by  $L$  value. In this study,  $L$  value varied from 97.87 to 99.18, which means that all films were bright even after the addition of zein. The  $a$  parameter expresses the red–green shade of film. The value  $a$  ranged from -0.17 (HPMC control) to -0.33 (Pectin–Gelatin) before adding zein, without statistically significant differences ( $P > 0.05$ ). By adding zein, the value of  $a$  decreased, which indicates the increase of green shade. The  $b$  parameter expresses the blue–yellow shade of film. Films based on pectin had higher  $b$  value  $2.15 \pm 0.61$  and  $4.21 \pm 0.48$  with and without zein, respectively. The  $\Delta E$  was slightly decreased by adding zein which means that the color changes were not visible to the naked eye.

The UV-Vis barrier properties were measured by spectrophotometer (VWR @ Double Beam UV × Vis 6300 PC spectrophotometer, China) at 190-800 nm wavelength range. The value of transmittance at 200 nm was lower the 0.1% for all films, which indicates great barrier properties at UVC. By adding zein, all the films showed lower transmittance at 280, 350, and 400 nm wavelength which indicates lower value for UVA and UVB wavelength. The transmittance in the visible wavelength range (400-800nm) was higher for the films without zein, which means that films were more transparent. Specifically, for pectin control and gelatin control films, the transmittance was higher than 70%, which means that all the films were clear and transparent.

In this study, the thickness of the films ranged from 31.72 to 48.69. The mechanical properties of the films that will be used as packaging materials are important in order to stand any external stress. Elastic modulus, tensile strength and elongation at break are the three more important parameters. Elastic modulus shows the flexibility of the films. Higher values of elastic modulus show less flexible biopolymers [6]. HPMC–gelatin films with zein had the highest elastic modulus (939.45 MPa), whereas gelatin films with zein had the lowest (396.19 MPa). Tensile strength shows how a film responds when it strengthens. Pure HPMC with and without zein films showed the highest values without statistically significant differences (26.92 MPa and 21.63 MPa, respectively). Pure gelatin films and Pectin–Gelatin films had the lowest value (~3.95 MPa). Elongation at break (%) determines the flexibility and the stretchability of the films. Pectin–HPMC and HPMC–gelatin showed the lowest values of elongation at break (less than 5 %), while pure gelatin films and pure HPMC films showed the highest values (~37 %). By combining the different types of polymers, the intermolecular forces are stronger and the free volume in the matrix is lower, thus, the flexibility is increased [6].

The aim of the study was to develop and synthesize edible packaging materials, as alternative food packaging systems to the conventional petroleum-based polymers. When a zein-based hydrophobic coating was used, the films showed lower water vapor permeability rates retaining the mechanical properties of the films. All the tested films showed excellent barrier properties in the UVC wavelengths and good performances in the UVA and UVB wavelengths range. The obtained results showed the potential of bilayer polysaccharide- and protein-based edible films with zein as green environmentally friendly packaging materials.

### Acknowledgement

This Project has received funding from the European Union's Horizon 2020 research and innovation program under the Marie Skłodowska-Curie Grant agreement 872217 (<https://www.ichthys-eu.org/about>).

### References

1. Plastic Europe Market Research Group and Conversion Market & Strategy GmbH.
2. C. Mellinas, M. Jimenez, M. C. Garrigos, *Materials*, **673** 13(3) (2020)
3. M. Ramos, A. Valdes, A. Beltran, M. C. Garrigos, *Coatings*, **41** 6(4) (2016)
4. M. Wrona, M. J. Cran, C. Nerin, S. W. Bigger, *Carbohydrate polymers*, **156** 108-117 (2017)

5. E. Corradini, P. S. Curti, A. B. Meniqueti, A. F. Martins, A. F. Rubira, E. C. Muniz, *International journal of molecular sciences*, **22445** 15(12) (2014)
6. Bigi, F., Haghghi, H., Siesler, H. W., Licciardello, F., & Pulvirenti, A. *Food Hydrocolloids*, **120**, 106979 (2021).

## Photocatalytic transformations of quinic acid derivatives

Antunes, M.B.,<sup>1,2,\*</sup> Candeias, N.R.,<sup>3</sup> Afonso, C.A.M.,<sup>1</sup> Gualandi, A.,<sup>2</sup> Cozzi, P.G.,<sup>2</sup>

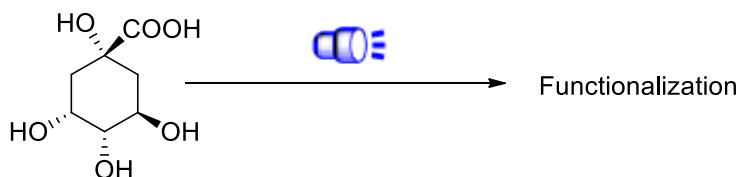
<sup>1</sup> Research Institute for Medicines (iMed.Ulisboa), Faculty of Pharmacy University of Lisbon, Avenida Professor Gama Pinto, 1649-003, Lisbon, Portugal. <sup>2</sup> Dipartimento di Chimica "G. Ciamician", Alma Mater Studiorum – Università di Bologna Via Selmi 2, 40126, Bologna, Italy <sup>3</sup> LAQV-REMQUIMTE, Department of Chemistry, University of Aveiro, 3810-193 Aveiro, Portugal.

\* miguelabarbara@campus.ul.pt

Abstract text:

Quinic acid (QA) is a widely occurring metabolite in plants and microorganisms<sup>1</sup>. The synthesis of Oseltamivir (Tamiflu)<sup>2</sup> and Bactobolin A<sup>3</sup> are probably the most distinct uses of QA in total synthesis. Exploration of stereoselective metal-free deoxygenation is a recent example of QA's synthetic value<sup>4</sup>. Additionally, the *O,O*-silyl group migration on a quinic acid-derived cyclitol gives suitable intermediate for the synthesis of a vitamin D receptor modulator (VS-105)<sup>5</sup>. Photoredox catalysis is a known sustainable alternative to the use of less environmentally superstoichiometric oxidants and reductants. Ruthenium and iridium complexes, in combination with visible light, are efficient photocatalysts when strong reductants or strong oxidants are needed, however, their toxicity and scarcity are a drawback for the evolution of photocatalysis to the next level. Organic dyes represent a good alternative to these metal complexes<sup>6</sup>.

The functionalization of QA and its derivatives via photoredox catalysis will be presented. Organic dyes under visible light irradiation can generate radical intermediates from QA under mild conditions. This radical generation unravels innovative ways for the synthetic modification of QA.



Scheme 9: Quinic acid functionalization under visible light

**Acknowledgements:** The authors acknowledge Fundação para a Ciência e Tecnologia (FCT) for financial support (PTDC/QUI-QOR/1131/2020, UIDB/04138/2020 and UIDP/04138/2020). The project leading to this application has received funding from the European Union's Horizon 2020 research and innovation programme under grant agreement No 951996.

### References

- Arceo, E.; Ellman, J. A.; Bergman, R. G., A direct, biomass-based synthesis of benzoic acid: formic acid-mediated deoxygenation of the glucose-derived materials quinic acid and shikimic acid. *ChemSusChem* **2010**, *3* (7), 811-3.
- Abrecht, S.; Federspiel, M. C.; Estermann, H.; Fischer, R.; Karpf, M.; Mair, H.-J.; Oberhauser, T.; Rimmler, G.; Trussardi, R.; Zutter, U. J. C. I. J. f. C., The synthetic-technical development of oseltamivir phosphate Tamiflu™: A race against time. *Chimia* **2007**, *61* (3), 93-99.
- Vojáčková, P.; Michalska, L.; Nečas, M.; Shcherbakov, D.; Böttger, E. C.; Šponer, J. i.; Šponer, J. E.; Švenda, J. J. J. o. t. A. C. S., Stereocontrolled synthesis of (–)-Bactobolin A. *Journal of the American Chemical Society* **2020**, *142* (16), 7306-7311.
- Holmstedt, S.; George, L.; Koivuporras, A.; Valkonen, A.; Candeias, N. R., Deoxygenative Divergent Synthesis: En Route to Quinic Acid Chirons. *J Organic Letters* **2020**, *22* (21), 8370-8375.
- Holmstedt, S.; Efimov, A.; Candeias, N. R., *O, O*-Silyl Group Migrations in Quinic Acid Derivatives: An Opportunity for Divergent Synthesis. *J Organic Letters* **2021**, *23* (8), 3083-3087.
- Gualandi, A.; Nenov, A.; Marchini, M.; Rodeghiero, G.; Conti, I.; Paltanin, E.; Balletti, M.; Ceroni, P.; Garavelli, M.; Cozzi, P. G., Tailored Coumarin Dyes for Photoredox Catalysis: Calculation, Synthesis, and Electronic Properties. *J ChemCatChem* **2021**, *13* (3), 981-989.

## Phenol-formaldehyde resins based on lignin functionalized with succinic anhydride

Emanuela Bellineto<sup>1\*</sup> and Gianmarco Griffini<sup>1</sup>

<sup>1</sup>Department of Chemistry, Materials and Chemical Engineering "Giulio Natta",  
Politecnico di Milano, Piazza Leonardo da Vinci 32, 20133 Milano, Italy

\*[emanuela.bellineto@polimi.it](mailto:emanuela.bellineto@polimi.it)

Phenol-formaldehyde (PF) resins are currently among the most widely used thermosetting materials, due to their excellent properties and relatively low production cost [1]. PF resins are characterized by high crosslinking density and high content of aromatic rings which are responsible for their superior thermal, chemical and mechanical stability, as well as moisture resistance and good mechanical strength. For these reasons, their fields of application include wood composites, isolating materials, adhesives and binders [2]. Since PF resins are obtained by polycondensation of phenol and formaldehyde, which are both fossil-based and toxic precursors, the need of employing more environmentally friendly, renewable and less hazardous raw materials for their production has recently emerged [1,3]. In this regard, lignin can be a promising alternative to oil-derived phenols, thanks to its polyphenolic structure [1,4]. Lignin is the most abundant natural aromatic polymer on Earth, largely available as by-product of the paper production process. The current limitations in its exploitation within the polymer industry are due to its large molecular weight, complex structure, and presence of few reactive sites. In light of this, different studies have focused on lignin functionalization/modification with the aim to increase its reactivity in polymeric systems [5,6]. In this work, the esterification of lignin with succinic anhydride (SAn) is proposed as a strategy to improve its reactivity, with the purpose to incorporate it in PF formulations, as a partial replacement of a novolac resin, up to 30% wt.

The softwood kraft lignin (KL) Indulin AT used was supplied by MeadWestvaco. For the functionalization reaction, SAn, 1-methylimidazole (1-MI) and tetrahydrofuran (THF) were used as received from Sigma Aldrich. The commercial PF resin formulation employed, provided by Camfart S.r.l, was composed by the novolac Bakelite® PF SM 1112, containing phenols and hexamethylenetetramine (HMTA) at 8.5-9.5% wt., in form of powder, and the liquid resole Bakelite® PF 2770, consisting of phenols and maximum 1% wt. of free formaldehyde. Before performing the SAn-based functionalization reaction, a THF-soluble fraction of KL (SKL) was obtained *via* Soxhlet extraction (24 h at 85 °C - 4 g of lignin per 150 ml of THF) to ensure the complete solubilization of KL in the reaction medium (THF). For the esterification reaction, SKL and SAn (SAn/lignin -OH molar ratio=2) were dissolved in THF in the presence of 1-MI as catalyst (0.2 mL/g of SKL) in a three-neck round-bottom flask and allowed to vigorously stir for 8 h at 60 °C in nitrogen atmosphere. The completion of the reaction was assessed by means of nuclear magnetic resonance (<sup>31</sup>P-NMR) and infrared spectroscopy (FT-IR). At the end of the reaction, the solvent was removed by rotary evaporation and the reaction products were washed with distilled water to remove the unreacted anhydride and then dried under vacuum for 24 h. Lignin-based PF resins (LPF) were produced employing 15% wt. of resole and 85% wt. of a combination of novolac resin and succinylated lignin (SAn-SKL) in 100/0, 95/5, 90/10, 80/20, 70/30 novolac/SAn-SKL wt. ratios. The three components were mixed and cured in a hydraulic press (50 bar) by means of the following thermal cycle: 15 min at 85 °C, 30 min at 150 °C and another 30 min at 180 °C. The curing activation energy, gel content, glass transition temperature (T<sub>g</sub>) and Vickers hardness were evaluated for all LPF thermosetting systems obtained.

FT-IR and <sup>31</sup>P-NMR analyses were used to characterize the esterification reaction product. Data obtained from <sup>31</sup>P-NMR (Table 1) show that the functionalization of SKL with SAn has effectively led to an increase of lignin COOH functionalities, with a consequent reduction in the abundance of aliphatic OH groups. In accordance with <sup>31</sup>P-NMR, FT-IR spectra (Figure 1) show that the signal related to OH group stretching vibrations in lignin (3400-3000 cm<sup>-1</sup>) broadens and decreases in intensity after the reaction with SAn, while a new band appears at 1730 cm<sup>-1</sup>, attributable to the stretching vibration of C=O carboxylic groups formed upon esterification [6].

Table 12 Concentration of lignin functionalities obtained by <sup>31</sup>P-NMR of SKL and SAn-SKL

Sample	Aliphatic OH [mmol/g]	Aromatic OH [mmol/g]	COOH [mmol/g]
SKL	1.50	4.02	0.43
SAn-SKL	0.42	4.27	2.86

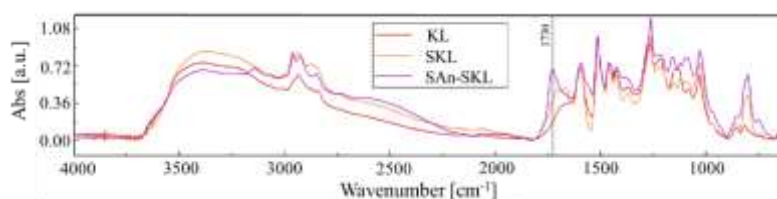


Figure 57 FT-IR of KL, SKL and SAn-SKL.

The main findings obtained from the characterization of the PF and LPF resins are reported in Table 2. The curing activation energy ( $E_a$ ) of LPF systems was studied by applying the Ozawa model. To this end, differential scanning calorimetry (DSC) analyses were carried out on the uncured lignin-resin blends at three heating rates ( $\beta=5, 10, 20$  °C/min, from room temperature to 300 °C) to detect the temperature of the exothermal peak ( $T_p$ ) associated with the crosslinking reaction. The activation energy of the systems corresponds to the slope of the straight line obtained by interpolating ( $-\log \beta$ ) vs. ( $1/T_p$ ) [7]. The results reported in Table 2 show that lignin-substituted samples are characterized by a higher  $E_a$  compared to the pristine PF resin. Actually, the kinetic parameter increases as the lignin content increases, meaning that lignin introduction in the PF formulation leads to an enhancement of the energy required for the LPF resin crosslinking reaction. These results can be attributed to two different aspects. On the one side, the different ortho and/or para vacant sites in the aromatic rings of phenol vs lignin, which are responsible for reacting with HMTA, yield different reaction mechanisms in the two systems. On the other side, the lignin complex and bulky polyphenolic structure may be held accountable for the lower lignin reactivity compared to that of the commercial novolac [8].

After the curing step, the amount of crosslinked material in resin samples was assessed by solvent resistance (gel content) tests submerging the cured resin samples in dimethyl sulfoxide for 24 h and evaluating the extracted sol fraction by gravimetry. Results show that lignin is well incorporated in the resin, which have a gel content value >95%, also in the case of high content of substituted lignin (i.e. 30% wt., Table 2).

DSC analyses were carried out on the resin samples to determine their  $T_g$ . Results reported in Table 2 show that the material results homogeneous with a single  $T_g$ , even for the highest amount of lignin substitution. Up to 10% wt. of substituted SAN-SKL,  $T_g$  of the PFL resins results unaffected by the lignin presence. On the contrary, for higher lignin content,  $T_g$  is reduced by up to 30 °C, highlighting the plasticization effect provided by the SAN-SKL system, the latter exhibiting a  $T_g$  at around 70 °C.

Microindentation tests were used to determine the Vickers surface hardness ( $H_{IT}$ ) of the PF and LPF resins. Analyses were performed in controlled-force mode, loading the samples at 5 mN for 30 seconds, while the test force and the corresponding indentation depth were recorded. The surface behaviour of a thermoset is highly influenced by its degree of crosslinking and  $T_g$ . Indeed, high hardness values are in general recorded for polymeric materials showing a high crosslinking degree and high  $T_g$  [9]. Data recorded and collected in Table 2 show that the Vickers indentation hardness of all LPF samples is comparable or even slightly higher than PF resin. These results represent further evidence of the high crosslinking degree reached in the lignin-substituted samples. Interestingly, despite the lower  $T_g$  values recorded for LPF samples substituted with 20 and 30 % wt. of SAN-SKL, their surface hardness remains in line with that of the pristine PF resins, demonstrating the optimal incorporation of high lignin content in the PF systems.

Table 13 Ozawa curing activation energy, gel content, glass transition temperature and Vickers hardness of PF and LPF resins.

Substituted SAN-SKL [% wt.]	Ozawa $E_a$ [kJ/mol]	Gel content [%]	$T_g$ [°C]	$H_{IT}$ [N/mm <sup>2</sup> ]
0	145	99	179	741 ± 140
5	148	97	176	712 ± 109
10	164	96	176	798 ± 129
20	165	96	157	831 ± 99
30	174	96	148	779 ± 60

Based on the results obtained, lignin functionalization with SAN can be considered as a successful strategy to introduce lignin in PF resins formulation. Indeed, functionalized lignin resulted well incorporated in the resins, leading to a thermosetting material characterized by optimal crosslinking degree and high surface hardness.

## Acknowledgements

This work has received funding from Regione Lombardia and Fondazione Cariplo (grant number 2018-1739, project: POLISTE) and from the European Union's Horizon 2020 Research and Innovation Programme (grant Agreement no. 952941, project: BIOMAC).

## References

1. A. Tejado, G. Kortaberria, C. Pena, J. Labidi, J. M. Echeverria, I. Mondragon, *J. Appl. Polym. Sci.*, **106** 2313 (2007).
2. Y. Zhang, Z. Yuan, C. Xu, *AIChE Journal*, **61** 1275 (2015).
3. B. Briou, S. Caillol, J. J. Robin, V. Lapinte, *Eur. J. Lipid Sci. Technol.*, **120** 1 (2018).
4. Y. Zhang, Z. Yuan, N. Mahmood, S. Huang, C. C. Xu, *Industrial Crops and Products*, **79** 84 (2016).
5. Z. Gao, X. Lang, S. Chen, C. Zhao, *Energy and Fuels*, **35** (2021).
6. C. Scarica, R. Suriano, M. Levi, S. Turri, G. Griffini, *ACS Sustain. Chem. Eng.*, **6** 3392 (2018).
7. E. S. De Medeiros, J. A. M. Agnelli, K. Joseph, L. H. De Carvalho, L. H. C. Mattoso, *J. Appl. Polym. Sci.*, **90** 1678 (2003).
8. J. M. Pérez, M. Oliet, M. V. Alonso, F. Rodríguez, *Thermochimica Acta*, **487** 39 (2009).



9. A. Caretto, V. Passoni, N. Brenna, M. Sitta, L. Ogliosi, G. Catel, S. Turri, G. Griffini, *ACS Sustain. Chem. Eng.*, **6** 14125 (2018).

## Polyolefin-lignin blends: Assessing lignin properties on post-consumer recycled polypropylene

Emanuela Bellineto<sup>1\*</sup>, Oussama Boumezgane<sup>1</sup> and Gianmarco Griffini<sup>1</sup>

<sup>1</sup>Department of Chemistry, Materials and Chemical Engineering "Giulio Natta",  
Politecnico di Milano, Piazza Leonardo da Vinci 32, 20133 Milano, Italy

\*emanuela.bellineto@polimi.it

The employment of renewable resources as feedstock for polymeric materials represents nowadays a valid way to reduce the environmental impact associated to plastic production [1]. Lignin is one of the most abundant natural biomasses on Earth that, at present, is mainly considered as a side-product of the paper industry [2]. Its large availability together with its excellent characteristics as high thermal stability, antioxidant activity and biodegradability, make lignin of great interest for high-value product applications [3]. Among these, polymer blending can be an attractive cost-effective method to produce new well-performing lignin-based materials [4]. In the field of polyolefins, a variety of works have already studied polypropylene-lignin composites [5]. However, no work to date has dealt with the production and comprehensive characterization of high-lignin content composites (up to 25% wt.) in which the thermoplastic matrix consists in commercial post-consumer polypropylene without using a compatibilizer. In view of this, in the current work, the effect of the introduction of kraft lignin in different amounts in second-life polypropylene compounds will be assessed from a morphological and thermo-mechanical point of view, with the twofold aim of valorizing the waste biomass by reducing the total amount of polypropylene employed.

The polypropylene used in this work (rPP), supplied by Electrolux S.p.A, is a post-consumer blend of polypropylene and a small fraction of polyethylene containing different inorganic filler (i.e. calcium carbonate, talc, alumina) recovered from food packaging recycling cycle. Kraft lignin Indulin AT (KL), by MeadWestvaco, was employed in this work after ball milling, in order to reduce its granulometry to few micrometers. Lignin was compounded with rPP at 5-10-15-20-25% wt. in a twin-screw extruder Process 11 by Thermo Fisher Scientific. The mechanical properties of the blends were assessed by tensile test, performed according to standard ISO-527-A. Rheology tests were carried out to study the viscoelastic behavior of the materials. Differential scanning calorimetry (DSC) and thermogravimetric analysis (TGA) were used to determine the thermal properties and thermal stability of the blends, respectively. Finally, in order to study their morphology, fracture surface of samples was analyzed by scanning electron microscopy (SEM).

Results of tensile tests are reported in Table 1. As expected, the tensile modulus increases with increasing lignin content. The stress at yield, which is of major importance in engineering applications, remains almost unchanged in the presence of lignin, while the tensile stress results moderately reduced. Both the strain at yield and the strain at break tend to decrease increasing the lignin percentage. Relying on literature, these outcomes are remarkable. Indeed, in various published works the maximum elongation of lignin-filled polypropylene is often not even reported [6] or, when reported, it turns out to be drastically reduced by lignin, due to lack of compatibility with PP [7]. On the contrary, the inorganic phase (i.e. oxides) contained in rPP seems to well interact with lignin, improving lignin-matrix affinity and allowing for larger deformations compared to those of virgin PP-lignin composites.

Table 14 Tensile modulus ( $E_t$ ), stress at yield ( $\sigma_y$ ), stress at break ( $\sigma_b$ ), strain at yield ( $\epsilon_y$ ) and strain at break ( $\epsilon_b$ ) of rPP-lignin blends.

Sample Code	$E_t$ [MPa]	$\sigma_y$ [MPa]	$\sigma_b$ [MPa]	$\epsilon_y$ [%]	$\epsilon_b$ [%]
rPP 0	1118.6 ± 79.8	26.0 ± 0.7	32.0 ± 0.3	12.7 ± 0.9	820.7 ± 35.2
rPP KL 5	1255.5 ± 145.3	26.8 ± 0.4	30.0 ± 0.2	10.7 ± 0.6	673.3 ± 37.7
rPP KL 10	1383.2 ± 42.8	25.9 ± 0.2	26.3 ± 0.2	8.9 ± 0.2	560.2 ± 20.4
rPP KL 15	1414.6 ± 107.6	24.7 ± 0.6	24.3 ± 0.3	8.4 ± 0.9	551.5 ± 28.4
rPP KL 20	1548.0 ± 41.3	24.6 ± 0.2	19.4 ± 2.1	6.9 ± 0.4	514.4 ± 14.5
rPP KL 25	1688.6 ± 52.6	25.2 ± 1.4	19.0 ± 2.3	5.4 ± 2.1	362.0 ± 147.3

Frequency sweep tests were performed with a rotational rheometer at 180 °C, from 1 Hz to 100 Hz, imposing a deformation of 1%, to evaluate the effect of lignin on rPP relaxation time. Results are summarized in Figure 1. Relaxation time increases with lignin content, for both lignins, up to 20%. The increase in relaxation times observed could be associated with longer chains in the polymer blends. In this case, the stabilizing effect in presence of lignin can be explained with an inhibition of molecular weight loss caused by thermal degradation during blend formation in the extruder. What is observed in the case of blends with 25% of lignin can be instead related to the non-perfect miscibility between lignin and rPP. Indeed, the high biomass content could lead to formation of voids and aggregates within the rPP matrix. The presence of voids allows the rPP chains to flow more easily, causing a decrease in the relaxation time of the material.

DSC was used to study the influence of lignin on the melting and crystallization behavior of rPP. Unfilled rPP shows two melting peaks: the first one around 130 °C, associated with the PE fraction contained in the recycled compound, and the second one around 165 °C, related to melting of the crystalline PP fraction. According to Mourad et al. [8], the degree of crystallinity of starting rPP is estimated to be 25%. In this case, rPP thermal properties are not significantly affected by the addition of lignin: both the melting temperatures and the degree of crystallization of the material remained almost unchanged, independently on lignin content.

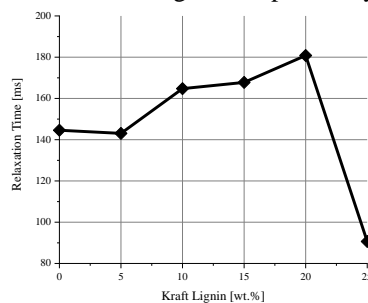


Figure 58 Relaxation times of rPP-lignin blends.

TGA were performed from 25 °C to 800 °C, at 20 °C/min, to understand how the presence of lignin affects the thermal degradation behavior of rPP. In Table 2 the temperature at which the highest weight loss is observed ( $DTG_{max}$ ) and the temperatures at which 5%, 10% and 50% of weight loss occurs ( $T_{5\%}$ ,  $T_{10\%}$ ,  $T_{50\%}$ ) are reported. Data show that the presence of lignin up to 20% wt. is able to stabilize rPP, in accordance with the results obtained from rheology tests. Indeed, all the characteristic mass loss temperatures shift at higher values and, in particular, they are found to increase as the lignin content increases, up to 20% wt. This effect is related to the well-known antioxidant effect of lignin, whose structure is characterized by hindered phenolic hydroxyl groups able to act as stabilizer for reactions induced by oxygen and its radical species [9].

Table 15 TGA characteristic temperatures of rPP-lignin blends.

Sample Code	$DTG_{max}$ (°C)	$T_{5\%}$ (°C)	$T_{10\%}$ (°C)	$T_{50\%}$ (°C)
rPP 0	411	313	338	399
rPP KL 5	429	332	356	414
rPP KL 10	431	326	351	413
rPP KL 15	440	320	347	416
rPP KL 20	437	322	354	419
rPP KL 25	417	308	333	398

SEM confirmed that the blends rPP-lignin containing up to 20% of lignin show a sufficiently smooth and homogenous surface, where it is difficult to distinguish lignin particles (Figure 2a). On the contrary, samples filled with higher lignin content (e.g., 25% wt.) show the presence of voids in the bulk and a more evidently rough fracture surface (Figure 2b).

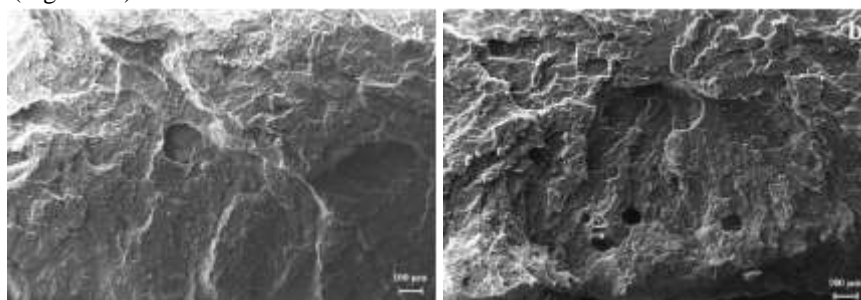


Figure 59 SEM images of (a) rPP KL 10 and (b) rPP KL 25.

This work represents the first example of the incorporation of high lignin loadings into polyolefin blends to achieve increased thermo-oxidative stability while maintaining excellent thermo-mechanical response without using a compatibilizer, and provides a demonstration of the potential of lignin as valuable biobased filler for post-consumer recycled thermoplastics.

### Acknowledgements

This work has received funding from Regione Lombardia and Fondazione Cariplo (grant number 2018-1739, project: POLISTE) and from the European Union's Horizon 2020 Research and Innovation Programme (grant Agreement no. 952941, project: BIOMAC).

## References

1. K. Müller, C. Zollfrank, M. Schmid, *Macromolecular Materials and Engineering*, **304** 1 (2019).
2. D. Kai, M. J. Tan, P. L. Chee, Y. K. Chua, Y. L. Yap, X. J. Loh, *Green Chemistry*, **18** 1175 (2016).
3. G. Griffini, V. Passoni, R. Suriano, M. Levi, S. Turri, *ACS Sustainable Chem. Eng.*, **3** 1145 (2015).
4. J. F. Kadla, S. Kubo, *Macromolecules*, **36** 7803 (2003).
5. M. A. Abdelwahab, M. Misra, A. K. Mohanty, **132** 497 (2019).
6. P. Alexy, B. Košíková, G. Podstránska, *Polymer*, **41** 4901 (2000).
7. O. A. T. Dias, M. Sain, I. Cesarino, A. L. Leão, *Polymers for Advanced Technologies*, **30** 70 (2019).
8. A. H. I. Mourad, R. O. Akkad, A. A. Soliman, T. M. Madkour, *Plastics, Rubber and Composites*, **38** 265 (2009).
9. A. Gregorová, Z. Cibulková, B. Košíková, P. Šimon, *Polymer Degradation and Stability*, **89** 553 (2005).

## Valorization of limonene in the presence of heterogenous catalysts

Madalena Frade<sup>1</sup>, PA. Mourão<sup>1</sup>, I. Cansado<sup>1,2</sup> and José E. Castanheiro<sup>1\*</sup>

<sup>1</sup>MED, Departamento de Química e Bioquímica, Escola de Ciências e Tecnologia, Universidade de Évora/, Portugal  
<sup>1</sup>LAQV-REQUIMTE, Departamento de Química e Bioquímica, Escola de Ciências e Tecnologia, Universidade de Évora/, Portugal

\*jefc@uevora.pt

Limonene is a monoterpene which is renewable feedstock. This terpene can be used in fine chemistry industries [1,2]. Etherification reactions of limonene are paths to synthesis of ethers with commercial value. These ethers can be applied in food, pharmaceutical industries [1-3]. Figure 1 shows a simplified scheme of limonene transformation in ethers [4-6].

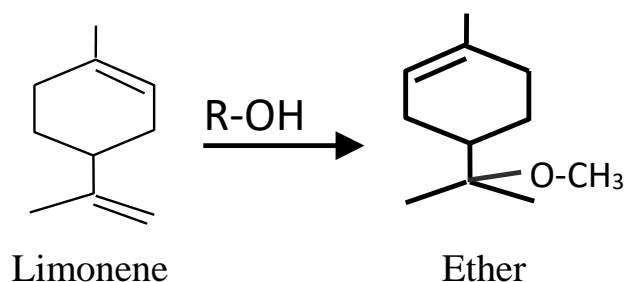


Figure 1. Scheme of limonene alkoxylation

Traditionally, limonene transformation in ethers have been performed using sulphuric acid, as homogeneous catalyst. However, this catalyst has some problems associated. Sometimes, they are used in stoichiometric quantities and the separation from reaction mixture is difficult. The heterogenous catalyst have some advantages over homogenous ones. The separation from reaction mixture it is easy (by decantation and filtration). These materials are reused, and they are more environmentally friendly.

The etherification of limonene to terpinyl ether have been done using beta zeolite, in batch and continuous reactors [7]. The methoxylation of limonene produced the main ether with yield of 85%. The methoxylation of limonene have been also carried out over heteropolyacid supported on silica. The selectivity to terpinyl methyl ether was about 81% (limonene conversion: 60%; temperature: 60°C and catalyst loading: 1.0 g; time reaction: 50 h) [8].

In a previous work, the methoxylation of limonene was carried out over composite catalysts (Chitosan/MCM-41-SO<sub>3</sub>H) [9].

In this work, we study the alkoxylation of limonene over chitosan with sulfonic acid groups. The sulfonic groups were introduced by reaction with chorosulfonic acid or sulfosuccinic acid.

The catalysts were characterized by CHNS Elemental Analyzer 1112 (Thermo Finnigan) was used to determine the sulphur. Also, the acid capacities of the materials were determined by ion-exchange with sodium chloride (NaCl)]. XRD spectra were recorded on a Bruker AXS-D8 Advance diffractometer. Zeiss Auriga scanning electron microscope was used to obtain SEM of composite.

The etherification of limonene with alcohol were performed using a batch reactor. The reactor was loaded with 3 mmol of limonene, 30 mL of alcohol and 0.1 g chitosan with sulphonic acid groups. The reaction was carried out at 60°C.

The catalytic activity of the materials was also studied.

During the reactions, some samples were pick up. The nonane was used as internal standard. It was used a KONIK HRGC-3000C gas chromatography. The column used is a DB-1.

It was observed that the catalytic activity increased with the amount of sulfonic acid groups present on polymeric matrix. High selectivity to alpha-terpinyl methyl ether was obtained.

## References

1. E. V. Gusevskaya. *ChemCatChem* **6** 1506 (2014) ..
2. P. Gupta, S. Paul. *Catal. Today* **236** 153 (2014).
3. L.M. Sanchez, H.J. Thomas, M.J. Climent, G.P. Romanelli, S. Iborra. *Catal. Rev.* **58** 497 (2016).
4. A. Corma, S. Iborra, A. Velty, *Chem. Rev.* **107** 2411 (2007).
5. P. Mäki-Arvela, B. Holmbom, T. Salmi, D. Y. Murzin, *Catal. Rev.* **49** 197 (2007).
6. J.L. Monteiro, C.O. Veloso, *Topics Catal.* **27** 169 (2004) 180.
7. K. Hensen, C. Mahaim, W.F. Hölderich, *Appl. Catal. A:Gen.* 149 311 (1997).
8. M. Caiado, D.S. Pito, J.E. Castanheiro (2013) Alkoxylation of terpenes over tungstophosphoric acid immobilized on silica. In: Patel A.U. (ed.) Environmentally benign catalysts: for clean organic reactions, Springer, Heidelberg, p 163-175.
9. J.E. Castanheiro, *Results in Materials* **12** 100233 (2021).

## Valorization of ruminant animal dung fiber: A sustainable natural resource of non-wood material for various applications.

Vinayak Fasake<sup>1\*</sup> and Kavya Dashora<sup>2</sup>

<sup>1</sup>Research scholar, Agri-Nano Technology Laboratory, Centre for Rural Development and Technology, Indian Institute of Technology, Delhi Hauz Khas, New Delhi 110016, India.

<sup>2</sup>Associate professor, Agri-Nano Technology Laboratory, Centre for Rural Development and Technology, Indian Institute of Technology, Delhi Hauz Khas, New Delhi 110016, India.

\*E-mail: [Vinayak.fasake@gmail.com](mailto:Vinayak.fasake@gmail.com)

### Abstract

A large part of the vegetation on the earth is unsuitable for human consumption but is fairly consumed by grazing and herbivorous animals. Cattle convert straw and stover into their rumen and the excreted waste from their body like dung and urine are subsidiary. Cattle-dung fiber is a lignocellulosic material abundant and sustainable non-wood source of polymeric components, which can be converted into high added-value products [1]. Increased urbanization and industrialization result in environmental degradation and increasing deforestation. Nowadays, although the utilization of wood is increasingly widespread, non-wood pulp production is also crucial in countries that do not have enough trees for the pulp industry such as China, India, Pakistan, Egypt, and Columbia. The authors have explored the potential and alternate sources of industrial pulp through ruminant animal dung, which is widely available as a rural and natural resource in India. Three types of undigested animal dung fibers from the Indigenous cow (IDF), Jersey cow (JDF), and Buffalo (BDF) were taken. Wheat straw (WS) was the main diet of all animals. The cellulose, hemicellulose, and lignin content for all animal dung samples were found in a range of (29-31.50%), (21-23.50%), and (11-13%), respectively [2].

The use of biomass by removing lignin and hemicellulose for paper production and packaging has become a subject of current attention due to the increased demand for green energy content and environmental protection. The proposed hydrothermal treatment is environmentally friendly because there was no chemical involvement during the cooking process [3]. The hydrothermally treated process valorizes the hemicellulose fraction of dung fiber but the delignification appeared to be done mildly. The objective of this research was to optimize the delignification parameters for waste cattle dung (or raw dung fibers) by using a central composite design (CCD). In this paper, the effect of independent factors viz. temperature and time on dependent variables viz. yield, cellulose hemicellulose, and lignin of dung fiber were investigated. The optimum conditions to produce maximum yield (78.15±1.5%), cellulose (48.08±0.96%), and lignin (30.05±1.83%) were obtained at 160°C, cooking time 5 min, and solid to water ratio 1:10. The paper sheet was prepared by using hydrothermally treated (HT) dung material and an additional blending material (paddy straw pulp and waste cotton rag material pulp) for various proportions. The paper was tested for physical and mechanical properties. Results show that (C50) a blend of 50% of dung fiber in waste cotton rag pulp exhibits maximum tensile and bursting index. But the quality of the paper obtained can be adjusted somewhere for single-use packaging according to the end-use application [4]. The main advantage of the proposed processing scheme is environmentally friendly, valorizes the hemicellulose fraction of dung fiber, and exhibited more yield.

Agricultural crop residues can be used directly as food for livestock, not directly in biorefinery or for energy generation. On the other hand, by separating the dung produced from livestock and setting aside undigested fiber, it can be further used as a non-wood material for various applications. This is a win-win situation to sustain the livestock of our large population and to meet other demands like energy, pulp, etc. from dung fiber without disturbing their existing uses. Cattle dung manure (or dung fiber) is an abundant, promising sustainable raw material, which will help in reducing deforestation [5].

**Keywords:** Cattle dung, Cellulose, Non-wood pulp, Pulp and paper, Response surface methodology (RSM), Ruminant animal, Tensile index.

### References:

1. Fasake, V., Dashora, K.: A sustainable potential source of ruminant animal waste material (dung fiber) for various industrial applications: A review. *Bioresour. Technol. Reports*. **15**, 100693 (2021). <https://doi.org/https://doi.org/10.1016/j.biteb.2021.100693>
2. Fasake, V., Dashora, K.: Characterization and Morphology of Natural Dung Polymer for Potential Industrial Application as Bio-Based Fillers. *Polymers (Basel)*. **12**, 3030 (2020). <https://doi.org/http://dx.doi.org/10.3390/polym12123030>
3. Fasake, V., Kaur, P.J., Dashora, K.: Physicochemical Characterization of Cattle Dung Fibre Under the Hydrothermal Process. (2021)
4. Fasake, V., Shelake, P.S., Srivastava, A., Dashora, K.: Characteristics of Different Plastic Materials, Properties and their Role in Food Packaging. *Curr. Nutr. Food Sci.* **17**, 944–954 (2021). <https://doi.org/https://doi.org/10.2174/1573401317666210505100139>
5. Fasake, V., Dashora, K.: Characterization of raw and anaerobic digested cattle dung fibers: a sustainable source of non-wood material. *Biomass Convers. Biorefinery*. 1–10 (2022).

<https://doi.org/http://dx.doi.org/10.1007/s13399-022-02487-0>



## Reinforcement and protection of marbles with composite epoxy-based adhesives using cellulose micro/nano-particles

Dimitris Gkiliopoulos<sup>1,2,\*</sup>, Eleni Psochia<sup>1</sup>, Konstantinos Simeonidis<sup>3</sup>, Filippos Boukas<sup>4</sup>, Doukas Efstathiadis<sup>4</sup>, Ioannis Polychroniadis<sup>4</sup>, Gian Raska<sup>4</sup>, and Konstantinos Triantafyllidis<sup>1,2,\*</sup>

<sup>1</sup> Department of Chemistry, Aristotle University of Thessaloniki, Thessaloniki, GR-54124, Greece

<sup>2</sup> Center for Interdisciplinary Research and Innovation (CIRI-AUTH), Balkan Center, 10th km Thessaloniki-Thermi Rd, P.O. Box 8318, 57001 Thessaloniki, Greece

<sup>3</sup> Department of Physics, Aristotle University of Thessaloniki, Thessaloniki, GR-54124, Greece

<sup>4</sup> Stone Group International, Thessaloniki, Kavaleri, GR-57200, Greece

\* Corresponding author: [ktrianta@chem.auth.gr](mailto:ktrianta@chem.auth.gr)

### Abstract

Marble is a material that has been used since antiquity as a building material, with a range of uses that extends from small structures to grand monuments that exist for centuries. Despite its particularly good properties, marble is vulnerable to various corrosive environmental factors (e.g., acid water and solvents) and it is necessary to protect it with anti-corrosion agents. Another problem in marble industry is the breaks and other types of damages that occur during the processing or transporting of the material, resulting in significant financial losses.

To prevent marble damaging during processing, transporting, and exposure to the environment, the use of protective agents has been implemented, which are either impregnated into the marbles to increase the consistency of the structure or used as coatings for corrosion protection. In their majority, the protective agents are epoxy resin/hardener systems, which have very good to excellent properties (thermal mechanical, dimensional stability, processing time, etc.) [1]. Despite the exceptional properties of epoxy polymers, there are some points in their use as protective agents of marble that could be improved, leading to a significant increase in the quality and commercial value of marble products. The most important of these points are color resistance due to UV radiation/oxidation, resistance to corrosion and chemicals, appropriate rheological properties for better penetration into the structure imperfections, reduction of liquid and gas permeability.

Aiming at addressing the aforementioned points, the present work focuses on the production of epoxy/cellulose composites and the study of the effect of cellulose addition on the properties of final composites. Concerning the composites production, initially, various cellulose micro- and nanoparticles were produced from biomass derived cellulose after treatment with different, environmentally friendly, physical or chemical methods, such as ball milling, ultrasonication, high shear blending, and acid hydrolysis. These cellulose micro- and nanoparticles were dispersed mechanically in diglycidyl ether of bisphenol A (DEGBA) type epoxy resin, and then the mixture was crosslinked with a polyether diamine curing agent. The thermal, mechanical, and thermomechanical properties of the epoxy/cellulose composites were determined via differential scanning calorimetry (DSC), tensile strength testing, and dynamic mechanical analysis (DMA), respectively. Finally, the effect of cellulose addition on the resistance of epoxy composites to yellowing was tested by applying UV radiation on the samples under a controlled environment of temperature and humidity.

### Acknowledgements

This research has been co-financed by the European Regional Development Fund of the European Union and Greek national funds through the Operational Program Competitiveness, Entrepreneurship and Innovation (EPAnEK 2014-2020), under the Action "RESEARCH – CREATE – INNOVATE B' CALL" (project code: T2EDK-02205).

### References

1. T.N. Kumar, B. Vikas, M.R. Krishna, Y. Jyothi, S.K. Imran, *Materials Today: Proceedings*, **5** 13031 (2018).

## Structural and morphological characterization of xerogels based on agar and gelatin.

Marta Goliszek<sup>1\*</sup> and Artur Chabros<sup>1\*</sup>

<sup>1</sup>Maria Curie-Skłodowska University, Faculty of Chemistry, Institute of Chemical Science, Analytical Laboratory, M. Curie-Skłodowska Sq. 3, 20-031 Lublin, Poland

\*e-mail addresses of corresponding authors:

marta.goliszek@mail.umcs.pl, artur.chabros@mail.umcs.pl

Xerogels are defined as dried gels that retain, at least in part, their porous texture after drying. They are advanced, functional, porous materials consisting of ambient, dried, cross-linked polymeric networks. Xerogels can be characterized by high porosity, great surface area, and an affordable preparation route. Nowadays, they are considered as new sustainable and eco-friendly materials with diverse potential applications. Xerogels based on agar and gelatin can be demonstrated as an example for this approach [1,2,3].

Numerous research articles considering the synthesis and utilization of hydrogels and corresponding xerogels in different fields have been published, and still restless labor is giving for the betterment of the product quality. The mechanism governing pore formation in xerogels is not well understood, limiting any control over pore size or distribution. The detailed investigation on xerogels considering current environmental issues will reach to its target of making the greener solution of sustainability [4,5,6,7].

In this research work to obtain the xerogels the previously obtained gels were drying. Traditional drying was preceded by the use of solvent exchange. Water and glycerol were replaced by ethyl alcohol and acetone. Surface morphologies of obtained xerogels were evaluated by scanning electron microscopy (SEM) and Fourier-transform infrared (FTIR) analyses. The main aim of our research was understanding the role played by the breaking/reforming of specific intermolecular H-bond interactions involving water molecules and the chemical groups present in the polymer network on their structures. By doing this, it is hoped that knowledge is gained regarding the structural features and stability of agar and gelatin based xerogels. Better understanding of structural and morphological properties will contribute to the improvement of their performance in various fields of application.

### References

1. G. Paladini, V. Venuti, V. Crupi, D. Majolino, A. Fiorati, C. Punta, *Cellulose*, **27**, 8605 (2020).
2. R. Naohara, K. Narita, T. Ikeda-Fukazawa, *Chem. Phys. Lett.*, **670**, 84 (2017).
3. H. P. S. Abdul Khalil, E. B. Yahya, H. A. Tajarudin, V. Balakrishnan, H. Nasution, *Gels*, **8(6)**, 334, (2022).
4. S. Yamasaki, W. Sakuma, H. Yasui, K. Daicho, T. Saito, S. Fujisawa, A. Isogai, K. Kanamori, *Front. Chem.*, **7**, 316 (2019).
5. Y. Fukui, R. Inamura, K. Fujimoto, *Polym. J.*, **53**, 815 (2021).
6. C. Scherdel, G. Reichenauer, *J. Supercrit. Fluids*, **106**, 160 (2015),
7. S. Yang, Y. Zhang, Ch. Zhang, T. Wang, W. Sun, Z. Tong, *Macromol. Rapid Commun.*, **40(18)**, 1900270 (2019).

## Lignin-containing polymer coatings – synthesis and characterization

B. Podkościelna<sup>1</sup>, M. Goliszek<sup>2\*</sup>, A. Lipke<sup>3</sup>, O. Sevastyanova<sup>4</sup>

<sup>1</sup>Maria Curie-Skłodowska University, Faculty of Chemistry, Institute of Chemical Science, Department of Polymer Chemistry, Lublin, Poland

<sup>2</sup>Maria Curie-Skłodowska University, Faculty of Chemistry, Institute of Chemical Science, Analytical Laboratory, Lublin, Poland;

<sup>3</sup>Maria Curie-Skłodowska University, Faculty of Chemistry, Institute of Chemical Science, Lublin, Poland;

<sup>4</sup>KTH Royal Institute of Technology, Department of Fibre and Polymer Technology, Stockholm, Sweden

\*e-mail address of corresponding author: marta.goliszek@mail.umcs.pl

Lignin, one of the component of lignocellulosic biomass, is produced mainly as a byproduct of the papermaking industry only <2% of it is recycled toward preparation of value-added products [1]. Therefore, high-valued utilization of lignin is very important for biomass utilization and environmental protection. Utilization of lignin not only avoids environmental pollution, but also provides a potential alternative for reducing our dependence on fossil fuel resources.

Lignin is considered as a perfect candidate for the development of polymer materials due to the presence of various functional groups in its structure - phenolic hydroxyl groups, alcoholic hydroxyl groups, and carboxyl groups, which can react with other polymers to form hybrid composites, making it a good source for the synthesis of various materials, e.g. polymer coatings. Lignin is frequently being used for the development of different types of coating materials due to its UV protection properties. Lignin has a remarkable ability to act as a blocker of ultraviolet radiation due to the large number of phenolic units, ketones, and other chromophores presents in its structure, which combined with the aromatic rings, are capable to form large conjugated  $\pi$  systems, which are capable of absorbing UV radiation. This property can become especially interesting for its use as a potential additive for epoxy resins, which are susceptible to degradation when exposed to UV radiation and have their durability substantially reduced when used in outdoors environments [2,3,4,5,6].

In this work unmodified kraft and organosolv lignin as well as methacrylated lignin were used in the polymerization process of coatings preparation. Commonly applied in industry Epidian 5 epoxy resin, triethylamine as a crosslinking agent and different amount of lignin (up to 50 wt.%) were applied. The spectroscopic characterization (ATR/FTIR) as well as thermal resistance (thermogravimetry) were studied in detail. The influence of lignin isolation process (kraft and organosolv), its chemical modification (methacrylation) on the properties of obtained polymer coatings will provide valuable information for the further development of this type of materials.

### Acknowledgements

The contribution of COST Action LignoCOST (CA17128), supported by COST (European Cooperation in Science and Technology, [www.cost.eu](http://www.cost.eu)), in promoting interaction, exchange of knowledge and collaborations in the field of lignin valorization is gratefully acknowledged.

### References

1. R. Kaur, N.S. Thakur, S. Chandna, J. Bhaumik, *ACS Sustainable Chem. Eng.* **9(33)** 11223 (2021).
2. O.B.F. Diógenes, D. R. de Oliveira, L. R.R. da Silva, Í. G. Pereira, S. E. Mazzetto, W.S. Araujo, D. Lomonaco, *Prog. Org. Coat.* **161** 106533 (2021).
3. M. Lin, L. Yang, H. Zhang, Y. Xia, Y. He, W. Lan, J.-j. Ren, F. Yue, F. Lu, *Ind. Crops Prod.*, **174** 114212 (2021).
4. H. Sadeghifar, A. Ragauskas, *Polymers*, **12(5)** 1134 (2020).
5. M. Yu, D. He, Y. Zhang, D. He, X. Wang, J. Zhou, *Int. J. Biol. Macromol.* **192** 498 (2021).
6. S. Tan, D. Liu, Y. Qian, J. Wang, J. Huang, C. Yi, X. Qiu, Y. Qin, *Holzforchung*, **73(5)** 485 (2019).

## Glycerol-based UV-curable resins for synthesis of vitrimers

Sigita Grauželiene\* and Jolita Ostrauskaitė

Department of Polymer Chemistry and Technology, Kaunas University of Technology, Radvilenu Rd. 19, LT-50254 Kaunas, Lithuania

\*sigita.grauzeliene@ktu.lt

Vitrimers have been defined as polymers with associative, dynamic covalent bonds which undergo exchange reactions upon an external stimulus [1]. Vitrimers are able to change their topology through thermoactivated bond exchange reactions: they behave like viscoelastic liquids at high temperature and like classical thermosets at low temperatures [2]. Transesterification reaction rate can be tuned by changing the amount and nature of the catalyst leading to the new possibilities in applications such as self-healing or processability in a wide temperature range [2]. Due to dynamic nature vitrimers can have unique properties such as recyclability, weldability, malleability, reshaping (shape-memory), and the ability for self-healing [3]. Consequently, they can be easily recycled and used again leading to environment protection. A huge increase of scientific publications with bio-based vitrimers has been observed during the last five years [4]. This intrigues to combine the attractive features of bio-based monomers and the properties of vitrimers for the synthesis of high-performance and sustainable materials. Biodiesel production from vegetable oils and animal fats generates about 10% (w/w) of glycerol as the main by-product which is a starting material for synthesis of various glycerol-based monomers [5]. Glycerol is attractive for synthesis of vitrimers as has properties such as low volatility, hygroscopicity, plasticizing effect, high miscibility, compatibility with a wide range of materials, stability, high viscosity, nontoxicity, [6] and has been used for the production of biodegradable plastics already [7-9].

The aim of this work was to combine the properties of glycerol and vitrimers for the synthesis of sustainable materials towards environmentally friendly strategy. Consequently, functionalized glycerol was used as a monomer in the UV-curable resins for synthesis of vitrimers with the other bio-based monomers at different ratios. A MCR302 rheometer from Anton Paar was used to monitor the evolution of photocross-linking and for stress relaxation experiments by real-time. The rigidity of the vitrimers decreased slightly and the viscosity of the resin was reduced with increasing the amount of functionalized glycerol. The dynamic networks were able to rapidly undergo thermo-activated rearrangements of their network topology as the resins had optimal amount of functional groups that were beneficial for transesterification reactions. The tensile test was performed to investigate the mechanical properties of glycerol-based vitrimers. The elasticity of vitrimers increased with the increase of the amount of functionalized glycerol. The synthesized vitrimers showed recyclability, shape memory and self-healing properties.

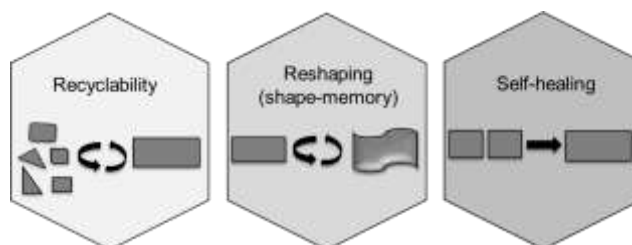


Figure 1. Properties of glycerol-based vitrimers.

### Acknowledgements

This project has received funding from the European Social Fund (project No. 09.9.9-LMT-K-712-23-0088) under grant agreement with the Research Council of Lithuania (LMTLT).

### References

1. J. Zheng, Z.M. Png, S.H. Ng, G.X. Tham, E. Ye, S.S. Goh, X.J. Loh, Z. Li, *Mater. Today*, **51** 586-625 (2021).
2. M. Capelot, M.M. Unterlass, F. Tournilhac, L. Leibler, *ACS Macro Lett.*, **1** 789-792 (2012).
3. M. Giebler, C. Sperling, S. Kaiser, I. Duretek, S. Schlögl, *Polymers*, **12** 1148 1-14 (2020).
4. M.A. Lucherelli, A. Duval, L. Avérou, *Prog. Polym. Sci.*, **127** 101515 1-24 (2022).
5. F. Yang, M.A. Hanna, R. Sun, *Biotechnol. Biofuels*, **5** 13 1-10 (2012).
6. M.R. Monteiro, C.L. Kugelmeier, R.S. Pinheiro, et al., *Renew. Sust. Energ. Rev.*, **88** 109-122 (2018).
7. S. Kasetaitė, J. Ostrauskaitė, V. Gražulevičienė, et al., *Polym. Bull.*, **72** 3191-3208 (2015).
8. S. Kasetaitė, J. Ostrauskaitė, V. Gražulevičienė, et al., *J. Compos. Mater.*, **51** (29) 4029-4039 (2017).
9. S. Kasetaitė, J. Ostrauskaitė, V. Gražulevičienė, D. Bridziuvienė, R. Budreckienė, E. Rainosalo, *React Funct Polym*, **122** 42-50 (2018).

## From ferulic acid and lignin to vanillin and other platform chemicals by hydrogen peroxide

Monika Horvat and Jernej Iskra\*

University of Ljubljana, Faculty of Chemistry and Chemical Technology, Večna pot 113, Ljubljana, Slovenia  
Monika.horvat@fkk.uni-lj.si

Selective oxidative cleavage of unsaturated bonds such as carbon-carbon double bonds is a synthetically important reaction to introduce oxygen functionality into molecules or to degrade complex compounds, especially those from natural sources and biomass. The production of aromatic compounds from biomass resources could provide a sustainable alternative to conventional methods. Thus, oxidative cleavage of olefins represents one of the most important reactions in organic chemistry. It is also a very fundamental reaction in industrial organic synthesis, as it can provide several important products, such as vanillin, benzaldehydes, and aromatic carboxylic acids. [1,2]

The standard methods for the conversion of cinnamic acid derivatives into corresponding carboxylic acids are oxidation with Oxone, m-CPBA, NaClO<sub>2</sub>, PIDA, O<sub>2</sub> and H<sub>2</sub>O<sub>2</sub>/OsO<sub>4</sub>. Several methods are also known for the conversion of ferulic acid to vanillin using various microorganisms (bacteria, microbial strains, fungal strains, enzymes, etc.), metal oxide catalysts, TiO<sub>2</sub>, WO<sub>3</sub>-loaded TiO<sub>2</sub> ... [3]

Herein, we have developed simple and cost-effective method for the conversion of ferulic acid related compounds to corresponding aromatic benzaldehydes, benzoquinones, or aromatic carboxylic acids. The reaction of oxidative cleavage of the carbon-carbon double bond takes place under mild reaction conditions with the green and environmentally friendly oxidant hydrogen peroxide. The choice of solvent significantly influences the course of the reaction. The process also offers a simple and cost-effective alternative for the conversion of natural compound ferulic acid to vanillin in high yield.

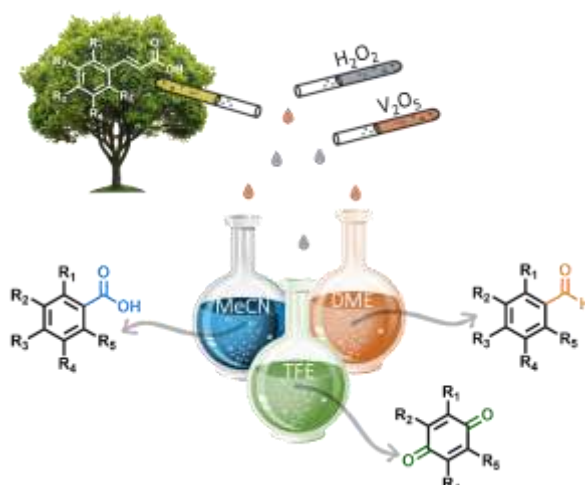


Figure 1. Oxidative degradation of the C-C double bond and conversion of ferulic acid and lignin into aromatic molecules.

### References

1. F. Chen, T. Wang, N. Jiao, *Chemical Reviews* **2014**, 114 (17), 8613-8661.
2. P. Sivaguru, Z. Wang, G. Zanoni, X. Bi, *Chemical Society Reviews* **2019**, 48 (9), 2615-2656.
3. K. Miyamoto, N. Tada, M. Ochiai, *Journal of the American Chemical Society* **2007**, 129 (10), 2772-2773.

## Augmenting the performance of eco-friendly greases using synergistic natural resources

Ankit Saxena<sup>1</sup>, Deepak Kumar<sup>1\*</sup>, Naresh Tandon<sup>1</sup>

<sup>1</sup> Centre for Automotive Research and Tribology (CART), Indian Institute of Technology Delhi, New Delhi, India

\*dkumar@iitd.ac.in

Grease industry extensively uses non-renewable, non-biodegradable, and toxic entities as ingredients that satisfy the performance goals and jeopardize the environment simultaneously. Several environmentally benign ingredients have been tried to formulate eco-friendly greases; however, a potential alternative is not yet reached. The present study explores, for the very first time, an effort to enhance the performance of eco-friendly greases (based on vegetable oil and organoclay) using biopolymers as additives. Two different series of greases containing 0 - 10 %w/w of two biopolymers (B1 and B2) are developed and evaluated for anti-wear (AW), and extreme-pressure (EP) tests as per ASTM standards.

B1-based greases displayed superior AW (upto  $\approx$  22% enhancement), frictional (upto  $\approx$  42% enhancement), and EP response (upto  $\approx$  60% enhancement). Whereas B2-based greases displayed superior EP characteristics (upto  $\approx$  60% enhancement), however, inferior AW response. The formation of an in-situ polymer-layered silicate nanocomposite film at the interface is attributed to the superior EP properties. The contradictory AW behavior of biopolymers is attributed to their distinct interfacial interaction tendencies (synergistic or antagonistic) with organoclay.

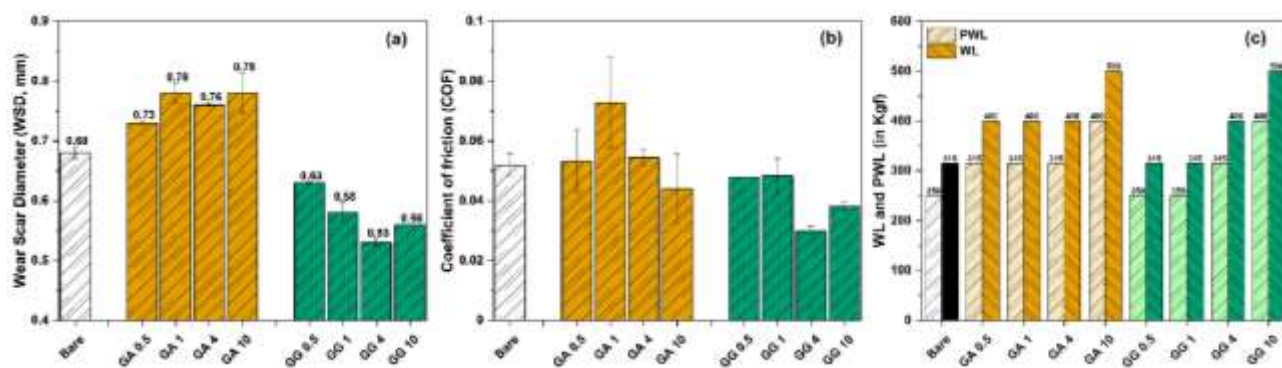


Figure 1. (a) Anti-wear (AW), (b) frictional, and (c) extreme-pressure (EP) performance characteristics of the formulated greases (WL: Weld load, and PWL: Pre-weld load)

This research is a step ahead in pursuing a sustainable solution of providing an efficient and thus commercially viable eco-friendly alternative to long-established harmful greases. The study explores and recommends biopolymers as performance additives to greases based on vegetable oil and organoclay.

### Acknowledgements

This research did not receive any specific grant from funding agencies in the public, commercial, or not-for-profit sectors. The authors are highly grateful to the Central Research Facility (CRF), IIT Delhi and Nano Research Facility (NRF), IIT Delhi for providing impressive support in the characterization work.

## pH indicator films based on renewable biodegradable polymers for food packaging applications

Julia Păușescu\*<sup>1</sup>, Diana Maria Dreavă<sup>1</sup>, Ioan Bîțcan<sup>1</sup>, Diana Dăescu<sup>1</sup>, Mihai Medeleanu<sup>1</sup>

<sup>1</sup>Politehnica University Timisoara, Faculty of Industrial Chemistry and Environmental Engineering, 6 Vasile Parvan Bvd, 300223, Timisoara, Romania

\* e-mail: iulia.pausescu@upt.ro

Active and intelligent systems produced from renewable biodegradable polymers for food packaging applications are increasingly attracting research interest because of the widespread concerns about the environmental problems caused by conventional plastic food packaging and food waste and the consumers demand for safe, functional, and convenient packaging to respond to their modern lifestyle [1].

Intelligent food packaging systems have the ability to track and record critical parameters for the food quality during transport and storage. One of the most used components in intelligent systems are indicators which can be incorporated into the matrix of the packaging materials and respond to different stimuli usually through a visual change. pH indicators are used in food packaging materials because food spoilage is often accompanied by pH changes, they are generally based on pH-sensitive dyes incorporated into a solid support [2].

One of the most used class of pH-sensitive dyes for pH indicator development are anthocyanins, which have the benefit of being safe and ecofriendly, with antioxidant and antimicrobial properties that make them suitable for active food packaging also [3]. However they have some significant disadvantages: their extraction, separation and purification imply high costs and time-consuming and laborious procedures, their stability and coloring properties are affected by their high sensitivity to degradation by temperature, light, oxygen, pH. To overcome some of these disadvantages bio-inspired synthetic dyes are developed [4].

In this work the synthesis of a new bio-inspired dye which was incorporated in renewable biodegradable polymeric matrices to develop pH indicators for food packaging applications is reported. The synthetic 3-deoxy-anthocyanidin was characterized by UV-Vis, FT-IR, 1D and 2D NMR spectroscopic analysis. An UV-Vis spectroscopy study proved that the dye exhibits halochromic properties that make it suitable as a pH-sensitive dye for pH indicators. The bio-inspired dye was used for the fabrication of intelligent systems based bio-polymers, namely chitosan, PVA and starch. The obtained polymeric films were characterized by FT-IR and UV-Vis spectroscopy. Their response to pH variation in buffer solutions was evaluated and color changes were observed. The pH indicator films were tested on food matrices stored in improper temperature conditions to evaluate their sensitivity to food spoilage, color changes were observed in these cases also.

### Acknowledgements

This work was supported by a grant of the Romanian Ministry of Education and Research, CCCDI - UEFISCDI, project number PN-III-P2-2.1-PED-2019-3037, within PNCDI III, contract number 385PED.

### References

1. N. Bhargava, V. S. Sharanagat, R. S. Mor, K. Kumar, *Trends in Food Sci Technol* 105, 385 (2020)
2. H. Cheng, H. Xu, D.J. McClements, L. Chen, A. Jiao, Y. Tian, M. Miao, Z. Jin, *Food Chem.* 375, 131738 (2022).
3. H. Yong, J. Liu, *Food Packag. Shelf* 26, 100550 (2020).
4. I. Păușescu, A. Todea, V. Badea, F. Peter, M. Medeleanu, I. Ledetî, G. Vlase, T. Vlase, *J Therm. Anal. Calorim.* 141, 999 (2020)

## Thermally insulating air- and ice-templated plant-based foams

Carina Schiele, Tamara L. Church, Lennart Bergström\*

Department of Materials and Environmental Chemistry, Stockholm University, Stockholm, 10691 Sweden

\*lennart.bergstrom@mmk.su.se

Applying renewable materials for efficient thermal insulation can both reduce the carbon footprint and lower the energy demand of buildings. Anisotropic nanocellulose-based foams can display a lower thermal conductivity than air ( $\sim 26.2 \text{ mW m}^{-1} \text{ K}^{-1}$ ) but the mechanical strength is sometimes low. (1) In this study, air- and ice templated plant-based hierarchical foams (AIT<sub>CNF-MC-TA</sub>) were produced by directionally freezing an aqueous foam consisting of: cellulose nanofibrils (CNF), methylcellulose, and tannic acid. The foams displayed a high stiffness both along and perpendicular to the ice-templating direction: this foam was indeed as stiff as nanocellulose–clay composites along the ice-templating direction. (2) The AIT<sub>CNF-MC-TA</sub> foams are superinsulating, i.e. displayed a thermal conductivity of  $\lambda_r < 25 \text{ mW m}^{-1} \text{ K}^{-1}$  for a relative humidity (RH) up to 65%, and the thermal conductivity was maintained at  $\lambda_r < 30 \text{ mW m}^{-1} \text{ K}^{-1}$  at 80% RH perpendicular to the ice-templating direction.

This work shows how the combination of two practical techniques, wet foaming and directional freezing can be used to produce a low-density anisotropic material that is plant-based, stiff and thermally insulating. The manufacturing strategy could be applied to other foam-forming aqueous systems.

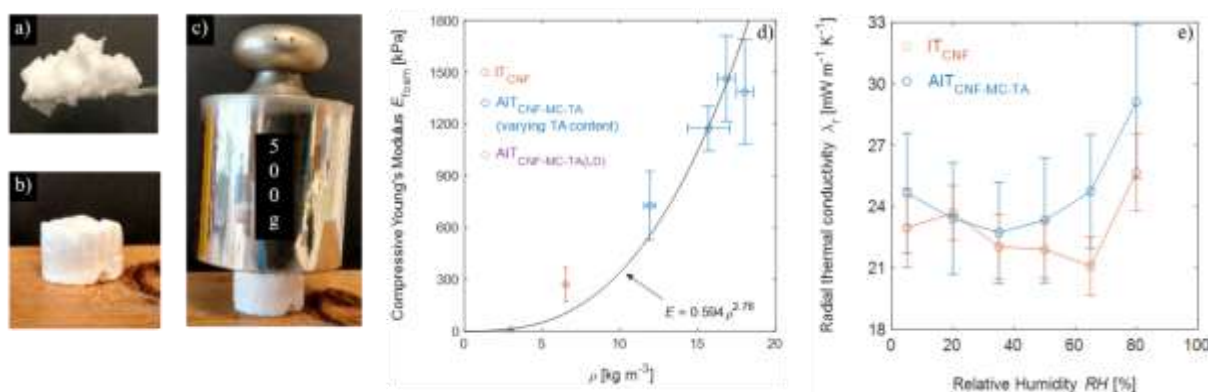


Figure 60: Properties of the air and ice templated foam. Digital photos of AIT<sub>CNF-MC-TA</sub> as a) wet foam b) dried foam c) dried foam with a mass of 72.3 mg carrying a weight of 500 g. d) Compressive Young's modulus as a function of density of the ice templated CNF foam (IT<sub>CNF</sub>) and AIT<sub>CNF-MC-TA</sub> along the direction of ice growth. e) Radial thermal conductivity  $\lambda_r$  of IT<sub>CNF</sub> and AIT<sub>CNF-MC-TA</sub> foams as functions of relative humidity.

### Acknowledgements

The authors acknowledge the ForestValue program, European Commission, and financial support from Vinnova, the Swedish Energy Agency and Formas for the StrongComposite project (2018-04979), as well as funding from the Swedish Energy Agency (Energimyndigheten, project 2019-006749).

### References

1. Apostolopoulou-Kalkavoura V, Munier P, Bergström L. Thermally Insulating Nanocellulose-Based Materials. *Adv Mater.* 2020;2001839.
2. Wicklein B, Kocjan A, Salazar-Alvarez G, Carosio F, Camino G, Antonietti M, et al. Thermally insulating and fire-retardant lightweight anisotropic foams based on nanocellulose and graphene oxide. *Nat Nanotechnol.* 2015;10(3):277–83.



## Synthesis and characterization of poly(lactic acid)/poly(ethylene adipate) copolymers for paclitaxel controlled delivery

Alexandra Zamboulis<sup>1\*</sup>, Evi Christodoulou<sup>1</sup>, Konstantinos Tsachouridis<sup>1</sup>, Dimitrios N. Bikiaris<sup>1</sup>

<sup>1</sup>Laboratory of Polymer Chemistry and Technology, Department of Chemistry, Aristotle University of Thessaloniki, Thessaloniki, Greece

\*azampouli@chem.auth.gr

Controlled drug delivery is a blooming field, promising to improve the efficacy of pharmaceutical treatments and alleviate their secondary effects, while decreasing the administration frequency. Owing to their good compatibility, aliphatic polyesters have attracted much attention in the biomedical field. Among them, poly(lactic acid) (PLA) and poly(lactic-co-glycolic acid) (PLGA) stand out and have already been approved by the FDA for use in several biomedical commercial products. Besides biocompatibility, biodegradability is an important criterion to select a polymer for drug delivery. Indeed, biodegradability is a crucial issue, as the accumulation of the polymeric carrier in the body can pose significant health risks. PLA is a linear biodegradable aliphatic polyester that can be derived from renewable biological resources such as rice and wheat through fermentation and polymerization. Despite the good biocompatibility of PLA, its slow biodegradability is a significant drawback, limiting its application for drug delivery.

In the present study, PLA/poly(ethylene adipate) (PEAd) copolymers were prepared to modulate PLA biodegradability. PEAd polyesters were synthesized by bulk polycondensation and two PLA/PEAd copolymers with different ratios were further prepared *via* reactive melt mixing. The copolymers were structurally characterized by infra-red and nuclear magnetic spectroscopy. The impact of the PLA/PEAd ratio on the enzymic hydrolysis of the newly synthesized copolymers was studied, while their cytocompatibility was also assessed. Finally, nanoparticles were further prepared to evaluate the performance of the PLA/PEAd copolymers in the delivery of paclitaxel. Smooth spherical nanoparticles were obtained via oil/water emulsification/solvent evaporation method, and the *in vitro* dissolution analysis of the paclitaxel-loaded nanoparticles showed a biphasic release of paclitaxel, dependent on the PLA/PEAd ratio of the copolymers.

### Acknowledgements

The authors wish to acknowledge co-funding of this research by European Union-European Regional Development Fund and Greek Ministry of Education, Research and Religions/EYDE-ETAK through program EPANAK 2014-2020/Action "EREVNO-DIMIOURGO-KAINOTOMO" (project T2EAK-00501).

Waste recycle and valorization –  
Circular economy (food waste,  
hazardous waste, municipal waste,  
plastic waste)

## Effect of a compatibilizer on the structural and mechanical properties of recycled HDPE/hemp composite materials

Nina Maria Ainali<sup>1</sup>, Eleftheria Xanthopoulou<sup>1</sup>, Georgia Michailidou<sup>1</sup>, Iouliana Chrysafi<sup>2</sup>, Alexandra Zamboulis<sup>1</sup>, Dimitrios N. Bikiaris<sup>1\*</sup>

<sup>1</sup> Department of Chemistry, Laboratory of Polymer Chemistry and Technology, Aristotle University of Thessaloniki, GR-541 24 Thessaloniki, Greece; [ainali.nina@gmail.com](mailto:ainali.nina@gmail.com)

<sup>2</sup> School of Physics, Aristotle University of Thessaloniki, GR-541 24 Thessaloniki, Greece

\* [ainali.nina@gmail.com](mailto:ainali.nina@gmail.com); [dbic@chem.auth.gr](mailto:dbic@chem.auth.gr)

High-density polyethylene (HDPE) is one of the most common-used synthetic polymers covering a wide spectrum of applications (e.g. packaging, piping, construction, fabrics, toys, etc.), due to its numerous advantages, such as its low cost, light weight, easy processing, high mechanical resistance, and durability. Nevertheless, the poor degradability of synthetic polymers in the natural habitats, in combination with the inadequate waste management, provokes their accumulation in the environment and especially in the marine ecosystems, leading to environmental pollution. As for the available literature data, approximately 13 Mts of these plastics end up in oceans, where they degrade further into smaller plastic particles under the action of several environmental stresses, called microplastics (plastic items with diameters  $\leq 5$ mm), which are characterized today as emerging contaminants. These microplastics, pose threat to aquatic and land-living organisms, whereas their consumption through the trophic chain and their effects on human health are still under severe examination. Nowadays, concentrated efforts toward the development of more eco-friendly materials and treatment processes have already been launched. In this framework, the recycling of HDPE and the exploitation of recycled HDPE (r-HDPE) has been a spot of great interest. Hemp fiber is one of the dominant classes of bast natural fibers, commonly derived from the hemp plant with the species of *Cannabis*. The common features of natural fibers along with the inherent mechanical, thermal, and acoustic properties of hemp fibers make them beneficial components for reinforcements in polymer composite materials.

In the present study, in order to exploit the use of r-HDPE and investigate the potential hemp fibers for its reinforcement, four composite materials with different filler concentrations (10-75 %wt. in hemp) using 1% wt. polypropylene-g-maleic anhydride as compatibilizer were prepared via melt-mixing. The structural properties of the r-HDPE/hemp composites were investigated using infra-red spectroscopy (ATR) and X-ray diffraction (XRD), while the dispersion of the fibers was examined with the implementation of stereomicroscopy and scanning electron microscopy (SEM). Finally, as the mechanical properties affect the final application of the materials, tensile and impact strength experiments were performed.

### Acknowledgements

This research has been co-financed by the European Union and Greek national funds through the Operational Program Competitiveness, Entrepreneurship and Innovation, under the call RESEARCH-CREATE-INNOVATE (project code: T2EDK – 00008).

## Laccases catalyzed dephenolization of raw wine lees and wine lees extract

Panagiotis E. Athanasiou, Michaela Patila, Angelos Papanikolaou, Theodora Bompotsiari, Angeliki C. Polydera, and Haralambos Stamatis\*

Laboratory of Biotechnology, Department of Biological Applications and Technologies, University of Ioannina, Ioannina, Greece

\*Corresponding author: hstamati@uoi.gr

### Abstract

Wine lees are one of the most common by-products of wine industry. They are defined as the remaining residues at the bottom of wine barrels during storage or ageing, and consist of a liquid and a solid fraction [1], [2]. Wine lees are mainly containing dead yeast cells, carbohydrates, proteins, inorganic and organic compounds, tartaric acid and high amount of phenolic compounds [1], [3]. Moreover, the low pH values, the high levels of biochemical and chemical oxygen demand (BOD & COD), and the high content of phenolic compounds make this by-product an environmental pollutant [4]. There are several methods that have been developed for phenol removal, like extraction, biological treatment, or use of adsorbents [5]. The enzymatic treatment of industry by-products has gained great interest as an environmentally friendly procedure. Oxidoreductases, such as, laccases can be used for wastewater treatment through oxidation of a variety of organic compounds, leading to their degradation and/or polymerization [5], [6]. Laccases are multi-copper oxidases that catalyze the one electron oxidation of a variety of substrates coupled with the reduction of molecular oxygen to water [6].

In the current study, ethanolic extract of red wine lees was prepared and the total phenolic content (TPC) was evaluated by the Folin–Ciocalteu assay. A variety of laccases, such as laccase from *Trametes versicolor* (TvL) and *Aspergillus sp.*, were used for the enzymatic treatment of the polyphenol extract, as well as, for the treatment of the raw wine lees. The remaining phenolic content was measured after the treatment, and the decrease of the TPC was expressed as dephenolization yield.

The early findings of the current study showed that several commercial laccases were able to efficiently catalyze the phenol removal of wine lees extract and raw wine lees.

### Methods

Red wine lees (WL) were provided by a winery located at regional unit of Ioannina, Epirus, Greece. Laccases from *Trametes versicolor* (TvL), *Rhus vernicifera* (RvL) and *Aspergillus sp.* (AsL), and Folin Ciocalteu reagent were purchased from Sigma-Aldrich. *White rot fungi* laccase (WrfL) was purchased from Creative enzymes and laccases Novozym 51003 and Suberose, were kindly provided by Novozymes. Histanol 70 (70% ethanol) was purchased from Biognost.

In order to prepare the wine lees extract (WLE), WL were centrifuged at 9,500 rpm for 10 min. The precipitate of the WL (40 g) was placed in a round bottom flask (250 mL) containing a 70% ethanol solution (200 mL) (solid to solvent ratio, 1:5), and placed for 20 min into a sonication bath. The sample was then centrifuged at 9,500 rpm for 10 min. The supernatant was filtered through a simple filter paper, rot evaporated to remove ethanol, and finally freeze-dried to remove water.

The enzymatic treatment of WLE, was carried out in 1 mL buffer solution, containing 2.5 mg of dry WLE and a certain amount of laccase, and the mixture was incubated at 30°C and 140 rpm, for 24 h. A same procedure was carried out for the enzymatic treatment of WL, but in this case, the reaction was performed in 1 mL of raw WL, instead of buffer solution. The TPC of WL and WLE before and after enzymatic treatment was determined by Folin Ciocalteu assay with some modifications [4].

### Results

Laccases from different origin were used for the dephenolization of WL and WLE. For the WL treatment, preliminary results showed that TvL and AsL were able to remove 41 and 5%, respectively, of the TPC of the raw wine lees. The results regarding the dephenolization of WLE are presented in Table 1. As it can be seen, most of the laccases that were used, were able to efficiently reduce the TPC of WLE. The highest dephenolization yield was achieved by TvL at 72%, while WrfL, Novozym 51003 and AsL were also able to catalyze the reduction of TPC in a high extent. On the contrary, it was shown that RvL and Suberose were not able to catalyze the dephenolization of WLE.

Table 1. Dephenolization capacity of different laccases on WLE.

Laccase	Dephenolization yield of WLE (%)
<i>TyL</i>	72
<i>Rhus vernicifera</i>	0
<i>Aspergillus sp.</i>	64
<i>Suberose</i>	9
<i>White rot fungi</i>	56
<i>Novozym51003</i>	65

## Conclusions

The present study reports the ability of different kind of laccase to catalyze the removal of the total phenolic content in raw wine lees, as well as, wine lees extracts. The results showed that the enzymatic treatment reduces the phenolic content in most cases, indicating that this procedure can be effectively applied in waste-treatment applications.

## Acknowledgements

This work is co-financed by the European Union (European Regional Development Fund) and National Resources, under the operational program “Competitiveness, Entrepreneurship and Innovation (EPAnEK)”, “NSRF 2014–2020”, Call 111: “Support for Regional Excellence” (project:MIS 5047215).

## References

- [1] M. J. Jara-Palacios, “Wine Lees as a Source of Antioxidant Compounds,” *Antioxidants*, vol. 8, no. 2, p. 45, Feb. 2019, doi: 10.3390/antiox8020045.
- [2] P. Sancho-Galán, A. Amores-Arrocha, A. Jiménez-Cantizano, and V. Palacios, “Physicochemical and nutritional characterization of winemaking lees: A new food ingredient,” *Agronomy*, vol. 10, no. 7, p. 996, Jul. 2020, doi: 10.3390/agronomy10070996.
- [3] Y. Tao, D. Wu, Q. A. Zhang, and D. W. Sun, “Ultrasound-assisted extraction of phenolics from wine lees: Modeling, optimization and stability of extracts during storage,” *Ultrason. Sonochem.*, vol. 21, no. 2, pp. 706–715, Mar. 2014, doi: 10.1016/j.ultsonch.2013.09.005.
- [4] Y. Zhijing, A. Shavandi, R. Harrison, and A. E.-D. Bekhit, “Characterization of Phenolic Compounds in Wine Lees,” *Antioxidants*, vol. 7, no. 4, p. 48, Mar. 2018, doi: 10.3390/antiox7040048.
- [5] J. Liu *et al.*, “Immobilization of laccase by 3D bioprinting and its application in the biodegradation of phenolic compounds,” *Int. J. Biol. Macromol.*, vol. 164, pp. 518–525, Dec. 2020, doi: 10.1016/j.ijbiomac.2020.07.144.
- [6] M. Patila *et al.*, “Immobilization of Laccase on Hybrid Super-Structured Nanomaterials for the Decolorization of Phenolic Dyes,” *Processes*, vol. 10, no. 2, 2022, doi: 10.3390/pr10020233.

## Laccase production using wine lees by submerged cultivation of *Pleurotus ostreatus*

Georgios Bakratsas, Kyriakos Antoniadis, Panagiotis E. Athanasiou, Angeliki C. Polydera, Petros Katapodis\*, Haralambos Stamatis\*

Biotechnology Laboratory, Department of Biological Applications and Technologies, University of Ioannina, 45110 Ioannina, Greece

\*Corresponding authors E-mail: hstamati@uoi.gr, Tel +30 26510 07116, pkatapo@uoi.gr Tel +30-2651007212

Laccases (EC 1.10.3.2) are multi-copper polyphenol oxidases that can be used for several biotechnological applications due to their high catalytic activity toward a broad range of aromatic substrates. *Pleurotus ostreatus*, one of the most cultivated fungi species in the world, belongs to a subclass of lignin-degrading microorganisms with a decoded genome that contains a laccase multi-gene family and could be characterized as a biotechnological model for the production of laccase[2,3]. Submerged cultivation of mushrooms is a method for rapid production of industrial enzymes. Different growth media and culture conditions could affect laccase production by mushroom mycelia [1].

Wine lees are wine industry wastewaters that are collected after the end of the fermentation, contain dead yeasts, grape skins, seed stems and are rich in phenolic compounds such as tartaric acid. Laccase induction using wine lees by submerged cultivation of fungi is something that is not been extensively studied until now[4].

In this study, we examined the effect of adding wine lees to the growth medium on laccase production by *Pleurotus ostreatus* strain. Different culture conditions, such as cultivation's initial pH, wine lees concentration, carbon, and nitrogen sources, on laccase production, were studied. Laccase activity, residual sugars, phenolic compounds consumption and decolorization were measured at various time intervals during fermentation.

According to the results, wine lees are a promising inducer for laccase production in contrast to a glucose basal medium by submerged cultivation of *Pleurotus ostreatus*. After the optimization of cultivation conditions, laccase production reached more than 70.000 Units/L. In addition, phenolic compounds consumption and decolorization reached a value up to 90%. In conclusion, a bioprocess using wastewater to produce a high-value enzyme used by industry could contribute to circular economy that is crucial nowadays.

### Acknowledgements

This work is co-financed by the European Union (European Regional Development Fund) and National Resources, under the operational program “Competitiveness, Entrepreneurship and Innovation (EPAnEK)”, “NSRF 2014–2020”, Call 111: “Support for Regional Excellence” (project:MIS 5047215)

### References

1. Papadaki, V. Kachrimanidou, S. Papanikolaou, A. Philippoussis, P. Diamantopoulou, *Microorganisms*,7, (2019)
2. G. Bakratsas, A. Polydera, P. Katapodis, H. Stamatis, *Future Foods*, **4**, 100086 (2021)
3. D. Dur, D. Suspes, E. Maestre, M. Alfaro, G. Perez, A.G. Pisabarro, *Journal of Fungi*, **8**, 7 (2022)
4. P.J. Strong, J.E Burgess, *Bioresource Technology* **99**, 6134–6142, (2008)

## Lab-scale production of grid-grade biomethane via supercritical water gasification of biowastes and sequential gas phase conversion according to a catalytic tandem approach

F. F. Frusteri, C. Cannilla, G. Giacoppo, S. Todaro, A. Cajumi and G. Bonura\*

CNR-ITAE, Via S. Lucia sopra Contesse 5, 98126, Messina, Italy

\*giuseppe.bonura@itae.cnr.it

Agricultural production and agro-food industry generate not only solid residues but also large volume of liquid wastes, severely determining pollution problems if not properly managed or treated. Indeed, the large amount of organics contained in the wastewaters can really represent a “fresh” energy resource suitable to be upgraded to alternative fuels, according to a bio-refinery approach [1]. Gasification in condition of supercritical water (SCWG) has received in the last years particular attention since it could offer the possibility to treat aqueous streams containing organic compounds without any preliminary expensive pre-treatment (*i.e.*, drying). Depending on the reaction conditions, a CH<sub>4</sub>-rich stream can be produced, which can undergo a sequential methanation step to deliver a grid-grade CH<sub>4</sub> stream, compatible with the injection in pipelines for energy purposes.

In this work, a catalytic process based on supercritical gasification of aqueous organic solutions coupled with a sequential methanation reactor is proposed. Preliminary experiments in SCWG were carried out by using acetone and cyclohexane as model molecules representative of some organic components, in order to investigate how activity and selectivity of the investigated catalysts could be changed as a function of the organic substrate employed. Regarding the solid catalyst, the identification of the key gasification features was made by considering the need of favoring the achievement of equilibrium for the water gas shift reaction and the hydrogenation of CO and CO<sub>2</sub> to CH<sub>4</sub> [2,3]. On this account, metal-supported catalysts were considered as suitable systems for the SCWG process, able to deliver high conversion level of organic compounds at relatively low temperature [2,3]. As regards the methanation reaction, recently a renewed attention has been paid in an attempt to develop new, more active and more stable catalytic systems. Indeed, methanation is an exothermic reaction because of the presence of carbon oxides in the feed gas [4,5]. So, the heat of reaction can induce metal sintering, which lowers the overall metal surface area and thus leads to poor activity. Moreover, catalytic deactivation can also occur through coking, which blocks the metal surface due to accumulated carbon [5]. Therefore, developing an efficient, low-temperature methanation catalyst with high thermal stability and coke resistance is necessary.

A customized 200 mL batch reactor Inconel 625 was used during SCWG experiments maintaining the catalyst fixed in a basket. The reactor was provided with valves for draining the liquid phase from the bottom, while sampling the gas phase at the end of reaction through a 1000 mL stainless steel tank AISI 316L. A 3-way valve located on the top of the vessel was used for introducing H<sub>2</sub> into the autoclave, as a sweep gas or catalyst pre-treatment prior to the run. The reactor was first fed with water and heated at supercritical temperature (374 °C); afterwards, organic model molecules (*i.e.*, acetone or cyclohexane) were quickly pumped (in 3 min) and the end of charging was considered as the starting time of reaction. Reaction was stopped after 20 min and the reactor was cooled down to room temperature by an ice bath. On the basis of the residual reactor pressure, the gas phase was transferred in the stainless-steel tank, in order to store the reaction stream for GC analysis. The liquid phase was drained from the bottom of the reactor and analysed.

The methanation runs were carried out in a micro-laboratory plant operating at atmospheric pressure, entirely realized in stainless steel AISI 316 and equipped with a tubular fixed bed reactor (*i.d.*, 6 mm; *l.*, 200 mm). The reaction stream was on-line analyzed by using the same GC apparatus for gaseous mixtures from SCWG. The catalytic tests were carried out under the following operating conditions: a) activation procedure in-situ at 500 °C for 1 h under pure H<sub>2</sub> fed at a space velocity of 22,000 ml<sub>N</sub>/g<sub>cat</sub>/h; b) catalytic testing at atmospheric pressure in the temperature range 200-350 °C and space velocity of 12,000 ml<sub>N</sub>/g<sub>cat</sub>/h, using two simulated mixtures at different H<sub>2</sub>/CO<sub>2</sub> volume ratios:

1. H<sub>2</sub>/CO<sub>2</sub>/CH<sub>4</sub> (10/40/50);
2. H<sub>2</sub>/CO<sub>2</sub>/CH<sub>4</sub> (20/30/50).

To perform the catalytic tests in both the experimental devices, a series of differently loaded Ru and Ni systems differently supported were used (see Table 1).

Table 1. Physico-chemical properties of the investigated SCWG and methanation catalysts.

SAMPLE	Metal loading <sup>[a]</sup> (wt%)	S <sub>ABET</sub> (m <sup>2</sup> /g)	MSA <sup>[b]</sup> (m <sup>2</sup> /g)	D <sub>Me</sub> <sup>[b]</sup> (%)	d <sub>Me</sub> <sup>[b]</sup> (nm)
1Ru/Al <sub>2</sub> O <sub>3</sub>	0.9	150	1.4	41.7	3
5Ru/Al <sub>2</sub> O <sub>3</sub>	4.7	100	3.1	16.8	8
15Ni/Al <sub>2</sub> O <sub>3</sub>	15.2	45	7.9	7.9	13
60Ni/Al <sub>2</sub> O <sub>3</sub>	60.1	198	28.0	7.5	14
Ni/MgO	48.0	31	18.1	11.9	9
Ni/HT	70.0	130	30.1	6.4	16

<sup>[a]</sup> From XRF analysis  
<sup>[b]</sup> From TPD measurements

In Figure 1 the catalytic behaviour of “noble” and “non-noble” metals has been compared under supercritical water gasification of acetone.

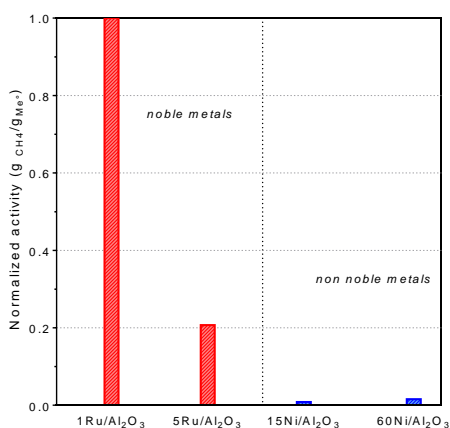


Figure 1. Relative activity during SCWG of acetone (acetone: 7.14 vol%; reaction time: 20 min;  $R_{cat/org}$ : 0.3 wt/wt).

The results obtained clearly demonstrate that, with an appropriate catalyst, the gasification of diluted organic solutions allows to obtain an outlet stream containing about 50% CH<sub>4</sub> / 40% CO<sub>2</sub> / 10% H<sub>2</sub>. In particular, what emerged is that the specific activity of Ru in the formation of methane was significantly higher than Ni, notwithstanding MSA values of the Ni/Al<sub>2</sub>O<sub>3</sub> samples significantly higher than Ru/Al<sub>2</sub>O<sub>3</sub> catalysts.

On the contrary, during methanation runs the Ni-based catalysts exhibited a superior behaviour than Ru catalysts in the entire temperature range investigated (225-350 °C). In particular, the Ni catalysts showed the maximum H<sub>2</sub> conversion (88-95%) at 275 °C, while at the same temperature the 1% Ru/Al<sub>2</sub>O<sub>3</sub> reached a conversion close to 20%. In Figure 2 some methanation results obtained over Ni catalysts in terms of H<sub>2</sub>/(H<sub>2</sub>+CH<sub>4</sub>) ratio are shown.

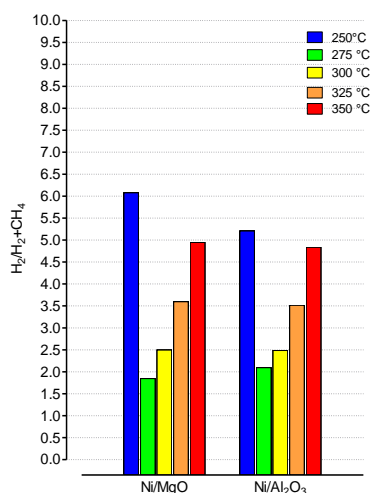


Fig. 2. Catalytic behavior of the Ni catalysts during methanation ( $P_R = 1$  atm; GHSV: 12,000 mlN/g<sub>cat</sub>/h; feed: H<sub>2</sub>/CO<sub>2</sub>/CH<sub>4</sub> (20/30/50 vol%).

Despite a Ni loading lower than Ni/Al<sub>2</sub>O<sub>3</sub>, Ni/MgO allowed to obtain mixtures richer in CH<sub>4</sub> even from streams with higher concentrations of H<sub>2</sub>, reaching a final H<sub>2</sub>/(H<sub>2</sub>+CH<sub>4</sub>) ratio less than 2 vol.%, clearly suggests that reaction is also affected by the metal carrier.



On the whole, these results demonstrate the feasibility of a two-step process based on gasification in supercritical phase of aqueous organic residues followed by selective conversion of the gas phase in grid-grade biomethane. In particular, using a Ru-based catalyst, a mixture containing 10% by volume of organic residues (alcohols, ketones, cyclic organics, etc...) can be converted into a gaseous stream containing approximately 60% CH<sub>4</sub>/30% CO<sub>2</sub>/10% H<sub>2</sub>. In the subsequent methanation step, using a Ni-based catalyst, it is possible to minimize the hydrogen concentration to get a CH<sub>4</sub>-rich mixture usable for energy purposes.

## References

1. A. Molino, S. De Gisi, L. Petta, A. Franzese, P. Casella, T. Marino, M. Notarnicola, *Chem. Eng. J.*, **370** 1101 (2019).
2. G. Salierno, F. Marinelli, B. Likozar, N. Ghavami, C. De Blasio, *Int. J. Heat Mass Tran.*, **183** 122200 (2022).
3. F. Frusteri, L. Frusteri, F. Costa, A. Mezzapica, C. Cannilla, G. Bonura, *Appl. Catal. A*, **545C** 24 (2017).
4. Z. Uddin, B.-Y. Yu, H.-Y. Lee, *J. CO<sub>2</sub> Util.*, **60** 101974 (2022).
5. C. Jeong-Potter, A. Porta, R. Matarrese, C.G. Visconti, L. Lietti, R. Farrauto, *Appl. Catal. B*, **310** 121294 (2022).

## Modified cross-linked pectin hydro-films for biomedical applications

Arkasubhro Chatterjee<sup>1,3\*</sup>, Antonio Patti<sup>2</sup>, Phil Andrews<sup>2</sup>, Amit Arora<sup>1,3</sup>

<sup>1</sup>IITB – Monash Research Academy, Indian Institute of Technology, Bombay, Powai, Mumbai 400076, India; <sup>2</sup>School of Chemistry, Monash University, Clayton, Victoria 3800, Australia ;<sup>3</sup>Centre for Technology Alternatives for Rural Areas (CTARA), Indian Institute of Technology, Bombay, Powai, Mumbai 400076

\*arkasubhro.chatterjee@monash.edu

**Background:** The global production of fresh fruit for the year 2021 was estimated to be around 870 million metric tons<sup>1</sup>. Approximately 20% of the total fruit produced are wasted due to post harvest losses<sup>2</sup>. Furthermore, processing of fruits by food industries generates a significant amount of waste as well, amounting to about 25-30% of the total product<sup>3</sup>. At the same time, there is a growing need for versatile, robust polymer-based hydrogels for applications in drug delivery, food preservation, biological implants etc<sup>4,5</sup>. in the current food and pharmaceutical industry. Pectin, a natural bio-polymer is a significant component in this waste, particularly in fruits. Pectin is a very viable component that could serve the growing need for versatile, robust polymer-based hydrogels for applications in drug delivery, food preservation and biological implants<sup>4,5</sup>. thus providing viable solutions for addressing the dual problem of food wastage and preservation<sup>6</sup>.

**Rationale:** Pectin is a natural polysaccharide derived from fruit peels that has been used extensively as a thickening agent for jams and jellies<sup>7</sup>. While it is able to dissolve in water and form hydro-films upon drying, the films themselves are of poor quality with low tensile strength. In order to improve the physico-chemical characteristics of the films, the pectin films were modified by blending with a complementary bio-polymer, carboxymethyl cellulose and a polyethylene glycol based cross-linker. The current work is aimed at using green approaches in the fabrication biodegradable pectin films from renewable fruit waste feedstocks for various applications. xxx

**Experimental:** Pectin from citrus peels (galacturonic acid content 84%) was obtained from Sigma Aldrich and combined with the sodium salt of carboxy methyl cellulose (Na CMC) and polyethylene glycol diglycidyl ether (PEGDE) obtained from Loba Chemie. Hydro films were prepared by mixing the components in water overnight. Three different pectin: CMC ratios were fabricated and characterized for a number of parameters such as solubility, Tensile strength and IR Spectral characteristics.



Image 1: Behavior of modified pectin films in water

**Results:** Depending upon ratio of polymers, the properties of the films were significantly different. The use of CMC and cross-linker led to the formation of films that were insoluble in water due to the high molecular weight of the polymer complex formed. This was also evident in the tensile strength of the films which were higher than that of standard pectin only films.



Image 2: Tensile strength of different pectin films tested.

**Conclusions:** A novel polymeric matrix with a unique cross-linked system was fabricated using green methods. The properties of the system are tunable based on the ratio of polymers used and could thus, have various potential application in diverse fields such as drug delivery, wound healing and active anti-microbial packaging.

**Acknowledgements:** The authors would like to thank the IITB-Monash Research Academy for funding this research.

### References:

1. STATISTICAL YEARBOOK WORLD FOOD AND AGRICULTURE 2021. <https://www.fao.org/3/cb4477en/online/cb4477en.html> doi:10.4060/CB4477EN.
2. Sm, Y. & Ay, M. Review of Post-Harvest Losses of Fruits and Vegetables. *Biomed. J. Sci. Tech. Res.* **13**, 001–009 (2019).
3. Kumar, H. *et al.* Fruit and Vegetable Peels: Utilization of High Value Horticultural Waste in Novel Industrial Applications. *Molecules* **25**, 2812 (2020).
4. Tang, X. Z., Kumar, P., Alavi, S. & Sandeep, K. P. Recent Advances in Biopolymers and Biopolymer-Based Nanocomposites for Food Packaging Materials. *Crit. Rev. Food Sci. Nutr.* **52**, 426–442 (2012).
5. Muir, V. G. & Burdick, J. A. Chemically Modified Biopolymers for the Formation of Biomedical Hydrogels. *Chem. Rev.* **121**, 10908–10949 (2021).
6. Mellinas, C., Ramos, M., Jiménez, A. & Garrigós, M. C. Recent Trends in the Use of Pectin from Agro-Waste Residues as a Natural-Based Biopolymer for Food Packaging Applications. *Materials* **13**, 673 (2020).
7. Chen, J. *et al.* Pectin Modifications: A Review. *Crit. Rev. Food Sci. Nutr.* **55**, 1684–1698 (2015).

## Optimization of enzymatic hydrolysis for utilization of food waste

Lisanne Krail, Tanmay Chaturvedi<sup>1\*</sup>, Eva Mie Lang Spedtsberg<sup>1</sup>, Jakob Lykke Stein<sup>1</sup> and Mette H. Thomsen<sup>1</sup>

<sup>1</sup>AAU Energy, Aalborg University, Niels Bohrs Vej 8 6700 Esbjerg, Denmark

\*tac@energy.aau.dk

Abstract text:

The generation and accumulation of municipal solid waste (MSW) is one of the fastest growing environmental problems worldwide [1]. MSW is produced in large quantities, it is one of the least exploited sources of lignocellulosic biomass [2]. In a circular economy the organic fraction of municipal solid waste (OFMSW), which accounts for nearly half of MSW [3], is used as a resource to produce secondary products such as biofuels. The main components of biomass that can be used for biofuel production are sugars (starches, simple sugars, and lignocelluloses) and lipids. These components are present in the OFMSW such as food waste (FW) and can be converted by hydrolysis to release smaller monomeric sugar compounds such as glucose, xylose, and arabinose.

To improve the utilization of FW, which accounts for 90 percent of the Danish OFMSW [4], the optimization of enzymatic hydrolysis was investigated, focusing on the enzyme combination and addition modes of two enzyme complexes (Cellic<sup>®</sup> CTec3 HS - cellulase and hemicellulase complex & AMG 300L - glucoamylase complex) which are shown in Table 1. Various experiments were performed to characterize the FW after performing enzymatic hydrolysis at 50°C for 24 hours. The characterization included performing strong acid on the solid fraction as well as weak acid hydrolysis and free sugar analysis on the liquid fraction of the food waste. Furthermore, the Klason lignin and the free acids content was determined.

Table 1. Enzyme combinations and addition modes of the performed enzymatic hydrolysis experiments

	Exp. 1	Exp. 2	Exp. 3	Exp. 4	Exp.5
CTec3	x		x	x (first)	x (second)
AMG 300L		x	x	x (second)	x (first)

The analysis showed a high sugar content in the raw FW (82g/ 100g dry matter), with a greater proportion in the solid fraction. After enzymatic hydrolysis with several enzyme combinations and addition modes of CTec3 and AMG 300L, differences in the sugar content were observed in the liquid and solid fraction, resulting in different enzymatic hydrolysis yields (see Figure 1). The analysis showed that the addition of CTec3 alone is the least efficient, while the enzyme combination of CTec3 and AMG 300L releases the largest amount of monomers that entered the liquid fraction. This indicates that this enzyme combination is the most optimal. However, due to the high starch content in the FW, the slightly less efficient enzyme combination AMG 300L could be chosen from an economical point of view.

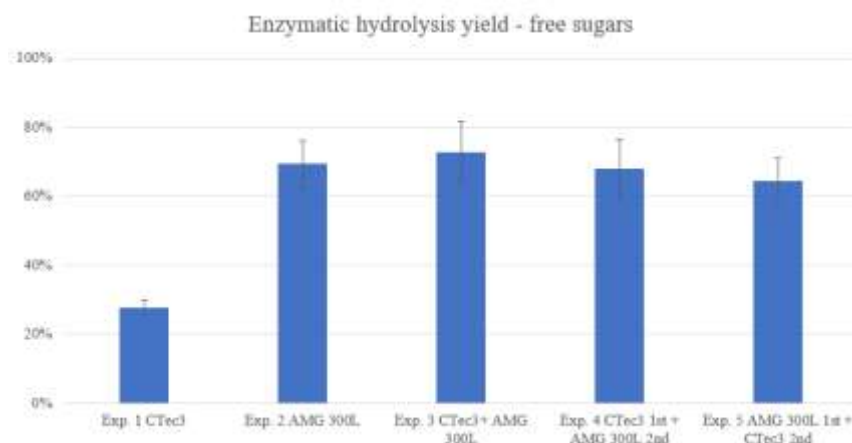


Figure 1. Diagram showing the enzymatic hydrolysis yield for all free sugars for the 5 different conducted experiments

### Acknowledgements

This project has received funding from the European Union's Horizon 2020 research and innovation programme under grant agreement No. 101007130

## References

- [1] A. M. Troschinetz and J. R. Mihelcic, “Sustainable recycling of municipal solid waste in developing countries,” *Waste Manag.*, vol. 29, no. 2, pp. 915–923, Feb. 2009, doi: 10.1016/J.WASMAN.2008.04.016.
- [2] J. W. Jensen, C. Felby, H. Jørgensen, G. Ø. Rønsch, and N. D. Nørholm, “Enzymatic processing of municipal solid waste,” *Waste Manag.*, vol. 30, no. 12, pp. 2497–2503, Dec. 2010, doi: 10.1016/J.WASMAN.2010.07.009.
- [3] T. Al Seadi, N. Owen, H. Hellström, and H. Kang, “Source separation of MSW: an overview of the source separation and separate collection of the digestible fraction of household waste, and other similar wastes from municipalities, aimed to be used as feedstock for anaerobic digestion in biogas plants,” *IEA Bioenergy Task 37 Energy from Biogas Rep.*, 2013.
- [4] A. Van der Linden and A. Reichel, “Bio-waste in Europe — turning challenges into opportunities,” 2020.

## Investigation and optimization of heat and enzymatic pretreatments of OFMSW and its combination with beechwood pulp

Stanislav Rudnyckyj<sup>1</sup>, Tanmay Chaturvedi<sup>1\*</sup>, and Mette H. Thomsen<sup>1</sup>

<sup>1</sup>AAU Energy, Aalborg University, Niels Bohrs Vej 8 6700 Esbjerg, Denmark

\*tac@energy.aau.dk

### Abstract text:

With the growing demand for alternative and more sustainable energy sources, biomass-based energy has received a great deal of attention. Promising feedstock OFMSW is currently investigated for bioenergy production as it is a cheap, renewable, abundant source of biomass that has been, to a large extent, unexplored for biotechnological applications compared to other traditional feedstocks. The main challenge for the application of OFMSW as a feedstock is the requirement to combine several preprocessing methods such as mechanical, physical, chemical, and biological in order to release a substantial amount of fermentable biomass components.

The composition of raw OFMSW was examined and found to have high sugar content, corresponding to 52 g of sugars/100 g DM of OFMSW, of which 15,4 g is starch. The starch gelatinization process was investigated at different reaction times and temperatures, and it was discovered that prolonging the reaction time and/or increasing the temperature results in a higher liberation of starch into the liquid fraction. The different heat pretreatment temperatures were investigated on sugar recovery and yield. The condition at 100°C for 4 hours resulted as the most promising one due to the fact that yields for higher temperatures were not statistically significant, and sugar recovery was the highest compared to other temperatures. Further, the composition of beechwood pulp was identified, corresponding to 84 g of glucose/100 g DM of beechwood pulp, and the remaining matter was classified as lignin. Enzymatic hydrolysis was conducted with a high enzymatic dosage of Cellic<sup>®</sup> CTec3 HS (Novozymes) and AMG<sup>®</sup> 300 L BrewQ (Novozymes) on raw OFMSW, beechwood pulp, and their mixtures. Analysis showed that hydrolysis of raw OFMSW and mixtures resulted in 90-100% yields. This brings an opportunity to enzymatically preprocess OFMSW and beechwood pulp together in a single step.

### Materials and methods:

Two methods investigated gelatinization of starch in OFMSW: 1) Iodometry method, which applies iodine reagent to form a colourful iodine-starch complex that can be detected by spectrophotometer; 2) Megazymes Total Starch HK Assay Kit is an enzymatic kit that was used to investigate total and liberated amount of starch in the OFMSW.

Heat pretreatment of OFMSW was further investigated on glucose, xylose, and arabinose content by HPLC. Raw and pretreated materials were separated into liquid and solid fractions by centrifugation. Liquid fractions were directly analyzed on HPLC for free sugar, weak acid, furfural, and HMF content as well as they underwent weak acid hydrolysis (8 w/w % H<sub>2</sub>SO<sub>4</sub>) for HPLC analysis of total sugar content. Solid fractions prior to HPLC analysis were acidly hydrolyzed (72 w/w % H<sub>2</sub>SO<sub>4</sub>) to completely liberate sugars from the majority of fibers.

For enzymatic hydrolysis Cellic<sup>®</sup> CTec3 HS (Novozymes) 6 w/w DM % and AMG<sup>®</sup> 300 L BrewQ (Novozymes) 2 w/w DM % were used on heat pretreated OFMSW, cellulose fraction from beechwood, and their mixtures. Liquid fractions of enzymatically hydrolyzed samples were directly analyzed on HPLC for free sugar, weak acid, furfural, and HMF content as well as they underwent weak acid hydrolysis (8 w/w % H<sub>2</sub>SO<sub>4</sub>) for HPLC analysis of total sugar content. Cellulose fraction from beechwood was hydrolyzed by strong acid (72 w/w % H<sub>2</sub>SO<sub>4</sub>) and examined by HPLC on the total amount of sugars.

Statistical tests such as ANOVA, Tuckey's HSD test, and the MLR model were performed by applying R.

### Key results:

The investigation of starch gelatinization revealed that the amount of liberated starch continuously rises with increasing reaction time (0-4 hours) and temperature (70-130°C). The analysis of heat pretreatment (100-130°C) showed that with increasing reaction temperature, the total sugar recovery decreases due to sugar degradation, but the difference in the total sugar yield was statistically insignificant for all reaction temperatures. The enzymatic hydrolysis of heat pretreated OFMSW, cellulose fraction from beechwood, and their mixtures showed that pretreated OFMSW and mixtures could be successfully hydrolyzed, resulting in 90-100% of the free sugar yield. On the other hand, enzymatic hydrolysis of cellulose fraction from beechwood resulted in lower performance of hydrolysis, corresponding to 50% of the free sugar yield.

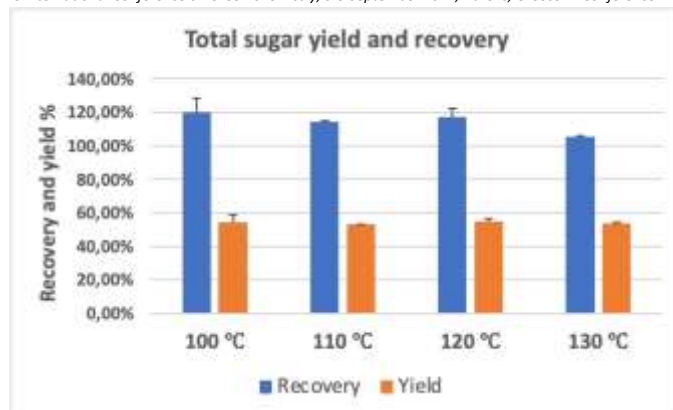


Figure 1. Recovery and yield of sugars, more specifically glucose, xylose, and arabinose, after heat pretreatment of OFMSW. The total sugar recovery is decreasing from 100°C to 130°C but for the total sugar yield there are not significant differences between reaction temperatures.

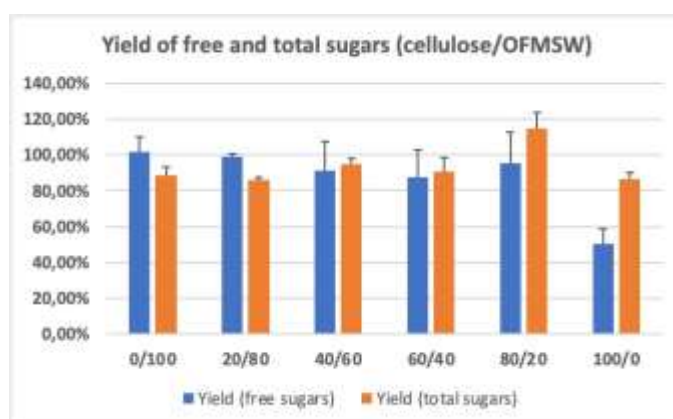


Figure 2. Yields of free and total sugars after enzymatic hydrolysis of heat pretreated OFMSW, cellulose fraction of beechwood, and their mixtures. All sample compositions, except the cellulose fraction of beechwood, showed high yields of 90-100% for the free and total sugar yield. The cellulose fraction of beechwood resulted in a 50% yield for the free sugars and over 80% for the total sugars.

## Acknowledgements

This project has received funding from the European Union's Horizon 2020 research and innovation programme under grant agreement No. 101007130

## Supercritical fluid extraction as a tool to isolate phytochemicals from rice (*Oryza sativa* L.) by-products

João P. Baixinho<sup>1,2</sup>, Andreia Bento-Silva<sup>3,4</sup>, Ana Maria Carvalho Partidário<sup>5</sup>, Maria do Rosário Bronze<sup>1,2,3</sup>,

Naiara Fernández<sup>2\*</sup>

<sup>1</sup>Instituto de Tecnologia Química e Biológica António Xavier, Universidade Nova de Lisboa, Av. da República, 2780-157 Oeiras, Portugal

<sup>2</sup>iBET, Instituto de Biologia Experimental e Tecnológica, Apartado 12, 2781-901 Oeiras, Portugal

<sup>3</sup>Faculdade de Farmácia da Universidade de Lisboa, Av. Prof. Gama Pinto, 1649-003 Lisboa, Portugal

<sup>4</sup>FCT NOVA, Faculdade de Ciências e Tecnologia, Universidade Nova de Lisboa, Campus da Caparica, Caparica, Portugal

<sup>5</sup>Instituto Nacional de Investigação Agrária e Veterinária, I.P., Unidade de Tecnologia e Inovação, Av. da República, Quinta do Marquês, 2780-157 Oeiras, Portugal

\*naiara.fernandez@ibet.pt

Rice production reaches more than 500 Mt annually. It represents 20% of the dietary energy intake of the global population and is the major source of carbohydrates, protein, vitamins, and minerals. Rice bran is an important byproduct of the rice milling industry and it is gaining attention due to its nutrient-rich composition, easy availability, low cost, and promising health benefits. Several bioactive components have shown antioxidant, anti-inflammatory, anti-cholesterolemic, anti-diabetic, anti-cancer activities and heart-related health benefits.<sup>1-4</sup>

We present an efficient supercritical fluid extraction (SFE) process to obtain bioactive phytochemicals from rice industry by-products (Figure 1). The effect of different process parameters on the extraction performance (extraction yield and chemical composition) were evaluated and optimized, including operating temperature and pressure, in order to maximize the extraction of high valued nutritional compounds (such as  $\gamma$ -oryzanol and fatty acids).

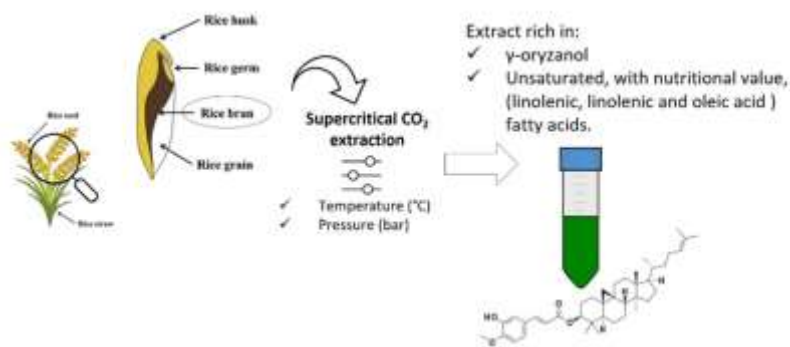


Figure 1. Bioactive extraction from rice by-products.

After a central composite design of experiments in which the raw material weight (20 g), flow rate (20 g/min), and extraction time (3 h) were fixed, temperature and pressure were varied (40-80 °C, 200-500 bar). The extraction yield obtained by the optimized SFE method was comparable to conventional Soxhlet extraction with *n*-hexane ( $\sim 18 \text{ g}_{\text{extract}}/100\text{g}_{\text{raw material}}$ ) and it was 2 times more selective for the  $\gamma$ -oryzanol extraction. Moreover, the fatty acid profile obtained by both methods were similar and the most abundant compounds were palmitic, oleic and linoleic acid.

This approach allows the isolation of  $\gamma$ -oryzanol rich extracts avoiding the use of organic solvents, which contributes to the valorization of food industry waste streams.

### Acknowledgements

The authors acknowledge the financial support received from the EU Horizon 2020 research & innovation programme under grant agreement TRACE-RICE (Grant n° 1934), part of the PRIMA programme. iNOVA4Health – UIDB/04462/2020 and UIDP/04462/2020, a program financially supported by Fundação para a Ciência e Tecnologia / Ministério da Ciência, Tecnologia e Ensino Superior, through national funds and funding from INTERFACE Programme, through the Innovation, Technology and Circular Economy Fund (FITEC), is also gratefully acknowledged. We also acknowledge the financial support from Fundação para a Ciência e Tecnologia and Portugal 2020 to the Portuguese Mass Spectrometry Network (LISBOA-01-0145-FEDER-402-022125).



## References

1. A. Mastinu, S.A. Bonini, W. Rungratanawanich, F. Aria, M. Marziano, G. Maccarinelli, G. Abate, M. Premoli, M. Memo, D. Uberti, *Nutrients*, **11**, 728 (2019).
2. N. Saji, N. Francis, L.J. Schwarz, C.L. Blanchard, A.B. Santhakumar, *Foods*, **9**, 829 (2020).
3. M. K. Sharif, M. S. Butt, F. M. Anjum, S. H. Khan, *Critical Reviews in Food Science and Nutrition*, **54**, 807 (2014).
4. M. Sohail, A. Rakha, M. S. Butt, M. J. Iqbal, S. Rashid, *Critical Reviews in Food Science and Nutrition*, **57**, 3771 (2017).

## Towards a kiwi waste valorization: optimization of extraction of phenolic compounds assisted by green chemistry tools

Sandra S. Silva<sup>1</sup>, Marina Justi<sup>1</sup>, Jean-Baptiste Chagnoleau<sup>2</sup>, Nicolas Papaiconomou<sup>2</sup>, Xavier Fernandez<sup>2</sup>, Sónia A. O. Santos<sup>1</sup>, Helena Passos<sup>1</sup>, Ana M. Ferreira<sup>1,\*</sup> and João A.P. Coutinho<sup>1</sup>  
<sup>1</sup>CICECO – Aveiro Institute of Materials, Department of Chemistry, University of Aveiro, 3810-193, Aveiro, Portugal.  
<sup>2</sup>Université Côte d'Azur, CNRS, Institut de Chimie de Nice, UMR 7272, 06108 Nice, France.  
\*ana.conceicao@ua.pt

The valorization of wastes rich in valuable compounds is one of the most relevant biorefinery and circular economy topics. Kiwifruit industry wastes are a potential source of bioactive compounds, such as phenolic compounds, which, in turn, exhibit many biological activities with potential health benefits. With the aim of developing a green approach for the valorization of kiwifruit waste, a study combining biobased solvents and alternative extraction techniques for the recovery of phenolic compounds from kiwifruits (*Actinidia deliciosa*) 'Hayward' by-products are presented. First, a pre-selection of the most suitable by-product for the recovery of phenolic compounds from kiwifruits was done, with kiwifruit peels being the most promising. After a screening of the most suitable biobased solvents to be used as mixtures along with ethanol and/or water was carried out. Gamma-valerolactone (GVL) mixtures yielded the highest phenolic compounds and antioxidant activity levels. The composition of GVL mixtures was optimized to GVL:ethanol in a ratio of 7:3 (wt/wt). Response surface methodology was used to optimize the operating conditions of different extraction techniques, namely, conventional extraction (CE) and the alternative techniques of ultrasound-assisted extraction (UAE) and microwave-assisted extraction (MAE), with MAE being identified as the most promising technique to obtain an extract with high levels of phenolic compounds (mainly epicatechin, caffeic acid and quercetin derivatives) and antioxidant activity, in a shorter extraction time. However, UAE demonstrated to be the preferable extraction technique, considering the estimated costs of the studied extraction processes. The obtained results showed for the first time the high potential of using GVL mixtures to extract phenolic compounds from biomass, while their combination with alternative extraction techniques could be the basis for the development of more effective extraction platforms.

### Acknowledgements

This work was developed within the scope of the project CICECO-Aveiro Institute of Materials, UIDB/50011/2020, UIDP/50011/2020 & LA/P/0006/2020, financed by national funds through the FCT/MEC (PIDDAC). J-B C. is grateful to the EUR Spectrum – Graduate school of Formal, Physical and Engineering Sciences- for his Ph.D. financing. H. Passos acknowledges FCT - Fundação para a Ciência e a Tecnologia, I.P. for the researcher contract CEECIND/00831/2017 under the Scientific Employment Stimulus -Individual Call 2017.

## New Compatibilizers from PET Residues

Hugo F. Gonçalves<sup>1\*</sup>, Pedro E. C. Nunes<sup>1</sup>, Rui Peneda<sup>2</sup>, Ana C. Fonseca<sup>1</sup> and Arménio C. Serra<sup>1</sup>

<sup>1</sup>CEMMPRE, Department of Chemical Engineering, University of Coimbra, 3030-790, Coimbra, Portugal

<sup>2</sup>GEPACK- Empresa Transformadora De Plásticos, S.A., Rua 1 de Abril Ed Gepack, 2050-182 Aveiras de Cima, Portugal

\*hugoferreiragoncalves1311@gmail.com

Abstract text:

Poly(ethylene terephthalate) (PET) is a widely used plastic for water and soft-drinks bottles, mainly because PET combines good mechanical properties with the excellent barrier properties to oxygen, carbon dioxide and humidity [1]. The high consumption of PET packaging combined with its non-biodegradability makes the recycling of this material essential to prevent its accumulation in the environment [2-3]. Usually, PET is mechanically recycled, where the original polymer structure is preserved. The recycled PET (RPET) may have lower mechanical properties, which may limit its application in certain types of packaging. These changes become more noticeable as the material recycling cycles increase [3]. These lower mechanical properties may result from chain scission reactions that decrease the polymer molecular weight [2-3]. To address this limitation, chemical recycling can be used. Here, PET is depolymerized into monomers, dimers or oligomers [4-5]. Then, high-quality materials can be produced using these lower molecular weight products as raw materials [4]. Based on the chemical agent used to break the polymer chains, chemical recycling can be achieved through methanolysis, glycolysis, hydrolysis, aminolysis or ammonolysis [4-5]. In glycolysis, it is employed an excess amount of glycol to perform the PET transesterification and produce bis(2-hydroxyethyl) terephthalate (BHET). Also, it is possible to separate the BHET monomers from the BHET dimers/oligomers. Due to its simplicity, broad range of operation conditions and lower reaction time, glycolysis is one of the best and most used methods to perform the PET depolymerization [5-6]. The main goal of this work is to valorize the PET residues by performing their chemical recycling by glycolysis and use the byproduct to synthesize a compatibilizer to use in the mixtures of immiscible polymers, such as poly(butylene adipate terephthalate) (PBAT) and poly(lactic acid) (PLA) blends. The compatibilizer needs to have a molecular structure that can physically interact with both polymers. For this, it was decided to synthesize the oligomers based on bis(2-hydroxyethyl) terephthalate lactic acid and lactic acid (BHET-LA) (Figure 1). The BHET-LA, due to the presence of LA moieties, can interact with PLA, and also with PBAT, due to the presence of aliphatic-aromatic moieties in the BHET dimers/oligomers. In this work, two approaches were studied: i) the BHET-LA was synthesized with only BHET dimers/oligomers and lactic acid, and ii) BHET-LA was end-capped with a branched aliphatic chain (Isofol32), as a way to counterbalance the rigidity of PLA in the chain and to increase the thermal stability of the BHET-LA oligomers.

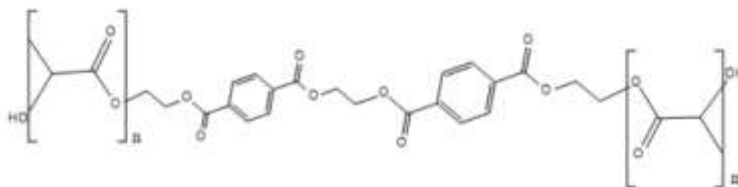


Figure 61 – BHET-LA molecular structure.

The synthesis of the BHET-LA is divided in two steps: PET glycolysis and obtainment of BHET-LA. In the first step, ethylene glycol and PET are placed in a three-neck round-bottom glass flask in a 3:1 molar ratio with 0.02% of Zn(Ac)<sub>2</sub> as the catalyst. The depolymerization was performed for 4 hours at 196 °C, in a nitrogen atmosphere. The solution is first filtered to retain possible PET pellets that do not depolymerize. To separate the BHET dimers/oligomers from the BHET monomers, boiling water was added to the liquid recovered from the filtration. This separation is possible due to the differences in the precipitation temperatures between the dimers/oligomers and the monomers. The solution was filtered and the precipitated was expected to be mainly constituted by BHET dimers/oligomers. Finally, the liquid part of the last filtration step was placed at 4°C to allow the precipitation of the BHET monomers. The products of the PET glycolysis were characterized by proton nuclear resonance (<sup>1</sup>H NMR). In the second step, the BHET-LA was synthesized through a bulk polymerization. The amount of acid lactic and BHET dimers/oligomers added to the reactor was calculated to have a polymer with a theoretical average molecular weight of 5000 g/mol. The reaction is performed in a nitrogen atmosphere at 180 °C with mechanical stirring. The reaction advance is inferred by measuring the reaction medium acid value following the European Standard norm ISO 2144. In the case of the BHET-LA with Isofol32, this compound was placed in the reactor during the reaction in function of the acid value. The products obtained were characterized by <sup>1</sup>H NMR, differential scanning calorimetry (DSC) and thermogravimetric analysis (TGA).

Through the  $^1\text{H}$  NMR analysis of the two products obtained in the PET depolymerization was possible to confirm that the 1<sup>st</sup> and 2<sup>nd</sup> precipitate are mainly constituted by BHET dimers/oligomers and BHET monomers, respectively. From the  $^1\text{H}$  NMR analysis was possible to identify the chemical structure of the BHET-LA in both products, that confirms that is compound was successfully synthesized. In the TGA analysis, it was verified that the BHET-LA has a very low thermal stability, presenting a  $T_{5\%}$  of about at 132°C. On the other hand, the BHET-LA with Isofol32 presented an improved thermal stability, with a  $T_{5\%}$  values of 288°C. This indicates that BHET-LA with Isofol32 is more suitable to be used as a compatibilizer in PLA and PBAT blends because does not thermally degrade at the processing temperature of these two polymers. The DSC analysis verified that BHET-LA has an amorphous morphology and BHET-LA with Isofol32 has a semicrystalline morphology.

### Acknowledgements

The authors gratefully acknowledge the project **GreenPack** (POCI-01-0247-FEDER-045282).

NMR data was collected at the UC-NMR facility which is supported in part by FEDER – European Regional Fund through the COMPETE Programme (Operational Programme for Competitiveness) and by National Funds through FCT – Fundação para a Ciência e a Tecnologia (Portuguese Foundation for Science and Technology) through grants REEQ/481/QUI/2006-RECI/QEQ-QFI/0168/2012, CENTRO-07-CT62-FEDER-002012, and Rede Nacional de Ressonância Magnética Nuclear (RNRRMN).

This research is sponsored by FEDER funds through the program COMPETE – Programa Operacional Factores de Competitividade – and by national funds through FCT – Fundação para a Ciência e a Tecnologia –, under the project UID/EMS/00285/2020.

### References

1. Frank Welle, *Conservation and Recycling*, **55** 865 (2011).
2. Firas Awaja, Dumitru Pavel, *European Polymer Journal*, **41** 1453 (2005).
3. Zoé O. G. Schyns, Michael P. Shaver, *Macromolecular Rapid Communications*, **42** (2021).
4. Daniela Carta, Giacomo Cao, Claudio D'Angeli, *Environmental Science and Pollution Research*, **10** 390 (2003).
5. Kim Ragaert, Laurens Delva, Kevin Van Geem, *Waste Management*, **69** 24(2017).
6. Mohammad Khoonkari, Amir Hossein Haghighi, Yahya Sefidbakht, Khadijeh Shekoohi, Abolfazl Ghaderian, *International Journal of Polymer Science*, **2015** (2015).

## Techno-economic evaluation and life cycle assessment for sustainable production of bio-based polyurethanes from the organic fraction of municipal solid waste

S.M. Ioannidou<sup>1</sup>, D. Ladakis<sup>1</sup>, A. Koutinas<sup>1,\*</sup>

<sup>1</sup>Department of Food Science and Human Nutrition, Agricultural University of Athens, Iera Odos 75, 118 55 Athens, Greece

\* [akoutinas@aua.gr](mailto:akoutinas@aua.gr)

Abstract text:

Municipal solid waste generation is continuously increasing worldwide, reaching 489 kg per capita in 2018 in EU-28 [1]. The organic fraction of municipal solid waste (OFMSW) contains high amounts of lipids, protein, pectins and polysaccharides [2]. Valorisation of OFMSW through a biorefinery approach could lead to the production of value-added bio-based products. Hydrolysis of OFMSW results in the production of a carbon and nutrient rich fermentation medium. A potential biorefinery concept focuses on the valorization of the OFMSW for the fermentative production of succinic acid from the sugar-rich OFMSW hydrolysate. The fermentation products and the remaining OFMSW fractions (e.g. protein, lipids/fats) are subsequently used for the production polyurethanes (PUD) and biosurfactants. The optimal results of the proposed biorefinery concept are evaluated via process design, techno-economic evaluation and Life Cycle Assessment (LCA).

Process design of each stage of the proposed biorefinery is carried out in order to estimate material and energy balances including validation using the process simulator UniSim (Honeywell). The developed inventory is used for the techno-economic evaluation and LCA study. Preliminary techno-economic evaluation (accuracy up to  $\pm 30\%$ ) is carried out for the estimation of the fixed capital investment (FCI) and the operating costs using literature-cited methodologies [3-4]. A discounted cash flow analysis is carried out to estimate important techno-economic indicators, namely net present value (NPV), minimum selling price (MSP) and discounted payback period (DPP). The environmental performance of the processes is assessed via LCA using the ISO 14040:2006 and the LCA software GaBi to construct the LCA model and perform the impact assessment calculations. The estimated results are compared to the environmental performance of the current OFMSW management practices.

FCI and COM for PUD production are calculated considering the following processes: the pretreatment process of OFMSW for succinic acid production, the succinic acid production, the polyester polyols formation and the polyurethane urea dispersions production process. Moreover, when the biorefinery approach is implemented, the economics of biosurfactants production are also considered. The values of FCI and COM per kilogram of produced PUD without the biorefinery development are \$0.85/kg<sub>PUD</sub> and \$2.18/kg<sub>PUD</sub>, respectively, while the same values with the biorefinery employment are \$1.41/kg<sub>PUD</sub> and \$2.43/kg<sub>PUD</sub>, respectively. After the discounted cash flow analysis, the MSP of the product is equal to \$2.15/kg<sub>PUD</sub> without the biorefinery development and \$1.75/kg<sub>PUD</sub> with the biorefinery approach for biosurfactants selling price equal to \$4.10/kg. The current selling price of PUD is approximately \$3.50/kg<sub>PUD</sub>, and when this price is implemented in the biorefinery concept, the payback period of the investment is 5 years. The most common environmental metrics of the PUD production process is the global warming potential (GWP) and is equal to 2.78 kg CO<sub>2</sub>-eq/ kg<sub>PUD</sub>. Succinic acid production has the lowest contribution to the final results, although it can be characterized as the main component of the PUD, while polyester polyols production is the main stage that affects environmental impact due to the impact of the two diols that are used for their formation. Finally, when the PUD from OFMSW is compared to the current management technique of OFMSW, savings in GHG emissions can be achieved reaching a percentage of 40%.

### Acknowledgements

The authors wish to acknowledge financial support from the LIFE EBP project (LIFE19 ENV/IT/000004) co-financed by European Commission through Life Programme.

### References

1. Eurostat, 2019. [https://ec.europa.eu/eurostat/statistics-explained/index.php/Municipal\\_waste\\_statistics](https://ec.europa.eu/eurostat/statistics-explained/index.php/Municipal_waste_statistics)
2. E. Stylianou, C. Pateraki, D. Ladakis, M. Cruz-Fernández, M. Latorre-Sánchez, C. Coll, A., Koutinas, A. *Biotechnol. Biofuels*, **13**(1) 1-16 (2020).
3. M.S. Peters, K.D. Timmerhaus, R.E. West. *Plant Design and Economics for Chemical Engineers*, 5th ed. (2003) McGraw-Hill.
4. R. Turton, R.C. Baile, W.B. Whiting, J.A. Shaeiwitz, D. Bhattacharyya. *Analysis, Synthesis, and Design of Chemical Processes*, 5th ed. Prentice Hall (2018), New Jersey.

## Tertiary treatment of municipal wastewater by microalgae technology for utilization in cooling towers of thermal power plants

Rahul J<sup>1\*</sup>, Anushree M<sup>1</sup>, Rajeev S<sup>2</sup>

<sup>1</sup> Applied Microbiology Laboratory, Centre for Rural Development and Technology, Indian Institute of Technology Delhi, New Delhi, India

<sup>2</sup> The NTPC Energy Technology Research Alliance (NETRA), Greater Noida, Uttar Pradesh, India

\*E-mail: rahul.jain@rdat.iitd.ac.in

**Abstract:** Increasing scarcity of water reserves with stringent restrictions on freshwater withdrawals have drawn thermal power plants attention towards alternate sources of water. The cooling towers contributing maximum to the water usage during electricity production process, provide significant opportunities to reduce the freshwater dependence and replace it with treated impaired water [1]. Secondary-treated municipal wastewater (MWW) available in adequate amount can be a promising alternative that can cater the cooling tower water demands. The major challenge associated with MWW reuse is its low quality due to presence of sufficient amount of dissolved solids, hardness, nitrate, and phosphate in comparison to freshwater [2]. Therefore, the utilization of MWW demands additional cleaning to remove these contaminants to mitigate corrosion and scaling of cooling tower infrastructure. In the present study, microalgae was utilized for tertiary treatment of MWW with an aim to remove contaminants and recover valuable biomass from it. Two algal species A1 (native consortium containing *chlorella* and *scenedesmus* sp) and PA6 (*chlorella*, *phormidium*, and *navicula* sp) were used to treat MWW collected from the sewage treatment plant of sector-50, Noida, Uttar Pradesh, India. The collected wastewater was found to be rich in nitrate-nitrogen ( $\text{NO}_3\text{-N}$ :  $9.5 \pm 0.4 \text{ mg L}^{-1}$ ), total dissolved phosphate (TDP:  $12.7 \pm 0.7 \text{ mg L}^{-1}$ ), Ca hardness ( $352 \text{ mg L}^{-1}$ ), Mg hardness ( $266 \text{ mg L}^{-1}$ ), sulphate ( $272 \text{ mg L}^{-1}$ ), and total dissolved solids (TDS:  $2479 \text{ mg L}^{-1}$ ). 1 L shake flasks with continuous aeration of  $2 \text{ L min}^{-1}$  were utilized for the bioremediation in the batch mode. The flasks were incubated at  $T = 25 \pm 2^\circ\text{C}$  and light intensity =  $48 \pm 6.5 \mu\text{mol m}^{-2} \text{ s}^{-1}$  with light: dark cycle of 16:8 h. During the 10 days treatment cycle, native A1 consortium gave better nutrient removals in comparison to PA6 consortium. With A1 consortium, the  $\text{Ca}^{2+}$  and  $\text{Mg}^{2+}$  hardness was reduced by 76.1% and 64.2%, respectively in comparison to PA6 which gave total hardness removal of about 20%. Interestingly, the sulphate ( $\text{SO}_4^{2-}$ ) was reduced by 98.6% and 82.9% in A1 and PA6 consortium. A1 further gave 99.2%, 85.1%, and 53% reduction in  $\text{PO}_4^{3-}$ ,  $\text{NO}_3\text{-N}$ , and COD. Though the removals were high, the TDS limit (<600 ppm) for make-up water in cooling towers was not reached. Overall, it was interpreted that the microalgae based bioremediation approach along with an integrated technology to reduce TDS could help to recycle treated MWW in cooling towers of power plants. The approach could significantly reduce the water footprint of thermal power plants along with the sustainable waste management.

**Acknowledgement:** The authors thank the Department of Science & Technology (DST), Government of India, for awarding the “Prime Minister Fellowship” to Mr. Rahul Jain. We gratefully acknowledge the support of our industrial partner: National Thermal Power Corporation (NTPC) Limited for funding the project.

### References:

- [1] Jain, R., Nigam, H., Mathur, M., Malik, A. and Arora, U.K., 2021. Towards green thermal power plants with blowdown water reuse and simultaneous biogenic nanostructures recovery from waste. *Resources, Conservation and Recycling*, 168, p.105283.
- [2] Chys, M., Demeestere, K., Nopens, I., Audenaert, W.T. and Van Hulle, S.W., 2018. Municipal wastewater effluent characterization and variability analysis in view of an ozone dose control strategy during tertiary treatment: The status in Belgium. *Science of the Total Environment*, 625, pp.1198-1207.

## Harnessing the potential of seaweed *Sargassum* spp. by treatment in acidic medium and anaerobic digestion

Luis Felipe Jiménez-Contreras<sup>1</sup> and María A. Fernández-Herrera.<sup>1\*</sup>

<sup>1</sup>Departamento de física aplicada, Cinvestav Mérida, 97310, Mérida, Yucatán; México

\*luis.jimenez@cinvestav.mx

Abstract text:

In recent years, the amount of seaweed reaching the coasts of the countries that share the Caribbean has considerably increased. This macro-alga represents an environmental, economic disaster and threatens human health [1]. Marine algae represent a rich source of biomass and biopolymers that can be used for a variety of applications, for example, in the field of materials or energy. Among the most abundant polymeric components present in marine algae is alginate. Alginate is a branched polymer found in the cell wall of brown algae, its primary function being to give them strength and flexibility [2]. The industrial extraction of alginate generates an organic waste that is mainly used as a fertilizer [3, 4]. Therefore, due to the problems caused by the arrival of marine algae and the fact that such products, with a wide range of applications, can be obtained from them.

The present work focuses on the extraction of sodium alginate from *Sargassum* spp. and its physicochemical characterization. Also, on the use of by-product generated from the extraction as a substrate to produce biogas through anaerobic digestion.

The samples were washed with tap water to remove sand residues. Subsequently, the algae were introduced into an ultrasonic washing machine with distilled water for 30 min. At the end of the washing, they were dried at 60 °C for 24 h. Finally, they were crushed and stored in a plastic bag at 3 °C. For the first experiment, 10 g of sample were weighed and placed in a beaker containing a 4% formaldehyde (CH<sub>2</sub>O) solution, this mixture was kept in constant agitation at 350 rpm [5]. The solid phase was extracted by filtering under vacuum and washed three times with distilled water. Again, the solid was placed in a beaker which now contained a 0.2 M HCl solution. The samples were again vacuum filtered and washed with distilled water. The resulting solid was placed in a 2% sodium carbonate (Na<sub>2</sub>CO<sub>3</sub>) solution at variable temperature and time (Table 1). At the end of this time, they were filtered under vacuum and centrifuged at 4500 rpm for 30 min in a centrifuge to remove the supernatant. The solution obtained was mixed with 96% v/v ethanol to precipitate the sodium alginate. After this treatment, a vacuum filtration was performed to obtain the sodium alginate and washed with ethanol and acetone (1 x 100 mL). Finally, the product was dried at room temperature.

Table 1. Parameters for each of the experiments for alginate extraction.

Samples	CH <sub>2</sub> O	HCl	Na <sub>2</sub> CO <sub>3</sub>	
	Time (min)	Time (min)	Time (h)	Temperature (°C)
1	30	30	5	60
2	30	120	3	80
3	1800	1800	3	80
4	30	120	3	90

For the anaerobic digestion of the waste, the experiments were performed in triplicate. The system consists of two reactors, reactor one (R1) contains the material and reactor two (R2) functions as a gas trap. R2 contained in all cases 100 mL of a 3% NaOH solution with 20 drops of phenolphthalein, which is used as a developer for the reaction of the base with the CO<sub>2</sub> present in the biogas. In R1 the samples were deposited in triplicate as follows: 1.- (B) Only 10 ml of brewing water was used in order to quantify the amount of biogas produced without any modification. Positive control (C+). In this condition, 1 g of sucrose was used as carbon source and 10 ml of brewery wastewater was added. The purpose of this experiment was to have a reference frame of biogas production that can be generated with a short carbon chain (disaccharide) and of easy acquisition. 3.- (S). In this condition, 1 g of the alginate extraction residue from *Sargassum* spp. was used as substrate. The substrate was washed with distilled water and then dried at 60 °C for 48 h to finally be crushed.

Sodium alginate was characterized by FTIR, X-ray diffraction and NMR. While the biogas was preliminarily characterized by infrared spectroscopy. Figure 1 shows the <sup>1</sup>H NMR spectrum of alginate, in this spectrum the characteristic signals of the anomeric proton of guluronic acid are observed at 4.94 ppm, the H-5 of guluronic acid at 4.33 ppm and the anomeric proton of mannuronic acid at 4.72 ppm.

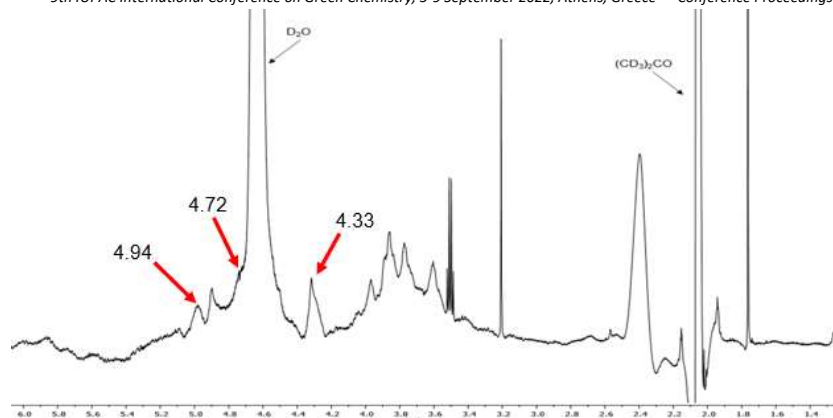
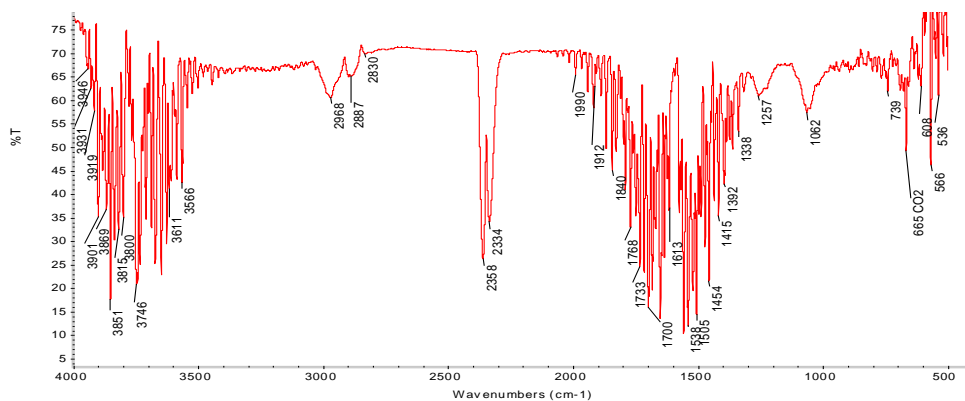
Figure 1.  $^1\text{H}$  NMR spectrum of sodium alginate.

Figure 2. IR spectrum of biogas.

The residue of the extraction generated an average of 23.73 mL of gas, such sample presented a significant difference (Anova 1 wat, post hoc Tukey) showing that more biogas was generated in comparison with substrates like sacarose.

### Acknowledgements

LFJC thank Conacyt for the PhD fellowship (254752)

### References

1. D. Resiere, R. Valentino, R. Nevière, R. Banydeen, P. Gueye, J. Florentin, A. Cabié, T. Lebrun, B. Mégarbane, G. Guerrier, H. Mehdaoui. *The Lancet*, **392** 2691 (2018)
2. R. Yabur Pacheco, G. Hernández Carmona. Doctorado, Instituto Politécnico Nacional, La Paz, Baja California Sur (2005).
3. C. Bertagnolli, A. P. D. M. Espindola, S. J. Kleinübing, L. Tasic, M. G. C. Silva. *Carbohydr Polym* **111** (2014).
4. B. Riaño, B. Molinuevo, M. C. García-González. *Bioresour Technol*, **102** 5 (2011).
5. T. A. Fenoradosoa, G. Ali, C. Delattre, C. Laroche, E. Petit, A. Wadouachi, P. Michaud. *J Appl Phycol* **22** 2 (2010).



## A new HPLC method for the detection and quantification of chemically recycled PET monomers in protic ionic liquids

Harriet Louise Judah<sup>1\*</sup>, Maariyah Suleman<sup>1</sup> and Agnieszka Brandt-Talbot<sup>1</sup>

<sup>1</sup>Imperial College London, Department of Chemistry, 82 Wood Ln, W12 0BZ, London, United Kingdom.

\*h.judah20@imperial.ac.uk

### 1. Abstract text:

Plastics are ubiquitous materials that have greatly improved the convenience and standard of modern-day living. Due to their low production cost, light weight and versatile properties, they are extensively used in building and construction, automotive and agriculture, but are most pervasive in the packaging industry. The rapid increase in plastic production combined with a lag in developing matching waste management has resulted in low recycling rates and environmental littering. At least 8 million tons of plastic leak into the ocean every year, which is expected to increase five-fold by 2050 if nothing changes.[1] This has a detrimental effect on marine life and encourages the production and proliferation of microplastics that have been detected in living organisms such as animals and humans.[2,3] In addition, 99% of plastics are petroleum derived, so there is a strong link between the plastic and fossil industries which is not sustainable.[4] The 9% of plastic that is collected for recycling is processed through what is called mechanical recycling. While mechanical recycling is useful for energy and resource preservation, the mechanical and optical properties of recycled plastic is reduced, even if carefully sorted and washed. Therefore, it merely delays discard of plastic waste and a significant amount of fossil raw materials are still required for producing plastic needed for high specification applications. Poly(ethylene terephthalate) (PET) is the most commonly recycled plastic and accounts for 8.4% of global production.[5] Depolymerization is a promising chemical recycling option for polyesters such as PET, to complement mechanical recycling technology.

The depolymerization of PET waste is an attractive process for the synthesis of terephthalic acid and ethylene glycol, the industrial monomers used in PET production. Ionic liquids are solvents composed of ions and have low melting temperatures, and have emerged as reactive solvents for PET depolymerization.[6] However, there is a lack of quantitative data on the solubility of terephthalic acid in ionic liquids, especially as a function of water content and acid-base ratio and also reliable measurements to determine the purity of the recovered terephthalic acid. Herein, we report the method development for the detection and quantification of terephthalic acid, dimethyl terephthalate and BHET in the presence of ionic liquids.

### 2. Materials and methods:

Ionic liquids were synthesized following a previously reported procedure via an acid-base neutralization reaction. Samples containing potential internal standard and terephthalic acid were prepared and measured via HPLC over the course of 1 – 8 days to determine the chemical compatibility of internal standard and analyte. A stock containing a certain amount of internal standard was prepared. This stock was used to prepare a stock of terephthalic acid. HPLC standards were then prepared by diluting the terephthalic acid stock further with the original internal standard stock. Saturated samples of terephthalic acid in ionic liquids at specific water content and acid:base ratio were prepared and left to stir for some time. These were centrifuged and a 50  $\mu$ L aliquot of supernatant was taken and 1 mL of internal standard stock added. This was run on the HPLC and the calibration curve used to determine concentration of terephthalic acid.

### 3. Key results

No new peaks were detected from stability test of 1,3,5-trimethoxybenzene with terephthalic acid, therefore it was selected as the internal standard for next set of experiments. A calibration plot of terephthalic acid (TPA) was prepared with 1,3,5-trimethoxybenzene (TMB) as internal standard. The R-squared value of the trend line from linear regression analysis was 0.99 which is acceptable, therefore will be used for TPA concentration determination. A preliminary test was done to determine qualitative, *relative* solubility of terephthalic acid in some protic ionic liquids at room temperature. [Hmim][OAc] appears to have the best solubilizing ability of the ionic liquids studied. This is just a preliminary test, quantitative determination experiments are currently underway and the protocol will be adapted for determining the purity of TPA obtained from hydrolysis of PET waste.

### Acknowledgements

We would like to thank the Engineering and Physical Sciences Research Council (EPSRC) for providing the funding of this project.

### References

- [1] E. M. Foundation, The new plastics economy: Rethinking the future of plastics, 2016.  
 [2] Anastasopoulou, A., Fortibuoni, T., Impact of Plastic Pollution on Marine Life in the Mediterranean Sea, 2019.

- [3] Heather A. Leslie, Martin J.M. van Velzen, Sicco H. Brandsma, A. Dick Vethaak, Juan J. Garcia-Vallejo, Marja H. Lamoree, Discovery and quantification of plastic particle pollution in human blood, 2022.
- [4] Nielsen, TD, Hasselbalch, J, Holmberg, K, Stripple, J. Politics and the plastic crisis: A review throughout the plastic life cycle, 2020
- [5] <https://ourworldindata.org/grapher/plastic-production-polymer> (accessed 27th June, 2022)
- [6] Liu, F., Cui, X., Yu, S., Li, Z. and Ge, X, Hydrolysis reaction of poly(ethylene terephthalate) using ionic liquids as solvent and catalyst, 2009

## Circular Economy Electrochemistry: Utilizing recycled materials for the development of 3D-printed electrochemical devices

Cristiane Kalinke<sup>1,2\*</sup>, Robert D. Crapnell<sup>2</sup>, Evelyn Sigley<sup>2</sup>, Matthew J. Whittingham<sup>2</sup>, Paulo R. de Oliveira<sup>3</sup>, Bruno C. Janegitz<sup>3</sup>, Craig E. Banks<sup>2</sup> and Juliano A. Bonacin<sup>1</sup>

<sup>1</sup>Institute of Chemistry, University of Campinas (Unicamp), 13083-859, Campinas, São Paulo, Brazil.

<sup>2</sup>Manchester Metropolitan University (MMU), Manchester, M1 5GD, United Kingdom.

<sup>3</sup>Federal University of São Carlos (UFSCar), 13600-970, Araras, São Paulo, Brazil.

\*cristiane.kalinke@gmail.com

The globalized world and growing consumerism have led to the search for more sustainable alternatives, for example using low toxicity materials, managing and recycling waste. Based on this concept, the circular economy has as its main objective the restoration and regeneration of material cycles, i.e., closing the material cycle through recycling [1]. Particular attention is focused on the use and re-use of plastics due to the effect that plastic accumulation has on the Earth's environment and in-particular wildlife and wildlife habitat. This has been the key objective for the TRANSFORM-CE project, led by Manchester Metropolitan University, which looked to take municipal plastic waste sources and repurpose it into high grade 3D printing feedstocks. This work included utilizing different plastic sources to create standard filament (PLA, ABS, PET, PETG, HDPE, LDPE, PE and PP), in addition to bespoke filament with interesting characteristics, such as electrical conductivity.

Parallel to this, additive manufacturing (3D printing) can be an allied for the use of these recycled materials, obtaining objects and devices by using polymeric filaments with low cost, low waste, speed, versatility, reproducibility for large-scale production, and portability [2]. Additive manufacturing (AM) has been applied to several areas of scientific research, including electrochemistry, where the main focus is the development of conductive and non-conductive materials for applications in energy storage and sensors [3]. The use of additively manufactured electrodes (AMEs) allows for bespoke electrode shapes to be produced rapidly, reproducibly and with little material wastage; however, due to the need to activate surfaces before use and poor regeneration of the interfacial surfaces they are often disposed of after a single use. Thus, the combination of waste recycling and additive manufacturing is an interesting strategy for the circular economy approach toward both AM electrochemical platforms and general lab management.

Based on this, we proposed recycling plastic waste to obtain new 3D printed electrochemical cells and sensors, and present two cases of fundamental research in this area. In the first instance, we utilize waste coffee cups based on the biopolymer polylactic acid (PLA), which were processed and re-extruded to manufacture both non-conducting filaments applied for the 3D printing of electrochemical cells and conductive filaments used to make bespoke AMEs for the cell. The cycling lifetime of the PLA base was evaluated through 3D-printing the in-house filament, processing it through granulation and re-extrusion through our in-house filament line to observe how many iterations of the electrochemical cell could be produced (Figure 1).

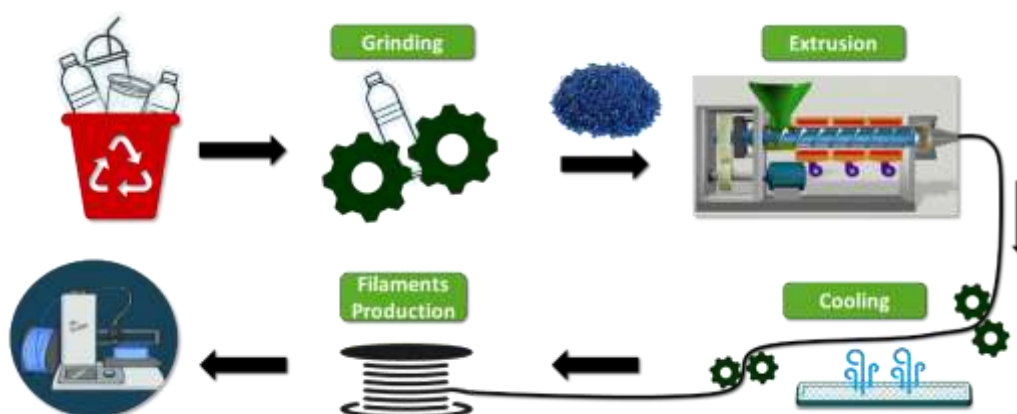


Figure 1. Scheme of the recycling of plastic materials for the in-house production of filaments for additive manufacturing

Additionally, the loading (Fill Factor) of the conductive material carbon black (CB) was evaluated alongside the type and amount of plasticizer used to stabilize the loaded filament, being directly compared to commercially available filaments. This fully AM electrochemical cell was then evaluated electrochemically and applied to the electrochemical detection of key environmental analytes, where it exhibited a significantly enhanced performance compared to commercially available, non-recycled counterparts. This design of electrochemical cell utilizes independent prints for the electrochemical cell and AMEs, allowing for them to be separated after use. Crucially,

this allows for the cell to be reused, even when the electrodes require replacing, and makes the recycling of each component simple as they can be separated into pure PLA recycling and CB contaminated recycling.

Secondly, we offer a solution to mixed material print recycling that allows for all prints to achieve at minimum one more life cycle. This builds on published work that highlighted the first single print fully AM electrochemical cell, where through the utilization of an independent dual-extruder 3D printer, it was possible to print the conductive electrodes embedded within the base of the cell [4]. Due to the electrodes being embedded within the non-conductive PLA cell, it is impractical to separate the two composites. Therefore, the production of new filament from a mix of these materials was shown. The electrochemical cells, comprising of ~90% pure PLA and ~10% conductive PLA, were processed in batches together through granulation, re-mixing at a raised temperature and then extrusion along an in-house filament line to produce a new non-conductive filament. This new filament comprised of approximately 2 wt% CB, from the commercial conductive filament, which was not a loading high enough to induce conductivity. It was then shown that new electrochemical sensing platforms can be produced using this as the non-conductive casing, in addition to the commercial conductive filament being used for the electrodes. As the electrode material remained unchanged in this case, the performance of the electrochemical cell remained consistent. To take this work further, the original cells were used to make a new conductive filament through the granulation of prints and thermal mixing with high loadings of CB. This utilized the residual plasticizer from the commercial filament and allowed for an enhanced bespoke conductive filament to be produced. This was utilized alongside the recycled non-conductive filament to produce fully recycled electrochemical cells, which had an improved performance to the original due to the higher loading of CB in the recycled conductive filament.

Thus, we present methods for the recycling of used municipal waste into 3D-printed electrochemical sensing platforms for the sensing and biosensing of environmental and biological species through the production of bespoke non-conductive and conductive filaments. It is shown how these platforms can then be recycled again into fresh electrochemical sensing platforms, completing the circular economy for these products. Additionally, evidence is provided that these bespoke filaments are an improvement on commercially available non-recycled filaments on the market. Finally, we highlight how mixed material electrochemical cells can also be recycled into the same product, in a circular approach, which can actually lead to enhancements over products made from commercially available filaments. This work overall highlights not only how AM can be used to create useful electrochemical platforms, but also suggests how research labs and companies can avoid unnecessary waste in their work by incorporating a circular economy approach.

### Acknowledgements

CK, PRO, BCJ and JAB would like to thank to São Paulo Research Foundation (FAPESP, Brazil. Grants# 2021/07989-4, 2019/00473-2, 2019/01844-4, 2017/21097-3, and 2013/22127-2) and Coordination of Improvement of Higher Education Personnel (Capes, Brazil. Finance Code 001, and 88887.504861/2020-00). RDC, ES and CEB would like to acknowledge TRANSFORM-CE, a transnational cooperation project supported by the Interreg North-West Europe program as part of the European Regional Development Fund.

### References

1. H. Salmenperä, K. Pitkänen, P. Kautto, L. Saikku. *Journal of Cleaner Production*, **280**, 124339 (2021).
2. R.M. Cardoso, C. Kalinke, R.G. Rocha, P.L. Santos, D.P. Rocha, P.R. Oliveira, B.C. Janegitz, J.A. Bonacin, E.M. Richter, R.A.A. Munoz. *Analytica Chimica Acta*, **1118**, 73-91 (2020).
3. M.J. Whittingham, R.D. Crapnell, E.J. Rothwell, N.J. Hurst, C.E. Banks. *Talanta*, **4**, 100051 (2021).
4. R.D. Crapnell, E. Bernalte, A.G.M. Ferrari, M.J. Whittingham, R.J. Williams, N.J. Hurst, C.E. Banks, *ACS Measurement Science AU*, **2** (2), 167-176 (2022).

# Catalytic upgrading of end-of-life tyre pyrolysis vapours for the production of highly aromatic pyrolysis oils

Stefanidis S.D.<sup>1</sup>, Karakouli S.A.<sup>1</sup>, Pachatouridou E.<sup>1</sup>, Heracleous E.<sup>1,2</sup> and Lappas A.A.<sup>1\*</sup>

<sup>1</sup> Chemical Process and Energy Resources Institute (CPERI), Centre for Research and Technology Hellas (CERTH), Thessaloniki, Greece

<sup>2</sup> School of Science and Technology, International Hellenic University, Thessaloniki, Greece

\*angel@cperi.certh.gr

## Introduction

Globally, around 1.6 billion tyres are sold annually and roughly an equal number of tyres enter the end-of-life tyre (ELT) category each year. ELTs are typically recycled into products that find applications in civil engineering or are used as fuel substitutes in kilns and boilers. However, there is currently an oversupply of ELTs and around 50% of them are not recycled. Moreover, ELT recycling is currently not circular, as the recycling products are not re-used to produce new tyres. However, ELTs can be pyrolysed to produce liquid, solid and gas products. The solid pyrolysis product, can be used as a substitute for carbon black (filler) for the production of new tyres. The heavy aromatic compounds in the liquid product can be used as feedstock in a furnace process to produce virgin carbon black, which can also be used for the production of new tyres. The gas product can be burned to produce electricity or to provide heat for the pyrolysis process. In this work, we investigated the catalytic upgrading of ELT pyrolysis vapours with the aim to produce highly aromatic pyrolysis oils. ELTs were pyrolysed in a bench-scale fixed bed reactor and the produced pyrolysis vapours were catalytically upgraded using various catalysts. The produced pyrolysis oils were thoroughly characterized and the effect of each catalyst on the composition of the pyrolysis oils was investigated. The most promising catalysts were also tested in a medium-scale continuous catalytic pyrolysis unit with two cascading bubbling bed reactors.

## Experimental

Two ELT feedstocks were used for the pyrolysis experiments and their properties are presented in Table 1. ELT1 was described as “granules of multi-brand truck tyres” and ELT2 was described as “granules of multi-brand all tyre”. The main difference between the two feedstocks was the particle size. ELT1 was used in the bench-scale pyrolysis runs, while ELT2 was used in the medium-scale pyrolysis runs. The catalysts used were a Y zeolite-based refinery equilibrium FCC catalyst (USY), a Y zeolite-based refinery catalyst poisoned with 1.6 wt% Ni (Ni/USY), a ZSM-5 zeolite-based refinery catalyst additive (ZSM-5), a ZSM-5 zeolite-based refinery catalyst additive wet-impregnated with 5.5 wt% Co (Co/ZSM-5) and a low-cost MgO catalyst derived from natural magnesite ore via simple calcination (MgO). The pyrolysis of the ELTs and the upgrading of the pyrolysis vapours were carried out at 500 °C. A detailed description of the bench-scale fixed bed reactor can be found at [1], while a detailed description of the continuous medium-scale catalytic pyrolysis unit can be found at [2]. The pyrolysis oils were thoroughly characterised by elemental analysis, simulated distillation, GC, GC-MS and HPLC to determine their elemental composition and content in aromatics.

Table 16. Properties of the ELT feedstocks used in this work.

Feedstock	Supplier	Particle size, mm	Moisture, wt%	Ash, wt%	C, wt%	H, wt%	S, wt%	O, wt%*
ELT1	Aliapur	1-3	1.0	8.0	80.7	7.6	1.1-3.6	0.1-2.6
ELT2	Michelin	0.2-0.8	0.5	6.1	81.2	7.7	1.2	3.8

\* by difference

## Results and Discussion

The pyrolysis product yields from the bench-scale catalyst screening results are presented in Figure 1. The non-catalytic pyrolysis of ELT1 yielded ~53 wt% pyrolysis oil, while the yield of the solid pyrolysis product was ~36 wt% (not shown). The catalytic upgrading of the pyrolysis vapours resulted in increased gas yields at the expense of the pyrolysis oil. Increasing the C/F ratio resulted in further increase of the gas products and reduction of the pyrolysis oil yield due to the catalytic cracking reactions. The Ni/USY and Co/ZSM-5 catalysts yielded significantly more hydrogen gas than the other catalyst, which was attributed to dehydrogenation reaction promoted by the transition metals on the catalysts. Overall, the zeolite-based catalysts appeared significantly more active than the MgO. The aromaticity of the produced pyrolysis oils vs. the pyrolysis oil yield is presented in Figure 2, both compared to the non-catalytic run at 500 °C, as well as to non-catalytic runs at elevated pyrolysis temperatures (550 °C and 600 °C). It was observed that pyrolysis at increased temperatures resulted in a notable reduction of the pyrolysis oil yield due to the thermal cracking of the pyrolysis vapours, accompanied by a small increase in the aromatics and the C/H molar ration. On the other hand, when using catalysts for the catalytic upgrading of the pyrolysis vapours, a notable reduction in the pyrolysis oil yield was also observed, however, it was accompanied by a significantly larger increase of the aromatics content and the C/H molar ratio. The most effective catalysts were the USY, Ni/USY, ZSM-5 and Co/ZSM-5 catalysts. MgO also showed some promise regarding the increase in the C/H molar ratio, but exhibited comparatively lower activity.

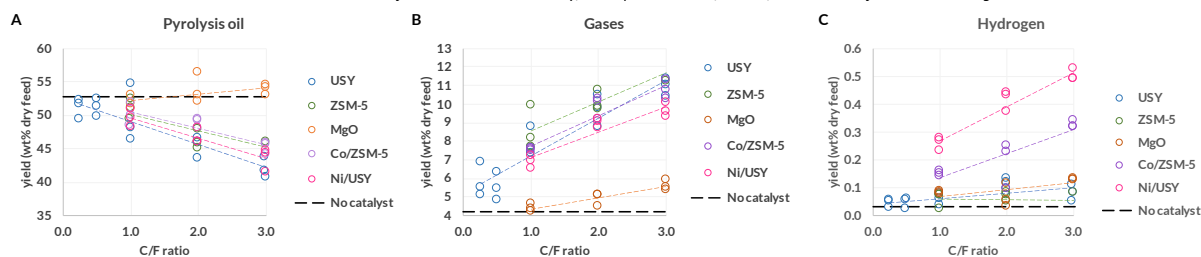


Figure 62. Pyrolysis product yields from the bench-scale catalyst screening runs as a function of the catalyst-to-feed (C/F) ratio.

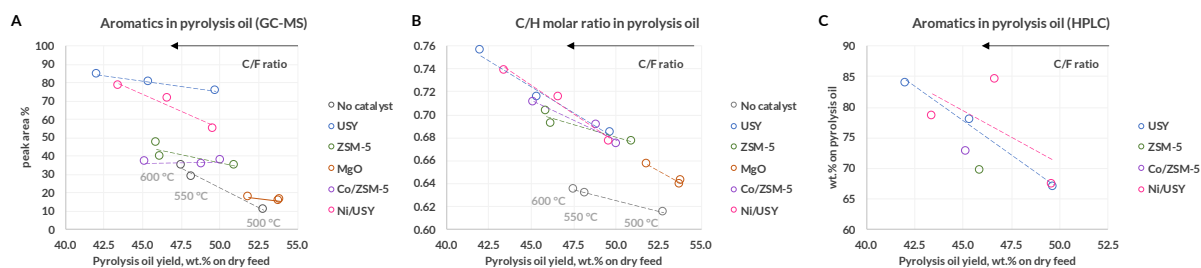


Figure 63. (A) Aromatics in the pyrolysis oils determined by GC-MS analysis, (B) C/H molar ratio determined by elemental analysis and (C) Aromatics determined by HPLC analysis, vs. the pyrolysis oil yield (bench-scale runs).

The pyrolysis product yields from the continuous medium-scale reactor tests are presented in Figure 3. The non-catalytic pyrolysis of ELT2 yielded ~51 wt% pyrolysis oil and ~38 wt% solid pyrolysis product (not shown). In agreement with the results from the bench-scale, the catalytic upgrading of the pyrolysis vapours resulted in increased gas yields at the expense of the pyrolysis oil. The aromaticity of the produced pyrolysis oils vs. the pyrolysis oil yield from the medium-scale runs is presented in Figure 4, compared to non-catalytic pyrolysis at 500 °C and 550 °C. In agreement with the bench-scale runs, increasing the pyrolysis temperature resulted in a decrease of the pyrolysis oil yield, accompanied by a small increase in the aromatics content of the pyrolysis oils and the C/H molar ratio. However, when using catalysts for the upgrading of the pyrolysis vapours, higher aromatics content and C/H molar ratios were achieved with a moderate reduction of the pyrolysis oil yields. The most aromatic pyrolysis oils in this work (up to 87 wt% aromatics) were produced with the Ni/USY and USY catalysts.

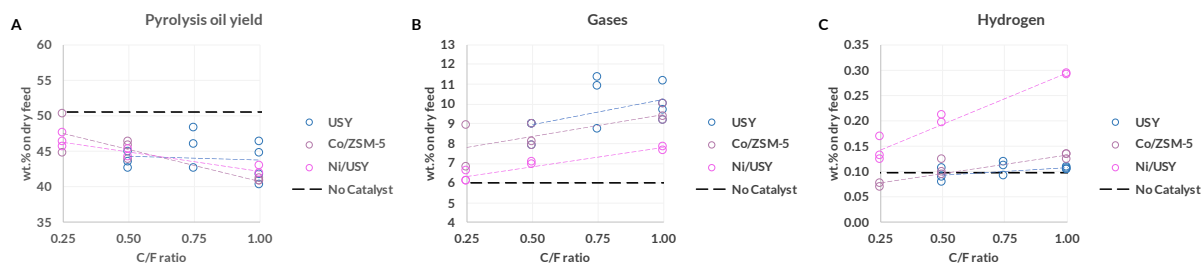


Figure 64. Pyrolysis product yields from the medium-scale runs as a function of the catalyst-to-feed (C/F) ratio.

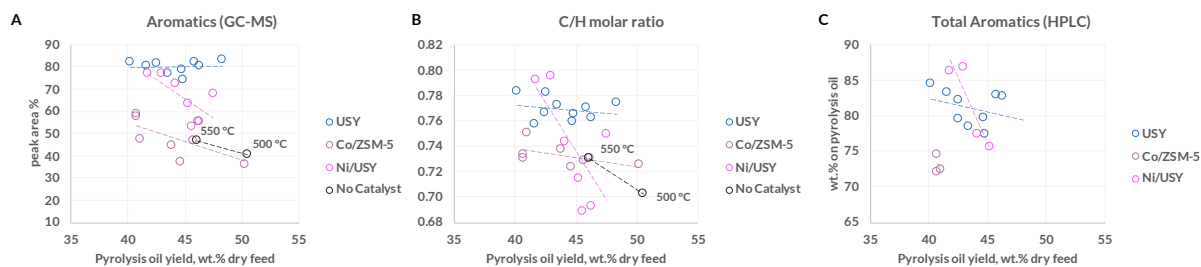


Figure 65. (A) Aromatics in the pyrolysis oils determined by GC-MS analysis, (B) C/H molar ratio determined by elemental analysis and (C) Aromatics determined by HPLC analysis, vs. the pyrolysis oil yield (medium-scale runs).

## Acknowledgements



This work has received funding from the European Union's Horizon 2020 research and innovation programme under grant agreement No. 869625.

## References

1. S.D. Stefanidis, K.G. Kalogiannis, E.F. Iliopoulou, et al., *Bioresource Technol.*, **102** 8261 (2011).
2. S.D. Stefanidis, K.G. Kalogiannis, P.A. Pilavachi, et al., *Catal. Sci. Technol.*, **6** 2807 (2016).

## Synthesis, ageing tests and flammability characterization of composites based on epoxy resin with different curing agents and flame retardant compounds

Krystyna Wnuczek<sup>1</sup>, Karolina Sowa<sup>1</sup>, Beata Podkościelna<sup>1</sup>, Tomasz Klepka<sup>2\*</sup>

<sup>1</sup>Department of Polymer Chemistry, Faculty of Chemistry, Institute of Chemical Sciences, Maria Curie-Skłodowska University, Gliniana 33, 20-614, Lublin, Poland

<sup>2</sup>Department of Technology and Polymer Processing, Faculty of Mechanical Engineering, Lublin University of Technology, Nadbystrzycka 36, 20-618 Lublin, Poland  
e-mail: t.klepka@pollub.pl

The majority of organic compounds, including polymers, will burn readily in air or oxygen. The flammability of polymers is a serious issue and limits their applications severely. The flame retardant additives are intended to inhibit or to stop the polymer combustion process acting either physically (such as cooling, fuel dilution, formation of a protective layer) or chemically (reaction in the solid or gaseous phase, the addition of flame retardant) [1].

As follows from the industrial practice, the phosphorous-containing flame retardants are used as an alternative to the commonly applied toxic halogenated flame retardants. These compounds can suppress fire in a polymer in two ways. The first mechanism proceeds through the thermal degradation of phosphorus flame retardants into phosphoric acid which converts the polymer into carbon, whereas the other one is based on migration into the vapour phase and quenching the radicals [2, 3]. Organophosphorous compounds are good flame retardants for polymeric materials [4]. There are several reports on thermal or thermo-oxidative degradation kinetics of flame-retarded polymeric materials [5]. The phosphorus-based flame retardants burn more intensively, especially when the conversion of both polymer and flame retardant into char decreases the formation of gaseous phase degradation products [1].

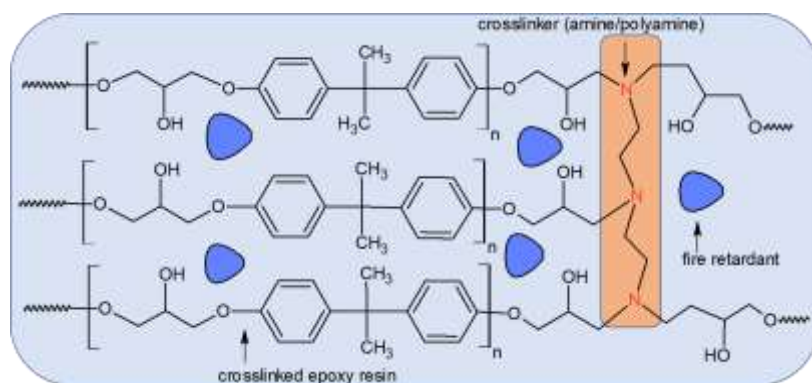


Figure 1. Fragment of composite structure.

This study presents the preparation and flammability characteristics of polymeric composites based on the epoxy resin Epidian® 601. The triethylenetetramine (TETA) and commercial curing agents based on polyamines (IDA and PAC) were used as crosslinking compounds. Moreover, two flame retardant compounds were added to this composition, the commercial Fire Retardant (FR) and triphenyl phosphate (TP). The chemical structure of the composites and the course of curing processes were confirmed by the ATR/FT-IR (Attenuated Total Reflection-Fourier Transform Infrared) analysis. The influence of different amounts of FR or TP on the flammability and thermal resistance was discussed in detail. After the flammability test the samples were also studied to assess their thermal destruction. In addition, the composites were subjected to the swelling tests, solvent resistance and microscopic observations. The DSC curves revealed that all materials were characterized by good thermal properties. All materials were temperature resistant up to 300 °C. Furthermore, the measurements of the composites hardness demonstrated that the material EP601+TETA+10% FR is the hardest. The addition of FR and RP influenced flammability of the composites increasing the thermal resistance. The ageing tests in methanol, acetone, hydrochloric acid and potassium hydroxide were also carried out.



## References

1. B. Podkościelna, K. Wnuczek, M. Goliszek, T. Klepka, K. Dziuba, *Molecules*. **25**, 5947 (2020)
2. E.D. Weil, M. Lewin, *CRC Press: Cambridge*, UK 31–68 (2001).
3. C. Hobbs, *Polymers* **11**, 224 (2019)
4. E. Feyz, Y. Jahani, M. Esfandeh, *Macromol. Symp.* 298 130–137 (2010)
5. G.J. Van Esch, *Report in WHO Library Cataloguing in Publication Data* (1997).

## From water for the water: food-waste based hydrogels for adsorption and photo-degradation of pollutants.

Marina Maddaloni<sup>1,2</sup> (m.maddaloni@unibs.it), Irene Vassalini<sup>2,3,4\*</sup>, Giammarco Roini<sup>1,4</sup>, Alessandra Gianoncelli<sup>2,5</sup>, Giovanni Ribaudò<sup>5</sup>, Alice de Villi and Ivano Alessandri<sup>2,3,4\*</sup>

<sup>1</sup>Chemistry for Technologies Laboratory, Department of Mechanical and Industrial Engineering, University of Brescia, via Branze 38, 25123 Brescia, Italy.

<sup>2</sup>National Interuniversity Consortium of Materials Science and Technology (INSTM), Florence, Italy

University of Brescia, via Branze 38, 25123 Brescia, Italy

<sup>3</sup>National Institute of Optics-Italian National Research Council (CNR-INO), University of Brescia, via Branze 38, 25123 Brescia, Italy

<sup>4</sup>Department of Information Engineering, University of Brescia, via Branze 38, 25123 Brescia, Italy

<sup>5</sup>Department of Molecular and Translational Medicine, University of Brescia, Viale Europa 11, 25123, Brescia, Italy  
ivano.alessandri@unibs.it\*  
irene.vassalini@unibs.it\*

### Introduction

A direct consequence of the increasing world population is the nonstop increment of food waste, which has a major impact not only on economy and society, but also on environment, as it severely contributes to greenhouse gas emissions. Nowadays, indeed, only 1% of the food waste is recycled for industrial uses [1]. At the same time, the supply of clean water to the growing population is becoming an urgent issue.

In this work, we exploit the possibility to merge these two aspects developing all-in one systems, based on materials derived from food waste, which are able to capture, degrade, and remove environmental pollutants in water.

### Materials and methods

Chitosan extracted from crustaceans' shells using chemical method with HCl and NaOH [2] is reutilized to obtain hydrogel bubbles, which act as adsorbents for organic dyes (e.g. methyl orange and methylene blue). The degree of deacetylation of the extracted chitosan, which is a key parameter for the preparation of the hydrogel bubbles, was characterized by IR and NMR spectroscopy and chemical titration. In order to enhance the adsorption capability towards specific class of pollutants and to exploit photo-catalytic properties, PEDOT:PSS, AuNPs, AgNPs and TiO<sub>2</sub> NPs at different concentration were introduced into chitosan bubbles.

Adsorption capability and photo-catalytic efficiency under direct sunlight irradiation were investigated by UV-Vis spectroscopy.

### Results and discussion

Each hydrogel system was employed to remove methylene blue (MB) and methyl orange (MO), two of the most common organic dyes, characterized by opposite charge (positive and negative, respectively). The possibility to use chitosan allowed us to combine its great absorption capability with antibacterial properties. Moreover, the adsorption tests showed that by incorporating PEDOT:PSS into the chitosan bubbles the adsorption capability of the system significantly increases up to reach a removal of more than 80% within 1 hour (Fig.1 shows data obtained using MB as target pollutant). These results demonstrate that the adsorption capability does not depend only on the chitosan matrix, but can be trimmed and further improved by adding biocompatible, environment-friendly polymeric blends, endowed with an extended  $\pi$ -conjugated system. This enhanced adsorption, combined with the natural antibacterial activity of chitosan, represents a major advancement with respect to our previous works on alginate bubbles [3,4].

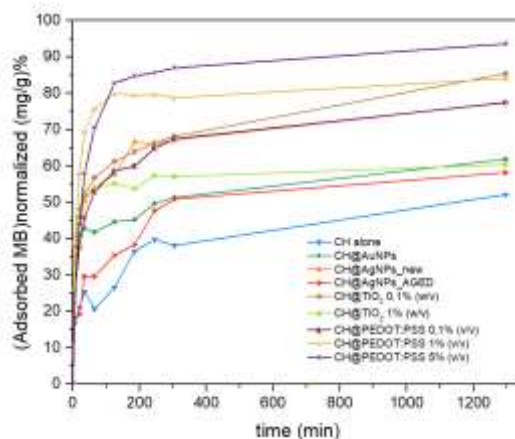


Figure 66: Adsorption curve of MB treated with the studied systems.

On the other end, the binary system composed of chitosan and TiO<sub>2</sub> Degussa P25 shows interesting photocatalytic properties that allow to eliminate the MB remaining into solution through photodegradation in less than 1 hour (Fig.2). In this regard, we noted the unexpected activity of bubbles containing only chitosan in MB photodegradation, which is comparable to that of analogous bubbles loaded with AuNPs and even better than bubbles with AgNPs. These results are confirmed by mass-spectrometry data. The origin of this enhanced activity is currently under investigation.

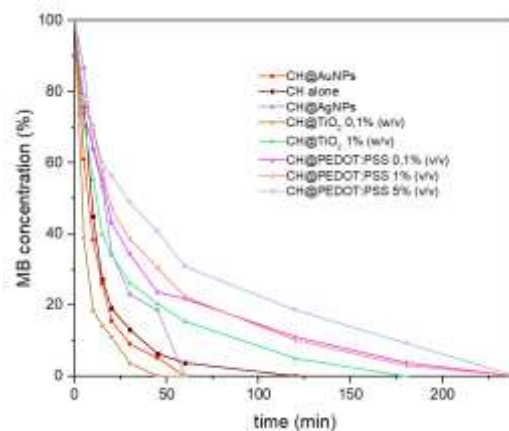


Figure 67: Photodegradation curve of MB treated with the studied systems under solar illumination.

All of the systems investigated in this study were less efficient in removal of MO, which is an anionic dye, with the only exception of the bubbles loaded with TiO<sub>2</sub>, which result in a full degradation of the dye.

This work demonstrates that food waste can be recovered and transformed into value-added materials for environmental remediation, whose functional properties can be rationally designed and controlled by a synergistic combination of individual, active components, such as polymer blends or photocatalytic nanoparticles.

## Acknowledgements

M. M. acknowledges ENEA for partially supporting her PhD scholarship in the framework of the program “Smart agriculture for the sustainability of the agro-food system”.

I.V.'s research activity was partially funded by the Italian Ministry of University and Research (MUR) through the PRIN project NOMEN (2017MP7F8F).

G.R. research activity is supported by DII, in the framework of “Dipartimento di Eccellenza 2018-2022” program.

## References

1. European Commission, Report T: *Preparatory Study on Food Waste Across Eu* 27. 2010.
2. Maddaloni M, Vassalini I, Alessandri I: **Green Routes for the Development of Chitin/Chitosan Sustainable Hydrogels**. *Sustain Chem* 2020, **1**:325–344.
3. Vassalini I, Ribaldo G, Gianoncelli A, Casula MF, Alessandri I: **Plasmonic hydrogels for capture, detection and removal of organic pollutants**. *Environ Sci Nano* 2020, **7**:3888–3900.
4. Vassalini I, Bontempi N, Federici S, Ferroni M, Gianoncelli A, Alessandri I: **Cyclodextrins enable indirect ultrasensitive Raman detection of polychlorinated biphenyls captured by plasmonic bubbles**. *Chem Phys Lett* 2021, **775**.

## Assessment of the H<sub>2</sub>S adsorption capacity of carbonaceous solids produced by pyrolysis of the major organic components of manure digestate

Á. Navarro-Gil\*, N. Gil-Lalaguna, I. Fonts, J. Ruiz, J. Ceamanos, J. Ábrego, G. Gea  
 Thermochemical Processes Group (GPT), Aragon Institute for Engineering Research (I3A)  
 University of Zaragoza, C/ Mariano Esquillor s/n, 50018 Zaragoza, Spain  
 africa@unizar.es

### Abstract

Manure is one of the main organic residues generated in intensive livestock farming. This residue, together with others from the livestock and agricultural sector, can be treated through anaerobic co-digestion to obtain combustible biogas that could be used as energy source on the farm itself. However, the concentration of some biogas pollutants, such as H<sub>2</sub>S, should be reduced to limit gas emission and broaden biogas fuel applications [1]. For example, high H<sub>2</sub>S concentration hinders biogas use for internal combustion engines. The content of H<sub>2</sub>S in biogas is directly related to the amount of sulfur introduced into the digester, which varies according to the raw material to be treated [2]. In the case of manure, it might have high sulfur content due to the presence of this element in the proteins that take part in its organic structure. During anaerobic co-digestion, a solid by-product (digestate) is produced, which, up to date, has been mainly used as a fertilizer in agricultural soils. However, exceeding nitrogen intake in vulnerable areas soils generates serious environmental issues. Therefore, alternative management ways for these agricultural residues should be developed. For instance, the integration of thermochemical treatments, such as pyrolysis, together with the anaerobic digester, to obtain a low-cost adsorbent useful for cleaning biogas will contribute to sustainable waste management and circular economy in livestock areas. Through pyrolysis of the solid digestate of manure (SDM), the biomass is thermally decomposed in an inert atmosphere to obtain a solid (char) with suitable structural and textural properties for its use in capturing H<sub>2</sub>S [3, 4]. The composition of SDM is highly variable depending on the type of farm, the residues co-digested with manure, animals feeding and even the season of the year in which it is collected. Therefore, it is necessary to analyze the effect of SDM composition on the preparation of the char and its capability to retain H<sub>2</sub>S. This study can be approached through the analysis of the H<sub>2</sub>S adsorption behavior of the carbonaceous solids obtained from the main organic components of SDM, such as cellulose, lignin and proteins.

Pyrolysis experiments of SDM and of its main organic components have been carried out in a fixed-bed reactor of 5 – 10 g capacity at two different temperatures (550 and 750 °C) with a heating rate of 10 °C/min and maintaining for 1 h the final temperature under 45 mL (STP)/min of N<sub>2</sub>. The H<sub>2</sub>S adsorption capacities of the produced pyrolysis chars have been studied in a fixed-bed reactor equipped with a mass spectrometer to monitor the effluent gas composition. In each experiment, 0.6 g of char was packed in the fixed-bed. The concentration of H<sub>2</sub>S in the gas was set at 1 % vol. The adsorption tests involved both an adsorption and desorption cycle of H<sub>2</sub>S. The H<sub>2</sub>S adsorption has been carried out during 3 h at 25 °C with a gas mixture of Ar, N<sub>2</sub> and H<sub>2</sub>S and the desorption process extended during 30 min at 150 °C with Ar. The total flow rate of gas passed through the adsorbent bed at a rate of 65 mL (STP)/min of gas. The content of sulfur remaining in the chars after the H<sub>2</sub>S adsorption – desorption cycle was analyzed (elemental analyzer LECO CHN628 with sulfur analyzer module) to quantify the sulfur chemically retained in the char. The adsorption capacity of each char was calculated by adding the amount desorbed, determined by the integration of the area below the desorption curve (mL (STP)/min of H<sub>2</sub>S leaving the reactor vs. time during the desorption step) and the S retained in the chars (expressed as H<sub>2</sub>S) after adsorption-desorption cycle. The breakthrough time was set as the time up to reaching a concentration of H<sub>2</sub>S in the exit gas of 1000 ppm, which represent 10 % of the inlet gas concentration.

The specific surface area of the chars has been determined by adsorption and desorption tests with N<sub>2</sub> at 77 K and CO<sub>2</sub> adsorption at 273 K. Data from N<sub>2</sub> adsorption isotherms have been analyzed according to Brunauer-Emmett-Teller (BET) model, while data from CO<sub>2</sub> isotherms have been analyzed with Dubinin-Radushkevich (DR) theory and non-local density functional theory (NLDFT), by assuming slit pore geometry, to determine the pore size distribution.

Table 1 shows the adsorption capacity (mg H<sub>2</sub>S/g char) and the amount desorbed (mg H<sub>2</sub>S des/g char) for all the char samples obtained at both pyrolysis temperatures. The pyrolysis temperature had a significant influence on the H<sub>2</sub>S adsorption capacities of the produced biochars. When the pyrolysis temperature increased from 500 to 750 °C, both the H<sub>2</sub>S adsorption total capacity and the content of sulfur retained in the chars after desorption increased, except for soybean protein char. The results also showed that as pyrolysis temperature increased, the breakthrough time was longer, moving from 4 min to 9 min for cellulose char, and from 1 min to 4 min for SDM char. This suggests that higher pyrolysis temperatures improve anyway the adsorption properties of biochar. Lignin and soybean protein chars hardly showed breakthrough times in any case, as H<sub>2</sub>S concentration in the inlet gas exceeded 1000 ppm almost instantly. However, this does not mean that H<sub>2</sub>S adsorption has not occurred, but that it occurs slowly. In fact, lignin char showed the highest adsorption capacity (37.6 mg/g), followed by SDM char (25.3 mg/g), cellulose char (23.1 mg/g) and soybean protein char (2.9 mg/g).

Table 2. Adsorption capacity of chars at 1 vol. % of H<sub>2</sub>S in the gas

	Char at 550 °C		Char at 750 °C	
	mg H <sub>2</sub> S ads / g char	mg H <sub>2</sub> S des / g char	mg H <sub>2</sub> S ads / g char	mg H <sub>2</sub> S des / g char
Cellulose	14.6	12.6	23.1	19.7
Lignin	29.1	11.2	37.6	15.1
Soybean Protein	5.4	2.1	2.9	1.3
SDM	12.2	2.2	25.3	5.8

If H<sub>2</sub>S is chemisorbed over the different solids, their sulfur contents after the H<sub>2</sub>S adsorption-desorption cycle should be greater than before the cycle. Figure 1 reports the sulfur content of the chars before and after the H<sub>2</sub>S adsorption – desorption cycle. The chars produced from lignin and SDM showed a greater chemical retention of sulfur (once the desorption step had been conducted), containing 1.8 and 3.2 wt. % of sulfur in the chars obtained at 750 °C, respectively, while the sulfur content in the cellulose and soybean protein chars was much lower (0.4 wt. % in all cases). These results suggest that the lignin-derived fraction is the organic component that contributes the most to H<sub>2</sub>S retention in SDM char. Taking into account the lignin fraction contained in SDM (< 20 wt.%) and the significant increase in sulfur content found in SDM (from 1.5% in the pristine char produced at 750 °C to more than 3% after the H<sub>2</sub>S adsorption-desorption cycle), it may be stated that other components in SDM, probably the ashes, may contribute greatly to the chemical retention of H<sub>2</sub>S.

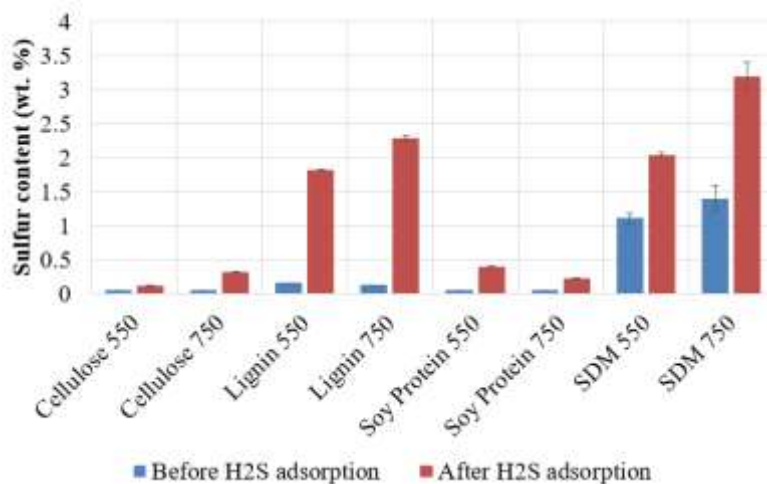


Figure 1. Sulfur content adsorbed on char before and after adsorption – desorption cycle of 1 % vol. of H<sub>2</sub>S

Cellulose and lignin chars present higher H<sub>2</sub>S adsorption capacities, BET surfaces and micropore volumes than char from soybean protein. In the case of these materials, the analysis of their structural properties showed a direct relationship between the H<sub>2</sub>S adsorption capacity and both the surface area and the micropore volume. However, the soybean protein and SDM chars showed the same microporous volume, but not the same adsorption capacity, so any other characteristics in these chars seem to affect the H<sub>2</sub>S adsorption process.

In summary, the results obtained show that chars from livestock waste, such as SDM, could be successfully used as low-cost adsorbent solids for the adsorption of H<sub>2</sub>S. Cellulose and lignin chars have higher adsorption capacities than soybean protein char, which barely retains H<sub>2</sub>S. Therefore, among the organic constituents, the lignocellulosic structure in SDM is the main responsible for its adsorption capacity. Moreover, lignin is the only one that produces a char able to retain chemically H<sub>2</sub>S in a significant proportion. Due to the presence of lignin, the H<sub>2</sub>S adsorption mechanism in SDM char combines physisorption and chemisorption processes.

## Acknowledgements

The authors would like to express their gratitude to the Aragon Government (Ref. T22\_20R) for financial support, co-financed by the FEDER 2014-2020 "Building Europe from Aragon" and the MICINN (PID2019-107200RB-100). A. Navarro acknowledges the FPI help received (PRE2020-093382). I. Fonts acknowledges the MINECO, European Social Fund, AEI and the University of Zaragoza for the post-doctoral contract awarded (RYC2020-030593-I).

## References

1. Ayiania, M., Carbajal-Gamarra, F. M., García-Perez, T., Frear, C., Suliman, W., Garcia-Perez, M. *Biomass and Bioenergy*, 120, 339-349 (2019)
2. Choudhury, A., Lansing, S. *Journal of Environmental Chemical Engineering*, 9, 104837 (2021)
3. Shang, G., li, Q., Liu, L., Chen, P. and Huang, X. *Journal of the Air & Waste Management Association*, 66:1, 8-16 (2016)
4. Hervey, M., Minh, D., Gérente, C., Weiss-Hortala, E., Nzihou, A., Villot, A., Le Coq, L. *Chemical Engineering Journal*, 334, 2179-2189 (2018)

## Determining antibacterial effect of liquid soaps from recycled cooking oil and distinct essential oils

Mira İcğören<sup>1</sup>, Zeynep Elif Ölmez<sup>2</sup> and Ceren Özçelik<sup>3</sup>

<sup>1,2</sup> Hisar School, Istanbul, Turkey; <sup>3</sup>Boğaziçi University, Istanbul, Turkey

mira.icgoren@hisarschool.k12.tr, zeynep.olmez@hisarschool.k12.tr, \*ceren.ozcelik@boun.edu.tr

### Abstract

This study aimed to determine bacterial growth in liquid soap produced from recycled cooking oil and different essential oils. The study further investigated the in vitro antibacterial effect of essential oils combined with the same liquid soap. The liquid soaps were made by a saponification reaction of KOH and recycled cooking oil. Three experimental groups of liquid soap containing clove, thyme, and peppermint essential oils were created along with a control group. Each sample was serially diluted properly with saline solution. The soap solutions were mixed with the gram-negative bacteria *Escherichia Coli* (*E. Coli*). These mixtures were inoculated into the agar medium. The streak plate method was utilized to see a possible bacterial growth in each soap sample, and the spread plate method was used to determine the antibacterial effect of the soaps at different concentrations and essential oils against *E. Coli*. A qualitative visual comparison of the plates was made to determine bacterial growth and the antibacterial effect of each sample. Overall, the results revealed no bacterial growth in the samples. The sample with the peppermint essential oil showed the highest antibacterial effect.

**Keywords:** antibacterial effect; essential oils; recycled soap

### Introduction

Soaps are cleaning agents which are essential for daily sanitary practices such as removing bacteria, foul odors, and stains. The antibacterial/antimicrobial property of soap signifies that it inhibits the growth of or kills bacteria, playing a significant role in human health. The main ingredients of soaps are oil, water, and lye. They are made as a result of a saponification reaction, consisting of the hydrolysis of triglycerides when they are reacted with an aqueous lye solution and the production of glycerol and a fatty acid salt, which is the soap. Besides the main ingredients, essential oils included in the final product may provide different properties to the soaps. In this investigation, recycled cooking oil, thyme, peppermint, and clove essential oils were utilized to produce liquid soap samples. Peppermint essential oil mainly contains menthol and menthone, showing significant antimicrobial and antiviral characteristics [4]. Thyme and its constituent thymol were also found to have an antibacterial effect against several bacteria [2]. Clove essential oil consists of phenylpropanoids such as carvacrol, thymol, eugenol and cinnamaldehyde, and it shows antibacterial activity [1].

### Significance of the Study

The aspect that distinguishes this study from other research with a similar objective is that recycled cooking oil is used when making the soap. While other research has determined the antibacterial effect of different essential oils with regular soap or different types of bacteria, the driving factor for this study was environmental concerns regarding waste management. Based on the literature, this study investigated the effectiveness of essential oils used as antibacterial agents in soaps made from recycled cooking oil and if bacterial growth is seen.

### Method













The two research questions that guide this study are: (1) Is there bacterial growth in soaps produced by recycled cooking oil and different essential oils? (2) Is there a difference between the antibacterial effectiveness of the soaps produced by recycled cooking oil and distinct essential oils on *Escherichia Coli* in vitro conditions? For sampling, three experimental groups of liquid soap separately containing clove (*Eugenia caryophyllus*), thyme (*Thymus vulgaris* L.), and peppermint essential oils (*Mentha piperita* L.), and a control group were created. The control group had only the liquid soap made of recycled cooking oil, without essential oils. The liquid soaps were made by a saponification reaction: the aqueous solution of KOH and 1000 grams of recycled cooking oil were combined and blended thoroughly. The essential oils were added respectively in the samples in the same amount. All the equipment used, the agar, and the salt solutions were autoclaved at 121°C for 15 minutes. The sample groups were serially diluted until 10<sup>-3</sup> with 0.85% isotonic sterile salt solution. The soap solutions were mixed with the gram-negative bacteria *Escherichia Coli* (*E. Coli*). Then, these mixtures were inoculated into the LB-Broth agar medium using the streak plate method to see the bacterial growth in each sample and using the spread plate method to determine the antibacterial effect of the soaps at different concentrations and essential oils against *E. Coli*. The soap samples mixed with *E. Coli* were incubated at 37 °C for 24 hours [3]. All data was analyzed qualitatively by visual comparison at the end of the 24 hours. The conclusions made were based on the fact that the antibacterial effect is inversely proportional to the number of bacterial colonies counted on the plate.

### Results and Conclusion

Overall, the results of the first research question of our study revealed no bacterial growth in the samples. All samples with different essential oils and the control group showed some antimicrobial properties. The liquid soap sample with the peppermint essential oil showed the highest antibacterial effect in higher concentrations, the

sample with clove essential oil exerted the second-highest, and the sample with thyme essential oil exerted the third-highest antibacterial effect. The control group showed an antimicrobial effect only in  $10^{-1}$  concentration. The findings of this study support that peppermint essential oil can be effectively used as an antibacterial agent with recycled cooking oil in soapmaking.

Table 1: The visuals of the *E.Coli* and soap samples incubated at 37 °C for 24 hours.

Sample Concentrations:	$10^{-1}$	$10^{-2}$	$10^{-3}$
The control group without essential oil			
Peppermint Essential Oil			
Thyme Essential Oil			
Clove Essential Oil			

## References

1. Chaieb, Kamel, et al. "The chemical composition and biological activity of clove essential oil, *Eugenia caryophyllata* (*Syzygium aromaticum* L. Myrtaceae): a short review." *Phytotherapy Research: An International Journal Devoted to Pharmacological and Toxicological Evaluation of Natural Product Derivatives* 21.6 (2007): 501-506.
2. Juven, B. J., et al. "Factors that interact with the antibacterial action of thyme essential oil and its active constituents." *Journal of applied bacteriology* 76.6 (1994): 626-631.
3. Lim, Ji Youn et al. "A brief overview of *Escherichia coli* O157:H7 and its plasmid O157." *Journal of microbiology and biotechnology*, 20,1 (2010): 5-14.
4. McKay, Diane L., and Jeffrey B. Blumberg. "A review of the bioactivity and potential health benefits of peppermint tea (*Mentha piperita* L.)." *Phytotherapy Research: An International Journal Devoted to Pharmacological and Toxicological Evaluation of Natural Product Derivatives* 20.8 (2006): 619-633.

## Sustainable resource recovery from waste printed circuit boards using green solvents

Snigdha Mishra<sup>1,2</sup>, K.K. Pant<sup>1\*</sup>, David Harbottle<sup>2</sup>, Bhoopesh Mishra<sup>3</sup>

<sup>1</sup>*Green and Sustainable Engineering lab*

*Department of Chemical Engineering, Indian Institute of Technology Delhi, India*

<sup>2</sup>*School of Chemical and Process Engineering, University of Leeds, Leeds, UK*

<sup>3</sup>*Illinois Institute of Technology, Chicago, IL*

\*kkpant@chemical.iitd.ac.in

### Abstract text:

Pyrometallurgy and Hydrometallurgy are abundantly used technologies to produce metals from ores. With certain drawbacks in terms of toxic gases discharge and excessive aqueous waste generation has led to emerging of an alternative greener route<sup>1-3</sup>. Solvometallurgy, is a branch which deals with non-aqueous solutions mainly deep eutectic solvents or ionic liquids. High selectivity, low water consumption makes solvometallurgy a suitable process for low concentration ores and also for heterogeneous waste mixture<sup>4</sup>.

Low grade ores or secondary urban mines are a challenging feedstock to extract out metals. Ores are present in various forms such as oxides, sulfides, carbonates, phosphates, silicates, etc. Oxide's form of metals is soluble in either strong acidic solution or basic solution<sup>4</sup>. In recent years, Ionic liquids has been explored as a potential solvent to recover metals but its highly complex synthesis process, high cost limits its use at industrial scale<sup>5</sup>. Deep eutectic solvents (DES) are simple mixture made up of cheap, readily available naturally occurring chemicals. DES is a mixture of Hydrogen Bond Donors which are generally alcohols, amides, organic acids and Hydrogen Bond Acceptors mainly ammonium salt. It can be tuned to certain property by varying molar ratio or altering Hydrogen Bond Donor.

Chemicals used in this work is used as received without purification. Choline Chloride (99 wt %), Oxalic Acid (99 wt %), Malonic Acid (99 wt%) were purchased from Merck. Copper oxide and silver oxide was purchased from Sigma Aldrich. Crushed printed circuit boards (PCB) are taken from Exigo India Pvt. Ltd. Change in viscosity of solvent was measured by Anton Paar MCR302 Rotational and Oscillatory Rheometer. Thermal degradation of solvents was studied by Thermo Gravimetric Analyser in range of 25°C to 800°C taking 10–20 mg of sample in nitrogen atmosphere. Infrared spectra were recorded on a Nicolet iS50 FTIR spectrophotometer equipped with ATR crystal detector. The metal concentration of the filtered sample was determined by Microwave Plasma Atomic Emission Spectroscopy (MPAES). The filtered sample were diluted by Millipore water. The samples were diluted upto 1000 times to have final metal concentration lower than 50 ppm. Triplicate experiments were conducted and was taken average to reach proper conclusion.



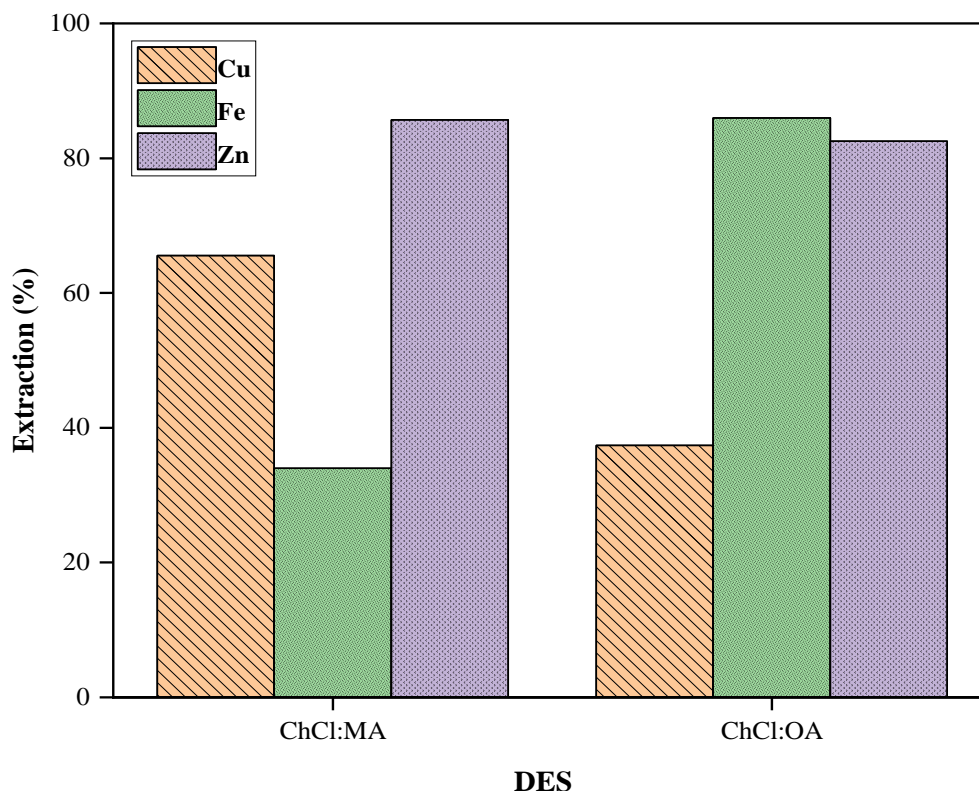


Figure 1. Metal extraction from waste PCB in Choline chloride: Oxalic acid and Choline chloride: Malonic acid-based DES 0.2 g oxidized PCB in 20 ml solution; 24 h; 50°C; 200 rpm

Figure 1 represents extraction of metals from oxidized printed circuit board into choline chloride dicarboxylic acid-based DES. It was observed that in malonic acid-based DES, 34 % extraction of iron took place, which is less as compared to oxalic acid extraction of 88 %. Copper extraction is 68 % in malonic acid-choline chloride DES while in oxalic acid-based DES, copper extraction is less than 40 %. Several factors play a role in the difference in solubility prominent one is pKa value of oxalic acid which is lower as compared to malonic acid.

#### Acknowledgements

Authors would like to thank the office of Principal Scientific Adviser to the Government of India for research grant under DRIIV scheme.

#### References

1. J. Heelan, E. Gratz, Z. Zheng, Q. Wang, M. Chen, D. Apelian and Y. Wang, *JOM*, 2016, 68, 2632–2638.
2. J. Cui and L. Zhang, *Journal of Hazardous Materials*, 2008, 158, 228–256.
3. A. Behnamfard, M. M. Salarirad and F. Veglio, *Waste Management*, 2013, **33**, 2354–2363.
4. A. Shishov, A. Gerasimov and A. Bulatov, *Food Chemistry*, 2021, 130634.
5. A. K. Jangir, P. Sethy, G. Verma, P. Bahadur and K. Kuperkar, *Journal of Molecular Liquids*, 2021, **332**, 115909.

## Transforming CO<sub>2</sub> and Sea Water to Green HYDROGEN & Green CEMENT Using Magnesium Waste Scrap

Rajesh Belgamwar, Vivek Polshettiwar

Department of Chemical Sciences, Tata Institute of Fundamental Research (TIFR), Mumbai,  
Email: vivekpol@tifr.res.in

### Abstract:

Excessive CO<sub>2</sub> emissions are a major cause of climate change, and hence reducing the CO<sub>2</sub> levels in the Earth's atmosphere is key to limit adverse environmental effects. Capture and then conversion of CO<sub>2</sub> to useful materials and fuels are the best ways to tackle these challenges. Our group has carried out several works in the field of catalysis & nanotechnology, such as DFNS<sup>1</sup>, Black Gold<sup>2</sup>, Defective Nanosilica<sup>3</sup>, Solid Acids<sup>4</sup>, LSN<sup>5</sup> to combat climate change.

Recently, we stumbled upon something truly unexpected and surprising. Magnesium Nanoparticles Convert CO<sub>2</sub> to Methane and Methanol using Pure Water as Hydrogen Source and at Room Temperature and Atmospheric Pressure (Figure 1).<sup>6</sup> This conversion took place within a few minutes.

Notably, no external energy (thermal, light or electric) was required, and reaction took place at room temperature. There was also no need of sacrificial reagent or co-catalysts for this conversion to proceed. Magnesium is the eighth most common element and the sixth most abundant metal, and hence this fundamental discovery has excellent potential to develop a commercial process for CO<sub>2</sub> conversion.

Although Magnesium is known as a powerful reducing agent but in the form of Grignard reagents and organometallic Mg-complexes. Pure magnesium was not used, and it was always assisted with a magnesium halide, hydride, and HgCl<sub>2</sub>, etc., for organic transformations. Few reports are also found in the literature on studies of CO<sub>2</sub> and Mg metal/metal oxide interactions, but no reports were found about Mg (metal, oxides or complexes) converting CO<sub>2</sub> to methane using water at room temperature and pressure.

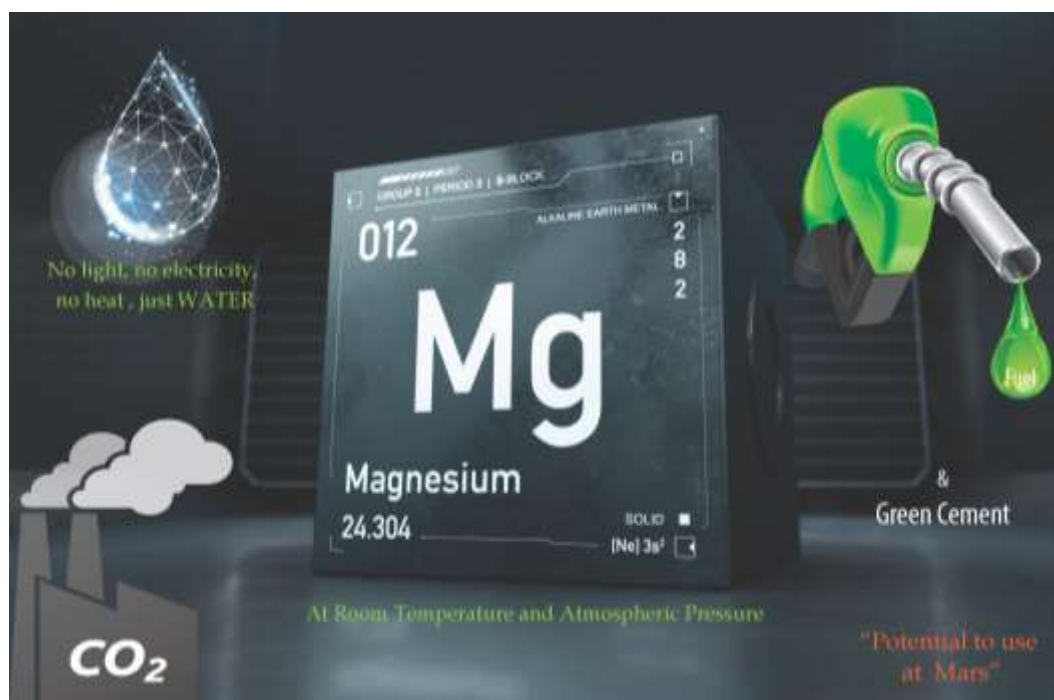


**Figure 1:** CO<sub>2</sub> Mitigation using Magnesium and water.

Our mechanistic studies indicate a unique cooperative act of magnesium, basic magnesium carbonate, CO<sub>2</sub> and water, to convert CO<sub>2</sub> to methane, methanol and formic acid. In the absence of any one of these, no CO<sub>2</sub> conversion takes place. Isotopic labeled <sup>13</sup>CO<sub>2</sub> experiment, PXRD, NMR, and FTIR studies allowed us to identify reaction intermediates and overall reaction pathway.<sup>6</sup>

I will present this work in the oral talk.

## References:

1. Maity, Polshettiwar et al. *Nature Protocol*, **2019**, *14*,2177.
2. Dhiman, Polshettiwar et al. *Chemical Science* **2019**, *10*, 6694.
3. Mishra, Polshettiwar et al. *Proc. Natl. Acad. Sci. U.S.A* **2020**, *117*, 6383.
4. Maity, Polshettiwar et al. *Nature Comm.* **2020**, *11*, 3828.
5. Belgamwar, Polshettiwar et al. *Chemical Science* **2021**, *12*, 4825.
6. Rawool, Polshettiwar et al. *Chemical Science* **2021**, *12*, 5774.

## Regulation of lignin-modifying enzymes production in lignocellulose fermentation by new white-rot basidiomycete *Trametes lactinea*

Mariam Rusitashvili\*, Vladimir Elisashvili

Institute of Microbial Biotechnology, Agricultural University of Georgia, 240 Aghmashenebeli alley, Tbilisi, Georgia

\*mrusi2010@agruni.edu.ge

White-rot basidiomycetes (WRB) are known to be efficient lignocellulose degraders and they are recognized for their unique capability to degrade lignin secreting lignin peroxidase (EC 1.11.1.14), manganese-dependent peroxidase (EC 1.11.1.13), and laccase (EC 1.10.3.2), which function together with hydrogen peroxide-producing oxidases. Besides their fundamental importance for efficient bioconversion of plant residues in nature, lignin-modifying enzymes (LME) may have a large variety of biotechnological and environmental applications requiring huge amounts of these biocatalysts at a low cost. These demands have intensified the search for new potent fungi overproducing LME with industrially relevant properties. Various approaches and strategies, such as supplementation of nutrient media with food industry wastes/by-products, favourable carbon and nitrogen sources at an appropriate concentration and addition of effective inducers have been explored to accelerate the LME synthesis and increase their yield [1, 2]. Hence, the main objective of the present work was to elucidate the features and modulation of LME activity of recently isolated Georgian fungus *Trametes lactinea* in response to different lignocellulosic materials, nitrogen sources and inducers.

The submerged cultivation of fungus was conducted in Innova 44 shaker (New Brunswick Scientific, USA) at 27°C and 160 rpm. The homogenized mycelium (3 mL) was used to inoculate the 250-mL flasks containing 100 mL of the basal medium (per litre): 1 g KH<sub>2</sub>PO<sub>4</sub>, 0.5 g MgSO<sub>4</sub> · 7H<sub>2</sub>O, 0.07 g CuSO<sub>4</sub> · 5H<sub>2</sub>O, 5 g glucose, 3 g peptone, 3 g yeast extract. Lignocellulosic materials in the amount of 40 g/L were used as growth substrates. All plant residues were dried at 50°C and milled to powder. Laccase activity was determined spectrophotometrically (Camspec M501, Cambridge, UK) at 420 nm as the rate of 0.25 mM ABTS (2,2'-azino-bis-(3-ethylthiazoline-6-sulfonate)) oxidation in 50 mM Na-acetate buffer (pH 3.8) at room temperature. MnP activity was measured by oxidation of Phenol Red in the presence of 0.1 mM H<sub>2</sub>O<sub>2</sub>. LiP activity was determined spectrophotometrically at 310 nm by the rate of oxidation of 2 mM veratryl alcohol in 0.1 M sodium tartrate buffer (pH 3.0) with 0.2 mM hydrogen peroxide. One unit (U) of LME activity was defined as the amount of enzyme that oxidized 1 µmol of substrate per minute.

Among twenty-four white-rot fungi belonging to different taxonomic groups and screened for the production of LME in submerged fermentation of mandarin pomace, *Trametes lactinea* appeared to be the best enzyme producer. This fungus was selected for subsequent study of the effect of chemically different lignocellulosic materials on LME production. Results presented in Table 1 show that this fungus is capable to secrete laccase activity in cultivation in a synthetic medium containing 0.5% glucose. However, supplementation of this medium with lignocellulosic substrates significantly increased laccase production. Especially mandarin pomace followed by wheat bran 13- and 9-fold stimulated this enzyme accumulation in the culture liquid. By contrast, vinasse was the poorest substrate for laccase production.

Table 1. Effect of lignocellulosic substrates on *T. lactinea* enzyme activity.

Carbon sources	Laccase (U/mL)	LiP (U/mL)	MnP (U/mL)
Glucose	3 ± 0.3 <sup>5</sup>	0	0
Mandarin pomace	38 ± 4.7 <sup>5</sup>	0.57 ± 0.08 <sup>14</sup>	0.29 ± 0.04 <sup>5</sup>
Wheat bran	26 ± 3.4 <sup>5</sup>	0.16 ± 0.02 <sup>12</sup>	0.10 ± 0.01 <sup>5</sup>
Vinasse	4 ± 0.4 <sup>5</sup>	0.26 ± 0.03 <sup>12</sup>	0.07 ± 0.01 <sup>5</sup>
Rosehip residue	11 ± 1.7 <sup>5</sup>	0.11 ± 0.01 <sup>5</sup>	0.16 ± 0.02 <sup>14</sup>
Pomegranate residue	13 ± 1.6 <sup>5</sup>	0	0.90 ± 0.15 <sup>8</sup>
Banana peels	12 ± 1.0 <sup>5</sup>	0.16 ± 0.02 <sup>14</sup>	0
Corn cobs	7 ± 0.6 <sup>5</sup>	0.12 ± 0.01 <sup>14</sup>	0.10 ± 0.01 <sup>5</sup>

\*The numbers indicate the days of the peak activity.

No LiP and no MnP activities were detected in the fungus cultivation in the basal medium. In the same medium, supplemented with mandarin pomace the highest LiP activity was revealed. At the same time, no LiP was observed during 14 days of the pomegranate residue fermentation. On the contrary, it was this substrate that provided the highest MnP activity. Unexpectedly, no enzyme activity was detected during the entire period of fungus cultivation in the banana peels-containing medium. Then the effect of nitrogen sources was tested; organic compounds (peptone, casein hydrolysate, and yeast extract) favoured laccase, MnP, and LiP production. Among them, casein hydrolysate at a concentration of 80 mM as nitrogen ensured the highest laccase activity.

Finally, the enzymatic activity of *T. lactinea* was evaluated in response to the addition of 0.5 mM of aromatic compounds to the optimised medium. All the tested aromatic compounds promoted the production of laccase (Table 2). Among them, 3,4-dimethyl benzene and xylydine appeared to be the most efficient inducers of laccase synthesis

(almost 10-fold increase in enzyme activity compared to control) while pyrogallol only weakly stimulated enzyme secretion. The effect of aromatic compounds on the fungus LiP activity varied depending on the nature of the chemical compound. In particular, guaiacol and dinitrotoluene two-fold increased the LiP activity of *T. lactinea*, other compounds inhibited the secretion of

Table 2. Effect of aromatic compounds on *T. lactinea* enzyme activity.

Aromatic compounds	Laccase (U/mL)	LiP (U/mL)	MnP (U/mL)
Control	67 ± 8 <sup>9</sup>	0.40 ± 0.05 <sup>9</sup>	0.50 ± 0.04 <sup>14</sup>
Catechol	104 ± 13 <sup>9</sup>	0.30 ± 0.05 <sup>14</sup>	0.53 ± 0.06 <sup>14</sup>
Pyrogallol	87 ± 10 <sup>9</sup>	0.20 ± 0.02 <sup>9</sup>	0.48 ± 0.06 <sup>14</sup>
Dinitrotoluene	210 ± 27 <sup>9</sup>	0.78 ± 0.11 <sup>14</sup>	0.57 ± 0.07 <sup>14</sup>
Guaiacol	244 ± 27 <sup>9</sup>	0.81 ± 0.10 <sup>14</sup>	0.58 ± 0.06 <sup>14</sup>
Ferulic Acid	563 ± 70 <sup>9</sup>	0.27 ± 0.04 <sup>14</sup>	0.54 ± 0.07 <sup>14</sup>
Xylidine	638 ± 81 <sup>9</sup>	0.19 ± 0.03 <sup>9</sup>	0.54 ± 0.08 <sup>14</sup>
3,4-Dimethyl benzene	672 ± 68 <sup>9</sup>	0.13 ± 0.02 <sup>4</sup>	0.55 ± 0.06 <sup>14</sup>

\*The numbers indicate the days of the peak activity.

the enzyme to varying degrees. Such a reaction of a fungal culture to various aromatic compounds makes it possible to obtain enzyme preparations with different ratios of laccase and LiP activities. As regards MnP activity, the production of this enzyme did not significantly depend on the presence of an aromatic compound. Thus, the data received indicate that *T. lactinea* is a promising candidate for scaled-up production of LME.

### Acknowledgements

This research PHDF-21-2806 has been supported by Shota Rustaveli National Science Foundation of Georgia (SRNSFG)

### References

1. P. Chowdhary, N. More, A. Yadav, R.N. Bharagava, *Enzymes in Food Biotechnology* (M. Kuddus, Ed.), Academic Press, Cambridge, MA, USA, 181–195 (2019)
2. V. Elisashvili, M.D. Asatiani, E. Kachlishvili, *Microbial Enzymes and Biotechniques*, (P. Shukla, ed). Springer, Singapore, 107-130 (2020).

## Bio-based thermoset derived from epoxidized soybean oil and agri-waste

M. Safarpour<sup>1,2</sup>, A. Zych<sup>1</sup>, M. Najafi<sup>1, 2</sup>, L. Bertolacci<sup>1</sup>, L. Ceseracciu<sup>3</sup>, A. Athanassiou<sup>1</sup>  
*1 Smart Materials, Istituto Italiano di Tecnologia, Via Morego 30, Genova 16163, Italy*  
*2 DIBRIS, University of Genoa, via Opera Pia 13, Genoa, Italy*  
*3 Materials Characterization Facility, Istituto Italiano di Tecnologia, Via Morego 30, Genova 16163, Italy*

### Abstract

Styrofoam™ is a petroleum-based material widely used in lightweight, protective packaging systems [1]. However, Styrofoam™ is made from non-renewable petroleum resources, is non-biodegradable, it is not recyclable in the vast majority of the existing recycling plants, and can cause chronic, low-level styrene migration into food [2]. As a result, to deal with the environmental pollution concerns, crude oil shortages, and possible serious adverse effects on human health, we propose as an alternative to Styrofoam™, biodegradable, naturally foamed soybean oil-based composites containing high amounts of agri-waste [3].

Bio-based thermosets were synthesized from epoxidized soybean oil (ESO) cross-linked with PRIPOL 1040, a fatty acid trimer. Thanks to the liquid cross-linker, curing of the composites can be performed at relatively low temperature of 80 °C, in the presence of agri-waste, like carrot residue after juice extraction, spinach stems, or tomato peel, without degrading them. Moreover, moisture present in the agri-waste, evaporates during the curing process creating gas bubbles and providing a natural way of foaming. To give a second life to agri-waste in added-value products, up to 50 % by wt. of vegetable waste was incorporated into the ESO-PRIPOL matrix, which in addition improved tensile and compression strength as well. Most importantly, the composites are biodegradable in marine environments preventing their long-term bioaccumulation in the ecosystem.

### References

1. B. Jethy, S. Paul, S. K. Das, A. Adesina, S. M. Mustakim, Critical review on the evolution, properties, and utilization of plastic wastes for construction applications, *Journal of Material Cycles and Waste Management*, 2022, 1-17.
2. N. Nismah, U. Suratman, A. Sheila Puspita, K. Mohammad, Effect of Styrofoam Waste Feeds on the Growth, Development and Fecundity of Mealworms (*Tenebrio molitor*), *OnLine Journal of Biological Sciences*, 2018, 18 (1).
3. R. Mustapha, A. R. Rahmat, R. Abdul Majid, S. N. H. Mustapha, Vegetable oil-based epoxy resins and their composites with bio-based hardener: a short review. *Polymer-Plastics Technology and Materials*, 2019, 58 (12), 1311-1326.

## Bio-based PLA/PHB plasticized blend films with eugenol for active food packaging applications

Aikaterini Spanou<sup>1\*</sup>, Francesco Bigi<sup>2</sup>, Enrico Maurizzi<sup>3</sup>, Andrea Quartieri<sup>2</sup> and Theofania Tsironi<sup>1</sup>

<sup>1</sup>Agricultural University of Athens, 75 Iera Odos 11855, Greece

<sup>2</sup> Packtin, Via Del Chionso, 14/I Reggio Emilia (RE), 42122, Italy

<sup>3</sup> Department of Life Sciences, University of Modena and Reggio Emilia, Via John Fitzgerald Kennedy 17/I, Reggio Emilia (RE), Italy

\* *sp.katerin@aua.gr*

### Abstract

Poly(lactic acid) (PLA) is a biopolymer obtained from renewable resources, with similar properties to several conventional synthetic polymers [1,2]. Poly(hydroxybutyrate) (PHB) is an aliphatic polyester, synthesized by microorganisms, with high biodegradability and biocompatibility [2]. PLA/PHB blends have gained significant interest, since the combination of the two biopolymers can create new biomaterials with interesting physical, thermal, and mechanical properties as compared to the single components [1,3]. Eugenol is the basic compound of clove essential oil, is “generally recognized as safe” (GRAS) and is known for its antimicrobial and antioxidant activities [4].

The objective of the study was to develop films by using a blend of PLA and PHB in a ratio 80/20 and glycerol monolaurate (GML) as a plasticizer (10% w/w of polymers). Eugenol was added as an active compound at different concentrations (0, 0.1, 0.25, 0.5 and 1.0% v/v). The films were evaluated regarding their mechanical properties (tensile strength, elastic modulus, elongation at break), optical (color, opacity value, light transmittance) and barrier properties (UV barrier), permeability properties (water vapor transmission rate, WVTR, and water vapor permeability, WVP), hydrophobicity (contact angle), and antimicrobial properties (*in vitro* testing & *in vivo* testing as packaging materials for fresh fish fillets). The overall aim of the study was to determine the optimum concentration of eugenol for the development of active packaging for food applications.

The PLA (TotalEnergies Corbion, Rayond, Thailand)/PHB (Kaneka Biopolymers, Tokio, Japan)/GML (BASF, Bologna, Italy)/Eugenol (Sigma-Aldrich, Milan, Italy) blended films were produced by solvent casting method, and chloroform (MERCCK, Milan, Italy) was used to dissolve all the materials (5% w/v sol.). All films were casted with the TQC Sheen, Automatic Film Applicator (Essen, Germany). The mechanical properties were determined using a dynamometer (Z1.0, Zwick/Roell, Ulm, Germany) according to ASTM standard method D882-02, and the software TestXpert®II (V3.31) (Zwick/Roell, Ulm, Germany) was used. The optical and UV barrier properties were estimated with the VWR®Double Beam UV-VIS 6300 PC spectrophotometer (China) and the CR-400 Minolta colorimeter (Minolta Camera, Co., Ltd., Osaka, Japan). For the determination of the hydrophobicity of the films, Theta Flow Optical Tensiometer (Biolin Scientific, Gothenburg, Sweden) was used. The WVTR was determined gravimetrically according to the ASTM E96 method, while the WVP was calculated with the use of the appropriate equations. The antimicrobial activity was determined with a disk diffusion assay (*P. fluorescens* ATCC 13525, *E. coli* UNIMORE 40522). The applicability of the developed films for food packaging applications was evaluated for fresh fish (gilthead seabream) fillets stored at refrigerated conditions (2 °C).

The key results of this research are summarized below. Regarding the mechanical properties, the tensile strength and the elastic modulus decreased as the concentration of eugenol increased, while elongation at break increased (*Figure 1*). The total color difference increased in parallel to the concentration of the active compound (*Table 1*). Moreover, the transmittance and the absorbance of the films in the UV-vis spectrum (190-1100 nm) can be reported in *Figure 2*. The WVP calculated for the control film was 1,46 g·mm/(m·day·kPa), and it was increased in films with higher eugenol concentrations. The contact angle decreased as the concentration of eugenol increased (*Table 2, Figure 3*), meaning that the addition of eugenol resulted in higher hydrophobicity of the films. The antimicrobial activity of the films against *P. fluorescens* was enhanced by increasing the concentration of eugenol, while eugenol was not effective against *E. coli*.

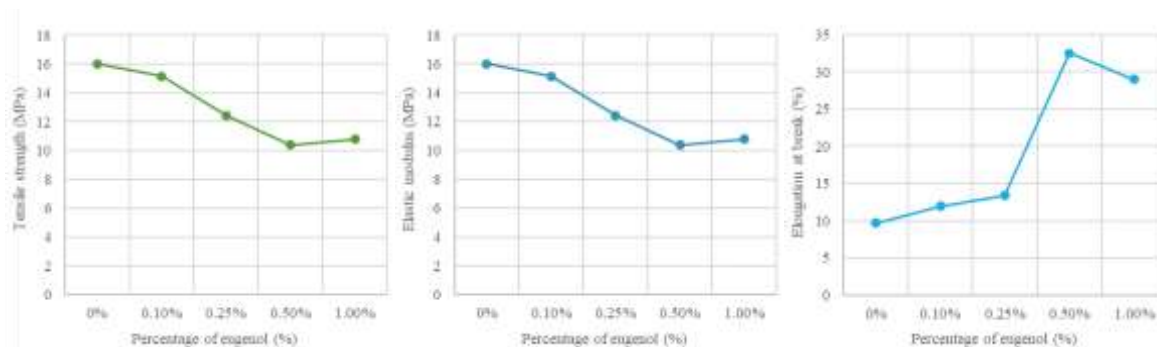


Figure 1. Mechanical properties of the films: i) tensile strength, ii) elastic modulus, iii) elongation at break.

Table 1. Color parameters ( $L^*$ ,  $a^*$  and  $b^*$ ) and total color difference ( $\Delta E^*$ ) of the films.

Film Sample	Color parameters			
	$L^*$	$a^*$	$b^*$	$\Delta E^*$
PLA/PHB	99.34	-0.19	-0.22	0.14
PLA/PHB 0.1% eugenol	99.28	-0.20	-0.10	0.13
PLA/PHB 0.25% eugenol	99.40	-0.15	-0.11	0.16
PLA/PHB 0.5% eugenol	99.28	-0.19	0.02	0.20
PLA/PHB 1.0 % eugenol	99.23	-0.26	0.00	0.23

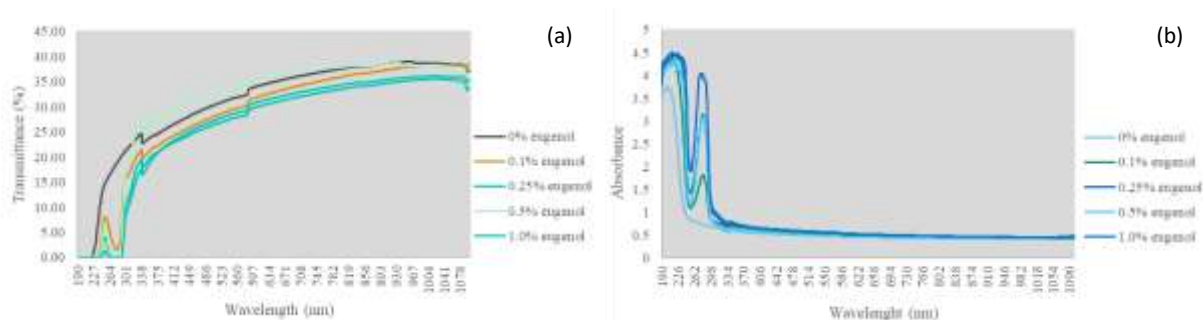


Figure 2. (a) Transmittance (%) and (b) Absorbance of the films in the UV-vis.

Table 2. Contact Angle of the films.

Eugenol (%)	0%	0.10%	0.25%	0.50%	1.00%
Contact Angle ( $^\circ$ )	65.30	69.79	73.61	76.98	80.33

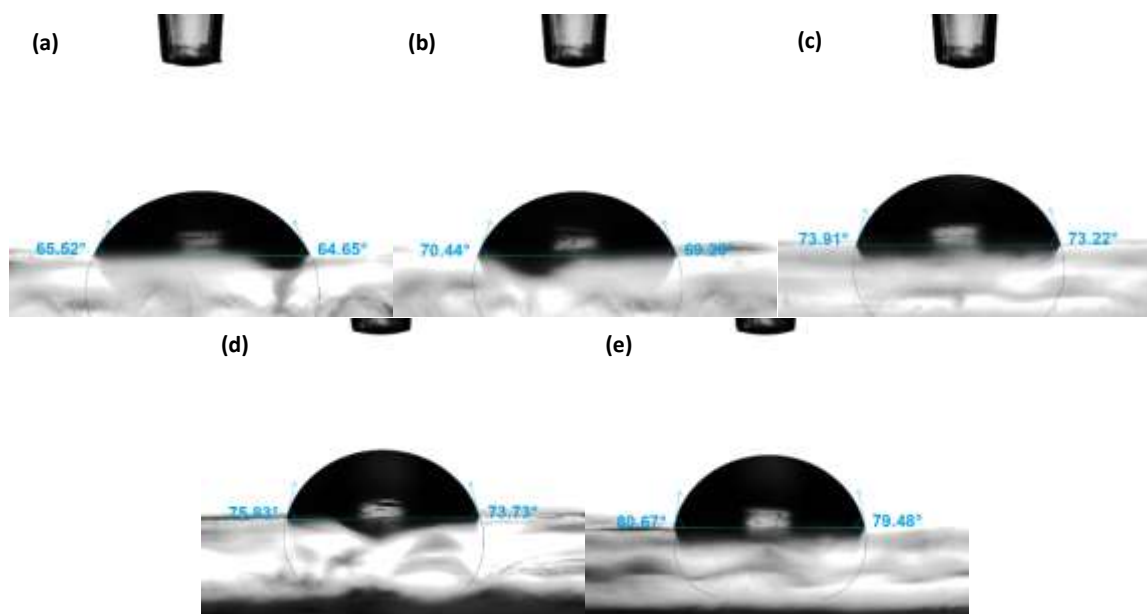


Figure 3. Contact angle of the films with (a) 0%, (b) 0.1%, (c) 0.25%, (d) 0.5% and (e) 1.0% eugenol.



The results of the study show the potential of the application of a bio-based PLA/PHB plasticized blend films with eugenol for the development of high-quality packaging materials, which can be used for the preservation of perishable food products such as fresh fish.

### **Acknowledgements**

This Project has received funding from the European Union's Horizon 2020 research and innovation program under the Marie Skłodowska-Curie Grant agreement 872217 (<https://www.ichthys-eu.org/about>).

### **References**

1. Y. Ma, L. Li, Y. Wang, *Packaging Technology and Science*, **31** (2018).
2. I. Armentano, E. Fortunati, N. Burgos, F. Dominici, F. Luzi, S. Fiori, A. Jiménez, K. Yoon, J. Ahn, S. Kang, J. M. Kenny, *Food Science and Technology*, **64** 2 (2015).
3. A. D'Anna, R. Arrigo, A. Frache, Alberto, *Polymers*, **1416** 11 (2019).
4. M. Li, H. Yu, Y. Xie, Y. Guo, Y. Cheng, H. Qian, W. Yao, *LWT*, **145** (2021).

## Optimization of production, antioxidant activity and stability of plant-based emulsions

Katarzyna Włodarczyk<sup>1\*</sup>, Karolina Stepińska<sup>1</sup>, Aleksandra Szydłowska-Czeraniak<sup>1</sup>

<sup>1</sup>Department of Analytical Chemistry and Applied Spectroscopy, Faculty of Chemistry, Nicolaus Copernicus University in Toruń, Gagarina 7, 87-100 Toruń, Poland

\*kwlodarczyk@doktorant.umk.pl

Food allergy is continually increasing problem nowadays. Up to 3.2% of children from USA and Western Europe have an allergy to eggs [1] also plant-based diet is getting more popular. Therefore, eggs in mayonnaise is replaced by plant protein isolates or soy drink [2,3]. In recent years, attention has been paid to sustainable development and “zero-waste” movement. Food industrial by-products like aquafaba can act as emulsifier in emulsions [4]. Also sesame and peanut meal milk was used as egg-yolk replacer in plant-based emulsions to improve nutritional value and rheological properties [5].

The aim of this study was to optimize production of low-fat plant-based mayonnaise based on rapeseed meal milk-like beverage. The emulsions consisted of oil (50%), egg replacer – rapeseed meal milk-like beverage (6-18%), guar gum (0-0.6%), mustard (4%), vinegar (1%), water (25.4 – 38%), salt and sugar (>1%). Response surface methodology was applied to estimate the effect of two independent variables, the amount of egg replacer (x) and amount of guar gum (y), on prepared plant-based emulsion parameters associated with antioxidant activity and stability. Antioxidant properties and total phenolic content of emulsion were determined using QUick, Easy, New, CHEap and Reproducible procedures using 2,2-diphenyl-1-picrylhydrazyl (QUENCHER-DPPH), 2,2'-azino-bis(3-ethylbenzothiazoline-6-sulfonic acid) (QUENCHER-ABTS) and Folin-Ciocalteu assay (QUENCHER-FC), respectively. The physical stability test was determined by the centrifugation method.

Increasing rapeseed meal milk (beverage) from 6 to 18% enhanced the radical scavenging activity measured by ABTS and DPPH methods. Also, the amount of total phenolic content determined by the Folin-Ciocalteu assay increased. The addition of a higher amount of guar gum (0 – 0.6%) improved the physical stability of the prepared emulsions, but it had a negative influence on antioxidant activity and total phenolic content. To evaluate the sufficiency of the proposed mathematical models, verification experiments were carried out at the predicted condition (x = 18%; y = 0.051%). The predicted and experimental values are listed in table 1. The novel vegan emulsion based on rapeseed meal beverage can be an interesting alternative to traditional and plant-based emulsions.

Table 1. Predicted and experimental values of the studied responses under the optimal conditions.

Response variables	Optimum ingredients amount		Predicted values	Experimental values ± SD
	Egg yolk replacer amount (%)	Guar gum amount (%)		
QUENCHER-DPPH (µmol TE/100 g)	18	0.0051	826.63	897.72 ± 2.4
QUENCHER-ABTS (µmol TE/100 g)			4335.58	4175.34 ± 1.68
QUENCHER-FC (µmol TE/100 g)			2014.61	1992.25 ± 1.91
Physical stability (%)			90.23	75.06 ± 0.74

### Acknowledgements

This research was financially supported by project “Grants4NCUStudents” (NCU Excellence Initiative – Research University).

### References

1. V.A. Gonzales-González et al. *Allergy Asthma Clin. Immunol.* **14**, 23 (2018).
2. M.H. Alu'datt et al. *J. Food Sci. Technol.* **54**, 1395–1405 (2017).
3. K. Rahmati, M. Mazaheri Tehrani, K. Daneshvar. *J. Food Sci. Technol.* **51**, 3341–3347 (2014).
4. T. F. Buhl, C.H. Christensen, M. Hammershøj. *Food Hydrocoll.* **96**, 354–364 (2019).
5. M. Karshenas, M. Goli, N. Zamindar. *Food Sci. Technol. Int.* **25**, 633–641 (2019).